

**ERCOFTAC Workshop on Data Bases and Testing of
Calculation Methods for Turbulent Flows**

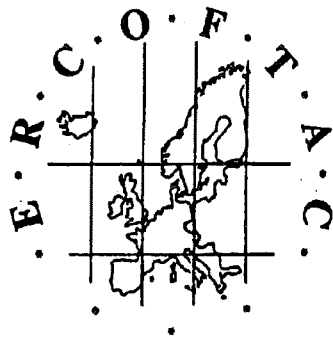
in association with

4th ERCOFTAC/IAHR Workshop on Refined Flow Modelling

April 3 - 7, 1995, University of Karlsruhe, Karlsruhe, Germany

supported by

COMETT II through UETP ERCOFTAC, COST, Electricité de France, University of Karlsruhe



**Revised
test case descriptions
and calculation results**

Organizers:

Professor W. Rodi
Dr. J.-C. Bonnin
Dipl.-Ing. T. Buchal

Institut für Hydromechanik, Universität Karlsruhe
Kaiserstr. 12, D-76128 Karlsruhe, F.R. Germany
Fax No.: +49-721-608-2202/4290
E-mail: rodi@bau-vern.uni-karlsruhe.de

TEST CASE DESCRIPTIONS

ERCOFTAC Workshop on Data Bases and Testing of Calculation Methods for Turbulent Flows

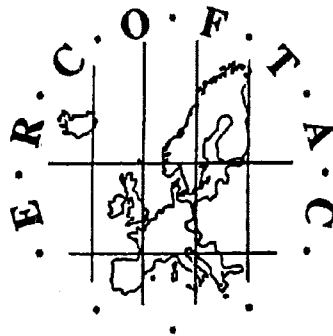
in association with

4th ERCOFTAC/IAHR Workshop on Refined Flow Modelling

April 3 - 7, 1995, University of Karlsruhe, Karlsruhe, Germany

supported by

COMETT II through UETP ERCOFTAC, COST, Electricité de France, University of Karlsruhe



Organizers:

Professor W. Rodi

Telephone: +49-721-608-3535

Dr. J.-C. Bonnin

Telephone: +49-721-608-3533

Institut für Hydromechanik, Universität Karlsruhe

Kaiserstr. 12, 76128 Karlsruhe, F.R. Germany

Fax No.: +49-721-608-2202/4290

E-mail: rodi@bau-verm.uni-karlsruhe.de

Nomenclature

| | |
|--|--|
| \bar{X} | time-averaged value of time-dependent quantity X |
| x' | fluctuating component of X |
| $S_x = \overline{x'^3} / \overline{x'^2}^{3/2}$ | skewness of X |
| $F_x = \overline{x'^4} / \overline{x'^2}^2$ | flatness of X |
| $R_{fg} = \frac{\overline{f'g'}}{\sqrt{\overline{f'^2}} \sqrt{\overline{g'^2}}}$ | temporal correlation coefficient |
| k | turbulent kinetic energy |
| ε | dissipation rate of turbulent kinetic energy |
| ν | kinematic viscosity |
| Re | Reynolds number |
| τ_w | wall shear stress |
| ρ | density |
| $U_\tau = U_* = (\tau_w / \rho)^{1/2}$ | friction velocity |
| $\overline{C_p}$ | time-averaged pressure coefficient |
| C_f | wall friction coefficient |
| $\delta(X)$ | uncertainty estimation of the quantity X |

PREFACE

This document contains the calculation results for 5 test cases and the description of calculation methods submitted to the ERCOFTAC Workshop on *Data Bases and Testing of Calculation Methods for Turbulent Flows* held in Karlsruhe from April 3 to 7, 1995. The workshop was an outcome and marked the end of the research project "Data Validation and Comparison in Fluid Mechanics" financed by the CEC programme SCIENCE, in which 7 ERCOFTAC members participated to collect experimental and numerical data on turbulent flows, to check their reliability and suitability for test cases, to set up test cases and perform calculations with various turbulence models, and finally to create a data bank from which the data can be accessed. This project, which was restricted to incompressible single-phase flows without chemical reactions, has yielded data for about 70 flows, and 10 well documented test cases have been set up from which 5 were chosen for the present workshop. The workshop follows three previous ERCOFTAC/IAHR Workshops on Refined Flow Modelling which have succeeded 14 IAHR workshops that were organised by the IAHR Working Group on Refined Flow Modelling in the years 1980 - 1991. Hence it is considered to be the 4th workshop in this series.

The following test cases have been chosen for the workshop:

Two-dimensional flows:

1. Couette flow with plane and wavy fixed walls
2. 2D model hill flows
3. Swirling boundary layer in conical diffuser

Three-dimensional flows:

4. Wing body junction with separation
5. Developing flow in a curved rectangular duct

The flows have been selected to range from relatively simple ones (Couette flow) to fairly complex 3D flows, to cover a number of different physical processes, and to be of practical relevance. Deliberately, only isothermal flows have been included; flows with heat transfer and buoyancy effects will be dealt with at future workshops.

Initially 101 groups intended to submit results to the workshop; in the end 36 groups managed to meet the deadline, submitting altogether 129 solutions for the 5 test cases. At the workshop, some inconsistencies and errors were detected and some information on the turbulence models, wall functions and inflow conditions used was missing. The contributors were asked to resupply corrected results and additional information. This document is a revised version of the original proceedings and contains the corrected results. A paper giving an interpretation of the results is in preparation.

The processing of the submitted data and the cross plotting required considerable effort. We are grateful to Dr. D. Laurence and his coworkers at EDF, Chatou, for helping us on this task by handling the originally submitted data for test cases 4 and 5.

Karlsruhe, July 1995

J.Ch. Bonnin, T. Buchal, W. Rodi

CONTENTS

Preface

Contents

The Test Cases D-1

Summary of Contributions with Key to Abbreviations

Description of Calculation Methods and Grids P-1

Results for:

Test Case 1: Couette Flow with Plane and Wavy Fixed Wall 1-1

Test Case 2: 2D Model Hill Flows 2-1

Test Case 3: Swirling Boundary Layer in Conical Diffuser 3-1

Test Case 4: Wing/Body Junction with Separation 4-1

Test Case 5: Developing Flow in a Curved Rectangular Duct 5-1

LIST OF CONTRIBUTIONS

| Name (Affiliation) | Alias | Convection Scheme | Mesh | Turbulence Model | Near-Wall Treatment | Key-Name |
|--------------------|-------|-------------------|------|------------------|---------------------|----------|
|--------------------|-------|-------------------|------|------------------|---------------------|----------|

TEST CASE 1A

| | | | | | | |
|---|----------|------------------------|---------|------------------------------------|-------------------------------|----------------|
| Cazalbou/Torres (ENSICA) | ENSICA | — | 1x100 | low-Re $k-\epsilon$ Yang-Shi | — | IKE_YaSh |
| | | MUSCL 1st-order | 96x102 | low-Re $k-\epsilon$ Launder-Sharma | — | IKE_LaSh(arco) |
| | | — | 1x100 | low-Re $k-\epsilon$ Launder-Sharma | — | IKE_LaSh |
| Craft (UMIST) | UMISTCra | Quick, MUSCL (turb.) | 120x80 | Reynolds-Stress Model Cubic | $k-\epsilon$ Launder-Sharma | RSM_Cub+2eq |
| | | | 120x80 | RSM Craft-Launder | $k-\epsilon$ Launder-Sharma | RSM_CrLa+2eq |
| Hanjalic/Hadzic/Jakirlic (TU Delft - Appl. Physics) | UDelftHa | UDS | 100x100 | RSM Hanjalic-Jakirlic-Hadzic | — | RSM_HJH |
| | | | 100x100 | low-Re $k-\epsilon$ Launder-Sharma | — | IKE_LaSh |
| Haroutunian (Fluid Dynamics Int.) | FluiDyna | streamline upwind | 200x69 | $k-\omega$ | — | kOm_Wil |
| Houzeaux (CERCA) | UConcord | 2nd-order FE | 200x70 | $k-\omega$ | — | kOm_Wil |
| Laurence et al. (EDF-DER-LNH) | EDFLNHLa | — | 1x200 | RSM Launder-Reece-Rodi | elliptic relaxation | RSM_LRR+elr |
| | | characteristics method | 200 FE | low-Re $k-\epsilon$ Launder-Sharma | — | IKE_LaSh |
| Stanislas/Hannani/Deldicque (Ecole Centrale Lille) | ECLille | — | 1x199 | RSM Jakirlic-Hanjalic | — | RSM_JaHa |
| | | — | 1x199 | RSM Launder-Shima | — | RSM_LaSh |
| | | Galerkin FE | 8000 FE | two-layer $k-\epsilon$ | Chien | hKE_std+Chi |
| | | — | 8000 FE | two-layer $k-\epsilon$ | Rodi-Mansour-Michelassi 1 eq. | hKE_std+RMM |
| Zaky (Univ. of Karlsruhe) | UKarlsru | Hybrid | 101x121 | two-layer $k-\epsilon$ | Norris-Reynolds 1 eq. | hKE_std+NoRe |

TEST CASE 1B

| | | | | | | |
|---|----------|----------------------|---------|------------------------------------|-----------------------------|----------------|
| Cazalbou/Torres (ENSICA) | ENSICA | — | 1x100 | low-Re $k-\epsilon$ Yang-Shi | — | IKE_YaSh |
| | | MUSCL 1st-order | 96x102 | low-Re $k-\epsilon$ Launder-Sharma | — | IKE_LaSh(arco) |
| | | — | 1x100 | low-Re $k-\epsilon$ Launder-Sharma | — | IKE_LaSh |
| Craft (UMIST) | UMISTCra | Quick, MUSCL (turb.) | 120x80 | Reynolds-Stress Model Cubic | $k-\epsilon$ Launder-Sharma | RSM_Cub+2eq |
| | | | 120x80 | RSM Craft-Launder | $k-\epsilon$ Launder-Sharma | RSM_CrLa+2eq |
| Hanjalic/Hadzic/Jakirlic (TU Delft - Appl. Physics) | UDelftHa | UDS | 100x100 | RSM Hanjalic-Jakirlic-Hadzic | — | RSM_HJH |

| Name (Affiliation) | Alias | Convection Scheme | Mesh | Turbulence Model | Near-Wall Treatment | Key-Name |
|--|----------|------------------------|---------|------------------------------------|-------------------------------|--------------|
| | | | 100x100 | low-Re $k-\epsilon$ Launder-Sharma | — | IKE_LaSh |
| Haroutunian (Fluid Dynamics Int.) | FluiDyna | streamline upwind | 200x69 | $k-\omega$ | — | kOm_Wil |
| Houzeaux (CERCA) | UConcord | 2nd-order FE | 200x70 | $k-\omega$ | — | kOm_Wil |
| Laurence et al. (EDF-DER-LNH) | EDFLNHLa | characteristics method | 200 FE | low-Re $k-\epsilon$ Launder-Sharma | — | IKE_LaSh |
| Stanislas/Hannani/Deldicque (Ecole Centrale Lille) | ECLille | — | 1x199 | RSM Jakirlic-Hanjalic | — | RSM_JaHa |
| | | — | 1x199 | RSM Launder-Shima | — | RSM_LaSh |
| | | Galerkin FE | 8000 FE | two-layer $k-\epsilon$ | Chien | hKE_std+Chi |
| | | — | 8000 FE | two-layer $k-\epsilon$ | Rodi-Mansour-Michelassi 1 eq. | hKE_std+RMM |
| Zaky (Univ. of Karlsruhe) | UKarlsru | Hybrid | 101x121 | two-layer $k-\epsilon$ | Norris-Reynolds 1 eq. | hKE_std+NoRe |

TEST CASE 1C

| | | | | | | |
|---|----------|-----------|--------|------------------------------------|-----------------------|----------------|
| Cazalbou/Torres (ENSICA) | ENSICA | McCormack | 52x102 | low-Re $k-\epsilon$ Launder-Sharma | — | IKE_LaSh |
| | | Roe+MUSCL | 52x102 | low-Re $k-\epsilon$ Launder-Sharma | — | IKE_LaSh(arco) |
| Hanjalic/Hadzic/Jakirlic (TU Delft - Appl. Physics) | UDelftHa | UDS | 180x80 | RSM Hanjalic-Jakirlic-Hadzic | — | RSM_HJH |
| | | — | 180x80 | low-Re $k-\epsilon$ Launder-Sharma | — | IKE_LaSh |
| Zaky (Univ. of Karlsruhe) | UKarlsru | Hybrid | 81x81 | two-layer $k-\epsilon$ | Norris-Reynolds 1 eq. | hKE_std+NoRe |

TEST CASE 2A

| | | | | | | |
|--|----------|--------------------------|---------|------------------------------------|------------------------|-----------------|
| Blom (Hokkaido R. D. P. Res. Center) | RCHokkai | upwind | 20x102 | standard $k-\epsilon$ | non-std wall functions | hKE_std+wf_nstd |
| Buchal (Univ. of Karlsruhe) | UKarlsru | Hybrid, HLP | 153x225 | two-layer $k-\epsilon$ | Norris-Reynolds 1 eq. | hKE_std+NoRe |
| | | HLP | 153x221 | standard $k-\epsilon$ | wall functions | hKE_std+wf |
| Castro/Palma (Univ. of Porto) | UPorto | Hybrid | 321x141 | standard $k-\epsilon$ | wall functions | hKE_std+wf |
| Davidson/Perzon et al. (Chalmers Univ. of Techn.) | UChalmer | Quick + HUW (turb.) | 122x50 | RSM Launder-Reece-Rodi | wall functions | RSM_LRR+wf |
| | | Quick + HUW (turb.) | 128x100 | RSM Hanjalic-Launder | — | RSM_HaLa |
| | | Quick + HUW (turb.) | 122x50 | RSM Speziale-Sarkar-Gatski | wall functions | RSM_SSG+wf |
| | | Quick + van Leer (turb.) | 128x100 | two-layer $k-\epsilon$ | Chen-Patel 1 eq. | hKE_std+ChPa |
| | | Quick + HUW (turb.) | 122x50 | standard $k-\epsilon$ | wall functions | hKE_std+wf |
| | | Quick + van Leer (turb.) | 128x100 | $k-\omega$ | — | kOm_Wil |
| | | Quick + HUW (turb.) | 128x100 | low-Re $k-\epsilon$ Launder-Sharma | — | IKE_LaSh |

| Name (Affiliation) | Alias | Convection Scheme | Mesh | Turbulence Model | Near-Wall Treatment | Key-Name |
|---|----------|--------------------------|------------|---|-------------------------------|-----------------|
| | | Quick + van Leer (turb.) | 128x100 | low-Re $k-\epsilon$ Lien-Leschziner | — | IKE_LiLe |
| Hanjalic/Hadzic/Jakirlic (TU Delft - Appl. Physics) | UDelftHa | UDS | 136x60 | RSM Launder-Reece-Rodi | wall functions | RSM_LRR+wf |
| | | | 136x60 | standard $k-\epsilon$ | wall functions | hKE_std+wf |
| Huurdean (Univ. of Stuttgart) | UStuttga | streamline upwind FE | 173x87 FE | two-layer $k-\epsilon$ | Chen-Patel 1 eq. | hKE_std+ChPa |
| | | | 211x101 FE | standard $k-\epsilon$ | non-std wall functions | hKE_std+wf_nstd |
| Issa/Leong/Sanatian (Computational Dynamics) | CompDyna | Hybrid | 48100 CV | two-layer RNG $k-\epsilon$ | Norris-Reynolds 1 eq. | hKE_RNG+NoRe |
| Jongen/Marx (EPFL) | EPFLausa | Roe+kappa | 85x100 CV | low-Re $k-\epsilon$ Lam-Bremhorst | — | IKE_LaBr |
| Kaczynski (Univ. of Gdansk) | UGdansk | monotized linear-upwind | 131x51 | standard $k-\epsilon$ | non-std wall functions | hKE_std+wf_nstd |
| Kessler (DLR Goettingen) | DLRGoett | Quick | 382x152 | $k-\omega$ | — | kOm_Wil |
| Laurence et al. (EDF-DER-LNH) | EDFLNHLa | characteristics method | 26856 FE | low-Re $k-\epsilon$ model LaSh | — | IKE_LaSh |
| Lien/Leschziner (UMIST) | UMISTLes | Quick, UMIST/TVD | 150x90 | RSM Gibson-Launder | Wolfshtein 1 eq. | RSM_GiLa+Wol |
| | | | 150x60 | RSM Gibson-Launder | wall functions | RSM_GiLa+wf |
| | | | 150x60 | RNG-modified $k-\epsilon$ | wall functions | hKE_RNG+wf |
| | | | 150x60 | standard $k-\epsilon$ | wall functions | hKE_std+wf |
| | | | 150x90 | low-Re $k-\epsilon$ Lien-Leschziner | — | IKE_LiLe |
| Michelassi/Chiaromonti (Univ. of Florence) | UFlorenc | centered finite-diff. | 160x71 | two-layer $k-\epsilon$ | Norris-Reynolds 1 eq. | hKE+NoRe |
| | | | 160x71 | two-layer $k-\epsilon$ | Rodi-Mansour-Michelassi 1 eq. | hKE+RMM |
| | | | 160x71 | $k-\omega$ | — | kOm_Wil |
| | | | 160x71 | two-layer $k-\epsilon$ | Kim model | hKE+Kim |
| | | | 160x71 | low-Re $k-\epsilon$ Nagano-Hishida | — | IKE_NaHi |
| | | | | | | |
| Sedlar (Pump Research Institute Olomouc) | IOlomouc | upwind FE | 101x61 FE | two-layer $k-\epsilon$ | Goldberg model | hKE_std+Gol |
| | | | 101x61 FE | standard $k-\epsilon$ | non-std wall functions | hKE_std+wf_nstd |
| | | | 101x61 FE | non-linear $k-\epsilon$ Speziale | wall functions | nKE_Spez+wf |
| Stubley (ASC) | ASC | UDS/CDS blended | 150x188 FE | non-linear $k-\epsilon$ Shih-Zhu-Lumley | wall functions | nKE_SZL+wf |
| | | | 150x188 FE | standard $k-\epsilon$ | non-std wall functions | hKE_std+wf_nstd |
| Zijlema (TU Delft) | UDelftZi | TVD + ISNAS (turb.) | 110x60 | standard $k-\epsilon$ | wall functions | hKE_std+wf |
| | | | 110x80 | $k-\omega$ | — | kOm_Wil |

| Name (Affiliation) | Alias | Convection Scheme | Mesh | Turbulence Model | Near-Wall Treatment | Key-Name |
|--------------------|-------|-------------------|------|------------------|---------------------|----------|
|--------------------|-------|-------------------|------|------------------|---------------------|----------|

TEST CASE 2B

| | | | | | | |
|---|----------|------------------------|----------|--------------------------------------|------------------------------|-----------------|
| Blom (Hokkaido R. D. P. Res. Center) | RCHokkai | upwind | 20x102 | standard k- ϵ | non-std wall functions | hKE_std+wf_nstd |
| Buchal (Univ. of Karlsruhe) | UKarlsru | HLPA | 153x225 | two-layer k- ϵ | Norris-Reynolds 1 eq. | hKE_std+NoRe |
| | | Hybrid | 153x225 | standard k- ϵ | wall functions | hKE_std+wf |
| Castro/Palma (Univ. of Porto) | UPorto | Hybrid | 241x161 | standard k- ϵ | wall functions | hKE_std+wf |
| | | | 241x161 | standard k- ϵ | wall functions | hKE_std+wf(fix) |
| | | | 181x181 | Leschziner-Rodi-modif. k- ϵ | wall functions | hKE_LeRo+wf |
| Craft (UMIST) | UMISTCra | Quick + MUSCL(turb.) | 80x120 | RSM Cubic | k- ϵ Launder-Sharma | RSM_Cub+2eq |
| | | | 80x120 | RSM Craft-Launder | k- ϵ Launder-Sharma | RSM_CrLa+2eq |
| Hanjalic/Hadzic/Jakirlic (TU Delft - Appl. Physics) | UDelftHa | UDS | 56x120 | RSM Launder-Reece-Rodi | wall functions | RSM_LRR+wf |
| | | | 243x120 | RSM Launder-Reece-Rodi | wall functions | RSM_LRR+wf(7th) |
| | | | 56x120 | standard k- ϵ | wall functions | hKE_std+wf |
| | | | 243x120 | standard k- ϵ | wall functions | hKE_std+wf(7th) |
| Issa/Leong/Sanatian (Computational Dynamics) | CompDyna | Hybrid | 13230 CV | RNG-modifided k- ϵ | wall functions | hKE_RNG+wf |
| | | | 13230 CV | RNG-modifided k- ϵ | wall functions | hKE_RNG+wf(7th) |
| Kessler (DLR Goettingen) | DLRGoett | Quick | 180x152 | k- ω | — | kOm_Wil |
| Laurence et al. (EDF-DER-LNH) | EDFLNHLa | characteristics method | 47556 FE | low-Re k- ϵ model LaSh | — | IKE_LaSh |
| | | | 47556 FE | RSM Launder-Reece-Rodi | wall functions | RSM_LRR |
| Maass (DLR Oberpfaffenhofen) | DLROberp | 2nd-order upwind | 96x48x48 | 2nd-order for SGS fluxes (LES) | logarithmic law | LES |
| Sedlar (Pump Research Institute Olomouc) | IOlomouc | upwind FE | 79x61 FE | two-layer k- ϵ | Goldberg model | hKE_std+Gol |
| | | | 79x61 FE | standard k- ϵ | non-std wall functions | hKE_std+wf_nstd |
| | | | 79x61 FE | non-linear k- ϵ Speziale | wall functions | nKE_Spez+wf |

TEST CASE 3

| | | | | | | |
|-------------------------------------|----------|----------------------|---------|--------------------------------------|----------------|-------------|
| Brison et al. (Ecole Centrale Lyon) | ECLyon | streamline upwind FE | 4800 FE | RSM Launder-Reece-Rodi (IP) | wall functions | RSM_LRR+wf |
| Gier/Krueger (RWTH Aachen) | THAachen | upwind | | RSM Launder-Reece-Rodi | wall functions | RSM_LRR+wf |
| | | | | Algebraic-Stress Model Clarke-Wilkes | wall functions | ASM_CiWi+wf |
| | | | | RNG-modified k- ϵ | wall functions | hKE_RNG+wf |

| Name (Affiliation) | Alias | Convection Scheme | Mesh | Turbulence Model | Near-Wall Treatment | Key-Name |
|---------------------------------------|----------|------------------------------|----------|--|---------------------|-------------|
| Kessler (DLR Goettingen) | DLRGoett | Quick | 248x152 | k- ω | — | kOm_Wil |
| Hirsch/Khodak (Univ. of Brussels) | UBrussel | 4th-order central diff. | 64x32 | non-linear k- ϵ Hirsch-Khodak | wall functions | nKE_HiKh+wf |
| | | | 64x32 | non-linear k- ϵ Shih-Zhu-Lumley | wall functions | nKE_HiKh+wf |
| | | | 64x32 | standard k- ϵ | wall functions | hKE_std+wf |
| Michelassi/Mugnai (Univ. of Florence) | UFlorenc | 2nd-order cent. finite-diff. | 419x150 | low-Re k- ϵ Jones-Launder | — | IKE_JoLa |
| Sick/Scheuerer (Sulzer Innotec/ASC) | ASC | 2nd-order upwind LPS | 13616 CV | standard k- ϵ | wall functions | hKE_std+wf |
| Vu/Shyy (GE Hydro/Univ. of Florida) | GEHydro | 2nd-order upwind | 35x35x75 | standard k- ϵ | wall functions | hKE_std+wf |

TEST CASE 4

| | | | | | | |
|--|----------|----------------------|-----------|---|--------------------------|--------------|
| Buchal (Univ. of Karlsruhe) | UKarlsru | HLLA, Hybrid | 81x81x81 | standard k- ϵ | wall functions | hKE_std+wf |
| Daunius (Volvo Data AB) | Volvo | CCCT 3rd-order | 176000 CV | RSM Launder-Reece-Rodi | wall functions | RSM_LRR+wf |
| Haroutunian (Fluid Dynamics International) | FluiDyna | streamline upwind | 114686 FE | two-layer modified k- ϵ | 0 eq.-model ¹ | hKE_mod+0eq |
| | | | 114686 FE | two-layer k- ϵ | 0 eq.-model | hKE_std+0eq |
| Issa/Leong/Sanatian (Computational Dynamics) | CompDyna | upwind | 177365 CV | RNG-modified k- ϵ | wall functions | hKE_RNG+wf |
| Mains/Muzaferija/Peric (Univ. of Hamburg) | UHamburg | 2nd-order/upwind | 525018 CV | RNG-modified k- ϵ | wall functions | hKE_RNG+wf |
| Ruprecht (Univ. of Stuttgart) | UStuttg2 | streamline upwind FE | 340000 FE | two-layer k- ϵ + Kato-Launder modif. | Mohammadi 1 eq. | hKE_KaLa+1eq |
| Scheuerer/Holzwarth (ASC) | ASC | 2nd-order upwind LPS | 92387 CV | standard k- ϵ | wall functions | hKE_std+wf |

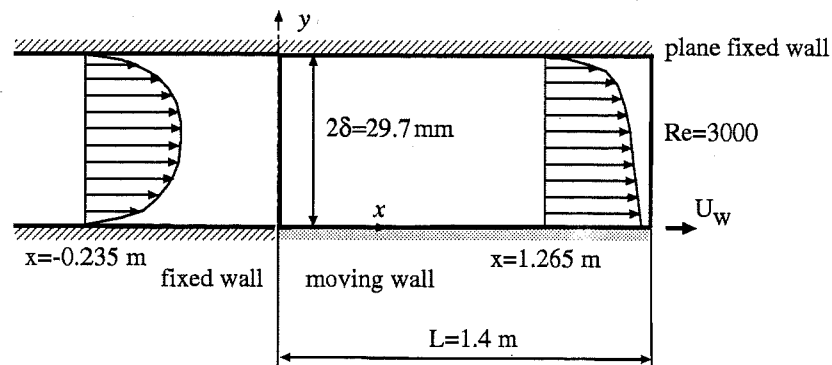
TEST CASE 5

| | | | | | | |
|--------------------------------------|----------|------------------------|-----------|--|----------------|-------------|
| Hedbergh/Chung (CERCA, McGill. Univ) | UMcGill | HLLA | 148x30x25 | RSM Gibson-Launder | wall functions | RSM_GiLa+wf |
| Hirsch/Khodak (Univ. of Brussels) | UBrussel | Quick | 96x16x32 | non-linear k- ϵ Hirsch-Khodak | wall functions | nKE_HiKh+wf |
| | | | 96x16x32 | non-linear k- ϵ Shih-Zhu-Lumley | wall functions | nKE_SZL+wf |
| | | | 96x16x32 | standard k- ϵ | wall functions | hKE_std+wf |
| Mattei/Minier (EDF-DER-LNH) | EDFLNHMi | characteristics method | | standard k- ϵ | wall functions | hKE_std+wf |
| Sick/Scheuerer (Sulzer Innotec/ASC) | ASC | 2nd-order upwind LPS | 163053 CV | standard k- ϵ | wall functions | hKE_std+wf |
| Zhang/Zhang (Univ. of Southampton) | USoutham | Hybrid | 163625 CV | Algebraic-Stress Model Clarke-Wilkes | wall functions | ASM_CiWi+wf |

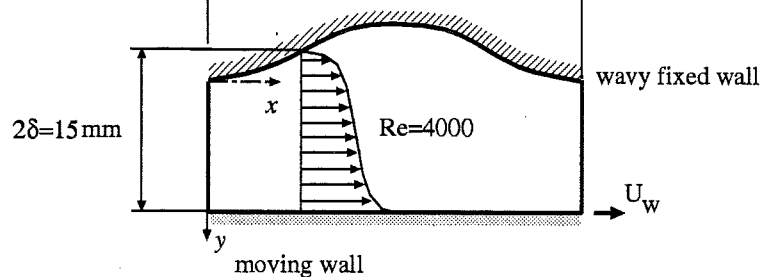
Test Case 1

Couette flow with plane and wavy fixed wall — *Experiments by Corenflos et al. and Nakabayashi et al. — Direct Numerical Simulations by Kuroda et al.*

cases A, B



case C



Flow description

Flow in a channel, between a plane (cases A, B) or wavy (case C) fixed wall and a plane moving wall.

Plane fixed wall, cases A and B

Distance between the two walls: $2\delta = 29.7$ mm.

Length of the domain: $L = 1.4$ m.

Wavy fixed wall, case C

Height of the channel close to the equation $h(x) = 2\delta - e\cos(2\pi x/L)$ with $e = 4.5$ mm, $2\delta = 15$ mm and $L = 1.4$ m (actual values stored in file `couette.prn` and recommended geometry data stored in `geom1c.dat`).

Flow characteristics

Case A, $Re = U_w\delta/\nu = 3000$

DNS by Kuroda *et al.* and experiments by Corenflos *et al.*

The channel flow develops from a pure Poiseuille flow (fixed bottom wall) to an established state (moving bottom wall) where the developed flow is of intermediate type. DNS data are available for the developed flow and experimental data are available for both the developing and developed flows. $\partial\bar{U}/\partial y = 0$ close to the moving wall (\bar{U} does not follow the logarithmic law of the wall) is the main feature of the developed flow.

Case B, $Re = 5000$

Experiments by Corenflos *et al.*

The channel flow develops from a pure Poiseuille flow (fixed bottom wall) to an established state (moving bottom wall) where the developed flow is of Couette type. Experimental data are available for both the developing and developed flows. For the developed flow, \bar{U} profile is close to the one of the pure Couette flow with a nearly symmetric shape but with higher values of $\partial\bar{U}/\partial y$ near the moving wall.

Case C, $Re = 4000$

Experiments by Nakabayashi *et al.*

The periodic behaviour of the flow is created by the periodic shape of the fixed upper wall. The wavy shape induces an alternating longitudinal pressure gradient which changes sign near the position where $h = 2\delta$. At these positions, the flow conditions are close to the ones of case B. Where $h \neq 2\delta$, the magnitude of the pressure gradient is insufficient to cause flow separation near the wavy wall but causes a distortion of the mean velocity profiles.

Flow parameters

Air with a kinematic viscosity:

$$\nu = 1.5 \times 10^{-5} \text{ m}^2/\text{s}.$$

Wall velocity: U_w .

Flow rate velocity, bulk velocity: U_q, U_b

Friction velocity on fixed wall: $U_{\tau f}$

Friction velocity on moving wall: $U_{\tau m}$

Non-dimensional pressure gradient:

$$a = (\delta/\rho U_w^2) \partial\bar{p}/\partial x$$

| case | A | B | C |
|---------------|------------------------|-------|--------|
| fixed wall | plane | plane | wavy |
| Re | 3000 | 5000 | 4000 |
| δ (mm) | 14.85 | 14.85 | 7.5 |
| U_w (m/s) | 3 | 5 | 7.9 |
| a | -1.18×10^{-3} | 0 | \sim |
| U_q/U_w | 0.812 | 0.490 | - |

Inflow conditions**Cases A and B**

In the plane fixed wall cases, the following measurements are provided at station 1, $x = -0.235$ m, upstream of the part of the channel where the bottom wall is moving, for a pure Poiseuille flow (fixed bottom wall). They can be used to calculate the developing flow.

Velocity measurements

Profiles from fixed to moving wall of: (file `poispr1.txt`)

First order moments

$$\bar{U}/U_q, \bar{V}/U_q, \bar{W}/U_q$$

Second order moments

Reynolds stresses:

$$\sqrt{u'^2}/U_{\tau f}, \sqrt{v'^2}/U_{\tau f}, \sqrt{w'^2}/U_{\tau f}$$

$$\overline{u'v'}/U_{\tau f}^2, \overline{w'v'}/U_{\tau f}^2$$

Measurement techniques**Cases A and B**

Measurements by Corenflos *et al.*

Hot wire velocity measurements have been carried out using single-wire and X-wire probes of boundary layer type.

Wall friction velocity $U_{\tau f}$ has been deduced from the $\overline{u'v'}$ profile close to the fixed wall.

Pressure measurements.

Case C

Measurements by Nakabayashi *et al.*

Hot-wire velocity measurements.

Pressure measurements.

Numerical techniques

Case A

DNS by Kuroda *et al.*

Direct Numerical Simulations have been performed using a spectral method with Fourier series in x and z directions and Chebyshev polynomials in y direction. The 3D computational domain is $5\pi\delta$ long, 2δ height and $2\pi\delta$ wide. Due to streamwise and spanwise homogeneities of the flow, the statistical values are only dependent on the distance from the wall.

Available data

- Case A, $Re = U_w\delta/\nu = 3000$

– Measurements by Corenflos *et al.*

The following measurements are available for the developing flow, at stations 2: $x = 0.165$ m, 3: $x = 0.265$ m and 4: $x = 1.165$ m.

Velocity measurements (file etabti.txt)

Profiles from fixed to moving wall of:

First order moment

$$\bar{U}/U_q$$

Second order moment

Reynolds stress:

$$\sqrt{u'^2}/U_{\tau f}$$

The following measurements are available for the established intermediate-type flow, at station 5: $x = 1.265$ m.

Velocity measurements (file typint5.txt)

Profiles from fixed to moving wall of:

First order moments

$$\bar{U}/U_q, \bar{V}/U_q, \bar{W}/U_q$$

Second order moments

Reynolds stresses:

$$\sqrt{u'^2}/U_{\tau f}, \sqrt{v'^2}/U_{\tau f}, \sqrt{w'^2}/U_{\tau f}$$

$$u'v'/U_{\tau f}^2, u'w'/U_{\tau f}^2$$

– DNS Calculations by Kuroda *et al.*

The following results are available for the statistical values (file pc12_pg.w13).

Velocity results

Profiles from fixed to moving wall of:

First order moments

Mean streamwise velocity:

$$\bar{U}/U_{\tau f}$$

Mean spanwise component of vorticity:

$$\bar{\Omega}_z$$

Second order moments

Reynolds stresses:

$$\sqrt{u'^2}/U_{\tau f}, \sqrt{v'^2}/U_{\tau f}, \sqrt{w'^2}/U_{\tau f}$$

$$u'v'/U_{\tau f}^2$$

Root mean square of vorticity components:

$$\sqrt{\omega_x'^2}/U_{\tau f}, \sqrt{\omega_y'^2}/U_{\tau f}, \sqrt{\omega_z'^2}/U_{\tau f}$$

Third order moments

Skewness:

$$S_u, S_v, S_w, S_{uv}$$

Fourth order moments

Flatness:

$$F_u, F_v, F_w, F_{uv}$$

Budgets of:

$$\overline{u'^2}, \overline{v'^2}, \overline{w'^2}, \overline{u'v'}, k, \varepsilon$$

Spectra of:

$$\overline{u'^2}, \overline{v'^2}, \overline{w'^2}$$

Two-point correlations:

$$R_{uu}, R_{vv}, R_{ww}$$

Pressure results

Profiles from fixed to moving wall of:

Second order moment

$$\overline{p'^2}$$

Third and fourth order moments

$$S_p, F_p$$

- Case B, $Re = U_w\delta/\nu = 5000$

– Measurements by Corenflos *et al.*

The same measurements as for case A are available for both the established Couette-type flow, at station 5: $x = 1.265$ m (file typcou5.txt), and the developing flow, at stations 2: $x = 0.165$ m, 3: $x = 0.265$ m and 4: $x = 1.165$ m (file etabtc.txt).

- Case C, $Re = U_w\delta/\nu = 4000$

– Measurements by Nakabayashi *et al.*

The following results are available at $x = 0., 0.175, 0.35, 0.525, 0.7, 0.875, 1.05, 1.225$ m. (file couette.prn)

Velocity measurements

Profiles of:

First order moments

$$\bar{U}/U_b, \bar{V}/U_b, \bar{U}/U_{\tau f}$$

Second order moments

Reynolds stresses:

$$\overline{u'^2}, \overline{v'^2}$$

Distribution of friction velocity along the wavy wall:

$$U_{\tau f}$$

Pressure measurements

Distribution of longitudinal pressure gradient along the wavy wall:

$$d\bar{p}/dx$$

Instructions for calculations**• 1st step: case A, developing flow****Inlet conditions:**

The calculation of the developing flow has to be started at $x = -0.235$ m, where the bottom wall is fixed, using the experimental values provided as inlet conditions for a pure Poiseuille flow (file `poispur1.txt`).

Moving wall:

The bottom wall is fixed between $x = -0.235$ m and $x = 0$ and is moving between $x = 0$ and $x = 1.4$ m with a velocity of $U_w = 3$ m/s ($Re = 3000$). $\partial\bar{U}/\partial y$ is nearly zero close to the moving wall. Therefore, a special treatment of this boundary might be considered.

Outlet conditions:

At $x = 1.4$ m, zero streamwise gradients may be assumed for the flow variables.

Presentation of the results:

The following results should be compared with the experimental data at $x = 0.165$ m, $x = 0.265$ m, $x = 1.165$ m and $x = 1.265$ m:

- mean velocity and Reynolds stress profiles, normalized by U_b

• 2nd step: case A, developed flow**One-dimensional flow:**

The calculation has to be performed for the one-dimensional established flow. If necessary, the flow rate may be derived from U_q and the longitudinal pressure gradient set to $a = -1.33 \times 10^{-3}$.

Presentation of the results:

The following results should be compared with the experimental data at $x = 1.265$ m and the DNS data:

- $d\bar{p}/dx$
- U_q/U_w
- mean velocity, Reynolds stress and k profiles, normalized by U_b

• 3rd step: case B, developing and developed flow

The same procedure as for the first step should be followed with a value of $U_w = 5$ m/s ($Re = 5000$). If possible, the computers should also calculate the developed flow with $U_w = 4$ m/s ($Re = 4000$). In this case, it is worth mentioning that neither measurements nor DNS data are provided.

• 4th step: case C, periodic flow**Periodicity:**

The calculation of the channel flow should be performed using periodicity conditions for both velocities and pressure gradient ($d\bar{p}(x+L)/dx = d\bar{p}(x)/dx$).

Presentation of the results:

The following results should be plotted and compared with the experimental data:

- mean velocity and Reynolds stress profiles at $x = 0, 0.175, 0.35, 0.525, 0.7, 0.875, 1.05, 1.225$ m, normalized by U_b
- $U_{\tau f}/U_b$ and $d\bar{p}/dx$ distributions along the wavy wall.

In case calculations have been performed for case B at $Re = 4000$, the following results should be plotted and compared with the experimental data:

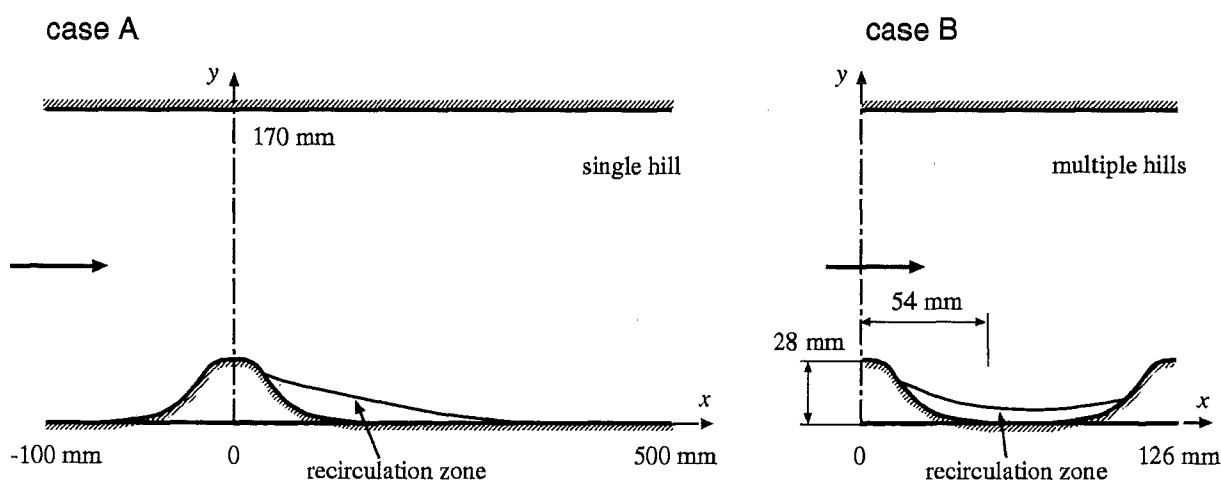
- mean velocity and Reynolds stress profiles at $x = 0.35$ m, normalized by U_b

Main references

1. K. NAKABAYASHI, O. KITOH and H. IWATA. Turbulent Couette type flow with an alternating pressure gradient. *Symp. on Turb. Shear Flows 8, Munich, poster I-13*, 1991.
2. K. CORENFLOS, S. RIDA, J.C. MONNIER, P. DUPONT, K. DANG TRAN, M. STANISLAS. Experimental and numerical study of a plane Couette-Poiseuille flow as a test case for turbulence modelling. *Engineering Turbulence Modelling and Experiments, Rodi and Martelli Eds, Elsevier Publ., 499-508*, 1993.
3. K. CORENFLOS. Etude expérimentale d'écoulements de Couette-Poiseuille turbulents à faible nombre de Reynolds. *PhD thesis - Lille, France*, 1993.
4. A. KURODA, N. KASAGI and M. HIRATA. Direct numerical simulation of turbulent plane Couette-Poiseuille flows: effect of mean shear on the near wall turbulence structures. *Symp. on Turb. Shear Flows 9, Kyoto, Japan, 8-4-1*, 1993.

Test Case 2

2D model hill flows — *Experiments by Almeida et al.*



Flow description

Flows over 2D polynomial-shaped obstacle(s) mounted on a flat plate with recirculation region in their wake.

In the first configuration, case A, a single hill is mounted on the bottom of the channel. In the second one, case B, a periodic flow is achieved over a series of consecutive hills mounted at the same location. The channel height is $H = 170$ mm and the maximum height and length of each hill are respectively $h_{max} = 28$ mm and $2R = 108$ mm. In the case of consecutive hills, the space between each of them is $4.5h_{max}$.

The shape of the hills was to be the inverse of a fourth-order polynomial but the actual shape is a bit different. The actual values of the height

$h(x)$ of the two-dimensional hills are stored in file `geom.dat`.

Flow characteristics

The hills are located about 6 m downstream of the tunnel inlet where a fully-developed channel flow is achieved in the absence of the obstacle(s). In case A, the measurements have been made around a single hill and, in case B, between two consecutive hills (the 7th and the 8th) located within an array of 10 equally spaced hills. The flow separates in the region of unfavourable pressure gradient on the downstream surface of the hills and, in the case of multiple hills, reattaches at an oblique angle on the upstream surface of the next hill. Very high levels of velocity fluctuations have been measured in

the shear layers surrounding the recirculation bubbles.

Flow parameters

Water with a kinematic viscosity:

$$\nu = 1 \times 10^{-6} \text{ m}^2/\text{s}.$$

Reference velocity: $U_0 = 2.147 \text{ m/s}$ in case A and $U_0 = 2.66 \text{ m/s}$ in case B

Mean centreline velocity at inlet in case A:
 $U_0 = 2.147 \text{ m/s}$.

Reynolds number: $U_0 h / \nu = 60,000$.

Inflow conditions

The following measurements are provided for a fully-developed channel flow in the absence of the hill(s) and at the same location. The centreline turbulence intensity is about 3%, the friction factor is $C_f = 0.0027$ and the wall friction velocity is $U_\tau = .079 \text{ m/s}$.

Velocity measurements

Profiles of: (stored in file ch000.dat)

First order moment

$$\bar{U}$$

Second order moments

Reynolds stresses:

$$\frac{\overline{u'^2}, \overline{v'^2}, \overline{w'^2}}{\overline{u'v'}}$$

Measurement techniques

Velocity measurements have been carried out using a Laser-Doppler Velocimeter up to 2 mm from the surface of the hill(s) and the bottom of the channel.

Measurement errors:

For a 95% confidence level:

$$\delta(\text{Mean values}) \quad 0.5\%$$

$$\delta(\text{Reynolds stresses}) \quad 3\%$$

Available measurements

The following profiles are available at 14 locations in case A (files 1h*.dat) and 11 locations in case B (files 2h*.dat).

Velocity measurements

Profiles of:

First order moments

$$\bar{U}, \bar{V}$$

Second order moments

Reynolds stresses:

$$\frac{\overline{u'^2}, \overline{v'^2}}{\overline{u'v'}}$$

Turbulent kinetic energy:

$$k/U_{ref}^2 \quad (k \text{ estimated as } \overline{u'^2} + 2\overline{v'^2})$$

Instructions for calculations

• Case A: single hill

Upper wall:

In both cases, the computational domain extends to the upper wall of the channel, $y = H = 170 \text{ mm}$.

Inlet conditions:

The calculation of the channel flow should be started at $x = -100 \text{ mm}$, upstream of the station $x = -50 \text{ mm}$ (where the flow is influenced by the presence of the hill), using the experimental values provided as inlet conditions.

Outlet conditions:

The outlet section must be placed sufficiently far downstream of the single hill ($x \geq 500 \text{ mm}$) in order to have the possibility of assuming zero streamwise gradients for the flow variables.

• Case B: consecutive hills

Periodicity:

Ideally the calculation of the channel flow should be performed using periodicity conditions for the flow variables.

• Presentation of results:

For both cases, the following results should be plotted and compared with the data:

– At $x/h_{max} = -1.785, -0.714, 0, 1.071, 1.786, 2.5, 3.214, 4.286, 4.786, 5.357, 6.607, 8.036, 10.714, 17.85$ in case A and at $x/h_{max} = 0,$

0.536, 0.714, 1.071, 1.786, 2.25, 2.715, 3.25, 3.429, 4.143, 4.5 in case B:

- mean velocity, Reynolds stress and k profiles against y , normalized by U_0

– In the whole computational domain:

- streamlines

Main references

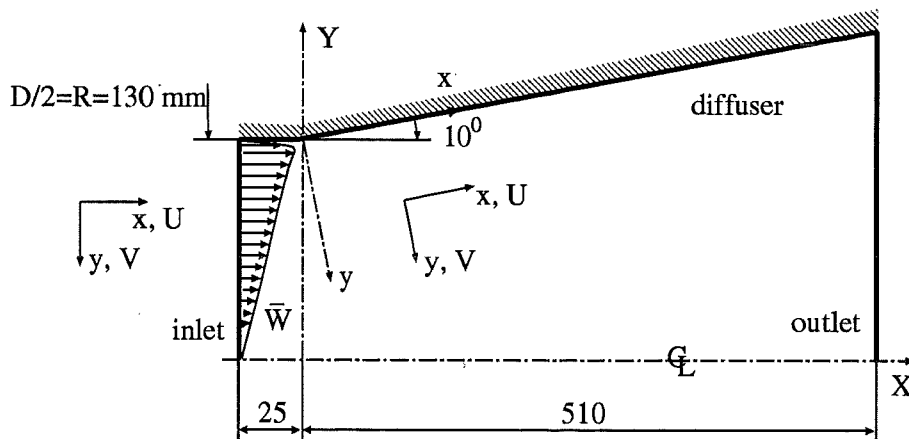
1. G.P. ALMEIDA, D.F.G. DURAO and M.V. HEITOR. Wake flows behind two-

dimensional model hills. *Exp. Thermal and Fluid Science*, 7, 87, 1993.

2. G.P. ALMEIDA, D.F.G. DURAO, M.V. HEITOR and J.P. SIMOES. LDV measurements of fully-developed turbulent channel flow. *Proc. 5th Int. Symp. Appl. Laser Techniques to Fluid Mechanics, Lisbon, pp. 9-12, 1990.*

Test Case 3

Swirling boundary layer in conical diffuser — *Experiments by Clausen et al.*



Flow description

Swirling boundary layer developing in a conical diffuser.

The conical diffuser is placed 100 mm downstream of a rotating swirl generator of diameter $D = 260$ mm and discharges into the atmosphere at $X = 510$ mm. It has a 20° included angle and an area ratio of 2.84.

Flow characteristics

The swirling flow is created by a rotating cylinder including a honeycomb screen at its inlet. At its outlet, the inlet swirl is close to solid-body rotation. Along the diffuser, the

swirl is of sufficient magnitude to prevent boundary layer separation but just insufficient to cause recirculation in the core flow. The axial pressure gradient and the curvature of the streamlines have been found to be the dominant perturbations imposed to the swirling boundary layer as it exits the cylindrical part and enters the conical diffuser. The swirl is responsible for severe radial gradients near the wall for most of the turbulence quantities.

Flow parameters

Air with a kinematic viscosity:

$$\nu = 1.5 \times 10^{-5} \text{ m}^2/\text{s}.$$

Average axial velocity at inlet ($x = -25$ mm):

$$U_0 = 11.6 \text{ m/s}.$$

Reynolds number: $U_0 D/\nu = 202,000$.
Atmospheric pressure at outlet.

Inflow conditions

The following measurements are provided at station -25, located at $x = -25$ mm, 75 mm downstream of the swirl generator and 25 mm upstream of the diffuser entrance. The swirl is close to solid-body rotation with a nearly uniform axial velocity in the core region outside the boundary layers. The swirl number is $W_{max}/U_0 = 0.59$ where W_{max} is the maximal circumferential velocity. The wall shear stress is $\tau_{wx}/U_0^2 = 0.00282$ in x direction and $\tau_{wz}/U_0^2 = 0.00190$ in z direction. The wall streamline angle is $\beta_w = \tan^{-1}(W/U)_{y=0} = 34^\circ$.

Velocity measurements

Profiles of:

First order moments from wall to centreline (files U-25.dat and W-25.dat)

$$\bar{U}/U_0, \bar{W}/U_0$$

Second order moments for y ranging from 4 to 20 mm (files usq-25.dat, vsq-25.dat, wsq-25.dat, uv-25.dat, uw-25.dat and vw-25.dat)

Reynolds stresses:

$$\overline{u'^2}/U_0^2, \overline{v'^2}/U_0^2, \overline{w'^2}/U_0^2$$

$$\overline{u'v'}/U_0^2, \overline{u'w'}/U_0^2, \overline{v'w'}/U_0^2$$

Turbulent kinetic energy:

$$k/U_0^2 \text{ (deduced)}$$

Measurement techniques

Hot-wire velocity measurements have been carried out using a single wire probe for the mean quantities and an X-wire probe for the turbulence quantities. It has been possible to measure all Reynolds stresses using the technique of rotating the probes $\pm 45^\circ$. It is worth mentioning that the velocity measurements are made in traverses normal to the diffuser wall along y axis (y is perpendicular to x but not to X).

Wall stress τ_w estimated using the logarithmic law of the wall. The two components τ_{wx} and τ_{wz} are determined using the value of β_w .

Static pressure measurements using wall taps.

The pressure coefficient is defined as $\bar{C}_p = 2\bar{p}/\rho U_0^2$.

Measurement errors:

| | |
|------------------------------------|---------------|
| $\delta(\bar{U}), \delta(\bar{W})$ | 2% |
| $\delta(\text{Reynolds stresses})$ | 10% |
| $\delta(\text{positions})$ | ± 0.01 mm |

Available measurements

The following measurements are available at 7 stations along the diffuser: $x = 025, 060, 100, 175, 250, 330, 405$ mm (\$\$\$ in the file names).

Velocity measurements

Profiles perpendicularly to diffuser wall of:

First order moments from wall to centreline (files U\$\$\$\$.dat and W\$\$\$\$.dat)

$$\bar{U}/U_0, \bar{W}/U_0$$

Second order moments for y ranging from 4 to 20 mm (files usq\$\$\$\$.dat, vsq\$\$\$\$.dat, wsq\$\$\$\$.dat, uv\$\$\$\$.dat, uw\$\$\$\$.dat and vw\$\$\$\$.dat)

Reynolds stresses:

$$\overline{u'^2}/U_0^2, \overline{v'^2}/U_0^2, \overline{w'^2}/U_0^2$$

$$\overline{u'v'}/U_0^2, \overline{u'w'}/U_0^2, \overline{v'w'}/U_0^2$$

Turbulent kinetic energy:

$$k/U_0^2 \text{ (deduced)}$$

Distribution along the diffuser of:

$$\beta_w \text{ (files Mm$$$$.dat)}$$

Distribution of the wall shear stress:

$$\tau_{wx}/U_0^2, \tau_{wz}/U_0^2 \text{ (files Mm$$$$.dat)}$$

The following measurements are available along the diffuser.

Pressure measurements (file Cp.dat)

Distribution of the static pressure coefficient:

$$\bar{C}_p$$

Instructions for calculations

Computational domain:

The calculations should be performed for the whole diffuser (not only for the boundary layer).

Inlet conditions:

The calculation of the duct flow should be started at station $x = -25$ mm using the experimental values provided as inlet conditions.

Outlet conditions:

The diffuser discharges to the atmosphere at $X = 510$ mm. Zero gradients may be assumed for the flow variables.

Presentation of results:

The following results should be plotted and compared with the data.

At $x = 025, 060, 100, 175, 250, 330, 405$ mm:

- normalized mean velocity, Reynolds stress and k profiles against y (perpendicular to diffuser wall)

Along the diffuser wall:

- $\overline{C_p}$ distribution
- τ_{wx}/U_o^2 and τ_{wz}/U_o^2 distributions

Previous numerical studies

Armfield *et al.* (ref. 2.) have used a $k - \epsilon$ and an algebraic Reynolds stress turbulence model with a two-layer wall function to calculate this case. The use of a two-layer, rather than a single-layer, wall function has been found to be necessary to accurately predict the level, location and the axial variation of the near-wall peak in turbulence quantities.

Main references**Description of experiments**

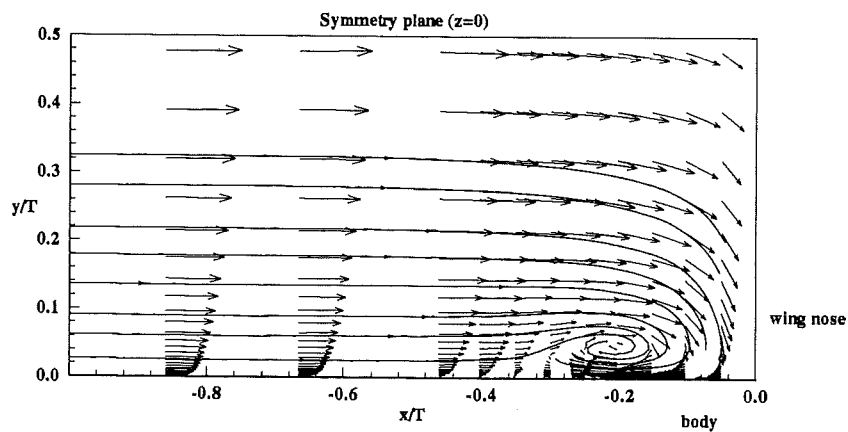
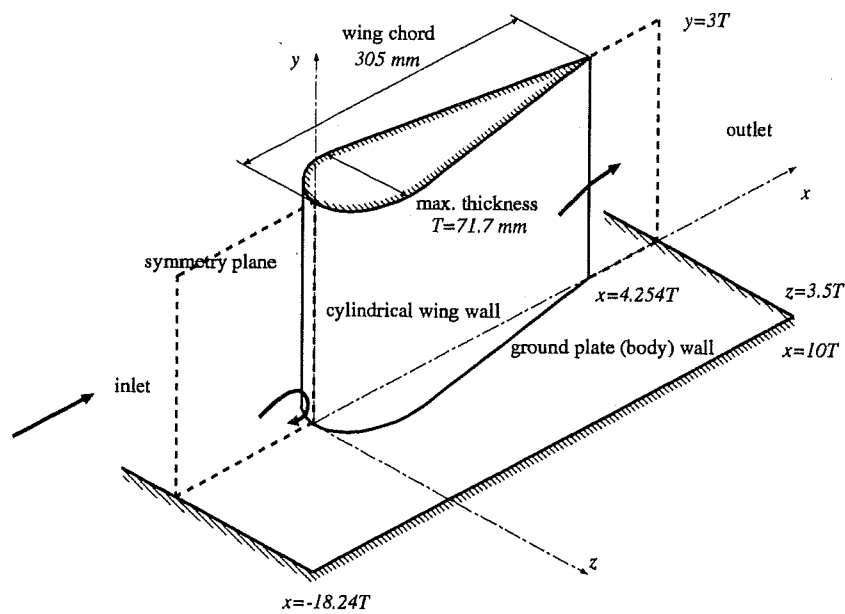
1. P.D. CLAUSEN, S.G. KOH and D.H. WOOD. Measurements of a swirling turbulent boundary layer developing in a conical diffuser. *Exp. Thermal and Fluid Science*, 6, 39, 1993.

Previous numerical studies

2. S.W. ARMFIELD, N.H. CHO and C.A.J. FLETCHER. Prediction of turbulence quantities for swirling flow in conical diffusers. *AIAA Journal*, 28, 3, 1990.

Test Case 4

Wing/body junction with separation — *Experiments by Fleming et al.*



Flow description

Turbulent flow at the junction of a flat surface and a normally-mounted cylindrical wing dominated by the presence of a horseshoe vortex.

The cylindrical wing has a maximum thickness of $T = 71.7$ mm and a chord length of $C = 305$ mm. It is situated $18.24 \times T$ downstream from the inlet and has its chord aligned with the x axis. Its cross-section consists of a 3:2 elliptical nose (major axis aligned with the chord) and NACA 0020 tail joined at the maximum thickness. x and z coordinates of the cross-section are given in file `geowing.dat`.

Flow characteristics

The adverse pressure gradient in the plane of symmetry causes the boundary layer approaching the wing to separate. Upstream of separation and in the vicinity of the separation point, mean velocity and Reynolds stress profiles are like those in a 2D boundary layer separating in an adverse pressure gradient. The junction vortex is observed as an intense approximately elliptical recirculation zone in this plane, centred about one-tenth of the undisturbed boundary-layer thickness from the wall. But this zone also appears as a region of intense turbulence production resulting from the large-scale unsteadiness of the flow. This unsteadiness is characterized by a bimodal velocity probability density function. According to the authors this feature is likely to make turbulence models assuming a Gaussian shape of the velocity p.d.f. perform poorly in this region.

Flow parameters

Air at temperature $\theta = 25^\circ\text{C}$
and pressure 94500 Pa.
Reference velocity: $U_{ref} = 26.75$ m/s.
Reynolds number: $Re_T = U_{ref}T/\nu = 115,000$.

Inflow conditions

At $x/T = -18.24$, the following measurements are provided for the two-dimensional boundary-

layer which has developed under zero pressure gradient conditions after being tripped.

Velocity measurements (stored in file `etabl.res`)

Profiles at $z = 0$ for y/T ranging from 0 to 0.87 of:

First order moment

$$\overline{U}/U_{ref}$$

Second order moments

Reynolds stresses:

$$\overline{u'^2}/U_{ref}^2, \overline{w'^2}/U_{ref}^2$$

$$\overline{u'w'}/U_{ref}^2$$

Measurement techniques

Ground plate and wing wall static pressure measurements by Devenport and Simpson (WJD) through 1 mm tappings. $\overline{C_p}$ is defined as $(\overline{p} - p_{ref})/(p_0 - p_{ref})$ where p_0 and p_{ref} are respectively the stagnation and static pressures of the undisturbed free stream. Results are stored in files `ebody.dat` and `ewing.dat`.

Velocity measurements by Fleming (JLF) using a boundary-layer type single-hot-wire probe. Results stored in files `f*.dat`.

Velocity measurements by Devenport and Simpson (WJD) using an argon-ion LDV system. Results stored in files `l*.dat` and `el*.dat`.

Measurement errors:

Uncertainty in wall static pressure measurements (by WJD):

$$\delta(\overline{C_p}) \pm 0.005$$

Uncertainty in single-hot-wire velocity measurements (by JLF):

$$\delta(\overline{U}/U_{ref}) \pm 1.5\%$$

$$\delta(\overline{W}/U_{ref}) \pm 3.0\%$$

$$\delta(\sqrt{\overline{u'^2}}/U_{ref}) \pm 1.5\%$$

$$\delta(\sqrt{\overline{w'^2}}/U_{ref}) \pm 5.0\%$$

$$\delta(\sqrt{|\overline{u'w'}|}/U_{ref}) \pm 5.0\%$$

Uncertainty in LDV velocity measurements (by WJD):

| | |
|--------------------------------------|--------------|
| $\delta(\overline{U}/U_{ref})$ | ± 0.035 |
| $\delta(\overline{V}/U_{ref})$ | ± 0.035 |
| $\delta(\overline{W}/U_{ref})$ | ± 0.035 |
| $\delta(\overline{u'^2}/U_{ref}^2)$ | ± 0.0002 |
| $\delta(\overline{v'^2}/U_{ref}^2)$ | ± 0.0007 |
| $\delta(\overline{w'^2}/U_{ref}^2)$ | ± 0.0004 |
| $\delta(\overline{-u'v'}/U_{ref}^2)$ | ± 0.0002 |
| $\delta(\overline{-u'w'}/U_{ref}^2)$ | ± 0.0009 |

Available measurements

• In the symmetry plane:

Velocity measurements (files e1*.dat)

Velocity vectors:

$$\overline{U}/U_{ref}, \overline{V}/U_{ref}$$

Contour maps of:

Second order moments

Reynolds stresses:

$$\overline{u'^2}/U_{ref}^2, \overline{v'^2}/U_{ref}^2$$

$$\overline{u'v'}/U_{ref}^2$$

Third and fourth order moments

Skewness and Flatness

$$S_u, S_v$$

$$F_u, F_v$$

• In $y - z$ planes:

Velocity measurements (files f*.dat and l*.dat)

Secondary velocity vectors in 3 $y - z$ planes (05, 08, 10):

$$\overline{V}/U_{ref}, \overline{W}/U_{ref}$$

Contour maps in 11 $y - z$ planes of:

First order moment

$$\overline{U}/U_{ref}$$

Second order moments

Reynolds stresses:

$$\overline{u'^2}/U_{ref}^2, \overline{v'^2}/U_{ref}^2, \overline{w'^2}/U_{ref}^2$$

$$\overline{u'v'}/U_{ref}^2, \overline{u'w'}/U_{ref}^2$$

Turbulent kinetic energy:

$$k/U_{ref}^2 \text{ (deduced)}$$

→ Availability

| plane | files | files | components |
|--------|--------|--------|------------|
| number | f*.dat | l*.dat | |
| 05 | + | + | u, v, w |
| 06 | + | | u, w |
| 07 | + | | u, w |
| 08 | | + | u, v, w |
| 09 | + | | u, w |
| 10 | + | + | u, v, w |
| 11 | + | | u, w |
| 12 | | + | u |
| 13 | + | | u |
| 14 | + | | u |
| 15 | + | | u |

• Wing wall:

Pressure measurements (file ewing.dat)

Contour map of pressure coefficient around wing wall for y/T ranging from 0.133 to 1.726

$$\overline{C_p}$$

• Ground plate wall:

Pressure measurements (file eboby.dat)

Contour map of pressure coefficient for x/T ranging from -2.0 to 4.75 and z/T up to 3.18

$$\overline{C_p}$$

Instructions for calculations

Inlet conditions:

The calculation of the boundary layer should be started at $x/T = -18.24$ using the experimental values provided as inlet conditions. These values are provided for the symmetry plane and correspond to a zero pressure gradient 2D boundary layer. Assume that the non-measured quantities \overline{V} and \overline{W} are negligible as expected in a 2D boundary layer. On the other hand, $\overline{v'^2}$ can be estimated as $2\overline{w'^2} - \overline{u'^2}$.

Symmetry:

Due to geometric symmetry with respect to the $z = 0$ plane – the plane containing the chord of the wing – one can use a computational domain including only one half of the wing.

Outlet conditions:

The outlet should be placed sufficiently far away, at $x = 10 \times T$, so that the vortex is developed and the boundary layer recovers its two-dimensionality. Zero gradients may be then assumed for the flow variables.

Conditions for the boundary parallel to the ground plate wall:

This boundary should be placed at $z = 3 \times T$. Symmetry condition for the flow variables may be assumed.

Conditions for the boundary parallel to the symmetry plane:

This boundary should be placed sufficiently far away, at $z = 3.5 \times T$, so that symmetry condition may be assumed for the flow variables.

Remark on outlet and symmetry conditions:

Computers are encouraged to also do calculations with these boundaries moved further away from the wing.

Presentation of results

The following results should be plotted and compared with the data:

– On both wing and ground plate walls:

- $\overline{C_p}$ contour maps

– In planes 12, 13, 14 and 15:

- \overline{U}/U_{ref} and $\overline{u'^2}/U_{ref}^2$ contour maps

– In planes 06, 07, 09 and 11:

- \overline{U}/U_{ref} , $\overline{u'^2}/U_{ref}^2$, $\overline{w'^2}/U_{ref}^2$ and $\overline{u'w'}/U_{ref}^2$ contour maps

– In planes 05, 08 and 10:

- mean secondary velocity vectors
- \overline{U}/U_{ref} , normalized Reynolds stress and k/U_{ref}^2 contour maps

– In the symmetry plane, in front of the nose:

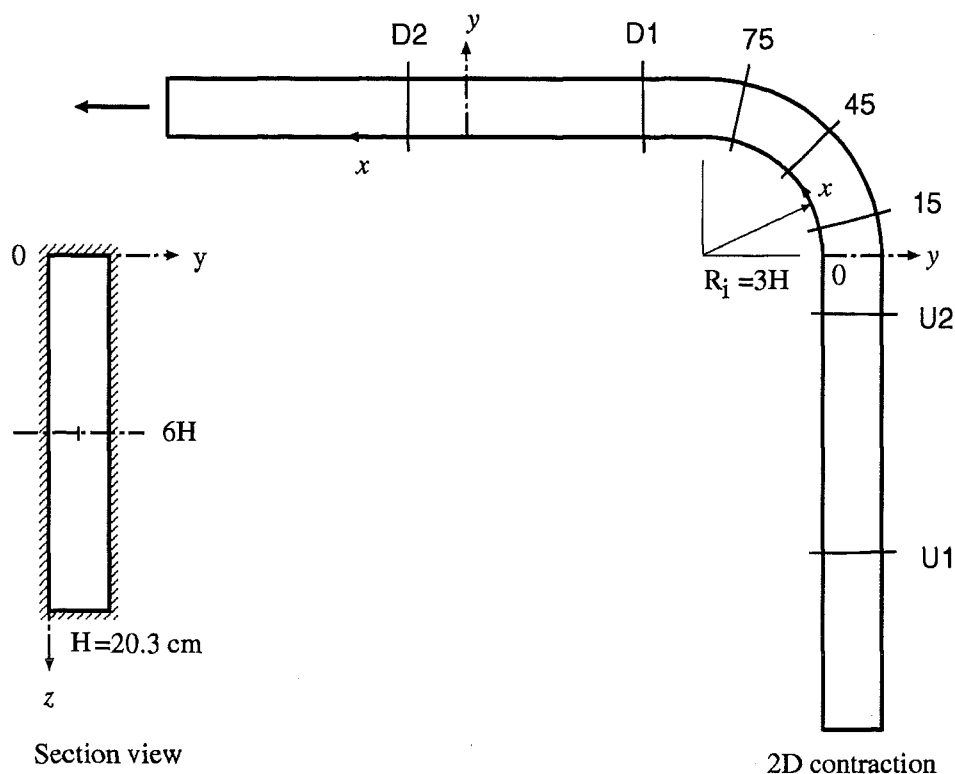
- mean streamwise velocity vectors
- $\overline{u'^2}/U_{ref}^2$, $\overline{v'^2}/U_{ref}^2$ and $\overline{u'v'}/U_{ref}^2$ contour maps

Main references

1. W.J. DEVENPORT and R.L. SIMPSON. An experimental investigation of the flow past an idealized wing-body junction: preliminary data report, Version 5. *Report of Virginia Polytechnic Institute and State University*, 1990.
2. W.J. DEVENPORT and R.L. SIMPSON. Time-dependent and time-averaged turbulence structure near the nose of a wing-body junction. *J. Fluid Mech.* 210, 23, 1990.
3. J.L. FLEMING, R.L. SIMPSON, J.E. COWLING and W.J. DEVENPORT. An experimental study of a turbulent wing-body junction and wake flow. *Exp. in Fluids* 14, 366, 1993.

Test Case 5

Developing flow in a curved rectangular duct — *Experiments by Kim and Patel*



Flow description

Developing turbulent flow in a 90 deg. curved duct of rectangular cross-section.

Duct with two straight and one curved sections. Rectangular cross-section of the duct with a

width of $H = 20.3$ cm and a height of $6 \times H$.

Inner radius of curvature of the bend:

$$R_i = 3 \times H.$$

Straight upstream section with a length of $7.5 \times H = 1.52$ m.

Straight downstream section with a length of $25.5 \times H = 5.18$ m.

Flow characteristics

The initially 2D boundary layers developing on the vertical lateral walls are subjected to strong streamwise curvatures and associated pressure gradients along the bend. On the other hand, the pressure-driven secondary motion in the corner regions eventually leads to the formation of a longitudinal vortex on the convex wall. The duct aspect ratio is such that these two features of the flow develop more or less independently, without interaction.

Flow parameters

Air with a kinematic viscosity:

$$\nu = 1.45 \times 10^{-5} \text{ m}^2/\text{s}.$$

Freestream velocity at station U1 ($x = -4.5 \times H$): $U_0 = 16 \text{ m/s}$.

Reynolds number: $U_0 H / \nu = 224,000$.

Inflow conditions

At station U1 ($x = -4.5 \times H$), the velocity is uniform in the core flow, outside the boundary layers, within a deviation less than 1%. On the vertical lateral walls, the boundary layers are of flat-plate type with a momentum thickness Reynolds number of 1650, a boundary layer thickness of $\delta = 0.08 \times H$ and a friction coefficient of $C_f = .0038$. The 2D wind-tunnel contraction located $3 \times H$ upstream of U1 introduces a secondary motion in the boundary layers on top and bottom flat walls but its magnitude reaches only 5% of the freestream velocity. The following measurements are then provided for a slightly three-dimensional duct flow but are sufficiently detailed to be used as inlet conditions.

Velocity measurements

Velocity vectors: (files mu1000.dat)

$$\bar{V}/U_0, \bar{W}/U_0$$

Contour maps of: (files mu1000.dat)

First order moment

$$\bar{U}/U_0$$

Second order moments

Reynolds stresses:

$$\overline{u'^2}/U_0^2, \overline{v'^2}/U_0^2, \overline{w'^2}/U_0^2$$

$$\overline{u'v'}/U_0^2, \overline{u'w'}/U_0^2$$

Turbulent kinetic energy:

$$k/U_0^2 \text{ (deduced)}$$

Wall friction coefficient distribution on each wall:

C_f (files su1in.dat, su1out.dat and su1up.dat)

Measurement techniques

Hot-wire velocity measurements have been carried out using a miniature X-wire probe for the turbulence quantities.

Mean velocity measurements have been carried out using a five-hole pressure probe of a diameter of 3 mm.

All velocity measurements have been made in the upper half of the duct divided into 5 different domains, namely in1, up1, ou1, in2, ou2 (see file readme.doc).

Wall stress τ_w measurements using two pressure probes in combination (only the magnitude is actually measured). The friction coefficient is defined as $C_f = 2\tau_w/\rho U_0^2$.

Static pressure measurements using wall taps. The pressure coefficient is defined as $\bar{C}_p = 2(\bar{p} - p_0)/\rho U_0^2$, where p_0 is the static pressure at $(0,0,3 \times H)$.

Measurement errors:

| | |
|--|------|
| $\delta(\bar{U})$ | 1.5% |
| $\delta(\bar{V}), \delta(\bar{W})$ | 3% |
| $\delta(\overline{u'^2})$ | 5% |
| $\delta(\text{other Reynolds stresses})$ | 10% |

Available measurements

The following measurements are available at 1 station upstream of the bend: U2 ($x = -0.5 \times H$); 3 stations along it: 15, 45, 75 and 2 stations downstream of it: D1 ($x = 0.5 \times H$), D2 ($x = 4.5 \times H$).

Velocity measurements

(\$\$ is the station and 000 the domain name)

Velocity vectors:

$$\bar{V}/U_0, \bar{W}/U_0$$

Contour maps of: (files m\$\$\$\$.dat)

First order moment

$$\bar{U}/U_0$$

Second order moments

Reynolds stresses:

$$\overline{u'^2}/U_0^2, \overline{v'^2}/U_0^2, \overline{w'^2}/U_0^2$$

$$\overline{u'v'}/U_0^2, \overline{u'w'}/U_0^2$$

Turbulent kinetic energy:

$$k/U_0^2 \text{ (deduced)}$$

Wall friction coefficient distribution on each wall:

C_f (files s\$\$in.dat, s\$\$out.dat and s\$\$up.dat)

The following measurements are available along the inner and the outer walls, in the plane of symmetry.

Pressure measurements (files pressure.dat and pressure.tab)

Distribution of the static pressure coefficient

$$\bar{C}_p$$

Instructions for calculations

Inlet conditions:

The calculation of the duct flow should be started at station U1 using the experimental values provided as inlet conditions. The non-measured quantity $\overline{v'w'}$ may be assumed as negligible.

Symmetry:

Due to geometric symmetry with respect to the $z = 0$ plane, one can use a computational domain including only the upper half of the duct.

Outlet conditions:

The outlet should be placed sufficiently far away ($x \geq 30 \times H$) so that zero gradients may be assumed for the flow variables.

Presentation of results:

The following results should be plotted and compared with the data:

- At all locations:

- mean secondary velocity vectors
- mean streamwise velocity, Reynolds stress and k contour maps, normalized by U_0
- circumferential distribution of C_f

- In the symmetry plane, along the lateral walls,

- \bar{C}_p distributions

Previous numerical studies

Sotiropoulos and Patel (ref 3.) have performed calculations of this case with the two-layer $k - \epsilon$ model using two different numerical methods: the "finite-analytic" and a finite-difference method. In both cases, the overall structure of the flow is well predicted but both the strength of the secondary motion, and consequently its effect on the streamwise flow development, and the effects of wall curvature on the turbulence within the lateral boundary layers are underestimated.

Main references

Description of experiments

1. W.J. KIM and V.C. PATEL. Origin and decay of longitudinal vortices in developing flow in a curved rectangular duct. *J. of Fluids Engineering*, 116, 45, 1994.
2. W.J. KIM. An experimental and computational study of longitudinal vortices in turbulent boundary layers. *PhD Thesis - Mechanical Engineering, University of Iowa*, 1991.

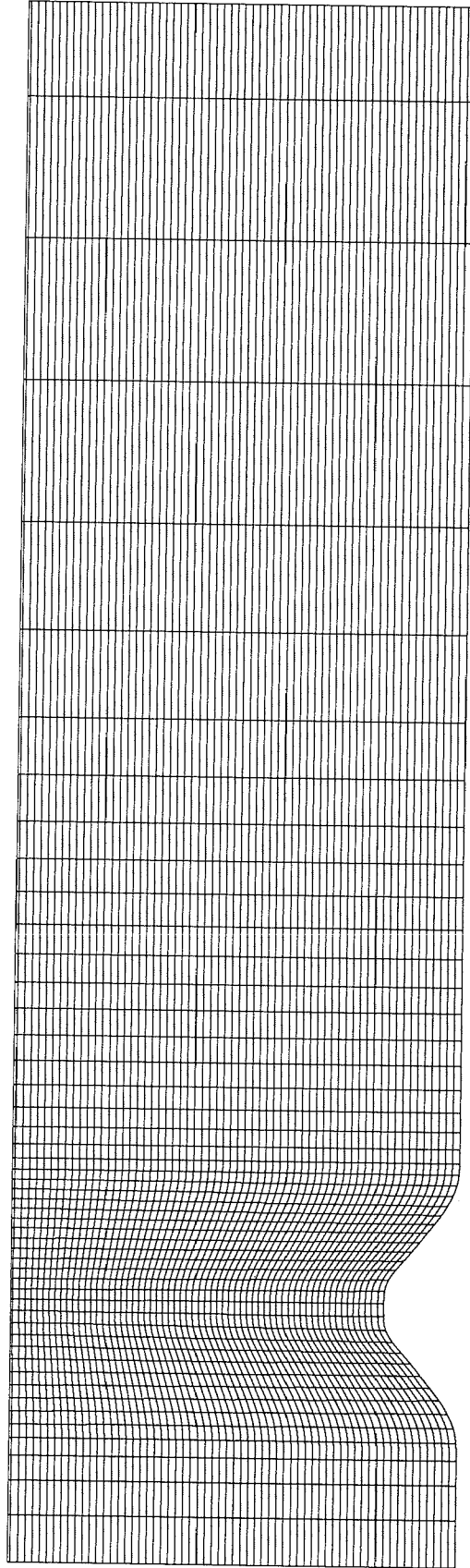
Previous numerical studies

3. F. SOTIROPOULOS and V.C. PATEL. Flow in curved ducts of varying cross-section. *Institute of Hydraulic Research, University of Iowa, IHR Report No. 358*, 1992.

Description of Numerical Methodology for Test Case #2a

- **Originator:** Gordon D. Stubbley
- **Affiliation:** Advanced Scientific Computing (ASC) Ltd.
- **General description:**
The calculations were performed with ASC's unstructured grid code. This code uses a finite element based finite volume method to discretize the transport equations. The code is fully conservative, including the treatment of boundary node control volumes. The code allows for mixed element types and uses an efficient coupled algebraic multigrid solver.
- **Convection scheme:**
Blending between UDS and CDS based on the grid Peclet number was used.
- **Mesh:**
A structured quadrilateral mesh with 150 nodes in the streamwise direction and 188 nodes in the transverse direction was used. The first interior node at the inlet was located at a y^+ of approximately 70.
- **Turbulence models:**
Calculations were performed with the standard isotropic $k - \epsilon$ model $\{C_\mu, C_{\epsilon 1}, C_{\epsilon 2}, \sigma_k, \sigma_\epsilon\} = \{0.09, 1.44, 1.92, 1.00, 1.30\}$ and a linear form of the fully realizable $k - \epsilon$ model developed by Shih et al [1]. The realizable model is identical to the standard $k - \epsilon$ model except for the form of the model coefficient C_μ . For 2 dimensional flows the model coefficient is given by

$$C_\mu = \frac{1}{A_0 + \frac{3}{\sqrt{2}} \frac{k}{\epsilon} \sqrt{S_{lk} S_{kl} + \Omega_{lk} \Omega_{kl}}} \quad (1)$$
 where S_{ij} is the deformation rate tensor, and Ω_{ij} is the rotation rate tensor. The model constant A_0 is set to 6.5.
- **Near-wall treatment:**
The near wall flow is resolved with a fully conservative wall function formulation. The wall shear stress is calculated by applying the log law velocity profile between the wall element centroid and the wall. The diffusion of k through the wall is neglected and the diffusive flux of ϵ at the wall is set to ensure a flux of ϵ into the first interior control volume that is consistent with local equilibrium. These approximations close the control volume equations for momentum, k , and ϵ at boundary nodes and are analogous to the standard wall function formulation.
- **Inlet Conditions:**
The inlet profiles for the streamwise velocity and k were interpolated from the experimental data. The inlet profile of ϵ was set to $k^{3/2}/L_t$ where L_t is the minimum of $\kappa y/C_\mu^{3/4}$ ($C_\mu = 0.09$) and $0.35H$.
- **Related publications/reports:**
[1] T.H. Shih, J. Zhu, and J.L. Lumley, 'A new Reynolds stress algebraic equation model', NASA Technical Memorandum 106644, August 1994.



Description of Numerical Methodology for Test Case #3

- **Originator:** Mirjam Sick^{#)}, Georg Scheuerer^{*)}

- **Affiliation:**

^{#)}Sulzer Innotec AG
CH-8401 Winterthur
Switzerland

^{*)}Advanced Scientific Computing GmbH
Münchner Str. 3, D-83607 Holzkirchen
Germany
Telephone: +49 8024 8852
Telefax: +49 8024 49304

- **General Description:**

The calculation is carried out with the element-based finite volume method **TASCflow**. **TASCflow** uses non-orthogonal numerical grids in combination with Cartesian velocity components and a co-located (non-staggered) variable arrangement. The mass and momentum equations are solved in a coupled manner, while the turbulence model equations are updated in a segregated, successive fashion. The linearized equation systems are relaxed using a solution algorithm based on incomplete LU factorization. For convergence rate enhancement, an algebraic multigrid scheme is incorporated.

The fluid flow is assumed to be incompressible. The calculation for the grid described below converged to maximum residuals of 10^{-4} , corresponding to an iteration accuracy of four significant digits.

- **Convection Scheme:**

The discretization scheme for the convective fluxes is based on the linear profile skew-upwind differencing method (LPS) (Raithby 1976), combined with the "Physical Advection Correction" (PAC) (Raw, 1994) method in order to obtain second order truncation error.

- **Mesh:**

The computational mesh is a block-structured, non-orthogonal grid. As the problem is considered as twodimensional, only two nodes are used in circumferential direction. Two solutions are calculated on a coarse and a fine grid, respectively, in order to estimate the numerical solution error. The fine grid consists of a total of 13616 nodes. Only results obtained from the fine grid are submitted.

- **Turbulence Models:**

The standard $k-\epsilon$ turbulence model is used (Launder and Spalding, 1974).

- **Near-Wall Treatment:**

In the near-wall regions a logarithmic law model is applied (Perić and Scheuerer, 1989).

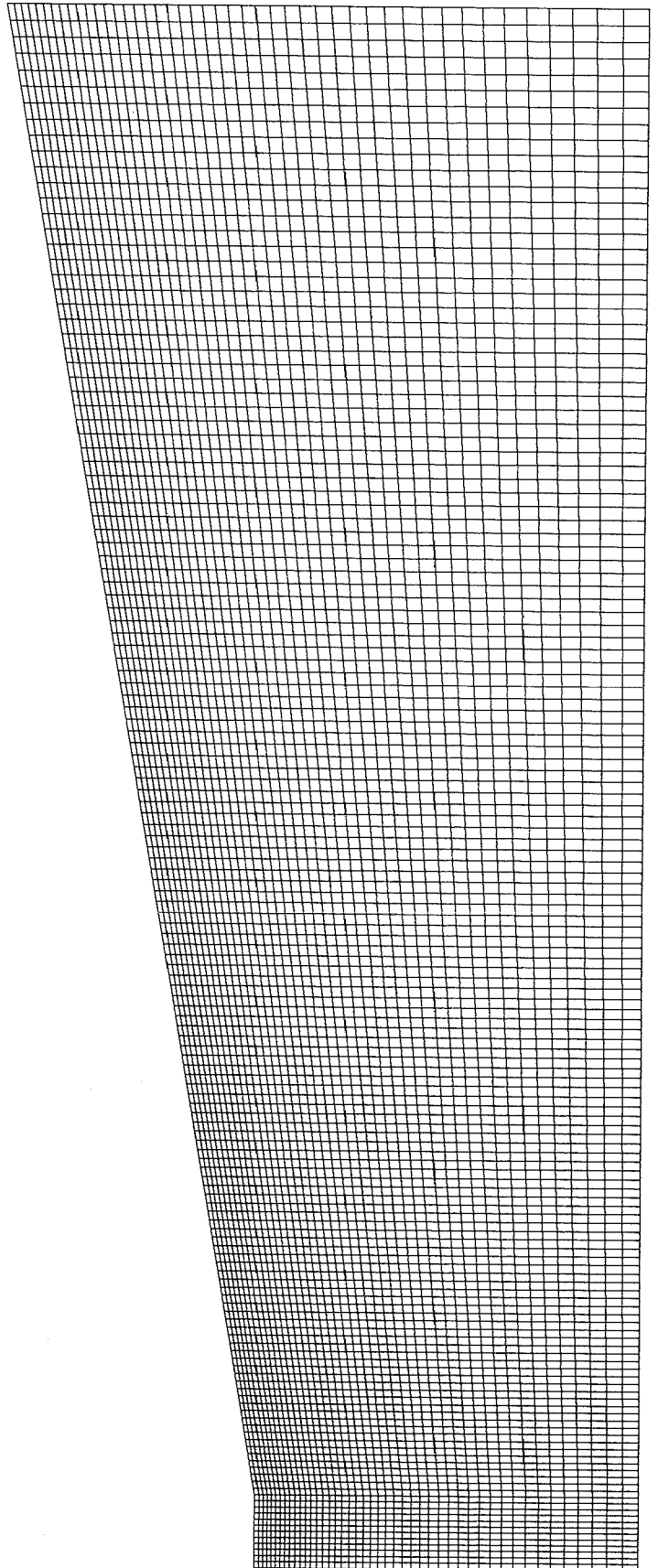
- **Related Publications/Reports:**

Raithby, G.D., 1976, "Skew Upstream Differencing Schemes for Problems Involving Fluid Flow", *Comput. Meth. Appl. Mech. Eng.*, Vol. 9, pp. 153-164.

Raw, M.J., Galpin, P.F., Hutchinson, B.R., Raithby, G.D., Van Doormaal, J.P., 1994, "An Element-Based Finite-Volume Method for Computing Viscous Flows", *Internal Report*, Advanced Scientific Computing Ltd., Waterloo, Ontario, Canada.

Launder, B.E. and D.B. Spalding, 1974, "The Numerical Computation of Turbulent Flows", *Comp. Meth. Appl. Mech. Eng.*, Vol. 3, pp 269 - 289.

Perić, M. and G. Scheuerer, 1989, "CAST — A Finite Volume Method for Predicting Two-Dimensional Flow and Heat Transfer Phenomena", *Technische Notiz SRR-89-01*, Gesellschaft für Reaktorsicherheit GmbH, Garching.



Description of Numerical Methodology for Test Case #4

- **Originator:** Achim Holzwarth, Georg Scheuerer

- **Affiliation:**

Advanced Scientific Computing GmbH
Münchner Str. 3, 83607 Holzkirchen
Telephone: +49 8024 8852, Telefax: +49 8024 49304

- **General Description:**

The calculation is carried out with the element-based finite volume method **TASCflow**. **TASCflow** uses non-orthogonal numerical grids in combination with Cartesian velocity components and a co-located (non-staggered) variable arrangement. The mass and momentum equations are solved in a coupled manner, while the turbulence model equations are updated in a segregated, successive fashion. The linearized equation systems are relaxed using a solution algorithm based on incomplete LU factorization. For convergence rate enhancement, an algebraic multigrid scheme is incorporated.

The fluid flow is assumed to be incompressible. The calculation for the grid described below took 47 iterations to converge to maximum residuals of 10^{-4} , corresponding to an iteration accuracy of four significant digits.

- **Convection Scheme:**

The discretization scheme for the convective fluxes is based on the linear profile skew-upwind differencing method (LPS) (Raithby 1976), combined with the "Physical Advection Correction" (PAC) (Raw, 1994) method in order to obtain second order truncation error.

- **Mesh:**

The computational mesh is a block-structured, non-orthogonal grid consisting of three subgrids. Two solutions are calculated on a coarse and a fine grid, respectively, in order to estimate the numerical solution error. The fine grid, which is obtained by doubling the number of flux elements in every grid direction, consists of a total of 92387 nodes. Only results obtained from the fine grid are submitted. The inflow and outflow boundaries are located at $x/T = -18.24$ and $x/T = 51$, respectively. The plane parallel to the symmetry plane is moved further outwards to $z/T = 10$. Results, however, are presented only in the range $z/T \leq 3.5$. The height of the wing is $y/T = 3$.

- **Turbulence Models:**

The standard k - ϵ turbulence model is used (Launder and Spalding, 1974). The empirical constants in the model equations have the standard values given by Launder and Spalding. They are compiled in the following table.

| c_μ | $c_{\epsilon 1}$ | $c_{\epsilon 2}$ | σ_k | σ_ϵ |
|---------|------------------|------------------|------------|-------------------|
| 0.09 | 1.44 | 1.92 | 1.0 | 1.3 |

Table 1: Constants used in the k - ϵ turbulence model.

- **Near-Wall Treatment:**

In the near-wall region a logarithmic law model is applied (Perić and Scheuerer, 1989). The law model is based upon the wall function approach derived by (Launder and Spalding, 1974). However, the wall function equations given by Launder and Spalding become singular at separation points. In order to avoid this problem, three assumptions are made which are consistent with the logarithmic profile. These are:

- Couette flow
- Local equilibrium (production equals dissipation)
- Constant stress layer

These assumptions produce the following relation between the wall shear stress and the kinetic energy:

$$\tau_w = \rho c_\mu^{1/2} k \quad (1)$$

Using this equation, the following explicit equation for the wall shear stress can be derived:

$$\tau_w = \tau_{visc} \frac{n^*}{u^+} \quad (2)$$

where

$$\begin{aligned} \tau_{visc} &= \mu u_t / \Delta n \\ n^* &= \rho c_\mu^{1/4} k^{1/2} \Delta n / \mu \\ u^+ &= \frac{1}{\kappa} \ln(n^*) + C \\ \tau_w &= \text{wall shear stress} \\ u_t &= \text{known velocity tangent to wall, at a distance } \Delta n \text{ from the wall} \\ \kappa, C &= \text{Constants depending on wall roughness} \end{aligned}$$

Thus the form of the wall functions used in **TASCflow** is based on a function of n^* . The constants of the logarithmic law model for smooth walls are $\kappa = 0.41$ and $C = 5.2$.

In the viscous sublayer very close to the wall, the logarithmic profile no longer holds. Therefore, the near wall region is divided into three sections, and the following definitions of u^+ and the associated regions of application are given below:

$$u^+ = n^* \quad n^* \leq 5 \quad (3)$$

$$u^+ = d_1 n^{*3} + d_2 n^{*2} + d_3 n^* + d_4 \quad 5 \leq n^* \leq 30 \quad (4)$$

$$u^+ = \frac{1}{\kappa} \ln(n^*) + C \quad n^* \geq 30 \quad (5)$$

The coefficients $d_1 \dots d_4$ are determined such that the three equations are continuous in value and first derivative. The coefficients depend on the values of n^* at which the equations are matched. For the values given above, the coefficients are as follows: $d_1 = 6.4264 \times 10^{-4}$, $d_2 = -5.2113 \times 10^{-2}$, $d_3 = 1.4729$, and $d_4 = -1.1422$.

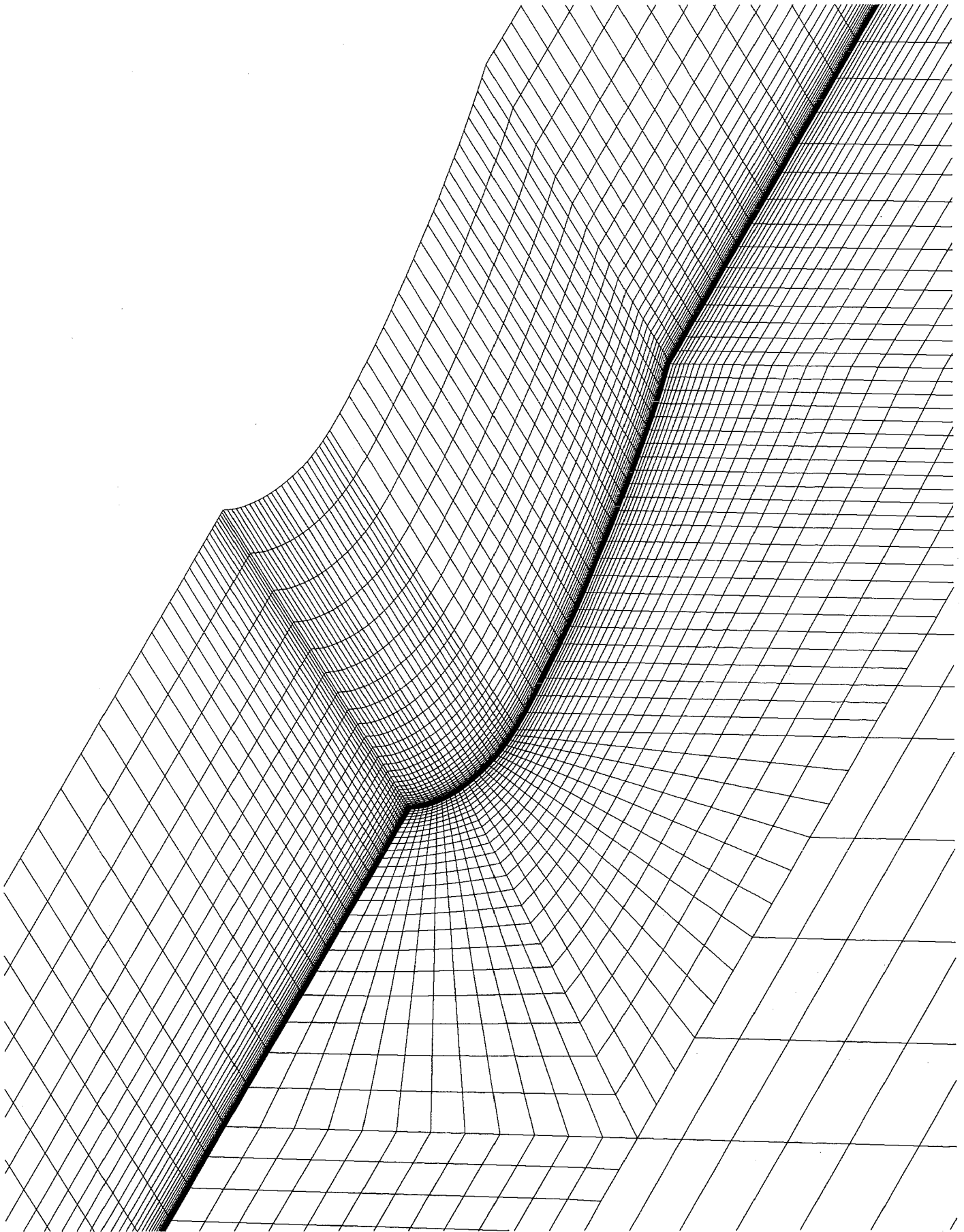
• Related Publications/Reports:

Raithby, G.D., 1976, "Skew Upstream Differencing Schemes for Problems Involving Fluid Flow", *Comput. Meth. Appl. Mech. Eng.*, Vol. 9, pp. 153-164.

Raw, M.J., Galpin, P.F., Hutchinson, B.R., Raithby, G.D., Van Doormaal, J.P., 1994, "An Element-Based Finite-Volume Method for Computing Viscous Flows", *Internal Report*, Advanced Scientific Computing Ltd., Waterloo, Ontario, Canada.

Launder, B.E. and D.B. Spalding, 1974, "The Numerical Computation of Turbulent Flows", *Comp. Meth. Appl. Mech. Eng.*, Vol. 3, pp 269 - 289.

Perić, M. and G. Scheuerer, 1989, "CAST — A Finite Volume Method for Predicting Two-Dimensional Flow and Heat Transfer Phenomena", *Technische Notiz SRR-89-01*, Gesellschaft für Reaktorsicherheit GmbH, Garching.



Description of Numerical Methodology for Test Case #5

- **Originator:** Mirjam Sick^{#)}, Georg Scheuerer^{*)}

- **Affiliation:**

^{#)}Sulzer Innotec AG
CH-8401 Winterthur
Switzerland

^{*)}Advanced Scientific Computing GmbH
Münchner Str. 3, D-83607 Holzkirchen
Germany
Telephone: +49 8024 8852
Telefax: +49 8024 49304

- **General Description:**

The calculation is carried out with the element-based finite volume method **TASCflow**. **TASCflow** uses non-orthogonal numerical grids in combination with Cartesian velocity components and a co-located (non-staggered) variable arrangement. The mass and momentum equations are solved in a coupled manner, while the turbulence model equations are updated in a segregated, successive fashion. The linearized equation systems are relaxed using a solution algorithm based on incomplete LU factorization. For convergence rate enhancement, an algebraic multigrid scheme is incorporated.

The fluid flow is assumed to be incompressible. The calculation for the grid described below converged to maximum residuals of 10^{-4} , corresponding to an iteration accuracy of four significant digits.

- **Convection Scheme:**

The discretization scheme for the convective fluxes is based on the linear profile skew-upwind differencing method (LPS) (Raithby 1976), combined with the "Physical Advection Correction" (PAC) (Raw, 1994) method in order to obtain second order truncation error.

- **Mesh:**

The computational mesh is a block-structured, non-orthogonal grid. The grid is refined towards the walls and also towards the symmetry plane. Two solutions are calculated on a coarse and a fine grid, respectively, in order to estimate the numerical solution error. The fine grid consists of a total of 163053 nodes. Only results obtained from the fine grid are submitted.

- **Turbulence Models:**

The standard $k-\epsilon$ turbulence model is used (Launder and Spalding, 1974).

- **Near-Wall Treatment:**

In the near-wall regions a logarithmic law model is applied (Perić and Scheuerer, 1989).

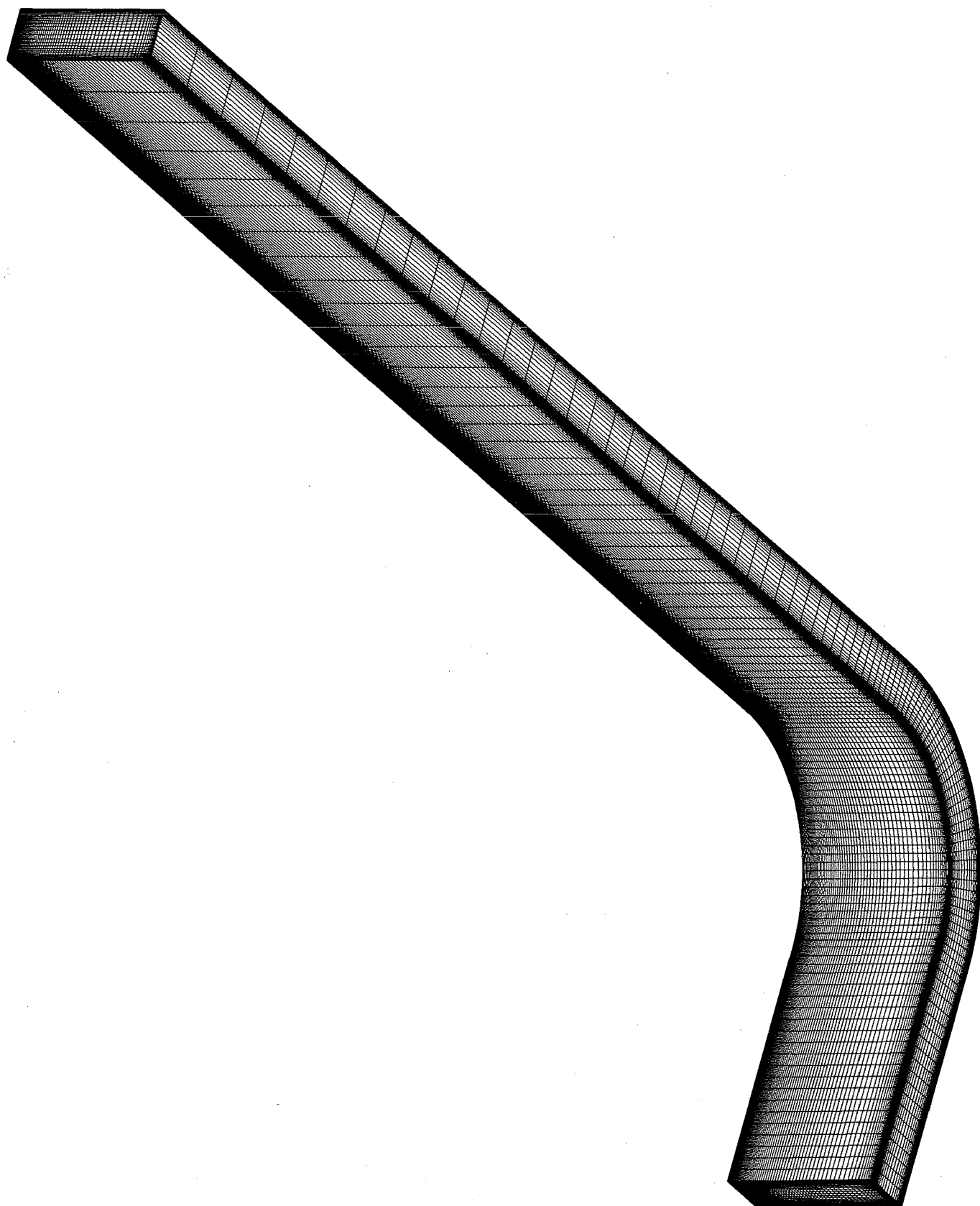
- **Related Publications/Reports:**

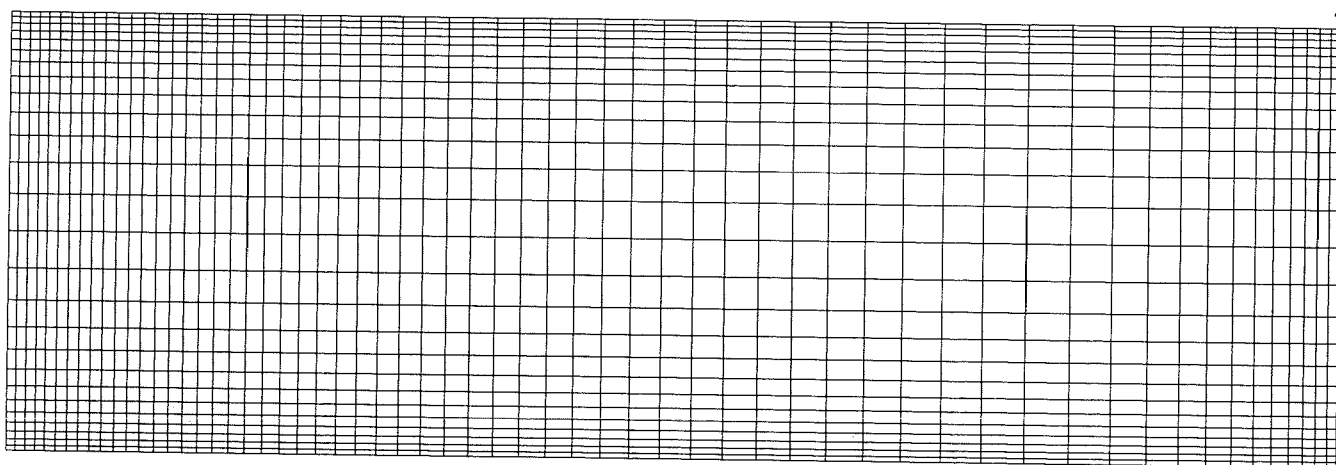
Raithby, G.D., 1976, "Skew Upstream Differencing Schemes for Problems Involving Fluid Flow", *Comput. Meth. Appl. Mech. Eng.*, Vol. 9, pp. 153-164.

Raw, M.J., Galpin, P.F., Hutchinson, B.R., Raithby, G.D., Van Doormaal, J.P., 1994, "An Element-Based Finite-Volume Method for Computing Viscous Flows", *Internal Report*, Advanced Scientific Computing Ltd., Waterloo, Ontario, Canada.

Launder, B.E. and D.B. Spalding, 1974, "The Numerical Computation of Turbulent Flows", *Comp. Meth. Appl. Mech. Eng.*, Vol. 3, pp 269 - 289.

Perić, M. and G. Scheuerer, 1989, "CAST — A Finite Volume Method for Predicting Two-Dimensional Flow and Heat Transfer Phenomena", *Technische Notiz SRR-89-01*, Gesellschaft für Reaktorsicherheit GmbH, Garching.





DESCRIPTION OF NUMERICAL METHODOLOGY FOR TEST CASE 2A
2D SINGLE MODEL HILL FLOWS

Originator:

R Issa, W U A Leong and R Sanatian

Affiliation:

Computational Dynamics (STAR-CD) Limited
Olympic House, 317 Latimer Road,
London W10 6RA

General description:

STAR-CD is a general-purpose thermofluid analysis code with extensive flow, heat and mass transfer capabilities including compressible, multiphase and chemically-reacting flows. It also has full pre/post processing facilities, encompassing mesh generation, results display and interfaces to external CAD systems. The code solves the Navier-Stokes' equation by employing an efficient finite-volume solution methodology in conjunction with a highly-flexible unstructured mesh system. This calculation simulated flow over a two-dimensional polynomial-shaped obstacle (hill) mounted on a flat plate with recirculation region in its wake.

Convection scheme:

Extended versions of the SIMPLE algorithm was used for steady-state calculations, in conjunction with either up-wind differencing or high order differencing (including central differencing) scheme.

Mesh:

The calculation meshes used for these simulations were based on unstructured grid with local mesh refinement. Calculations were performed for three different mesh resolutions, they were;

Grid 1: 15600 cells

Grid 2: 37700 cells

Grid 3: 48100 cells

The near wall treatment for calculations using Grid 1 and 2 was log-law based wall function. The inlet channel length in Grid 2 and 3 was extended from the specified 100mm to 300 mm. Although the number of cells used in Grid 2 was double the amount used in Grid 1, no significant change was observed in the results. The additional cells used in Grid 3 was the result of the grid refinement at the near wall region (for applying the two-layer near wall treatment). The presented results were believed to be practically grid independent.

Turbulence models:

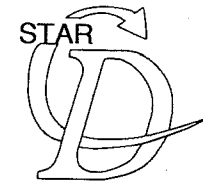
The model used the 'RNG' variant of k-epsilon turbulence model [1].

Near-wall treatment:

A 'two-layer' variant of k-epsilon, in which the near-wall flow is simulated via a so-called one-equation low Reynolds number model [2] consisting of a transport equation for k and an algebraic prescription for the turbulence dissipation rate; and the solution is matched to that of the standard k-epsilon equations at the 'edge' of the viscosity-influenced region. The f_{μ} coefficient of the turbulent viscosity equation is used as a basis for switching between the near-wall flow region (where viscosity dominates) and outer flow region (where viscous effects become negligible). The default transition is set at $f_{\mu} = 0.95$.

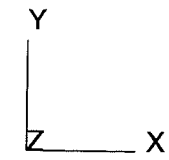
Related publications/reports:

- [1] Yakhot, V, Orszag, S A, Thangam, S, Gatski, T B and Speziale C G (1992) 'Development of turbulence models for shear flows by a double expansion technique', Phys. Fluids, A4, No. 7, pp. 1510-1520.
- [2] Norris, L H and Reynolds W C (1975) 'Turbulent channel flow with a moving wavy boundary' Report No. FM-10, Department of Mechanical Engineering, Stanford University, USA.

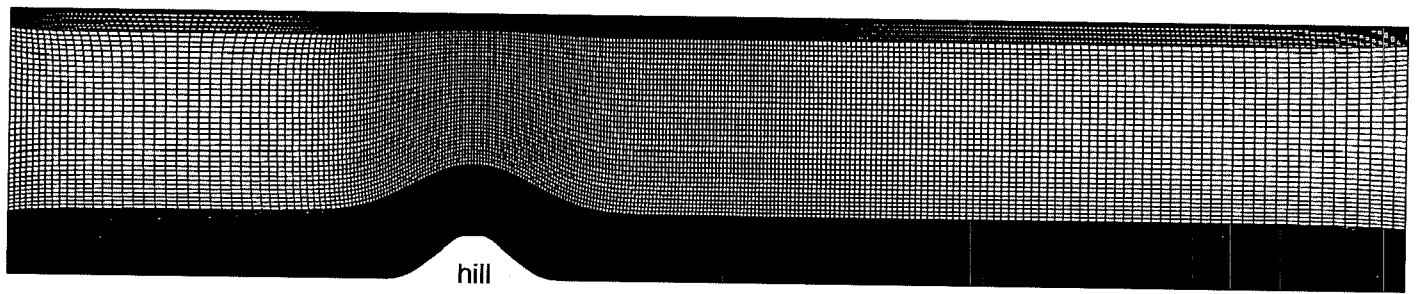


PROSTAR 2.21

VIEW
0.000
0.000
1.000
ANGLE
0.000
DISTANCE
0.464
CENTER
0.150
0.085
0.005
EHIDDEN PLOT



Flow direction
→



wall

hill

wall

ERCOFTAC Case 2a: 2D single hill

DESCRIPTION OF NUMERICAL METHODOLOGY FOR TEST CASE 2B
2D MULTI HILLS MODEL FLOWS

Originator:

R Issa, W U A Leong and R Sanatian

Affiliation:

Computational Dynamics (STAR-CD) Limited
Olympic House, 317 Latimer Road,
London W10 6RA

General description:

STAR-CD is a general-purpose thermofluid analysis code with extensive flow, heat and mass transfer capabilities including compressible, multiphase and chemically-reacting flows. It also has full pre/post processing facilities, encompassing mesh generation, results display and interfaces to external CAD systems. The code solves the Navier-Stokes' equation by employing an efficient finite-volume solution methodology in conjunction with a highly-flexible unstructured mesh system. The results presented here represent the simulations of flow over ten consecutive polynomial-shaped obstacles (hills) mounted on a flat plate with recirculation region in their wake. Two sets of results were produced. The first set (in directory hill2_1-dir) was obtained from calculations based on a domain which comprised the nine consecutive hills plus an inlet channel (which length is 300mm). The experimental inlet flow conditions used in the single hill case was used in this calculation. The results presented were extracted from a region between the 7th and 8th hills. The second set of results (in directory hill2_2-dir) was obtained from calculations using the cyclic boundary conditions which were applied at the inlet and outlet of the calculation domain (between the peaks of the 7th and 8th hills).

Convection scheme:

Extended versions of the SIMPLE algorithm was used for steady-state calculations, in conjunction with either up-wind differencing or high order differencing (including central differencing) scheme.

Mesh:

To start with, we developed a grid for simulating the flows between hill no. 7 and 8, using cyclic type boundary conditions. This grid was based on the coarse grid used in the single hill case (with log-law based wall function) in which the results were almost independent of the grid refinement. The number of cells used was 13230 cells. For the full domain model which comprised the first nine hills and the inlet section, the total number of cells used was 116039.

Turbulence models:

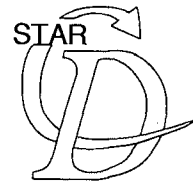
The model used the 'RNG' variant of k-epsilon turbulence model [1].

Near-wall treatment:

This model used the log-law based wall function. Details of the assumptions and resulting formulae can be found in [2].

Related publications/reports:

- [1] Yakhot, V, Orszag, S A, Thangam, S, Gatski, T B and Speziale C G (1992)
'Development of turbulence models for shear flows by a double expansion technique', Phys. Fluids, A4, No. 7, pp. 1510-1520.
- [2] 'Manuals for STAR-CD Version 2.2', (1994)
Computational Dynamics Ltd., Olympic House, 317 Latimer Rd., London W10 6RA.



PROSTAR 2.21

VIEW

0.000

0.000

1.000

ANGLE

0.000

DISTANCE

0.707

CENTER

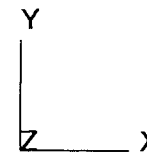
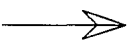
0.386

0.085

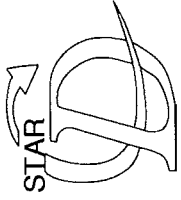
0.005

EHIDDEN PLOT

Flow direction

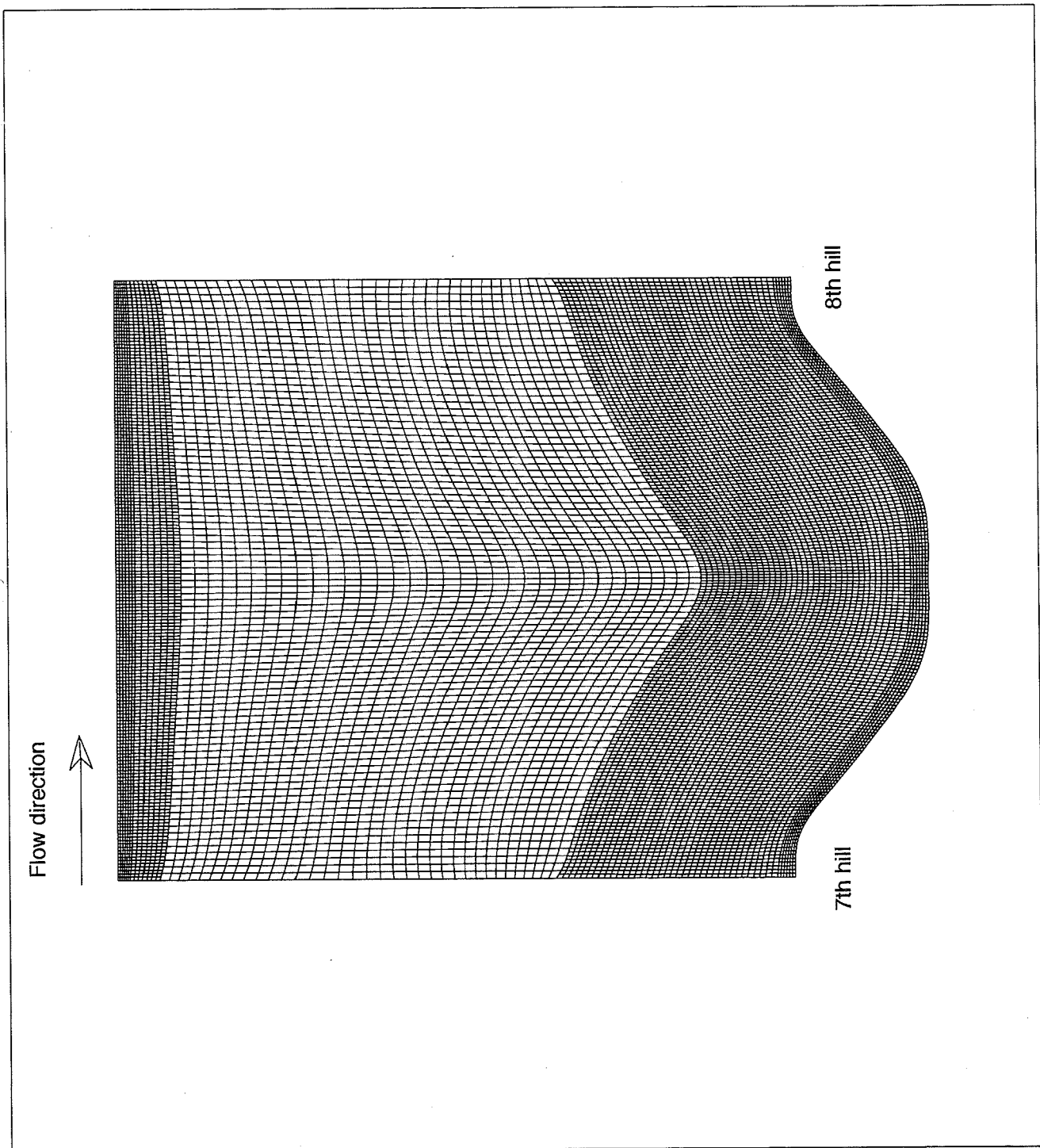
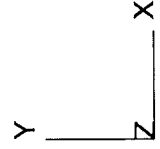


ERCOFTAC CASE 2b1: 2D multi hill flows



PROSTAR 2.21

VIEW 0.000
0.000
1.000
ANGLE 0.000
DISTANCE 0.120
CENTER 0.000
0.085
0.005
EHIDDEN PLOT



ERCOFTAC CASE 2b: 2D consecutive hills
This calculation used the cyclic boundary conditions

DESCRIPTION OF NUMERICAL METHODOLOGY FOR TEST CASE 4 WING/BODY JUNCTION WITH SEPARATION

Originator:

R Issa, W U A Leong and R Sanatian

Affiliation:

Computational Dynamics (STAR-CD) Limited
Olympic House, 317 Latimer Road,
London W10 6RA

General description:

STAR-CD is a general-purpose thermofluid analysis code with extensive flow, heat and mass transfer capabilities including compressible, multiphase and chemically-reacting flows. It also has full pre/post processing facilities, encompassing mesh generation, results display and interfaces to external CAD systems. The code solves the Navier-Stokes' equation by employing an efficient finite-volume solution methodology in conjunction with a highly-flexible unstructured mesh system. These calculations simulated three-dimensional flow over a surface-mounted cylindrical wing. Due to geometric symmetry, only one half of the wing was used in the computational domain. The calculational domain was extended to 25 times the wing's thickness in the x-direction and 7 times the wing's thickness in the z-direction.

Convection scheme:

Extended versions of the SIMPLE algorithm was used for steady-state calculations, in conjunction with up-wind differencing scheme.

Mesh:

The calculations were performed for three different mesh resolutions, they were;

Grid 1: 67290 cells

Grid 2: 129760 cells

Grid 3: 177365 cells

All the calculations performed with these meshes were based on log-law type wall function. The refinements were the results of our attempts to capture the development of boundary layer near the wall and the development of vortex near the wing/body junction. The results presented here were based on Grid 3.

Turbulence models:

The model used the 'RNG' variant of k-epsilon turbulence model [1].

Near-wall treatment:

This model used log-law based wall function. Details of the assumptions and resulting formulae can be found in [2].

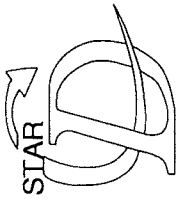
Related publications/reports:

[1] Yakhot, V, Orszag, S A, Thangam, S, Gatski, T B and Speziale C G (1992)

'Development of turbulence models for shear flows by a double expansion technique', Phys. Fluids, A4, No. 7, pp. 1510-1520.

[2] 'Manuals for STAR-CD Version 2.2', (1994)

Computational Dynamics Ltd., Olympic House, 317 Latimer Rd., London W10 6RA.



PROSTAR 2.26

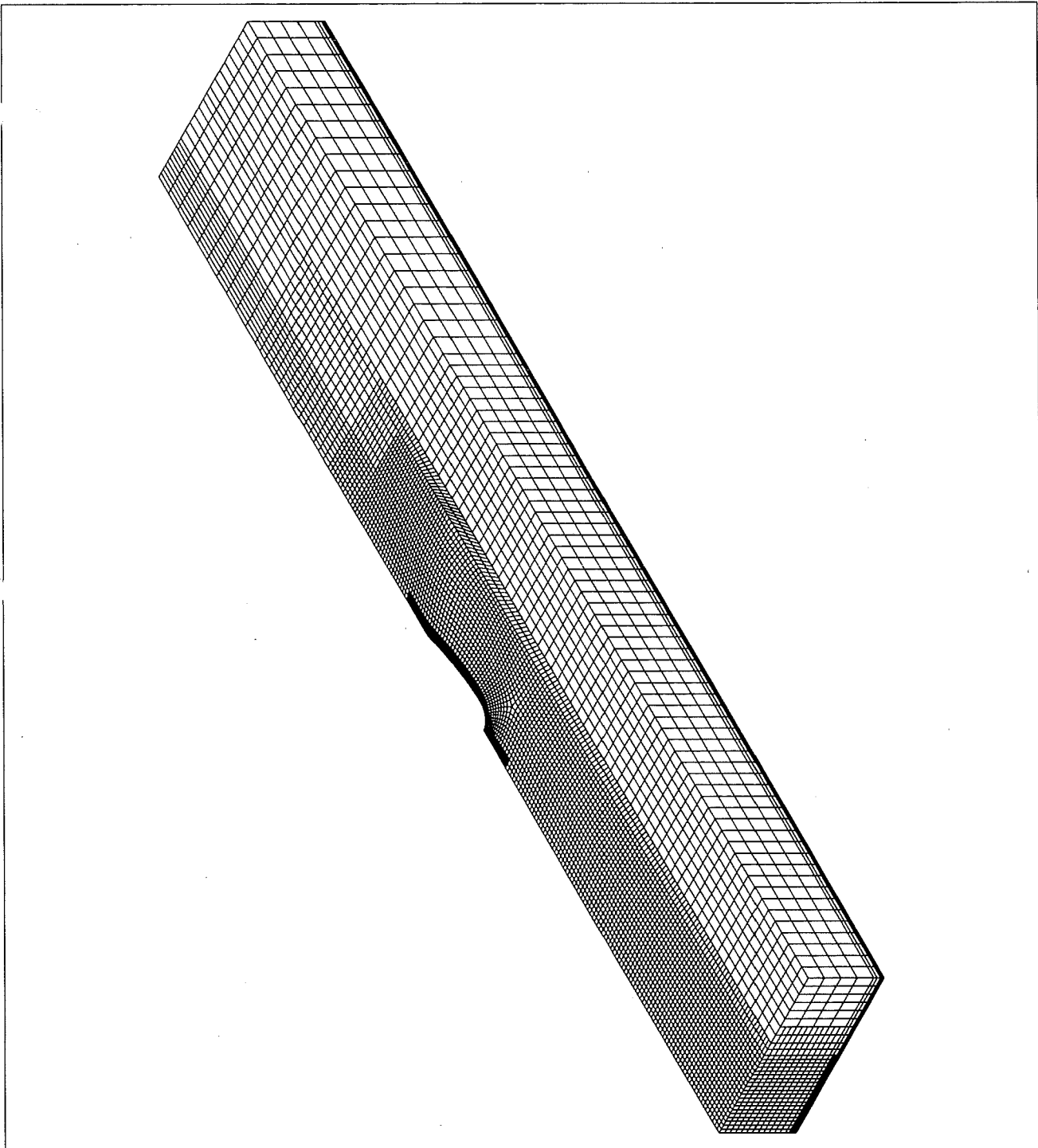
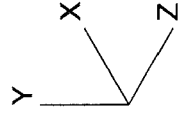
28-Feb-95

VIEW
-1.000
1.000
1.000

ANGLE
0.000
DISTANCE
1312.962

CENTER
242.345
107.520
250.950

EHIDDEN PLOT



ERCOFTAC Case 4: Wing/body junction with separation

DESCRIPTION OF NUMERICAL METHODOLOGY FOR TEST CASES 2 AND 3

Originator:

Dr.-Ing. R. Kessler

Affiliation:

DLR – Goettingen, Bunsenstr. 10, 37081 Goettingen

General description:

Finite-Volume method for non-orthogonal grids, non-staggered variable arrangement, SIMPLE algorithm, incomplete LU-decomposition, multigrid acceleration.

Convection scheme:

3rd order QUICK scheme

Mesh:

case 2a: 328 x 152 control volumes, typical y^+ : .08 – .5
case 2b: 180 x 152 control volumes, typical y^+ : .16 – .6
case 3 : 248 x 152 control volumes, typical y^+ : .13 – .2

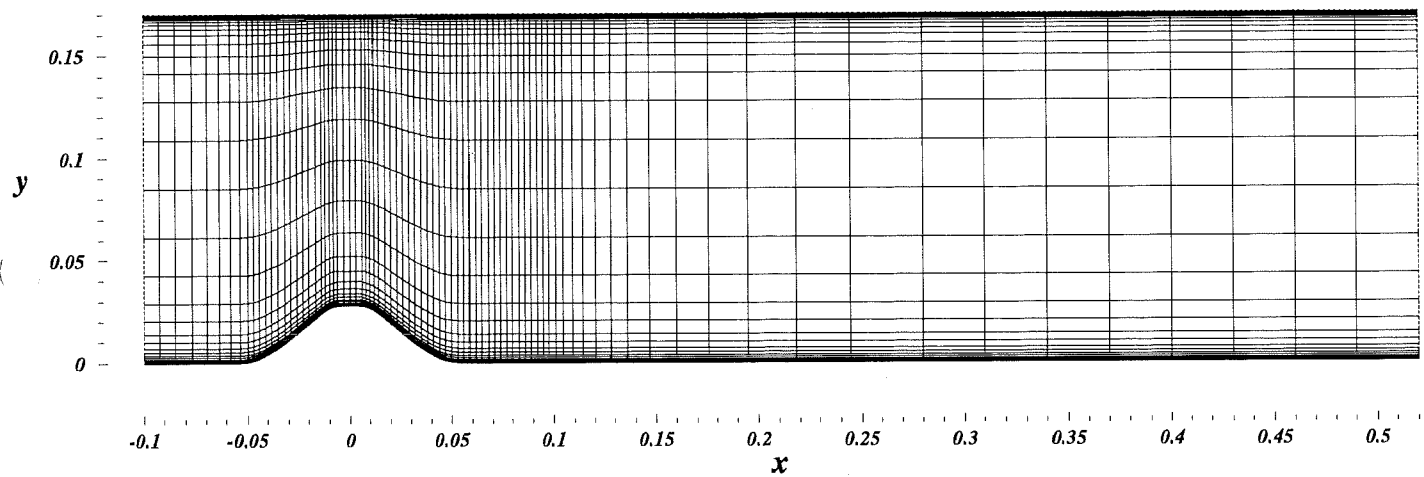
Turbulence models:

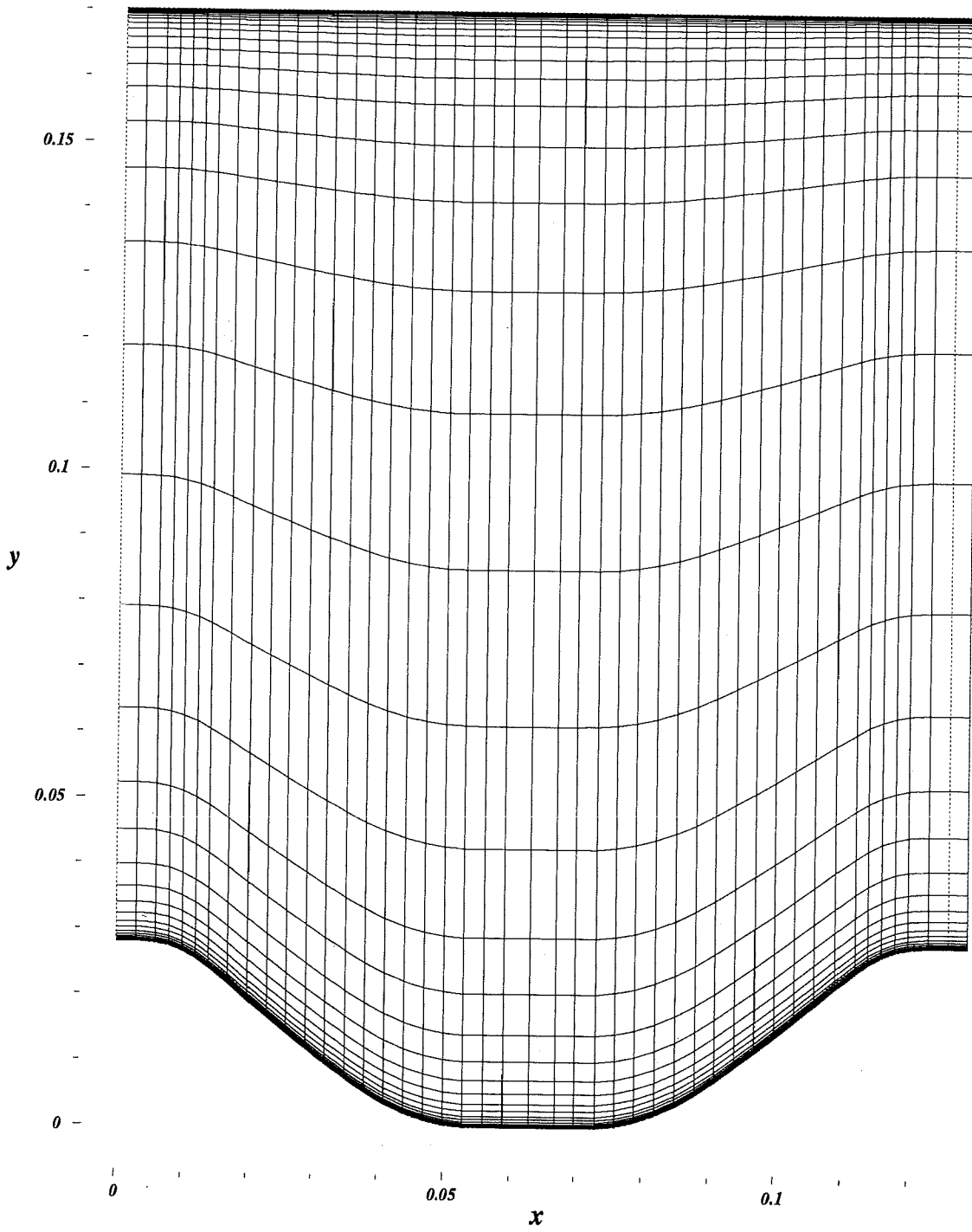
different two equation models implemented.

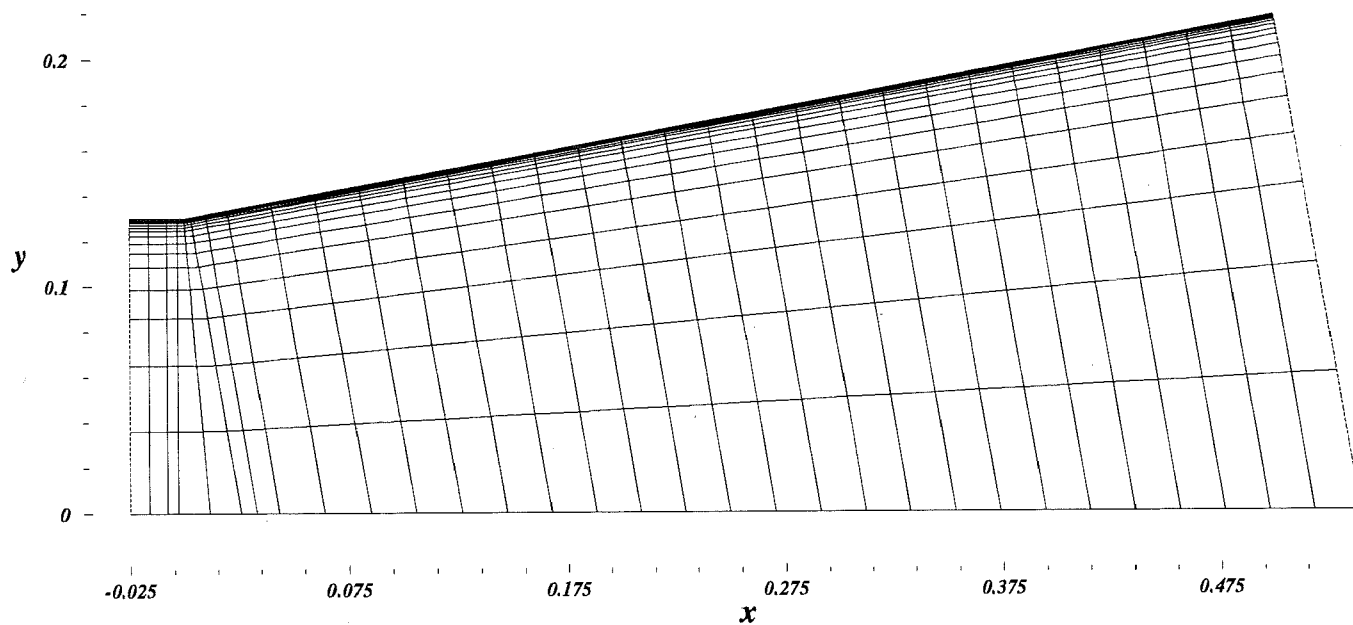
all present calculation are done with the k-omega model of Wilcox.

Near-wall treatment:

Related publications/reports:







DESCRIPTION OF NUMERICAL METHODOLOGY FOR TEST CASE 2B

Originator: C. Maaß

Affiliation: DLR, Institut für Physik der Atmosphäre D-82230 Oberpfaffenhofen

General description:

The numerical scheme integrates the full primitive equations of motion for incompressible flows in three dimensions and as a function of time. The subgrid-scale (SGS) fluxes are determined by means of eddy diffusivities as a function of the grid scale and the square root of the SGS kinetic energy. The latter is computed from a separate transport equation including shear and dissipation. The differential equations are approximated by finite differences in a spatial staggered grid. The momentum equation is integrated in time using the Adams-Bashforth scheme. The mean velocity U_m is defined as the average velocity in the x -direction across a y - z plane. After each time step Δt , the actual mean velocity is tested and a mean pressure gradient P_x in the axial direction is determined such that U_m remains constant. At the lateral boundaries, periodicity conditions are used. At the rigid surfaces, the frictional momentum flux is computed locally from the horizontal velocity in the lowest grid cell using the Prandtl relationships for a rough surface. The initial conditions prescribe uniform velocities with additional random perturbations. The LES Method is explained in detail in Krettenauer and Schumann (1992).

For this test case various boundary conditions, grids, and Smagorinsky constants have been considered but no set of parameters allowed the prediction of this reversed flow correctly. The presented results of Almeida et al. as well as the discussions at the workshop have shown that the flow in case of the consecutive hills is not fully periodic. In the simulation we consider a time dependent flow. If we define $t_{ref} = \lambda/U_b$, where U_b is the bulk velocity, then there will be an approximate equivalence between the channel flow at distance $n \lambda$ from the start of the waves and the spatially periodic simulated flow after a time $n t_{ref}$. We will assume this similarity in comparing simulation and experiment. We find that results at an early stage corresponding to the location of measurement (7th trough) match the experimental results much better as the results at a later state, which would correspond to the 40th trough. We conclude that parts of the differences between the experiment and the simulations are due to this instationarity.

Convection scheme: Second-order upwind scheme.

Mesh:

The equations of motion are formulated for the Cartesian velocity components (u, v, w) as a function of curvilinear coordinates $(\bar{x}, \bar{y}, \bar{z})$ which are related to the Cartesian coordinates according to the transformation $\bar{x} = x$, $\bar{y} = y$, $\bar{z} = \eta(x, y, z)$. Here,

$$\eta = H \frac{z - h}{H - h} \quad (1)$$

maps the domain above the model hills and below a plane top surface at $z = H$ onto a rectangular transformed domain. In this simulation we use $96 \times 48 \times 48$ grid cells. The computational domain extends over 4 hills. The horizontal grid spacings are refined near the walls.

Turbulence models: Second-order closure for the SGS fluxes using a separate transport equation for the SGS kinetic energy.

Near-wall treatment:

Flat wall: Boundary condition from Werner and Wengle (1991) with $u^+ = 10.6(z^+)^{1/9}$.

Wavy wall: $u_* = |u| \kappa / \ln(z/z_0)$ with roughness height $z_0/H = 0.0002$.

Related publications/reports:

K. Krettenauer and U. Schumann (1992), Numerical simulation of turbulent flow over wavy terrain. J. Fluid Mech. 237, pp. 261-299

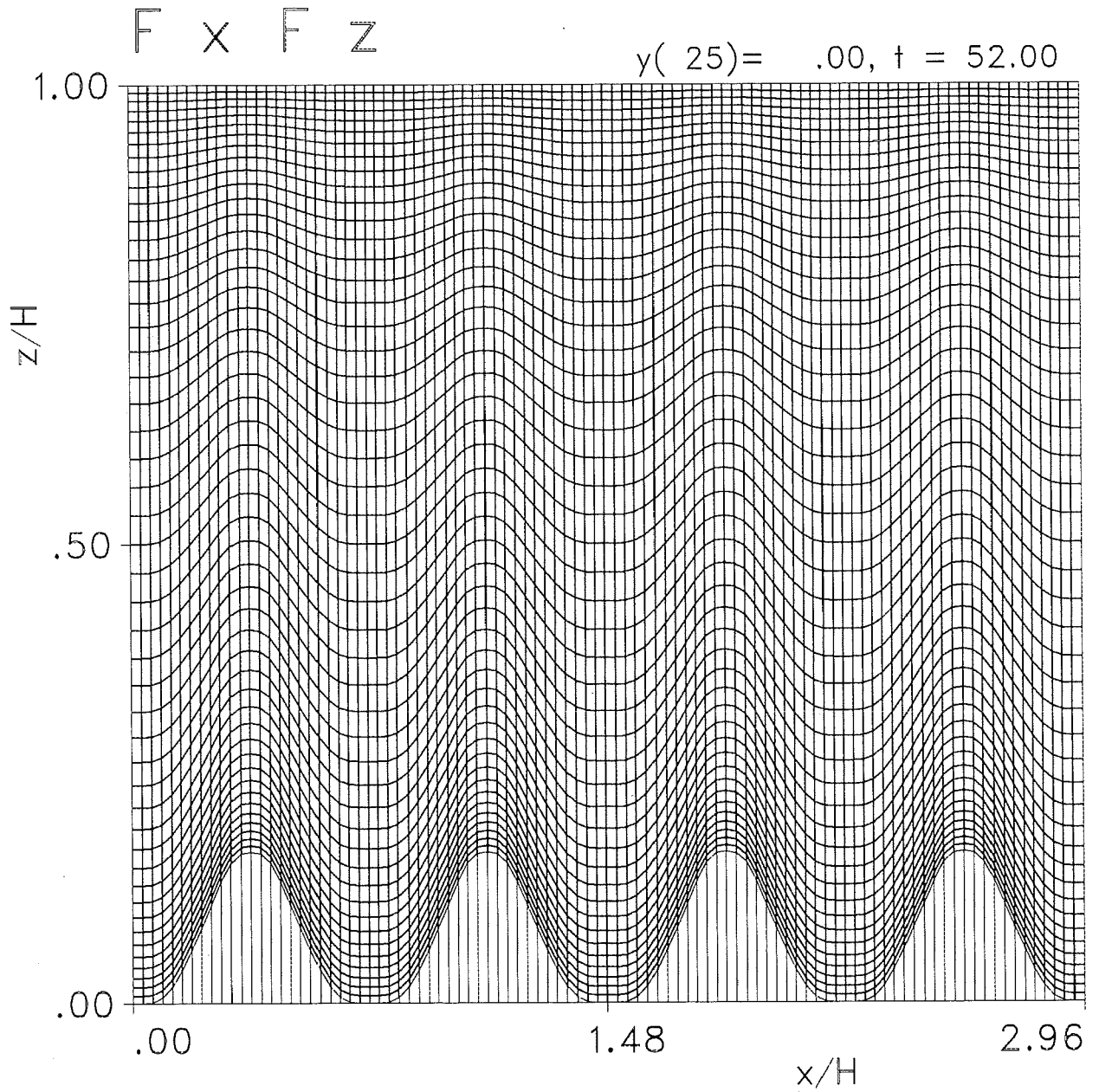
A. Dörnbrack and U. Schumann (1993), Numerical simulation of turbulent convective flow over wavy terrain. Boundary-Layer Meteorology 65, pp. 323-355

Werner H. and H. Wengle (1991), Large-eddy simulation of turbulent flow over and around a cube in a plate channel. Proc. 8th Turbulent Shear Flow Symp. Munich, Sept 9-11, pp. 19.4.1-6

FRAME 1 +0

LES31, 12/7/95, Cs=0.165, 96x48x48, Almeida, RHUSCC=0.93

MESOSC 95-07-16 19:27:30 (3)
CONTOUR FROM 2 TO 08 BY 1



DESCRIPTION OF NUMERICAL METHODOLOGY FOR TEST CASE 1A

Originators: Stanislas M., Hannani K. S. , and Deldicque A.

Affiliation: Ecole Centrale de Lille, Laboratoire de Mécanique de Lille,

URA CNRS-1441, BP-48, F59651 Villeneuve d'Acsq, France

General description:

A Galerkin finite element formulation is used to study the development of a two dimensional Couette-Poiseuille turbulent flow in a rectangular channel. To specify the eddy viscosity a two equation $k - \epsilon$ model is implemented and solved in conjunction with the Reynolds averaged incompressible Navier-Stokes equations. The near wall region is also modeled and resolved using a "low Reynolds number" extension of the $k - \epsilon$ model.

Bilinear elements for velocity components and constant pressure elements are employed. A penalty function approach has been used to eliminate the pressure at the element level. Bilinear elements have been also used for the k and ϵ . The system of steady state non-linear equations is solved using a Newton-Raphson and Picard method. At the walls no-slip boundary conditions are imposed for the velocity variables and $k = 0$ and $(\epsilon - D) = 0$ where $D = 2\nu k/y^2$ (see below). At the outlet boundary the streamwise gradients of all variables are set to zero. For the inlet boundary condition, experimental profiles did not seem to be consistent with the model used. Therefore, one-dimensional calculations are done for the pure Poiseuille flow in order to obtain the numerical inlet boundary profiles. The calculations are also performed with experimental profiles as inlet boundary conditions. Using experimental profiles, the kinetic energy profiles oscillate in the region $-.235 < x < 0$ and before reaching the moving wall they switch back to the profiles predicted by the model. It seems that results at the developed section (developing length) are not sensitive to the inlet boundary conditions.

Convection scheme: Standard Galerkin finite element (centered) scheme.

Mesh: The computational domain has been discretized by 8000 (80×100) non-uniform elements between $x = -.235$ m and $x = 2.673$ m. The mesh system consists of 101 points in the y direction and 81 points in the x direction. The mesh system is highly refined in the wall region and at $x = 0.0$ where the lower wall starts moving. A moving wall length of 2.673 m (90 times the channel height) is needed to obtain a fully developed flow (fully developed velocity, k , and ϵ). Using a moving wall length of less than 70 times the channel height, the kinetic energy will not reach a fully developed condition and will be under-estimated compared to the fully developed case.

Turbulence model: Standard $k - \epsilon$ turbulence model has been opted.

Near wall treatment: The near wall region is modeled and resolved using a "low Reynolds number" extended version of the $k - \epsilon$ model. In this study Chien's model (1982) is used. This is indeed a $k - \tilde{\epsilon}$ model where the $\tilde{\epsilon}$ goes to zero at walls. The two $k - \tilde{\epsilon}$ transport equations are written as:

$$\begin{aligned} \rho(\nabla k) \cdot u - \nabla \cdot ((\mu + \mu_t / \sigma_k)(\nabla k)) &= \\ & \mu_t (\nabla u + (\nabla u)^T) : \nabla u - \rho \tilde{\epsilon} - D \\ \rho(\nabla \tilde{\epsilon}) \cdot u - \nabla \cdot ((\mu + \mu_t / \sigma_\epsilon)(\nabla \tilde{\epsilon})) &= \\ & c_{\epsilon 1} \mu_t \tilde{\epsilon} / k (\nabla u + (\nabla u)^T) : \nabla u - c_{\epsilon 2} f \tilde{\epsilon}^2 / k - E \end{aligned}$$

where

$$D = 2\mu k / y^2$$

$$\epsilon = \tilde{\epsilon} + D$$

$$E = f_2 \mu \tilde{\epsilon} / y^2$$

| | | | | |
|---------|------------------|------------------|------------|-------------------|
| c_μ | $c_{\epsilon 1}$ | $c_{\epsilon 2}$ | σ_k | σ_ϵ |
| 0.09 | 1.35 | 1.88 | 1.0 | 1.3 |

| | | |
|------------------------------|---|---------------------|
| f_μ | f_1 | f_2 |
| $(1 - \exp(-.0115u^*y/\nu))$ | $(1 - .22\exp(-(k^2/6\nu\tilde{\epsilon}))$ | $\exp(-.5u^*y/\nu)$ |

Recently, Michelassi, Rodi and Zhu (1993), based on the DNS data, recommended the following f_μ function:

$$f_\mu = (1 - \exp(-2.10^{-4}y^+ - 4.5.10^{-4}y^{+2}))$$

In the same reference the value of σ_k is changed to 1.3 to predict correctly the turbulent kinetic energy at the center of the channel. Here, calculation are also performed with the above f_μ and σ_k implemented to the Chien's model.

References:

- K.Y. Chien, " Predictions of channel and boundary-layer flow with a low-Reynolds-number turbulence model", AIAA Journal, Vol. 20, No. 1, January, 1982.
- V. Michelassi, W. Rodi, and J. Zhu, " Testing a low Reynolds number $k - \epsilon$ turbulence model based on Direct Simulation Data ", AIAA Journal, Vol. 31, No. 9, September, 1993.

DESCRIPTION OF NUMERICAL METHODOLOGY FOR TEST CASE 1B

Originators: Stanislas M., Hannani K. S. , and Deldicque A.

Affiliation: Ecole Centrale de Lille, Laboratoire de Mécanique de Lille,

URA CNRS-1441, BP-48, F59651 Villeneuve d'Acsq, France

General description:

A Galerkin finite element formulation is used to study the development of a two-dimensional Couette-Poiseuille turbulent flow in a rectangular channel. To specify the eddy viscosity a two equation $k - \epsilon$ model is implemented and solved in conjunction with the Reynolds averaged incompressible Navier-Stokes equations. The near wall region is also modeled and resolved using a "low Reynolds number" extension of the $k - \epsilon$ model.

Bilinear elements for velocity components and constant pressure elements are employed. A penalty function approach has been used to eliminate the pressure at the element level. Bilinear elements have been also used for the k and ϵ . The system of steady state non-linear equations is solved using a Newton-Raphson and Picard method. At the walls no-slip boundary conditions are imposed for the velocity variables and $k = 0$ and $(\epsilon - D) = 0$ where $D = 2\nu k/y^2$ (see below). At the outlet boundary the streamwise gradients of all variables are set to zero. For the inlet boundary condition, experimental profiles did not seem to be consistent with the model used. Therefore, one-dimensional calculations are done for the pure Poiseuille flow in order to obtain the numerical inlet boundary profiles. The calculations are also performed with experimental profiles as inlet boundary conditions. Using experimental profiles, the kinetic energy profiles oscillate in the region $-.235 < x < 0$ and before reaching the moving wall they switch back to the profiles predicted by the model. It seems that results at the developed section (developing length) are not sensitive to the inlet boundary conditions.

Convection scheme: Standard Galerkin finite element (centered) scheme.

Mesh: The computational domain has been discretized by 8000 (80×100) graded elements between $x = -.235$ m and $x = 3.58$ m. The mesh system consists of 101 points in the y direction and 81 points in the x direction. The mesh system is highly refined in the wall region and at $x = 0.0$ where the lower wall starts moving. A moving wall length of $3.58m$ (120 times the channel height) is needed to obtain a fully developed flow (fully developed velocity). However, even using a moving wall length of 120 times the channel height, the turbulent kinetic energy did not reach a completely fully developed condition.

Turbulence model: Standard $k - \epsilon$ turbulence model has been opted.

Near wall treatment: The near wall region is modeled and resolved using a "low Reynolds number" extended version of the $k - \epsilon$ model. In this study Chien's model (1982) is used. This is indeed a $k - \tilde{\epsilon}$ model where the $\tilde{\epsilon}$ goes to zero at walls. The two $k - \tilde{\epsilon}$ transport equations are written as:

$$\rho(\nabla k) \cdot u - \nabla \cdot ((\mu + \mu_t / \sigma_k)(\nabla k)) =$$

$$\mu_t (\nabla u + (\nabla u)^T) : \nabla u - \rho \tilde{\epsilon} - D$$

$$\rho(\nabla \tilde{\epsilon}) \cdot u - \nabla \cdot ((\mu + \mu_t / \sigma_\epsilon)(\nabla \tilde{\epsilon})) =$$

$$c_{\epsilon 1} \mu_t \tilde{\epsilon} / k (\nabla u + (\nabla u)^T) : \nabla u - c_{\epsilon 2} f \tilde{\epsilon}^2 / k - E$$

where

$$D = 2\mu k/y^2$$

$$\epsilon = \tilde{\epsilon} + D$$

$$E = f2\mu\tilde{\epsilon}/y^2$$

| c_μ | $c_{\epsilon 1}$ | $c_{\epsilon 2}$ | σ_k | σ_ϵ |
|---------|------------------|------------------|------------|-------------------|
| 0.09 | 1.35 | 1.88 | 1.0 | 1.3 |

| f_μ | f_1 | f_2 |
|------------------------------|---|---------------------|
| $(1 - \exp(-.0115u^*y/\nu))$ | $(1 - .22\exp(-(k^2/6\nu\tilde{\epsilon}))$ | $\exp(-.5u^*y/\nu)$ |

Recently, Michelassi, Rodi and Zhu (1993), based on the DNS results, recommended the following f_μ function :

$$f_\mu = (1 - \exp(-2.10^{-4}y^+ - 4.5.10^{-4}y^{+2}))$$

In the same reference the value of σ_k is changed to 1.3 to predict correctly the turbulent kinetic energy at the center of the channel. Here, calculation are also performed with the above f_μ and σ_k implemented to the Chien's model.

References:

- K.Y. Chien, " Predictions of channel and boundary-layer flow with a low-Reynolds-number turbulence model", AIAA Journal, Vol. 20, No. 1, January, 1982.
 V. Michelassi, W. Rodi, and J. Zhu, " Testing a low Reynolds number $k - \epsilon$ turbulence model based on Direct Simulation Data ", AIAA Journal, Vol. 31, No. 9, September, 1993.

DESCRIPTION OF METHODOLOGY FOR TEST CASES 1A AND 1B

Originator: Stanislas.M, Deldicque A., Hannani S.

Affiliation: Ecole Centrale de Lille, LML URA CNRS 1441, BP48 F59651 Villeneuve d'Ascq, FRANCE

General Description: When the flow is developed, the problem reduces to the one dimensional problem:

$$\frac{d}{dy} \left(K \frac{d\Phi}{dy} \right) + S = 0$$

Using a finite volume formulation, at a node j the discretized equation is obtained (a second order scheme is used for the derivatives)

$$A\Phi_{j+1} + B\Phi_j + C\Phi_{j-1} = D$$

Using Thomas Algorithm, the tri-diagonal set of equations for Φ is solved.

Convection scheme: No scheme has been used because of the absence of convection when the flow is developed.

Mesh: The mesh used to perform the calculation for the two cases is symmetrical and exponential. The number of nodes used in the y direction is 199. For example, near the fixed wall, ten points lie in the viscous layer (the first point is about 0.4 viscous length) and thirty points in the buffer layer.

Turbulence model: The model of JAKIRLIC & HANJALIC (proceedings of the 5 International Symposium on refined flow modelling and turbulence measurements) has been used to perform the calculation for the case 1a and 1b. The equation of ϵ has been slightly modified; $C_{\epsilon 4}$ has been set equal to zero. Their model differs essentially in the expression of the ϵ equation from LAUNDER & SHIMA's model. The stress transport model is a version of LAUNDER & SHIMA model though the anisotropy of the dissipation tensor is explicitly modeled. Several constants are made function of the invariants of the anisotropic stress tensor a_{ij} and of the anisotropic dissipation tensor e_{ij} . The wall reflection effects are taken in account through the pressure strain term. The way to model this phenomena involves the use of wall function based on the turbulent energy k , the dissipation ϵ , and a characteristic length. In the present case, at a location, the length to consider is the nearest normal distance; that means that only the nearest wall is felt at a location point.

Near wall treatment: For each wall, mirror conditions have been used to impose the no slip condition on the first moment and the second moments. At each wall, the dissipation ϵ is deduced from the kinetic energy k through the relation:

$$\epsilon_{wall} = 2\nu \left(\frac{dk^{1/2}}{dy} \right)_{wall}^2$$

References:

Jakirlic S., Hanjalic K., Durst F. *Proc. 5th Symposium on Refined Flow Modelling and Turbulence Measurements*

Set of equations and constants:

Stress transport equation:

$$\frac{D}{Dt} \overline{u_i u_j} = P_{ij} + \Phi_{ij}^1 + \Phi_{ij}^2 + \Phi_{ij}^{w1} + \Phi_{ij}^{w2} + \frac{\partial}{\partial x_k} (-J_{ijk} + \nu \frac{\partial}{\partial x_k} \overline{u_i u_j}) - \epsilon_{ij}$$

$$P_{ij} = - \left(\overline{u_j u_k} \frac{\partial \overline{U_i}}{\partial x_k} + \overline{u_i u_k} \frac{\partial \overline{U_j}}{\partial x_k} \right)$$

$$\Phi_{ij}^1 = -C_1 \frac{\epsilon}{k} \left(\overline{u_i u_j} - \frac{2}{3} k \delta_{ij} \right)$$

$$\begin{aligned}\Phi_{ij}^2 &= -C_2 \left(P_{ij} - \frac{2}{3} P \delta_{ij} \right) \\ \Phi_{ij}^{w1} &= C_{w1} \frac{\epsilon}{k} \left(\overline{u_k u_m n_k n_m} \delta_{ij} - \frac{3}{2} \overline{u_k u_i n_k n_j} - \frac{3}{2} \overline{u_k u_j n_k n_i} \right) \frac{k^{3/2}}{\epsilon d} \\ \Phi_{ij}^{w2} &= C_{w2} \left(\Phi_{km}^2 n_k n_m \delta_{ij} - \frac{3}{2} \Phi_{ik}^2 n_k n_j - \frac{3}{2} \Phi_{jk}^2 n_k n_i \right) \frac{k^{3/2}}{\epsilon d} \\ J_{ijk} &= -C_s \frac{k}{\epsilon} \overline{u_k u_l} \frac{\partial \overline{u_i u_j}}{\partial x_l} \\ \epsilon_{ij} &= f_s \epsilon_{ij}^* + (1 - f_s) \frac{2}{3} \epsilon \delta_{ij} \\ \epsilon_{ij}^* &= \frac{\epsilon}{k} \frac{(\overline{u_i u_j} + (\overline{u_i u_k n_j n_k} + \overline{u_j u_k n_i n_k} + \overline{u_k u_l n_k n_l n_i n_j}) f_d)}{(1 + \frac{3}{2} \frac{\overline{u_p u_q}}{k} n_p n_q f_d)}\end{aligned}$$

ϵ transport equation

$$\begin{aligned}\frac{D}{Dt} \epsilon &= C_{\epsilon 1} \frac{\epsilon}{k} P - C_{\epsilon 2} f \frac{\epsilon \tilde{\epsilon}}{k} + C_{\epsilon 3} \nu \frac{k}{\epsilon} \overline{u_j u_k} \frac{\partial^2 \overline{U_i}}{\partial x_j \partial x_l} \frac{\partial^2 \overline{U_i}}{\partial x_k \partial x_l} \\ &\quad + \frac{\partial}{\partial x_k} \left(C_\epsilon \frac{k}{\epsilon} \overline{u_k u_l} \frac{\epsilon}{\partial x_l} + \nu \frac{\partial \epsilon}{\partial x_k} \right)\end{aligned}$$

Classical constants:

| c_s | c_ϵ | $c_{\epsilon 1}$ | $c_{\epsilon 2}$ | $c_{\epsilon 3}$ |
|-------|--------------|------------------|------------------|------------------|
| 0.22 | 0.18 | 1.44 | 1.92 | 0.3 |

Other constants:

| | |
|--------------------------------------|---|
| $C_1 = 1 - f_s + C$ | $C = 2.5 A F^{1/4} f$ |
| $F = \min(A_2, 0.6)$ | $f = \min[(R_t/140)^4, 1]$ |
| $C_2 = 0.75 A^{1/2}$ | $C_{w1} = 2/5 - 4C/15$ |
| $C_{w2} = \max[4/15 - 1/(15C_2), 0]$ | $f_s = 1 - A^{1/2} E^2$ |
| $f_d = 1/(1 + 0.1 R_t)$ | $f_\epsilon = 1 - \frac{C_{\epsilon 2} - 1}{C_{\epsilon 2}} \left(\exp(-\frac{R_t^2}{36}) \right)$ |

where

$$\begin{cases} A = 1 - 9A_2/8 + 9A_3/8 & A_2 = a_{ij} a_{ij} \\ A_3 = a_{ij} a_{jk} a_{ki} & a_{ij} = \overline{u_i u_j} / k - 2/3 \delta_{ij} \\ R_t = k^2 / \nu \epsilon \\ E = 1 - 9/8 E_2 + 9/8 E_3 & E_2 = e_{ij} e_{ij} \\ E_3 = e_{ij} e_{jk} e_{ki} & e_{ij} = \epsilon_{ij} / \epsilon - 2/3 \delta_{ij} \end{cases}$$

Description of methodology for test cases 1a and 1b

Originator: Stanislas.M, Deldicque A., Hannani S.

Affiliation: Ecole Centrale de Lille, LML URA CNRS 1441, BP48 F59651 Villeneuve d'Ascq, FRANCE

General Description: When the flow is developed, the problem reduces to the one dimensional problem:

$$\frac{d}{dy} \left(K \frac{d\Phi}{dy} \right) + S = 0$$

Using a finite volume formulation, at a node j the discretized equation is obtained (a second order scheme is used for the derivatives)

$$A\Phi_{j+1} + B\Phi_j + C\Phi_{j-1} = D$$

Using Thomas Algorithm, the tri-diagonal set of equations for Φ is solved.

Convection scheme: No scheme has been used because of the absence of convection when the flow is developed.

Mesh: The mesh used to perform the calculation for the two cases is symmetrical and exponential. The number of nodes used in the y direction is 199. For example, near the fixed wall, ten points lie in the viscous layer (the first point is about 0.4 viscous length) and thirty points in the buffer layer.

Turbulence model: The model of SHIMA (&LAUNDER) (proceedings of the eight symposium on turbulent shear flows session 8-2) has been used to perform the calculation for the case 1a and 1b. The wall reflection effects are taken in account through the pressure strain term. The way to model this phenomena involves the use of wall function based on the turbulent energy k , the dissipation ϵ , and a characteristic length. In the present case, at a location, the length to consider is the nearest normal distance; that means that only the nearest wall is felt at a location point.

Near wall treatment: For each wall, mirror conditions have been used to impose the no slip condition on the first moment and the second moments. At each wall, the dissipation ϵ is deduced from the kinetic energy k through the relation:

$$\epsilon_{wall} = 2\nu \left(\frac{dk^{1/2}}{dy} \right)_{wall}^2$$

References:

Shima N. 1991 *Proc. 8th Symposium on Turbulent Shear Flows*

Lauder B.E. & Shima N. 1989 *AIAA J.* 27, 1319-1325

Set of equations and constants:

Stress transport equation:

$$\frac{D}{Dt} \overline{u_i u_j} = P_{ij} + \Phi_{ij}^1 + \Phi_{ij}^2 + \Phi_{ij}^{w1} + \Phi_{ij}^{w2} + \frac{\partial}{\partial x_k} \left(-J_{ijk} + \nu \frac{\partial}{\partial x_k} \overline{u_i u_j} \right) - \epsilon_{ij}$$

$$P_{ij} = - \left(\overline{u_j u_k} \frac{\partial \overline{U_i}}{\partial x_k} + \overline{u_i u_k} \frac{\partial \overline{U_j}}{\partial x_k} \right)$$

$$\Phi_{ij}^1 = -C_1 \frac{\epsilon}{k} \left(\overline{u_i u_j} - \frac{2}{3} k \delta_{ij} \right)$$

$$\Phi_{ij}^2 = -C_2 \left(P_{ij} - \frac{2}{3} P \delta_{ij} \right)$$

$$\Phi_{ij}^{w1} = C_{w1} \frac{\epsilon}{k} \left(\overline{u_k u_m} n_k n_m \delta_{ij} - \frac{3}{2} \overline{u_k u_i} n_k n_j - \frac{3}{2} \overline{u_k u_j} n_k n_i \right) \frac{k^{3/2}}{2.5 \epsilon d}$$

$$\Phi_{ij}^{w2} = C_{w2} \left(\Phi_{km}^2 n_k n_m \delta_{ij} - \frac{3}{2} \Phi_{ik}^2 n_k n_j - \frac{3}{2} \Phi_{jk}^2 n_k n_i \right) \frac{k^{3/2}}{2.5 \epsilon d}$$

$$J_{ijk} = -C_s \frac{k}{\epsilon} \overline{u_k u_l} \frac{\partial \overline{u_i u_j}}{\partial x_l}$$

$$\epsilon_{ij} = \frac{2}{3} \epsilon \delta_{ij}$$

ϵ transport equation

$$\frac{D}{Dt}\epsilon = (C_{\epsilon 1} + \Psi_1 + \Psi_2)\frac{\epsilon}{k}P - C_{\epsilon 2}\frac{\epsilon \tilde{\epsilon}}{k} + \frac{\partial}{\partial x_k} \left(C_{\epsilon} \frac{k}{\epsilon} \overline{u_k u_l} \frac{\epsilon}{\partial x_l} + \nu \frac{\partial \epsilon}{\partial x_k} \right)$$

Classical constants:

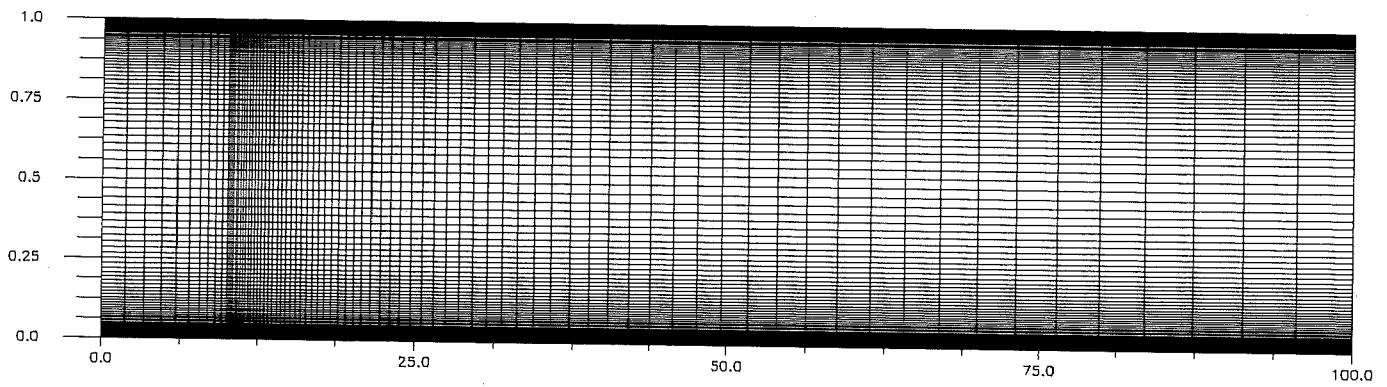
| C_s | C_{ϵ} | $C_{\epsilon 1}$ | $C_{\epsilon 2}$ |
|-------|----------------|------------------|------------------|
| 0.22 | 0.18 | 1.45 | 1.9 |

Other constants:

| | | |
|----------|-----|---|
| C_1 | $=$ | $1 + 2.58AA_2^{1/4} [1 - \exp(-(0.0067R_t)^2)]$ |
| C_2 | $=$ | $0.75A^{1/2}$ |
| C_{w1} | $=$ | $-2C_1/3 + 1.67$ |
| C_{w2} | $=$ | $\max[2(C_2 - 1)/3 + 0.5, 0]/C_2$ |
| Ψ_1 | $=$ | $1.5A(\frac{P}{\epsilon} - 1)$ |
| Ψ_2 | $=$ | $0.35(1 - 0.3A_2)\exp(-(0.002R_t)^{1/2})$ |

where

$$\begin{cases} A & = 1 - 9A_2/8 + 9A_3/8 & A_2 & = a_{ij}a_{ij} \\ A_3 & = a_{ij}a_{jk}a_{ki} & a_{ij} & = \overline{u_i u_j}/k - 2/3\delta_{ij} \\ R_t & = k^2/\nu\epsilon \end{cases}$$



DESCRIPTION OF NUMERICAL METHODOLOGY FOR TEST CASE 3

Originator:

P.Debaty, J.F.Brisson, G.Brun, O.Leroy

Affiliation:

laboratoire de mecanique des fluides et d'acoustique
Ecole Centrale de Lyon 69131 ECULLY Cedex France

General description:

- NATUR : Navier–stokes TURbulent code
 - elliptic solver of the Navier–Stokes equations using rsm model of turbulence for calculating flows with complex geometries with or without swirl
 - finite element discretisation with two grids (P1 interpolation of pressure on a coarse grid, P1isoP2 interp. of all other quant. on finer grid)
 - non stationary formulation, semi–implicit time scheme ensuring linearisation of the differential operators
 - resolution of linear systems by a CGS method
-

Convection scheme:

streamline–upwind finite element technique[TJ.Hughes]

Mesh: 651 nodes,1200 triangular elements on pressure grid
2501 nodes,4800 triangular elements on the finer grid

Inlet conditions

boundary conditions at the inlet(located at $x=-25$ mm) are taken from experimental profiles(some of them are extrapolated to reach $y=1$ mm)

Turbulence models:

standard simplified form of Launder,Reece,Rodi [1974] model with $C1=1.5$ and $\text{gama}=0.6$, using isotropisation of production hypothesis (IP model) wall echo terms are discarded here

Near–wall treatment:

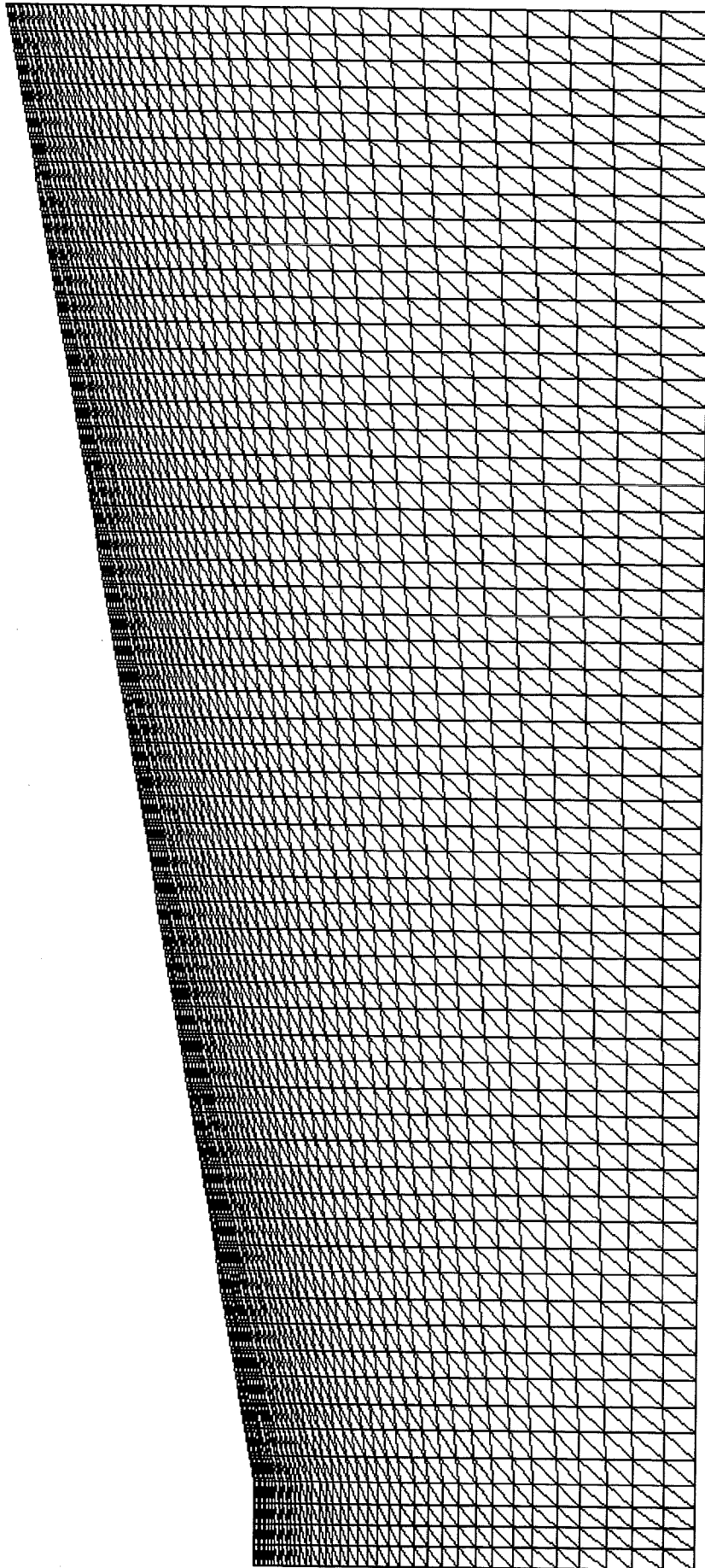
wall functions

logarithmic law for velocity

the first point is located at $y=1$ mm from the wall to ensure a $y+$ value between 40 and 80

Related publications/reports:

P.Debaty "Performances des modeles de turbulence au second ordre appliques a des configurations axisyme– triques simulees par elements finis" these E.C.L. 16/12/94



Velocity Grid

DESCRIPTION OF NUMERICAL METHODOLOGY FOR TEST CASE 1A_1D

Originator: Laurence D.

Affiliation: EDF-LNH, 6 quai watier, 7840 Chatou, France.

General description:

1D finite difference code for fully developed channel flow. The diffusion and elliptic operators are solved as coupled tri-diagonal systems : k and ϵ , u_2 and ϕ_2 etc.

Convection scheme:

none

Mesh:

200 nodes, with clustering in the near wall region.

Turbulence models:

IP second moment closure of Lunder-Reece-Rodi with no wall echo terms.

The damping of the redistributive pressure-strain terms is obtained by an elliptic relaxation of the latter which is most effective in the near wall layer ($y^+ < 50$).

The timescale k/ϵ is prevented from going to zero by setting a lower bound based on a Kolmogorov time-scale.

The rotta constant is decreased from its standard value to capture the log-law without wall echo terms: $C_1 = 1.22$, $C_2 = 0.6$, $\sigma_{\epsilon} = 1.2$, $\sigma_{\epsilon} = 1.65$, $\sigma_{\epsilon} = 1.44$, $\sigma_{\epsilon} = 1.9$

Near-wall treatment:

elliptic relaxation avoids use of damping functions. k and u_2 are parabolic at $y^+ = 0$ and dissipation floats to whatever level is needed to balance diffusion. uv and v_2 decrease as y^{*4} .

Related publications/reports:

. P. Durbin

A Reynolds Stress model for near-wall turbulence. JFM (1993) vol 249 p465.

. D. Laurence, P. Durbin

Modelling near wall effects in second moment closures by elliptic relaxation. Center for Turbulence Research, Proceedings of the 1992 summer program.

DESCRIPTION OF NUMERICAL METHODOLOGY FOR TEST CASE 1&2

Originator:

N.E. Bouchama, E. Razafindrakoto, D. Laurence, G. Pot

Affiliation:

EDF-LNH, 6 quai watier, 7840 Chatou, France.

General description:

- Finite element N3S code,
- Time and space discretization : Fractional steps method with convection step, diffusion step and pressure-continuity problem. Convection step is solved by characteristics method and the two remaining stages are solved by a Galerkin finite element method with P1-IsoP2 triangles (pressure is P1 on the element and other variables are P1 on each sub-element),

Convection Scheme:

Characteristics method

Mesh:

200 nodes, with clustering in the near wall region.

Turbulence models:

Launder Sharma low Re k-epsilon model

Near-wall treatment:

$U=0.$, $k=0.$, $\epsilon=0.$

Related publications/reports:

- CHABARD, METIVET, POT, THOMAS : "An efficient finite element method for the computation of 3D turbulent incompressible flows", Finite Element in Fluids , Vol.8, 1992.

DESCRIPTION OF NUMERICAL METHODOLOGY FOR TEST CASE 2 (RSTM)

Originator:

N.E. Bouchama, E. Razafindrakoto, D. Laurence, G. Pot

Affiliation: EDF-LNH, 6 quai watier, 7840 Chatou, France.

General description:

– Finite element N3S code,

– Time and space discretization : Fractional steps method with convection step, stress step and pressure–continuity problem. Convection step is solved by a characteristics method and the two remaining stages are solved by a Galerkin finite element method with P1–IsoP2 triangles (pressure is P1 on the element and other variables are P2 on each sub–element). The Re Stresses equations are solved coupled with the momentum equations, under an incremental linearized form. The linear system is solved by a conjugate residual method.

Convection scheme:

Characteristics method. The upstream trajectory is computed by Runge Kutta, and advected variables interpolated by the quadratic P2 discretization.

Mesh:

3721 P1 nodes, with clustering in the near wall region.

Turbulence models:

IP version of the LRR Reynolds Stress Transport model, without "wall echo" terms. The "law of the wall" is applied for the shear stress and constant values are given to the normal stresses.

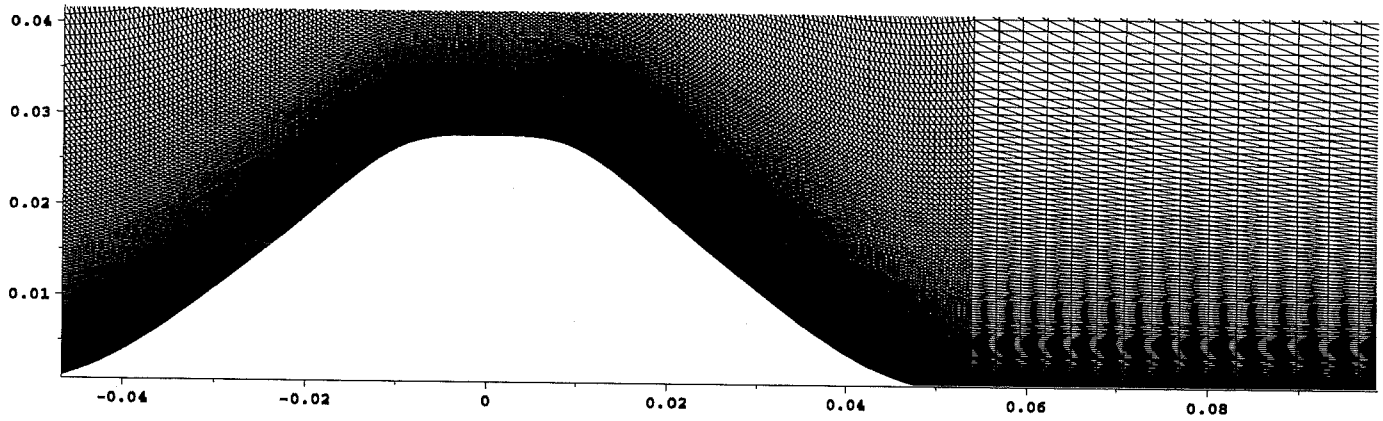
Near–wall treatment:

High Re form $U(y)=f(y,u^*) \Rightarrow u^* \Rightarrow$ Re stresses

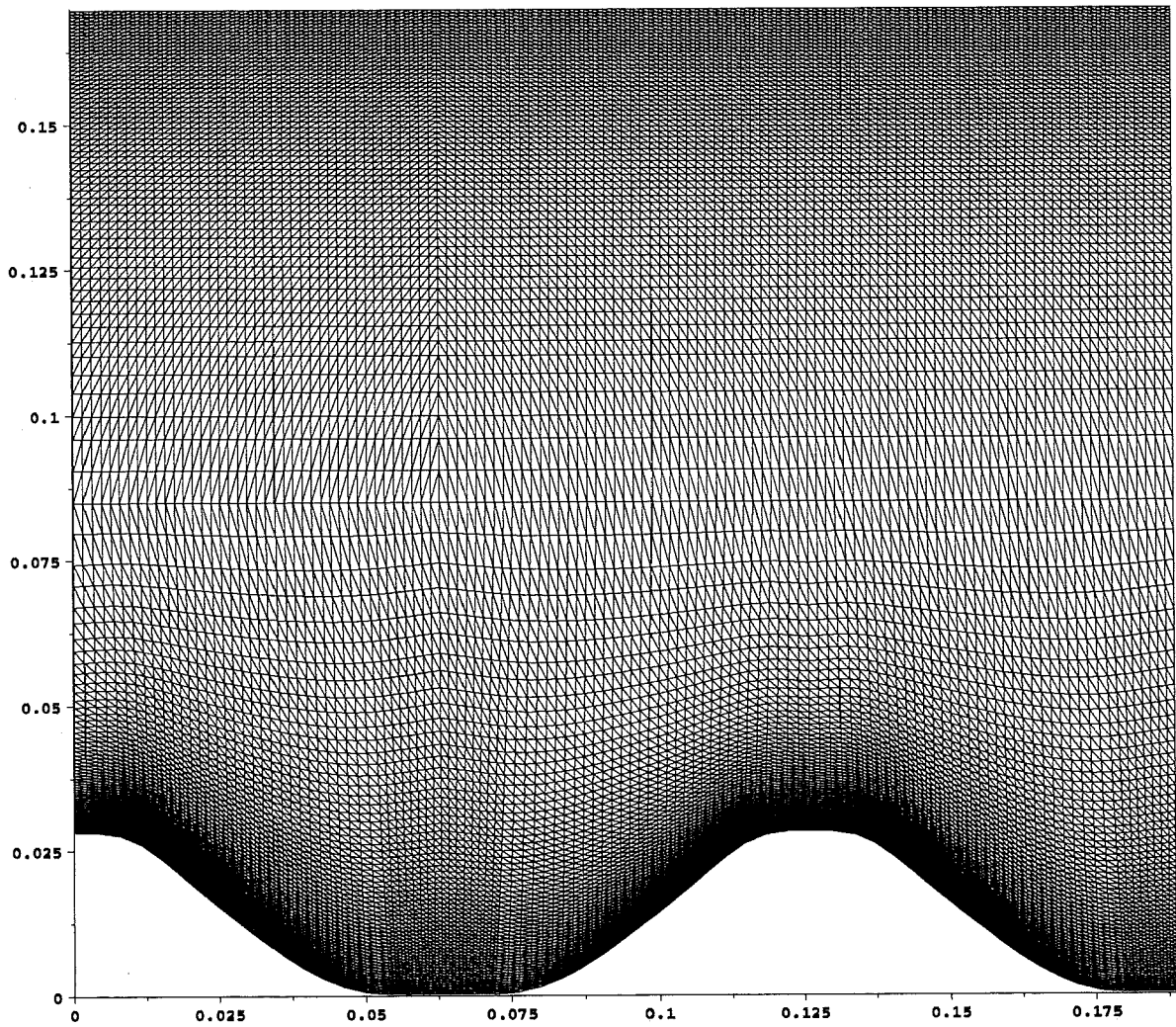
Related publications/reports:

– CHABARD, METIVET, POT, THOMAS : "An efficient finite element method for the computation of 3D turbulent incompressible flows", Finite Element in Fluids , Vol.8, 1992.

Structured Mesh for Test Case 2A
13536 P1 Nodes (pressure)
53671 P2 Nodes (velocity)



Structured Mesh for Test Case 2B
3721 P1 Nodes (pressure)
14641 P2 Nodes (velocity)



DESCRIPTION OF NUMERICAL METHODOLOGY FOR TEST CASE 5

Originator : J.D. Mattei, J.P. Minier

Affiliation : EDF/DER/LNH

General description : ESTET is a multi-purpose software using single block structured mesh. Coordinates are cartesian or orthogonal curvilinear. Laminar and turbulent flows can be simulated using $k-\epsilon$ or $k-\epsilon$ low Reynolds modelling (Launder-Sharma model). Compressible or incompressible can be computed, a Lagrangian treatment of the dispersed phase (if any) can be used as well as radiative transfer, porous media The numerical scheme is based on a half-staggered grid and makes use of the separation of operators (advection, diffusion + source terms, mass balance). Advection for velocity components, k and ϵ is performed by the characteristics method. The $k - \epsilon$ system is solved in a coupled manner. The mass balance step is treated by Finite Volume discretization while for scalars a quick-upwind Finite Volume discretization is applied.

Convection scheme : Characteristics method with cubic interpolation at their feet. The interpolation scheme is based on Hermite interpolation.

Mesh : Structured single block mesh.

Turbulence models : $k - \epsilon$ standard model with constants equal to $C_{\epsilon 1} = 1.44$, $C_{\epsilon 2} = 1.92$, $\sigma_k = 1$, $\sigma_\epsilon = 1.3$ and $C_\mu = 0.09$.

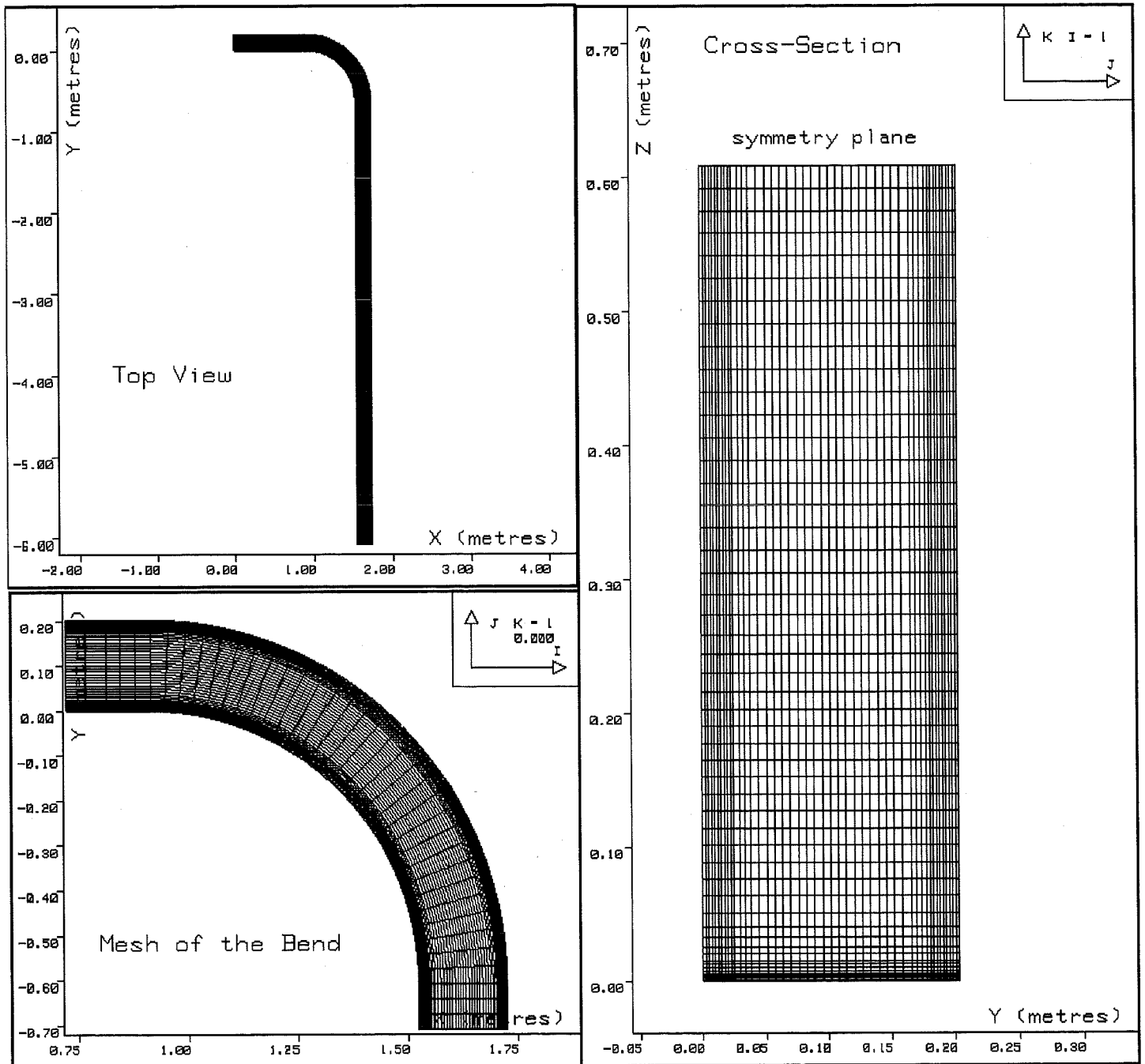
Near-wall treatment : Use of wall functions with a logarithmic law for the velocity based on two regions :

$$\text{if } y^+ \leq 5 \text{ then } \bar{u} = 0, k = 0, \frac{\partial \epsilon}{\partial n} = 0.$$

if $y^+ \leq 5$ then wall functions.

Related publications/reports :

- [1] Gabillard, M. and Viollet, P.L., 1988, "The 3D computation of secondary flow and density currents in a curved pipe", *3rd International Symposium of Refined Flow Modelling and Turbulence Measurements*, Tokyo 1988.
- [2] Peniguel, C. and Rupp, I., 1993, "A Numerical Method for Thermally Coupled Fluid and Solid Problems", *8rd International Conference on Numerical Methods in Thermal Problems*, 11-16 July 1993.
- [3] Mattei, J.D., Lionnet, B. and Laurence, D., 1994, "Computations of Turbulent Mixed Convection in Square Cavities", *International Symposium on Turbulence, Heat and Mass Transfer*, 9-12 August 1994.
- [4] Peniguel, C., 1994, "Numerical Study of a Thermally Stratified Flow and its Interaction with a Conducting Wall", *4th International Symposium on Stratified Flows*, 29 June-2 July 1994.
- [5] Bailly, C., Lafon, P. and Candel, S., 1994, "Computation of Subsonic and Supersonic Jet Mixing Noise Using a Modified $k - \epsilon$ Model for Compressible Free Shear Flows", *Acta Acustica 2* (1994), pp 101-112.



DESCRIPTION OF NUMERICAL METHODOLOGY FOR TEST CASE 1A, B & C
“Developing flow”

Originators:

Jean-Bernard CAZALBOU and Florence TORRES.

Affiliation:

ENSICA, Département de Mécanique de Fluides,
49 avenue L. BLUM, 31056 TOULOUSE Cedex.

General description:

An “artificial compressibility code” is used to generate all developing-flow results in Case 1A, 1B and 1C. The steady Reynolds-averaged Navier-Stokes equations, written for an incompressible fluid, are supplemented with fictitious-time evolution terms including a pressure temporal derivative in the continuity equation. Time-marching until convergence gives the solution for the steady incompressible flow. The method is based on a finite-volume spatial discretization of the partial-differential equations written in vector form for the dynamics and in scalar form for the closure transport equations. Approximations to the diffusion terms are centered while that of the convection terms are based on a flux-difference splitting procedure that can be precise up to the third order. Time discretization is explicit.

Convection scheme:

Roe’s approximate Riemann Solver [J. Comput. Phys., Vol.43, 1981] implemented with the MUSCL approach (Van Leer, J. Comput. Phys., Vol. 43, 1981) limited to first-order precision.

Mesh:

Two orthogonal grids are used:

- Grid #1 for Cases A and B, (96,102) points in (x, y) clustered in the x -direction at the beginning of the moving belt and following a cosine distribution in y , (Cartesian grid);
 - Grid #2 for Case C, (52,102) points in (x, y) evenly spaced in the x -direction and following a cosine distribution in y , (non-Cartesian grid).
-

Turbulence models:

The (k, ϵ) model with the standard set of constants [Launder and Sharma, Letters in Heat and Mass Transfer, Vol. 1, 1974].

Near-wall treatment:

Low-Reynolds-number version of the (k, ϵ) model according to Launder and Sharma (Ibid.)

Related publications/reports:

J.-B. CAZALBOU,

“Calcul d’écoulement turbulents de fluide incompressible par une méthode de compressibilité artificielle”,
Internal rpt. ENSICA/DFR/MF, 1991.

DESCRIPTION OF NUMERICAL METHODOLOGY FOR TEST CASE 1A & 1B
“Developed flow”

Originators:

Jean-Bernard CAZALBOU and Florence TORRES.

Affiliation: ENSICA, Département de Mécanique de Fluides,
49 avenue L. BLUM, 31056 TOULOUSE Cedex.

General description:

A “One-dimensional channel flow code” is used to generate all developed-flow results in Case 1A and 1B. It is based on a simple finite-volume spatial discretization of the differential equations of the 1-D case (obtained from the Reynolds-averaged equations). A fictitious-time marching is performed that gives the solution after time convergence. All approximation are centered, diffusion terms are implicitly treated and, in order to improve convergence, the evaluation of the source terms is either explicit or implicit depending on their sign.

Convection scheme:

No convection terms in the 1-D differential equations.

Mesh:

100 discretization points with a cosine distribution (clustered near the upper and lower walls) ensures grid independence.

Turbulence models:

The (k, ϵ) model with the standard set of constants [Launder and Sharma, Letters in Heat and Mass Transfer, Vol. 1, 1974].

Near-wall treatment:

Low-Reynolds-number form of the (k, ϵ) model in two versions:

- 1) Launder and Sharma (Ibid.)
 - 2) Yang and Shi [AIAA J., Vol. 31, 1993]
-

Related publications/reports:

DESCRIPTION OF NUMERICAL METHODOLOGY FOR TEST CASE 1C
"Developing flow"

Originators:

Jean-Bernard CAZALBOU and Florence TORRES.

Affiliation:

ENSICA, Département de Mécanique de Fluides,
49 avenue Leon Blum, 31056 TOULOUSE Cedex.

General description:

A code solving the compressible two-dimensional mass-weighted averaged Navier-Stokes equations is used to generate results in Case 1C. The numerical method is based on a finite volume formulation of the explicit implicit Mac Cormack scheme, which is second order accurate in time and space. At each time step, forward or backward approximations are used for the inviscid terms whereas viscous terms are centered. The implicit operator implemented leads to the inversion of a block-matrix which is performed by a line Gauss-Seidel relaxation technique.

Calculations are performed at $Re_w = U_w \delta \rho / \mu = 4000$, with $U_w = 30\text{m/s}$ and $\delta = 7.5\text{mm}$. The initial conditions assumed a uniform flow at Mach number 0.10 with pressure and temperature set everywhere. The initial temperature equals 225K and μ is calculated with the Sutherland's law. It was necessary to adopt such values for the different parameters in order to perform the calculations with a compressible code, we believe that the low value retained for the Mach number allows a valid comparison with experimental data.

Convection scheme:

Mac Cormack's predictor-corrector scheme implemented with the flux splitting procedure of Steger and Warming [AIAA Paper 81-0110, St Louis Missouri, 1981].

Mesh:

The grid used is orthogonal and contains (52,102) points in (x, y) evenly spaced in the x -direction and following a cosine distribution in y , (non-Cartesian grid).

Turbulence models:

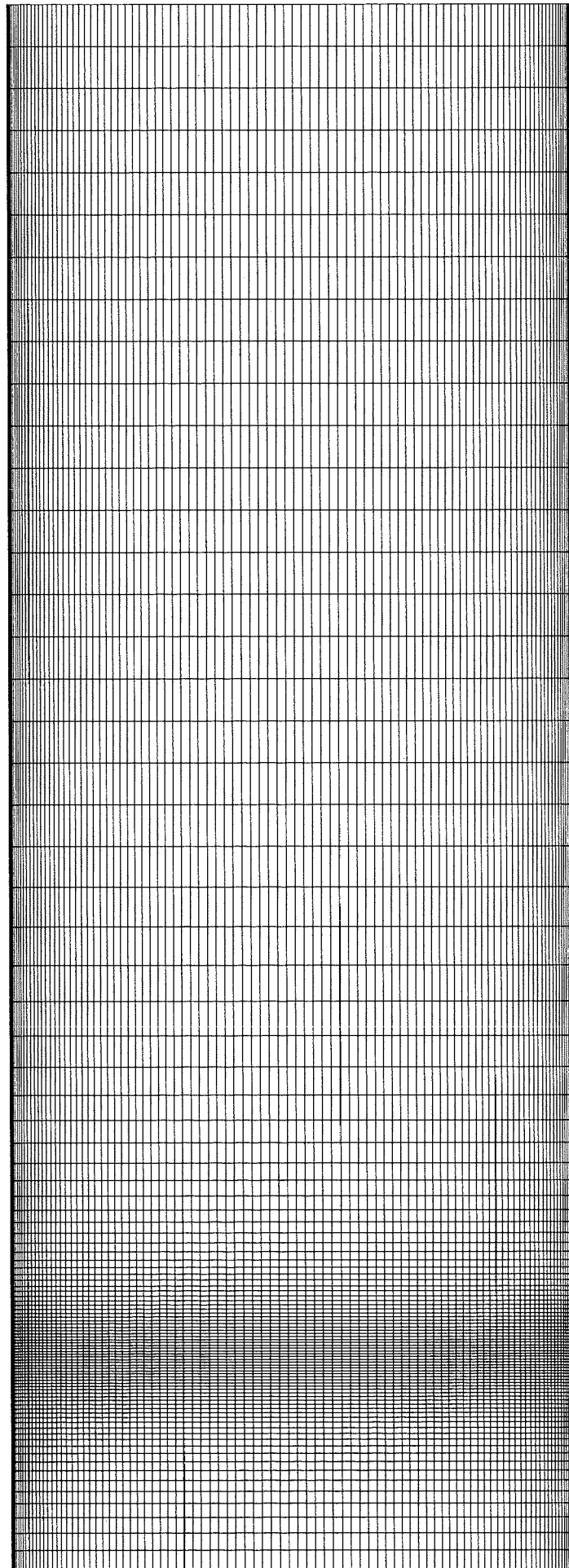
The (k, ϵ) model with the standard set of constants [Launder and Sharma, Letters in Heat and Mass Transfer, Vol. 1, 1974].

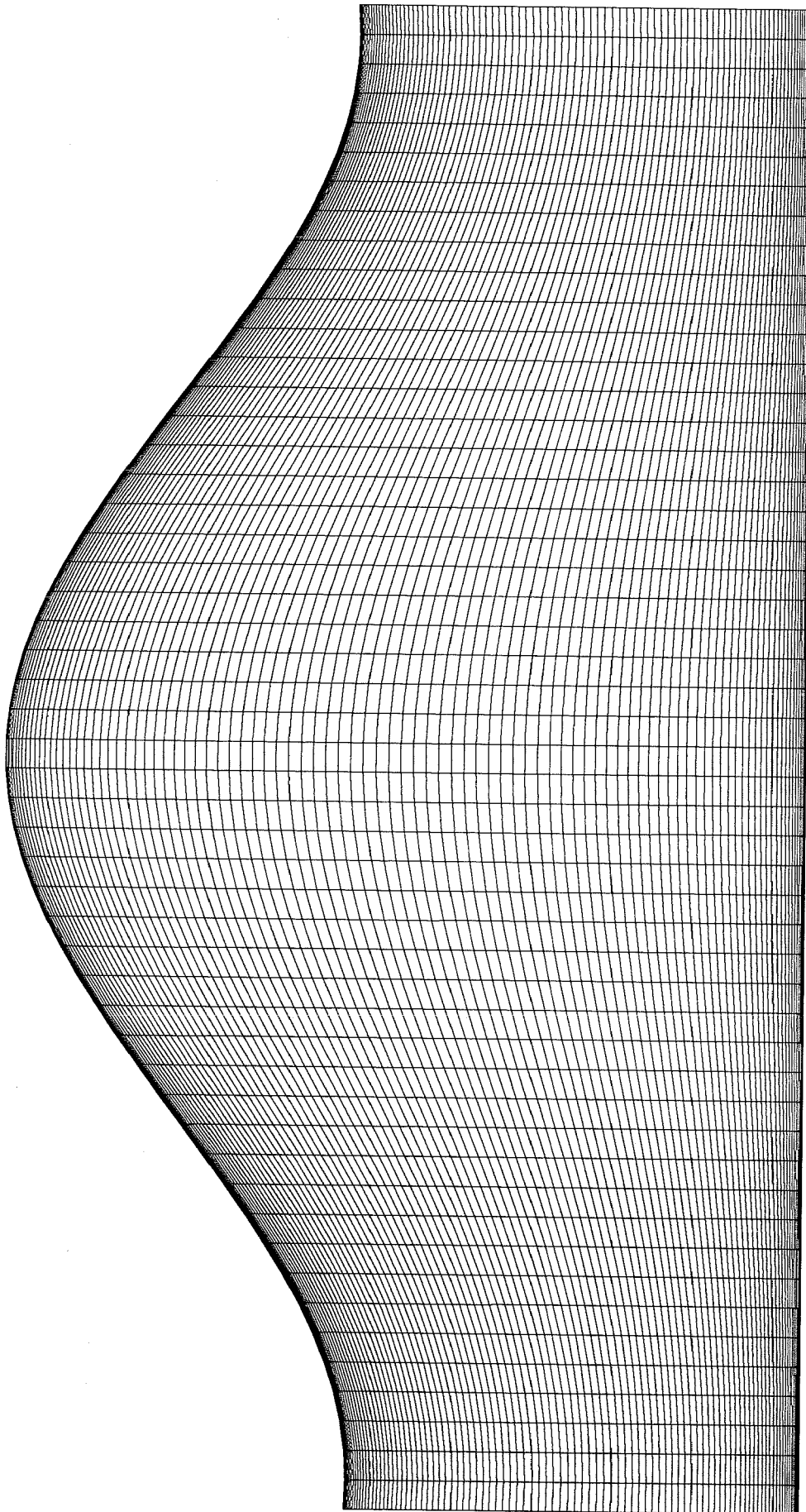
Near-wall treatment:

Low-Reynolds-number version of the (k, ϵ) model according to Launder and Sharma (Ibid.)

Related publications/reports:

F. PAVIE-TORRES, J.-B. CAZALBOU, A. KOURTA, H. HAMINH "Numerical study of heat transfer for unsteady viscous supersonic blunt body flows", Proceedings of the fifth International Symposium on Numerical Methods in Engineering, Lausanne, Sept. 1989, Springer Verlag, Vol. 1, p.595-600.





DESCRIPTION OF NUMERICAL METHODOLOGY FOR TEST CASE 2

Originator: T. Jongen & Y. Marx

Affiliation: EPFL-IMHEF

General description:

Finite-volume method/ Cell-centered / Artificial compressibility method Fully implicit / ADI method for the implicit step Nine-points molecule for the diffusive terms

Convection scheme:

High order upwind (Roe scheme + kappa scheme)

Mesh:

85x100 points, made of trapezoids.

Bottom: 1st point $y/h_{\max}=1.09e-3$ (cell-center)

Top : 1st point $y/h_{\max}=6.23e-3$ (cell-center)

Towards the center of the domain: geometrical progression of ratio 1.07 (top) and 1.08 (bottom)

Turbulence models:

Low Reynolds formulation of the k-epsilon turbulence model. The k-epsilon equations are solved every iupdate steps for the momentum equations. (here, iupdate=2) The equations for k and for epsilon are treated in a coupled fashion. All the terms are treated implicitly. The ADI method is used to solve the linear systems

Near-wall treatment:

Combination of Lam_Bremhorst damping functions and the ones proposed by C.G. Speciale and al. in "A Critical Evaluation of Two Equations Models for Near Wall Turbulence", AIAA 90-1481:

$$f_{\mu}=(1+3.45/\sqrt{\text{Re}_t})\cdot\tanh(y^+/70)$$

$$f_1=(1+0.05/f_{\mu})^2$$

$$f_2=(1-2/9\cdot\exp(-\text{Re}_t^2/36))\cdot(1-\exp(-y^+/4.9))$$

$$\text{and } \text{Re}_t=k^2/\nu/\epsilon$$

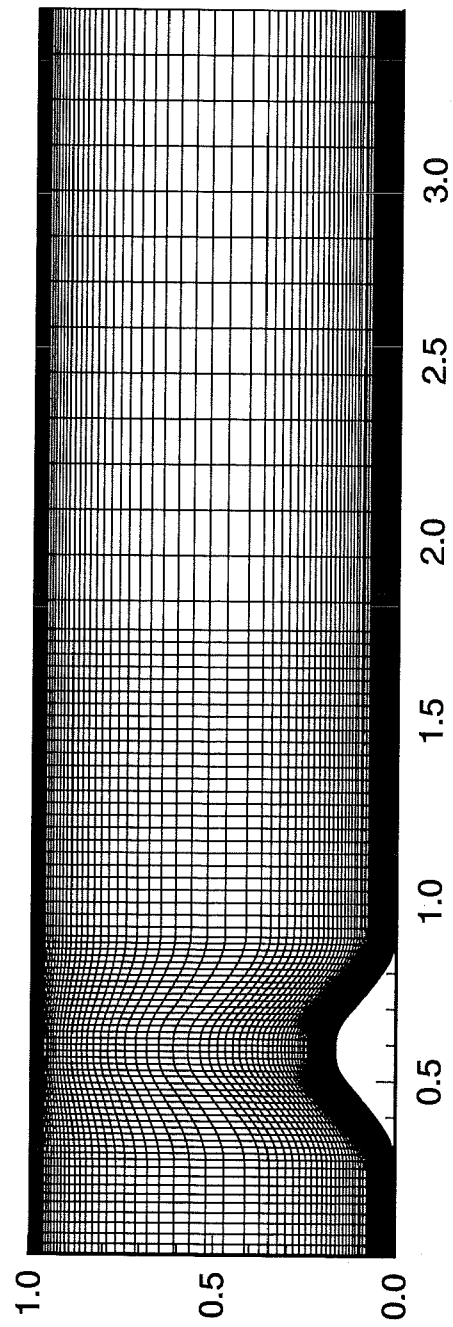
Related publications/reports:

Yves P. Marx, "Time integration schemes for the unsteady incompressible Navier- Stokes equations", Journal of Comput. Phys., Vol. 112, No. 1, May 1994.

contributor: T.Jongen

code: Sagarmatha

k-epsilon model, low Reynolds formulation



DESCRIPTION OF NUMERICAL METHODOLOGY FOR TEST CASE 1

Originator: Vahe' Haroutunian

Affiliation: Fluid Dynamics International
500 Davis Street, Suite 600
Evanston, IL 60201, USA

General description:

Computations are performed with the general purpose finite element CFD code FIDAP. FIDAP employs a range of solution algorithms and linear equation solvers. Turbulence modeling capabilities are primarily based on two-equation models. The two-equation models in the current version of FIDAP include: the standard k - ϵ model of Launder and Spalding (1974), the extended k - ϵ model of Chen and Kim (1987), the RNG k - ϵ model of Yakhot et al (1992), an anisotropic version of the standard k - ϵ model (1995) and Wilcox's k - ω model (1988). These two-equation models may be used in conjunction with one of three available eddy-viscosity models. These are: the linear (isotropic) Boussinesq EVM, the nonlinear (anisotropic) EVM of Speziale (1987) and the nonlinear (anisotropic) EVM of Craft et al (1993). The four k - ϵ model variants in FIDAP are of the high- Re type and are used with a two-layer near-wall model. Wilcox's k - ω model is a low- Re model and does not require the use of a near-wall model. Wilcox's model is primarily intended for use in internal flows at low Reynolds numbers (say, $Re < 10,000$). The near-wall model in FIDAP is a finite element implementation of a two-layer approach. This consists of a single layer of specialized finite elements which fully contains the viscous sub-layers. Specialized shape functions based on the universal near-wall flow profiles are used to accurately resolve the flow profiles. van Driest's low- Re mixing-length model is used to predict the variation of the turbulent viscosity in the layer of special elements. This near-wall model is fully described by Haroutunian and Engelman (1991). A segregated solution algorithm is used to solve the discretized flow equations resulting from case 1. The algorithm which is a consistent finite element implementation of the SIMPLER algorithm is fully described by Haroutunian et al (1993). The systems of linear equations resulting from the discretizations can be solved using either a direct Gaussian elimination solver or a choice of conjugate gradient type iterative solvers. Test cases 1a and 1b are simulated only. Owing to the low Reynolds numbers involved Wilcox's k - ω model is used to simulate these examples. Boundary conditions for u , k and ω at the inlet to the computational domain ($x = -0.235$ m) were obtained from a separate 1-D run of fully developed Poiseuille channel flow. The pressure drop was iteratively adjusted to obtain a mean flow velocity of $U_q = 2.3906$ m/s. The velocity profile obtained in this manner compares closely with the experimental velocity profile available at $x = -0.235$ m. For test case 1a, two separate runs were performed to obtain the fully developed 1-D flow at $x = \text{infinity}$. The first case corresponded to the DNS simulation of Kuroda et al where a prescribed normalized pressure gradient of $a = -1.33e-3$ is used. The second case was simulated using $a = -1.18e-3$ which corresponds to the experiments of Corenflos et al. One separate run was performed to obtain the 1-D established Couette flow of case 1-b. The pressure drop was set to zero.

Convection scheme:

A purely streamline upwind scheme is employed. This scheme is described by Hughes and Brooks (1979).

Mesh:

A regular Cartesian grid of 13800 4-node elements is used. 69 elements are placed across the flow and 200 along the flow direction. Grading is applied towards the walls and the $x=0$ location on the bottom wall at which the velocity jump occurs. 30 elements are used between $-0.235 < x < 0$, and 170 elements are used between $0 < x < 1.4$. The $y+$ values of the first grid points removed from the walls are everywhere less than 0.3.

Turbulence models:

Wilcox's k - ω model

Near-wall treatment:

Wilcox's k - ω model used to integrate through viscous sub-layers. The wall boundary condition of ω is applied based on the recommendation of Menter (1993).

Related publications/reports:

Launder and Spalding, (1974), "The Numerical Computation of Turbulent Flows", Comp. in Applied Mech. and Engng., Vol. 3, 269-289.

Chen and Kim, (1987), "Computations of Turbulent Flows Using an Extended k - ϵ Turbulence Closure Model", NASA CR-179204.

Yakhot et al, (1992), "Development of Turbulence Models for Shear Flows by a Double Expansion Technique", Physics of Fluids, A4, 7.

FIDAP 7.5 Update Manual, (1995), Fluid Dynamics Int. Evanston, IL.

Wilcox, (1988), "Reassessment of the Scale-Determining Equation for Advanced Turbulence Models", AIAA Journal, Vol., 26, No. 11.

Speziale, (1987), "On Nonlinear k - l and k - ϵ Models of Turbulence", JFM, Vol. 178.

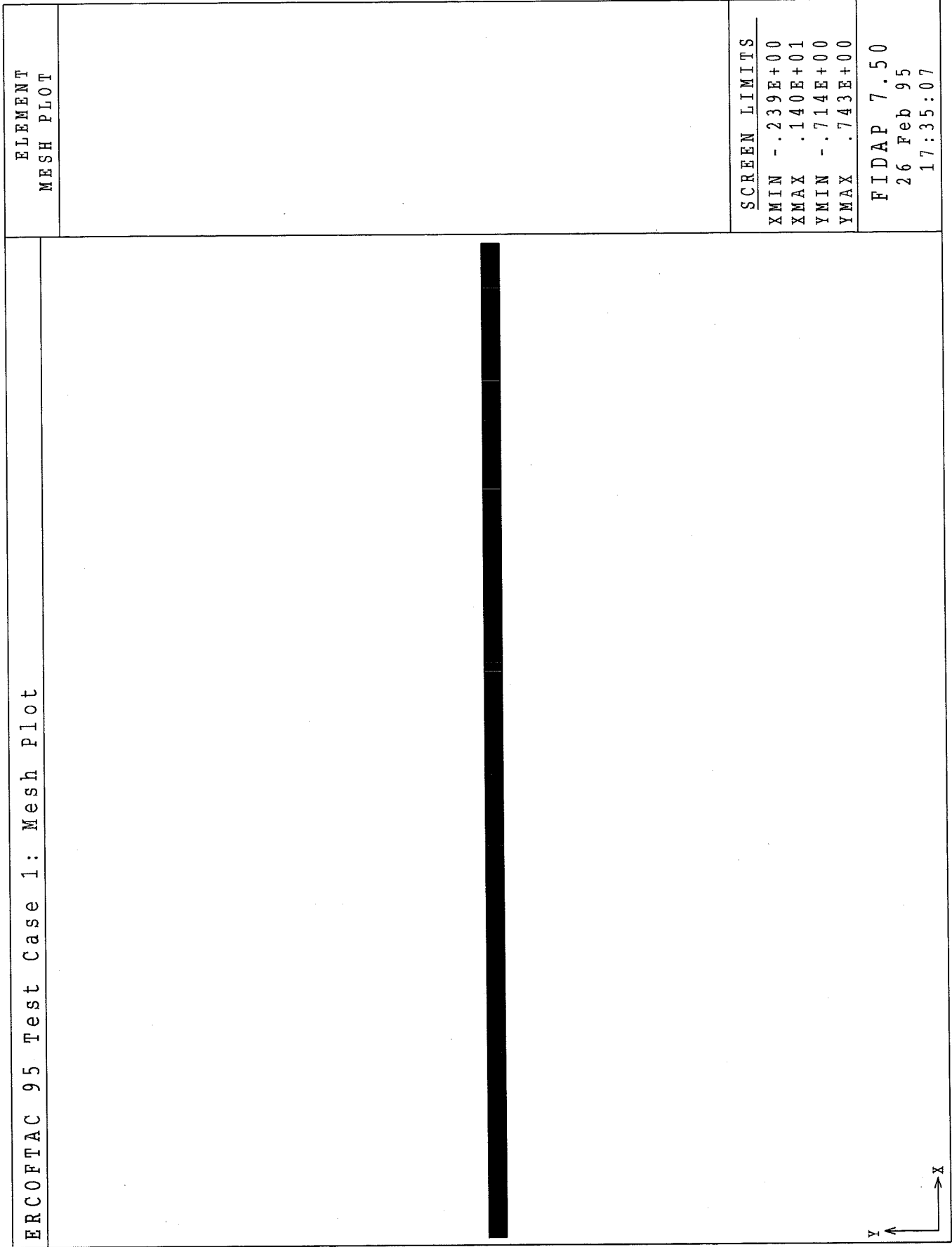
Craft, Launder and Suga (1993), "Extending the Applicability of Eddy Viscosity Models Through the use of Deformation Invariants and Nonlinear Elements", Proc. 5th IAHR Conf. on Refined Flow Modeling and Turbulence Measurements.

Haroutunian and Engelman, (1991), "On Modeling Wall-Bound Turbulent Flows Using Specialized Near-Wall Finite Elements and the Standard k - ϵ Model", Advances in Numerical Simulation of Turbulent Flows, ASME Pub. FED-Vol. 117.

Haroutunian, Engelman and Hasbani, (1993), "Segregated Finite Element Algorithms for the Numerical Solution of Large-Scale Incompressible Flow Problems", Int. J. Numerical Methods in Fluids, Vol 17.

Menter, (1993), "Zonal Two-Equation k - ω Turbulence Models for Aerodynamic Flows", AIAA Paper 93-2906.

Hughes and Brooks, (1979), "A Multidimensional upwind scheme with no cross-wind diffusion", in Finite Element Methods for Advection Dominated Flows, ASME Pub. AMD-Vol. 34.



DESCRIPTION OF NUMERICAL METHODOLOGY FOR TEST CASE 4

Originator: Dr. Vahe' Haroutunian

Affiliation: Fluid Dynamics International
500 Davis Street, Suite 600
Evanston, IL 60201, USA

General description:

Computations are performed with the general purpose finite element CFD code FIDAP. FIDAP employs a range of solution algorithms and linear equation solvers. Turbulence modeling capabilities are primarily based on two-equation models. The two-equation models in the current version of FIDAP include: the standard k-e model of Launder and Spalding (1974), the extended k-e model of Chen and Kim (1987), the RNG k-e model of Yakhot et al (1992), an anisotropic version of the standard k-e model (1995) and Wilcox's k-omega model (1988). These two-equation models may be used in conjunction with one of three available eddy-viscosity models. These are: the linear (isotropic) Boussinesq EVM, the nonlinear (anisotropic) EVM of Speziale (1987) and the nonlinear (anisotropic) EVM of Craft et al (1993). The four k-e model variants in FIDAP are of the high-Re type and are used with a two-layer near-wall model. Wilcox's k-omega model is a low-Re model and does not require the use of a near-wall model. Wilcox's model is primarily intended for use in internal flows at low Reynolds numbers (say, $Re < 10,000$). The near-wall model in FIDAP is a finite element implementation of a two-layer approach. This consists of a single layer of specialized finite elements which fully contains the viscous sub-layers. Specialized shape functions based on the universal near-wall flow profiles are used to accurately resolve the flow profiles. van Driest's low-Re mixing-length model is used to predict the variation of the turbulent viscosity in the layer of special elements. This near-wall model is fully described by Haroutunian and Engelman (1991). A segregated solution algorithm is used to solve the discretized flow equations resulting from case 1. The algorithm which is a consistent finite element implementation of the SIMPLER algorithm is fully described by Haroutunian et al (1993). The systems of linear equations resulting from the discretizations can be solved using either a direct Gaussian elimination solver or a choice of conjugate gradient type iterative solvers. Two simulations of test case 4 were performed using the standard k-e and the extended k-e models, respectively. The near-wall model was employed in both simulations.

Convection scheme:

A purely streamline upwind scheme is employed. This scheme is described by Hughes and Brooks (1979).

Mesh:

A non-regular mesh comprising of 114686 nodes is constructed using 8-node brick elements. Grading is applied towards the wing and body surfaces.

Turbulence models:

The standard and extended k-e models. The extended model in FIDAP employs slightly revised values for model coefficients c_1 and c_3 . Chen and Kim recommend $c_1=1.15$ and $c_3=0.25$. In our testing of this model in FIDAP, we find that $c_1=1.35$ and $c_3=0.05$ gives consistently better results over a wide range of flows. (Chen and Kim's recommended values of c_1 and c_3 produce significantly underdiffuse predictions). The revised values which are the defaults in FIDAP are used in the simulation of test case 4.

Near-wall treatment:

The two-layer near-wall model of FIDAP

Related publications/reports:

Launder and Spalding, (1974), "The Numerical Computation of Turbulent Flows", *Comp. in Applied Mech. and Engng.*, Vol. 3, 269-289.

Chen and Kim, (1987), "Computations of Turbulent Flows Using an Extended k-e Turbulence Closure Model", NASA CR-179204.

Yakhot et al, (1992), "Development of Turbulence Models for Shear Flows by a Double Expansion Technique", *Physics of Fluids*, A4, 7.

FIDAP 7.5 Update Manual, (1995), Fluid Dynamics Int. Evanston, IL.

Wilcox, (1988), "Reassessment of the Scale-Determining Equation for Advanced Turbulence Models", *AIAA Journal*, Vol., 26, No. 11.

Speziale, (1987), "On Nonlinear k-l and k-e Models of Turbulence", *JFM*, Vol. 178.

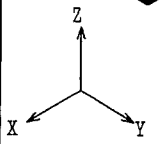
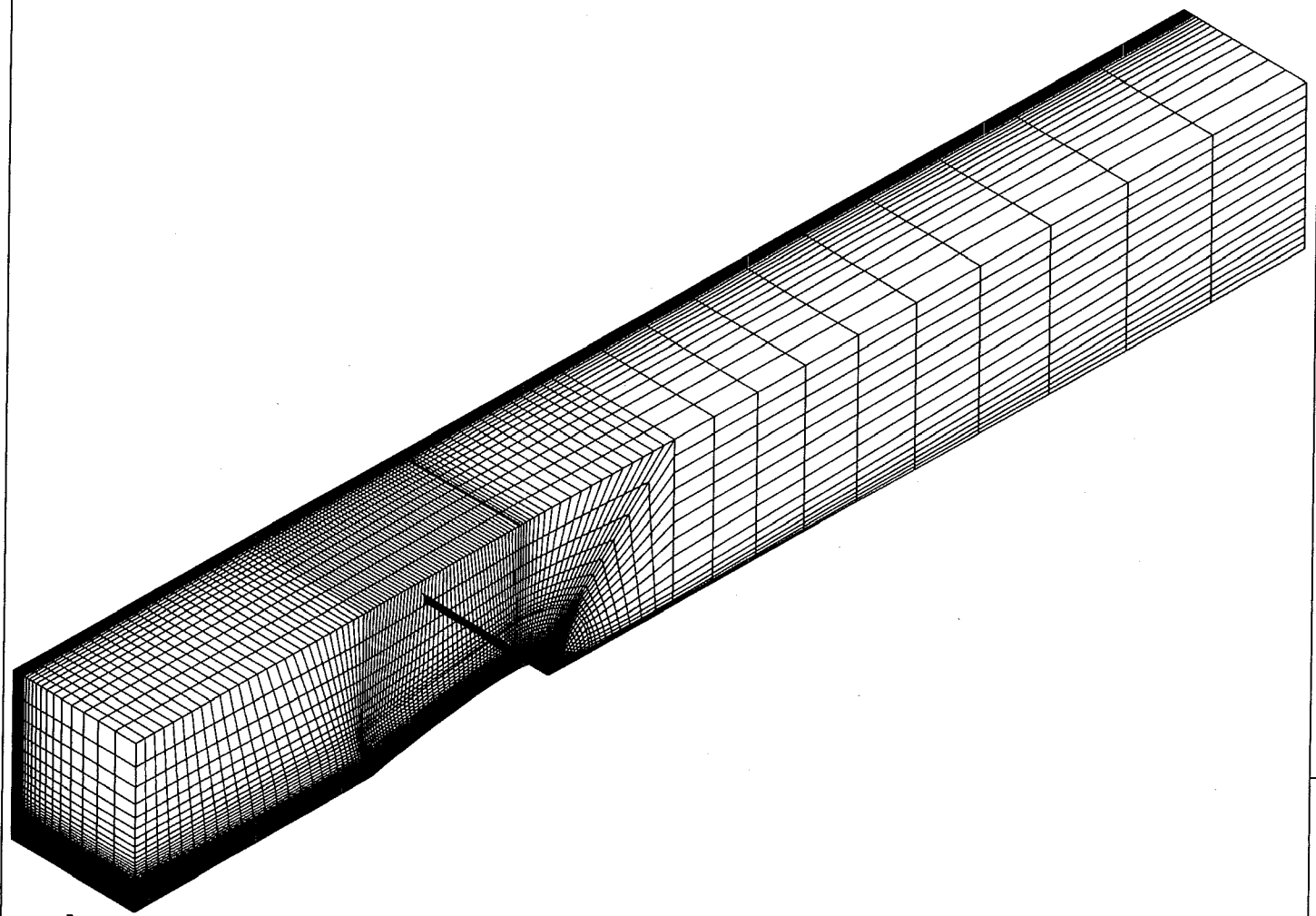
Craft, Launder and Suga (1993), "Extending the Applicability of Eddy Viscosity Models Through the use of Deformation Invariants and Nonlinear Elements", *Proc. 5th IAHR Conf. on Refined Flow Modeling and Turbulence Measurements*.

Haroutunian and Engelman, (1991), "On Modeling Wall-Bound Turbulent Flows Using Specialized Near-Wall Finite Elements and the Standard k-e Model", *Advances in Numerical Simulation of Turbulent Flows*, ASME Pub. FED-Vol. 117.

Haroutunian, Engelman and Hasbani, (1993), "Segregated Finite Element Algorithms for the Numerical Solution of Large-Scale Incompressible Flow Problems", *Int. J. Numerical Methods in Fluids*, Vol 17.

Hughes and Brooks, (1979), "A Multidimensional upwind scheme with no cross-wind diffusion", in *Finite Element Methods for Advection Dominated Flows*, ASME Pub. AMD-Vol. 34.

ERCOFTAC 95 Test Case 4: Mesh Plot



ELEMENT
MESH PLOT

| VIEW DIRECTION | |
|----------------|-----------|
| VX | 0.100E+01 |
| VY | 0.100E+01 |
| VZ | 0.100E+01 |
| ANG | 0.000E+00 |

FIDAP 7.50
26 Feb 95
16:46:25

ERCOFTAC Workshop
CASE 3: SWIRLING BOUNDARY LAYER
IN CONICAL DIFFUSER

Originator & Affiliation:

T.C. Vu GE Hydro
795 George V, Lachine, Quebec, H8S 2S8
vutc@hydro.ge.com
W.Shyy University of Florida, Dept. of Aerospace Eng.,
Mechanics and Eng. Science.
231 Aerospace Bldg., Gainesville, Florida, 32611
wss@tiger.aero.ufl.edu

General description:

The code used for the test case 3 has been developed by the authors to predict 3D flow characteristics and energy losses in hydraulic turbine components: spiral case, distributor (radial cascades), runner (Francis and Kaplan) and draft tube (elbow diffuser). Since the code is used for a wide range of applications, the original k-epsilon turbulence model is adopted.

Convection scheme:

The conservative control volume formulation and the Semi-Implicit Method for Pressure Linked Equations (SIMPLE) algorithm are extended and implemented in a general curvilinear coordinate system. A staggered grid arrangement is adopted for the discretization. Both Cartesian and contravariant velocity components are located at the midpoint of the control volume faces and the pressure is located at the arithmetic center of the volume. The second order upwind scheme, cast in a conservative form, has been adopted for the convection terms, and second order central difference schemes have been applied for all other terms.

Turbulence models:

The original k-epsilon two equation turbulence model is adopted as the closure form. Constants used for the standard k-epsilon model are as follows:

$C_{\mu} = 0.09$
 $C_{\epsilon_1} = 1.44$
 $C_{\epsilon_2} = 1.92$
 $\sigma_k = 1.$
 $\sigma_{\epsilon} = 1.3$

Near-wall treatment:

Wall function

Mesh:

The test case 3 was analysed in 3D with 4 different grid sizes: 23x23x55, 27x27x75, 35x35x75 and 45x45x75. Numerical result obtained with the 35x35x75 grid is presented here (Figure 1).

Three-dimensional, instead of two-dimensional, geometry is used here mainly to assess whether a truly axisymmetric flowfield can be obtained on a stretched quadrilateral mesh system. Since our computations are based on structured grid in all three directions, it is of interest to ensure that, for example, the corner meshes on a circular cross section do not adversely affect the solution accuracy. This issue is practically important. As can be observed from our solutions, the present approach, while costly, has not prevented us from obtaining solutions with poor spatial resolutions. It does help us answer question about both turbulence models and complex geometries.

Inlet condition

The profiles of U and W are specified following Mm-25.dat file and are normalized by $U_0 = 11.6$ m/s. The turbulence kinetic energy is defined as $k = 0.5(u^2 + v^2 + w^2)/3$ where u, v and w are specified in usq-25.dat, vsq-25.dat and wsq-25.dat. The turbulence kinetic energy dissipation at the inlet is calculated as $\epsilon = C_\mu k^{3/2}/0.075$

The profile of V (radial component) is set equal to zero at the inlet for the submitted solution. This assumption is not a realistic one because the specified inlet section is too close to the divergence section ($x = -25$ mm), therefore V can not be zero at this location.

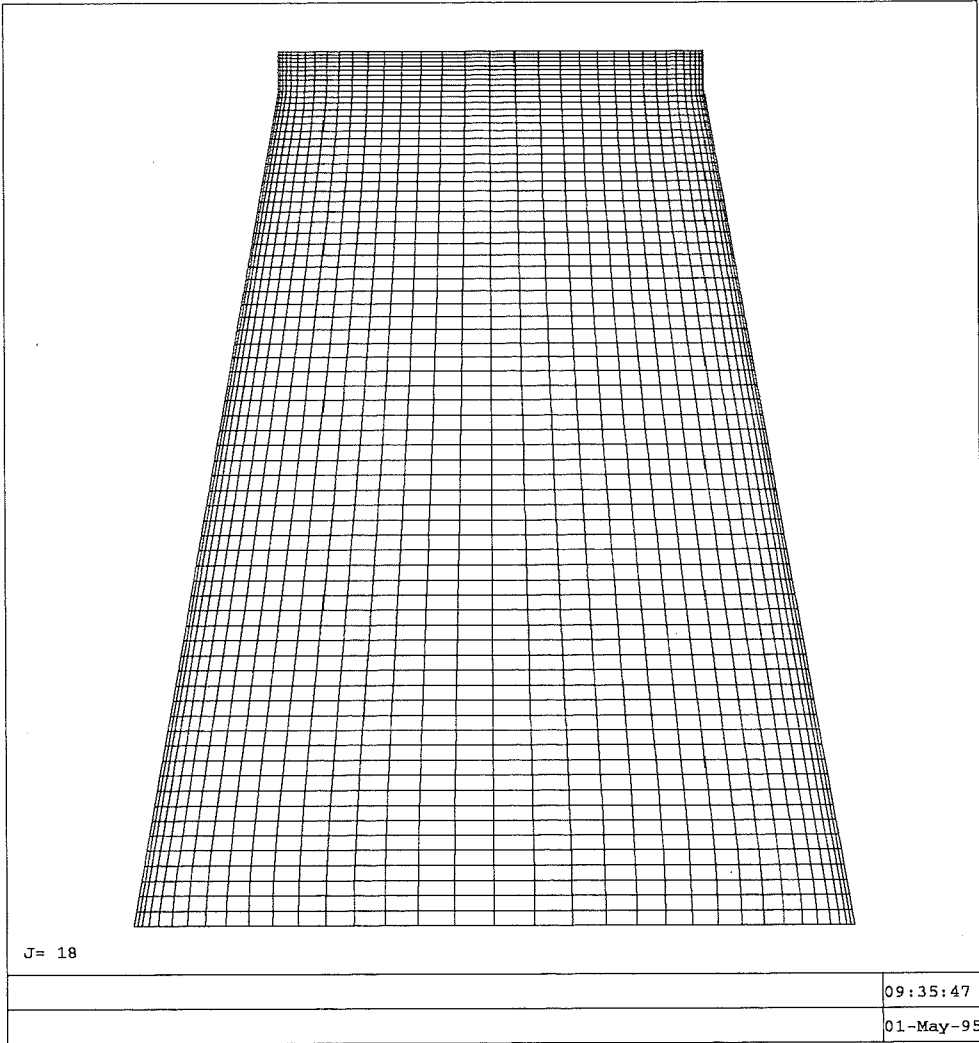
The profile of V can be estimated numerically by the following manner. First, a preliminary flow analysis is performed for the conical diffuser, but the inlet is extended further upstream to $x = -100$ mm where the radial component is specified as zero (Figure2). Then from the preliminary solution, we could determine the radial component profile at $x = -25$ mm for the final flow analysis with the original inlet (Figure3).

Related publications/reports:

- Vu, T.C. and Shyy, W., 1988, "Viscous Flow Analysis for Hydraulic Turbine Draft Tubes.", Proceedings 14th Symposium of the IAHR, Trondheim, Norway, 1988, pp.915-926, also published in the Journal of Fluids Engineering, Vol. 112, 1990, pp.199-206.
- Vu, T.C., Heon, K. and Shyy, W., 1994, "A CFD-based Computer Aided Engineering System for Hydraulic Turbines", Proceedings 17th Symposium of the IAHR, Beijing, China, Vol. 1, pp.329-340.
- Shyy, W., 1994, "Computational Modeling for Fluid Flow and Interfacial Transport", Elsevier, Amsterdam, The Netherlands.
- Braaten, M.E. and Shyy, W., 1986, "A Study of Recirculating Flow Computation using Body-fitted Coordinates: Consistency Aspects and Skewness.", Numerical Heat Transfer, Vol. 9, pp.559-574.
- Shyy, W., Tong, S.S. and Correa, S.M., 1985, "Numerical Recirculating Flow Computation Using Body-Fitted Coordinates", Numerical Heat Transfer, Vol. 8, pp.99-113
- Shyy, W. and Vu, T.C., 1991, "On the Adoption of Velocity Variable and Grid System for Fluid Flow Computation in Curvilinear Coordinates", Journal of Computational Physics, Vol. 92, pp.82-105.

```
| SYSTEME 4DF |  
| BANC D'ESSAI NUMERIQUE |
```

```
MAILLAGE : diffu3v.grid  
dir : /usr/people/thi/diffuser  
Dimension de Maillage = 75 35 35  
J = 18
```



ZOOM IN ? <Y/N>, [N]

Description of Numerical Methodology for Test Case 2

Originator: Dr. Milan Sedlar
 Pump Research Institute of Olomouc
 Kosmonautu 6a, CZ-77223 OLOMOUC

Affiliation: Independent Research Worker
 CFD Branch

General description: NEPTUNE is the finite element based system for the solution of two-dimensional, quasi-three-dimensional and three-dimensional viscous incompressible flow problems, especially in hydromachinery applications. It has been developed in the Pump Research Institute of Olomouc as the entry-level system able to run on personal computers. As a finite element, the quadratic triangle is used for the test case 2. To eliminate the pressure unknown from the system of equations, the penalisation and reduced integration method is applied. The code enables to use both the structured and the unstructured and hybrid grids.

Convection scheme: The nonlinear equations are solved by the successive approximation and under-relaxation. The upwinding method is based on the artificial viscosity operator that is constructed so as to operate in the flow direction only and to eliminate any crosswind artificial diffusion (Sedlar, 1993a, 1993b).

Mesh: Case 2A: the structured non-uniform grid of 3000 (50x30x2) quadratic elements (101x61 nodal points arrangement)
 Case 2B: the structured non-uniform grid of 2340 (39x30x2) quadratic elements (79x61 nodal points arrangement)

Turbulence models: The turbulence is modelled through the high Reynolds k - ϵ model:

$$(\mathbf{u} \cdot \nabla)k = \nabla \cdot \left(\left(\nu + \frac{\nu_t}{\sigma_k} \right) \nabla k \right) + P - \epsilon$$

$$(\mathbf{u} \cdot \nabla)\epsilon = \nabla \cdot \left(\left(\nu + \frac{\nu_t}{\sigma_\epsilon} \right) \nabla \epsilon \right) + \frac{\epsilon}{k} (C_{\epsilon 1} P - C_{\epsilon 2} \epsilon)$$

$$\nu_t = C_\mu \frac{k^2}{\epsilon}, \quad P = \nu_t (\nabla \mathbf{u} + (\nabla \mathbf{u})^*) \cdot \nabla \mathbf{u}$$

$$C_\mu = 0.09, \quad \sigma_k = 1.0, \quad \sigma_\epsilon = 1.3, \quad C_{\epsilon 1} = 1.44, \quad C_{\epsilon 2} = 1.92$$

To predict better eddy viscosity distribution in the separation region, the Goldberg's model for separated flows can be used (Goldberg, 1992).

Another turbulence model used in this study is the nonlinear k - ϵ model of Speziale (Speziale, 1987). The simple form for

two-dimensional flow (Acharya et al., 1994) has been adopted in the test case 2.

Near-wall treatment: wall functions

$$\frac{u}{u_{\tau}} = y_0^+ \quad \text{for } y_0^+ < 12$$

$$\frac{u}{u_{\tau}} = \frac{1}{\kappa} \ln(Ey_0^+) \quad \text{for } y_0^+ > 12, \quad E = 9, \quad \kappa = 0.4$$

$$k_0 = \frac{u_{\tau}^2}{\sqrt{C_{\mu}}}, \quad \varepsilon_0 = \frac{u_{\tau}^3}{\kappa y_0}$$

$$y^+ = \frac{yu_{\tau}}{\nu}, \quad u_{\tau} = \sqrt{\tau_w/\rho}$$

Inlet boundary conditions:

mean velocity in x direction \bar{U} ...from the experimental data

mean velocity in y direction \bar{V} ...zero value

turbulent kinetic energy kfrom the experimental data

$$(k = (\overline{u'u'} + \overline{v'v'})/2)$$

dissipation rate ε $\varepsilon = k^{3/2} C_{\mu}^{3/4} / l_m$

$$l_m = \kappa y \quad \text{for } y \leq C_{\mu} \delta / \kappa$$

$$l_m = C_{\mu} \delta \quad \text{for } y > C_{\mu} \delta / \kappa$$

Related publications/reports:

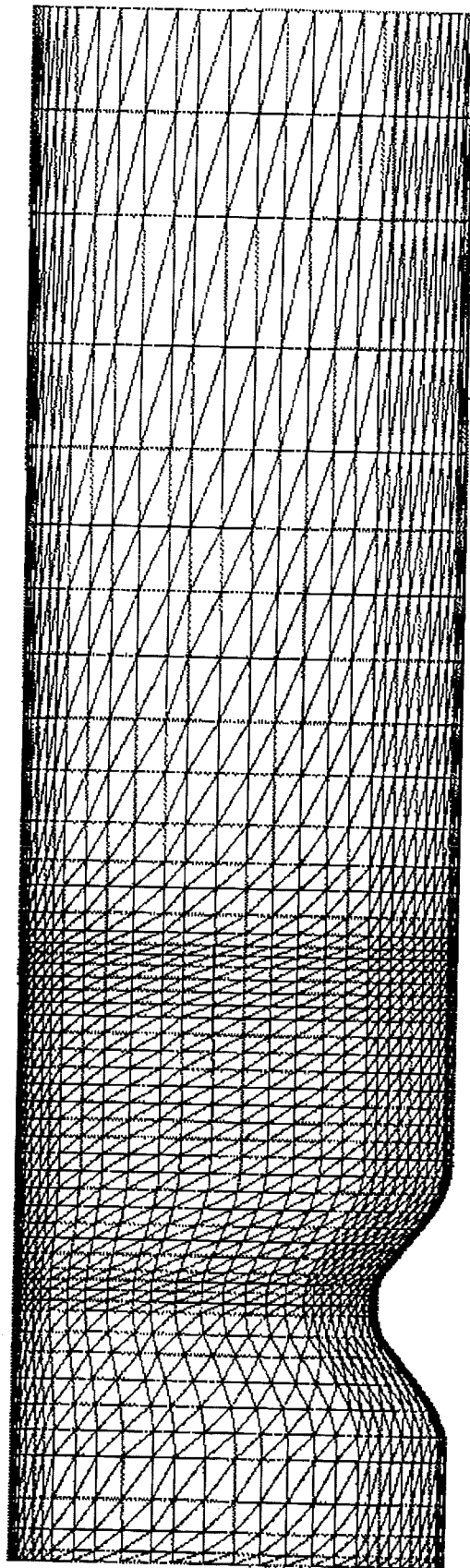
Acharya, S., Dutta, S., Myrum, T.A., Baker, R.S., 1994, "Turbulent Flow Past a Surface-Mounted Two-Dimensional Rib". Journ. Fluids Engng., Vol. 116, pp. 238-246.

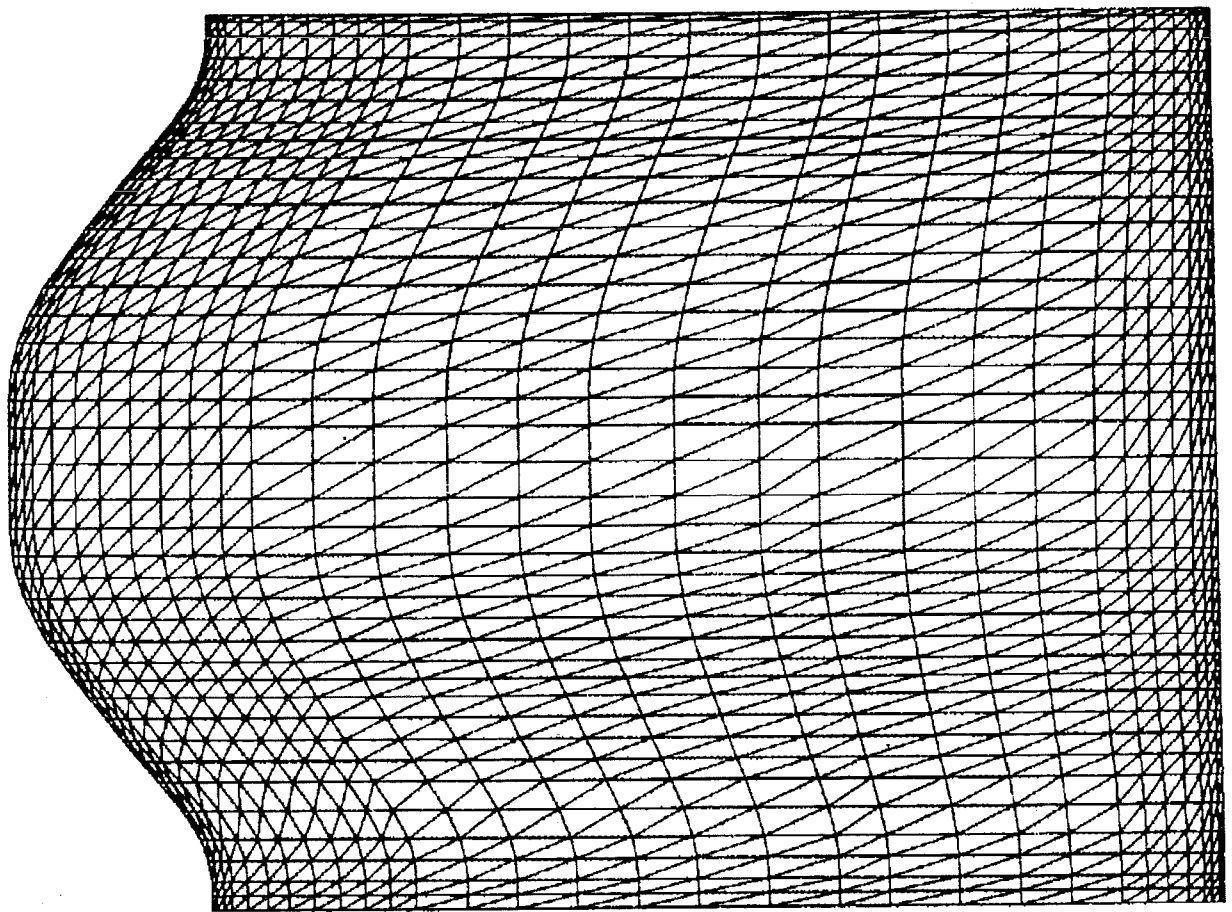
Goldberg, U.C., 1992, "A Near-Wall Model for Separated Turbulent Flows". Journ. Fluids Engng., Vol. 114, pp. 694-697.

Sedlar, M., 1993a, "Calculation of Quasi-Three-Dimensional Incompressible Viscous Flows by the Finite Element Method". Journ. Num. Meth. Fluids, Vol. 16, pp. 953-966.

Sedlar, M., 1993b, "Using Quasi-Three-Dimensional Viscous Flow Modeling in Pump Design". Proc. 8th Int. Conf. Numerical Methods in Laminar and Turbulent Flow, Swansea, pp. 924-934.

Speziale, C.G., 1987, "On Nonlinear k-l and k-eps Models of Turbulence". Journ. Fluid Mech., Vol. 178, pp. 459-475.





DESCRIPTION OF NUMERICAL METHODOLOGY FOR TEST CASE 2.

Originator: Pieter Blom* and Robert Booij**

Affiliation:

* Hokkaido River Disaster Prevention Research Center
S-1, W-1, Chuo-ku, 2nd Yuraku Bldg.
Sapporo City, Hokkaido, Japan, 060

** Department of Civil Engineering
Delft University of Technology
P.O. Box 5048, 2600 GA Delft
The Netherlands

General description:

The calculations were made using the PHOENICS flow-simulation software, PC version 2.1, of CHAM Limited. PHOENICS is a computer code which simulates fluid-flow, heat-transfer, chemical-reaction and related phenomena. It is a 3D finite-volume system that solves convection-diffusion equations. It is equipped to be used for two-phase flow while up to 50 dependent variables can be solved. PHOENICS solves sets of algebraic equations which represent the consequences of integrating the differential equation over the finite-volume of a computational cell and over a finite-time and approximating the resulting volume, area and time by way of interpolation assumptions.

Convection scheme:

The default interpolation assumption is the "fully-implicit upwind" scheme. This implies that:

In time-dependent terms, all fluid properties are presumed to be independent of position within the cell.

In the convection term, all fluid properties are uniform over cell faces; "new" values are supposed to prevail throughout the time interval; and the values prevailing at the cell face are those at the nearest grid node on the 'upwind' side of the face.

In diffusion terms, the property gradients and the transport properties are uniform over cell faces; "new" values are supposed to prevail throughout the time interval; the gradients are based on the supposition that the properties vary linearly, and the transport properties are arithmetic averaged of those on either side of the cell faces.

In source terms, the nodal values are supposed to prevail over the cell volume; "new" values are supposed to prevail throughout the time interval.

Mesh:

Case 2a, Staggered grid, 480*50 elements.

Case 2b, Staggered grid, 180*50 elements. To avoid influence of the outflow boundary at the location $x = 126$ mm, the outflow boundary is located half way the 8th and 9th hill.

Calculation time:

Case 2a, 8 hours on Compaq Pentium 66 MHz

Case 2b, 24 hours on Compaq Pentium 66 MHz

Turbulence models:

Standard k-epsilon turbulence model

Coefficients: Von Karman coefficient = 0.41

$C_{\mu} = 0.5478$

$C_d = 0.1643$

$C_{\mu cd} = C_{\mu} * C_d$

C1e = 1.44
C2e = 1.92

Near-wall treatment:

BOTTOM: "Law of the wall" to calculate the friction velocity.

$U_{\tau f} = (u_1 * Karman) / (\log(d_1/z_0) - 1)$ with u_1 velocity in element closest to the wall, d_1 height of element closest to the wall, z_0 roughness length.

- Source term in momentum equation in flow direction to simulate the friction.

$S = U_{\tau f} * \text{abs}(U_{\tau f}) * \rho$, ρ is the density.

- Prescribed values for the turbulence energy and the dissipation.

$k = (U_{\tau f}^2) / (C_{\mu} * d^{.5})$

$\epsilon = (U_{\tau f}^3) / (Karman * z)$

WATER SURFACE:

- Symmetry condition for the turbulence energy.

$dk/dz = 0$.

- Prescribed value for the dissipation to counteract large length scales near the water surface.

$\epsilon = (C_{\mu} * d^{.75} * k^{1.5}) / (Karman * (z + 0.07 * h))$ z is the vertical coordinate and h is the water depth.

- Adaptation of the rigid water surface, by iterative calculations of the new water level.

$\Delta D = \Delta p / (\rho * g)$, ΔD is rise of the water surface, Δp is the excess pressure with respect to pressure in the inflow element at the rigid lid, and g the gravitational acceleration.

Apart from the adaptation of the surface a source term has to be introduced to simulate the hydrostatic pressure due to the rise of the water: $S = \rho * g * \Delta D$.

For Case 2a as well as for Case 2b at both walls the BOTTOM near-wall treatment is used.

Inflow condition:

Case 2a

- Velocity: measured velocity profile

- k : measured velocity profile

- ϵ : calculated from an assumed parabolic eddy-viscosity profile,
 $\epsilon = (C_{\mu} * k^2) / \text{viscosity}$, with the
 $\text{viscosity} = (U_{\tau f} * Karman * z * (1 - z / h))$

Case 2b

- Velocity, k and ϵ of the location $x = 126$ mm. 7 calculations were made, the 7th calculation is presented.

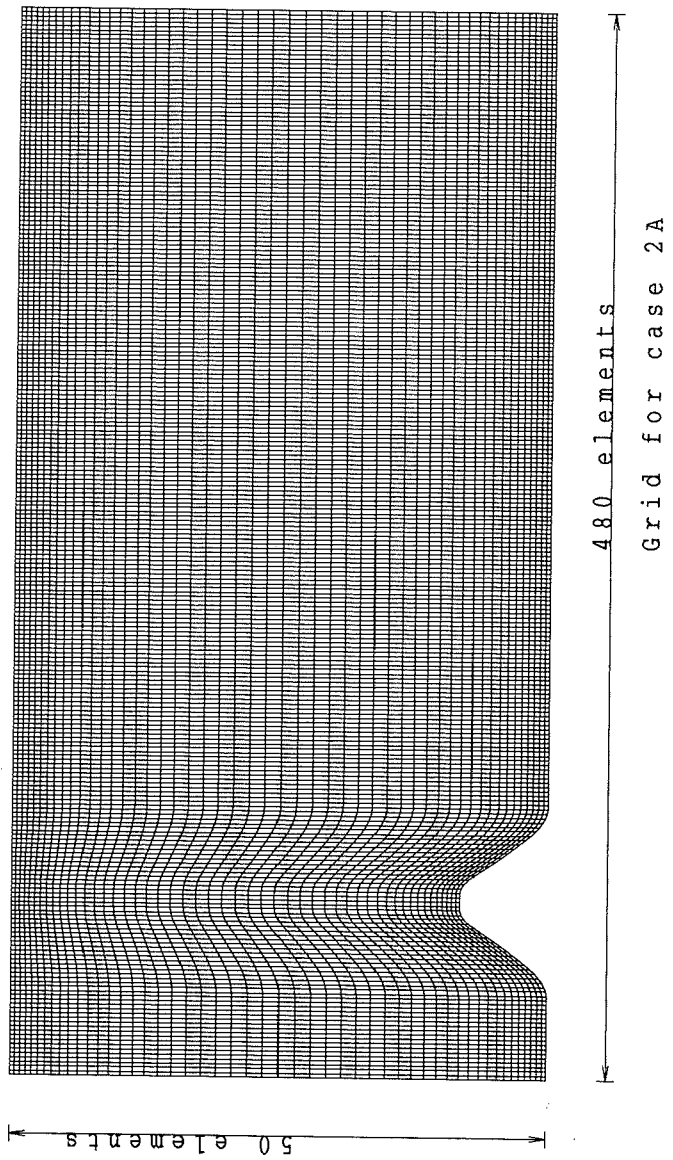
Related publications/reports:

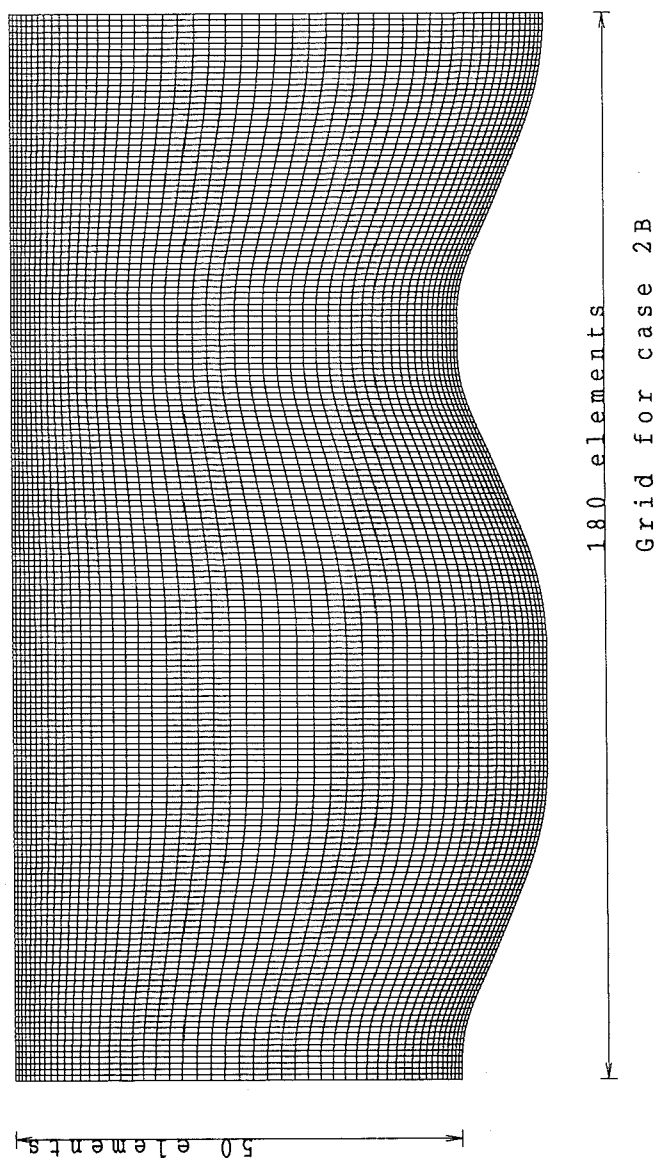
P. Blom, "Turbulent flow over a sill", Proceedings XXIV IAHR congress Madrid, 1991.

P. Blom, "Turbulent free-surface flow over sill", Ph. D-thesis Delft University of Technology, Faculty of Civil Engineering, Communication on hydraulic and geometrical engineering 93-1, 1993

P. Blom, R. Booij, J.A. Battjes, "Turbulent free-surface flow over a sill", Proceedings Second National Mechanics Congress Kerkrade, Kluwer Academic Publishers, 1993.

P. Blom and R. Booij, "Turbulent free-surface flow over sills", submitted for publication in Journal of Hydraulic Research.





DESCRIPTION OF NUMERICAL METHODOLOGY FOR TEST CASE 3

Originator:

Dipl.-Ing. Jochen Gier, Dipl.-Ing. Uwe Krueger

Affiliation: Institut fuer Dampf- und Gasturbinen,
RWTH Aachen
Direktor: Univ. Prof. Dr.-Ing. D. Bohn

General description:

Program FLOW3D. Fully implicit, structured finite volume scheme for body-fitted, multiblock meshes. SIMPLEC pressure correction (Van Doormal and Raithby) algorithm on non-staggered grid together with improved Rhie-Chow interpolation method to avoid checkerboard oscillations. Central differencing for diffusion terms.

Inlet Conditions:

Given physical information was used for the inlet boundary condition including the turbulence quantities. For determination of epsilon the following relationship was employed:
 $\epsilon = k^{1.5} / ((CMU^{0.75}) * (D * 0.01))$ with $CMU = 0.09$, $D = 0.26$

Convection scheme:

Higher-order upwind differencing

Mesh:

Algebraically generated mesh with appropriate refinement near the wall. (Cylindrical coordinate system)

Turbulence models:

Algebraic Reynolds Stress Model (Clarke, D.S. and Wilkes, N.S. (1987), 'Turbulent flow predictions using Algebraic stress models', AERE-R 12694) (based on work at UMIST by Launder)

Near-wall treatment:

One layer logarithmic velocity profile

Related publications/reports:

Van Doormal, J.P. and Raithby, G.D. (1984), "Enhancements of the SIMPLE method for predicting incompressible fluid flows", Numer. Heat Transfer, 7 pp 147-163

Thompson, C.P. and Wilkes, N.S. (1982), "Experiments with Higher-Order Finite Difference Formulae", AERE-R 10493

DESCRIPTION OF NUMERICAL METHODOLOGY FOR TEST CASE 3

Originator:

Dipl.-Ing. Jochen Gier, Dipl.-Ing. Uwe Krueger

Affiliation: Institut fuer Dampf- und Gasturbinen,
RWTH Aachen

Direktor: Univ. Prof. Dr.-Ing. D. Bohn

General description:

Program FLOW3D. Fully implicit, structured finite volume scheme for body-fitted, multiblock meshes. SIMPLEC pressure correction (Van Doormal and Raithby) algorithm on non-staggered grid together with improved Rhie-Chow interpolation method to avoid checkerboard oscillations. Central differencing for diffusion terms.

Inlet Conditions:

Given physical information was used for the inlet boundary condition including the turbulence quantities. For determination of epsilon the following relationship was employed:
 $\epsilon = k^{1.5} / ((CMU^{0.75}) * (D * 0.01))$ with $CMU = 0.09$, $D = 0.26$

Convection scheme:

Higher-order upwind differencing

Mesh:

Algebraically generated mesh with appropriate refinement near the wall. (Cylindrical coordinate system)

Turbulence models:

Differential Reynolds Stress Model (Clarke, D.S. and Wilkes, N.S. (1989), 'The calculation of turbulent flows in complex geometries using a Differential Stress Model', AERE-R 13428)

(Launder, Reece, Rodi (1975) 'Progress in the development of a Reynolds Stress Turbulence Closure', J. Fluid Mech.)

Near-wall treatment:

One layer logarithmic velocity profile

Related publications/reports:

Van Doormal, J.P. and Raithby, G.D. (1984), "Enhancements of the SIMPLE method for predicting incompressible fluid flows", Numer. Heat Transfer, 7 pp 147-163

Thompson, C.P. and Wilkes, N.S. (1982), "Experiments with Higher-Order Finite Difference Formulae", AERE-R 10493

DESCRIPTION OF NUMERICAL METHODOLOGY FOR TEST CASE 3

Originator:

Dipl.-Ing. Jochen Gier, Dipl.-Ing. Uwe Krueger

Affiliation: Institut fuer Dampf- und Gasturbinen,
RWTH Aachen
Direktor: Univ. Prof. Dr.-Ing. D. Bohn

General description:

Program FLOW3D. Fully implicit, structured finite volume scheme for body-fitted, multiblock meshes. SIMPLEC pressure correction (Van Doormal and Raithby) algorithm on non-staggered grid together with improved Rhie-Chow interpolation method to avoid checkerboard oscillations. Central differencing for diffusion terms.

Inlet Conditions:

Given physical information was used for the inlet boundary condition including the turbulence quantities. For determination of epsilon the following relationship was employed:
 $\epsilon = k^{1.5} / ((CMU^{0.75}) * (D * 0.01))$ with $CMU = 0.09$, $D = 0.26$

Convection scheme:

Higher-order upwind differencing

Mesh:

Algebraically generated mesh with appropriate refinement near the wall. (Cylindrical coordinate system)

Turbulence models:

RNG k-epsilon model Modification of standard k-epsilon model, derived from a renormalization group analysis of the Navier-Stokes equations.

Constants:

CMU 0.09
C1 1.42
C2 1.68
BETA 0.015
ETA0 4.38

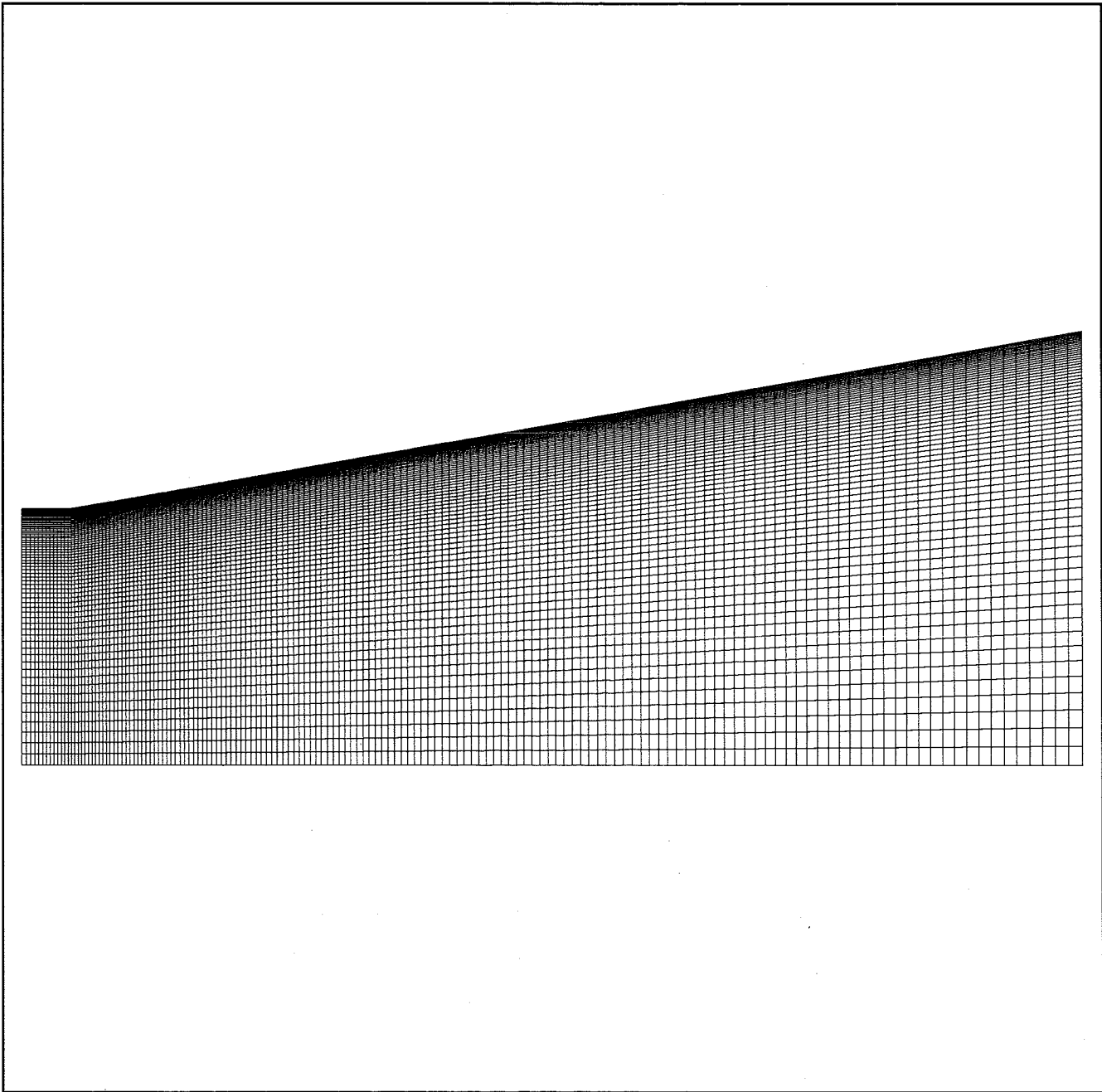
Near-wall treatment:

One layer logarithmic velocity profile

Related publications/reports:

Van Doormal, J.P. and Raithby, G.D. (1984), "Enhancements of the SIMPLE method for predicting incompressible fluid flows", Numer. Heat Transfer, 7 pp 147-163

Thompson, C.P. and Wilkes, N.S. (1982), "Experiments with Higher-Order Finite Difference Formulae", AERE-R 10493



DESCRIPTION OF NUMERICAL METHODOLOGY FOR TEST CASE 3

Originators: Charles Hirsch and Andrei E. Khodak

Affiliation: Department of Fluid Mechanics
Vrije Univeriteit Brussel, B-1050 Brussels, Belgium

General description:

Full Reynolds averaged Navier–Stokes computations were performed with the three–dimensional Navier–Stokes solver EURANUS (EUropean Aerodynamic NUmerical Simulator) Equations are formulated in generalized non–orthogonal coordinates for Cartesian velocity components This code has essentially a compressible time–marching formulation with Runge–Kutta time integration. The low–Mach– number computations apply a preconditioning technique with an artificial compressibility approach.

Convection scheme:

Central schemes with fourth order numerical dissipation

Mesh:

64x32 non–orthogonal. Unknown parameters are placed in the cell centers

Turbulence models:

Standard high–Reynolds–number turbulent kinetic energy – dissipation rate turbulence model. Original constants

Near–wall treatment:

Wall functions: velocity field is connected with a log–law dependence near the wall. Von Karman constant 0.42, $E=9.0$. Friction velocity is obtained from the solution of the transcendental equation for the velocity in the center of the first inner cell. Turbulent kinetic energy and dissipation rate are imposed in the center of the first inner cell according to the standard formulas.

Inlet conditions:

Experimental data for streamwise and swirl velocities and turbulent kinetic energy. Radial velocity equal zero. Dissipation rate is obtained from three–layer approach as described in Hirsch and Khodak (1995).

Related publications/reports:

Hirsch Ch., and Khodak A., 1995 "Modeling of Complex Internal Flows with Reynolds Stress Algebraic Equation Model" AIAA Paper 95–2246

DESCRIPTION OF NUMERICAL METHODOLOGY FOR TEST CASE 3

Originators:

Charles Hirsch and Andrei E. Khodak

Affiliation:

Department of Fluid Mechanics Vrije Univeriteit Brussel, B-1050 Brussels, Belgium

General description:

Full Reynolds averaged Navier–Stokes computations were performed with the three–dimensional Navier–Stokes solver EURANUS (EUropean Aerodynamic NUmerical Simulator) Equations are formulated in generalized non–orthogonal coordinates for Cartesian velocity components This code has essentially a compressible time–marching formulation with Runge–Kutta time integration. The low–Mach– number computations apply a preconditioning technique with an artificial compressibility approach.

Convection scheme:

Central schemes with fourth order numerical dissipation

Mesh:

64x32 non–orthogonal. Unknown parameters are placed in the cell centers

Turbulence models:

Reynolds stress algebraic equation model or non–linear turbulent kinetic energy – dissipation rate turbulence model (Shih, Zhu, and Lumley, 1994) Original constants except $A1=4$.

Near–wall treatment:

Wall functions: velocity field is connected with a log–law dependence near the wall. Von Karman constant 0.42, $E=9.0$. Friction velocity is obtained from the solution of the transcendental equation for the velocity in the center of the first inner cell. Turbulent kinetic energy and dissipation rate are imposed in the center of the first inner cell according to the standard formulas.

Inlet conditions:

Experimental data for streamwise and swirl velocities and turbulent kinetic energy. Radial velocity equal zero. Dissipation rate is obtained from three–layer approach as described in Hirsch and Khodak (1995).

Related publications/reports:

Hirsch Ch., and Khodak A., 1995 "Modeling of Complex Internal Flows with Reynolds Stress Algebraic Equation Model" AIAA Paper 95–2246

Shih, T.–H., Zhu, J., and Lumley, J.L., 1994 "Modeling of the Wall–Bounded Complex Flows and Free Shear Flows" NASA TM 106513

DESCRIPTION OF NUMERICAL METHODOLOGY FOR TEST CASE 3

Originators:

Charles Hirsch and Andrei E. Khodak

Affiliation:

Department of Fluid Mechanics Vrije Univeriteit Brussel, B-1050 Brussels, Belgium

General description:

Full Reynolds averaged Navier-Stokes computations were performed with the three-dimensional Navier-Stokes solver EURANUS (EUropean Aerodynamic NUmerical Simulator) Equations are formulated in generalized non-orthogonal coordinates for Cartesian velocity components This code has essentially a compressible time-marching formulation with Runge-Kutta time integration. The low-Mach- number computations apply a preconditioning technique with an artificial compressibility approach.

Convection scheme:

Central schemes with fourth order numerical dissipation

Mesh:

64x32 non-orthogonal. Unknown parameters are placed in the cell centers

Turbulence models:

Reynolds stress algebraic equation model (Hirsch, and Khodak, 1995). Original constants

Near-wall treatment:

Wall functions: velocity field is connected with a log-law dependence near the wall. Von Karman constant 0.42, $E=9.0$. Friction velocity is obtained from the solution of the transcendental equation for the velocity in the center of the first inner cell. Turbulent kinetic energy and dissipation rate are imposed in the center of the first inner cell according to the standard formulas.

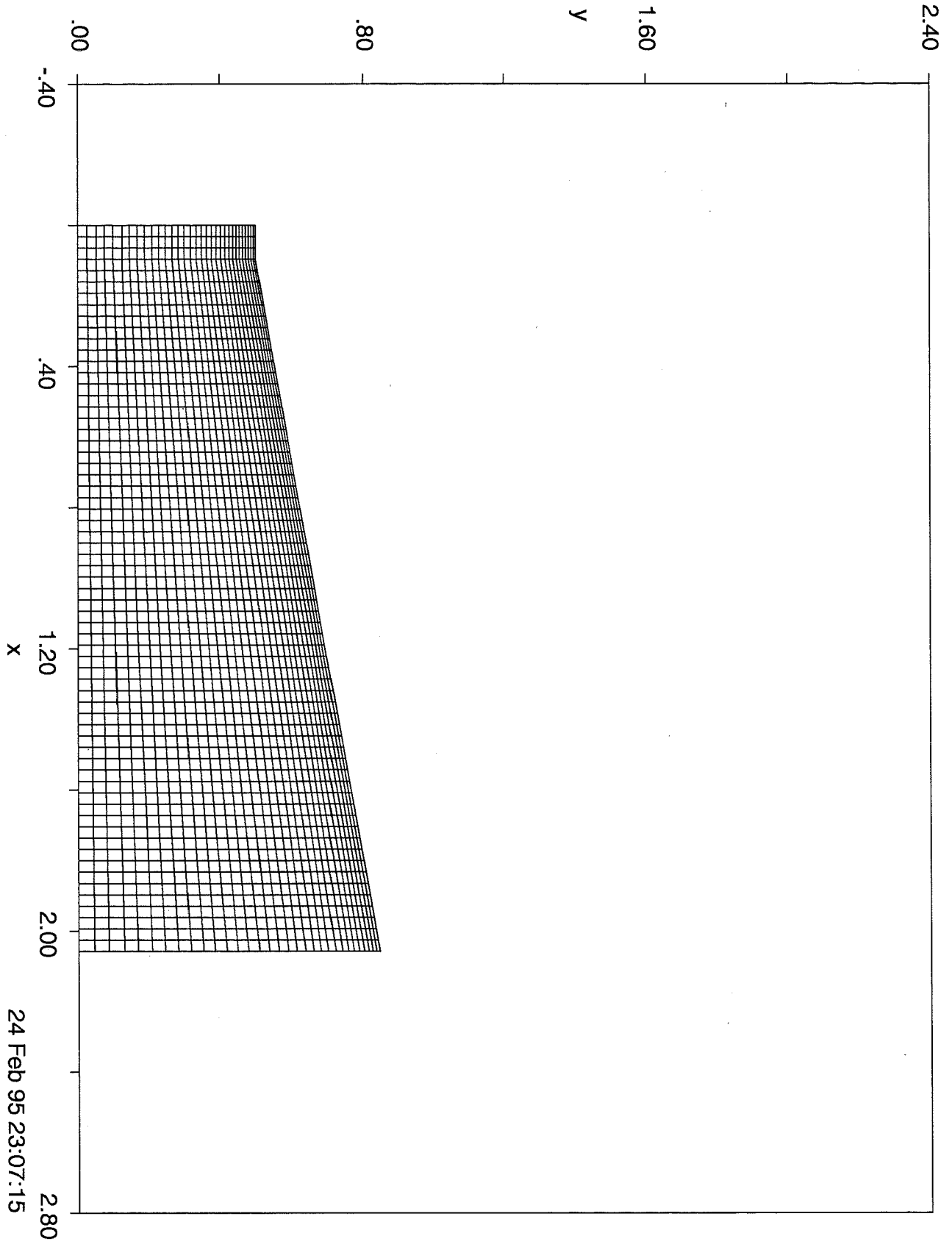
Inlet conditions:

Experimental data for streamwise and swirl velocities and turbulent kinetic energy. Radial velocity equal zero. Dissipation rate is obtained from three-layer approach as described in Hirsch and Khodak (1995).

Related publications/reports:

Hirsch Ch., and Khodak A., 1995 "Modeling of Complex Internal Flows with Reynolds Stress Algebraic Equation Model" AIAA Paper 95-2246

The Mesh :



DESCRIPTION OF NUMERICAL METHODOLOGY FOR TEST CASE 5

Originators:Charles Hirsch and Andrei E. Khodak

Affiliation:

Department of Fluid Mechanics Vrije Univeriteit Brussel, Brussels, Belgium

General description:

Reduced Reynolds averaged Navier–Stokes computations were performed with the three–dimensional Navier–Stokes solver – called CF (Channel Flow) in partially–parabolic approach (Hirsch, and Khodak, 1995) Equations for incompressible flow are formulated in generalized orthogonal coordinates. This code has implicate time–marching formulation with approximate factorisation and artificial compressibility approach.

Convection scheme:QUICK

Mesh:

96x16x32 orthogonal. Unknown parameters are placed according to staggering representation

Turbulence models:

Standard high–Reynolds–number turbulent kinetic energy – dissipation rate turbulence model.
Original constants

Near–wall treatment:

Wall functions: velocity field is connected with a log–law dependence near the wall. Von Karman constant 0.42, $E=9.0$. Friction velocity is obtained from the solution of the transcendental equation for the velocity in the center of the first inner cell. Turbulent kinetic energy and dissipation rate are imposed in the center of the first inner cell according to the standard formulas.

Inlet conditions:

Experimental data for velocity and turbulent kinetic energy. Dissipation rate is obtained from the assumption of the constant turbulent mixing length as described in Hirsch and Khodak (1995).

Related publications/reports:

Hirsch Ch., and Khodak A., 1995 "Application of Different Turbulent Models for Duct flow Simulation with Reduced and Full Navier–Stokes Equations" ASME Paper 95–GT–145

Hirsch Ch., and Khodak A., 1995 "Modeling of Complex Internal Flows with Reynolds Stress Algebraic Equation Model" AIAA Paper 95–2246

DESCRIPTION OF NUMERICAL METHODOLOGY FOR TEST CASE 5

Originators:

Charles Hirsch and Andrei E. Khodak

Affiliation:

Department of Fluid Mechanics Vrije Universiteit Brussel, Brussels, Belgium

General description:

Reduced Reynolds averaged Navier–Stokes computations were performed with the three–dimensional Navier–Stokes solver – called CF (Channel Flow) in partially–parabolic approach (Hirsch, and Khodak, 1995) Equations for incompressible flow are formulated in generalized orthogonal coordinates. This code has implicate time–marching formulation with approximate factorisation and artificial compressibility approach.

Convection scheme:

QUICK

Mesh:

96x16x32 orthogonal. Unknown parameters are placed according to staggering representation

Turbulence models:

Reynolds stress algebraic equation model or non–linear turbulent kinetic energy – dissipation rate turbulence model (Shih, Zhu, and Lumley, 1994) Original constants except $A1=4$.

Near–wall treatment:

Wall functions: velocity field is connected with a log–law dependence near the wall. Von Karman constant 0.42, $E=9.0$. Friction velocity is obtained from the solution of the transcendental equation for the velocity in the center of the first inner cell. Turbulent kinetic energy and dissipation rate are imposed in the center of the first inner cell according to the standard formulas.

Inlet conditions:

Experimental data for velocity and turbulent kinetic energy. Dissipation rate is obtained from the assumption of the constant turbulent mixing length as described in Hirsch and Khodak (1995).

Related publications/reports:

Hirsch Ch., and Khodak A., 1995 "Application of Different Turbulent Models for Duct flow Simulation with Reduced and Full Navier–Stokes Equations" ASME Paper 95–GT–145

Hirsch Ch., and Khodak A., 1995 "Modeling of Complex Internal Flows with Reynolds Stress Algebraic Equation Model" AIAA Paper 95–2246

Shih, T.–H., Zhu, J., and Lumley, J.L., 1994 "Modeling of the Wall–Bounded Complex Flows and Free Shear Flows" NASA TM 106513

DESCRIPTION OF NUMERICAL METHODOLOGY FOR TEST CASE 5

Originators:

Charles Hirsch and Andrei E. Khodak

Affiliation:

Department of Fluid Mechanics Vrije Univeriteit Brussel, Brussels, Belgium

General description:

Reduced Reynolds averaged Navier–Stokes computations were performed with the three–dimensional Navier–Stokes solver – called CF (Channel Flow) in partially–parabolic approach (Hirsch, and Khodak, 1995) Equations for incompressible flow are formulated in generalized orthogonal coordinates. This code has implicate time–marching formulation with approximate factorisation and artificial compressibility approach.

Convection scheme:

QUICK

Mesh:

96x16x32 orthogonal. Unknown parameters are placed according to staggering representation

Turbulence models:

Reynolds stress algebraic equation model (Hirsch, and Khodak, 1995). Original constants

Near–wall treatment:

Wall functions: velocity field is connected with a log–law dependence near the wall. Von Karman constant 0.42, $E=9.0$. Friction velocity is obtained from the solution of the transcendental equation for the velocity in the center of the first inner cell. Turbulent kinetic energy and dissipation rate are imposed in the center of the first inner cell according to the standard formulas.

Inlet conditions:

Experimental data for velocity and turbulent kinetic energy. Dissipation rate is obtained from the assumption of the constant turbulent mixing length as described in Hirsch and Khodak (1995).

Related publications/reports:

Hirsch Ch., and Khodak A., 1995 "Application of Different Turbulent Models for Duct flow Simulation with Reduced and Full Navier–Stokes Equations" ASME Paper 95–GT–145

Hirsch Ch., and Khodak A., 1995 "Modeling of Complex Internal Flows with Reynolds Stress Algebraic Equation Model" AIAA Paper 95–2246

DESCRIPTION OF NUMERICAL METHODOLOGY FOR TEST CASE 2

Originator:

Jerome Renard, Dominique Gresser, Sven Perzon and Lars Davidson

Affiliation:

Thermo and Fluid Dynamics
Chalmers University of Technology
S-412 96 Gothenburg
SWEDEN

phone: (+46)31-7721404/1400

Fax number : (+46)31-180976

E-mail : lada@tfd.chalmers.se

General description:

The CALC-BFC code [1, 2] is used. It is a general three-dimensional finite volume computer program CALC-BFC (**B**oundary **F**itted **C**oordinates) for three-dimensional complex geometries. The program uses Cartesian velocity components, and the pressure-velocity coupling is handled with the SIMPLEC procedure. Collocated grid arrangement is used, which means that velocities are stored along with all scalar variables like p, k, ε at the center of the control volume.

Convection scheme:

The QUICK scheme is used for the velocities and a second-order bounded scheme of van Leer (see Ref. 3) is used for the turbulent quantities.

Mesh:

128 × 100 interior cells (128 in streamwise direction).

Turbulence models:

$k - \varepsilon$ and $k - \omega$ models.

Near-wall treatment:

Two-layer $k - \varepsilon$ model:

The standard $k - \varepsilon$ model is used in the fully turbulent region. The one-equation model by Chen and Patel [4], is used near the walls. In this model, the standard k equation is solved and the turbulent length scales are prescribed. The matching line between the two regions is defined as where the damping function in the expression for the turbulent viscosity takes the value 0.95.

Low-Re $k - \varepsilon$ model:

The low-Re $k - \varepsilon$ model of Lien & Leschziner [5] is used

Low-Re $k - \omega$ model:

The low-Re $k - \omega$ model of Wilcox [6] is used.

Inlet conditions

Inlet conditions was taken according to experiments except for ε which can be set as

$$\varepsilon_{\text{in}} = -2\bar{u}v \frac{\partial U}{\partial y}$$

References

- [1] DAVIDSON, L. and FARHANIEH, B., CALC-BFC: A Finite-Volume Code Employing Collocated Variable Arrangement and Cartesian Velocity Components for Computation of Fluid Flow and Heat Transfer in Complex Three-Dimensional Geometries, Rept. 92/4, Thermo and Fluid Dynamics, Chalmers University of Technology, Göteborg, 1992.
- [2] JOHANSSON, S., DAVIDSON, L. and OLSSON, E., "Numerical Simulation of Vortex Shedding Past Triangular Cylinders at High Reynolds Number", *Int. J. Numer. Meth. Fluids*, Vol. 16, pp. 859-878, 1993.
- [3] JANSSON, S., "Turbulence Modelling of Flows Related to Wall-Cooling Application", PhD thesis, Dept. of Thermo and Fluid Dynamics, Chalmers Univ. of Tech., Göteborg, 1994.
- [4] CHEN, H.C. and PATEL, V.C., Near-Wall Turbulence Models for Complex Flows Including Separation, *AIAA J.*, Vol. 26, p. 641, 1988.
- [5] LIEN, F.S. and LESCHZINER, M.A., Assessment of Turbulence-Transport Models Including Non-Linear RNG Eddy-Viscosity Formulation and Second-Moment Closure for Flow Over a Backward-Facing Step, *Computers & Fluids*, Vol. 23, pp. 983-1004, 1994.
- [6] WILCOX, D.C., Reassessment of the Scale-Determining Equation for Advanced Turbulence Models, *AIAA J.*, Vol. 26, pp. 1299-1309, 1988.

DESCRIPTION OF NUMERICAL METHODOLOGY FOR TEST CASE 2

Originator:

Sven Perzon^{*}, Lars Davidson^{*} and Mats Ramnefors^{**}

Affiliation:

^{*}Thermo and Fluid Dynamics
Chalmers University of Technology
S-412 96 Gothenburg
SWEDEN

phone: (+46)31-7721413/1400
Fax number : (+46)31-180976
E-mail : svpe@tfd.chalmers.se

^{**}Volvo Data AB
2620 CAE
405 08 Gothenburg
SWEDEN

General description:

The commercial code, CFDS-FLOW3D [1] was used. It is a general three-dimensional finite volume computer program using body fitted coordinates for three-dimensional complex geometries. The program uses Cartesian velocity components, and the pressure-velocity coupling is handled with a SIMPLEC algorithm. A non-staggered grid arrangement is used, which means that velocities are stored along with all scalar variables like p, k, ε etc. at the center of the control volume.

Convection scheme:

The QUICK scheme is used for the velocities and a second-order upwind scheme named Higher-order upwind, (HUU), (see Ref. [1]) is used for k and ε . The Reynolds stresses, in the differential stress models were solved for using the first order accurate Hybrid scheme. This was due to stability problems.

Mesh:

The grids used were created using the ICEM-CFD mesh generator. The dimensions are for the different near wall treatments,

- Wall function models: **122 x 50**
- Low Reynolds number models: **128 x 100**

The work has been focused on test case 2a only.

Turbulence models:

Two equation models:

The standard $k - \varepsilon$ model [3] has been used with constants as follows:
 $c_{\varepsilon 1} = 1.44$, $c_{\varepsilon 2} = 1.92$, $c_{\mu} = 0.09$, $\sigma_{\varepsilon} = 1.217$ and $\sigma_k = 1.0$. A low Reynolds number formulation of the model has also been tried.

Reynolds Stress Models (RSM):

Two pressure strain models have been used in the Reynolds stress model which are adopted for high Reynolds number flows and these are:

A common and simple linear proposal based upon the slow pressure strain term by Rotta [8] and the rapid pressure strain term by Naot *et al.* [7]. The model is described thoroughly in [2].

The non linear proposal by Speziale, Sarkar and Gatski [9] (the SSG-model) has also been used. The LRR [5] linear pressure strain model has been used for low Reynolds number flows.

Near-wall treatment:

Wall functions:

Standard wall functions [3] are used in the standard k - ϵ model and the model is summarized in [1]. k is solved for the node adjacent to the wall using modified production terms. ϵ is set according to,

$$\epsilon = \frac{c_\mu^{3/4} k^{3/2}}{\kappa x_n}$$

at the node next to the wall. All is default settings in CFDS-FLOW3D [1]. For the high Reynolds number RSMs the wall functions of Lien and Leschziner [11] are used for the stresses together with the procedure described above for the mean-velocities and ϵ .

Low-Re k - ϵ model:

The low-Re k - ϵ model of Launder and Sharma [4] was used.

Low-Re formulation of a Reynolds stress model.

The low-Re RSM of Hanjalic and Launder [6], also referenced to as the HL-model, was used. This model was slightly modified though and the turbulent diffusion was instead modeled according to Daly and Harlows gradient hypothesis [10].

Inlet conditions

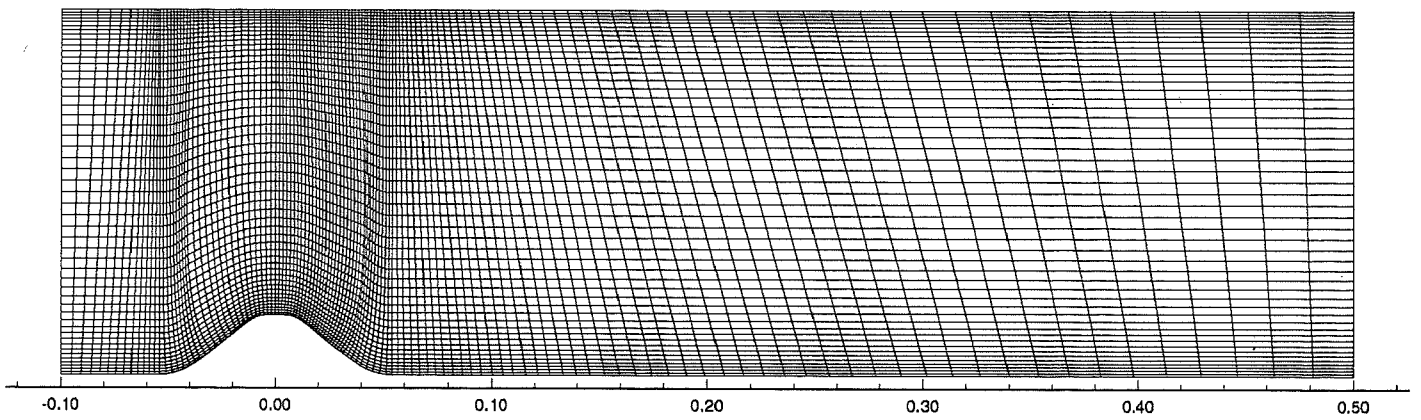
Inlet conditions was taken according to experiments except for ϵ which can be set as

$$\epsilon_{\text{in}} = -2\bar{uv} \frac{\partial U}{\partial y}$$

References

- [1] CFDS-FLOW3D 3.3 User Guide, AEA Technology, Harwell Laboratory, UK, 1994.
- [2] CLARKE, D.S. and WILKES, N.S., The Calculation of Turbulent Flows in Complex Geometries using a Differential Stress Model, AERE-R 13428, 1989.
- [3] LAUNDER, B.E. and SPALDING, D.P., The Numerical Computation of Turbulent Flows, Comp. Methods in Applied Mech. and Engineering 3, 269-289, 1974
- [4] LAUNDER, B.E. and SHARMA, B.T., Application of the Energy Dissipation Model of Turbulence to the Calculation of Flow Near a Spinning Disc, *Lett. Heat and Mass Transfer* 1, 131-138, 1974.
- [5] LAUNDER, B.E., REECE, G.J. and RODI, W., Progress in the Development of a Reynolds-Stress Turbulence Closure, *J. Fluid Mech.*, Vol. 68, 537-566, 1975.
- [6] HANJALIĆ, K. and LAUNDER, B.E., Contribution Towards a Reynolds-stress Closure for Low-Reynolds-Number Turbulence, *J. Fluid Mech.*, Vol. 74, 593-610, 1976.
- [7] NAOT, D., SHAVIT, A., and WOLFSHTEIN, M., Interactions Between Components of the Turbulent Velocity Correlation Tensor, *Israel J. Techn.*, 8, 259, 1970.
- [8] ROTTA, J.C., Statistische Theorie Nichthomogener Turbulenz, *Zeitschrift für Physik*, Vol. 129, 547-572, 1951.
- [9] SPEZIALE, C.G., SARKAR, S. and GATSKI, T.B., Modeling the Pressure-Strain Correlation of Turbulence, *J. Fluid Mech.*, Vol 227, 245-272, 1991.
- [10] DALY, B.J. and HARLOW, F.H., Transport equation in turbulence, *Phys. Fluids*, 13, 2634-2649, 1970.
- [11] LIEN, F.S. and LESCHZINER, M.A., Second-Moment Modelling of Recirculating Flow with a Non-Orthogonal Collocated Finite-Volume Algorithm, Eighth symposium on turbulent shear flows, Technical University of Munich, Sept 9-11, 1991.

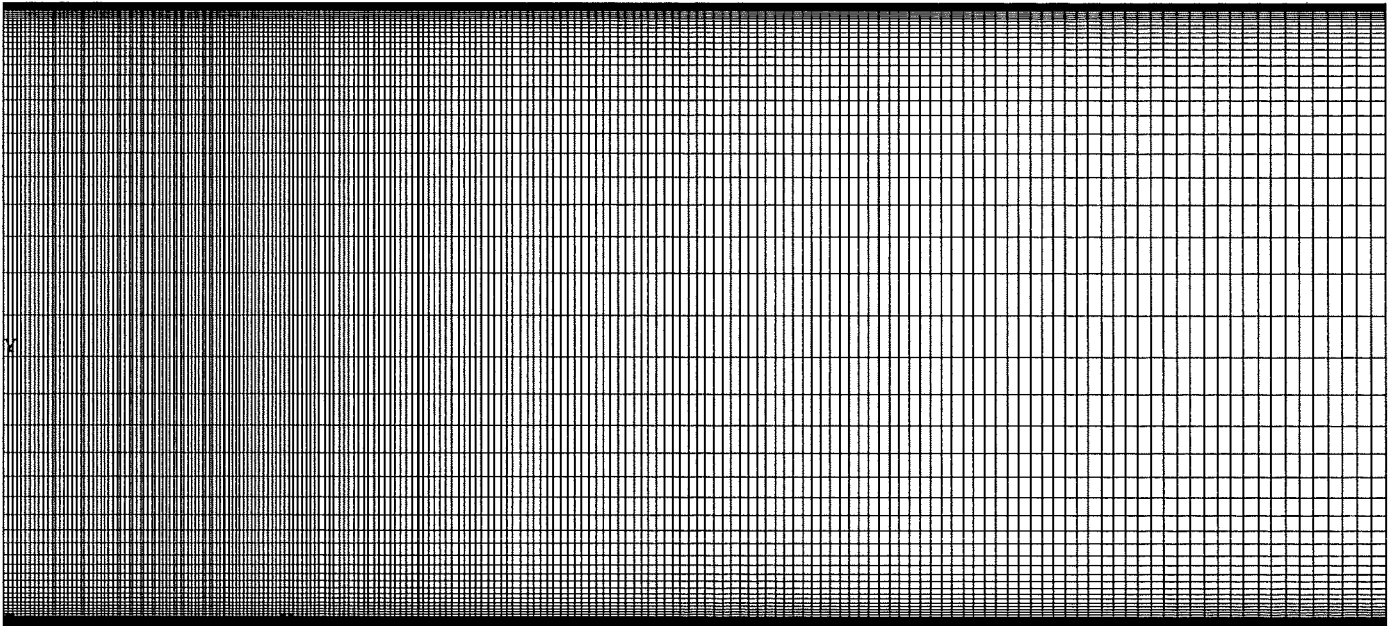
122 X 50 cells



DESCRIPTION OF NUMERICAL METHODOLOGY FOR TEST CASES 1A AND 1B

- **Originator:** Guillaume Houzeaux, Wagdi G. Habashi and Guido Baruzzi
- **Affiliation:** CFD Lab. Concordia University and CERCA, Montréal (Canada)
- **General description:** Navier-Stokes compressible solver based on a finite element approximation with equal order linear interpolation for velocities and pressure. The scheme is stabilized by the addition of a second order explicit artificial viscosity in the momentum equation, and an explicit artificial dissipation in the continuity equation. The nonlinearity is treated with a Newton linearization; its convergence is based on the L^2 norm of the residual of the governing equations. For simplification, the energy equation is replaced by a constant total enthalpy approximation. As the test case flow is incompressible, simulations were carried out with a Mach number = 0.8×10^{-2} .
- **Mesh:** Grid convergence was tested in both x and y directions; to achieve grid independence, five grids were tested ($(x) \times (y)$): 100×60 , 200×60 , 200×70 , 350×80 . The computations were finally carried out on the 200×70 structured mesh, for which convergence was achieved (residual below 10^{-12} for all equations including turbulence).
- **Turbulence model:** k - ω turbulence model: k and ω were solved at the four nodes of the quadrilaterals. The low-Reynolds number Wilcox corrections were implemented to capture the sharp peak of the fluctuating quantities near the wall. The k and ω systems are decoupled from the momentum and continuity equation and are solved sequentially. The turbulent viscosity was underrelaxed, as well as the ω value on the boundary.
- **Near-wall treatment:** k and ω were integrated up to the wall. On the wall, k was set to zero and ω to $\omega_{wall} = \frac{u_\tau^2}{\nu} S_R$, where $u_\tau = \sqrt{\nu \frac{\partial u}{\partial y} \Big|_{wall}}$ is the friction velocity and S_R is given in terms of the sand-grain roughness k_R^+ : $S_R = (50/k_R^+)^2$. As suggested by Wilcox, k_R^+ was set to a value below 5; in the present computations, $k_R^+ = 4.0$.
- **Inlet conditions:** The inlet conditions for all variables were computed for a fully-developed channel flow at $Re = 5000$; they do not affect the flow in the region of interest (i.e beyond the point $x=0$).
- **Related publications/reports:**
 - G.S. Baruzzi, W.G. Habashi and M.M. Hafez (1995): "A Second Order Method for the Finite Element Solution of the Euler and Navier-Stokes equations", Invited paper in special issue of the Int. Journ. Numer. Meths. in Fluids.
 - G.S. Baruzzi, W.G. Habashi and M.M. Hafez (1991): "Finite Element Solutions of the Euler Equations for Transonic External Flows", AIAA Journal, 29 (11), pp.1886-1893.
 - W.G. Habashi, G.S. Baruzzi, M.F. Peeters and M.M. Hafez (1991): "Finite Element Method in the Solution of the Euler and Navier-Stokes equations for Internal Flows", Journal Num. Meths. Part. Diff. Equ., 7, pp.193-207.
 - Wilcox D. C. (1993): "Turbulence Modeling for CFD", DCW Industries, Inc.

VU: Grid for test case 1B. Distances on y are multiplied by 25.



*4th ERCOFTAC/IAHR Workshop on Refined Flow Modelling, April 3-7, 1995,
University of Karlsruhe, Karlsruhe, Germany*

Description of the Models and Computational Method

Originators I. Hadžić¹, K. Hanjalić¹ and S. Jakirlić²

Affiliation ¹Faculty of Applied Physics, Delft University of Technology, The Netherlands

²Lehrstuhl für Strömungsmechanik, University of Erlangen, Germany

General Description Computation of the considered test cases have been performed with a finite volume 2-dimensional Navier-Stokes code which uses body-fitted mesh, cartesian vector and tensor components, and colocated variable arrangement, [1]. The cell face values of variables and gradients featuring in surface integrals are approximated using linear interpolation and central differences, respectively. The equations are linearised and solved sequentially using ILU method after Stone (1968). A pressure-correction method based on SIMPLE algorithm (Patankar and Spalding, 1972) is used for pressure-velocity coupling. Outer iterations with under-relaxation are used to account for non-linearity and coupling of transport equations. Upwind differencing scheme (UDS) is used for convection of all properties. Computed were the test cases 1 and 2, each with several turbulence models, as outlined below.

Test case 1: Couette flow with plane and wavy fixed walls The solutions were obtained by using a non-uniform numerical mesh, clustered near the walls and in the middle of the channel (cases 1A and 1B). The number of control volumes for each sub-case is shown in the table below:

| Case | A and B developed | A and B developing | C |
|-------------|----------------------|-----------------------|-------------|
| | 5 x 100 | 100 x 100 | 180 x 80 CV |
| x-direction | uniform | non-uniform | uniform |
| y-direction | non-uniform | non-uniform | non-uniform |

The grid dependence test was performed with grids: 50x80, 100x100 and 90x60 and 180x80 CV for the cases 1A, 1B and 1C respectively. The fully grid-independent solution was not achieved. Presented are the results obtained with the following models of turbulence:

- Launder and Sharma low Re-number $k - \varepsilon$ model (LS low $k - \varepsilon$), [1], [2],
- Hanjalić and Jakirlić low Re-number full stress model (HJ low RSM), [3], [4].

The latter model is summarised in the Appendix.

Test case 2: 2D model hill flows The solutions were obtained by using a non-uniform numerical mesh, clustered near the walls with 136x60 and 56x60 CV for the cases 2A and 2B respectively. The grid dependence test was performed with grids: 68x30 and 136x60 CV for the 2A and 28x30 and 56x60 CV for the 2B (other grids have also been used in some cases, as explained below). The fully grid-independent solution was not achieved, though the differences between the results for two considered grid sizes is tolerable. Presented are the results obtained with the following models of turbulence:

- Standard $k - \varepsilon$ model with wall functions approach ($k - \varepsilon + \text{WF}$),
- Launder, Reece, Rodi and Gibson full stress model with wall functions approach (LRRG + WF), [5], [6] and
- LRRG + WF + S_l . The term S_l , introduced specifically to deal with the separating and reattaching flows, is the additional source term in the dissipation equation:

$$S_l = \max \left\{ \left[\left(\frac{1}{C_l} \frac{\partial l}{\partial x_n} \right)^2 - 1 \right] \left(\frac{1}{C_l} \frac{\partial l}{\partial x_n} \right)^2 ; 0 \right\} \frac{\tilde{\varepsilon} \varepsilon}{k} A; \quad C_l = 2.5; \quad l = \frac{k^{3/2}}{\varepsilon} \quad (1)$$

This term has been described in more details in [5].

The test case 2B was computed in three different ways, which differ in the treatment of the flow development, i.e. in the specification of the inlet conditions:

- Approach 1: The flow was considered as *fully developed* and periodic conditions have been applied, as suggested by the Workshop organizers.
 - Computational grid (Fig. 1): 56×120 CV
 - Inlet conditions: irrelevant
- Approach 2: Developing flow over a series of hills: The computational domain covers a sequence of 9 consecutive hills (Fig. 2).
 - Computational grid: 243×60 CV (in x-direction $\approx 8.5 \times 28$)
 - Initial conditions: Solution of the fully developed channel flow imposed at the channel inlet cross-section ($x=-100 \text{ mm}$).
- Approach 3: Hill-by-hill consecutive solutions of the flow domain covering a valley between the two neighbouring hills, until the 7th valley is reached. For each valley a convergent solution was achieved. For the first valley the solutions at the hill top for the case 2A (isolated hill), preceded by a fully developed channel flow, were used as the inlet conditions. The convergent exit profiles were then used as the inlet profiles for the next valley, etc. A small error is introduced here since the exit boundary conditions are defined in terms of zero gradients, which is not fully correct, considering that the flow is developing. However, the width of the last control volume in streamwise direction was made small, minimizing the error.

The solutions with the two latter approaches agree well in between (peak k within the 10%), in spite of approximations in the Approach 3 regarding the inlet and exit conditions, and twice coarser grid in the Approach 2 in the x -direction. Although these solution differ considerably from the measurements, particularly in the near-wall region, they are qualitatively much closer to experiments than the fully developed solutions obtained by the application of the fully periodic conditions. A further confirmation to this is the streamline field which shows in both latter cases that the boundary layer grows steadily.

References:

- [1] Peric M. (1993): *Private communication*,
- [2] Jones W.P., Launder B.E., (1972): *Prediction of laminarization with a two-equation model of turbulence*, Int. J. Heat Mass Transfer, Vol. 15, pp 301-314,
- [3] Launder B.E, Sharma B.I., (1974): *Application of the energy-dissipation model of turbulence to the calculation of the flow near a spinning disk*, Letters in Heat and Mass Transfer, Vol. 1, pp 131-138,
- [4] Hanjalic K., Jakirlic S., Hadzic I., (1995.): *Computation of Oscillating Turbulent Flows at Transitional Re-Numbers*, Turbulent Shear Flows, Vol. 9, pp 323-342, Eds. F.Durst et al., Springer Berlin,
- [5] Jakirlic S., Hanjalic K., (1994.): *On the Performance of the Second-Moment High- and Low-Re-Number Closures in Reattaching Flows*, Proc. Int. Symposium on Turbulence, Heat and Mass Transfer, Lisbon, 9-12 August,
- [6] Launder B.E., Reece G.J., Rodi W., (1975): *Progress in the development of a Reynolds-stress turbulence closure*, J. of Fluid Mech., Vol. 68, pp 537-566,
- [7] Gibson M.M., Launder B.E., (1978): *Ground effects on pressure fluctuations in the atmospheric boundary layer*, J. of Fluid Mech., Vol. 86, pp 491-511.

Turbulence model:

$$\frac{D\overline{u_i u_j}}{Dt} = \frac{\partial}{\partial x_k} \left[\left(\nu \delta_{kl} + C_s \frac{k}{\varepsilon} \overline{u_k u_l} \right) \frac{\partial \overline{u_i u_j}}{\partial x_l} \right] - \left(\overline{u_i u_k} \frac{\partial U_j}{\partial x_k} + \overline{u_j u_k} \frac{\partial U_i}{\partial x_k} \right) + \Phi_{ij} - \varepsilon_{ij}$$

$$\begin{aligned} \frac{D\varepsilon}{Dt} = \frac{\partial}{\partial x_k} \left[\left(\nu \delta_{kl} + C_\varepsilon \frac{k}{\varepsilon} \overline{u_k u_l} \right) \frac{\partial \varepsilon}{\partial x_l} \right] - C_{\varepsilon_1} \frac{\varepsilon}{k} \overline{u_i u_j} \frac{\partial U_i}{\partial x_j} - C_{\varepsilon_2} f_\varepsilon \frac{\varepsilon \tilde{\varepsilon}}{k} \\ + C_{\varepsilon_3} \nu \frac{k}{\varepsilon} \overline{u_j u_k} \frac{\partial^2 U_i}{\partial x_j \partial x_l} \cdot \frac{\partial^2 U_i}{\partial x_k \partial x_l} \end{aligned}$$

$$\Phi_{ij,1} = -C_1 \varepsilon a_{ij} \quad \Phi_{ij,2} = -C_2 \left(P_{ij} - \frac{2}{3} P_k \delta_{ij} \right)$$

$$\Phi_{ij,1}^w = C_1^w f_w \frac{\varepsilon}{k} \left(\overline{u_k u_m n_k n_m} \delta_{ij} - \frac{3}{2} \overline{u_i u_k n_k n_j} - \frac{3}{2} \overline{u_k u_j n_k n_i} \right)$$

$$\Phi_{ij,2}^w = C_2^w f_w \left(\Phi_{km,2} n_k n_m \delta_{ij} - \frac{3}{2} \Phi_{ik,2} n_k n_j - \frac{3}{2} \Phi_{kj,2} n_k n_i \right)$$

$$C_1 = C + \sqrt{AE^2} \quad C = 2.5AF^{1/4} f \quad F = \min\{0.6; A_2\}$$

$$f = \min \left\{ \left(\frac{Re_t}{150} \right)^{3/2}; 1 \right\} \quad f_w = \min \left[\frac{k^{3/2}}{2.5\varepsilon x_n}; 1.4 \right]$$

$$C_2 = 0.8A^{1/2} \quad C_1^w = \max(1 - 0.7C; 0.3) \quad C_2^w = \min(A; 0.3)$$

$$A = 1 - \frac{9}{8}(A_2 - A_3) \quad A_2 = a_{ij} a_{ji} \quad A_3 = a_{ij} a_{jk} a_{ki}$$

$$E = 1 - \frac{9}{8}(E_2 - E_3) \quad E_2 = e_{ij} e_{ji} \quad E_3 = e_{ij} e_{jk} e_{ki}$$

$$a_{ij} = \frac{\overline{u_i u_j}}{k} - \frac{2}{3} \delta_{ij} \quad e_{ij} = \frac{\varepsilon_{ij}}{\varepsilon} - \frac{2}{3} \delta_{ij}$$

$$\varepsilon_{ij} = f_s \varepsilon_{ij}^* + (1 - f_s) \frac{2}{3} \delta_{ij} \varepsilon$$

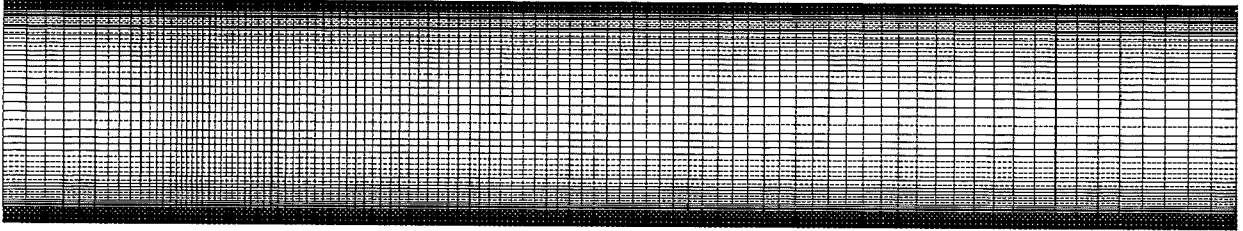
$$\varepsilon_{ij}^* = \frac{\varepsilon}{k} \frac{[\overline{u_i u_j} + (\overline{u_i u_k n_j n_k} + \overline{u_j u_k n_i n_k} + \overline{u_k u_l n_k n_l n_i n_j}) f_d]}{1 + \frac{3}{2} \frac{\overline{u_p u_q}}{k} n_p n_q f_d}$$

$$f_s = 1 - \sqrt{AE^2} \quad f_d = (1 + 0.1Re_t)^{-1}$$

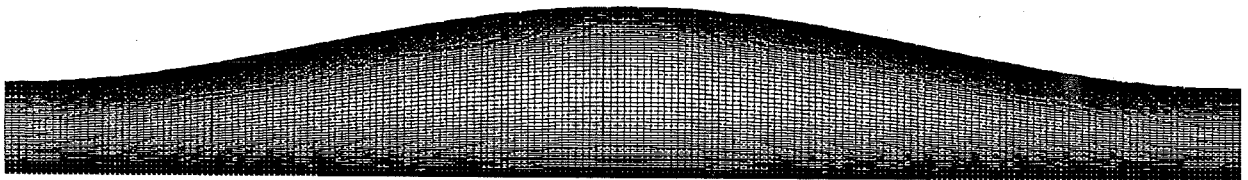
$$f_\varepsilon = 1 - \frac{C_{\varepsilon_2} - 1.4}{C_{\varepsilon_2}} \exp \left[- \left(\frac{Re_t}{6} \right)^2 \right]$$

$$C_s = 0.22 \quad C_\varepsilon = 0.18 \quad C_{\varepsilon_1} = 1.44 \quad C_{\varepsilon_2} = 1.92 \quad C_{\varepsilon_3} = 0.25$$

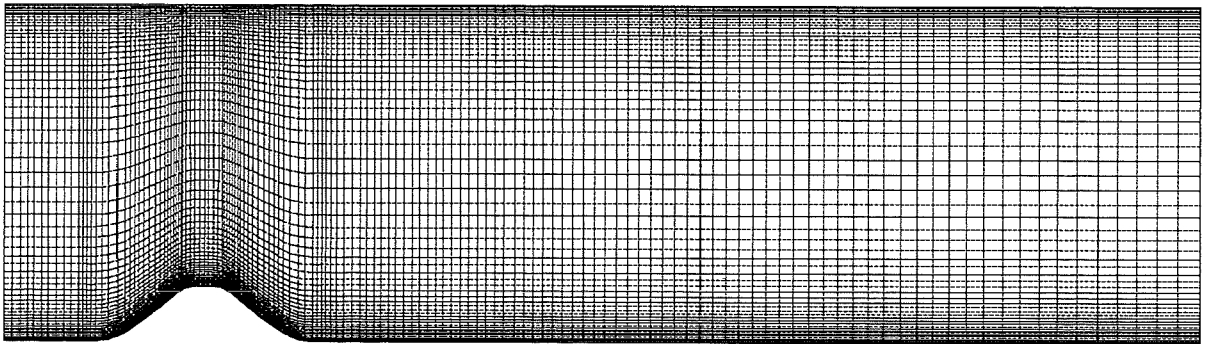
Mesh arrangement for Test cases 1A and 1B (100×100 CV)



Mesh arrangement for Test case 1C (180×80 CV)



Mesh arrangement for Test case 2A (136×60 CV)



Mesh arrangement for Test case 2B (56×60 CV)

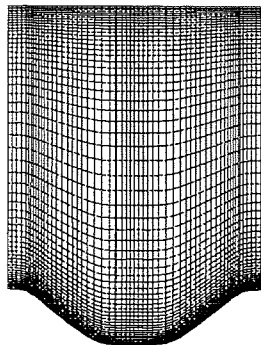


Figure 1. Approach 1: Grid 56×120 CV

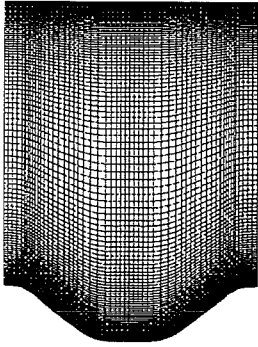
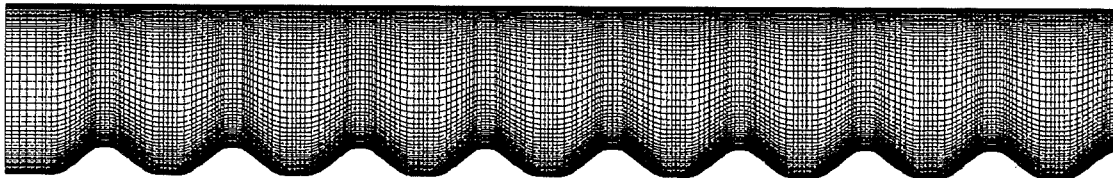


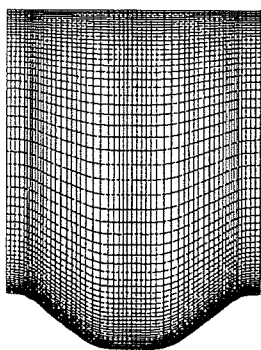
Figure 2. Approach 2: Grid 243×60 CV



High-Re k-ε Std
 UDS+UDS 243x60 9 blocks

Grid No. 1
 Time = 0.

Figure 3. Approach 3: Grid 56×60 CV



DESCRIPTION OF NUMERICAL METHODOLOGY FOR 2D MODEL HILL FLOWS

Originator:

M. Zijlema

Affiliation:

Delft University of Technology
 Faculty of Technical Mathematics and Informatics
 P.O. Box 5031, 2600 GA Delft, the Netherlands
 Email: m.zijlema@math.tudelft.nl

General Description:

Results have been obtained with the ISNaS code (Information System for solving Navier-Stokes equations) developed by our group at DUT. A list of our recent publications is [2], [8], [5], [3], [7], [11], [13] and [14].

The ISNaS code is based on a coordinate invariant finite volume discretization on a staggered non-orthogonal grid of the incompressible Reynolds-averaged Navier-Stokes equations. Three types of eddy-viscosity models are embedded in the code: the standard high-Re k - ϵ model with wall functions [1], an RNG based k - ϵ variant [10] and the Wilcox's k - ω closure without viscous corrections near a solid wall [9].

The governing equations are solved numerically using a finite volume technique on a staggered grid in the computational domain. These equations have to be recast in a form in which both independent and dependent variables are invariant with respect to change of coordinates. The mean flow equations are integrated over a cell to yield the equations containing unknown cell-face fluxes, which necessitates the use of central differences and bilinear interpolations. Discretization of the turbulence transport equations is done similarly, except that the convection terms are approximated with a third-order accurate TVD/ISNAS (Interpolation Scheme which is Nonoscillatory for Advective Scalars) scheme, recently derived by the present author [12].

Time discretization is done by the implicit Euler method and linearization is carried out with the Newton method. A second-order pressure-correction scheme [6] is used to obtain a divergence-free velocity field. The three linear systems, namely momentum, pressure and transport equations, are solved in each time step by a preconditioned GMRES solver [4]. For preconditioners we use incomplete LU factorizations. In every time step first the momentum and continuity equations are solved and then each turbulence equation. The whole process is repeated until convergence to a stationary solution is achieved.

The inlet boundary conditions for the longitudinal velocity and the turbulent kinetic energy are prescribed according to the experimental data. The inlet dissipation of the turbulent energy and the specific dissipation rate are estimated from

$$\epsilon_{in} = \frac{c_\mu^{3/4} k_{in}^{3/2}}{l}, \quad \omega_{in} = \frac{\sqrt{k_{in}}}{l}$$

where the length scale l is given by:

$$l = \min(\kappa y, 0.1H)$$

with $\kappa = 0.41$ the Von Karman constant and H is half the inlet depth. At the outflow section it is assumed that the tangential and normal stresses and normal gradients of turbulence quantities are all zero.

Convection scheme:

- Mean flow: central differences
- Turbulence quantities: TVD/ISNAS

Mesh:

For the single hill case the number of grid points is 110×60 for the k - ϵ model, whereas for the k - ω model a 110×80 grid has been employed. The solutions are then found to be nearly grid-independent.

Turbulence models:

- Standard high-Re k - ϵ model; $\{ c_\mu, c_{\epsilon 1}, c_{\epsilon 2}, \sigma_k, \sigma_\epsilon \} = \{ 0.09, 1.44, 1.92, 1.0, 1.3 \}$
- Wilcox's k - ω model; $\{ \alpha, \beta, \beta^*, \sigma, \sigma^* \} = \{ \frac{5}{9}, \frac{3}{40}, \frac{9}{100}, \frac{1}{2}, \frac{1}{2} \}$

Near-wall treatment:

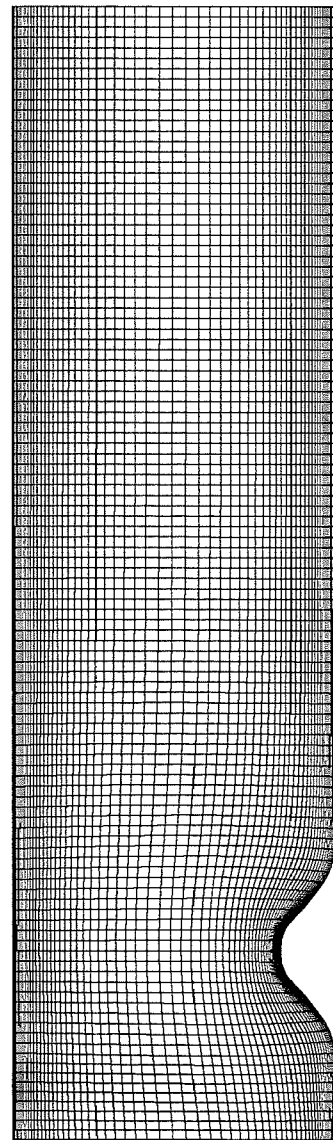
For the standard k - ε model log-law based wall laws for a smooth wall, as described by Launder and Spalding [1], are used. In the case of the k - ω model standard boundary conditions are employed, i.e. for the momentum equations noslip conditions are imposed on the solid wall, whereas for turbulent energy a homogeneous Dirichlet condition is taken (in order to avoid non-positive values of k , $k = 10^{-6}$ may be taken as boundary condition on the wall). Due to the singular behaviour of ω at the wall, a special condition for ω has been used, which is given by

$$\omega = \frac{6\nu}{\beta y^2}, \quad y^+ < 2.5$$

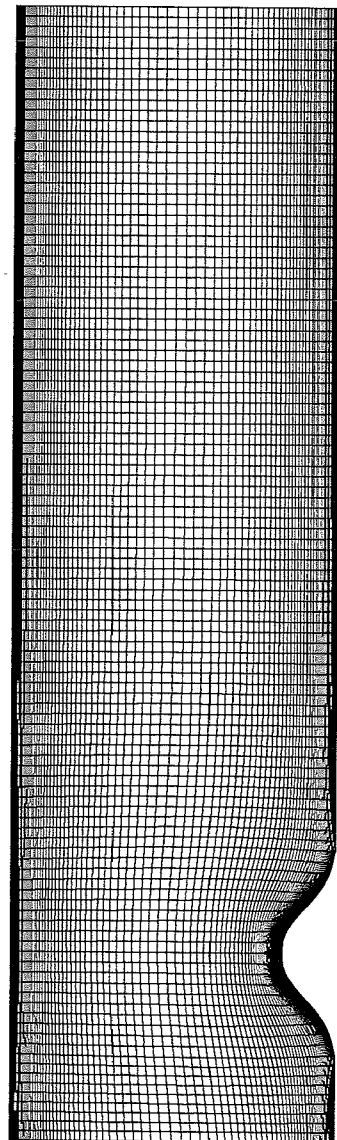
where y is the distance perpendicular to the wall, ν is the kinematic viscosity and β is a closure constant belonging to the k - ω model.

Related publications/reports:**References**

- [1] B.E. Launder and D.B. Spalding, The numerical computation of turbulent flows. *Comput. Meth. Appl. Mech. Engng.* **3**, 269-289 (1974).
- [2] A.E. Mynett, P. Wesseling, A. Segal and C.G.M. Kassels, The ISNaS incompressible Navier-Stokes solver: invariant discretization. *Appl. Sci. Res.* **48**, 175-191 (1991).
- [3] C.W. Oosterlee, P. Wesseling, A. Segal and E. Brakkee, Benchmark solutions for the incompressible Navier-Stokes equations in general coordinates on staggered grids. *Int. J. Numer. Meth. Fluids* **17**, 301-321 (1993).
- [4] Y. Saad and M.H. Schultz, GMRES: a generalized minimal residual algorithm for solving non symmetric linear systems. *SIAM J. Sci. Stat. Comput.* **7**, 856-869 (1986).
- [5] A. Segal, P. Wesseling, J. van Kan, C.W. Oosterlee and K. Kassels, Invariant discretization of the incompressible Navier-Stokes equations in boundary fitted co-ordinates. *Int. J. Numer. Meth. Fluids* **15**, 411-426 (1992).
- [6] J.J.I.M. van Kan, A second-order accurate pressure correction method for viscous incompressible flow. *SIAM J. Sci. Stat. Comput.* **7**, 870-891 (1986).
- [7] P. Wesseling, C.G.M. Kassels, C.W. Oosterlee, A. Segal, C. Vuik, S. Zeng and M. Zijlema, Computing incompressible flows in general domains. In *Numerical Methods for the Navier-Stokes equations*, (edited by F.-K. Hebeker, R. Rannacher and G. Wittum), Vieweg, Braunschweig/Wiesbaden, 298-314 (1994).
- [8] P. Wesseling, A. Segal, J.J.I.M. van Kan, C.W. Oosterlee and C.G.M. Kassels, Finite volume discretization of the incompressible Navier-Stokes equations in general coordinates on staggered grids. *Comput. Fluid Dyn. J.* **1**, 27-33 (1992).
- [9] D.C. Wilcox, Reassessment of the scale determining equation for advanced turbulence models. *AIAA J.* **26**, 1299-1310 (1988).
- [10] V. Yakhot, S.A. Orszag, S. Thangam, T.B. Gatski and C.G. Speziale, Development of turbulence models for shear flows by a double expansion technique. *Phys. Fluids A* **4**, 1510-1520 (1992).
- [11] S. Zeng and P. Wesseling, Multigrid solution of the incompressible Navier-Stokes equations in general coordinates. *SIAM J. Numer. Anal.* **31**, 1764-1784 (1994).
- [12] M. Zijlema, On the construction of a third-order accurate TVD scheme using Leonard's normalized variable diagram with application to turbulent flows in general domains. Report No. 94-104, Delft University of Technology, Faculty of Technical Mathematics and Informatics, Delft, The Netherlands (1994).
- [13] M. Zijlema, A. Segal and P. Wesseling, Invariant discretization of the k - ε model in general coordinates for prediction of turbulent flow in complicated geometries. *Comput. Fluids* **24**, 209-225 (1995).
- [14] M. Zijlema, A. Segal and P. Wesseling, Finite volume computation of incompressible turbulent flows in general co-ordinates on staggered grids. *Int. J. Numer. Meth. Fluids* **20**, 621-640 (1995).



110 x 60



110 x 80

DESCRIPTION OF NUMERICAL METHODOLOGY FOR TEST CASE 2

Originators:

Vittorio Michelassi and David Chiaramonti

Affiliation:

Energetics Department Engineering University of Florence Via di S.Marta 3, 50139 – Florence ITALY

General Description:

The flow over the single hill (Test 2, Case A) has been solved by the twodimensional solver "tdns". The solver is based on the implicit approximate factorization technique. Mass conservation is enforced by the artificial compressibility method. The conservation equation are discretized by means of centered finite differences. The Continuity and Momentum equation are decoupled from the turbulence model equations which are solved in a decoupled manner, thereby lagging one time step with respect to the flow field solution. Particular care is devoted to the linearization of the turbulence model source terms which are accounted for implicitly to improve numerical stability and robustness. Artificial dissipation terms are introduced in the artificial compressibility equation because of the natural tendency of this formulation to produce pressure wiggles. The artificial terms, which are also included in the implicit side of the operator, do not increase the overall mass conservation error which is kept under 0.1% inlet-outlet.

Convection Scheme:

Centered Finite Difference Scheme (second order accurate) with Artificial Dissipation. NO UPWIND is introduced.

Mesh:

The mesh that was used to simulate the flow over the hill has been stretched in the vertical direction by a factor of 1.08: it means that the first grid point is located at approximately $y^+ = 2.1$, whereas the refined one places the same grid point at $y^+ = 0.9$. Along the x-axis (direction of the flow entering the tunnel) mesh size has also been reduced approaching the hill: it has been then kept constant over the hill and then it has finally been increased after the hill. Two grids have been investigated. A first 160x71 and a refined 291x136. No significative differences are detected between the two grids, so that only the coarse solution is presented.

Turbulence Models:

Five different turbulence models have been studied. All the models are based on the transport of two quantities. Four k-epsilon models are used which allow the integration down to the solid wall, and the k-omega Model by Wilcox. All the models belong to the Low-Reynolds Number forms. Among the five models, three of them follow a two-layer formulation. This form defines an inner layer close to the solid boundary in which the dissipation rate is computed by means of an algebraic expression which replaces the dissipation rate transport equation. This algebraic expression is based on a length scale distribution which changes in the three models (TL, TV, KI) Observe that the near wall model proposed by Norris and Reynolds was integrated with the k-eps model by Rodi who proposed to solve for the standard dissipation rate equation in the outer layer. The dissipation rate equation is also kept unchanged in the outer layer by the other two models too, namely TV and KI.

Near-Wall Treatment:

TL: Norris-Reynolds

TV: Rodi-Mansour-Michelassi (see ref. [4])

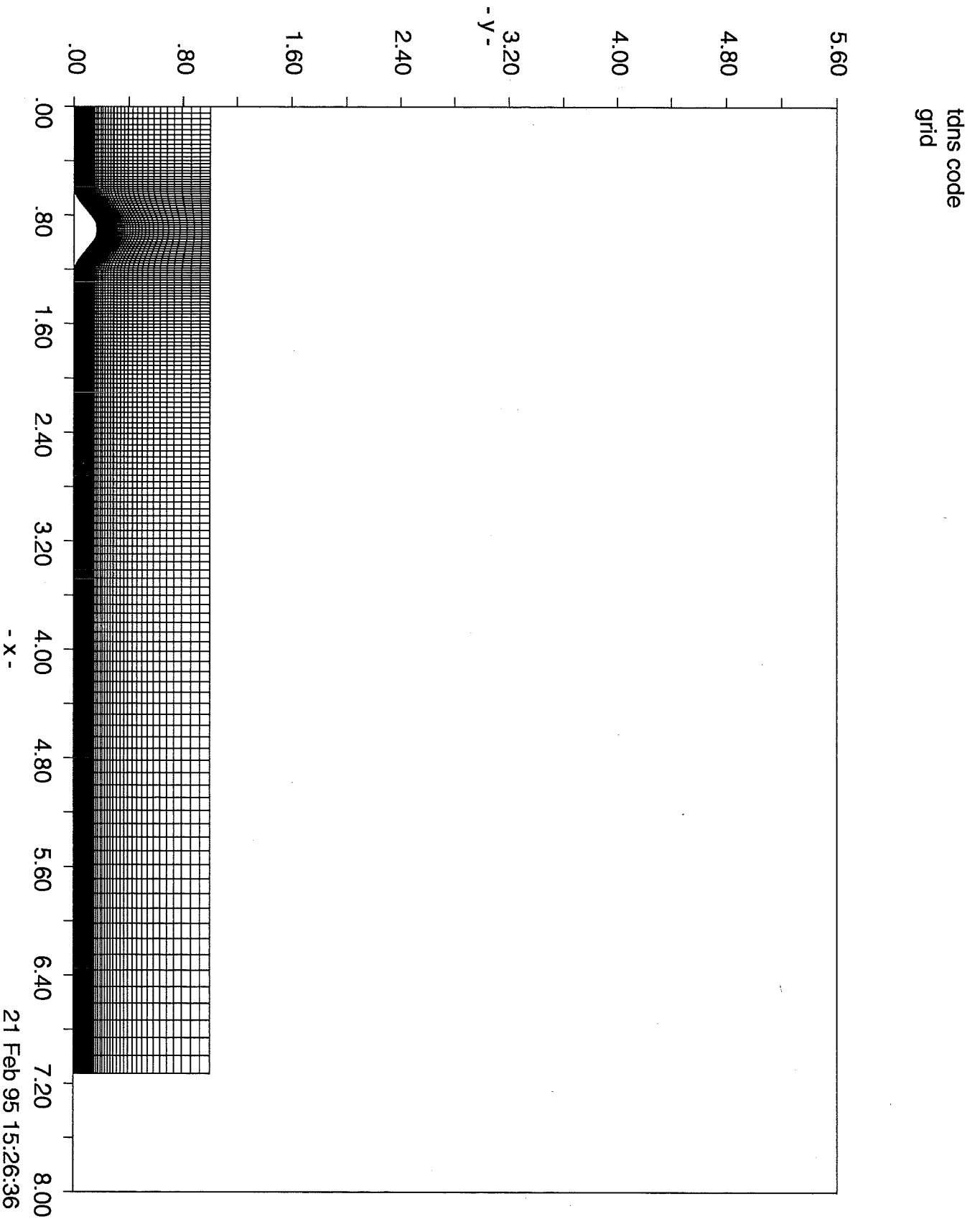
KO: Wilcox

KI: S.W.Kim

NH: Nagano-Hishida

Related Publications/reports:

- [1] Michelassi, V., Benocci, C., "Prediction of Incompressible Flow Separation with the Approximate Factorization Technique", International Journal of Numerical Methods in Fluids, vol.7, 1987.
- [2] Martelli, F. Michelassi, V., "Using Viscous Calculations in Pump Designs", 3-rd Joint ASCE/ASME Mechanics Conference, July 9-12 1989, San Diego, and Transaction of the ASME, Journal of Fluids Engineering September 1990, Vol.112, pp.272-280.
- [3] Michelassi, V., Martelli, F., "Efficient Solution of Turbulent Incompressible Separated Flows". Eighth GAMM Conference on Numerical Methods in Fluid Mechanics, September 27-29, 1989 (published in the series "Notes on Numerical Fluid Mechanics", by Vieweg Verlag).
- [4] Rodi, W., Mansour, N.N., Michelassi, V., "One-Equation Near-Wall Modelling with the Aid of Direct Simulation Data", ASME Journal of Fluids Engineering, vol.115, June 1993, pp.196-205.
- [5] Michelassi, V., "Testing of Turbulence Models by an Artificial Compressibility Solution Method", University of Karlsruhe, report SFB 210/T/49, 1988.
- [6] Michelassi, V., Shih, T.-H., "Elliptic Flow Computation by Low Reynolds Number Two-Equation Turbulence Models", NASA TM-105376, ICOMP-91-28, CMOTT-91-11.
- [7] Michelassi, V., "Adverse Pressure Gradient Flow Computation by Two-Equation Turbulence Models", Proceedings 2-nd International Symposium on Engineering Turbulence Modelling and Measurements", May 31-June 2, 1993, Florence, Italy.



DESCRIPTION OF NUMERICAL METHODOLOGY FOR TEST CASE 3

Originators:

Vittorio Michelassi and Stefano Mugnai

Affiliation:

Energetics Department Engineering University of Florence Via di S.Marta 3, 50139 – Florence ITALY

General Description:

The flow in the swirling diffuser (Test 3) has been solved by the twodimensional solver "tdns". The solver is based on the implicit approximate factorization technique. Mass conservation is enforced by the artificial compressibility method. The conservation equation are discretized by means of centered finite differences. The Continuity and Momentum equation are decoupled from the turbulence model equations which are solved in a decoupled manner, thereby lagging one time step with respect to the flow field solution. Particular care is devoted to the linearization of the turbulence model source terms which are accounted for implicitly to improve numerical stability and robustness. Artificial dissipation terms are introduced in the artificial compressibility equation because of the natural tendency of this formulation to produce pressure wiggles. The artificial terms, which are also included in the implicit side of the operator, do not increase the overall mass conservation error which is kept under 0.1% inlet-outlet. The solver introduces the angular momentum equation in the axisymmetric form which is solved decoupled from all the other transport equations.

Convection Scheme:

Centered Finite Difference Scheme (second order accurate) with Artificial Dissipation. NO UPWIND is introduced.

Mesh:

The mesh that was used to simulate the diffuser flow has been stretched in the vertical direction by using a geometric expansion ratio. Two curvilinear grids have been used. A first coarse 209x75 grid places the first grid point at the wall at $y^+=24$, while the second refined 419x150 has the first grid point at the wall at $y^+=0.075$. The results obtained with the first grid were still largely grid dependent, so that only the refined grid calculations will be reported.

Turbulence Model:

The Low-Reynolds-number form of the k - ϵ s proposed by Jones and Launder is introduced without changes in the constants. The model allows the integration down to the solid wall.

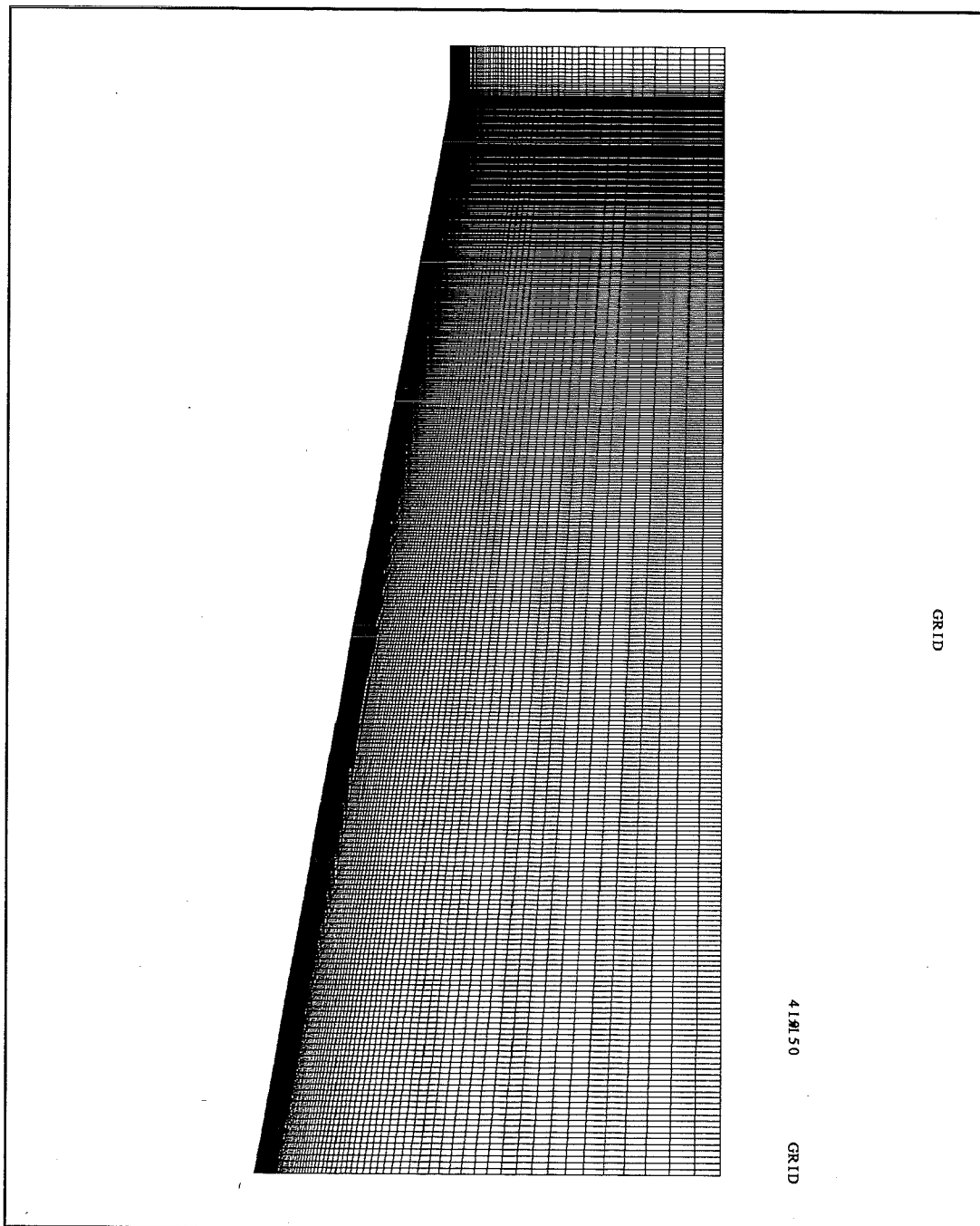
Near-Wall Treatment:

JL: Jones-Launder

Related Publications/reports:

- [1] Michelassi, V., Benocci, C., "Prediction of Incompressible Flow Separation with the Approximate Factorization Technique", International Journal of Numerical Methods in Fluids, vol.7, 1987.

- [2] Martelli, F. Michelassi, V., "Using Viscous Calculations in Pump Designs", 3-rd Joint ASCE/ASME Mechanics Conference, July 9-12 1989, San Diego, and Transaction of the ASME, Journal of Fluids Engineering September 1990, Vol.112, pp.272-280.
- [3] Michelassi, V., Martelli, F., "Efficient Solution of Turbulent Incompressible Separated Flows". Eighth GAMM Conference on Numerical Methods in Fluid Mechanics, September 27-29, 1989 (published in the series "Notes on Numerical Fluid Mechanics", by Vieweg Verlag).
- [4] Rodi, W., Mansour, N.N., Michelassi, V., "One-Equation Near-Wall Modelling with the Aid of Direct Simulation Data", ASME Journal of Fluids Engineering, vol.115, June 1993, pp.196-205.
- [5] Michelassi, V., "Testing of Turbulence Models by an Artificial Compressibility Solution Method", University of Karlsruhe, report SFB 210/T/49, 1988.
- [6] Michelassi, V., Shih, T.-H., "Elliptic Flow Computation by Low Reynolds Number Two-Equation Turbulence Models", NASA TM-105376, ICOMP-91-28, CMOTT-91-11.
- [7] Michelassi, V., "Adverse Pressure Gradient Flow Computation by Two-Equation Turbulence Models", Proceedings 2-nd International Symposium on Engineering Turbulence Modelling and Measurements", May 31-June 2, 1993, Florence, Italy.



DESCRIPTION OF NUMERICAL METHODOLOGY FOR TEST CASE 2A

Originator:

Jaroslaw Kaczynski, M. Sc.

Affiliation:

Institut of Fluid Flow Machinery (IFFM) Polish Academy of Sciences ul.Fiszera 14 80-952 Gdansk, Poland

General description:

The numerical solution procedure is a conservative finite – volume method in primitive variables using non-staggered variable arrangement (Peric, et al., 1988).

Convection scheme:

Monotized Linear-Upwind Scheme (Noll, 1992)

Mesh:

131 (in x direction) x 51, non-orthogonal, generated with an algebraic method

Turbulence models:

standard k-eps model (Launder and Spalding, 1974)

Near-wall treatment:

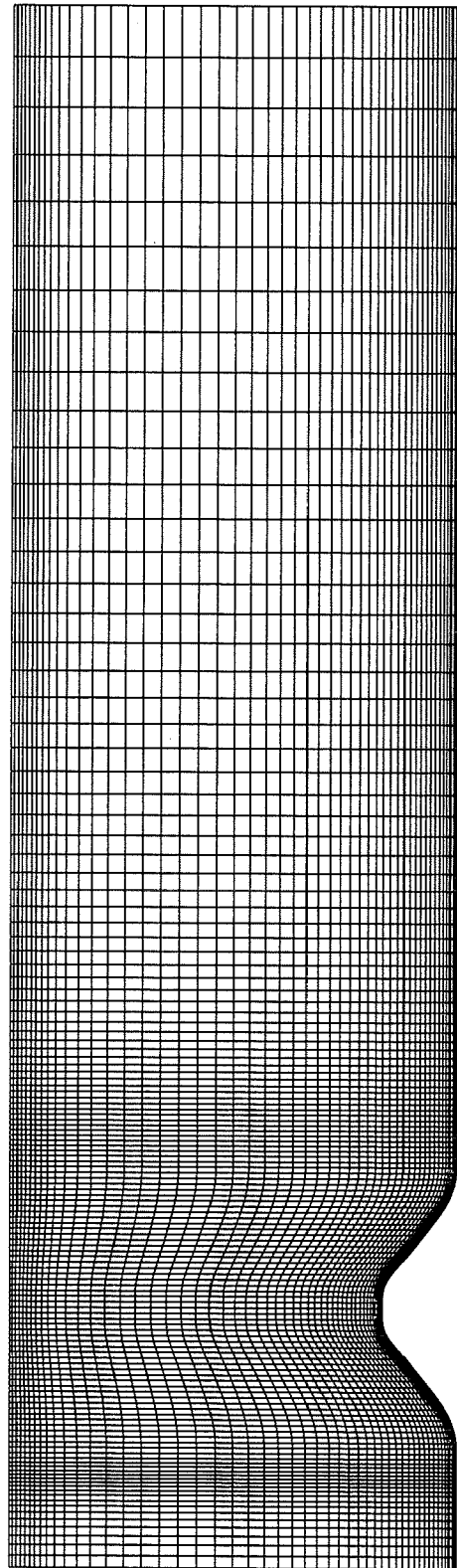
"wall functions" (Turner and Jennions, 1993)

Related publications/reports:

Peric, M., Kessler, R., Scheuerer, G., 1988, *Compt. Fluid*, 16, 389-403. Noll, B., 1992, *AIAA J.*, 30, 64-69.

Launder, B.E., Spalding, D.B., 1974, *Comp. Meth. Appl. Mech. Eng.*, 3, 269-289.

Turner, M.G., Jennions, I.K., 1993, *J. of Turbomachinery*, 249-260.



DESCRIPTION OF NUMERICAL METHODOLOGY FOR TEST CASE 4:

Originators: C. Mains, S. Muzaferija and M. Perić

Affiliation: Institut für Schiffbau, Universität Hamburg, Lämmersieth 90, D-22305 Hamburg

General description: Calculation is performed with the COMET (CONTINUUM MECHANICS ENGINEERING TOOL) computer code. The method is based on the finite volume approach and allows the use of unstructured grids with control volumes of arbitrary shape. Working variables are the cartesian velocity components and pressure, leading to a fully conservative discretisation. The solution method is iterative and solves sequentially linearized equations for each dependent variable using a preconditioned conjugate gradient solver. The coupling of pressure and velocity is achieved via SIMPLE algorithm using colocated variable arrangement. Discretization is based on midpoint rule integration, while the interpolation and differentiation are based on polynomial fitting functions whose one formulation leads to second-order approximations of convective and diffusive fluxes on non-uniform grids.

Convection scheme: Convection fluxes are calculated by blending the first-order upwind and a second-order scheme, which reduces to central differencing on cartesian grids. Results presented here are obtained using 80% of the second-order and 20% of the upwind scheme.

Mesh: The mesh is unstructured and composed of cells with different topology (hexaedra and prisms). Three meshes were used: 10478 CV, 98199 CV and 525018 CV. The results from the finest grid are presented. Monotonic convergence towards grid-independent solution is observed. Discretization errors are estimated to be below 5%.

Turbulence models: Standard $k - \epsilon$ model and its RNG version (see Yakhot *et al*, 1992) were used. Presented are results with the RNG-version, which show slightly better agreement with experimental data.

Near-wall treatment: Standard wall functions are used for modelling near-wall effects.

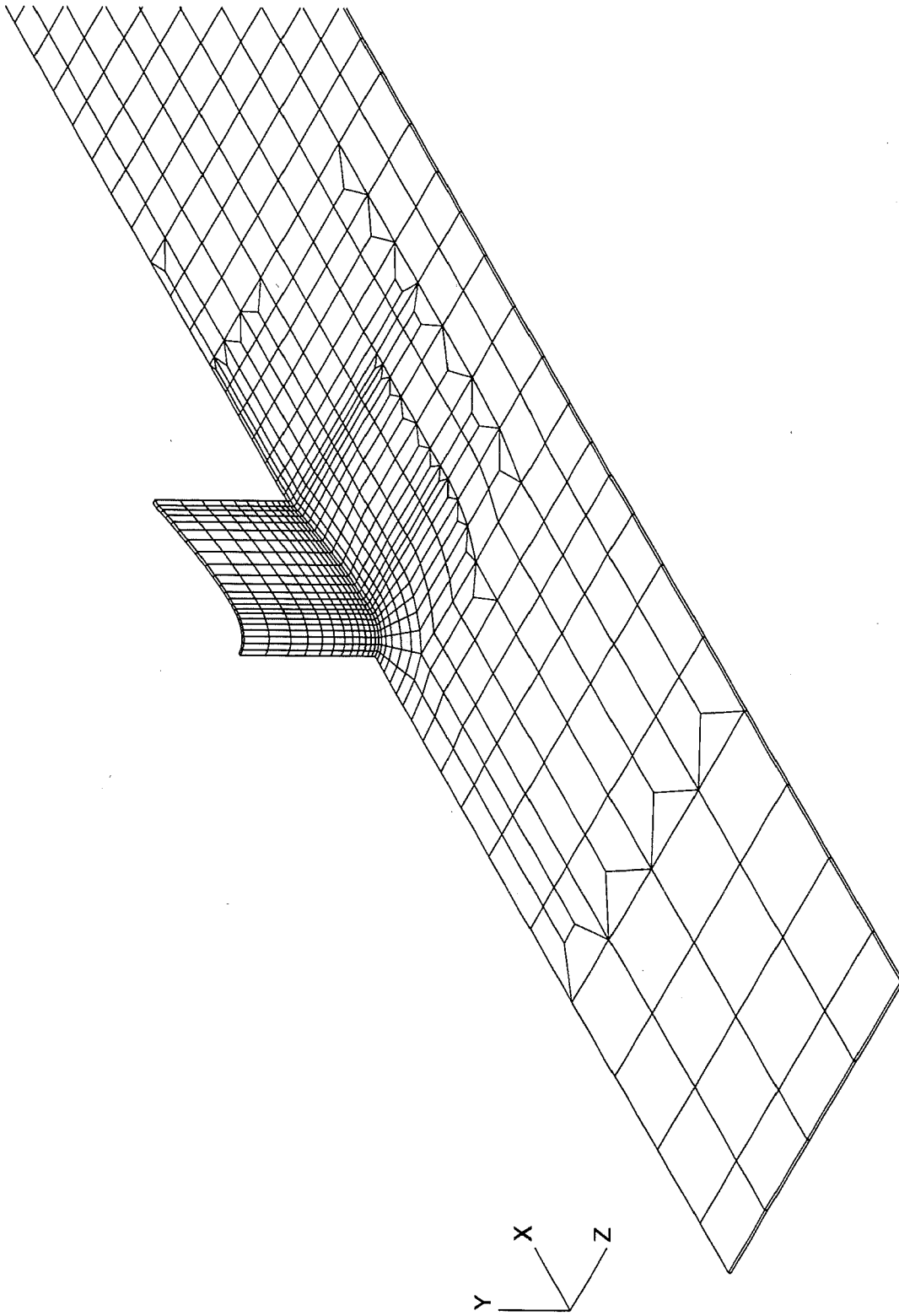
Related publications:

Demirdžić I., Perić M.: Finite volume method for prediction of fluid flow in arbitrarily shaped domains with moving boundaries, *Int. J. Num. Methods in Fluids*, Vol. 10, pp. 771-790 (1990).

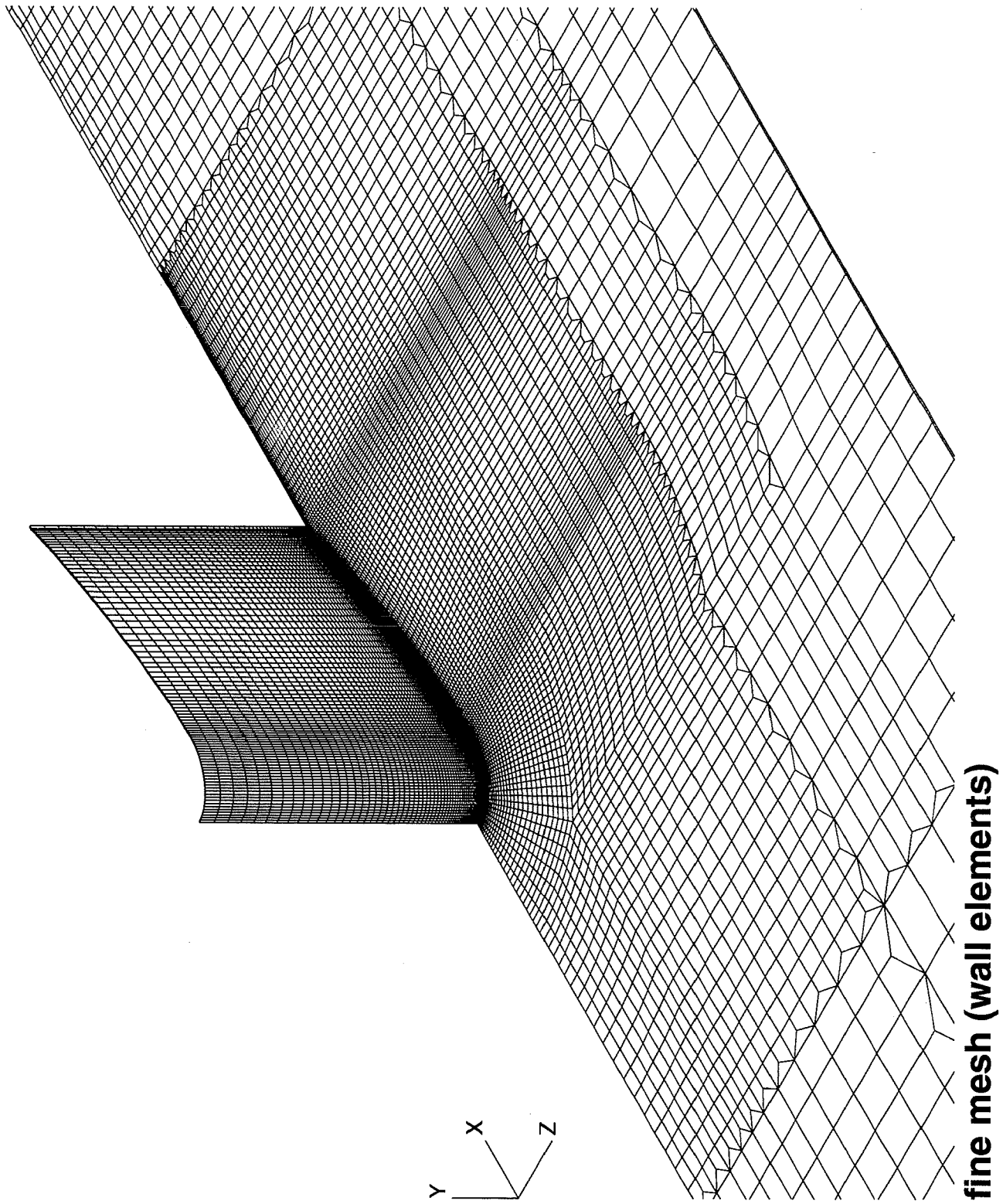
Yakhot V., Orszag S.A., Thangam S., Gatski T.B., Speziale C.G.: Development of turbulence models for shear flows by a double expansion technique, *Phys. Fluids*, A4, No.7, pp. 1510-1520 (1992).

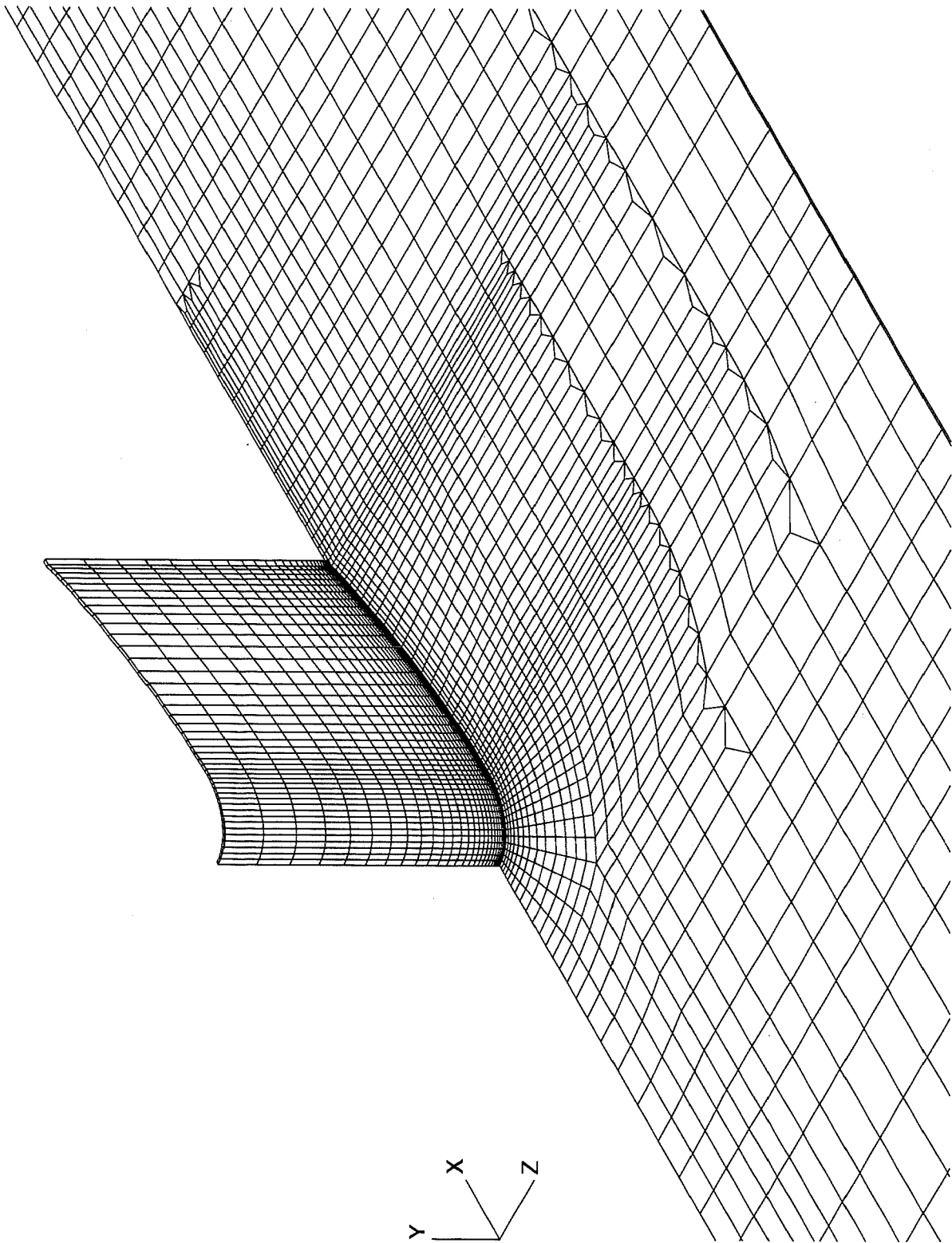
Demirdžić I., Muzaferija S.: Finite volume method for stress analysis in complex domains, *Int. J. Numer. Methods Engineering*, Vol. 37, pp. 3751-3766 (1994).

Demirdžić I., Muzaferija S.: Numerical method for coupled fluid flow, heat transfer and stress analysis using unstructured moving meshes with cells of arbitrary topology, *Comput. Methods Appl. Mech. Eng.*, in print (1995).



coarse mesh (wall elements)





middle mesh (wall elements)

Description of numerical methodology for test case1 [a, b and c]

Originators: Zaky (El-Said Mohamed Zaky Barghouth)

Affiliation: Institute for Hydromechanics, University of Karlsruhe,
Kaiserstr. 12 . Postfach 6980, D-76128 Karlsruhe, Germany

General description:

Code: FAST2D (Flow Analysis Simulation Tool of 2-Dimensions)

- 2D Finite-volume Navier-Stokes code for calculating 2D or axisymmetric flows with or without swirling,
- designed for use of non-orthogonal, curvilinear, boundary-fitted numerical grids,
- strong conservation form of the governing equations,
- cartesian velocity and tensor components,
- non-staggered variable arrangement, with cell-face velocities determined by momentum interpolation,
- pressure-correction method (SIMPLEC) for pressure-velocity coupling,
- The equations are linearised and solved sequentially using the strongly implicit procedure (SIP) of Stone.
- used relaxation factors: velocities and viscosity:0.6; kinetic energy and its dissipation rate:0.5; pressure and pressure correction:1.0;

Convection scheme:

Hybrid central/upwind differencing scheme

Mesh:

Structured quadrilateral smoothly spaced ($0.93 < x_i/x_{i+1} < 1.07$) mesh.

Case a/b: developing flow: 101 * 121 nodes, developed flow: 81 * 81 nodes;

Case c: 81 * 81 nodes.

Turbulence model:

Standard $k - \epsilon$ turbulence model (Launder and Spalding, 1974)

with $C_\mu = 0.09$, $C_{1\epsilon} = 1.44$, $C_{2\epsilon} = 1.92$, $\sigma_k = 1$, $\sigma_\epsilon = 1.3$

Near wall treatment:

Two-layer model (Rodi, 1991):

The viscosity-affected near-wall region is resolved with the one-equation model of Norris and Reynolds (1975) while the outer region is determined with the standard $k-\epsilon$ model. The two model components are matched at locations where the damping function $f_\mu = 0.95$ or $\mu_t/\mu = 36$ which corresponds to $y^+ = 80 - 90$. In the one-equation model the turbulent kinetic energy k is calculated with the k equation of the $k-\epsilon$ model while the eddy-viscosity μ_t and the dissipation rate ϵ are calculated by

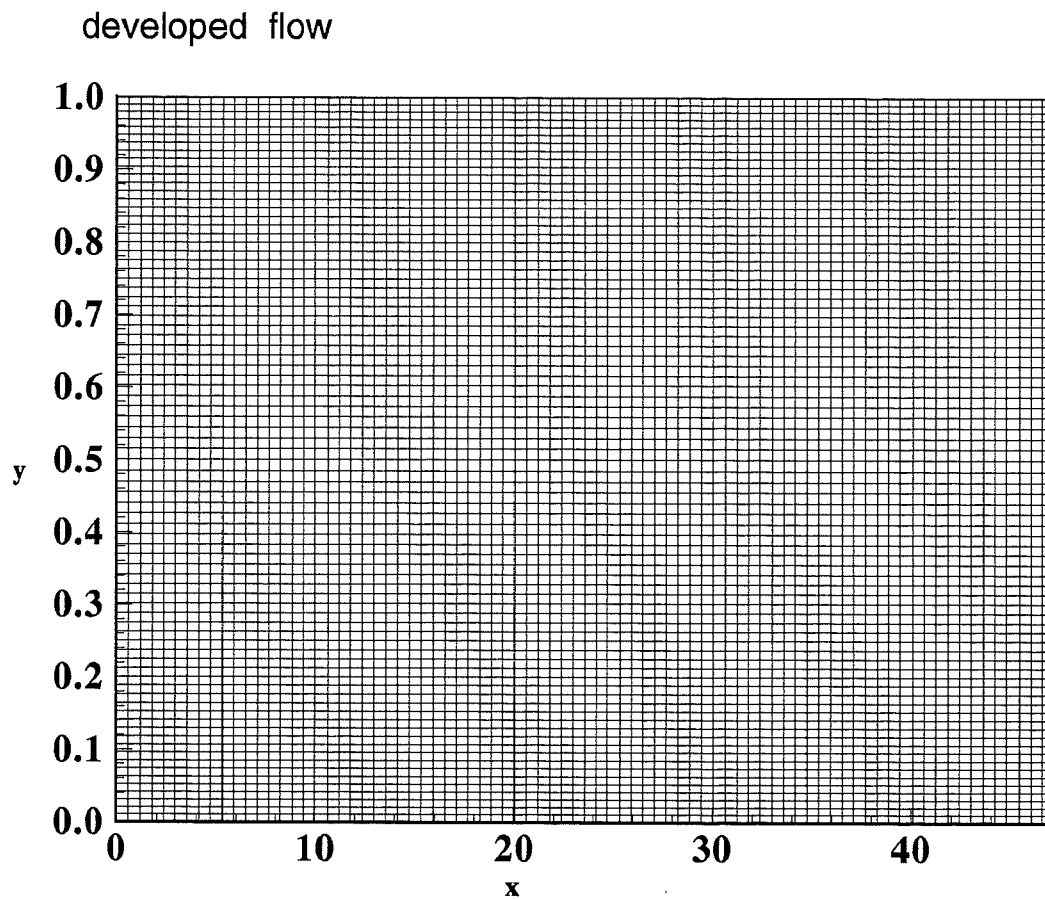
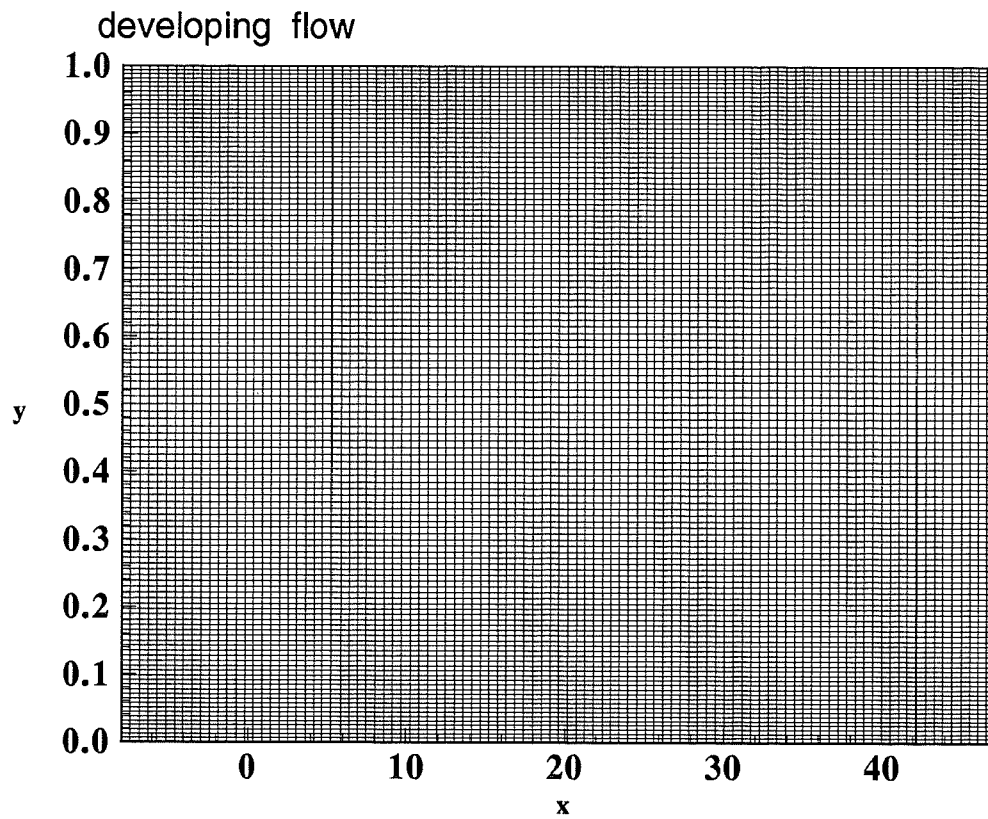
$$\mu_t = \rho f_\mu C'_\mu \sqrt{k} L \quad , \quad \epsilon = \frac{k^{3/2}}{L} \left(1 + \frac{\mu C_\epsilon}{\sqrt{k} L \rho} \right)$$

$$\text{where } f_{\mu} = 1 - \exp(-0.0198 R_y), \quad R_y = \frac{\sqrt{k} y_n \rho}{\mu}$$
$$C'_{\mu} = 0.084 \quad C_{\epsilon} = 13.2 \quad L = C_D \kappa y_n, \quad C_D = 6.41, \quad \kappa = 0.41$$

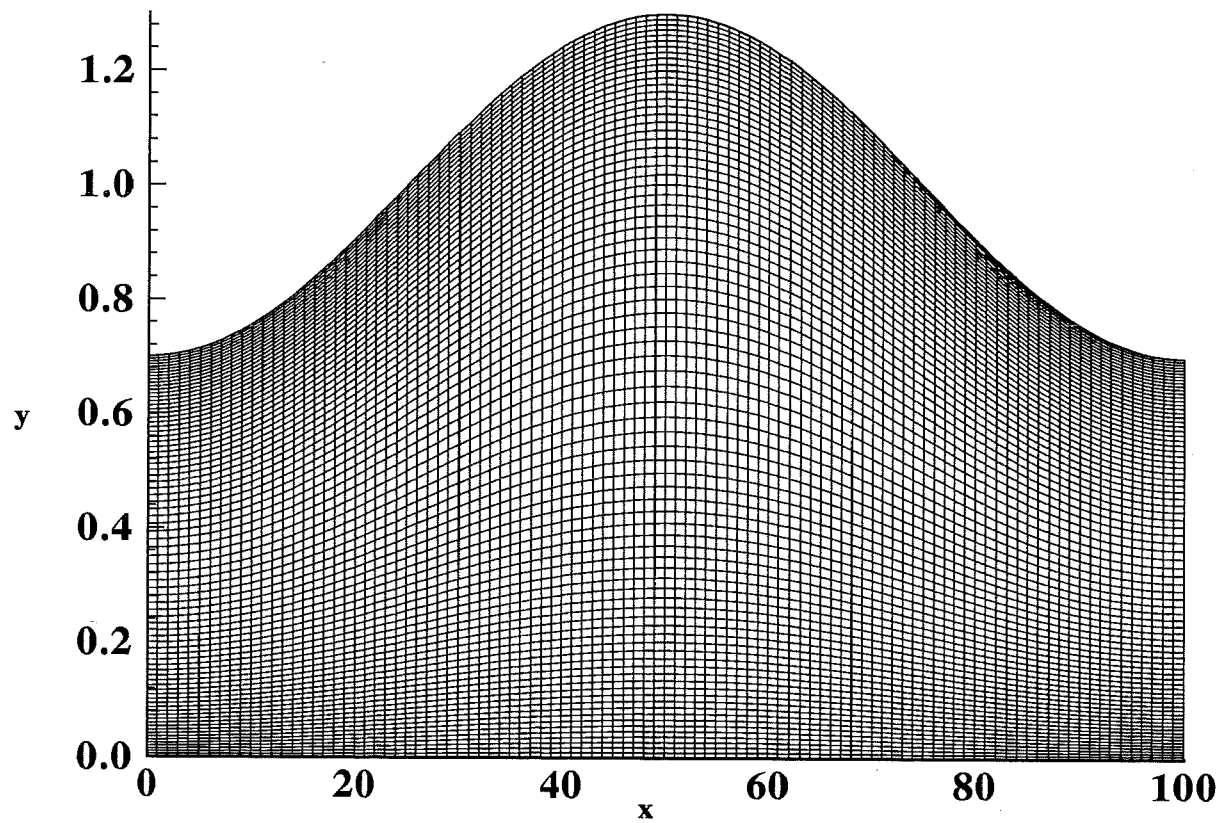
Related publications/reports:

1. Fletcher, C.A.J., 1988, "Computational Techniques for Fluid Dynamics", Springer-Verlag, Vol.1, Chapter 6.
2. Launder, B.P. and Spalding, D.P., 1974, "The numerical computation of turbulent flows", Comput. Meths. Appl. Mech. Eng., Vol.3, pp.269-289.
3. Majumdar, S., 1986, "Development of a finite-volume procedure for prediction of fluid flow problems with complex irregular boundaries", Report SFB 210/T/29, University of Karlsruhe.
4. Rodi, W., Majumdar, S. and Schönung, B., 1989, "Finite-volume method for two-dimensional incompressible flows with complex boundaries", Comput. Meths. Appl. Mech. Eng. Vol.75, pp.369-392.
5. Stone, H.L., 1968, "Iterative solution of implicit approximation multidimensional partial differential equations", SIAM J. on Num. Analysis, pp.530-558.
6. Van Doormal, J.P. and Raithby, G.D., 1984, "Enhancements of the SIMPLE method for predicting incompressible fluid flow", Numerical Heat transfer, Vol.7, pp.147-163.
7. Rodi, W., 1991, "Experience with two-layer models combining the k- ϵ model with a one-equation model near the wall," AIAA 91-0216.

Grids for test case 1 a/b



Grid for test case 1 c (wavy fixed wall)



Description of numerical methodology for test case 2 [a and b]

Originators: Tobias Buchal (Tobias.Buchal@bau-verm.uni-karlsruhe.de)

Affiliation: Institute for Hydromechanics, University of Karlsruhe,
Kaiserstr. 12 . Postfach 6980, D-76128 Karlsruhe, Germany

General description:

Code: FAST2D (Flow Analysis Simulation Tool of 2-Dimensions)

- 2D Finite-volume Navier-Stokes code for calculating 2D or axisymmetric flows with or without swirling,
- designed for use of non-orthogonal, curvilinear, boundary-fitted numerical grids,
- strong conservation form of the governing equations,
- cartesian velocity and tensor components,
- non-staggered variable arrangement, with cell-face velocities determined by momentum interpolation,
- pressure-correction method (SIMPLEC) for pressure-velocity coupling,
- The equations are linearised and solved sequentially using the strongly implicit procedure (SIP) of Stone.
- used relaxation factors: velocities and viscosity: 0.8; kinetic energy and its dissipation rate: 0.7; pressure and pressure correction: 1.0;

Convection scheme:

Hybrid central/upwind differencing scheme

HLP (Hybrid linear/parabolic Approximation; Zhu 1991)

Mesh:

Structured quadrilateral smoothly spaced ($0.93 < x_i/x_{i+1} < 1.07$) mesh.

Wall-function: single hill: 101 * 121 nodes ; periodic configuration: 153 * 225 nodes

12 < y^+ < 60 at the first interior node at inlet

two-layer model: 153 * 225 nodes. (for configuration a and b)

$y^+ < 1$ at the first interior node at inlet

Turbulence model:

Standard $k - \epsilon$ turbulence model (Launder and Spalding, 1974)

with $C_\mu = 0.09$, $C_{1\epsilon} = 1.44$, $C_{2\epsilon} = 1.92$, $\sigma_k = 1$, $\sigma_\epsilon = 1.3$

Near wall treatment:

standard wall-function (Launder and Spalding, 1974):

The resultant wall shear stress $\vec{\tau}_w$ is related to the flow velocity vector \vec{V} at near-wall point P by

$$\vec{\tau}_w = -\lambda_w \vec{V}_P \quad \text{with} \quad \lambda_w = \begin{cases} \rho C_\mu^{1/4} \sqrt{k_P} \kappa / \ln(E y_P^+) & \text{if } y_P^+ \geq 11.6 \\ \mu / y_P & \text{otherwise} \end{cases}$$

where

$$y_P^{\dagger} = \rho C_{\mu}^{1/4} \sqrt{k_P} y_P / \mu, \quad \kappa = 0.41, \quad E = 8.43$$

The diffusive flux of k is set to zero at the wall. The near-wall of the generation G and the dissipation rate ϵ are determined from

$$G_P = \frac{\tau_w^2}{\kappa \mu y_P^{\dagger}}, \quad \epsilon_P = \frac{C_{\mu}^{3/4} k_P^{3/2}}{\kappa y_P}$$

Two-layer model (Rodi, 1991):

The viscosity-affected near-wall region is resolved with the one-equation model of Norris and Reynolds (1975) while the outer region is determined with the standard k - ϵ model. The two model components are matched at locations where the damping function $f_{\mu} = 0.95$ or $\mu_t/\mu = 36$ which corresponds to $y^{\dagger} = 80 - 90$. In the one-equation model the turbulent kinetic energy k is calculated with the k equation of the k - ϵ model while the eddy-viscosity μ_t and the dissipation rate ϵ are calculated by

$$\mu_t = \rho f_{\mu} C'_{\mu} \sqrt{k} L, \quad \epsilon = \frac{k^{3/2}}{L} \left(1 + \frac{\mu C_{\epsilon}}{\sqrt{k} L \rho} \right)$$

$$\text{where } f_{\mu} = 1 - \exp(-0.0198 R_y), \quad R_y = \frac{\sqrt{k} y_n \rho}{\mu}$$

$$C'_{\mu} = 0.084 \quad C_{\epsilon} = 13.2 \quad L = C_D \kappa y_n, \quad C_D = 6.41, \quad \kappa = 0.41$$

Periodic boundary conditions:

In the periodic case 2 additional columns of control-volumes were added at the inlet and outlet. The equations were not solved for these control-volumes, but all variables (velocities, pressure-correction, k and ϵ) were updated by copying their counterparts from inside the solution-domain after each sweep of the solver. To achieve a constant total massflow (the one of the experimental inlet profile), the massflow had to be corrected regularly. The residuals decreased in less than 2.000 iterations nearly to their final values (mass and v-velocity: 1.E-6, u-velocity, k and ϵ : 1.E-4), while the flowfield still changed slightly up to 20.000 iterations. But after 2.000 Iterations the best agreement with the experiment was reached, while for larger iteration numbers the maximum of the u-velocity was shifted to the upper wall. This might be a hint that the measured flowfield was not fully periodic.

Related publications/reports:

1. Fletcher, C.A.J., 1988, "Computational Techniques for Fluid Dynamics", Springer-Verlag, Vol.1, Chapter 6.
2. Launder, B.P. and Spalding, D.P., 1974, "The numerical computation of turbulent flows", Comput. Meths. Appl. Mech. Eng., Vol.3, pp.269-289.
3. Majumdar, S., 1986, "Development of a finite-volume procedure for prediction of fluid flow problems with complex irregular boundaries", Report SFB 210/T/29, University of Karlsruhe.

4. Rodi, W., Majumdar, S. and Schönung, B., 1989, "Finite-volume method for two-dimensional incompressible flows with complex boundaries", *Comput. Meths. Appl. Mech. Eng.* Vol.75, pp.369-392.
5. Stone, H.L., 1968, "Iterative solution of implicit approximation multidimensional partial differential equations", *SIAM J. on Num. Analysis*, pp.530-558.
6. Van Doormal, J.P. and Raithby, G.D., 1984, "Enhancements of the SIMPLE method for predicting incompressible fluid flow", *Numerical Heat transfer*, Vol.7, pp.147-163.
7. Zhu, J., 1991, "A low diffusive and oscillation-free convection scheme", *Communications in Applied Numerical Methods.*, Vol.7, pp.225-232.
8. Rodi, W., 1991, "Experience with two-layer models combining the k- ϵ model with a one-equation model near the wall," *AIAA 91-0216*.

Description of numerical methodology for test case 4

Originators: Tobias Buchal (Tobias.Buchal@bau-verm.uni-karlsruhe.de)

Affiliation: Institute for Hydromechanics, University of Karlsruhe,
Kaiserstr. 12 . Postfach 6980, D-76128 Karlsruhe, Germany

General description:

Code: FAST3D (Flow Analysis Simulation Tool of 3-Dimensions)

- 3D Finite-volume Navier-Stokes code,
- designed for use of non-orthogonal, curvilinear, boundary-fitted numerical grids,
- strong conservation form of the governing equations,
- cartesian velocity and tensor components,
- non-staggered variable arrangement, with cell-face velocities determined by momentum interpolation,
- pressure-correction method (SIMPLEC) for pressure-velocity coupling,
- The equations are linearised and solved sequentially using the strongly implicit procedure (SIP) of Stone.
- used relaxation factors: velocities and viscosity: 0.8; kinetic energy and its dissipation rate: 0.5; pressure and pressure correction: 1.0;

Convection scheme:

Hybrid central/upwind differencing scheme

HLPA (Hybrid linear/parabolic Approximation; Zhu 1991)

Mesh:

Structured quadrilateral smoothly spaced ($0.93 < x_i/x_{i+1} < 1.07$) mesh.
81 * 81 * 81 nodes.

Turbulence model:

Standard $k - \epsilon$ turbulence model (Lauder and Spalding, 1974)
with $C_\mu = 0.09$, $C_{1\epsilon} = 1.44$, $C_{2\epsilon} = 1.92$, $\sigma_k = 1$, $\sigma_\epsilon = 1.3$

Near wall treatment:

standard wall-function (Lauder and Spalding, 1974):

The resultant wall shear stress $\vec{\tau}_w$ is related to the flow velocity vector \vec{V} at near-wall point P by

$$\vec{\tau}_w = -\lambda_w \vec{V}_P \quad \text{with} \quad \lambda_w = \begin{cases} \rho C_\mu^{1/4} \sqrt{k_P} \kappa / \ln(E y_P^+) & \text{if } y_P^+ \geq 11.6 \\ \mu / y_P & \text{otherwise} \end{cases}$$

where

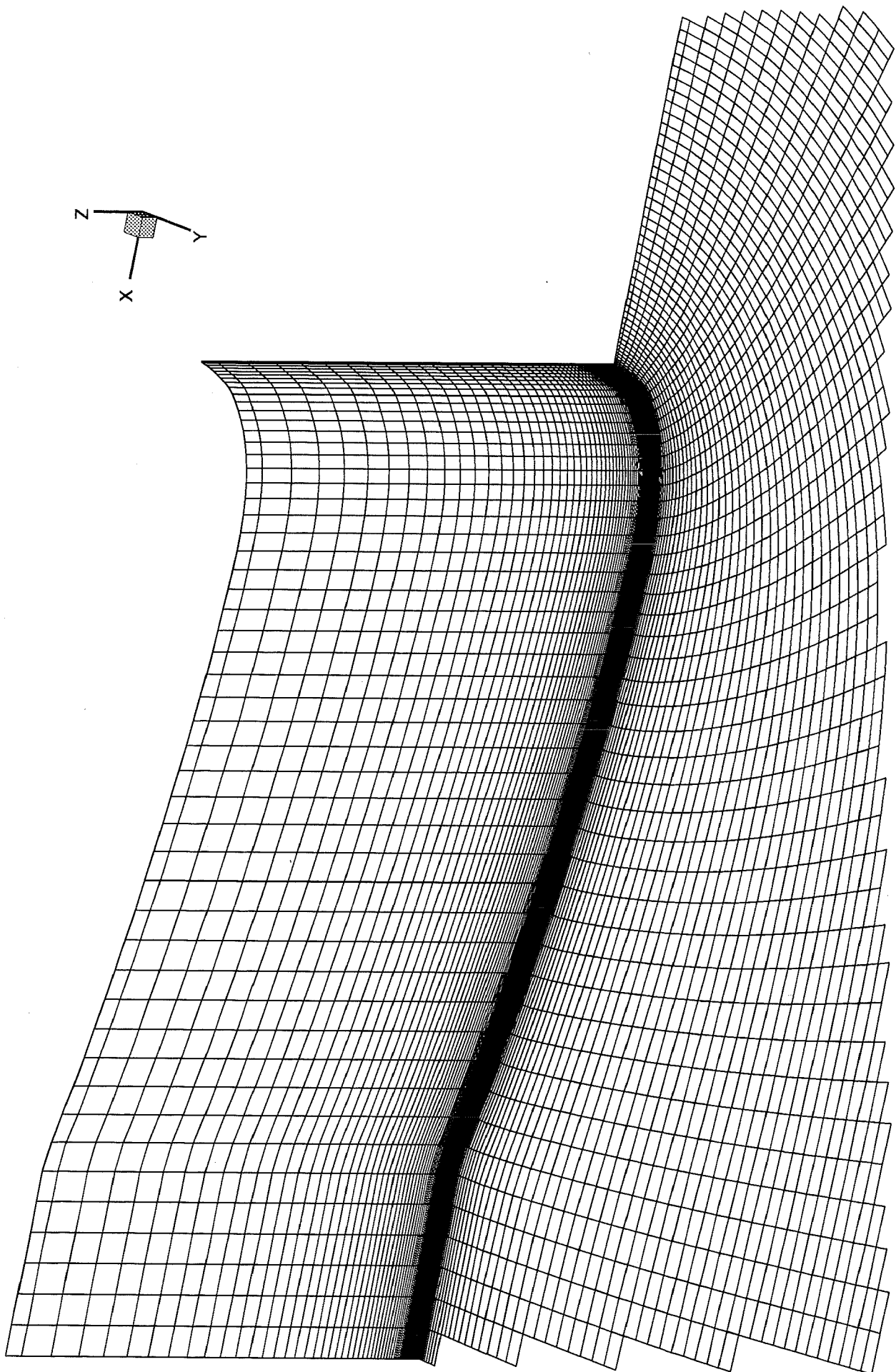
$$y_P^+ = \rho C_\mu^{1/4} \sqrt{k_P} y_P / \mu, \quad \kappa = 0.41, \quad E = 8.43$$

The diffusive flux of k is set to zero at the wall. The near-wall of the generation G and the dissipation rate ϵ are determined from

$$G_P = \frac{\tau_w^2}{\kappa \mu y_P^+} \quad , \quad \epsilon_P = \frac{C_\mu^{3/4} k_P^{3/2}}{\kappa y_P}$$

Related publications/reports:

1. Fletcher, C.A.J., 1988, "Computational Techniques for Fluid Dynamics", Springer-Verlag, Vol.1, Chapter 6.
2. Launder, B.P. and Spalding, D.P., 1974, "The numerical computation of turbulent flows", Comput. Meths. Appl. Mech. Eng., Vol.3, pp.269-289.
3. Majumdar, S., 1986, "Development of a finite-volume procedure for prediction of fluid flow problems with complex irregular boundaries", Report SFB 210/T/29, University of Karlsruhe.
4. Rodi, W., Majumdar, S. and Schönung, B., 1989, "Finite-volume method for two-dimensional incompressible flows with complex boundaries", Comput. Meths. Appl. Mech. Eng. Vol.75, pp.369-392.
5. Stone, H.L., 1968, "Iterative solution of implicit approximation multidimensional partial differential equations", SIAM J. on Num. Analysis, pp.530-558.
6. Van Doormal, J.P. and Raithby, G.D., 1984, "Enhancements of the SIMPLE method for predicting incompressible fluid flow", Numerical Heat transfer, Vol.7, pp.147-163.
7. Zhu, J., 1991, "A low diffusive and oscillation-free convection scheme", Communications in Applied Numerical Methods., Vol.7, pp.225-232.



DESCRIPTION OF NUMERICAL METHODOLOGY FOR TEST CASE 1a,b

Originators:

T.J. Craft

Affiliation:

UMIST

General description:

The flow is computed using an elliptic solver applying fully periodic boundary conditions between the inlet and outlet boundaries.

The code is a modified version of STREAM [4] which is a finite volume solver employing a fully collocated grid arrangement.

A Reynolds stress model is used in the region away from the wall, and is interfaced to a low-Reynolds-number k-e model in the near-wall region. The switch-over between models is placed where the turbulent Reynolds number is around 150.

Convection scheme:

QUICK for mean quantities; MUSCL for turbulence quantities.

Mesh:

120 (cross-stream) x 80 (streamwise)

Turbulence models:

In the fully turbulent region away from the wall, the Gibson-Lauder RSM is used in conjunction with the Craft-Lauder wall-reflection terms. (Referred to as the Basic model in results file) In the near-wall region, the Launder-Sharma k-e model is used.

Near-wall treatment:

Employing a fine near-wall grid, with the Launder-Sharma low-Reynolds number k-e model used in the near-wall layer where viscous effects are important.

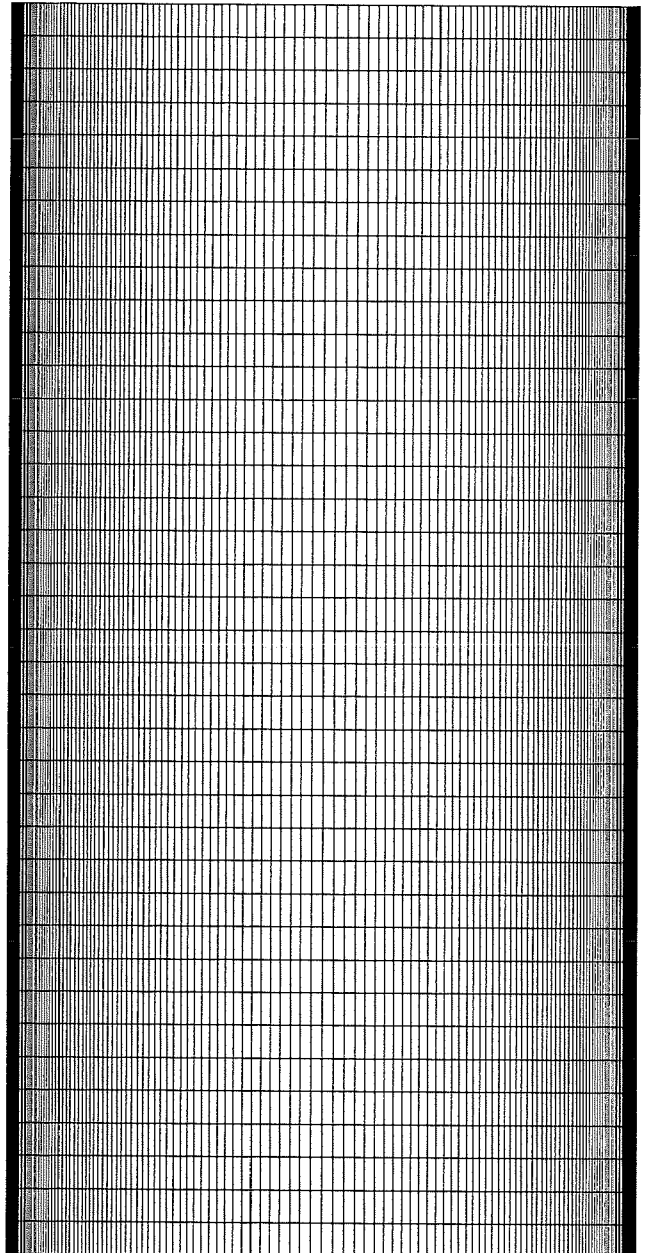
Related publications/reports:

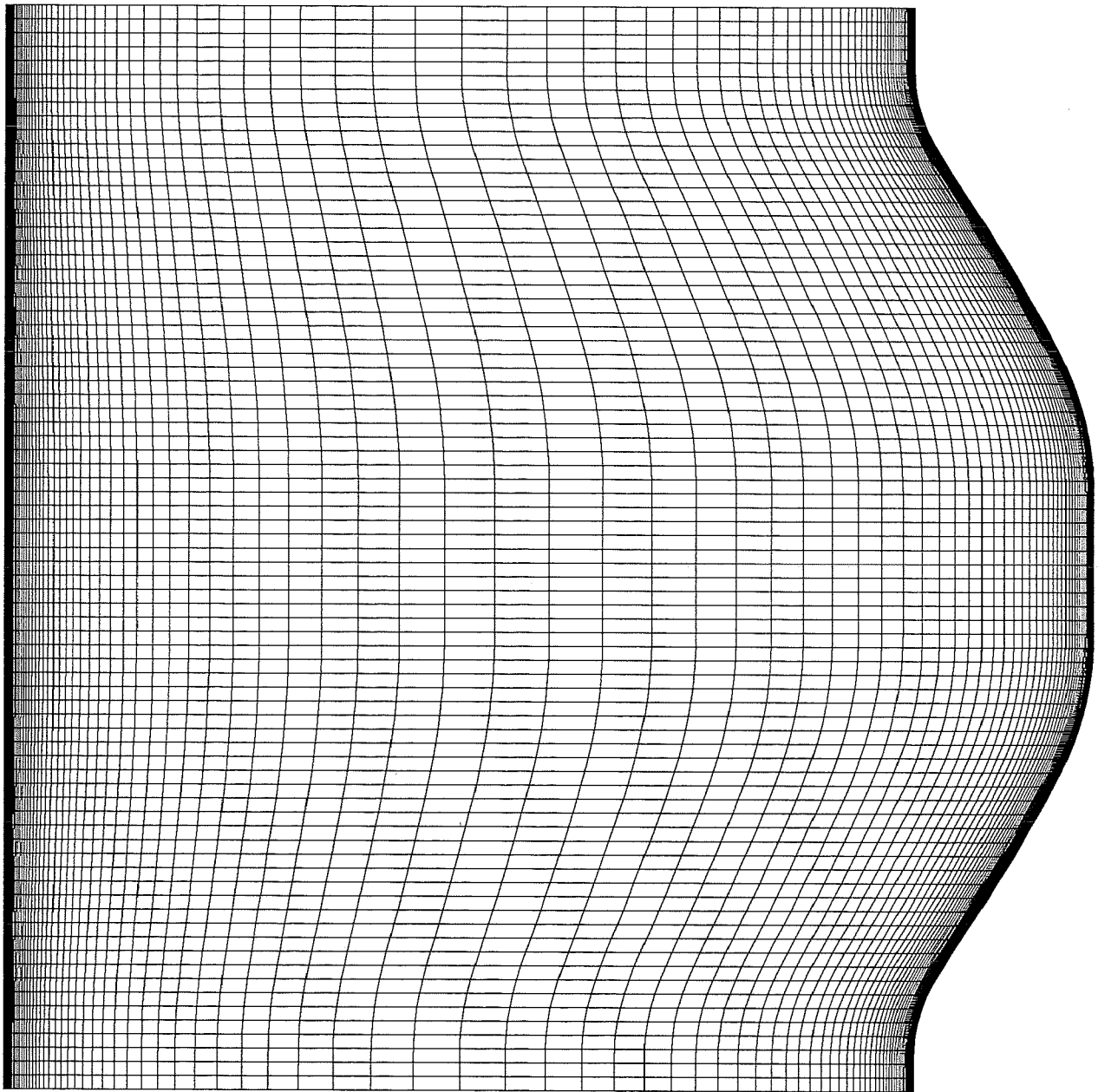
Craft T.J., Launder B.E. 1992 AIAA J. v30 p2970.

Craft T.J. 1991 PhD Thesis, Faculty of Technology, Univ. of Manchester.

Gibson M.M., Launder B.E. 1978 J. Fluid Mech. v86 p491.

Lien F-S., Leschziner M.A. 1993 Turbulent Shear Flows 8, p205.





DESCRIPTION OF NUMERICAL METHODOLOGY FOR TEST CASE 2

 Originator:

F.S. Lien and M.A. Leschziner

 Affiliation:

UMIST

 General Description:

Results have been obtained with the general 2D/3D-flow code STREAM (Lien & Leschziner, 1994). This is based on a non-orthogonal, structured-grid, collocated finite-volume method. The solution is advanced, iteratively, towards the steady state via a pressure-correction algorithm. Convection is approximated by the quadratic QUICK scheme or UMIST/TVD scheme (Lien & Leschziner, 1994), the latter applied principally to the turbulence-model equations. Various turbulence models are embedded in the code, including linear/non-linear eddy-viscosity models and second-moment closure variants. A FAS multigrid convergence acceleration scheme is an optional feature, as is a shock-capturing methodology for transonic conditions, based on density-retardation.

 Convection scheme:

QUICK and UMIST/TVD

 Mesh:

150 × 60 for high-Re models and 150 × 90 for low-Re models

 Turbulence models:

standard high-Re $k - \epsilon$ model, low-Re $k - \epsilon$ model of Lien & Leschziner (1993), high-Re RNG $k - \epsilon$ model of Yakhot et al (1992) and Reynolds-stress model of Gibson & Launder (1978)

 Near-wall treatment:

wall function:

using wall laws constants: $kappa = 0.4187$ and $E=9.7930$ The y^+ value at outlet for high-Re model is 60.0.The y^+ value at outlet for low-Re model is 0.65.

 one-equation model of Wolfshtein (1969):
the interface was chosen at y^+ value at outlet equal to 70.

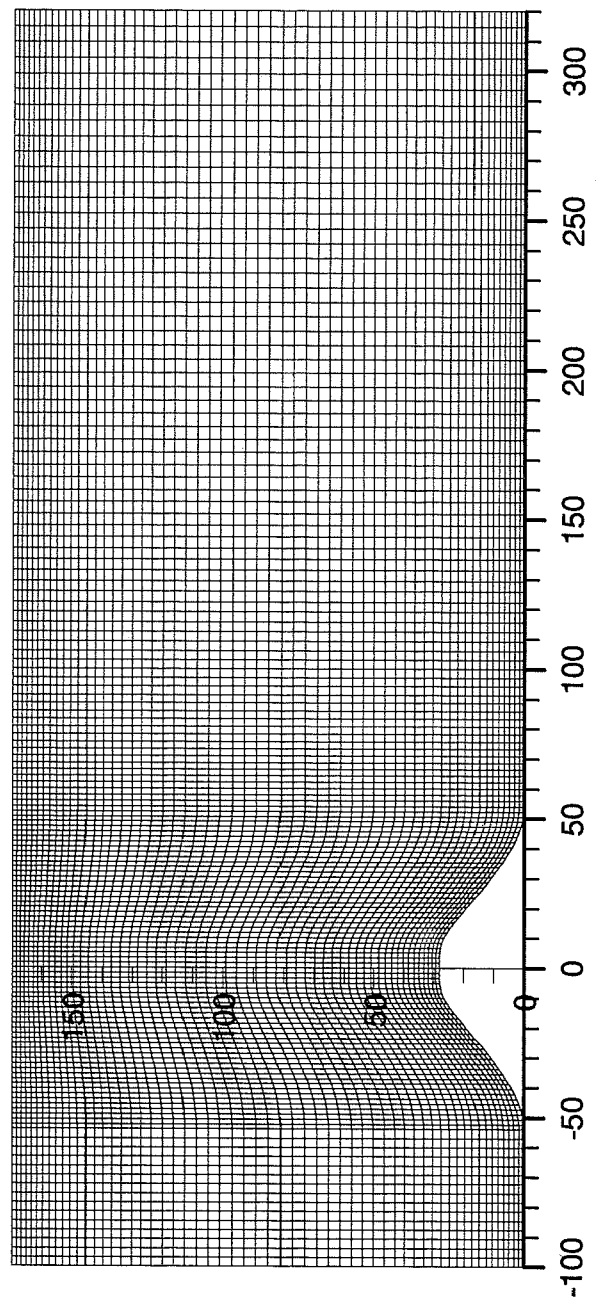
 Related publications/reports:

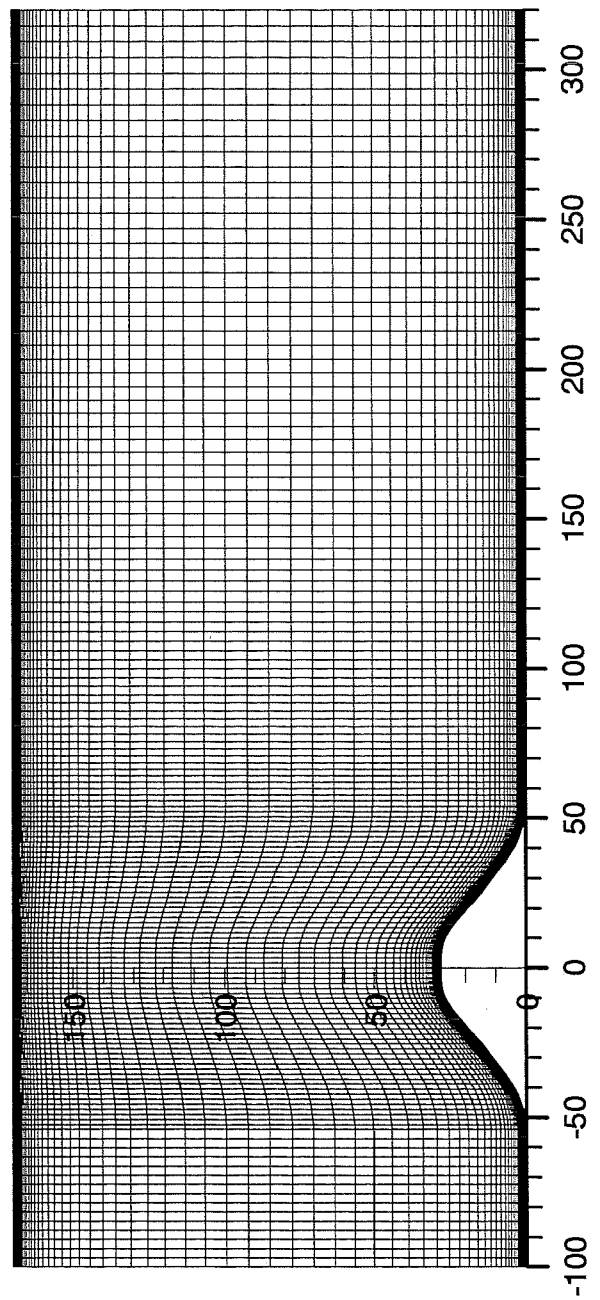
F.S. Lien and M.A. Leschziner (1993), "Computation in Diffusers and Complex Ducts With Non-Orthogonal FV Procedure", **2nd Int. Sym. on Engineering Turbulence Modelling and Measurements**, May 31-June 2, Florence, Italy.

F.S. Lien and M.A. Leschziner (1994), "A General Non-Orthogonal Collocated FV Algorithm for Turbulent Flow at All Speeds Incorporating Second-Moment Closure, Part 1: Computational Implementation and Part 2: Applications", **Comp. Meth. Appl. Mech. Eng.**, Vol. 114, p. 123 and p. 149.

F.S. Lien and M.A. Leschziner (1994), "Multigrid Acceleration for Turbulent Flow with a Non-Orthogonal, Collocated Scheme", **Comp. Meth. Appl. Mech. Eng.**, Vol. 118, p. 351.

F.S. Lien and M.A. Leschziner (1994), "Upstream Monotonic Interpolation for Scalar Transport with Application in Complex Turbulent Flows", **Int. J. Num. Meth. Fluids**, Vol. 19, p. 527.





DESCRIPTION OF NUMERICAL METHODOLOGY FOR TEST CASE 5

Originators:

Peter Hedberg / Chi Hang Chung

Affiliation:

CERCA / McGill University

General description:

A RSM model using a control volume/ finite difference method. Symmetric conditions are applied at the midspan position. Fully developed outflow boundary conditions are applied.

Convection scheme:

J. Zhu, "COMMUNICATIONS IN APPLIED NUMERICAL METHODS", VOL 7, 225-232 (1991)

Mesh:

Structured, 148 X 30 X 25 (longitudinal, transverse, spanwise).

Longitudinal

upstream 40 regularly spaced control volumes in the bend 30 regularly spaced control volumes downstream 78 control volumes (non regular)

Transverse

2 sets of geometrically increasing control volumes from walls, symmetric about centreline

Spanwise

geometrically increasing control volumes from wall

Turbulence models:

Gibson & Launder "Ground Effects on Pressure Fluctuations in the Atmospheric Boundary Layer", Journal of Fluid Mechanics, Vol 86 pp 491-511 (1978)

Cs=0.22 , C1=1.8 , C2=0.6 , C1w=0.5 , C2w=0.3, Ce1=1.45 , Ce2=1.9 , Ce3=0.16

Near-wall treatment:

wall function

$$k = (u_{\tau})^2 / C_{\tau} \quad u_{\tau} = \text{friction velocity}$$

$$C_{\tau} = (C_{\mu})^{0.5}$$

Kappa = 0.400

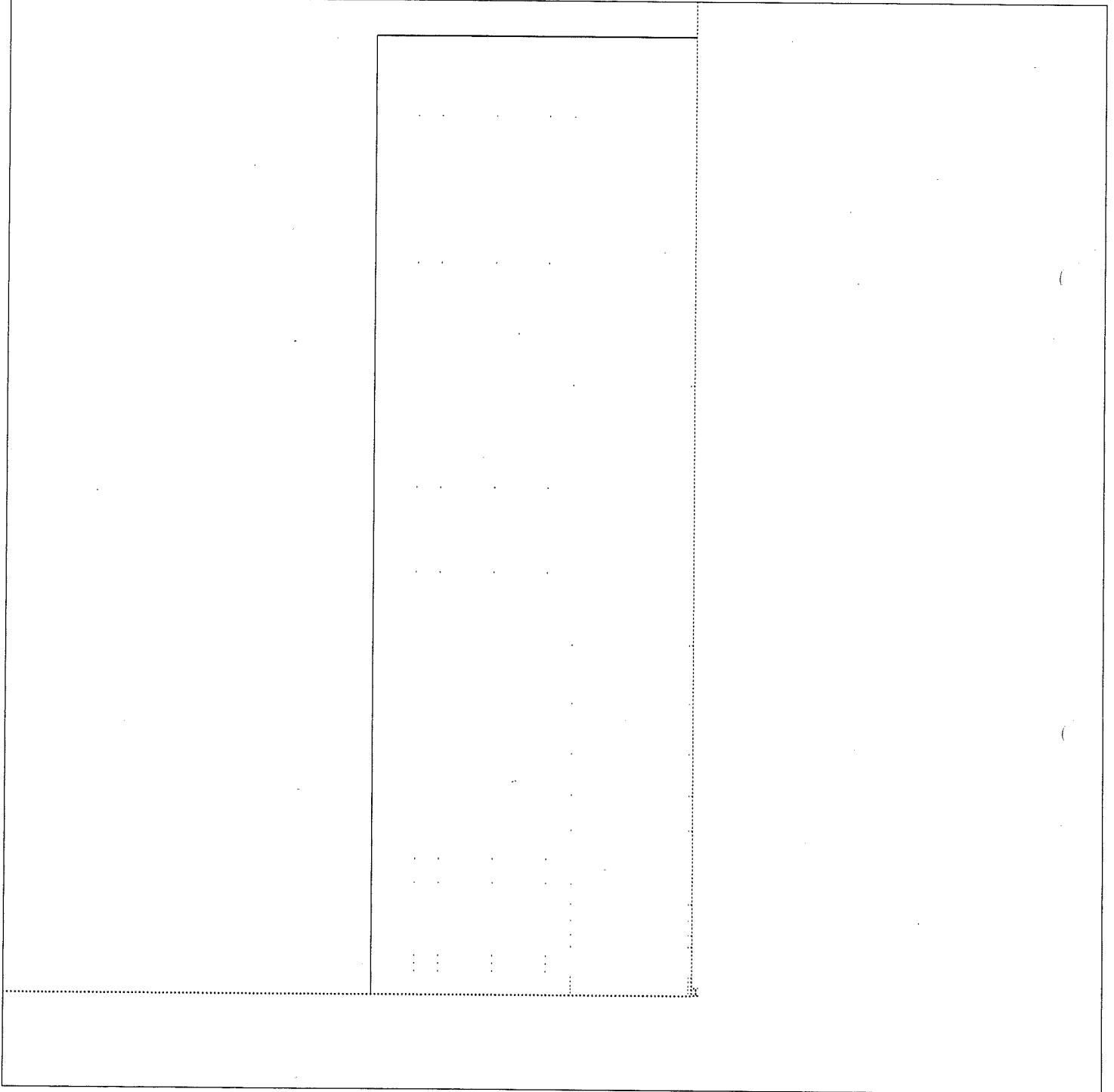
B = 5.05

Stresses in the streamwise / near wall local coordinate system

uu = 1.098 k vv = 0.247 k

-uv = 0.255 k ww = 0.653 k

grid geometry - section view (x direction)



DESCRIPTION FILE FOR CASE 2

1 Originators:

F. A. Castro and J. M. L. M. Palma

2 Affiliation:

IDMEC - Instituto de Engenharia Mecânica, Department of Mechanical Engineering and Industrial Management, Faculty of Engineering, Rua dos Bragas, 4099 Porto, Portugal

3 General description:

Finite differences (finite volume formulation). SIMPLE algorithm for non-staggered mesh in a curvilinear non-orthogonal coordinate system.

- Case 2A: The outlet boundary condition was zero axial gradient for all variables. At the inlet boundary the experimental values of U , V , and k were used. The experimental values of k were obtained using the experimental values of the normal Reynolds stresses. The dissipation of turbulence kinetic energy at the inlet boundary was specified using $\epsilon = 3k^{1.5}/(D_h/2)$, where D_h is the hydraulic diameter. Standard $k - \epsilon$ model of [1].
- Case 2B: Three simulations were performed
 1. Using periodic boundary conditions and the standard $k - \epsilon$ model.
 2. As above, but using a c_μ correction of [2] to account for streamline curvature.
 3. Fixed values (experimental data) for U , V and k at the inlet and outlet boundaries. The ϵ boundary condition was periodic. Standard $k - \epsilon$ model.

4 Convection scheme:

Hybrid

5 Mesh

Along the vertical direction the mesh is concentrated near the bottom boundary.

- Case 2A: The horizontal domain goes from $x = -100$ mm to $x = 600$ mm (321×141 grid nodes). Along the horizontal direction the mesh is concentrated around $x = 0$ mm.
- Case 2B: In all meshes the grid is regularly spaced along the horizontal direction.
 1. 241×161 grid nodes
 2. As above
 3. 181×181 grid nodes

6 Turbulence models:

- Case 2A: Standard $k - \epsilon$ model. The constants of the standard turbulence model are $C1 = 1.44$, $C2 = 1.92$, $c_\mu = 0.09$, $\sigma_k = 1.0$ and $\sigma_\epsilon = 1.22$.
- Case 2B: Three simulations were performed
 1. Standard $k - \epsilon$ model.
 2. Standard $k - \epsilon$ model with a c_μ correction of [2] to account for streamline curvature. The limits of variation of c_μ were 0.03 and 0.12.
 3. Standard $k - \epsilon$ model. Values of k fixed at the inlet and outlet boundaries, according to the experimental data.

7 Near-wall treatment:

At the solid boundaries we use wall functions with a switch criterion of $y^+ = 11.63$. At the first node near the wall it is assumed that the flow is parallel to the wall. In the momentum equations we calculate the shear stress at the wall,

$$\tau_{wall} = \mu \frac{\partial U_{//}}{\partial \eta} \text{ for } y^+ < 11.63 \quad (1)$$

and

$$\tau_{wall} = \rho k c_\mu^{1/2} \text{ for } y^+ \geq 11.63 \quad (2)$$

where $U_{//}$ is the velocity parallel to the wall. In the calculation of the production of k the shear stress at the wall is computed in agreement with equations (1) and (2). The dissipation rate is calculated using,

$$\int \rho \epsilon dV = \frac{\rho k^{3/2} c_\mu^{3/4} u^+}{y} \Delta V \quad (3)$$

where,

$$u^+ = \frac{1}{\kappa} \log(Ey^+) \text{ for } y^+ \geq 11.63 \quad (4)$$

and

$$u^+ = y^+ \text{ for } y^+ < 11.63 \quad (5)$$

with $\kappa = 0.4187$ $E = 9.793$. In the transport equation of ϵ the value in the first node near the wall is prescribed using,

$$\epsilon = \frac{c_\mu^{3/4} k^{3/2}}{\kappa y} \quad (6)$$

8 Periodic boundary conditions:

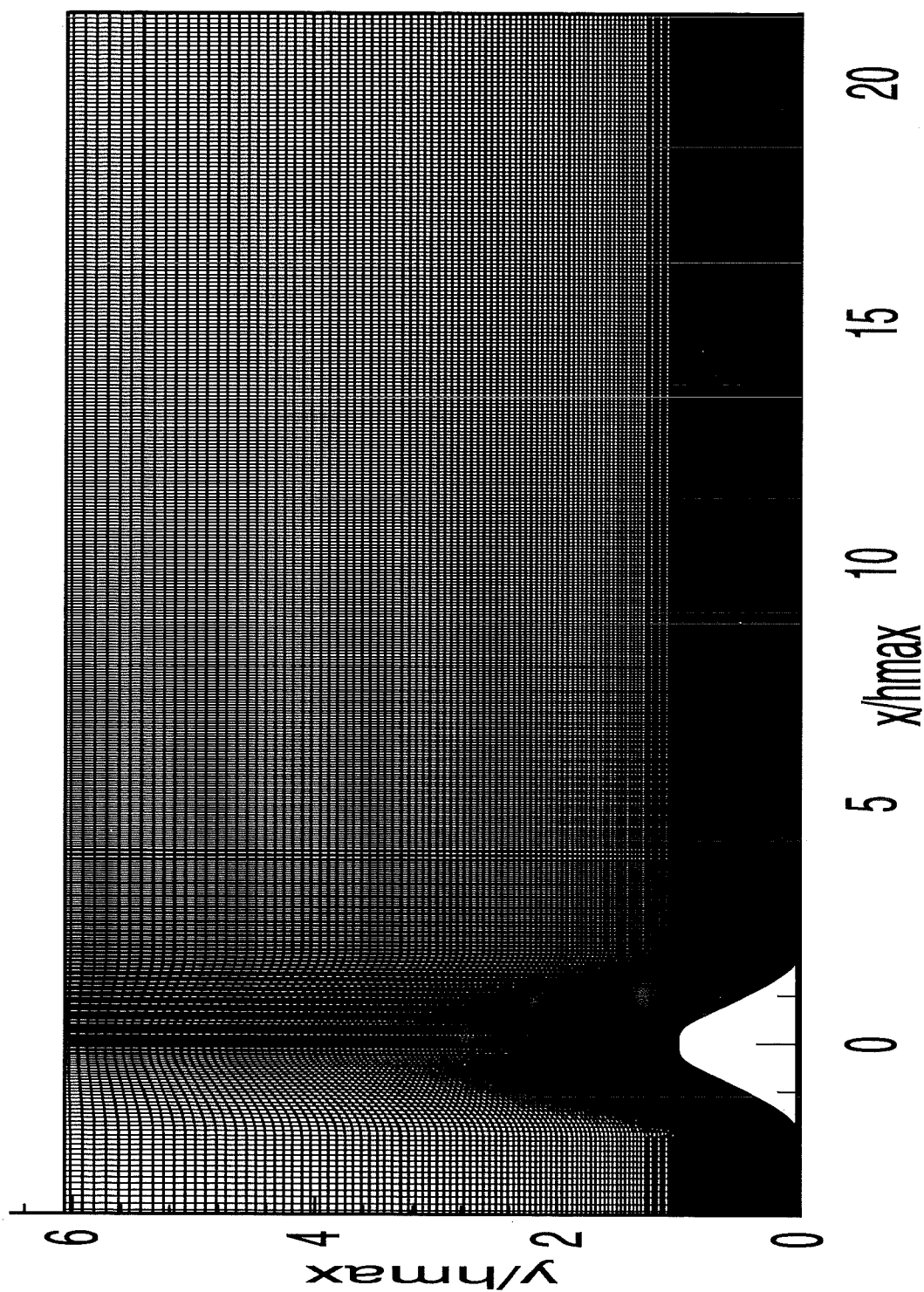
For simulations (1) and (2) of case 2B we use periodic boundary condition for all variables. For these cases the first vertical line of grid nodes ($I=1$) is located to the left of $x = 0$, and the last vertical line of grid nodes ($I=NI$) is located to the right of $x = 126$ mm. NI is the grid dimension in the longitudinal direction. The $I=2$ and $I=NI-1$ indexes correspond to vertical lines of grid nodes passing at $x = 0$ mm and $x = 126$ mm, respectively.

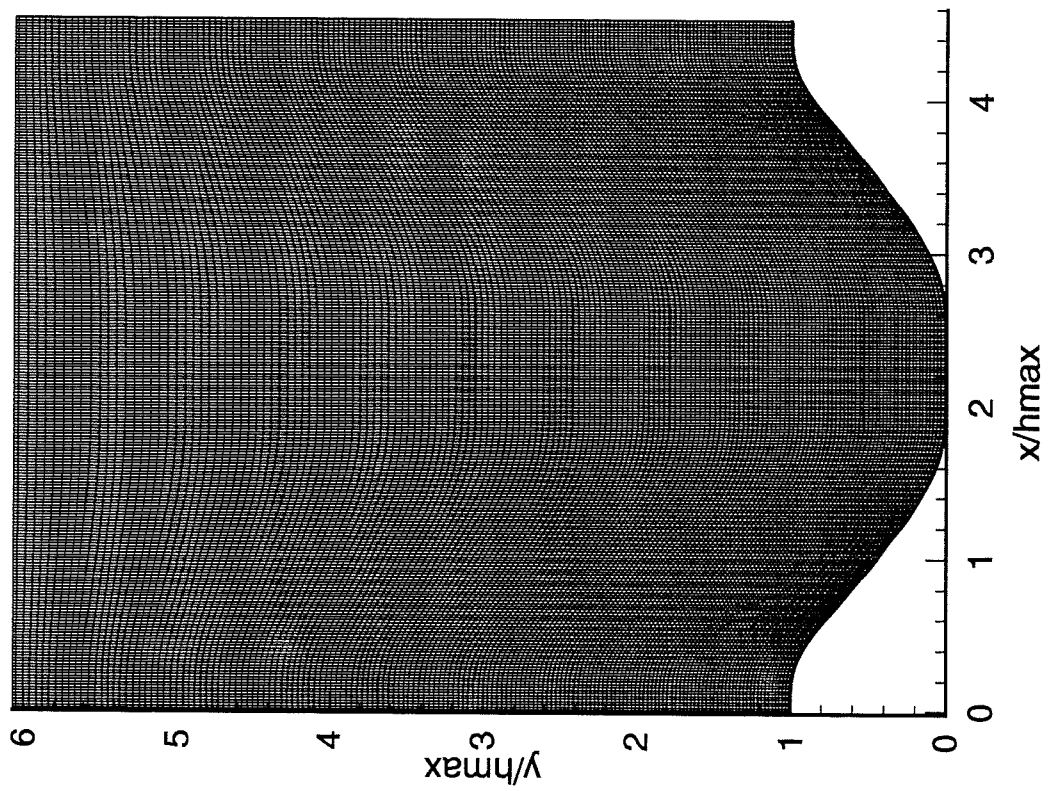
At the beginning of the simulation the experimental data for U , V and k are fixed at $I=1$ and $I=NI$ until a percentual error of 1×10^{-2} is obtained for all variables. During this stage we apply periodic boundary conditions to ϵ and extrapolate the pressure to the boundaries. After the error has decreased to levels below 1×10^{-2} periodic boundary conditions are applied to all variables. This error is the sum of the absolute values of the residual over the all field, and made nondimensional using the inlet fluxes.

The periodic boundary conditions are applied simply by copying the values calculated at $I=NI-2$ to the $I=1$ section and the values calculated at the $I=3$ to the $I=NI$ section, for U , V , k and ϵ . The inlet pressure ($P_{I=1,J}$) is calculated imposing that $P_{I=1,J} - P_{I=2,J} = P_{I=NI-2,J} - P_{I=NI-1,J}$ and the pressure at the outlet boundary ($P_{I=NI,J}$) is calculated imposing that $P_{I=NI-1,J} - P_{I=NI,J} = P_{I=2,J} - P_{I=3,J}$.

References

- [1] B. E. Launder and D. B. Spalding. *Mathematical models of turbulence*. Academic Press Inc. (London) Ltd., 1972.
- [2] M. A. Leschziner and W. Rodi. Calculation of annular and twin parallel jets using various discretization schemes and turbulence-model variations. *Journal of Fluids Engineering*, 103:352-360, 1981.





Developing Flow in a Curved Rectangular Duct (Test Case 5)

Originators:

Hui-Liu ZHANG and Xin ZHANG

Affiliation:

Department of Aeronautics and Astronautics
University of Southampton
Southampton SO17 1BJ, United Kingdom

General description

The CFD software FLOW3D version 3.3 by AEA Industrial Technology, Harwell Laboratory, UK, has been used to predict the flow field in a curved rectangular duct.

Governing equations

The basic set of equations used to describe incompressible turbulent flow are the continuity and Navier-Stokes equations. Applying the so-called Reynolds averaging, we have:

$$\nabla \cdot U = 0, \quad (1)$$

$$\frac{\partial U}{\partial t} + \nabla \cdot (U \otimes U) = \nabla \cdot (\sigma - \overline{u \otimes u}) \quad (2)$$

with

$$\sigma = -\frac{p}{\rho} \delta + \frac{\mu}{\rho} (\nabla U + (\nabla U)^T),$$

where p and ρ are the pressure and density, respectively, μ the molecular viscosity, U the mean fluid velocity and \otimes denotes the tensor product. The Reynolds stresses, $\overline{u \otimes u}$, can be obtained by using different turbulence models.

Reynolds stress turbulence model

In the differential form of the Reynolds stress turbulence model [1], $\overline{u \otimes u}$ satisfies the following equation:

$$\frac{\partial \overline{u \otimes u}}{\partial t} + \nabla \cdot (\overline{u \otimes u} \otimes U) - \nabla \cdot \left(\frac{C_S}{\sigma_{DS}} \frac{k}{\varepsilon} \overline{u \otimes u} (\nabla \overline{u \otimes u})^T \right) = P + \phi - \frac{2}{3} \varepsilon I, \quad (3)$$

where C_S and σ_{DS} are two model constants, and P is the shear stress production given by

$$P = -\overline{u \otimes u} (\nabla U)^T + (\nabla U) \overline{u \otimes u}.$$

The pressure-strain correlation, ϕ , can be divided into two terms, $\phi = \phi_1 + \phi_2$, which are given by:

$$\phi_1 = -C_{1S} \frac{\varepsilon}{k} (\overline{u \otimes u} - \frac{2}{3} k I),$$

$$\phi_2 = -C_{2S} (P - \frac{2}{3} P I)$$

where P is the shear production of turbulence kinetic energy:

$$P = -\overline{u \otimes u} \cdot \nabla U,$$

and C_{1S} and C_{2S} are another two turbulent model constants.

As the turbulence dissipation rate ε and turbulence kinetic energy k appear in the stress equation (3), two equations for ε and k are still required:

$$\frac{\partial \varepsilon}{\partial t} + \nabla \cdot (U \varepsilon) - \nabla \cdot \left(\frac{C_S}{\sigma_\varepsilon} \frac{k}{\varepsilon} \overline{u \otimes u} \nabla \varepsilon \right) = C_1 \frac{\varepsilon}{k} P - C_2 \frac{\varepsilon^2}{k}, \quad (4)$$

$$\frac{\partial k}{\partial t} = \nabla \cdot (U k) - \nabla \cdot \left(\frac{C_S}{\sigma_k} \frac{k}{\varepsilon} \overline{u \otimes u} \nabla k \right) = P - \varepsilon^2, \quad (5)$$

where C_S , σ_ε and σ_k are turbulent model constants. Therefore, Equations (1), (2), (3), (4) and (5) are closed for solving the incompressible turbulent flow.

In the algebraic Reynolds stress Turbulence model [2], Equation (3) is replaced by an algebraic relation:

$$\overline{u \otimes u} = \frac{2}{3} k I + \frac{(1 - C_{2s})k(P - \frac{2}{3}PI)}{\rho(C_{1s} - 1)\epsilon + P} \quad (6)$$

with ϵ and k obtained again from Equations (4) and (5).

Near-wall treatment

To avoid using an excessive number of grid points to resolve the steep velocity gradients near the wall, a wall function is used to relate the velocity to the wall shear stress τ , turbulence kinetic energy k and the distance from the wall y :

$$u^+ = \begin{cases} \frac{1}{\kappa} \log(Ey^+), & \text{when } y^+ > 11.225; \\ \frac{\kappa}{y^+}, & \text{when } y^+ < 11.225, \end{cases} \quad (7)$$

where κ is the Karman constant and

$$u^+ = C_w^{-\frac{1}{4}} \frac{U}{k^{\frac{1}{2}}}, \quad y^+ = C_w^{-\frac{1}{4}} k^{\frac{1}{2}} \frac{y}{(\mu/\rho)}.$$

The standard transport equation for the turbulent kinetic energy k is solved as usual, but the dissipation rate ϵ in the wall region is explicitly determined from a prescribed length-scale distribution:

$$\epsilon = k^{\frac{3}{2}} / C_w^{\frac{3}{4}} y \quad (8)$$

In equation (8) the value of the model constant c_w is listed in Table I, together with all other constants appeared in the turbulence model thus far.

| C_S | σ_{DS} | C_{1S} | C_{2S} | σ_ϵ | σ_k | C_w |
|-------|---------------|----------|----------|-------------------|------------|-------|
| 0.22 | 1.0 | 1.8 | 0.6 | 1.375 | 1.0 | 0.065 |

Table I. Constants in the Reynolds stress turbulence model.

Numerical Implementation

A multi-block structured grid system is applied in the software. The grid is non-orthogonal and non-staggered, with all variables stored at the centers of the grid cells. A total of 163,625 cells have been used in three blocks (15(upstream)x, 30(bend)x and 40(downstream)x35x55, respectively) and the size of the smallest cell in the yz -plane is $0.00154H \times 0.00052H$, see Figure 1 for the mesh on one section. The discretisation of the advection-diffusion type equations (1)-(5) is straightforward on the non-staggered grid. The diffusion terms are discretised by the central differencing, while the convection terms by the HYBRID differencing. A fully implicit backward difference time stepping procedure is implemented to the time terms. After discretisation, the sets of linearised difference equations are solved iteratively with a line relaxation algorithm.

The treatment of pressure is different from the other governing equations, since it does not obey a transport equation. In fact, the momentum equations are substituted into the continuity equation and thus a Poisson equation governing the variable pressure can be derived. The SIMPLE algorithm was used to give the pressure and velocity corrections.

Inlet boundary conditions

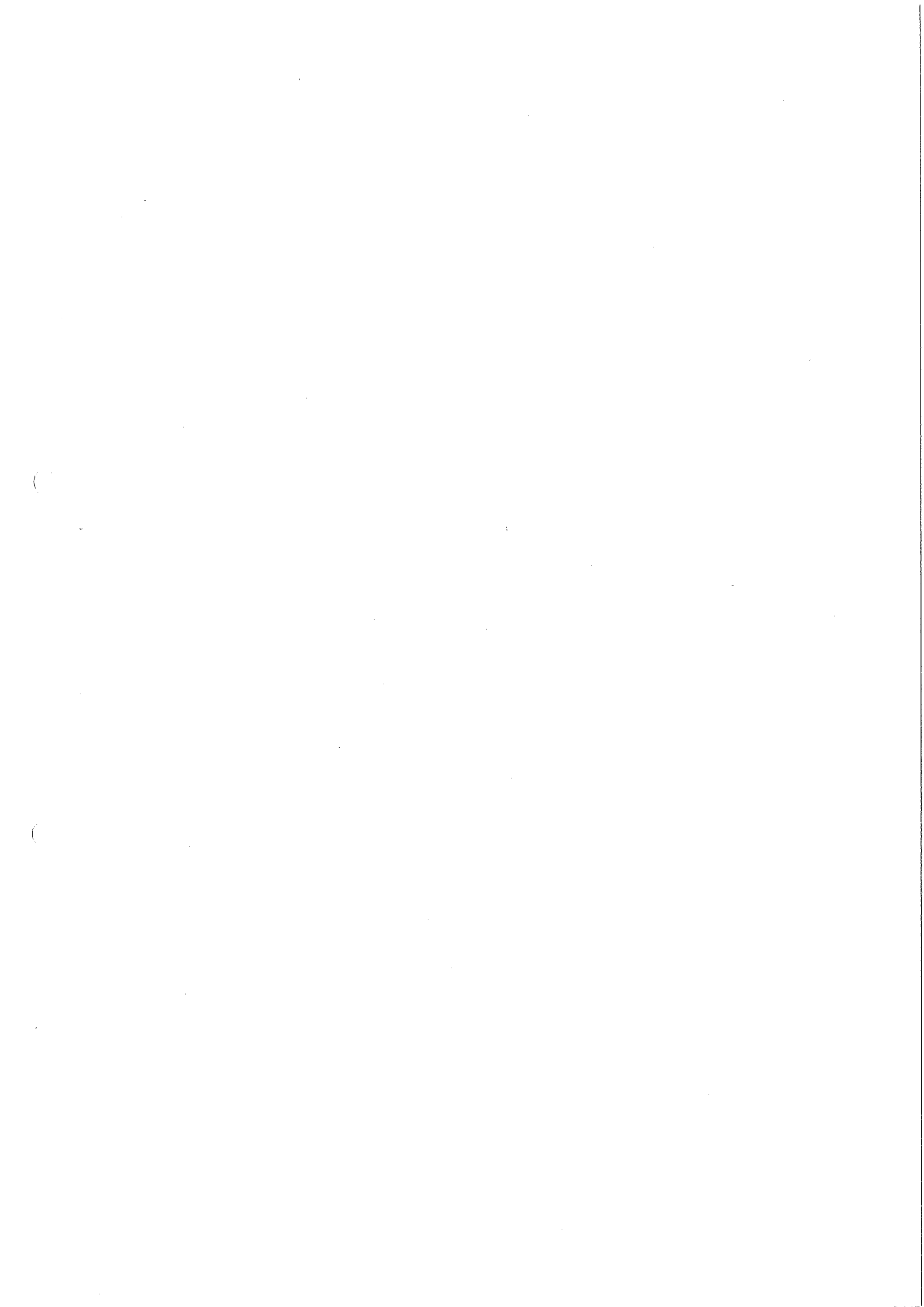
The incoming flow measured at the section $U1$ in the experiments was used as the inlet boundary conditions in the computation.

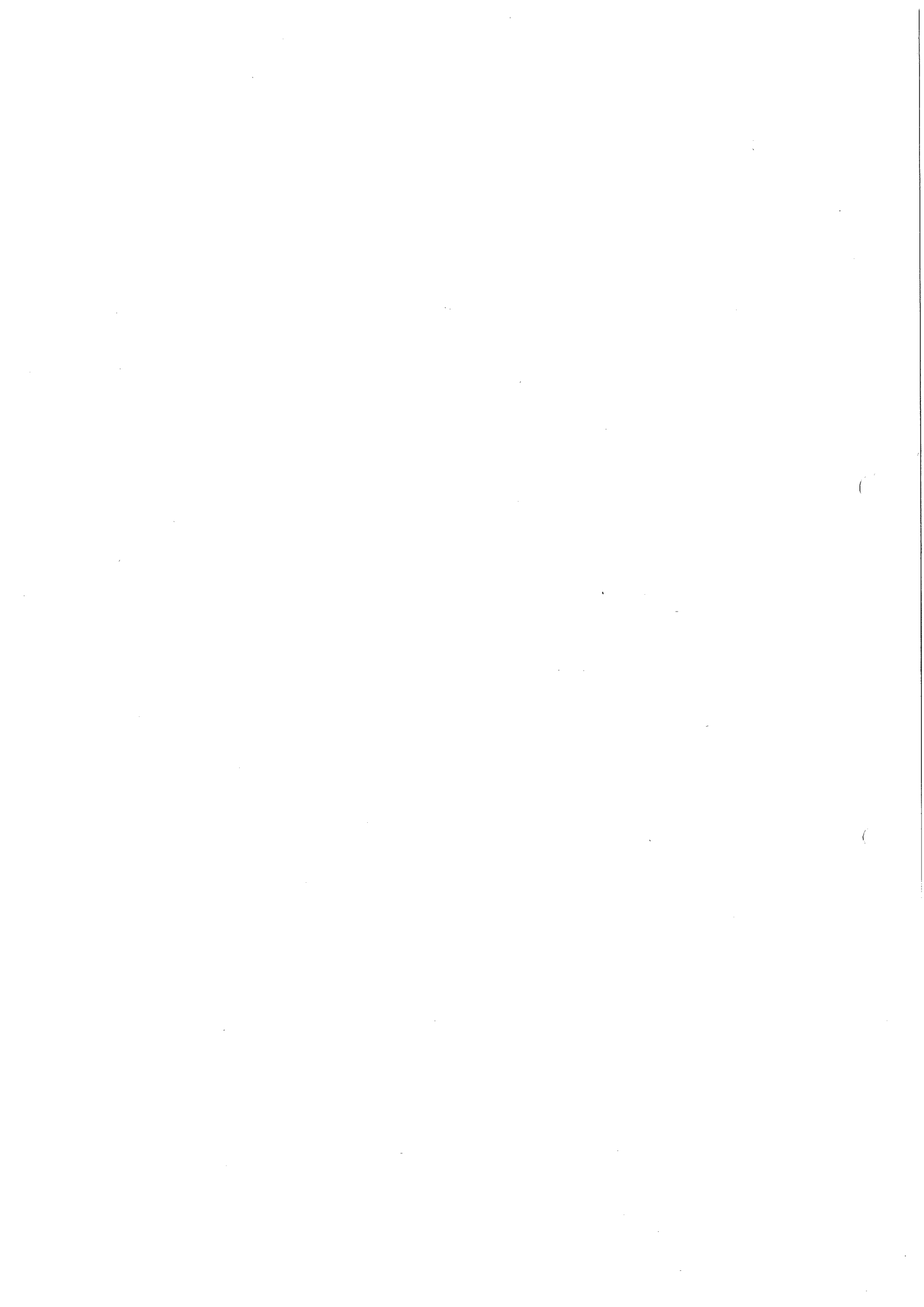
Computer resources

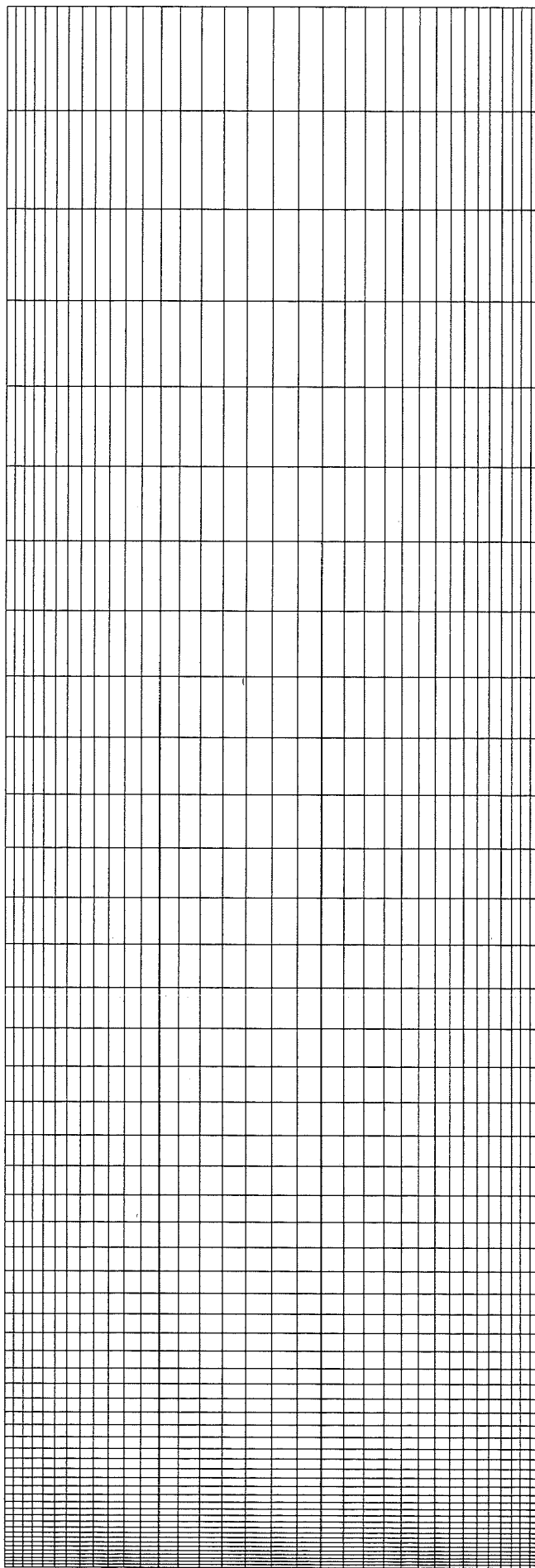
The software was installed on a SUN SPARC 2 workstation. Totally 500 iterations are necessary to reduce all residuals by three orders of magnitude within about 36 hours CPU time (260 seconds for each iteration). Total real, integer and character workspaces used are about 21.5mB, 7.5mB and 0.5kB, respectively.

References

- [1] Clarke, D.S. and Wilkes, N.S. (1989): The Calculation of Turbulent Flows in Complex Geometries Using a Differential Stress Model, *AERE-R 13428*, Harwell Laboratory Report
- [2] Clarke, D.S. and Wilkes, N.S. (1987): Turbulent Flow Predictions Using Algebraic Stress Models, Using a Differential Stress Model, *AERE-R 12694*, Harwell Laboratory Report







DESCRIPTION OF THE NUMERICAL METHODOLOGY FOR TEST CASE 4

Originator:

A. Ruprecht
Institut für Strömungsmechanik und Hydraulische
Strömungsmaschinen
Universität Stuttgart
Pfaffenwaldring 10, 70550 Stuttgart

Numerical method:

Galerkin-finite-element method

Type of elements: tri-linear 8-node brick elements with constant pressure
segregated solution algorithm

ILU-preconditioned conjugate gradient method (BI-CGSTAB2) for non-symmetric sparse matrices [1]
Streamline upwinding.

Mesh:

Unstructured mesh with 340,000 nodes.

Turbulence models:

Modified k-epsilon model, hybrid model [2], which is a combination of standard k-epsilon model and the k-epsilon model with Kato-Lauder correction [3].

The weighting factor was chosen to be 0.85 similar to [2].

Near wall treatment:

Two-layer approximation according to Mohammadi [4].

Computer:

CRAY C94

Time (4 processors): approximately 8 h starting from a 2D solution.

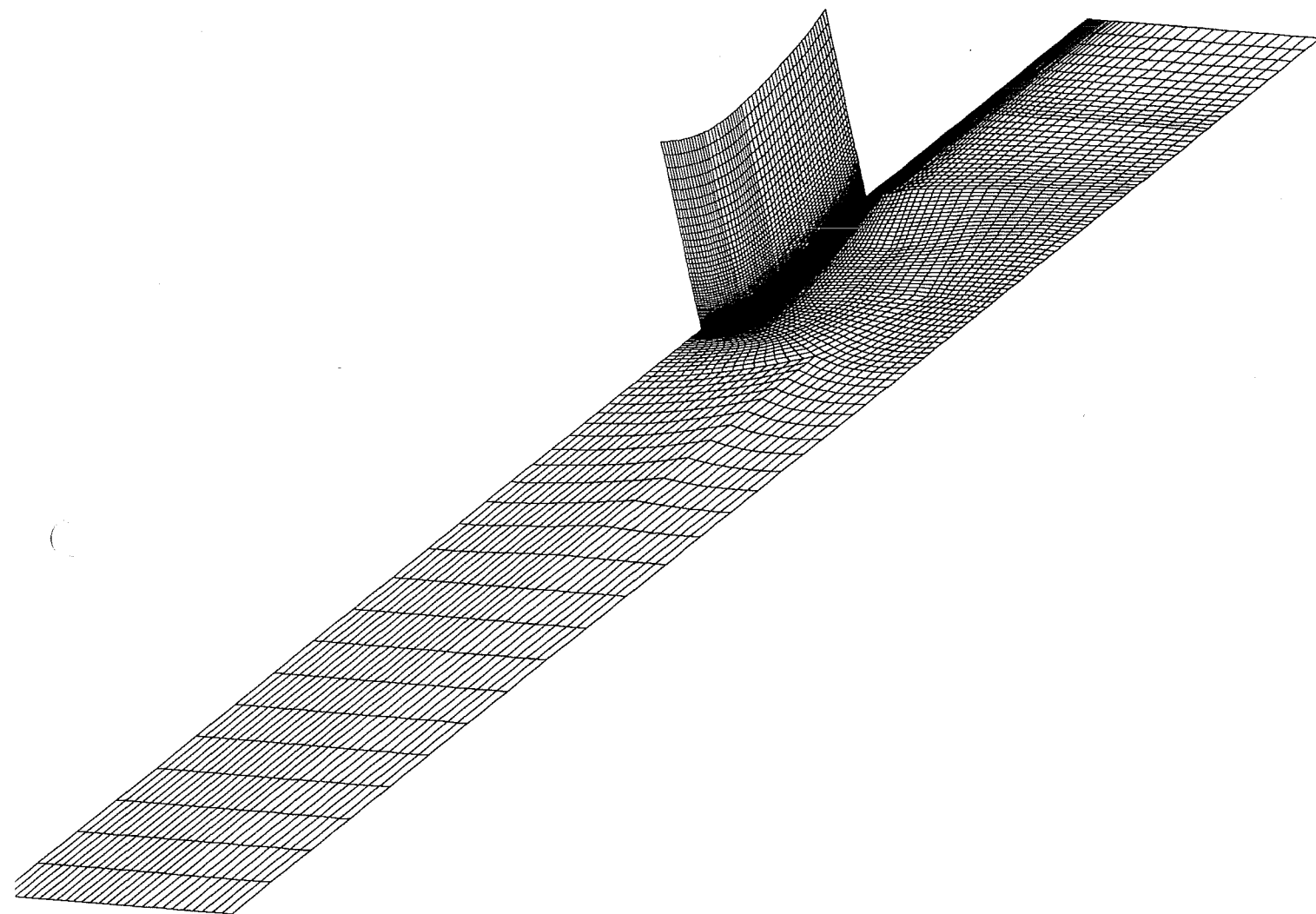
Literature:

[1] Van der Vorst, H. A.: Recent Developments in Hybrid CG Methods, High-Performance Computing and Networking, 1994.

[2] Chen, W. L., Lien, F. S., Leschziner, M.A.: Computational Modelling of Turbulent Flow in Turbomachine Passage with Low-Re Two-equation Models, ECCOMAS, 1994.

[3] Kato, M., Launder, B.E.: The Modelling of Turbulent Flow around Stationary and Vibrating Square Cylinders, Proc. Turbulent Shear Flows, 1993.

[4] Mohammadi, B.: Complex Turbulent Flows Computation with Two-Layer Approach, Int. Num. Meth. Fluids, Vol. 15, 1992.



DESCRIPTION OF NUMERICAL METHODOLOGY FOR TEST CASE 2A

Originator: Bernhard Huurdeman

Affiliation: Institute for Computer Applications, University of Stuttgart, Pfaffenwaldring 27,
D-70569 Stuttgart

General description

The spatial discretization of the transport equations for momentum and scalar quantities is derived using a variational formulation by employing finite element approximations. The application of the weighted residual method requires suitable weighting functions. Here the streamline upwind / Petrov-Galerkin method is adopted, which is appropriate for convection dominated flows (Argyris 1993). In order to satisfy the Babuska-Brezzi condition we use piecewise linear interpolation for the velocity and scalar components and let the pressure constant on each element (Q1-P0 element).

The time discretization follows a first order semi-implicit scheme. Then a linearisation of the equations at each time step is possible and only momentum and continuity equations are coupled. So all scalar variables can be solved successively in order to minimize memory requirements.

For the iterative solution of the linear systems for the momentum and scalar transport equations a SSOR preconditioner and a BCGS accelerator is used. The solution of the pressure correction equation can be obtained with an direct solver using a Cholesky method for banded matrices.

Boundary conditions are Dirichlet conditions at walls and at the inlet for Velocity and turbulent properties and a constant pressure condition at the outlet, achieved by a weak formulation for the pressure deviation.

At inlet, for u and k the experimental values were used.

For ϵ the following formula was used:

$$\epsilon^+ = (0.1 + 0.003y^{+2}) / (1.0 + 0.00125y^{+3}) \text{ with } \epsilon^+ = \epsilon\nu/u_\tau^4 \text{ and } u_\tau = 0.079 \text{ m/s (exp. value)}$$

Convection scheme

Streamline upwind / Petrov-Galerkin formulation (Brooks 1982)

Mesh

Model 1: 211 x 101 grid points (21000 QUAD4-Elements)

Model 2: 173 x 87 grid points (14792 QUAD4-Elements)

Turbulence models

Model 1 (kepsw): Standard k-epsilon model with wall functions (Launder 1974)

Model 2 (kepslay): Inner region: Standard k-epsilon model (Launder 1974)

Upper wall : wall functions

Lower wall : Two layer model (Chen 1988)

Near-wall treatment

Wall-functions for k - ϵ model

A modified form of the standard wall-function method is used. The Dirichlet boundary conditions for U , k and ϵ at the near-wall grid points are given as:

$$U = u_\tau y^+ \text{ for } y^+ < 11.6, \quad U = u_\tau \frac{1}{\kappa} \ln(Ey^+) \text{ for } y^+ > 11.6,$$

$$k = 0.05u_\tau^2 y^{+2} \text{ for } y^+ < 8.12, \quad k = 3.3u_\tau^2 \text{ for } y^+ > 8.12,$$

$$\epsilon = \text{Min} \left(\frac{c_\mu^{3/4} k^{1.5}}{y\kappa}, 0.2 \frac{\rho u_\tau^4}{\mu} \right)$$

where $u_\tau = \sqrt{\tau_w/\rho}$ is the wall friction velocity, τ_w is the wall shearing stress and $y^+ = u_\tau y \rho / \mu$ is the non-dimensional wall coordinate. The wall shearing stress is obtained from the flow properties at the point next to the near wall point with:

$$\tau_w = \frac{\mu U}{y} \quad \text{for } y^+ < 11.6, \quad \tau_w = \frac{\rho U \kappa c_\mu^{1/4} k^{1/2}}{\ln(E c_\mu^{1/4} \rho y k^{1/2} / \mu)} \quad \text{for } y^+ > 11.6.$$

The constants are given by $c_\mu = 0.09$, $\kappa = 0.41$ and $E = 9$.

Near wall region in two-layer k - ϵ model

In the near-wall region, which comprises the viscous sublayer, the buffer zone and a part of the fully turbulent region, only the transport equation for k needs to be solved. The dissipation rate and the eddy-viscosity are specified by $\epsilon = k^{3/2}/l_\epsilon$ and $\mu_t = \rho c_\mu \sqrt{k} l_\mu$, where the length scales l_ϵ and l_μ are obtained in terms of the turbulent Reynolds number $R_y = \rho \sqrt{k} y / \mu$

$$l_\epsilon = c_l y [1 - \exp(-R_y/A_\epsilon)] \quad \text{and} \quad l_\mu = c_l y [1 - \exp(-R_y/A_\mu)].$$

The model constants are given by $c_l = \kappa c_\mu^{-3/4}$, $A_\epsilon = 2c_l$ and $A_\mu = 70$.

In the outer region, the standard k - ϵ model is applied and the match boundary between the near-wall region and the outer region is chosen along a line where the Reynolds number R_y exceeds the value of 250. In the course of the calculation, the location of the dividing boundary is repeatedly checked and, if required, the near-wall region will be expanded or decreased. Thus, even for complex geometries, the correct fitting of the dividing boundary is always ensured.

Related publications/reports

J. Argyris, H. Friz, B. Huurdeman and A. Laxander, Turbulent fluid flow and its incorporation into combustion processes, *Comp. Meth. Appl. Mech. Engrg.* 110 (1993) p. 1

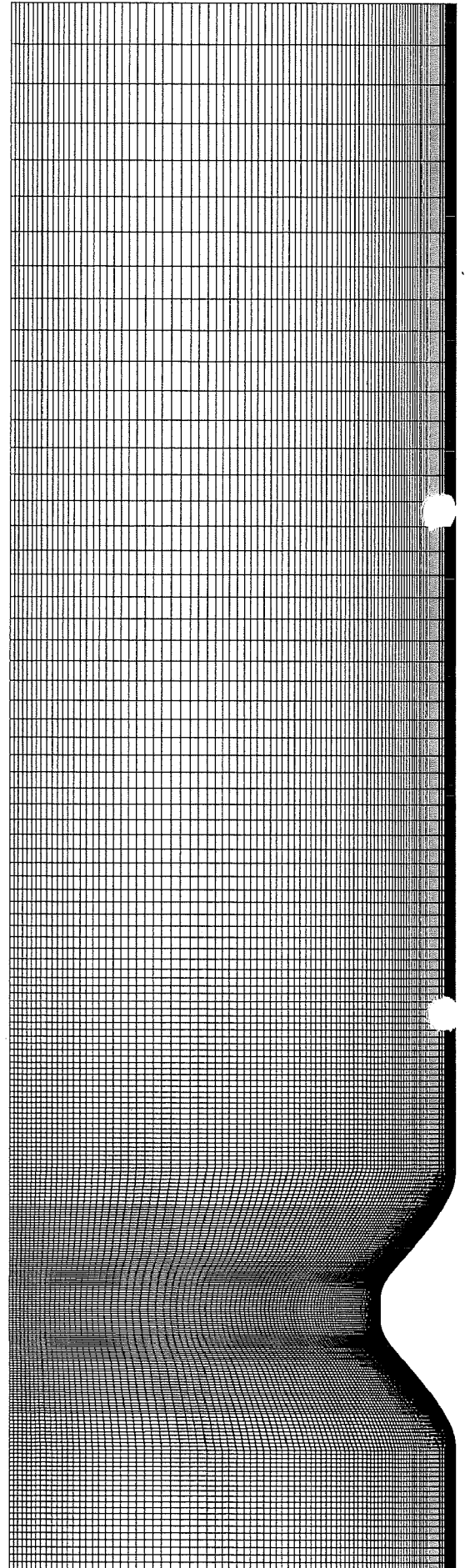
A.N. Brooks and T.J.T. Hughes, Streamline upwind / Petrov-Galerkin formulations for convection dominated flows with particular emphasis on the incompressible Navier-Stokes equations, *Comp. Meth. Appl. Mech. Engrg.* 59 (1982) p. 199

H.C. Chen and V.C. Patel, Near wall turbulence models for complex flows including separation, *AIAA J.* 26 (1988) p. 641

M.M. Gibson and B.E. Launder, Ground effects on pressure fluctuations in the atmospheric boundary layer, *J. Fluid Mech.* 1978, Vol. 86, p. 491

B.E. Launder and D.B. Spalding, The numerical computation of turbulent flows, *Comp. Meth. Appl. Mech. Engrg.* 3 (1974) p. 269

S. Obi, M. Peric and G. Scheuerer, Second moment calculation procedure for turbulent flows with collocated variable arrangement, *AIAA J.* 29 (1991) p. 585



DESCRIPTION OF NUMERICAL METHODOLOGY FOR TEST CASE 4

Originator:
Olof Daunius

Affiliation:
Volvo Data corp., Gothenburg, Sweden

General description:

Three different calculations are submitted. Two of them uses the same mesh and are a comparison of RSM with and without wall correction to the pressure– strain correlation. This wall reflection is described in [1]. The third calculation is on a mesh derived from the first two, but with the outlet located further downstream (at $x=60*T$). The wall reflection terms are included in this case.

The flow solver used is CFDS–FLOW3D [2], a structured multi–block finite volume solver using boundary–fitted coordinates and collocated variable storage (Rhie–Chow). The SIMPLEC pressure correction algorithm was used.

The measured inlet values of u , uu , vv and uw at $x/T=-18.24$ were interpolated to the inlet boundary. The quantity vv was taken as $\max(2.0*ww-uu, 1.0e-3)$ to prevent negative values. The energy dissipation at the inlet boundary was derived from an assumed length scale of $0.1*T$. At the outlet boundary, zero axial gradients were imposed.

The axial velocity residuals were converged to 0.1% of inlet momentum.

Convection scheme:

CCCT scheme [2]: a bounded third order upwind scheme of QUICK–type.

Mesh:

Mesh 'rsm' and 'rsmrfl' are C–type meshes, wrapping the wing profile, embedded in an H–type structure. They consist of three blocks, and 160 000 interior cells. There are 24 cells in the y –direction. Mesh stretching were kept below 1.1.

Mesh 'rsmrfl2' was created by adding a fourth block and placing the outlet at $x=60*T$. Some coarsening of the original three blocks were made to restrict this mesh to 176 000 interior cells

Turbulence models:

A standard RSM [2] with 'slow' pressure–strain term from Rotta [3], and 'rapid' isotropization from Naot et al. [4].

Near–wall treatment:

Log–law based wall function and near–wall correction to pressure– strain terms as described by Clarke and Wilkes [1].

Related publications/reports:

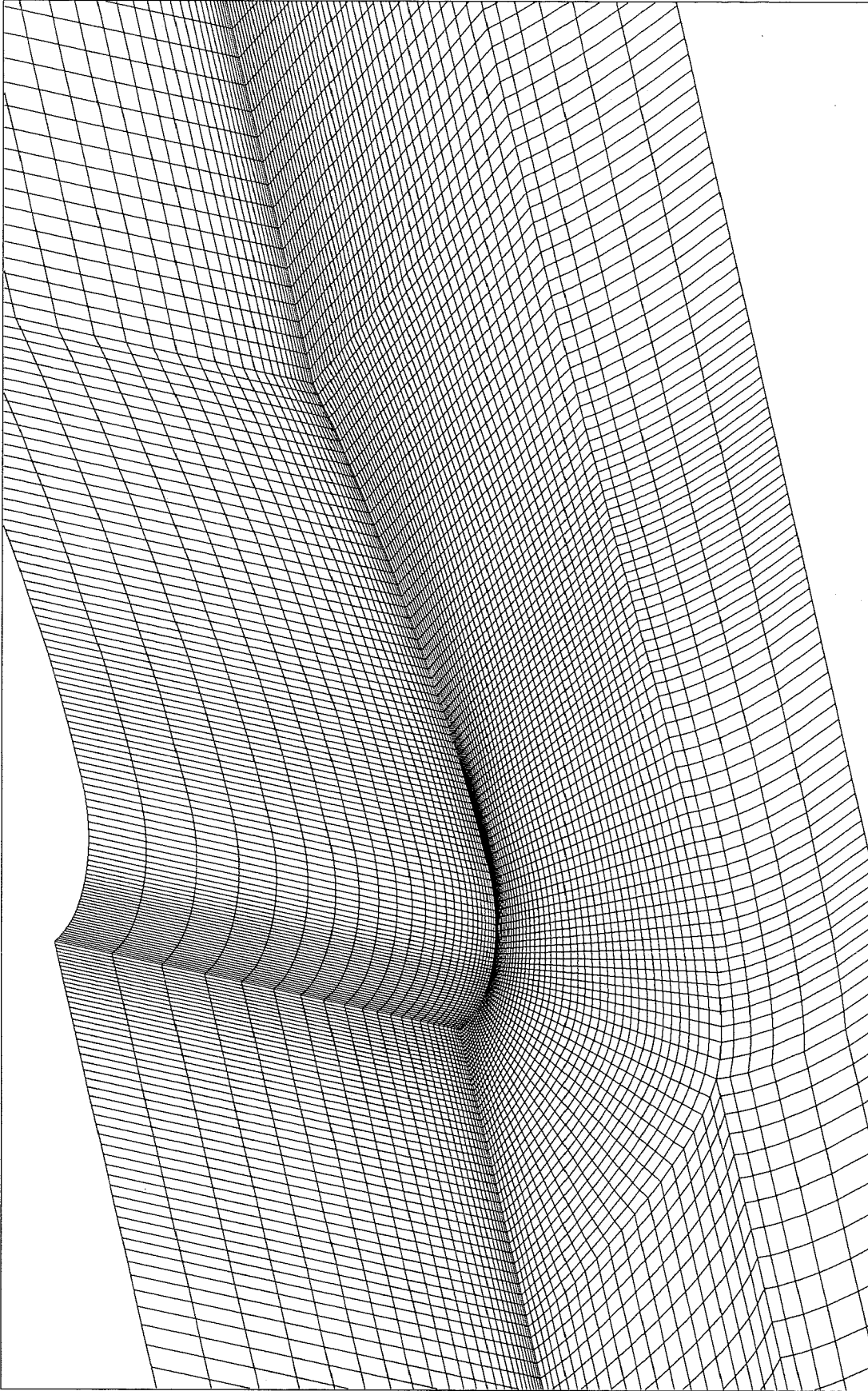
[1]: Clarke, D.S. and Wilkes, N.S., "The Calculation of Turbulent Flows in Complex Geometries Using a Differential Stress Model", AERE–R 13428, 1989.

[2]: CFDS–FLOW3D Release 3.3 User Manual, 1994.

[3]: Rotta, J.C., "Turbulente Stromungen", B.G Teubner, Stuttgart, 1972.

[4]: Naot, D., Shavit, A. and Wolfshtein, M., "Interactions Between Components of the Turbulent Velocity Correlation Tensor due to Pressure Fluctuations", J. of Technology, 8, pp. 259, 1970

Case 4, C-type mesh embedded in H, three blocks.



Plotted by v047904@sluggo on Tue Feb 28 16:28:48 PST 1995, using the ICFD CFD LEO Grid Visualizer 3.1.2.4.

KEY TO TEST CASE 1A

| Contributor | Key-Name | Gr. | Name (Affiliation) | Turbulence Model | Near-Wall Treatment |
|-------------|----------------|------|--|---|-------------------------------|
| ECLille | RSM_JaHa | 3 | Stanislas/Hannani/Deldicque (Ecole Centrale Lille) | Reynolds-Stress Model Jakirlic-Hanjalic | — |
| | RSM_LaSh | 3 | | Reynolds-Stress Model Launder-Shima | — |
| | hKE_std+Chi | 1, 2 | | two-layer k- ϵ | Chien |
| | hKE_std+RMM | 1, 2 | | two-layer k- ϵ | Rodi-Mansour-Michelassi 1 eq. |
| EDFLNHLa | RSM_LRR+elr | 3 | Laurence et al. (EDF-DER-LNH) | RSM Launder-Reece-Rodi | elliptic relaxation |
| | IKE_LaSh | 1 | | low-Re k- ϵ Launder-Sharma | — |
| ENSICA | IKE_YaSh | 1 | Cazalbou/Torres (ENSICA) | low-Re k- ϵ Yang-Shi | — |
| | IKE_LaSh(arco) | 1 | | low-Re k- ϵ Launder-Sharma | — |
| | IKE_LaSh | 1 | | low-Re k- ϵ Launder-Sharma | — |
| FluiDyna | kOm_Wil | 2, 1 | Haroutunian (Fluid Dynamics Int.) | k- ω | — |
| UConcord | kOm_Wil | 2, 1 | Houzeaux (CERCA) | k- ω | — |
| UDelftHa | RSM_HJH | 2, 3 | Hanjalic/Hadzic/Jakirlic (TU Delft, Appl. Physics) | RSM Hanjalic-Jakirlic-Hadzic | — |
| | IKE_LaSh | 1 | | low-Re k- ϵ Launder-Sharma | — |
| UKarlsru | hKE_std+NoRe | 1, 2 | Zaky (Univ. of Karlsruhe) | two-layer k- ϵ | Norris-Reynolds 1 eq.-model |
| UMISTCra | RSM_Cub+2eq | 3 | Craft (UMIST) | Reynolds-Stress Model Cubic | k- ϵ Launder-Sharma |
| | RSM_CrLa+2eq | 3 | | Reynolds-Stress Model Craft-Launder | k- ϵ Launder-Sharma |

KEY TO TEST CASE 1B

| Contributor | Key-Name | Gr. | Name (Affiliation) | Turbulence Model | Near-Wall Treatment |
|-------------|-------------|------|--|---|-------------------------------|
| ECLille | RSM_JaHa | 3 | Stanislas/Hannani/Deldicque (Ecole Centrale Lille) | Reynolds-Stress Model Jakirlic-Hanjalic | — |
| | RSM_LaSh | 3 | | Reynolds-Stress Model Launder-Shima | — |
| | hKE_std+Chi | 1, 2 | | two-layer k- ϵ | Chien |
| | hKE_std+RMM | 1, 2 | | two-layer k- ϵ | Rodi-Mansour-Michelassi 1 eq. |

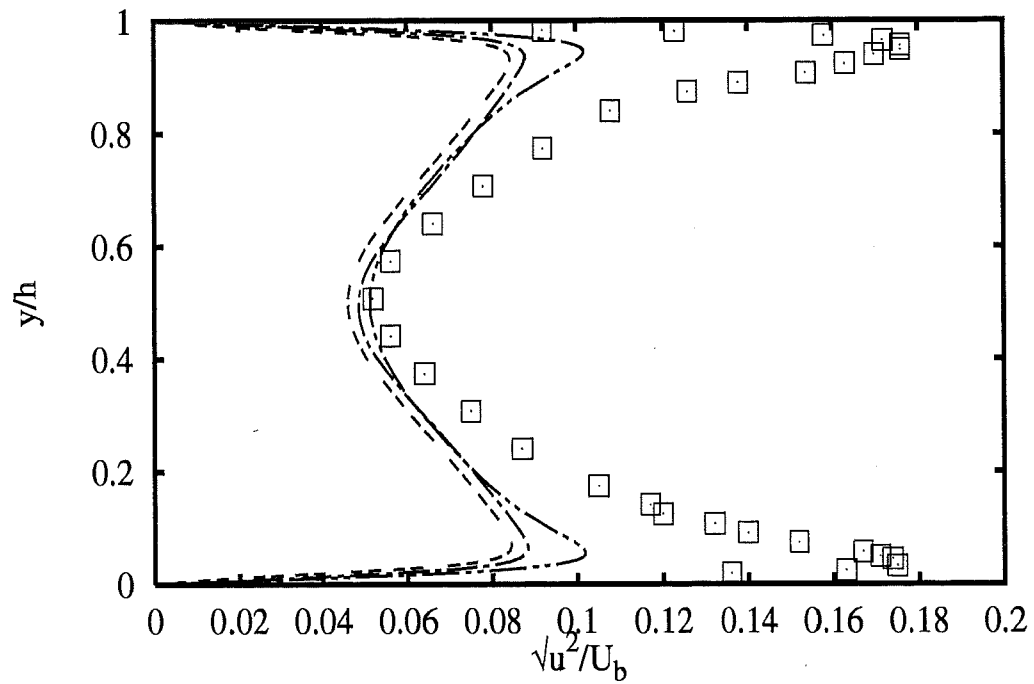
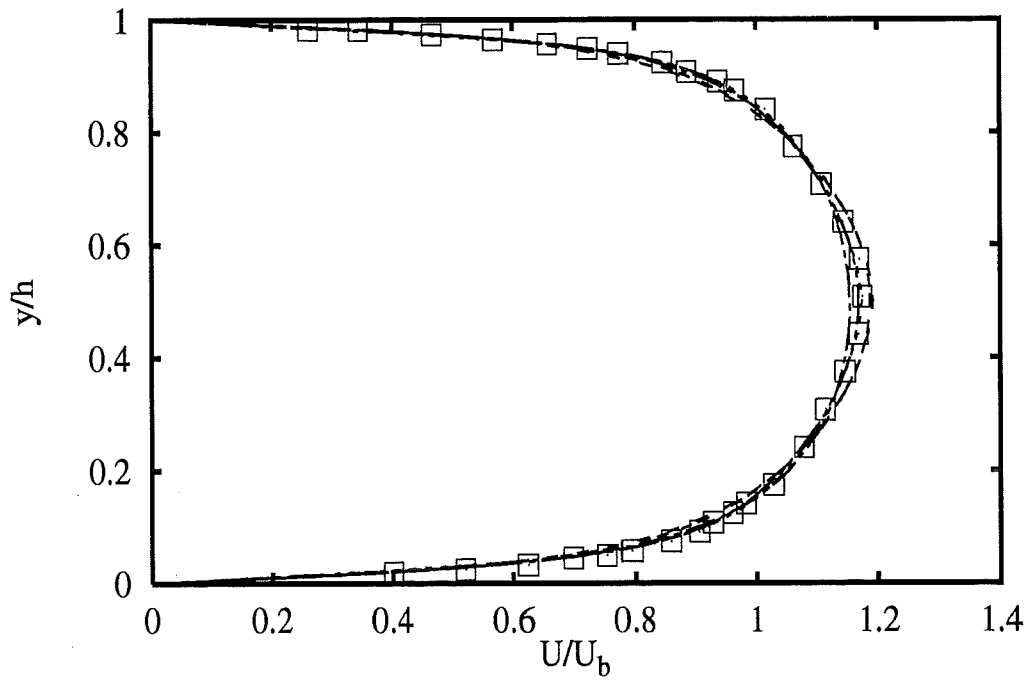
| | | | | | |
|----------|----------------|------|--|-------------------------------------|------------------------------|
| EDFLNHLa | IKE_LaSh | 1 | Laurence et al. (EDF-DER-LNH) | low-Re k- ϵ Launder-Sharma | — |
| ENSICA | IKE_YaSh | 1 | Cazalbou/Torres (ENSICA) | low-Re k- ϵ Yang-Shi | — |
| | IKE_LaSh(arco) | 1 | | low-Re k- ϵ Launder-Sharma | — |
| | IKE_LaSh | 1 | | low-Re k- ϵ Launder-Sharma | — |
| FluiDyna | kOm_Wil | 2, 1 | Haroutunian (Fluid Dynamics Int.) | k- ω | — |
| UConcord | kOm_Wil | 2, 1 | Houzeaux (CERCA) | k- ω | — |
| UDelftHa | RSM_HJH | 2, 3 | Hanjalic/Hadzic/Jakirlic (TU Delft, Appl. Physics) | RSM Hanjalic-Jakirlic-Hadzic | — |
| | IKE_LaSh | 1 | | low-Re k- ϵ Launder-Sharma | — |
| UKarlsru | hKE_std+NoRe | 1, 2 | Zaky (Univ. of Karlsruhe) | two-layer k- ϵ | Norris-Reynolds 1 eq.-model |
| UMISTCra | RSM_Cub+2eq | 3 | Craft (UMIST) | Reynolds-Stress Model Cubic | k- ϵ Launder-Sharma |
| | RSM_CrLa+2eq | 3 | | Reynolds-Stress Model Craft-Launder | k- ϵ Launder-Sharma |

KEY TO TEST CASE 1C

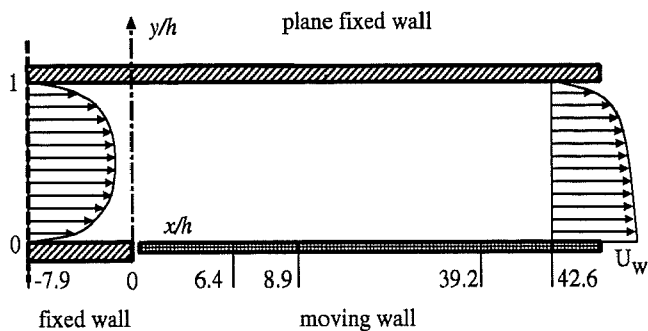
| Contributor | Key-Name | Name (Affiliation) | Turbulence Model | Near-Wall Treatment |
|-------------|----------------|--|-------------------------------------|-----------------------------|
| ENSICA | IKE_LaSh | Cazalbou/Torres (ENSICA) | low-Re k- ϵ Launder-Sharma | — |
| | IKE_LaSh(arco) | | low-Re k- ϵ Launder-Sharma | — |
| UDelftHa | RSM_HJH | Hanjalic/Hadzic/Jakirlic (TU Delft, Appl. Physics) | RSM Hanjalic-Jakirlic-Hadzic | — |
| | IKE_LaSh | | low-Re k- ϵ Launder-Sharma | — |
| UKarlsru | hKE_std+NoRe | Zaky (Univ. of Karlsruhe) | two-layer k- ϵ | Norris-Reynolds 1 eq.-model |

In key-names:

(arco): artificial compressibility code

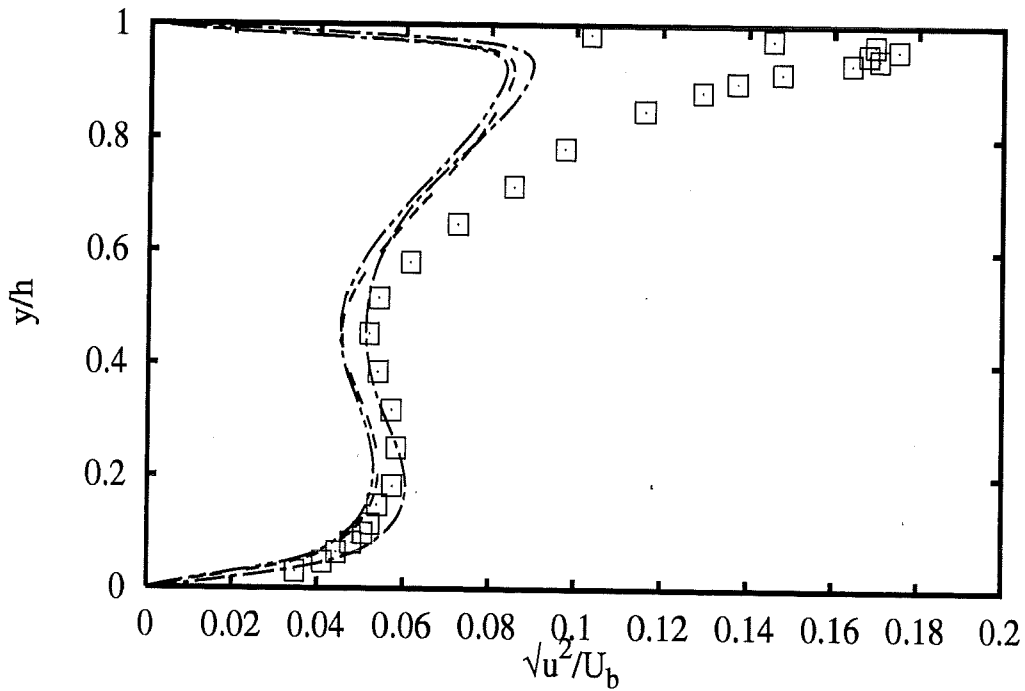
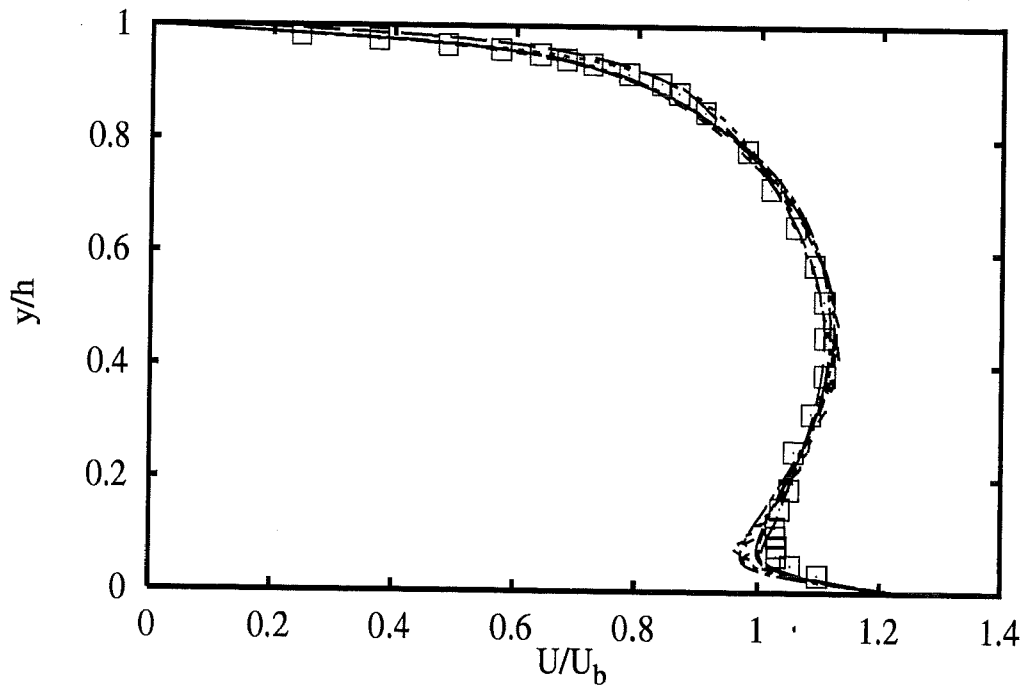


Profiles at $x/h = -7.9$

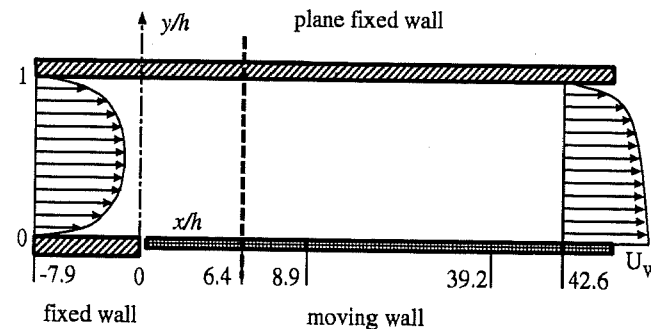


- Experiments** □
- ECLille hKE std+Chi** ---
- ECLille hKE std+RMM** -.-.-
- EDFLNHLA lKE LaSh** - - -
- UDeftHa lKE LaSh** - - -
- ENSICA lKE LaSh (arco)** - - -

1A - 1

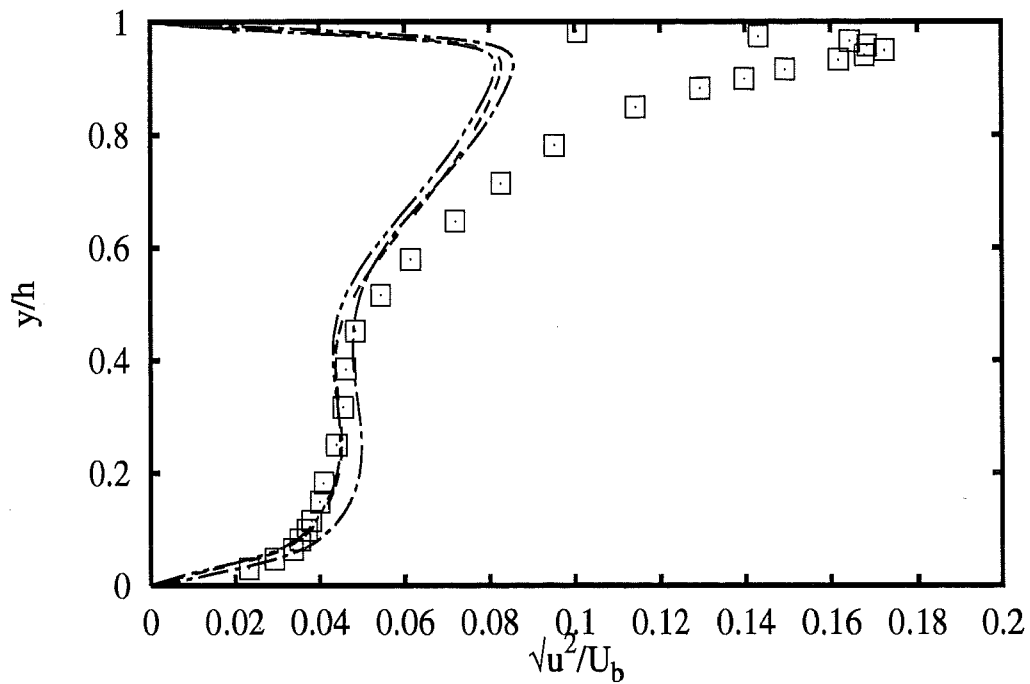
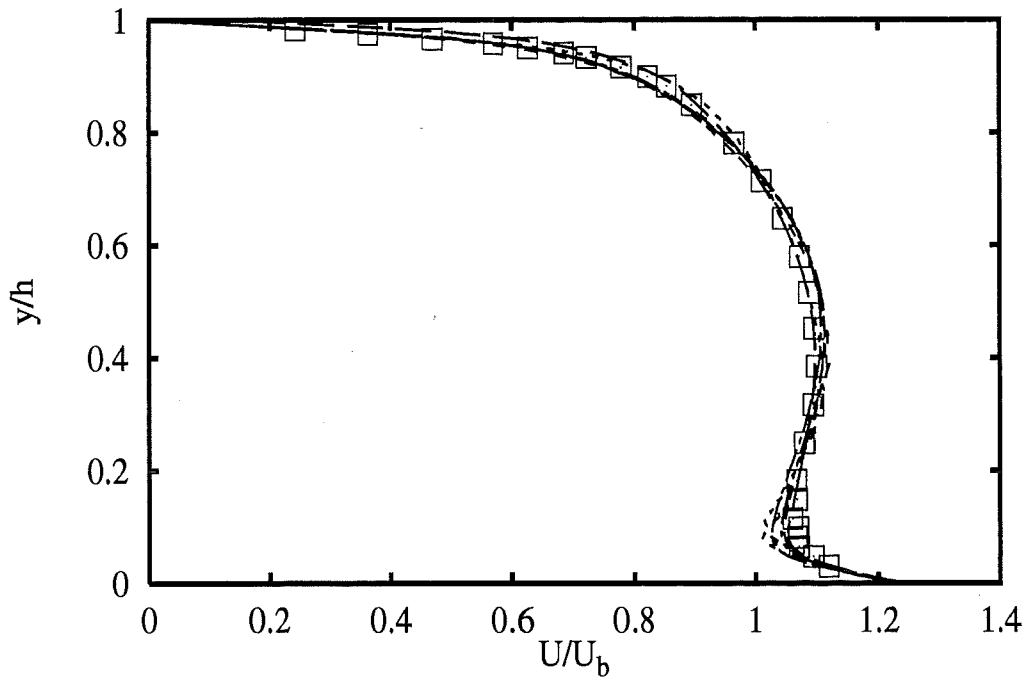


Profiles at $x/h=5.6$

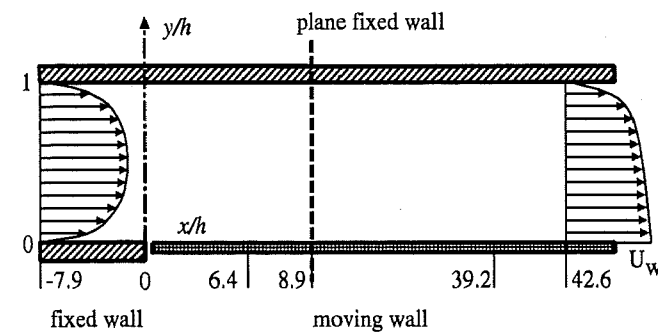


- | | |
|-------------------------------|-----------|
| Experiments | □ |
| UKarlsru hKE std+NoRe | — |
| ECLille hKE std+Chi | - - - |
| ECLille hKE std+RMM | · · · · · |
| EDFLNHLA lKE LaSh | — · — |
| UDELftHa lKE LaSh | - · - · - |
| ENSICA lKE LaSh (arco) | - - - - - |

1A - 2

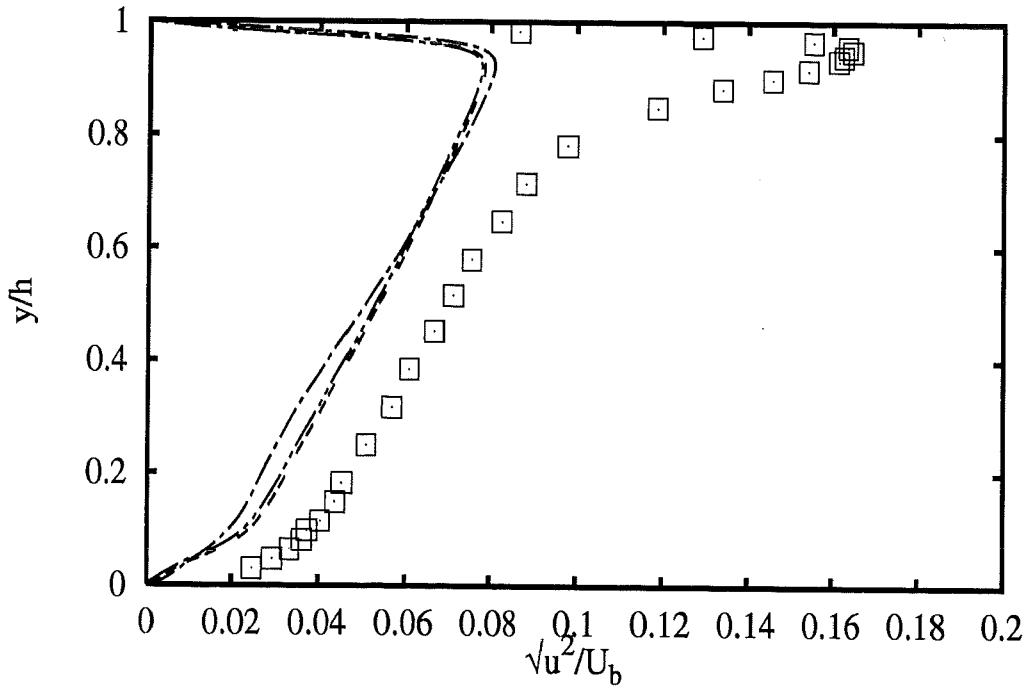
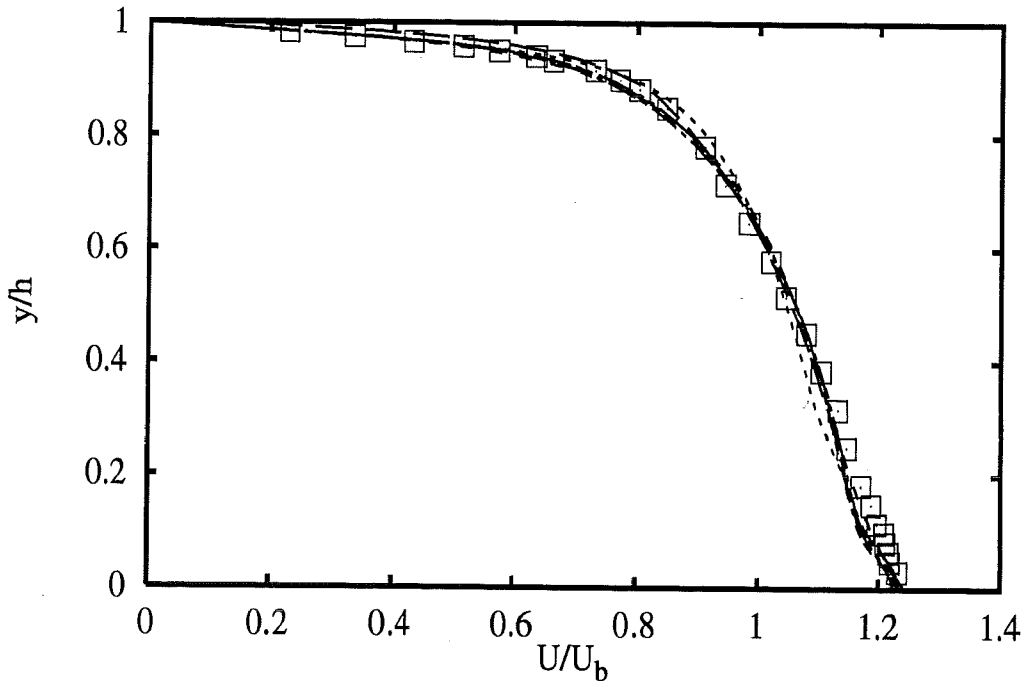


Profiles at $x/h=8.9$

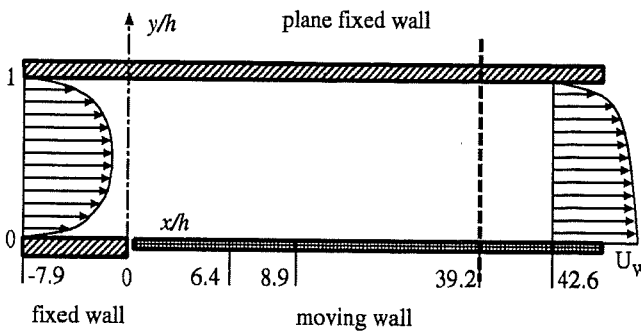


- | | |
|------------------------|-----|
| Experiments | □ |
| UKarlsru hKE std+NoRe | --- |
| ECLille hKE std+Chi | --- |
| ECLille hKE std+RMM | --- |
| EDFLNHLa lKE LaSh | --- |
| UDelftHa lKE LaSh | --- |
| ENSICA lKE LaSh (arco) | --- |

1A - 3

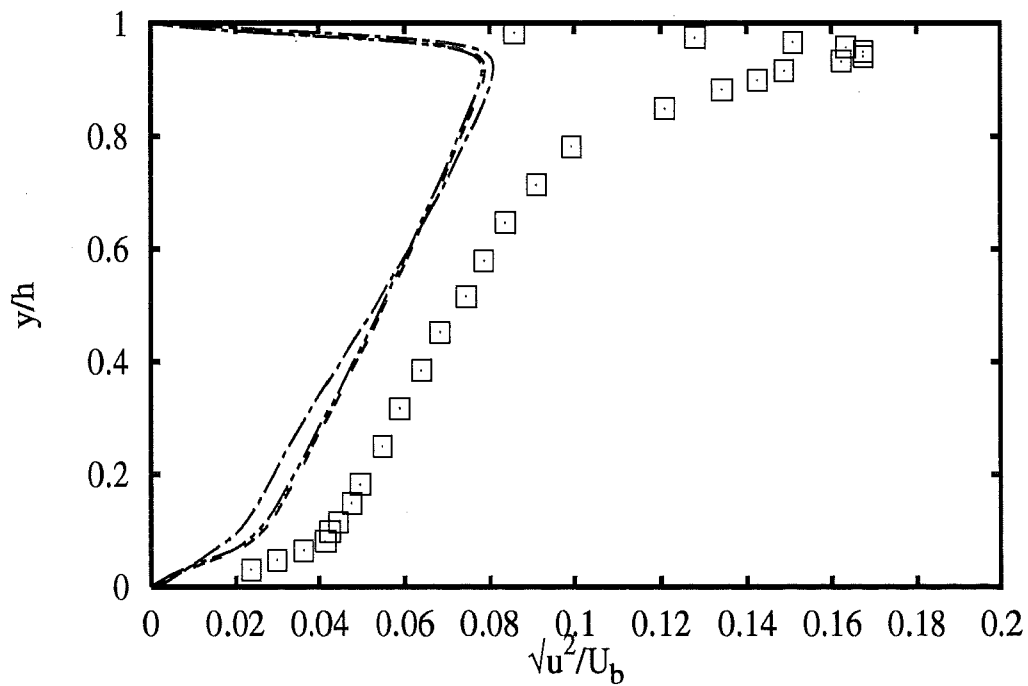
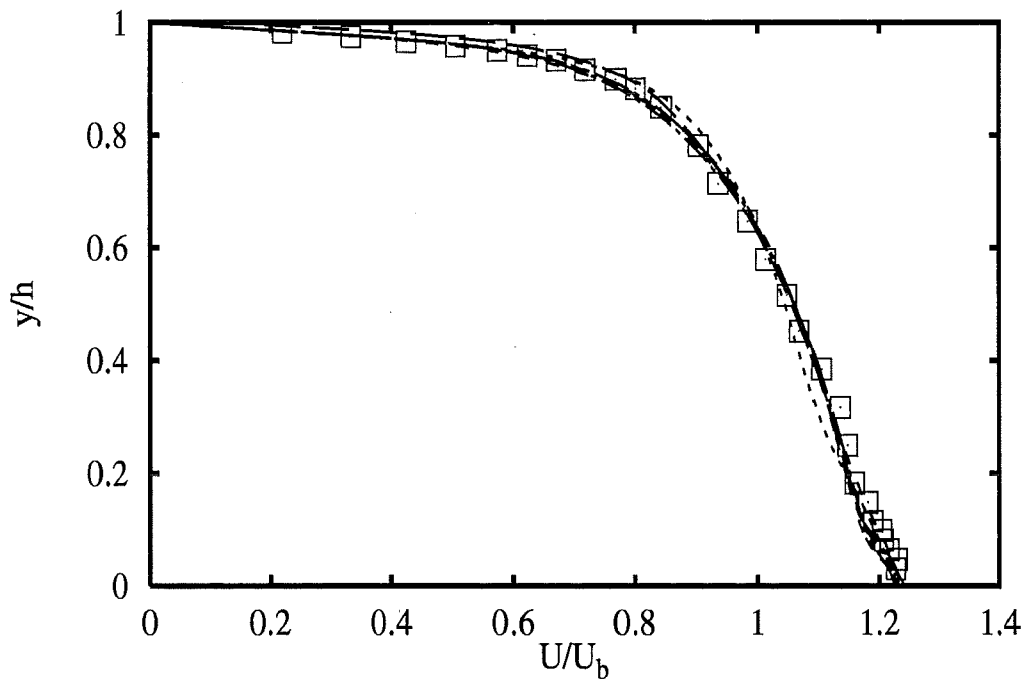


Profiles at $x/h=39.2$

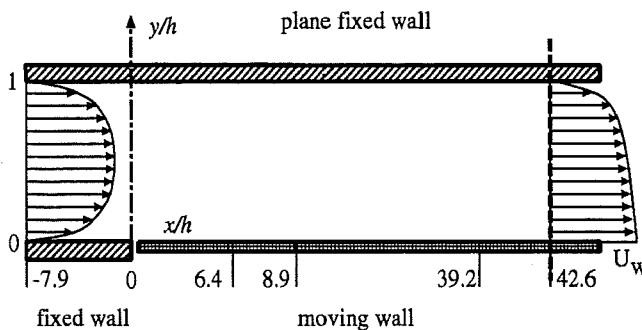


- | | |
|-------------------------|-----------|
| Experiments | □ |
| UKarlsruhe hKE std+NoRe | — — |
| ECLille hKE std+Chi | - - - |
| ECLille hKE std+RMM | · · · · · |
| EDFLNHLa lKE LaSh | - · - · - |
| UDelftHa lKE LaSh | - · - · - |
| ENSICA lKE LaSh (arco) | - - - |

1A - 4

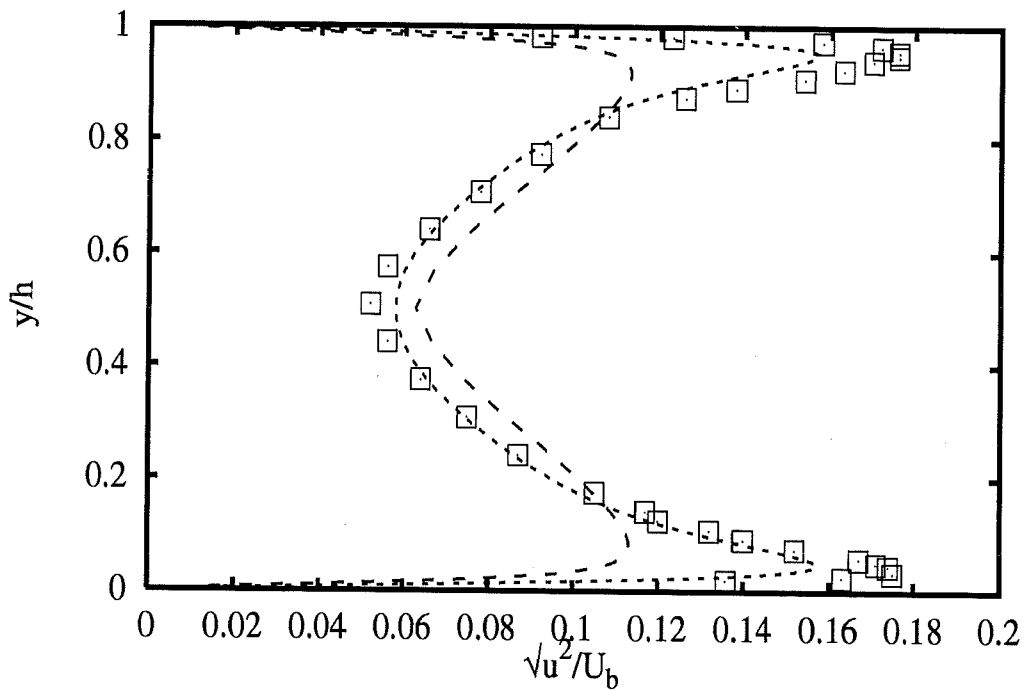
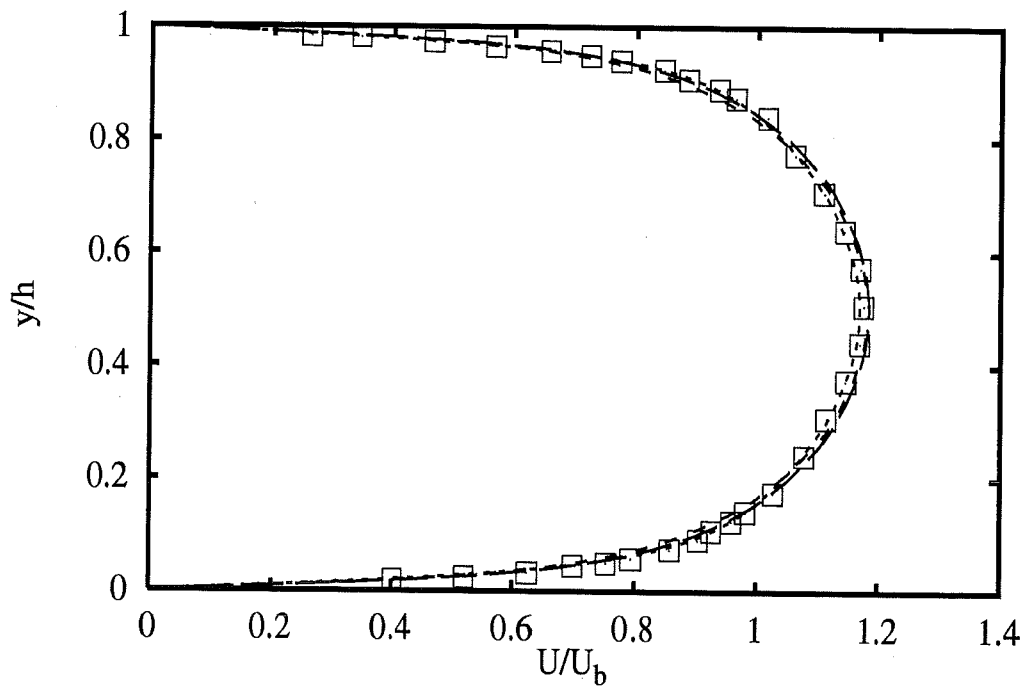


Profiles at $x/h=42.6$

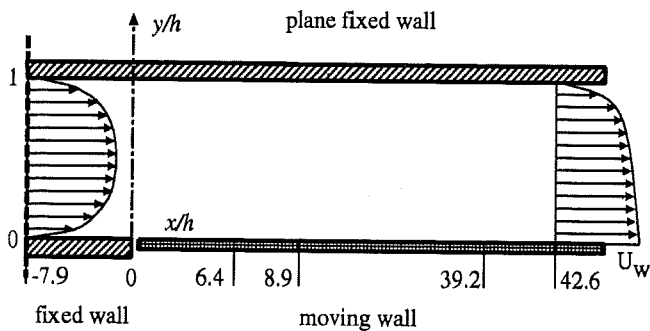


- | | |
|--------------------------------------|-------|
| Experiments | □ |
| UKarlsru <i>hKE std+NoRe</i> | — — |
| ECLille <i>hKE std+Chi</i> | - - - |
| ECLille <i>hKE std+RMM</i> | ⋯⋯⋯ |
| EDFLNHLA <i>lKE LaSh</i> | - - - |
| UdelftHa <i>lKE LaSh</i> | - - - |
| ENSICA <i>lKE LaSh (arco)</i> | - - - |

1A - 5

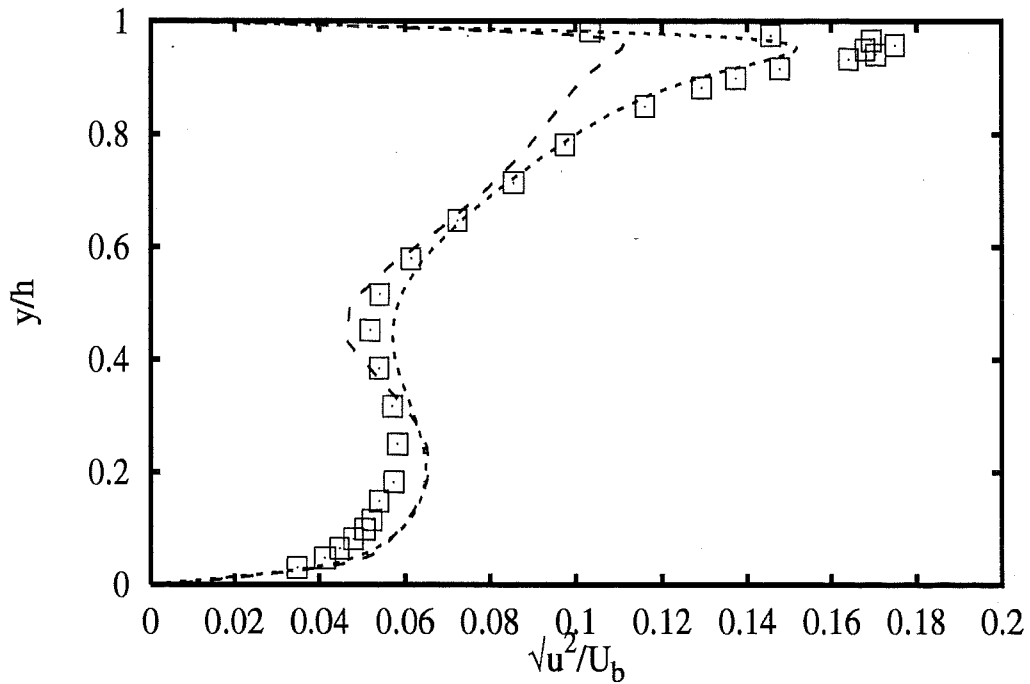
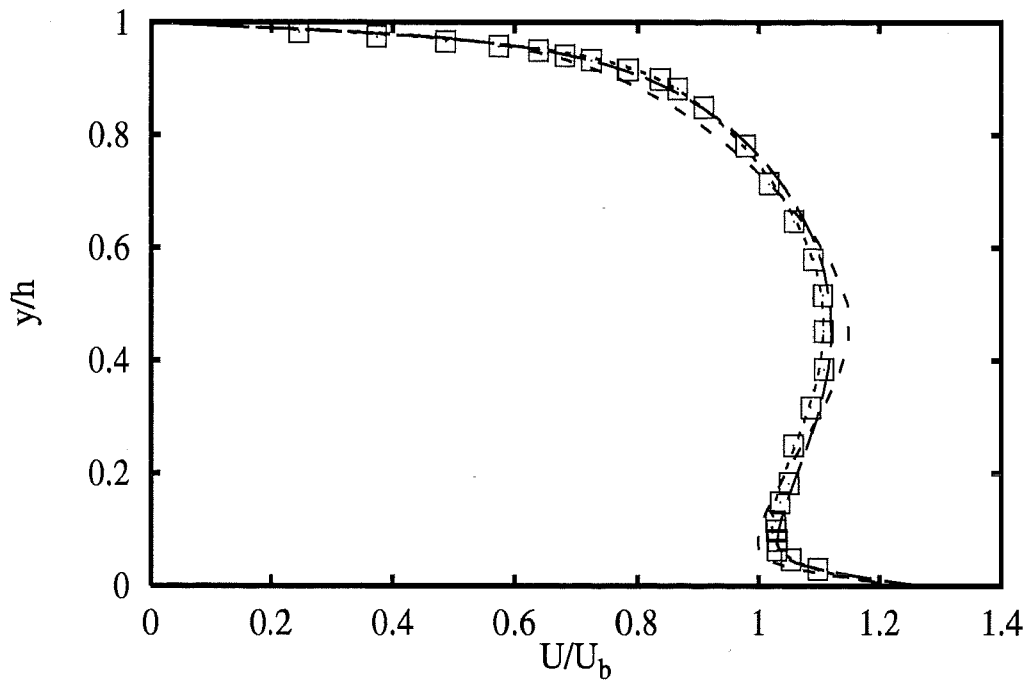


Profiles at $x/h = -7.9$

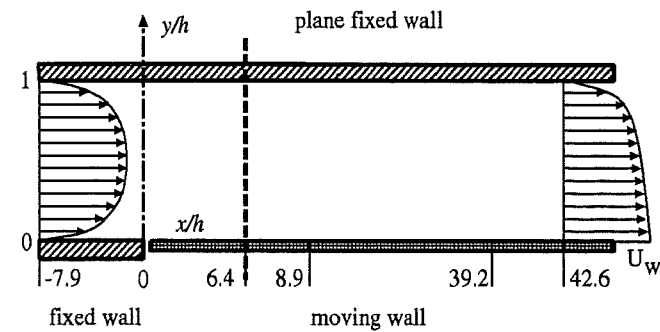


- Experiments** □
- Fluidyna** *kOm Wil* — —
 - UConcord** *kOm Wil* - - -
 - UDelftHa** *RSM HJH* ·····

1A - 6

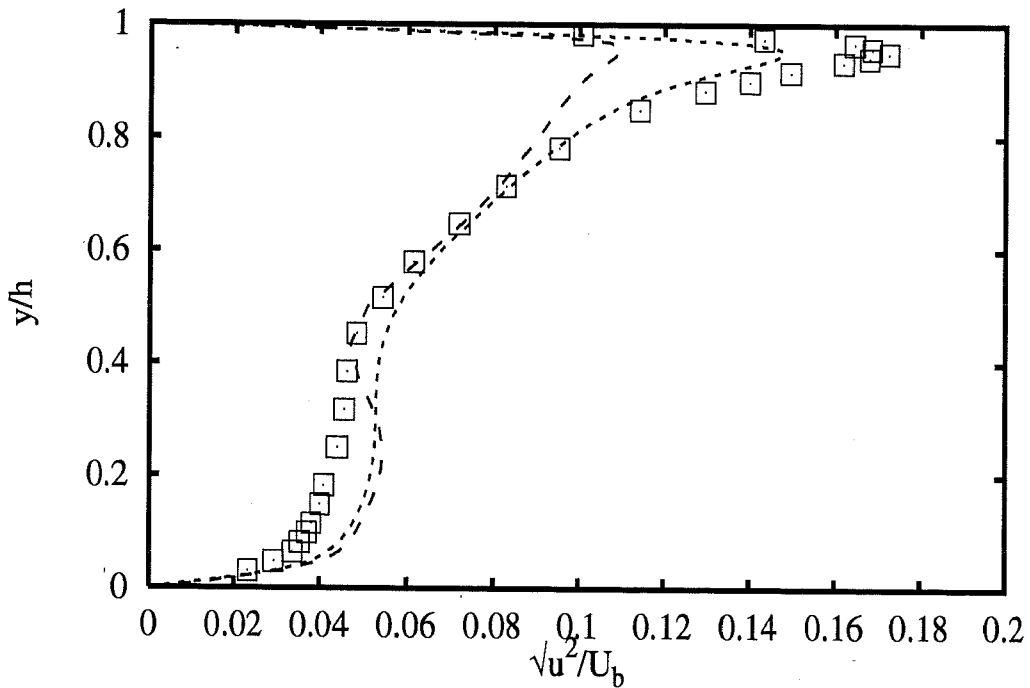
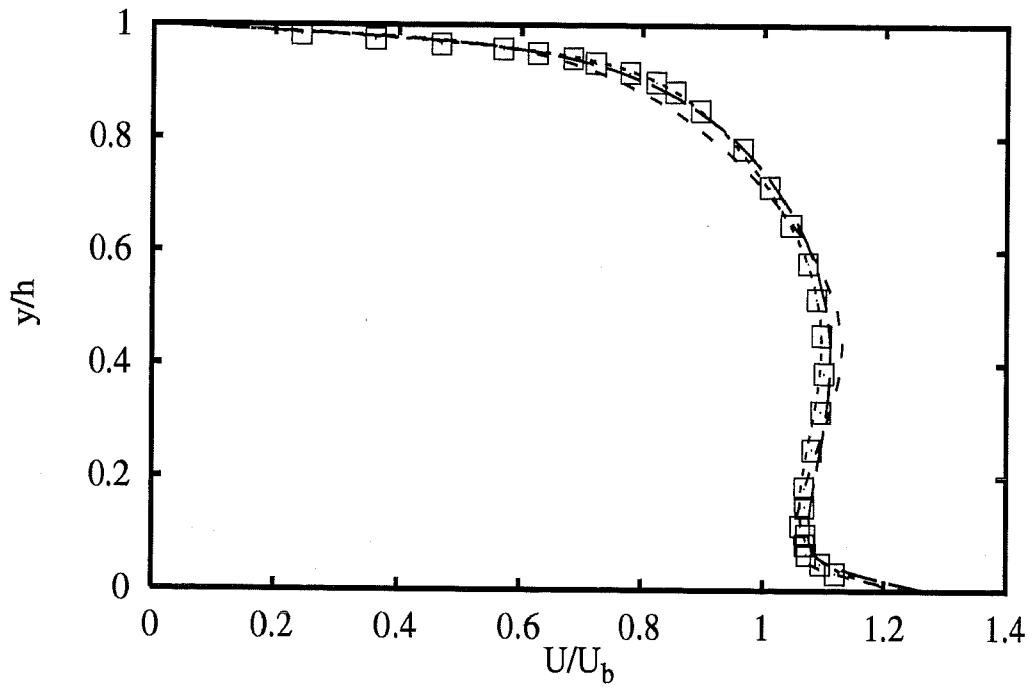


Profiles at $x/h=5.6$

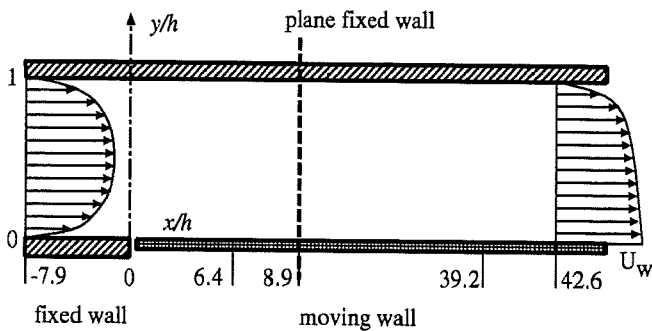


- | | |
|--------------------------------|-------|
| Experiments | □ |
| <i>Fluidyna</i> <i>kOm Wil</i> | --- |
| <i>UConcord</i> <i>kOm Wil</i> | ---- |
| <i>UDelftHa</i> <i>RSM HJH</i> | |

1A - 7

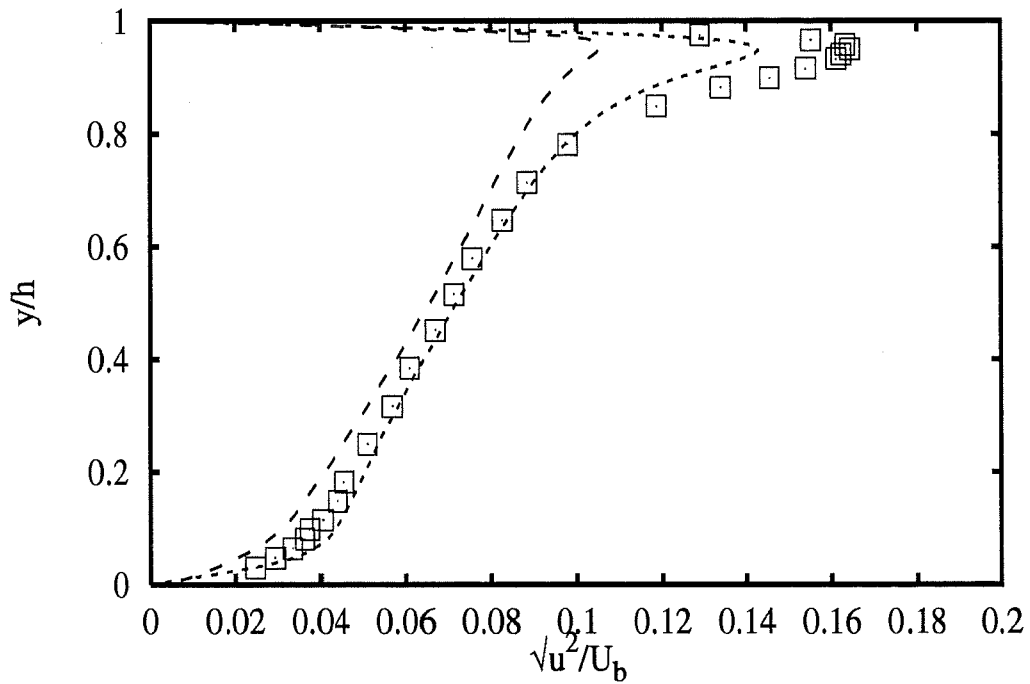
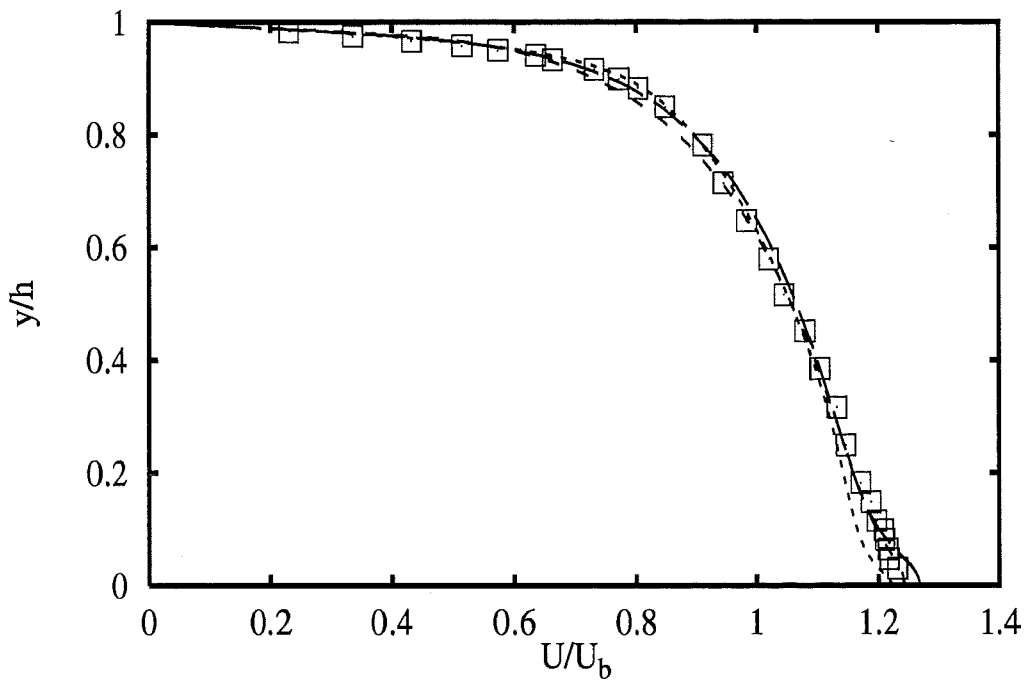


Profiles at $x/h=8.9$

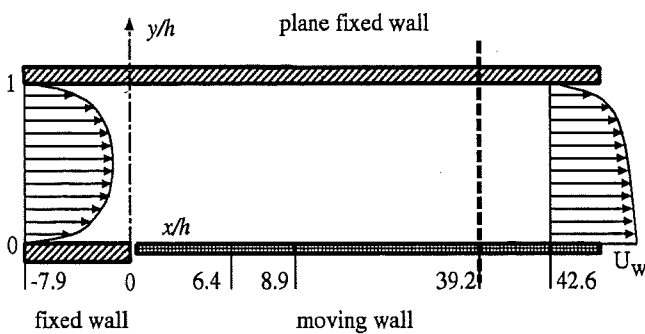


- Experiments** □
- Fluidyna kOm Wil — —
 - UConcord kOm Wil - - -
 - UDelftHa RSM HJH ·····

1A - 8

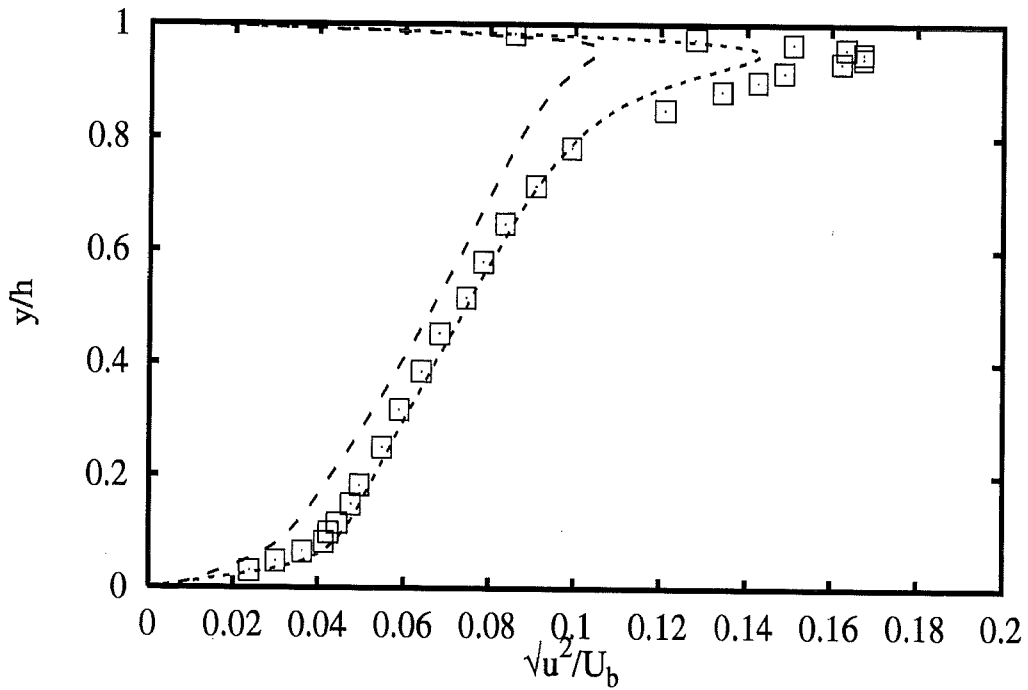
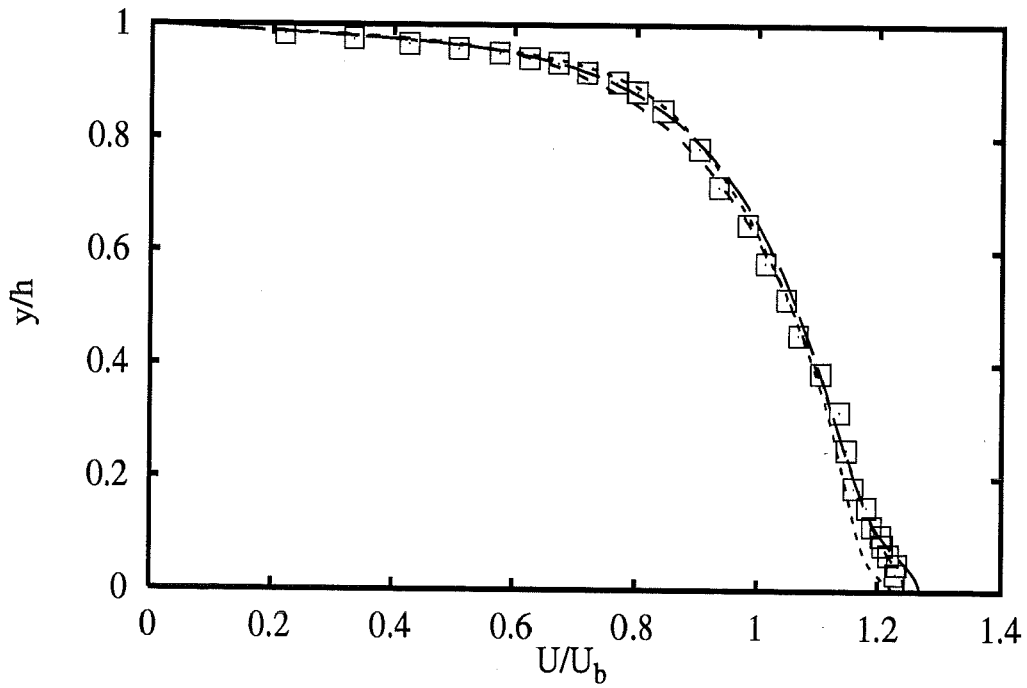


Profiles at $x/h=39.2$

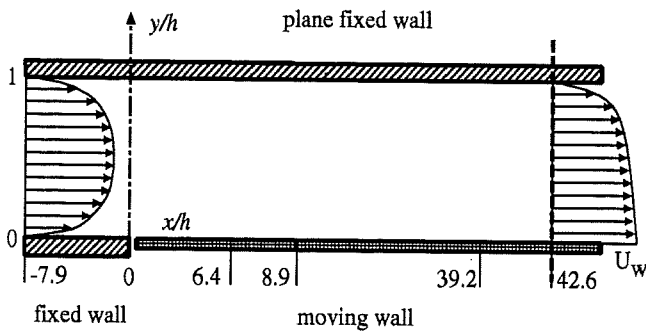


- Experiments** □
- Fluidyna kOm Wil** —
- UConcord kOm Wil** - - -
- UDelftHa RSM HJH** ·····

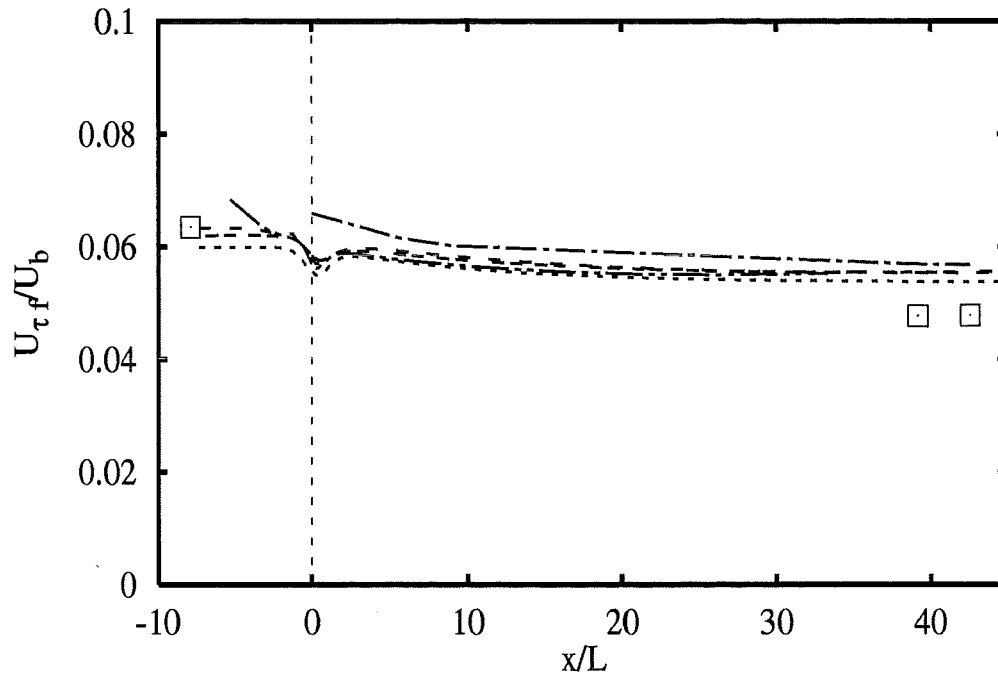
1A - 9



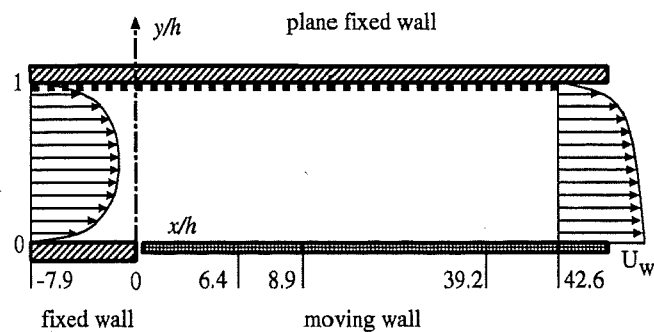
Profiles at $x/h=42.6$



- Experiments** □
- FluidDyna** *kOm Wil* — —
- UConcord** *kOm Wil* - - -
- UdelftHa** *RSM HJH* ·····

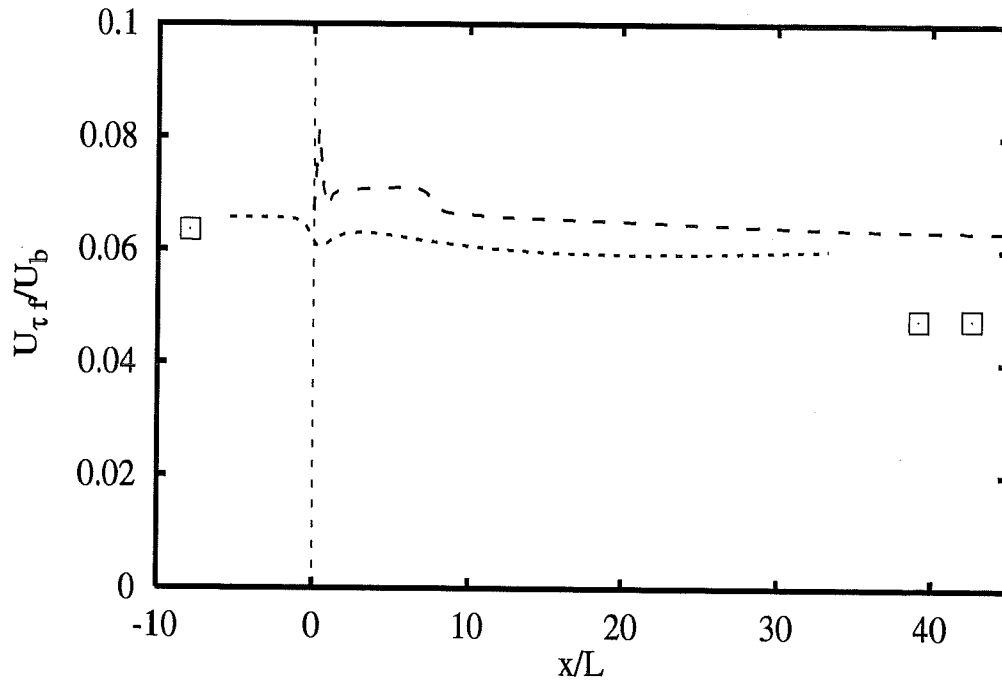


Distribution along fixed wall

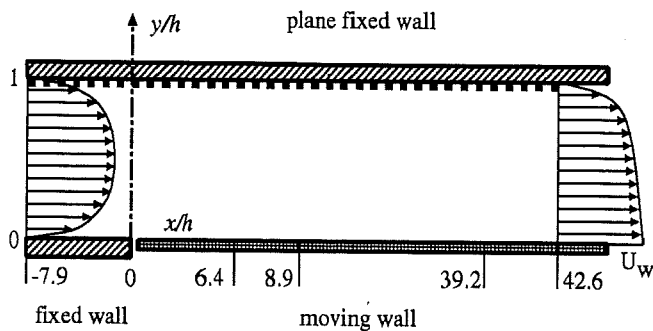


- | | |
|-------------------------------|-------|
| Experiments | □ |
| ECLille hKE std+Chi | --- |
| ECLille hKE std+RMM | |
| EDFLNHLA lKE LaSh | ---- |
| UDelftHa lKE LaSh | ----- |
| ENSICA lKE LaSh (arco) | ----- |

1A - 11

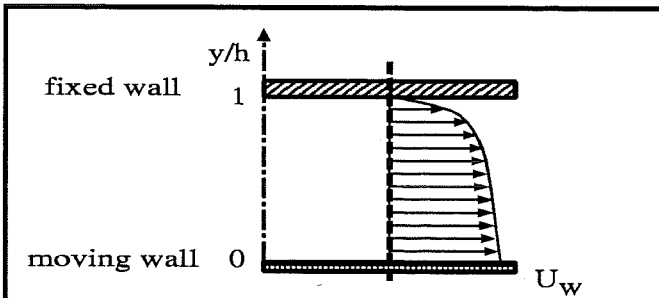
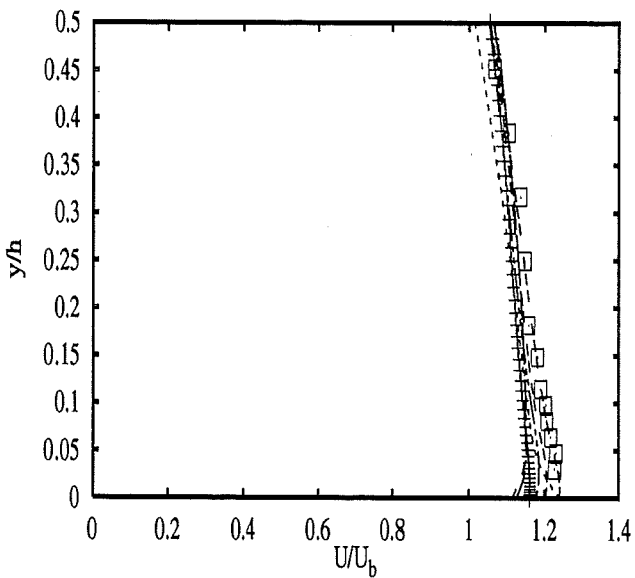
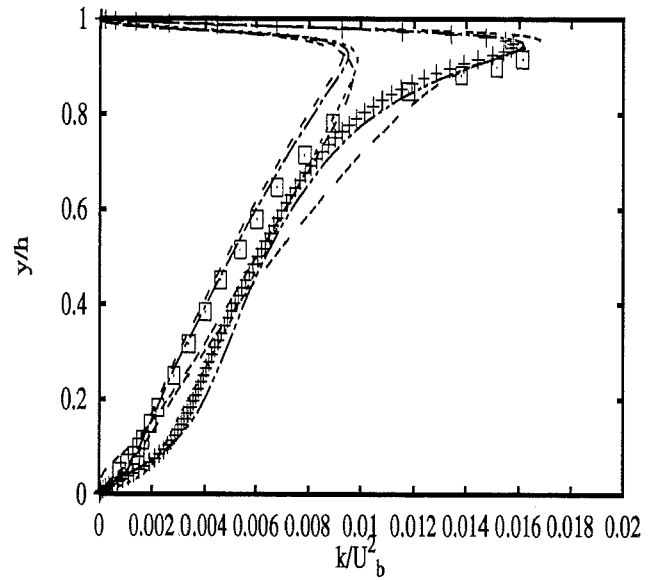
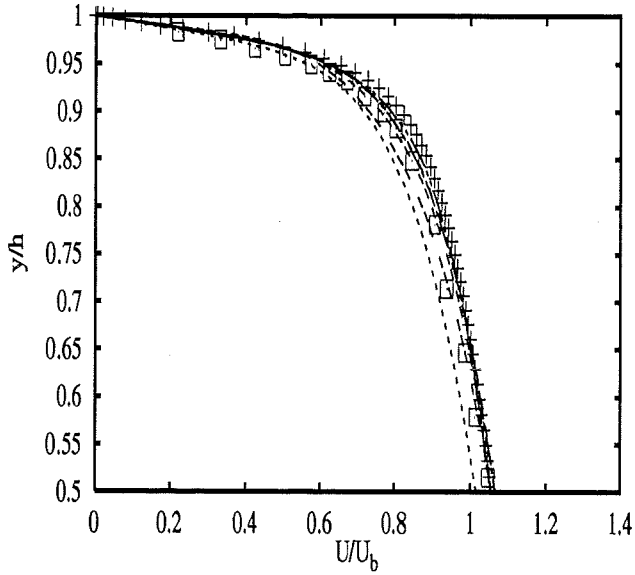


Distribution along fixed wall



Experiments □
Fluidyna *kOm Wil* — —
UConcord *kOm Wil* - - -
UDelftHa *RSM HJH* ·····

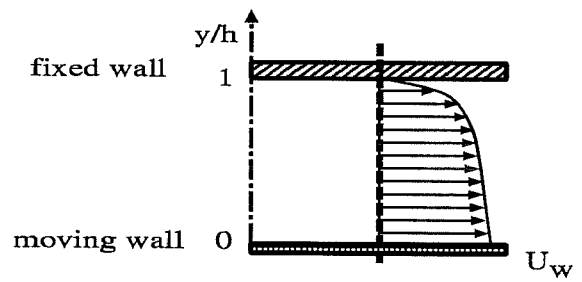
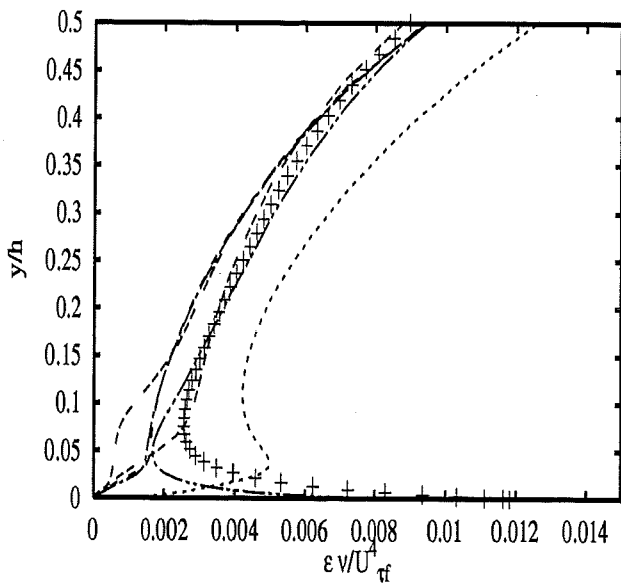
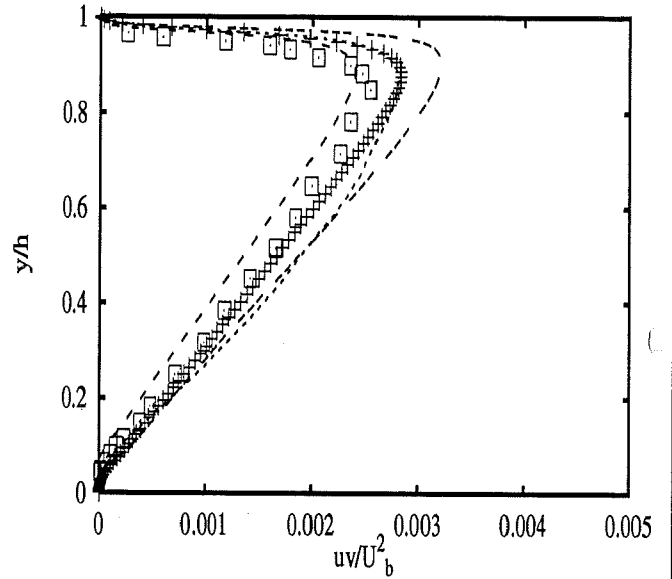
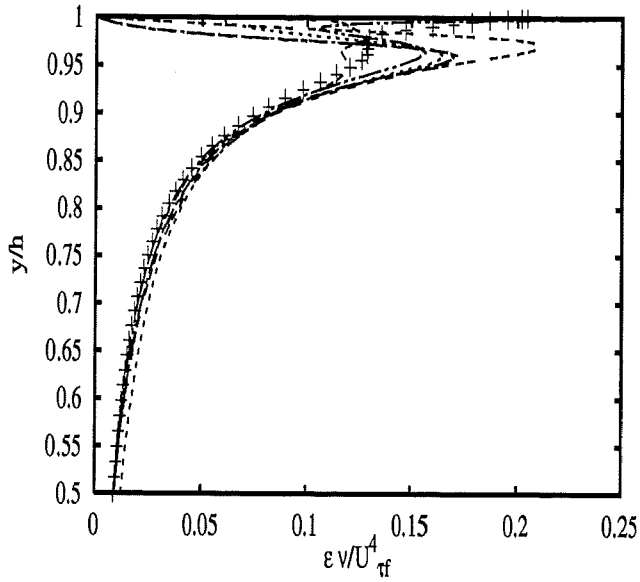
1A - 12



Developed flow

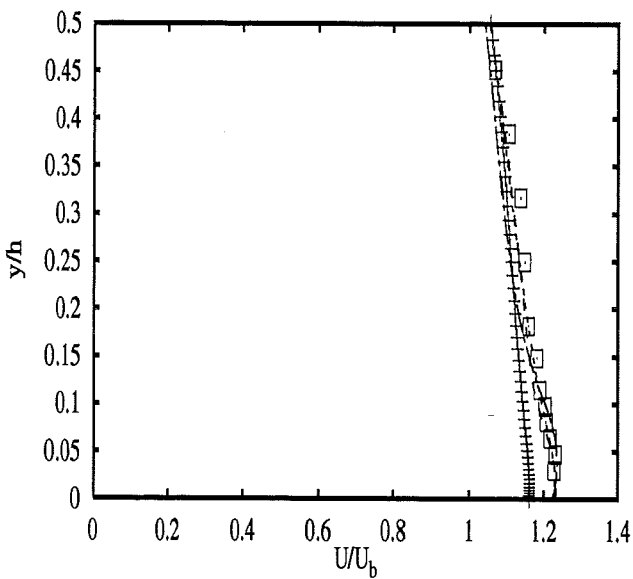
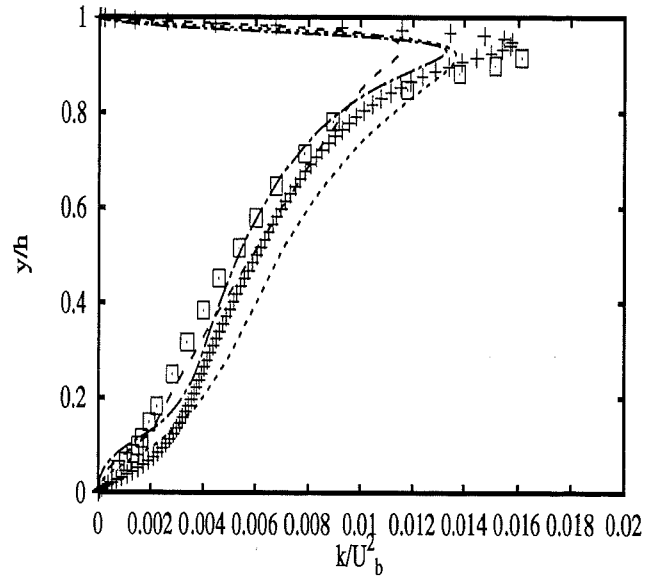
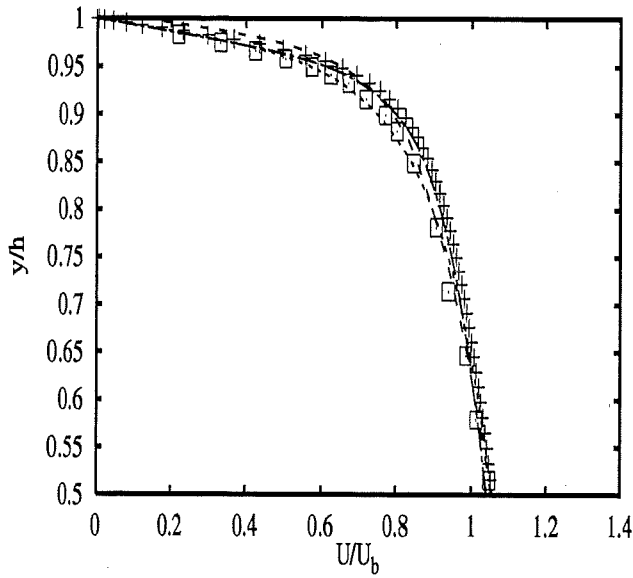
- Experiments** □
- DNS (Kuroda et al.)** +
- UdelftHa lKE LaSh** ---
- EDFLNHLA lKE LaSh** ·····
- ENSICA lKE LaSh** - - -
- ENSICA lKE YaSh** - · - ·
- Fluidyna kOm Wil** - - - -
- UConcord kOm Wil** - - - -

1A - 13



Developed flow

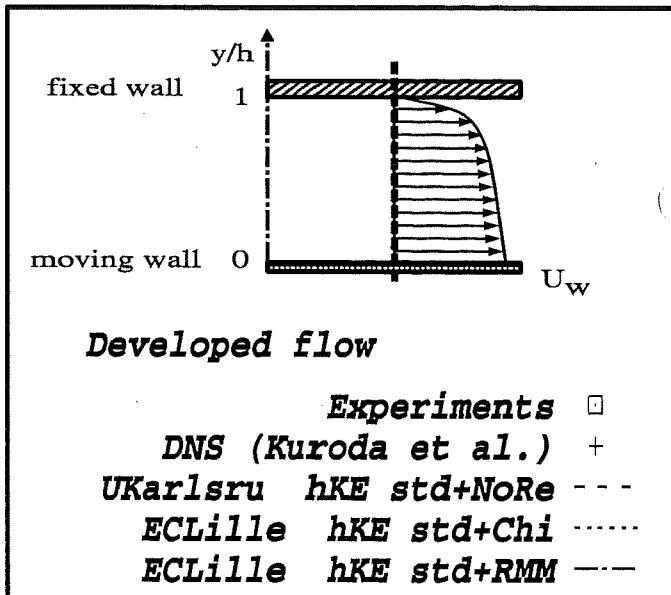
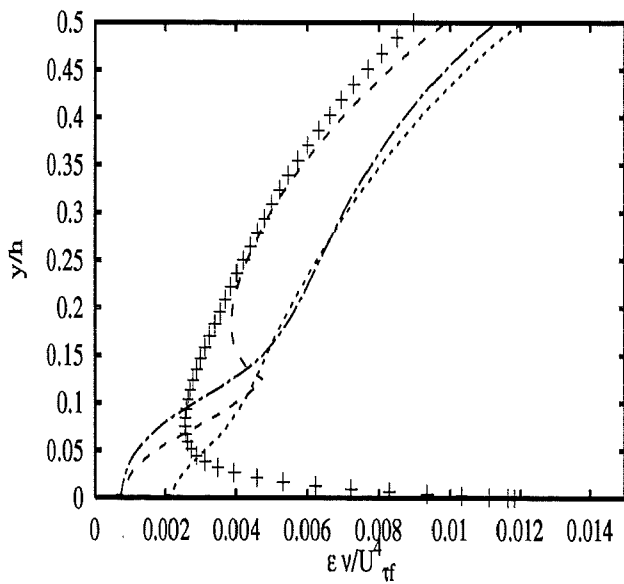
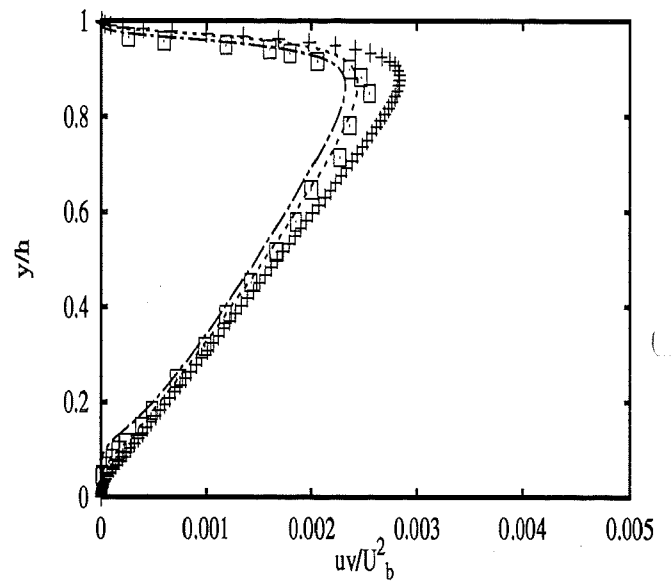
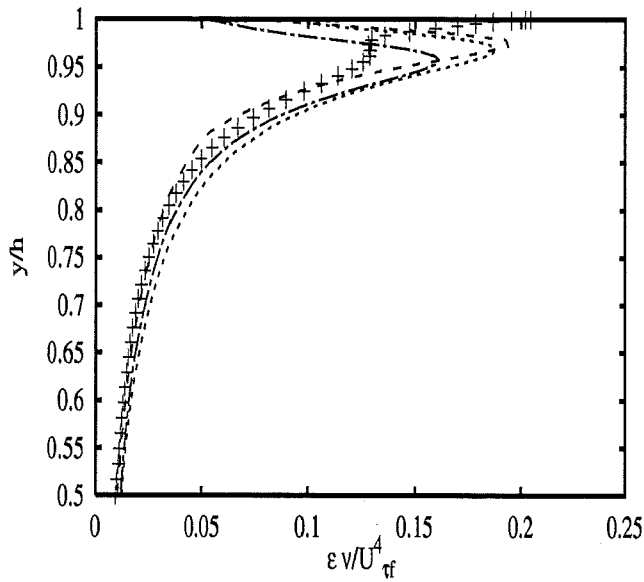
- Experiments** □
- DNS (Kuroda et al.)** +
- UDelftHa IKE LaSh** ---
- EDFLNHLa IKE LaSh** - - - -
- ENSICA IKE LaSh** - - -
- ENSICA IKE YaSh** - - - -
- Fluidyna kOm Wil** - - - -
- UConcord kOm Wil** - - - -

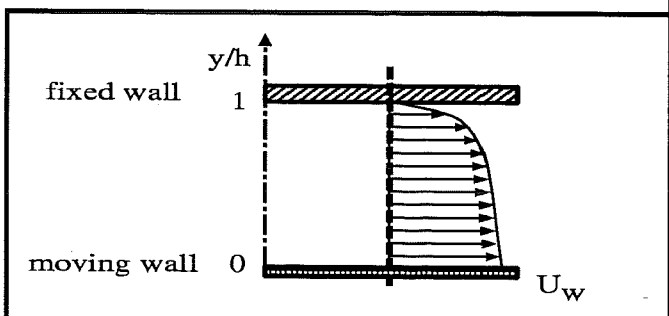
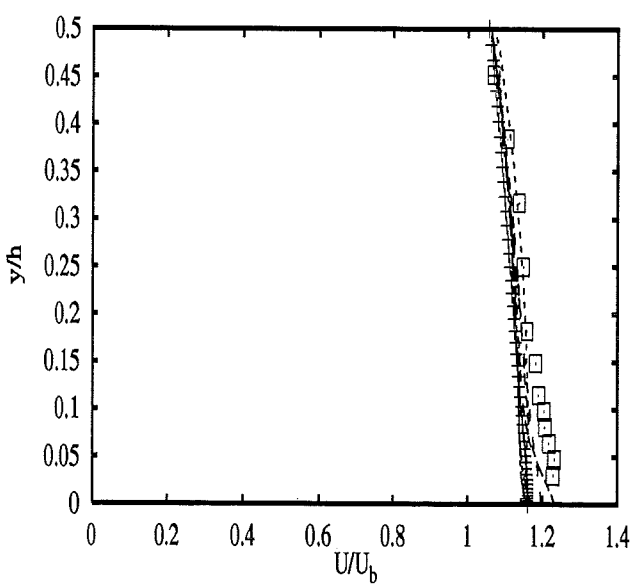
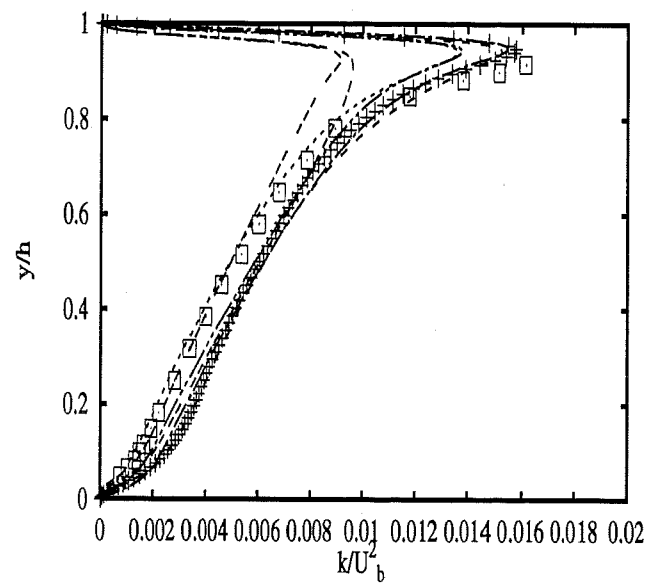
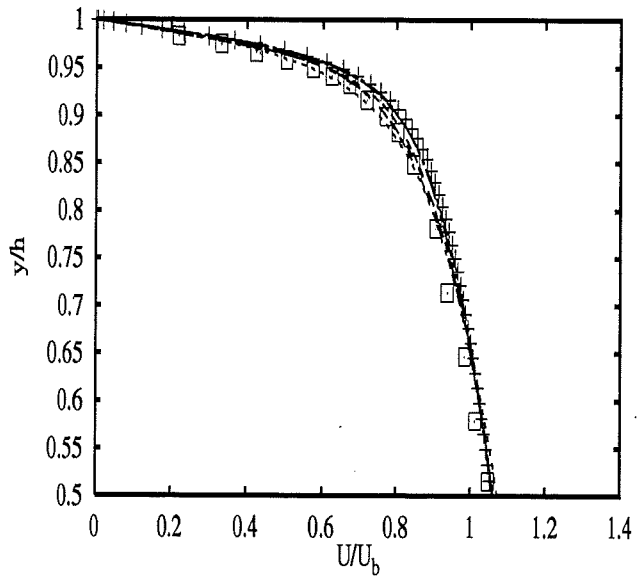


Developed flow

Experiments □
DNS (Kuroda et al.) +
UKarlsruhe hKE std+NoRe ---
ECLille hKE std+Chi
ECLille hKE std+RMM - - -

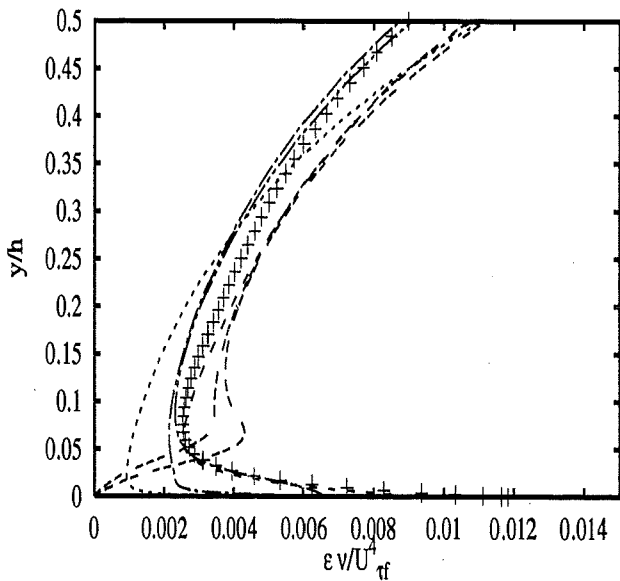
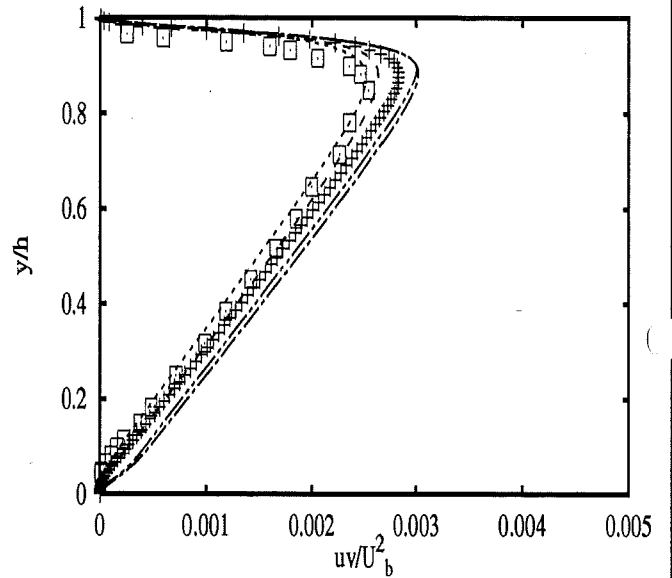
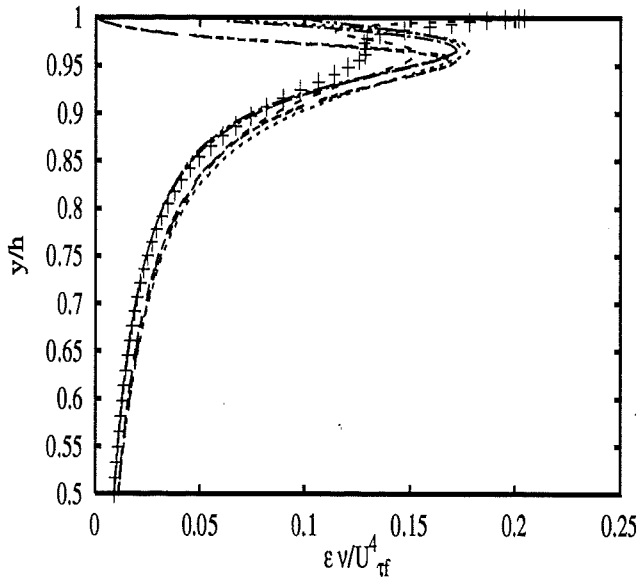
1A - 15





Developed flow

- Experiments** □
- DNS (Kuroda et al.)** +
- EDFLNHLa RSM LRR+elr** ---
- ECLille RSM LaSh** ·····
- ECLille RSM JaHa** - - - -
- UDeftHa RSM HJH** - · - · -
- UMISTCra RSM CrLa+2eq** - - - -
- UMISTCra RSM Cub+2eq** - - - -

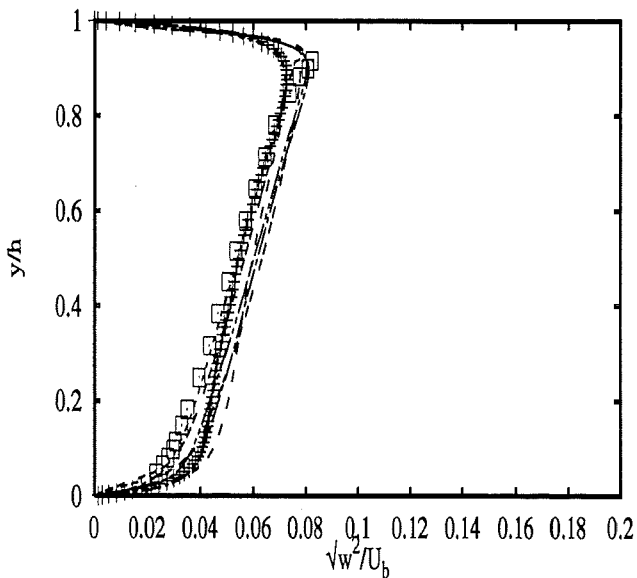
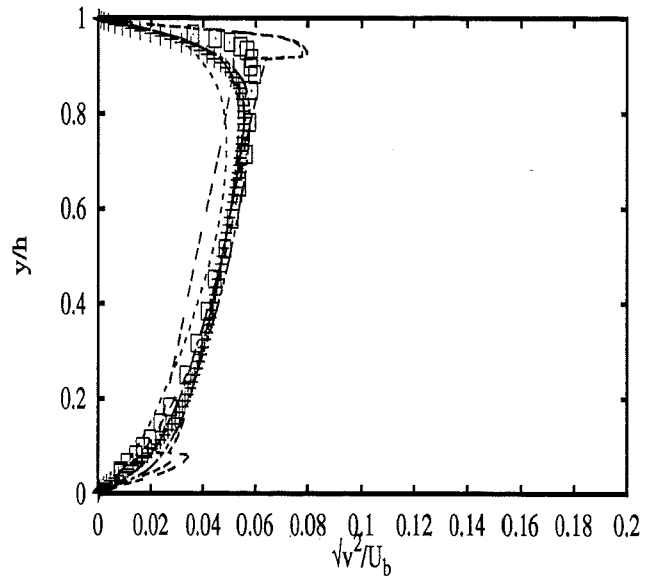
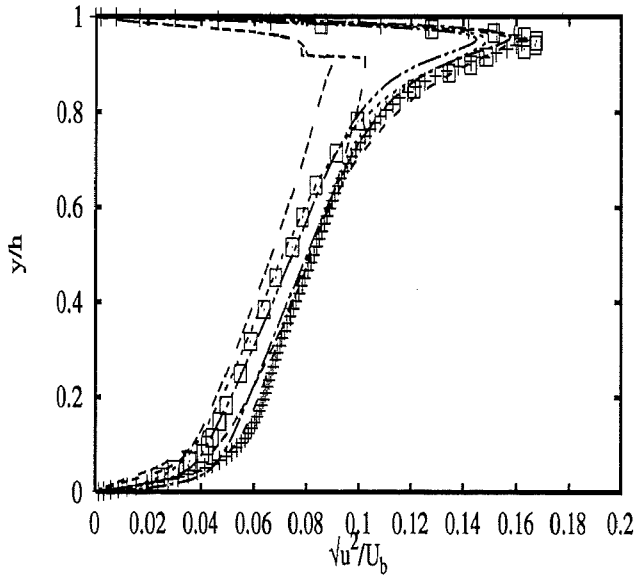


fixed wall 1
moving wall 0
 U_w

Developed flow

Experiments □
DNS (Kuroda et al.) +
EDFLNHLa RSM LRR+elr - - -
ECLille RSM LaSh ·····
ECLille RSM JaHa — — —
UDELfthHa RSM HJH - · - · -
UMISTCra RSM CrLa+2eq - - -
UMISTCra RSM Cub+2eq - · - · -

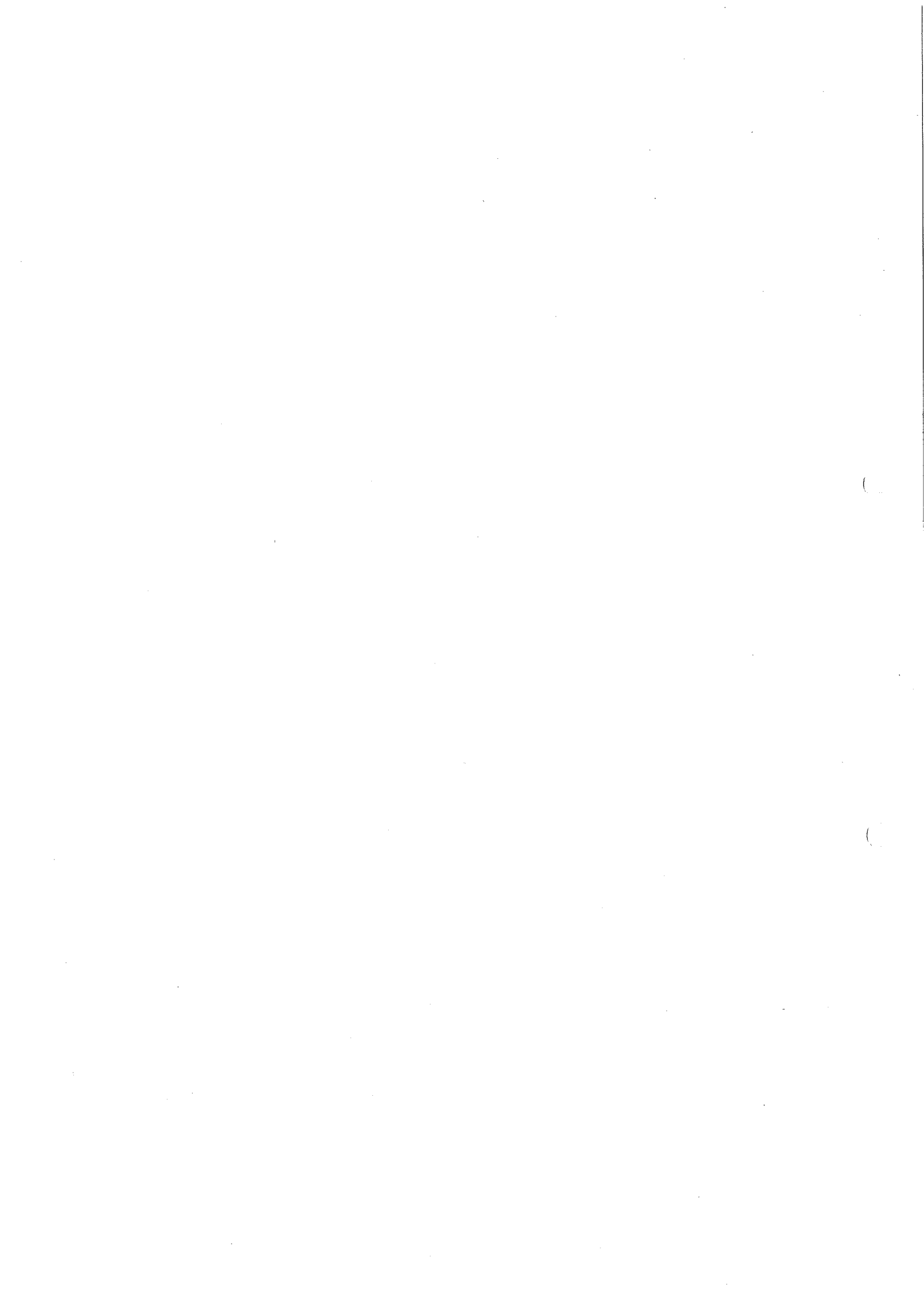
1A - 18

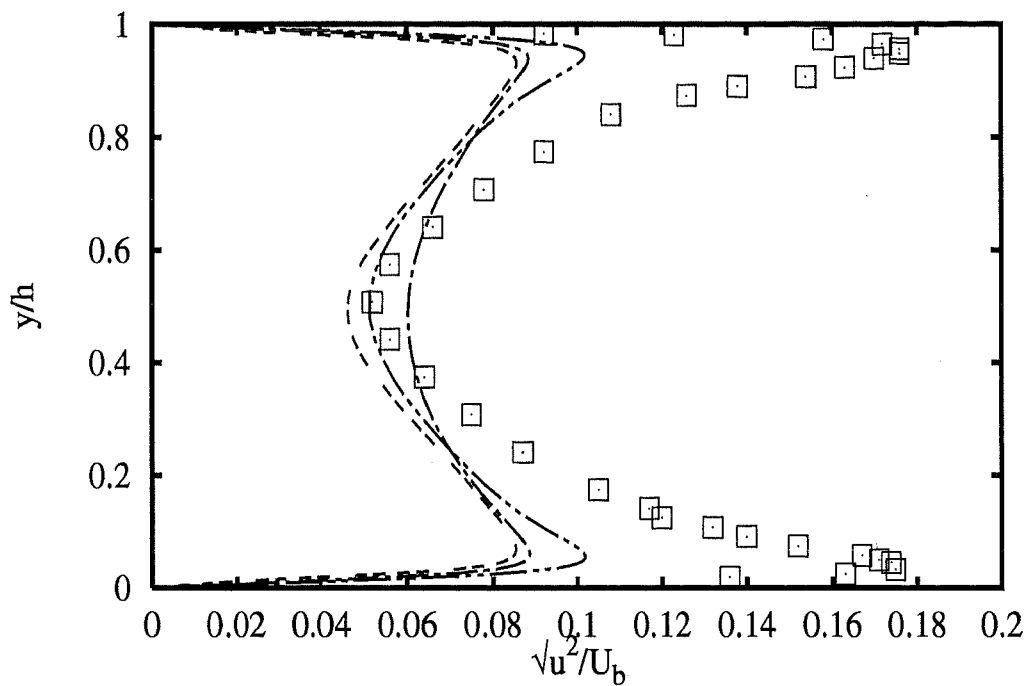
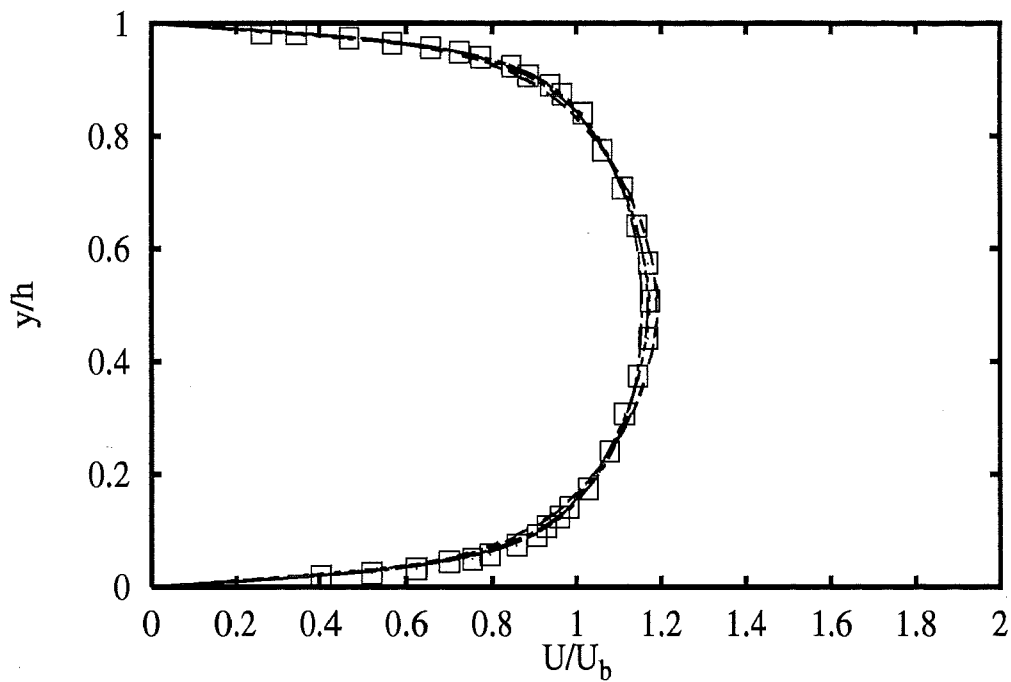


Developed flow

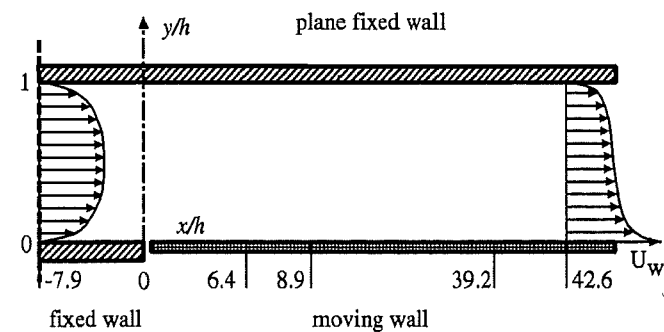
| | |
|------------------------------|-------|
| Experiments | □ |
| DNS (Kuroda et al.) | + |
| EDFLNHLa RSM LRR+elr | --- |
| ECLille RSM LaSh | |
| ECLille RSM JaHa | ---- |
| UDeflthHa RSM HJH | ---- |
| UMISTCra RSM CrLa+2eq | --- |
| UMISTCra RSM Cub+2eq | --- |

1A - 19



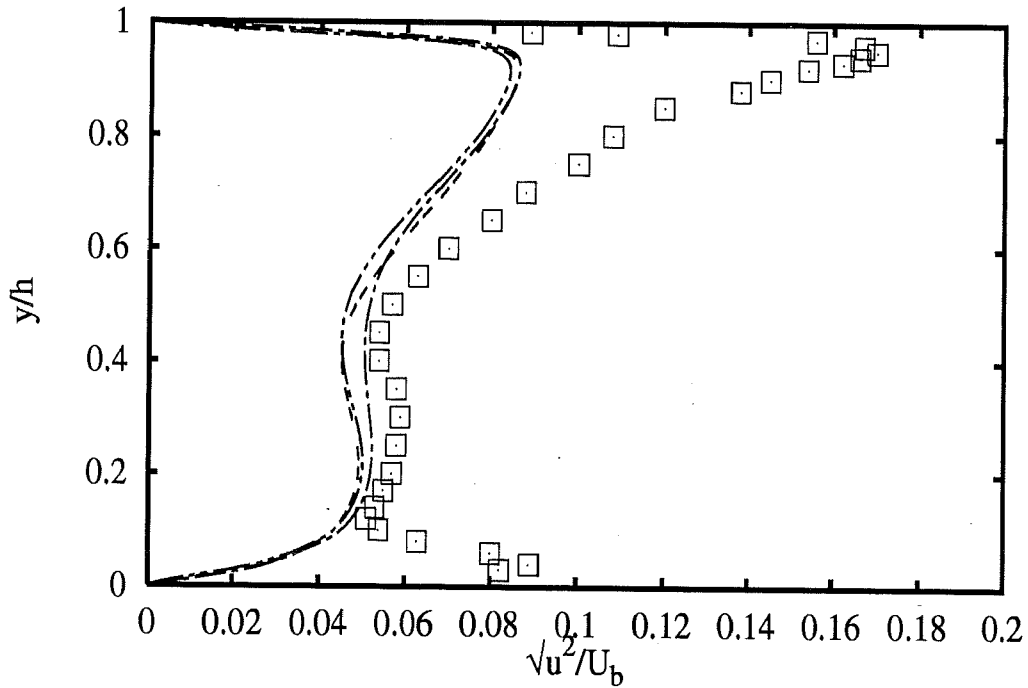
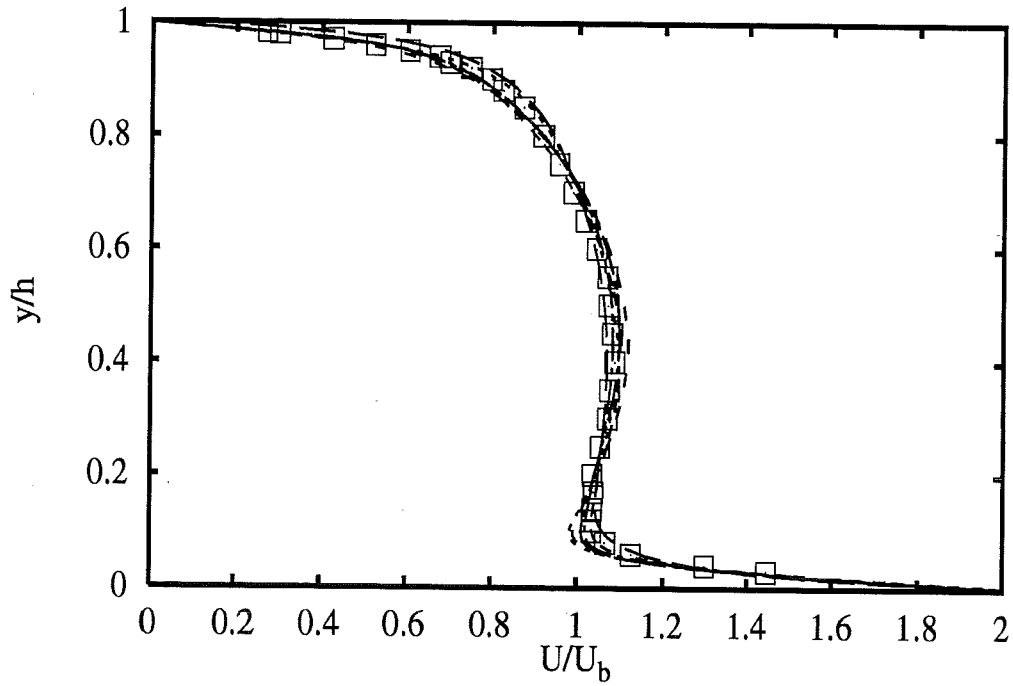


Profiles at $x/h = -7.9$

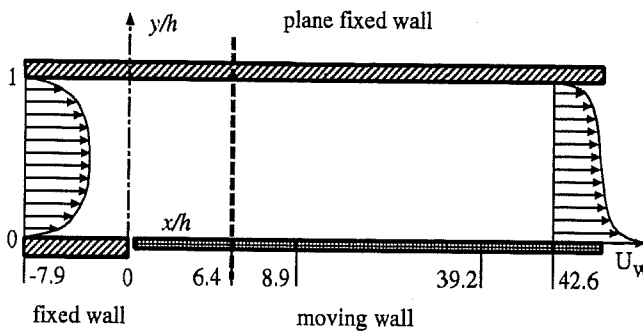


- | | |
|-------------------------------|-------|
| Experiments | □ |
| ECLille hKE std+Chi | --- |
| ECLille hKE std+RMM | |
| EDFLNHLA lKE LaSh | ---- |
| UDeflthHa lKE LaSh | ----- |
| ENSICA lKE LaSh (arco) | ----- |

1B - 1

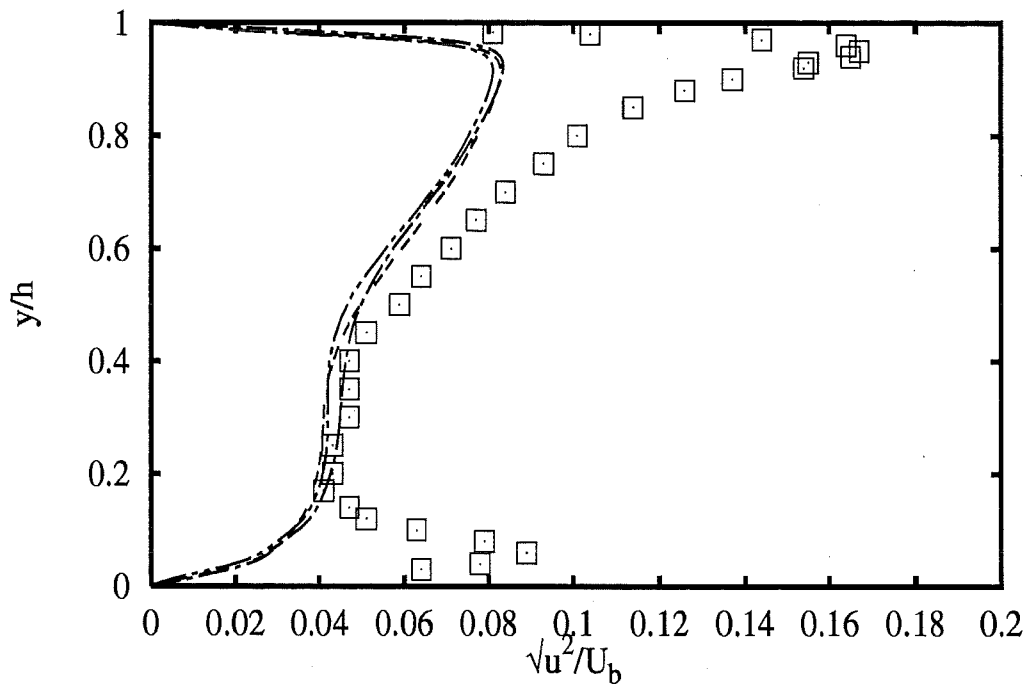
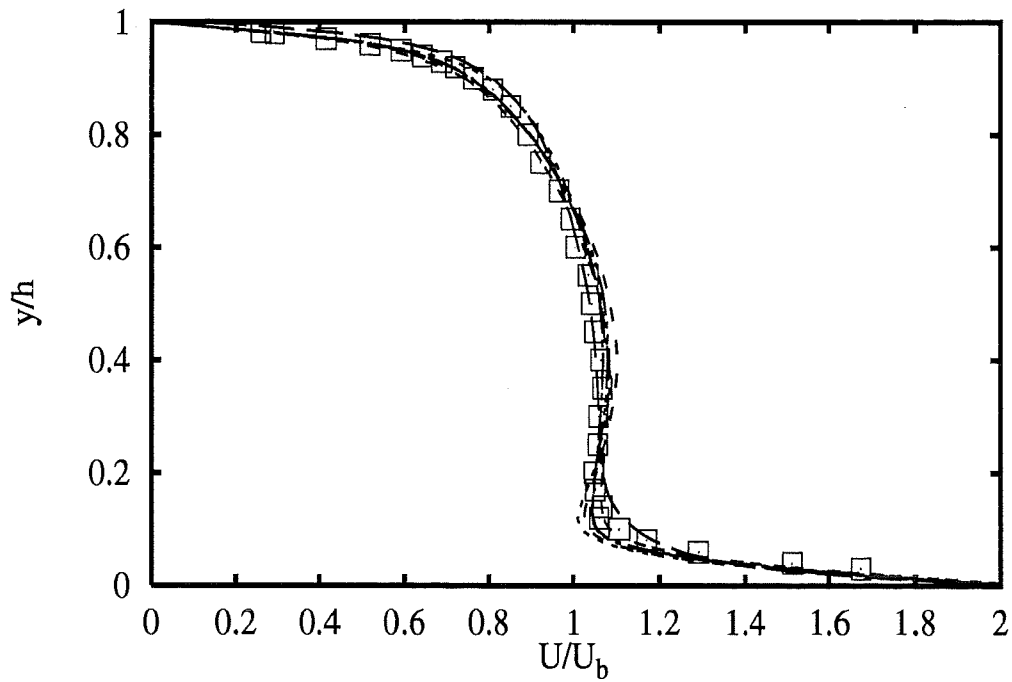


Profiles at $x/h=5.6$

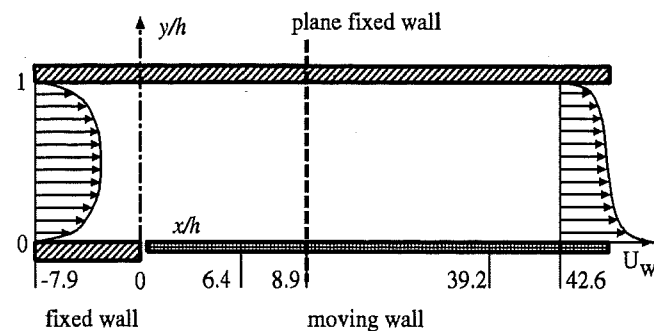


- | | |
|--------------------|------------------------------|
| Experiments | □ |
| UKarlsru | <i>hKE std+NoRe</i> --- |
| ECLille | <i>hKE std+Chi</i> - - - |
| ECLille | <i>hKE std+RMM</i> ····· |
| EDFLNHLa | <i>lKE LaSh</i> - - - |
| UdelftHa | <i>lKE LaSh</i> - - - |
| ENSICA | <i>lKE LaSh (arco)</i> - - - |

1B - 2

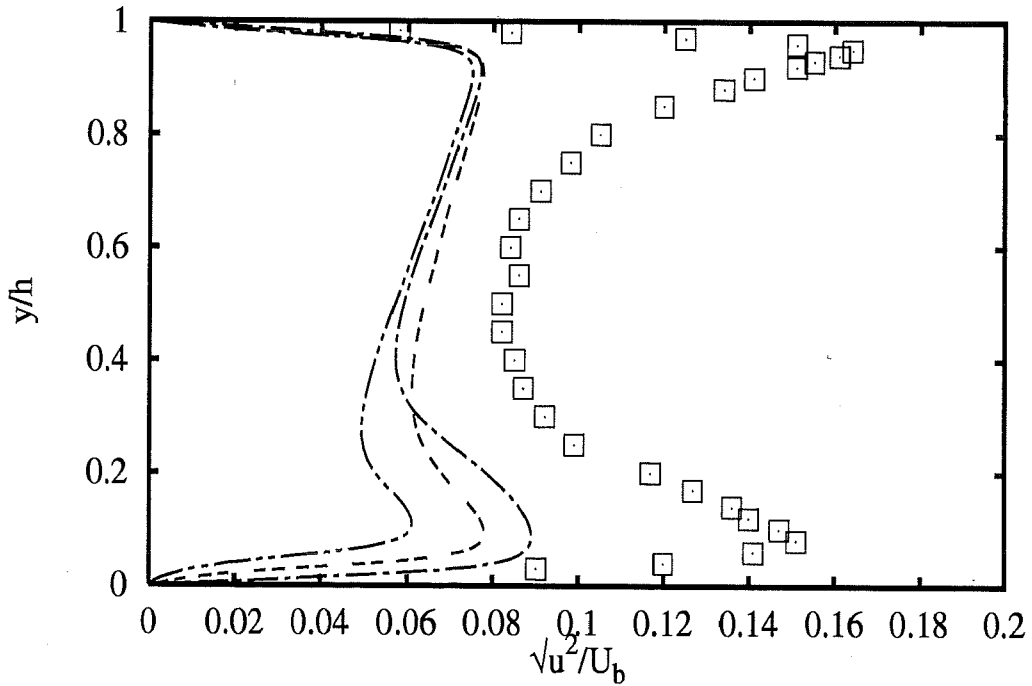
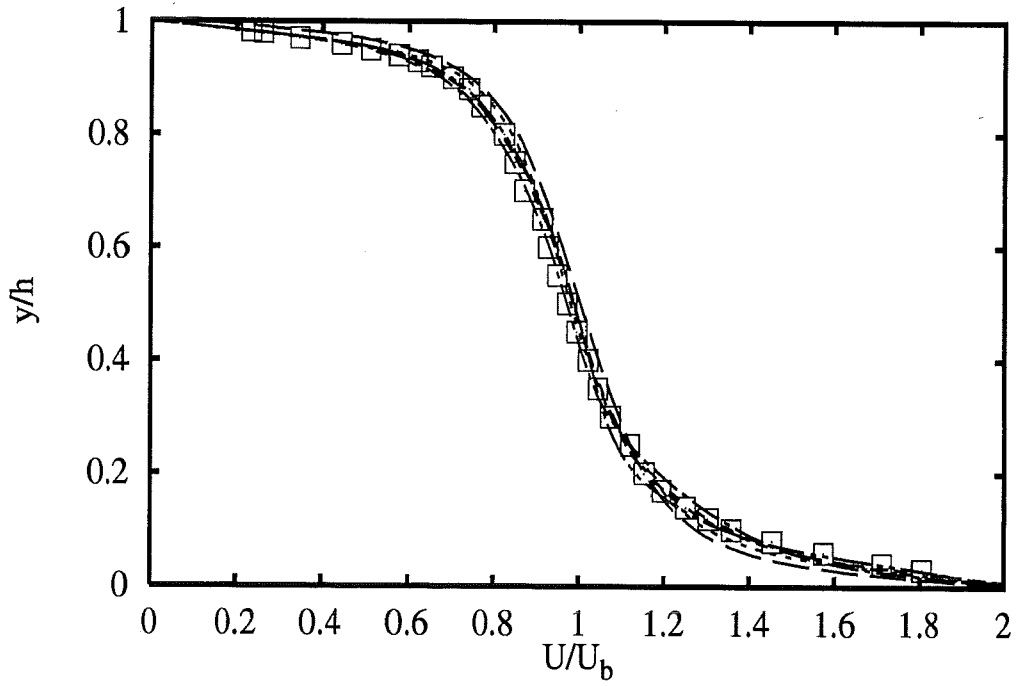


Profiles at $x/h=8.9$

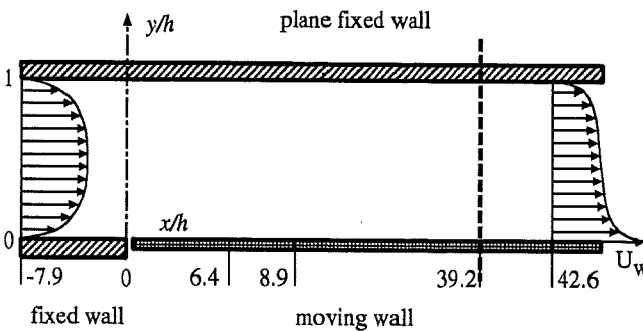


- | | |
|--------------------------------|-----|
| Experiments | □ |
| UKarlsruhe hKE std+NoRe | --- |
| ECLille hKE std+Chi | --- |
| ECLille hKE std+RMM | --- |
| EDFLNHLa lKE LaSh | --- |
| UdelftHa lKE LaSh | --- |
| ENSICA lKE LaSh (arco) | --- |

1B - 3

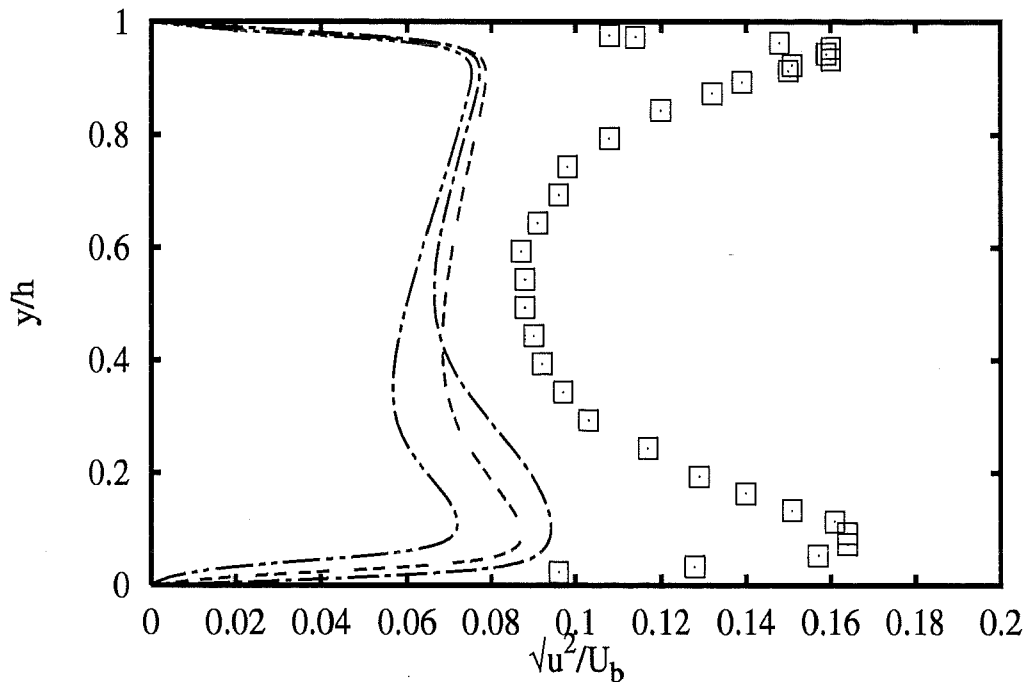
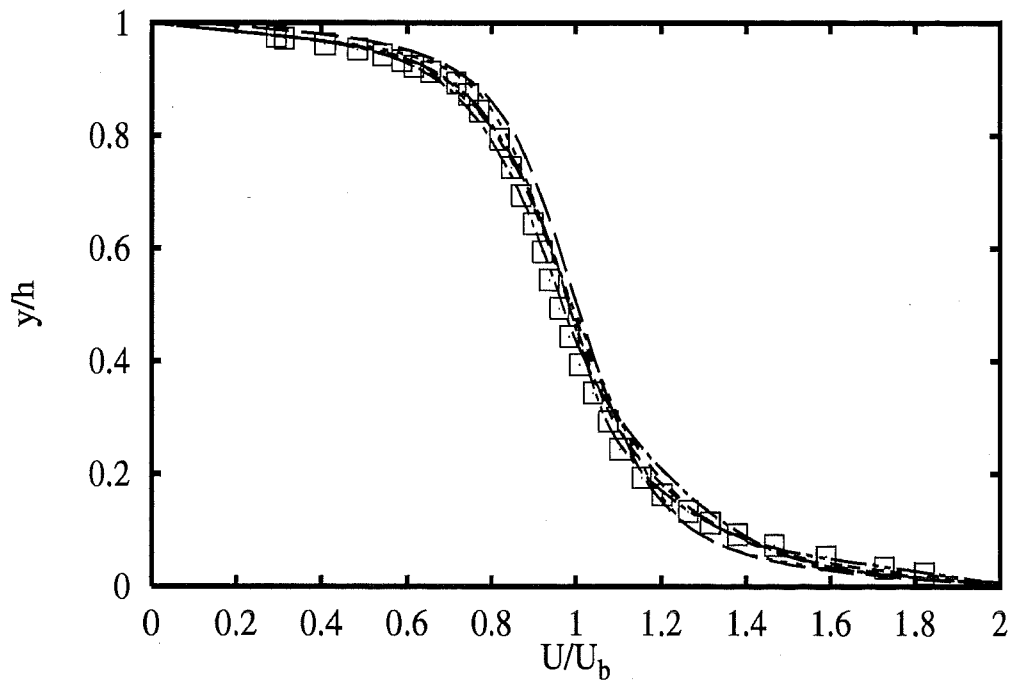


Profiles at $x/h=39.2$

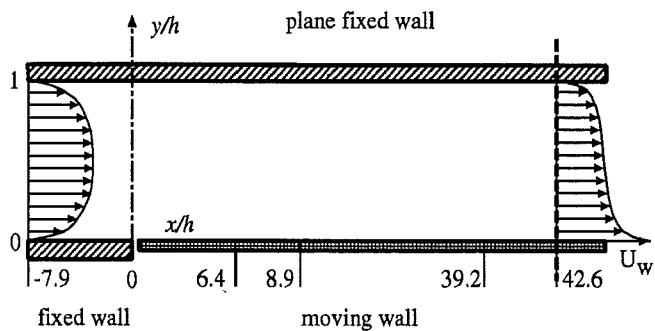


- | | | |
|----------|------------------------|-----|
| | Experiments | □ |
| UKarlsru | hKE std+NoRe | --- |
| ECLille | hKE std+Chi | --- |
| ECLille | hKE std+RMM | --- |
| EDFLNHLa | lKE LaSh | --- |
| UdelftHa | lKE LaSh | --- |
| ENSICA | lKE LaSh (arco) | --- |

1B - 4

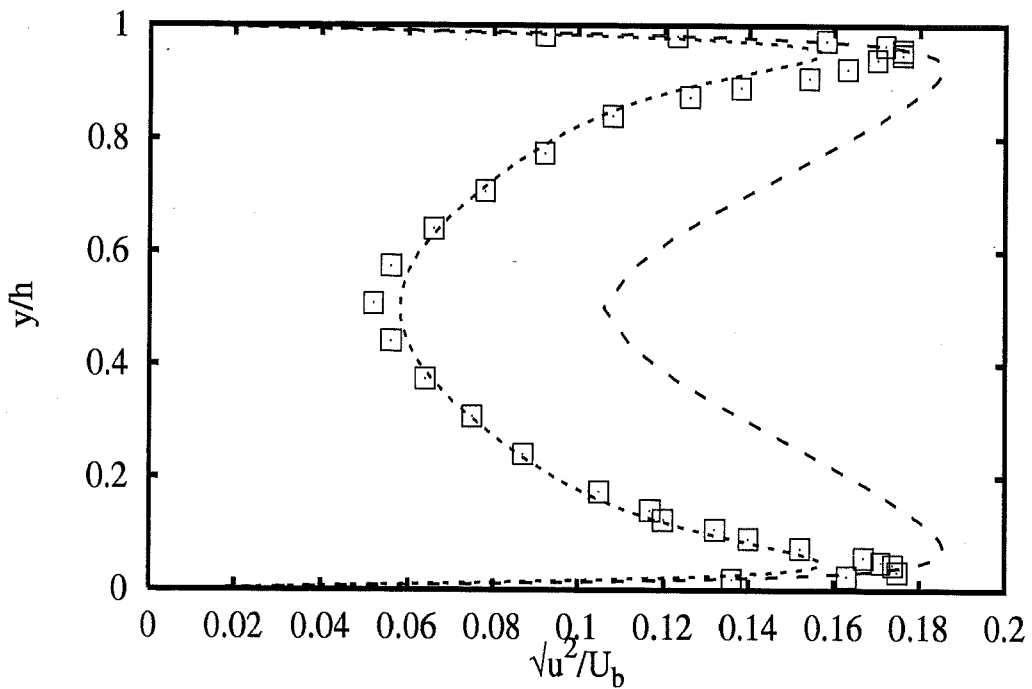
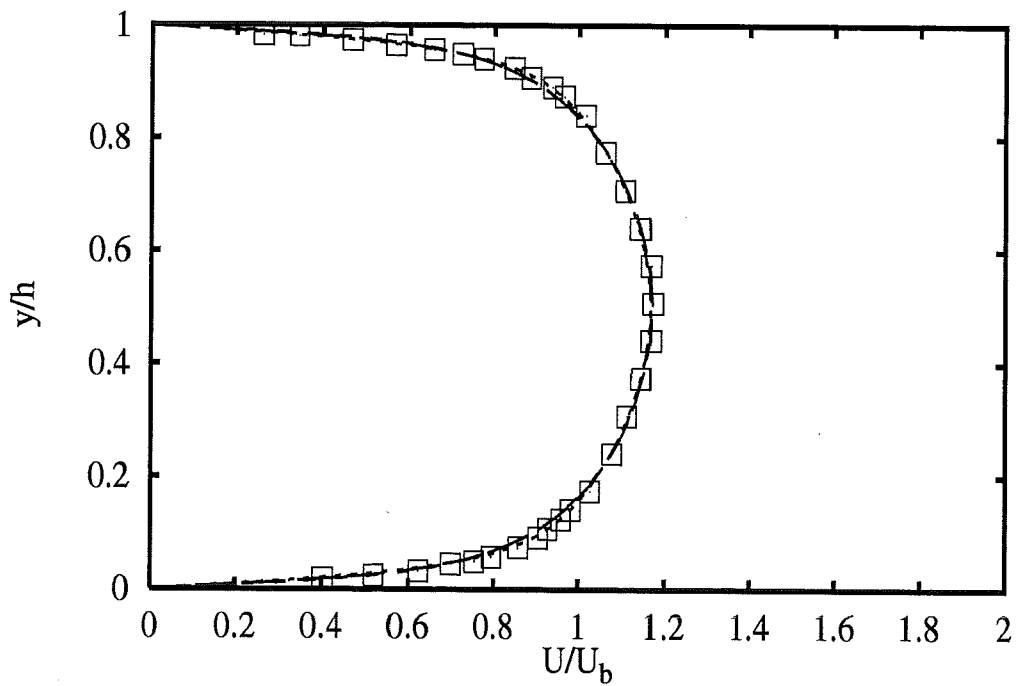


Profiles at $x/h=42.6$

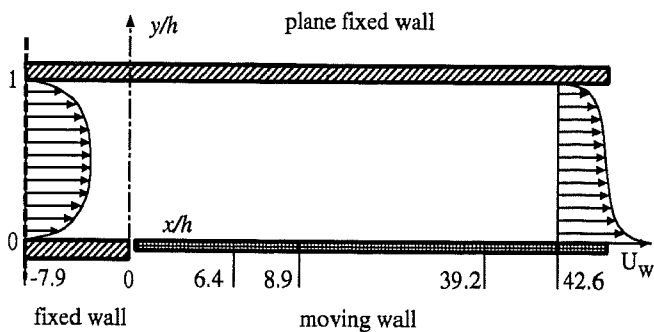


- | | |
|--------------------------------------|---------|
| Experiments | □ |
| UKarlsru <i>hKE std+NoRe</i> | --- |
| ECLille <i>hKE std+Chi</i> | ---- |
| ECLille <i>hKE std+RMM</i> | |
| EDFLNHLA <i>lKE LaSh</i> | -.-.- |
| UdelftHa <i>lKE LaSh</i> | -.-.-.- |
| ENSICA <i>lKE LaSh (arco)</i> | -.-.-.- |

1B - 5

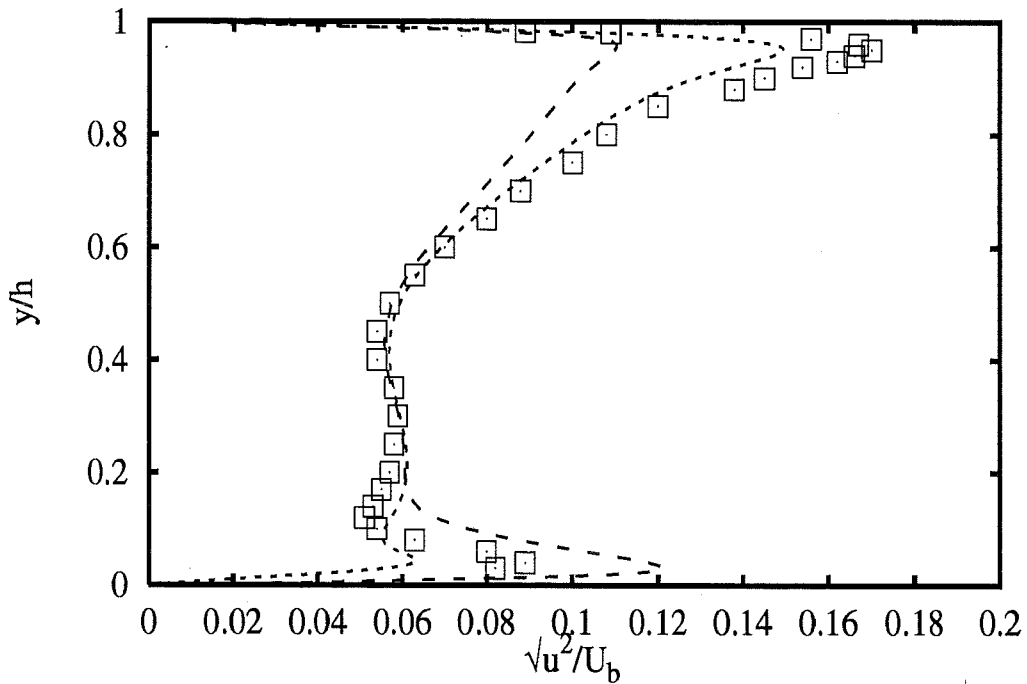
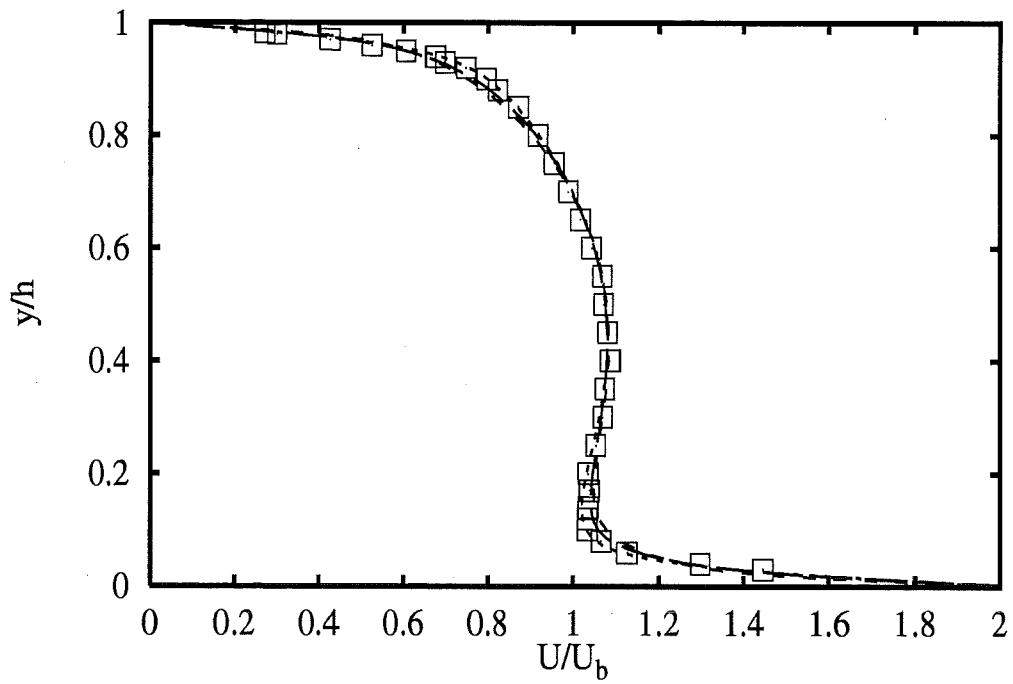


Profiles at $x/h = -7.9$

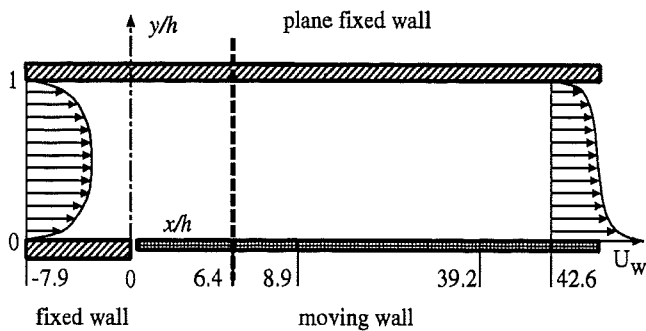


- | | |
|--------------------|-------|
| Experiments | □ |
| Fluidyna kOm Wil | --- |
| UConcord kOm Wil | ---- |
| UDelftHa RSM HJH | |

1B - 6

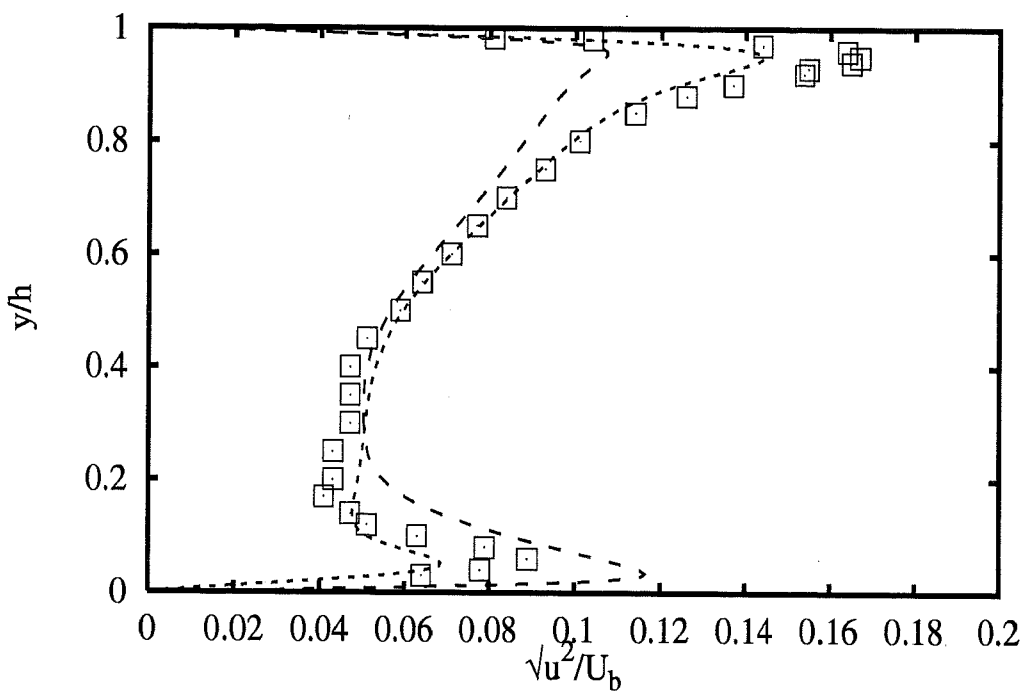
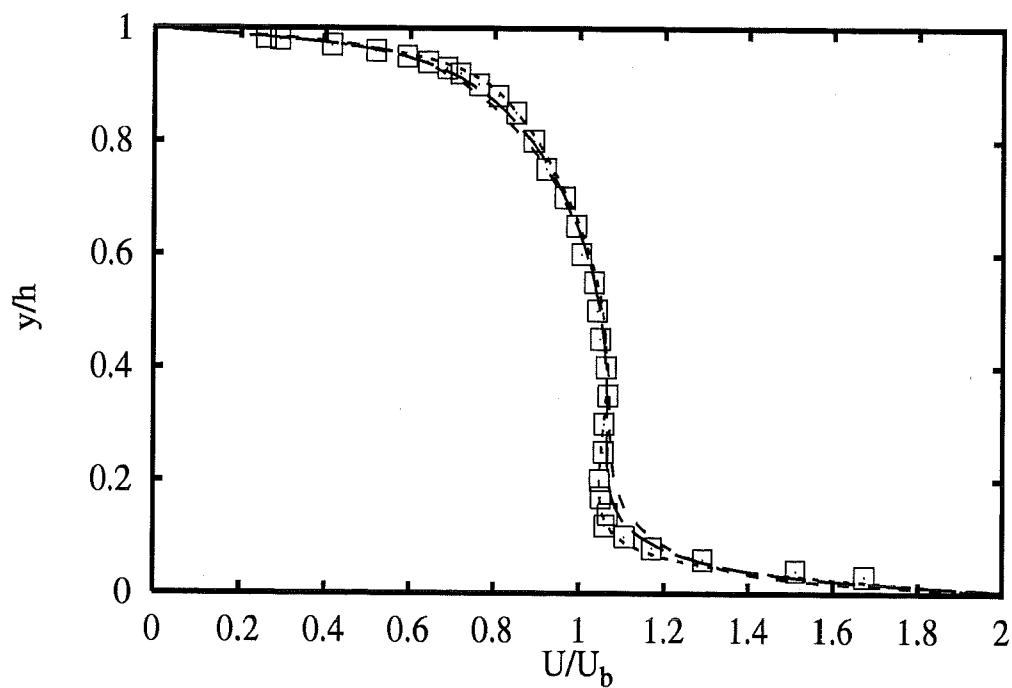


Profiles at $x/h=5.6$

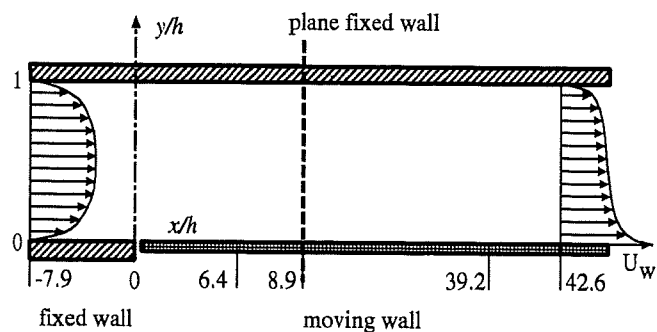


Experiments □
Fluidyna kOm Wil — —
UConcord kOm Wil - - -
UDelftHa RSM HJH ·····

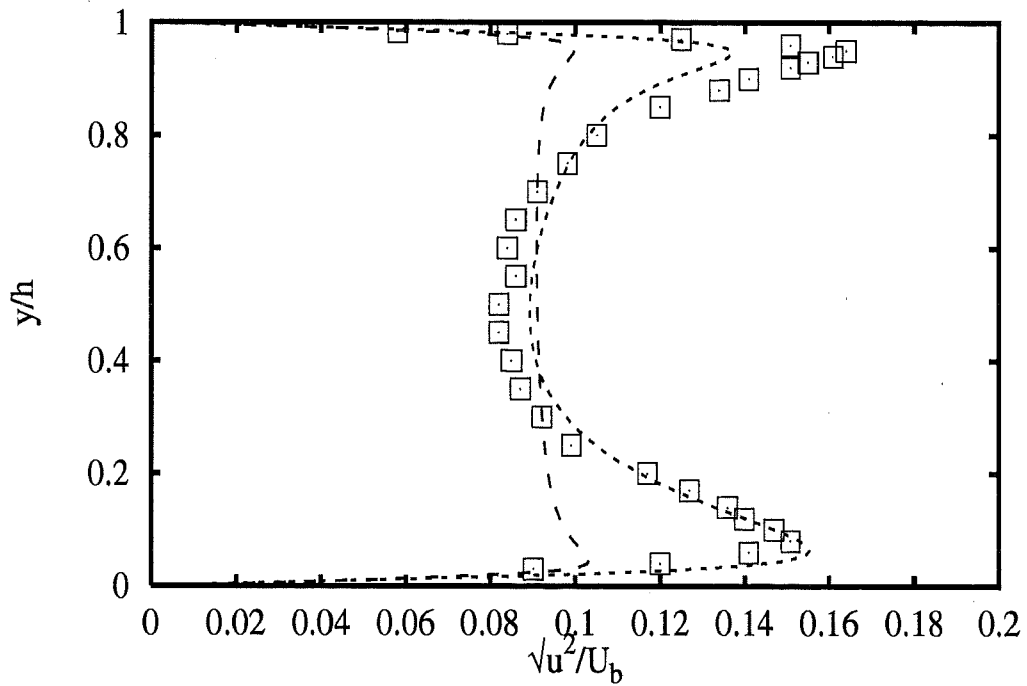
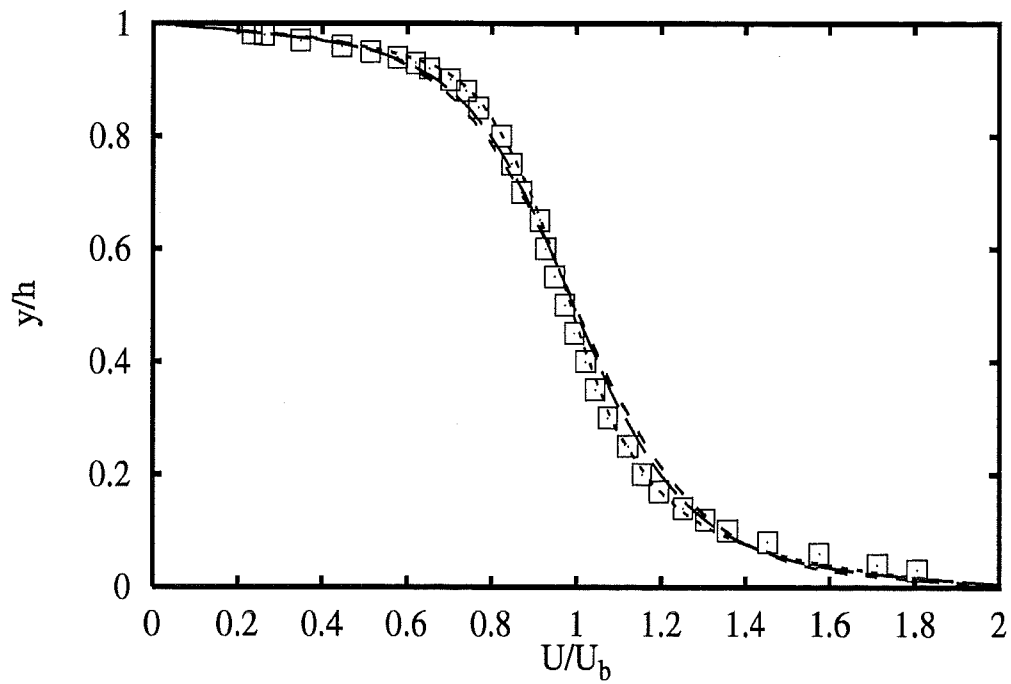
1B - 7



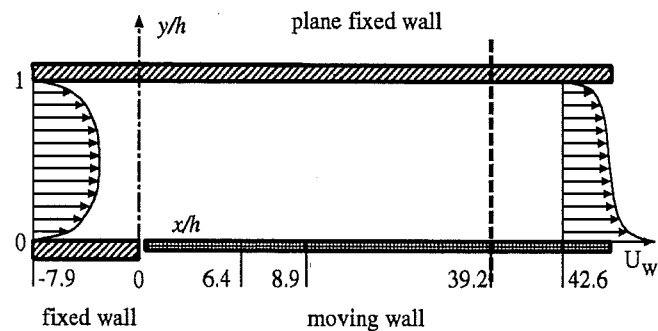
Profiles at $x/h=8.9$



Experiments □
Fluidyna *kOm Wil* ---
UConcord *kOm Wil* - - -
UDelftHa *RSM HJH* ·····

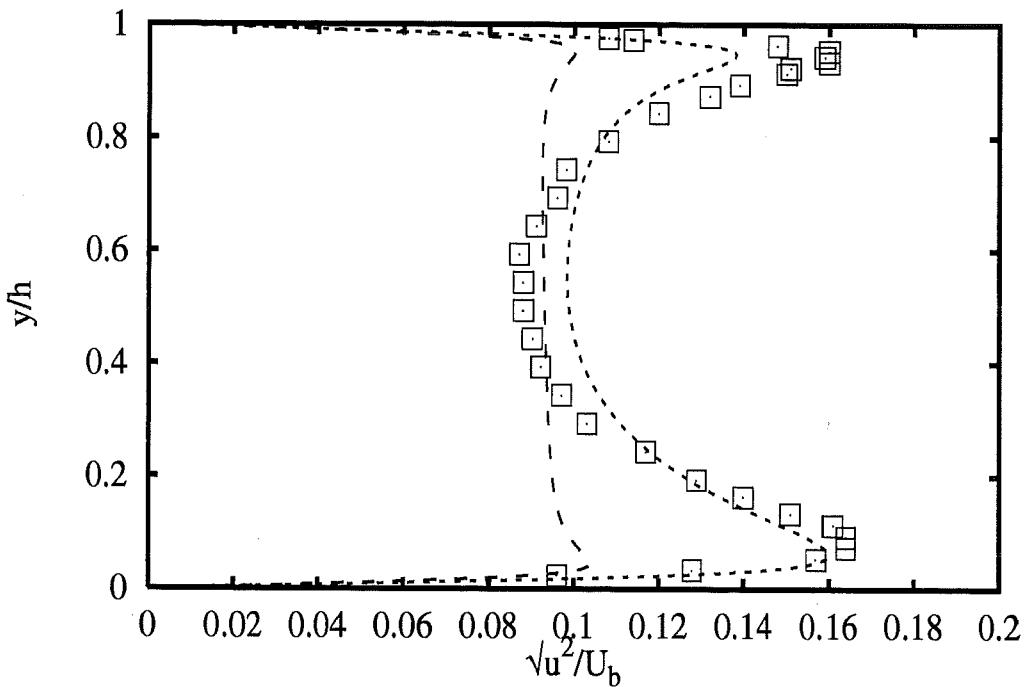
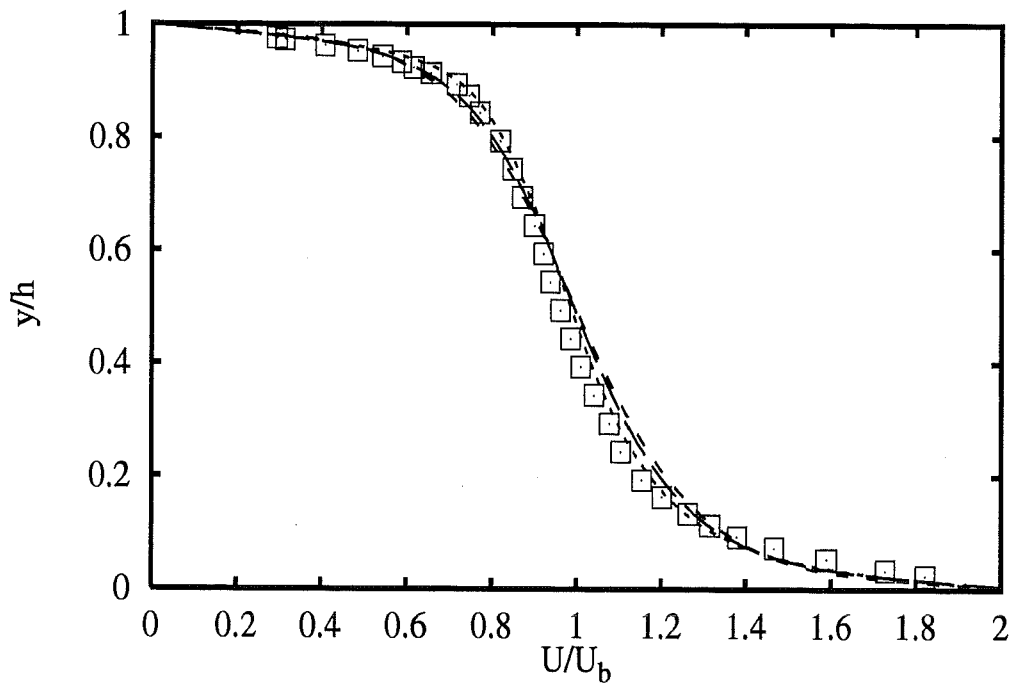


Profiles at $x/h=39.2$

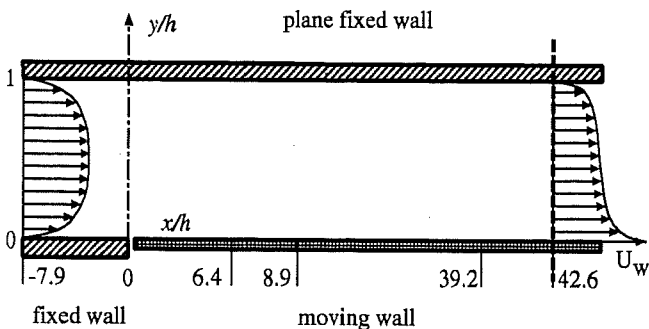


- | | |
|--------------------|---------------------|
| Experiments | □ |
| Fluidyna | $k\Omega$ Wil — — |
| UConcord | $k\Omega$ Wil - - - |
| UDelftHa | RSM HJH ····· |

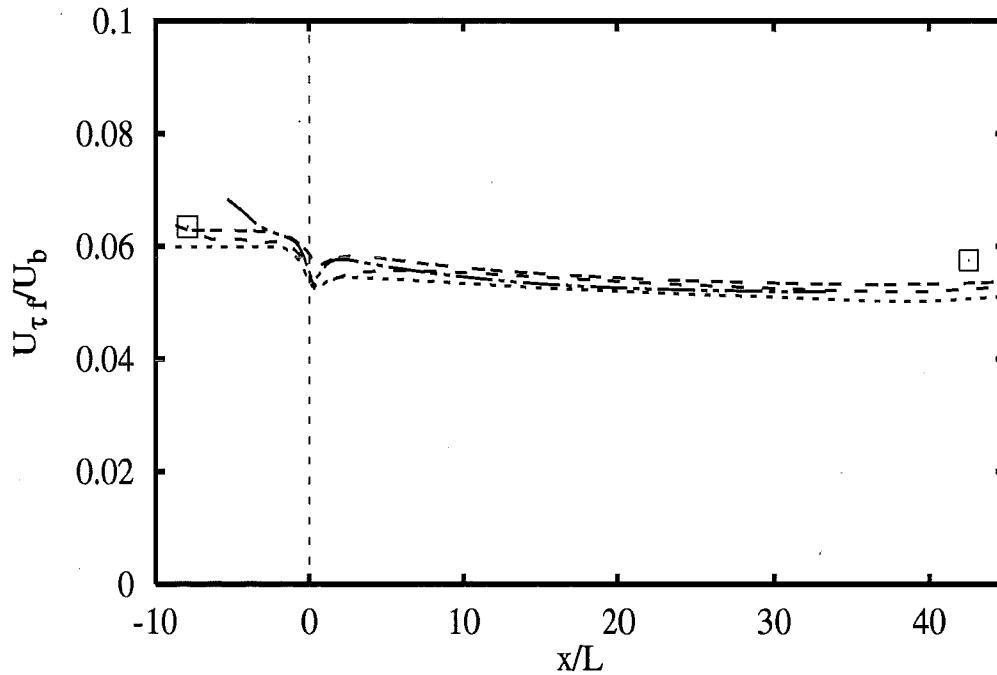
1B - 9



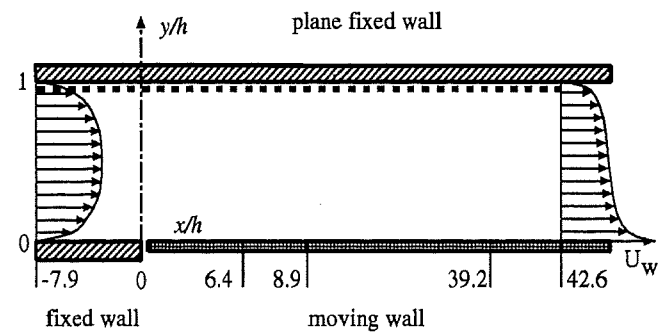
Profiles at $x/h=42.6$



- Experiments** □
- Fluidyna kOm Wil ---
 - UConcord kOm Wil - - -
 - UDelftHa RSM HJH ·····

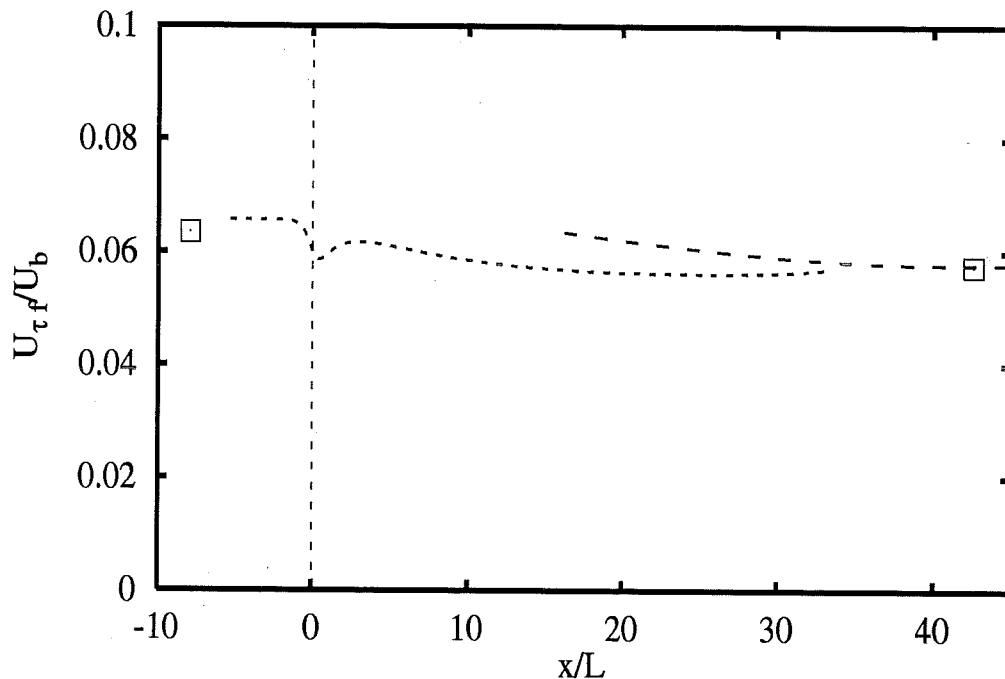


Distribution along fixed wall

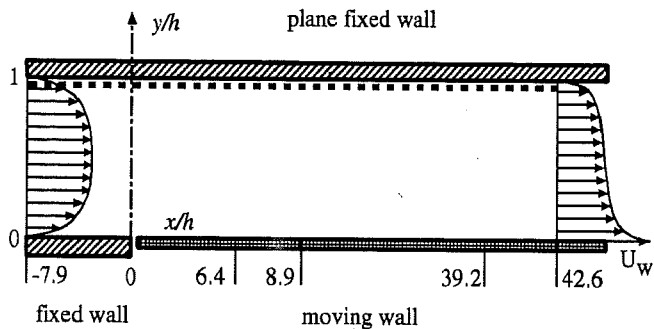


- | | |
|-------------------------------|-------|
| Experiments | □ |
| ECLille hKE std+Chi | --- |
| ECLille hKE std+RMM | |
| UDelftHa lKE LaSh | -.-.- |
| ENSICA lKE LaSh (arco) | --- |

1B - 11

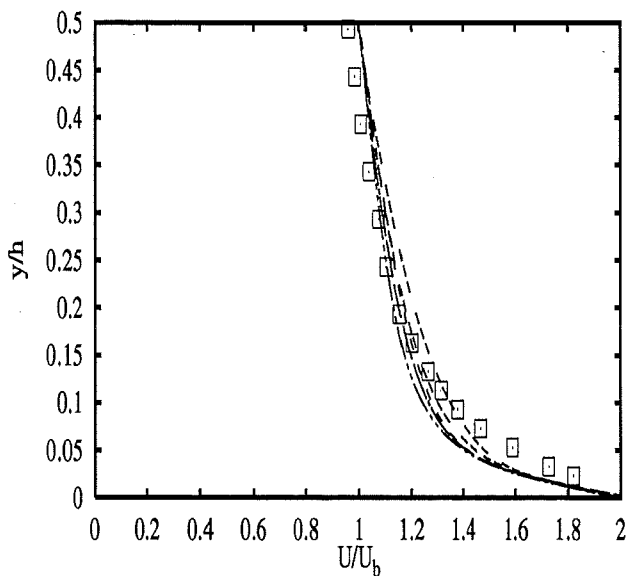
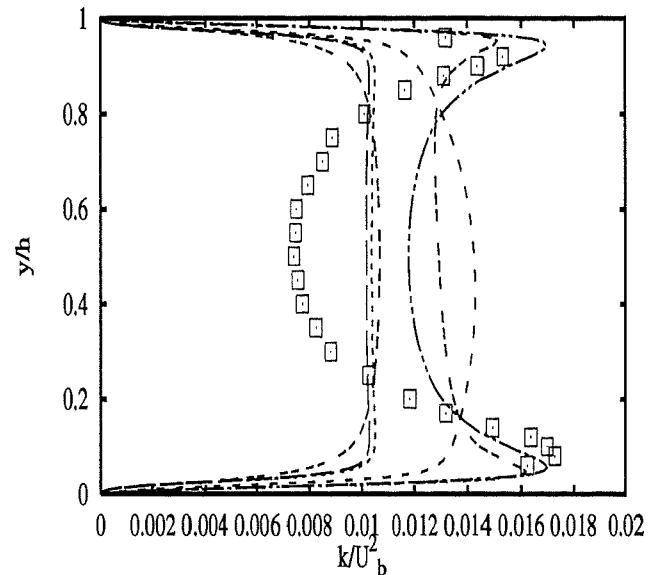
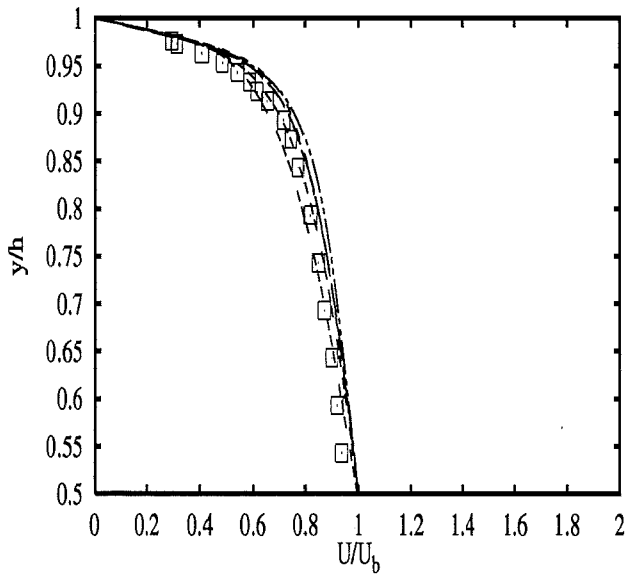


Distribution along fixed wall



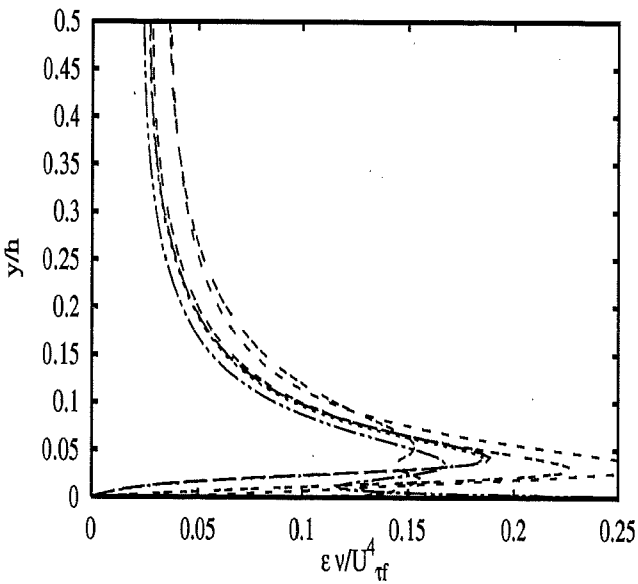
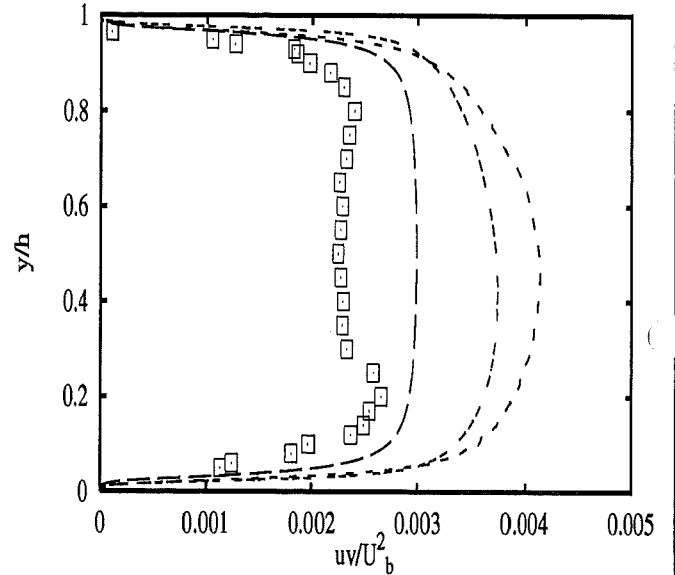
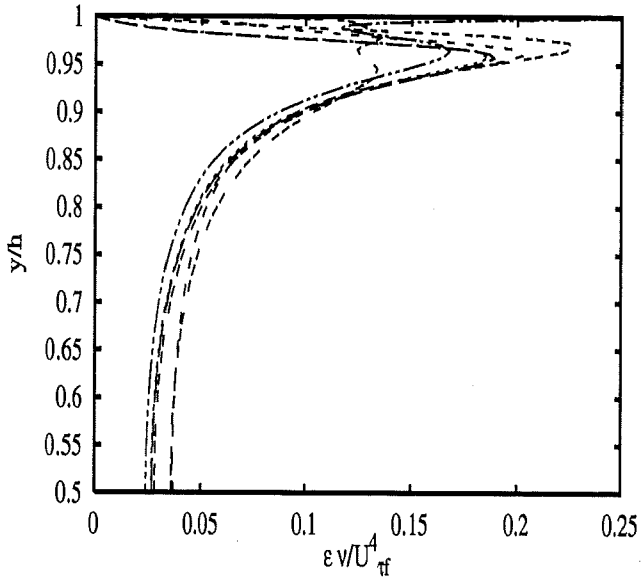
Experiments □
 Fluidyna kOm Wil — —
 UConcord kOm Wil - - -
 UDelftHa RSM HJH ·····

1B - 12



Developed flow

| | | |
|-----------------|--------------------|---------|
| | Experiments | □ |
| <i>UDelftHa</i> | <i>lKE LaSh</i> | — — |
| <i>EDFLNHLA</i> | <i>lKE LaSh</i> | - - - |
| <i>ENSICA</i> | <i>lKE LaSh</i> | |
| <i>ENSICA</i> | <i>lKE YaSh</i> | — · — · |
| <i>Fluidyna</i> | <i>kOm Wil</i> | - - - - |
| <i>UConcord</i> | <i>kOm Wil</i> | - - - - |

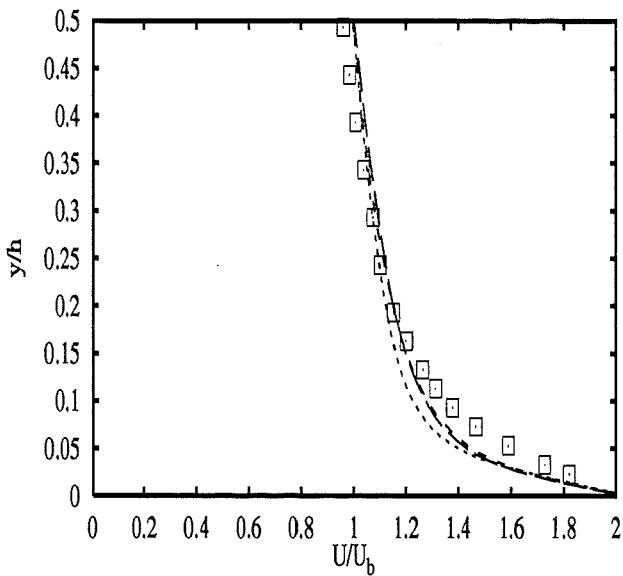
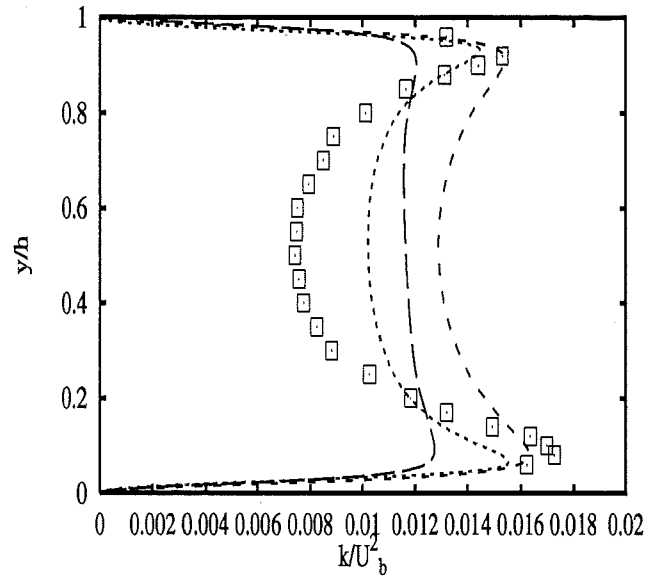
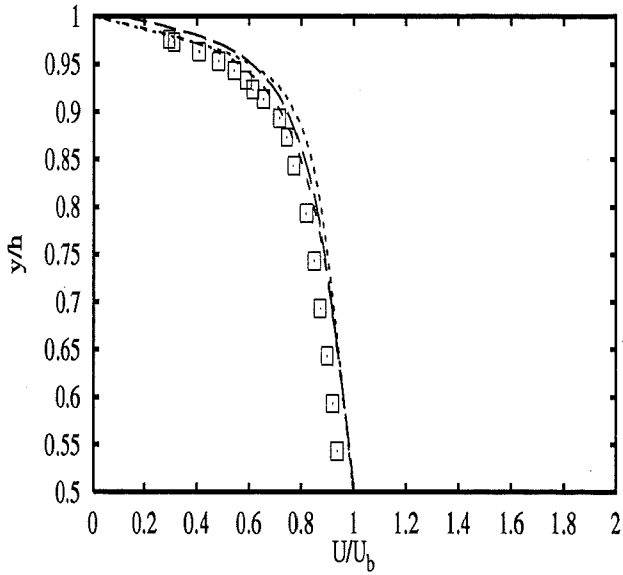


Developed flow

Experiments □

| | | |
|------------------|--------------------------|-------|
| <i>U</i> DelftHa | <i>l</i> KE <i>La</i> Sh | --- |
| <i>E</i> DfLNHLA | <i>l</i> KE <i>La</i> Sh | --- |
| <i>E</i> NSICA | <i>l</i> KE <i>La</i> Sh | |
| <i>E</i> NSICA | <i>l</i> KE <i>Ya</i> Sh | ---- |
| <i>F</i> luidYna | <i>k</i> Om <i>Wil</i> | ---- |
| <i>U</i> Concord | <i>k</i> Om <i>Wil</i> | ---- |

1B - 14



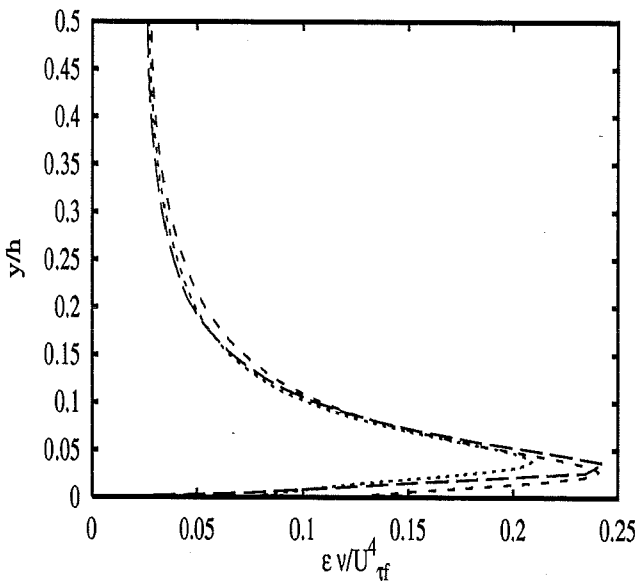
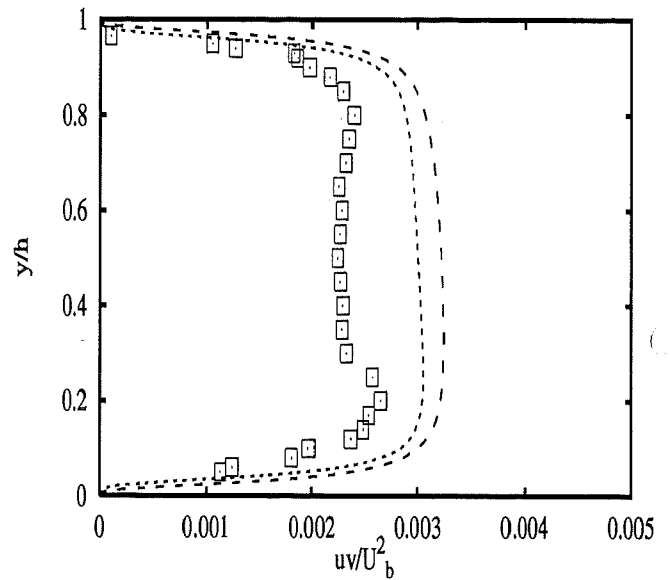
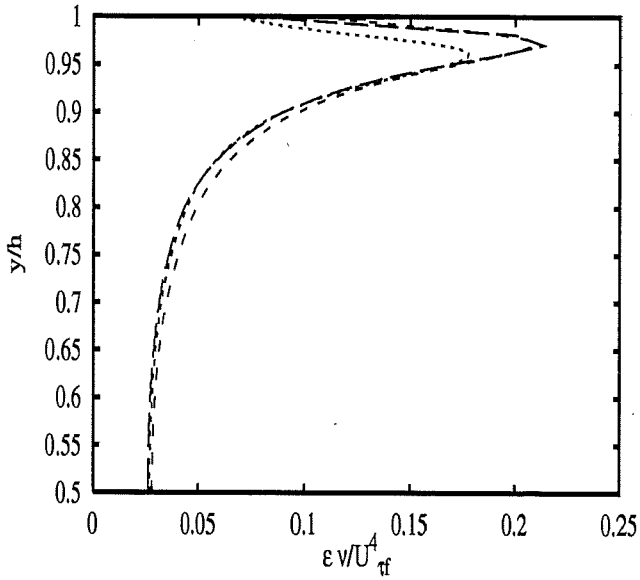
Developed flow

Experiments □

UKarlsruhe hKE std+NoRe - - -

ECLille hKE std+Chi - - -

ECLille hKE std+RMM ·····



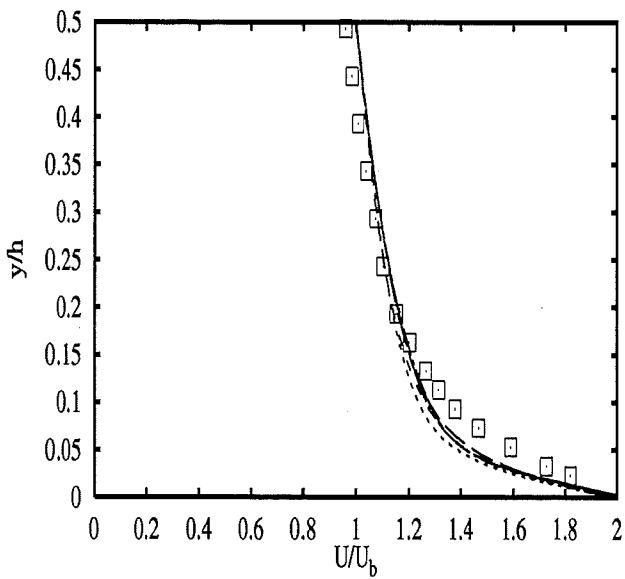
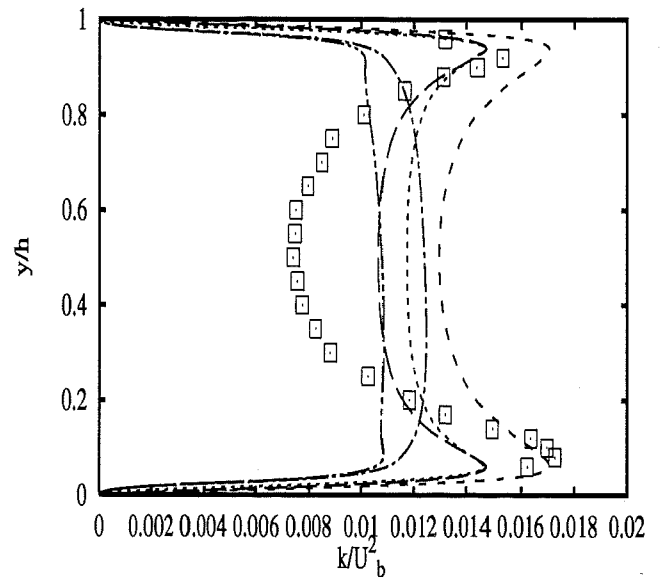
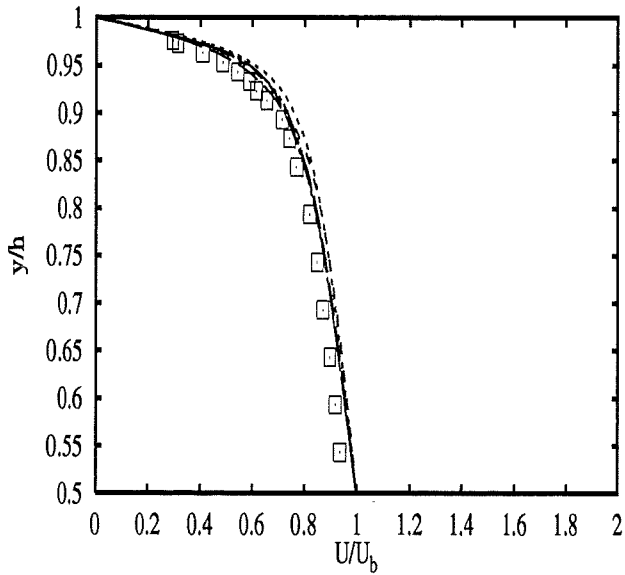
Developed flow

Experiments □

UKarlsruhe hKE std+NoRe ---

ECLille hKE std+Chi - - -

ECLille hKE std+RMM ·····



Developed flow

Experiments □

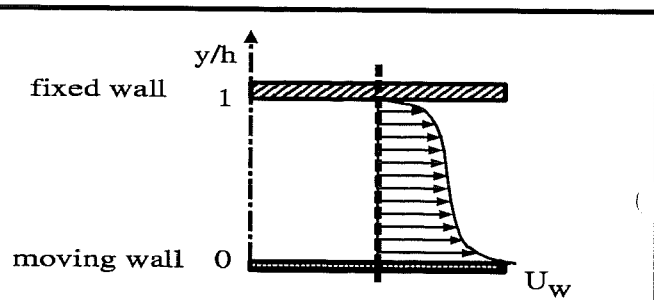
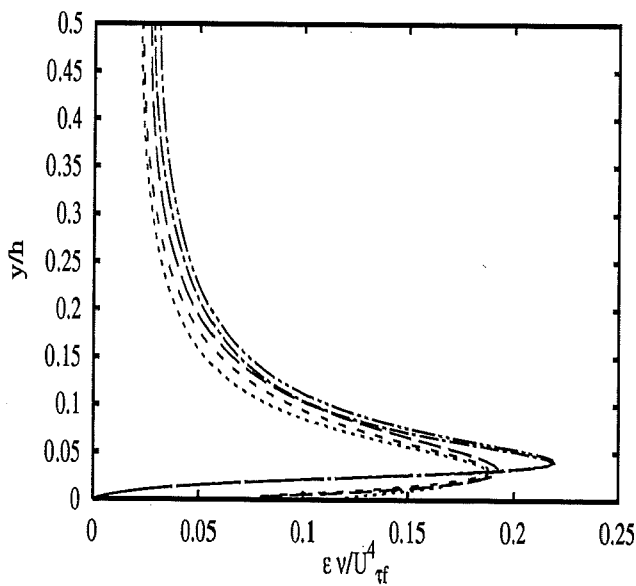
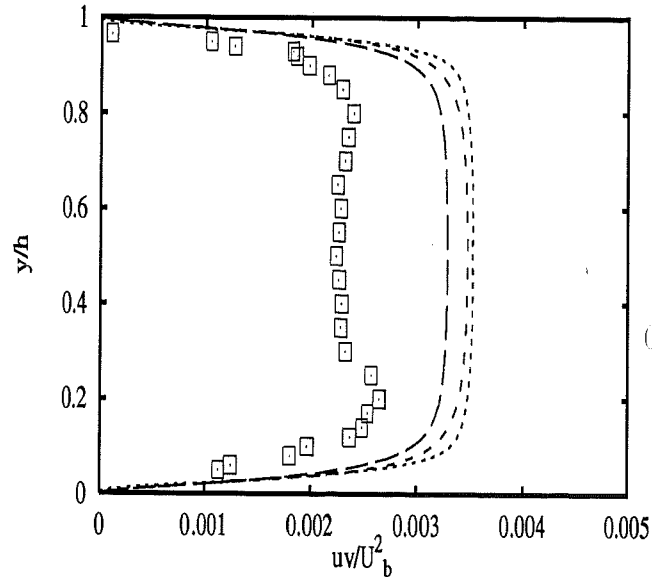
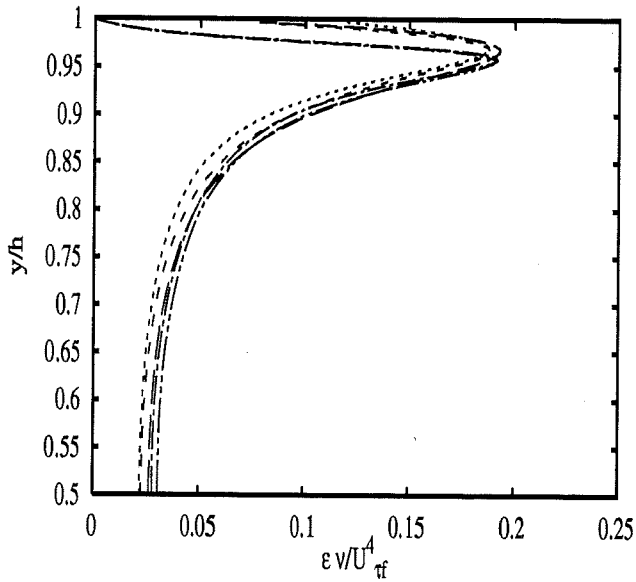
ECLille RSM LaSh ---

ECLille RSM JaHa - - -

UdelftHa RSM HJH ·····

UMISTCra RSM CrLa+2eq - · - ·

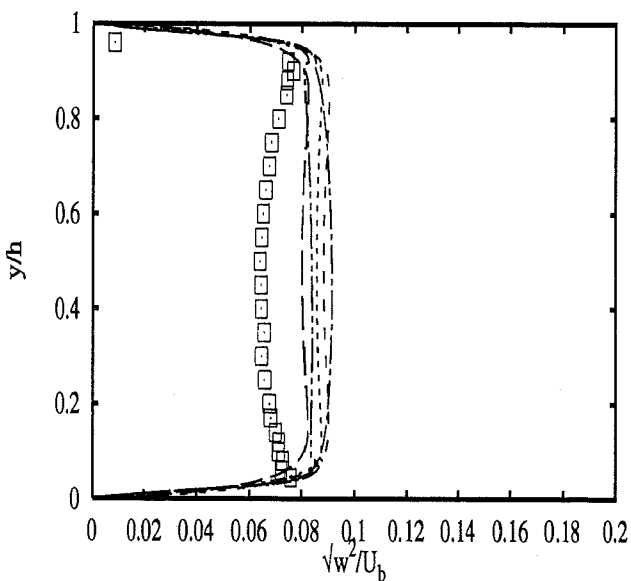
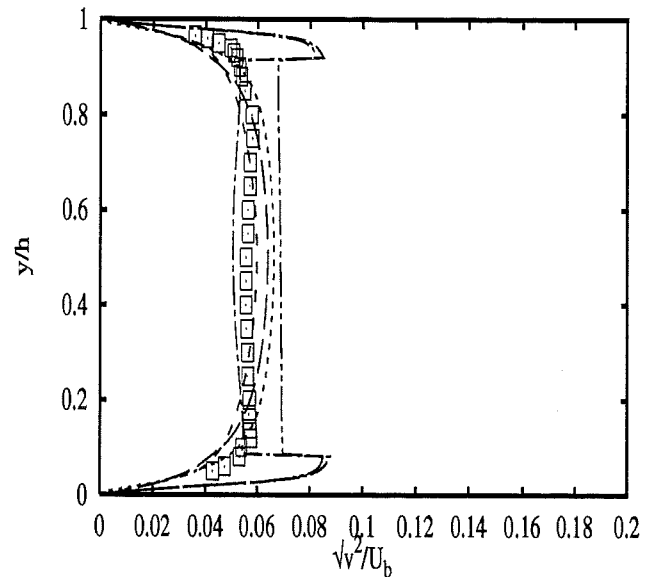
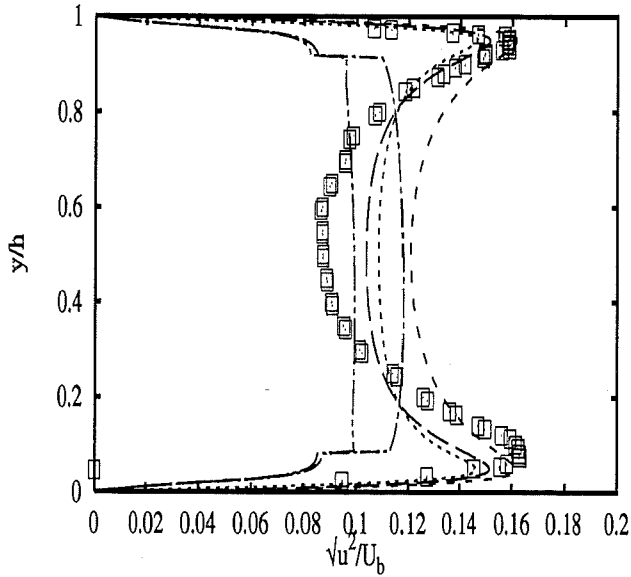
UMISTCra RSM Cub+2eq - · - ·



Developed flow

- Experiments** \square
- ECLille RSM LaSh** ---
- ECLille RSM JaHa** - - -
- UdelftHa RSM HJH** ·····
- UMISTCra RSM CrLa+2eq** - - -
- UMISTCra RSM Cub+2eq** - - -

1B - 18



Developed flow

Experiments □

ECLille RSM LaSh ---

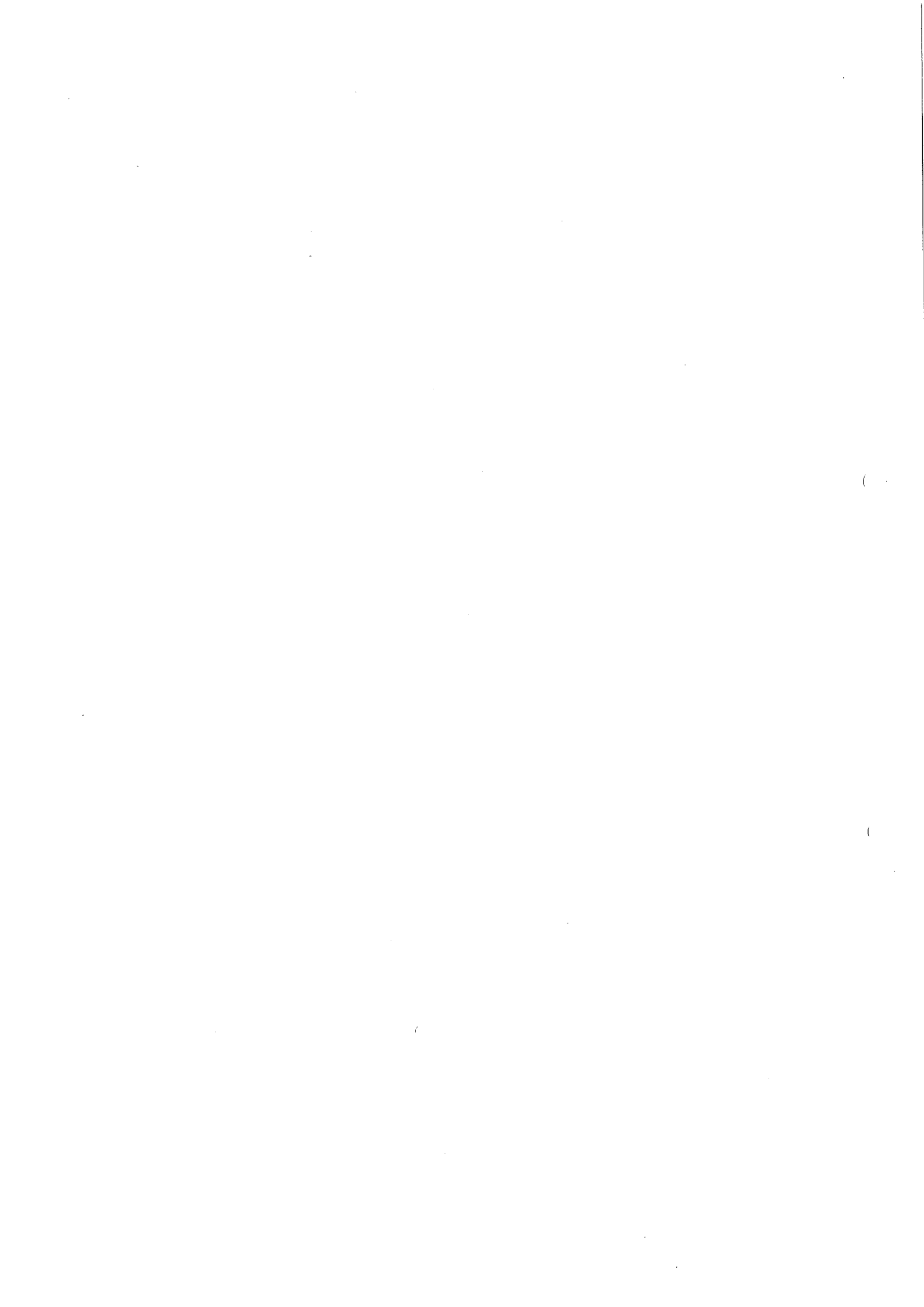
ECLille RSM JaHa - - -

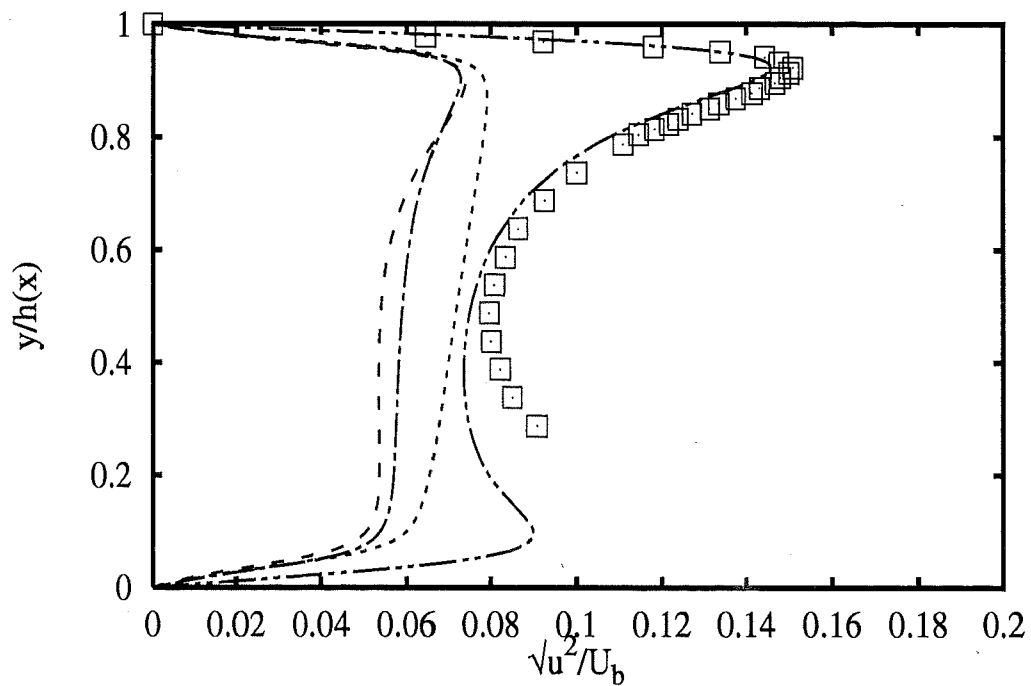
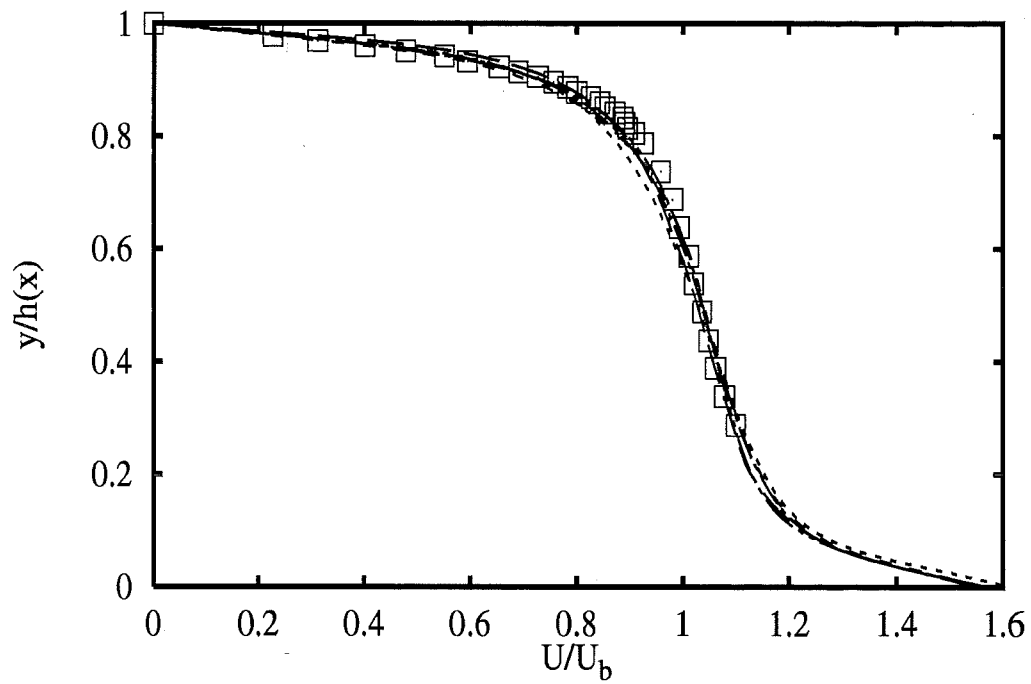
UDeftHa RSM HJH ·····

UMISTCra RSM CrLa+2eq - · - ·

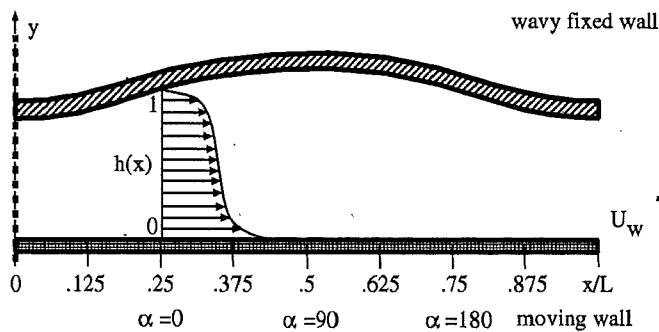
UMISTCra RSM Cub+2eq - · - ·

1B - 19



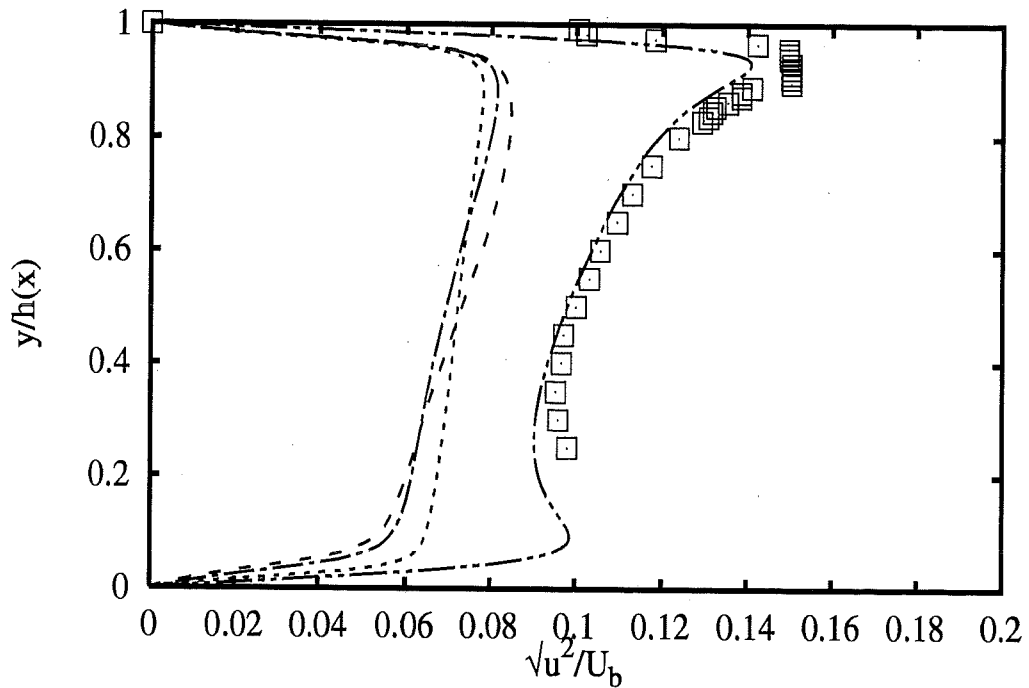
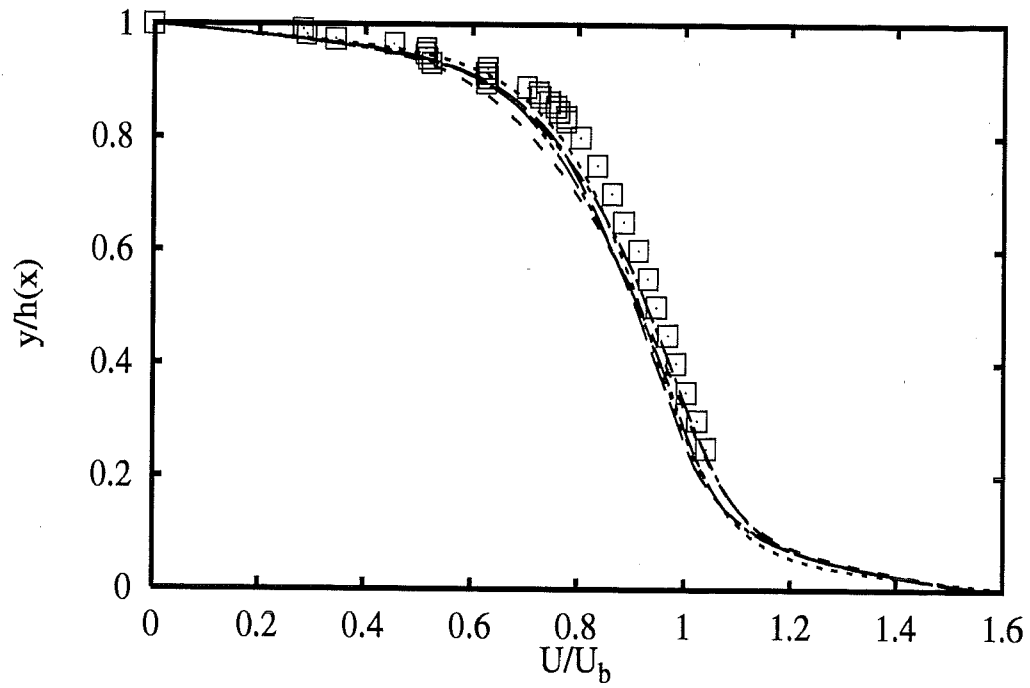


Profiles at $x/L=0$ ($\alpha=-90^0$)

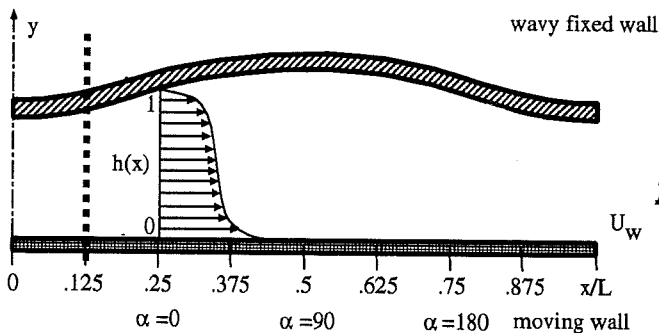


- Experiments** \square
- UKarlsru** **hKE std+NoRe** — —
- UDelftHa** **lKE LaSh** - - -
- ENSICA** **lKE LaSh** ·····
- ENSICA** **lKE LaSh (arco)** - · - · -
- UDelftHa** **RSM HJH** - · - · -

1C - 1

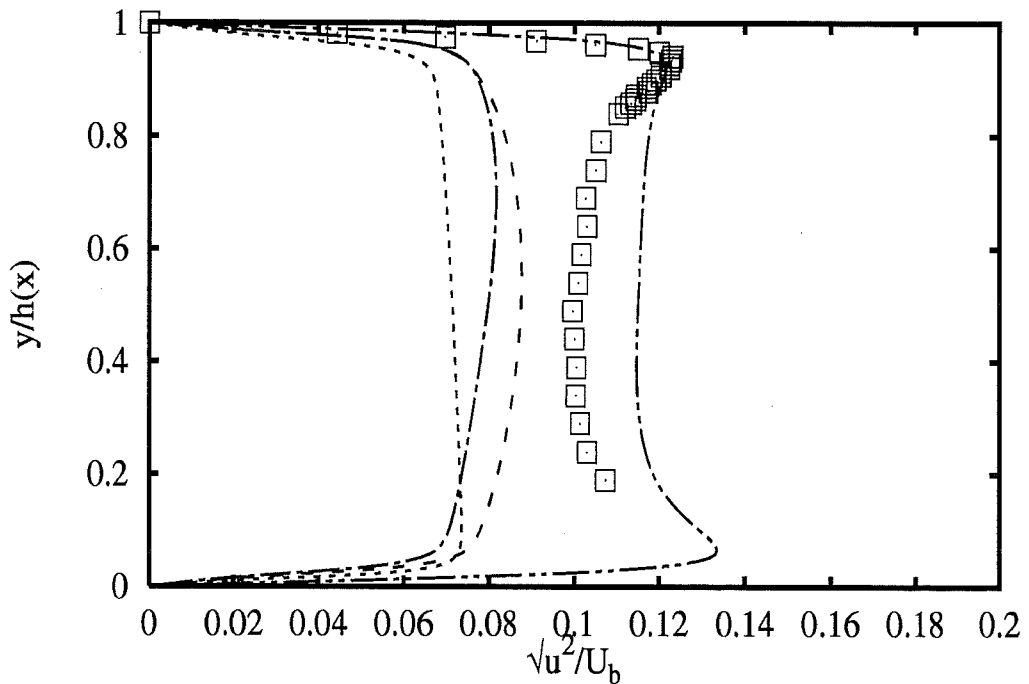
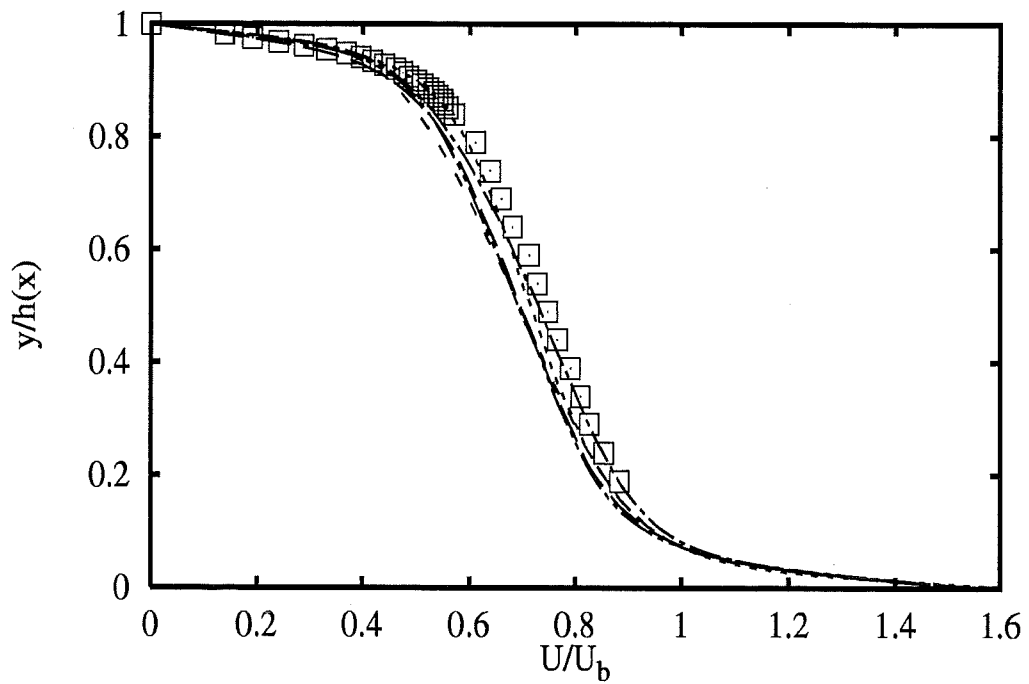


Profiles at $x/L=0.125$ ($\alpha=-45^0$)

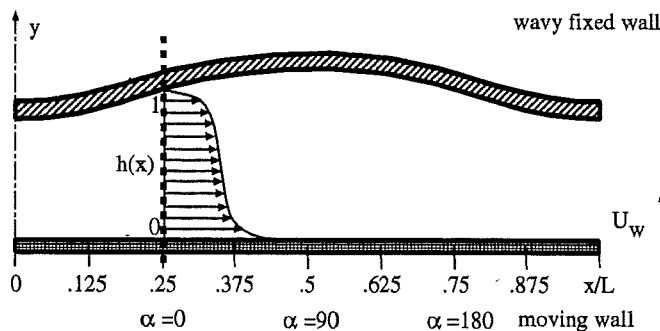


- | | |
|--------------------|----------------------------------|
| Experiments | □ |
| UKarlsru | <i>hKE std+NoRe</i> --- |
| UDelftHa | <i>lKE LaSh</i> - - - |
| ENSICA | <i>lKE LaSh</i> ····· |
| ENSICA | <i>lKE LaSh (arco)</i> - · - · - |
| UDelftHa | <i>RSM HJH</i> - · - · - |

1C - 2

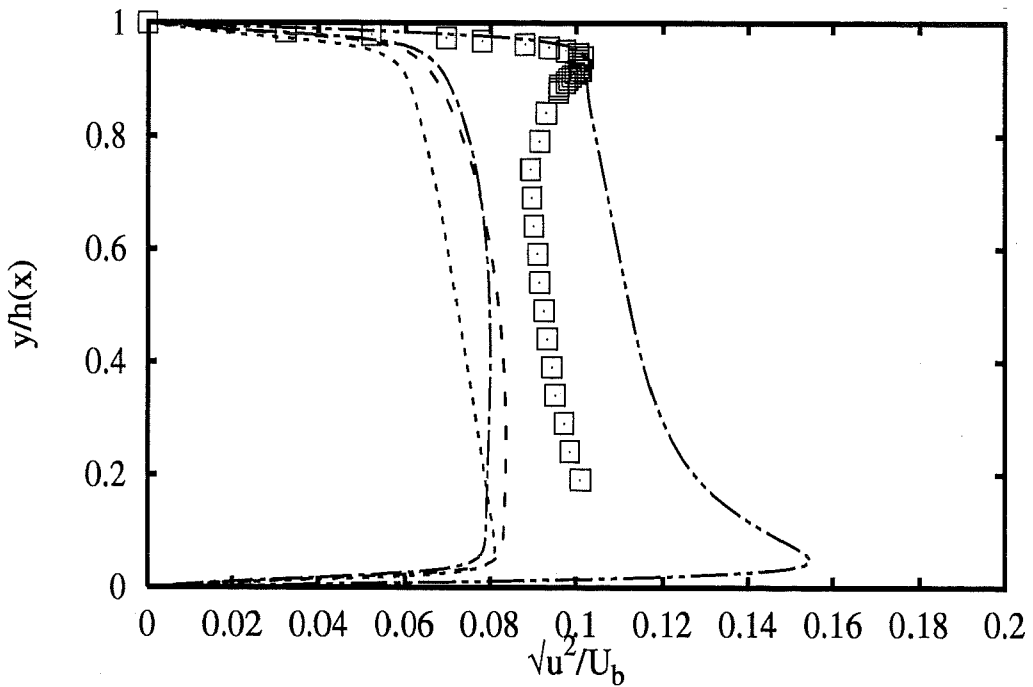
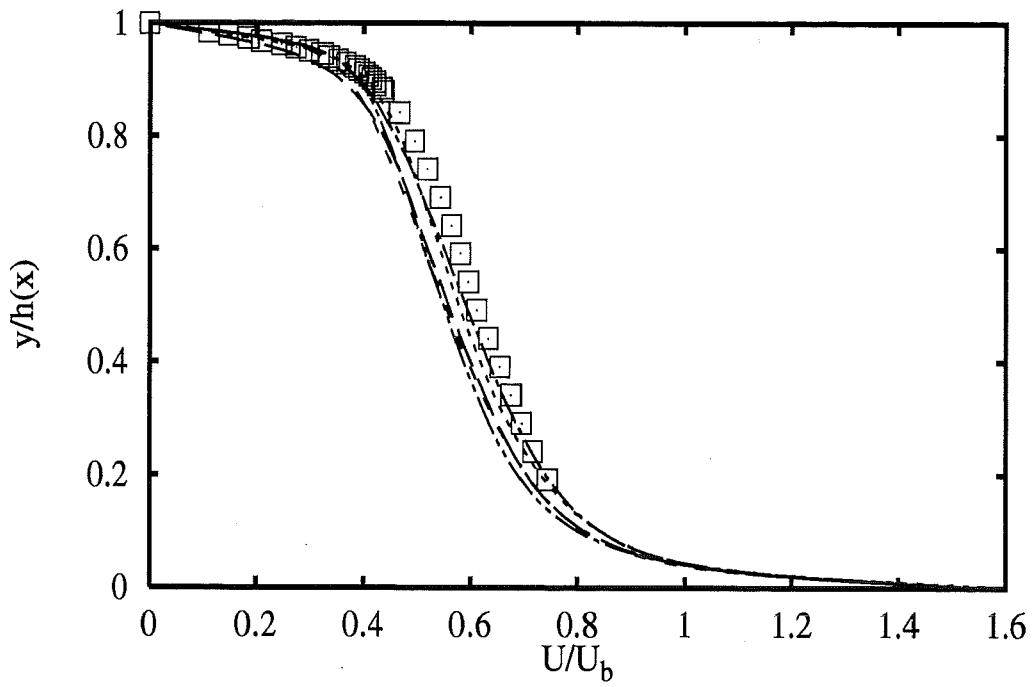


Profiles at $x/L=0.25$ ($\alpha=0^0$)

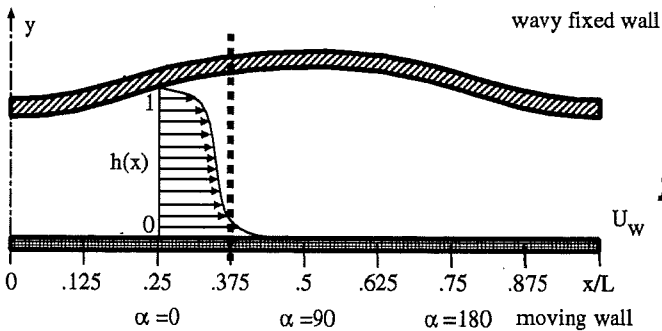


- Experiments** □
- UKarlsru** **hKE std+NoRe** ---
- UDelftHa** **lKE LaSh** - - -
- ENSICA** **lKE LaSh** ·····
- ENSICA** **lKE LaSh (arco)** - - -
- UDelftHa** **RSM HJH** ·····

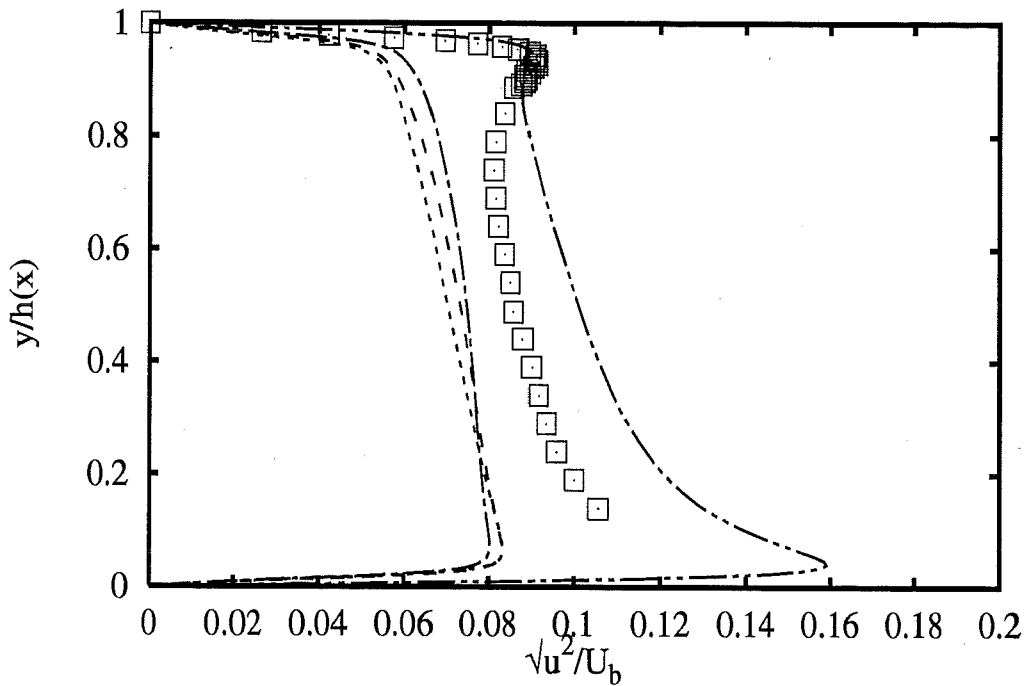
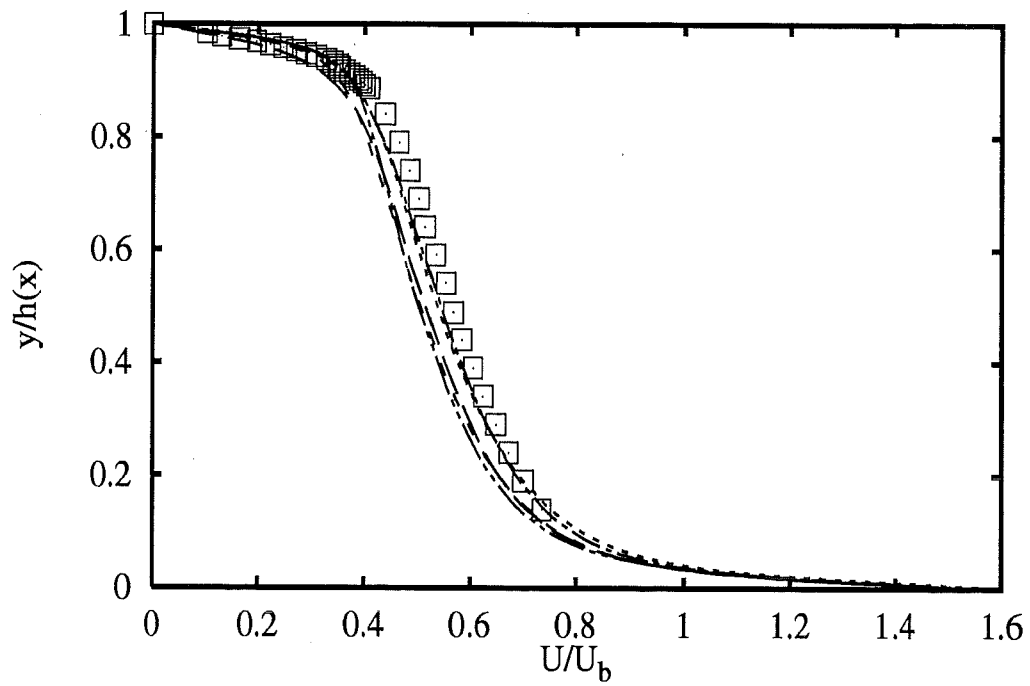
1C - 3



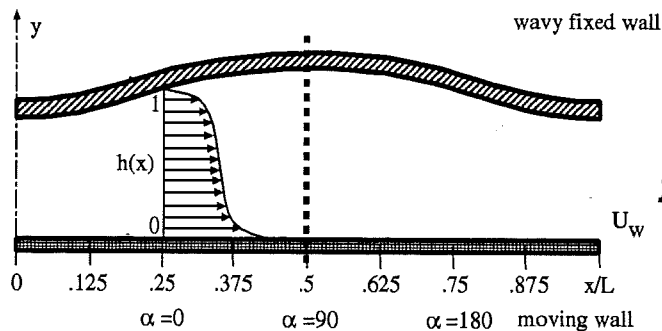
Profiles at $x/L=0.375$ ($\alpha=45^\circ$)



- | | |
|------------------------|-------|
| Experiments | □ |
| UKarlsru hKE std+NoRe | --- |
| UDelftHa lKE LaSh | --- |
| ENSICA lKE LaSh | |
| ENSICA lKE LaSh (arco) | --- |
| UDelftHa RSM HJH | --- |

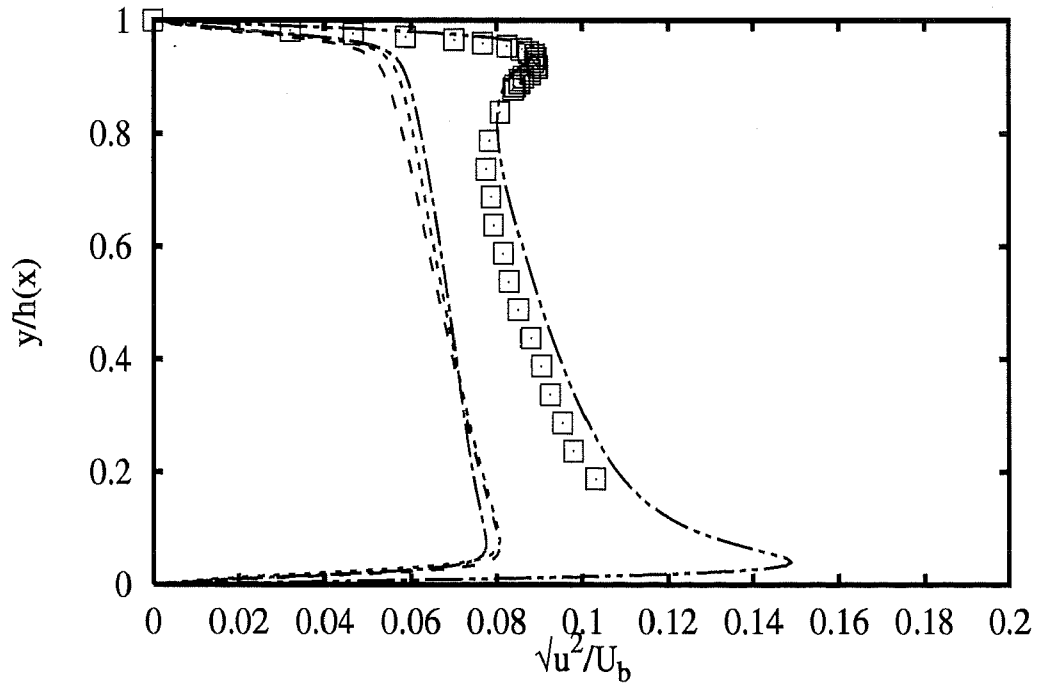
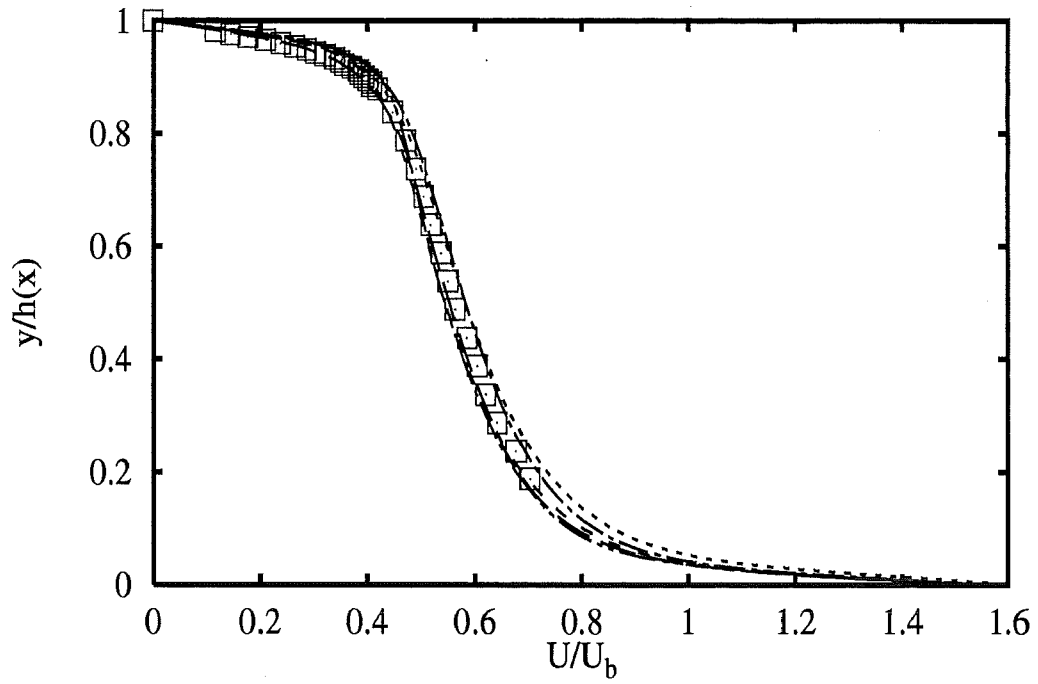


Profiles at $x/L=0.5$ ($\alpha=90^\circ$)

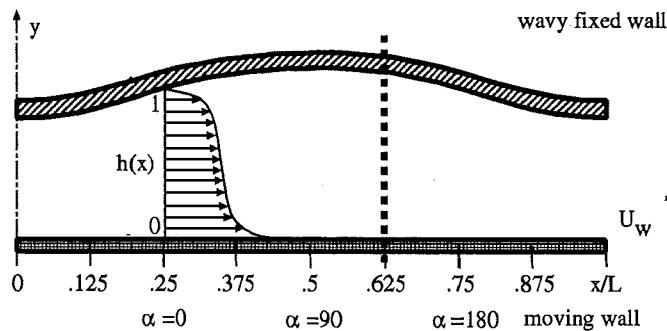


- Experiments** □
- UKarlsru** *hKE std+NoRe* — —
- UDelftHa** *lKE LaSh* - - -
- ENSICA** *lKE LaSh* ·····
- ENSICA** *lKE LaSh (arco)* - · - ·
- UDelftHa** *RSM HJH* - · - ·

1C - 5

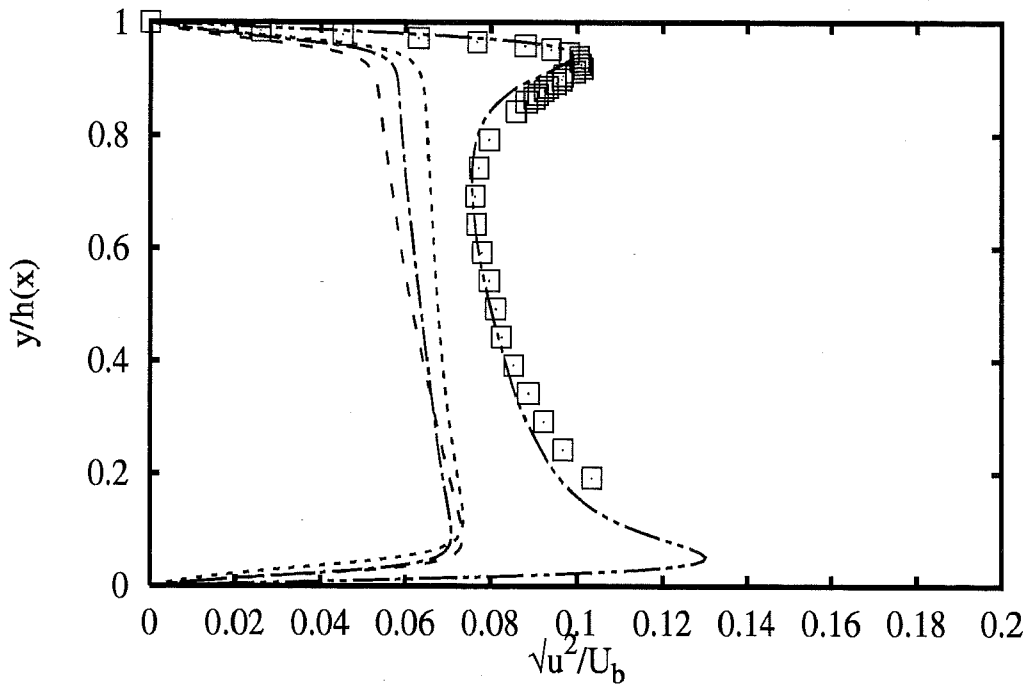
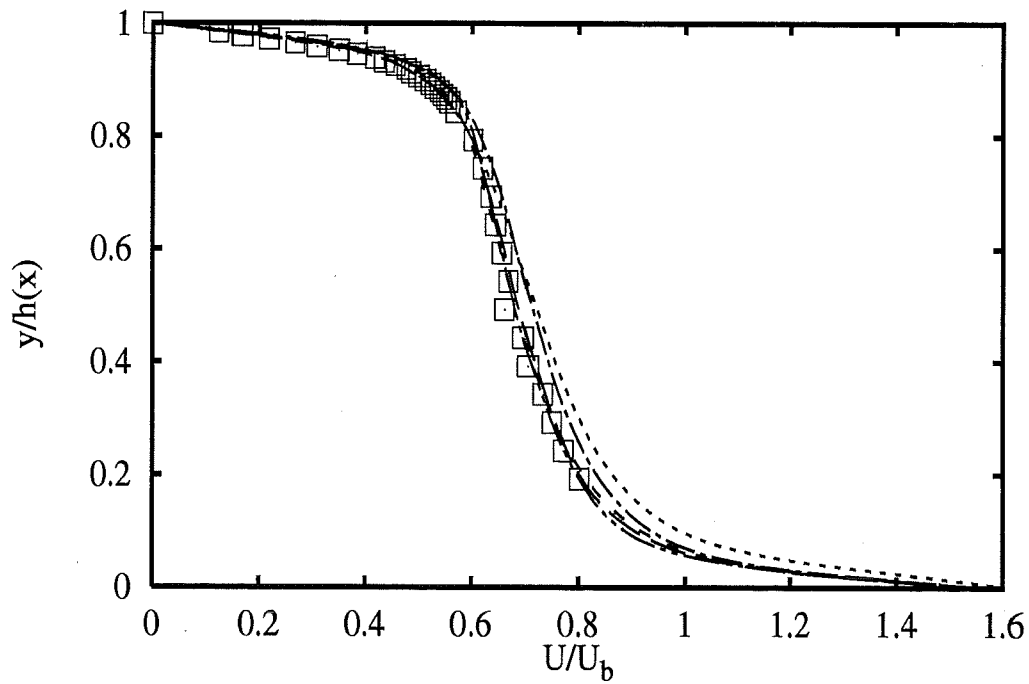


Profiles at $x/L=0.625$ ($\alpha=135^\circ$)

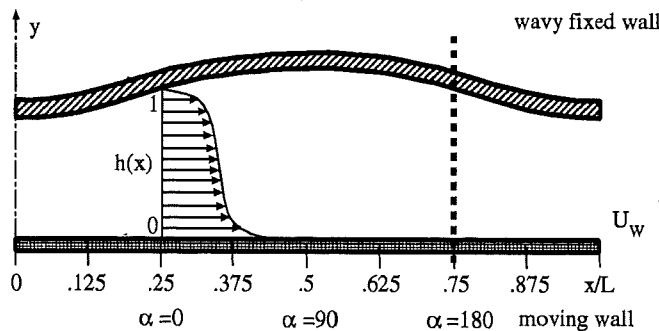


- | | |
|------------------------|-----|
| Experiments | □ |
| UKarlsru hKE std+NoRe | --- |
| UDelftHa lKE LaSh | --- |
| ENSICA lKE LaSh | --- |
| ENSICA lKE LaSh (arco) | --- |
| UDelftHa RSM HJH | --- |

1C - 6

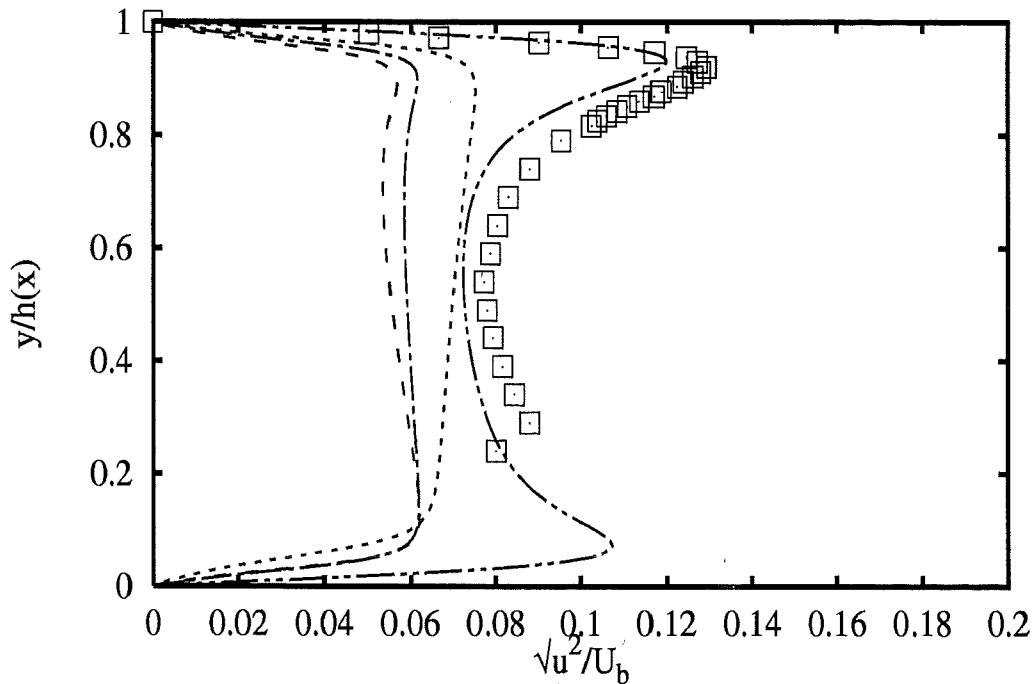
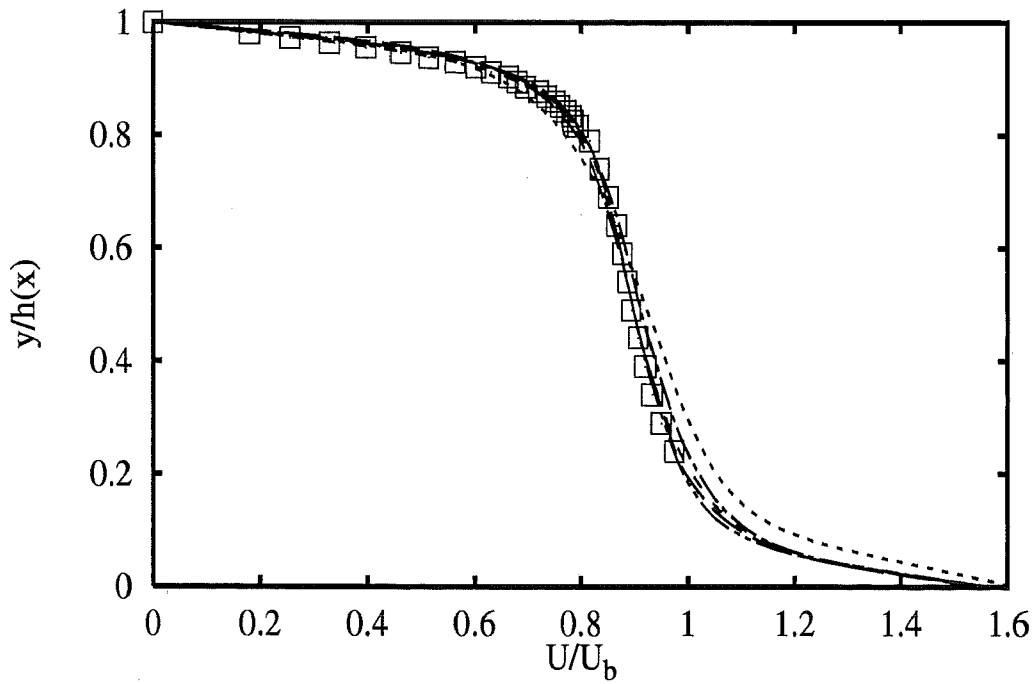


Profiles at $x/L=0.75$ ($\alpha=180^\circ$)

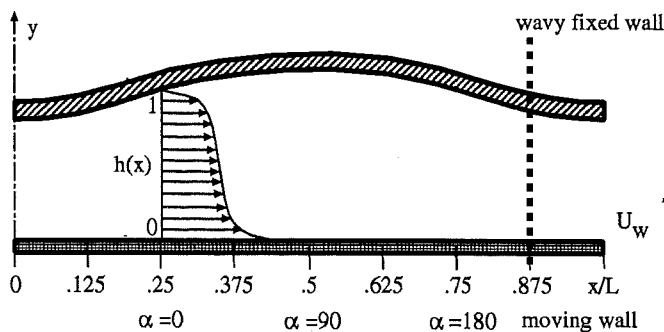


- Experiments \square
- UKarlsru hKE std+NoRe $---$
- UDelftHa lKE LaSh $---$
- ENSICA lKE LaSh \cdots
- ENSICA lKE LaSh (arco) $---$
- UDelftHa RSM HJH $---$

1C-7

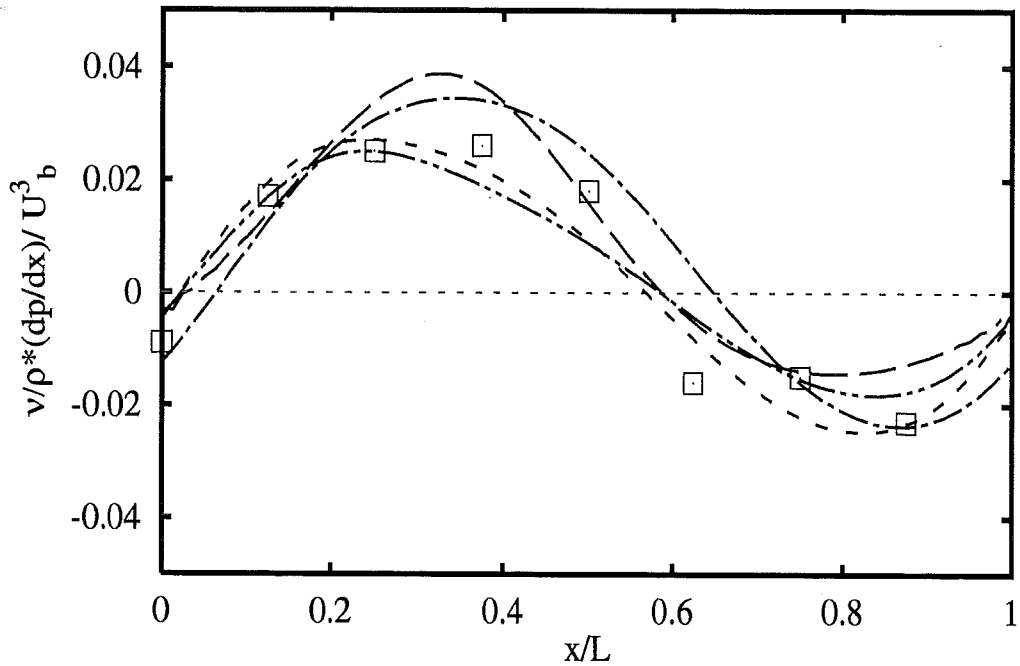
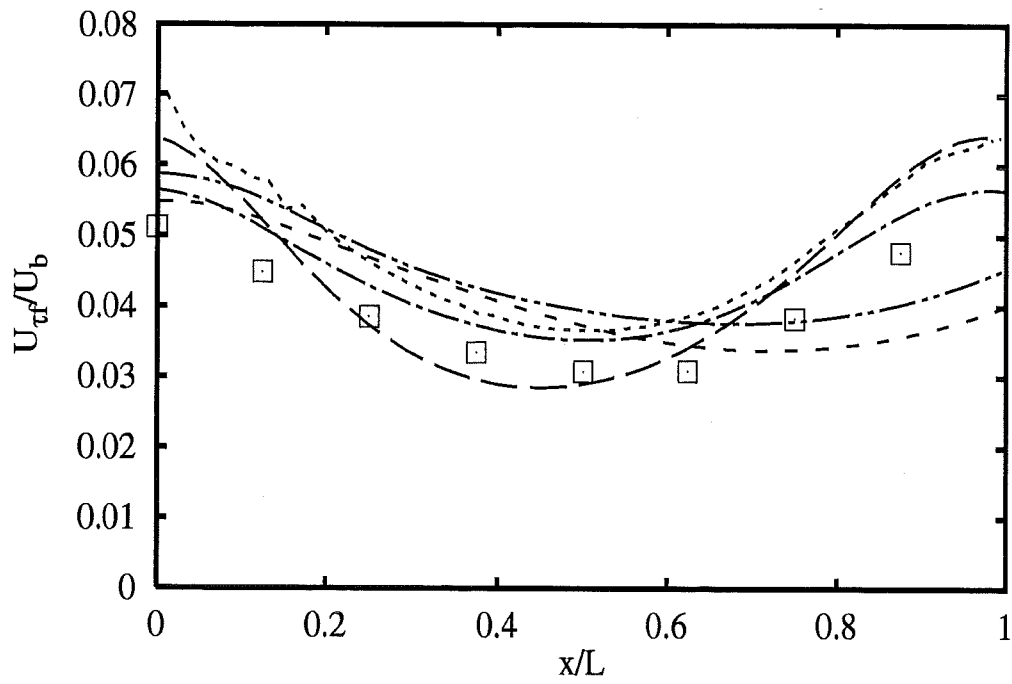


Profiles at $x/L=0.875$ ($\alpha=225^0$)

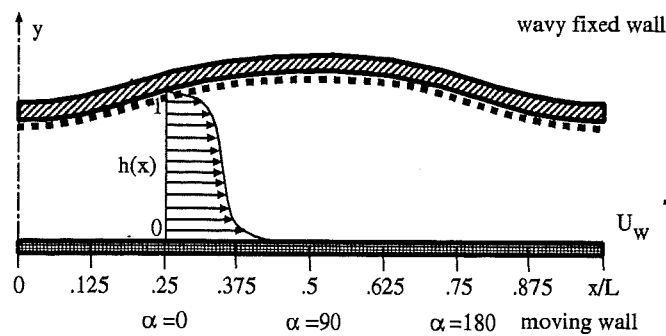


- | | |
|------------------------|-----------|
| Experiments | □ |
| UKarlsru hKE std+NoRe | — |
| UdelftHa lKE LaSh | - - - |
| ENSICA lKE LaSh | ⋯⋯⋯ |
| ENSICA lKE LaSh (arco) | - · - · - |
| UdelftHa RSM HJH | · - - · - |

1C - 8



Distributions along wavy wall



- Experiments** \square
- UKarlsru** **hKE std+NoRe** — —
- UDelftHa** **lKE LaSh** - - -
- ENSICA** **lKE LaSh** ·····
- ENSICA** **lKE LaSh (arco)** - · - · -
- UDelftHa** **RSM HJH** - · - · -

1C - 9



KEY TO TEST CASE 2A

| Contributor | Key-Name | Gr. | Name (Affiliation) | Turbulence Model | Near-Wall Treatment |
|-------------|-----------------|-----|---|--|-------------------------------|
| ASC | nKE_SZL+wf | 6 | Stubley (ASC) | non-linear k-ε Shih-Zhu-Lumley | wall functions |
| | hKE_std+wf_nstd | 2 | | standard k-ε | non-standard wall functions |
| | hKE_RNG+NoRe | 4 | | two-layer RNG k-ε | Norris-Reynolds 1 eq.-model |
| | kOm_Wil | 6 | | k-ω | — |
| | IKE_LaSh | 5 | | low-Re k-ε model LaSh | — |
| | IKE_LaBr | 5 | | low-Re k-ε Lam-Bremhorst | — |
| IOlomouc | hKE_std+Gol | 4 | Sedlar (Pump Research Institute Olomouc) | two-layer k-ε | Goldberg model |
| | hKE_std+wf_nstd | 2 | | standard k-ε | non-standard wall functions |
| | nKE_Spez+wf | 6 | | non-linear k-ε Speziale | wall functions |
| | hKE_std+wf_nstd | 2 | | standard k-ε | non-standard wall functions |
| | RSM_LRR+wf | 7 | | RSM Launder-Reece-Rodi | wall functions |
| | RSM_HaLa | 7 | | Reynolds-Stress Model Hanjalic-Launder | — |
| UChalmer | RSM_SSG+wf | 7 | Blom (Hokkaido R. D. P. Res. Center) Davidson/Perzon et al. (Chalmers Univ.) | RSM Speziale-Sarkar-Gatski | wall functions |
| | hKE_std+ChPa | 3 | | two-layer k-ε | Chen-Patel 1 eq.-model |
| | hKE_std+wf | 1 | | standard k-ε | wall functions |
| | kOm_Wil | 6 | | k-ω | — |
| | IKE_LaSh | 5 | | low-Re k-ε Launder-Sharma | — |
| | IKE_LiLe | 5 | | low-Re k-ε Lien-Leschziner | — |
| | RSM_LRR+wf | 7 | | RSM Launder-Reece-Rodi | wall functions |
| | hKE_std+wf | 1 | | standard k-ε | wall functions |
| UDelftHa | hKE_std+wf | 1 | Hanjalic/Hadzic/Jakirlic (TU Delft, Appl. Physics) Zijlema (TU Delft) | standard k-ε | wall functions |
| | hKE_std+wf | 1 | | standard k-ε | wall functions |
| | kOm_Wil | 6 | | k-ω | — |
| UFlorenc | hKE+NoRe | 3 | Michelassi/Chiaramonti (Univ. of Florence) | two-layer k-ε | Norris-Reynolds 1 eq.-model |
| | hKE+RMM | 4 | | two-layer k-ε | Rodi-Mansour-Michelassi 1 eq. |
| | kOm_Wil | 6 | | k-ω | — |
| | hKE+Kim | 4 | | two-layer k-ε | Kim model |
| | IKE_NaHi | 5 | | low-Re k-ε Nagano-Hishida | — |

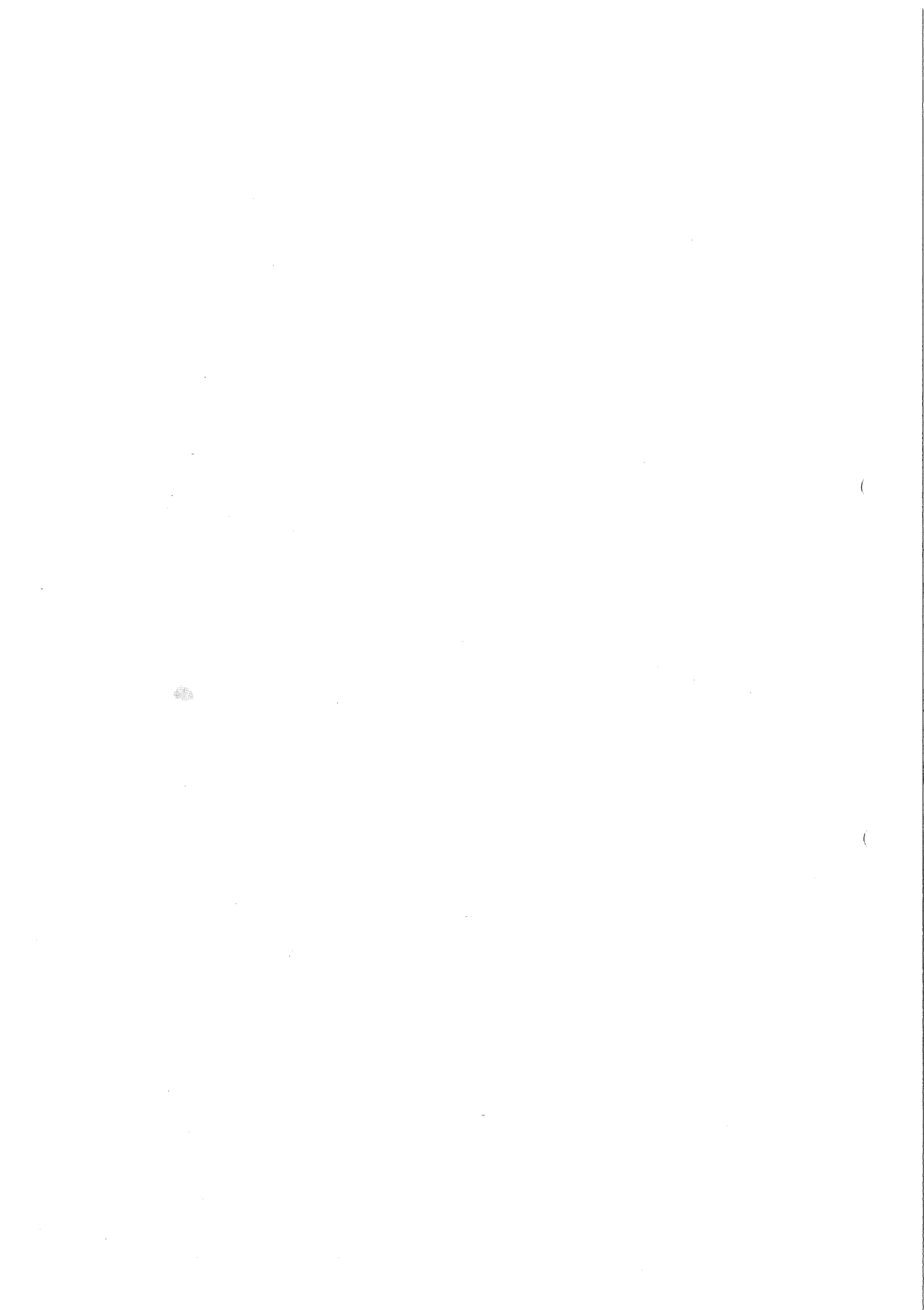
| | | | | |
|----------|-------------------|---------------------------------|-------------------------------------|-----------------------------|
| UGdansk | hKE_std+wf_nstd 2 | Kaczynski (Univ. of Gdansk) | standard k-ε | non-standard wall functions |
| UKarlsru | hKE_std+NoRe 3 | Buchal (Univ. of Karlsruhe) | two-layer k-ε | Norris-Reynolds 1 eq.-model |
| | hKE_std+wf 1 | | standard k-ε | wall functions |
| UMISTLes | RSM_GiLa+Wol 7 | Lien/Leschziner (UMIST) | Reynolds-Stress Model Gibson-Lauder | Wolfshtein 1 eq.-model |
| | RSM_GiLa+wf 7 | | Reynolds-Stress Model Gibson-Lauder | wall functions |
| | hKE_RNG+wf 2 | | RNG-modified k-ε | wall functions |
| | hKE_std+wf 1 | | standard k-ε | wall functions |
| | IKE_LiLe 5 | | low-Re k-ε Lien-Leschziner | — |
| UPorto | hKE_std+wf 1 | Castro/Palma (Univ. of Porto) | standard k-ε | wall functions |
| UStuttga | hKE_std+ChPa 3 | Huurdeeman (Univ. of Stuttgart) | two-layer k-ε | Chen-Patel 1 eq.-model |
| | hKE_std+wf_nstd 2 | | standard k-ε | non-standard wall functions |

Notes:

- experimental values of k evaluated as $k = \frac{1}{4}(3\overline{u'^2} + 2\overline{v'^2})$
- stream lines not equally distributed according to stream function values

TEST CASE 2A

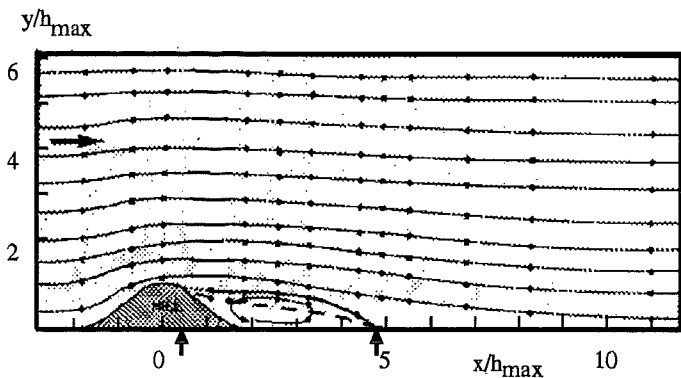
| Group | Turbulence Model | Separation (x/h_{max}) | Reattachment (x/h_{max}) |
|---|--------------------|-------------------------------|---------------------------------|
| Exp | | 0.43 | 4.82 |
| Group 1: standard k-ϵ model with standard wall functions | | | |
| UChalmer | hKE_std+wf | 1.24 | 2.32 |
| UDelftHa | hKE_std+wf | 0.55 | 3.13 |
| UDelftZi | hKE_std+wf | 0.46 | 3.61 |
| UKarlsru | hKE_std+wf | 0.68 | 3.16 |
| UMISTLes | hKE_std+wf | 0.6 | 3.9 |
| UPorto | hKE_std+wf | 0.52 | 3.57 |
| Group 2: k-ϵ model with wall functions, non-standard | | | |
| ASC | hKE_std+wf_nstd | 0.68 | 2.64 |
| IOlomouc | hKE_std+wf_nstd | 0.74 | 3.34 |
| RCHokkai | hKE_std+wf_nstd | 0.83 | 2.52 |
| UGdansk | hKE_std+wf_nstd | 0.48 | 4.72 |
| UStuttga | hKE_std+wf_nstd | 0.5 | 5.6 |
| UMISTLes | hKE_RNG+wf | 0.55 | 5.50 |
| Group 3: two-layer models | | | |
| UFlorenc | hKE_std+NoRe | 0.40 | 4.80 |
| UKarlsru | hKE_std+NoRe(HLPA) | 0.32 | 5.34 |
| UKarlsru | hKE_std+NoRe(Hyb) | 0.36 | 4.92 |
| UChalmer | hKE_std+ChPa | 0.30 | 4.62 |
| UStuttga | hKE_std+ChPa | 0.3 | 6.0 |
| Group 4: two-layer models | | | |
| UFlorenc | hKE_std+RMM | 0.34 | 4.94 |
| IOlomouc | hKE_std+Gol | 0.73 | 4.26 |
| UFlorenc | hKE_std+Kim | 0.35 | 6.23 |
| CompDyna | hKE_RNG+NoRe | 0.31 | 6.36 |
| Group 5: low-Re k-ϵ models | | | |
| UChalmer | IKE_LaSh | 0.35 | 5.42 |
| EDFLNHLa | IKE_LaSh | 0.41 | 4.29 |
| EPFLausa | IKE_LaBr | 0.21 | 6.62 |
| UChalmer | IKE_LiLe | 0.29 | 5.41 |
| UMISTLes | IKE_LiLe | 0.40 | 4.50 |
| UFlorenc | IKE_NaHi | 0.32 | 4.64 |
| Group 6: non-linear k-ϵ and k-ω models | | | |
| ASC | nKE_SZL+wf | 0.68 | 2.36 |
| IOlomouc | nKE_Spez+wf | 0.55 | 5.22 |
| UChalmer | kOm_Wil | 0.24 | 6.54 |
| UDelftZi | kOm_Wil | 0.14 | 6.43 |
| UFlorenc | kOm_Wil | 0.33 | 6.38 |
| DLRGoett | kOm_Wil | 0.3 | 6.3 |
| Group 7: Reynolds-stress models | | | |
| UDelftHa | RSM_LRR+wf | 0.45 | 4.13 |
| UChalmer | RSM_LRR+wf | 1.29 | 2.21 |
| UMISTLes | RSM_GiLa+wf | 0.55 | 5.60 |
| UChalmer | RSM_SSG+wf | 0.95 | 3.52 |
| UMISTLes | RSM_GiLa+Wol | 0.40 | 6.00 |
| UChalmer | RSM_HaLa | 0.36 | 3.89 |



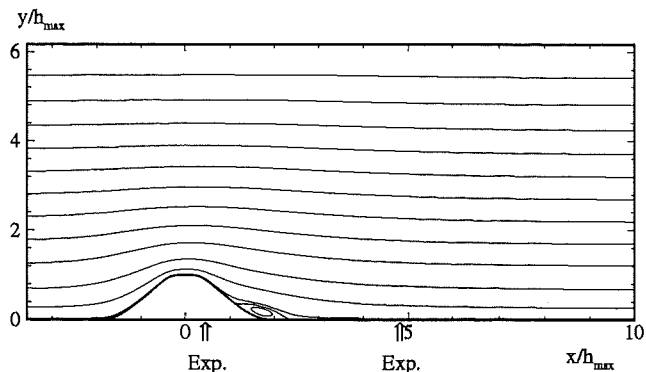
2D Model Hill Flow - Case 2A: Single Hill

Field Distribution of Stream Lines

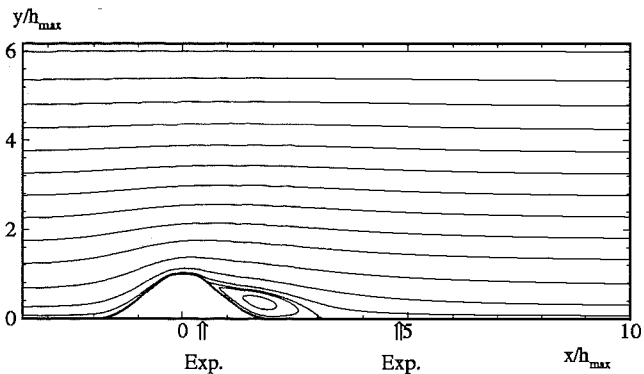
standard k-epsilon model with standard wall function



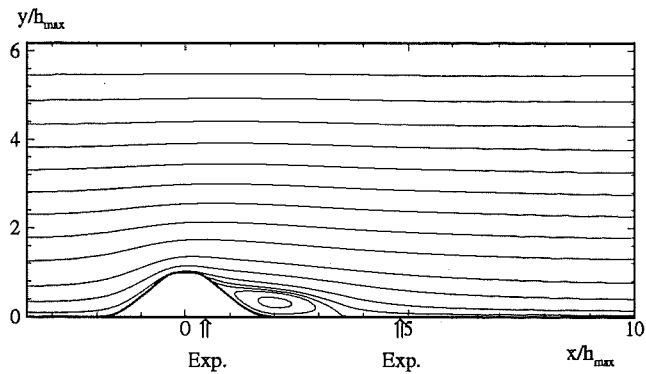
Experiments



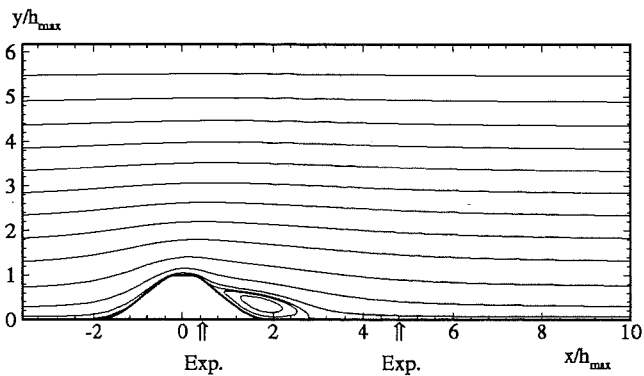
UChalmer:hKE_std+wf



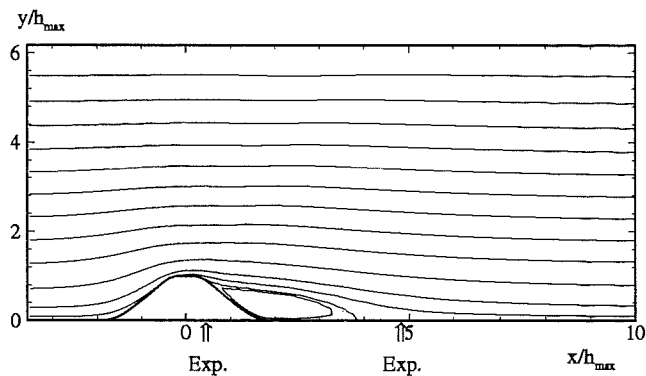
UDelftHa:hKE_std+wf



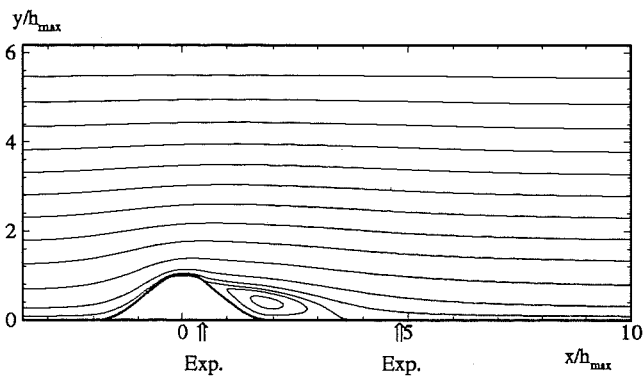
UDelftZi:hKE_std+wf



UKarlsru:hKE_std+wf



UMISTLes:hKE_std+wf

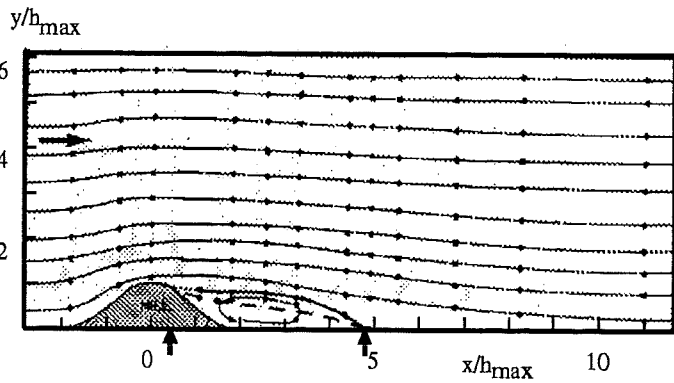


UPorto:hKE_std+wf

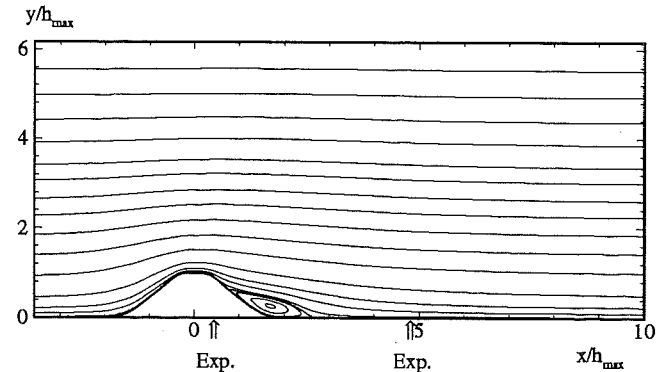
2D Model Hill Flow - Case 2A: Single Hill

Field Distribution of Stream Lines

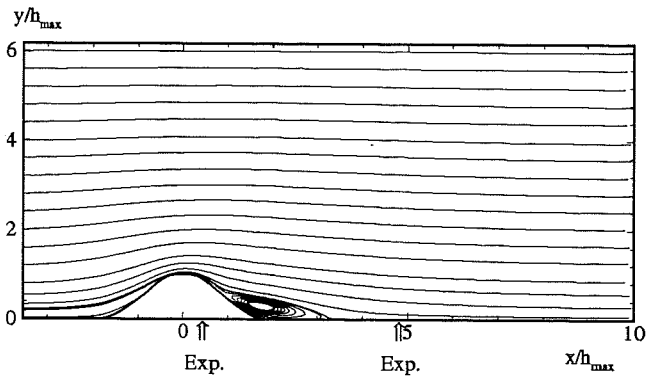
k-epsilon model with wall functions, non-standard



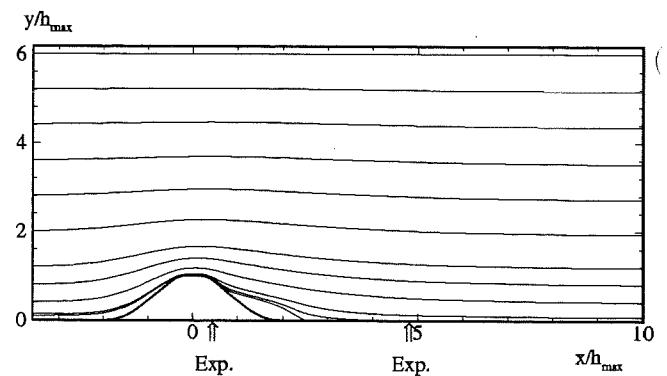
Experiments



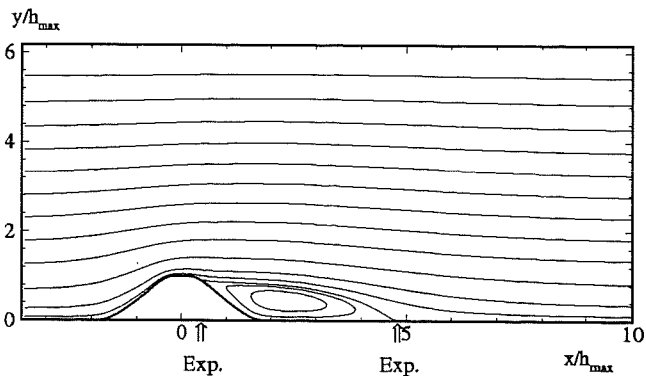
ASC:hKE_std+wf_nstd



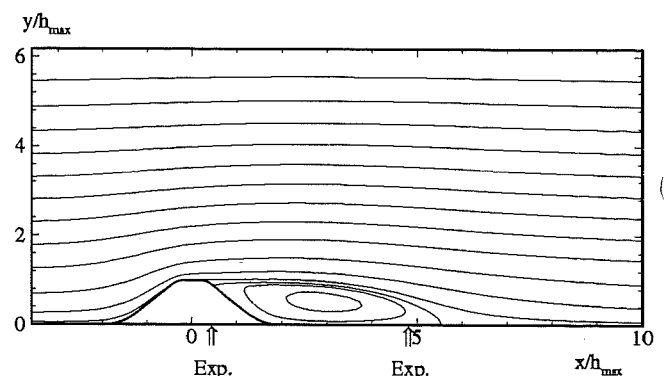
IOlomouc:hKE_std+wf_nstd



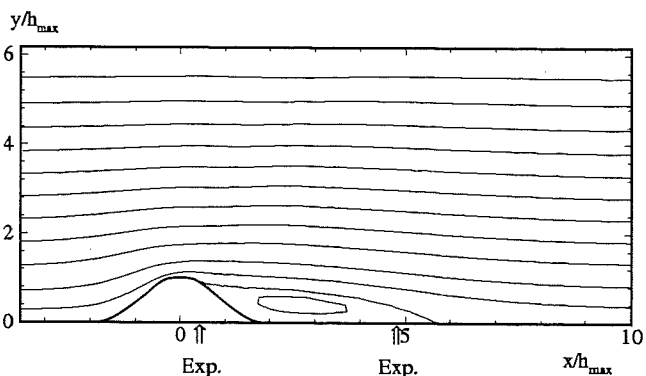
RCHokkai:hKE_std+wf_nstd



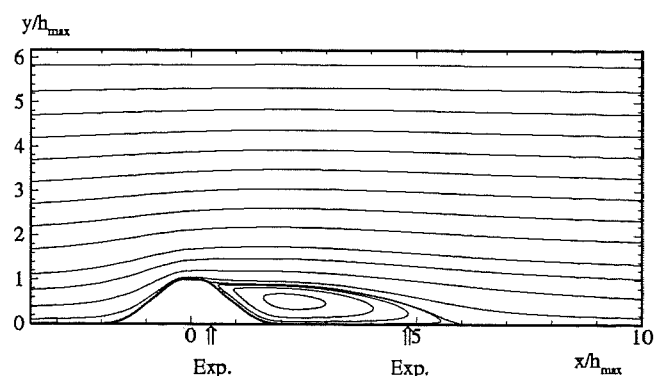
UGdansk:hKE_std+wf_nstd



UStuttga:hKE_std+wf_nstd



UMISTLes:hKE_RNG+wf

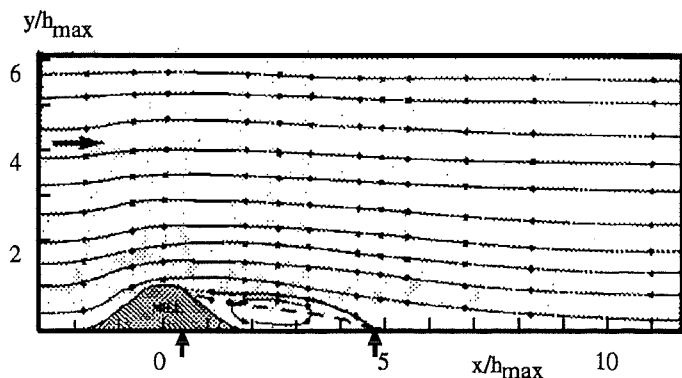


CompDyna:hKE_RNG+NoRe

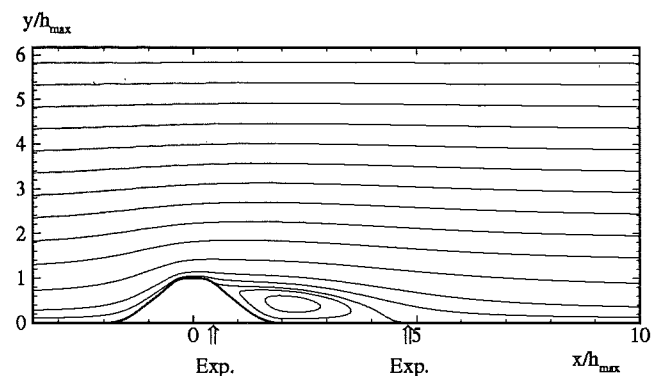
2D Model Hill Flow - Case 2A: Single Hill

Field Distribution of Stream Lines

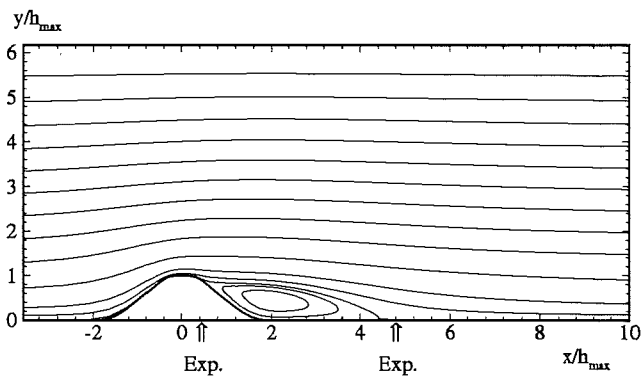
two-layer models



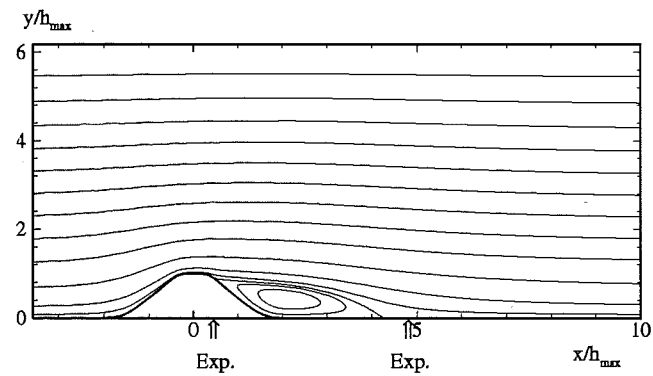
Experiments



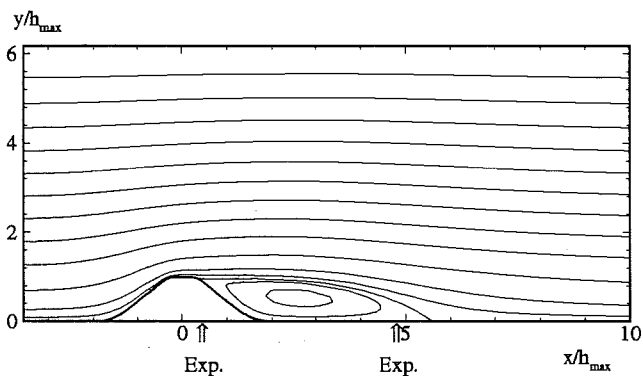
UFlorenc:hKE_std+NoRe



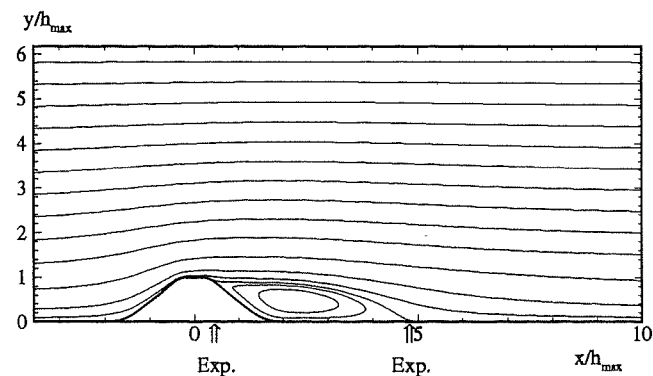
UKarlsru:hKE_std+NoRe(Hyb)



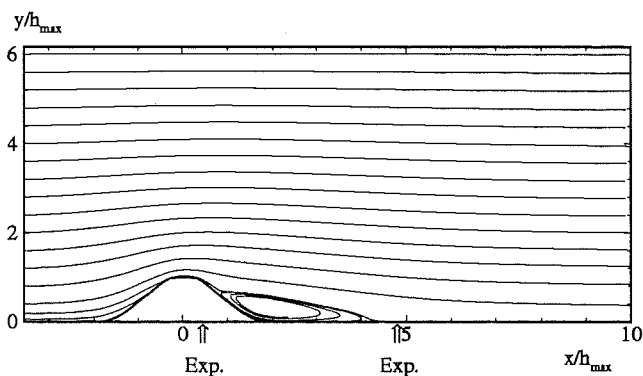
UChalmer:hKE_std+ChPa



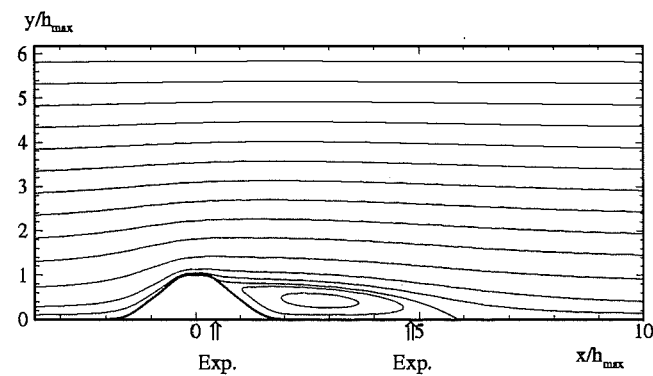
UStuttga:hKE_std+ChPa



UFlorenc:hKE_std+RMM



IOlomouc:hKE_std+Gol

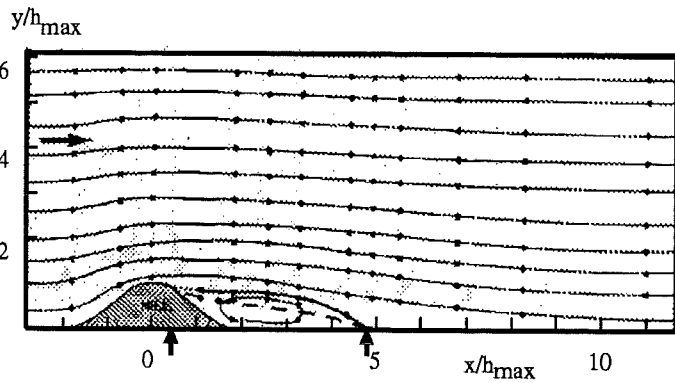


UFlorenc:hKE_std+Kim

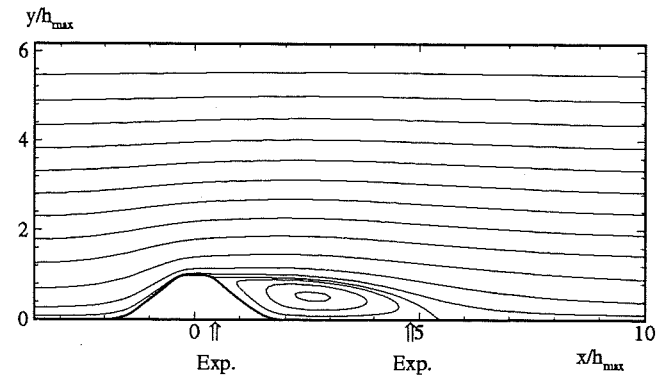
2D Model Hill Flow - Case 2A: Single Hill

Field Distribution of Stream Lines

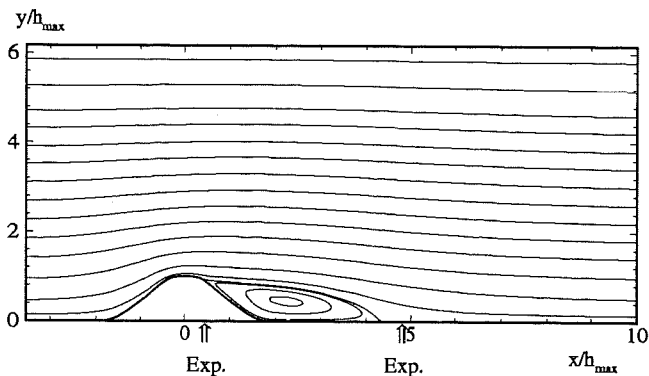
low-Re k-epsilon models



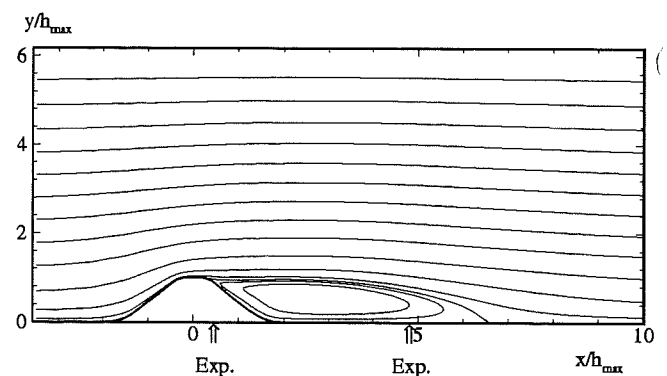
Experiments



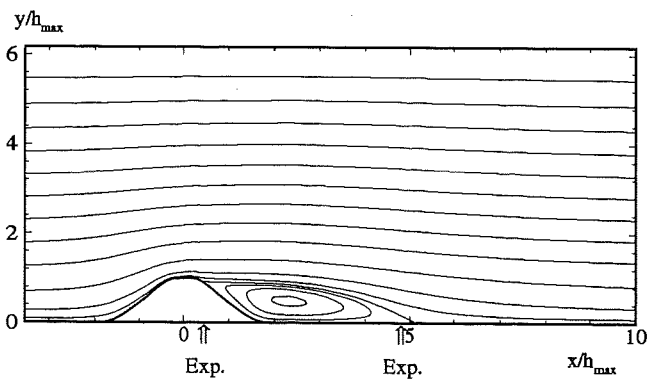
UChalmer:lKE_LaSh



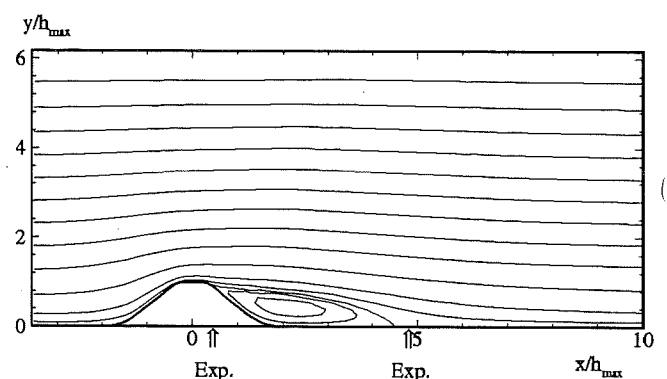
EDFLNHLa:lKE_LaSh



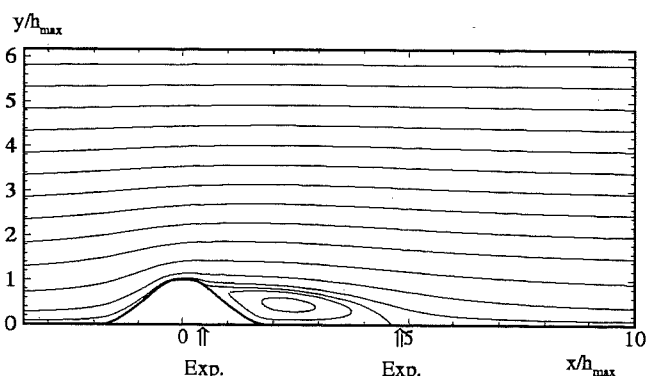
EPFLausa:lKE_LaBr



UChalmer:lKE_LiLe



UMISTLes:lKE_LiLe

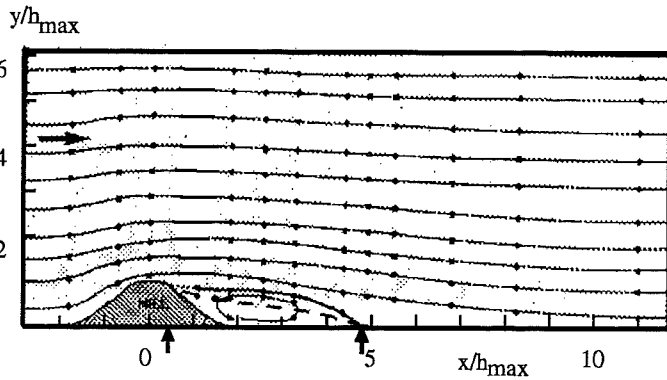


UFlorenc:lKE_NaHi

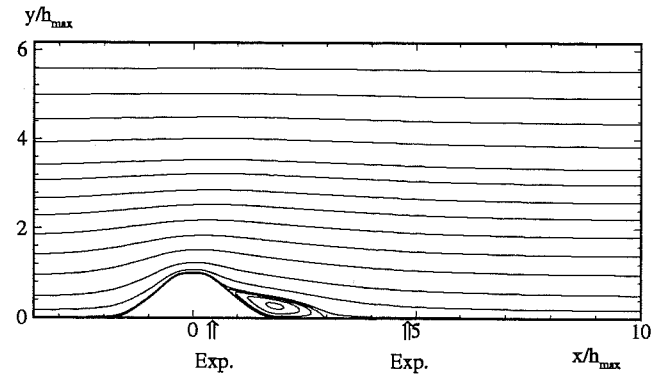
2D Model Hill Flow - Case 2A: Single Hill

Field Distribution of Stream Lines

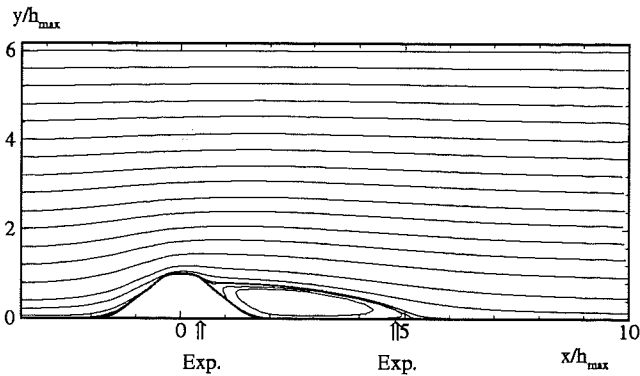
non-linear k-epsilon and k-omega models



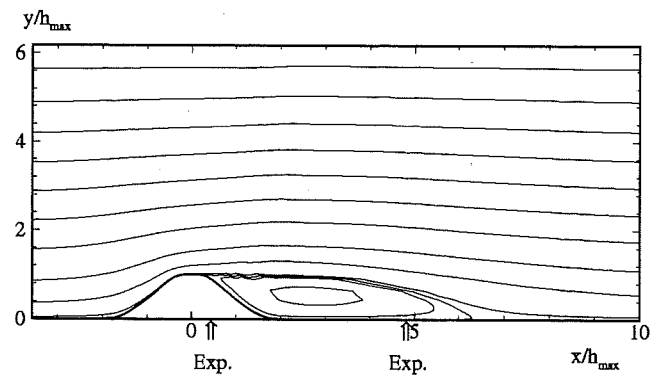
Experiments



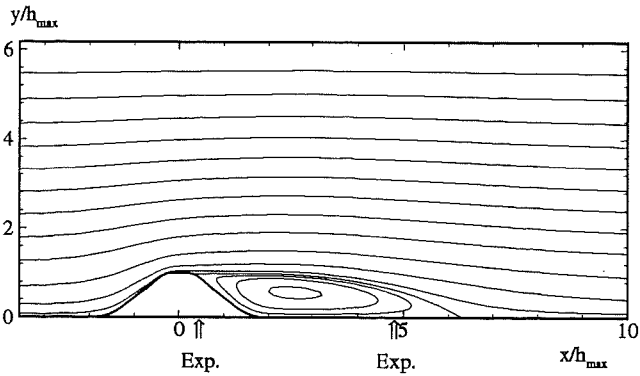
ASC:nKE_SZL+wf



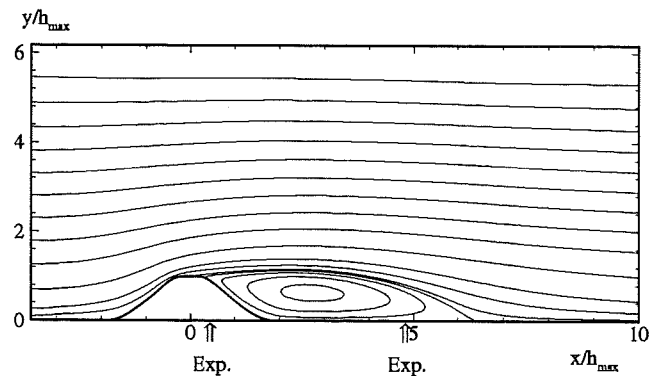
IOlomouc:nKE_Spez+wf



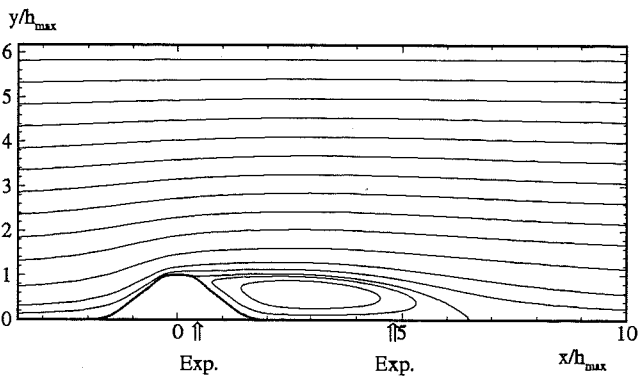
DLRGoett:kOm_Wil



UChalmer:kOm_Wil



UDelftZi:kOm_Wil

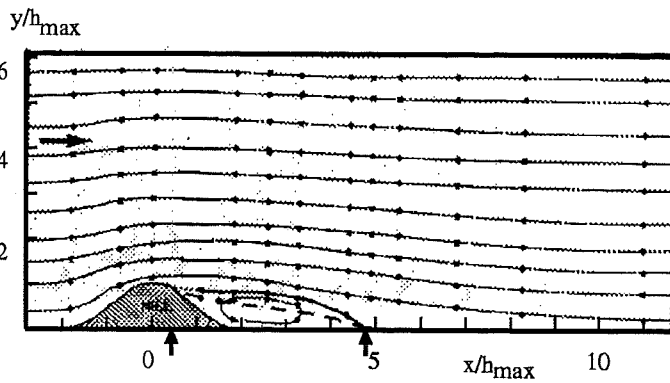


UFlorenc:kOm_Wil

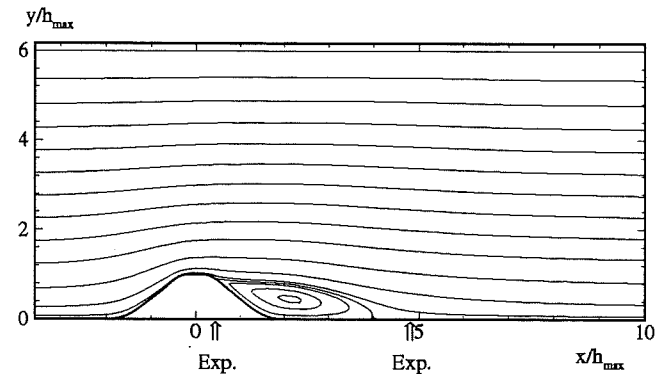
2D Model Hill Flow - Case 2A: Single Hill

Field Distribution of Stream Lines

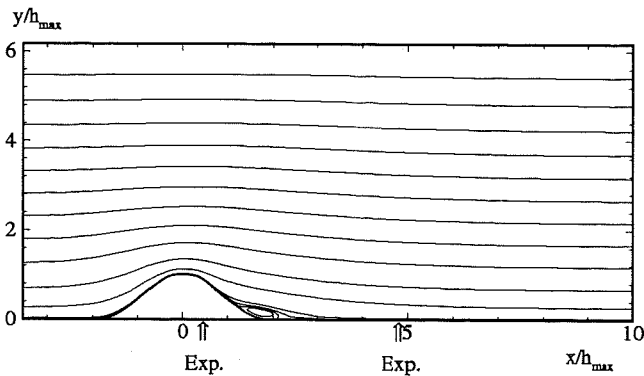
Reynolds-stress models



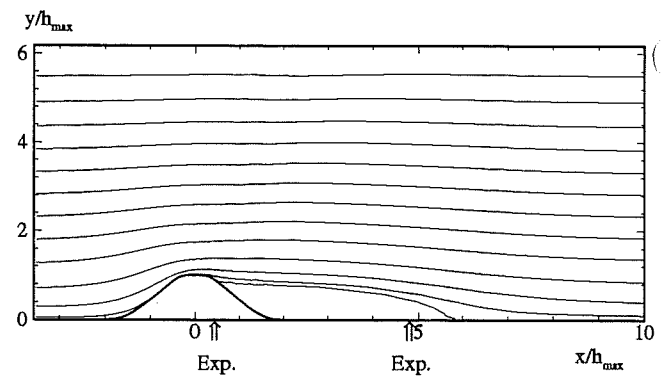
Experiments



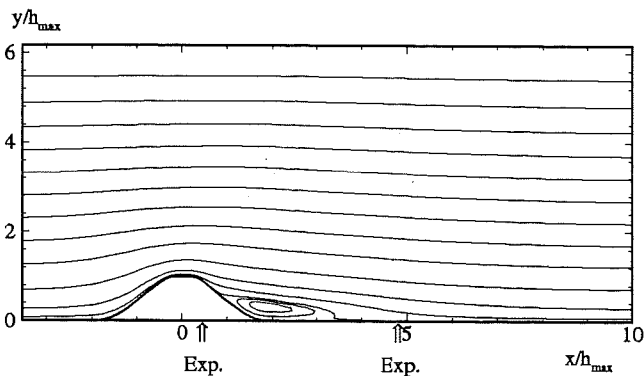
UDelftHa:RSM_LRR+wf



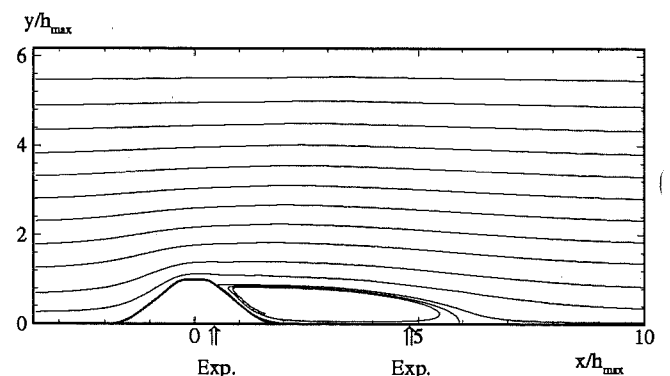
UChalmer:RSM_LRR+wf



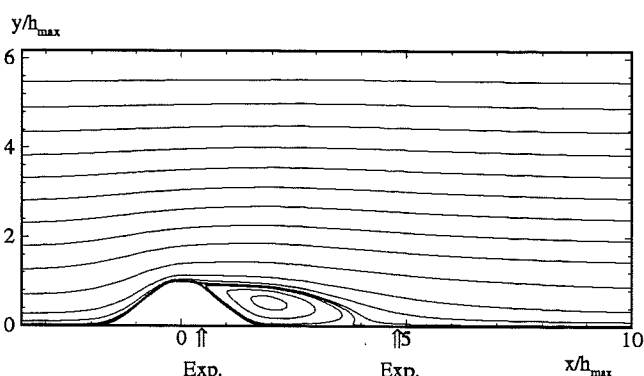
UMISTLes:RSM_GiLa+wf



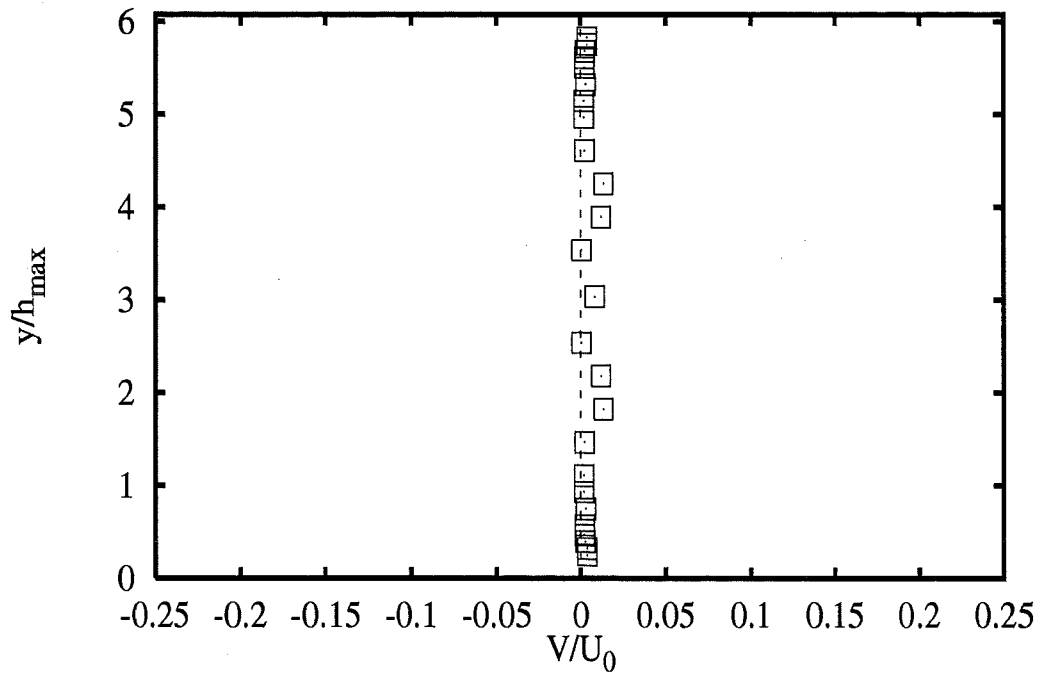
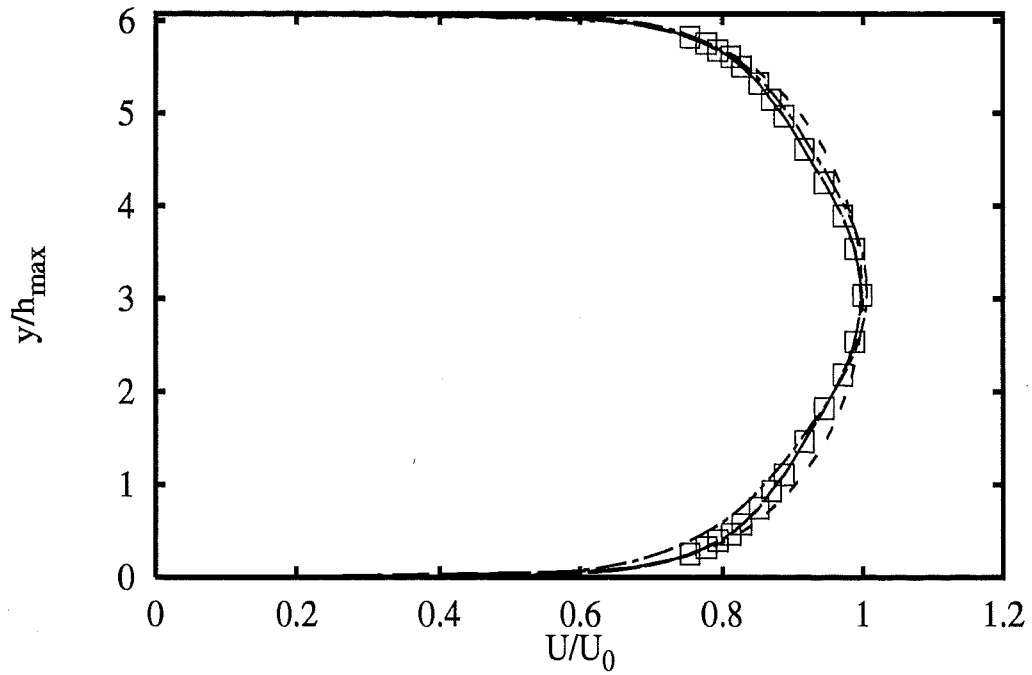
UChalmer:RSM_SSG+wf



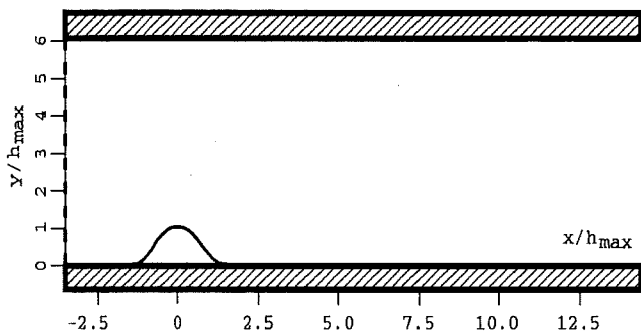
UMISTLes:RSM_GiLa+Wol



UChalmer:RSM_HaLa

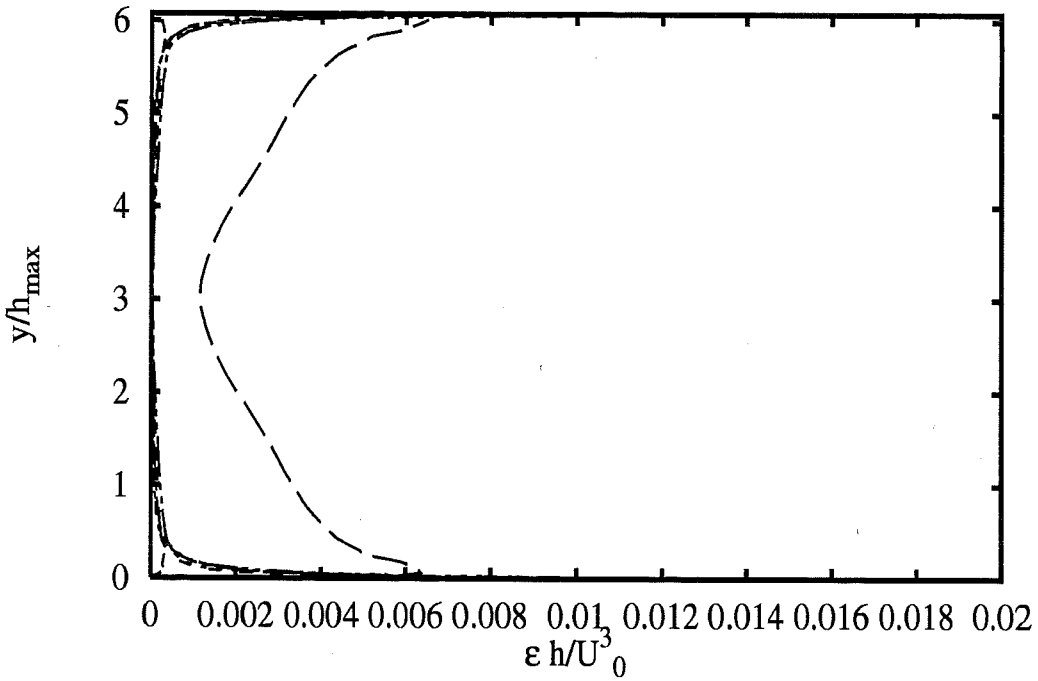
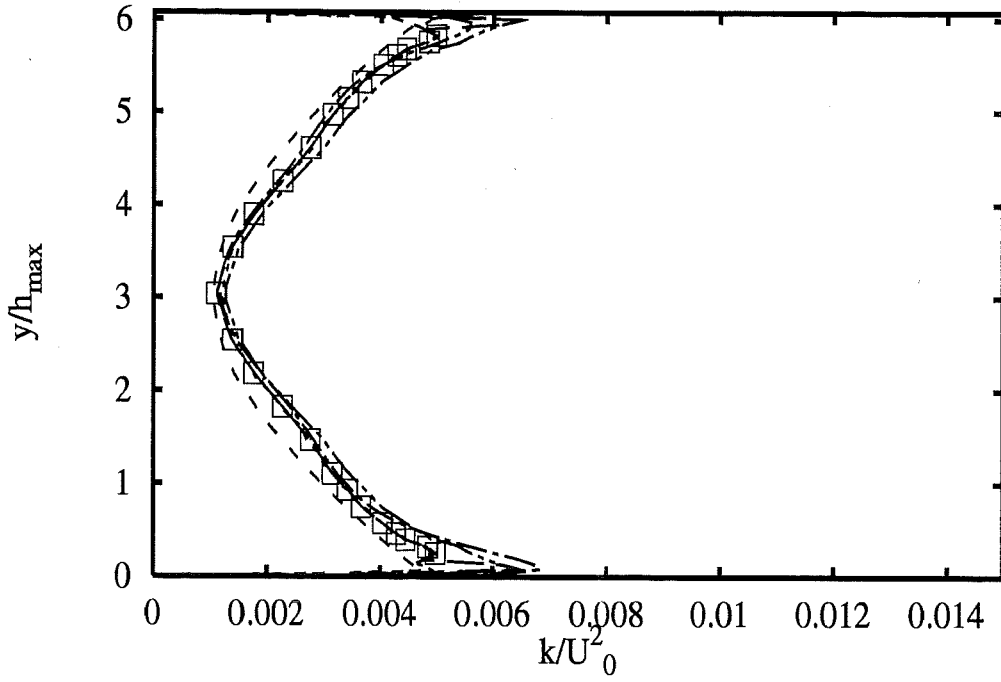


Profiles at $x/h_{max} = -3.57$

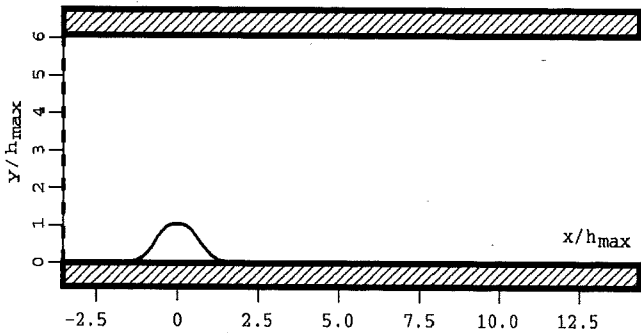


| | | Experiments | □ |
|----------|------------|-------------|-------|
| UChalmer | hKE std+wf | — | — |
| UDelftHa | hKE std+wf | - - - | - - - |
| UDelftZi | hKE std+wf | | |
| UKarlsru | hKE std+wf | — | — |
| UMISTLes | hKE std+wf | - - - | - - - |
| UPorto | hKE std+wf | - - - | - - - |

2A - 7

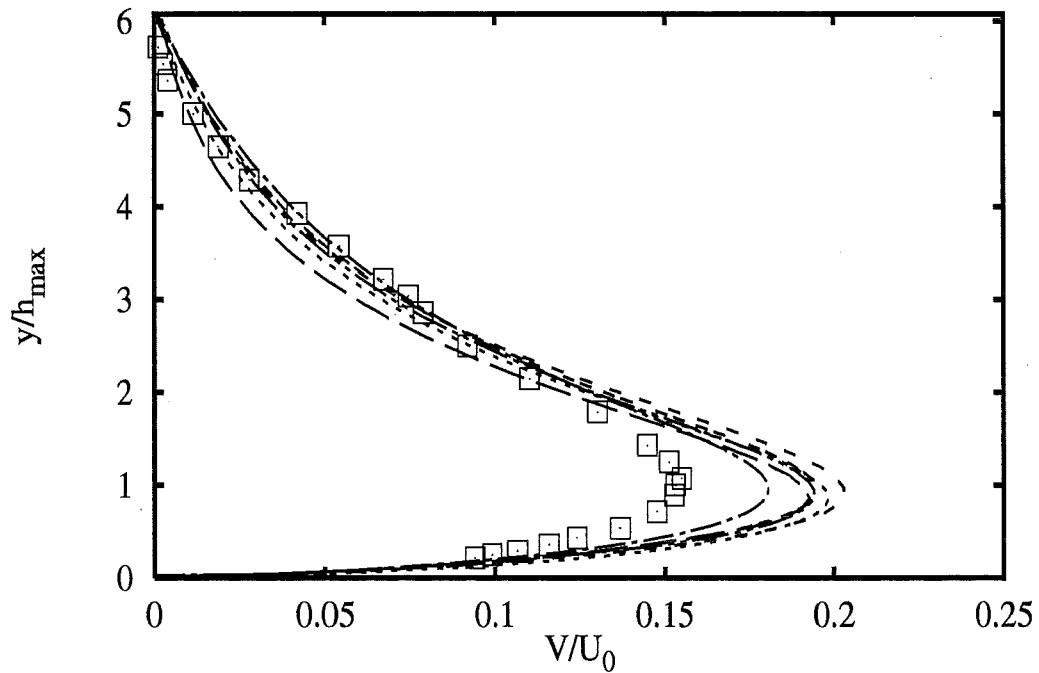
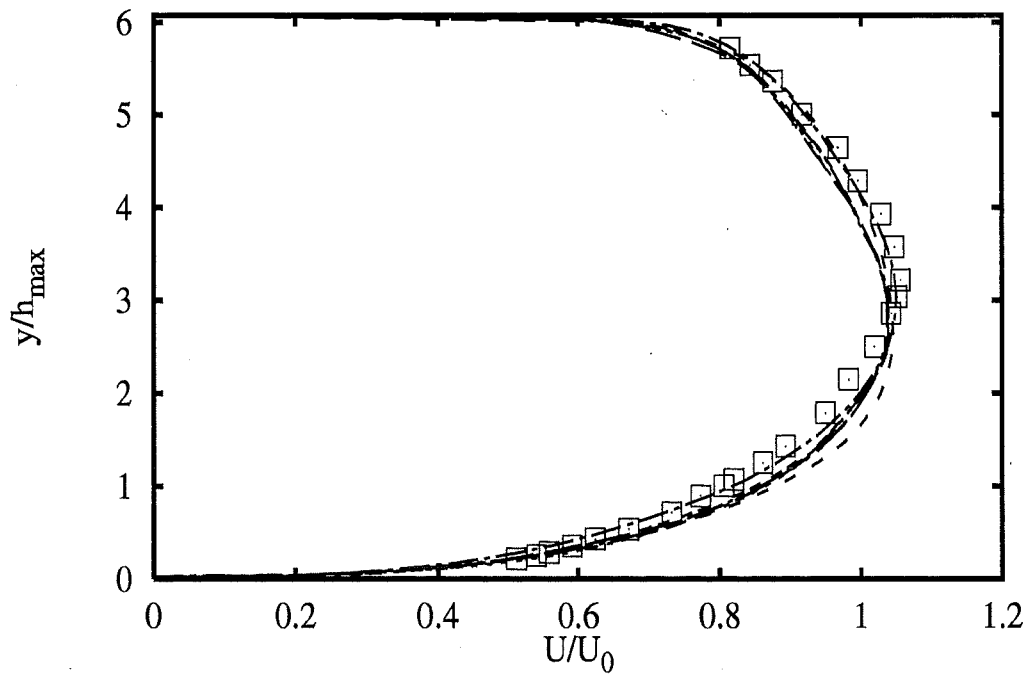


Profiles at $x/h_{max} = -3.57$

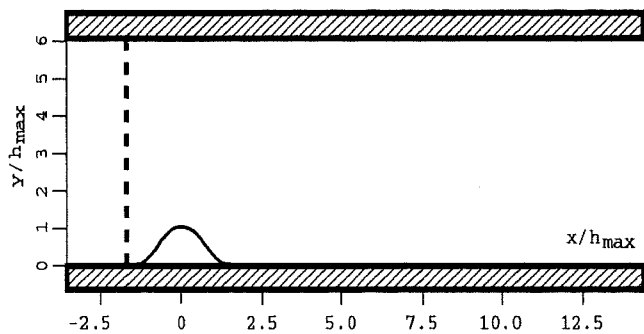


| | | Experiments | □ |
|----------|------------|-------------|---|
| UChalmer | hKE std+wf | --- | |
| UDelftHa | hKE std+wf | --- | |
| UDelftZi | hKE std+wf | --- | |
| UKarlsru | hKE std+wf | --- | |
| UMISTLes | hKE std+wf | --- | |
| UPorto | hKE std+wf | --- | |

2A - 8

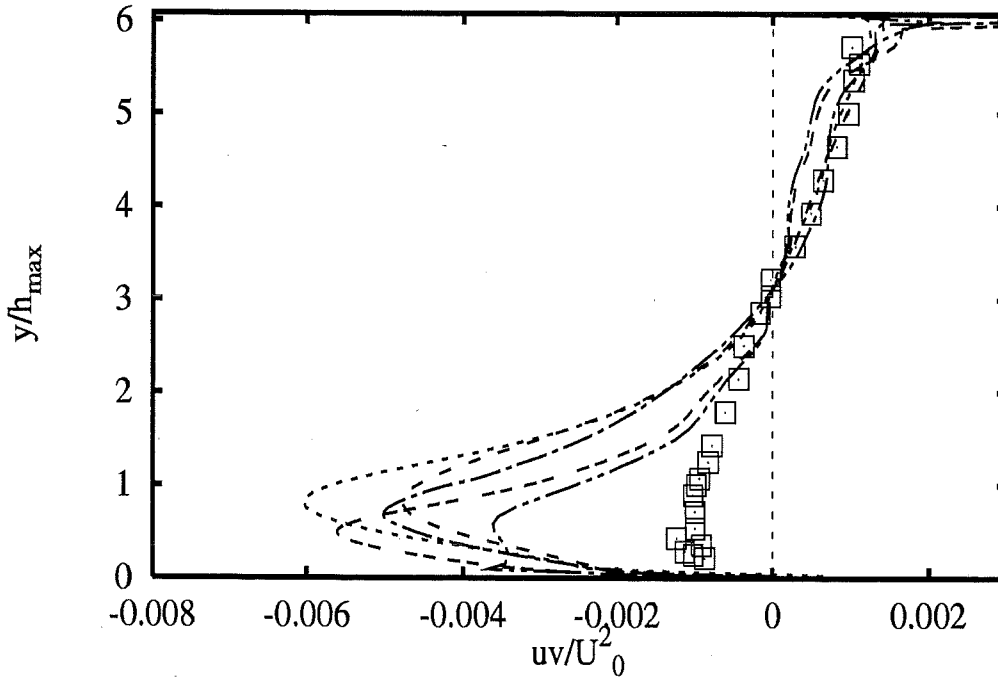
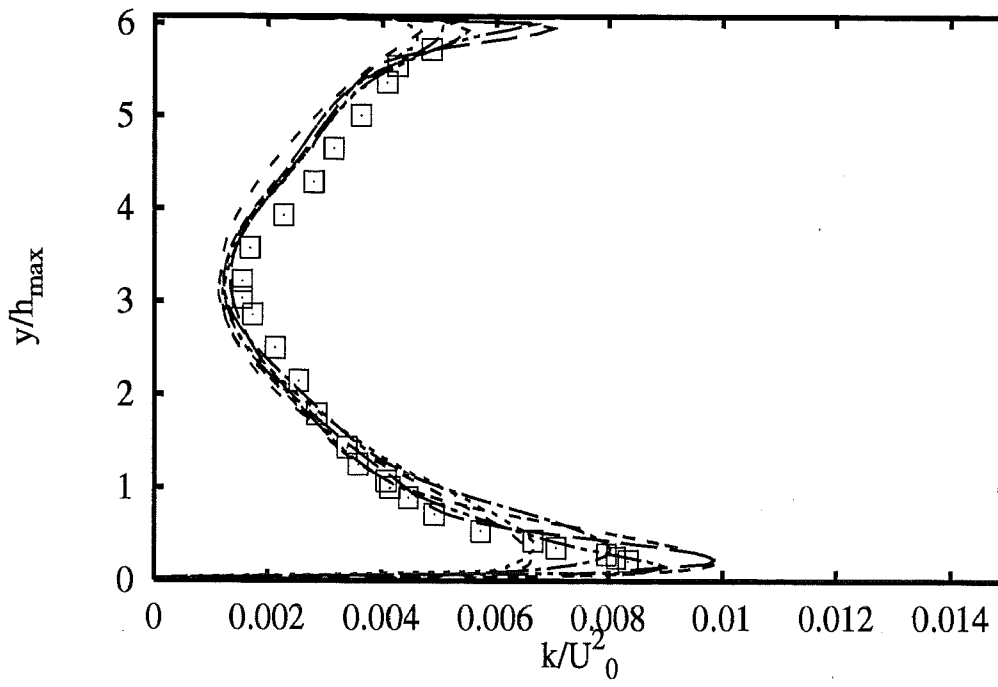


Profiles at $x/h_{max} = -1.78$

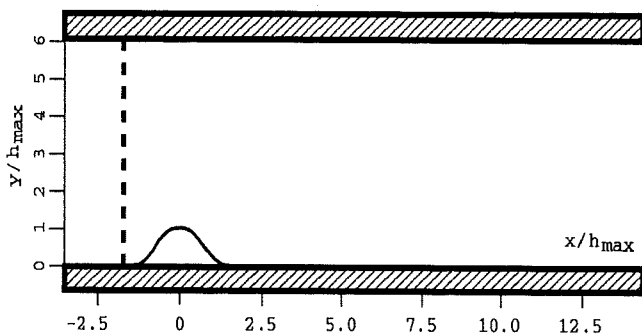


| | | Experiments | □ |
|-----------------|-------------------|-------------|---|
| <i>UChalmer</i> | <i>hKE std+wf</i> | --- | |
| <i>UDelftHa</i> | <i>hKE std+wf</i> | --- | |
| <i>UDelftZi</i> | <i>hKE std+wf</i> | --- | |
| <i>UKarlsru</i> | <i>hKE std+wf</i> | --- | |
| <i>UMISTLes</i> | <i>hKE std+wf</i> | --- | |
| <i>UPorto</i> | <i>hKE std+wf</i> | --- | |

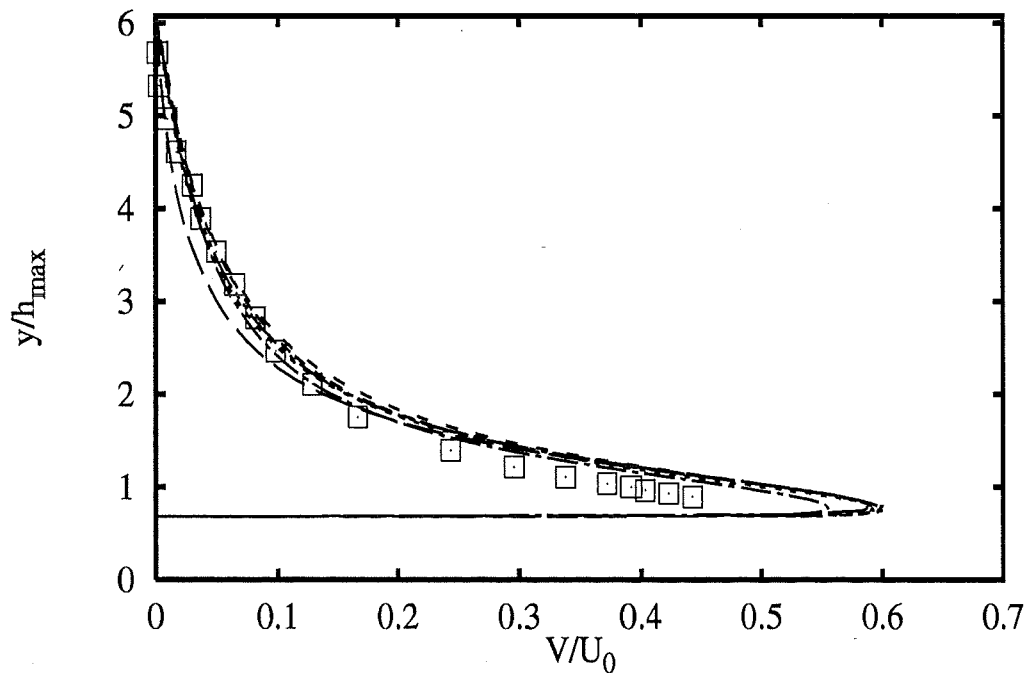
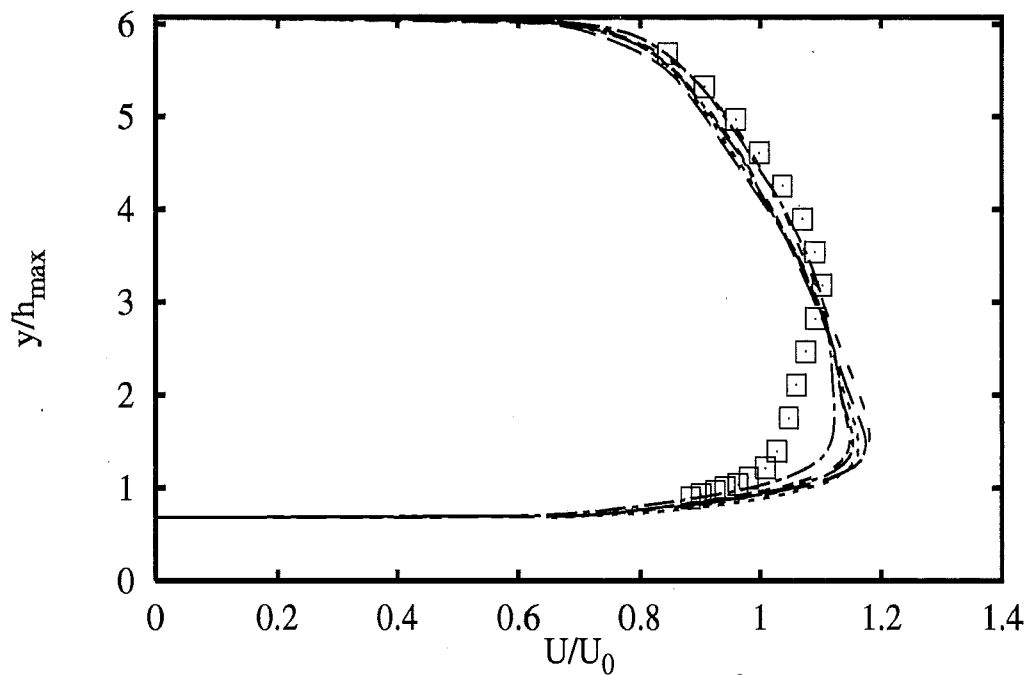
2A - 9



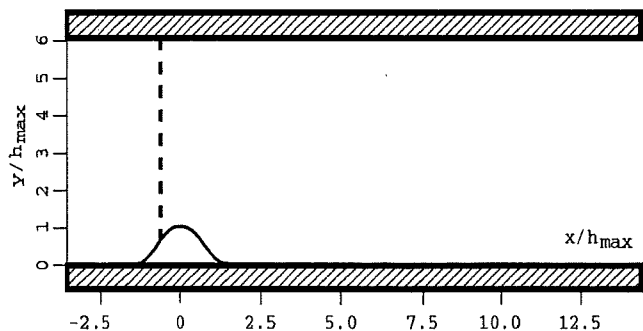
Profiles at $x/h_{max} = -1.78$



| | | Experiments | | |
|-----------------|-------------------|--------------------|--|---|
| <i>UChalmer</i> | <i>hKE std+wf</i> | --- | | □ |
| <i>UDelftHa</i> | <i>hKE std+wf</i> | --- | | |
| <i>UDelftZi</i> | <i>hKE std+wf</i> | --- | | |
| <i>UKarlsru</i> | <i>hKE std+wf</i> | --- | | |
| <i>UMISTLes</i> | <i>hKE std+wf</i> | --- | | |
| <i>UPorto</i> | <i>hKE std+wf</i> | --- | | |

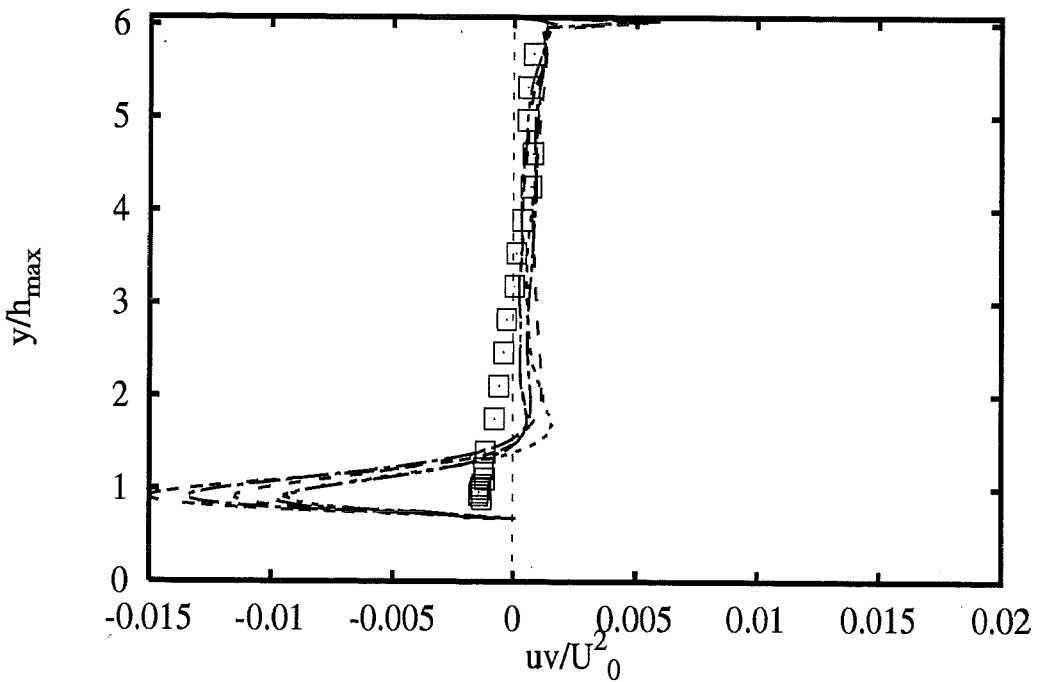
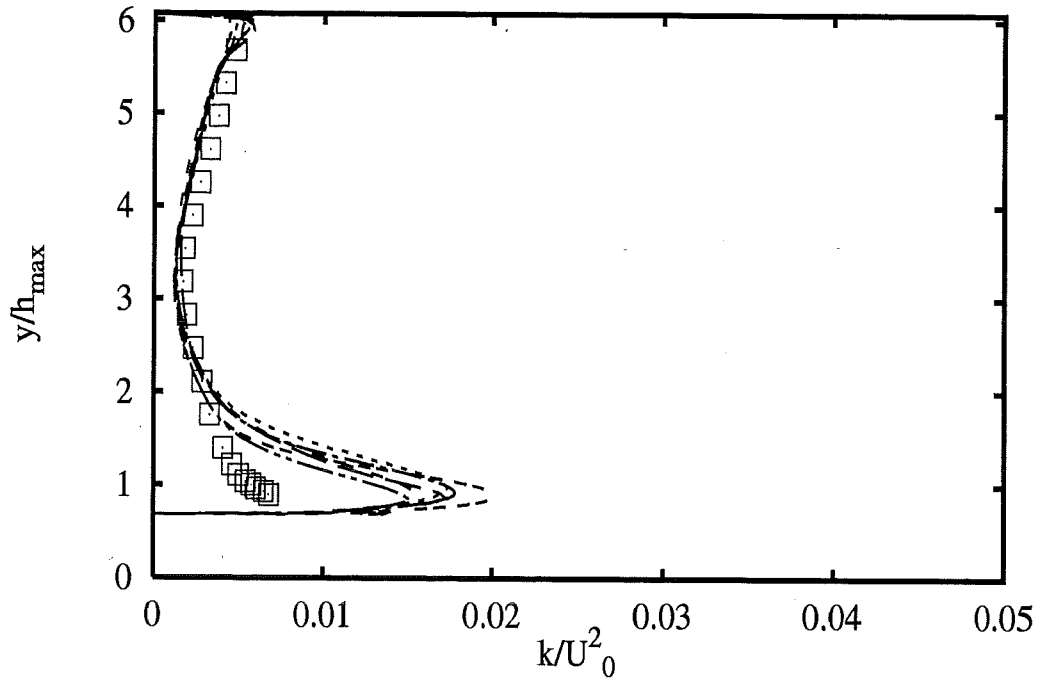


Profiles at $x/h_{max} = -0.71$

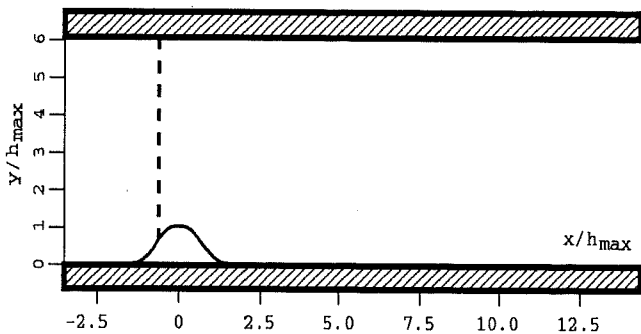


| | | Experiments | □ |
|-----------------|-------------------|-------------|---|
| <i>UChalmer</i> | <i>hKE std+wf</i> | --- | |
| <i>UDelftHa</i> | <i>hKE std+wf</i> | --- | |
| <i>UDelftZi</i> | <i>hKE std+wf</i> | | |
| <i>UKarlsru</i> | <i>hKE std+wf</i> | --- | |
| <i>UMISTLes</i> | <i>hKE std+wf</i> | --- | |
| <i>UPorto</i> | <i>hKE std+wf</i> | --- | |

2A - 11

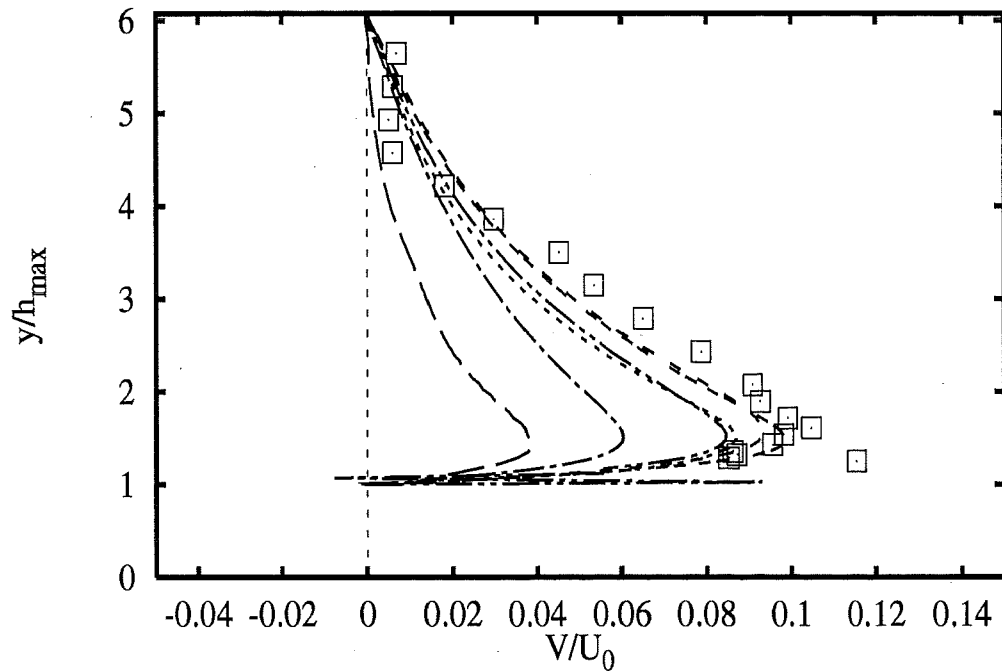
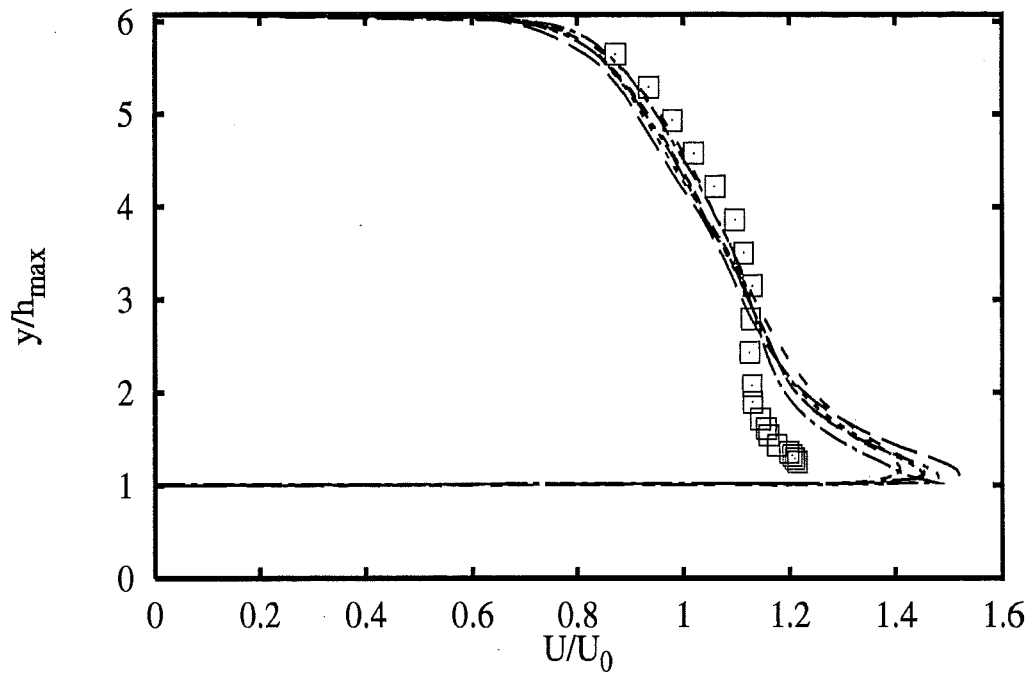


Profiles at $x/h_{max} = -0.71$

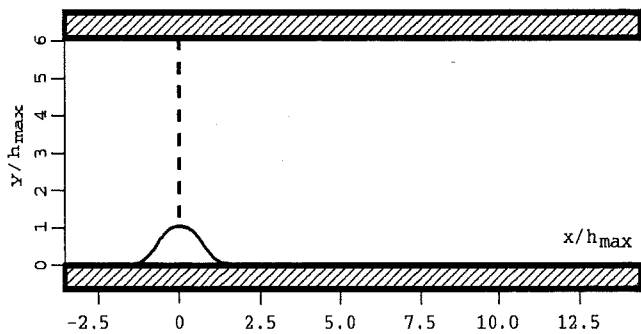


| | | Experiments | □ |
|----------|------------|-------------|---|
| UChalmer | hKE std+wf | --- | |
| UDelftHa | hKE std+wf | --- | |
| UDelftZi | hKE std+wf | --- | |
| UKarlsru | hKE std+wf | --- | |
| UMISTLes | hKE std+wf | --- | |
| UPorto | hKE std+wf | --- | |

2A - 12

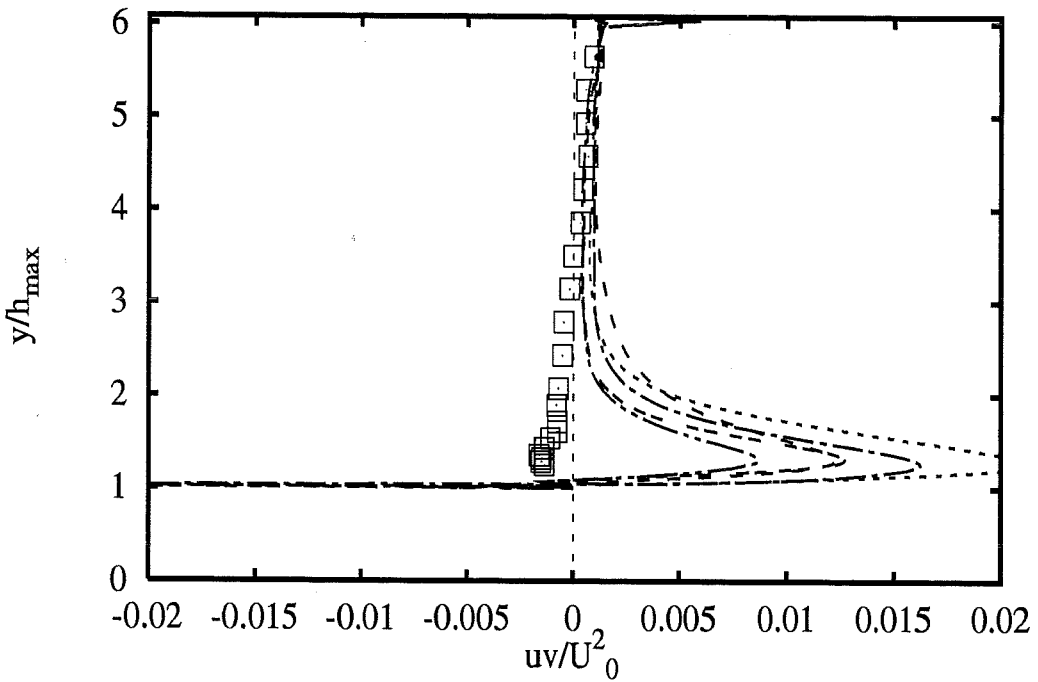
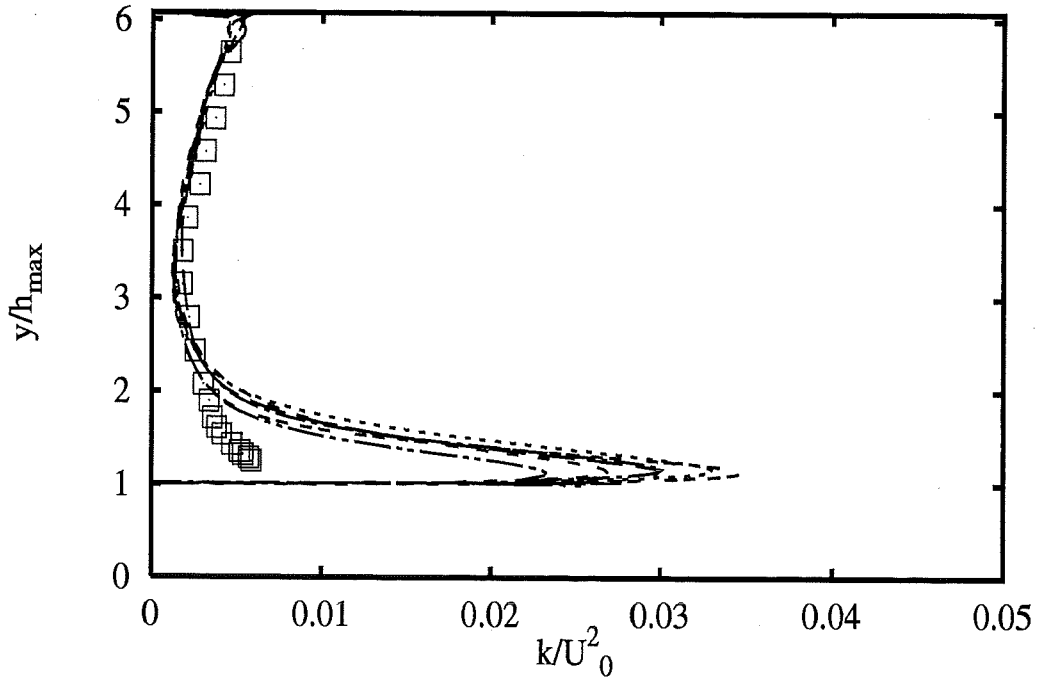


Profiles at $x/h_{max} = 0$

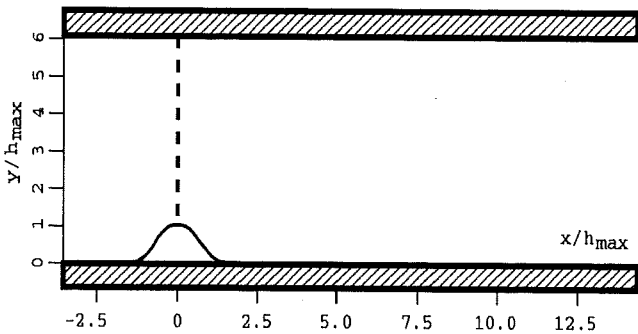


| | | Experiments | □ |
|-----------------|-------------------|-------------|---|
| <i>UChalmer</i> | <i>hKE std+wf</i> | — — | |
| <i>UDelftHa</i> | <i>hKE std+wf</i> | - - - | |
| <i>UDelftZi</i> | <i>hKE std+wf</i> | · · · · · | |
| <i>UKarlsru</i> | <i>hKE std+wf</i> | - - - - | |
| <i>UMISTLes</i> | <i>hKE std+wf</i> | - · - · - | |
| <i>UPorto</i> | <i>hKE std+wf</i> | - - - | |

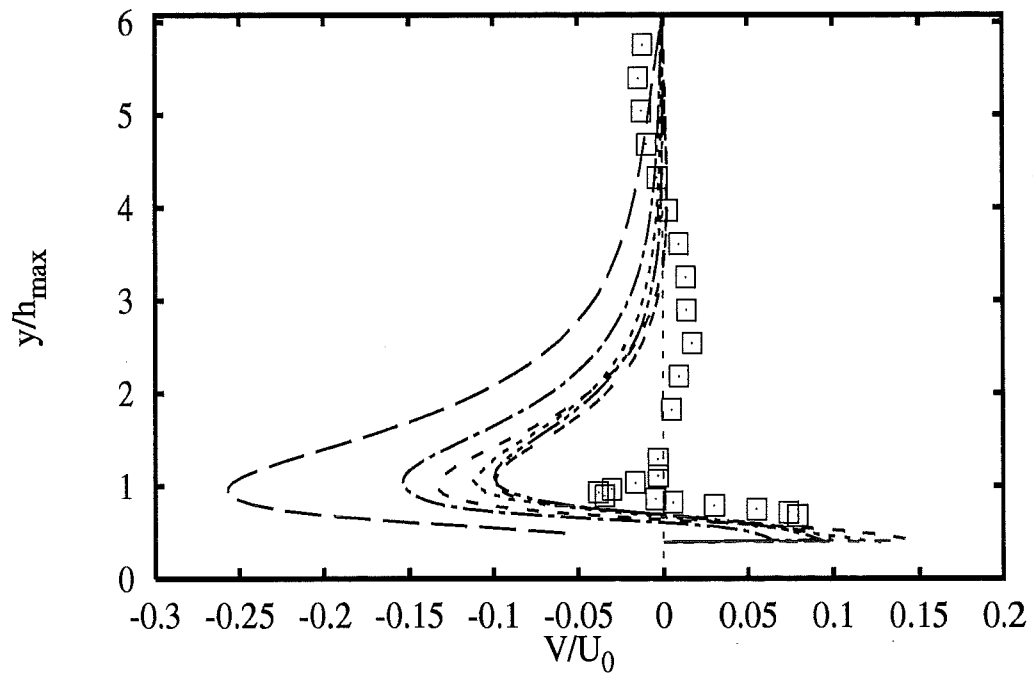
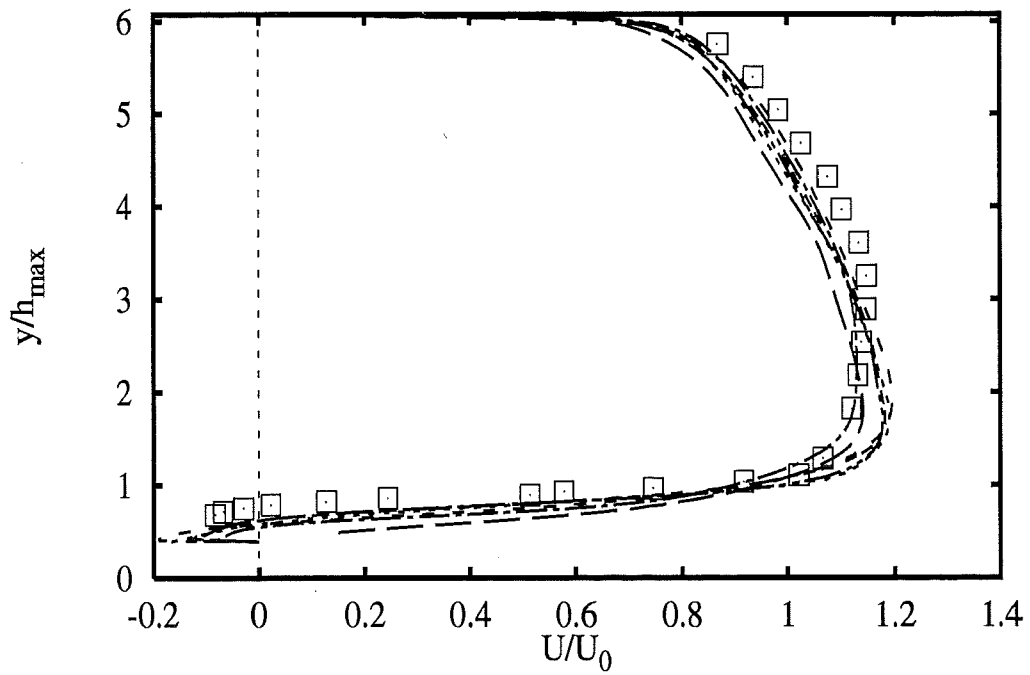
2A - 13



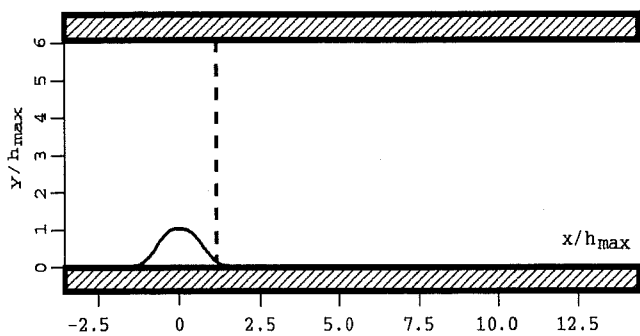
Profiles at $x/h_{max} = 0$



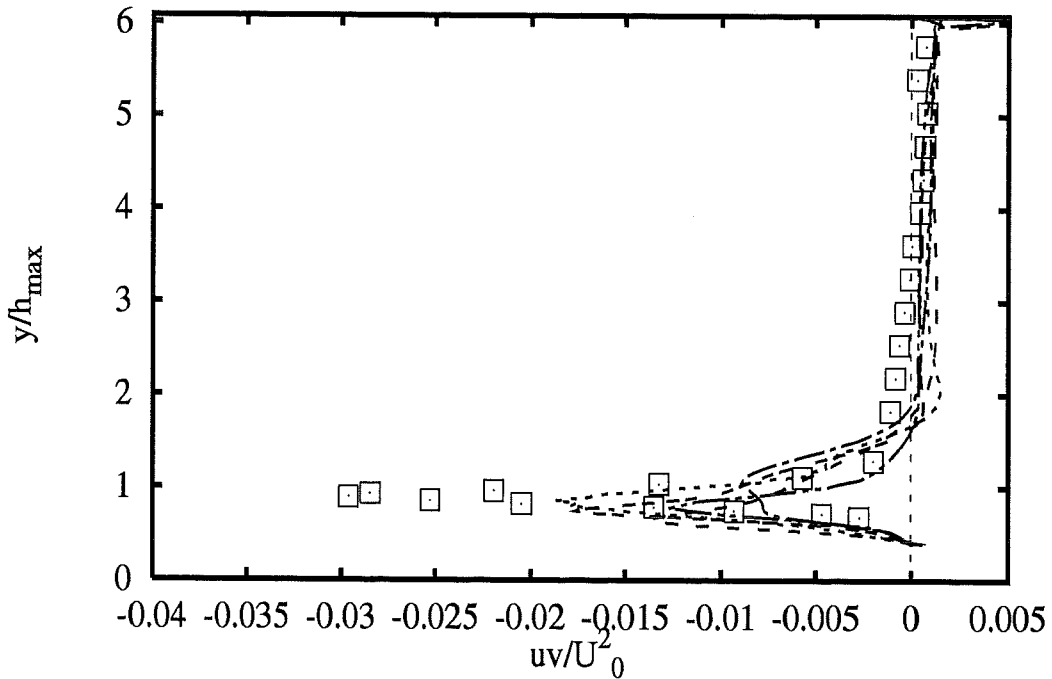
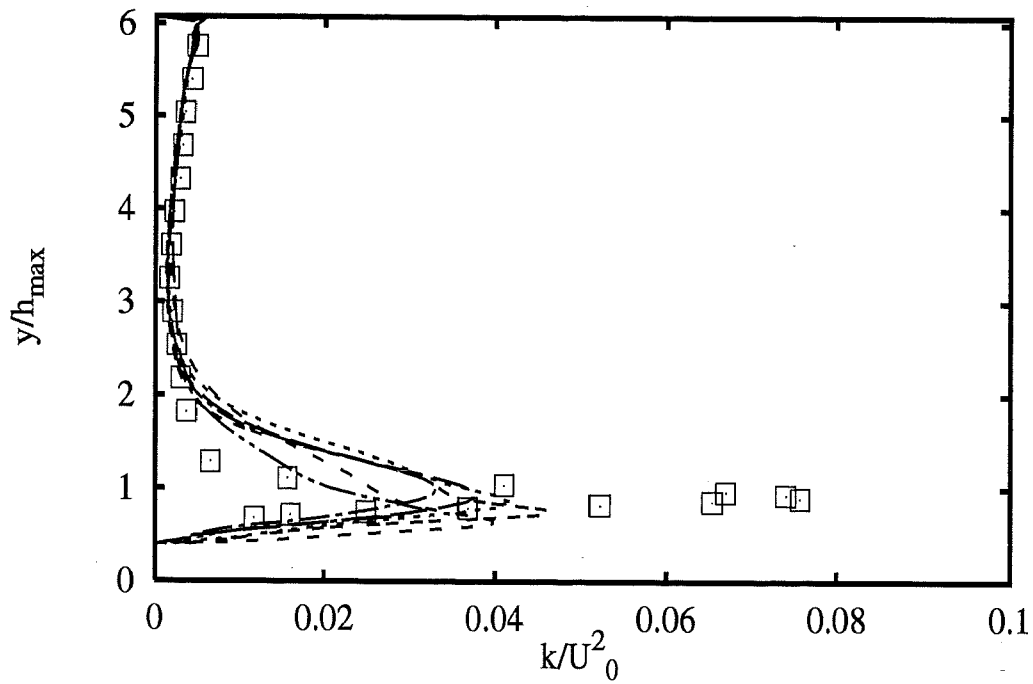
| | | Experiments | □ |
|----------|------------|-------------|---|
| UChalmer | hKE std+wf | --- | |
| UDelftHa | hKE std+wf | --- | |
| UDelftZi | hKE std+wf | --- | |
| UKarlsru | hKE std+wf | --- | |
| UMISTLes | hKE std+wf | --- | |
| UPorto | hKE std+wf | --- | |



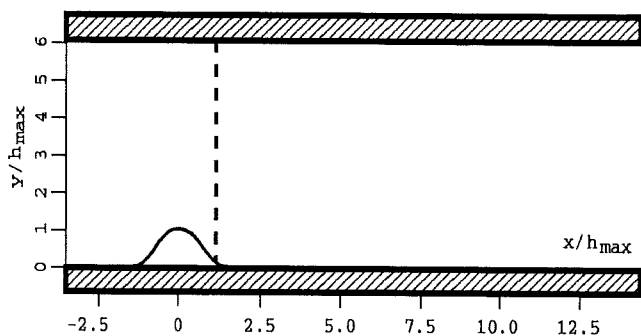
Profiles at $x/h_{max} = 1.07$



| | | Experiments | □ |
|----------|------------|-------------|---|
| UChalmer | hKE std+wf | --- | |
| UDelftHa | hKE std+wf | --- | |
| UDelftZi | hKE std+wf | --- | |
| UKarlsru | hKE std+wf | --- | |
| UMISTLes | hKE std+wf | --- | |
| UPorto | hKE std+wf | --- | |

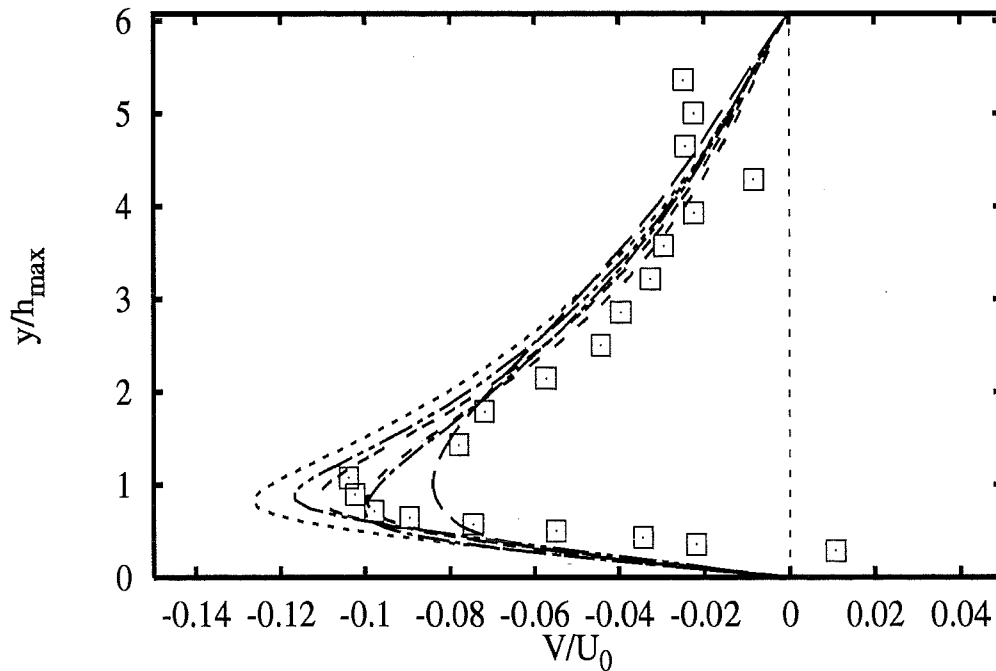
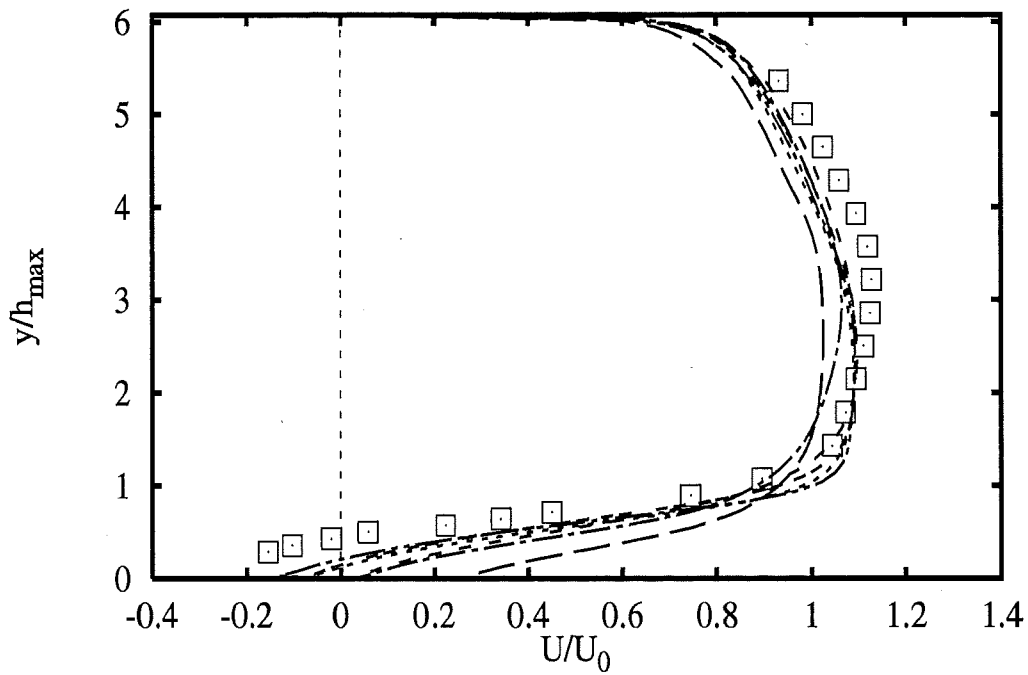


Profiles at $x/h_{max} = 1.07$

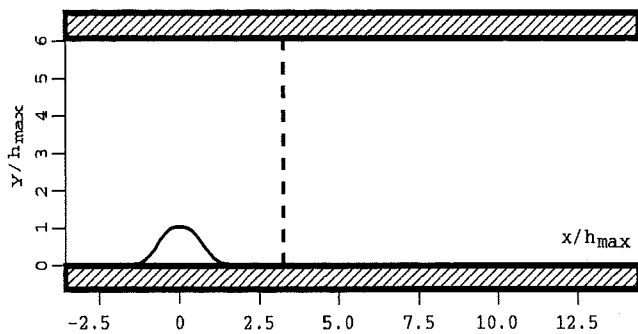


| | | Experiments | □ |
|----------|------------|-------------|---|
| UChalmer | hKE std+wf | --- | |
| UDelftHa | hKE std+wf | --- | |
| UDelftZi | hKE std+wf | --- | |
| UKarlsru | hKE std+wf | --- | |
| UMISTLes | hKE std+wf | --- | |
| UPorto | hKE std+wf | --- | |

2A - 16

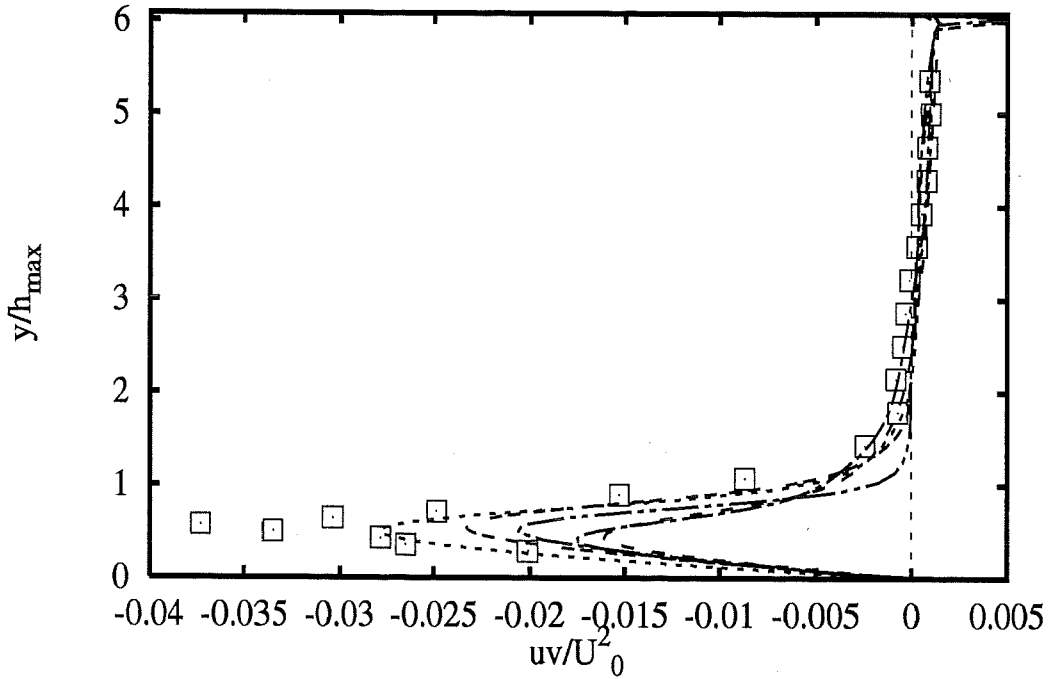
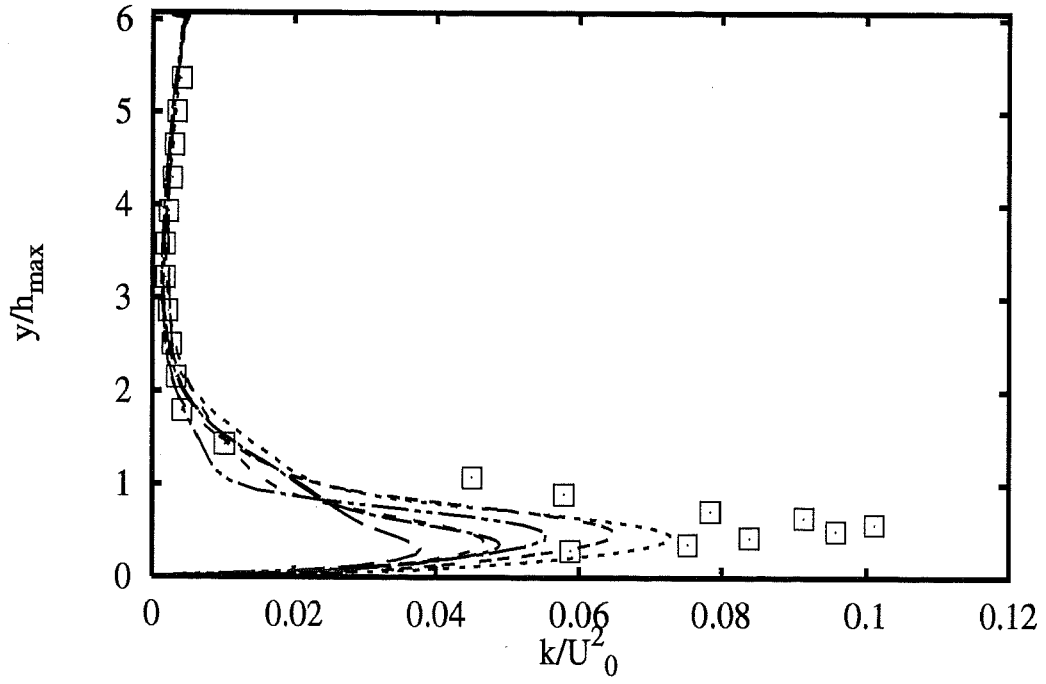


Profiles at $x/h_{max} = 3.21$

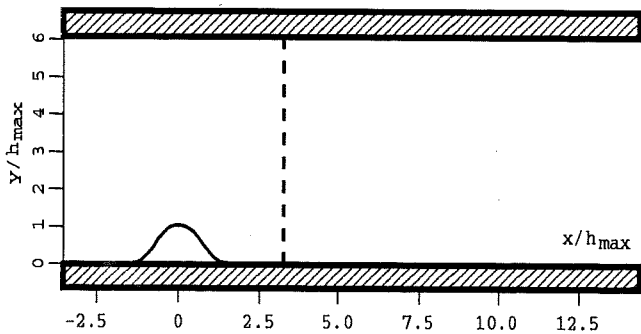


| | | Experiments | □ |
|-----------------|-------------------|-------------|---|
| <i>UChalmer</i> | <i>hKE std+wf</i> | --- | |
| <i>UDelftHa</i> | <i>hKE std+wf</i> | --- | |
| <i>UDelftZi</i> | <i>hKE std+wf</i> | --- | |
| <i>UKarlsru</i> | <i>hKE std+wf</i> | --- | |
| <i>UMISTLes</i> | <i>hKE std+wf</i> | --- | |
| <i>UPorto</i> | <i>hKE std+wf</i> | --- | |

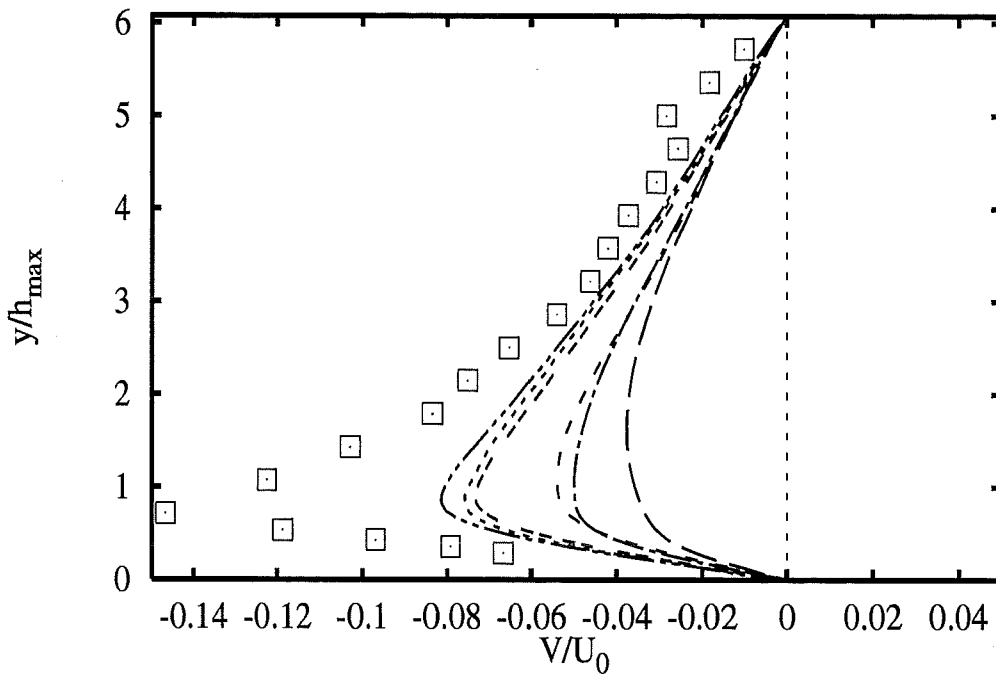
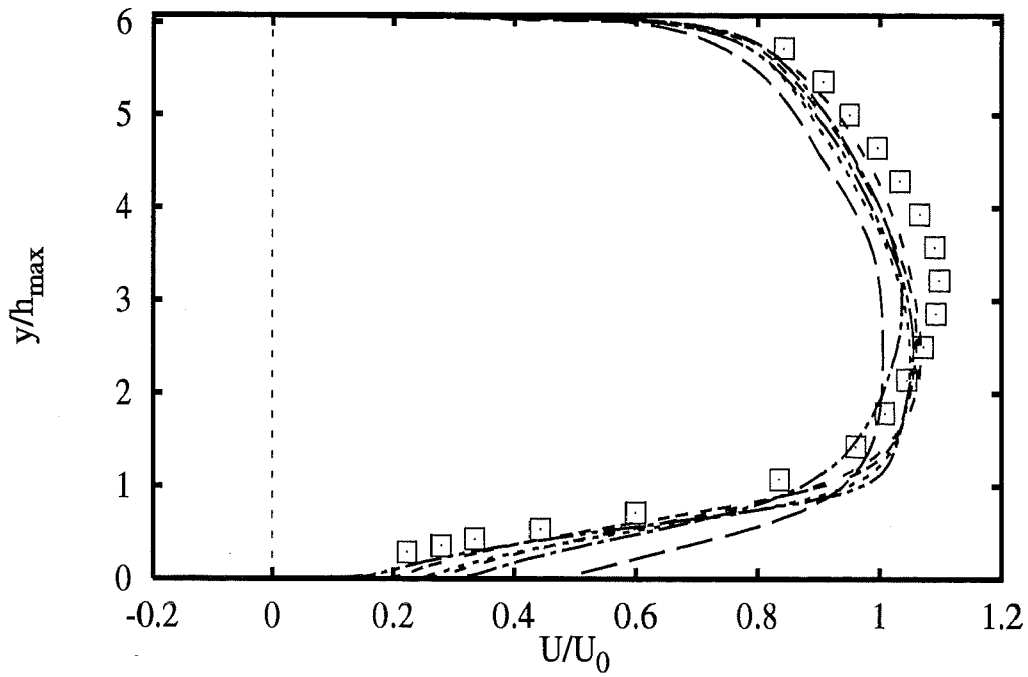
2A - 17



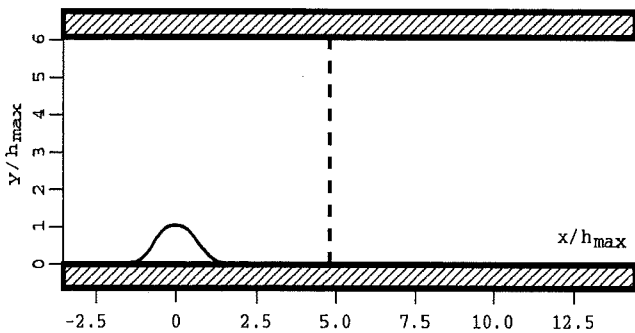
Profiles at $x/h_{max} = 3.21$



| Experiments | | |
|-------------|-------------------|-----|
| UChalmer | <i>hKE std+wf</i> | --- |
| UdelftHa | <i>hKE std+wf</i> | --- |
| UdelftZi | <i>hKE std+wf</i> | --- |
| UKarlsru | <i>hKE std+wf</i> | --- |
| UMISTLes | <i>hKE std+wf</i> | --- |
| UPorto | <i>hKE std+wf</i> | --- |

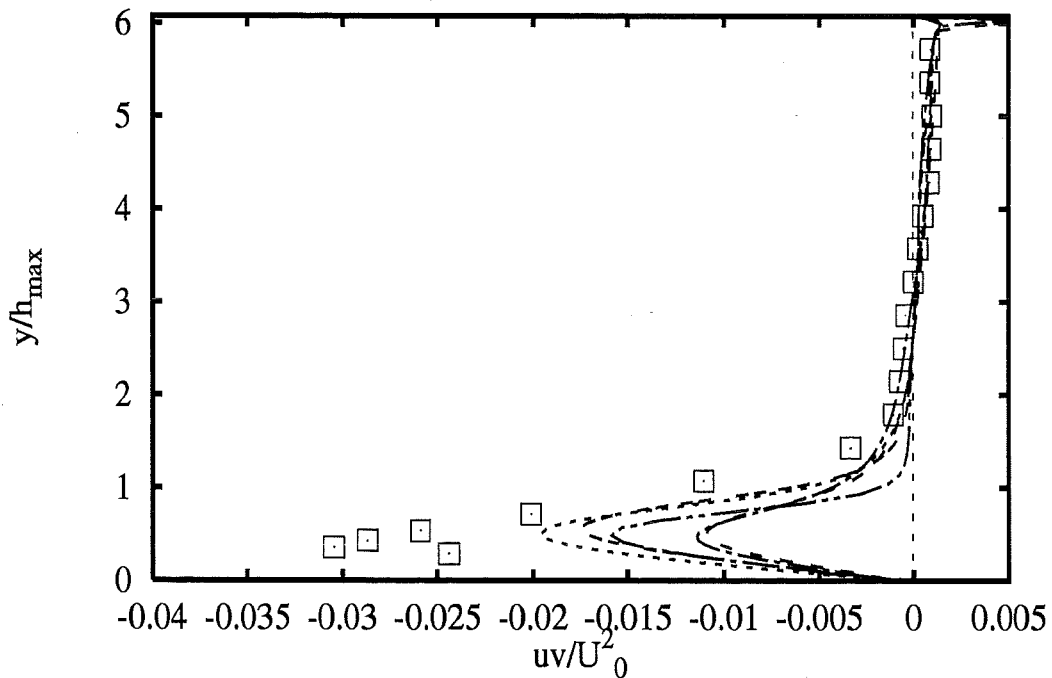
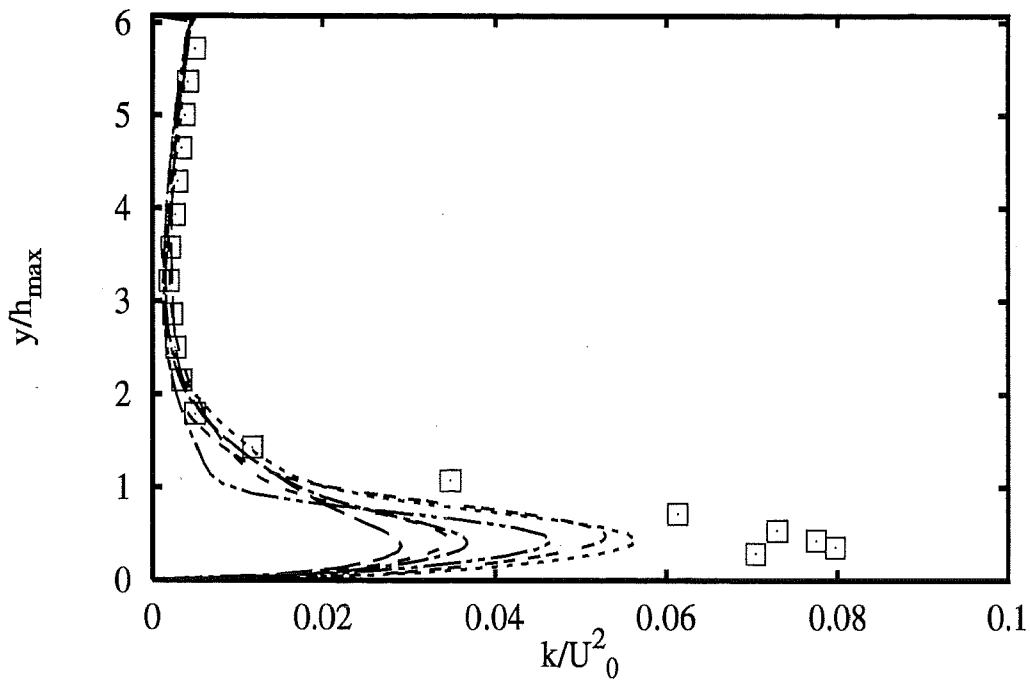


Profiles at $x/h_{max} = 4.79$

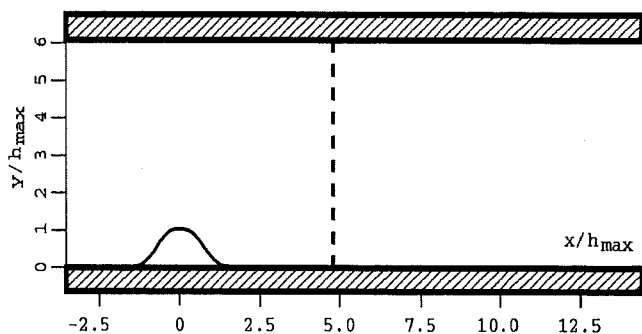


| | | Experiments | □ |
|----------|-------------------|-------------|---|
| UChalmer | <i>hKE std+wf</i> | --- | |
| UDelftHa | <i>hKE std+wf</i> | ---- | |
| UDelftZi | <i>hKE std+wf</i> | | |
| UKarlsru | <i>hKE std+wf</i> | ---- | |
| UMISTLes | <i>hKE std+wf</i> | | |
| UPorto | <i>hKE std+wf</i> | ---- | |

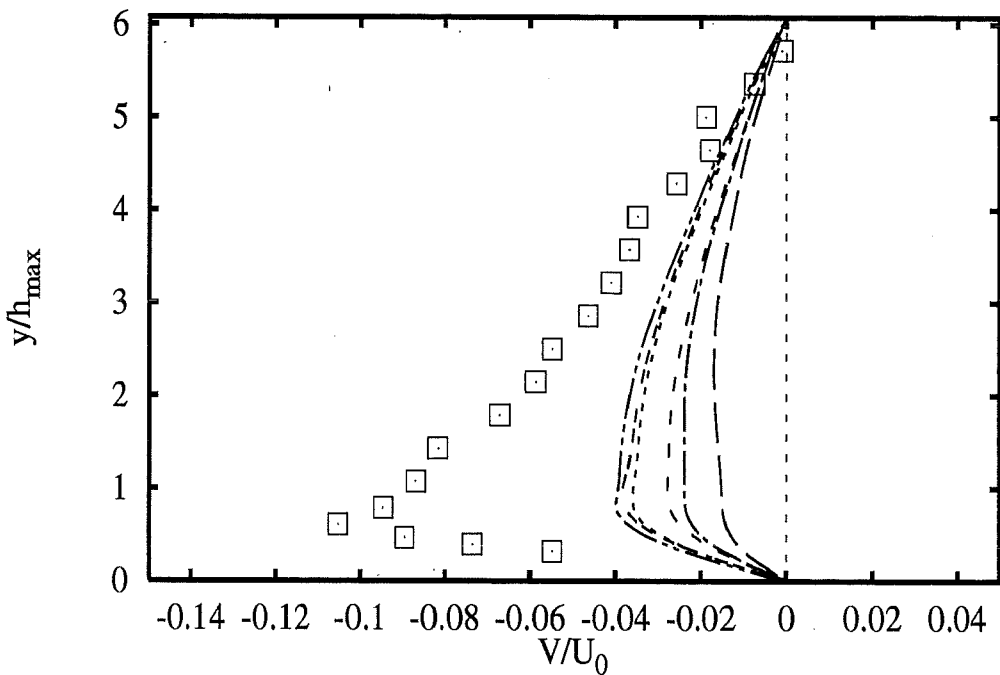
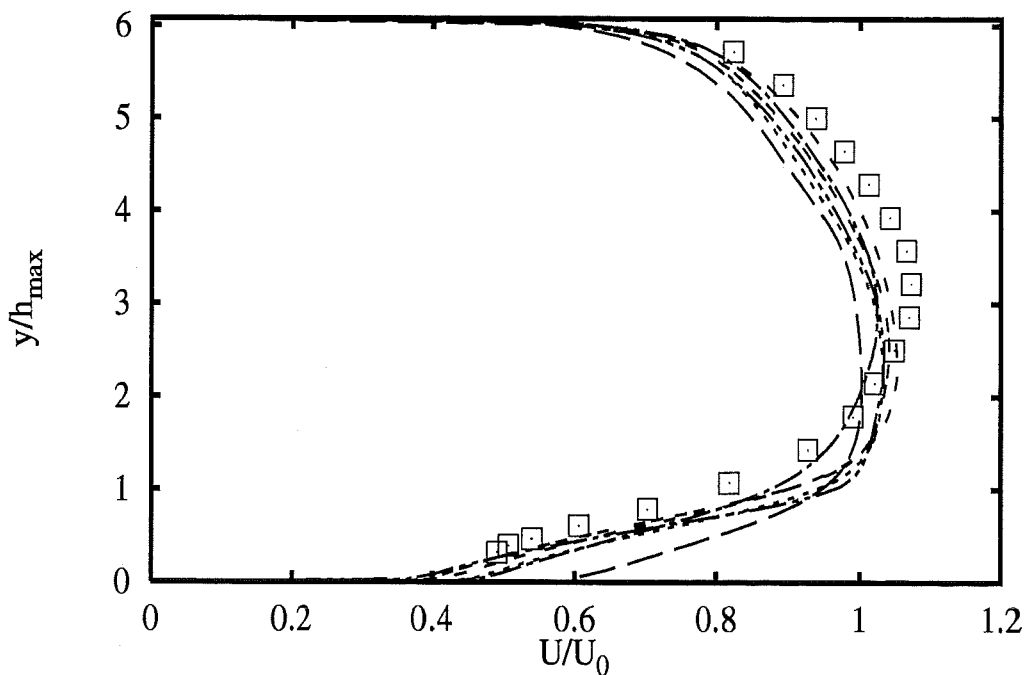
2A - 19



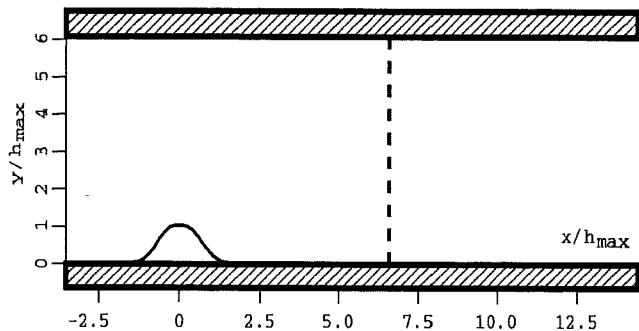
Profiles at $x/h_{max} = 4.79$



| | | Experiments | □ |
|-----------------|-------------------|-------------|---|
| <i>UChalmer</i> | <i>hKE std+wf</i> | --- | |
| <i>UdelftHa</i> | <i>hKE std+wf</i> | --- | |
| <i>UdelftZi</i> | <i>hKE std+wf</i> | --- | |
| <i>UKarlsru</i> | <i>hKE std+wf</i> | --- | |
| <i>UMISTLes</i> | <i>hKE std+wf</i> | --- | |
| <i>UPorto</i> | <i>hKE std+wf</i> | --- | |

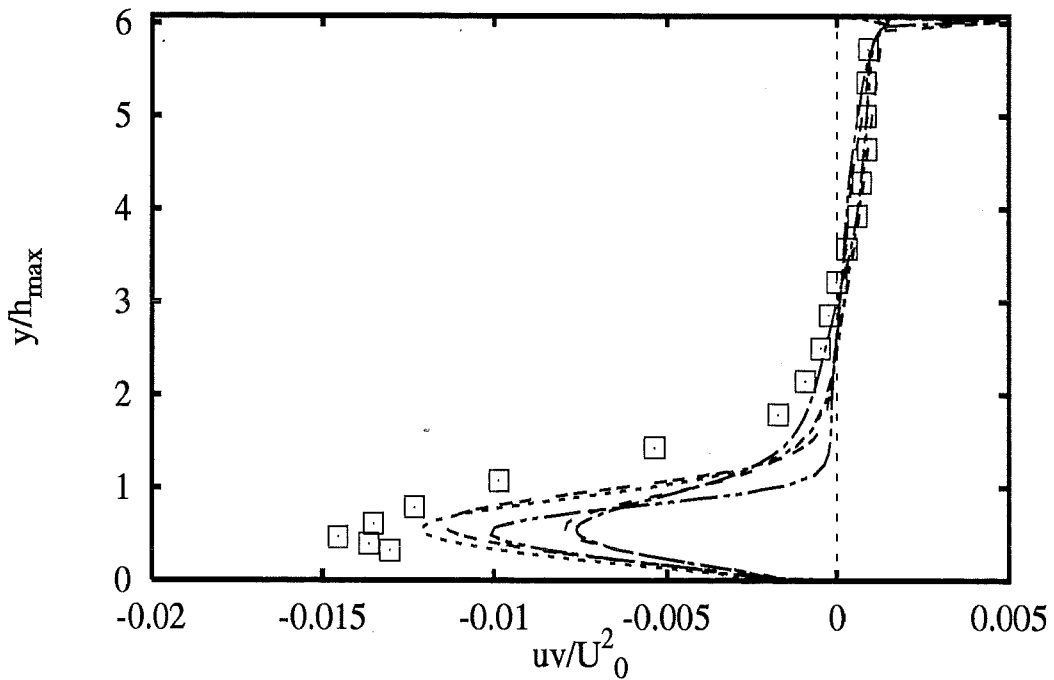
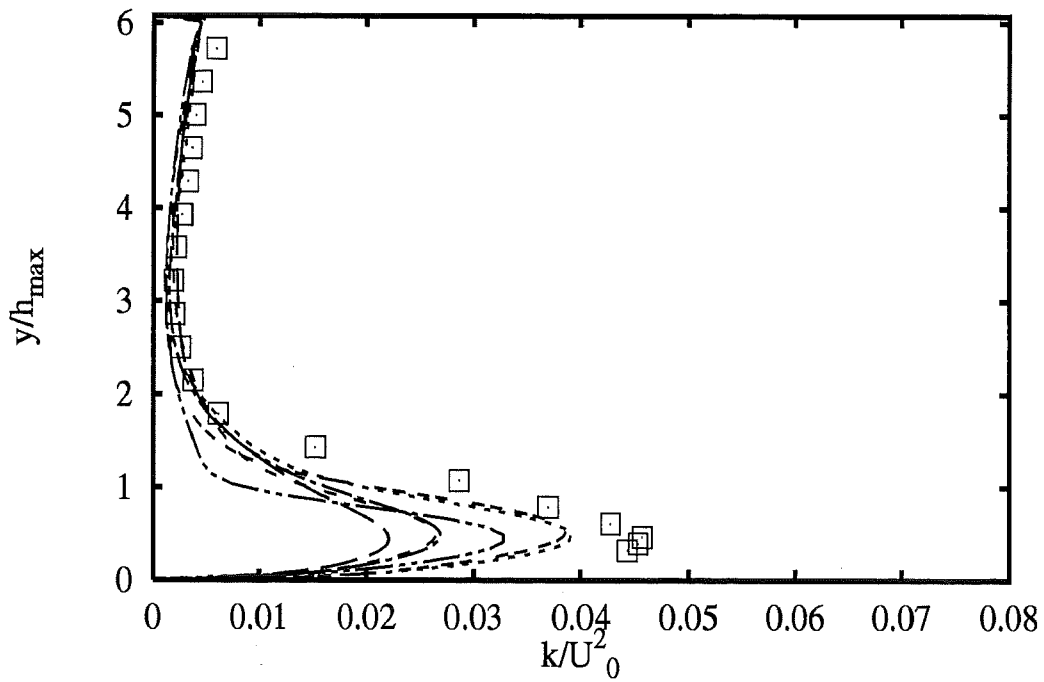


Profiles at $x/h_{max} = 6.61$

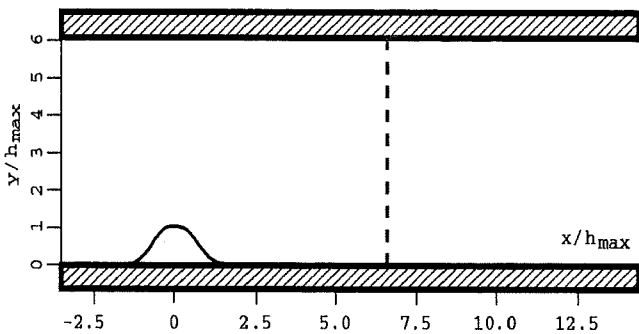


| Experiments | | |
|-------------|------------|-----|
| UChalmer | hKE std+wf | --- |
| UDelftHa | hKE std+wf | --- |
| UDelftZi | hKE std+wf | --- |
| UKarlsru | hKE std+wf | --- |
| UMISTLes | hKE std+wf | --- |
| UPorto | hKE std+wf | --- |

2A - 21

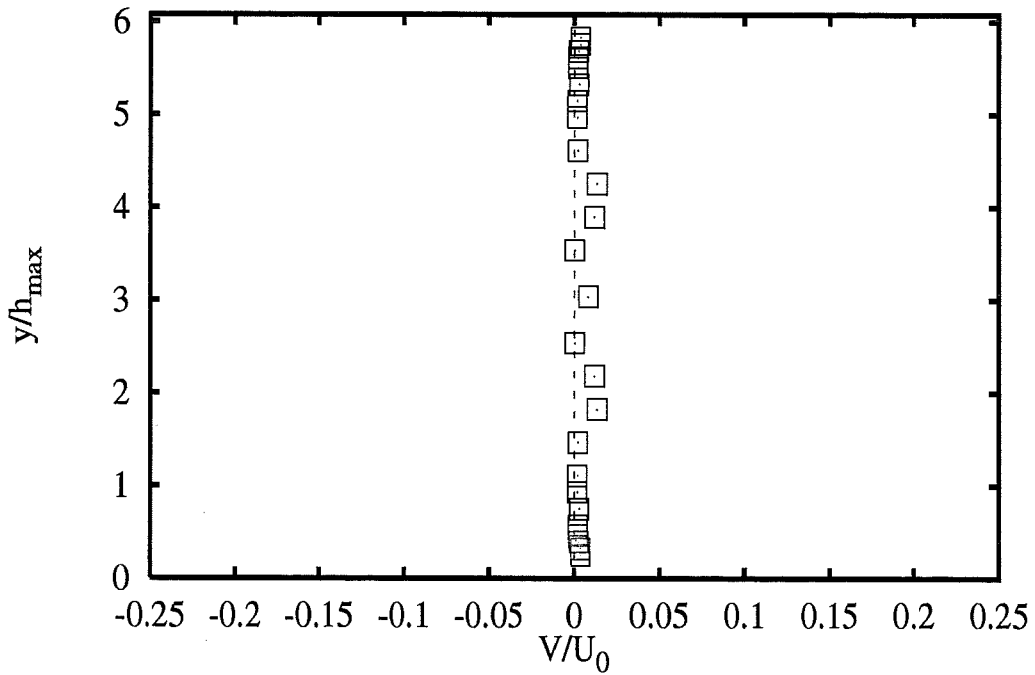
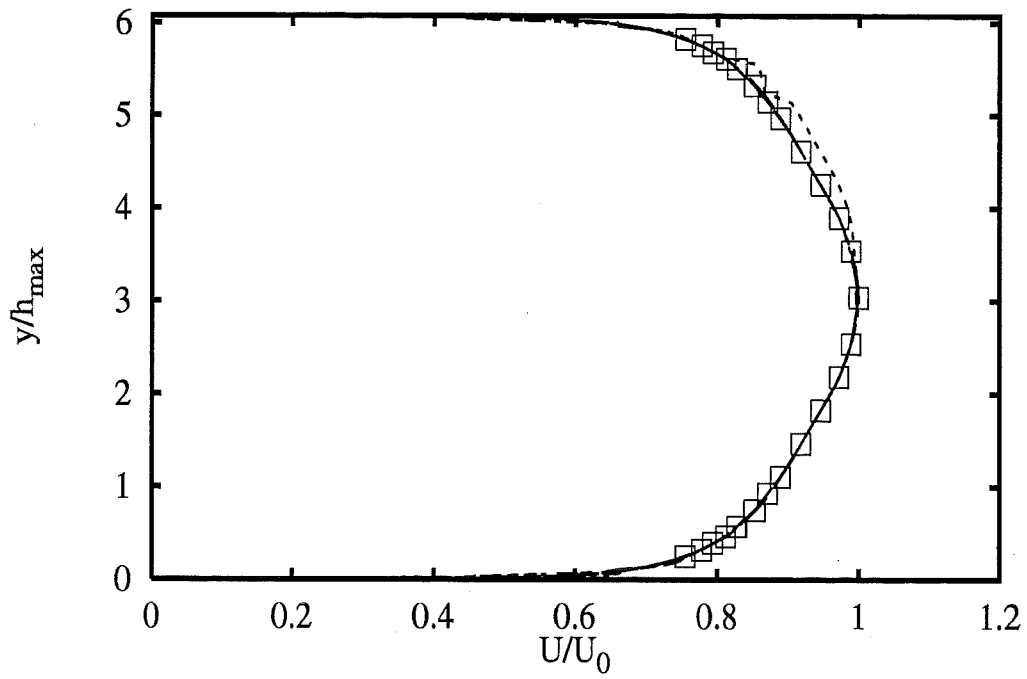


Profiles at $x/h_{max} = 6.61$

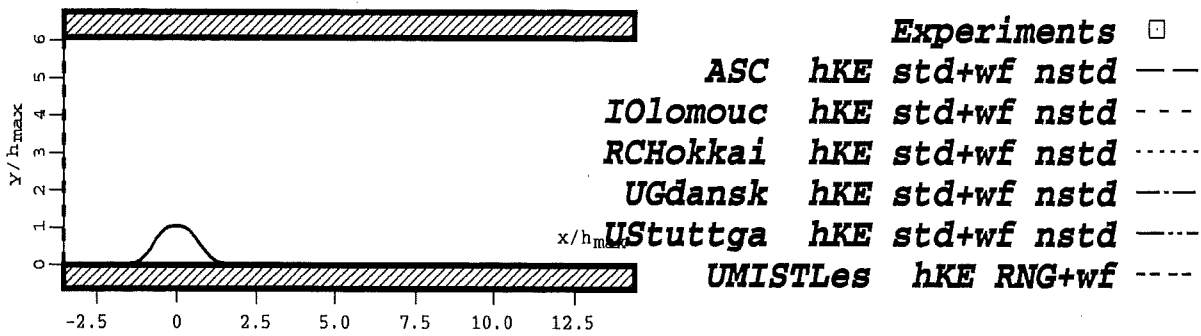


| | | Experiments | □ |
|-----------------|-------------------|-------------|---|
| <i>UChalmer</i> | <i>hKE std+wf</i> | --- | |
| <i>UDelftHa</i> | <i>hKE std+wf</i> | ---- | |
| <i>UDelftZi</i> | <i>hKE std+wf</i> | | |
| <i>UKarlsru</i> | <i>hKE std+wf</i> | ---- | |
| <i>UMISTLes</i> | <i>hKE std+wf</i> | ----- | |
| <i>UPorto</i> | <i>hKE std+wf</i> | ----- | |

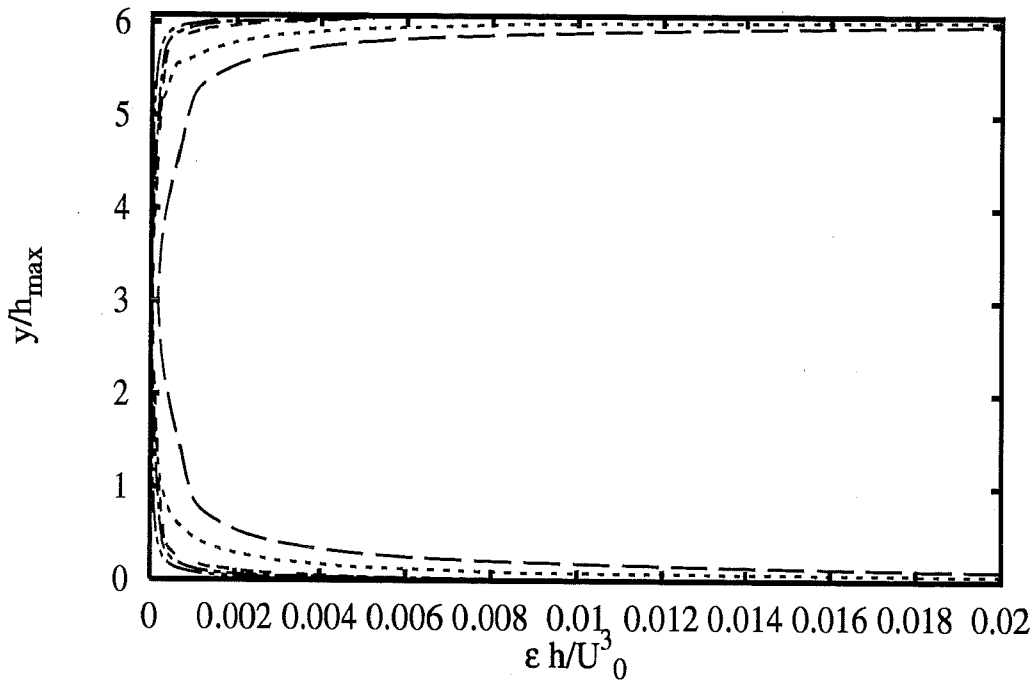
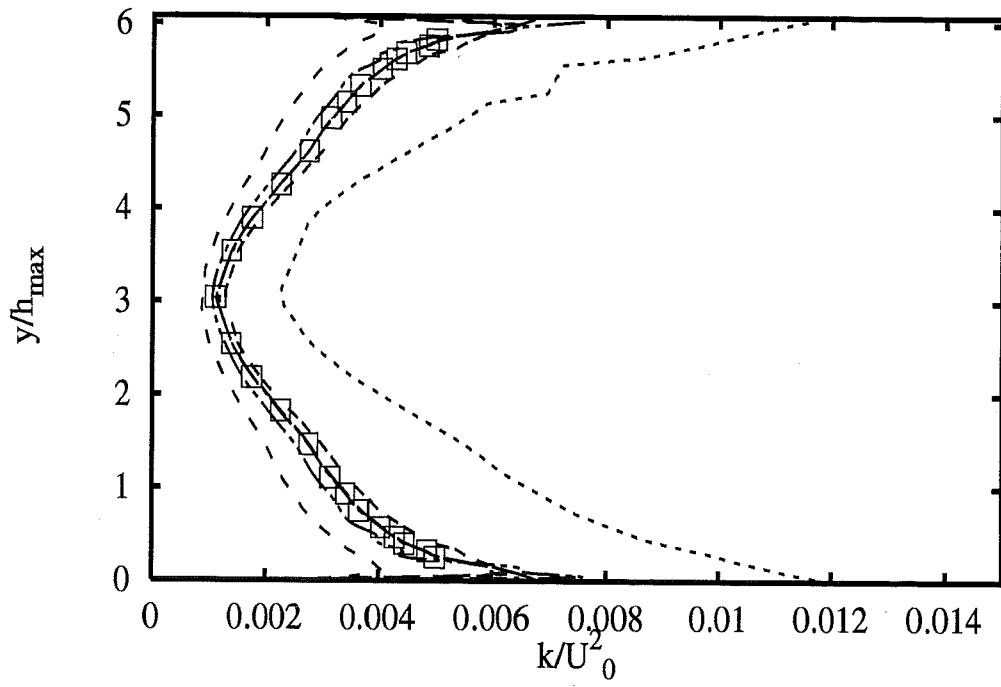




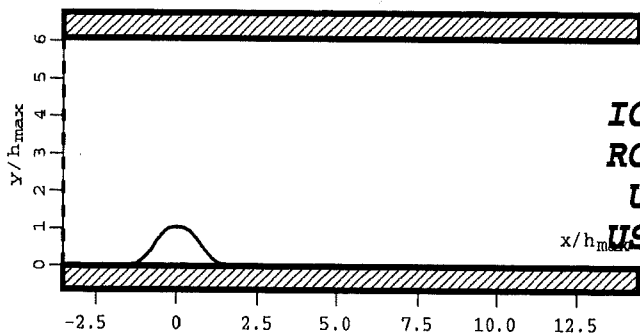
Profiles at $x/h_{max} = -3.57$



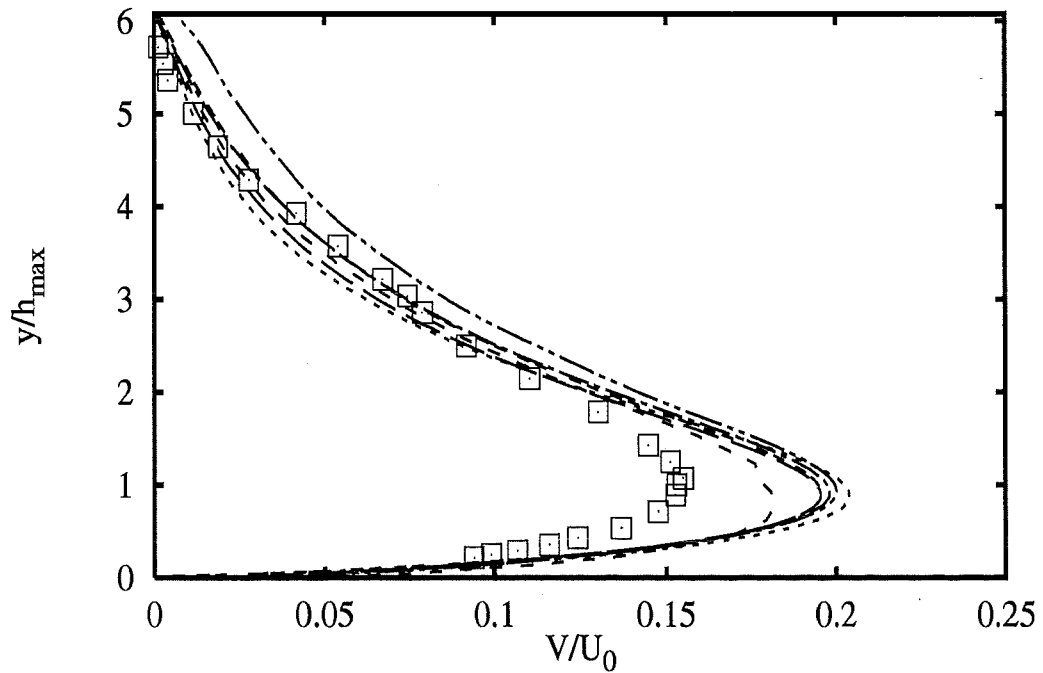
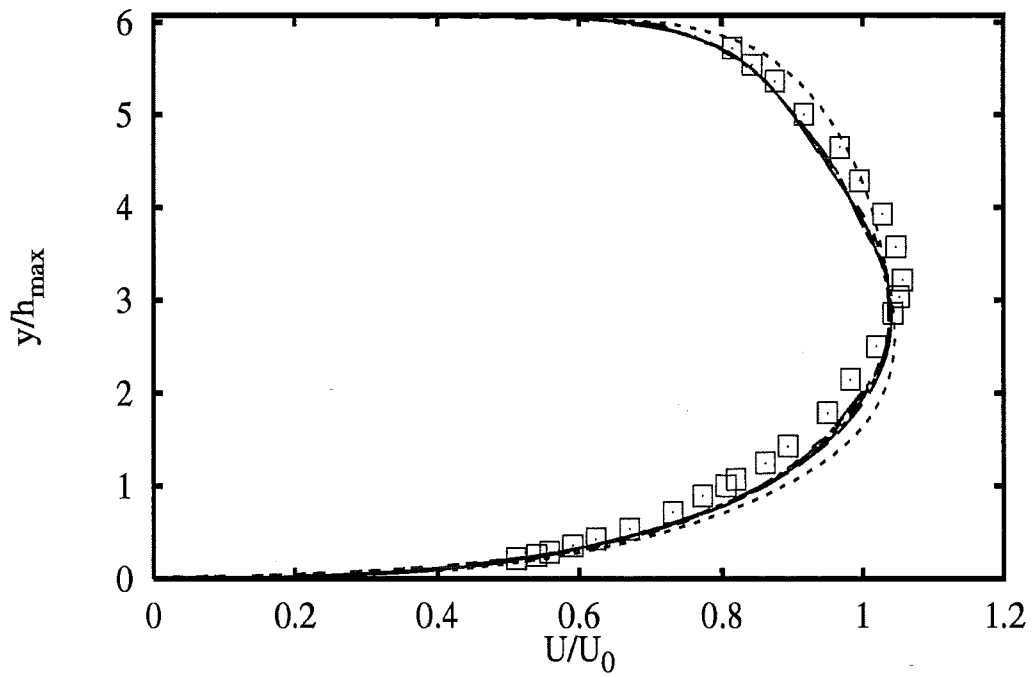
2A - 23



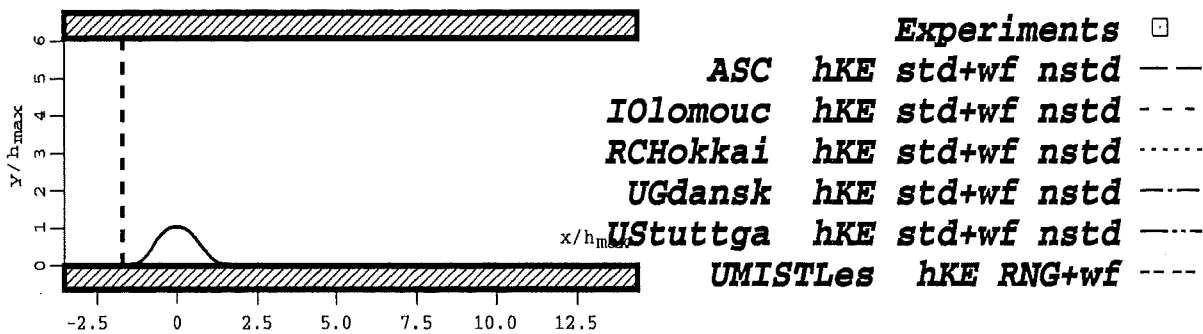
Profiles at $x/h_{max} = -3.57$



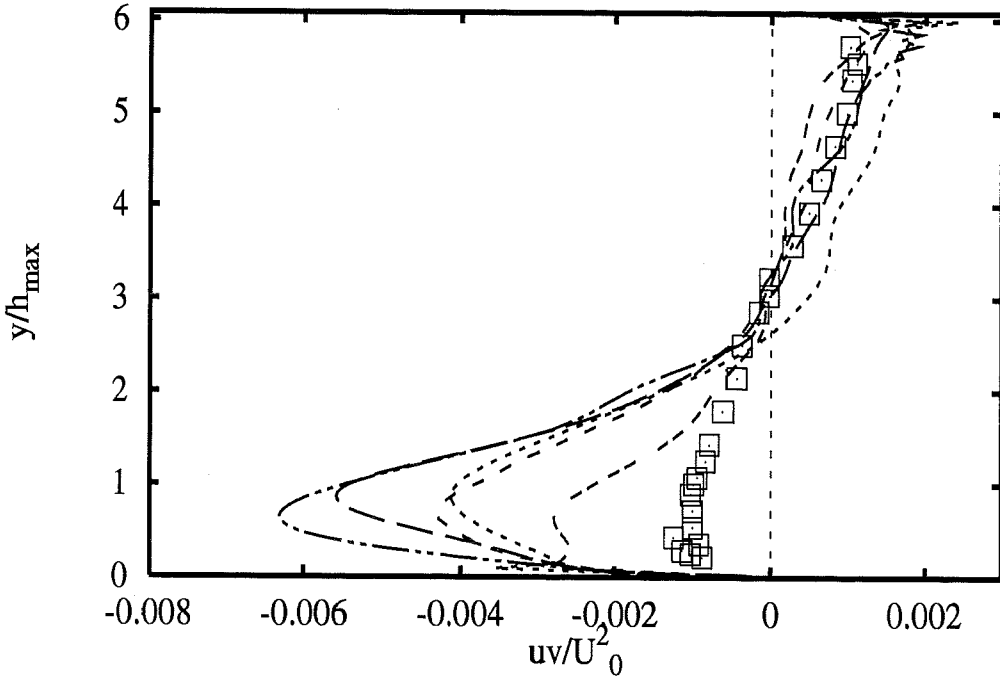
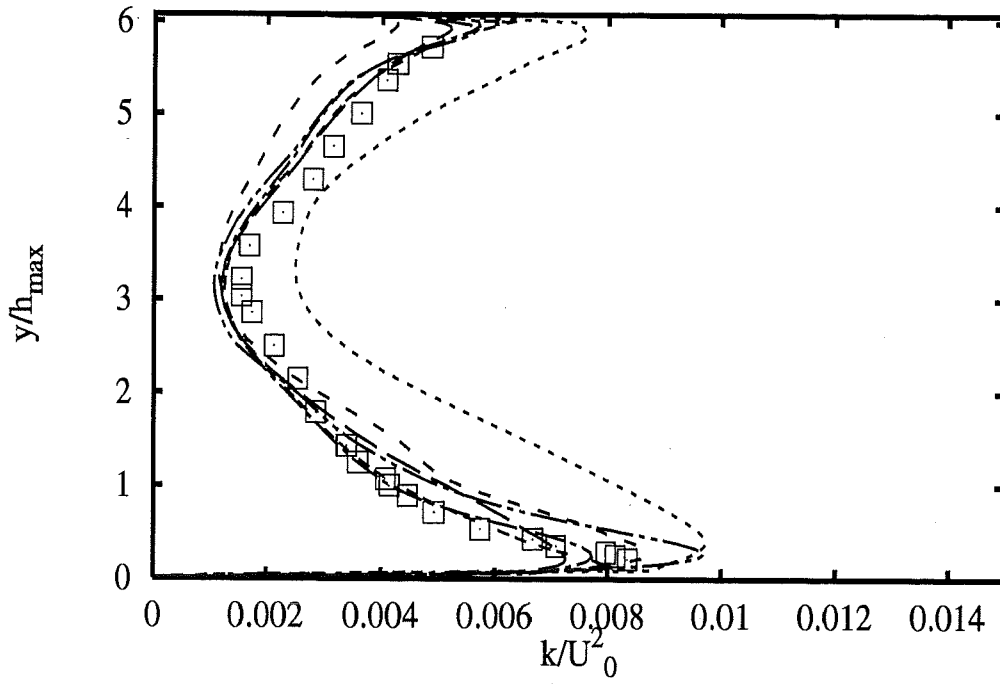
| | | | |
|----------|-----------------|--------------------|---|
| | | Experiments | □ |
| ASC | hKE std+wf nstd | --- | |
| IOlomouc | hKE std+wf nstd | --- | |
| RCHokkai | hKE std+wf nstd | --- | |
| UGdansk | hKE std+wf nstd | --- | |
| USTuttga | hKE std+wf nstd | --- | |
| UMISTLes | hKE RNG+wf | --- | |



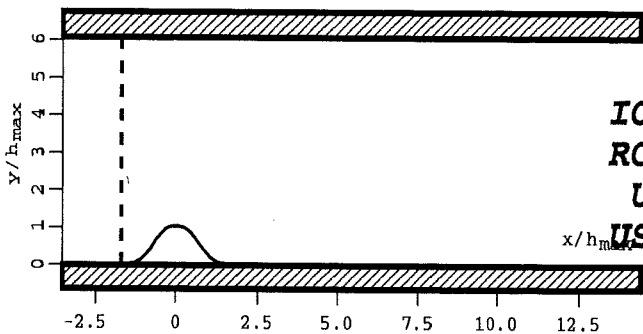
Profiles at $x/h_{max} = -1.78$



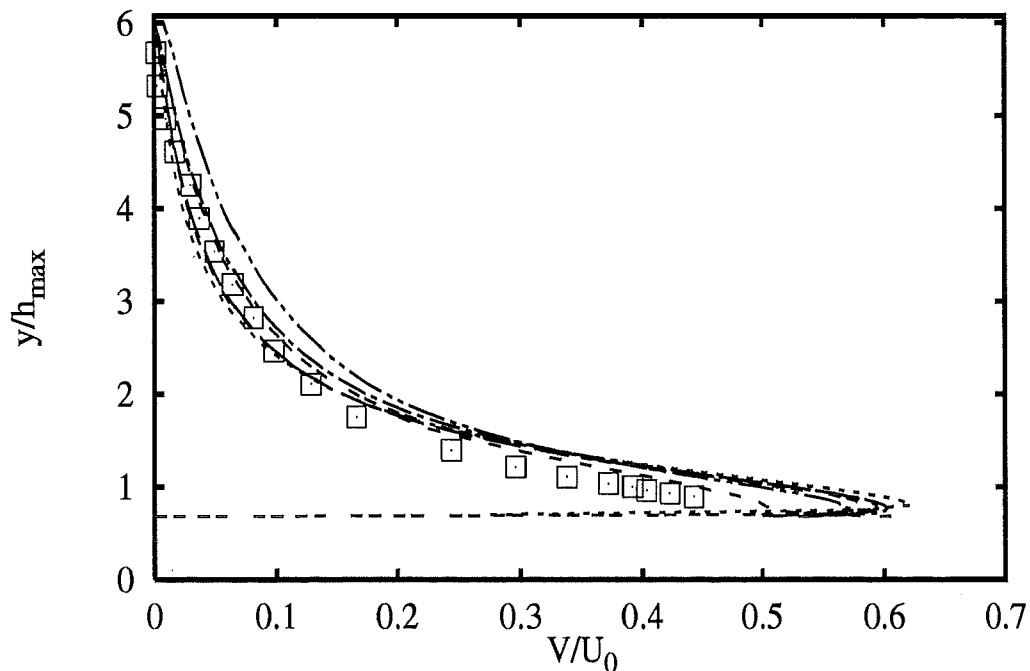
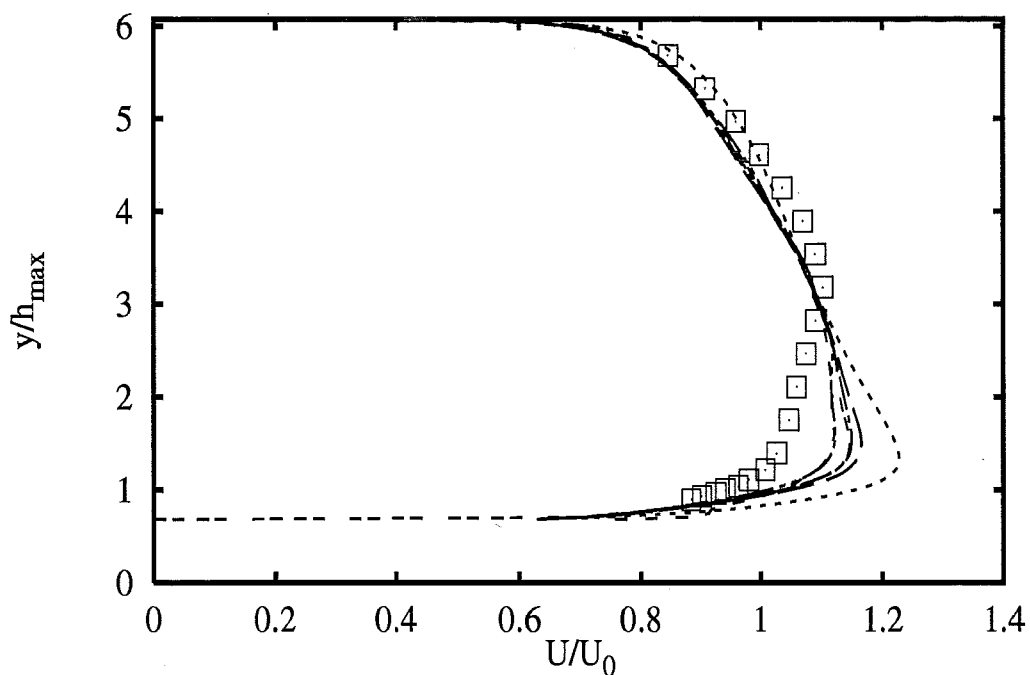
2A - 25



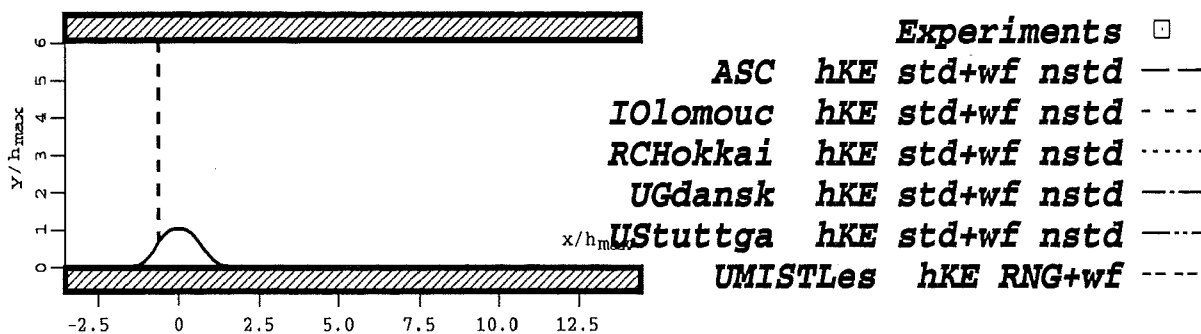
Profiles at $x/h_{max} = -1.78$



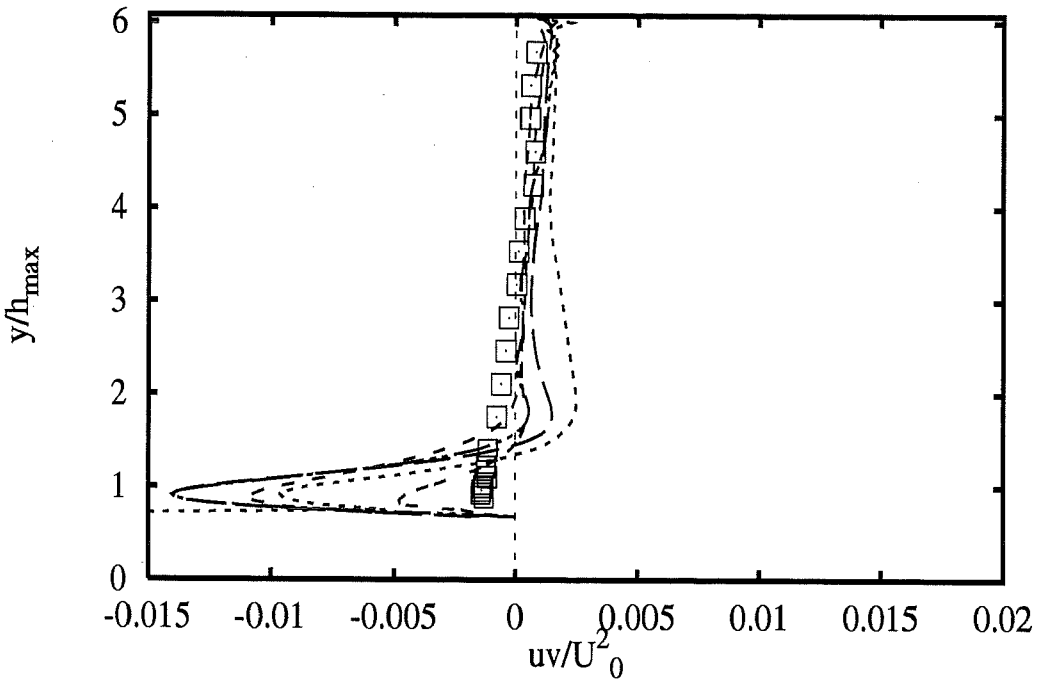
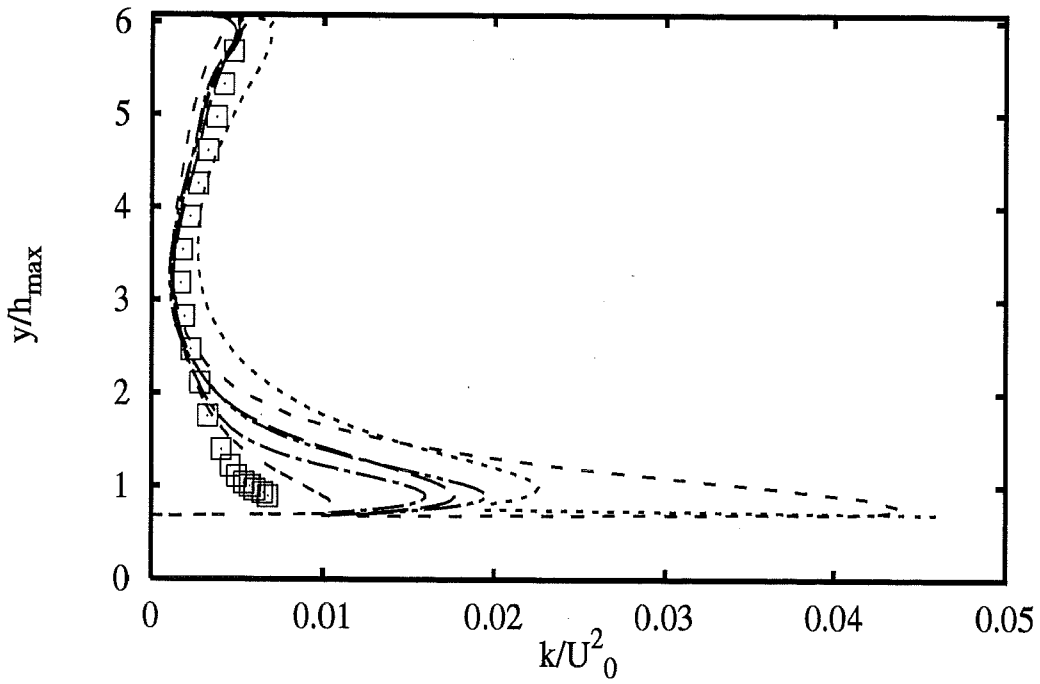
| | | |
|----------|------------------------|-----|
| | Experiments | □ |
| ASC | <i>hKE std+wf nstd</i> | --- |
| IOlomouc | <i>hKE std+wf nstd</i> | --- |
| RCHokkai | <i>hKE std+wf nstd</i> | --- |
| UGdansk | <i>hKE std+wf nstd</i> | --- |
| UStuttga | <i>hKE std+wf nstd</i> | --- |
| UMISTLes | <i>hKE RNG+wf</i> | --- |



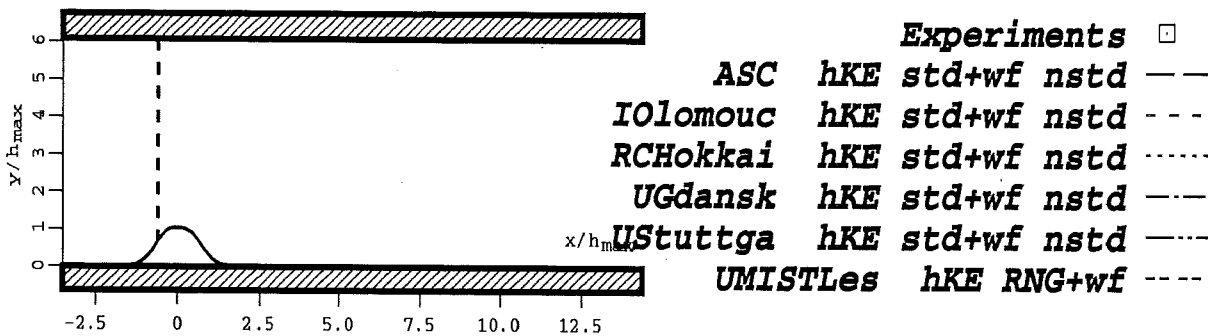
Profiles at $x/h_{max} = -0.71$

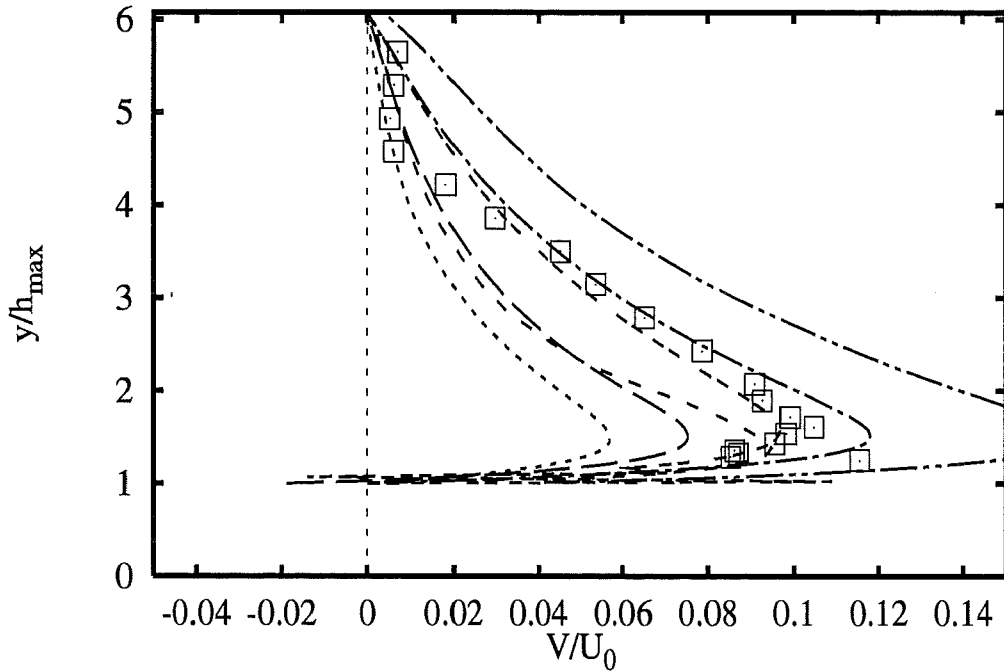
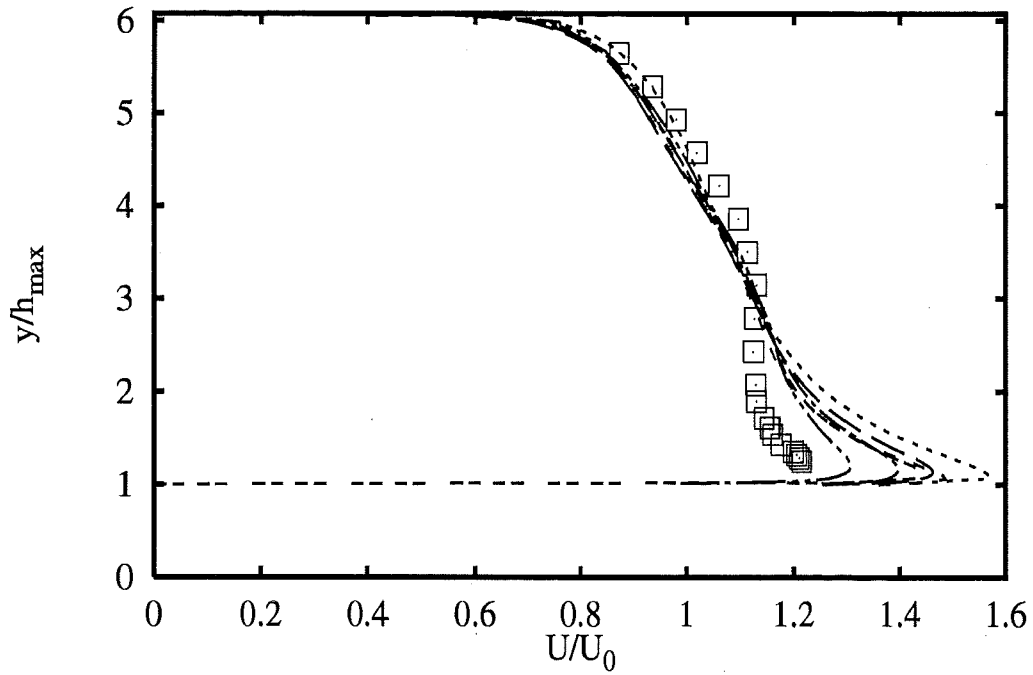


2A - 27

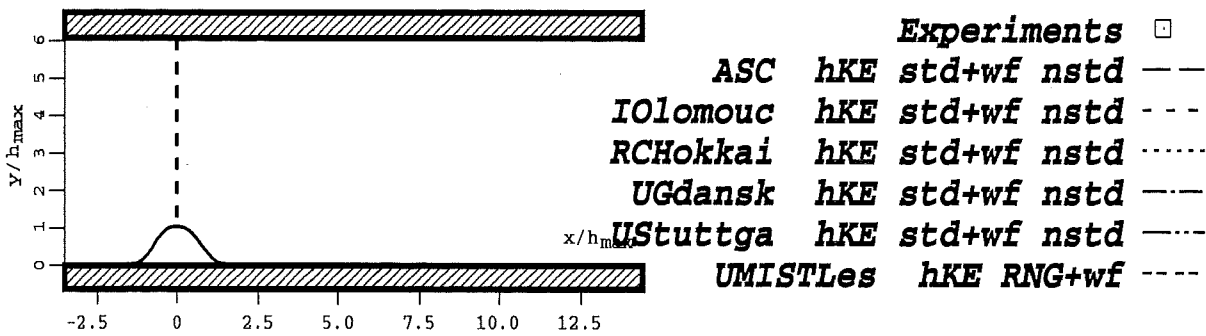


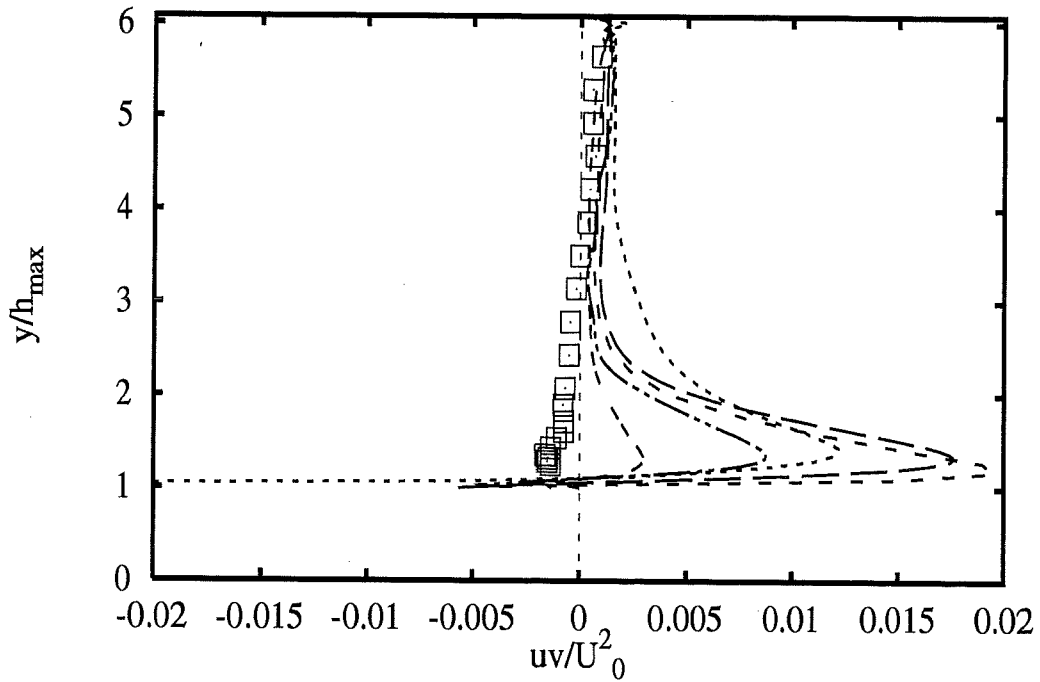
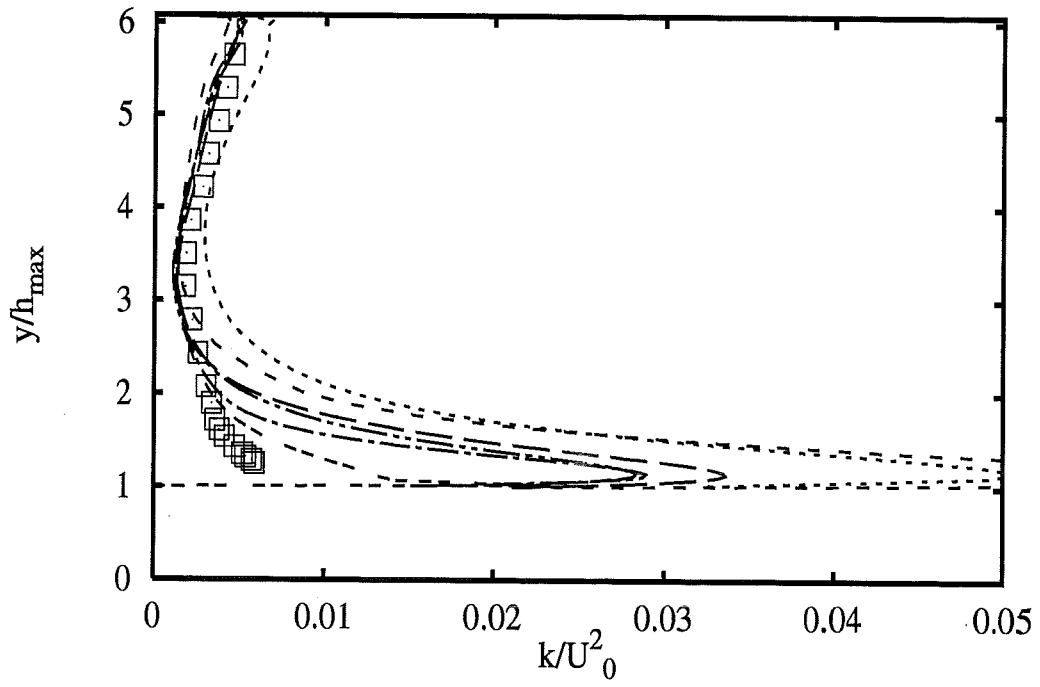
Profiles at $x/h_{max} = -0.71$



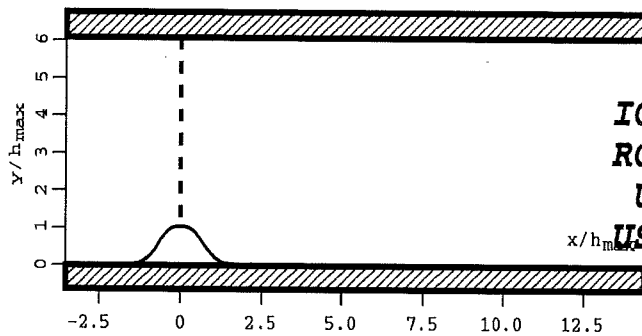


Profiles at $x/h_{max} = 0$



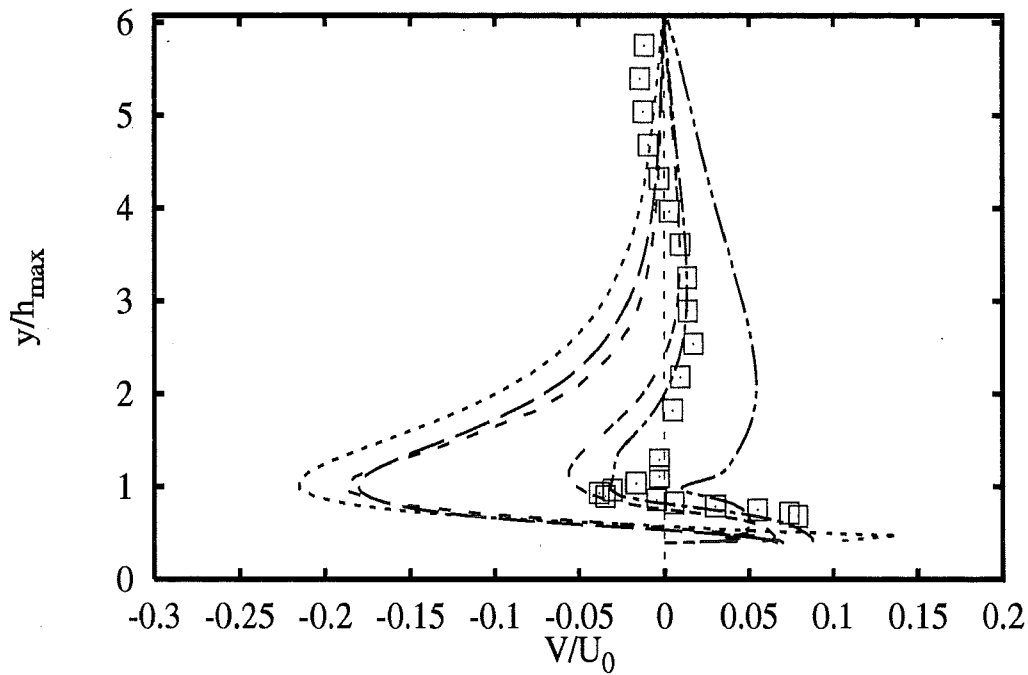
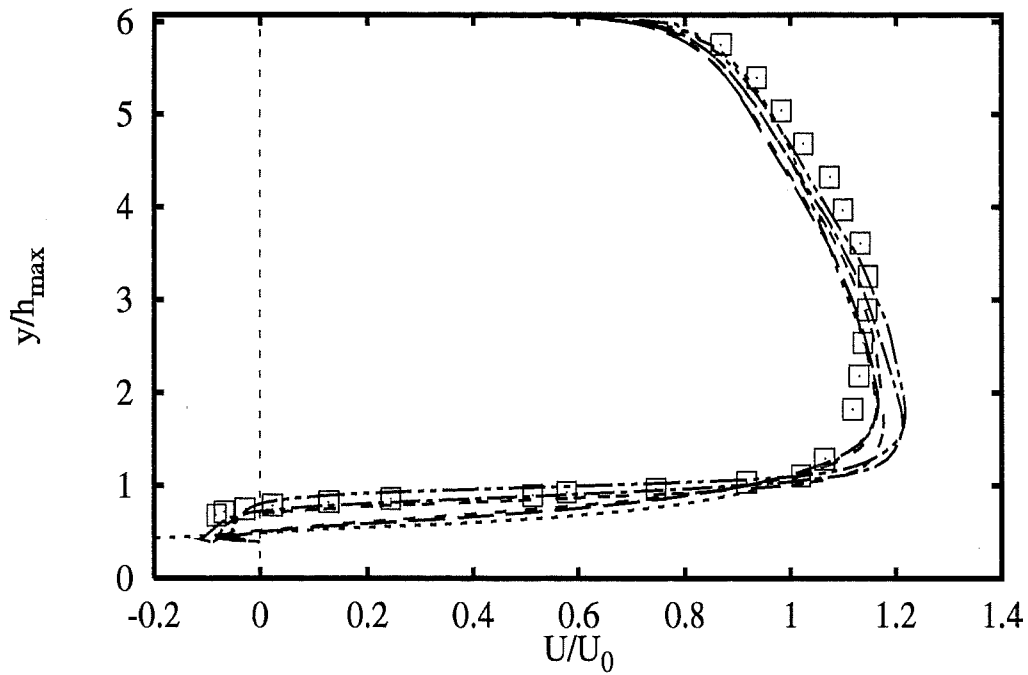


Profiles at $x/h_{max} = 0$

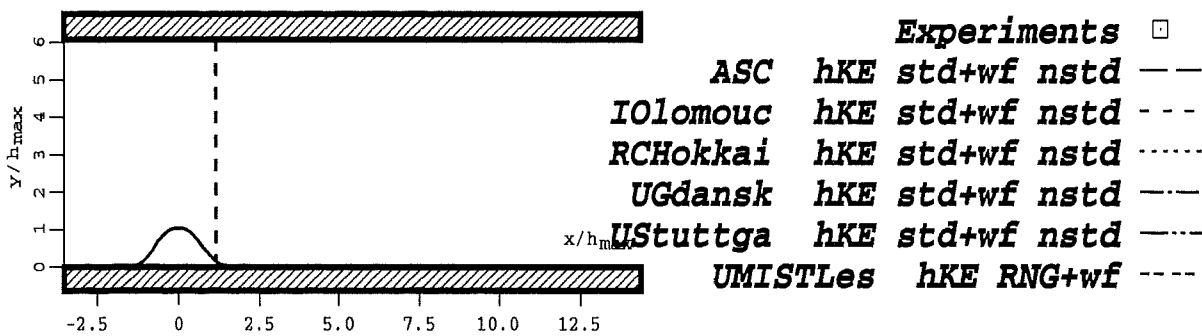


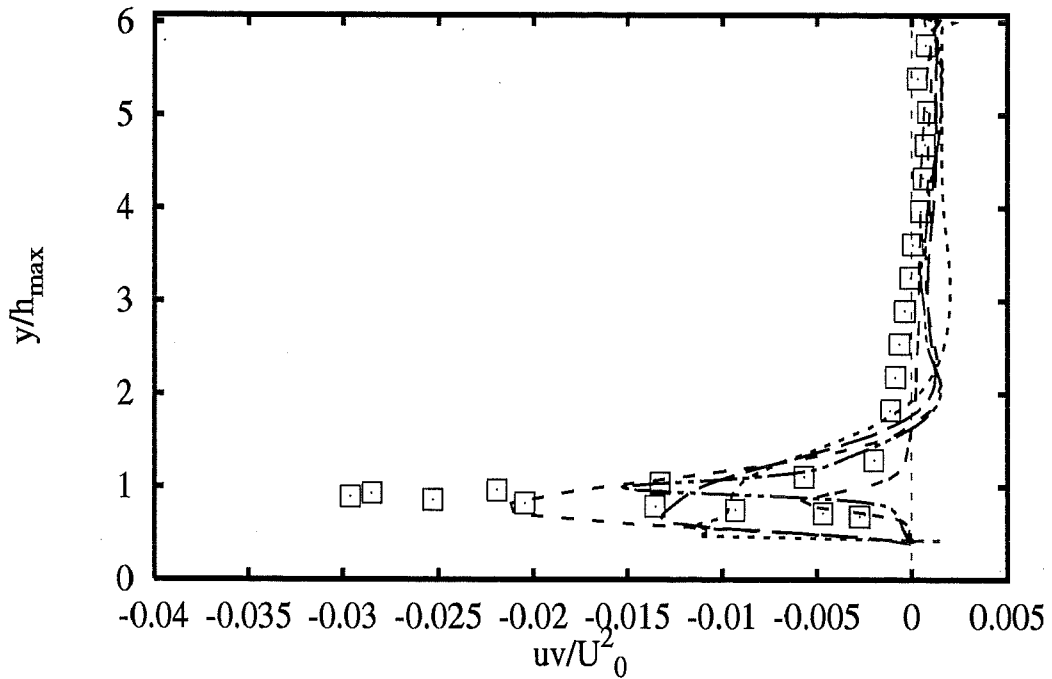
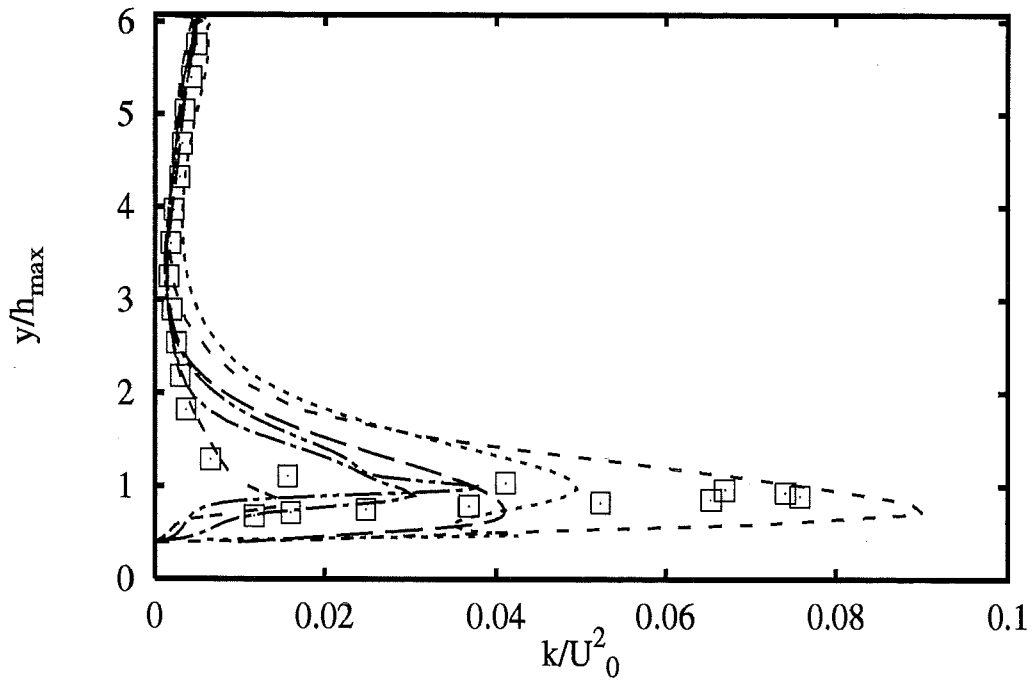
| | | |
|----------|------------------------|-------|
| | Experiments | □ |
| ASC | <i>hKE std+wf nstd</i> | --- |
| Iolomouc | <i>hKE std+wf nstd</i> | --- |
| RCHokkai | <i>hKE std+wf nstd</i> | |
| UGdansk | <i>hKE std+wf nstd</i> | --- |
| UStuttga | <i>hKE std+wf nstd</i> | --- |
| UMISTLes | <i>hKE RNG+wf</i> | --- |

2A - 30

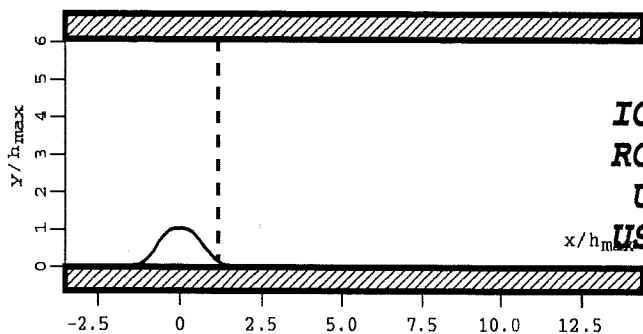


Profiles at $x/h_{max} = 1.07$

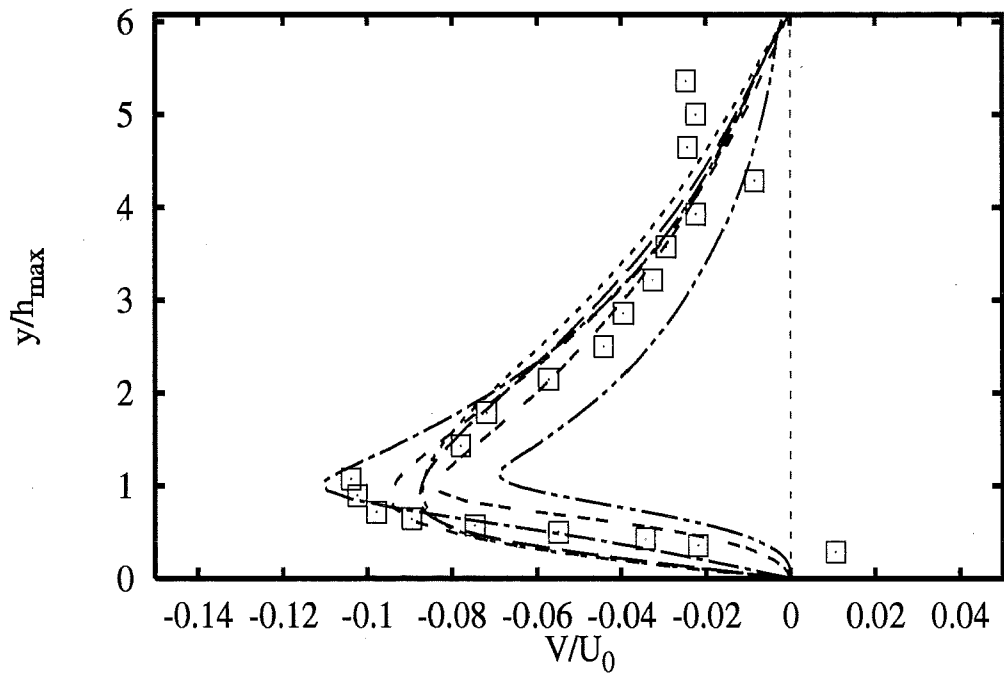
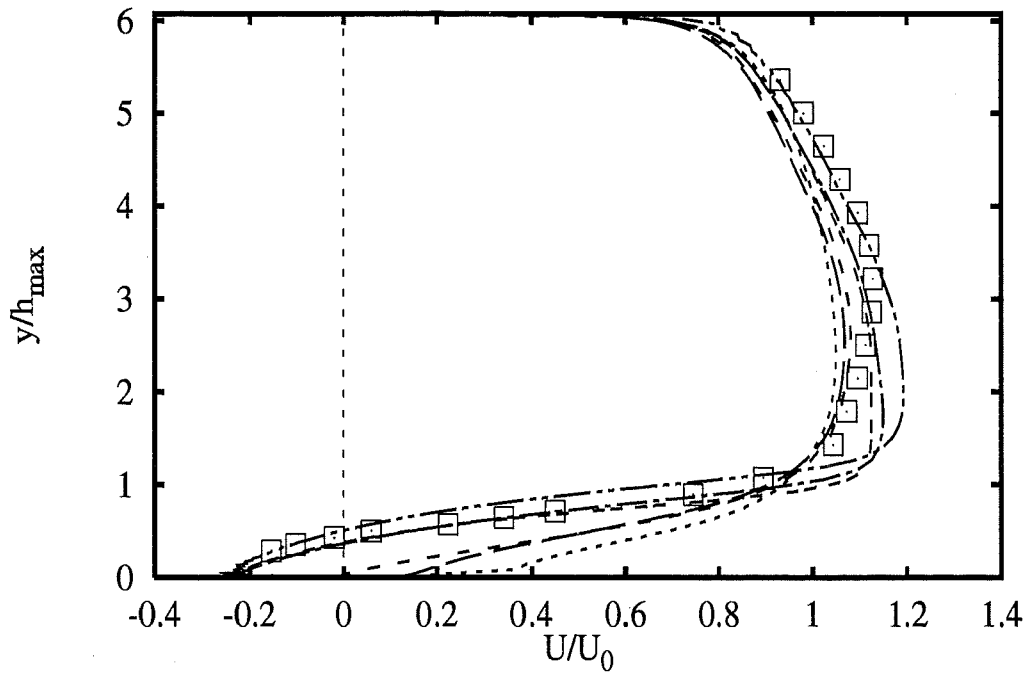




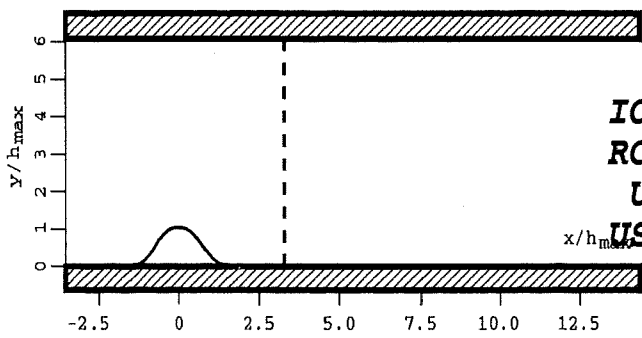
Profiles at $x/h_{max} = 1.07$



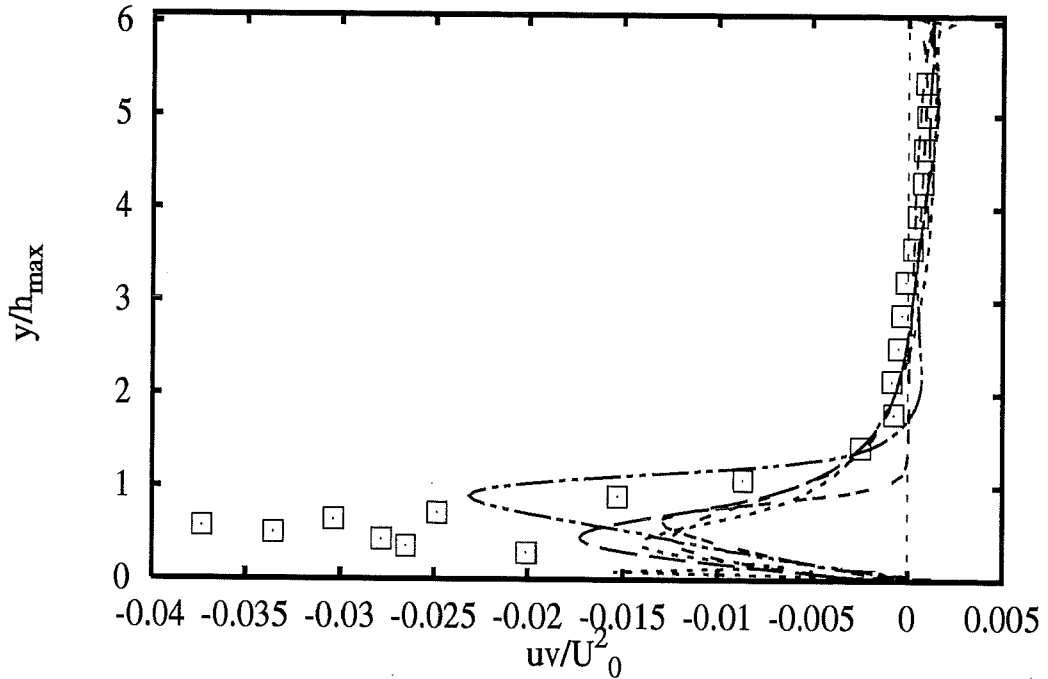
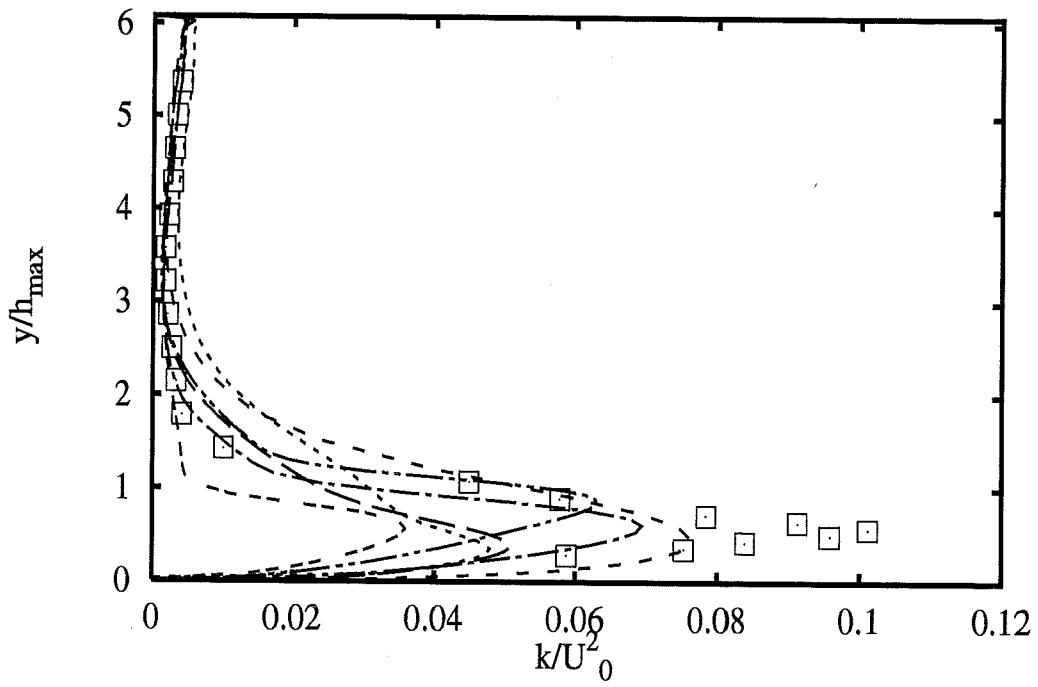
| | | |
|----------|------------------------|-----|
| | Experiments | □ |
| ASC | <i>hKE std+wf nstd</i> | --- |
| IOlomouc | <i>hKE std+wf nstd</i> | --- |
| RCHokkai | <i>hKE std+wf nstd</i> | --- |
| UGdansk | <i>hKE std+wf nstd</i> | --- |
| UStuttga | <i>hKE std+wf nstd</i> | --- |
| UMISTLes | <i>hKE RNG+wf</i> | --- |



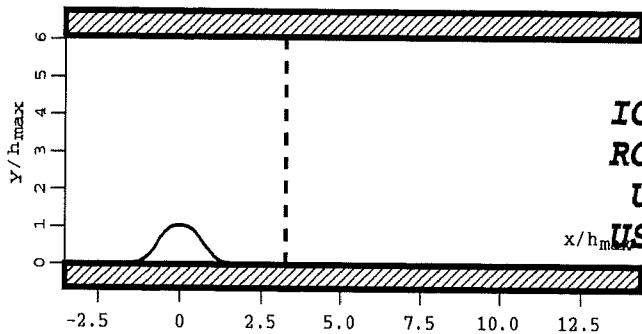
Profiles at $x/h_{max} = 3.21$



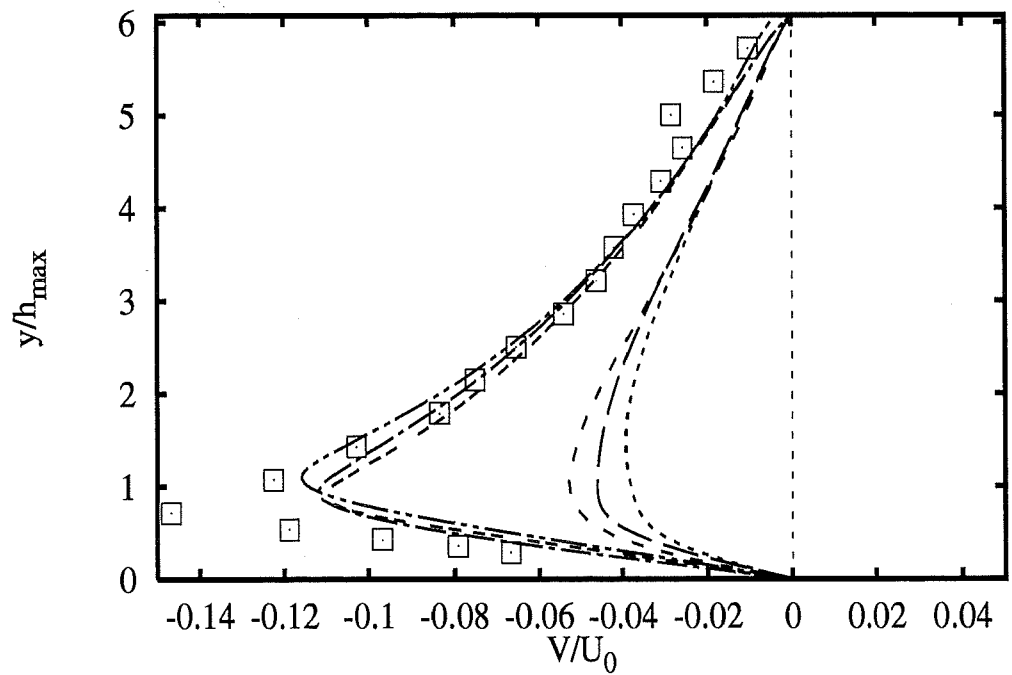
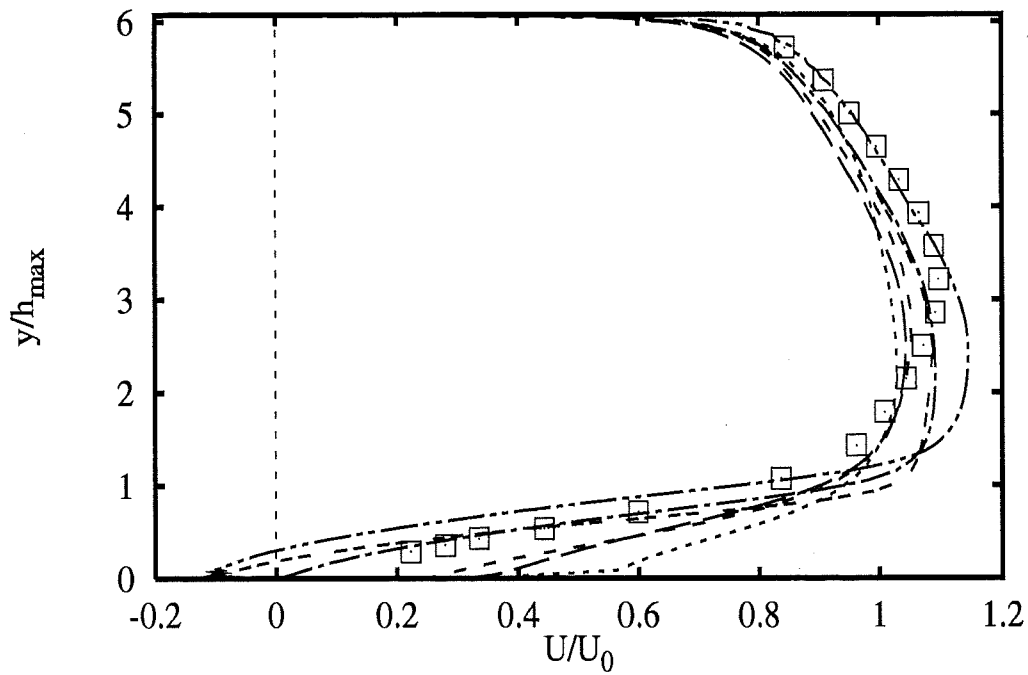
| | | |
|----------|------------------------|---------|
| | Experiments | □ |
| ASC | <i>hKE std+wf nstd</i> | — — |
| IOlomouc | <i>hKE std+wf nstd</i> | - - - |
| RCHokkai | <i>hKE std+wf nstd</i> | |
| UGdansk | <i>hKE std+wf nstd</i> | — · — |
| UStuttga | <i>hKE std+wf nstd</i> | — · · — |
| UMISTLes | <i>hKE RNG+wf</i> | - - - |



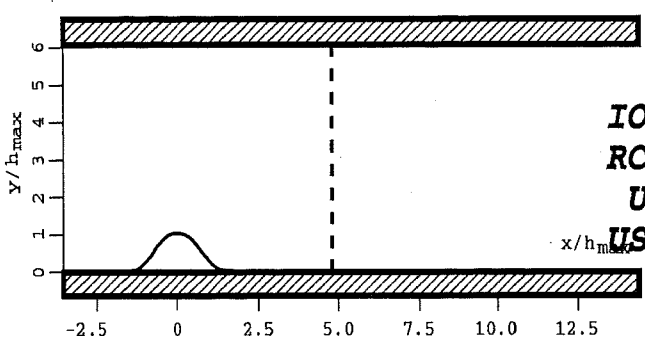
Profiles at $x/h_{max} = 3.21$



| | | |
|----------|------------------------|---------|
| | Experiments | □ |
| ASC | <i>hKE std+wf nstd</i> | — — |
| Iolomouc | <i>hKE std+wf nstd</i> | - - - |
| RCHokkai | <i>hKE std+wf nstd</i> | ⋯⋯⋯ |
| UGdansk | <i>hKE std+wf nstd</i> | — · — · |
| UStuttga | <i>hKE std+wf nstd</i> | — · — · |
| UMISTLes | <i>hKE RNG+wf</i> | - - - |

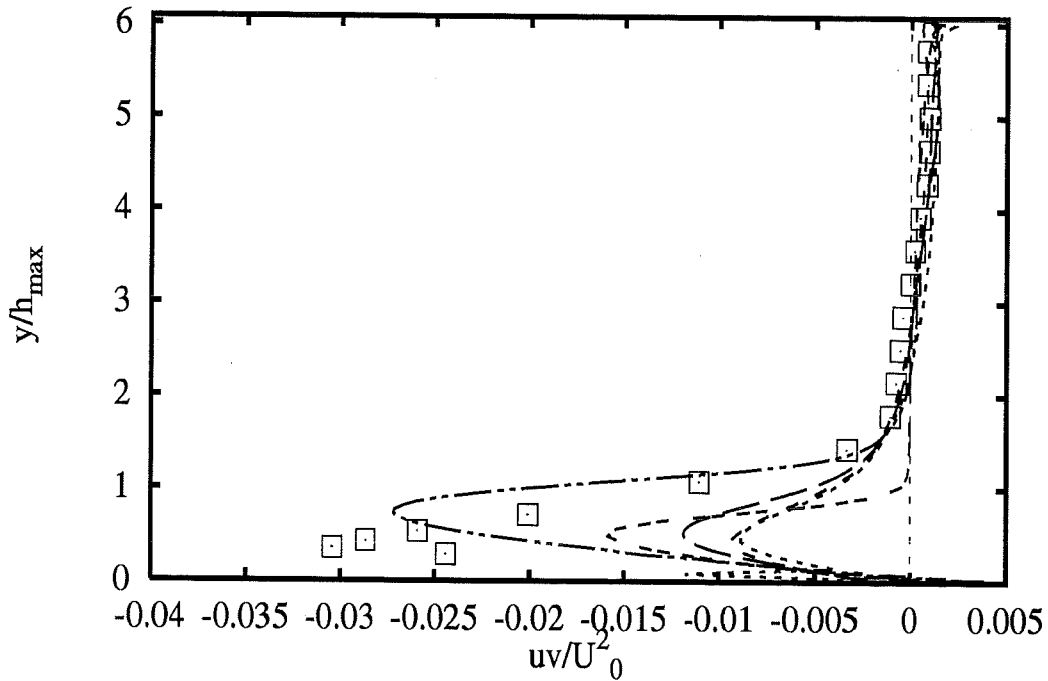
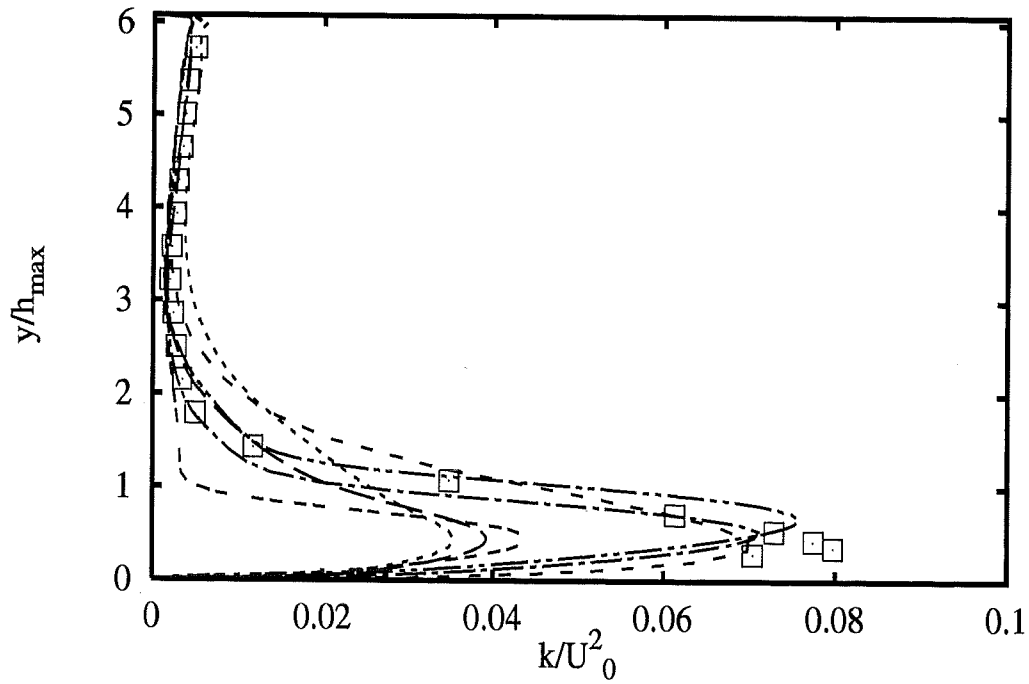


Profiles at $x/h_{max} = 4.79$

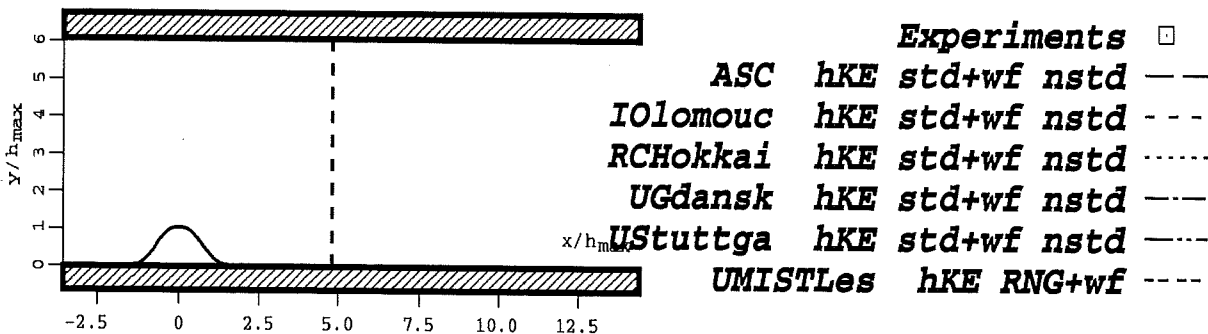


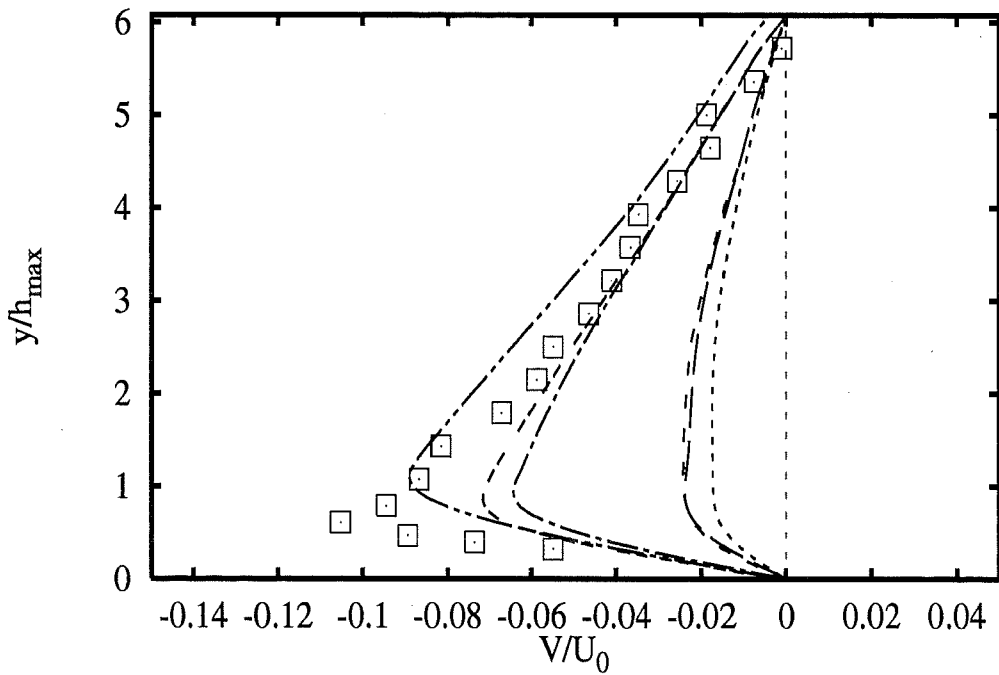
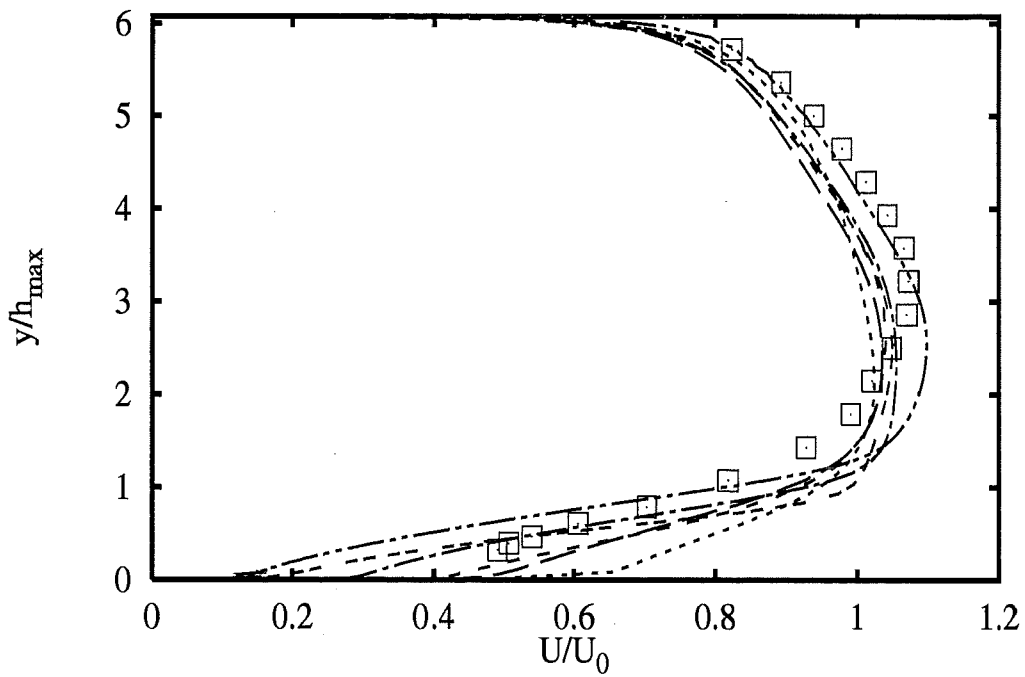
| | | | |
|----------|------------------------|--------------------|---|
| | | Experiments | □ |
| ASC | <i>hKE std+wf nstd</i> | — — | |
| Iolomouc | <i>hKE std+wf nstd</i> | - - - | |
| RCHokkai | <i>hKE std+wf nstd</i> | ⋯⋯⋯ | |
| UGdansk | <i>hKE std+wf nstd</i> | — — | |
| UStuttga | <i>hKE std+wf nstd</i> | - · - · - | |
| UMISTLes | <i>hKE RNG+wf</i> | - - - | |

2A - 35

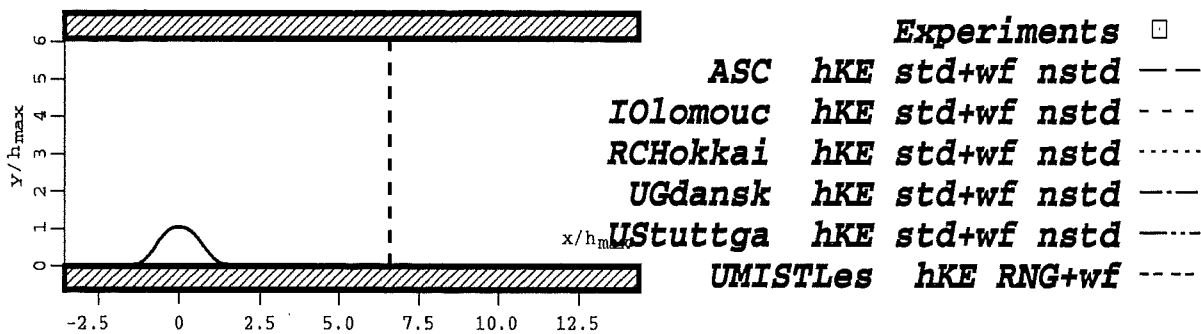


Profiles at $x/h_{max} = 4.79$

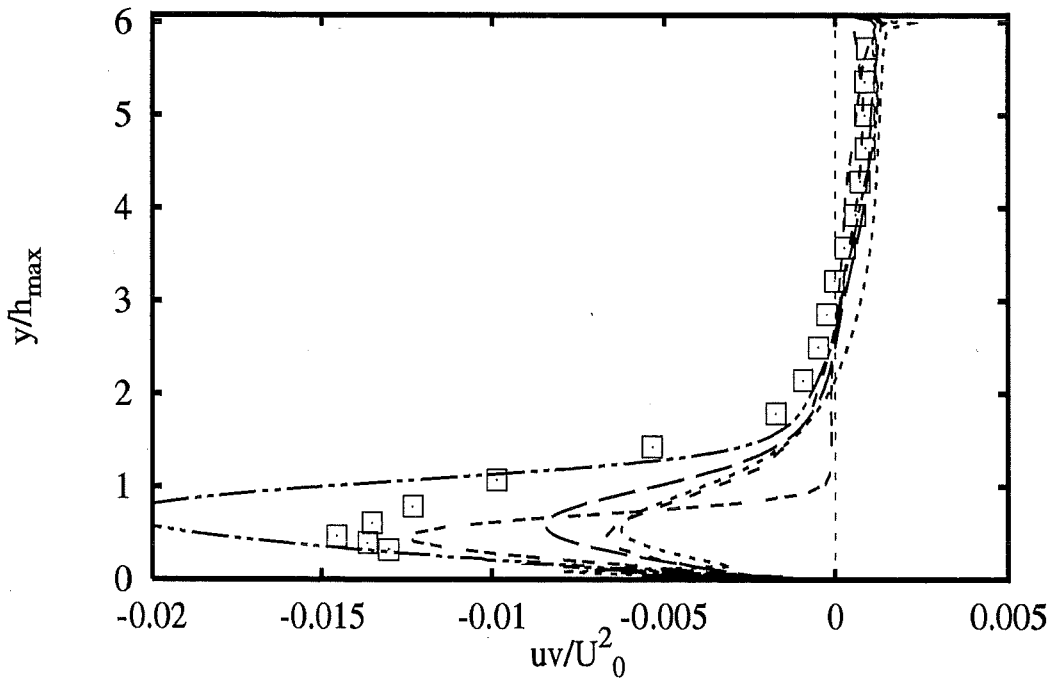
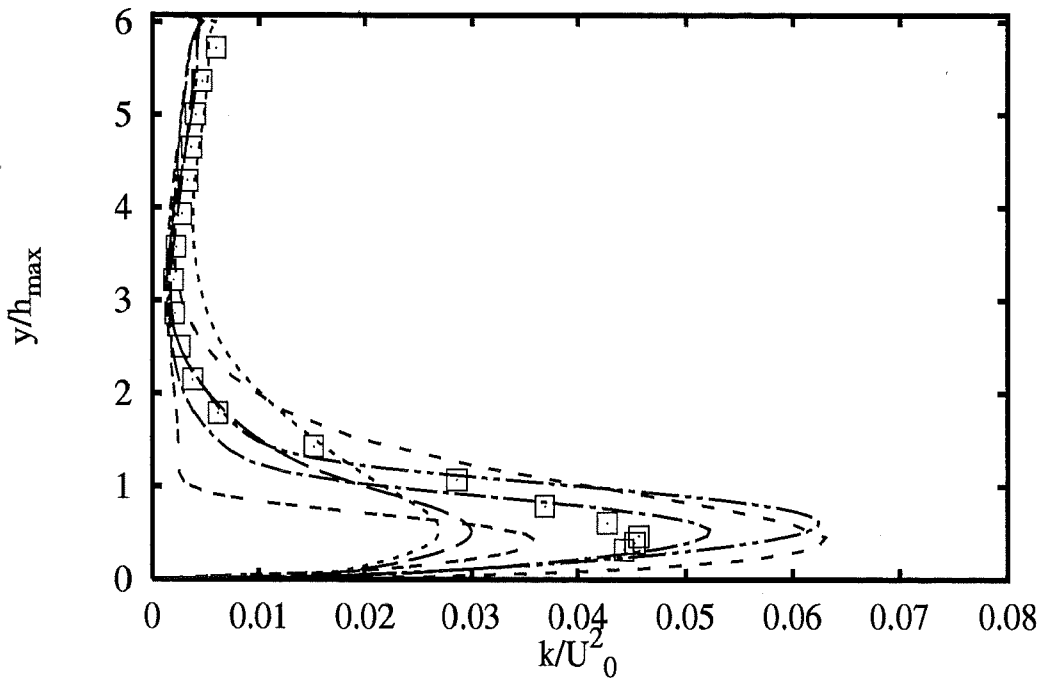




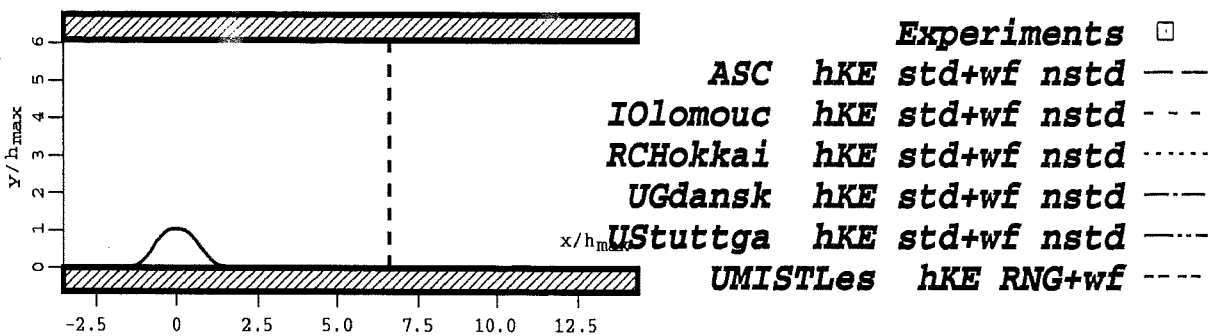
Profiles at $x/h_{max} = 6.61$



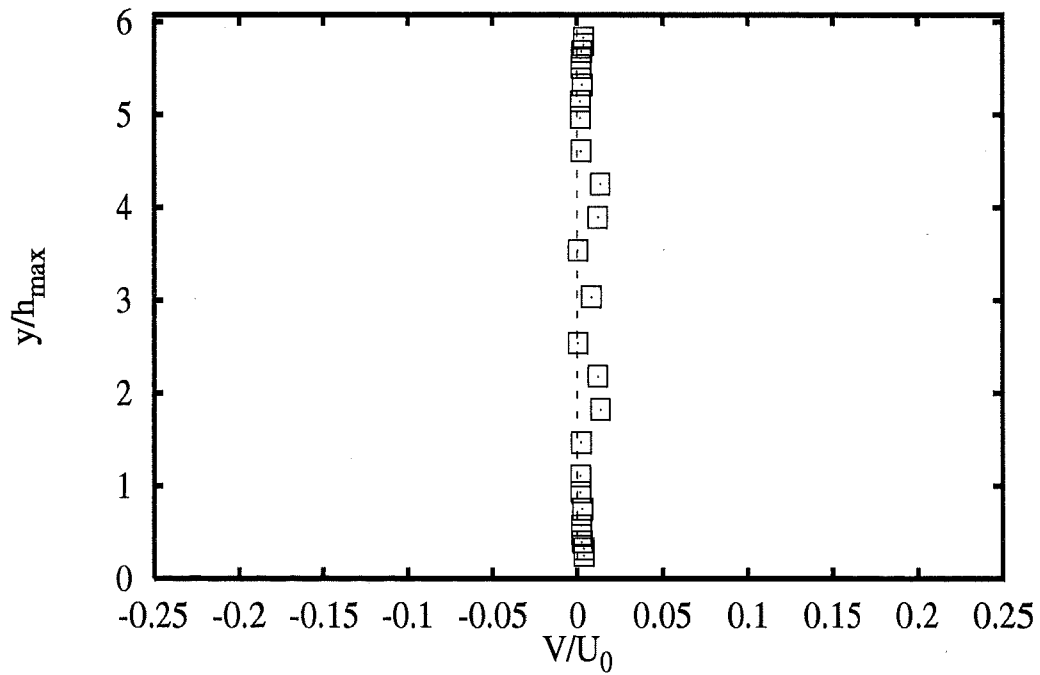
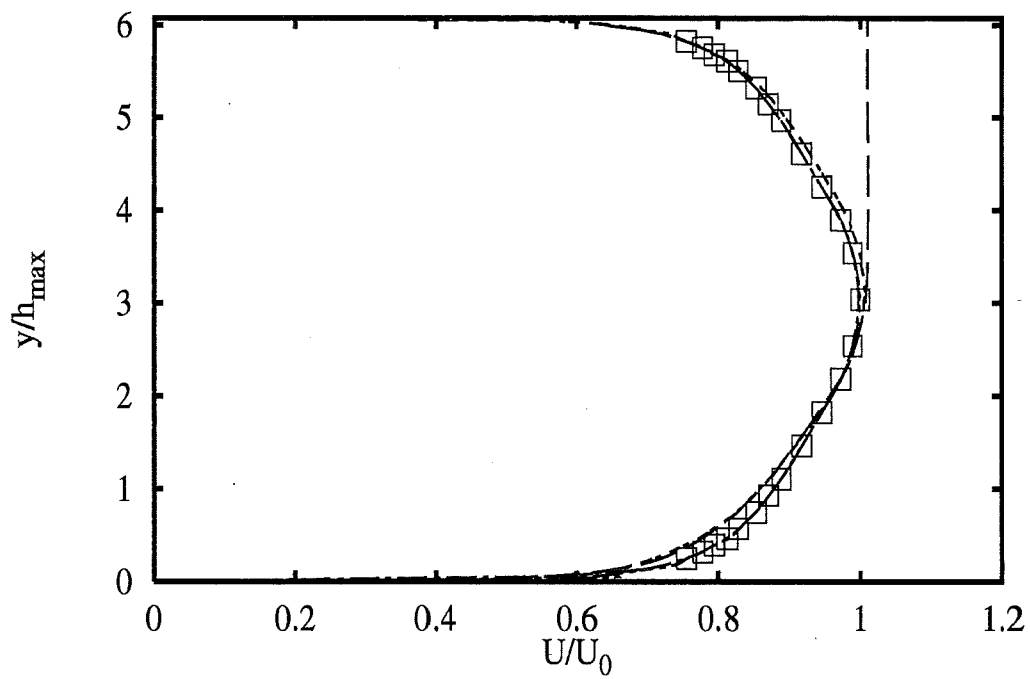
2A - 37



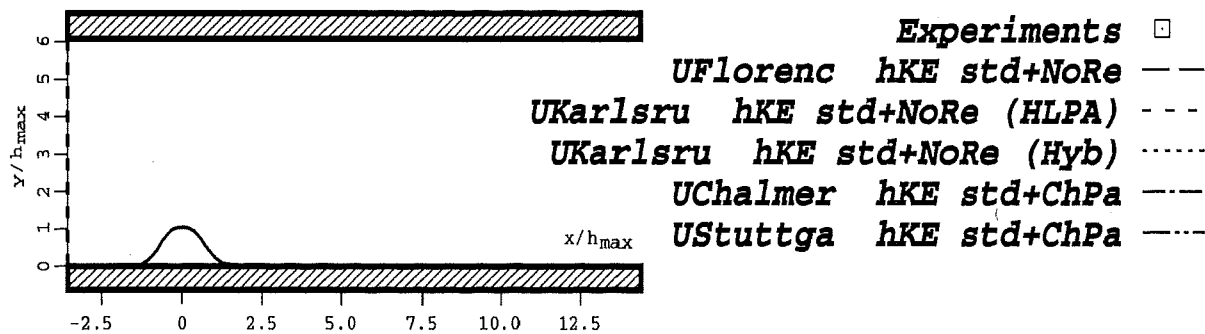
Profiles at $x/h_{max} = 6.61$



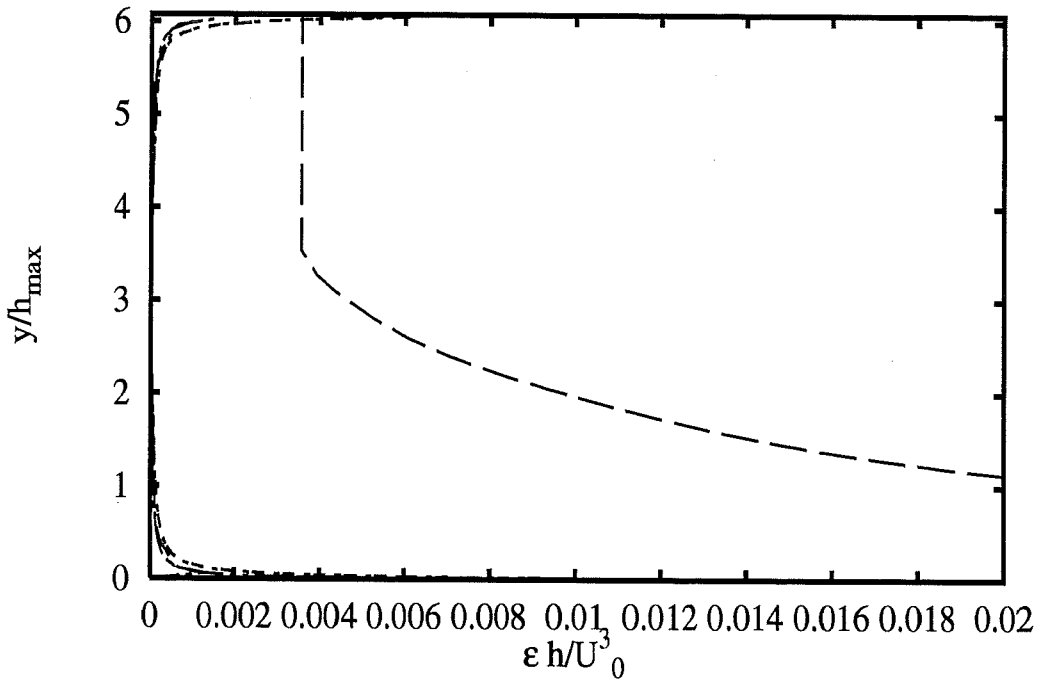
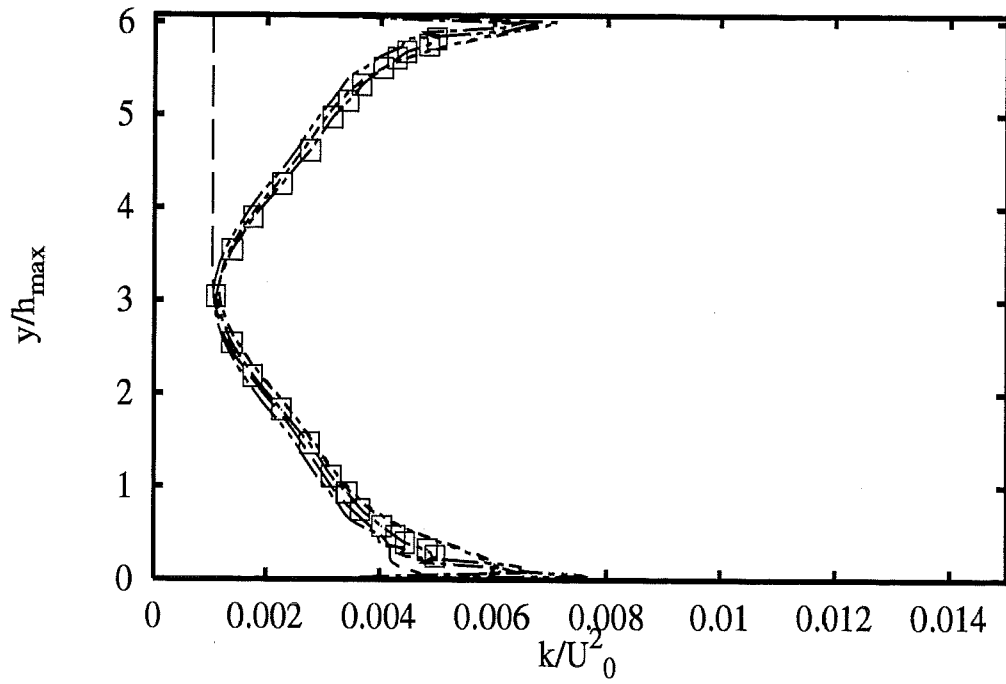




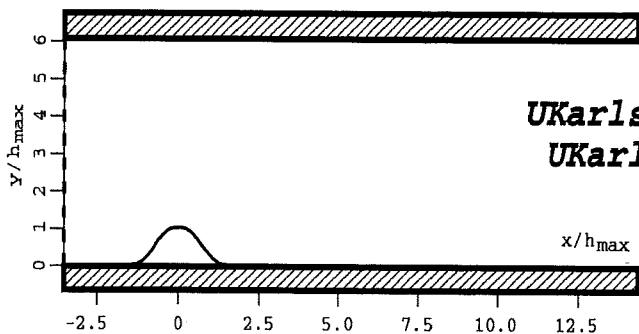
Profiles at $x/h_{max} = -3.57$



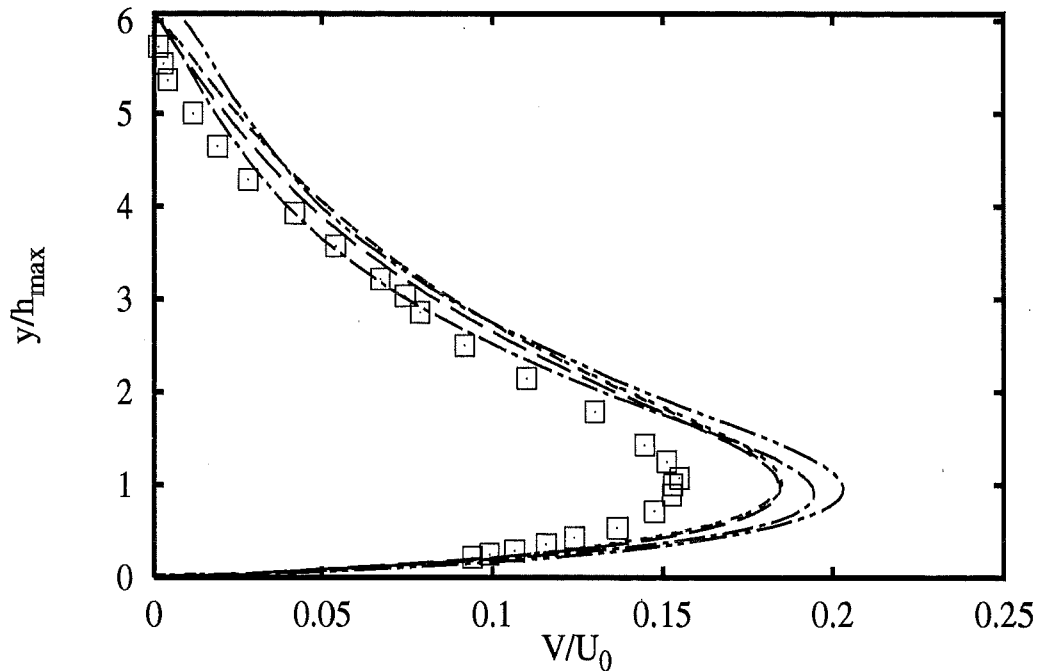
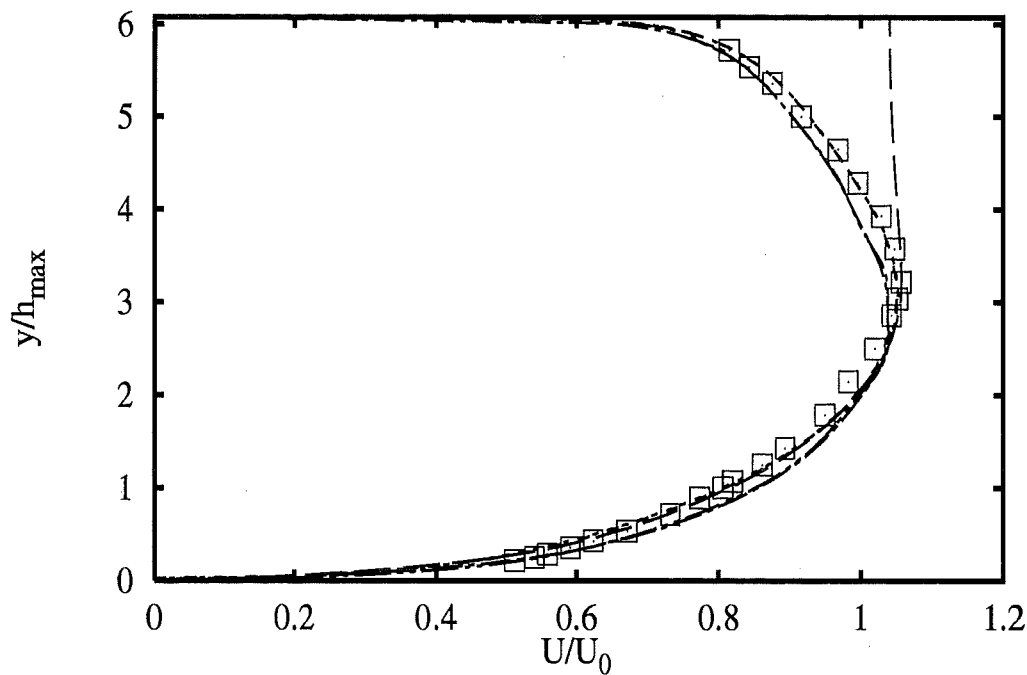
2A - 39



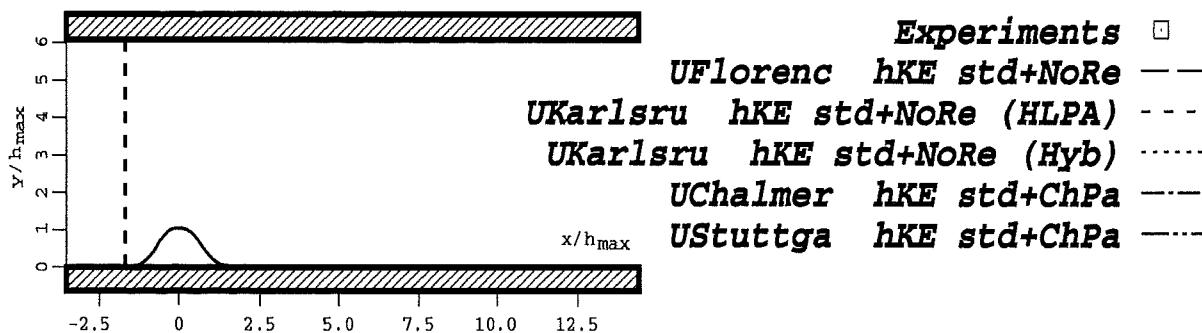
Profiles at $x/h_{max} = -3.57$



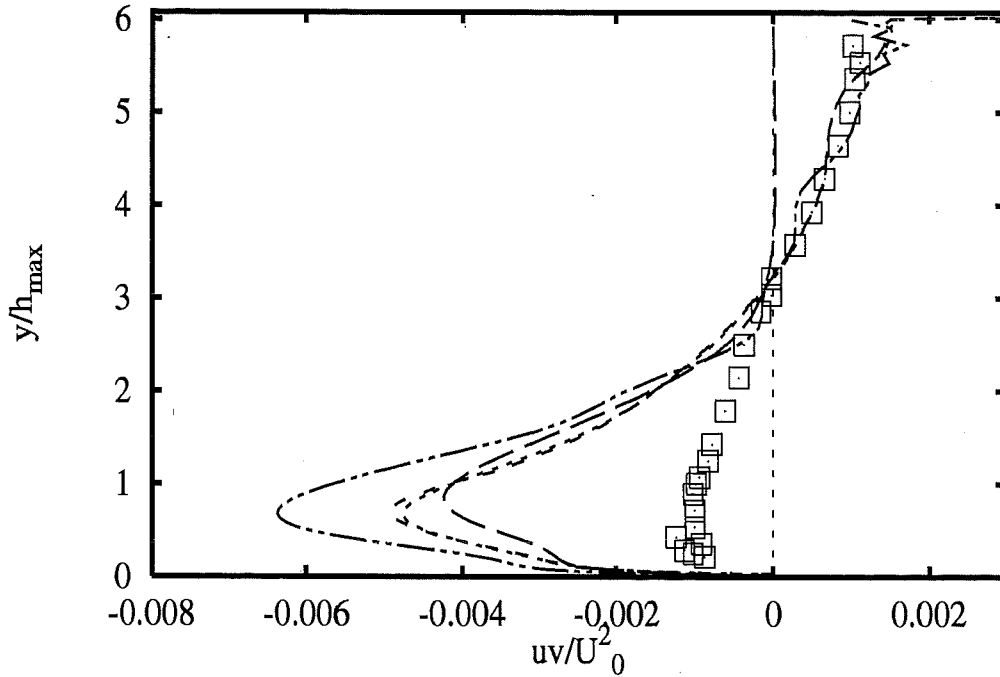
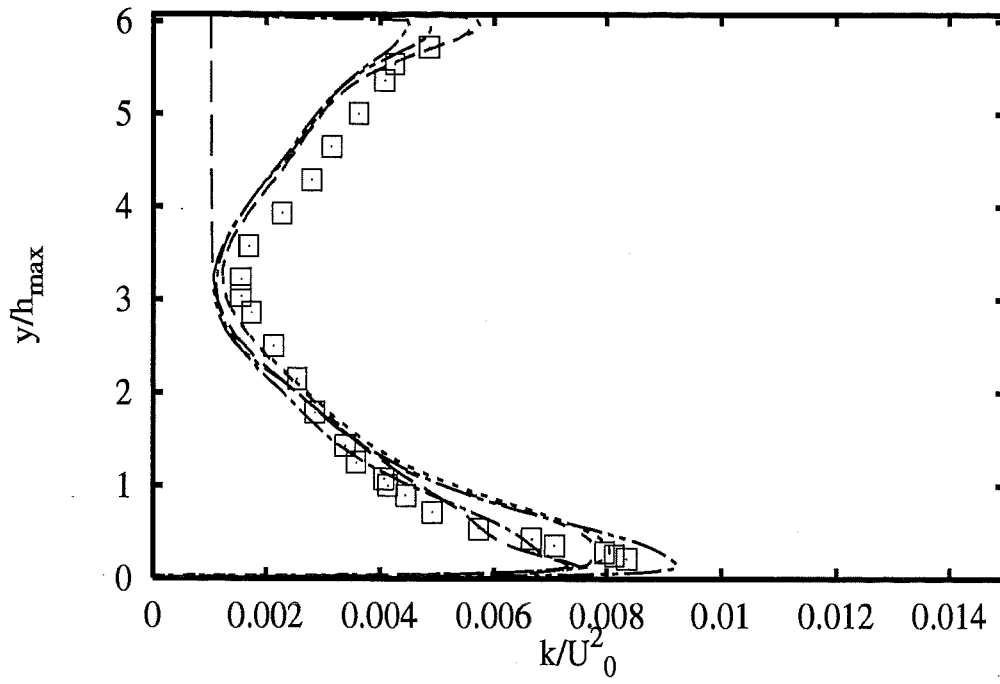
- Experiments** □
- UFlorenc hKE std+NoRe ---
 - UKarlsru hKE std+NoRe (HLPA) - - -
 - UKarlsru hKE std+NoRe (Hyb) ·····
 - UChalmer hKE std+ChPa - · - ·
 - UStuttga hKE std+ChPa - · - ·



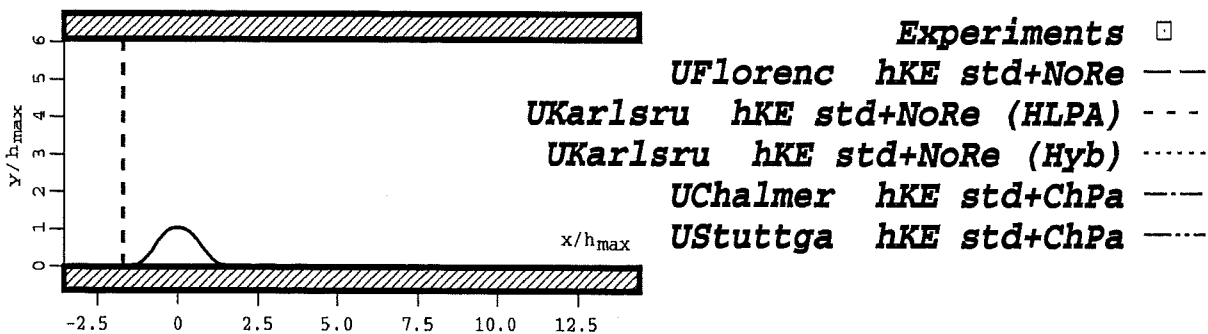
Profiles at $x/h_{max} = -1.78$

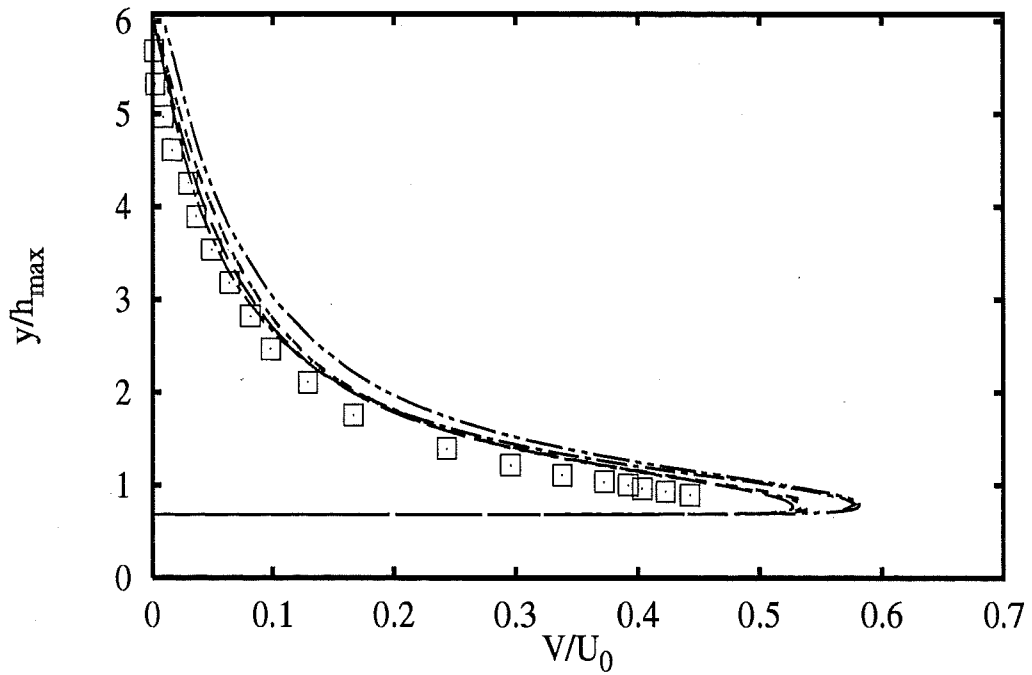
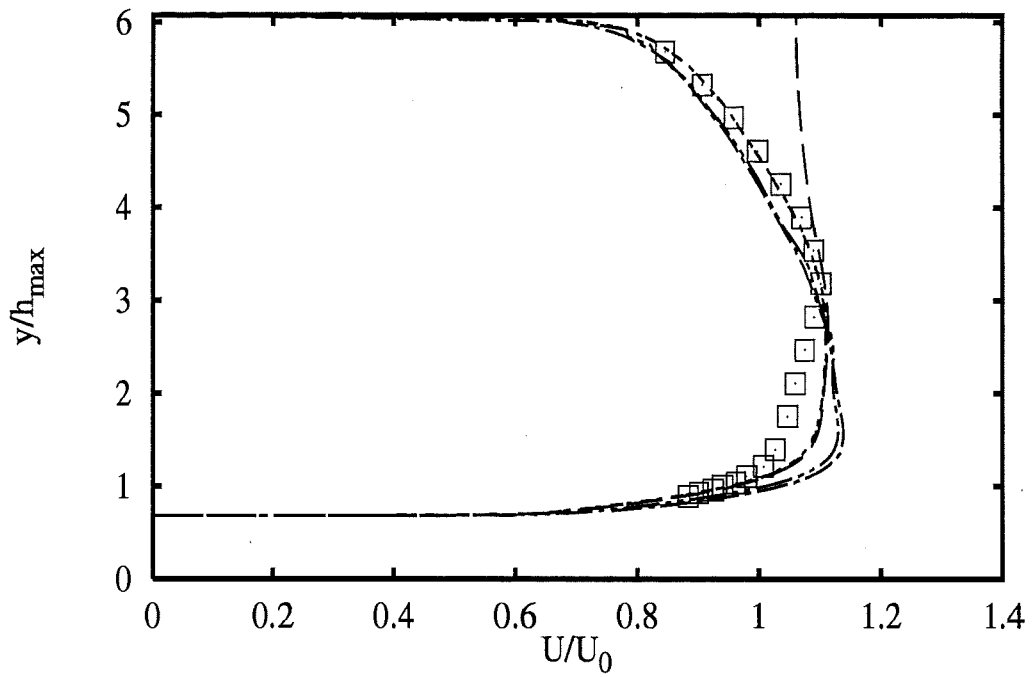


2A - 41

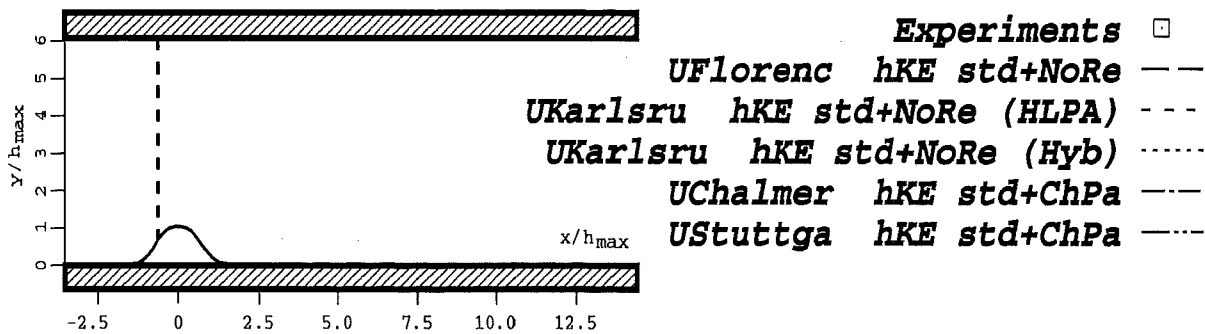


Profiles at $x/h_{max} = -1.78$

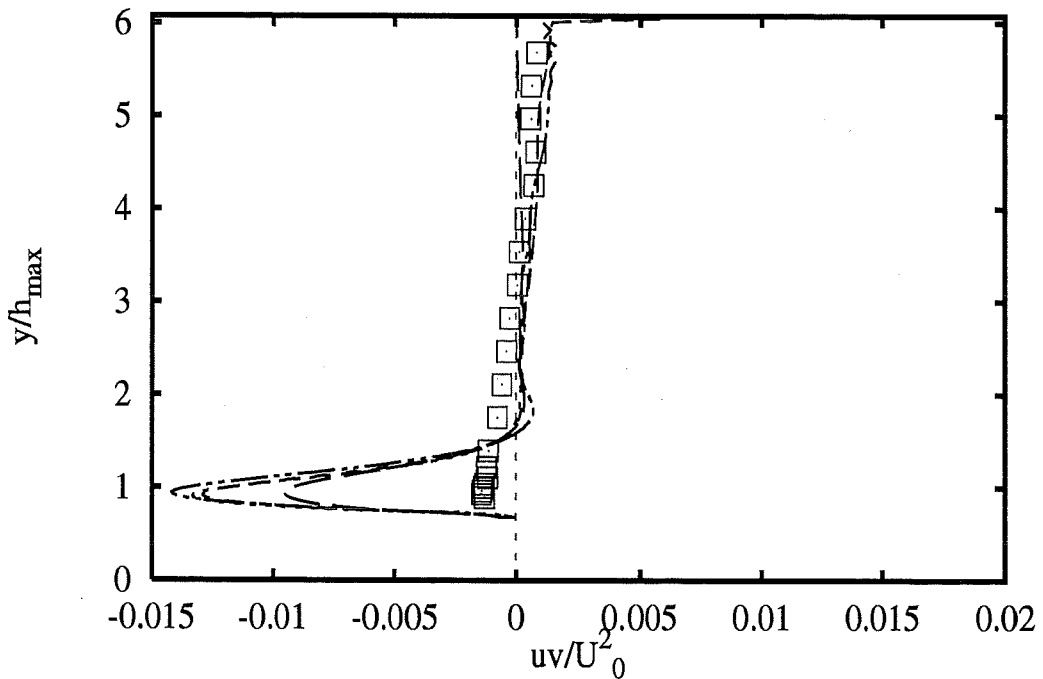
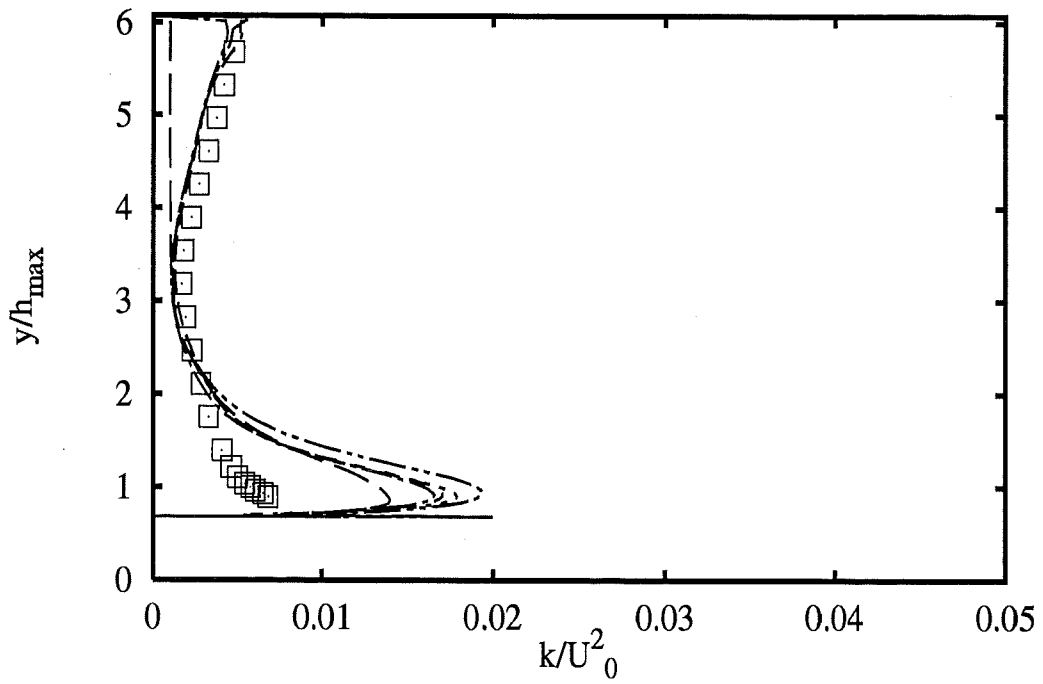




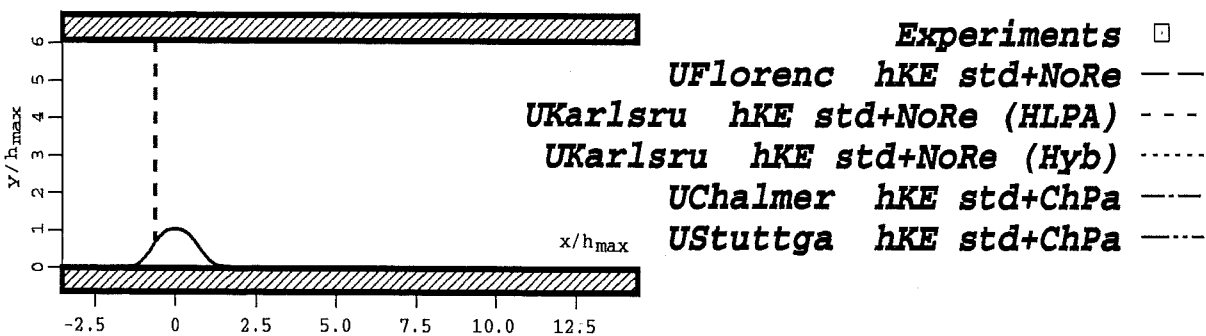
Profiles at $x/h_{max} = -0.71$

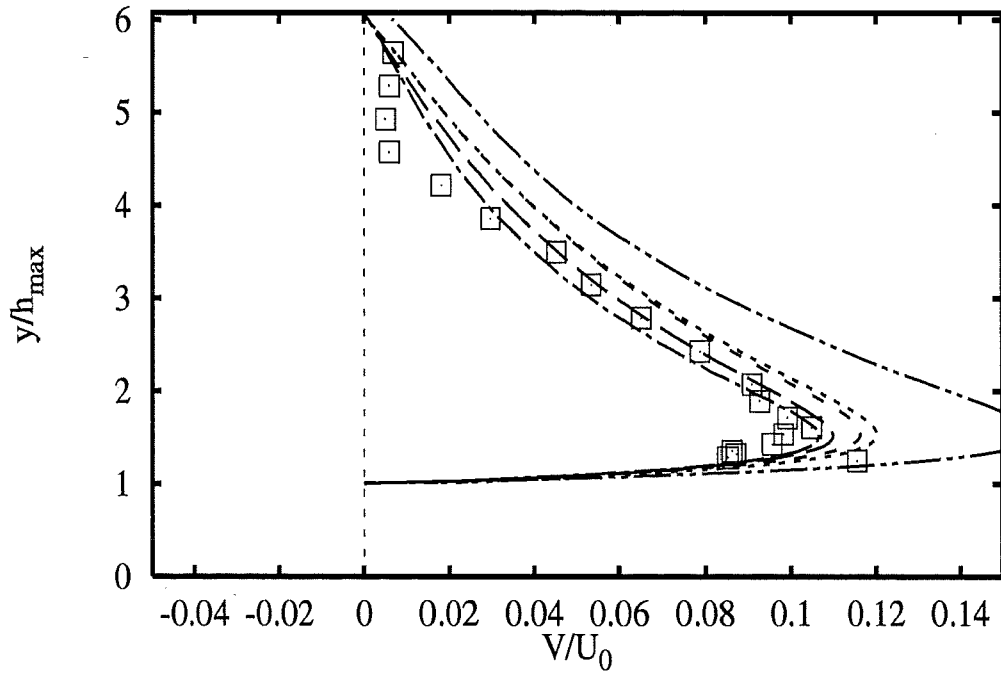
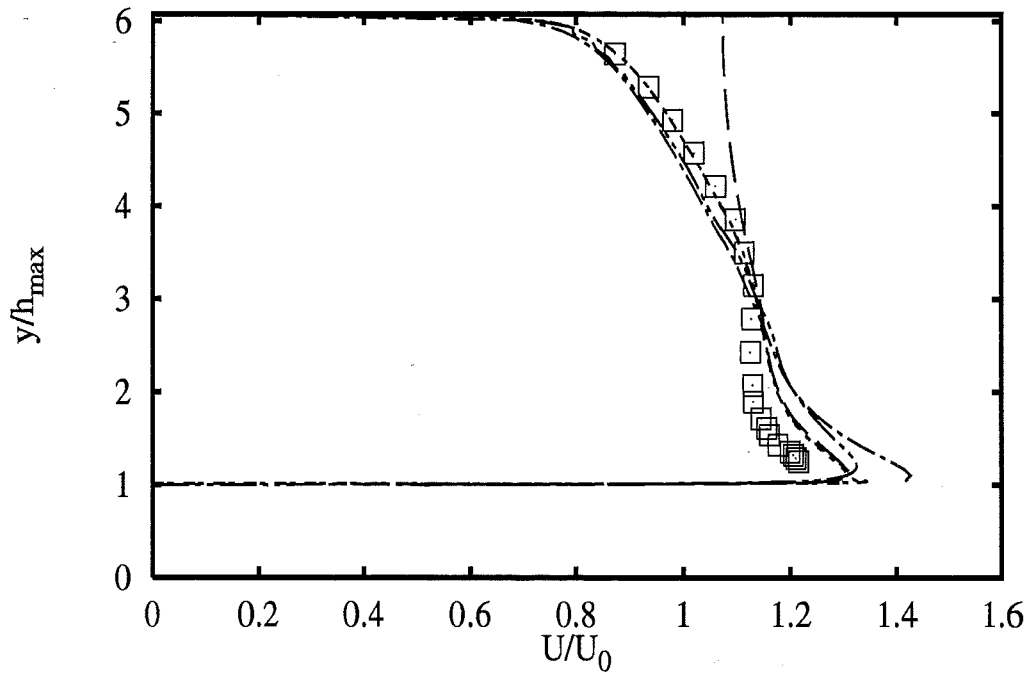


2A - 43

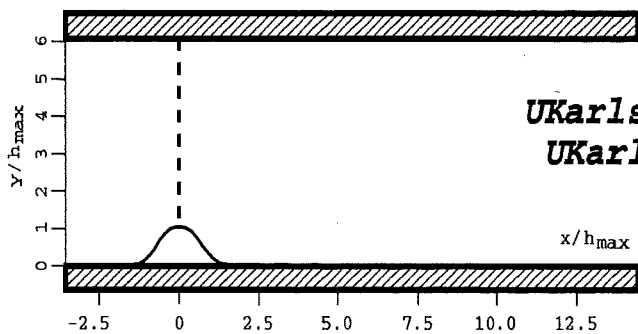


Profiles at $x/h_{max} = -0.71$

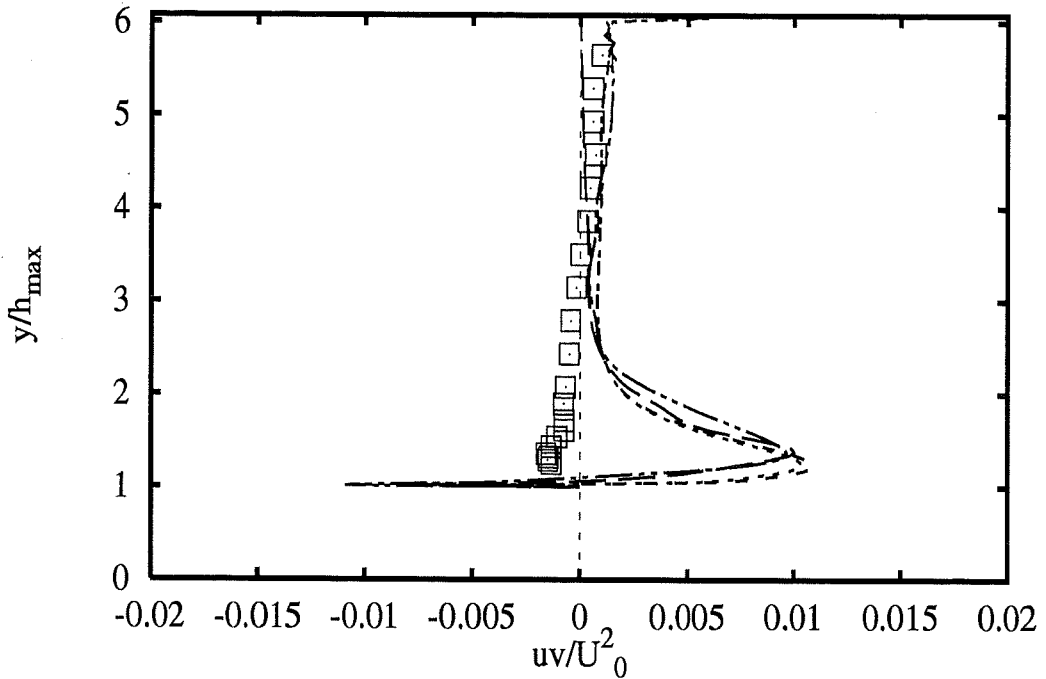
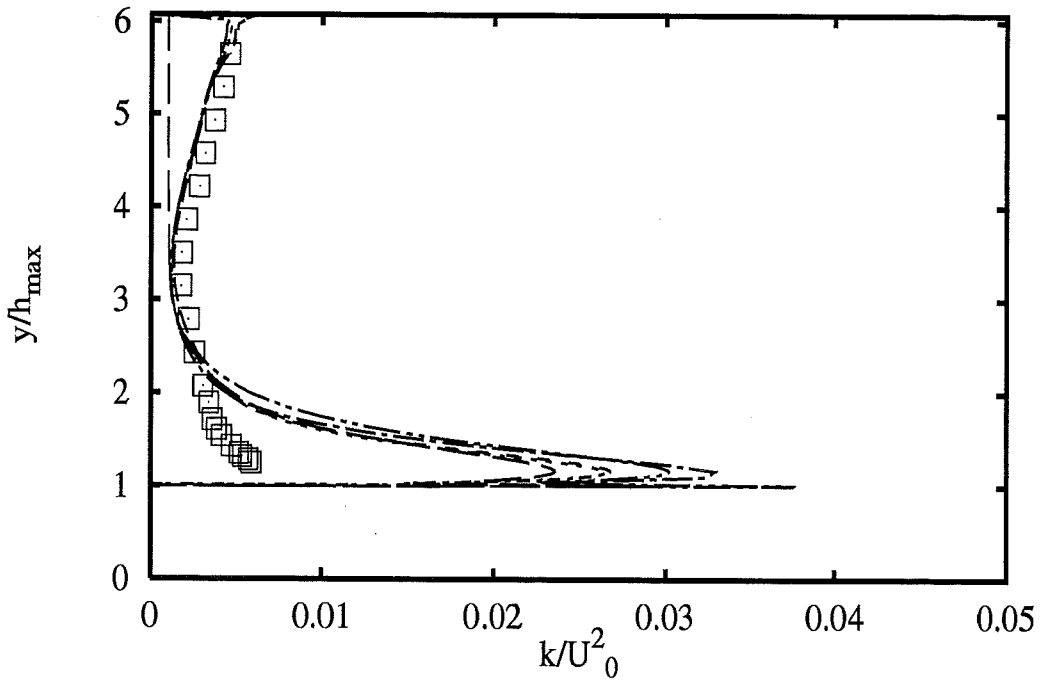




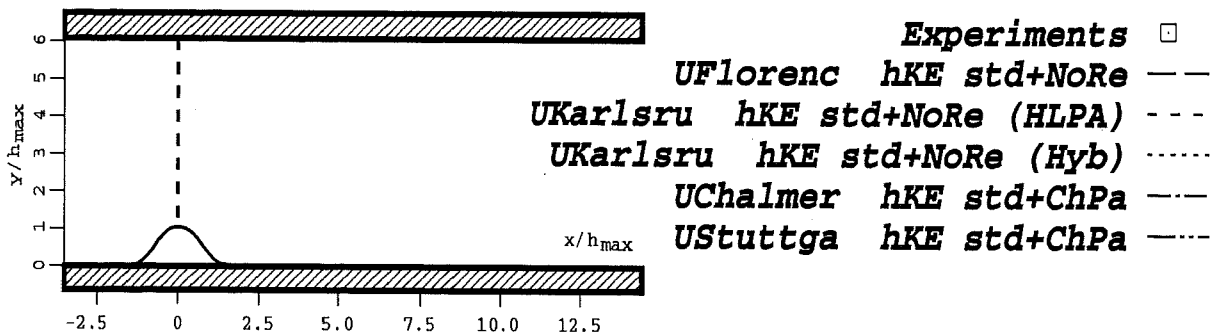
Profiles at $x/h_{max} = 0$

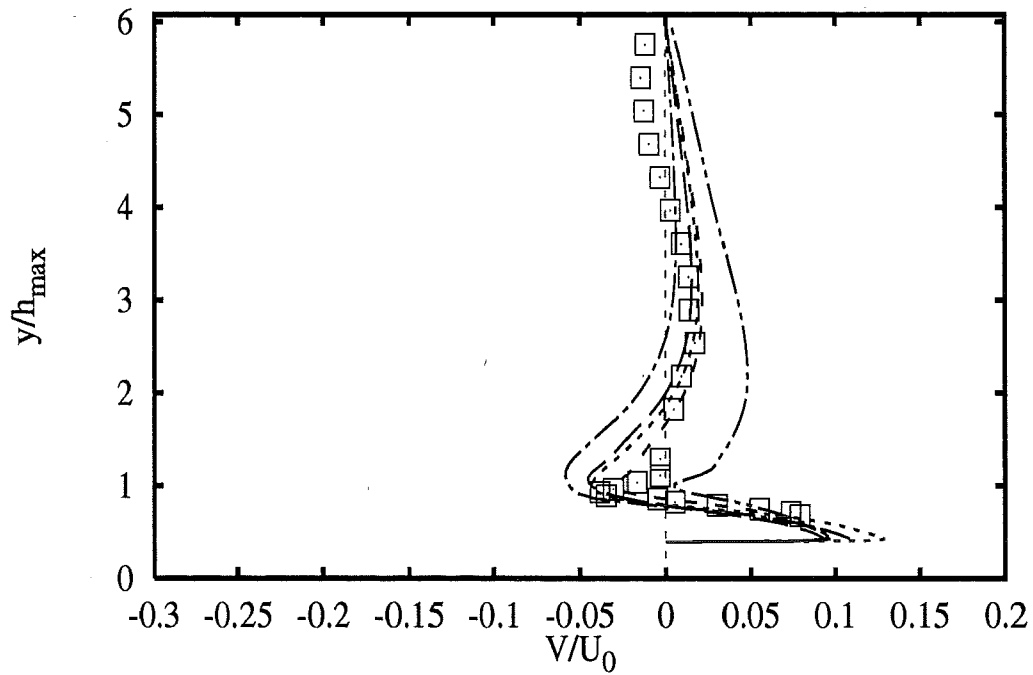
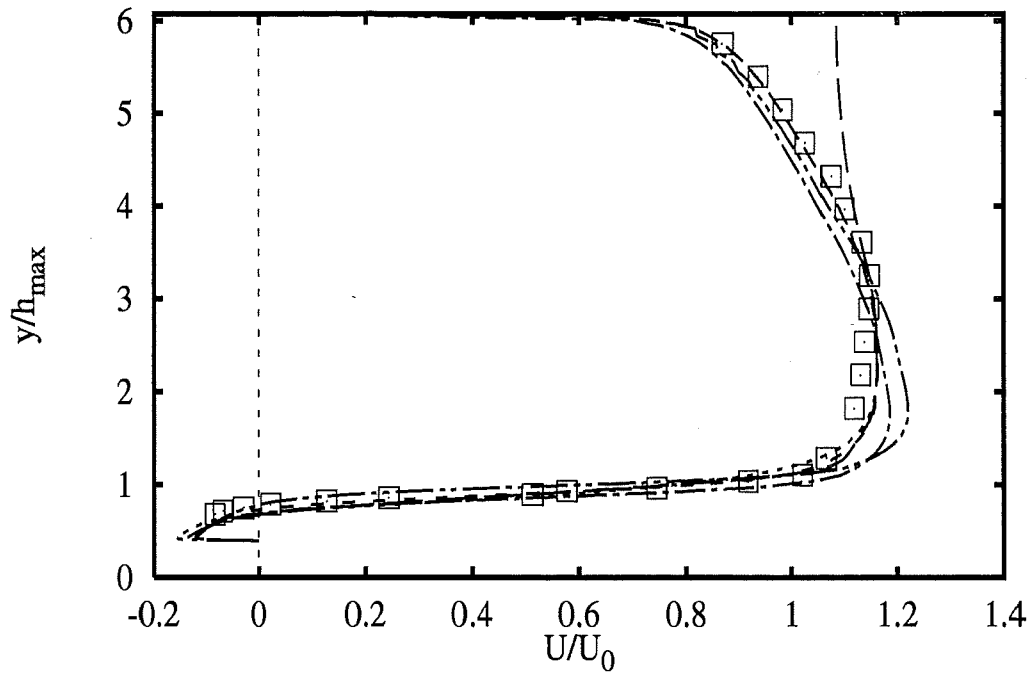


- | | | |
|----------|----------------------------|-------|
| | Experiments | □ |
| UFlorenc | hKE std+NoRe | — — |
| UKarlsru | hKE std+NoRe (HLPa) | - - - |
| UKarlsru | hKE std+NoRe (Hyb) | ⋯⋯⋯ |
| UChalmer | hKE std+ChPa | - - - |
| UStuttga | hKE std+ChPa | - - - |

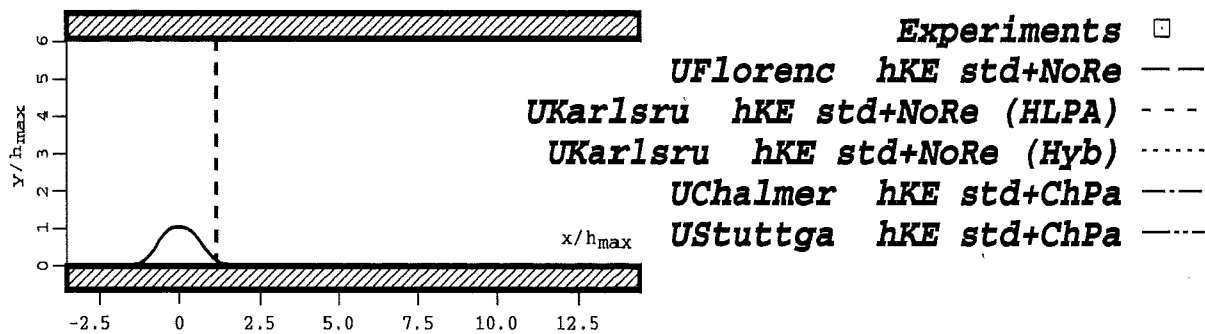


Profiles at $x/h_{max} = 0$

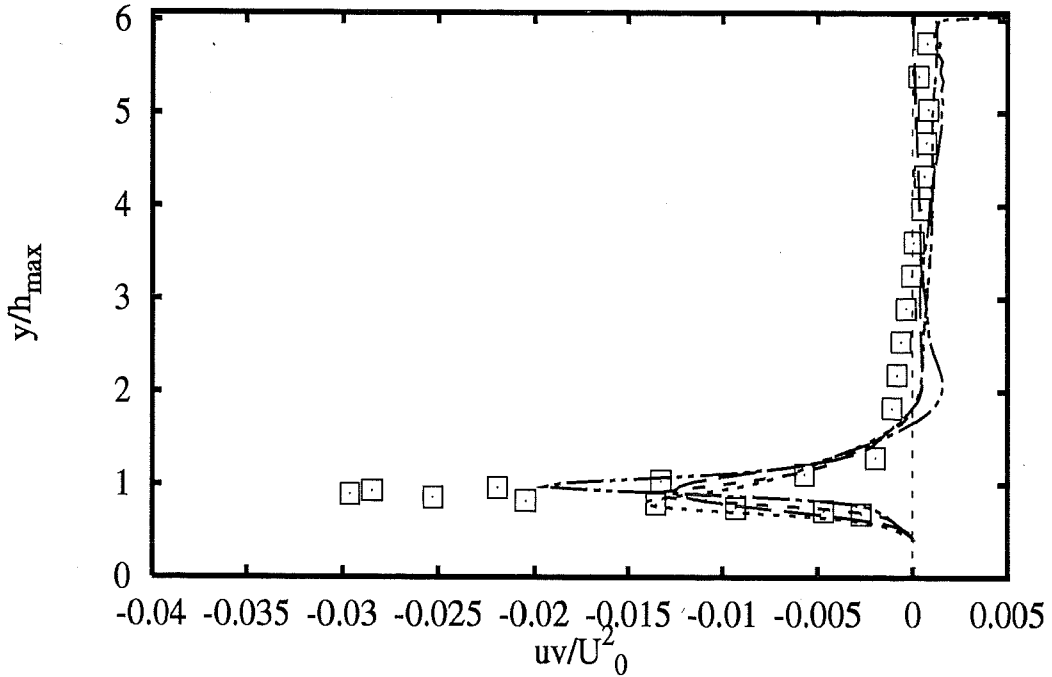
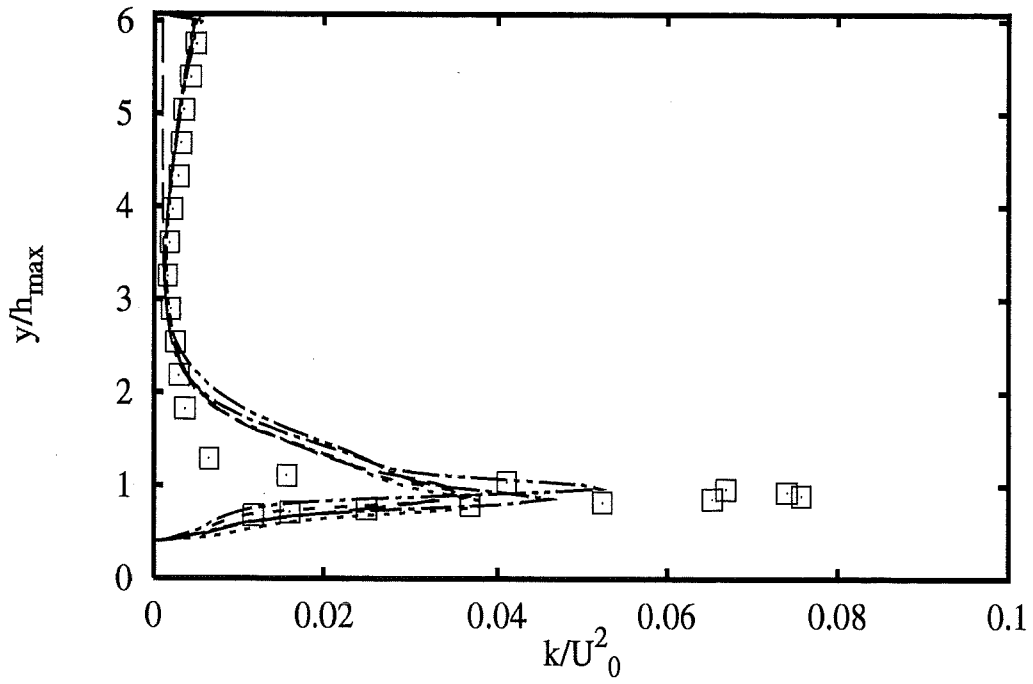




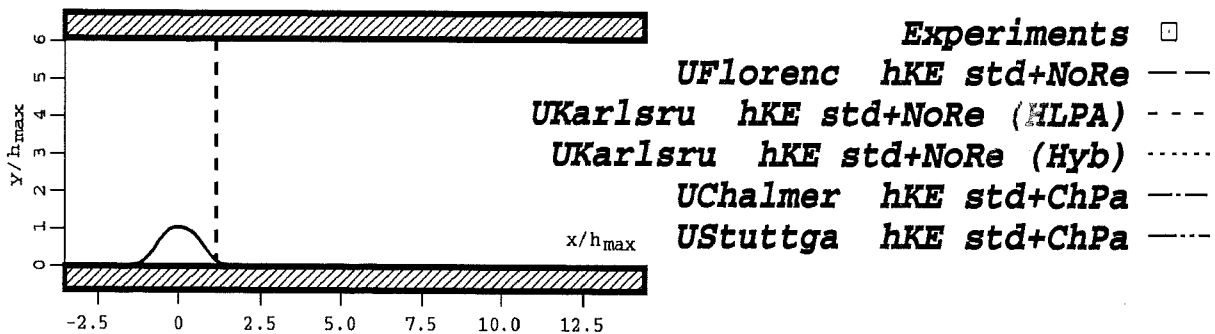
Profiles at $x/h_{max} = 1.07$

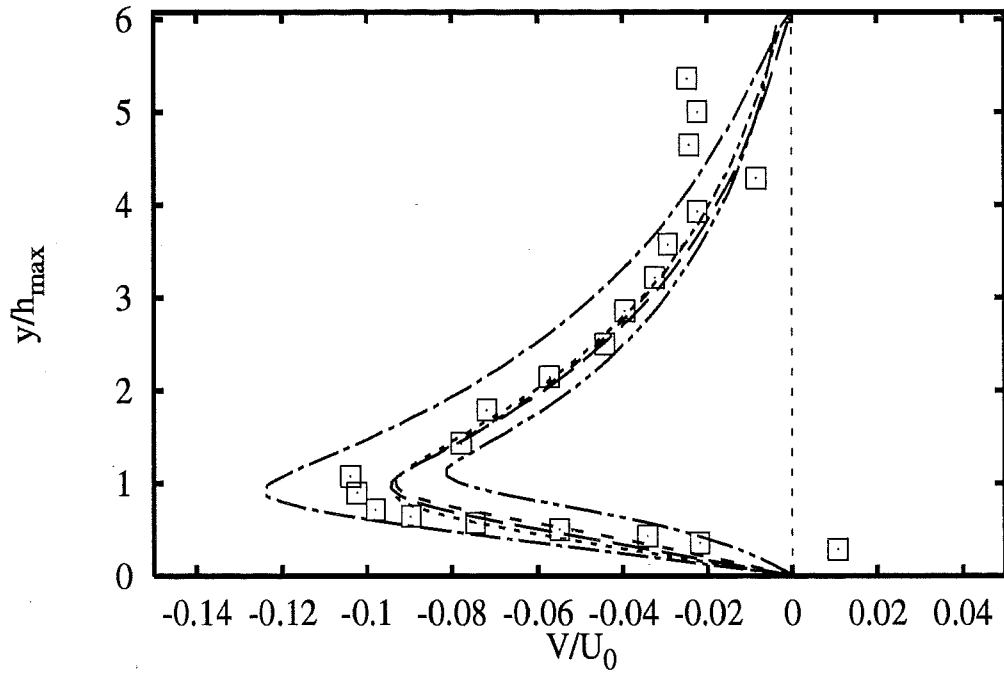
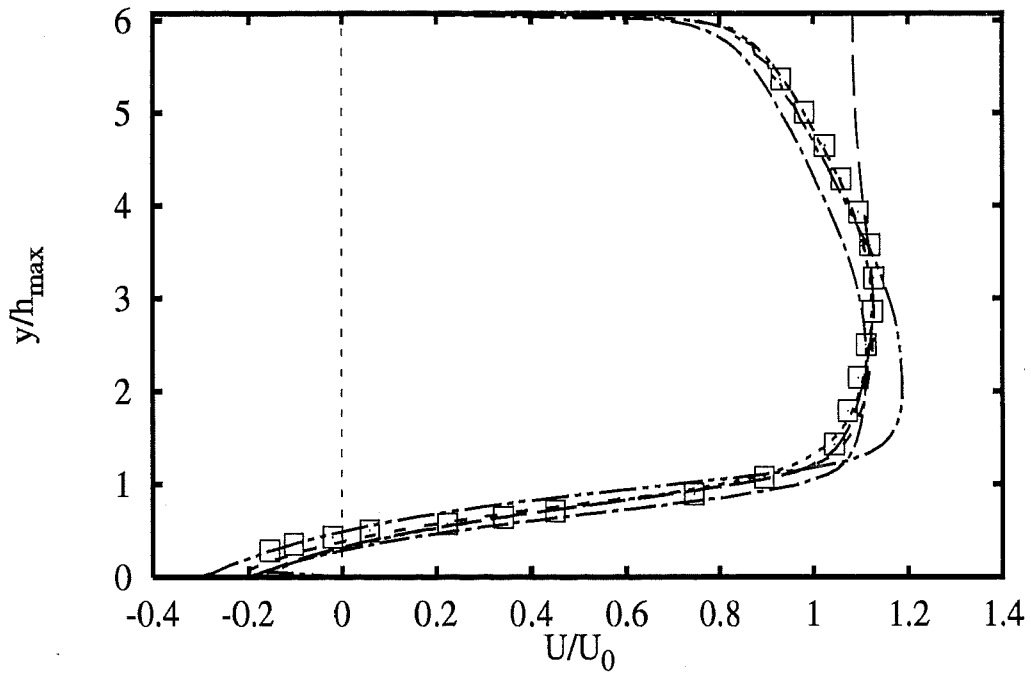


2A - 47

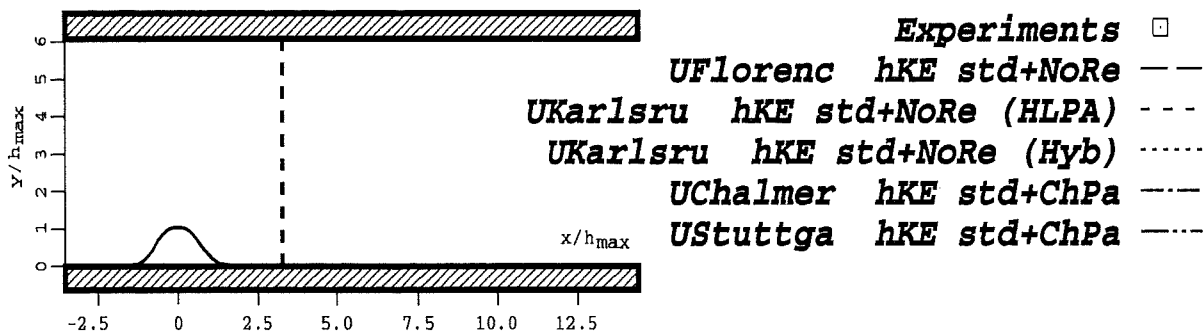


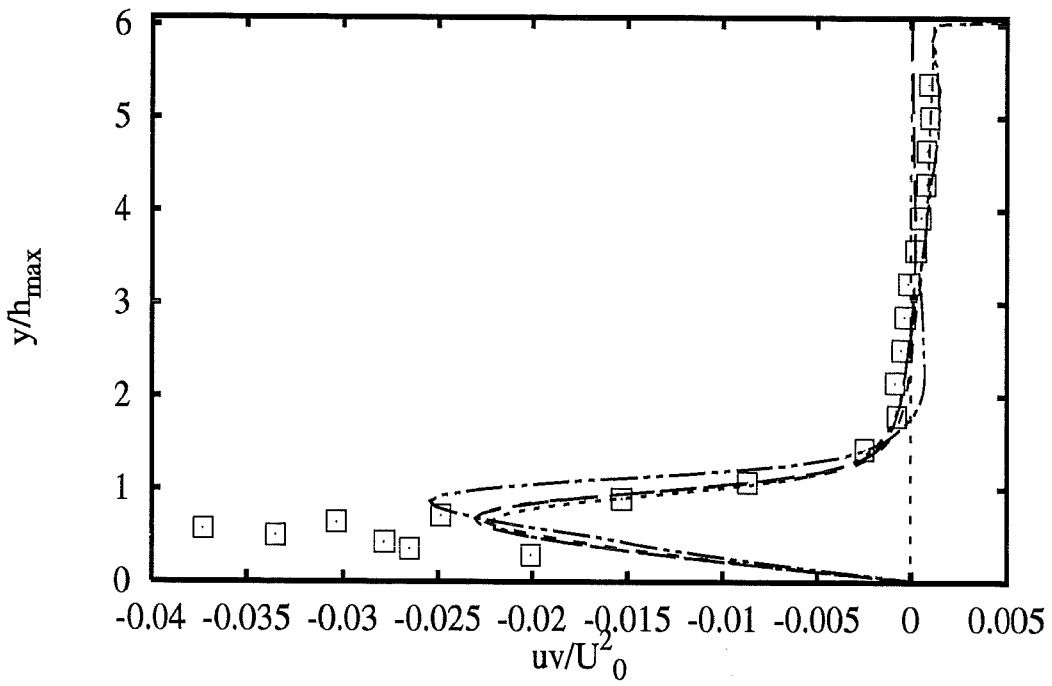
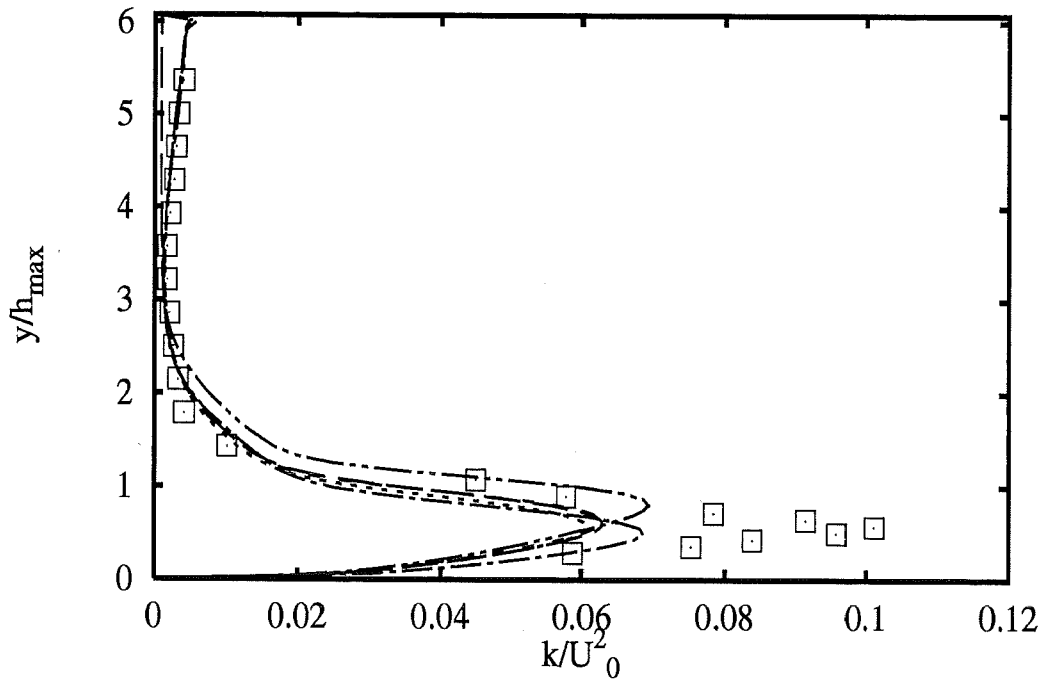
Profiles at $x/h_{max} = 1.07$



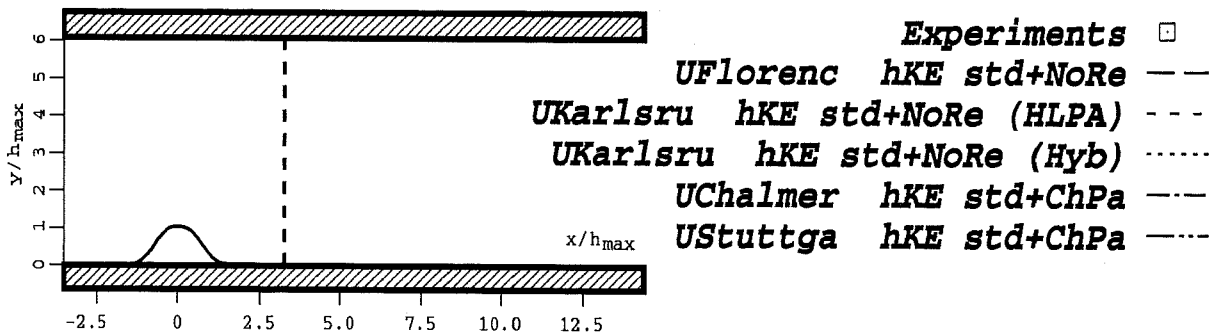


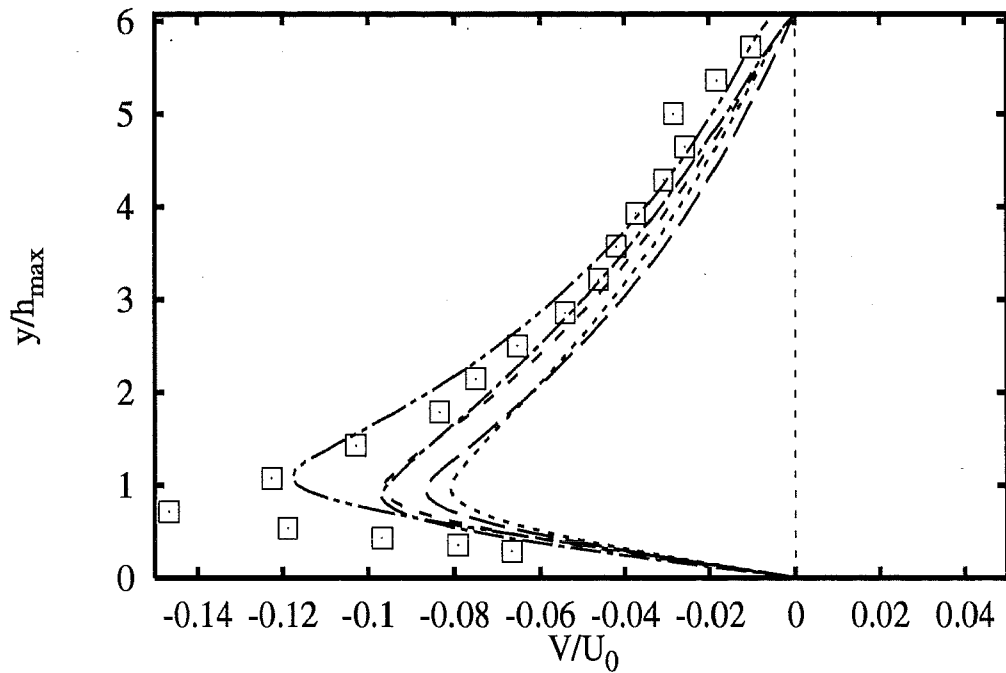
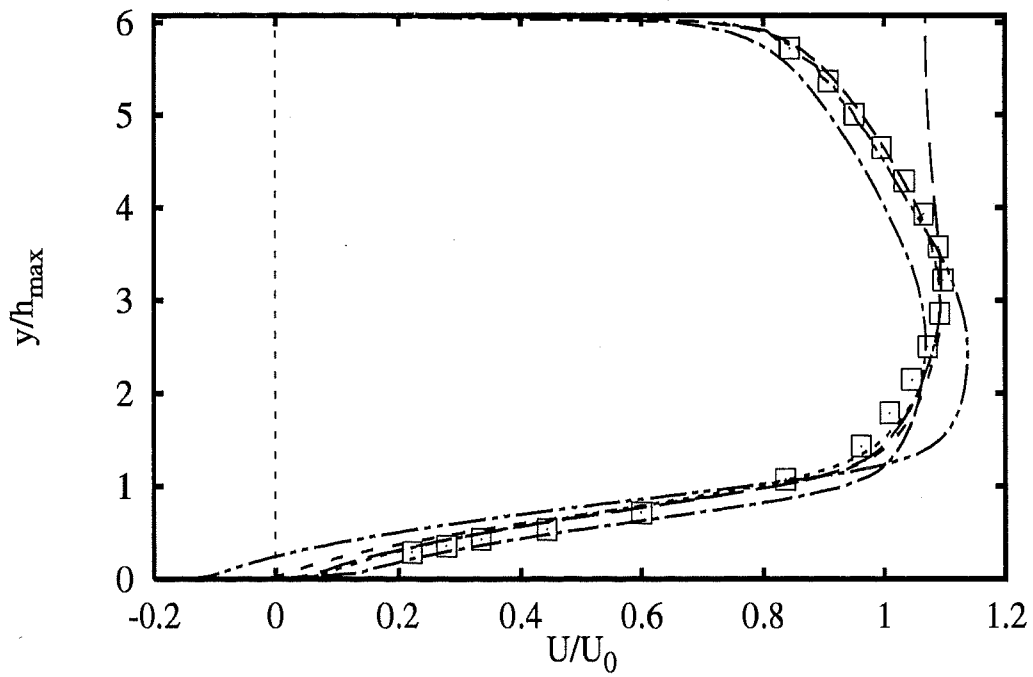
Profiles at $x/h_{max} = 3.21$



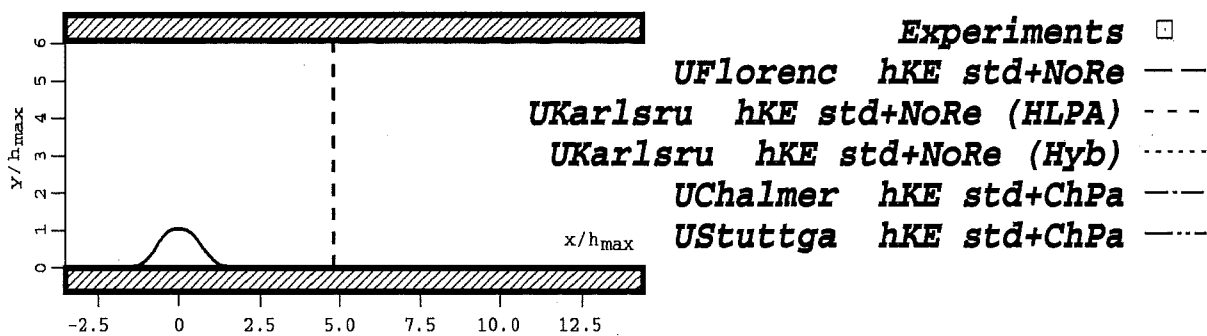


Profiles at $x/h_{max} = 3.21$

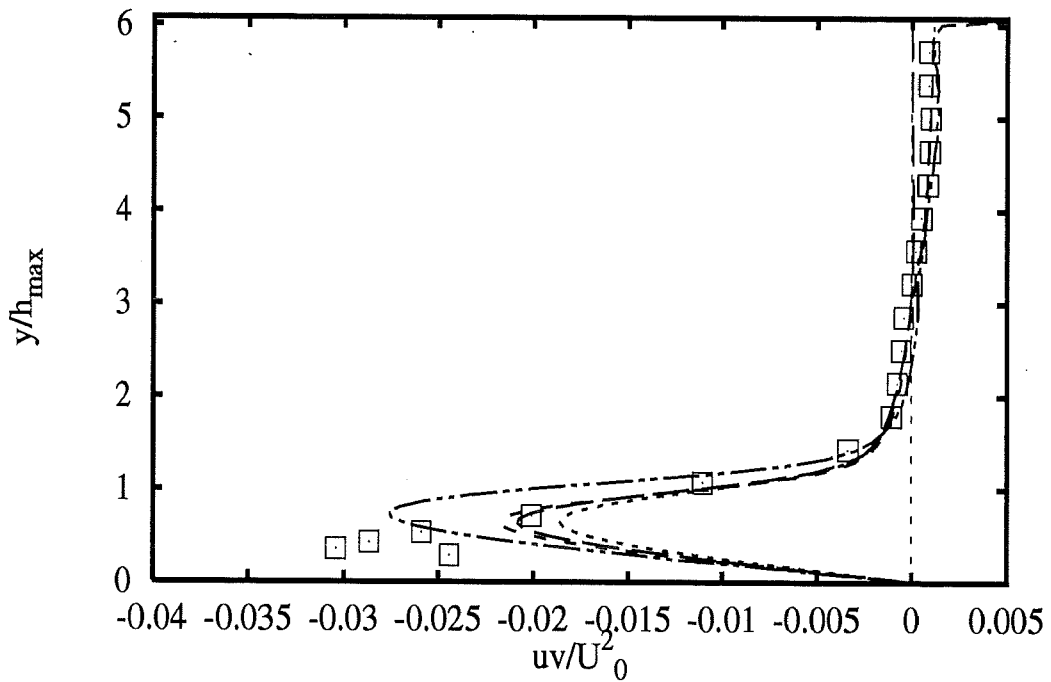
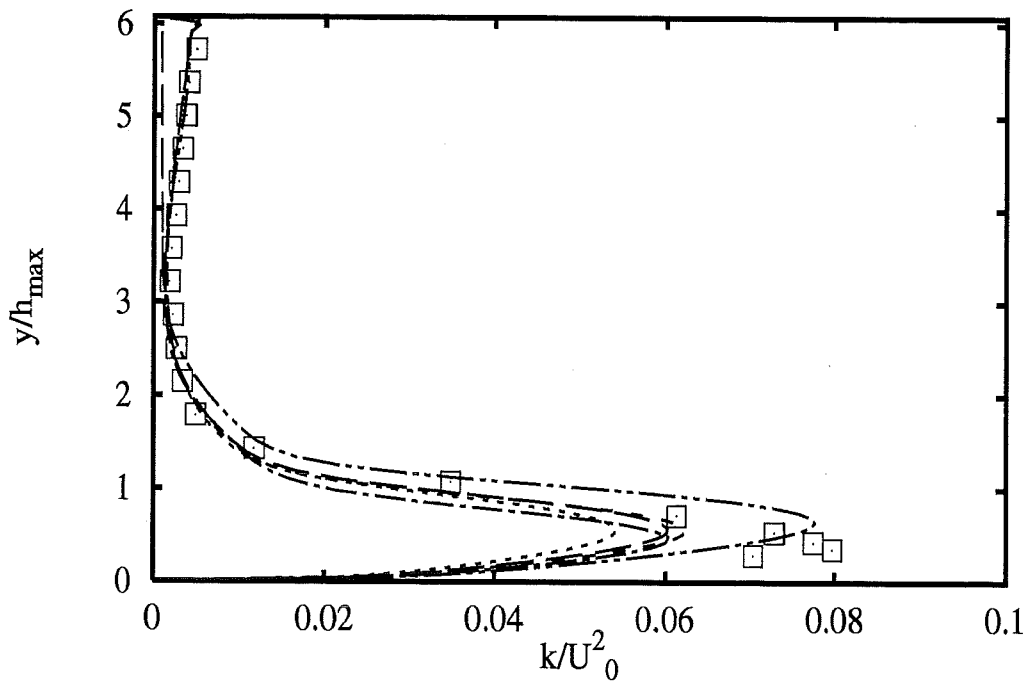




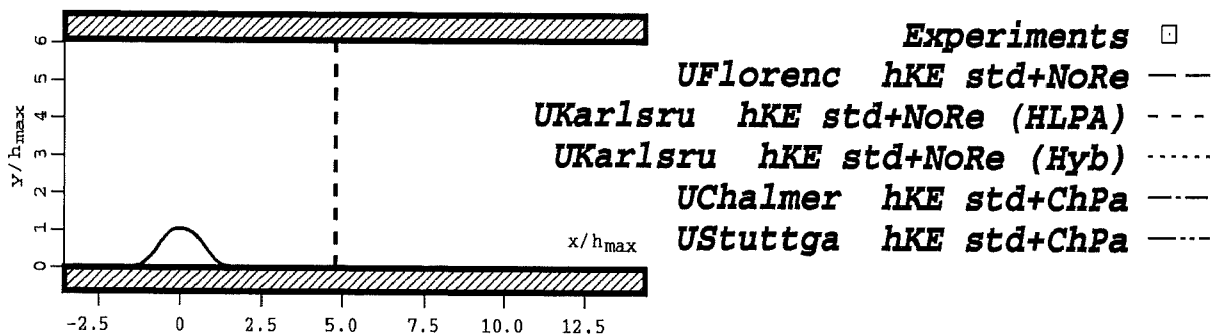
Profiles at $x/h_{max} = 4.79$

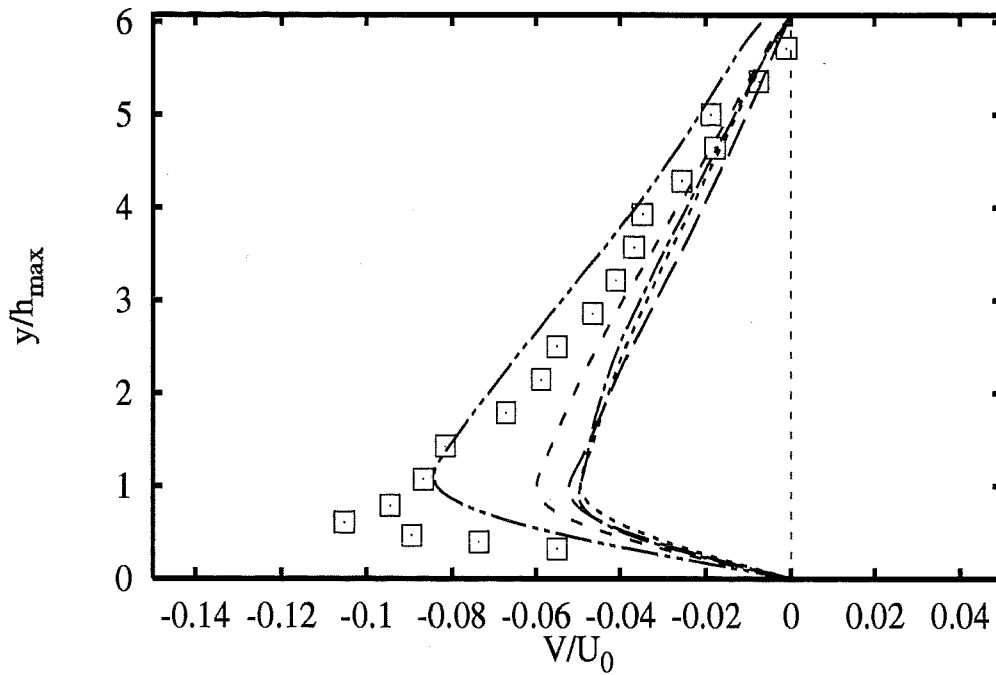
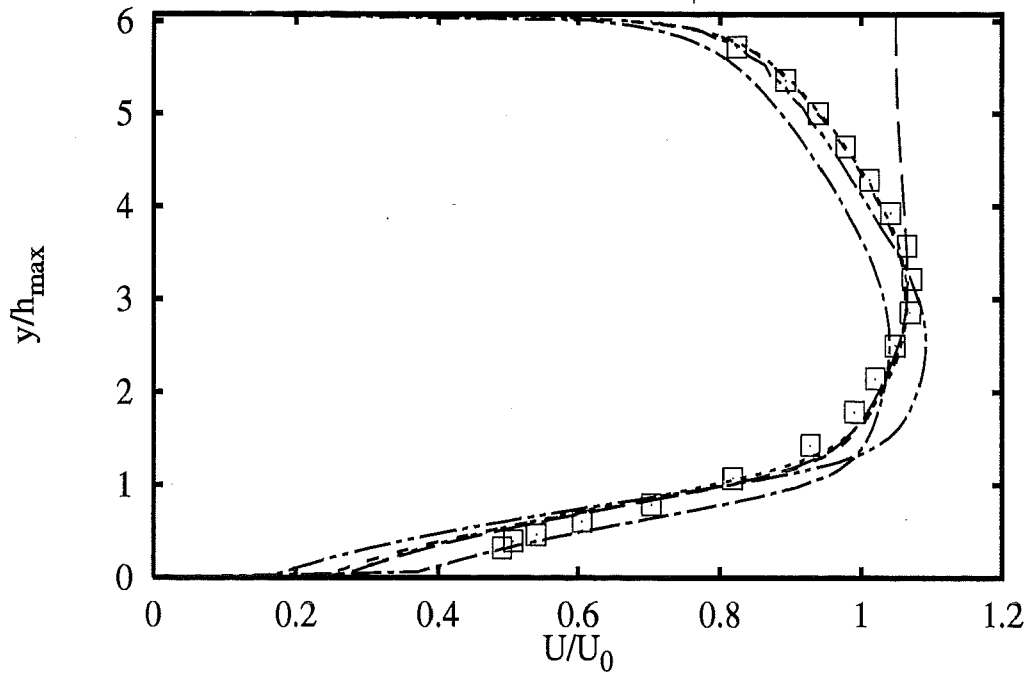


2A - 51

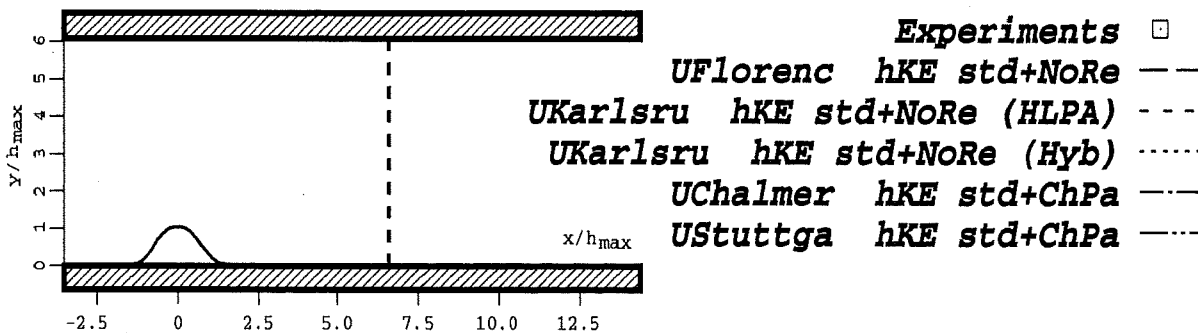


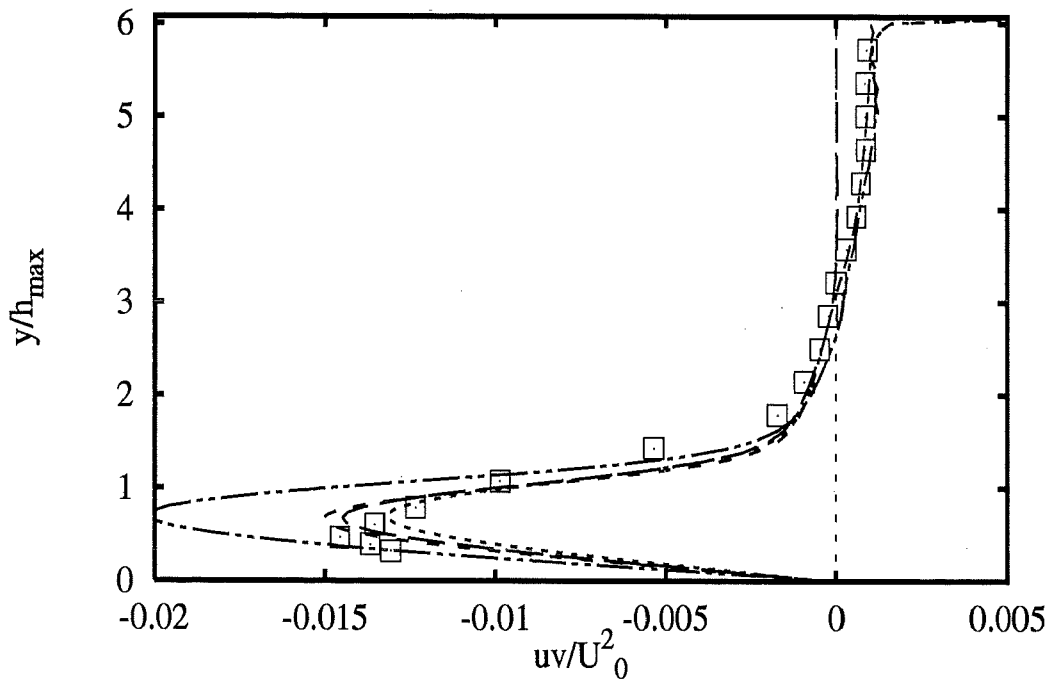
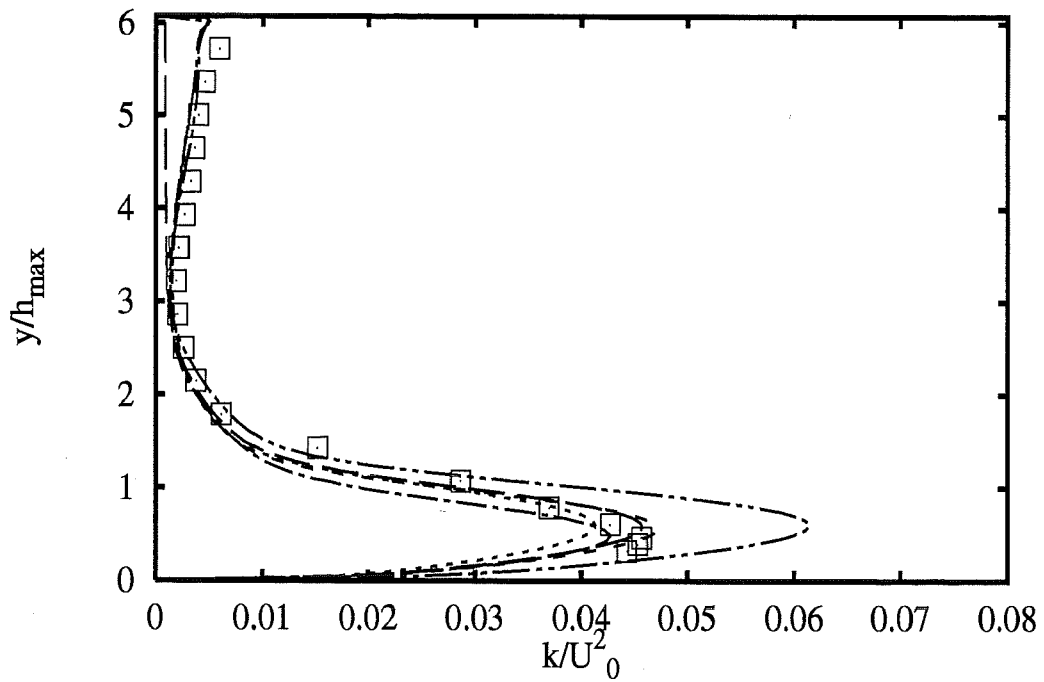
Profiles at $x/h_{max} = 4.79$



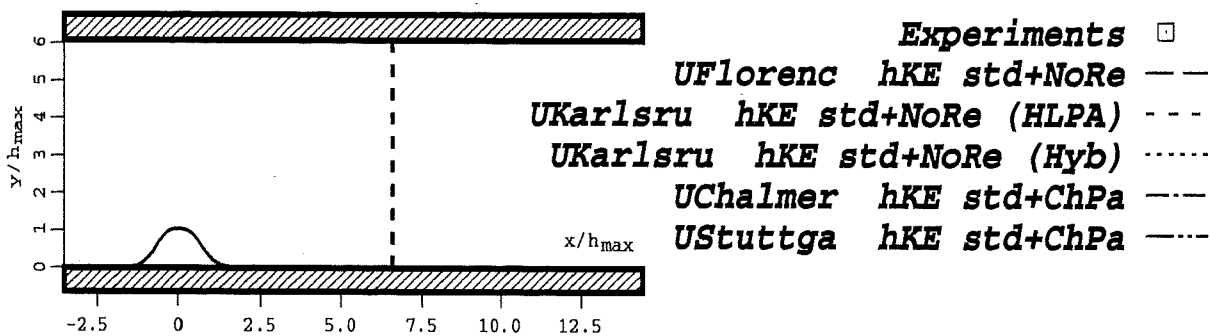


Profiles at $x/h_{max} = 6.61$

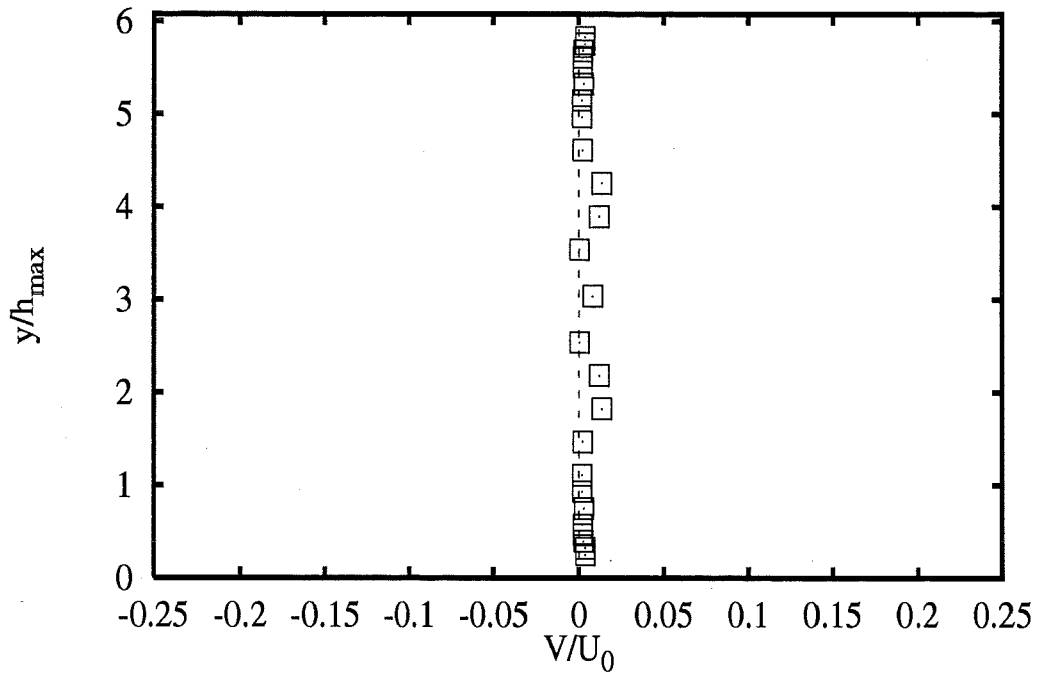
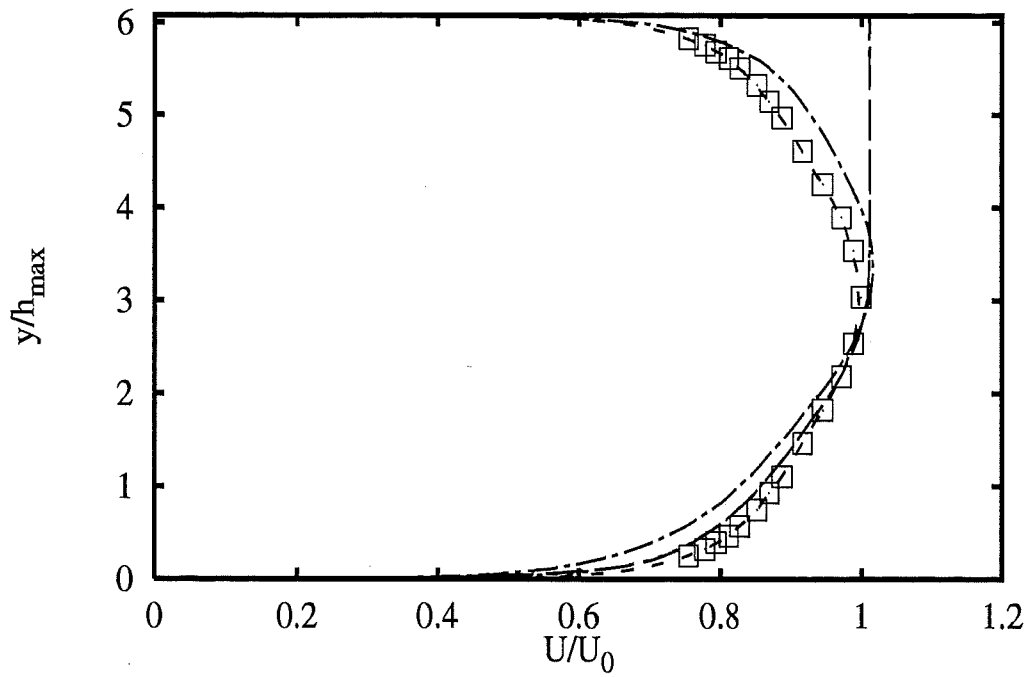




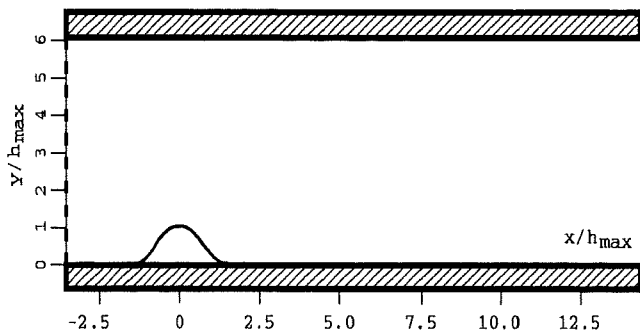
Profiles at $x/h_{max} = 6.61$





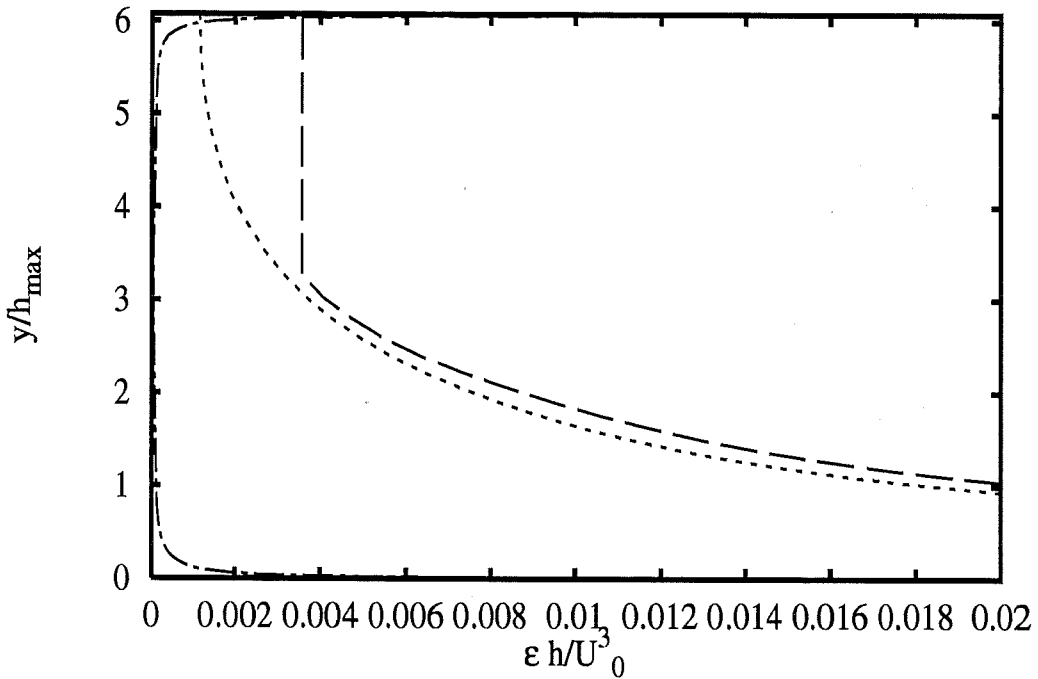
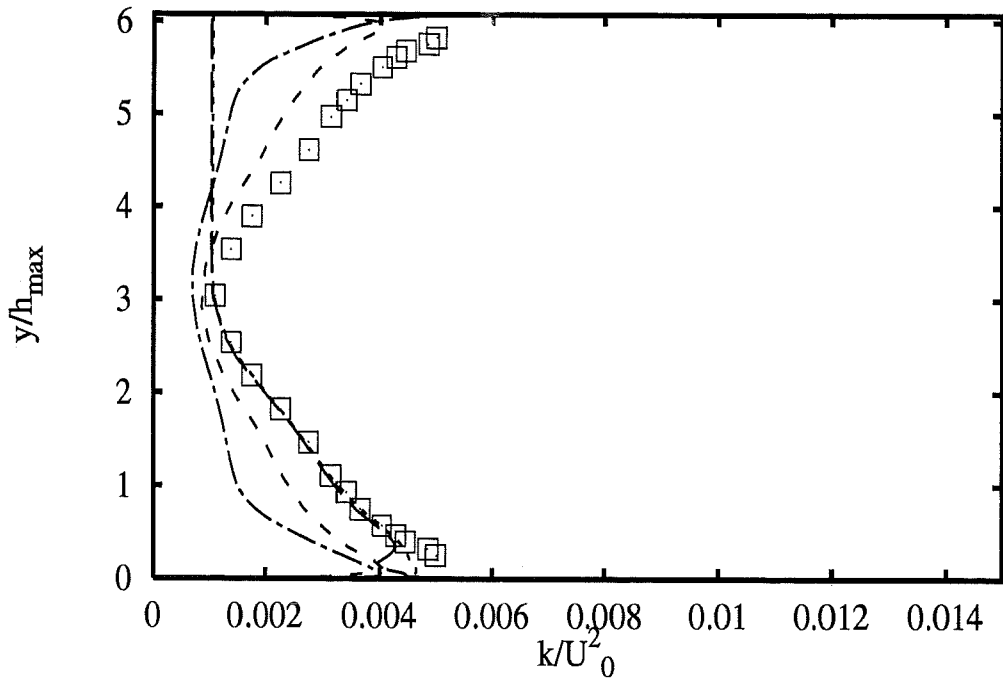


Profiles at $x/h_{max} = -3.57$

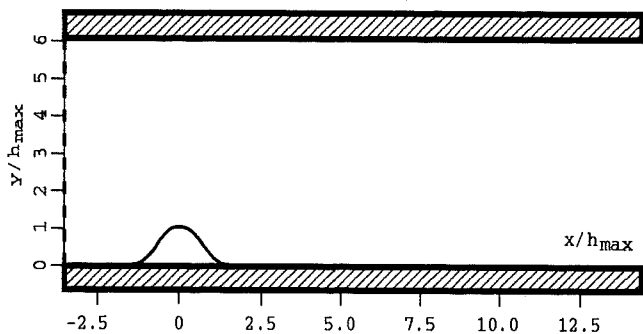


| | | |
|-----------------|---------------------|-------|
| | Experiments | □ |
| <i>UFlorenc</i> | <i>hKE std+RMM</i> | — — |
| <i>Iolomouc</i> | <i>hKE std+Gol</i> | - - - |
| <i>UFlorenc</i> | <i>hKE std+Kim</i> | ⋯⋯⋯ |
| <i>CompDyna</i> | <i>hKE RNG+NoRe</i> | - - - |

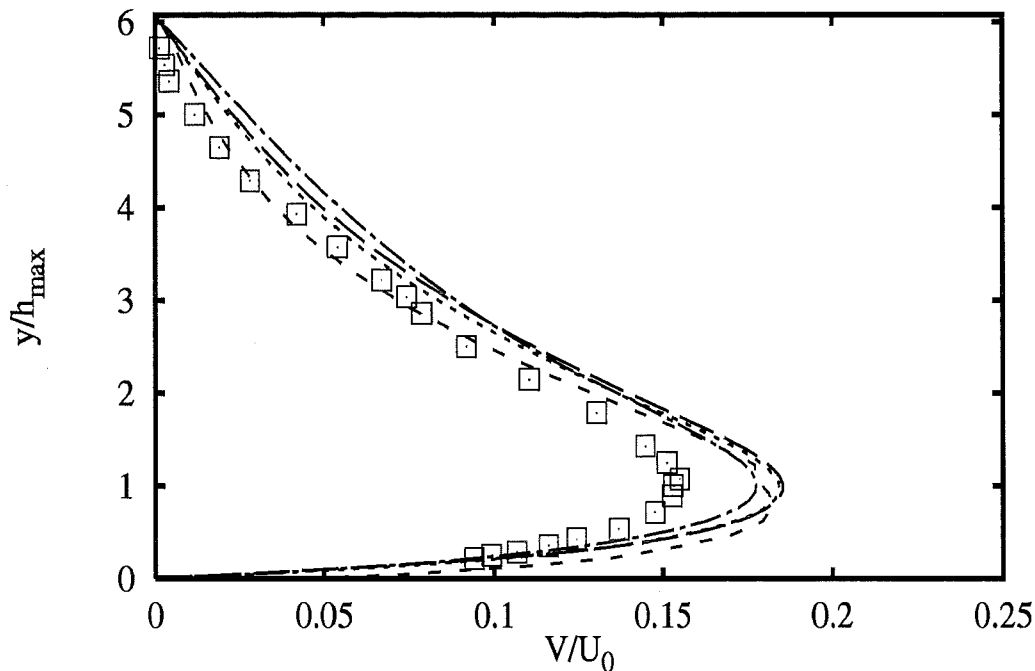
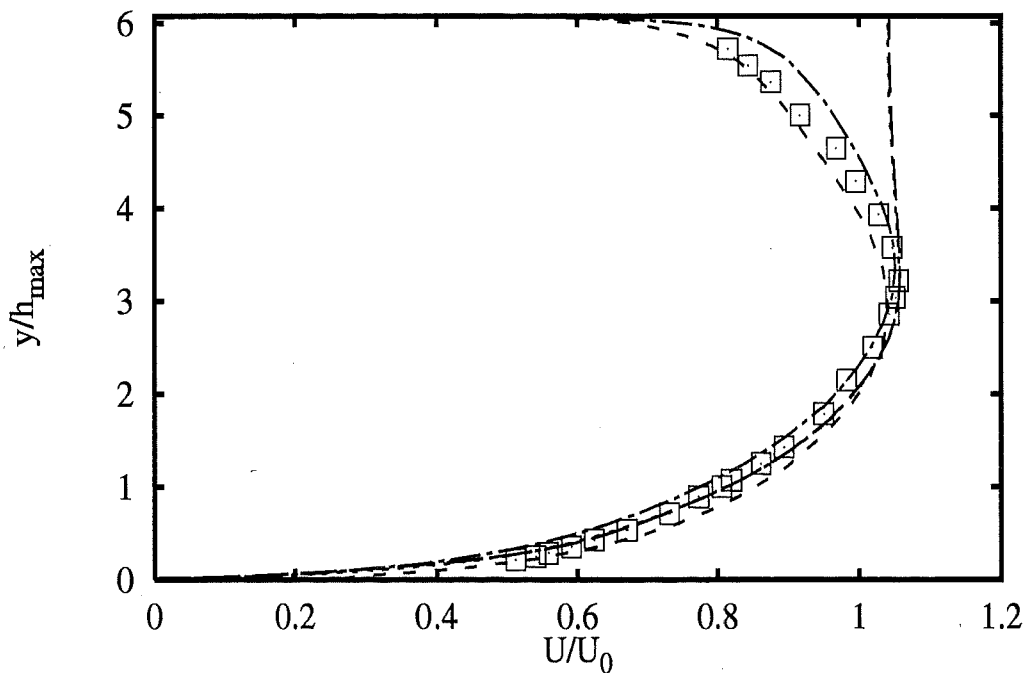
2A - 55



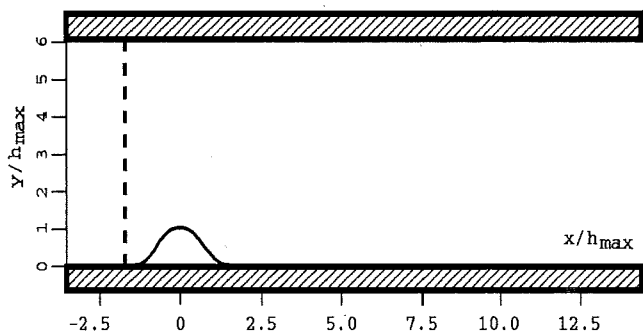
Profiles at $x/h_{max} = -3.57$



- | | | |
|-----------------|---------------------|-------|
| | Experiments | □ |
| <i>UFlorenc</i> | <i>hKE std+RMM</i> | --- |
| <i>Iolomouc</i> | <i>hKE std+Gol</i> | --- |
| <i>UFlorenc</i> | <i>hKE std+Kim</i> | |
| <i>CompDyna</i> | <i>hKE RNG+NoRe</i> | --- |

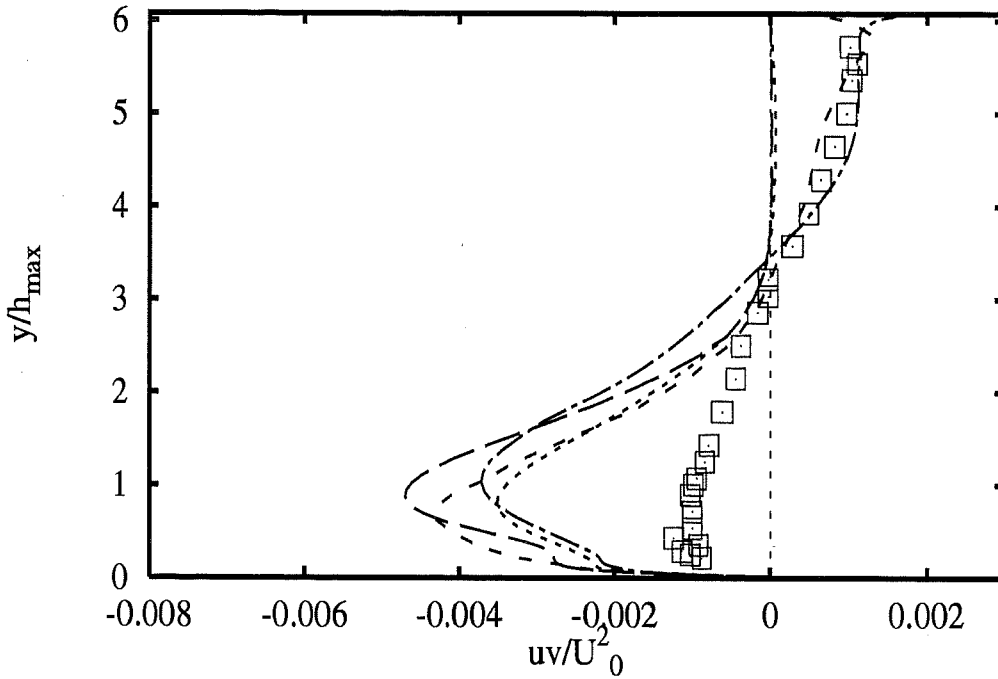
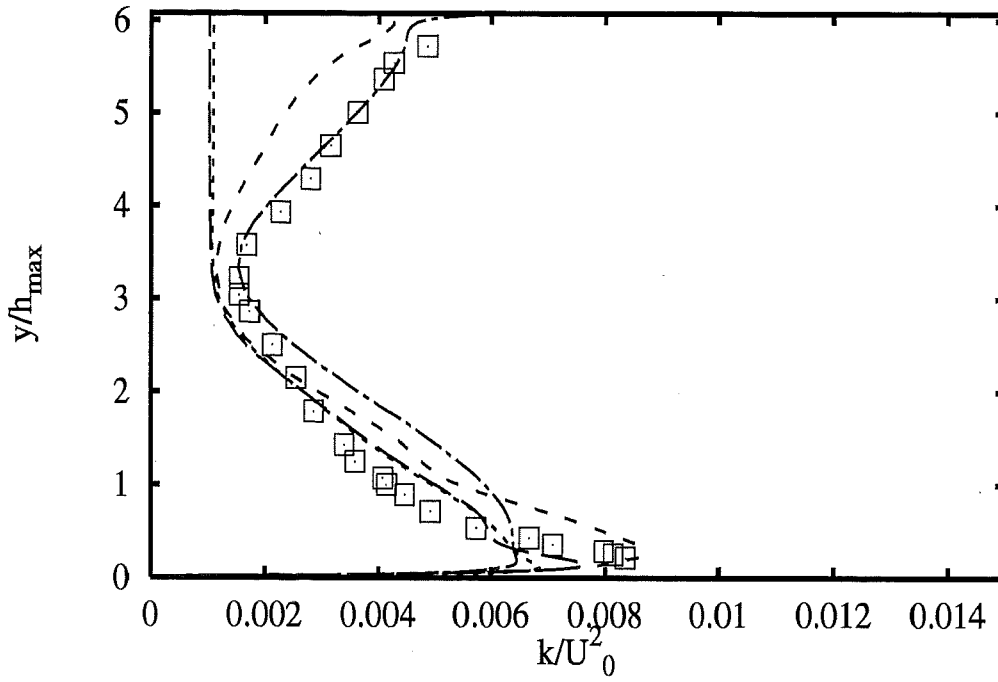


Profiles at $x/h_{max} = -1.78$

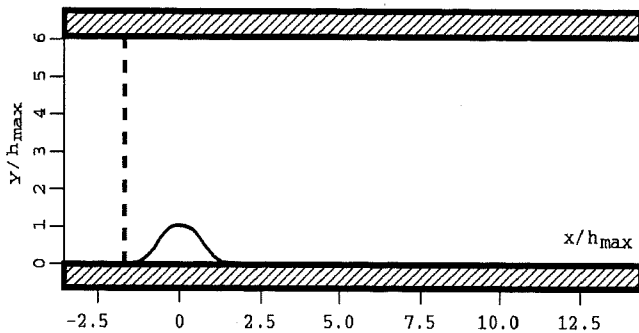


| | | |
|-----------------|---------------------|-----------|
| | Experiments | □ |
| <i>UFlorenc</i> | <i>hKE std+RMM</i> | — — |
| <i>Iolomouc</i> | <i>hKE std+Gol</i> | - - - |
| <i>UFlorenc</i> | <i>hKE std+Kim</i> | ⋯⋯⋯ |
| <i>CompDyna</i> | <i>hKE RNG+NoRe</i> | - · - · - |

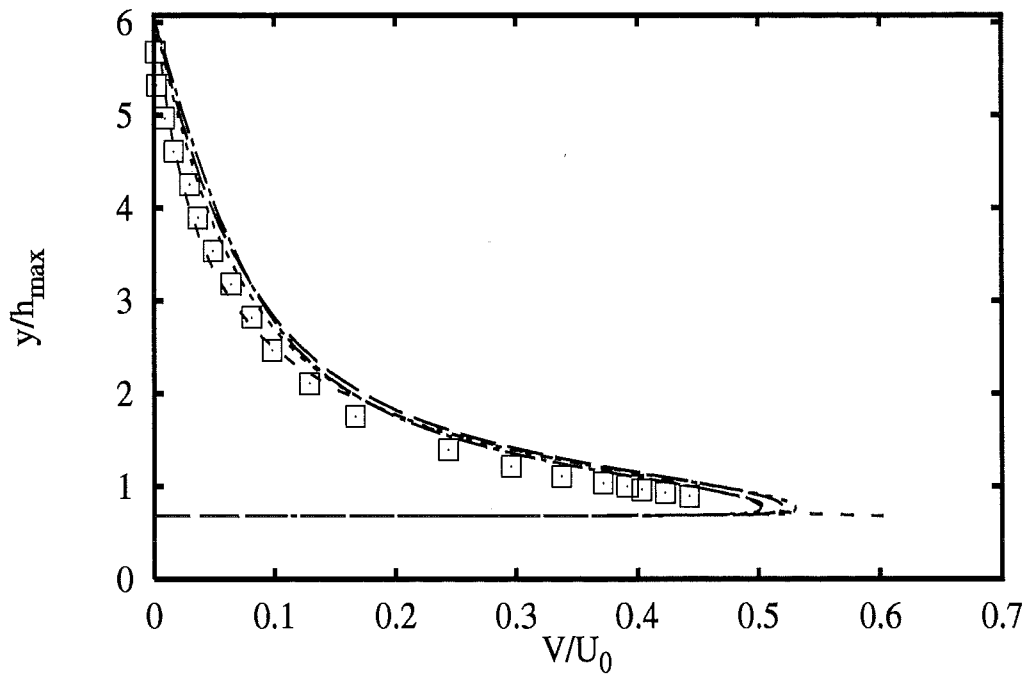
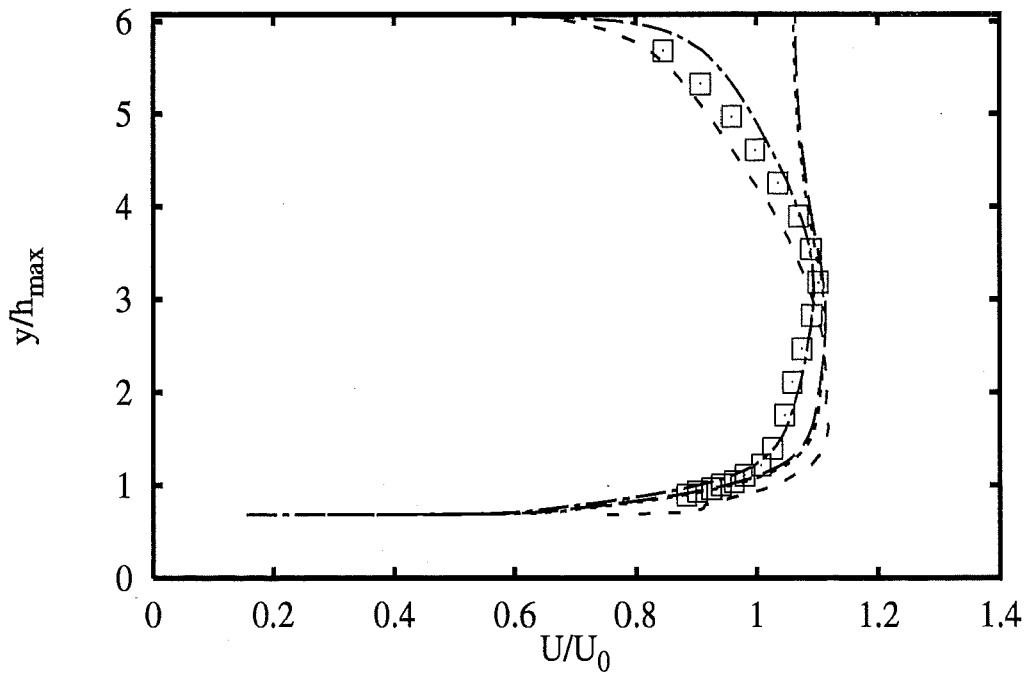
2A - 57



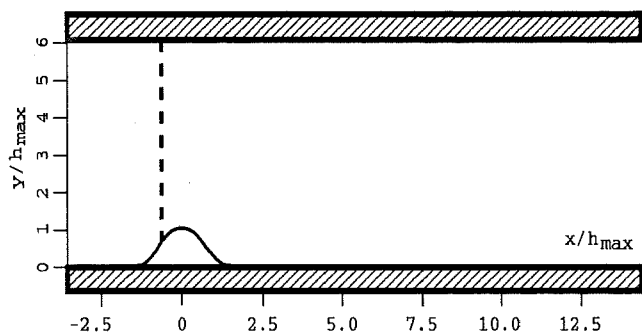
Profiles at $x/h_{max} = -1.78$



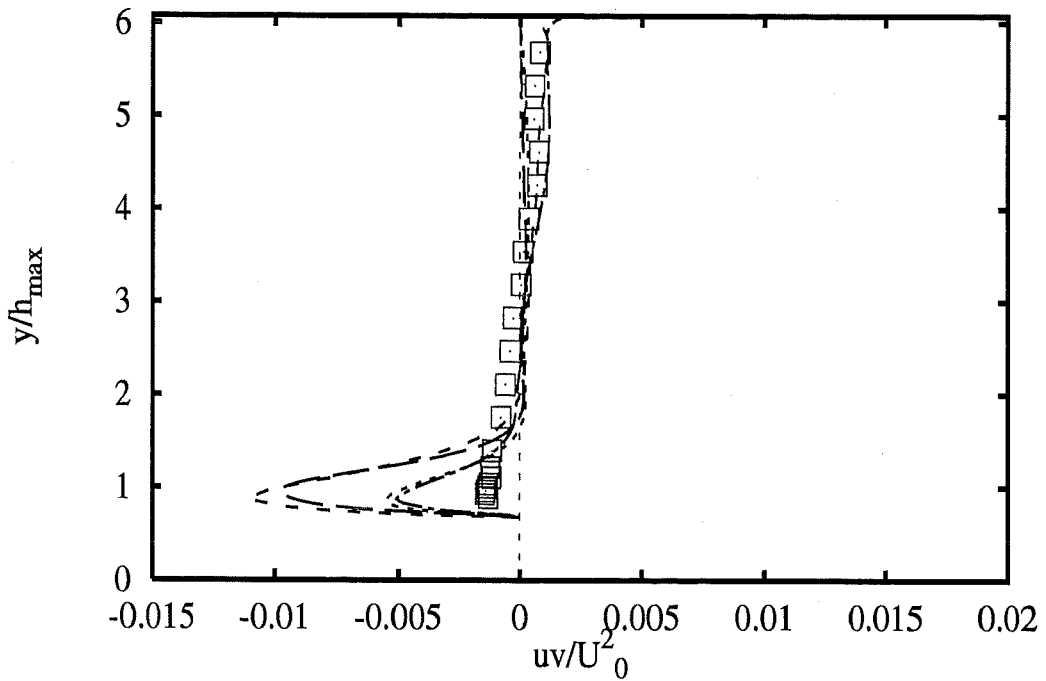
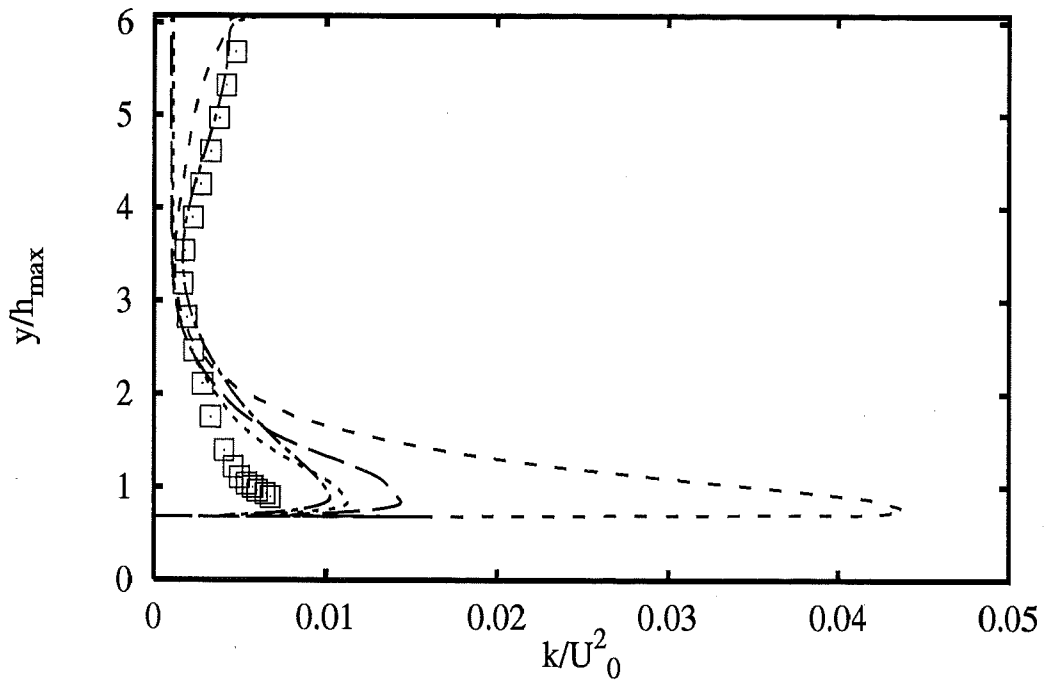
- Experiments \square
- UFlorenc hKE std+RMM ---
- Iolomouc hKE std+Gol - - -
- UFlorenc hKE std+Kim ·····
- CompDyna hKE RNG+NoRe - · - ·



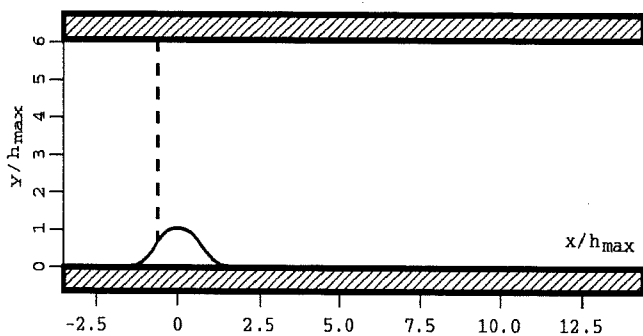
Profiles at $x/h_{max} = -0.71$



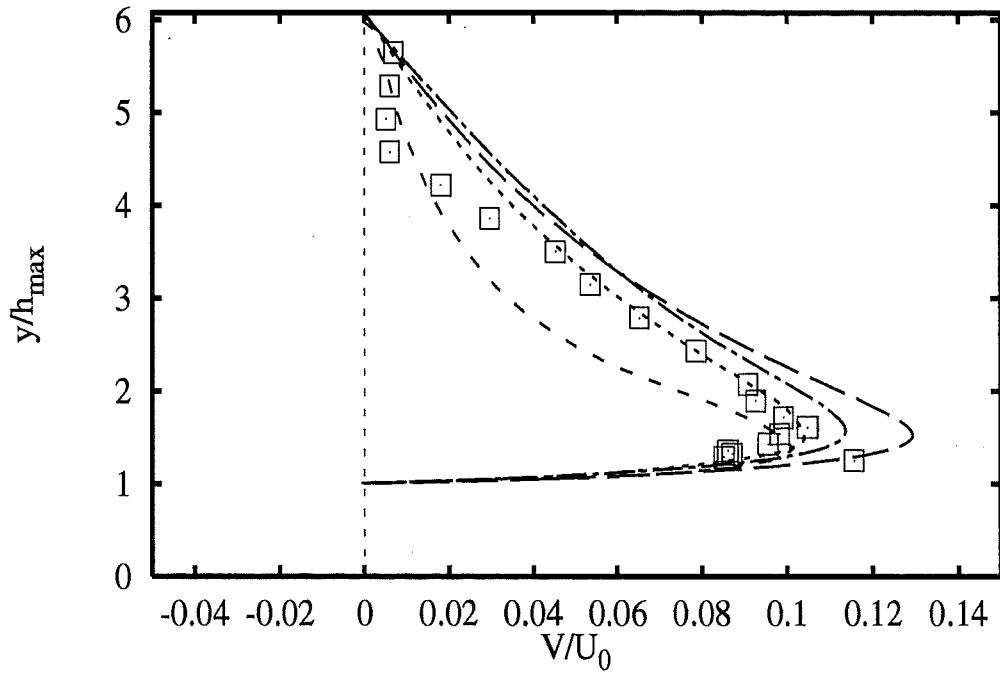
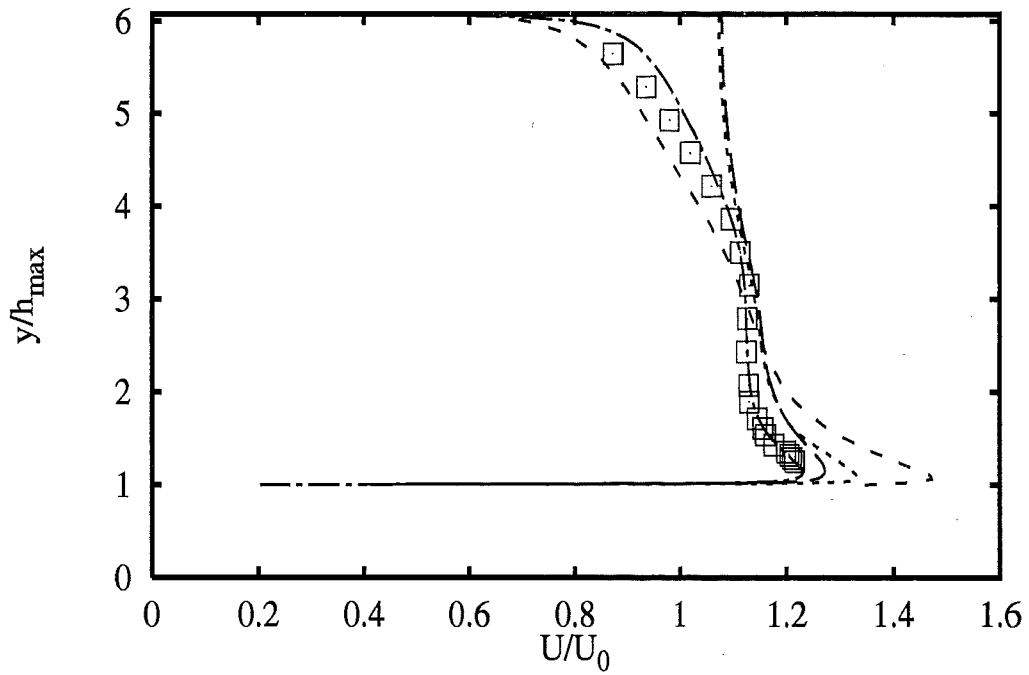
| | | |
|-----------------|---------------------|-----|
| | Experiments | □ |
| <i>UFlorenc</i> | <i>hKE std+RMM</i> | --- |
| <i>Iolomouc</i> | <i>hKE std+Gol</i> | --- |
| <i>UFlorenc</i> | <i>hKE std+Kim</i> | --- |
| <i>CompDyna</i> | <i>hKE RNG+NoRe</i> | --- |



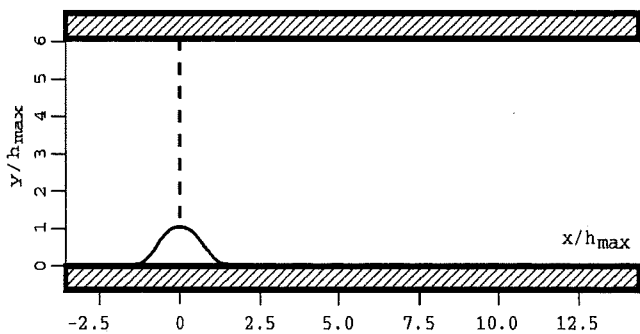
Profiles at $x/h_{max} = -0.71$



- | | | |
|-----------------|---------------------|-------|
| | Experiments | □ |
| <i>UFlorenc</i> | <i>hKE std+RMM</i> | --- |
| <i>Iolomouc</i> | <i>hKE std+Gol</i> | --- |
| <i>UFlorenc</i> | <i>hKE std+Kim</i> | |
| <i>CompDyna</i> | <i>hKE RNG+NoRe</i> | --- |

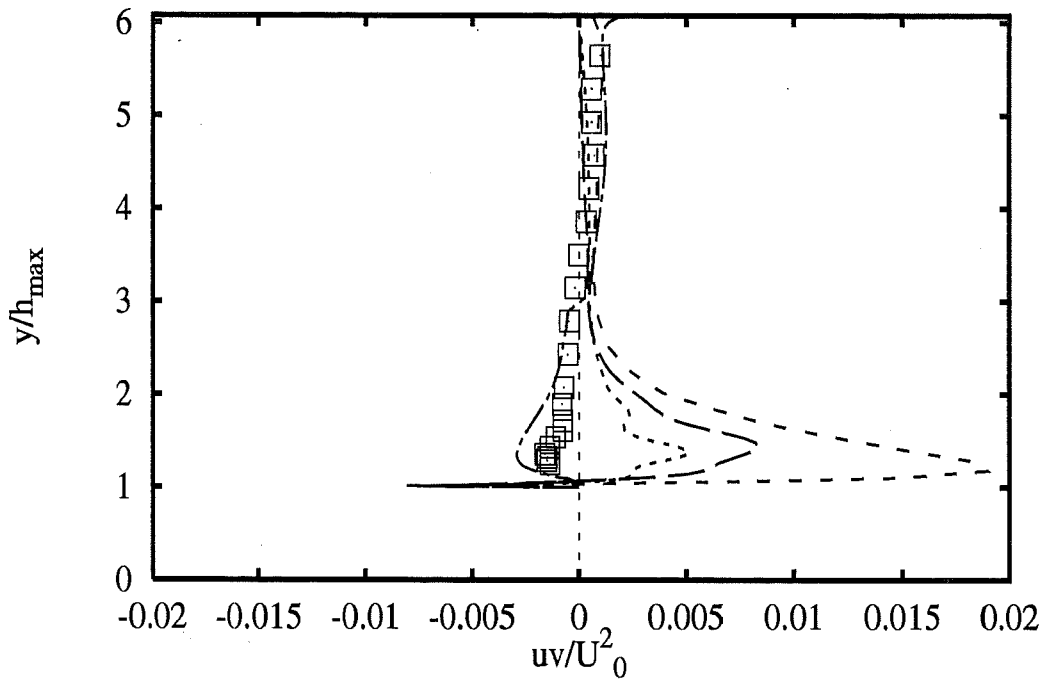
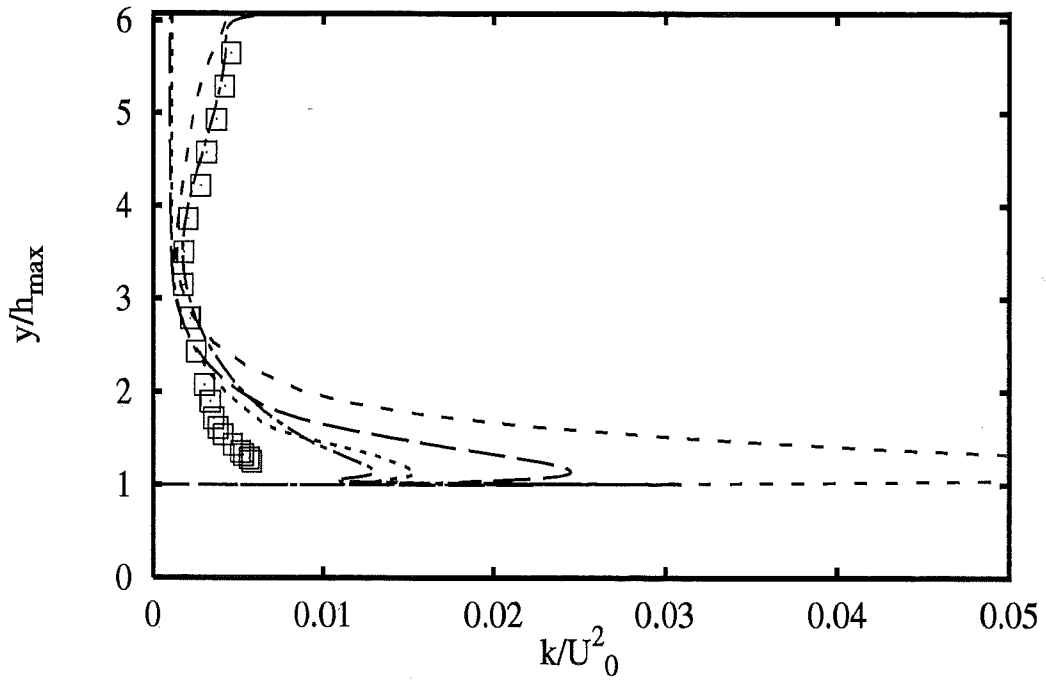


Profiles at $x/h_{max} = 0$

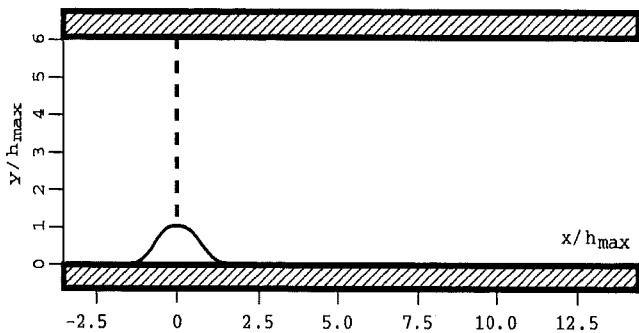


| | | |
|-----------------|---------------------|-----------|
| | Experiments | □ |
| <i>UFlorenc</i> | <i>hKE std+RMM</i> | — — |
| <i>Iolomouc</i> | <i>hKE std+Gol</i> | - - - |
| <i>UFlorenc</i> | <i>hKE std+Kim</i> | ⋯⋯⋯ |
| <i>CompDyna</i> | <i>hKE RNG+NoRe</i> | - · - · - |

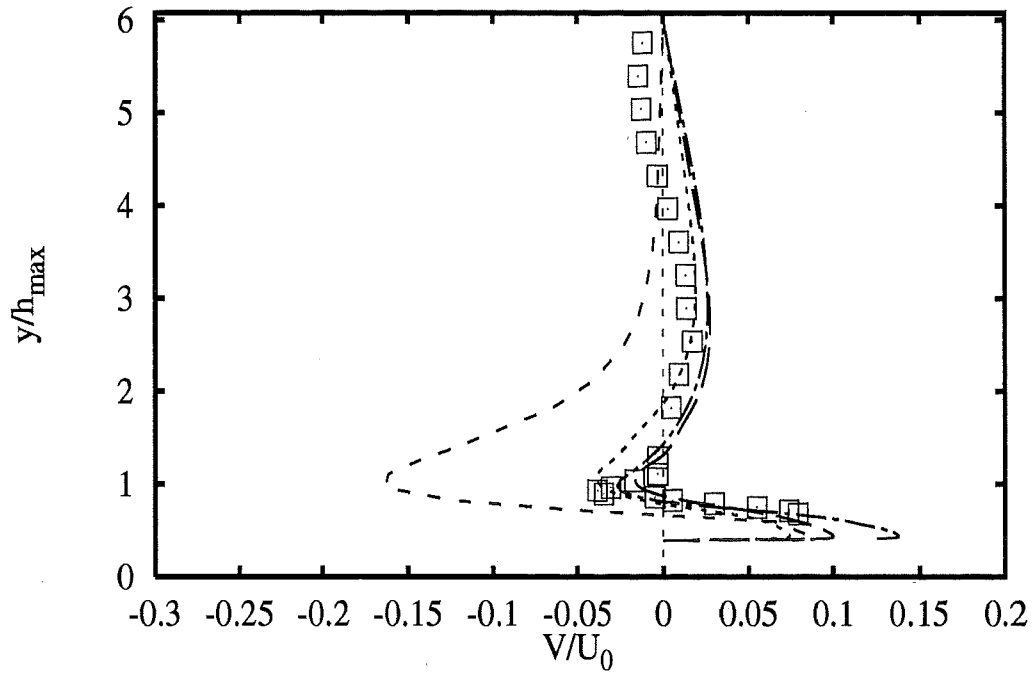
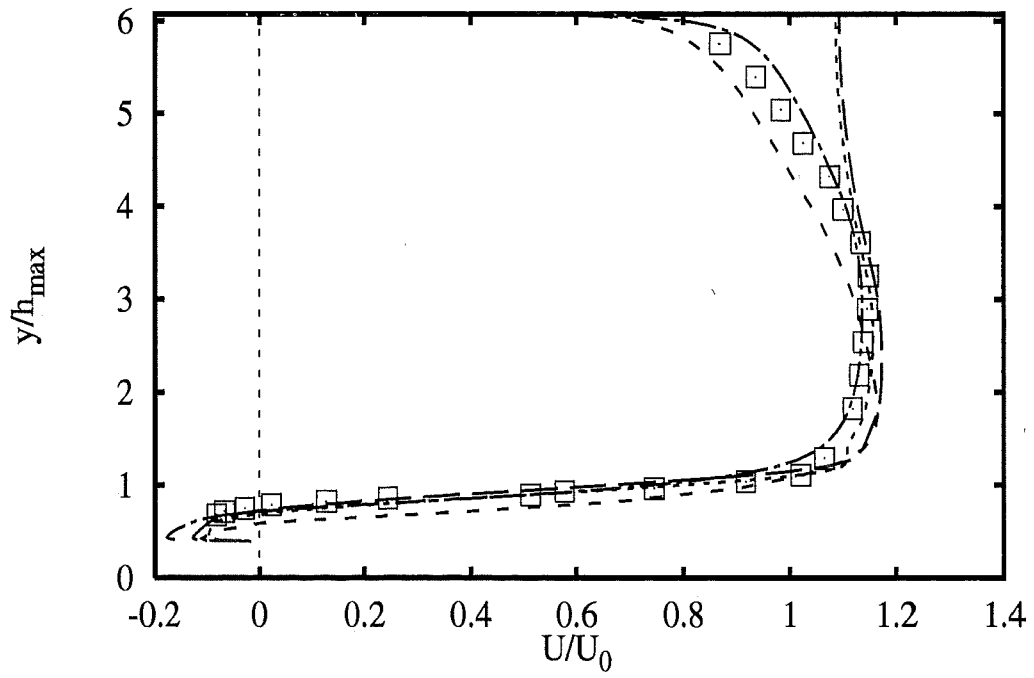
2A - 61



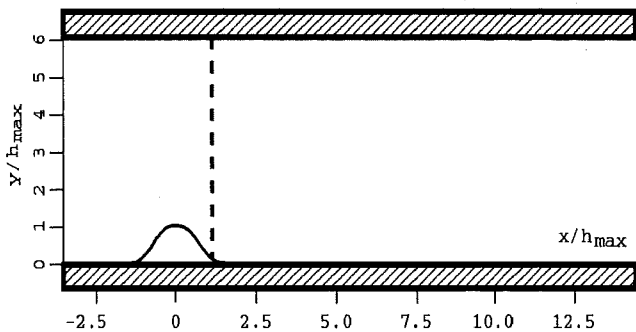
Profiles at $x/h_{max} = 0$



- | | | |
|-----------------|---------------------|-----|
| | Experiments | □ |
| <i>UFlorenc</i> | <i>hKE std+RMM</i> | --- |
| <i>Iolomouc</i> | <i>hKE std+Gol</i> | --- |
| <i>UFlorenc</i> | <i>hKE std+Kim</i> | --- |
| <i>CompDyna</i> | <i>hKE RNG+NoRe</i> | --- |

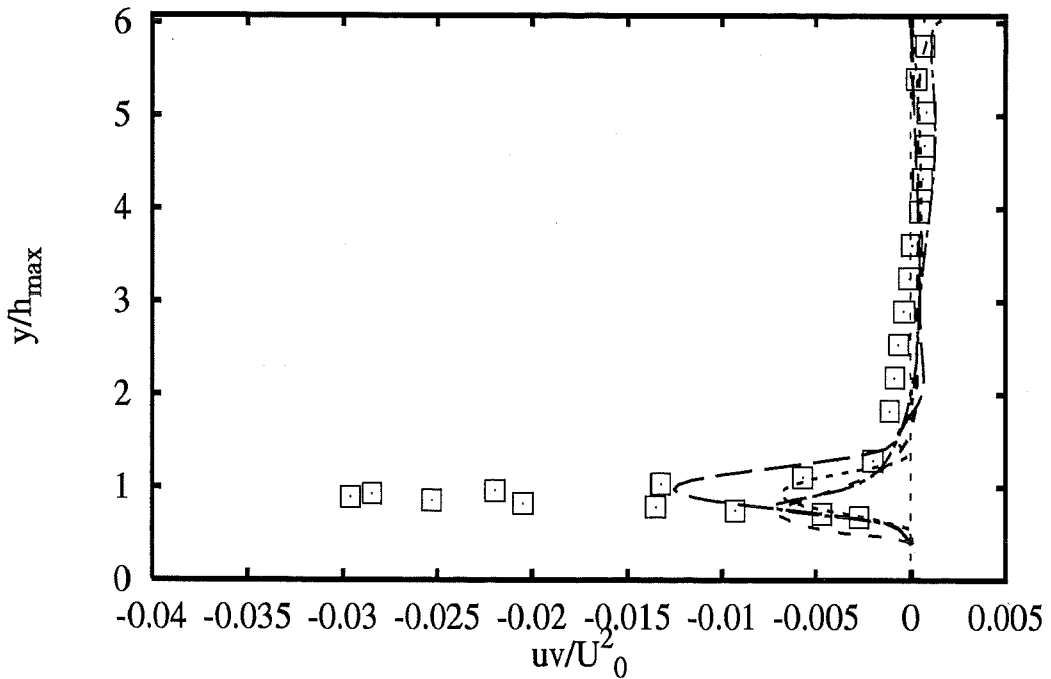
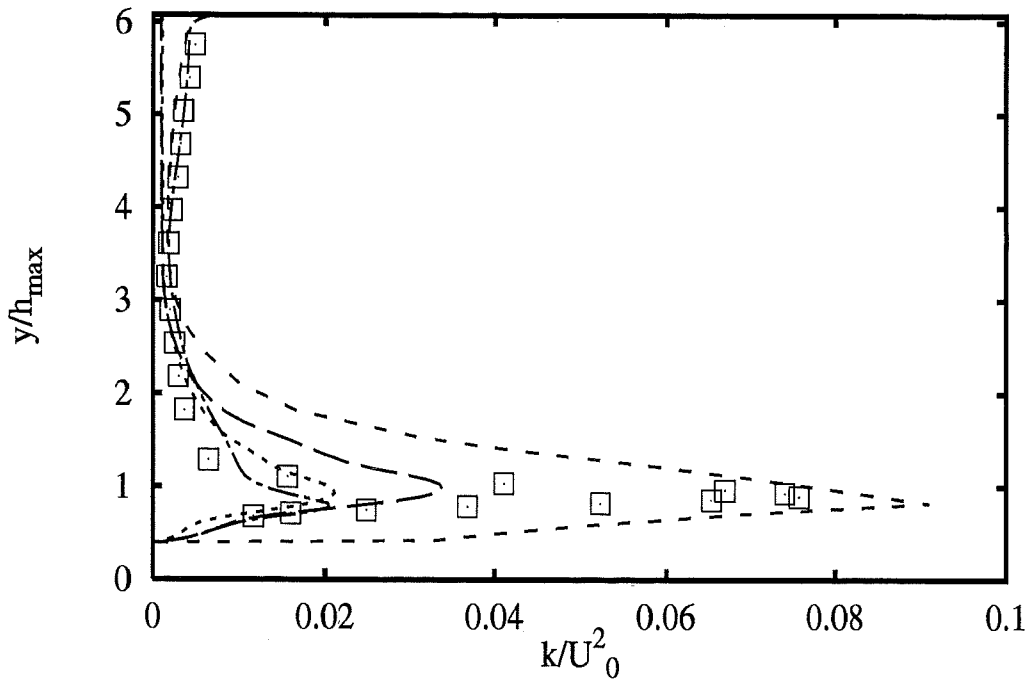


Profiles at $x/h_{max} = 1.07$

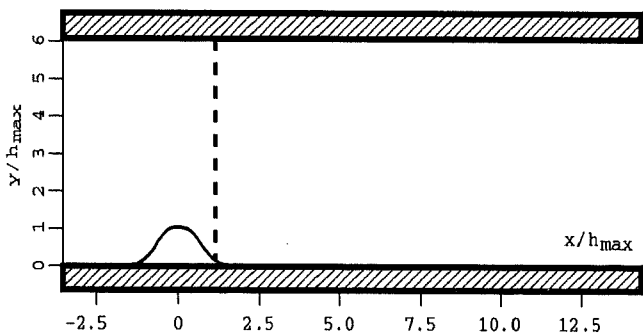


- | | | |
|-----------------|---------------------|-----------|
| | Experiments | □ |
| <i>UFlorenc</i> | <i>hKE std+RMM</i> | — |
| <i>Iolomouc</i> | <i>hKE std+Gol</i> | - - - |
| <i>UFlorenc</i> | <i>hKE std+Kim</i> | · · · · · |
| <i>CompDyna</i> | <i>hKE RNG+NoRe</i> | - - - - - |

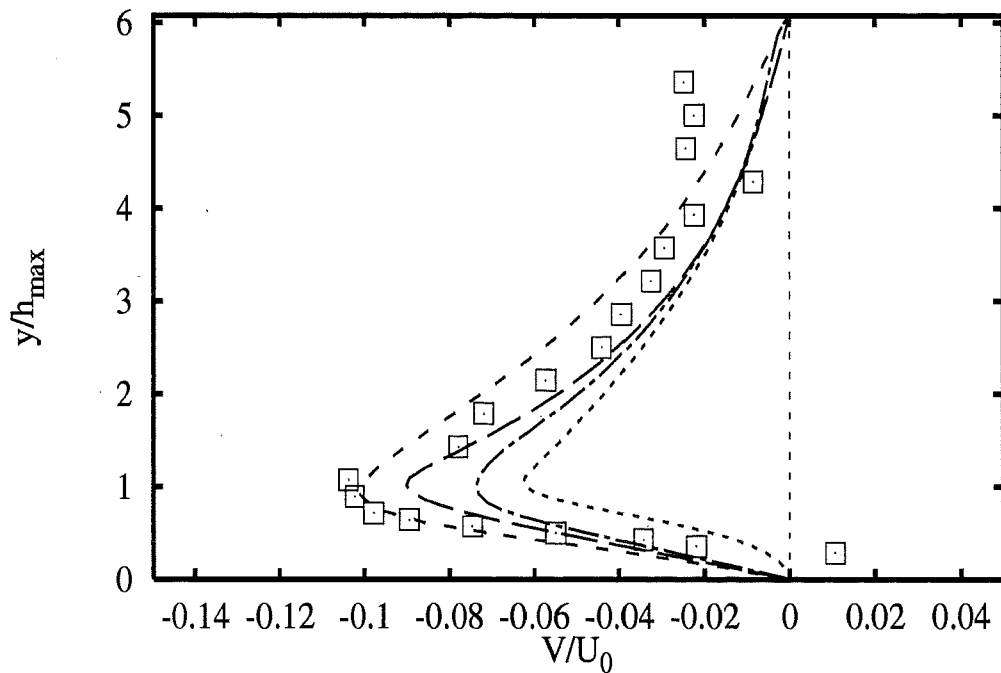
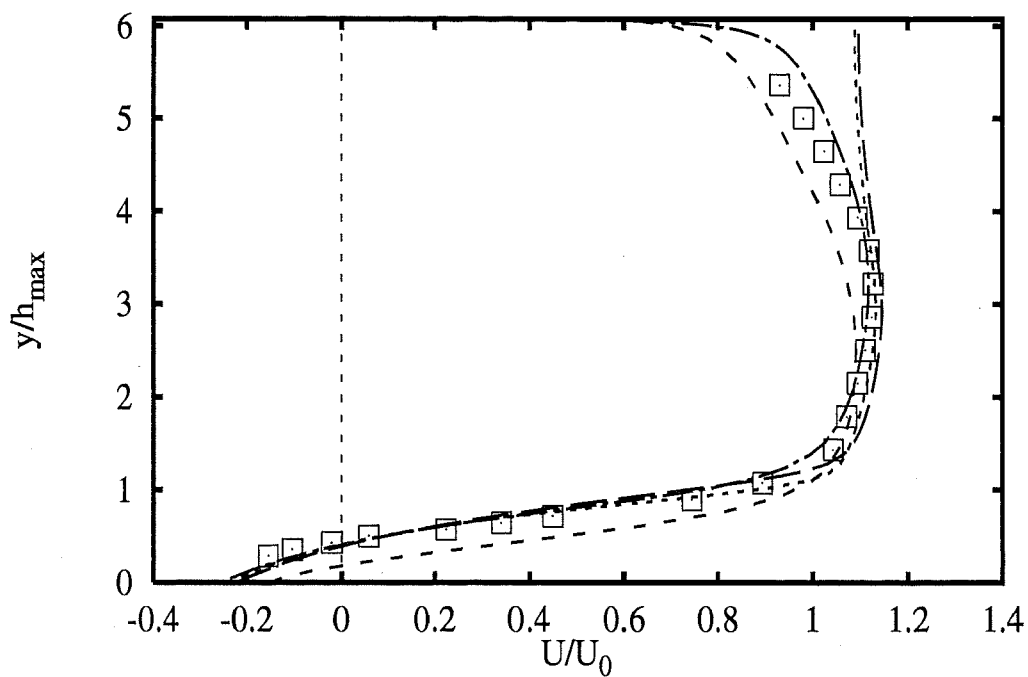
2A - 63



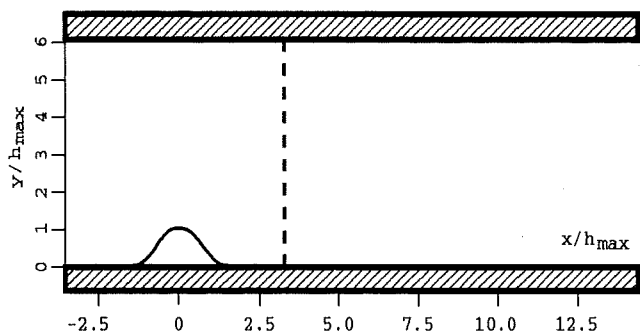
Profiles at $x/h_{max} = 1.07$



- | | | |
|-----------------|---------------------|-----|
| | Experiments | □ |
| <i>UFlorenc</i> | <i>hKE std+RMM</i> | --- |
| <i>Iolomouc</i> | <i>hKE std+Gol</i> | --- |
| <i>UFlorenc</i> | <i>hKE std+Kim</i> | --- |
| <i>CompDyna</i> | <i>hKE RNG+NoRe</i> | --- |

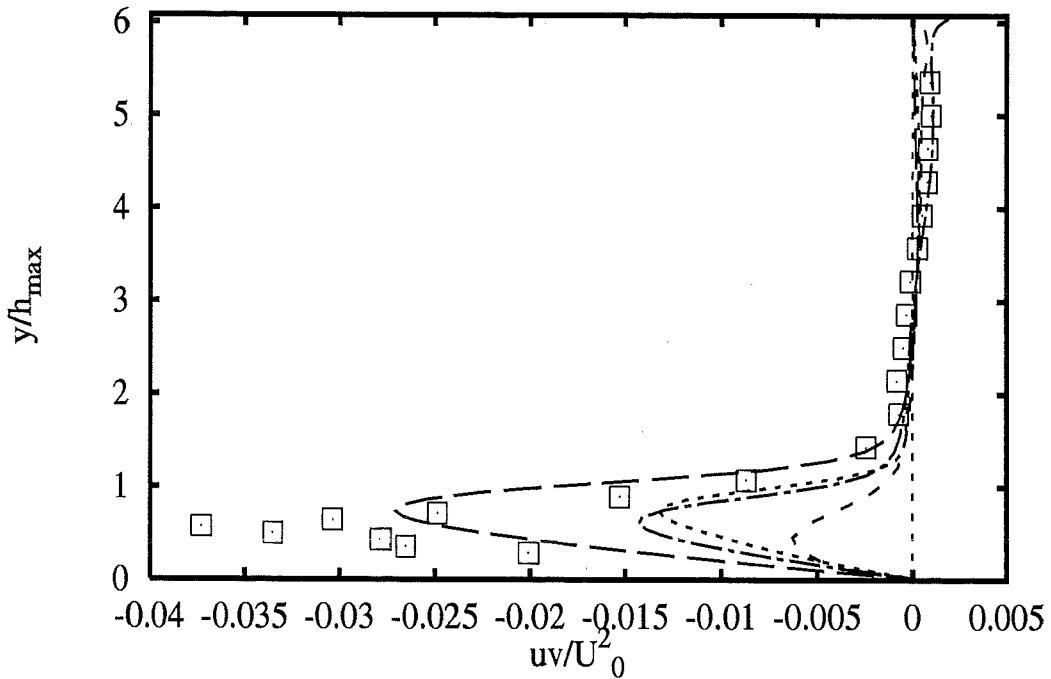
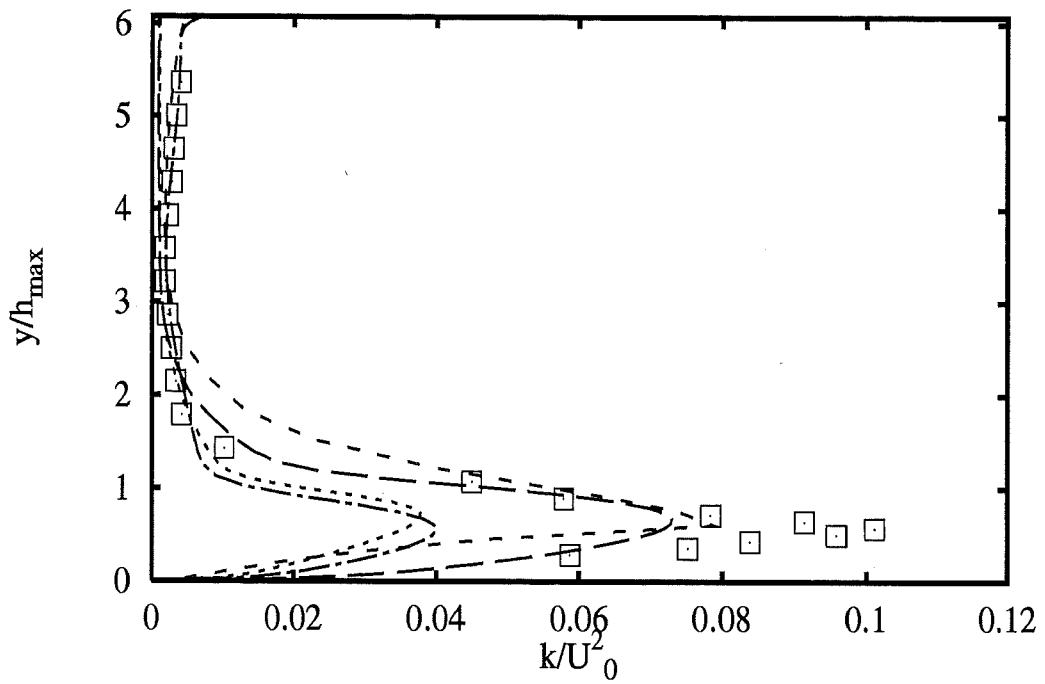


Profiles at $x/h_{max} = 3.21$

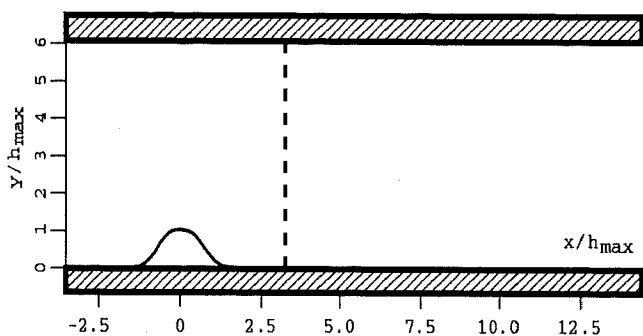


- | | |
|-------------------------------------|-------|
| Experiments | □ |
| <i>UFlorenc</i> hKE std+RMM | --- |
| <i>Iolomouc</i> hKE std+Gol | ---- |
| <i>UFlorenc</i> hKE std+Kim | |
| <i>CompDyna</i> hKE RNG+NoRe | ----- |

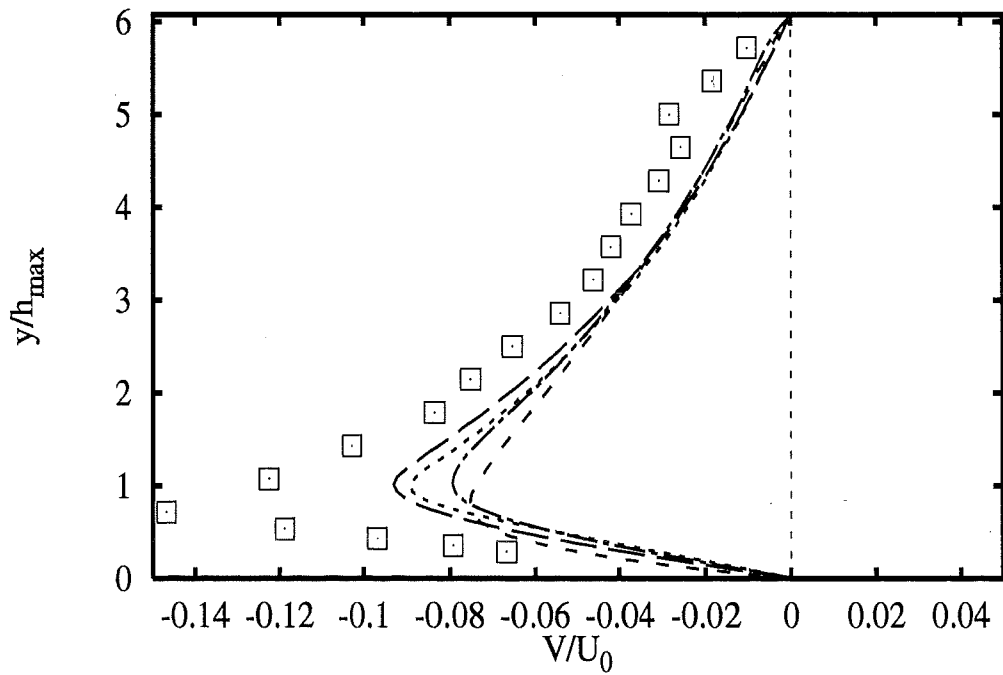
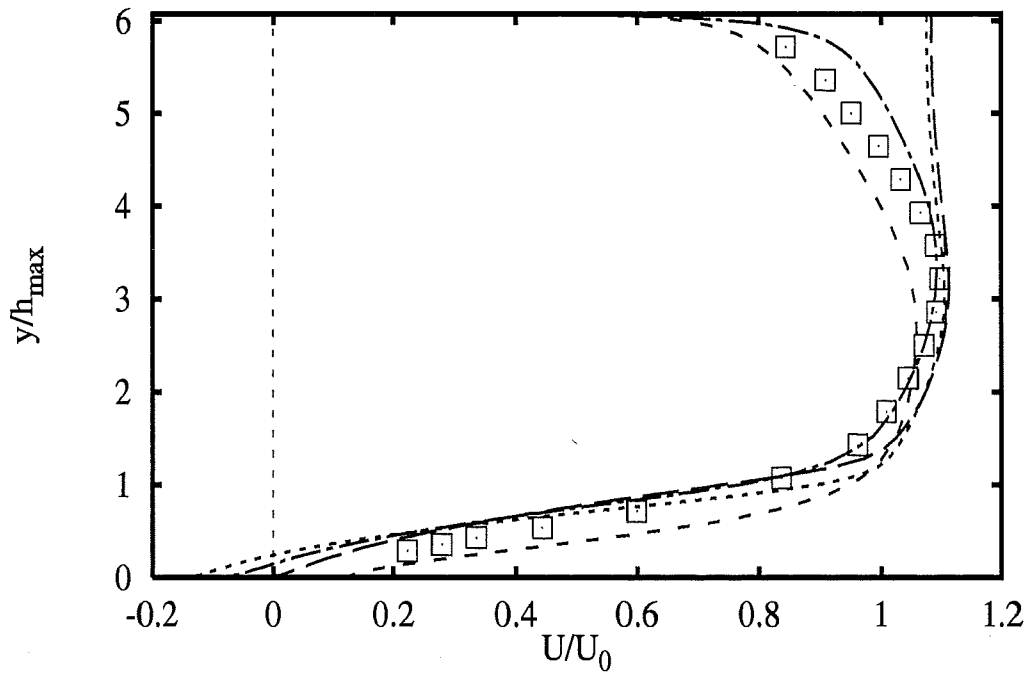
2A - 65



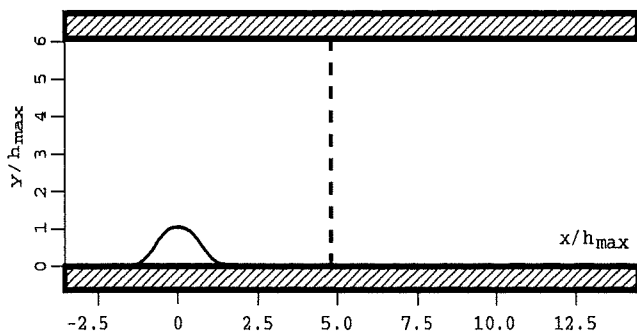
Profiles at $x/h_{max} = 3.21$



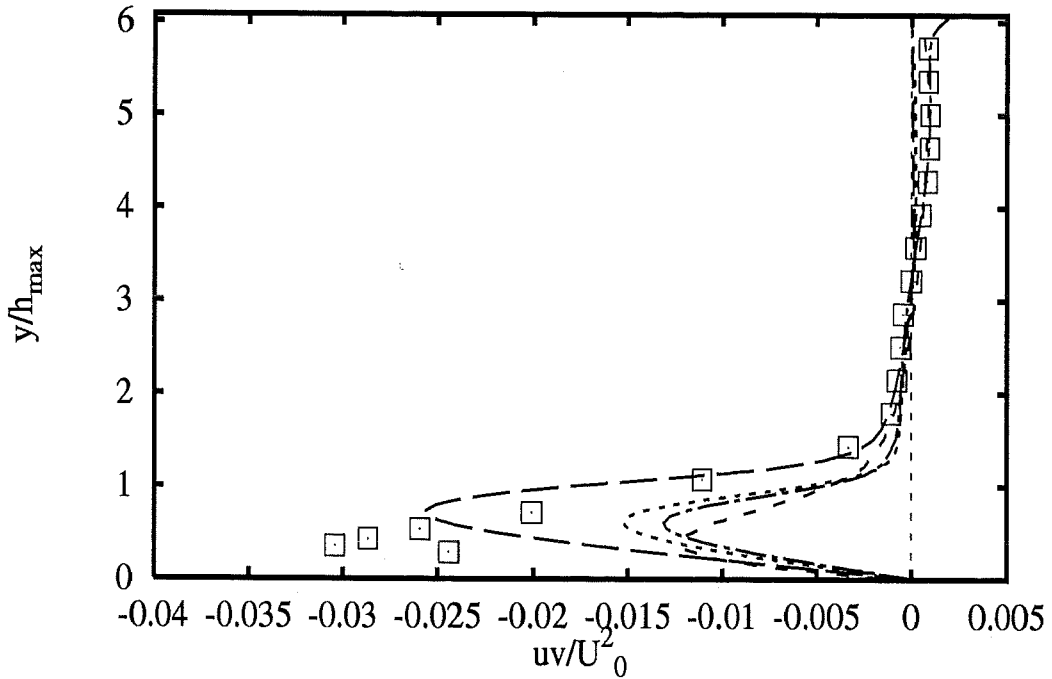
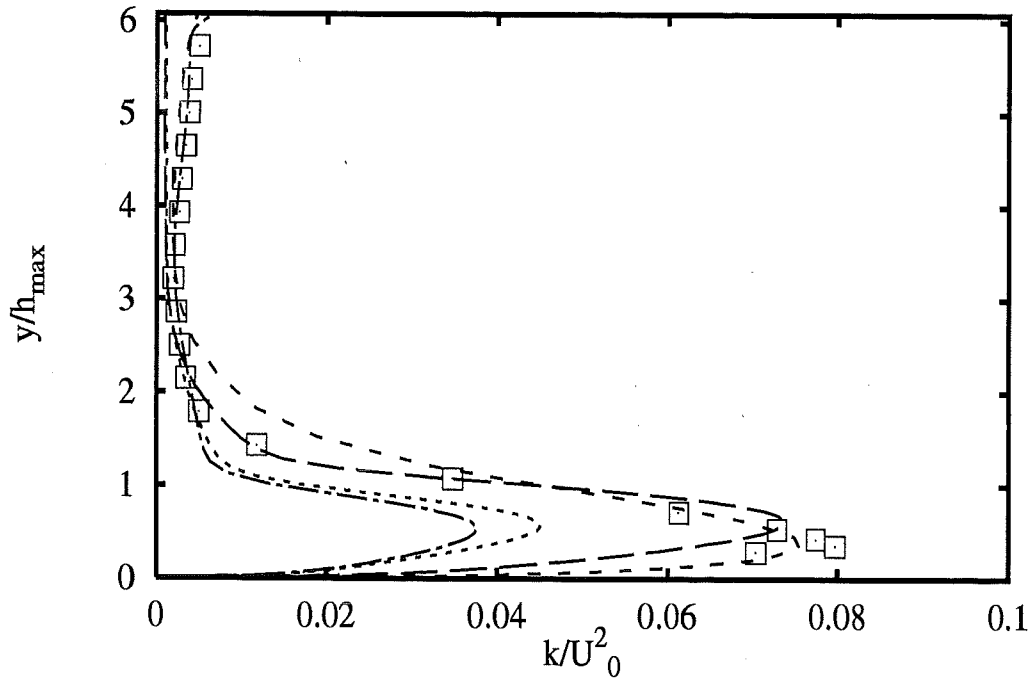
- | | |
|-----------------------|-----------|
| Experiments | □ |
| UFlorenc hKE std+RMM | --- |
| IOlomouc hKE std+Gol | - - - |
| UFlorenc hKE std+Kim | |
| CompDyna hKE RNG+NoRe | - · - · - |



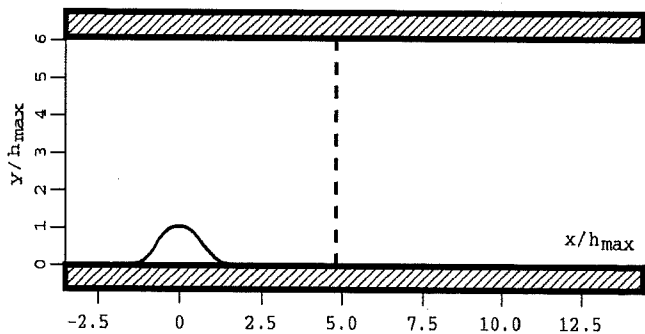
Profiles at $x/h_{max} = 4.79$



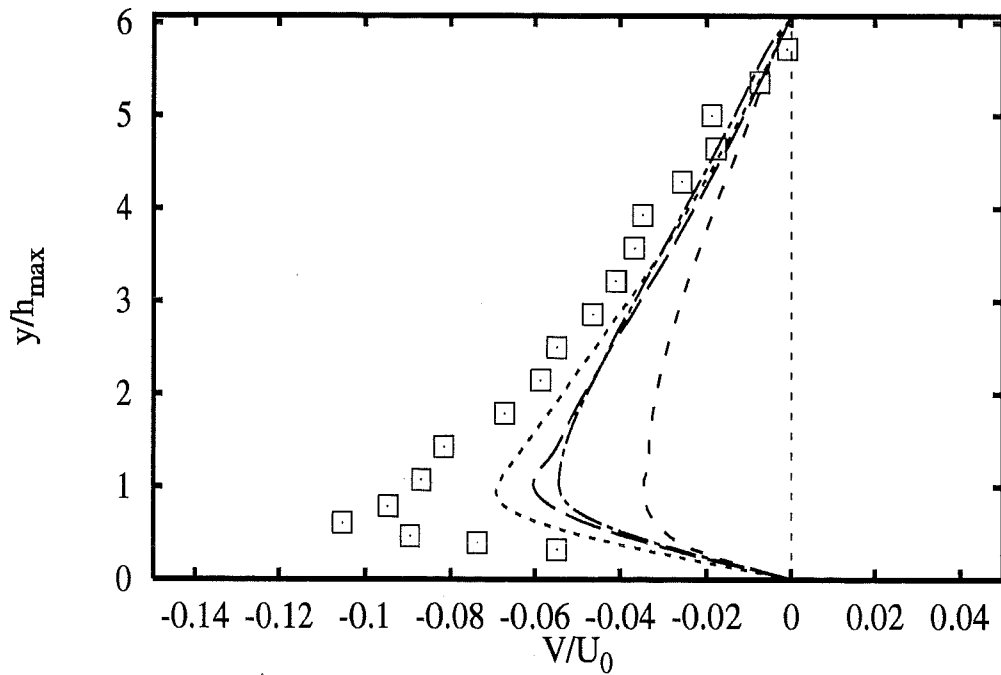
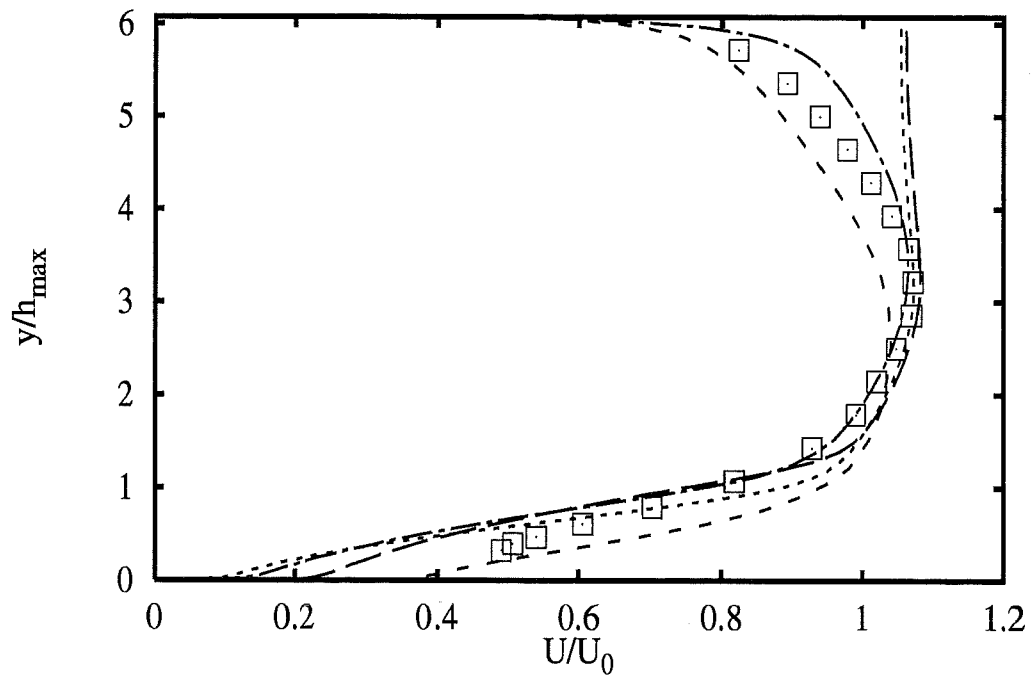
- | | | |
|-----------------|---------------------|-------|
| | Experiments | □ |
| <i>UFlorenc</i> | <i>hKE std+RMM</i> | — — |
| <i>Iolomouc</i> | <i>hKE std+Gol</i> | - - - |
| <i>UFlorenc</i> | <i>hKE std+Kim</i> | ⋯⋯⋯ |
| <i>CompDyna</i> | <i>hKE RNG+NoRe</i> | — · — |



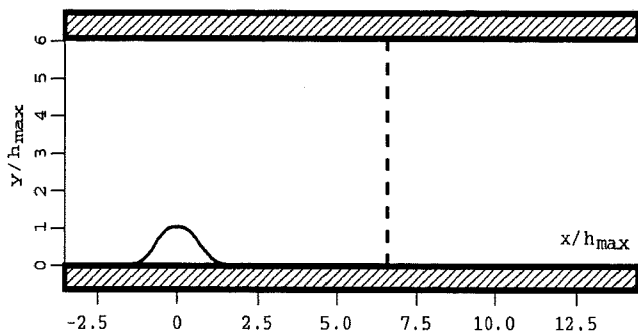
Profiles at $x/h_{max} = 4.79$



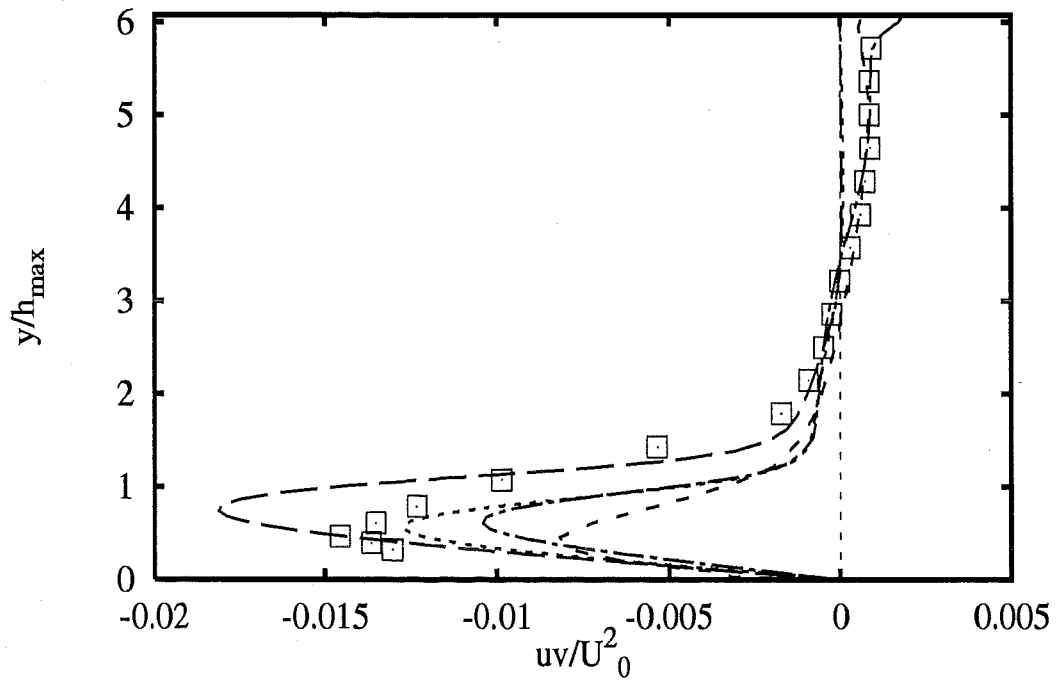
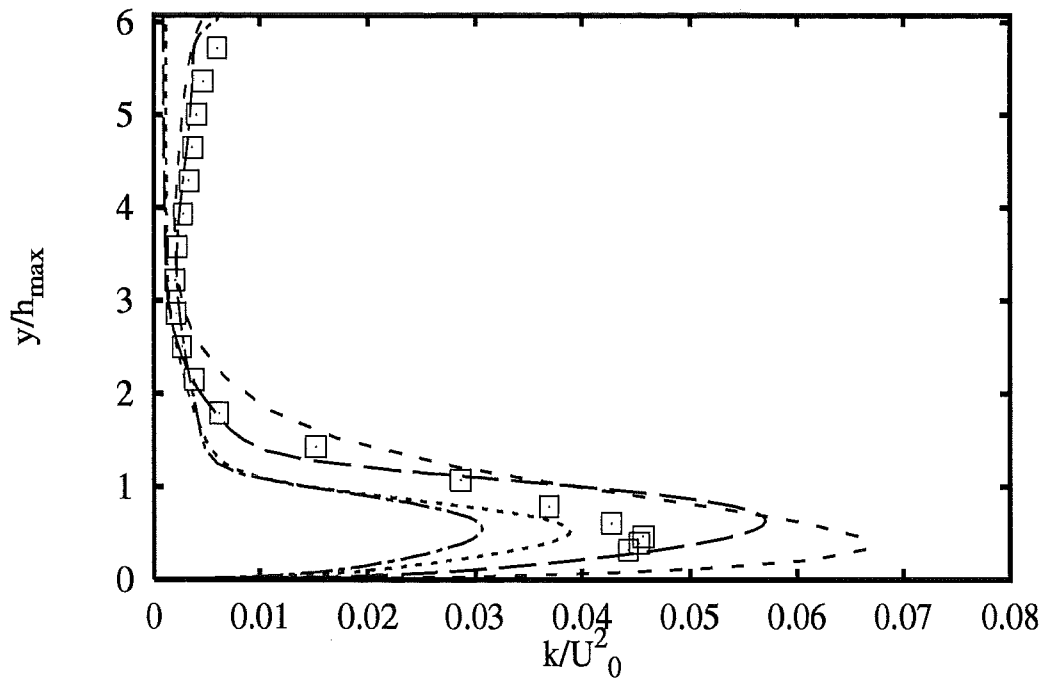
- | | | |
|-----------------|---------------------|-------|
| | Experiments | □ |
| <i>UFlorenc</i> | <i>hKE std+RMM</i> | --- |
| <i>Iolomouc</i> | <i>hKE std+Gol</i> | ---- |
| <i>UFlorenc</i> | <i>hKE std+Kim</i> | |
| <i>CompDyna</i> | <i>hKE RNG+NoRe</i> | -.-.- |



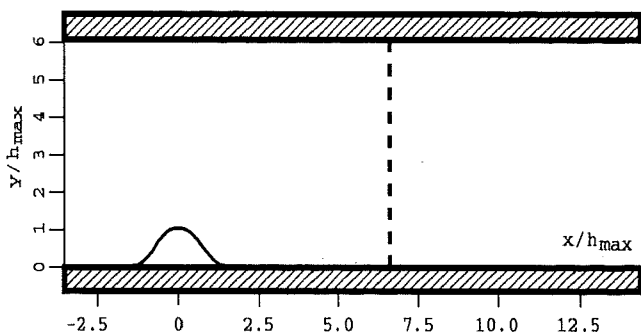
Profiles at $x/h_{max} = 6.61$



- | | |
|-------------------------------------|-------|
| Experiments | □ |
| <i>UFlorenc</i> hKE std+RMM | — — |
| <i>Iolomouc</i> hKE std+Gol | - - - |
| <i>UFlorenc</i> hKE std+Kim | · · · |
| <i>CompDyna</i> hKE RNG+NoRe | - · - |

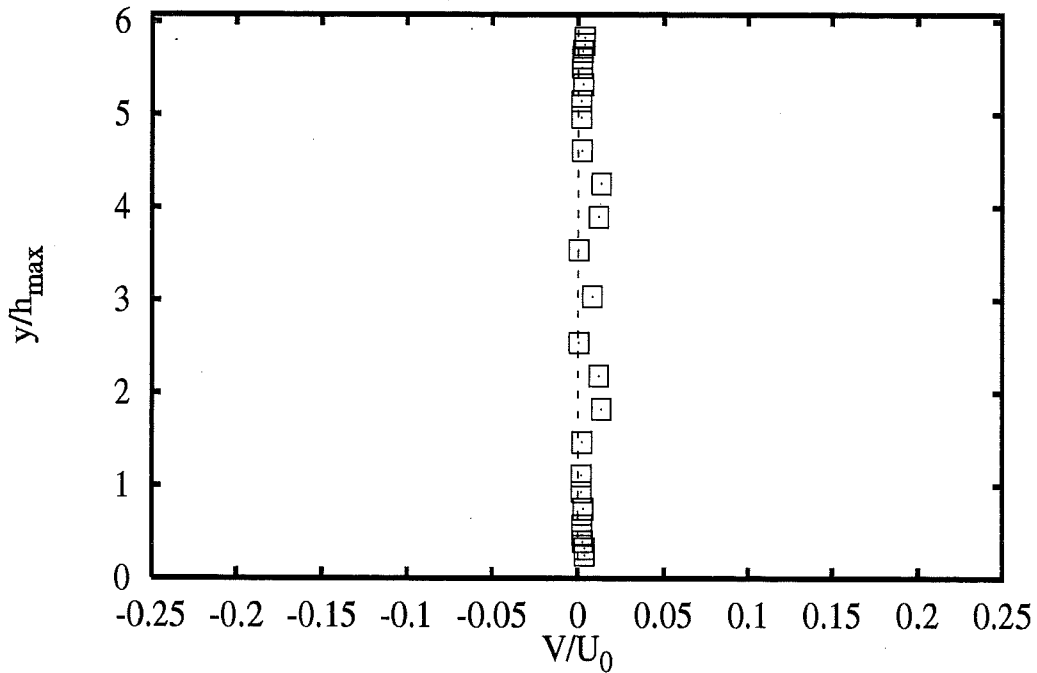
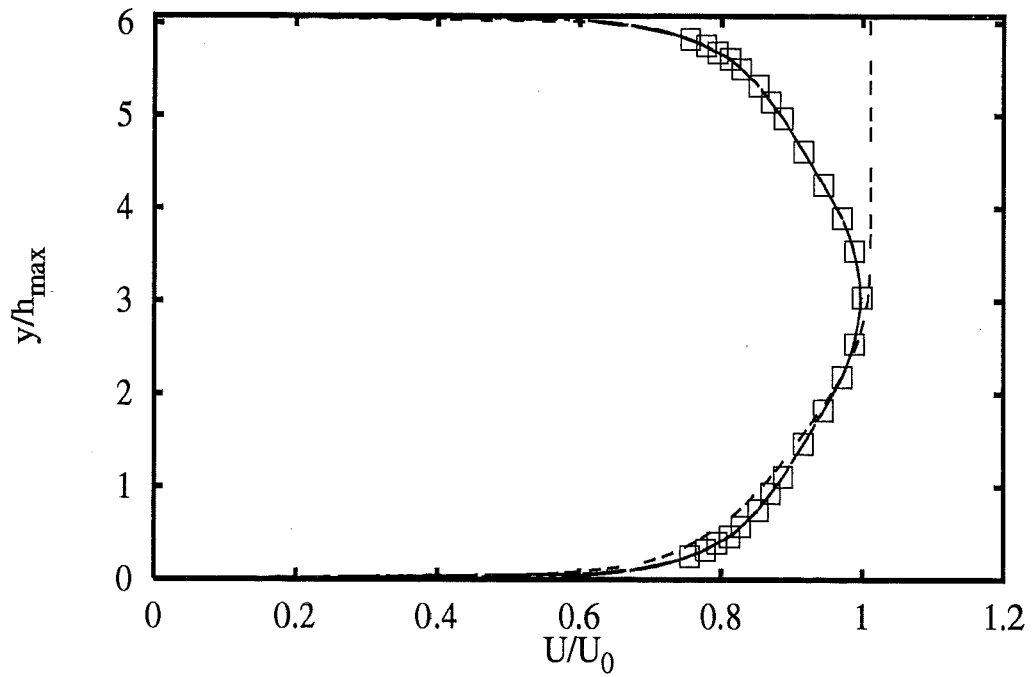


Profiles at $x/h_{max} = 6.61$

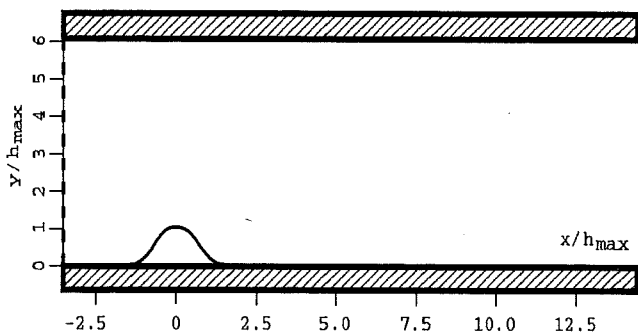


- | | | |
|-----------------|---------------------|-------|
| | Experiments | □ |
| <i>UFlorenc</i> | <i>hKE std+RMM</i> | — |
| <i>Iolomouc</i> | <i>hKE std+Gol</i> | - - - |
| <i>UFlorenc</i> | <i>hKE std+Kim</i> | ⋯ |
| <i>CompDyna</i> | <i>hKE RNG+NoRe</i> | - · - |

2A - 70

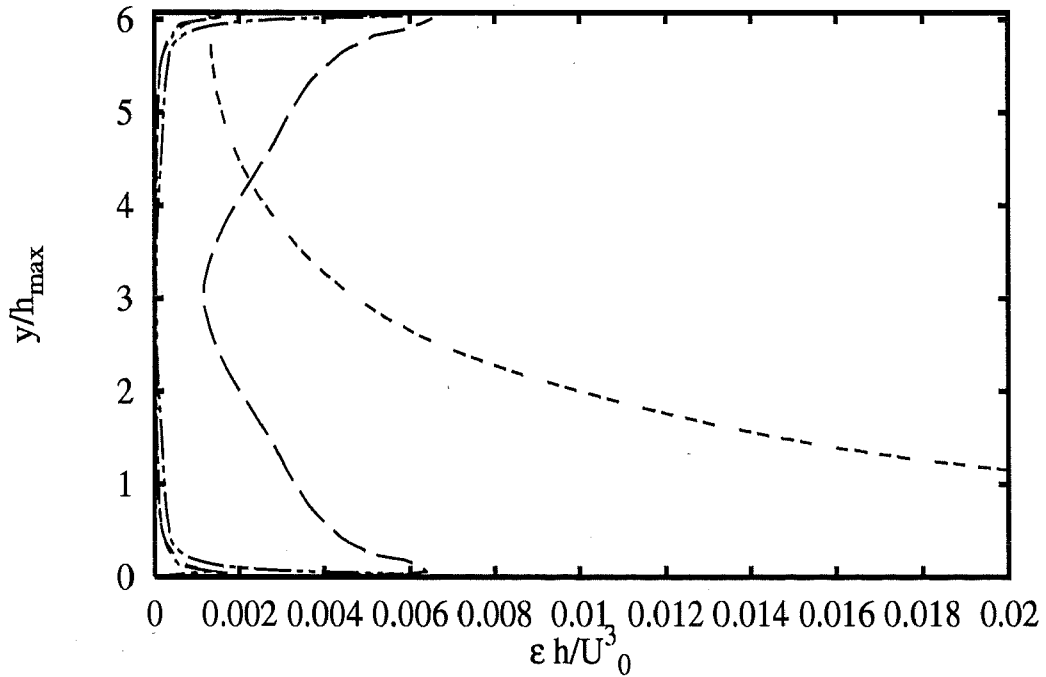
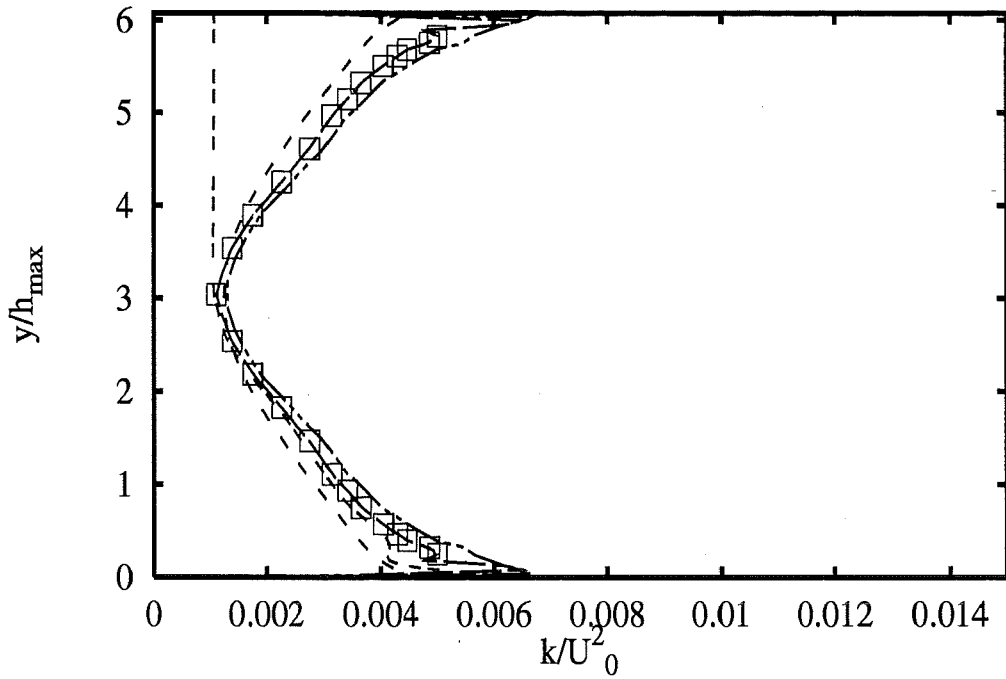


Profiles at $x/h_{max} = -3.57$

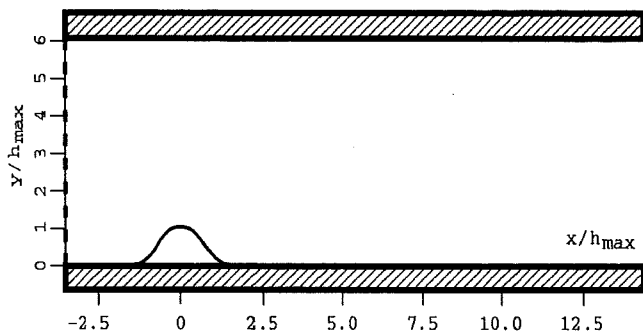


- Experiments** □
- UChalmer lKE LaSh ---
 - EDFLNHLa lKE LaSh ---
 - UChalmer lKE LiLe ---
 - UMISTLes lKE LiLe ---
 - UFlorenc lKE NaHi ---

2A - 71



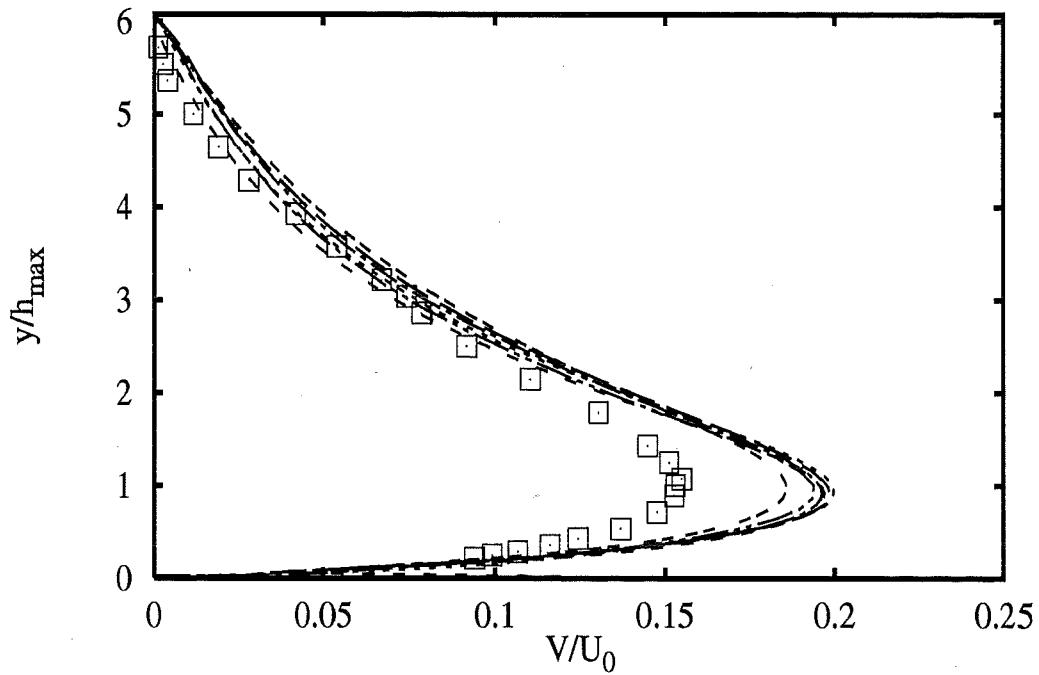
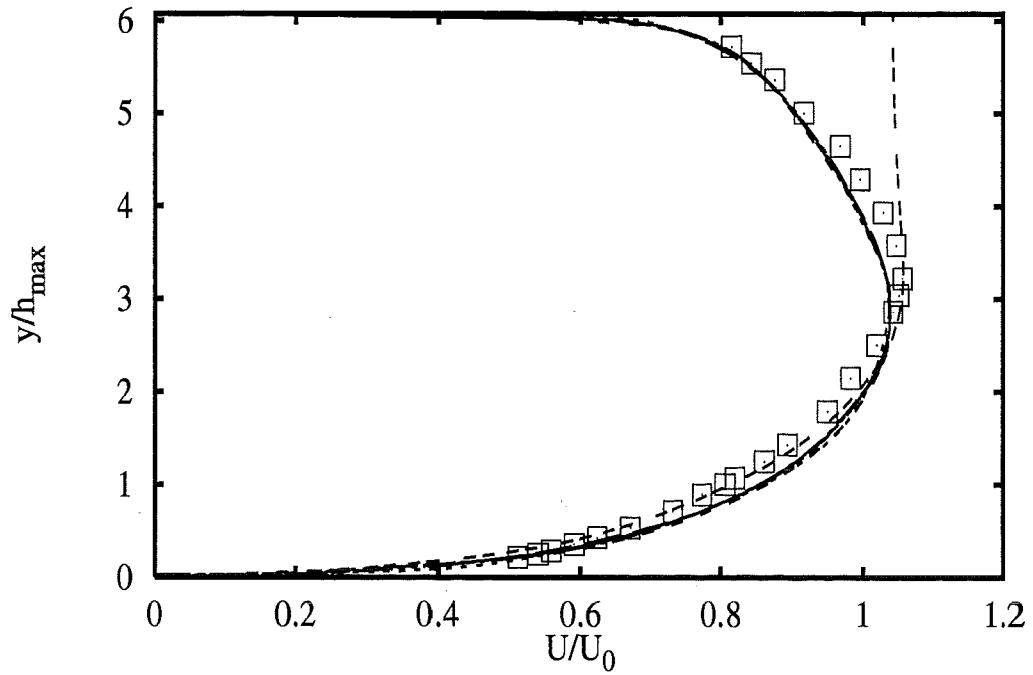
Profiles at $x/h_{max} = -3.57$



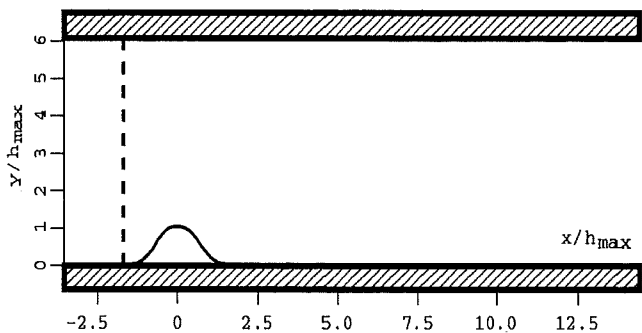
Experiments □

| | | | |
|-----------------|------------|-------------|-----|
| UChalmer | lKE | LaSh | --- |
| EDFLNHLa | lKE | LaSh | --- |
| UChalmer | lKE | LiLe | --- |
| UMISTLes | lKE | LiLe | --- |
| UFlorenc | lKE | NaHi | --- |

2A - 72

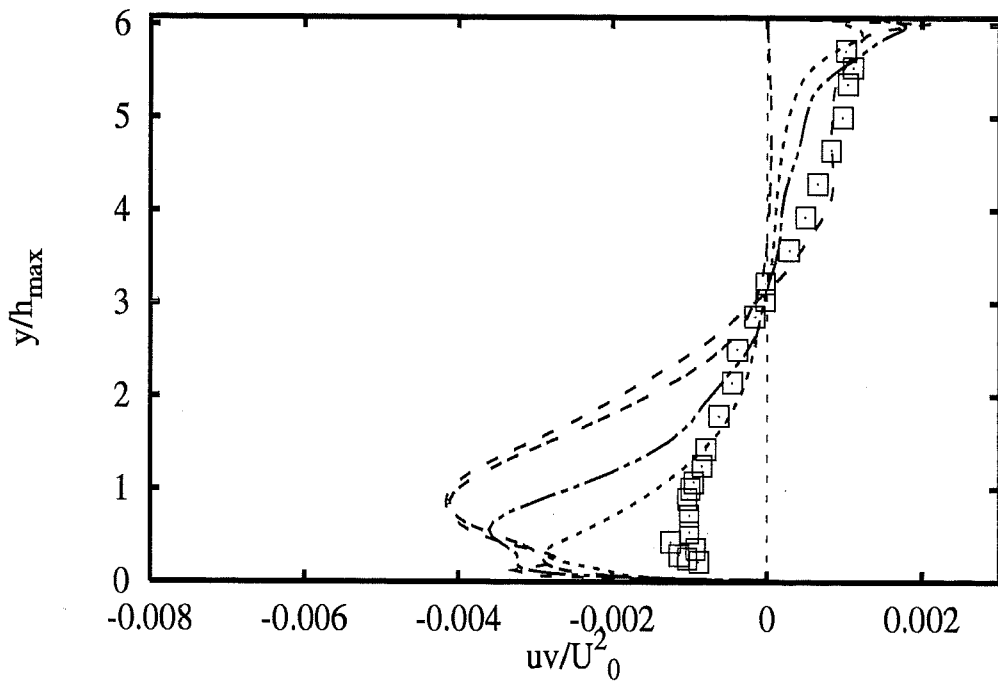
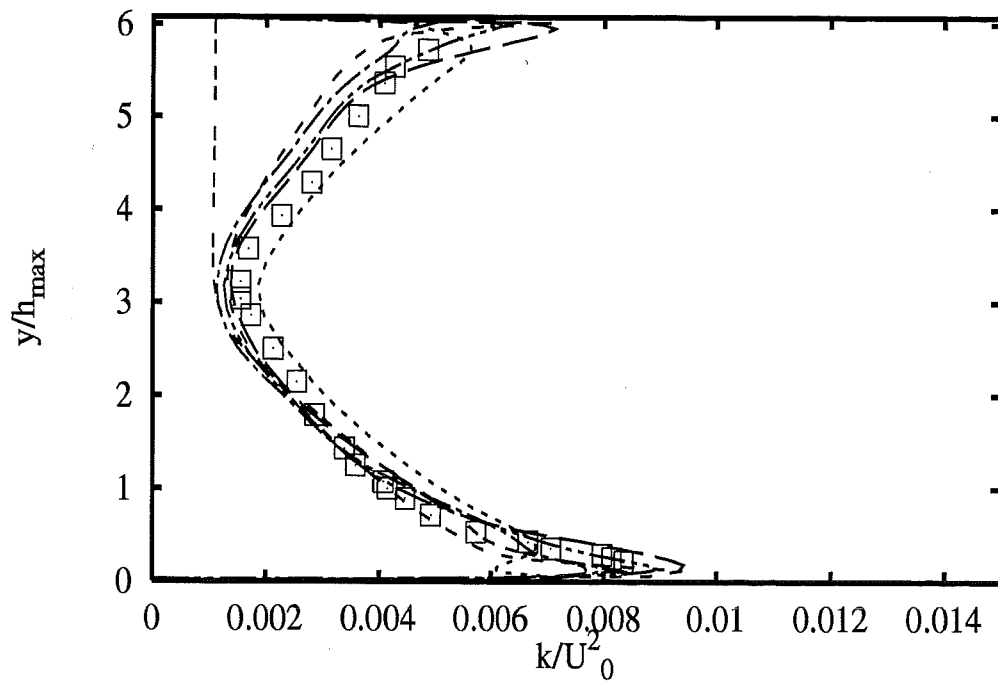


Profiles at $x/h_{max} = -1.78$

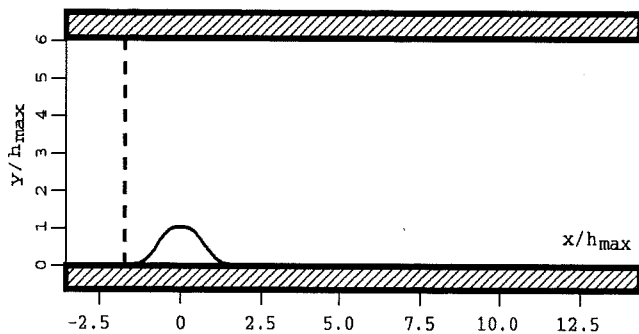


- Experiments** □
- UChalmer lKE LaSh ---
 - EDFLNHLA lKE LaSh - - -
 - EPFLausa lKE LaBr ·····
 - UChalmer lKE LiLe - - -
 - UMISTLes lKE LiLe ·····
 - UFlorenc lKE NaHi - - -

2A - 73

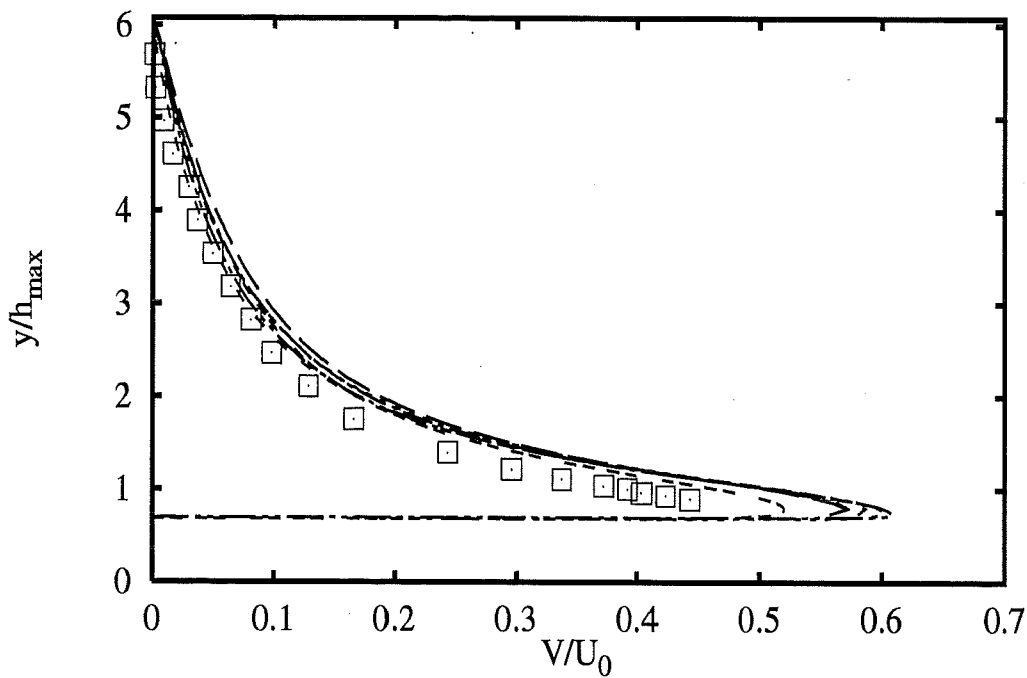
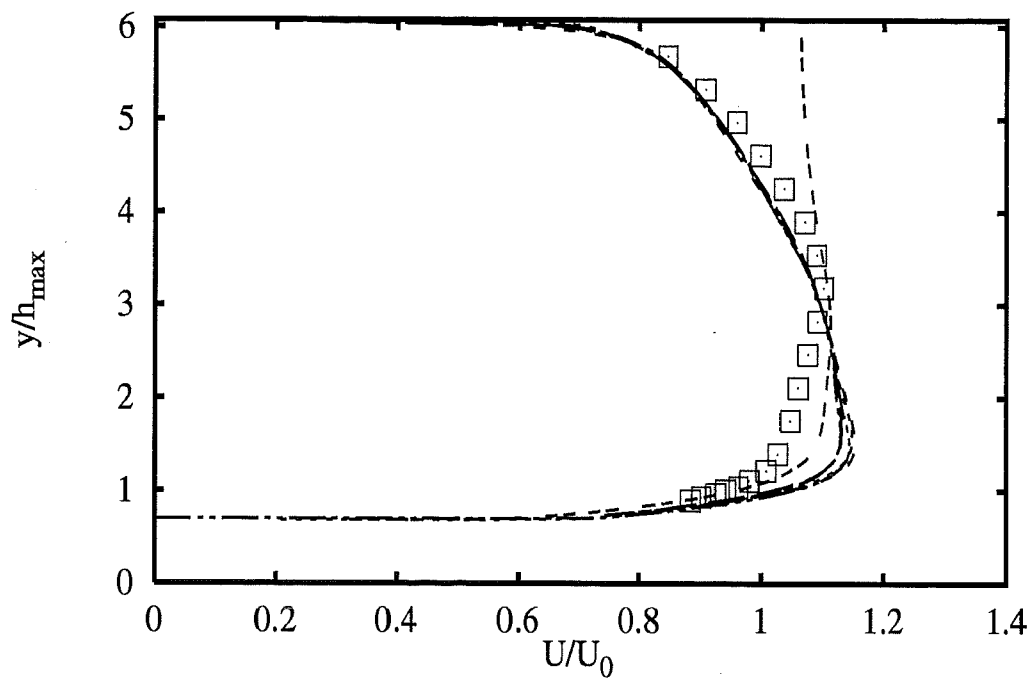


Profiles at $x/h_{max} = -1.78$

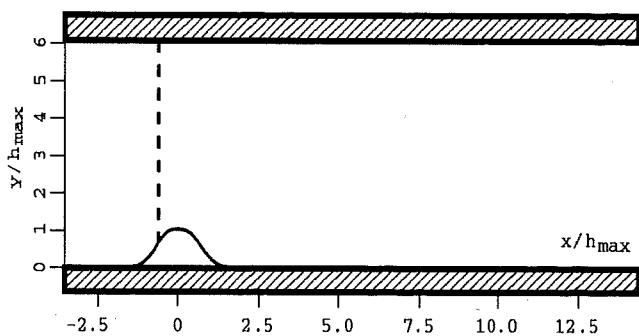


- Experiments** □
- UChalmer IKE LaSh ---
 - EDFLNHLA IKE LaSh - - -
 - EPFLausa IKE LaBr ·····
 - UChalmer IKE LiLe - · - ·
 - UMISTLes IKE LiLe - · - ·
 - UFlorenc IKE NaHi - - -

2A - 74

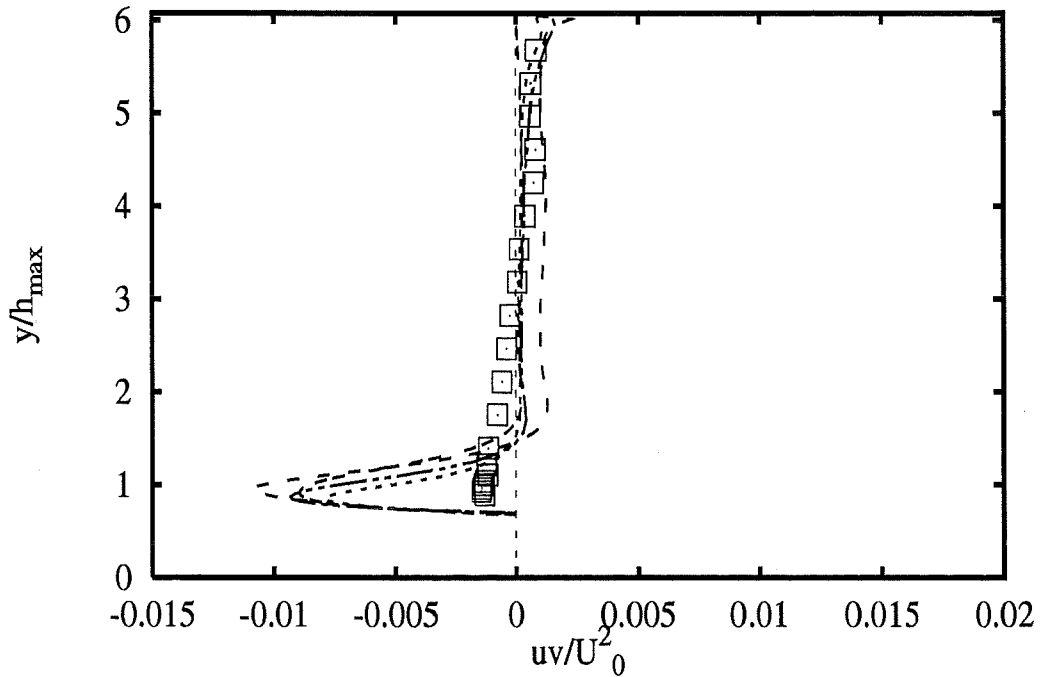
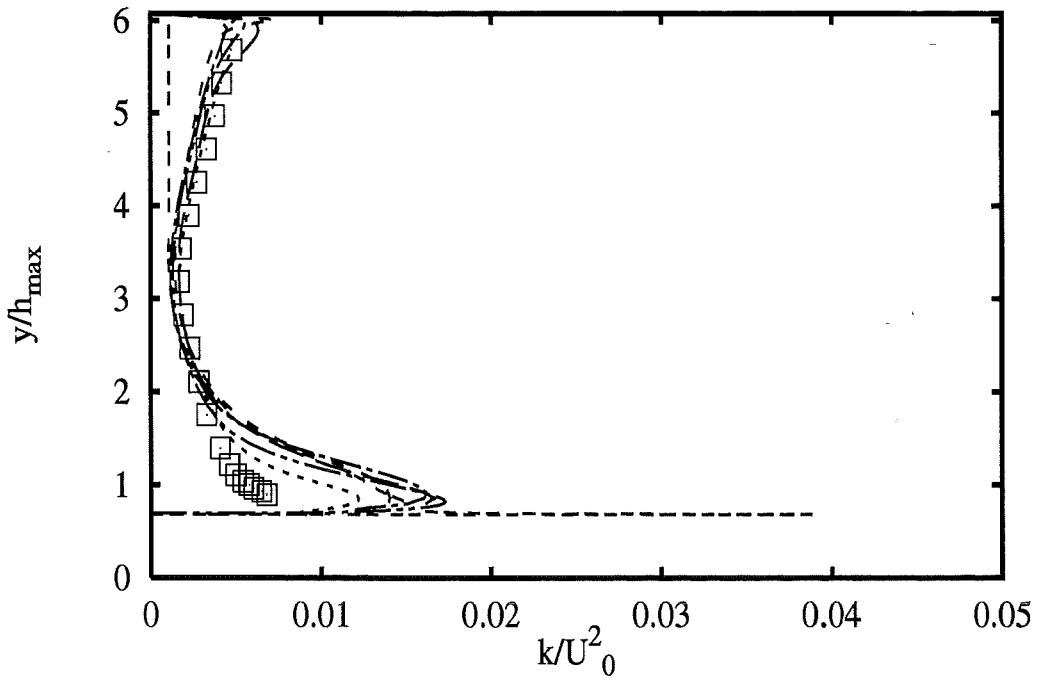


Profiles at $x/h_{max} = -0.71$

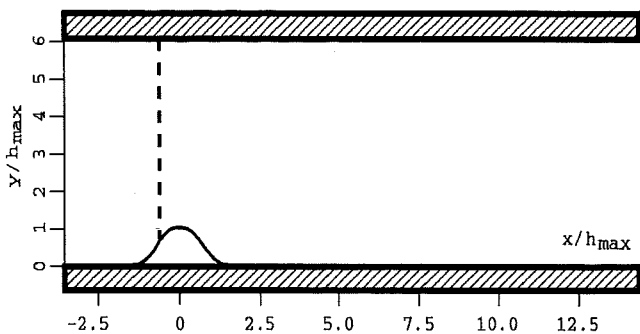


- Experiments** □
- UChalmer IKE LaSh ---
 - EDFLNHLa IKE LaSh - - -
 - EPFLausa IKE LaBr ·····
 - UChalmer IKE LiLe - - -
 - UMISTLes IKE LiLe - - -
 - UFlorenc IKE NaHi - - -

2A - 75

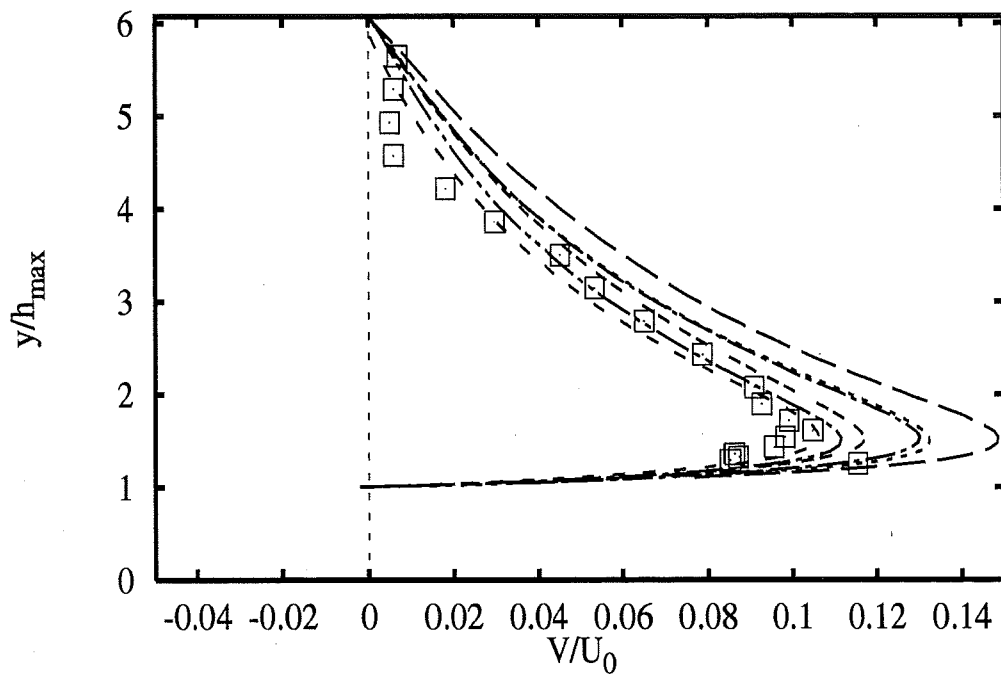
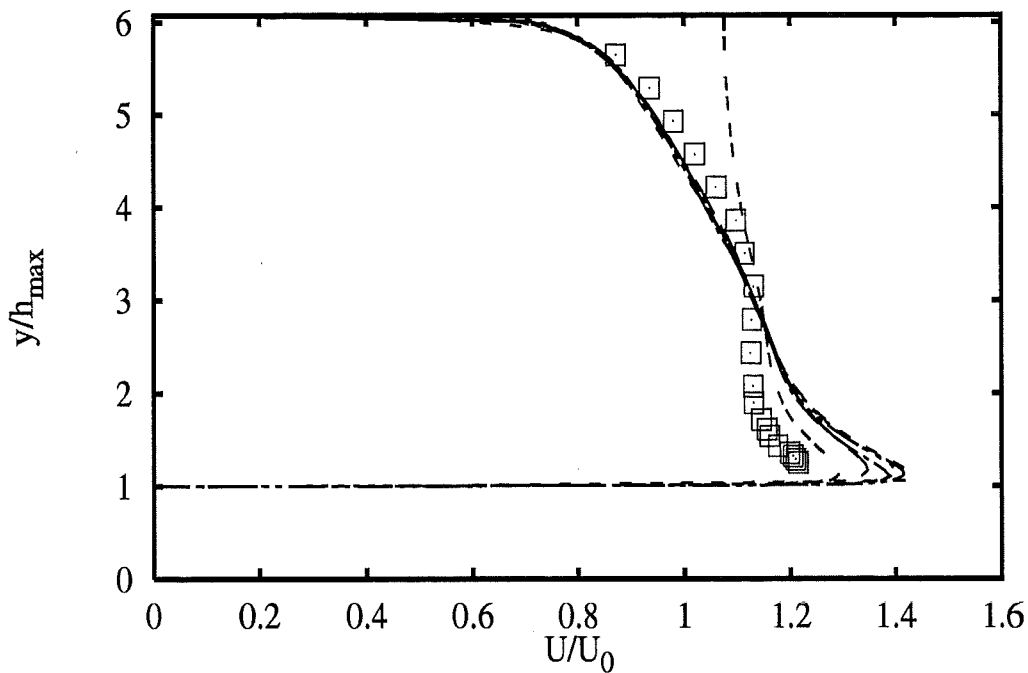


Profiles at $x/h_{max} = -0.71$

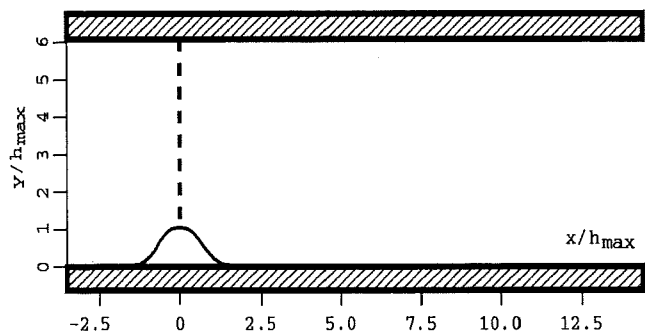


- Experiments** □
- UChalmer IKE LaSh ---
 - EDFLNHLa IKE LaSh - - -
 - EPFLausa IKE LaBr ·····
 - UChalmer IKE LiLe - · - ·
 - UMISTLes IKE LiLe - · - ·
 - UFlorenc IKE NaHi - - -

2A - 76

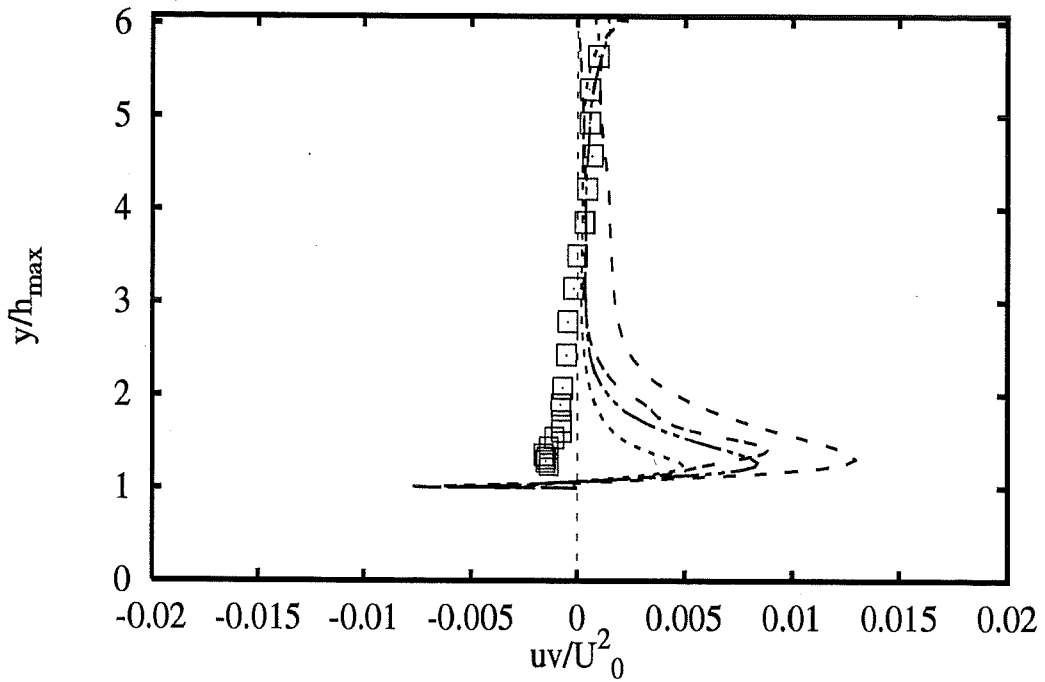
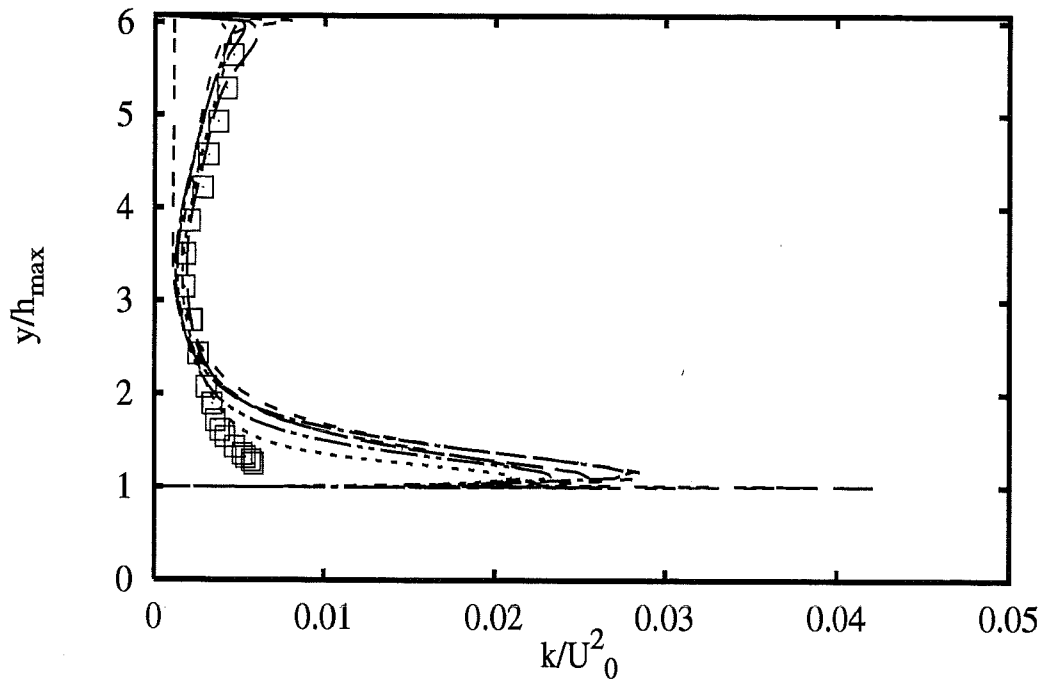


Profiles at $x/h_{max} = 0$

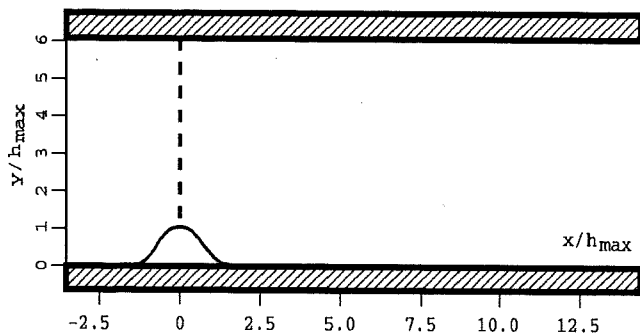


- | Experiments | | \square |
|--------------------|-----------------|-----------|
| <i>UChalmer</i> | <i>lKE LaSh</i> | --- |
| <i>EDFLNHLa</i> | <i>lKE LaSh</i> | --- |
| <i>EPFLausa</i> | <i>lKE LaBr</i> | --- |
| <i>UChalmer</i> | <i>lKE LiLe</i> | --- |
| <i>UMISTLes</i> | <i>lKE LiLe</i> | --- |
| <i>UFlorenc</i> | <i>lKE NaHi</i> | --- |

2A - 77

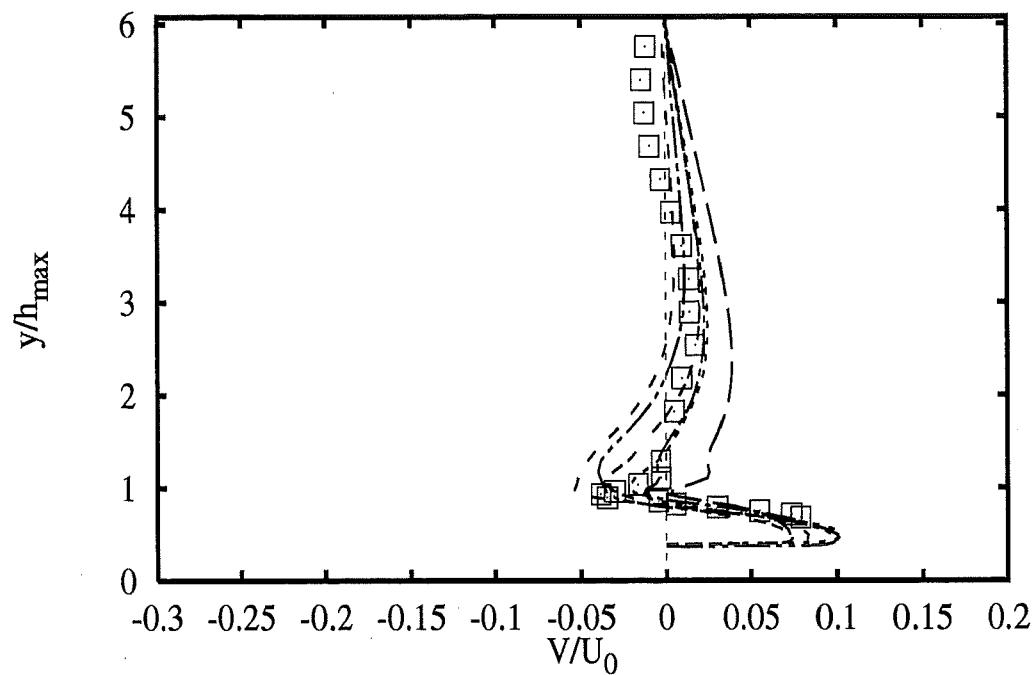
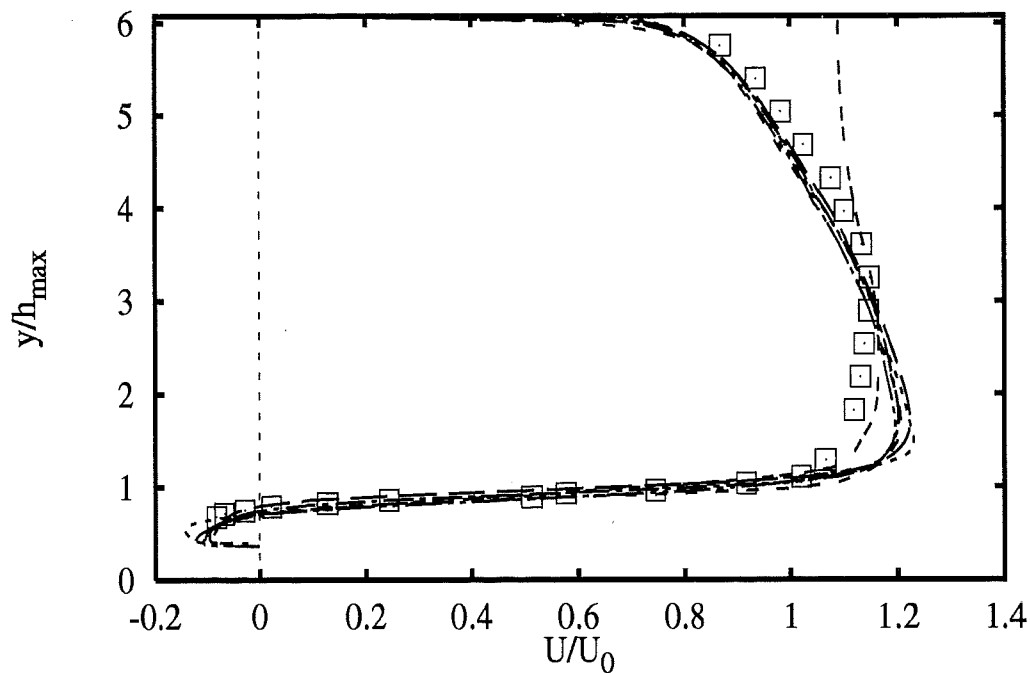


Profiles at $x/h_{max} = 0$

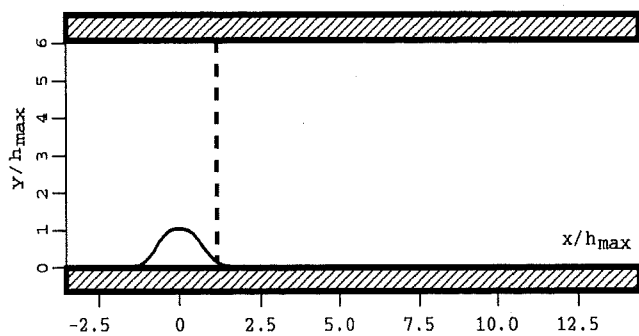


- Experiments** □
- UChalmer IKE LaSh ---
 - EDFLNHLa IKE LaSh - - -
 - EPFLausa IKE LaBr ·····
 - UChalmer IKE LiLe - · - ·
 - UMISTLes IKE LiLe - · - ·
 - UFlorenc IKE NaHi - - -

2A - 78

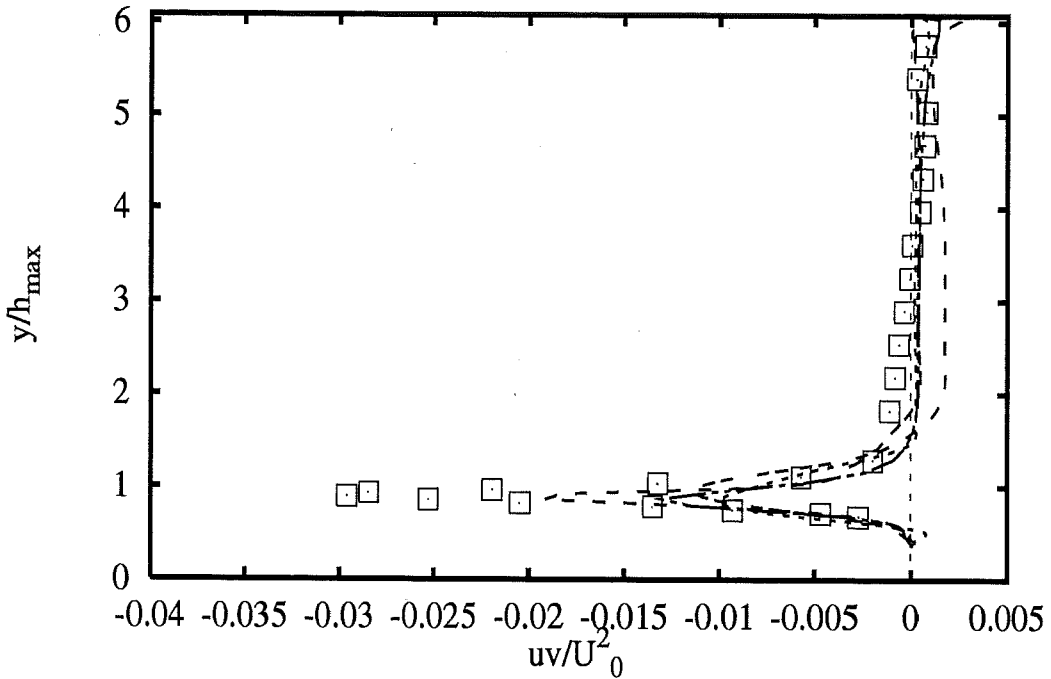
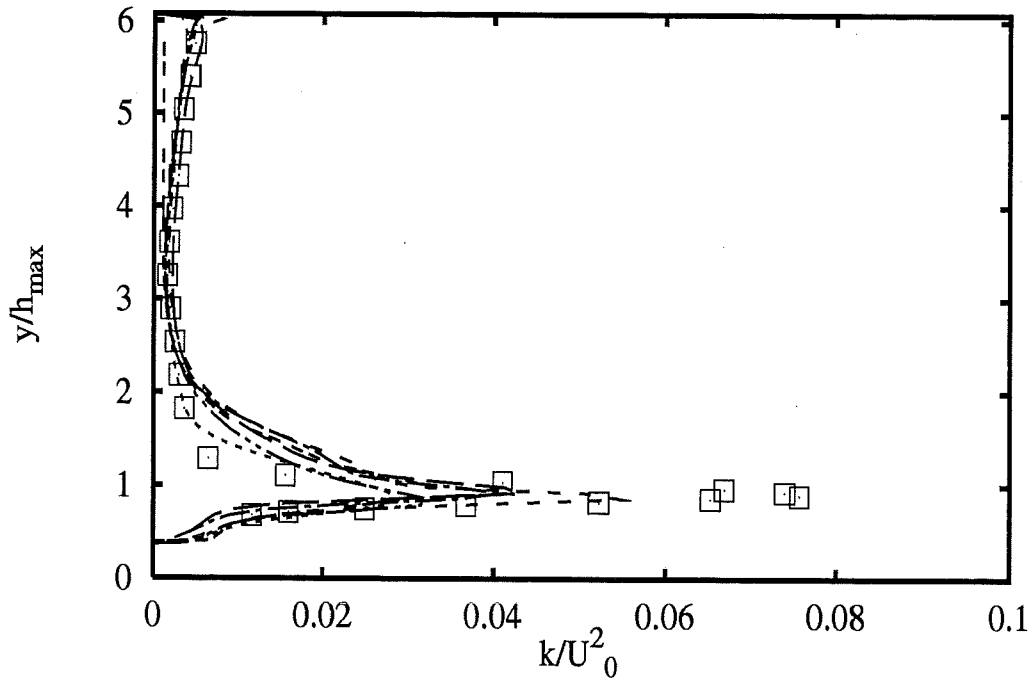


Profiles at $x/h_{max} = 1.07$

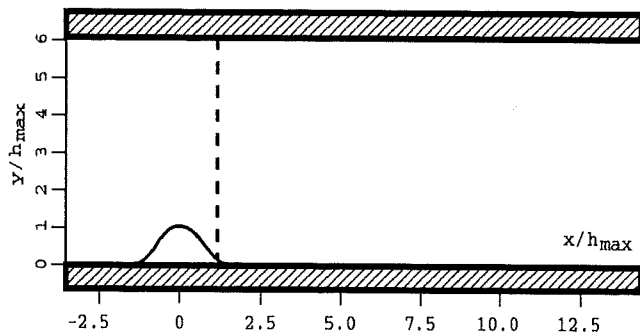


- Experiments** □
- UChalmer** *lKE LaSh* — —
 - EDFLNHLa** *lKE LaSh* - - -
 - EPFLausa** *lKE LaBr* ·····
 - UChalmer** *lKE LiLe* - - -
 - UMISTLes** *lKE LiLe* - - -
 - UFlorenc** *lKE NaHi* - - -

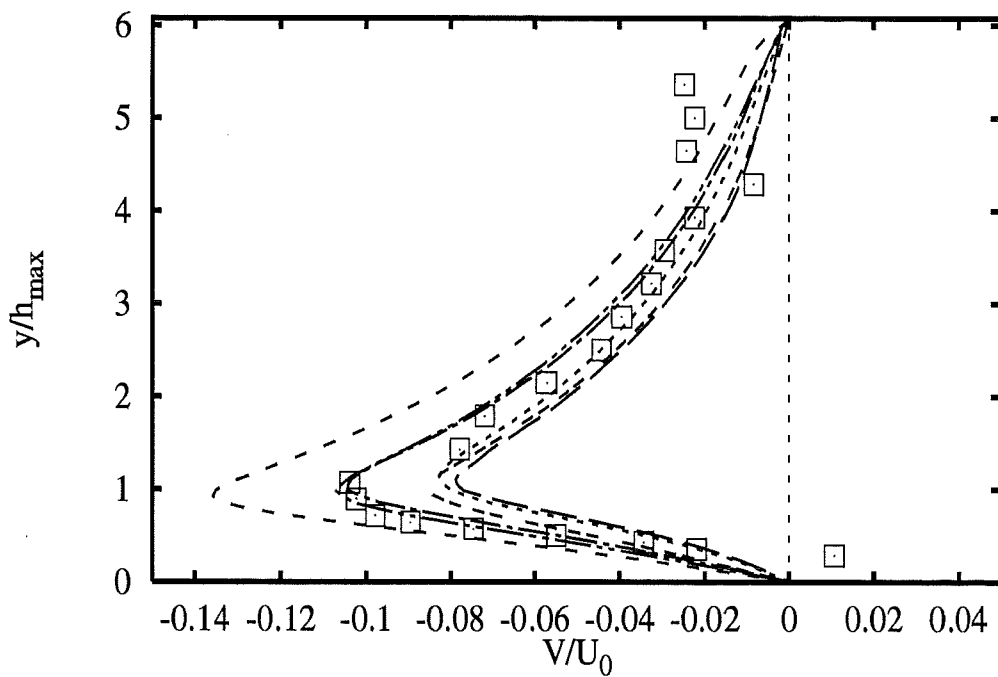
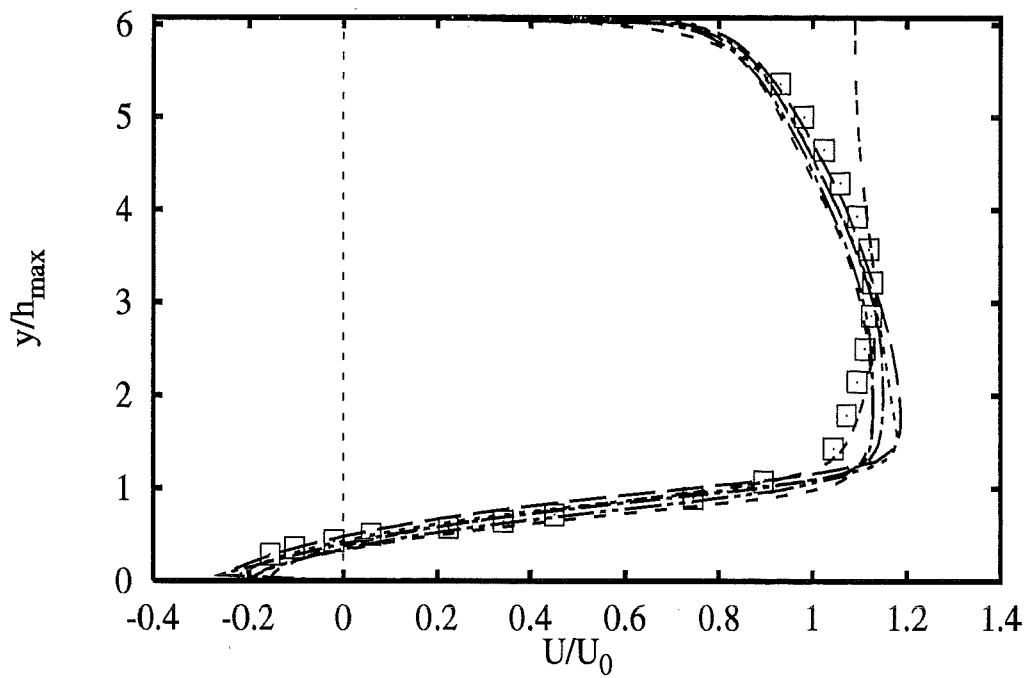
2A - 79



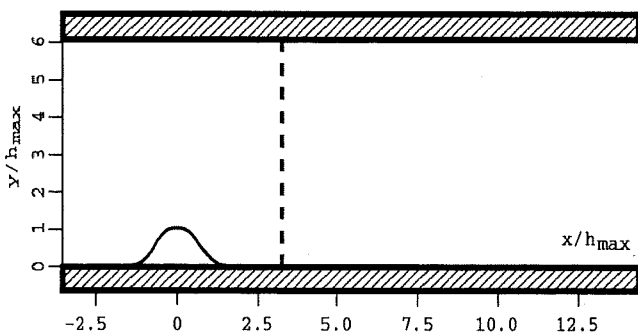
Profiles at $x/h_{max} = 1.07$



- Experiments** □
- UChalmer IKE LaSh ---
 - EDFLNHLa IKE LaSh - - -
 - EPFLausa IKE LaBr ·····
 - UChalmer IKE LiLe - · - ·
 - UMISTLes IKE LiLe - · - ·
 - UFlorenc IKE NaHi - - -

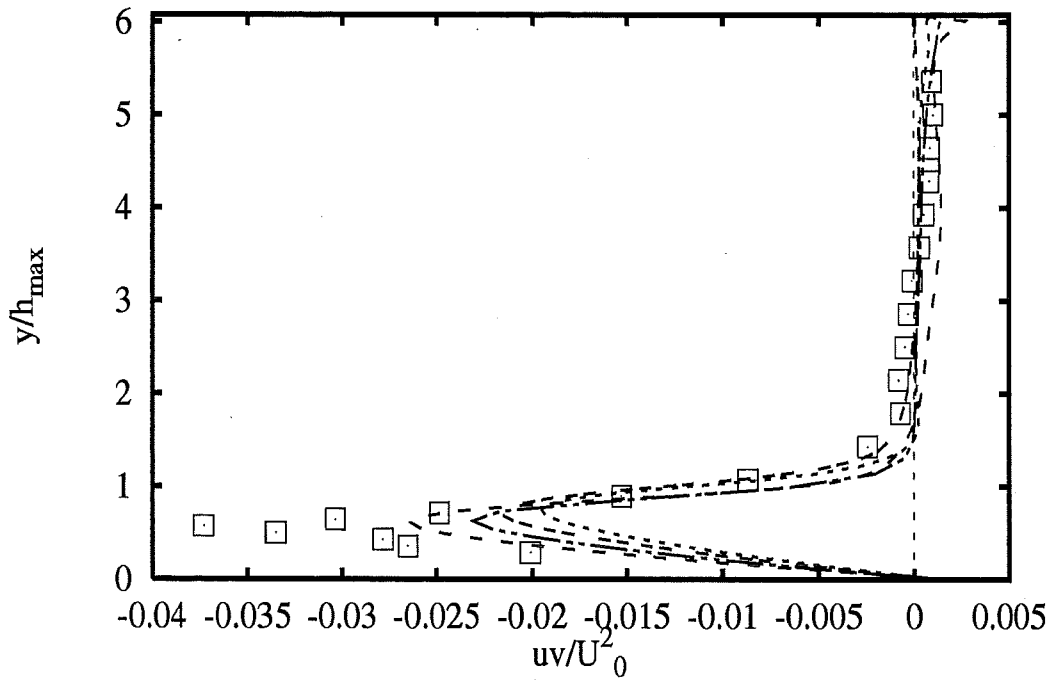
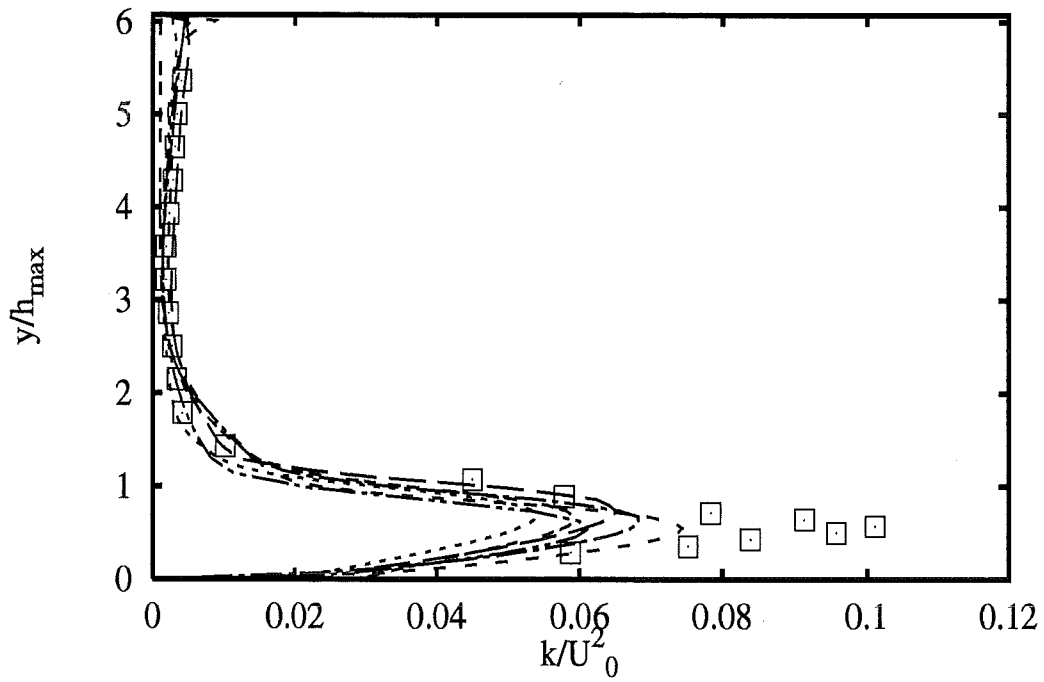


Profiles at $x/h_{max} = 3.21$

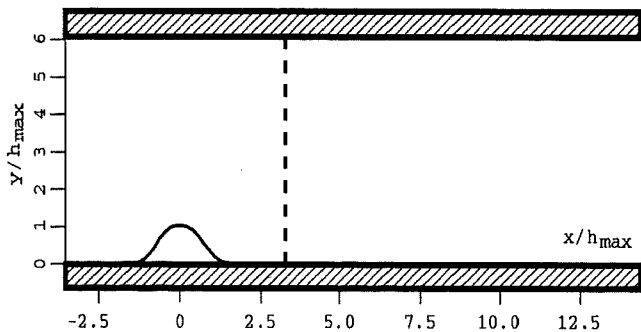


| Experiments | | □ |
|--------------------|-----------------|-------|
| UChalmer | lKE LaSh | --- |
| EDFLNHLa | lKE LaSh | --- |
| EPFLausa | lKE LaBr | |
| UChalmer | lKE LiLe | --- |
| UMISTLes | lKE LiLe | |
| UFlorenc | lKE NaHi | --- |

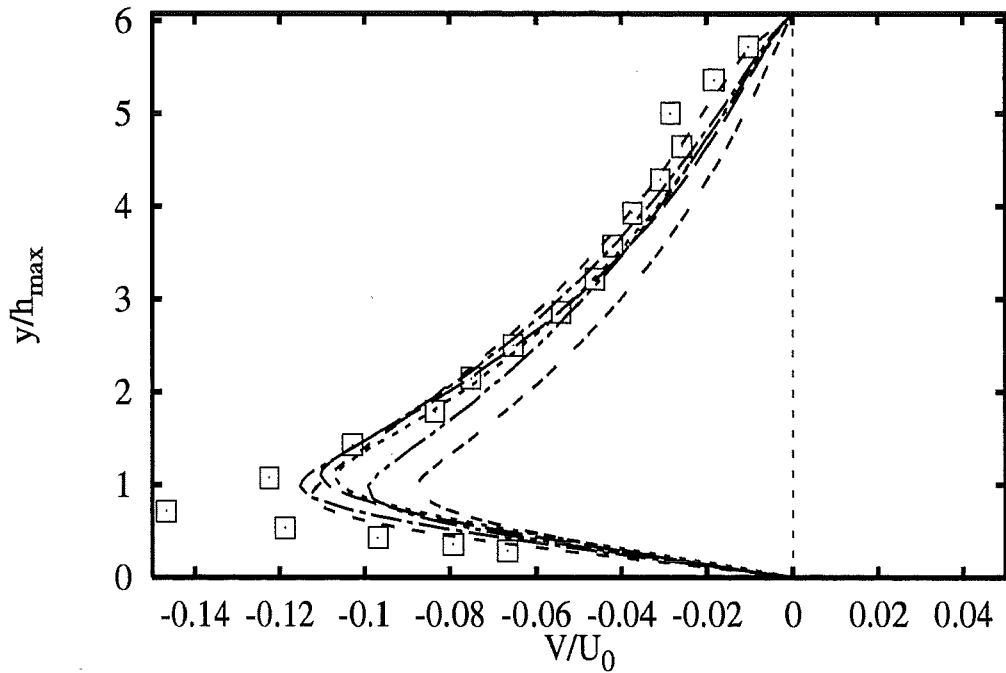
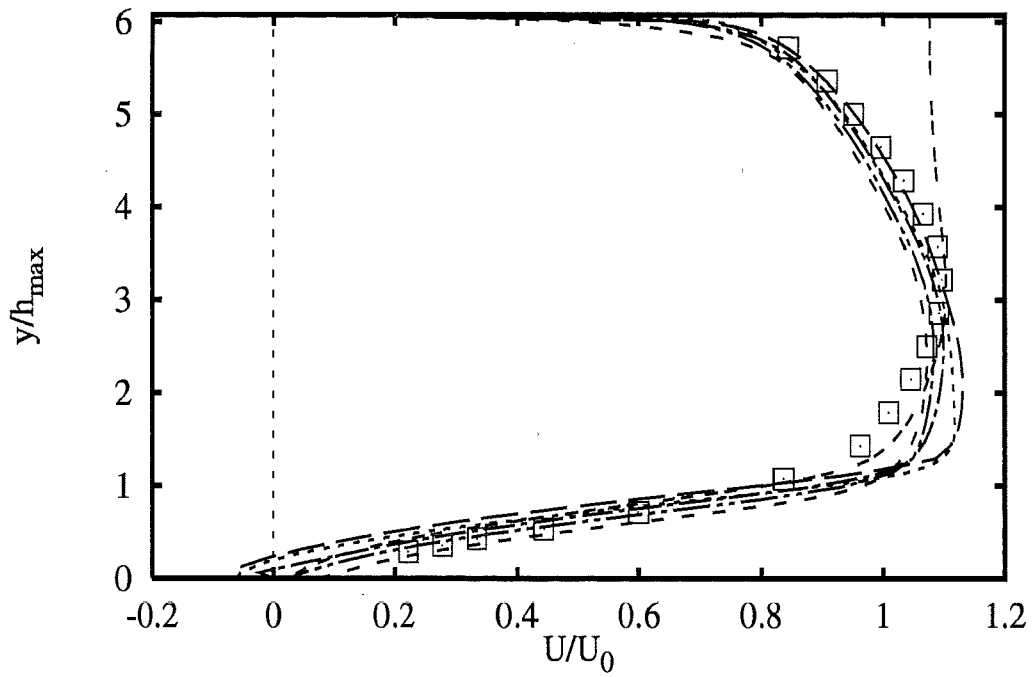
2A - 81



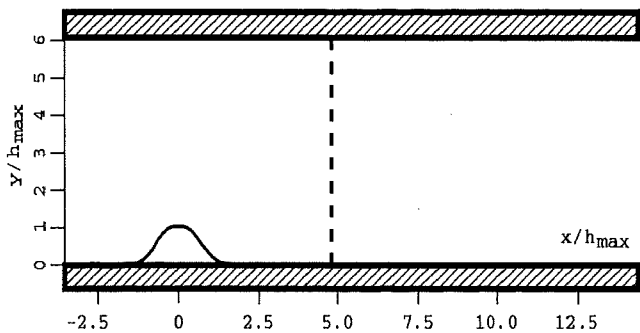
Profiles at $x/h_{max} = 3.21$



- Experiments** □
- UChalmer** **lKE** **LaSh** — —
 - EDFLNHLA** **lKE** **LaSh** - - -
 - EPFLausa** **lKE** **LaBr** ·····
 - UChalmer** **lKE** **LiLe** — · —
 - UMISTLes** **lKE** **LiLe** — · · ·
 - UFlorenc** **lKE** **NaHi** - - -

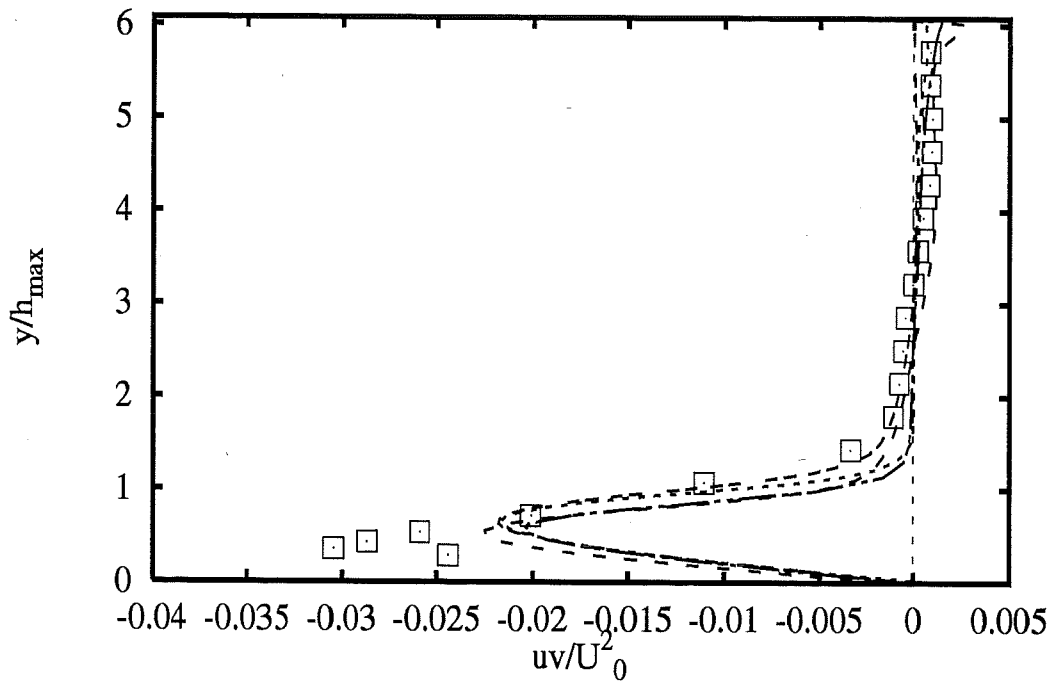
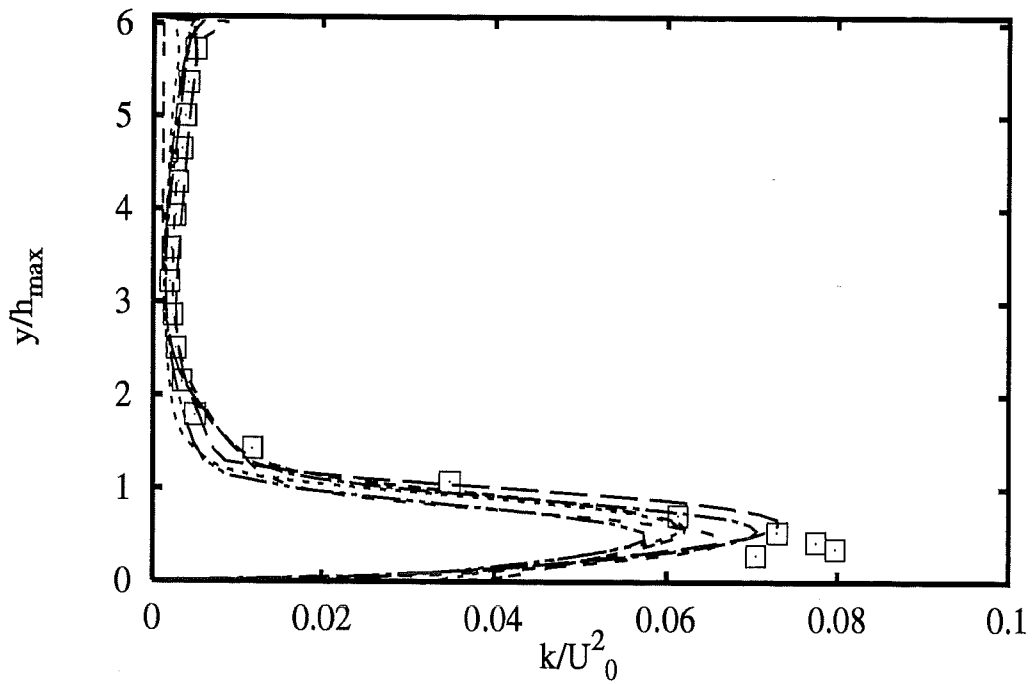


Profiles at $x/h_{max} = 4.79$

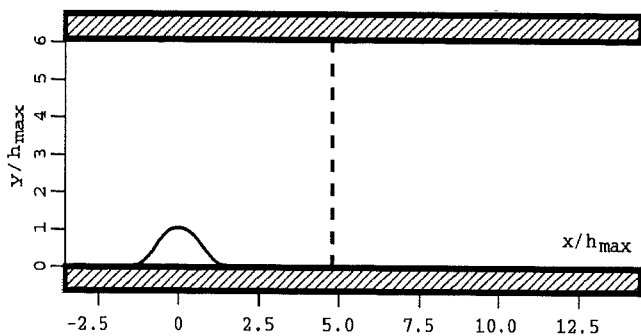


- Experiments** □
- UChalmer** *lKE* *LaSh* —
 - EDFLNHLA** *lKE* *LaSh* - - -
 - EPFLausa** *lKE* *LaBr* ·····
 - UChalmer** *lKE* *LiLe* - - -
 - UMISTLes** *lKE* *LiLe* ·····
 - UFlorenc** *lKE* *NaHi* - - -

2A - 83

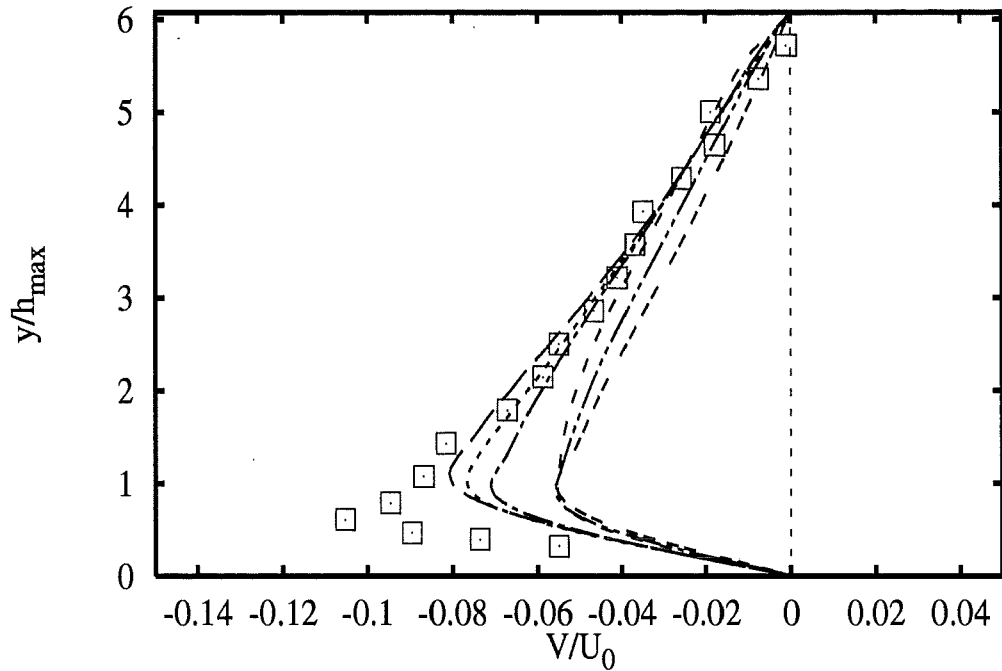
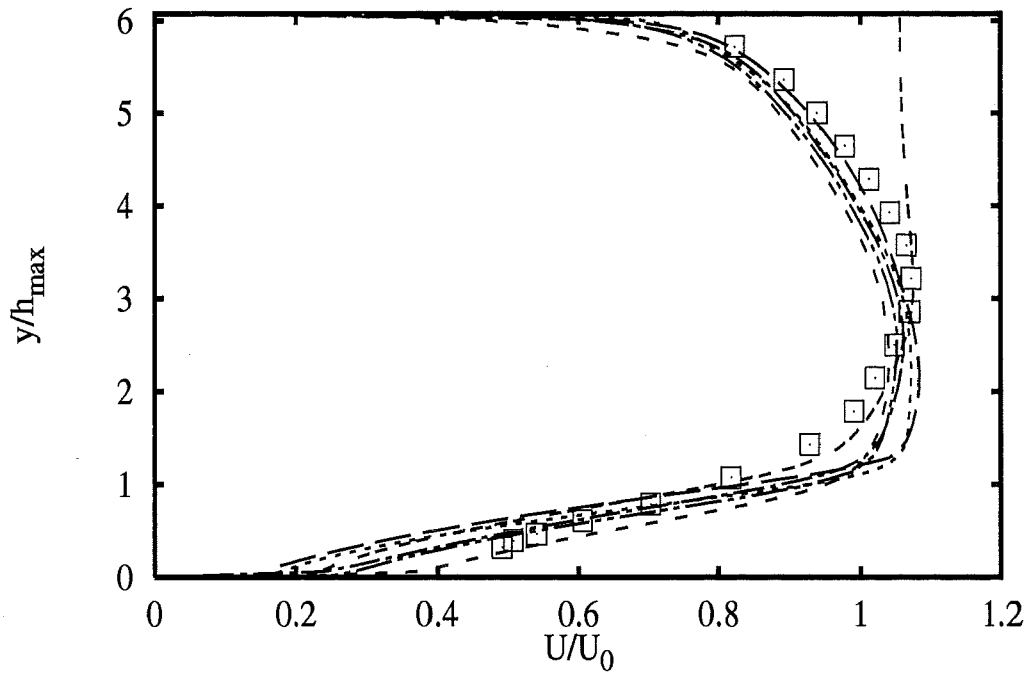


Profiles at $x/h_{max} = 4.79$

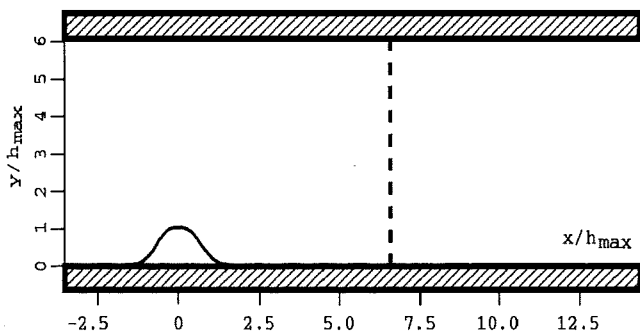


- Experiments** □
- UChalmer* *lKE* *LaSh* ---
 - EDFLNHLa* *lKE* *LaSh* - - -
 - EPFLausa* *lKE* *LaBr* ·····
 - UChalmer* *lKE* *LiLe* - · - ·
 - UMISTLes* *lKE* *LiLe* - · - ·
 - UFlorenc* *lKE* *NaHi* - - -

2A - 84

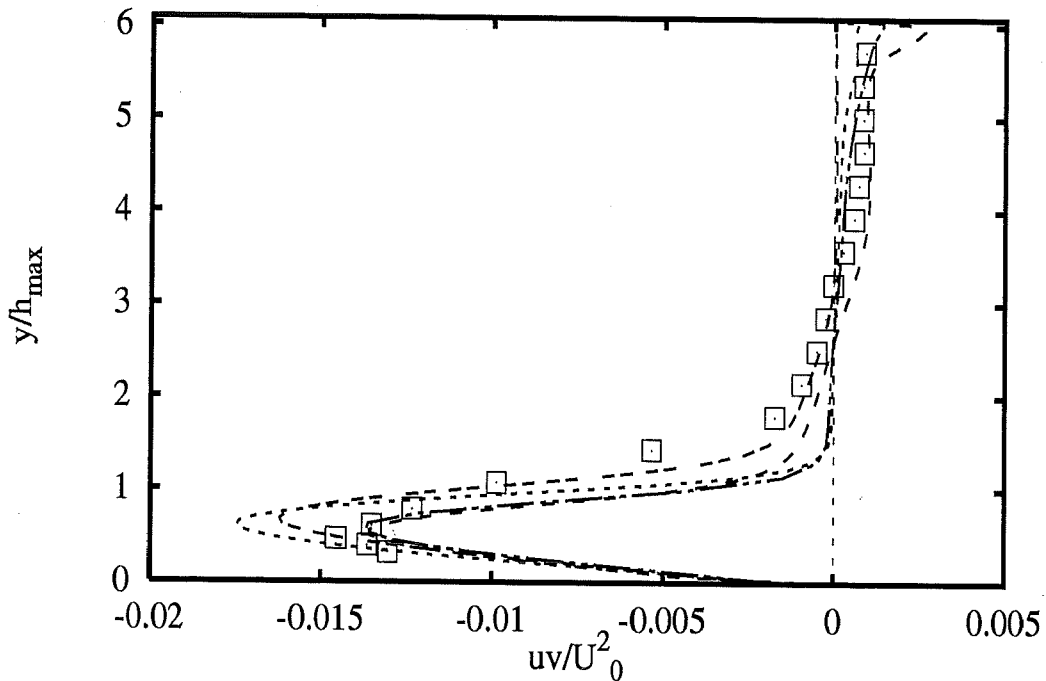
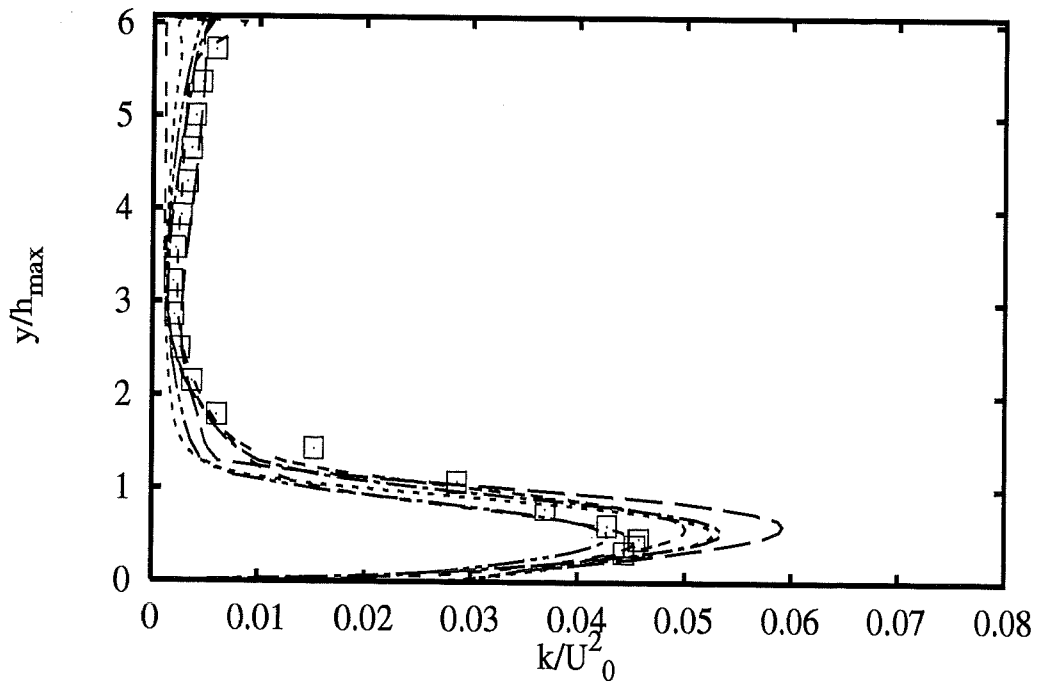


Profiles at $x/h_{max} = 6.61$

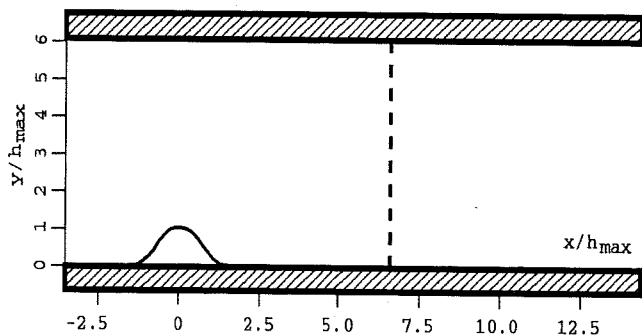


| Experiments | | □ |
|--------------------|-----------------|-------|
| <i>UChalmer</i> | <i>lKE LaSh</i> | --- |
| <i>EDFLNHLa</i> | <i>lKE LaSh</i> | --- |
| <i>EPFLausa</i> | <i>lKE LaBr</i> | |
| <i>UChalmer</i> | <i>lKE LiLe</i> | --- |
| <i>UMISTLes</i> | <i>lKE LiLe</i> | --- |
| <i>UFlorenc</i> | <i>lKE NaHi</i> | --- |

2A - 85

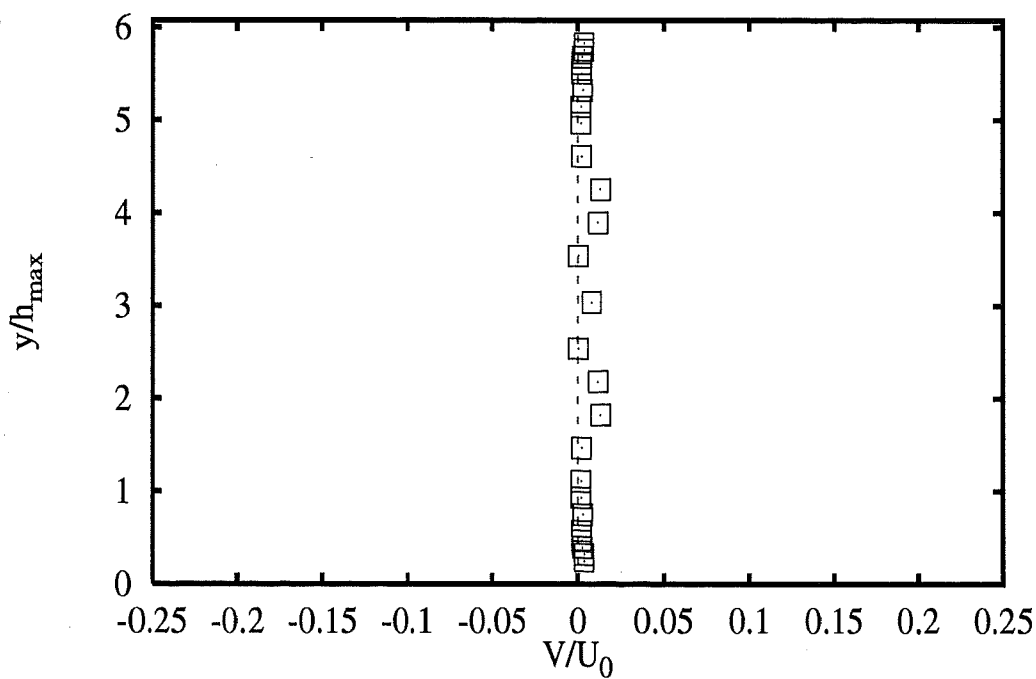
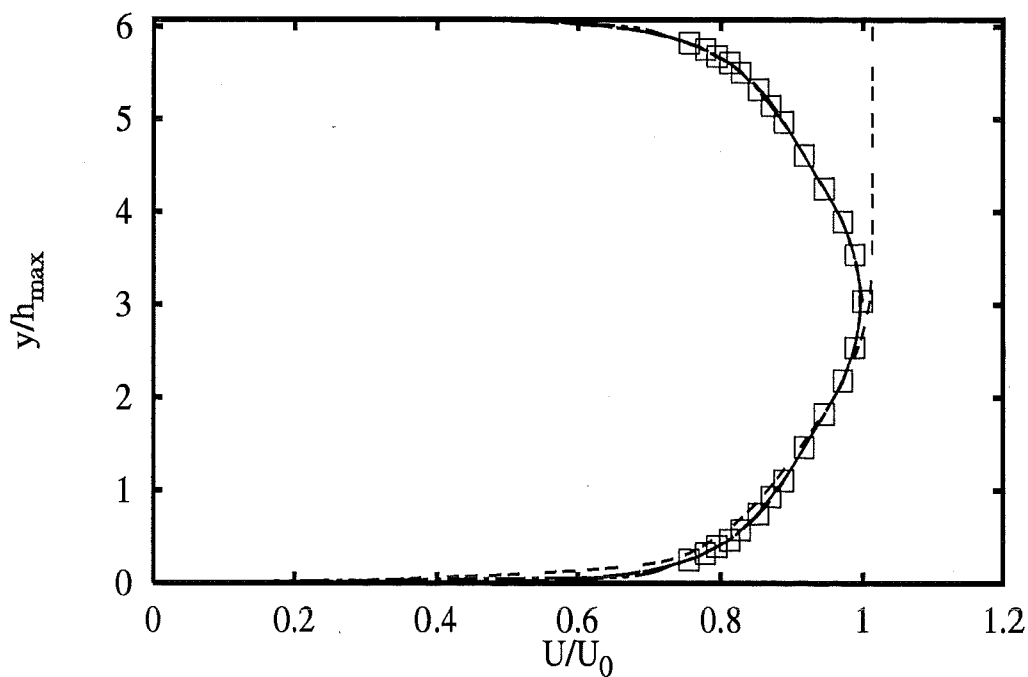


Profiles at $x/h_{max} = 6.61$

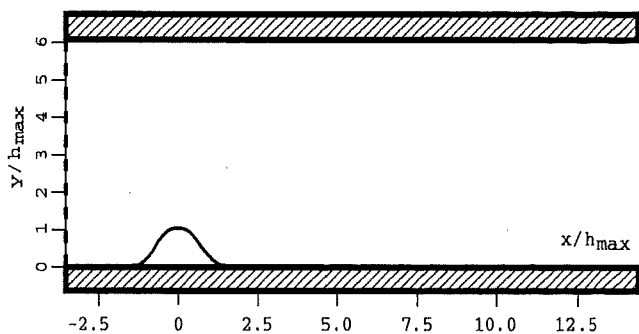


- Experiments** □
- UChalmer* *lKE* *LaSh* — —
 - EDFLNHLa* *lKE* *LaSh* - - -
 - EPFLausa* *lKE* *LaBr* ·····
 - UChalmer* *lKE* *LiLe* - - -
 - UMISTLes* *lKE* *LiLe* - - -
 - UFlorenc* *lKE* *NaHi* - - -

2A - 86

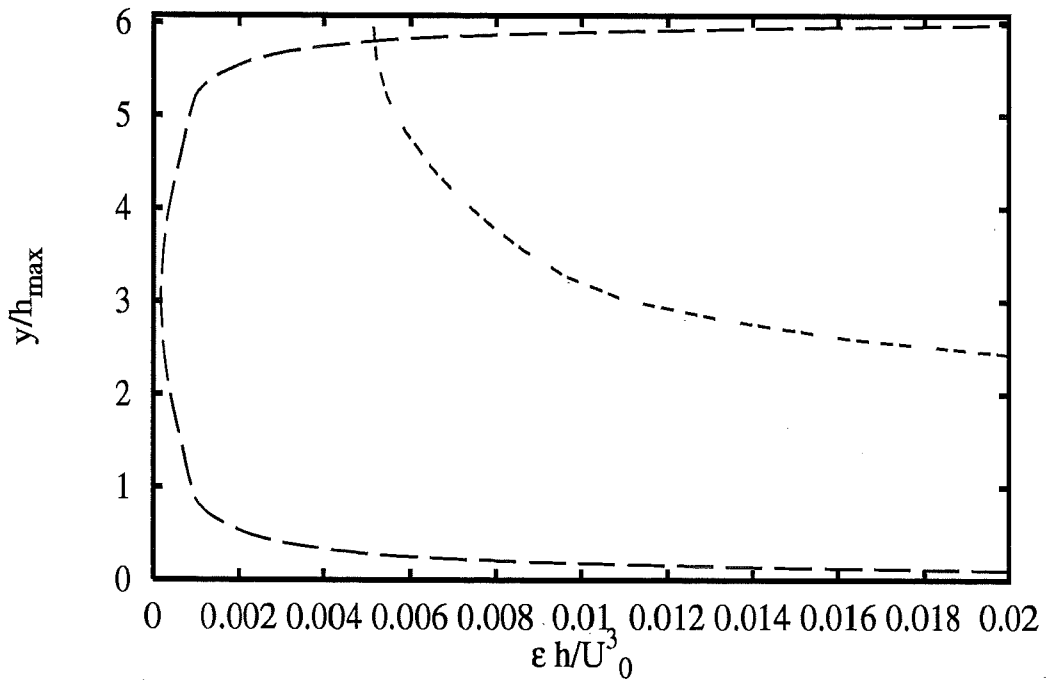
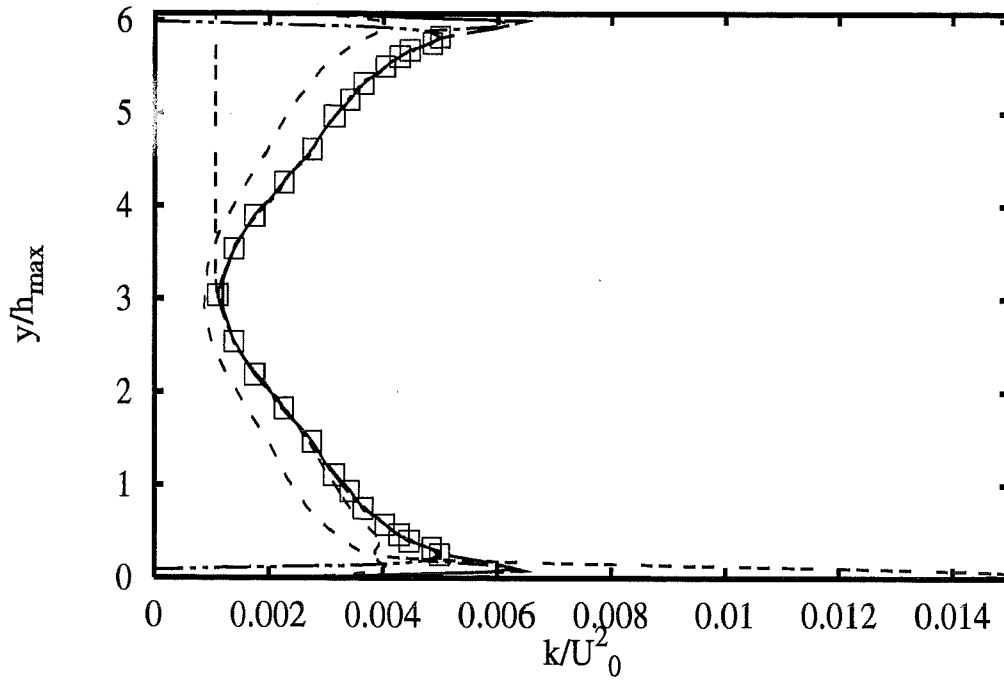


Profiles at $x/h_{max} = -3.57$

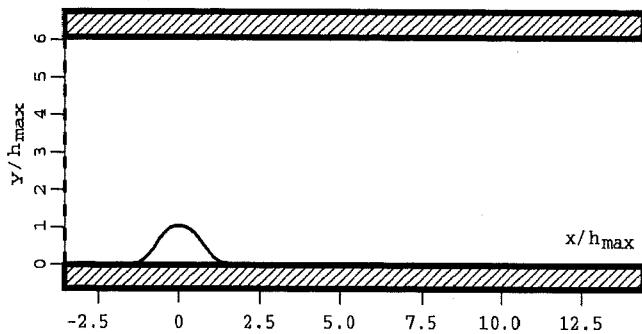


- | | |
|----------------------|-------------|
| Experiments | □ |
| ASC nKE SZL+wf | --- |
| IOlomouc nKE Spez+wf | - - - |
| UChalmer kOm Wil | - · - · - |
| UDelftZi kOm Wil | - · · - · - |
| UFlorenc kOm Wil | - · · · - |

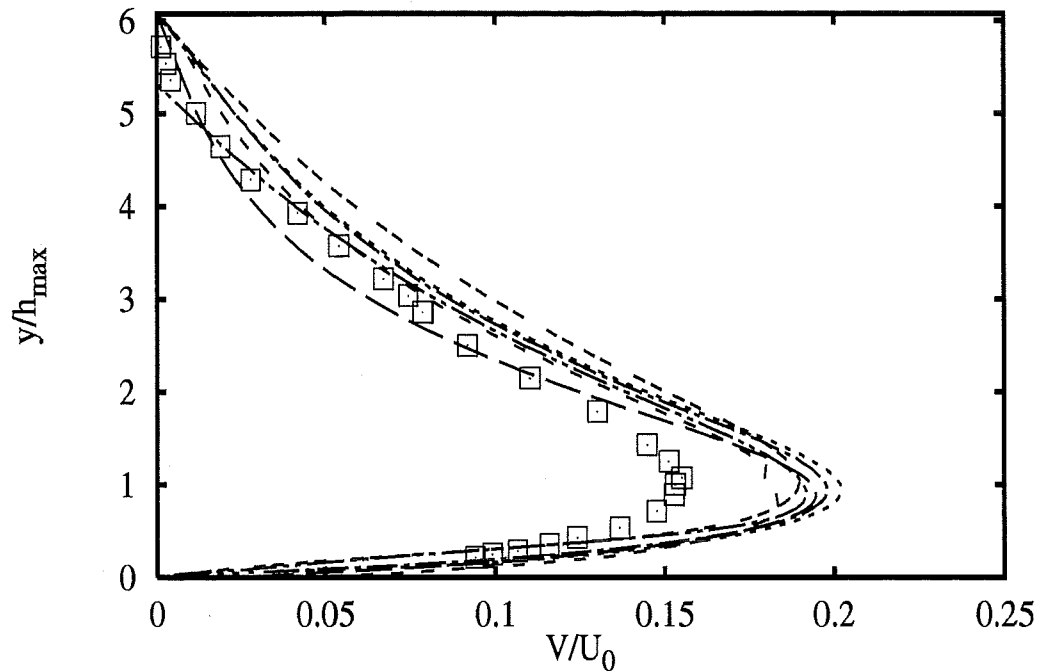
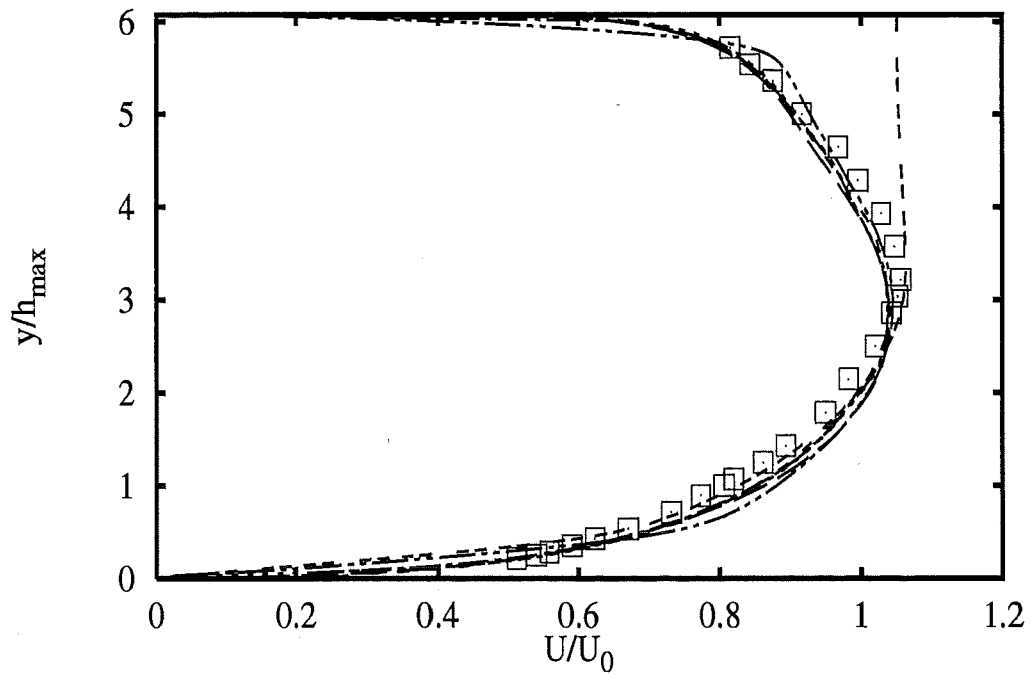
2A - 87



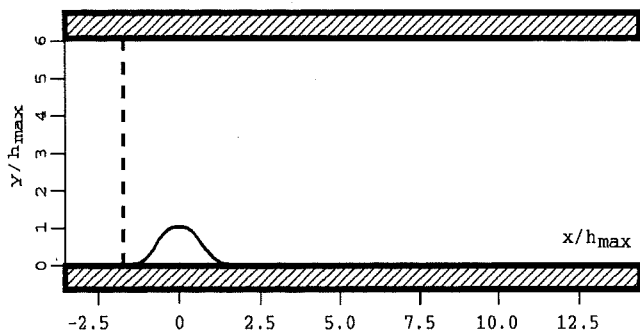
Profiles at $x/h_{max} = -3.57$



- Experiments
- ASC nKE SZL+wf ---
 - Iolomouc nKE Spez+wf - - -
 - UChalmer kOm Wil - - - -
 - UdelftZi kOm Wil - - - -
 - UFlorenc kOm Wil - - - -

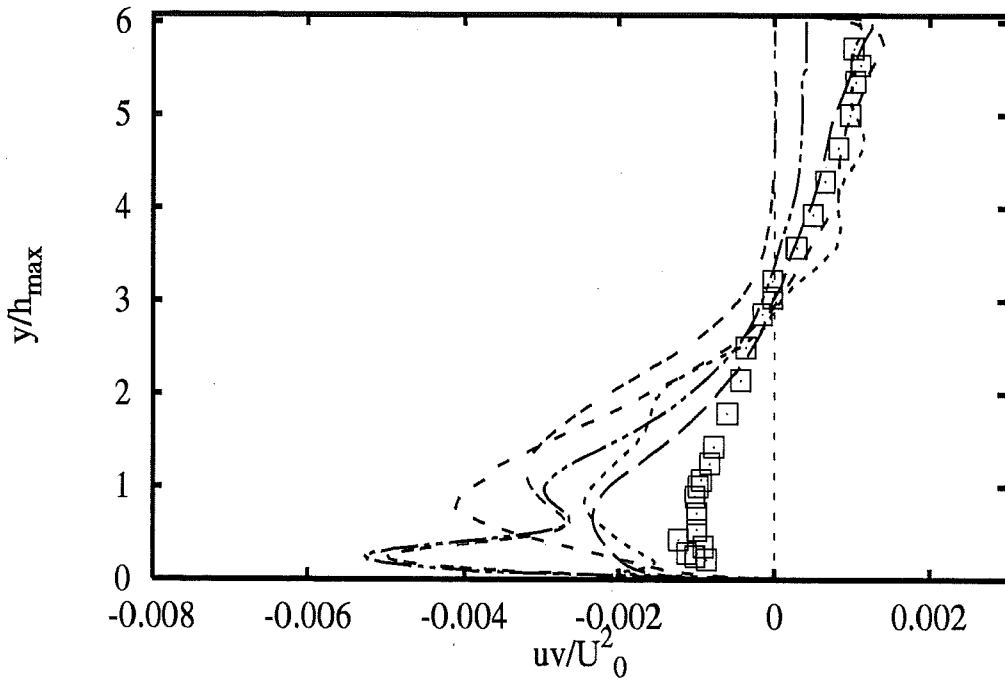
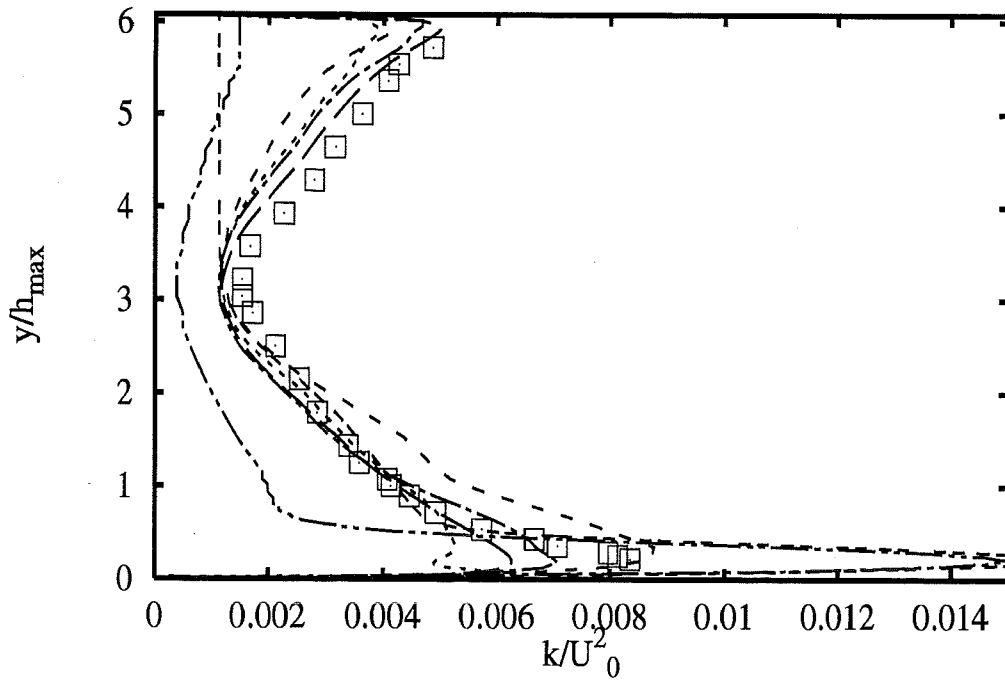


Profiles at $x/h_{max} = -1.78$

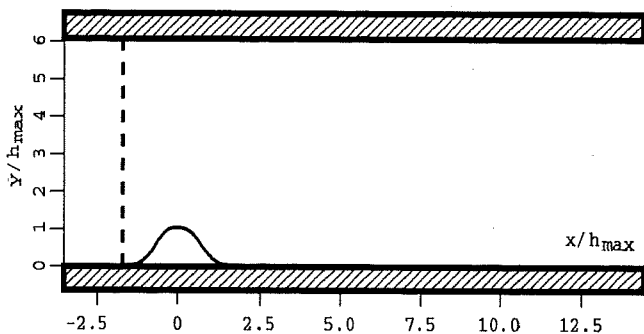


- | | |
|----------------------|-------|
| Experiments | □ |
| ASC nKE SZL+wf | --- |
| Iolomouc nKE Spez+wf | ---- |
| DLRGoett kOm Wil | |
| UChalmer kOm Wil | ----- |
| UDelftZi kOm Wil | ----- |
| UFlorenc kOm Wil | ----- |

2A - 89

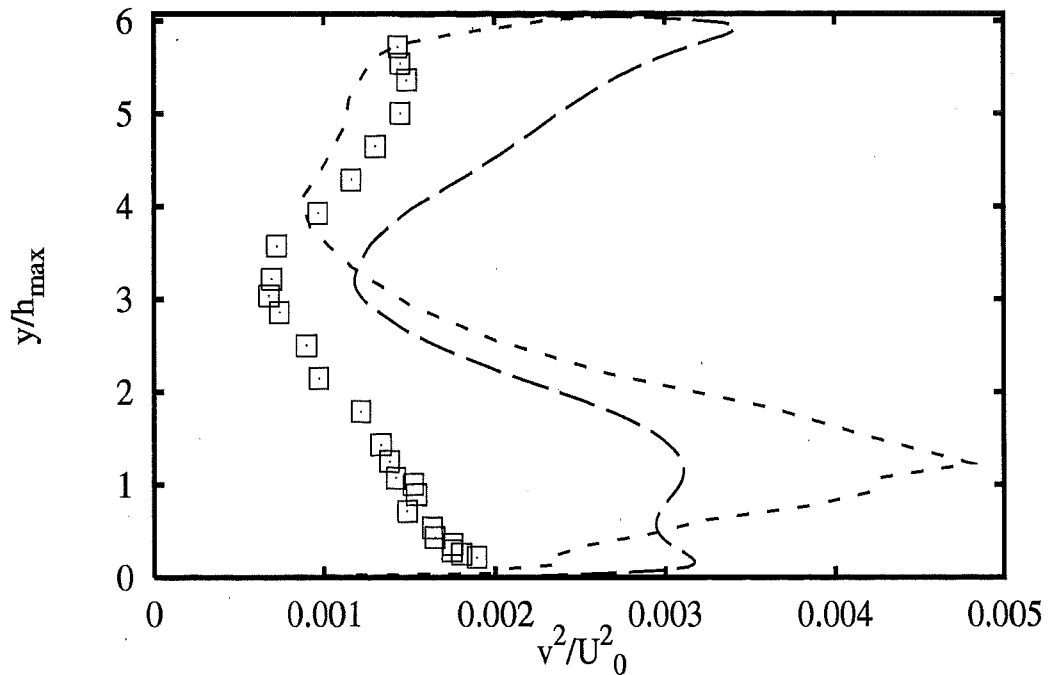
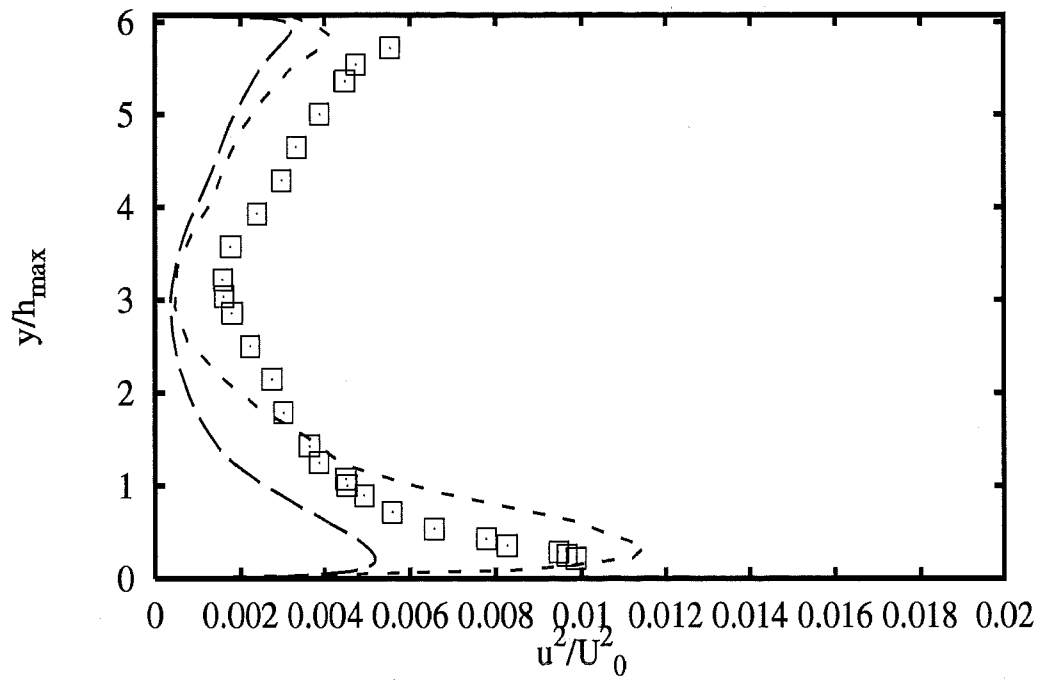


Profiles at $x/h_{max} = -1.78$

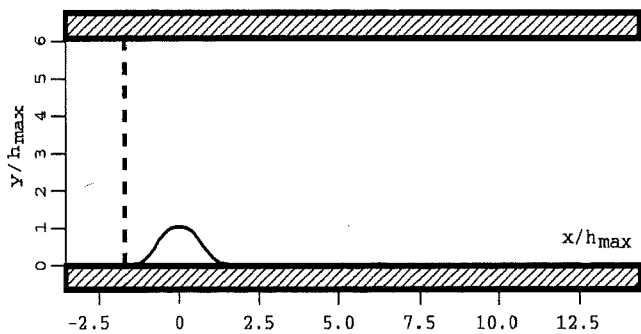


- Experiments \square
- ASC nKE SZL+wf ---
 - Iolomouc nKE Spez+wf - - -
 - DLRGoett kOm Wil (dash-dot-dot)
 - UChalmer kOm Wil --- (long-dash)
 - UDelftZi kOm Wil - - - (short-dash)
 - UFlorenc kOm Wil - - - (short-dash)

2A - 90

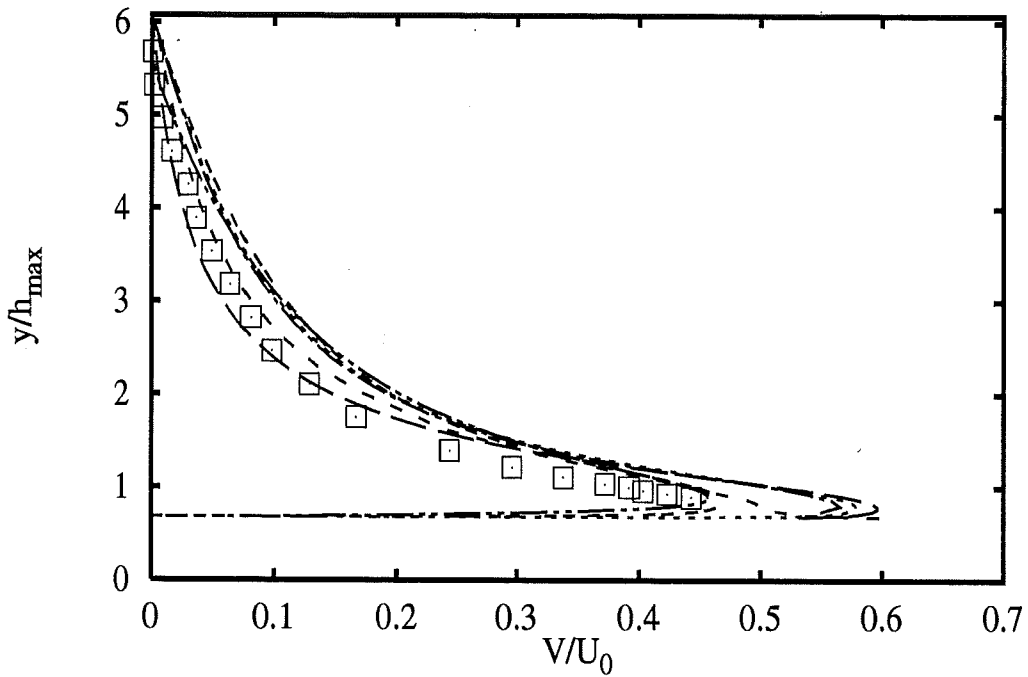
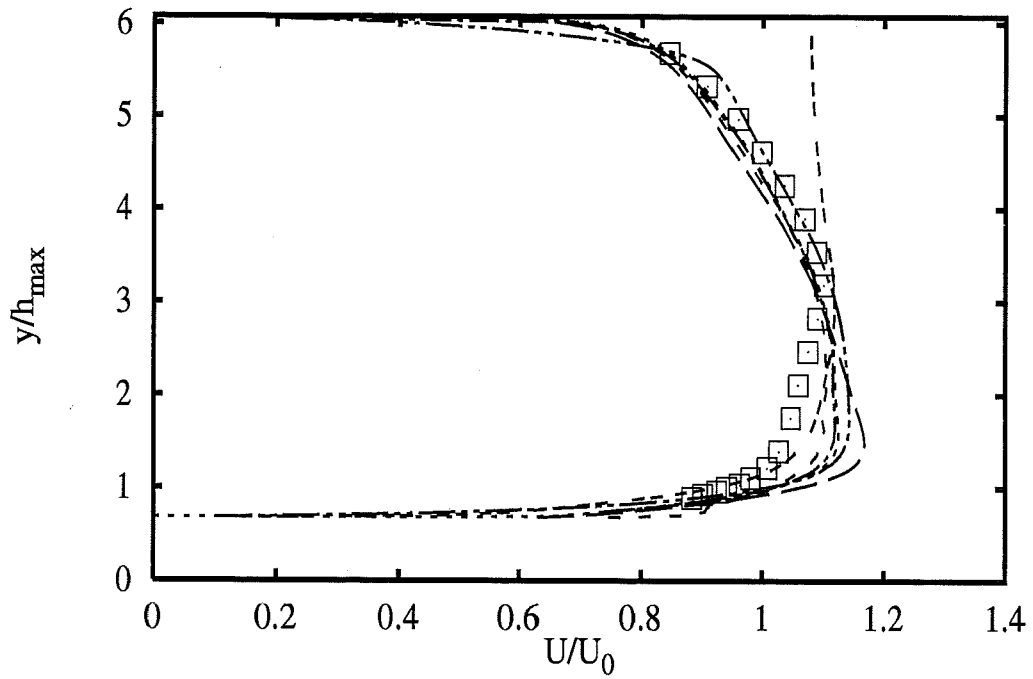


Profiles at $x/h_{max} = -1.78$

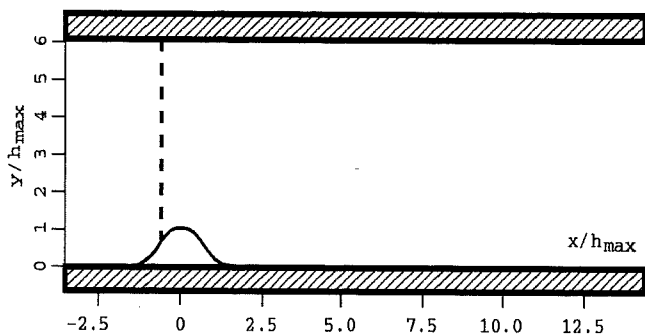


Experiments \square
 ASC nKE SZL+wf $---$
 IOlomouc nKE Spez+wf $---$

2A - 91

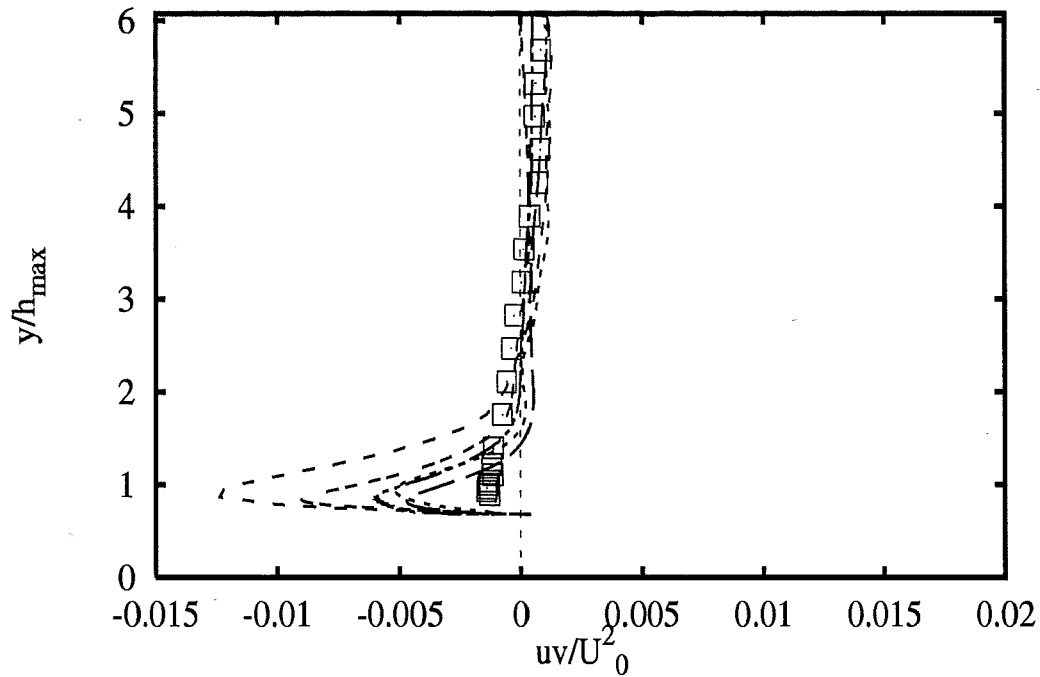
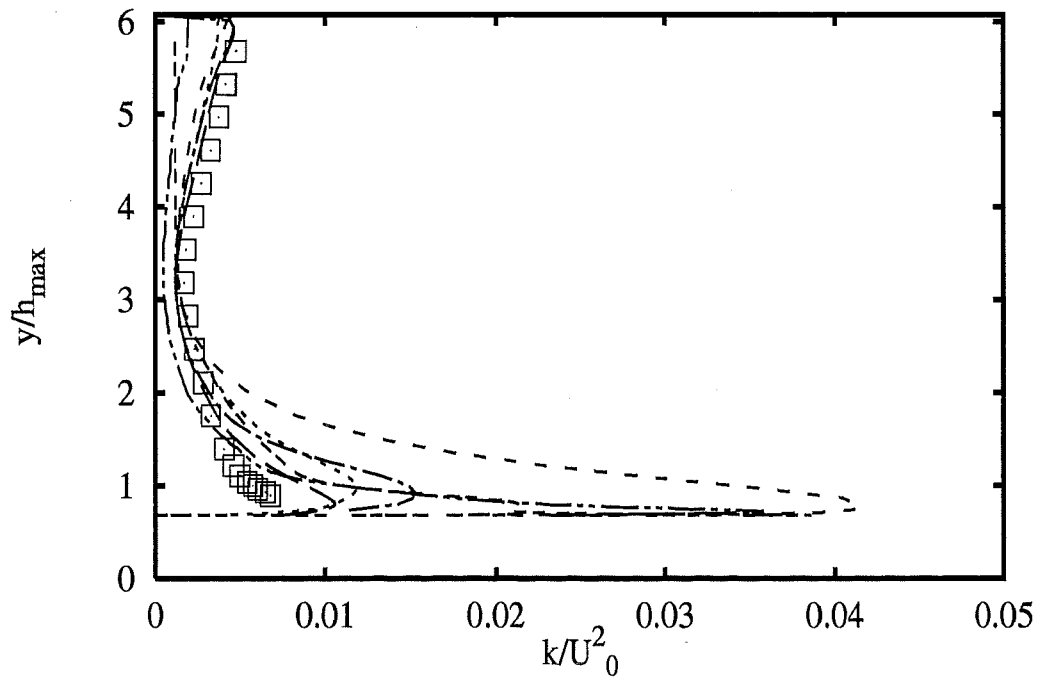


Profiles at $x/h_{max} = -0.71$

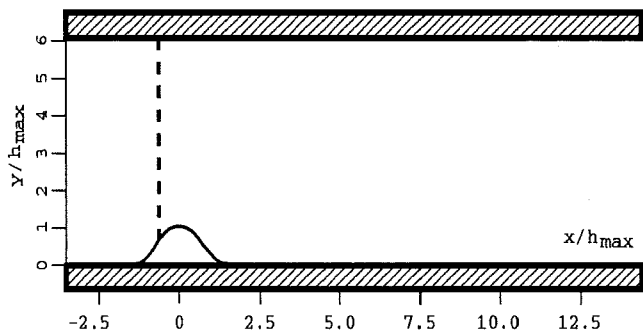


- | | | |
|--------------------|-------------|-------|
| Experiments | | □ |
| ASC | nKE SZL+wf | --- |
| IOlomouc | nKE Spez+wf | --- |
| DLRGoett | kOm Wil | |
| UChalmer | kOm Wil | --- |
| UDelftZi | kOm Wil | --- |
| UFlorenc | kOm Wil | --- |

2A - 92

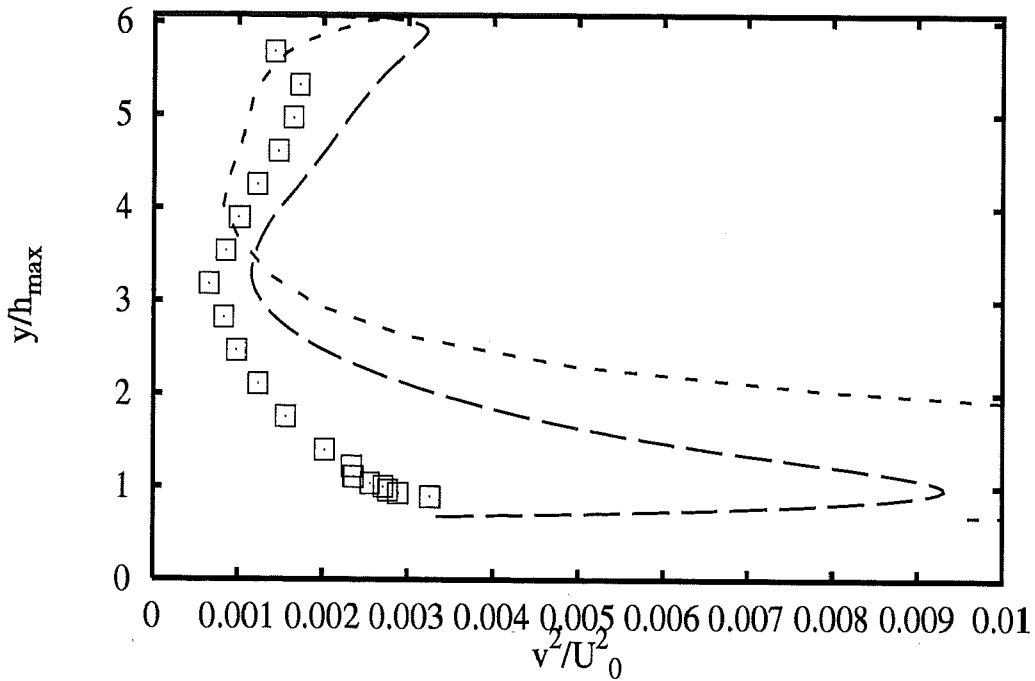
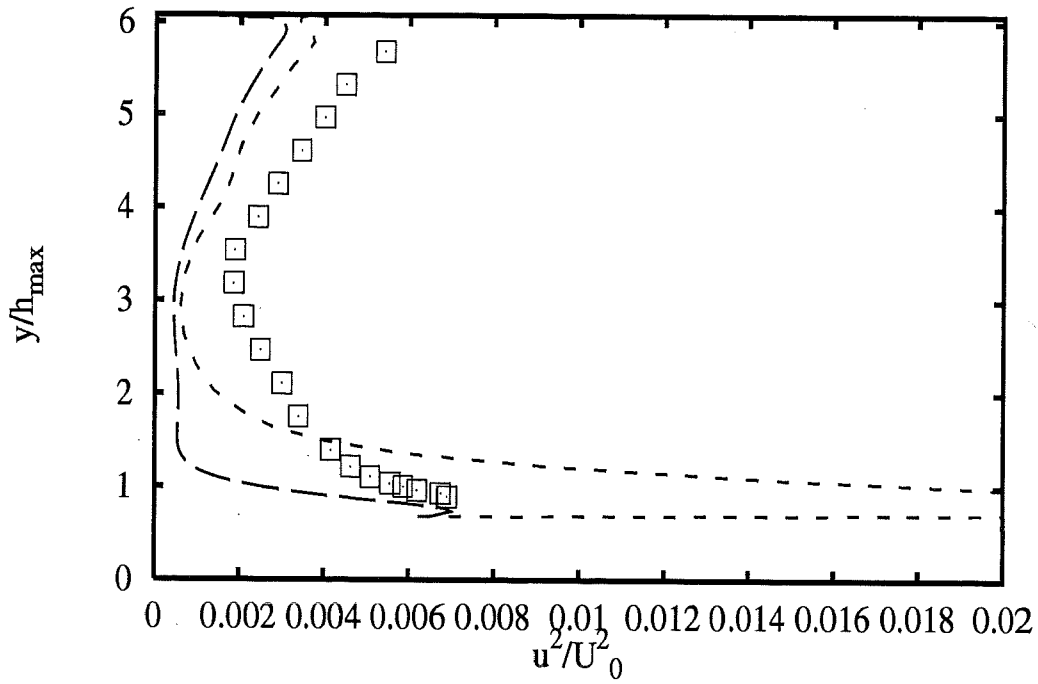


Profiles at $x/h_{max} = -0.71$

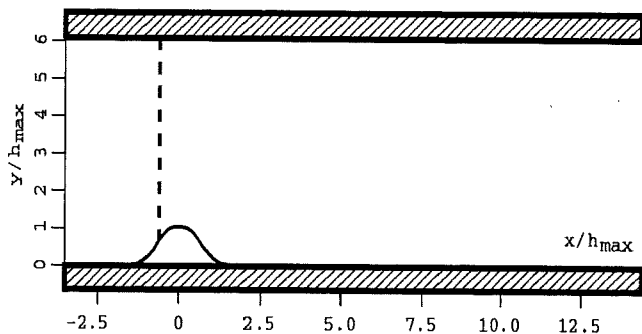


- | | |
|----------------------|---------------|
| Experiments | □ |
| ASC nKE SZL+wf | — — |
| IOlomouc nKE Spez+wf | - - - |
| DLRGoett kOm Wil | · · · · · |
| UChalmer kOm Wil | — · — |
| UDelftZi kOm Wil | - · - · - |
| UFlorenc kOm Wil | - - - · - - - |

2A - 93

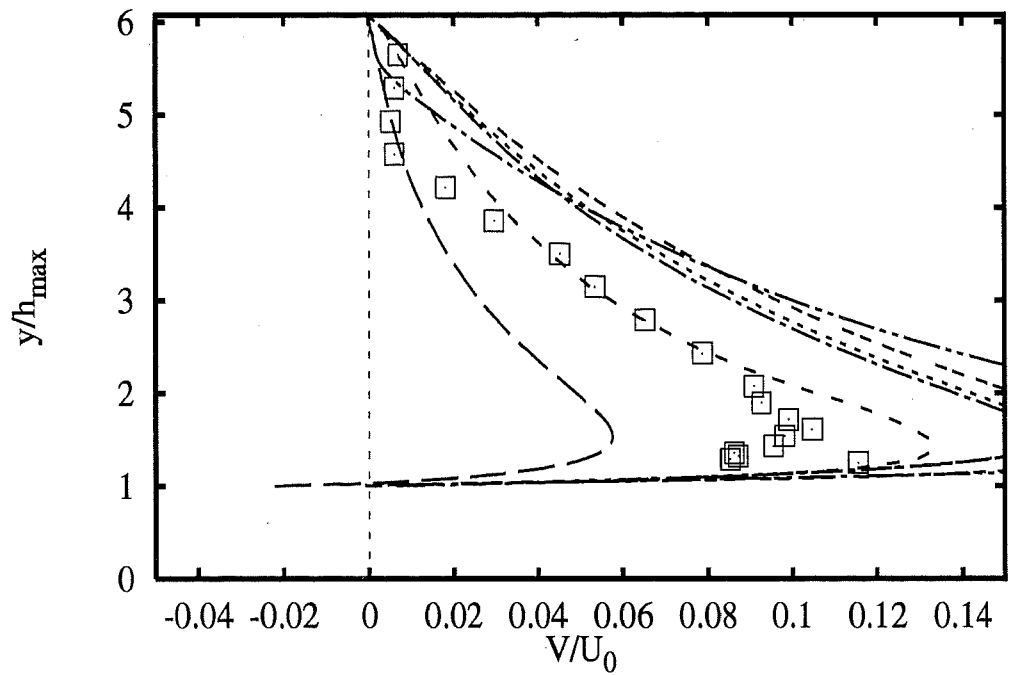
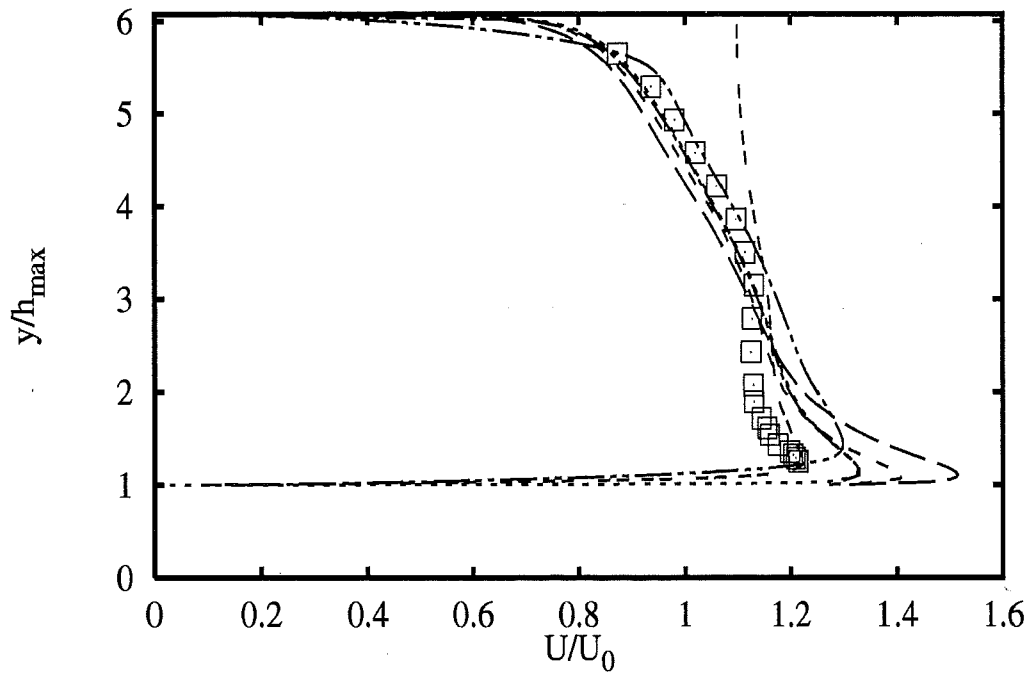


Profiles at $x/h_{max} = -0.71$

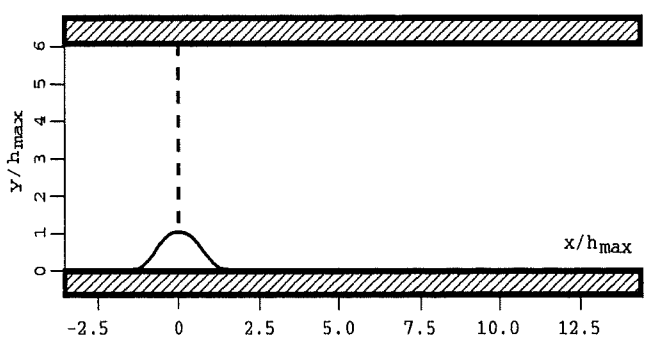


Experiments \square
ASC nKE SZL+wf ---
IOlomouc nKE Spez+wf - - -

2A - 94

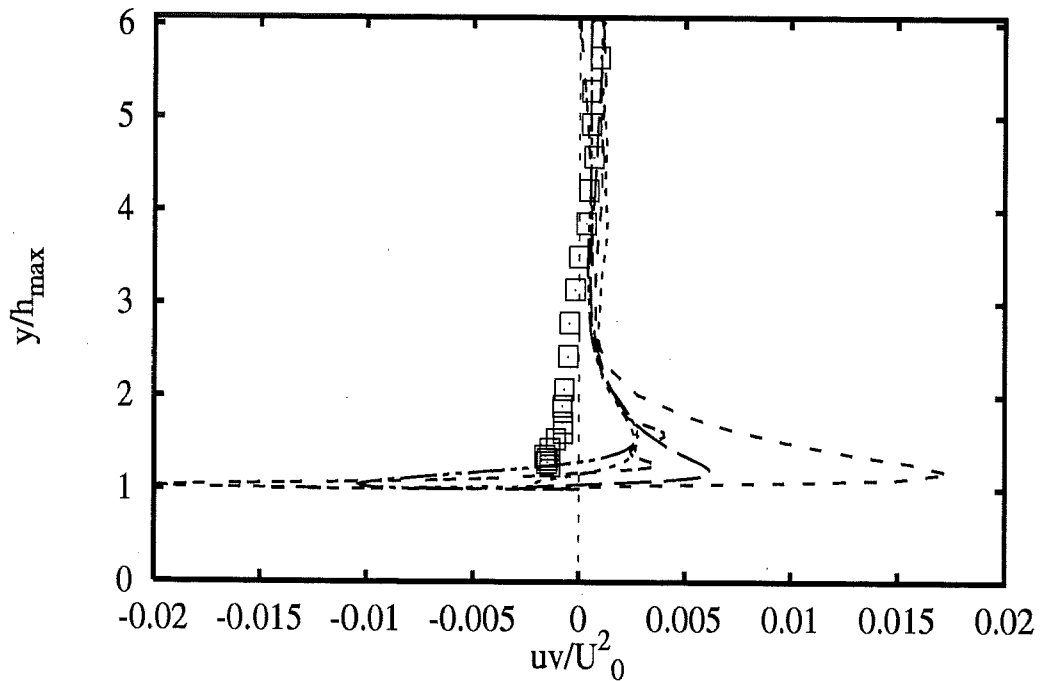
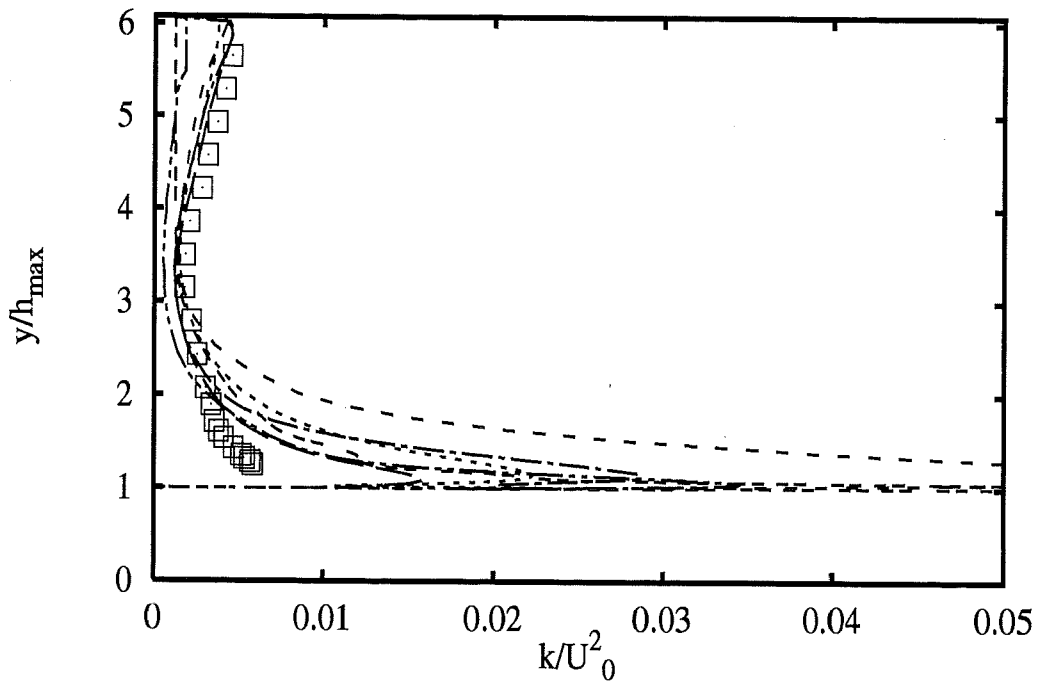


Profiles at $x/h_{max} = 0$

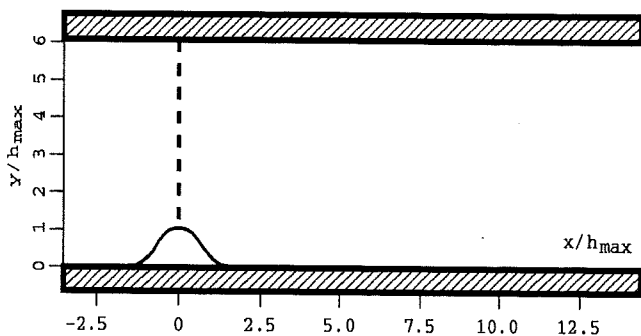


- | | |
|----------------------|-------|
| Experiments | □ |
| ASC nKE SZL+wf | --- |
| IOlomouc nKE Spez+wf | ---- |
| DLRGoett kOm Wil | |
| UChalmer kOm Wil | ---- |
| UDelftZi kOm Wil | ----- |
| UFlorenc kOm Wil | ----- |

2A - 95

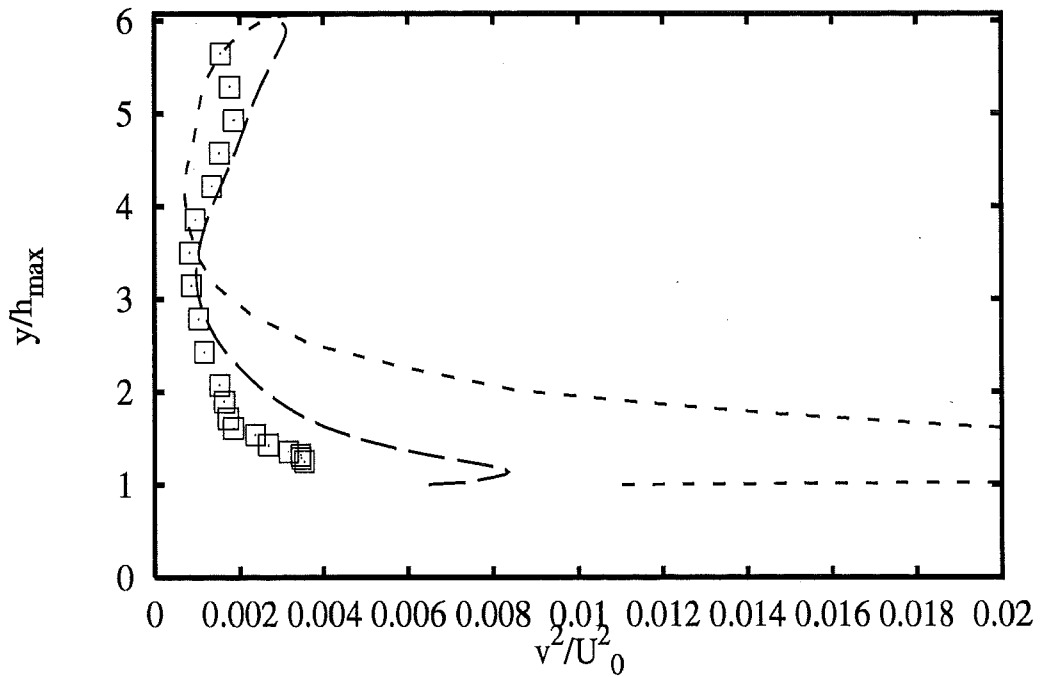
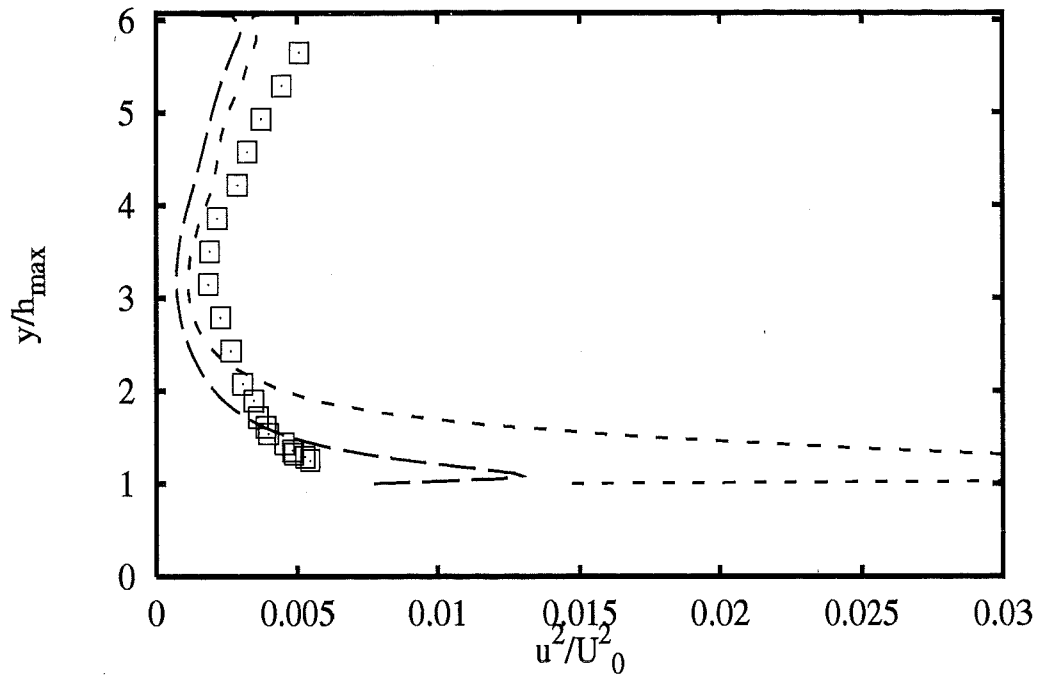


Profiles at $x/h_{max} = 0$

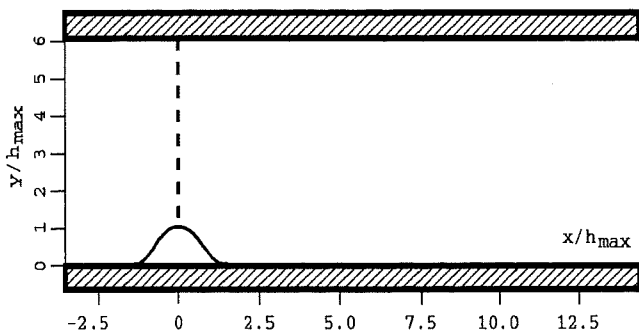


- | | |
|----------------------|-----------|
| Experiments | □ |
| ASC nKE SZL+wf | — — |
| Iolomouc nKE Spez+wf | - - - |
| DLRGoett kOm Wil | · · · · · |
| UChalmer kOm Wil | — · — |
| UDelftZi kOm Wil | - · - · - |
| UFlorenc kOm Wil | - · - - - |

2A - 96

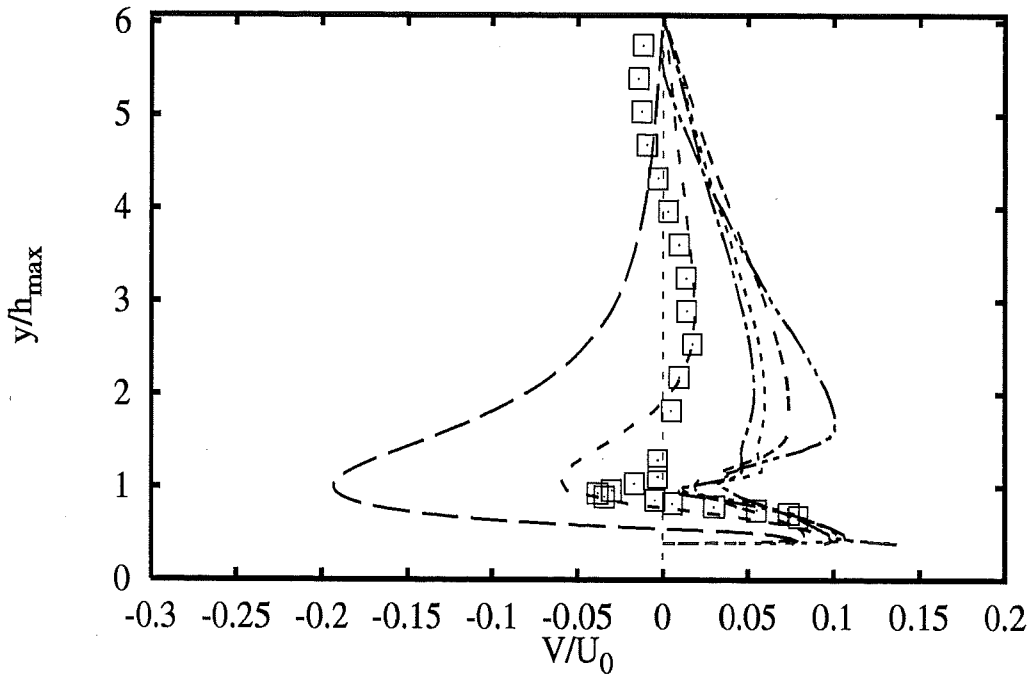
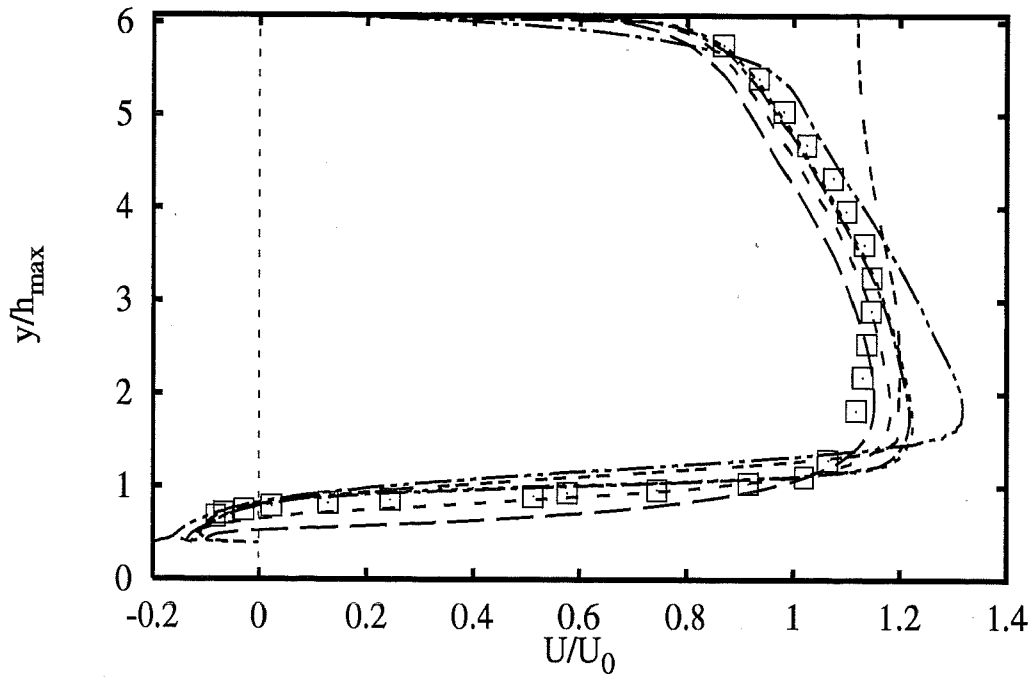


Profiles at $x/h_{max} = 0$

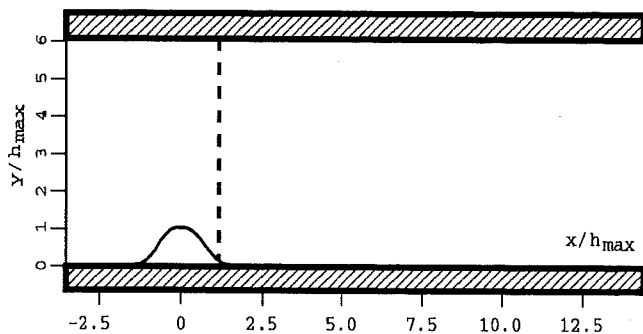


Experiments \square
ASC nKE SZL+wf - - -
IOlomouc nKE Spez+wf - - -

2A - 97

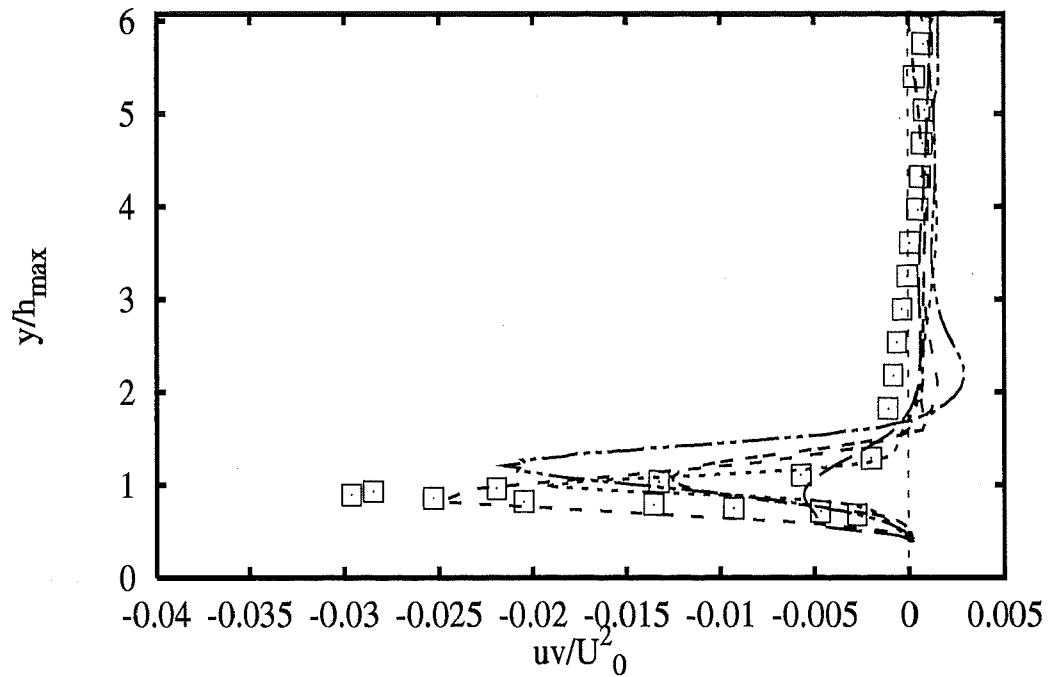
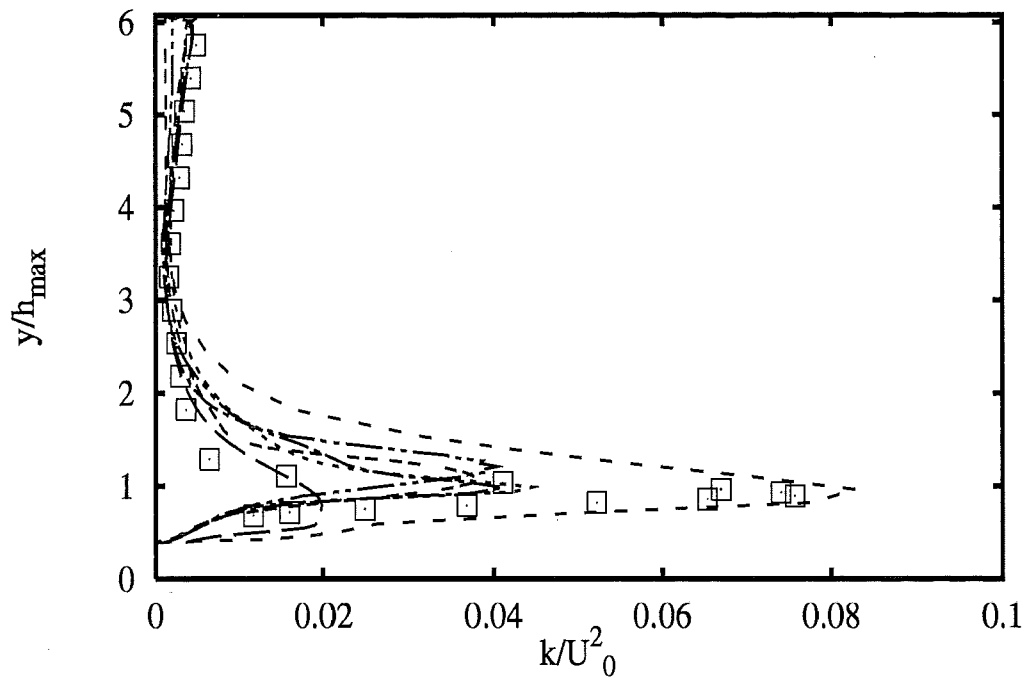


Profiles at $x/h_{max} = 1.07$

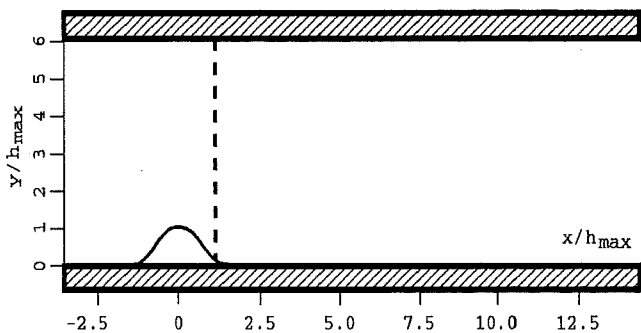


- | | | |
|-----------------|--------------------|-------|
| | Experiments | □ |
| ASC | nKE SZL+wf | --- |
| Iolomouc | nKE Spez+wf | --- |
| DLRGoett | kOm Wil | |
| UChalmer | kOm Wil | --- |
| UDelftZi | kOm Wil | --- |
| UFlorenc | kOm Wil | --- |

2A - 98

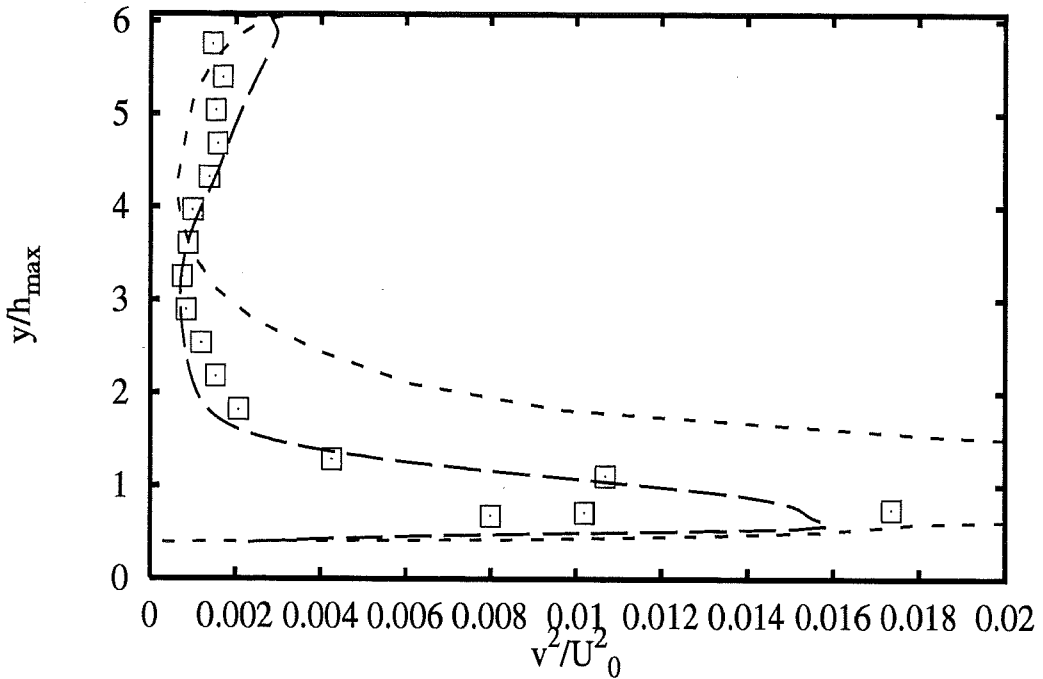
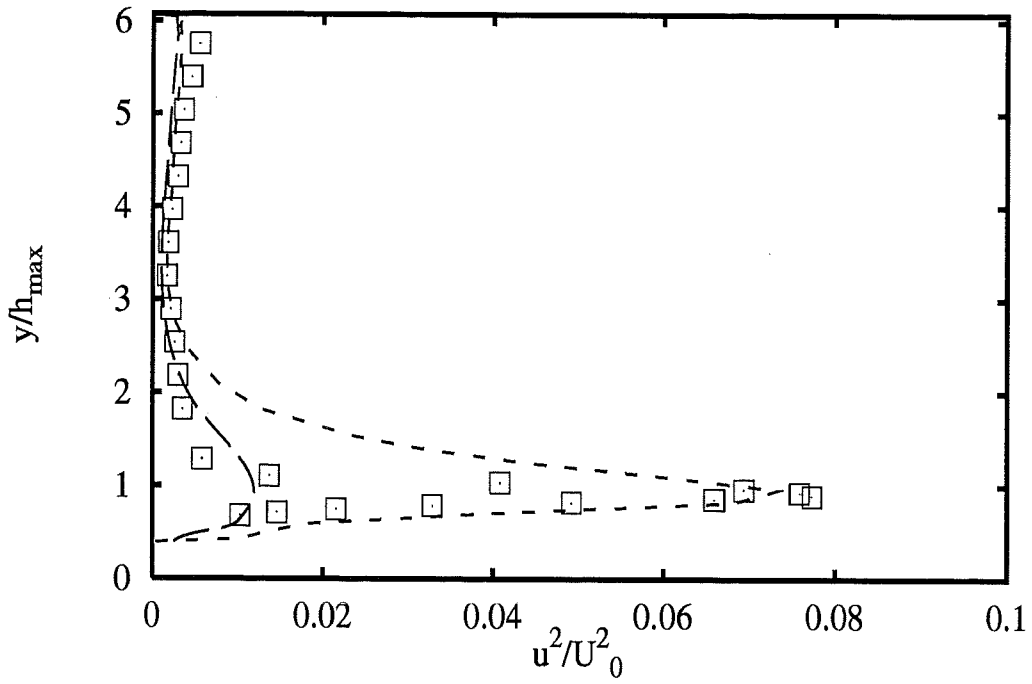


Profiles at $x/h_{max} = 1.07$

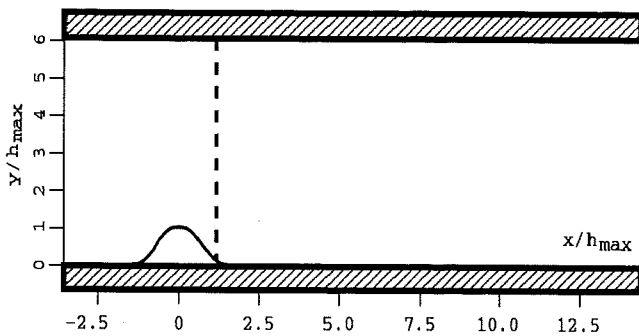


- | | |
|----------------------|-------|
| Experiments | □ |
| ASC nKE SZL+wf | — |
| Iolomouc nKE Spez+wf | - - - |
| DLRGoett kOm Wil | ⋯⋯⋯ |
| UChalmer kOm Wil | - - - |
| UDelftZi kOm Wil | ⋯⋯⋯ |
| UFlorenc kOm Wil | - - - |

2A - 99

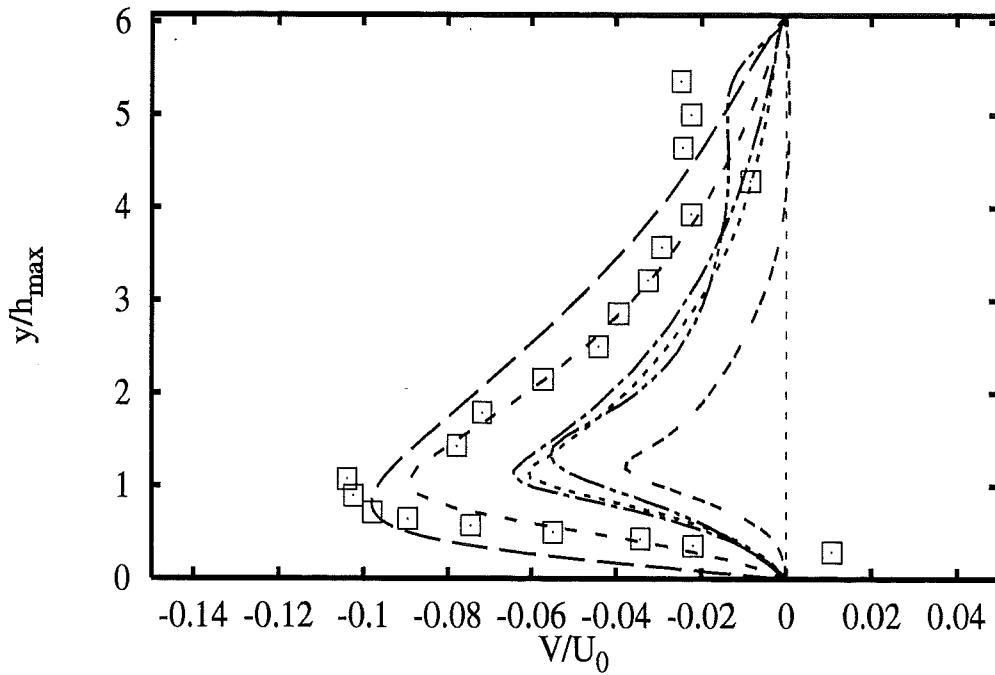
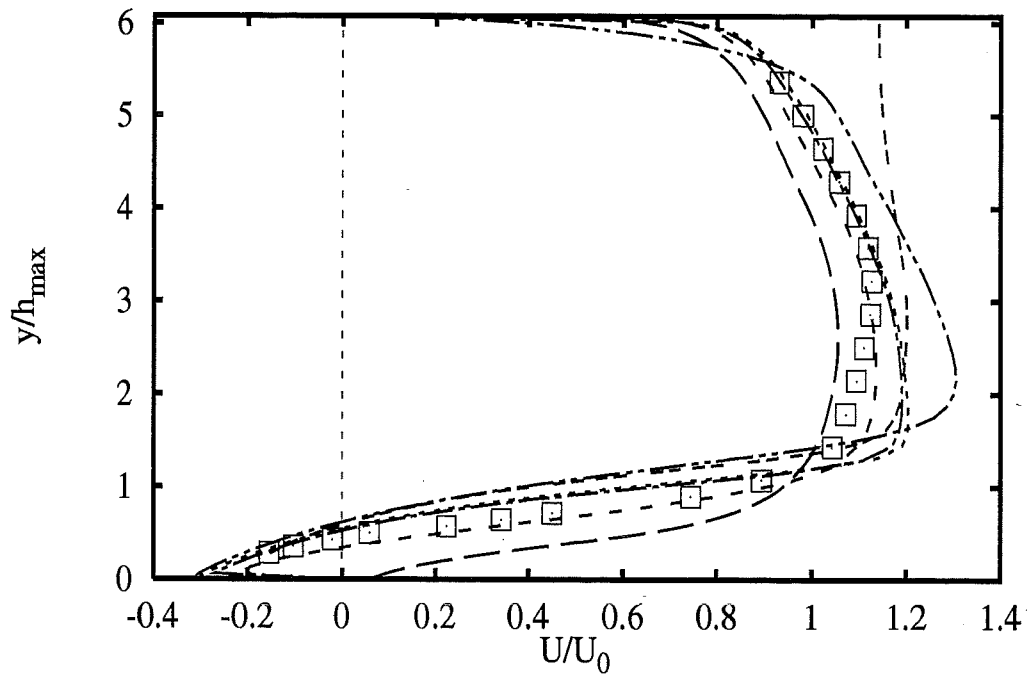


Profiles at $x/h_{max} = 1.07$

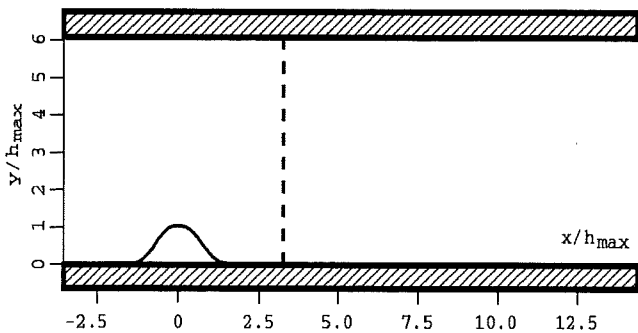


Experiments □
ASC nKE SZL+wf ---
Iolomouc nKE Spez+wf - - -

2A - 100

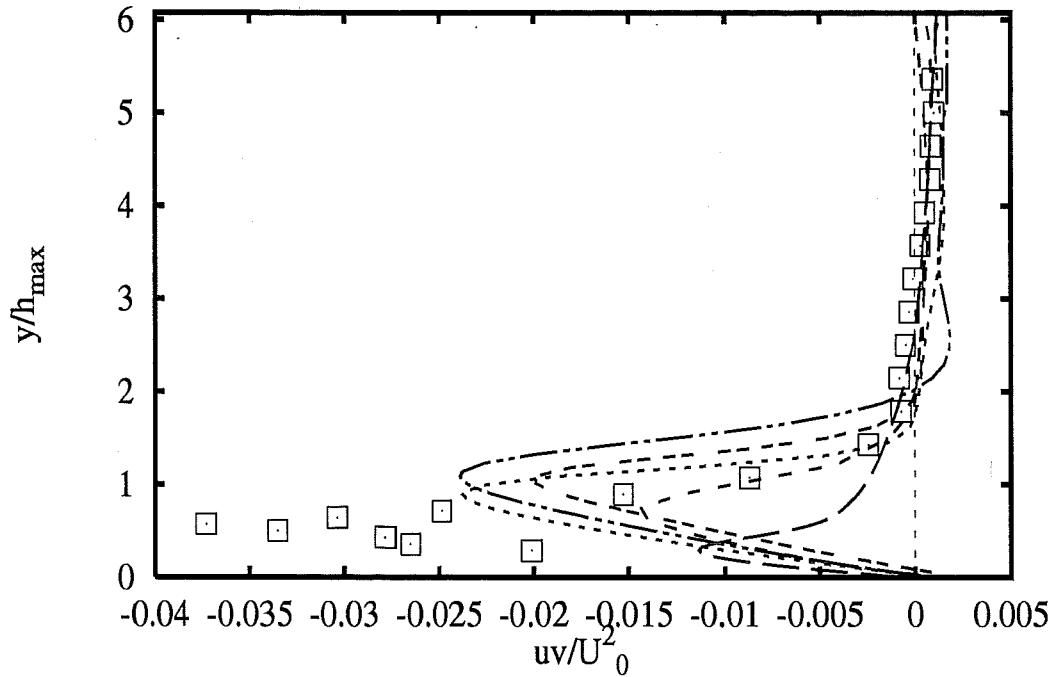
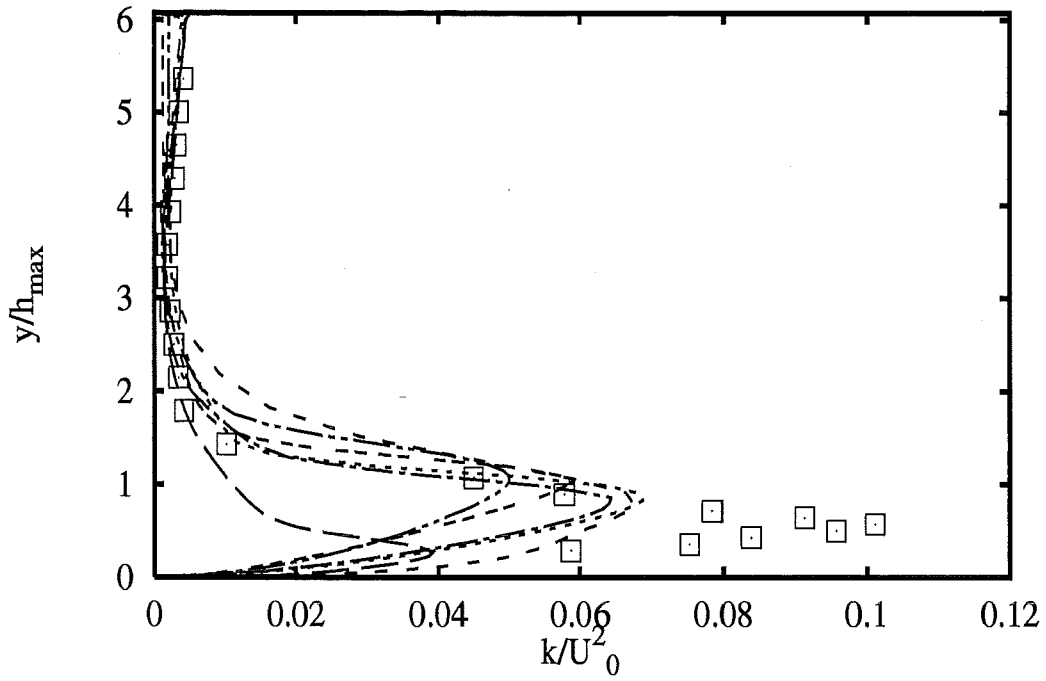


Profiles at $x/h_{max} = 3.21$

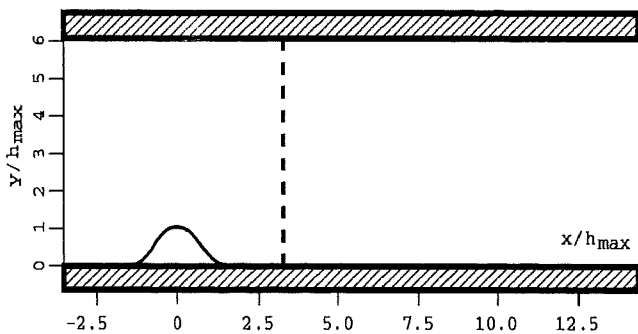


- | | |
|-----------------------------|-------|
| Experiments | □ |
| ASC nKE SZL+wf | --- |
| Iolomouc nKE Spez+wf | ---- |
| DLRGoett kOm Wil | |
| UChalmer kOm Wil | ---- |
| UDefltzi kOm Wil | |
| UFlorenc kOm Wil | ---- |

2A - 101

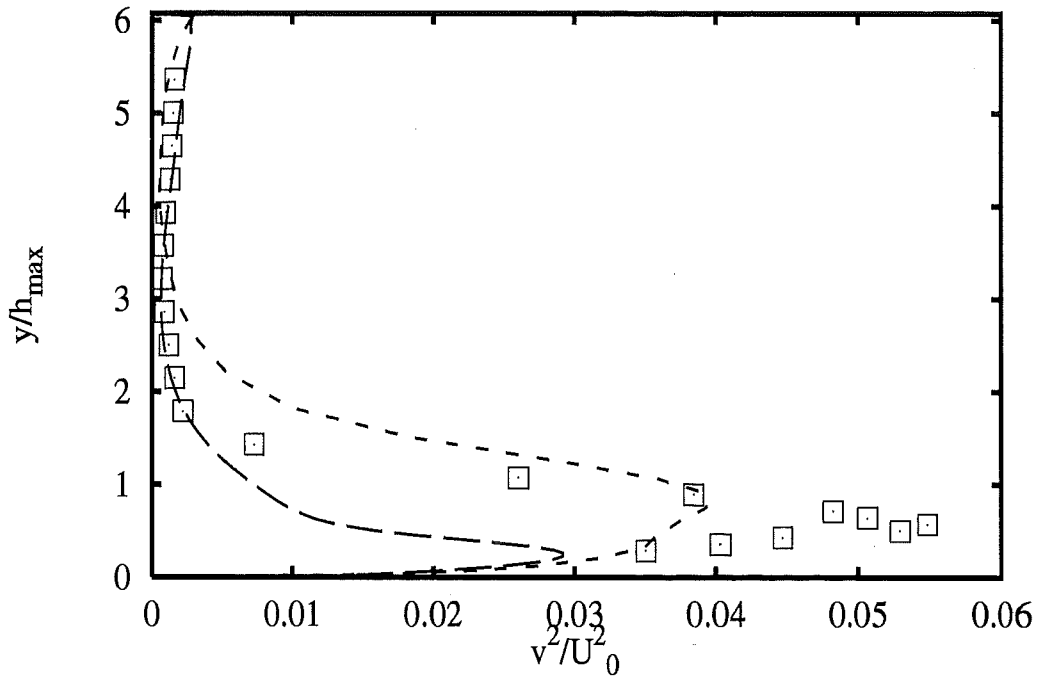
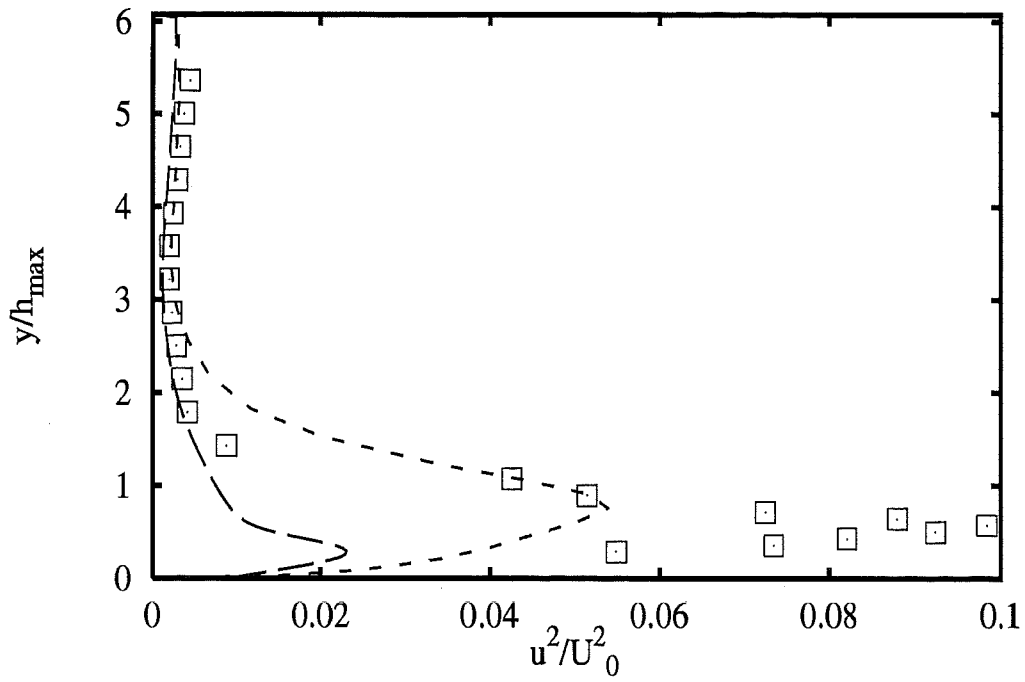


Profiles at $x/h_{max} = 3.21$

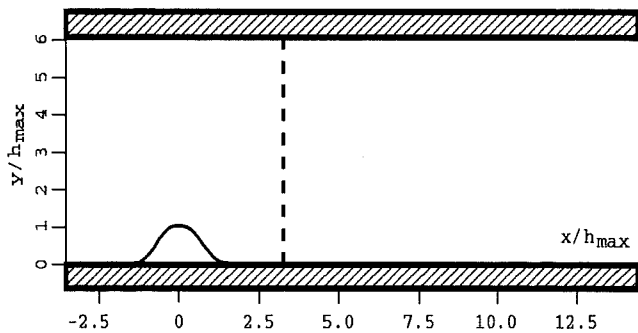


- | | |
|----------------------|-------|
| Experiments | □ |
| ASC nKE SZL+wf | --- |
| Iolomouc nKE Spez+wf | ---- |
| DLRGoett kOm Wil | |
| UChalmer kOm Wil | ----- |
| UDelftZi kOm Wil | ----- |
| UFlorenc kOm Wil | ----- |

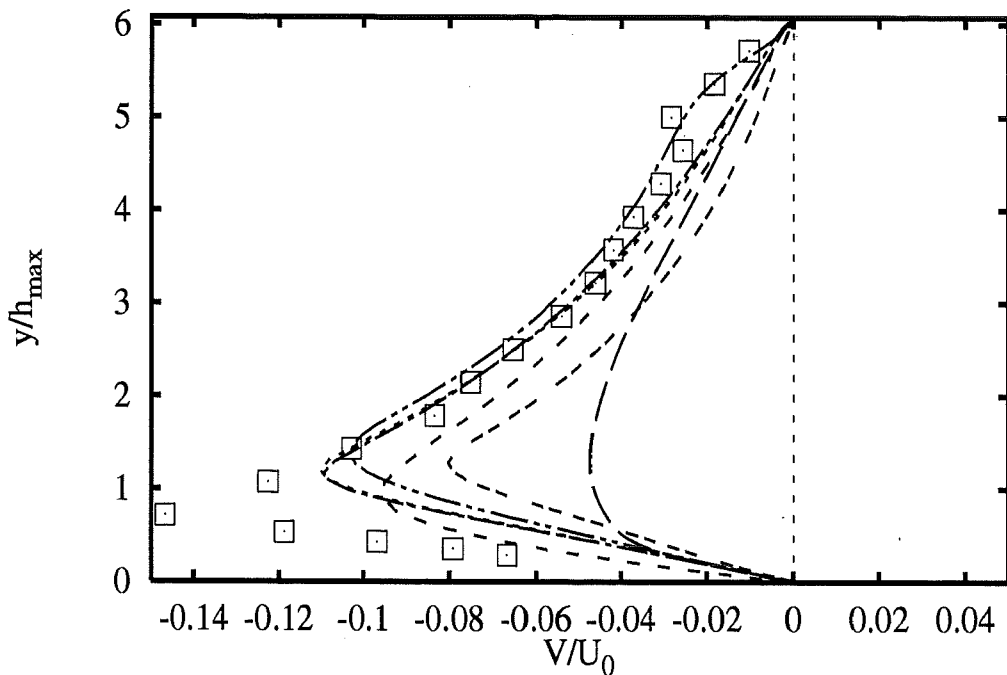
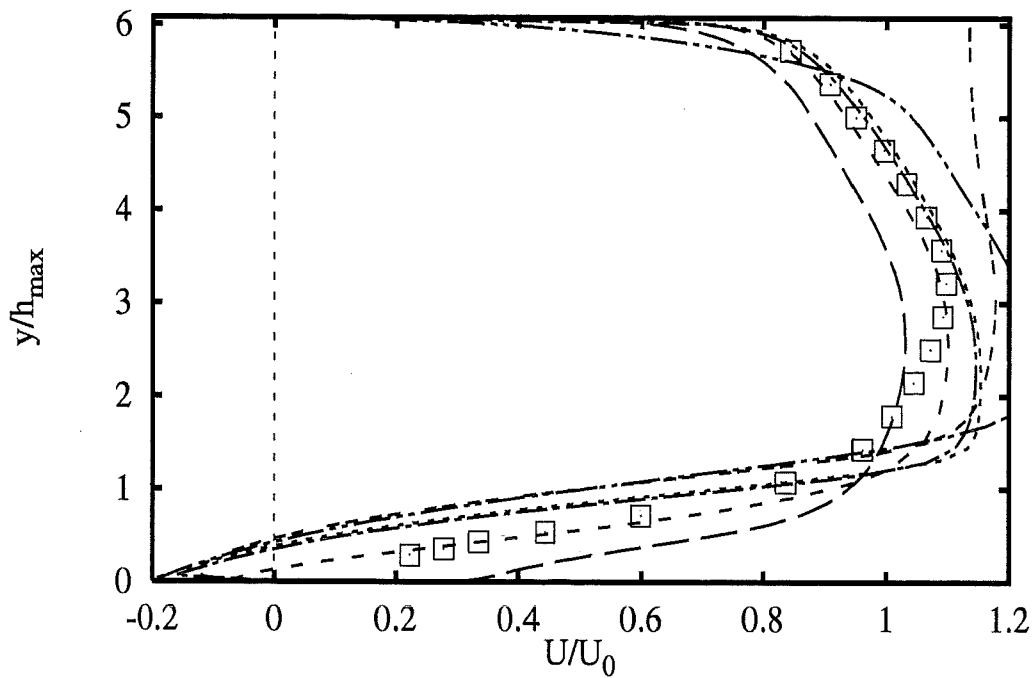
2A - 102



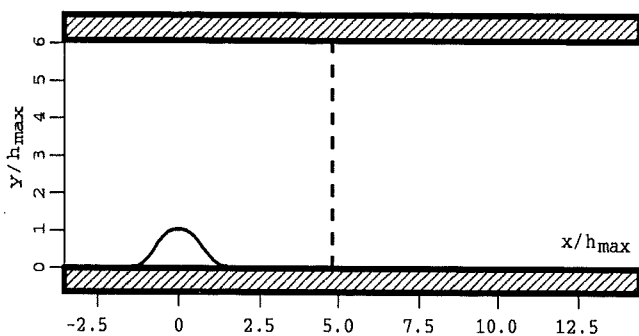
Profiles at $x/h_{max} = 3.21$



Experiments \square
ASC nKE SZL+wf - - -
Iolomouc nKE Spez+wf - - -

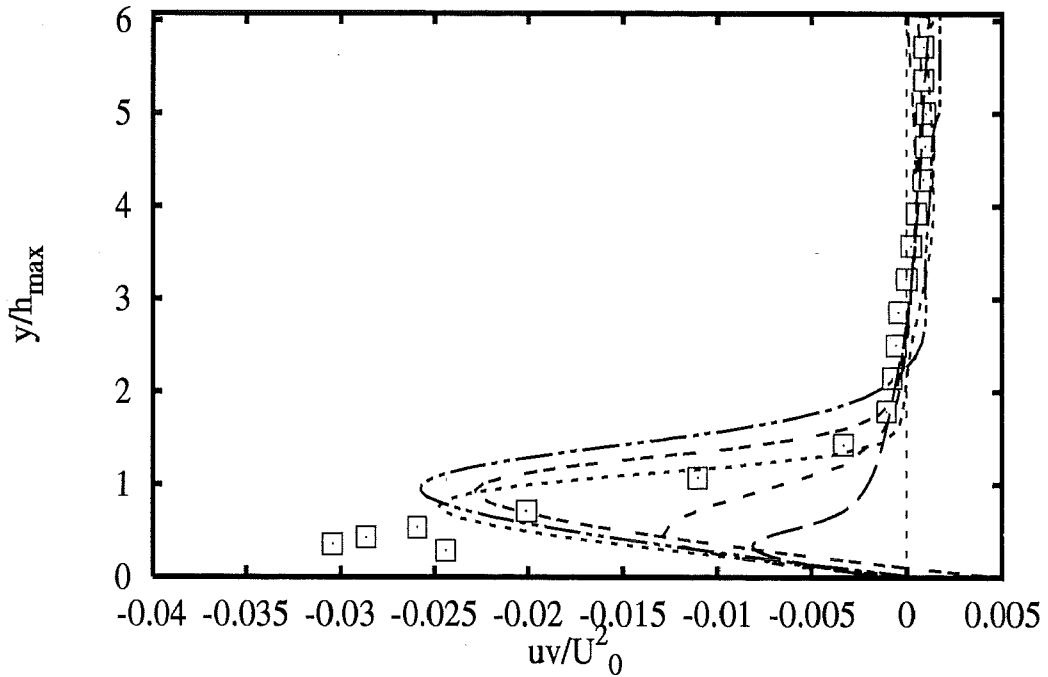
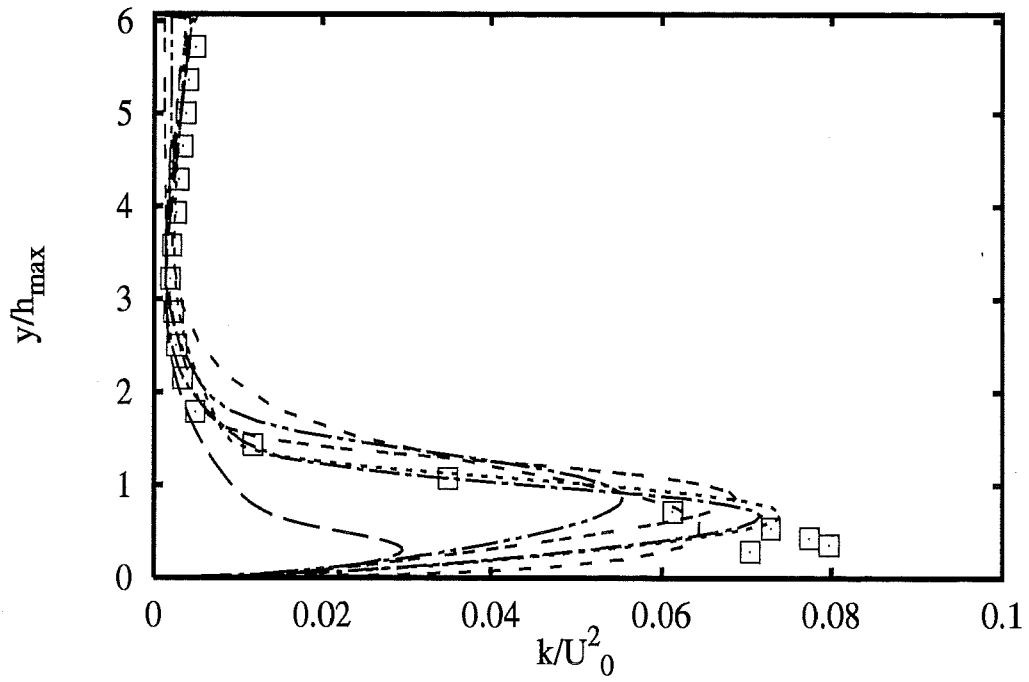


Profiles at $x/h_{max} = 4.79$

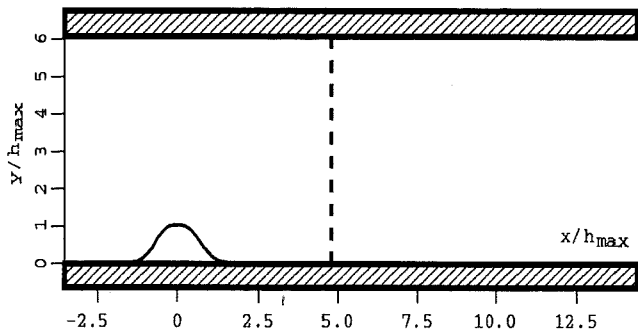


- | | |
|----------------------|-------|
| Experiments | □ |
| ASC nKE SZL+wf | --- |
| Iolomouc nKE Spez+wf | ---- |
| DLRGoett kOm Wil | |
| UChalmer kOm Wil | ----- |
| UDelftZi kOm Wil | ----- |
| UFlorenc kOm Wil | ----- |

2A - 104

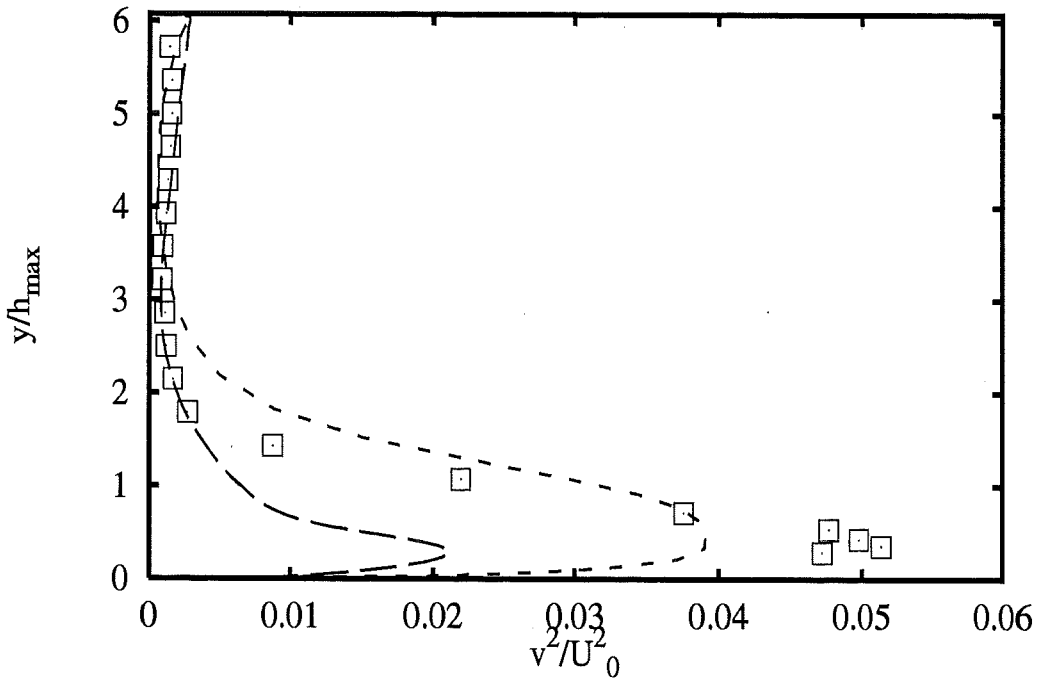
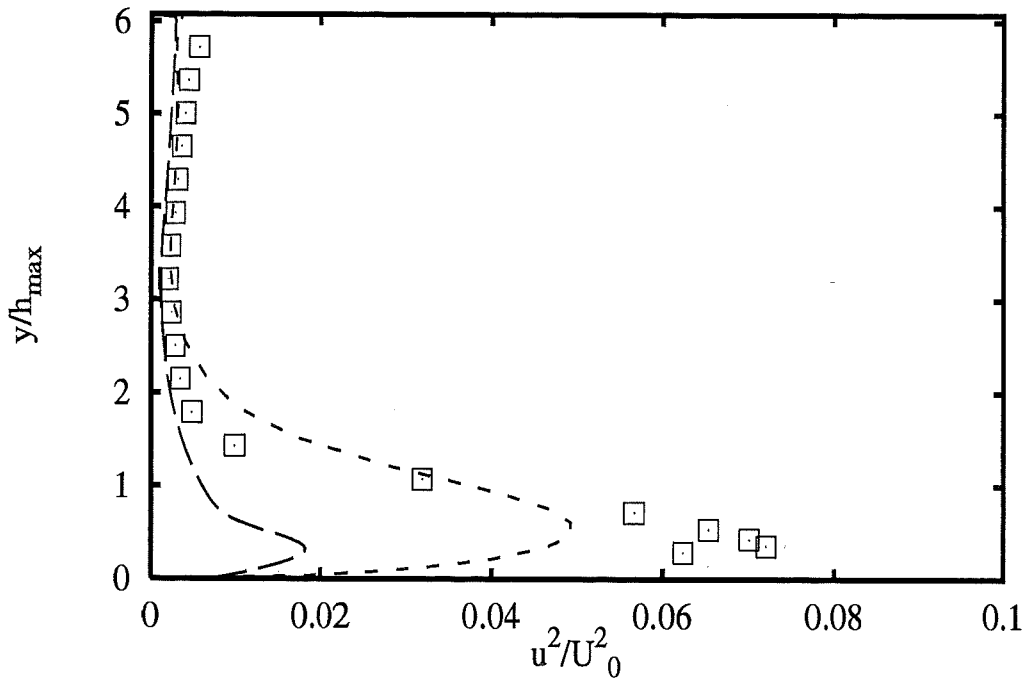


Profiles at $x/h_{max} = 4.79$

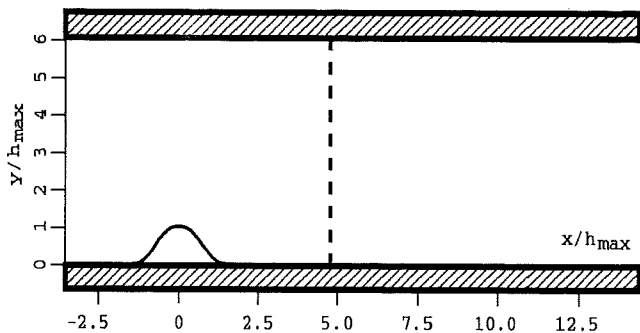


- | | |
|----------------------|-----------|
| Experiments | □ |
| ASC nKE SZL+wf | — |
| Iolomouc nKE Spez+wf | - - - |
| DLRGoett kOm Wil | · · · · · |
| UChalmer kOm Wil | - - - - - |
| UDelftZi kOm Wil | - · - · - |
| UFlorenc kOm Wil | - - - - - |

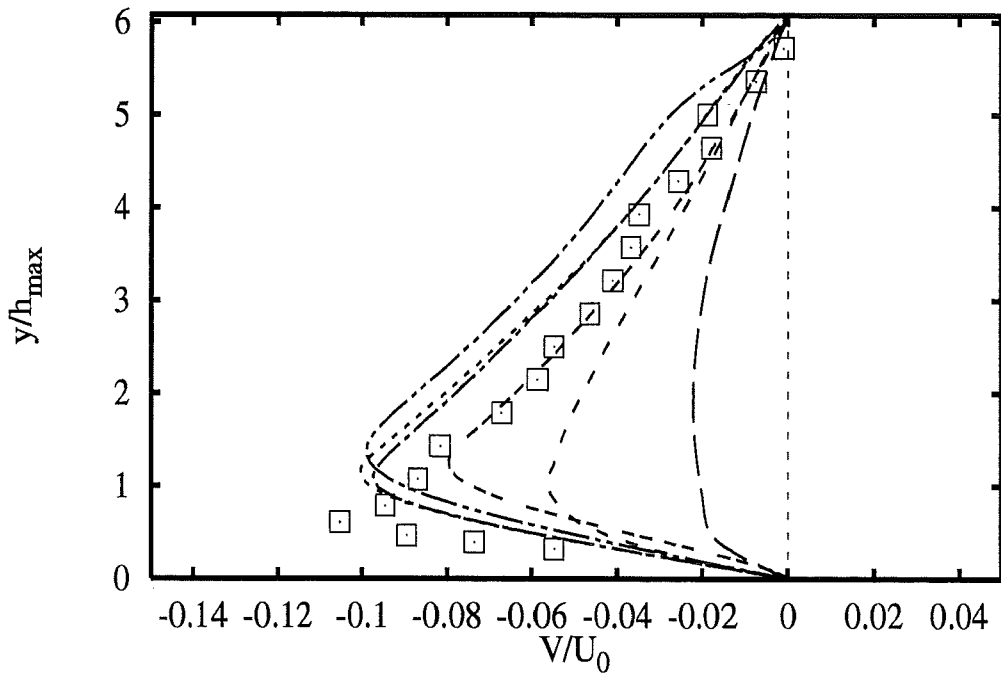
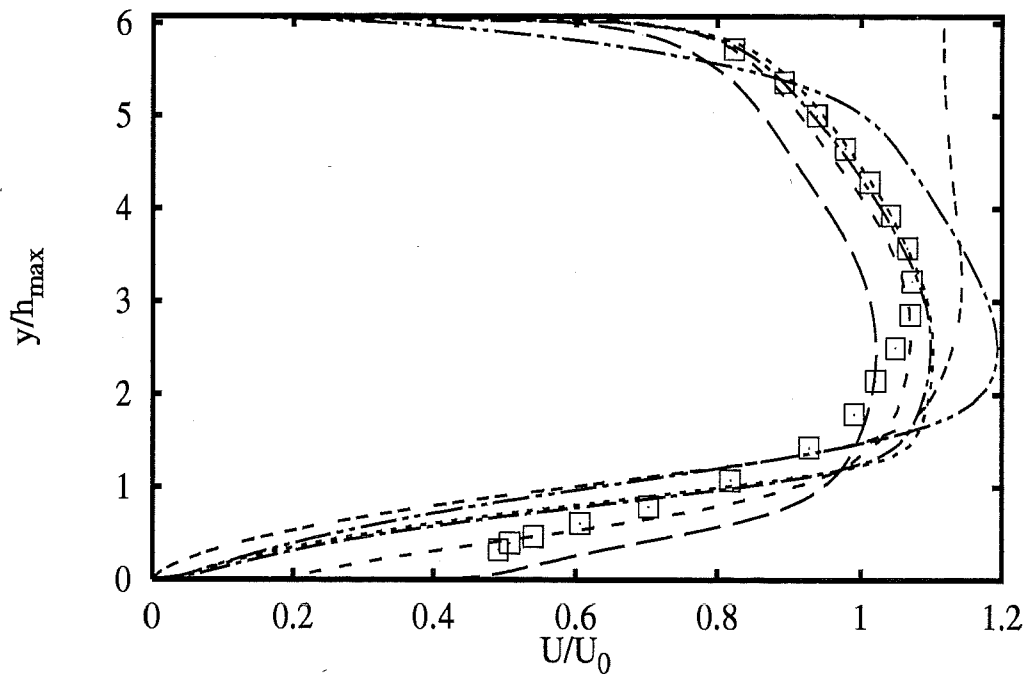
2A - 105



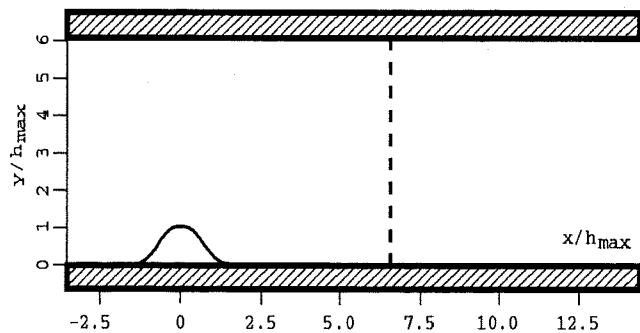
Profiles at $x/h_{max} = 4.79$



Experiments □
ASC nKE SZL+wf ---
IOlomouc nKE Spez+wf - - -

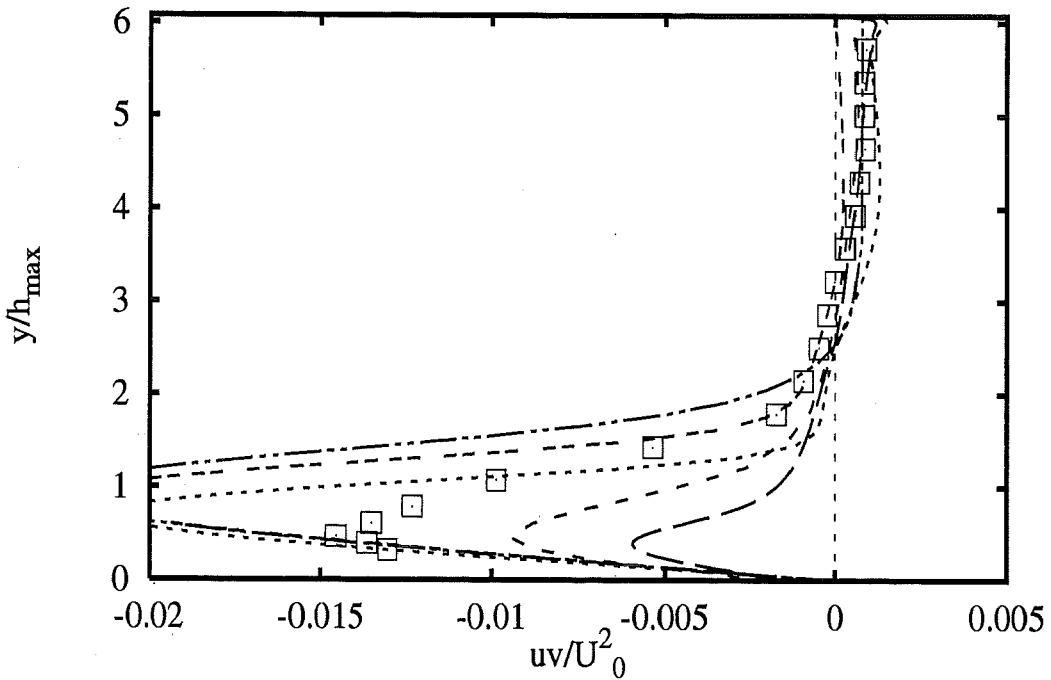
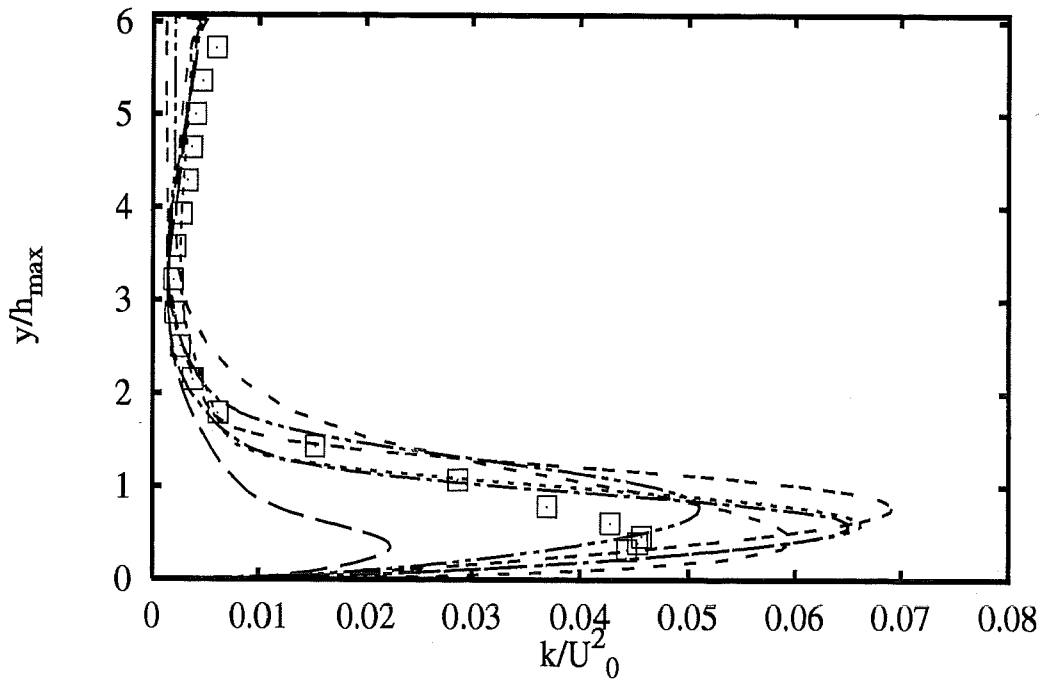


Profiles at $x/h_{max} = 6.61$

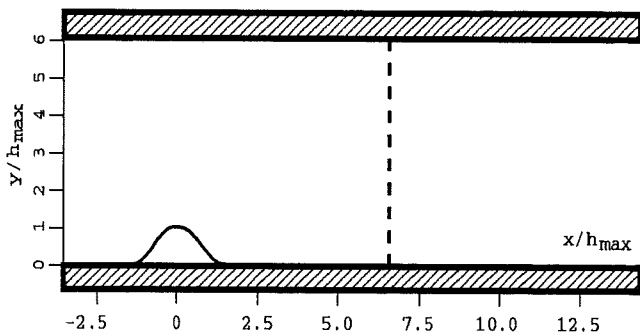


- | | |
|----------------------|-------|
| Experiments | □ |
| ASC nKE SZL+wf | --- |
| IOLomouc nKE Spez+wf | ---- |
| DLRGoett kOm Wil | |
| UChalmer kOm Wil | ----- |
| UDelftZi kOm Wil | ----- |
| UFlorenc kOm Wil | ----- |

2A - 107

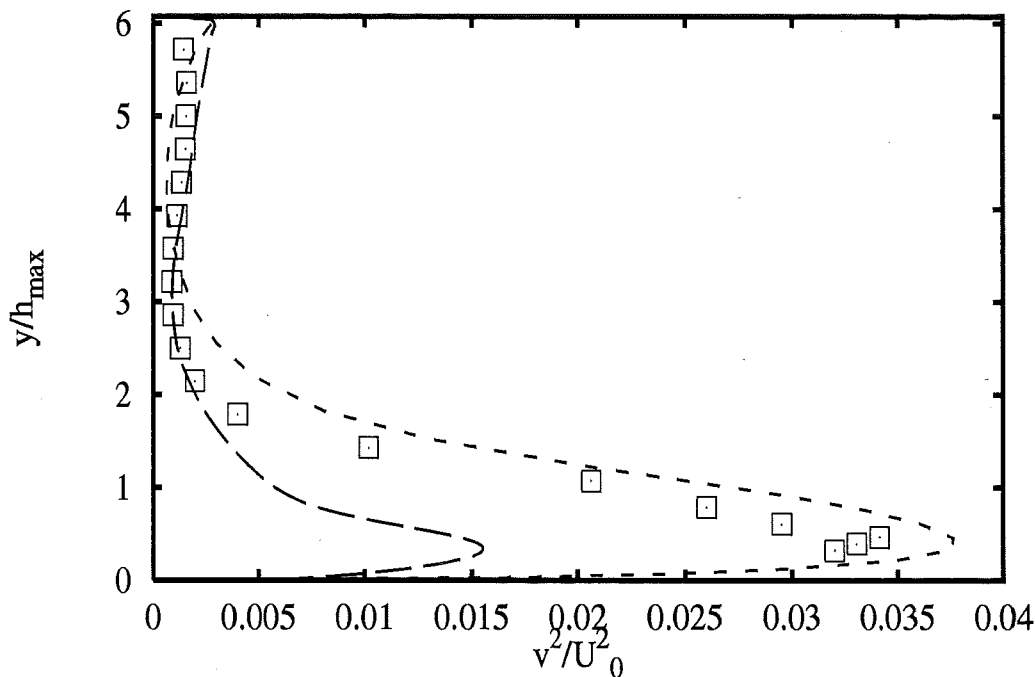
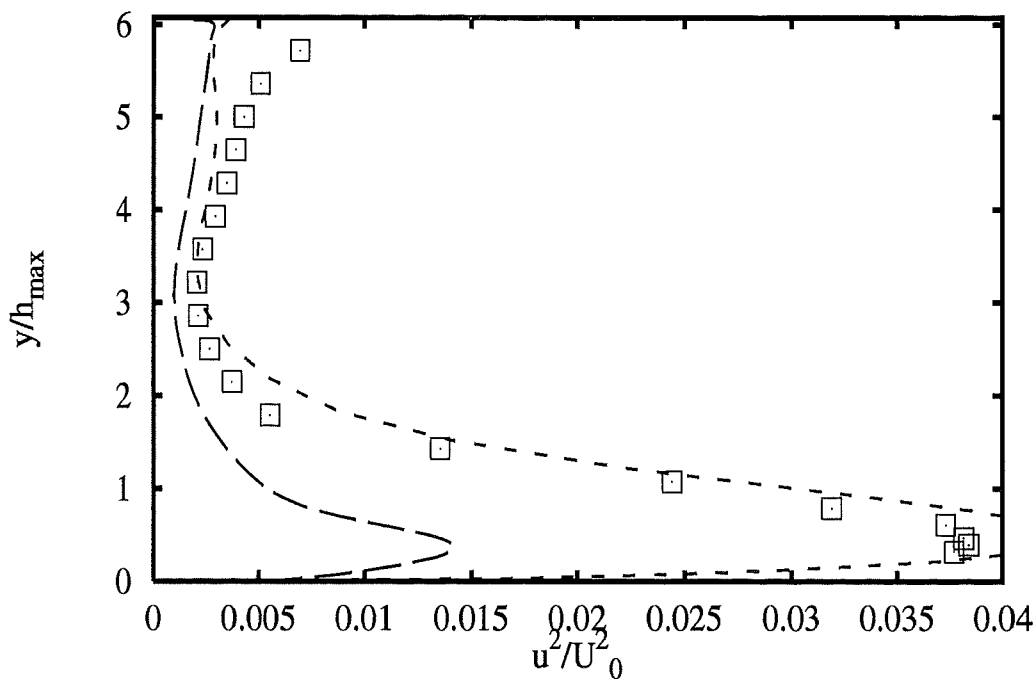


Profiles at $x/h_{max} = 6.61$

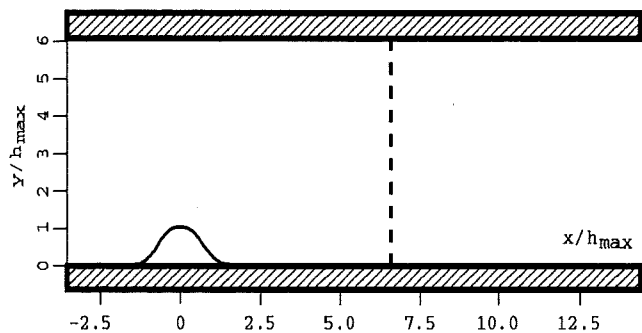


- | | |
|----------------------|-------|
| Experiments | □ |
| ASC nKE SZL+wf | --- |
| Iolomouc nKE Spez+wf | ---- |
| DLRGoett kOm Wil | |
| UChalmer kOm Wil | ---- |
| UDelftZi kOm Wil | ---- |
| UFlorenc kOm Wil | ---- |



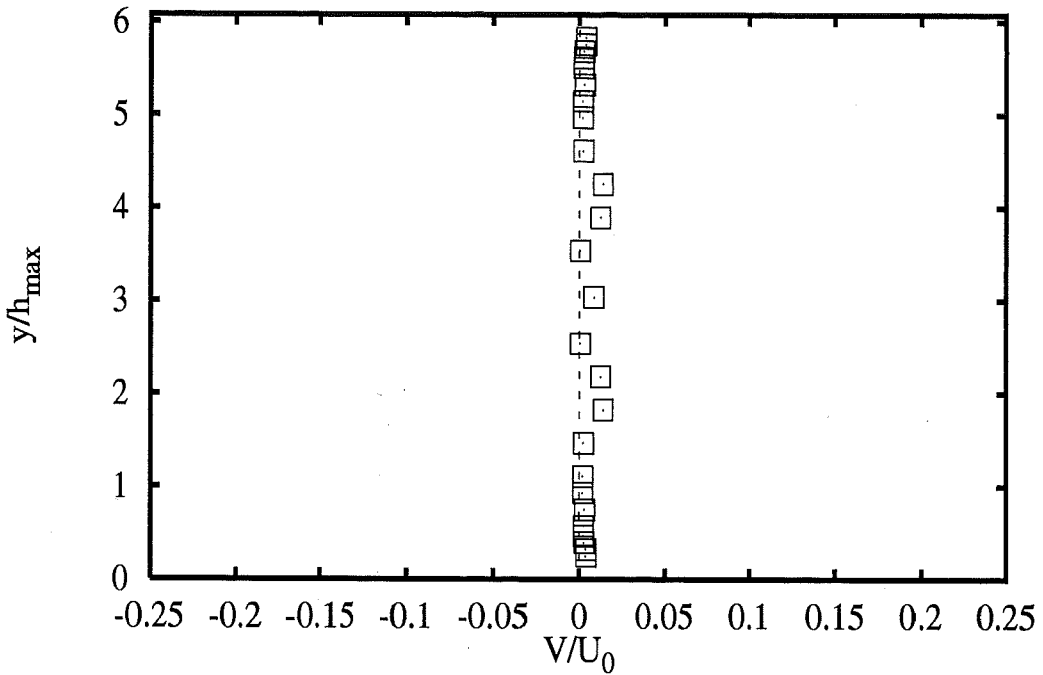
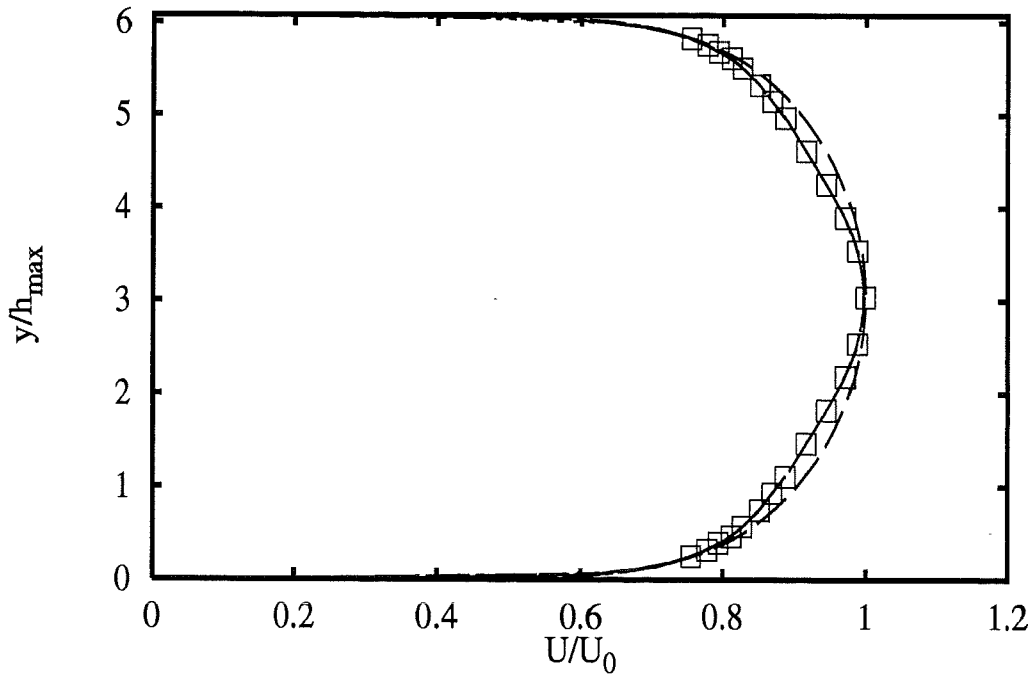


Profiles at $x/h_{max} = 6.61$

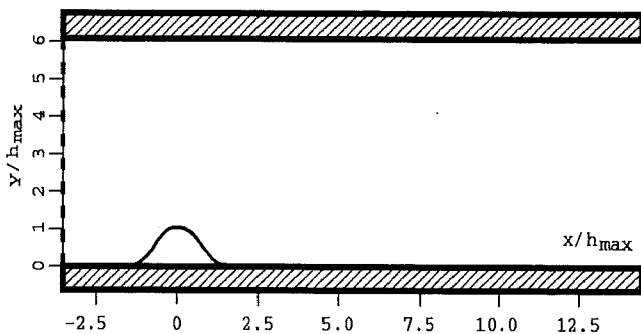


Experiments \square
ASC nKE SZL+wf $-\cdot-$
Iolomouc nKE Spez+wf $---$

2A - 109

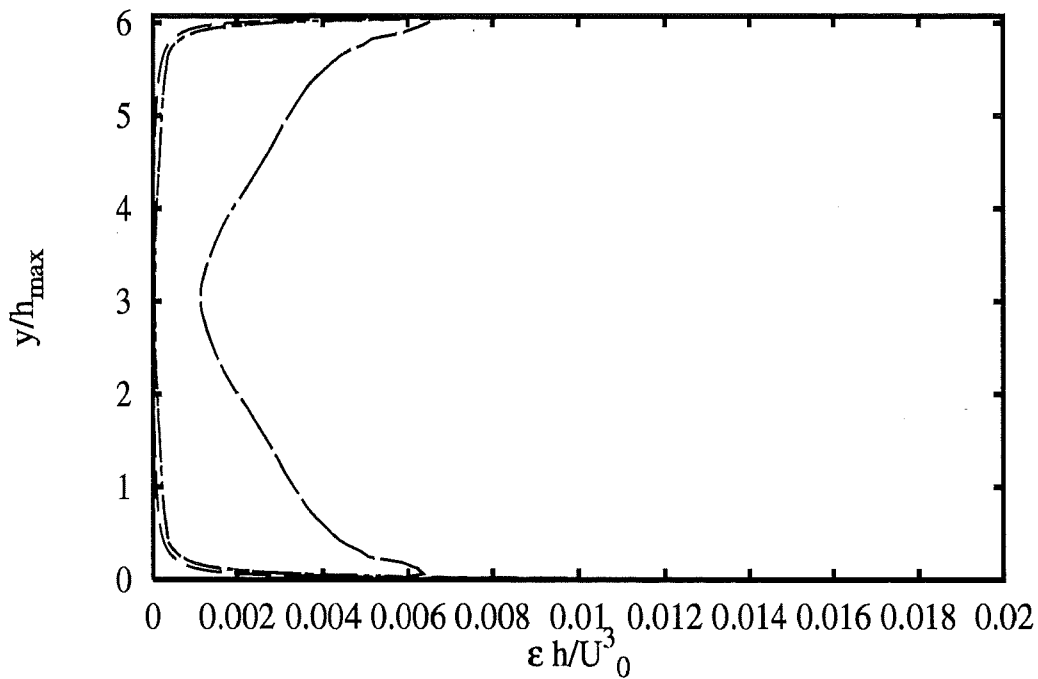
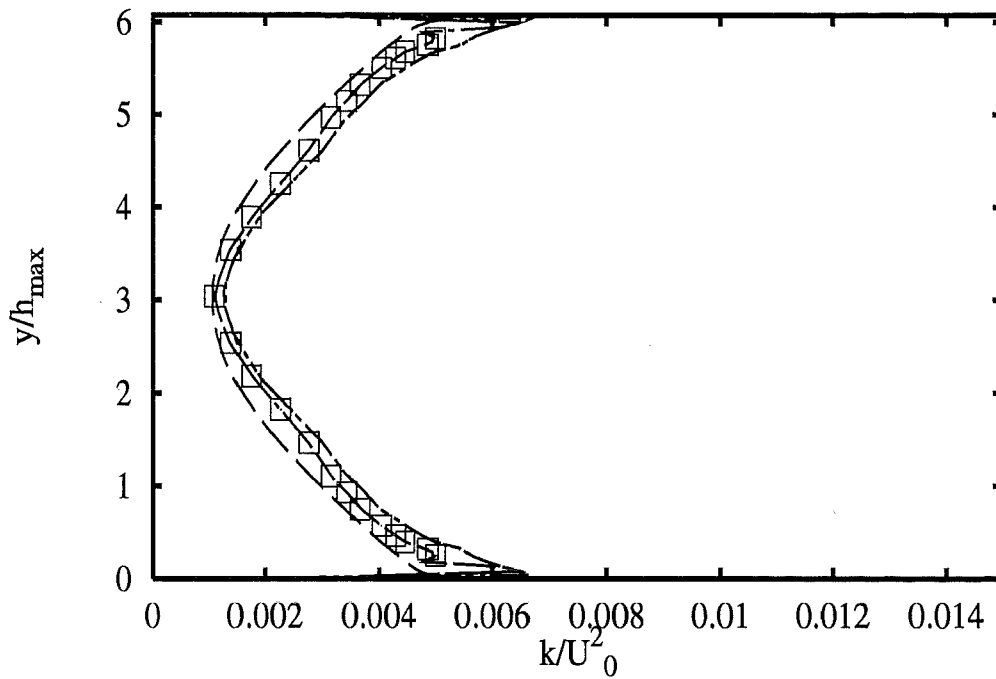


Profiles at $x/h_{max} = -3.57$

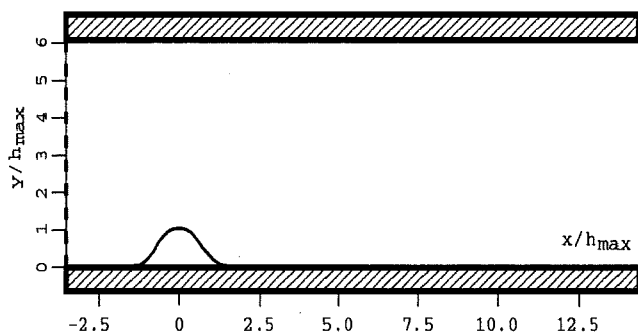


- | | |
|-----------------------|-------|
| Experiments | □ |
| UdelftHa RSM LRR+wf | --- |
| UChalmer RSM LRR+wf | --- |
| UMISTLes RSM GiLa+wf | |
| UChalmer RSM SSG+wf | --- |
| UMISTLes RSM GiLa+Wol | --- |
| UChalmer RSM HaLa | --- |

2A - 110

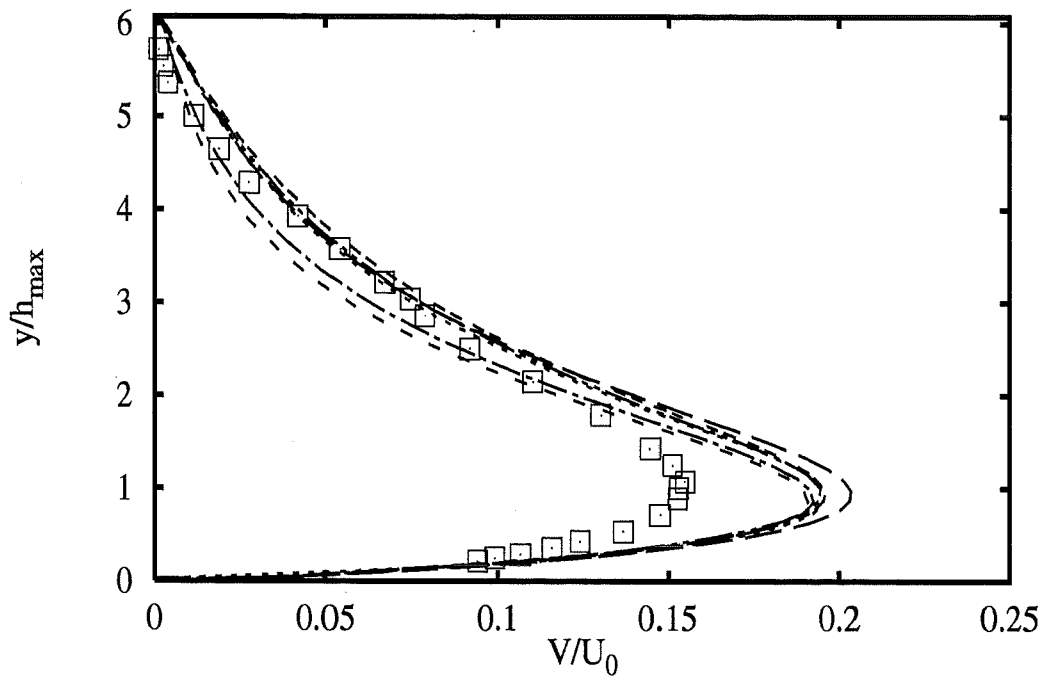
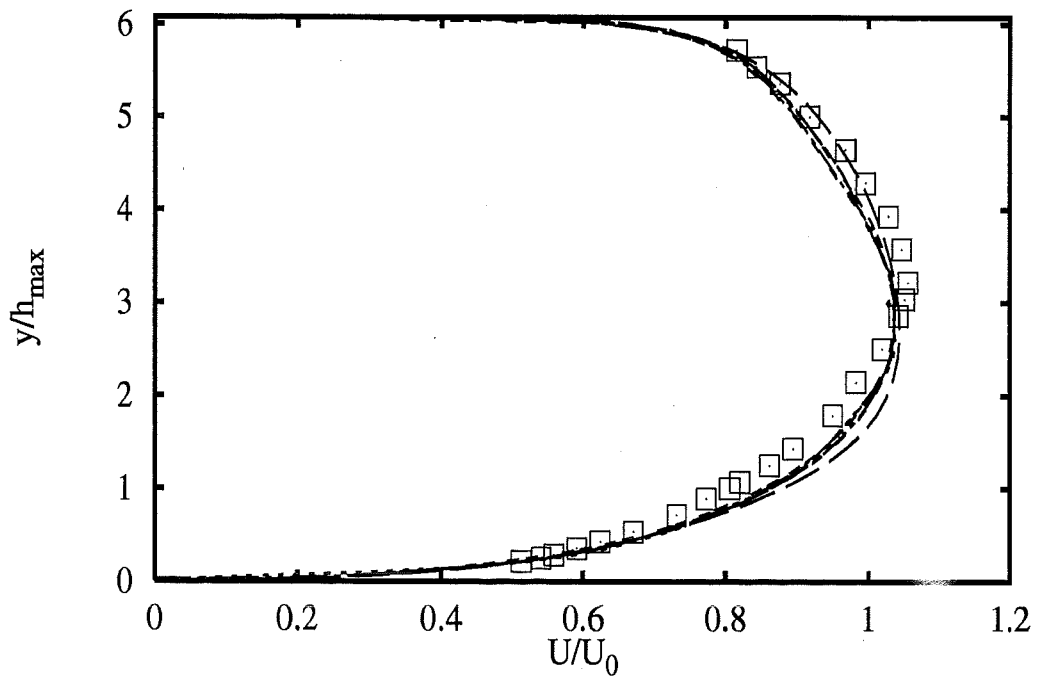


Profiles at $x/h_{max} = -3.57$

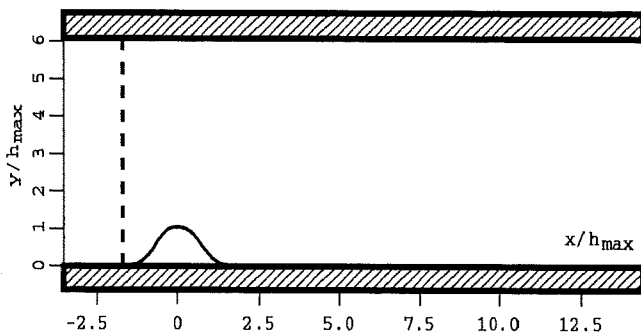


- | | | |
|----------|--------------------|-------|
| | Experiments | □ |
| UdelftHa | RSM LRR+wf | --- |
| UChalmer | RSM LRR+wf | - - - |
| UMISTLes | RSM GiLa+wf | |
| UChalmer | RSM SSG+wf | ---- |
| UMISTLes | RSM GiLa+Wol | ---- |
| UChalmer | RSM HaLa | ---- |

2A - 111

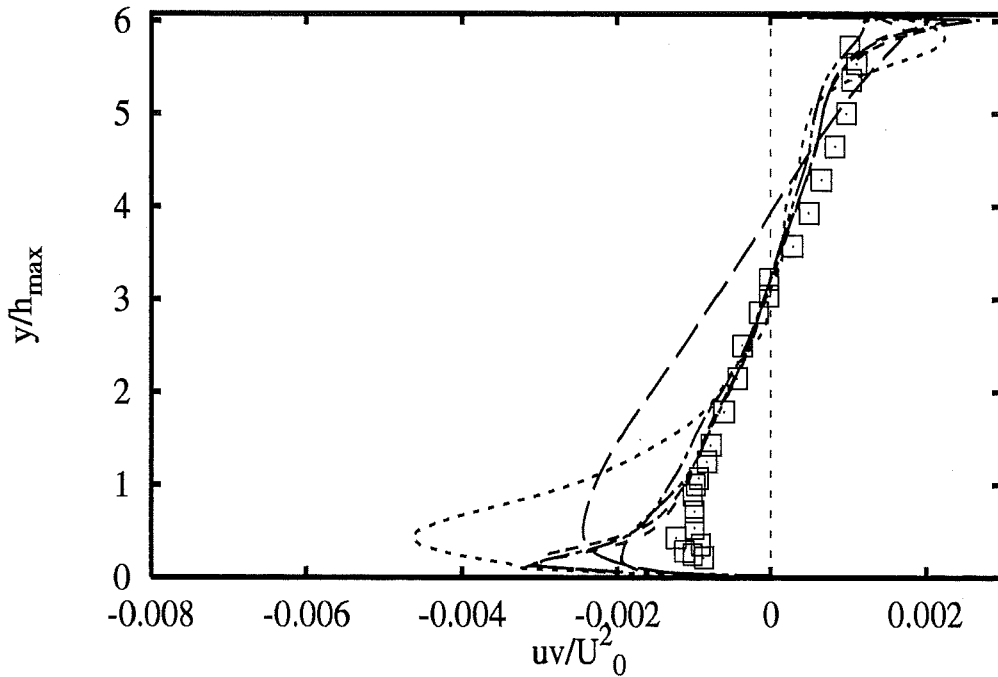
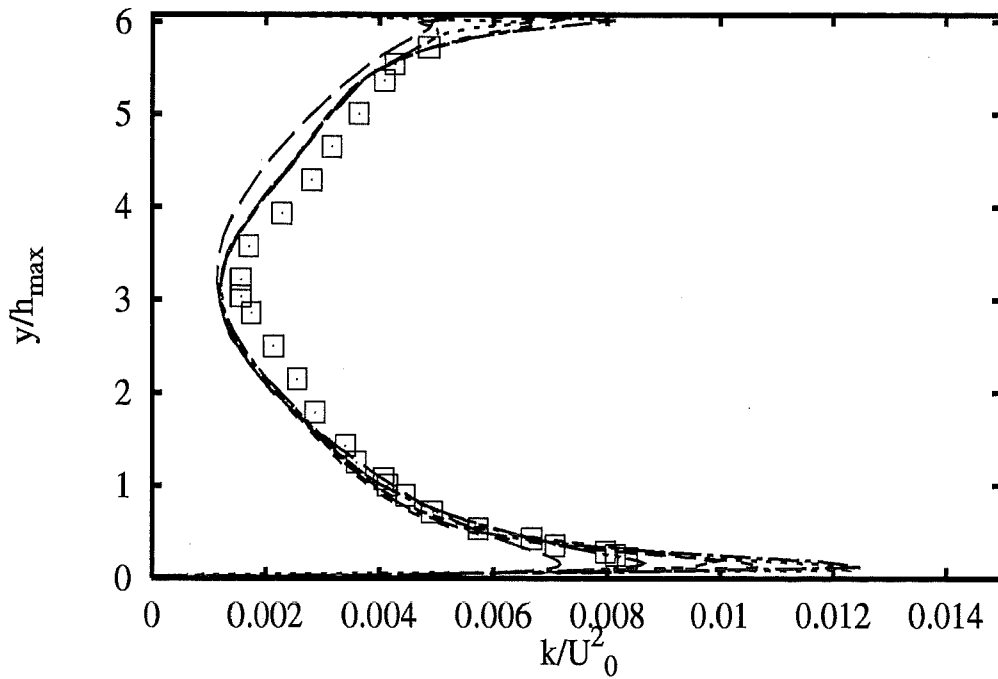


Profiles at $x/h_{max} = -1.78$

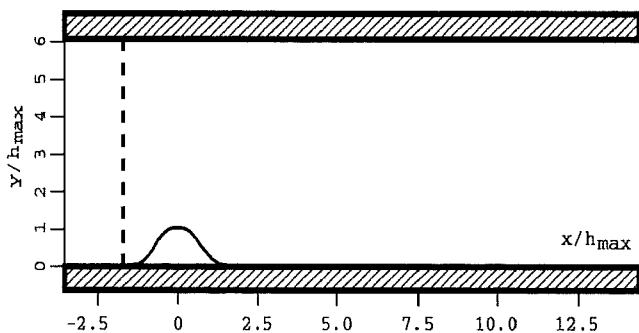


- | | | |
|----------|--------------------|-------|
| | Experiments | □ |
| UDelftHa | RSM LRR+wf | --- |
| UChalmer | RSM LRR+wf | ---- |
| UMISTLes | RSM GiLa+wf | |
| UChalmer | RSM SSG+wf | ---- |
| UMISTLes | RSM GiLa+Wol | ---- |
| UChalmer | RSM HaLa | ---- |

2A - 112

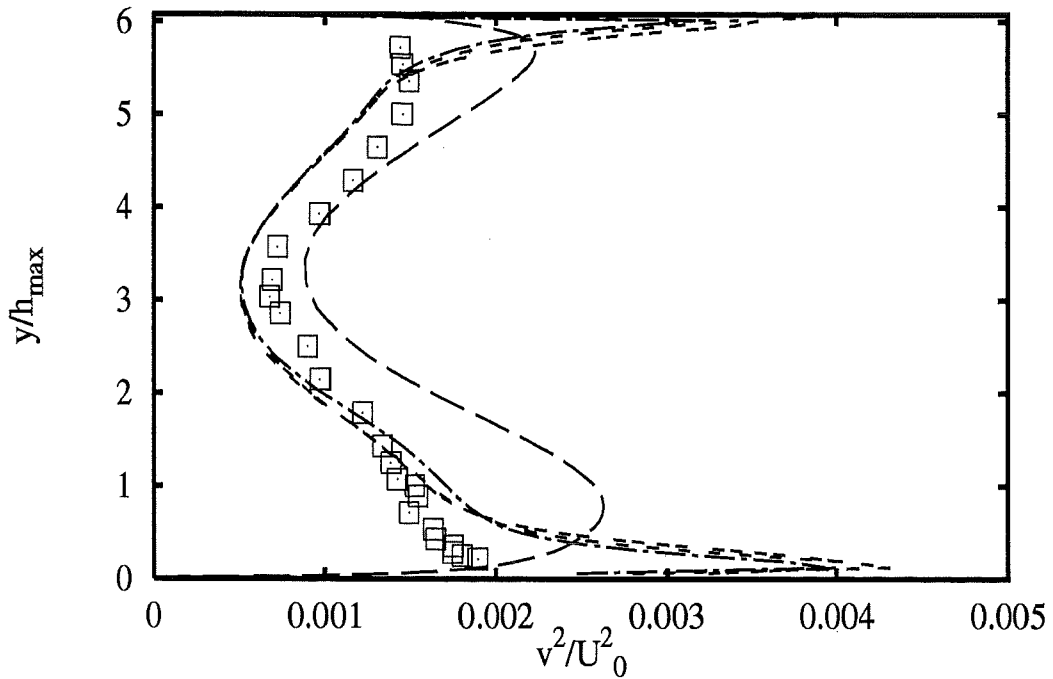
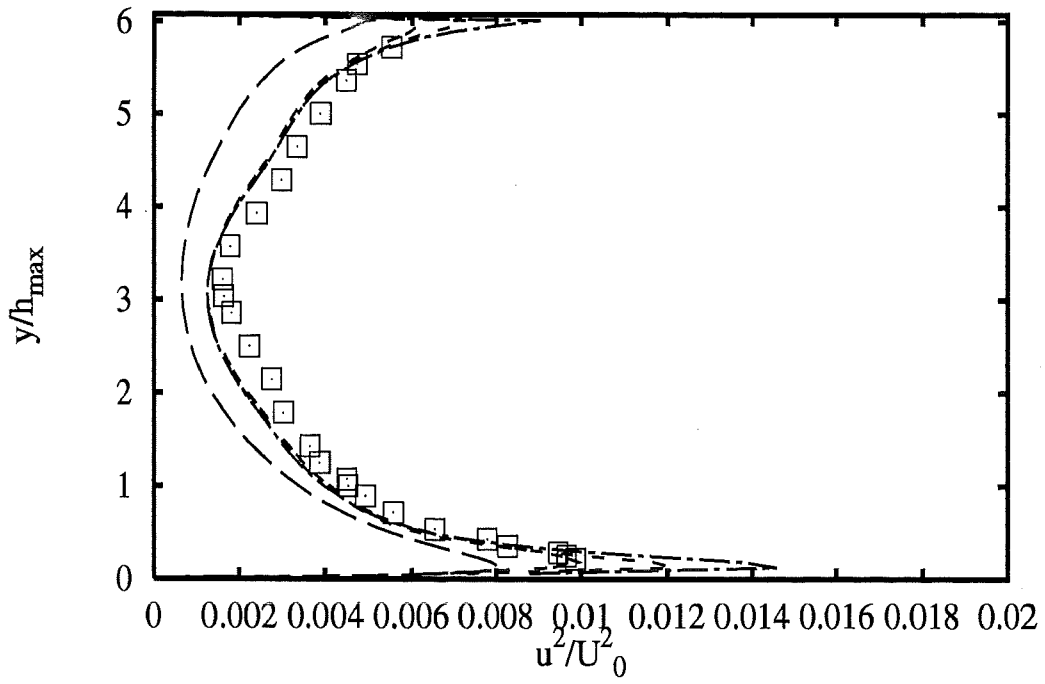


Profiles at $x/h_{max} = -1.78$

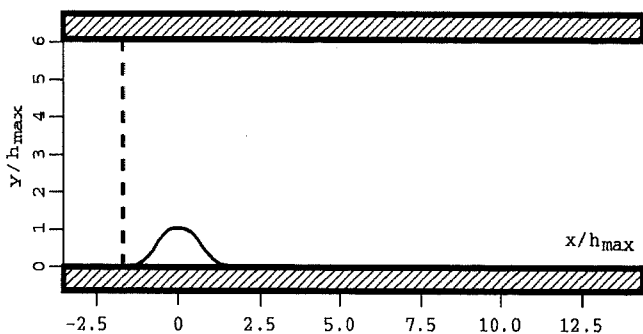


- | | |
|------------------------------|-----------|
| Experiments | □ |
| UdelftHa RSM LRR+wf | — |
| UChalmer RSM LRR+wf | - - - |
| UMISTLes RSM GiLa+wf | · · · · · |
| UChalmer RSM SSG+wf | - - - |
| UMISTLes RSM GiLa+Wol | · · · · · |
| UChalmer RSM HaLa | - - - |

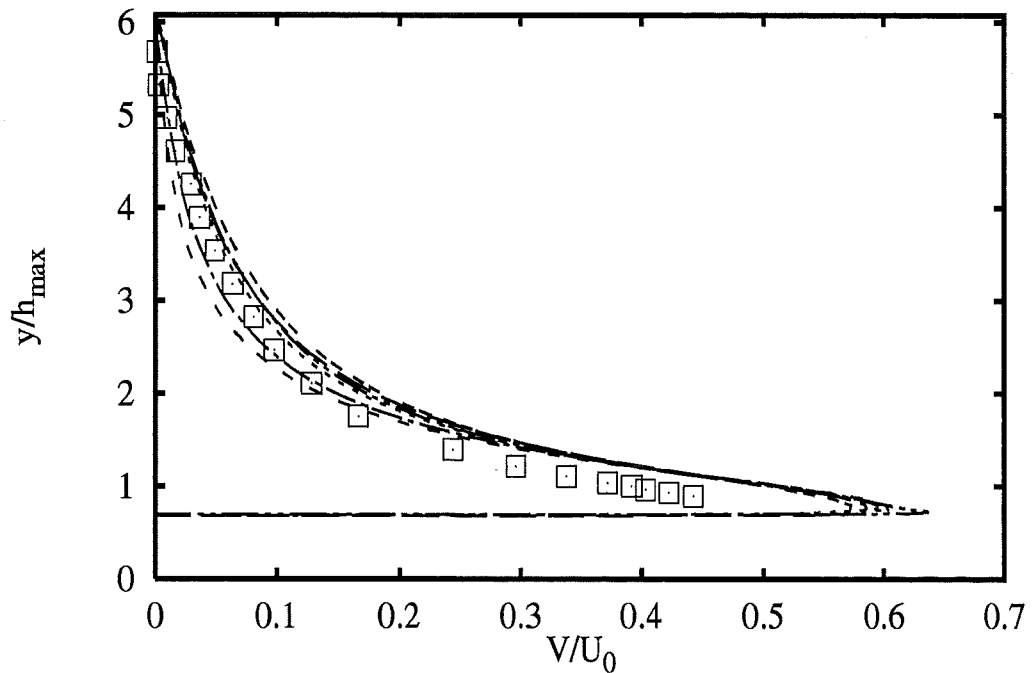
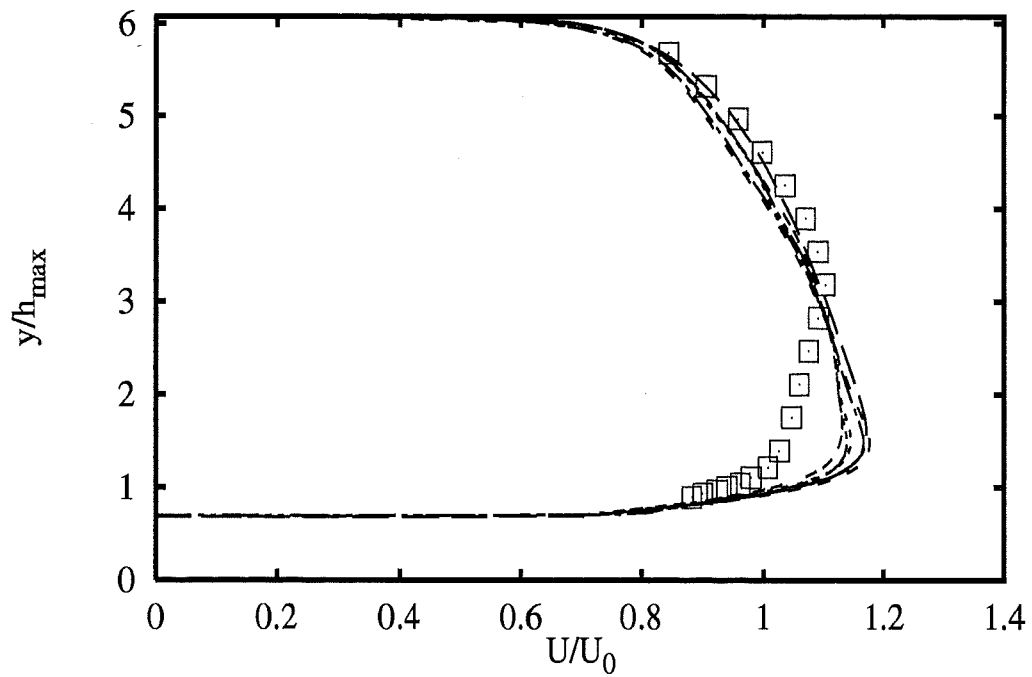
2A - 113



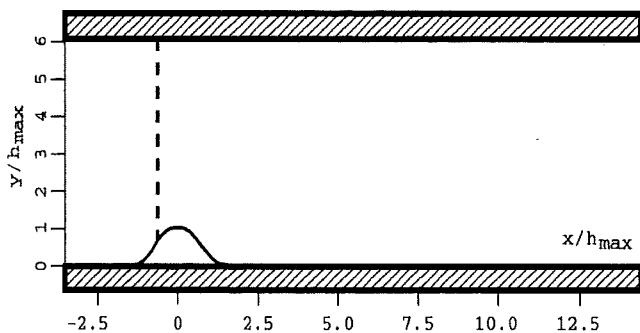
Profiles at $x/h_{max} = -1.78$



- Experiments** □
- UDelftHa RSM LRR+wf ---
 - UChalmer RSM LRR+wf - - -
 - UChalmer RSM SSG+wf - · - · -
 - UChalmer RSM HaLa - - -

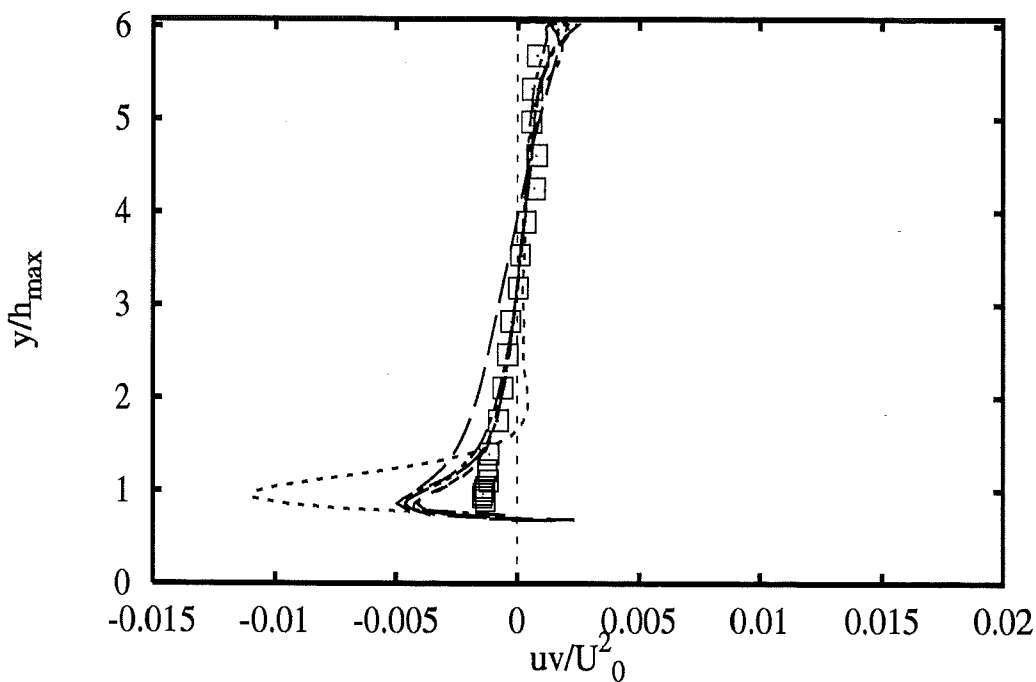
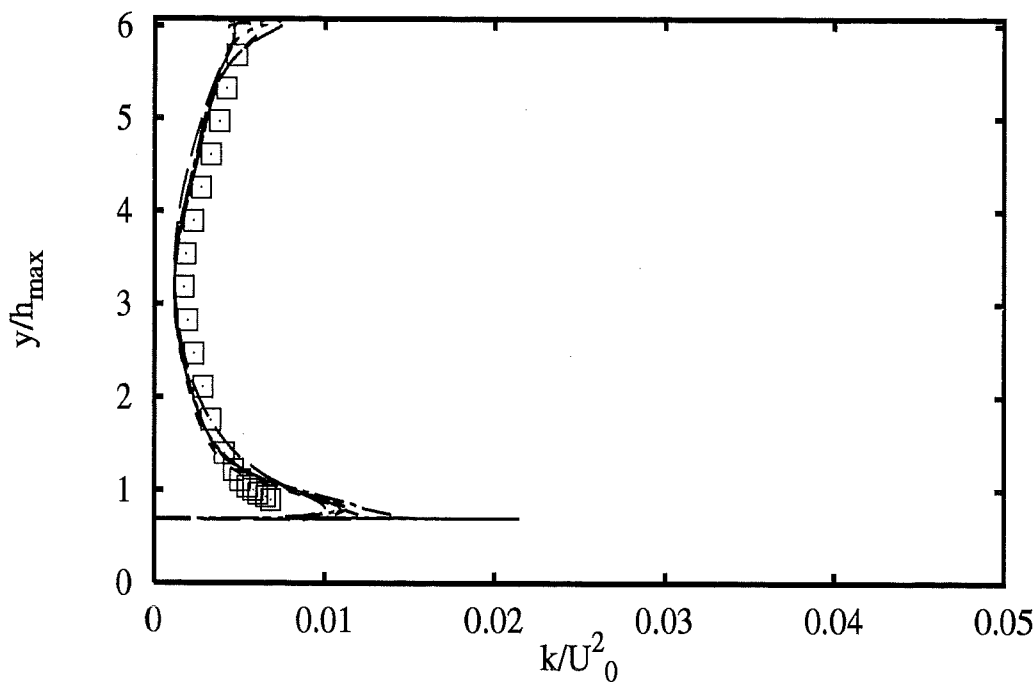


Profiles at $x/h_{max} = -0.71$

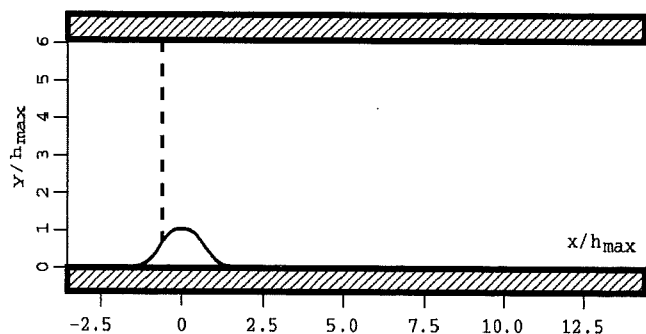


- | | |
|------------------------------|-----------|
| Experiments | □ |
| UDeftHa RSM LRR+wf | — — |
| UChalmer RSM LRR+wf | - - - |
| UMISTLes RSM GiLa+wf | |
| UChalmer RSM SSG+wf | — · — |
| UMISTLes RSM GiLa+Wol | - · - · - |
| UChalmer RSM HaLa | - - - - |

2A - 115

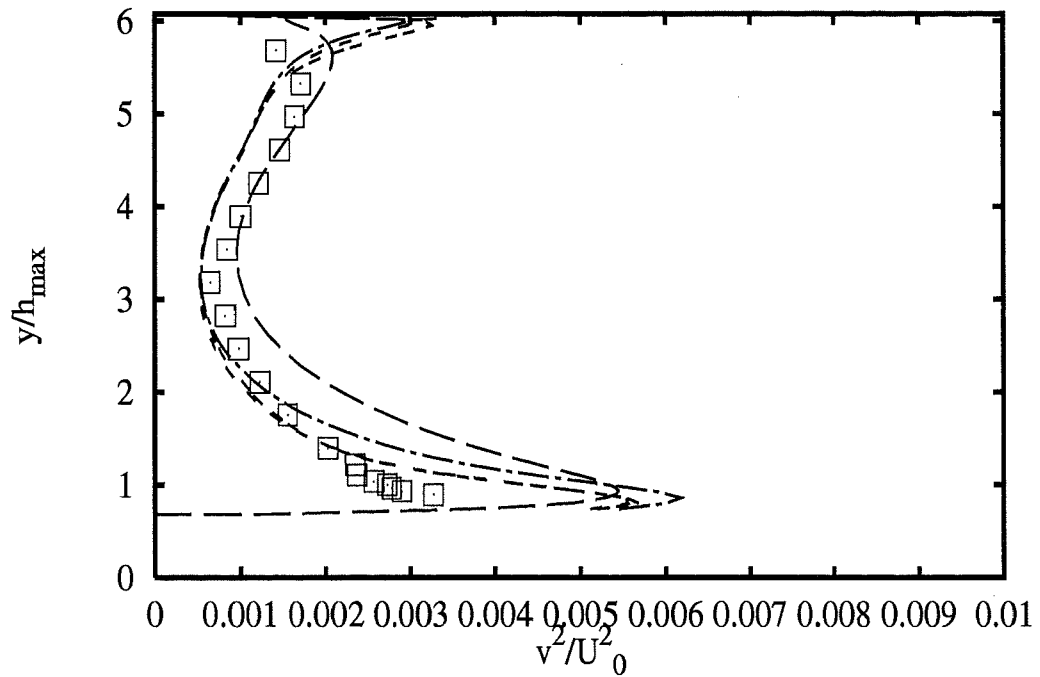
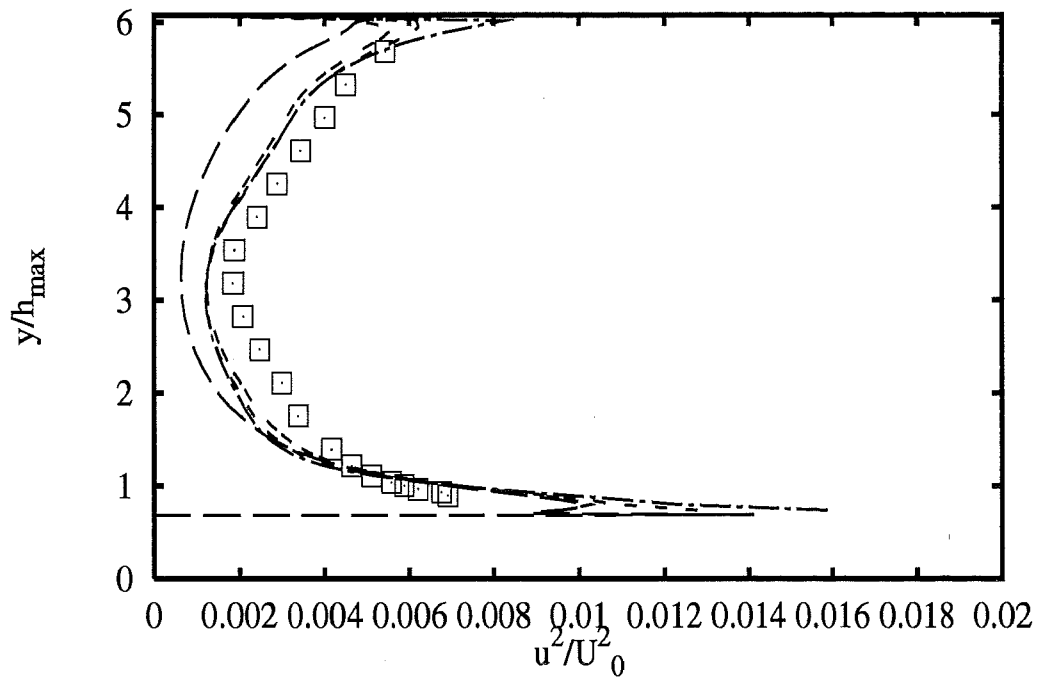


Profiles at $x/h_{max} = -0.71$

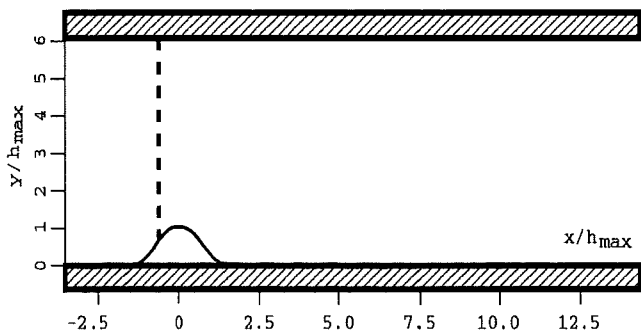


- | | |
|-----------------------|-------|
| Experiments | □ |
| UDelftHa RSM LRR+wf | --- |
| UChalmer RSM LRR+wf | --- |
| UMISTLes RSM GiLa+wf | |
| UChalmer RSM SSG+wf | --- |
| UMISTLes RSM GiLa+Wol | --- |
| UChalmer RSM HaLa | --- |

2A - 116

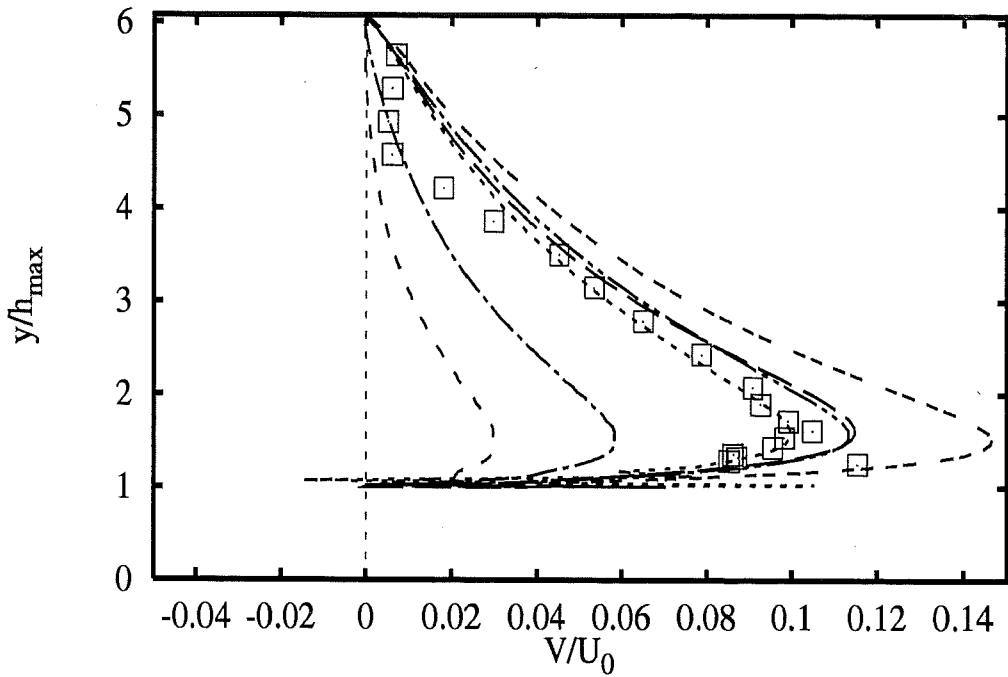
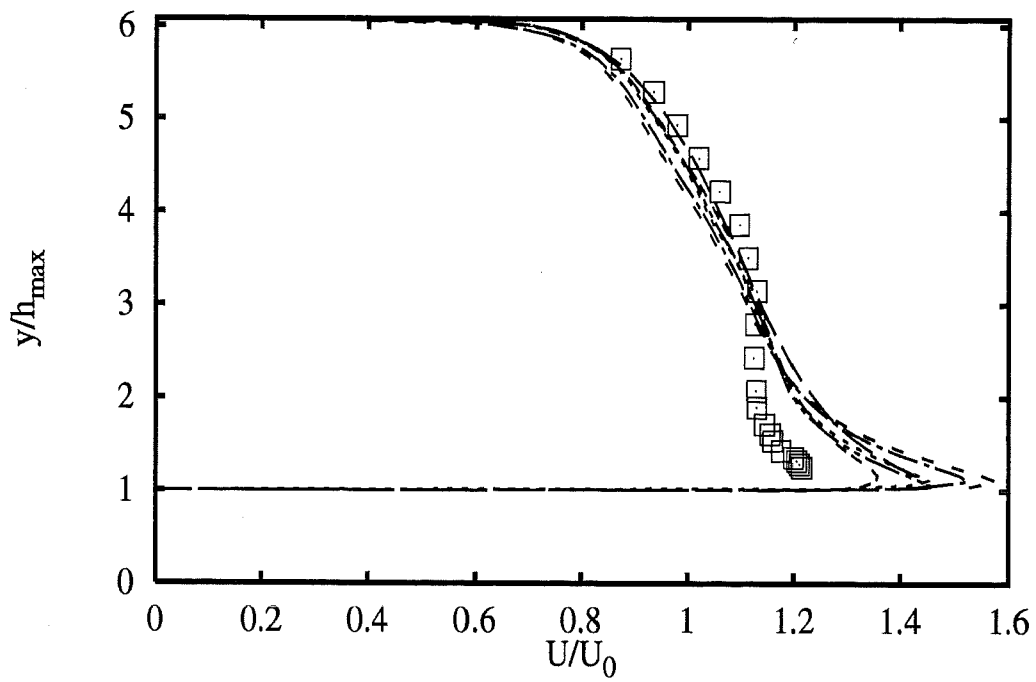


Profiles at $x/h_{max} = -0.71$

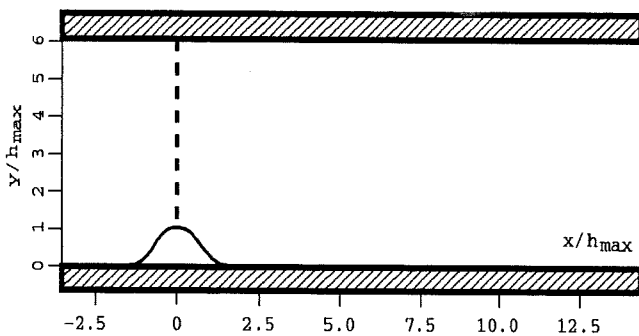


- Experiments \square
- UDelftHa RSM LRR+wf $---$
- UChalmer RSM LRR+wf $---$
- UChalmer RSM SSG+wf $---$
- UChalmer RSM HaLa $---$

2A - 117

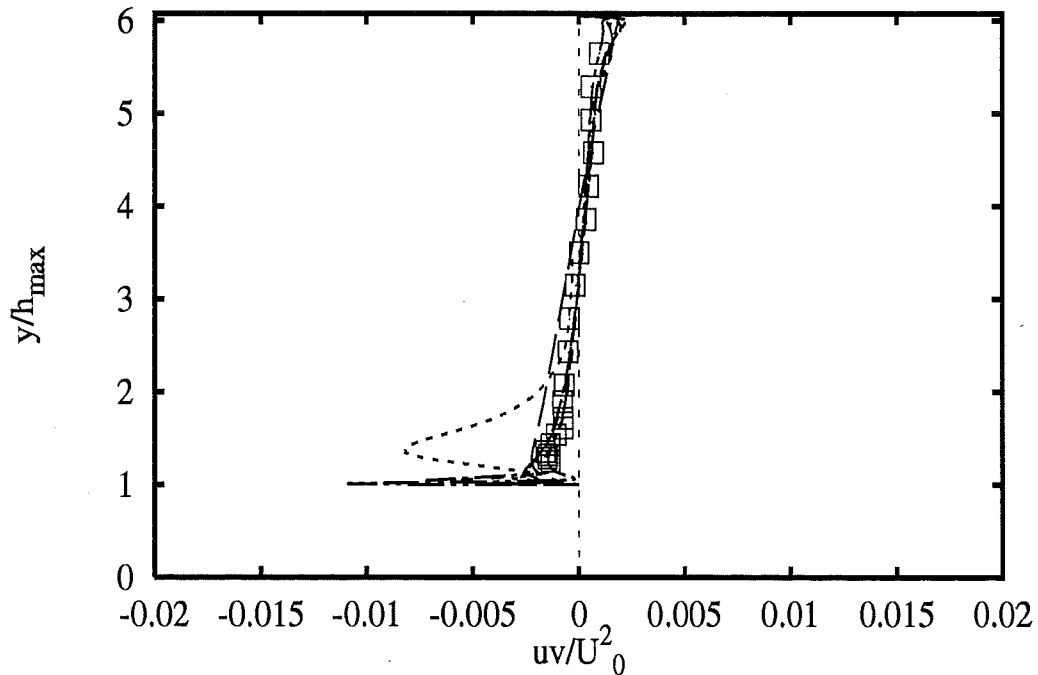
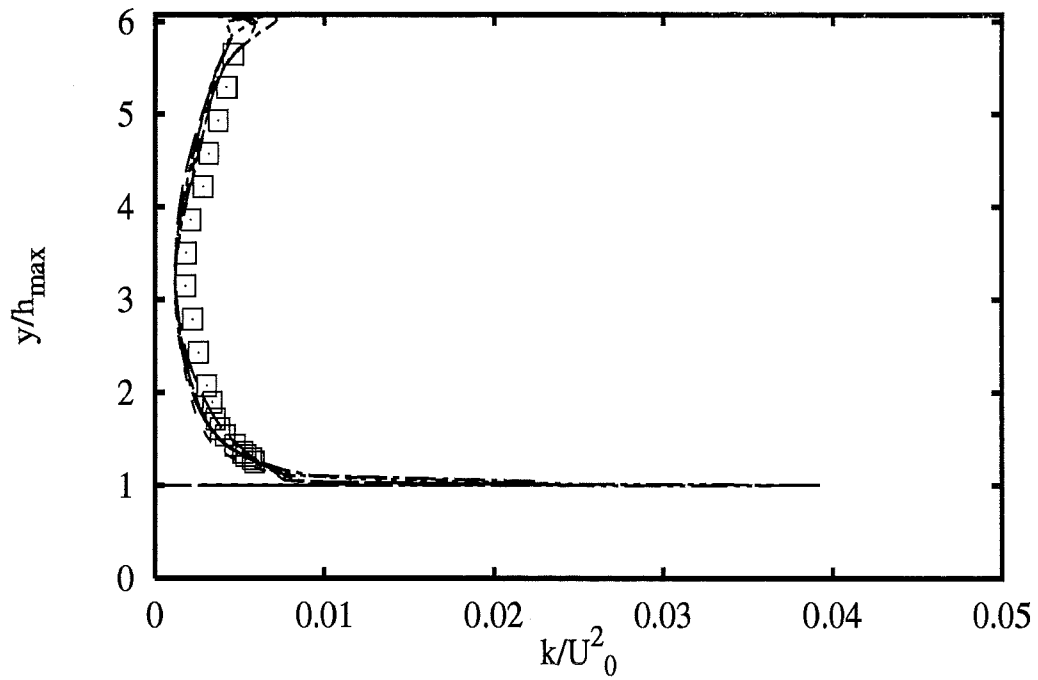


Profiles at $x/h_{max} = 0$

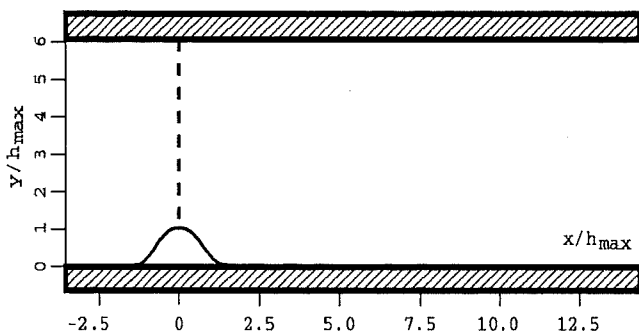


| | | |
|----------|--------------------|-------|
| | Experiments | □ |
| UDelftHa | RSM LRR+wf | --- |
| UChalmer | RSM LRR+wf | --- |
| UMISTLes | RSM GiLa+wf | |
| UChalmer | RSM SSG+wf | --- |
| UMISTLes | RSM GiLa+Wol | --- |
| UChalmer | RSM HaLa | --- |

2A - 118

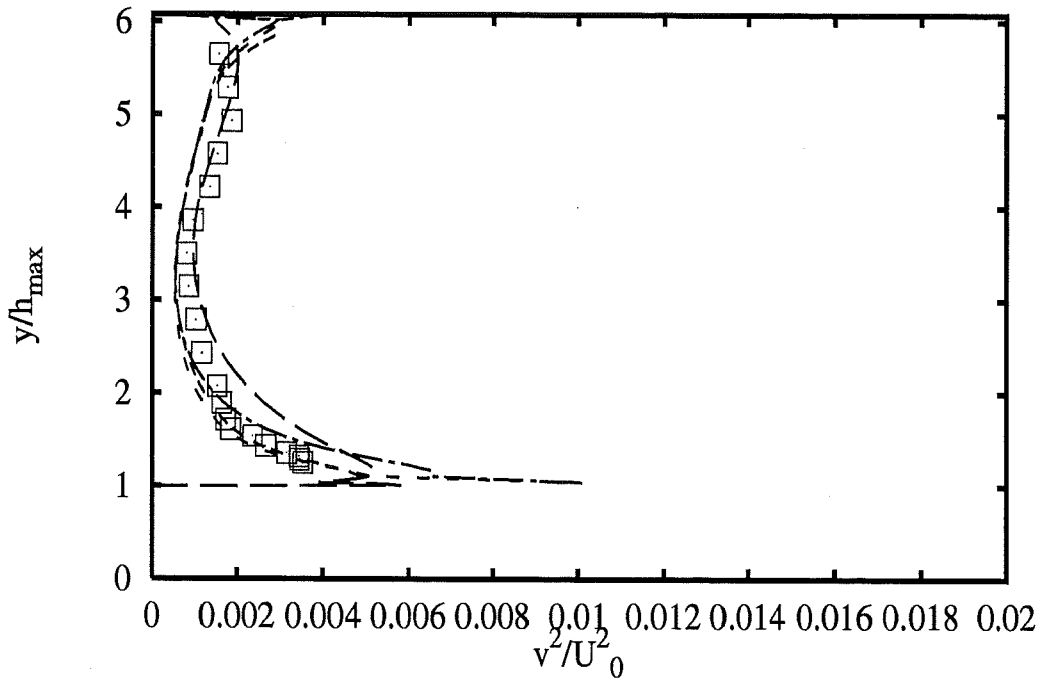
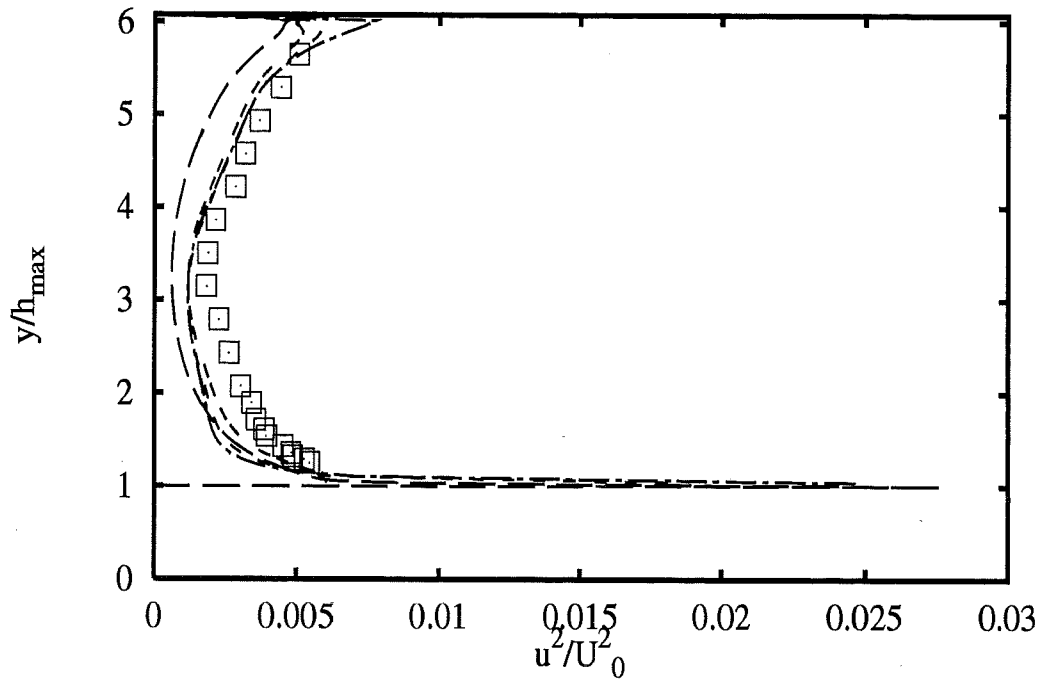


Profiles at $x/h_{max} = 0$

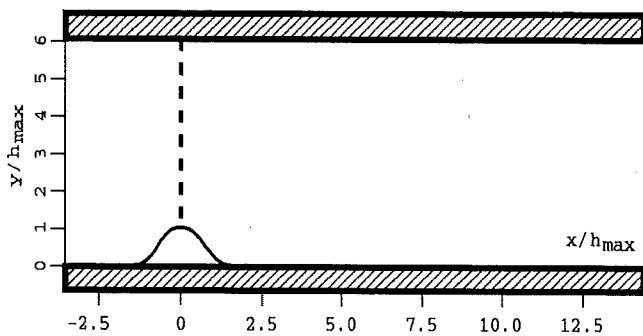


- | | |
|-----------------------|-------|
| Experiments | □ |
| UDelftHa RSM LRR+wf | — — |
| UChalmer RSM LRR+wf | - - - |
| UMISTLes RSM GiLa+wf | |
| UChalmer RSM SSG+wf | — · — |
| UMISTLes RSM GiLa+Wol | — · — |
| UChalmer RSM HaLa | - - - |

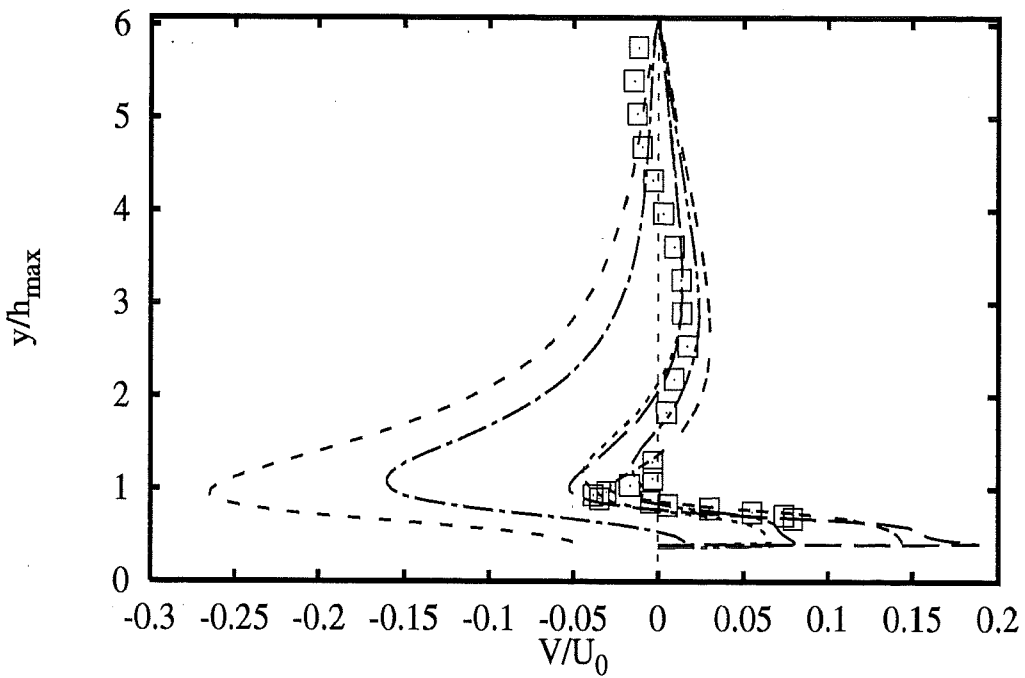
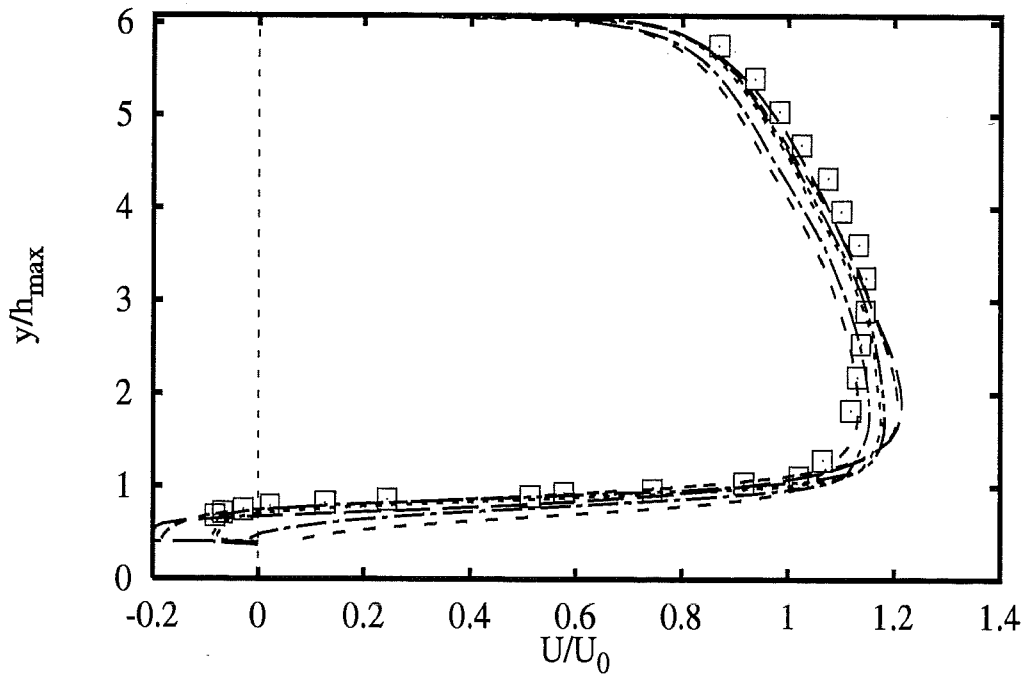
2A - 119



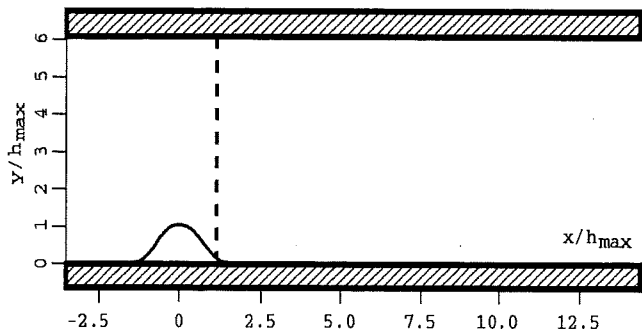
Profiles at $x/h_{max} = 0$



- Experiments** □
- UdelftHa RSM LRR+wf ---
 - UChalmer RSM LRR+wf - - -
 - UChalmer RSM SSG+wf - · - ·
 - UChalmer RSM HaLa - - - -

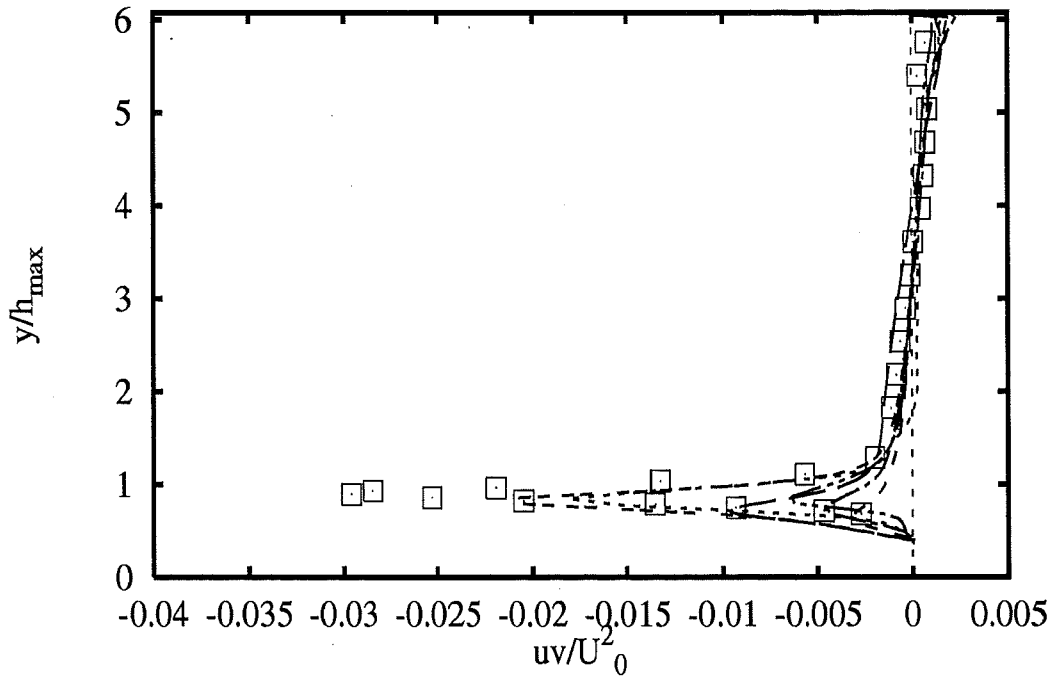
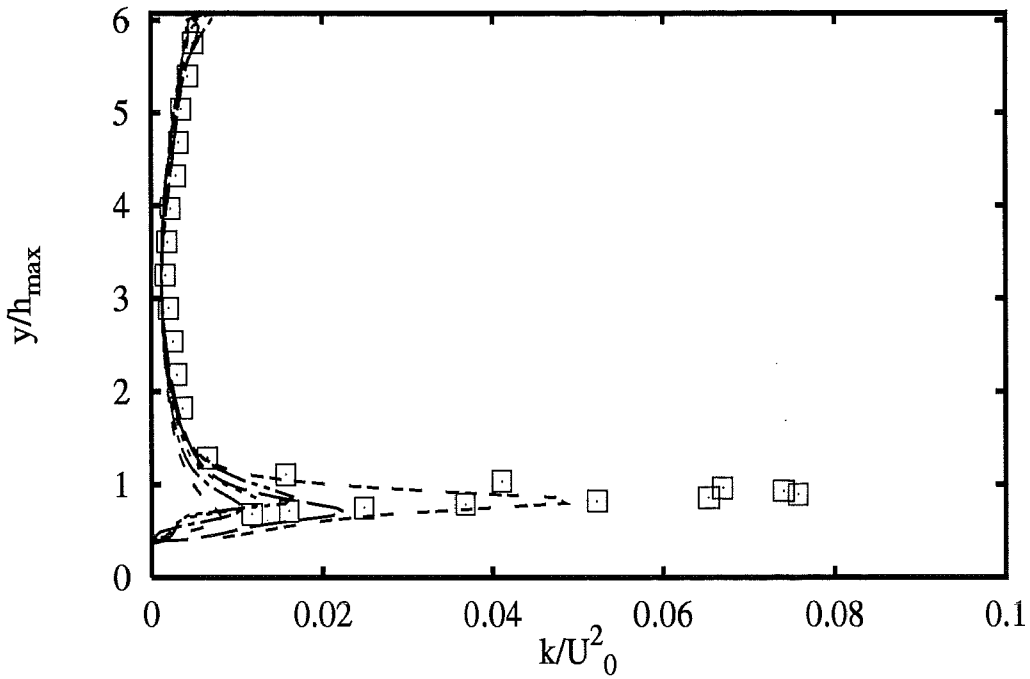


Profiles at $x/h_{max} = 1.07$

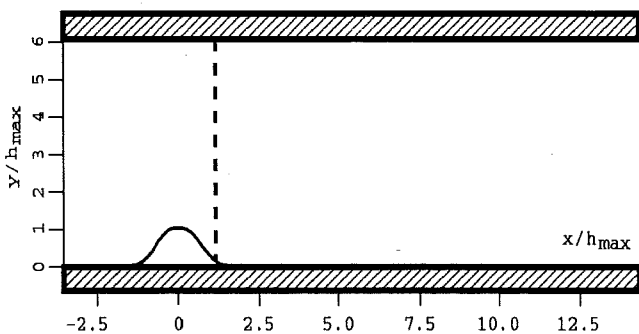


- | | | |
|----------|--------------------|-------|
| | Experiments | □ |
| UdelftHa | RSM LRR+wf | --- |
| UChalmer | RSM LRR+wf | ---- |
| UMISTLes | RSM GiLa+wf | |
| UChalmer | RSM SSG+wf | -.-.- |
| UMISTLes | RSM GiLa+Wol | ----- |
| UChalmer | RSM HaLa | ----- |

2A - 121

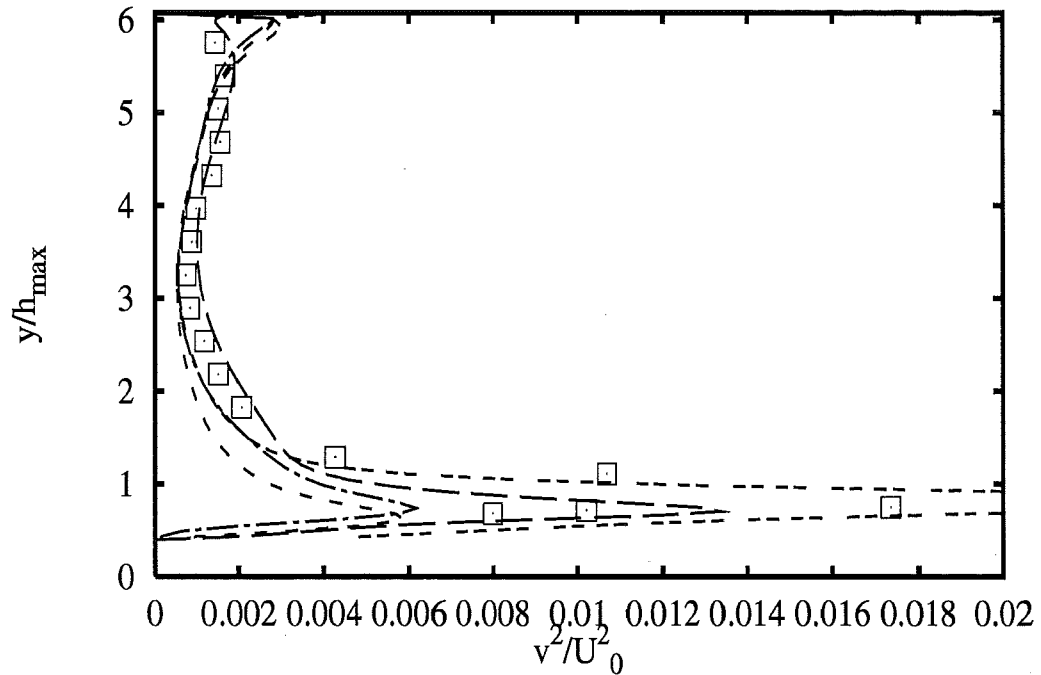
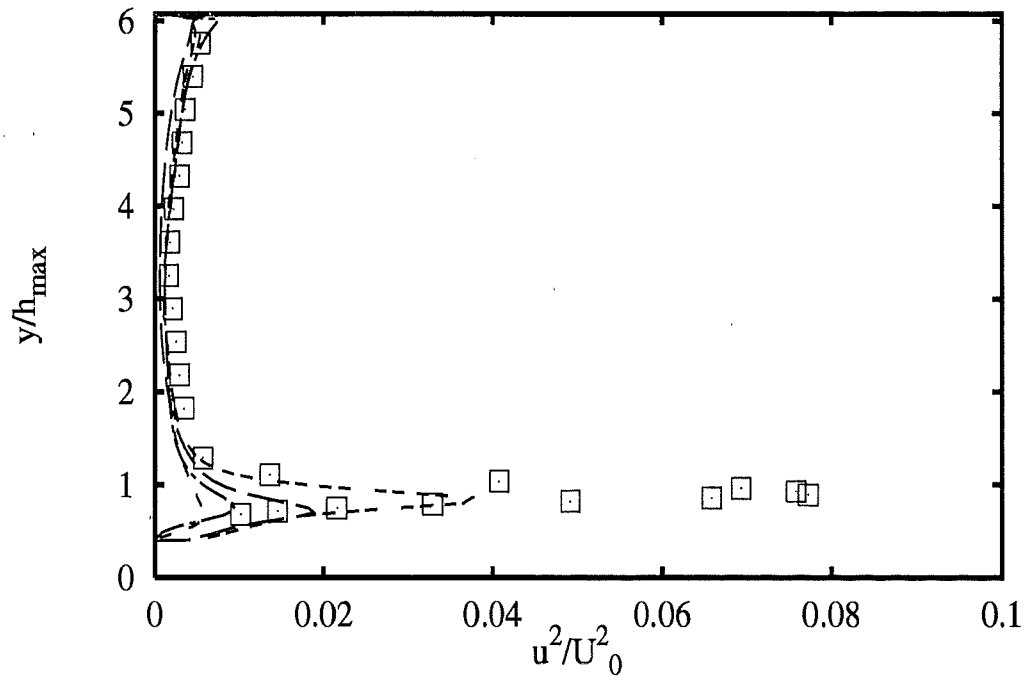


Profiles at $x/h_{max} = 1.07$

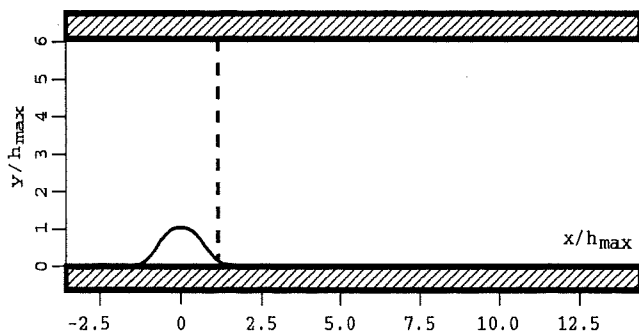


- | | |
|-----------------------|-----|
| Experiments | □ |
| UDelftHa RSM LRR+wf | --- |
| UChalmer RSM LRR+wf | --- |
| UMISTLes RSM GiLa+wf | --- |
| UChalmer RSM SSG+wf | --- |
| UMISTLes RSM GiLa+Wol | --- |
| UChalmer RSM HaLa | --- |

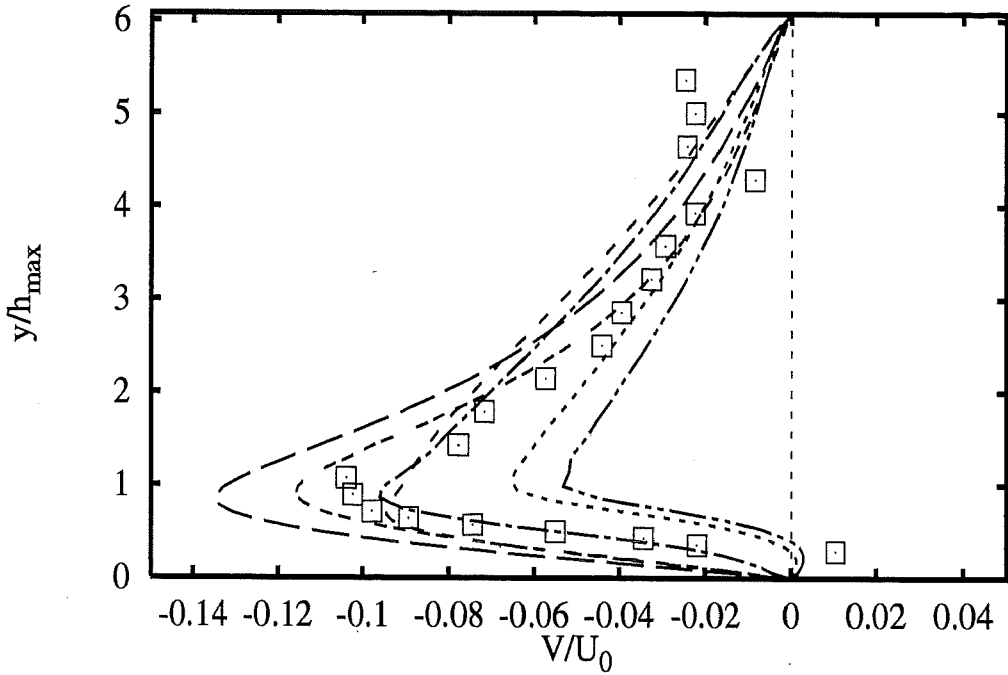
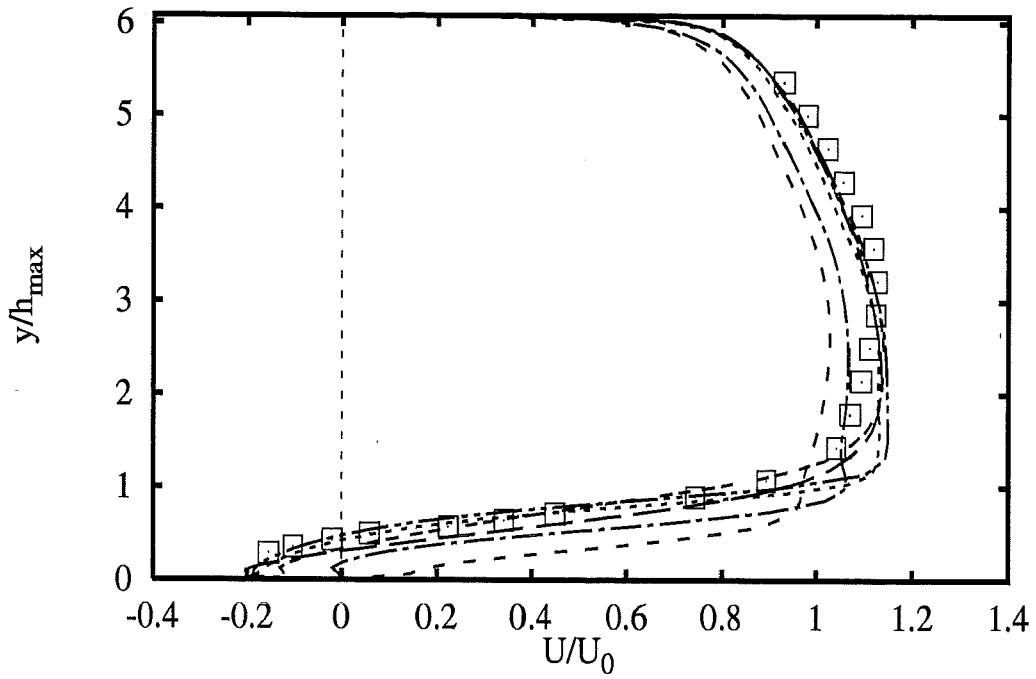
2A - 122



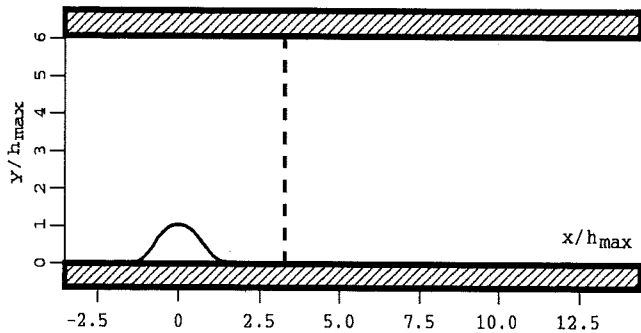
Profiles at $x/h_{max} = 1.07$



- | | | |
|------------------|--------------------|---------|
| | Experiments | □ |
| U DelftHa | RSM LRR+wf | — — |
| U Chalmer | RSM LRR+wf | - - - |
| U Chalmer | RSM SSG+wf | - · - · |
| U Chalmer | RSM HaLa | · · · · |

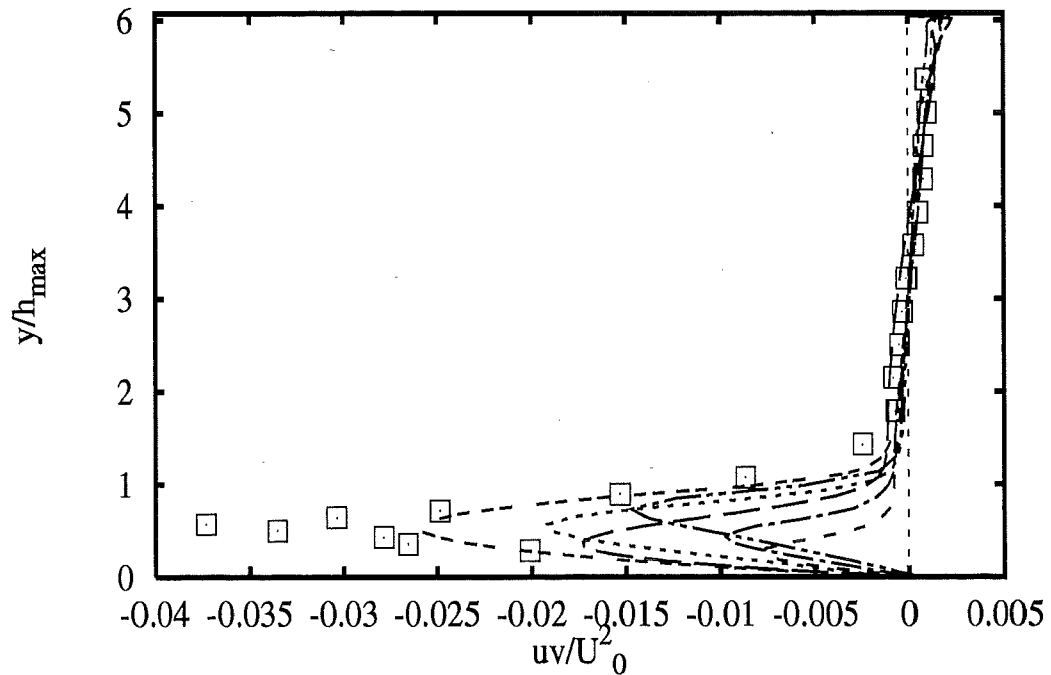
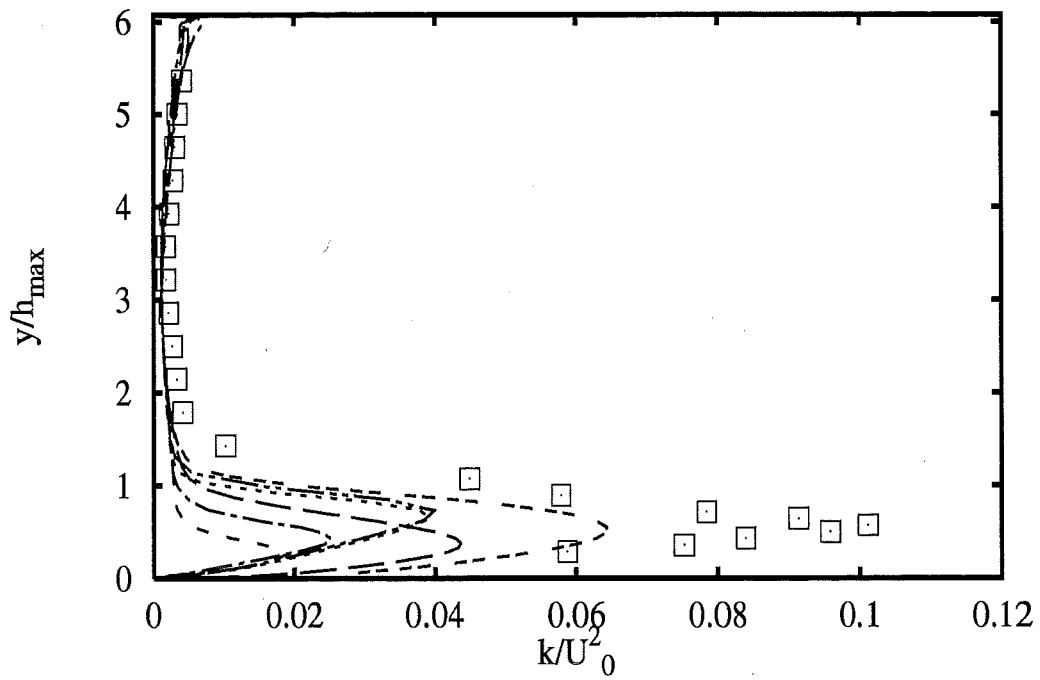


Profiles at $x/h_{max} = 3.21$

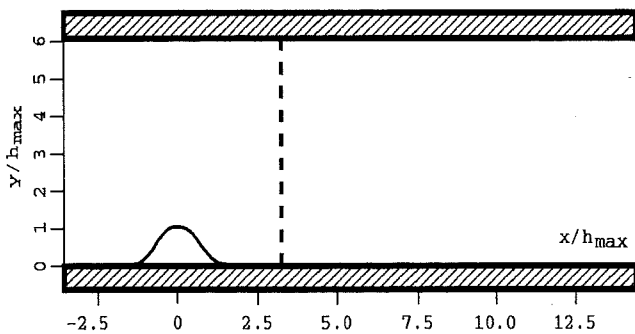


- | | |
|-----------------------|-------|
| Experiments | □ |
| UDelftHa RSM LRR+wf | --- |
| UChalmer RSM LRR+wf | ---- |
| UMISTLes RSM GiLa+wf | |
| UChalmer RSM SSG+wf | -.-.- |
| UMISTLes RSM GiLa+Wol | ---- |
| UChalmer RSM HaLa | ---- |

2A - 124

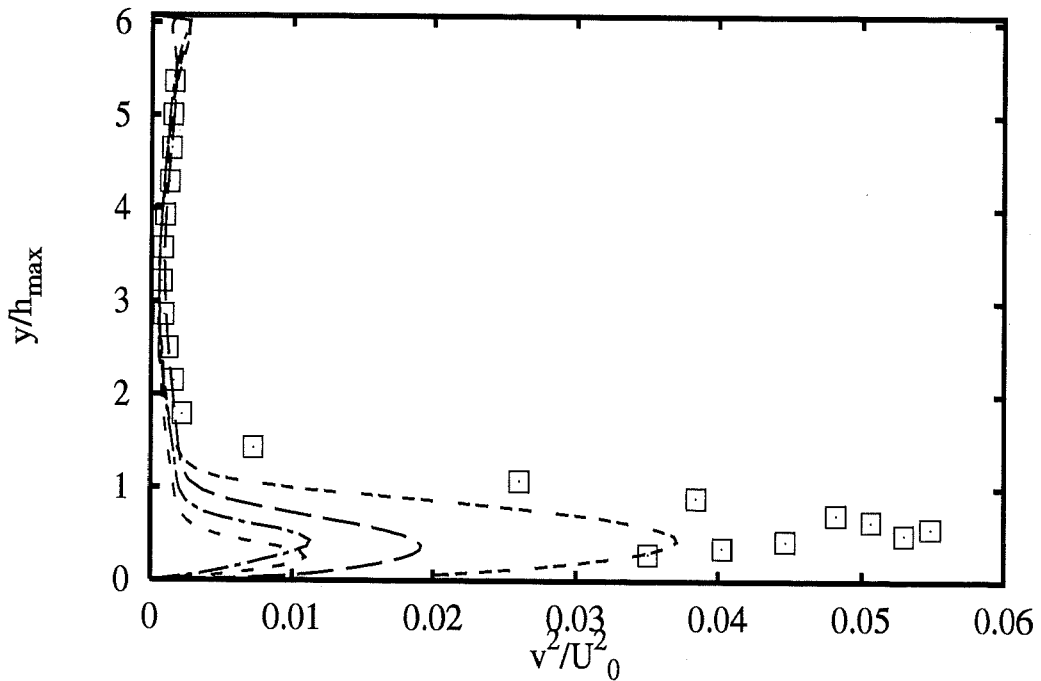
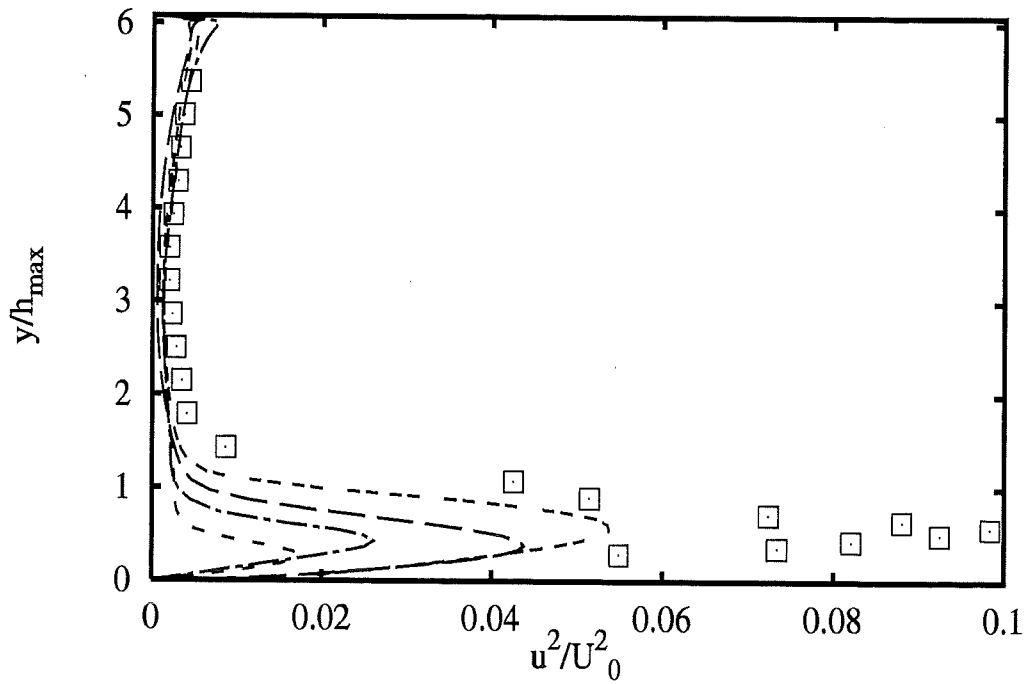


Profiles at $x/h_{max} = 3.21$

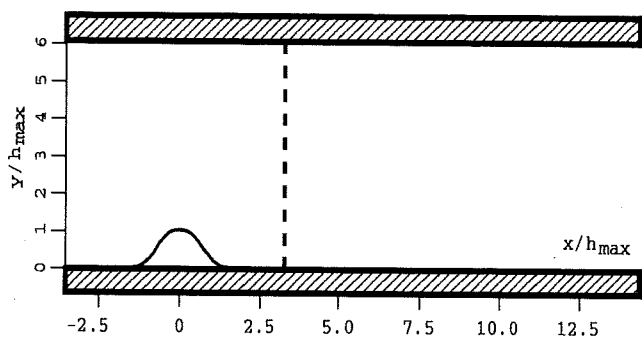


- | | | |
|----------|--------------------|-----------|
| | Experiments | □ |
| UDelftHa | RSM LRR+wf | — — |
| UChalmer | RSM LRR+wf | - - - |
| UMISTLes | RSM GiLa+wf | · · · · · |
| UChalmer | RSM SSG+wf | - · - · - |
| UMISTLes | RSM GiLa+Wol | - · - · - |
| UChalmer | RSM HaLa | - - - |

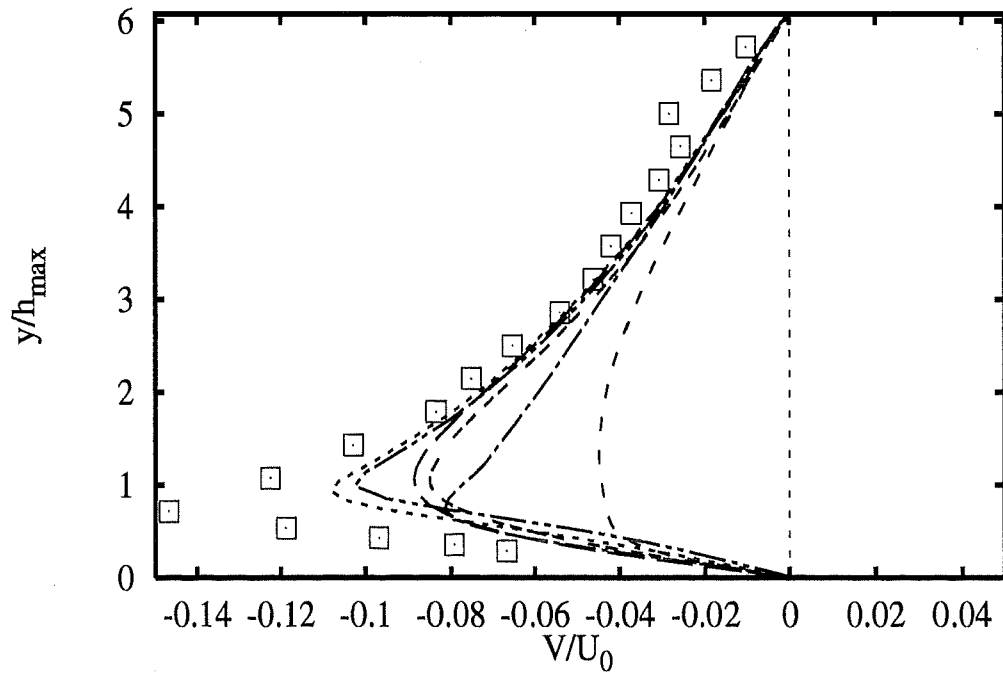
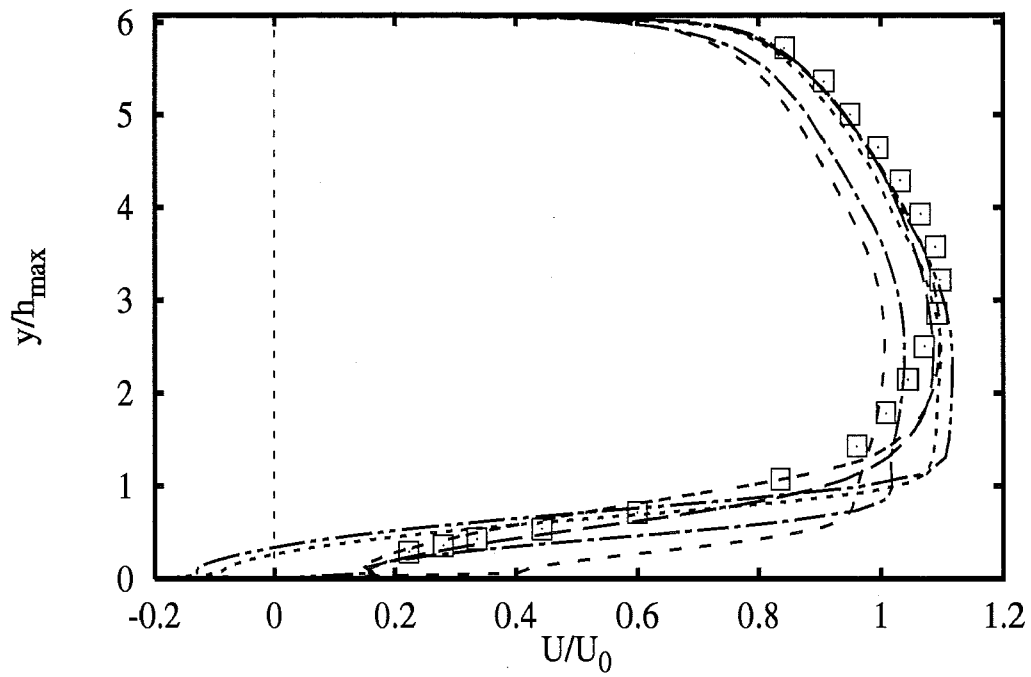
2A - 125



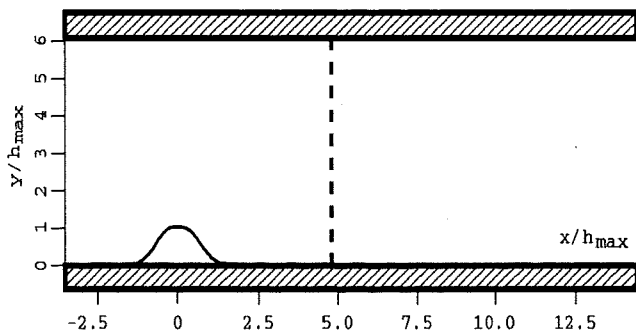
Profiles at $x/h_{max} = 3.21$



- | | | |
|-----------------|--------------------|-----|
| | Experiments | □ |
| <i>UdelftHa</i> | RSM LRR+wf | --- |
| <i>UChalmer</i> | RSM LRR+wf | --- |
| <i>UChalmer</i> | RSM SSG+wf | --- |
| <i>UChalmer</i> | RSM HaLa | --- |

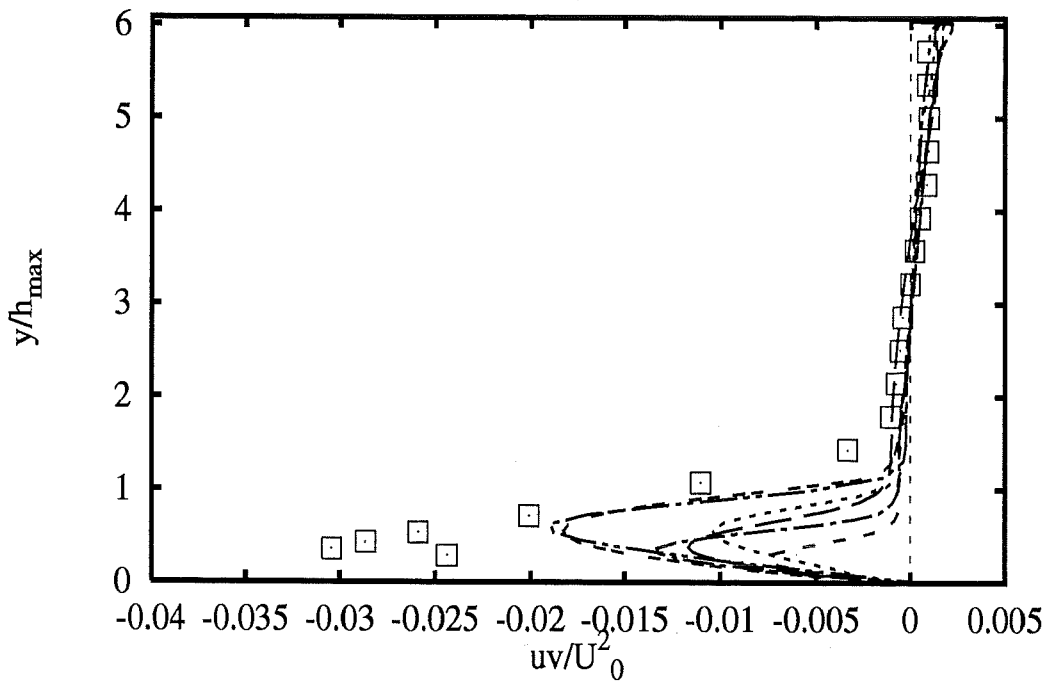
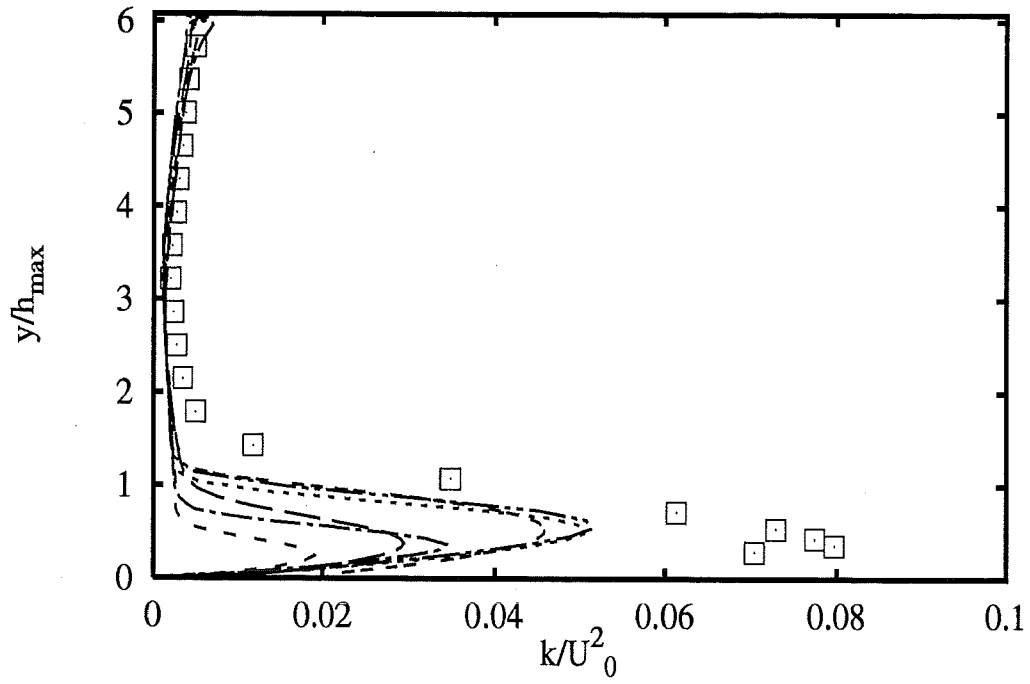


Profiles at $x/h_{max} = 4.79$

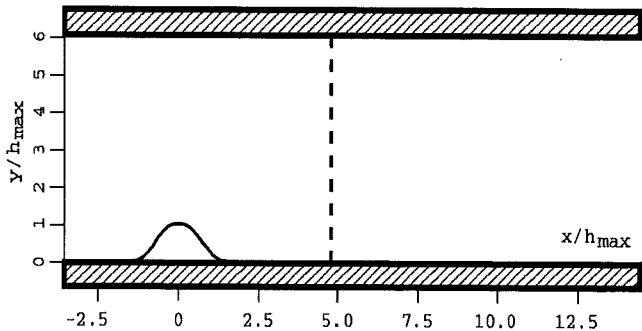


- | | |
|-------------------------------|-----------|
| Experiments | □ |
| <i>U</i> DelftHa RSM LRR+wf | — — |
| <i>U</i> Chalmer RSM LRR+wf | - - - |
| <i>UMIST</i> Les RSM GiLa+wf | ⋯⋯⋯ |
| <i>U</i> Chalmer RSM SSG+wf | - · - · - |
| <i>UMIST</i> Les RSM GiLa+Wol | - · - · - |
| <i>U</i> Chalmer RSM HaLa | - · - · - |

2A - 127

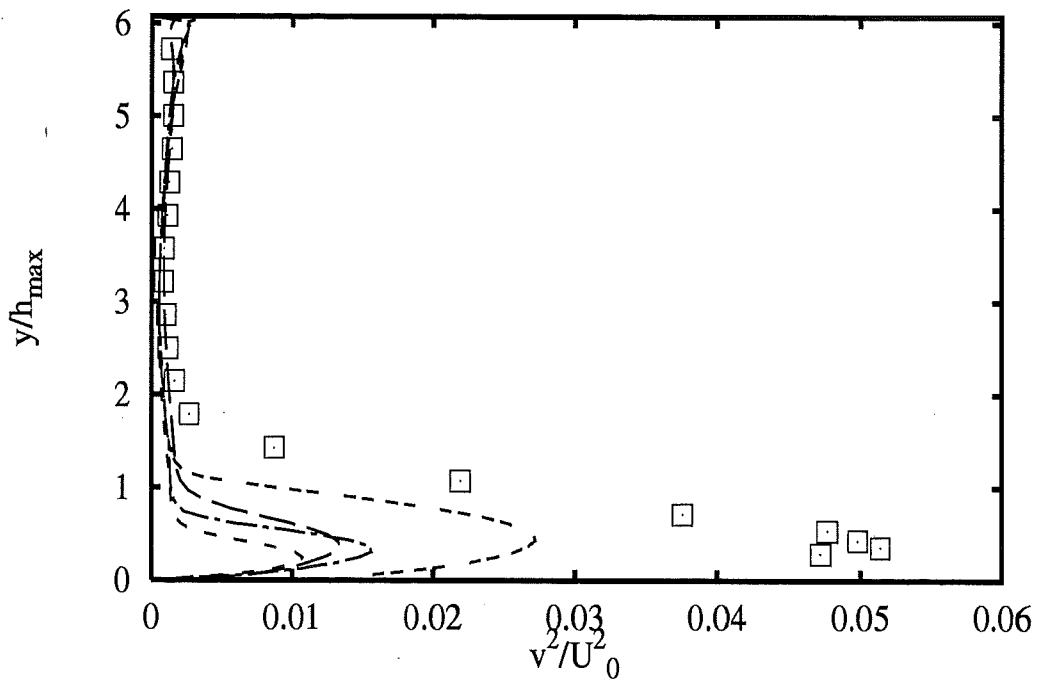
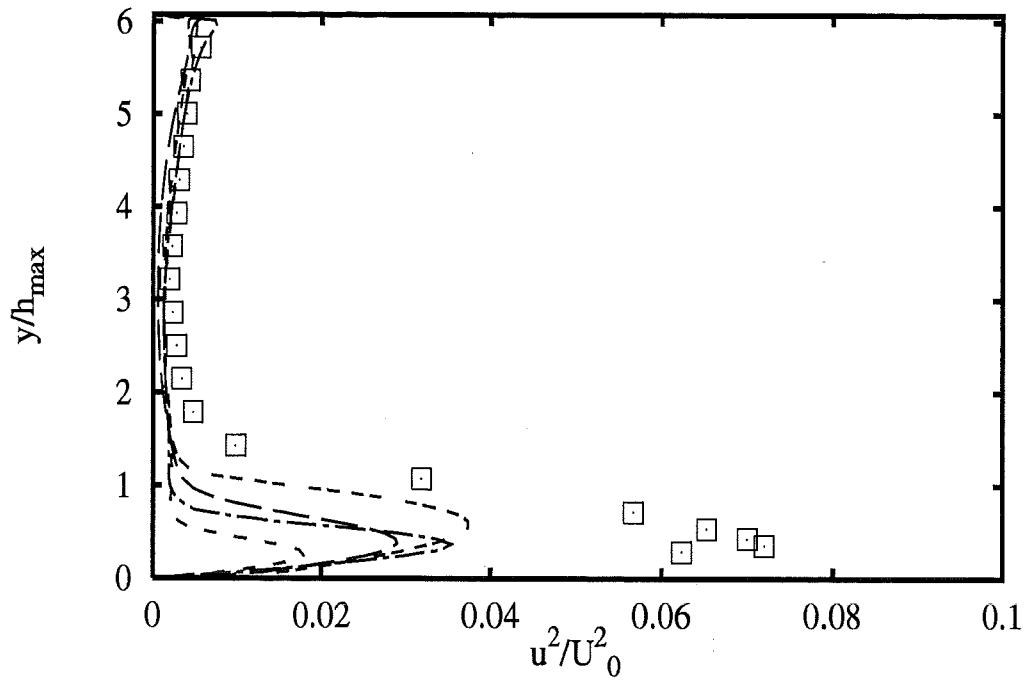


Profiles at $x/h_{max} = 4.79$

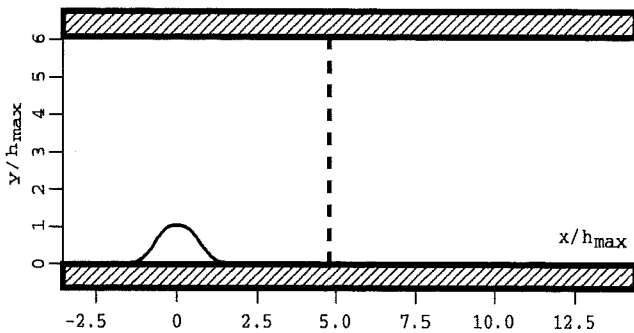


- | | |
|-------------------------------|-------|
| Experiments | □ |
| <i>U</i> DelftHa RSM LRR+wf | --- |
| <i>U</i> Chalmer RSM LRR+wf | --- |
| <i>UMIST</i> Les RSM GiLa+wf | |
| <i>U</i> Chalmer RSM SSG+wf | --- |
| <i>UMIST</i> Les RSM GiLa+Wol | --- |
| <i>U</i> Chalmer RSM HaLa | --- |

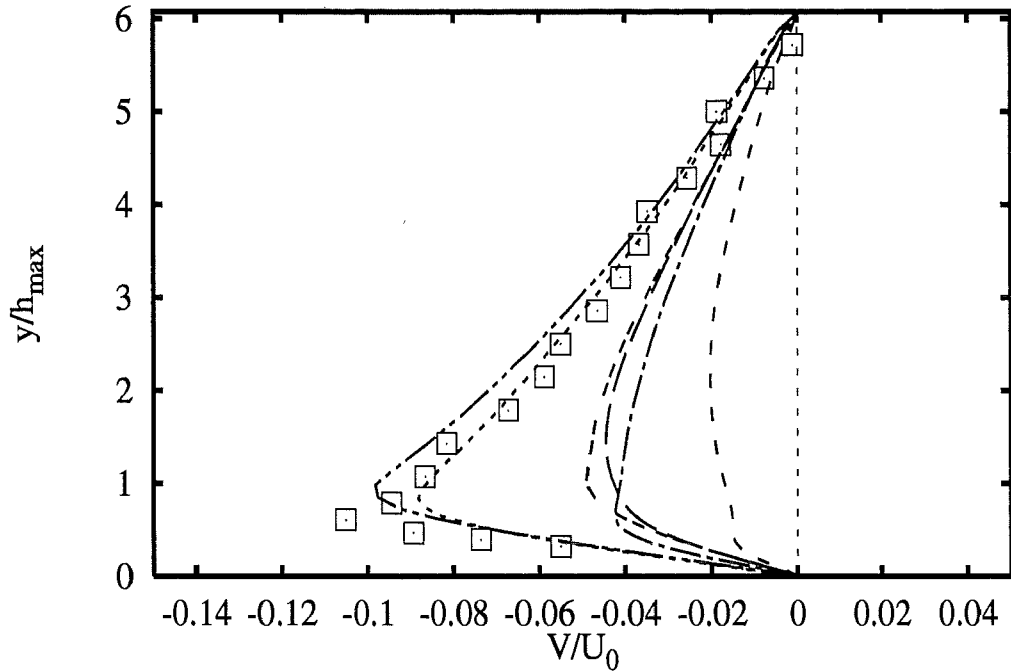
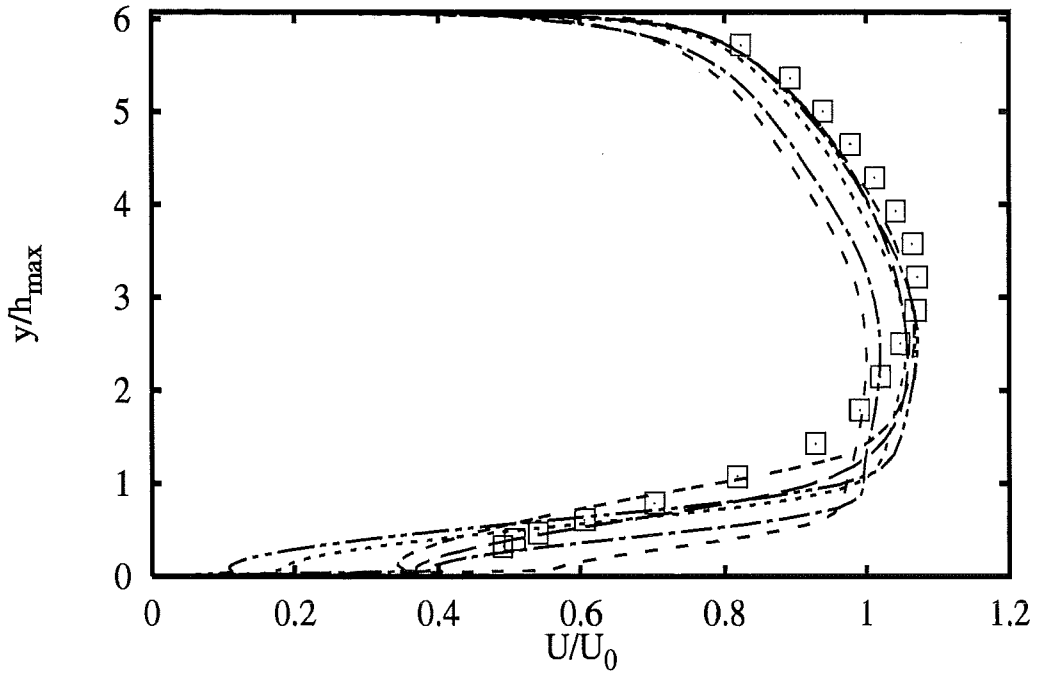
2A - 128



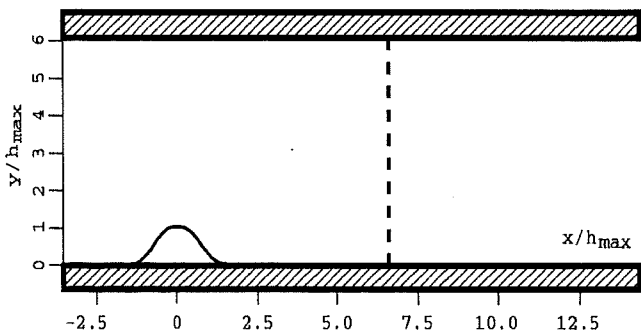
Profiles at $x/h_{max} = 4.79$



- Experiments** □
- UdelftHa RSM LRR+wf — —
 - UChalmer RSM LRR+wf - - -
 - UChalmer RSM SSG+wf - · -
 - UChalmer RSM HaLa - - -

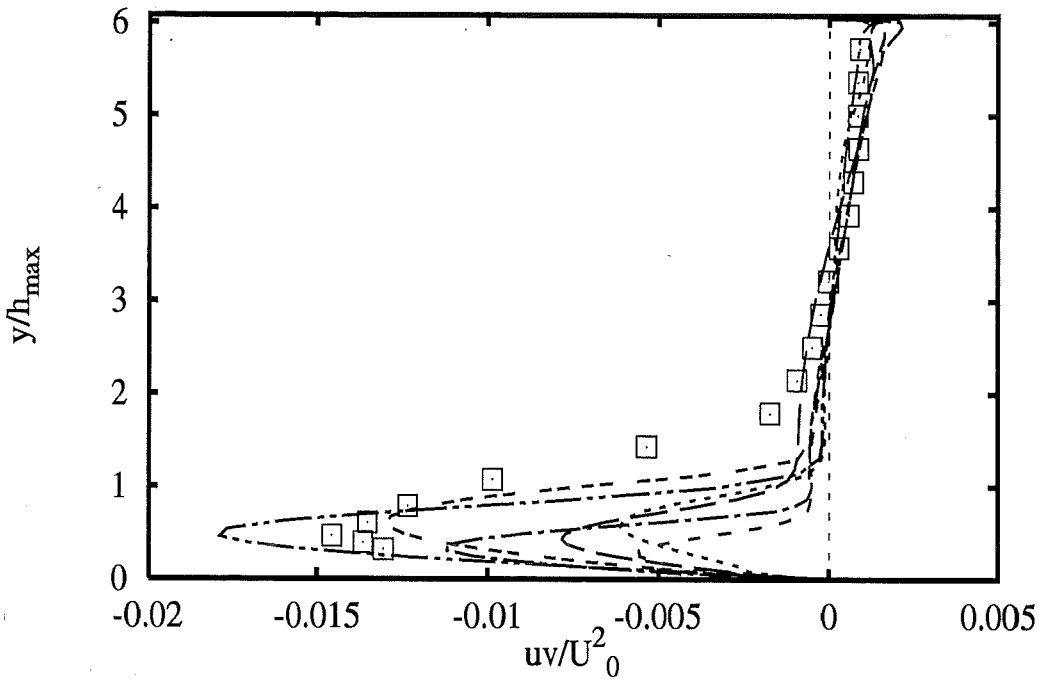
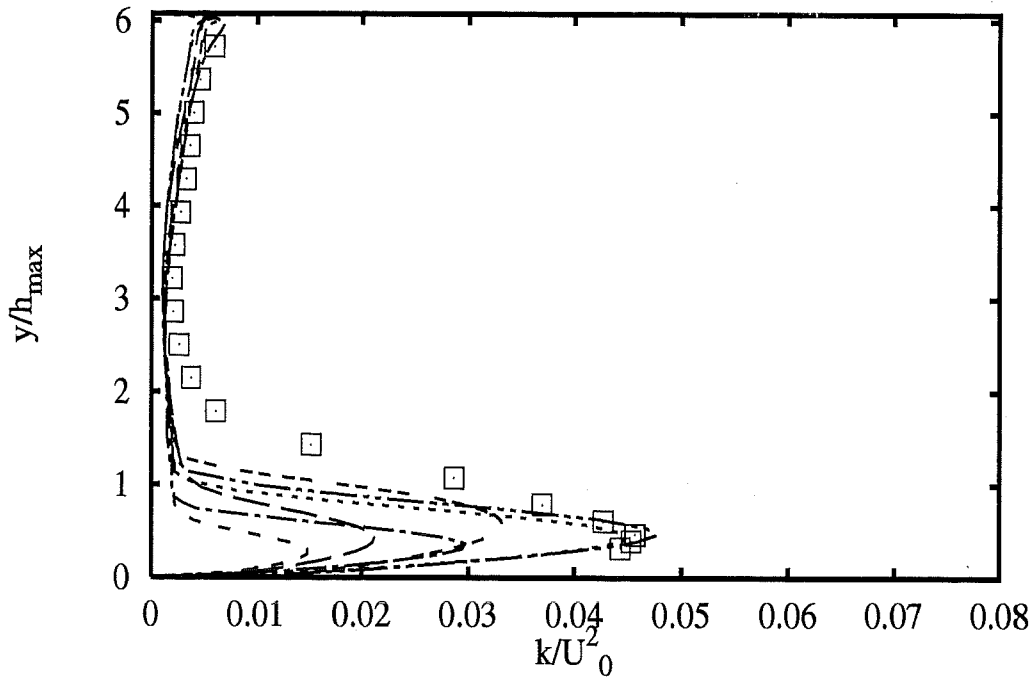


Profiles at $x/h_{max} = 6.61$

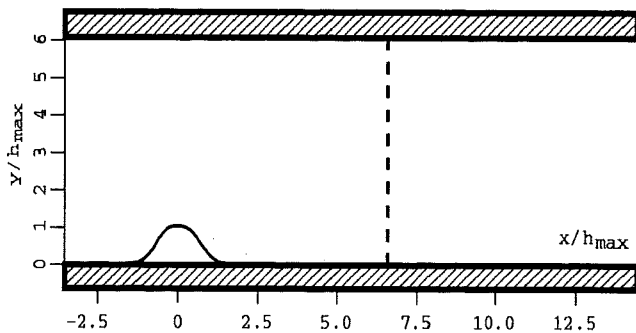


- | | | |
|-----------------|---------------------|-------|
| | Experiments | □ |
| UdelftHa | RSM LRR+wf | --- |
| UChalmer | RSM LRR+wf | ---- |
| UMISTLes | RSM GiLa+wf | |
| UChalmer | RSM SSG+wf | ----- |
| UMISTLes | RSM GiLa+Wol | ----- |
| UChalmer | RSM HaLa | ----- |

2A - 130

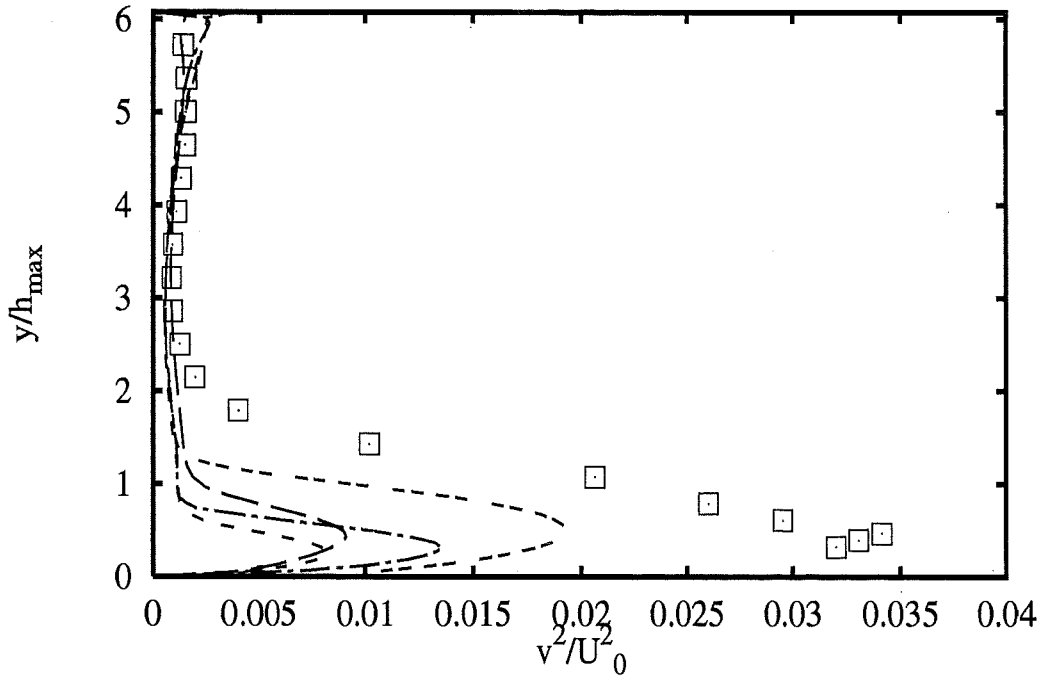
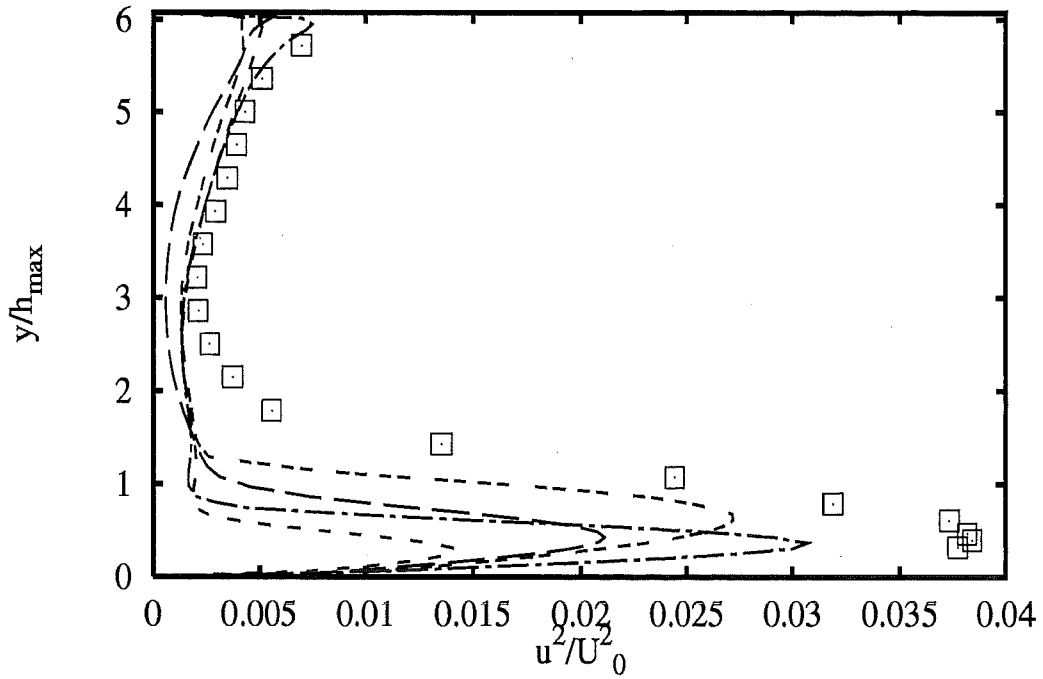


Profiles at $x/h_{max} = 6.61$

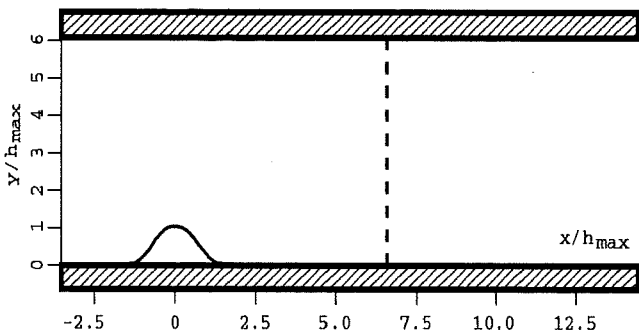


- | | | |
|-----------------|---------------------|-------|
| | Experiments | □ |
| UdelftHa | RSM LRR+wf | --- |
| UChalmer | RSM LRR+wf | ---- |
| UMISTLes | RSM GiLa+wf | |
| UChalmer | RSM SSG+wf | -.-.- |
| UMISTLes | RSM GiLa+Wol | ----- |
| UChalmer | RSM HaLa | ----- |

2A - 131



Profiles at $x/h_{max} = 6.61$



- | | | |
|-----------------|--------------------|------|
| | Experiments | □ |
| UdelftHa | RSM LRR+wf | --- |
| UChalmer | RSM LRR+wf | ---- |
| UChalmer | RSM SSG+wf | ---- |
| UChalmer | RSM HaLa | ---- |

| KEY TO TEST CASE 2B | | | | | |
|---------------------|-----------------|-----|--|-------------------------------------|-----------------------------|
| Contributor | Key-Name | Gr. | Name (Affiliation) | Turbulence Model | Near-Wall Treatment |
| CompDyna | hKE_RNG+wf | 2 | Issa/Leong/Sanatian (Computational Dynamics) | RNG-modifided k-ε | wall functions |
| | hKE_RNG+wf(7th) | 4 | | RNG-modifided k-ε | wall functions |
| DLRGoett | kOm_Wil | 2 | Kessler (DLR Goettingen) | k-ω | — |
| DLROberp | LES | 3 | Maass (DLR Oberpfaffenhofen) | 2nd-order for SGS fluxes (LES) | logarithmic law |
| EDFLNHLa | IKE_LaSh | 2 | Laurence et al. (EDF-DER-LNH) | low-Re k-ε model LaSh | — |
| | RSM_LRR | 3 | | RSM Launder-Reece-Rodi | wall functions |
| IOlomouc | hKE_std+Gol | 2 | Sedlar (Pump Research Institute Olomouc) | two-layer k-ε | Goldberg model |
| | hKE_std+wf_nstd | 1 | | standard k-ε | non-standard wall functions |
| | nKE_Spez+wf | 2 | | non-linear k-ε Speziale | wall functions |
| RCHokkai | hKE_std+wf_nstd | 4 | Blom (Hokkaido R. D. P. Res. Center) | standard k-ε | non-standard wall functions |
| UDelftHa | RSM_LRR+wf | 3 | Hanjalic/Hadzic/Jakirlic (TU Delft, Appl. Physics) | RSM Launder-Reece-Rodi | wall functions |
| | RSM_LRR+wf(7th) | 4 | | RSM Launder-Reece-Rodi | wall functions |
| | hKE_std+wf | 1 | | standard k-ε | wall functions |
| | hKE_std+wf(7th) | 4 | | standard k-ε | wall functions |
| UKarlsru | hKE_std+NoRe | 2 | Buchal (Univ. of Karlsruhe) | two-layer k-ε | Norris-Reynolds 1 eq.-model |
| | hKE_std+wf | 1 | | standard k-ε | wall functions |
| UMISTCra | RSM_Cub+2eq | 3 | Craft (UMIST) | Reynolds-Stress Model Cubic | k-ε Launder-Sharma |
| | RSM_CrLa+2eq | 3 | | Reynolds-Stress Model Craft-Launder | k-ε Launder-Sharma |
| UPorto | hKE_std+wf | 1 | Castro/Palma (Univ. of Porto) | standard k-ε | wall functions |
| | hKE_std+wf(fix) | 1 | | standard k-ε | wall functions |
| | hKE_LeRo+wf | 2 | | Leschziner-Rodi-modif. k-ε | wall functions |

In key-names:

(fix): k value fixed at inlet and outlet

(Hyb.2000): HYBRID numerical scheme after 2000 iterations

(Hyb.12000): HYBRID numerical scheme after 12000 iterations

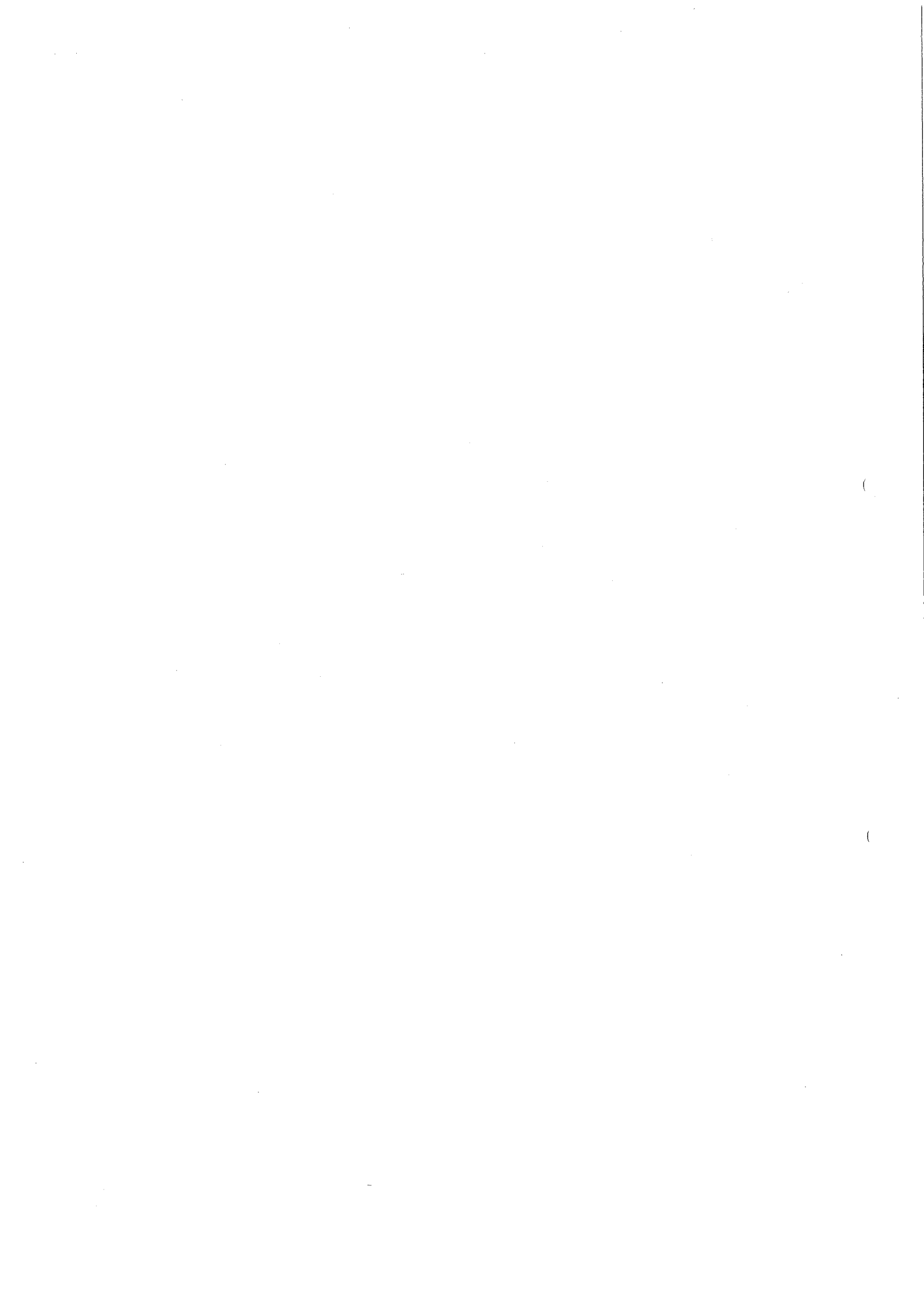
(Hyb.30000): HYBRID numerical scheme after 30000 iterations

Notes:

- experimental values of k evaluated as $k = \frac{1}{4}(3\overline{u'^2} + 2\overline{v'^2})$
- stream lines not equally distributed according to stream function values

TEST CASE 2B

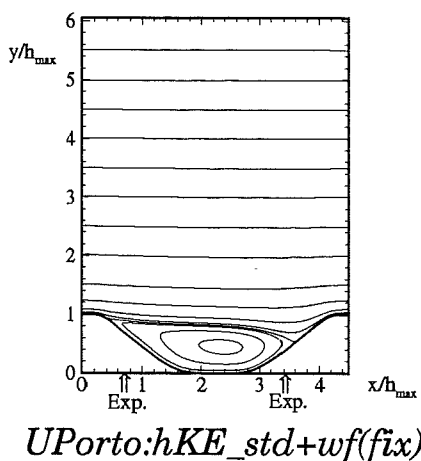
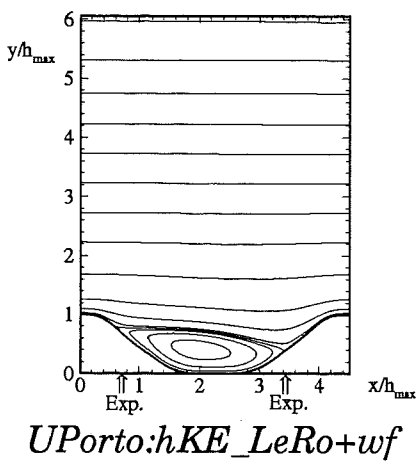
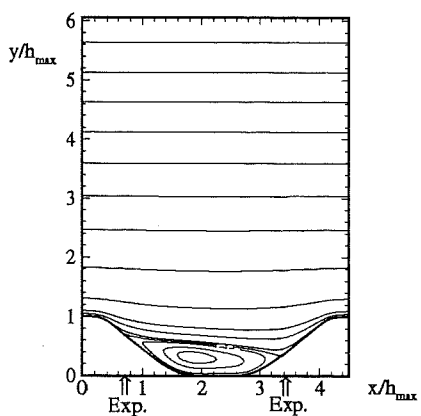
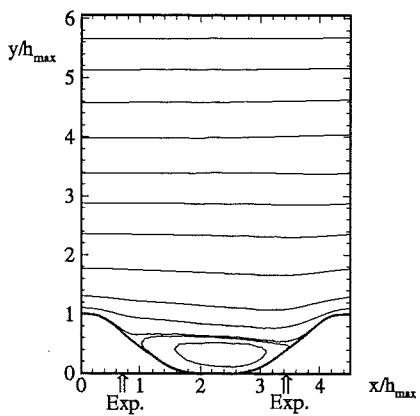
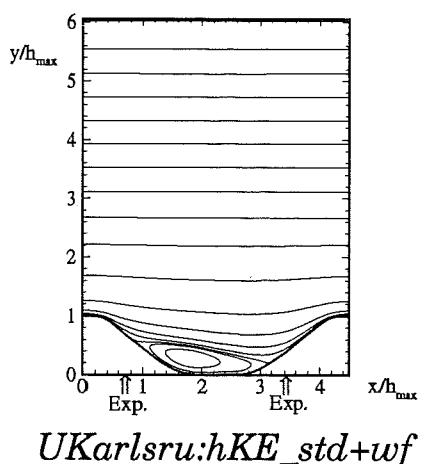
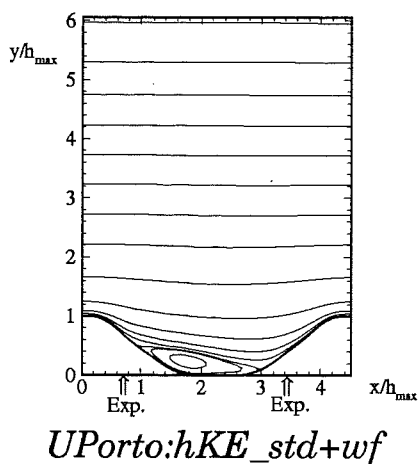
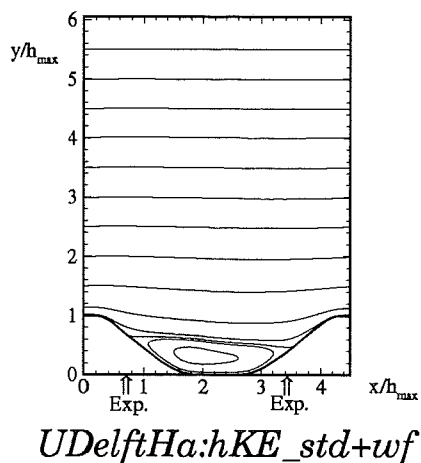
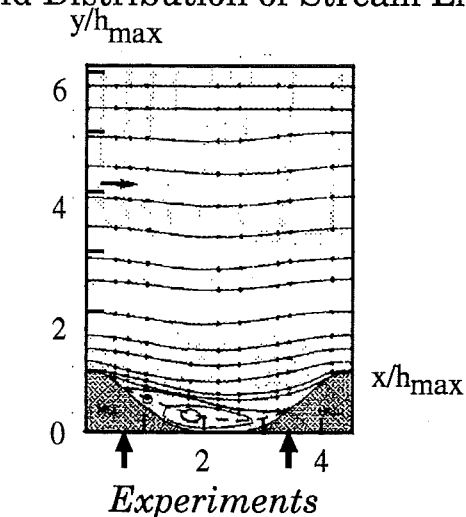
| Group | Turbulence Model | Separation (x/h_{max}) | Reattachment (x/h_{max}) |
|---|----------------------------|-------------------------------|---------------------------------|
| Exp | | 0.71 | 3.43 |
| Group 1: k-ϵ model with wall functions | | | |
| UDelftHa | hKE_std+wf | 0.75 | 3.54 |
| UPorto | hKE_std+wf | 0.93 | 3.05 |
| UKarlsru | hKE_std+wf | 0.85 | 3.05 |
| IOlomouc | hKE_std+wf_nstd | 0.85 | 3.50 |
| UPorto | hKE_std+wf_(k fixed) | 0.42 | 3.57 |
| Group 2: various two-equation models | | | |
| CompDyna | hKE_RNG+wf | 0.72 | 3.35 |
| UPorto | hKE_LeRo+wf | 0.61 | 3.45 |
| EDFLNHLa | IKE_LaSh | 0.52 | 3.61 |
| IOlomouc | hKE_std+Gol | 0.75 | 3.52 |
| UKarlsru | hKE_std+NoRe | 0.34 | 3.75 |
| DLRGoett | kOm_Wil | 0.5 | 3.7 |
| IOlomouc | nKE_Spez+wf | 0.64 | 3.50 |
| Group 3: Reynolds-stress models and LES | | | |
| EDFLNHLa | RSM_LRR+wf | 0.52 | 3.61 |
| UDelftHa | RSM_LRR+wf | 0.36 | 3.43 |
| UMISTCra | RSM_CrLa+2eq | 0.40 | 3.60 |
| UMISTCra | RSM_Cub+2eq | 0.59 | 2.03 |
| DLROberp | LES | 0.56 | 3.18 |
| Group 4: non-periodic calculations | | | |
| UDelftHa | hKE_std+wf_(7th hill) | 0.75 | 3.54 |
| RCHokkai | hKE_std+wf_nstd_(7th hill) | 0.45 | 3.49 |
| CompDyna | hKE_RNG+wf_(7th hill) | 0.39 | 3.46 |
| UDelftHa | RSM_LRR+wf_(7th hill) | 0.46 | 3.59 |
| DLROberp | LES_(7th hill) | 0.47 | 3.36 |



2D Model Hill Flow - Case 2B: Consecutive Hills

Field Distribution of Stream Lines

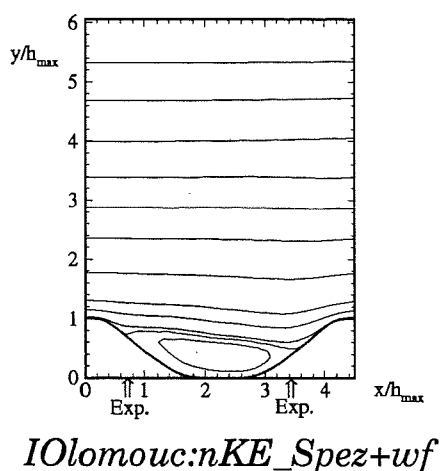
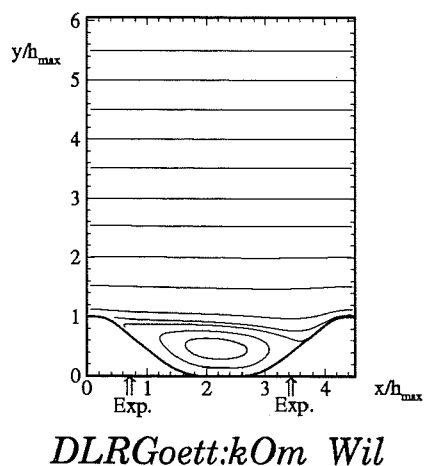
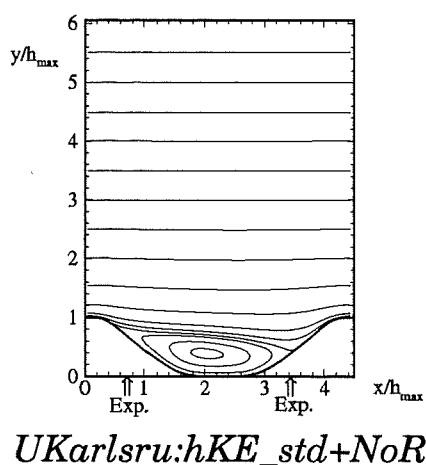
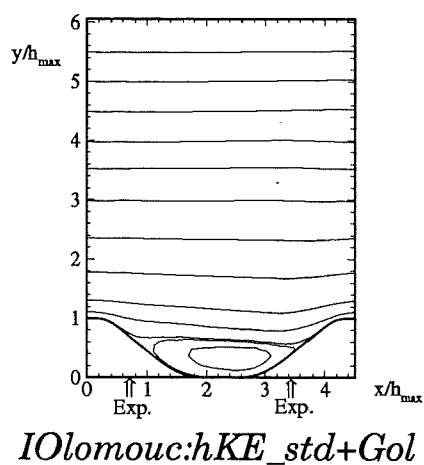
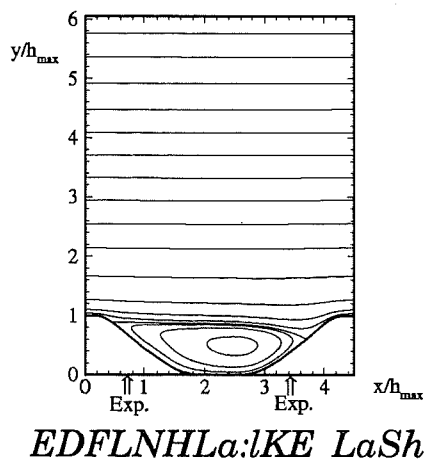
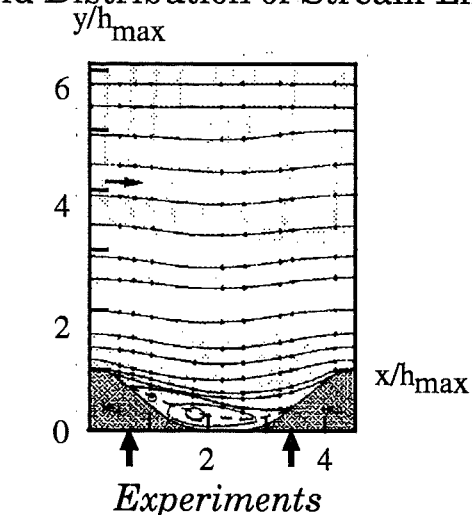
k-epsilon model with wall functions



2D Model Hill Flow - Case 2B: Consecutive Hills

Field Distribution of Stream Lines

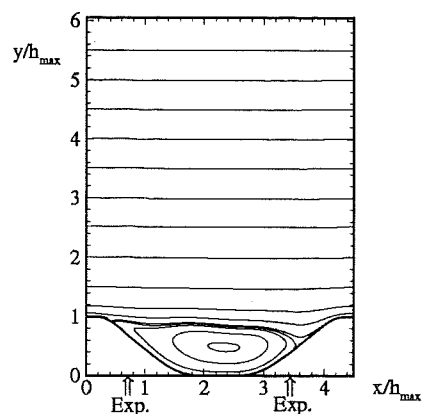
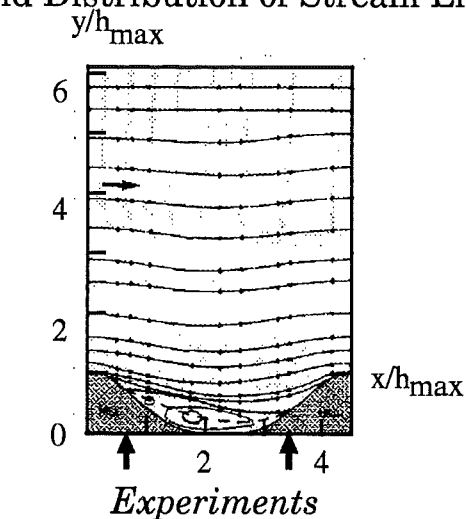
various two-equation models



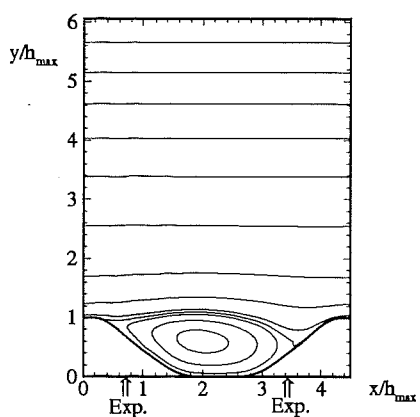
2D Model Hill Flow - Case 2B: Consecutive Hills

Field Distribution of Stream Lines

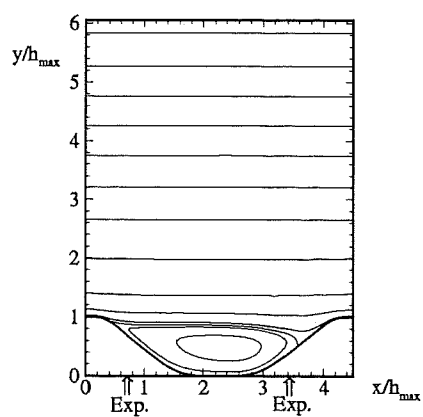
Reynolds-stress models and LES



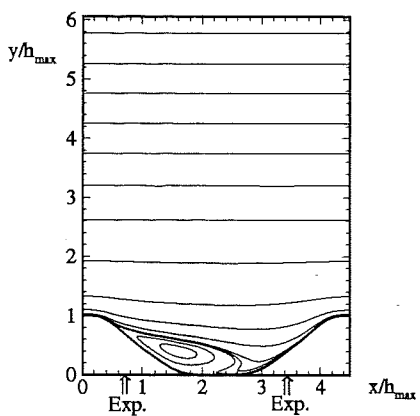
EDFLNHL α :RSM_LRR+wf



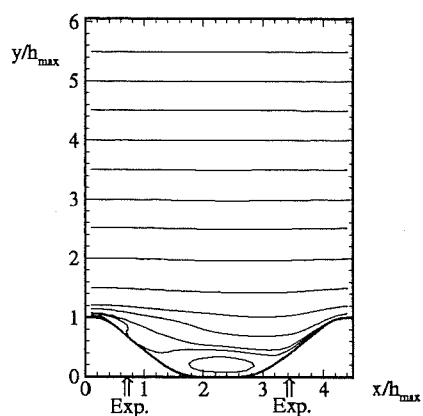
UDelftHa:RSM_LRR+wf



UMISTCr α :RSM_CrLa+2eq



UMISTCr α :RSM_Cub+2eq

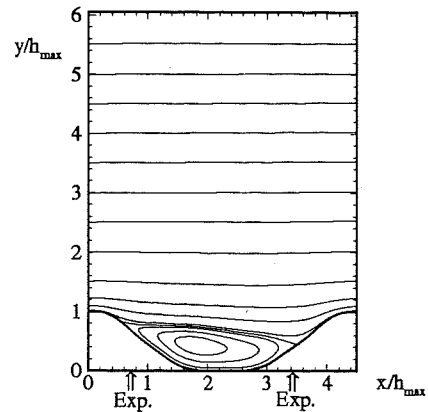
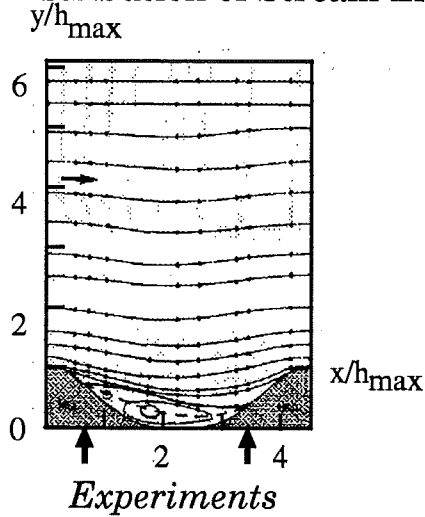


DLROberp:LES

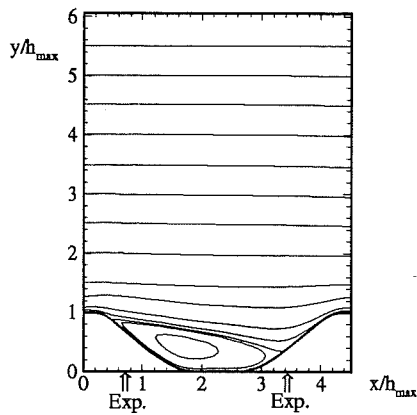
2D Model Hill Flow - Case 2B: Consecutive Hills

Field Distribution of Stream Lines

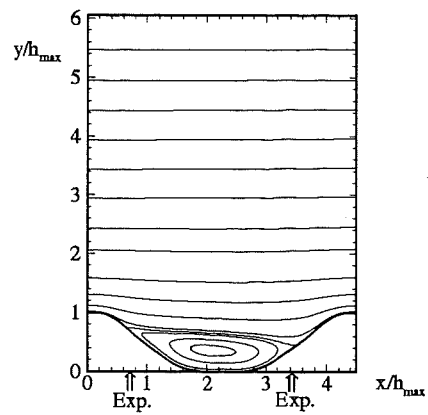
non-periodic calculations



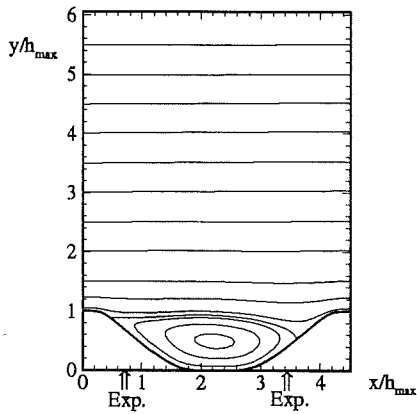
UDelftHa:hKE_std+wf_(7th)



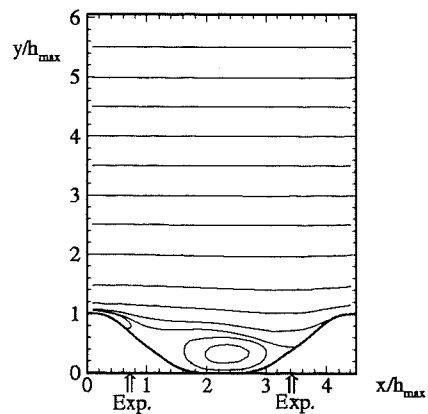
RCHokkai:hKE_std+wf_nstd_(7th)



CompDyna:hKE_RNG+wf_(7th)



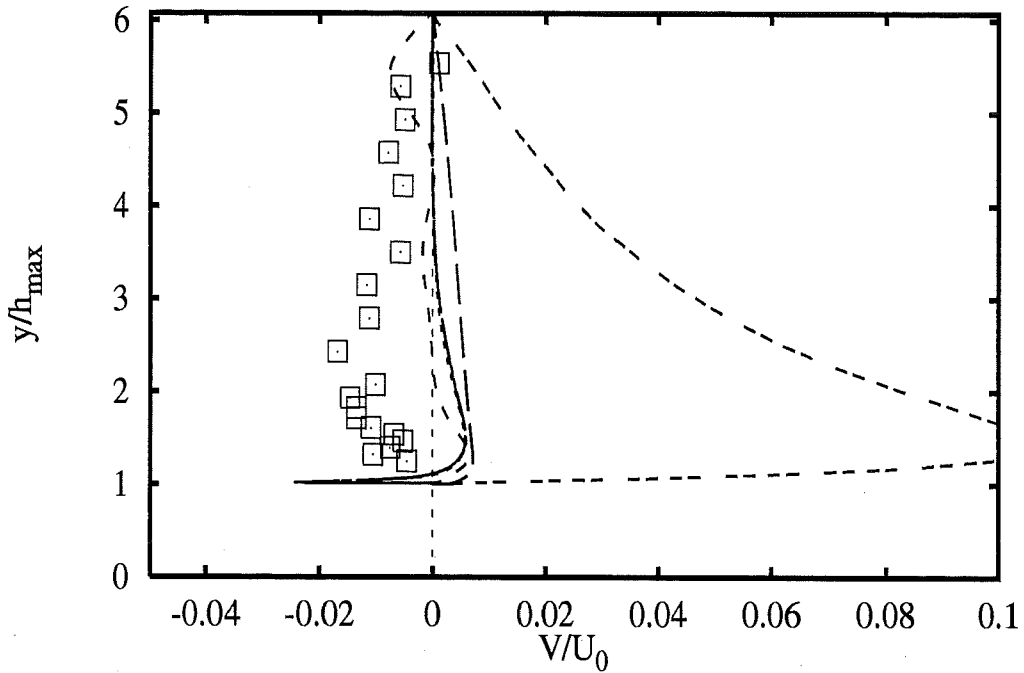
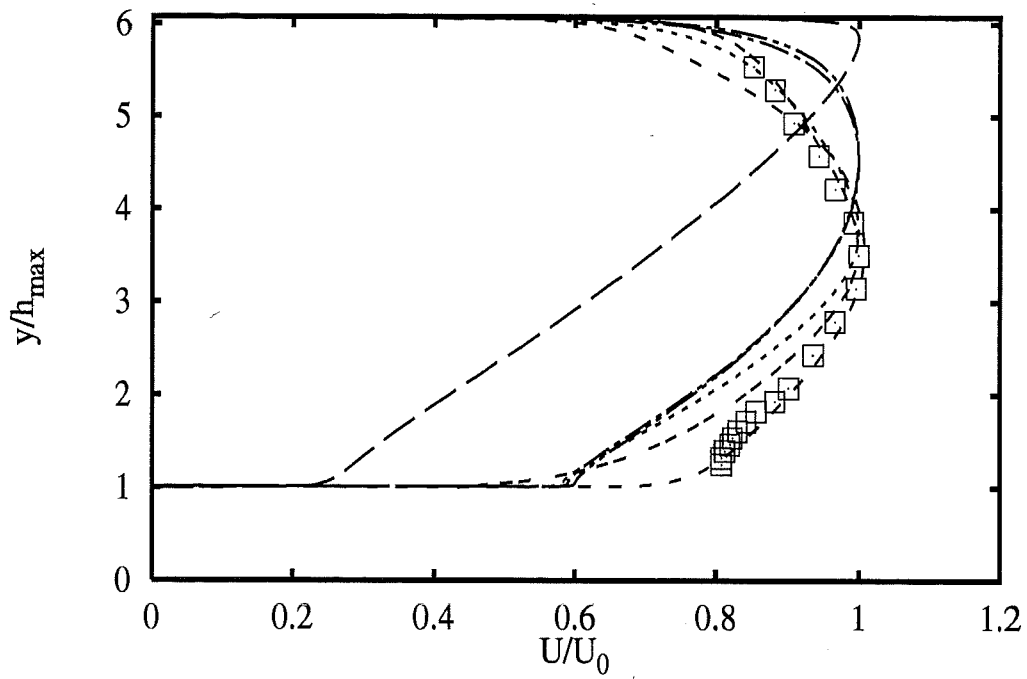
UDelftHa:RSM_LRR+wf_(7th)



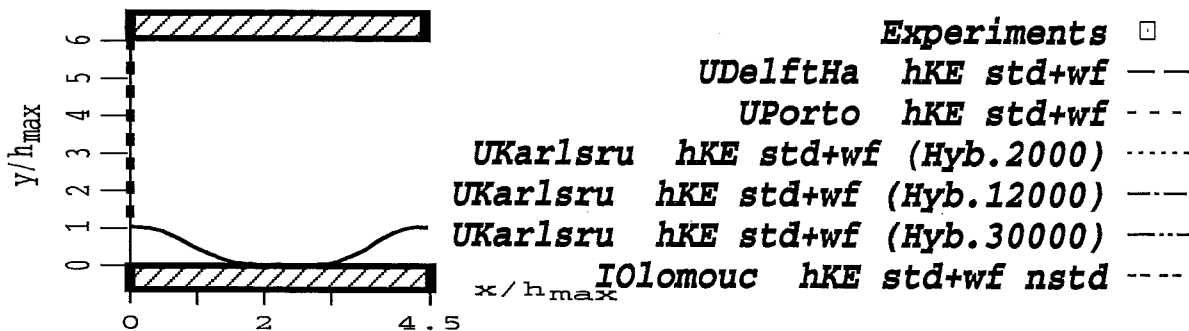
DLROberp:LES_(7th)



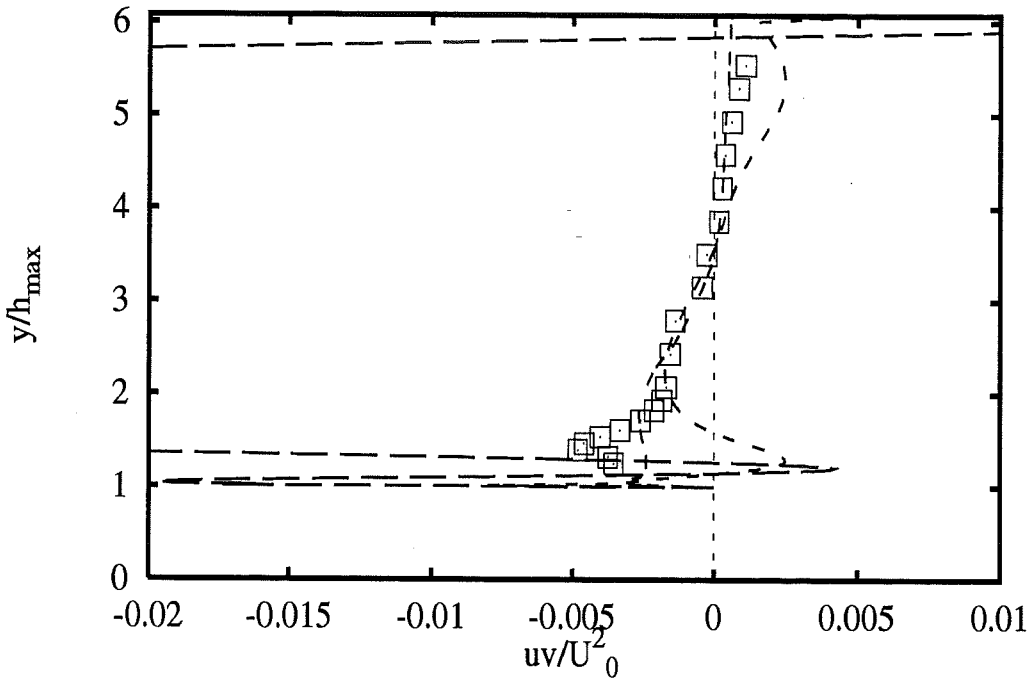
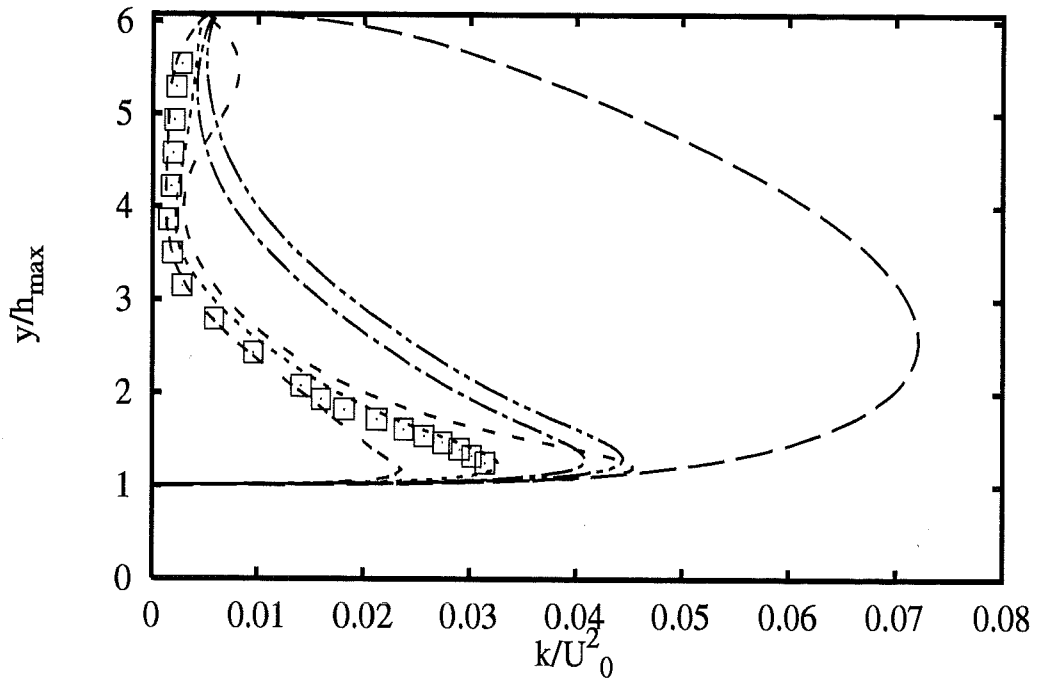




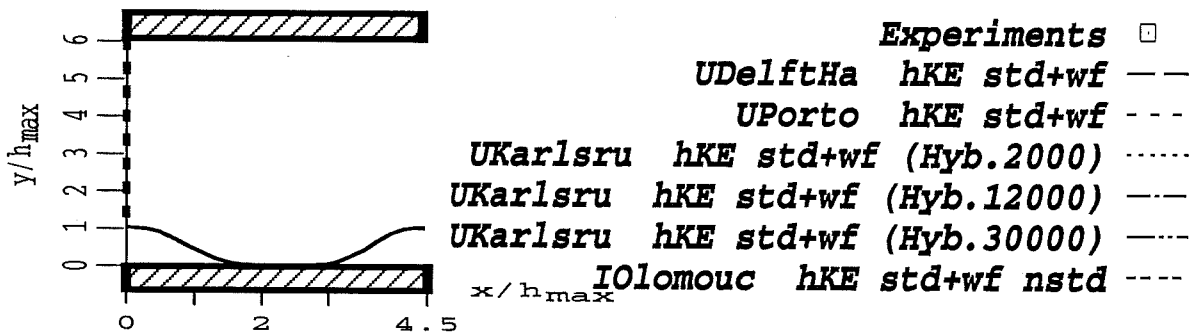
Profiles at $x/h_{max} = 0$



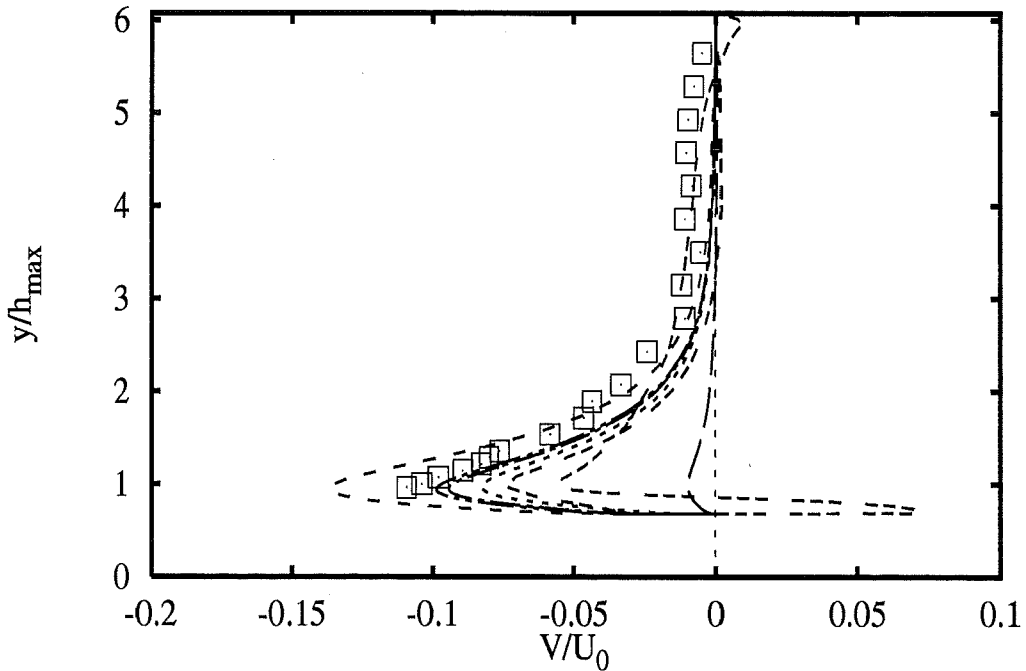
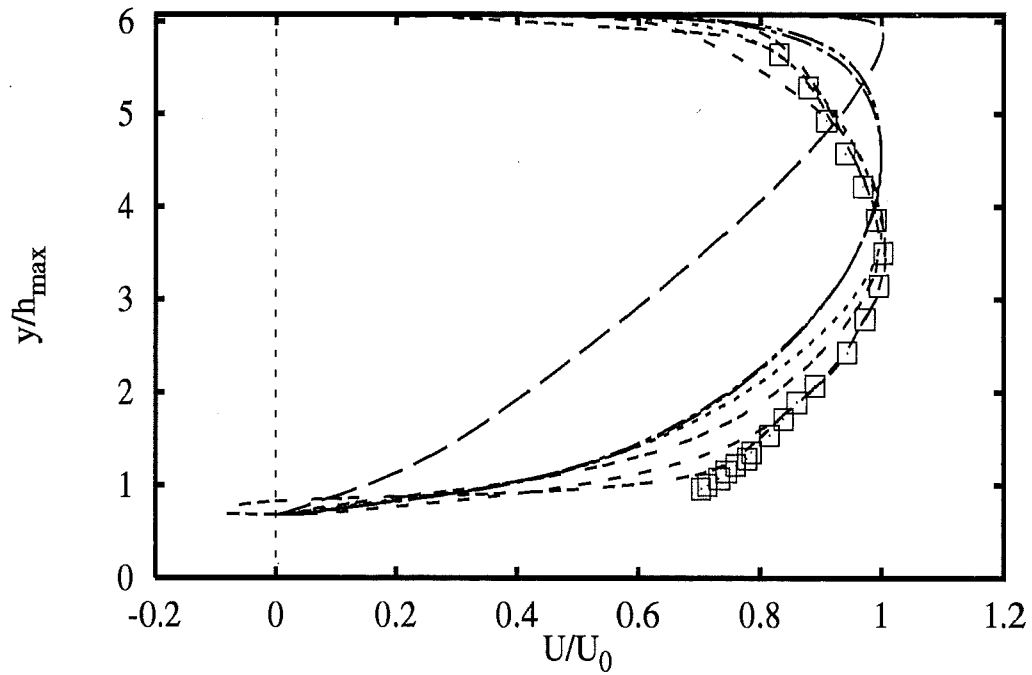
2B - 5



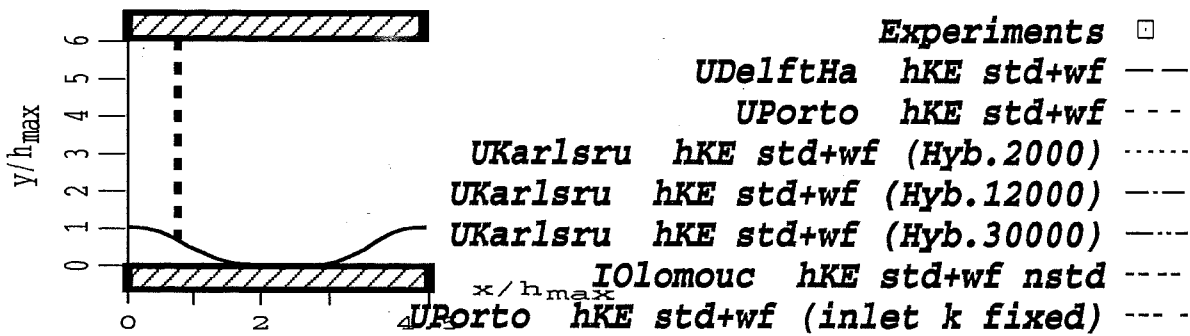
Profiles at $x/h_{max} = 0$



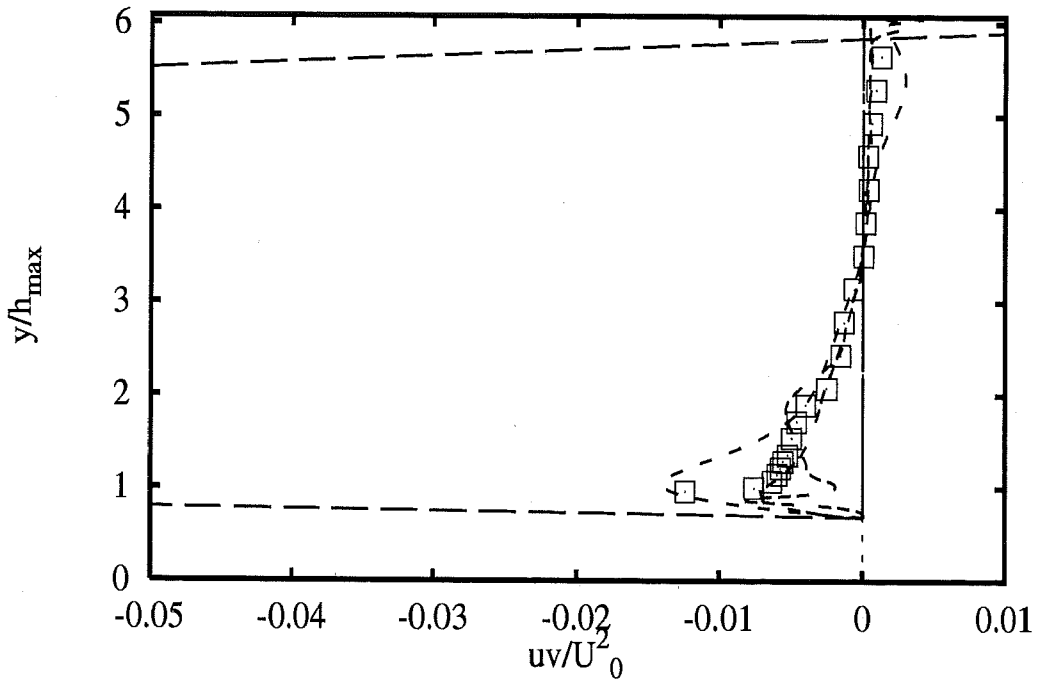
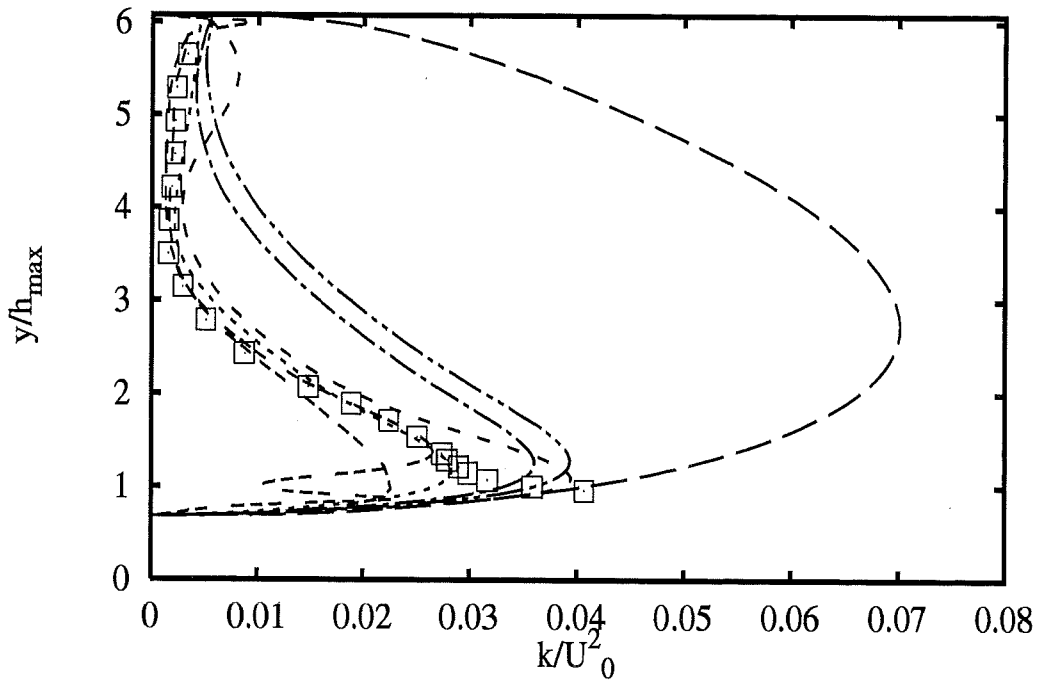
2B - 6



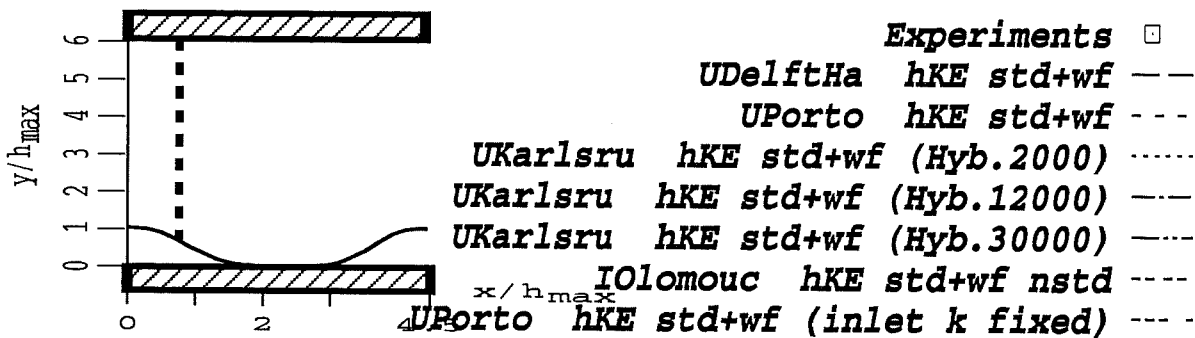
Profiles at $x/h_{max} = 0.71$



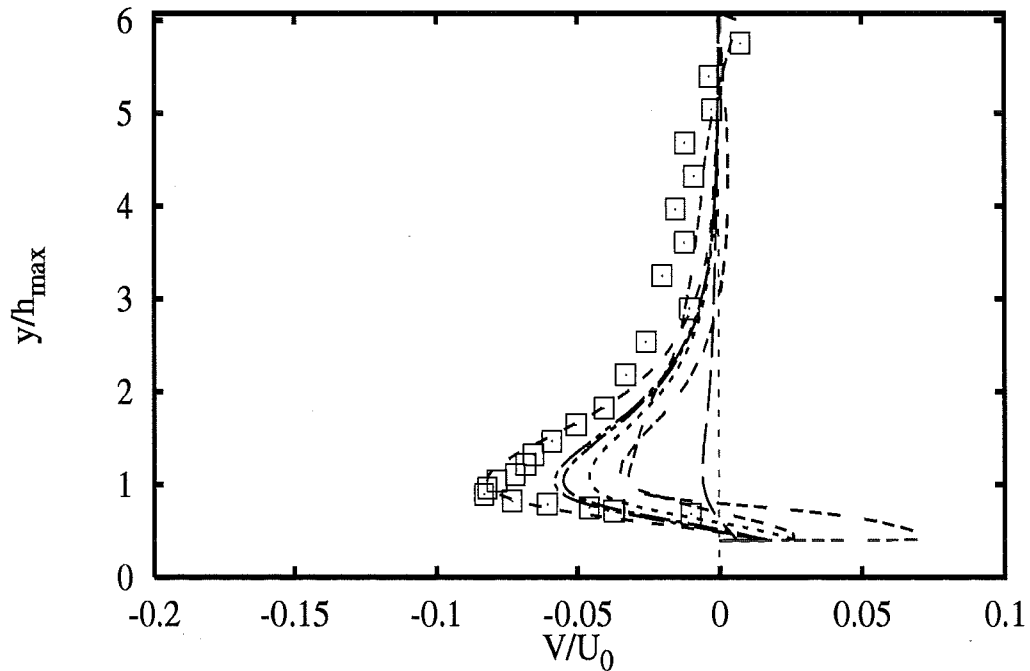
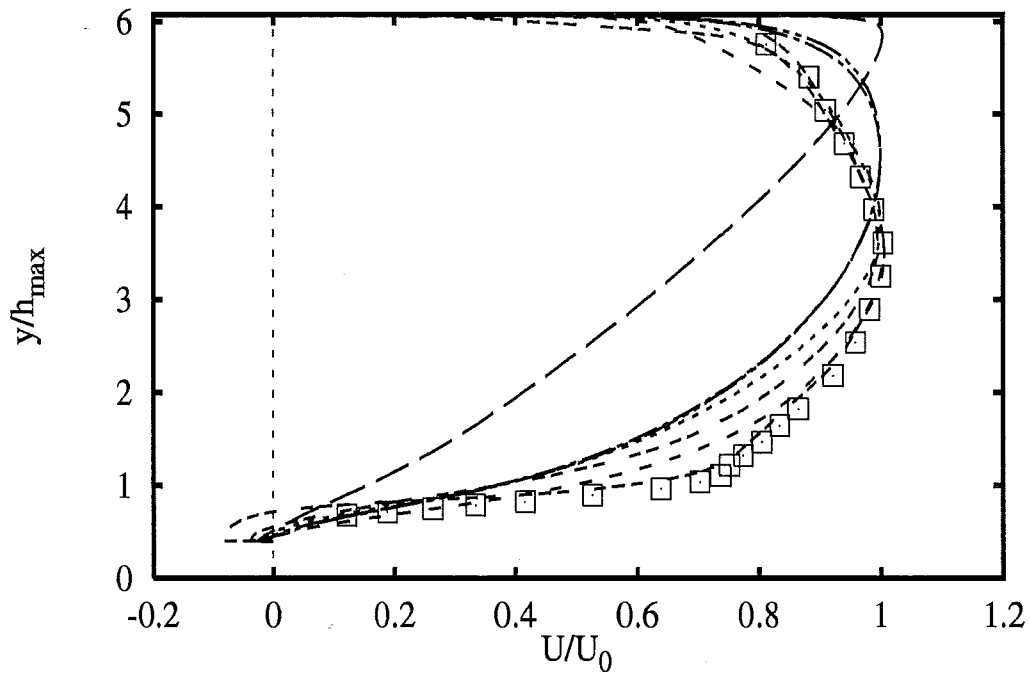
2B - 7



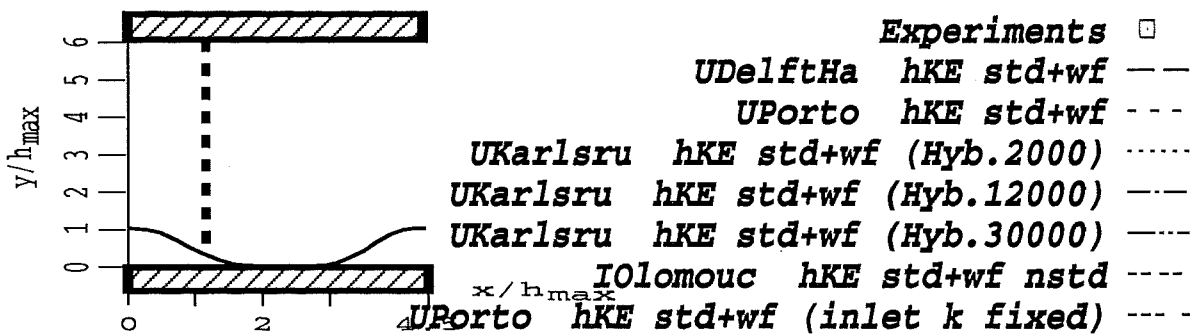
Profiles at $x/h_{max} = 0.71$



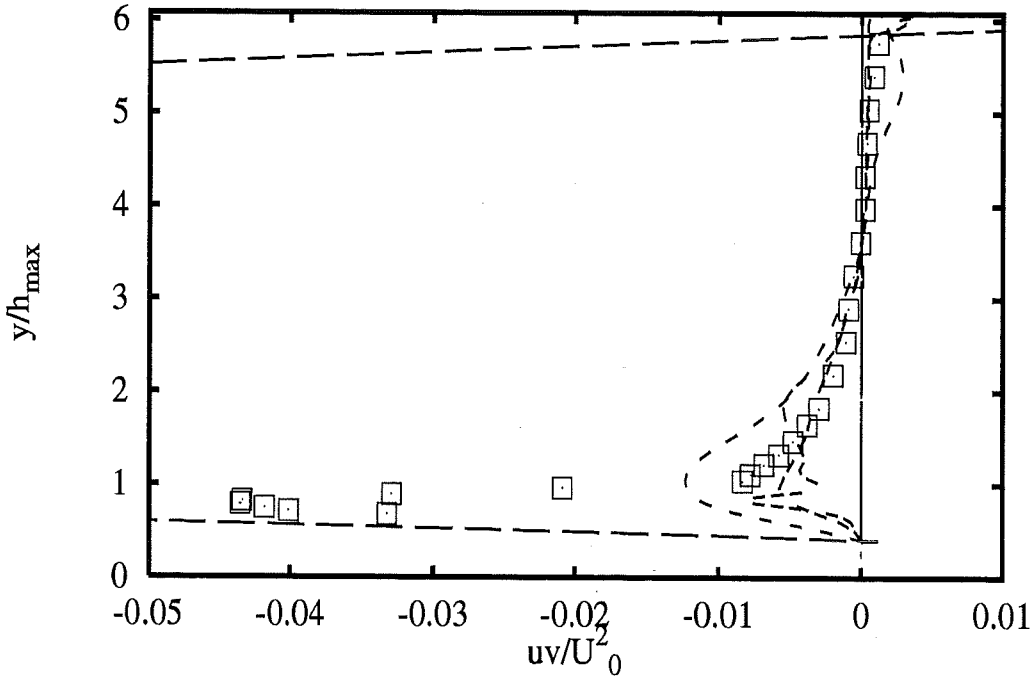
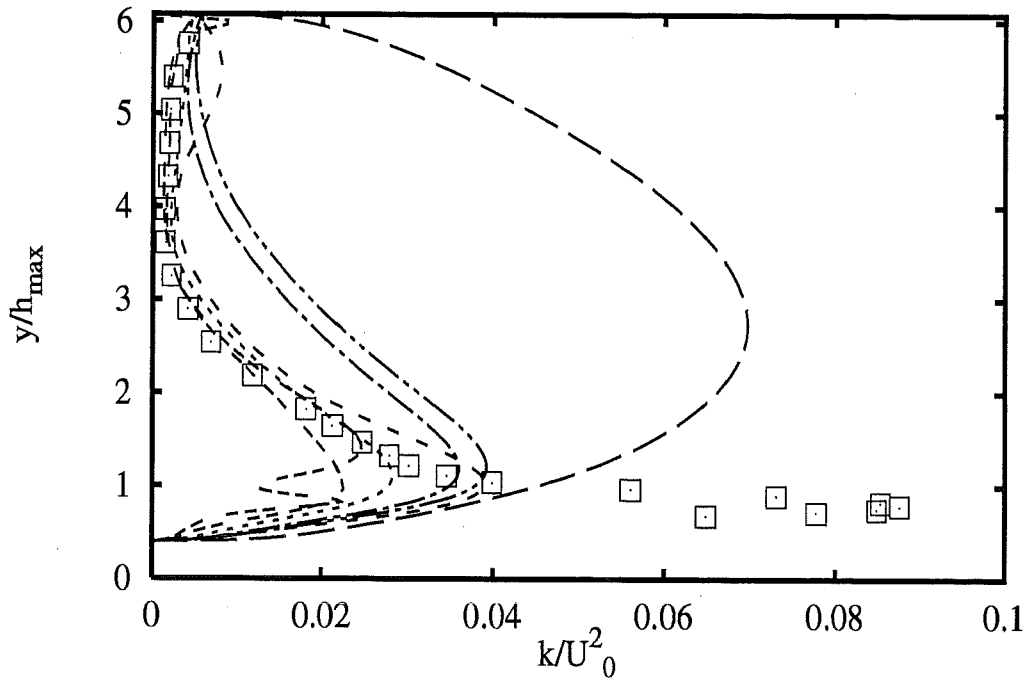
2B - 8



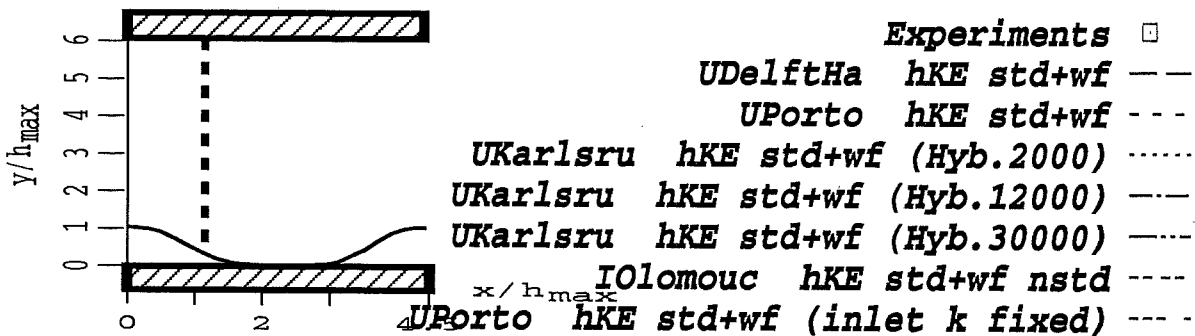
Profiles at $x/h_{max} = 1.07$



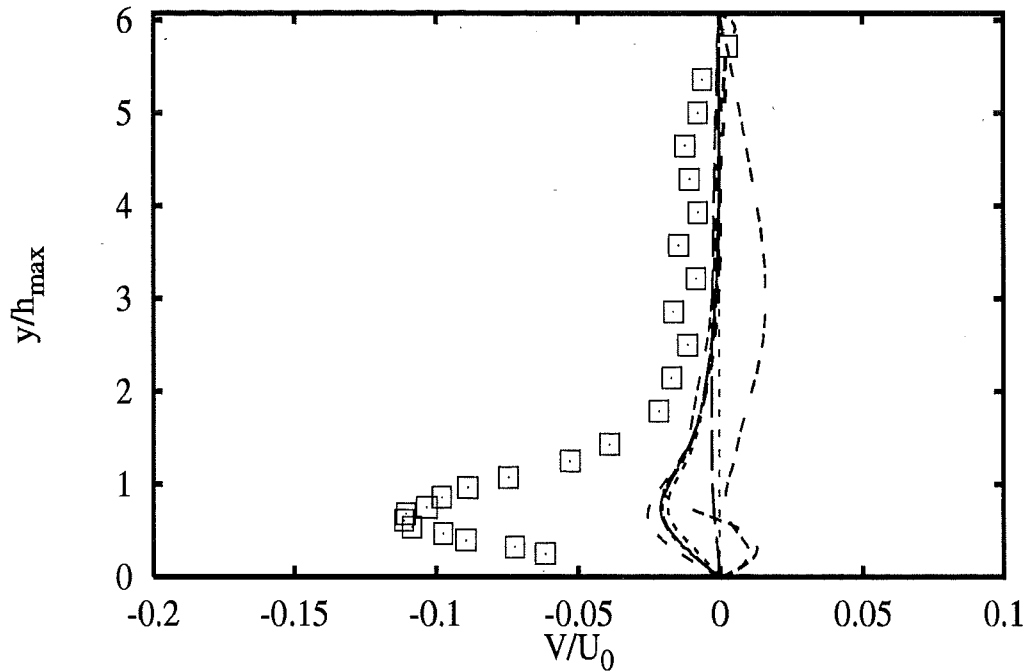
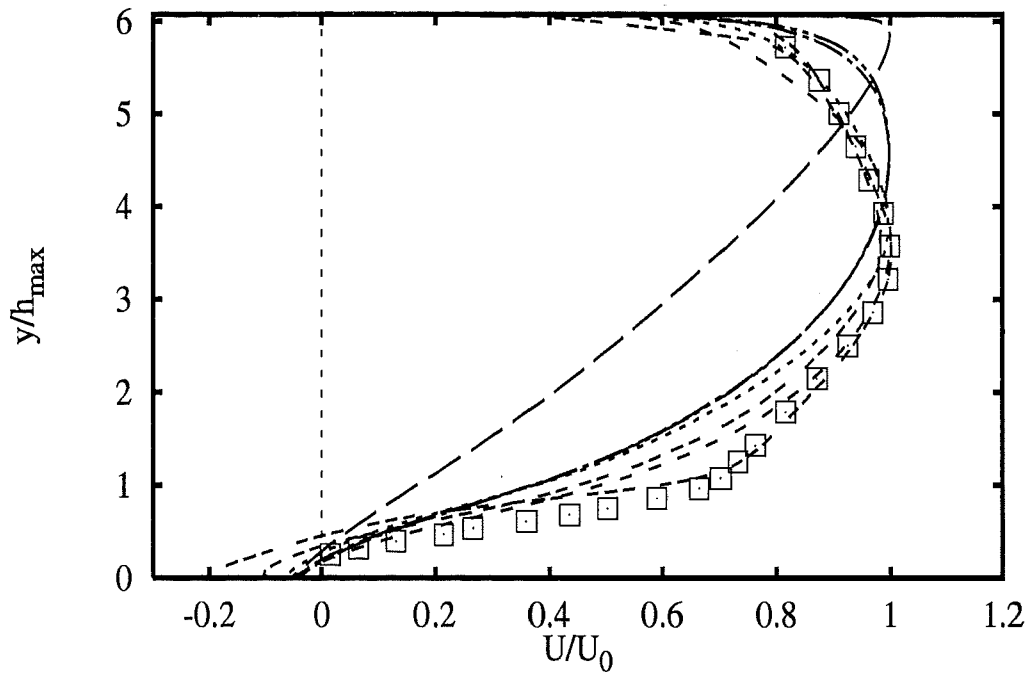
2B - 9



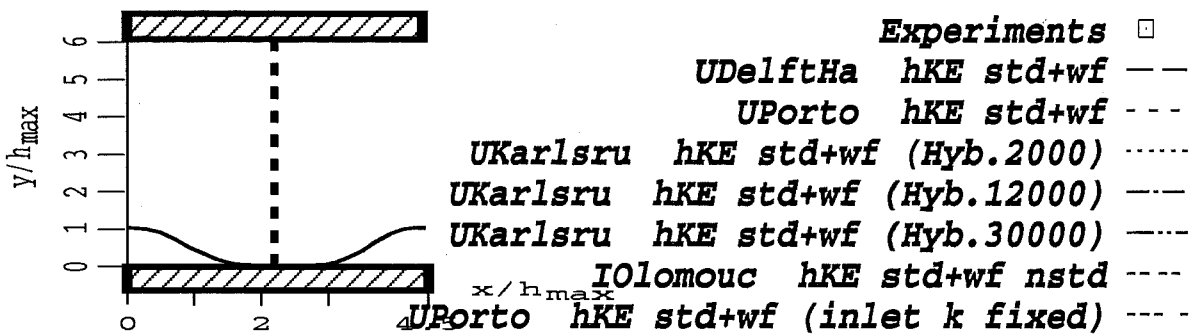
Profiles at $x/h_{max} = 1.07$



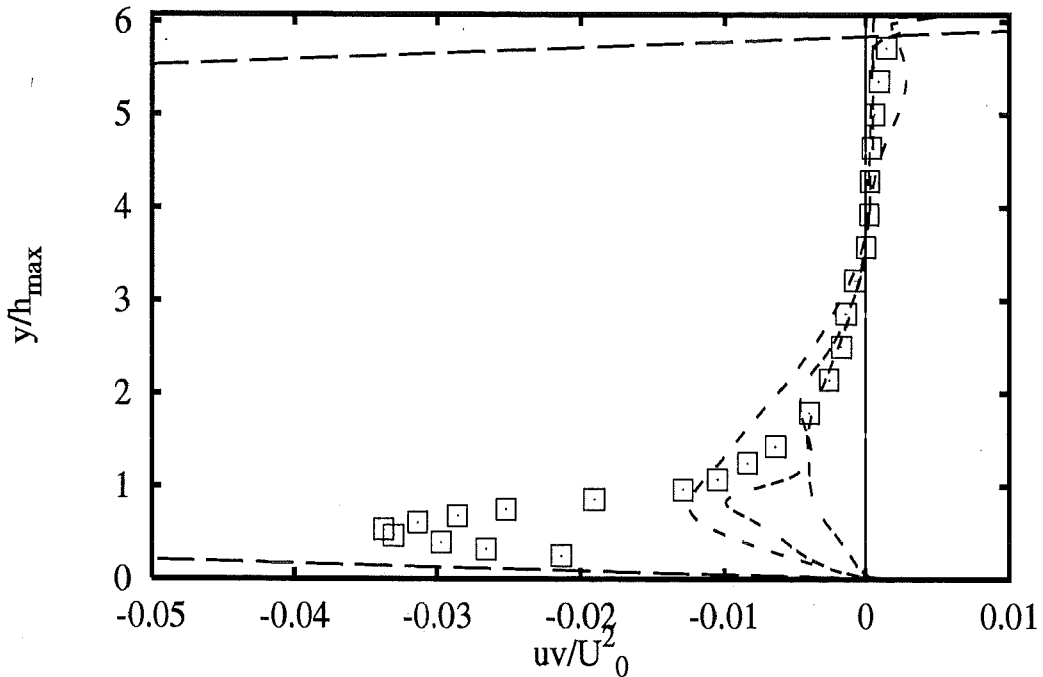
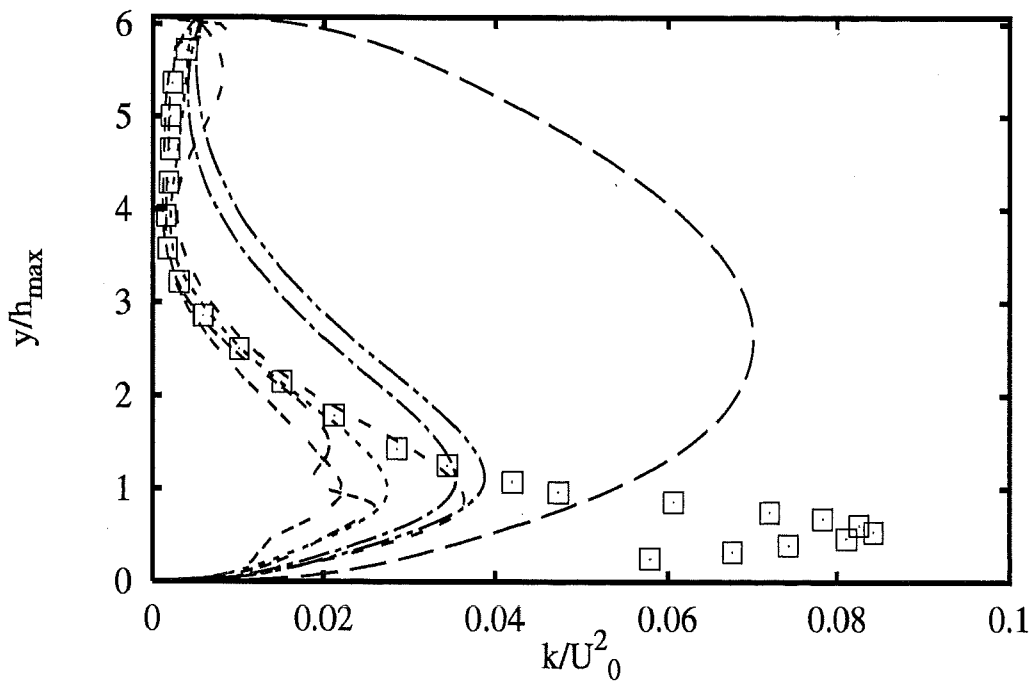
2B - 10



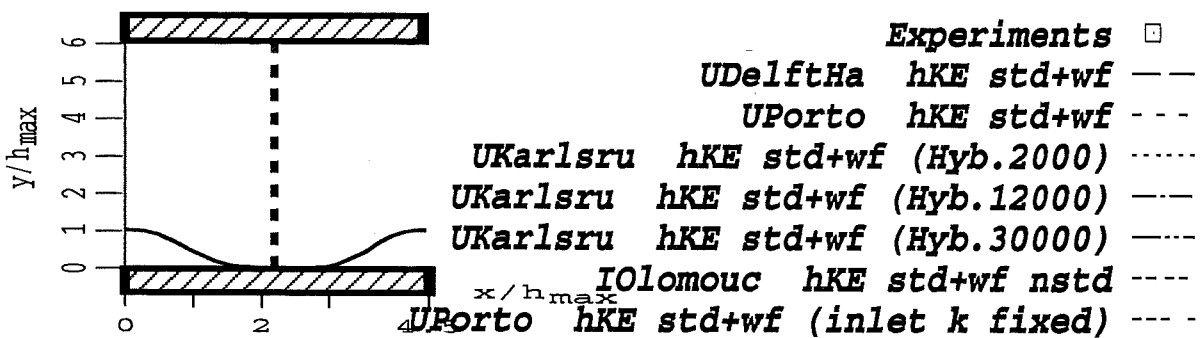
Profiles at $x/h_{max} = 2.25$

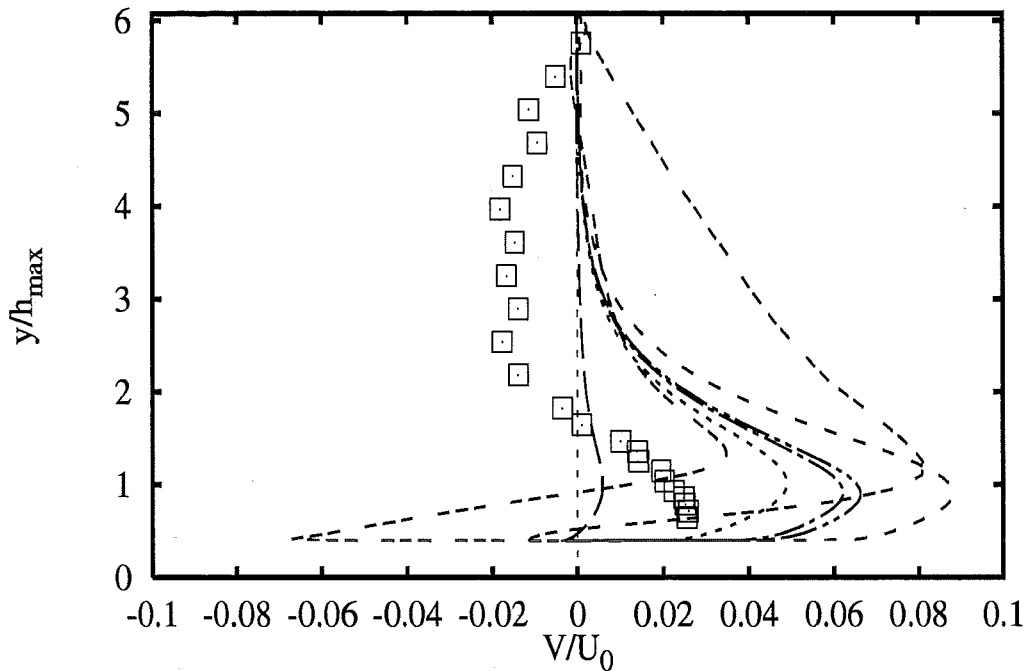
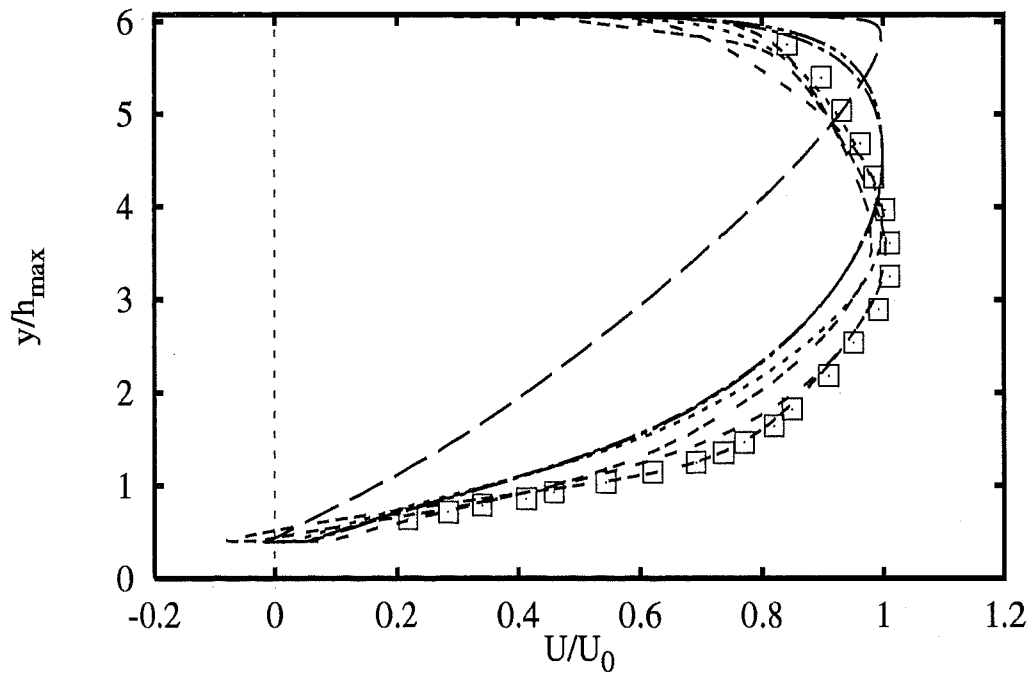


2B - 11

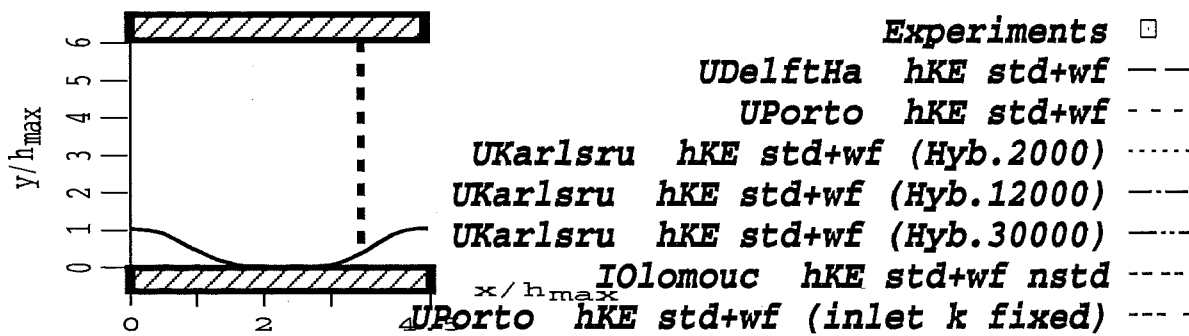


Profiles at $x/h_{max} = 2.25$

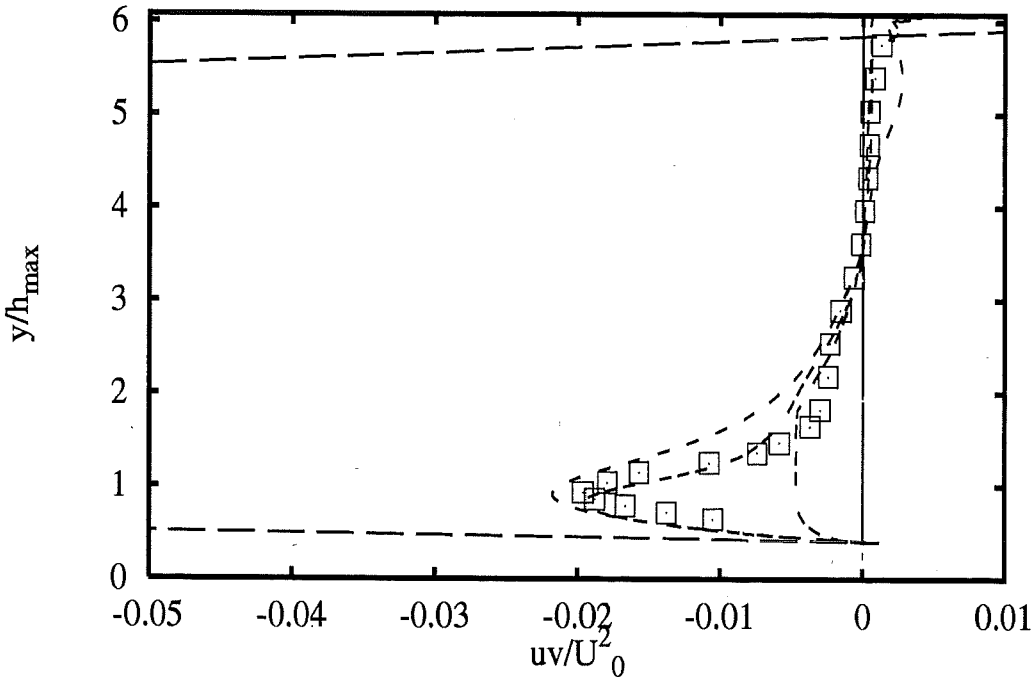
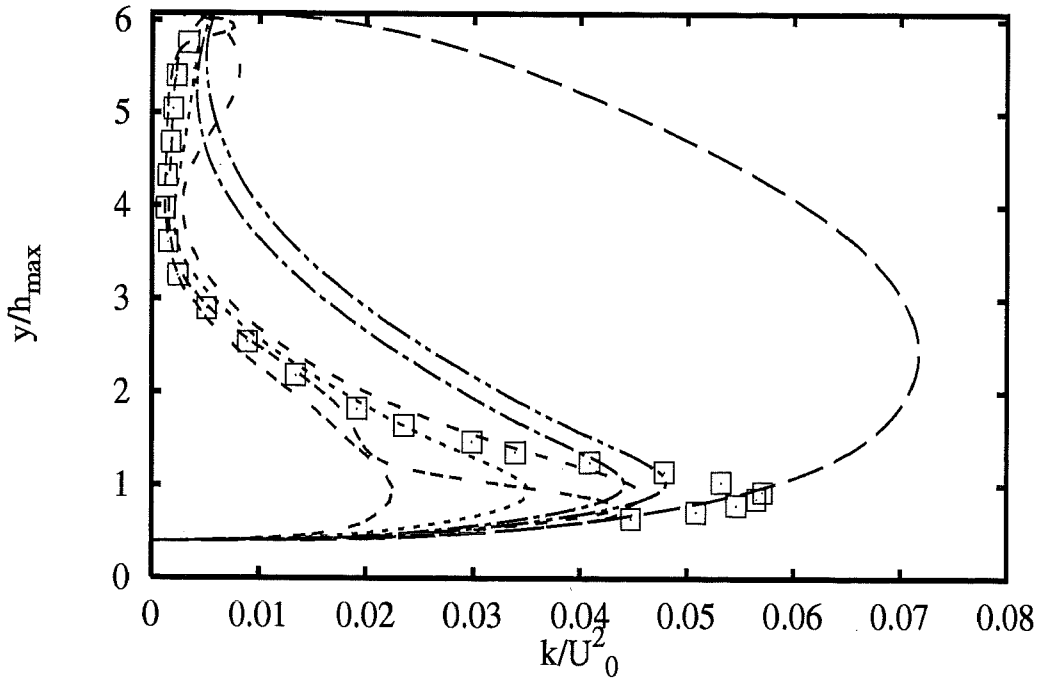




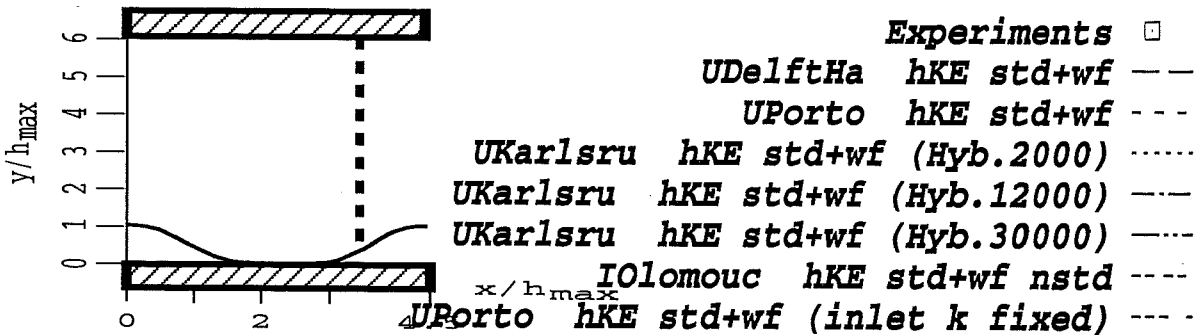
Profiles at $x/h_{max} = 3.43$

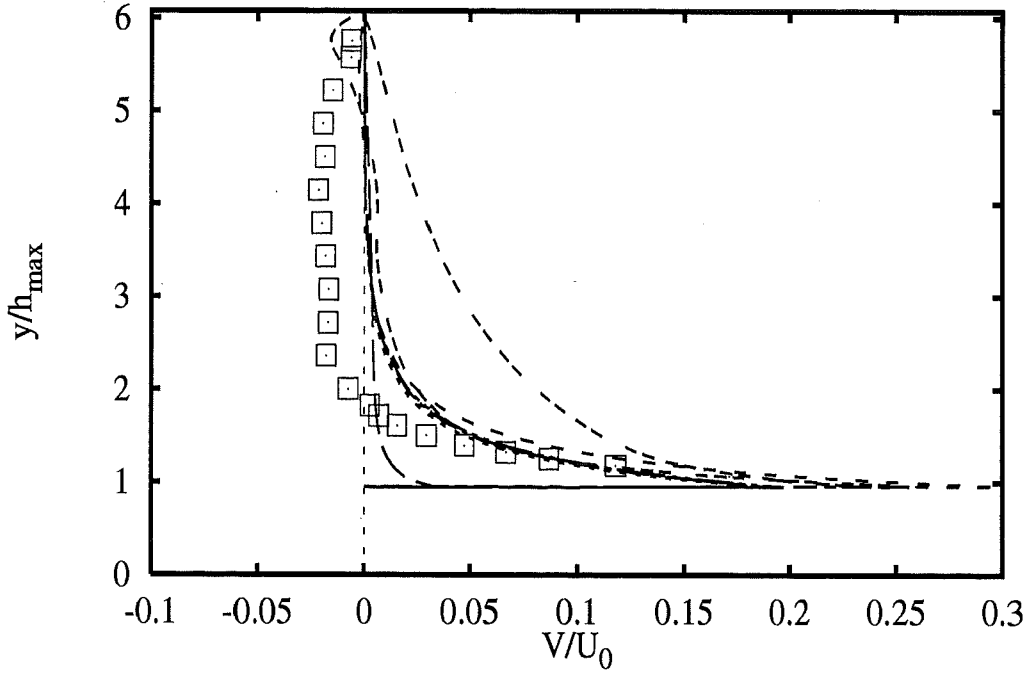
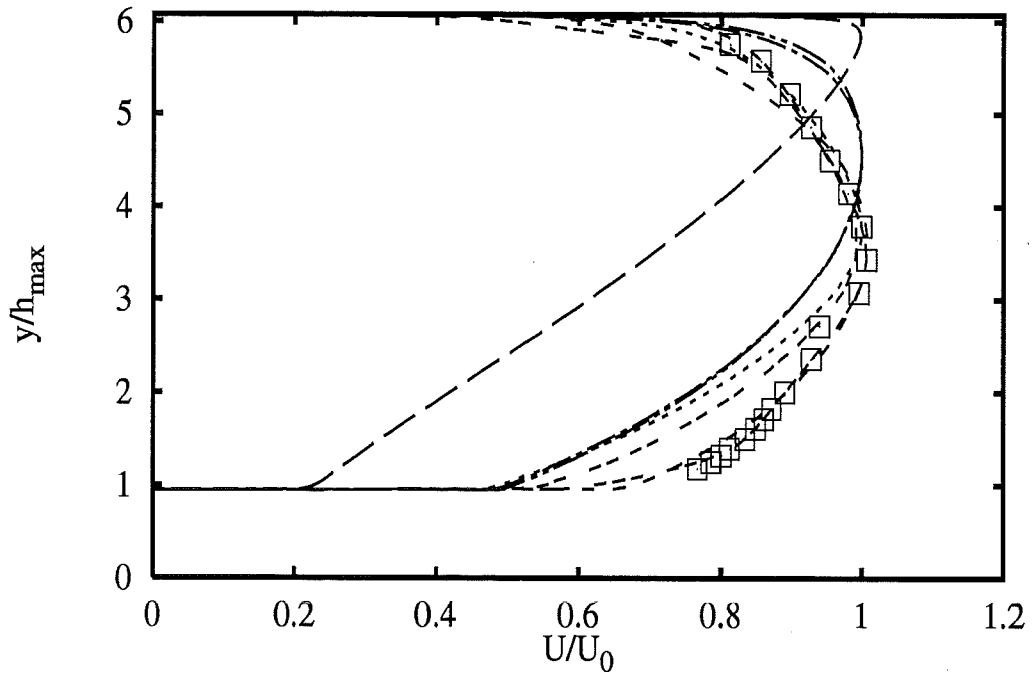


2B - 13

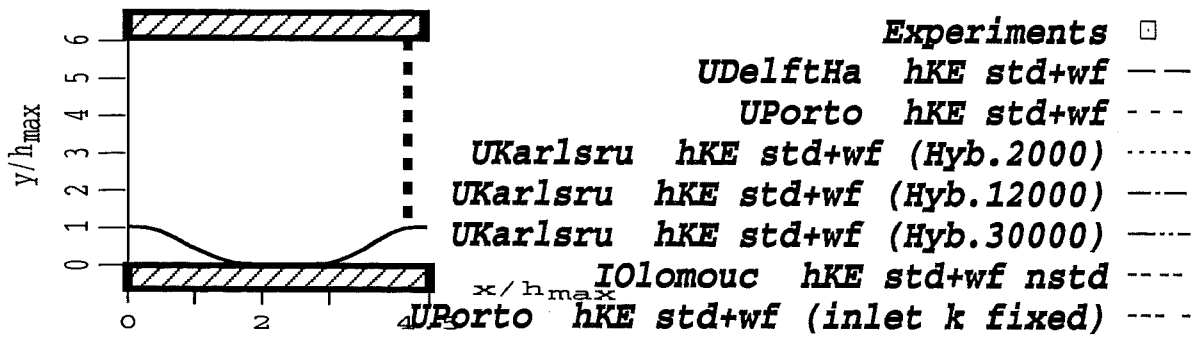


Profiles at $x/h_{max} = 3.43$

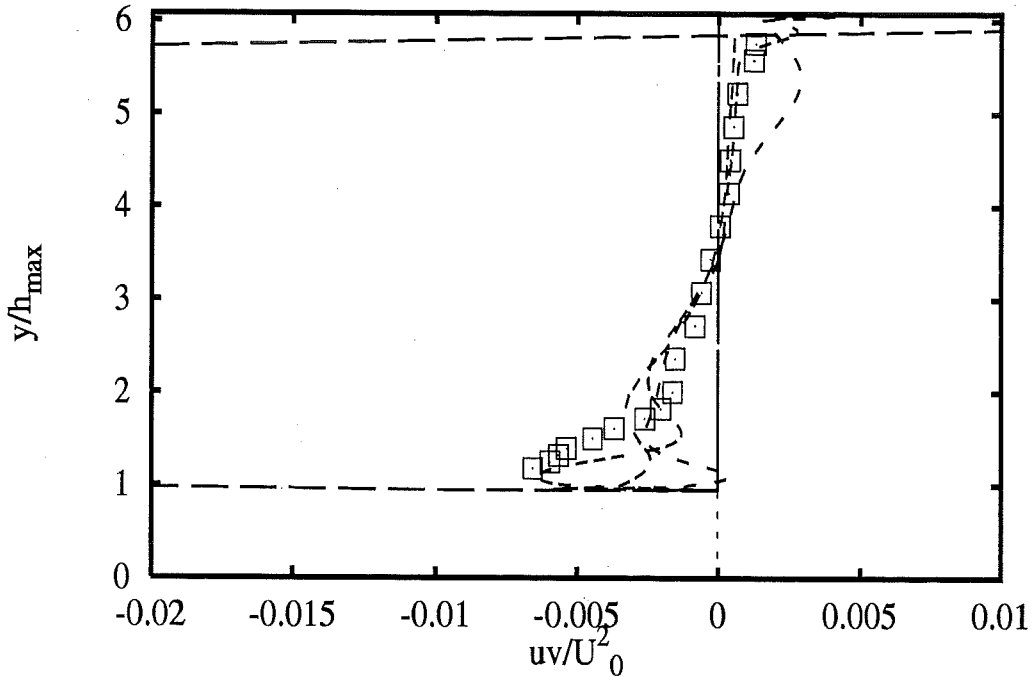
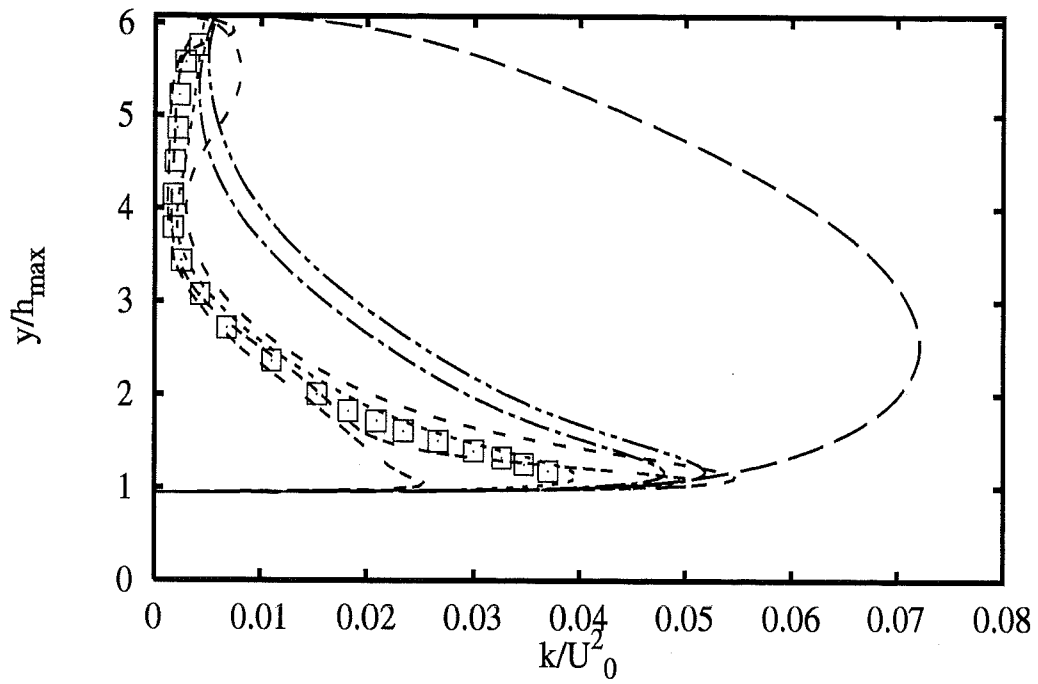




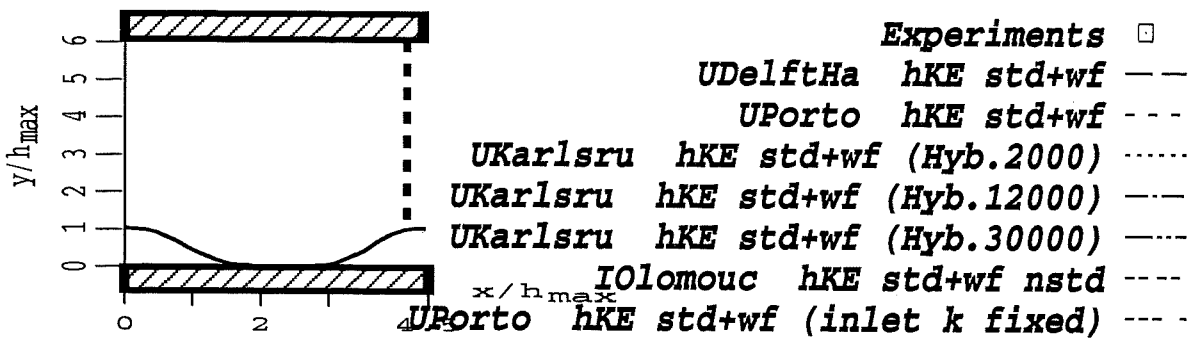
Profiles at $x/h_{max} = 4.14$

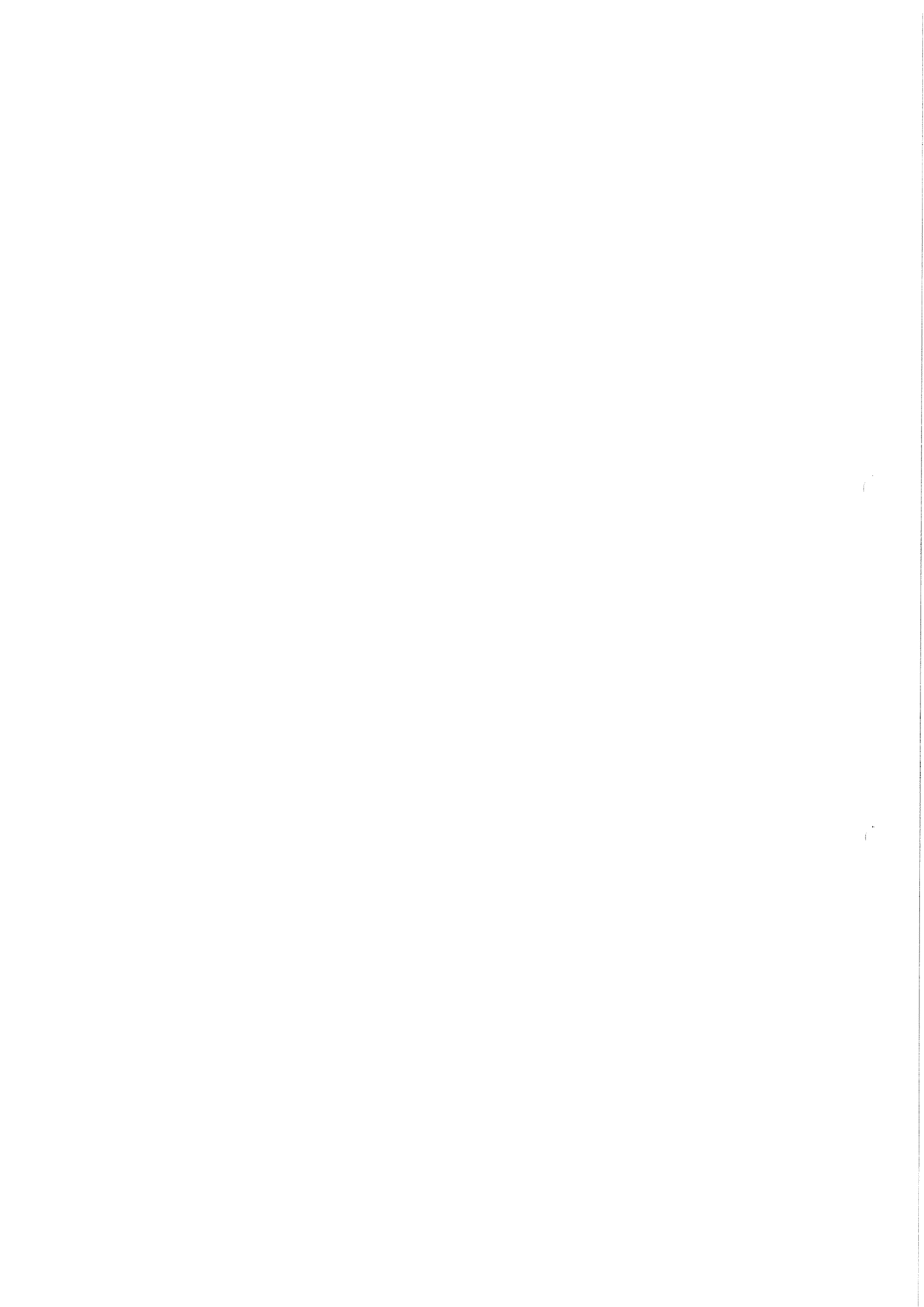


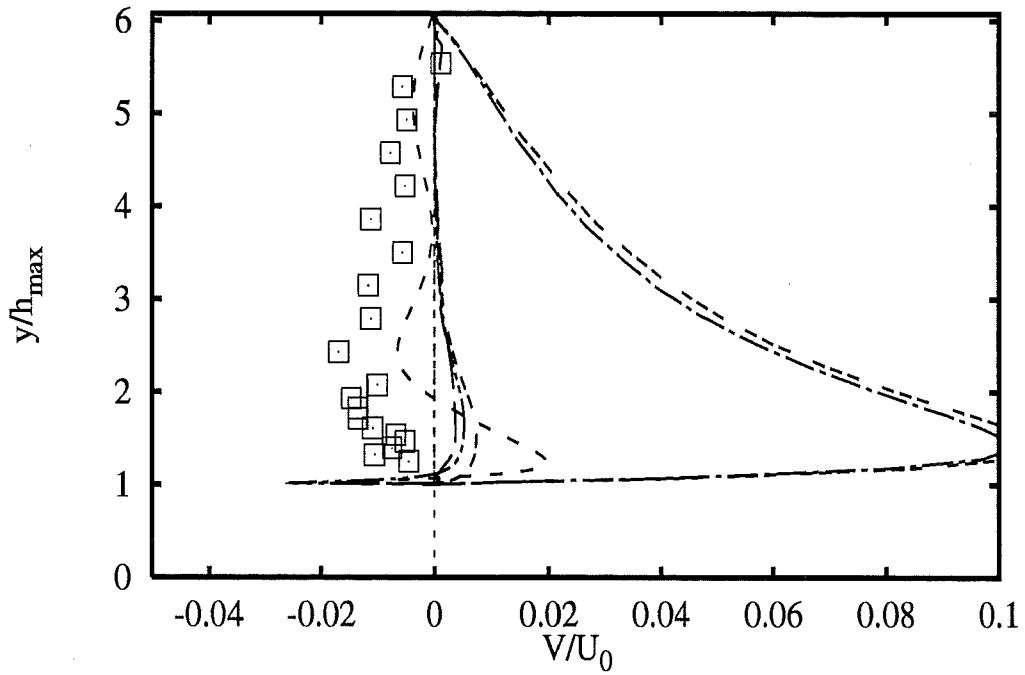
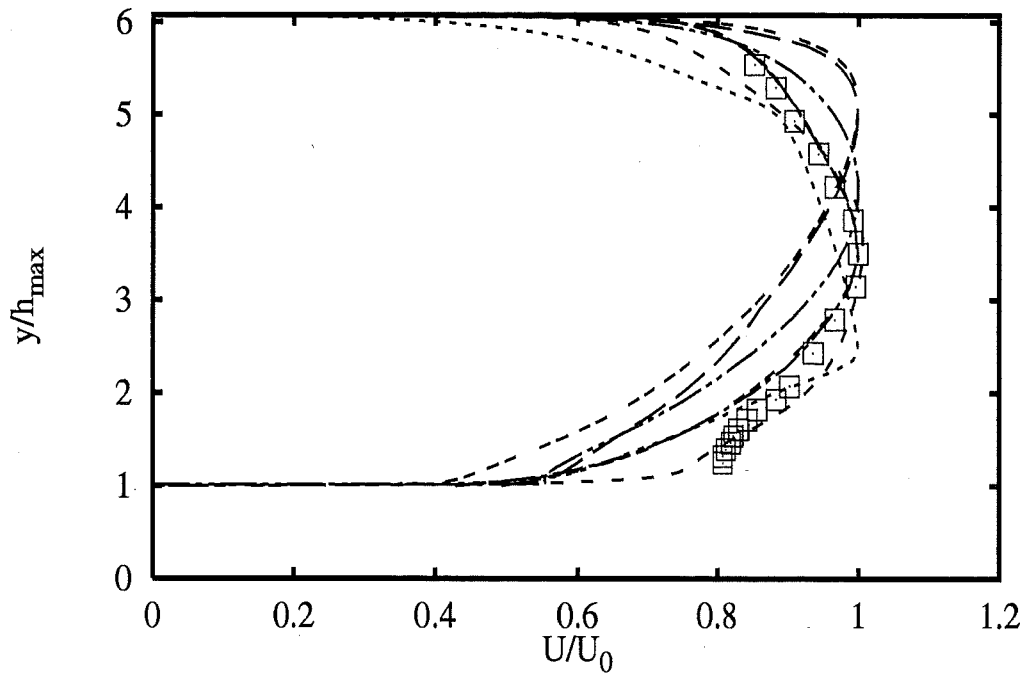
2B - 15



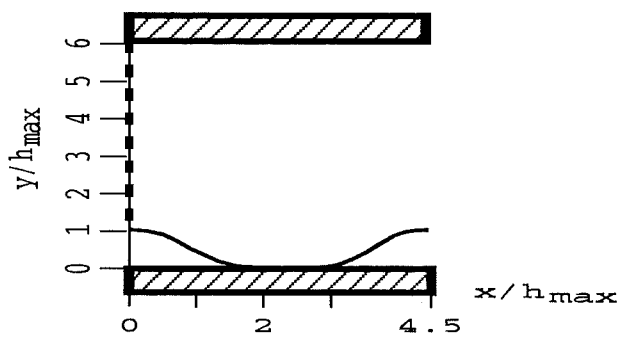
Profiles at $x/h_{max} = 4.14$





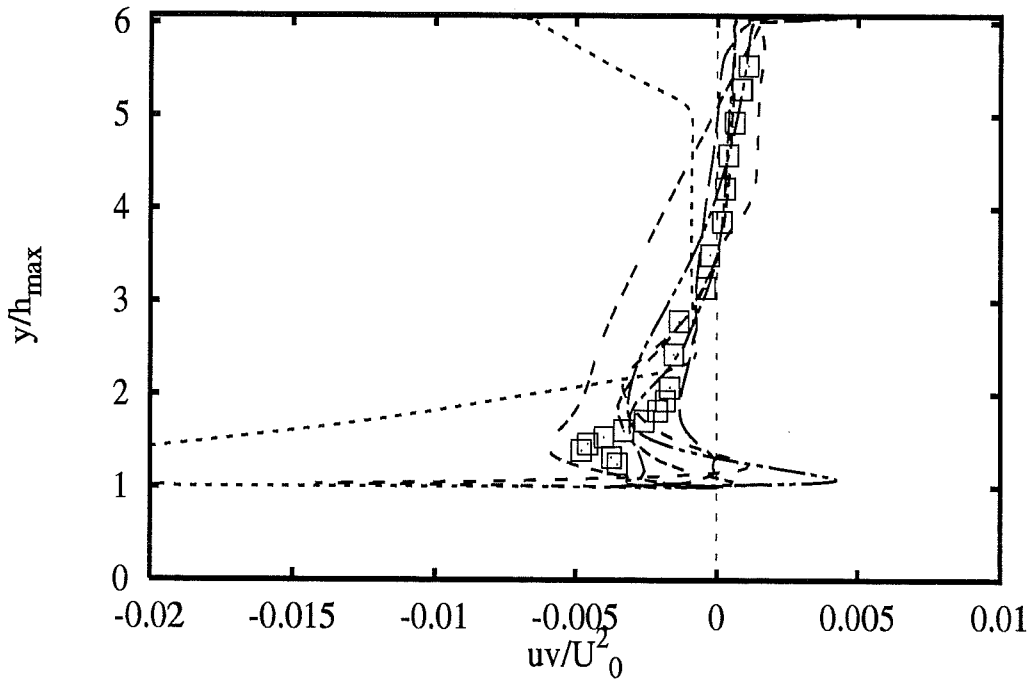
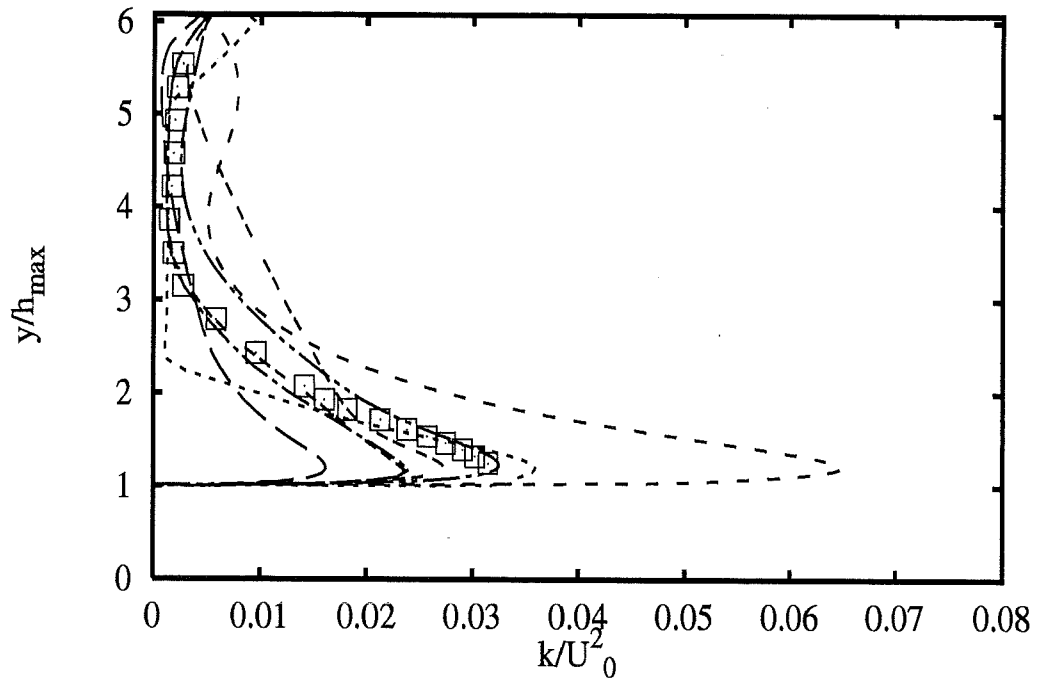


Profiles at $x/h_{max} = 0$

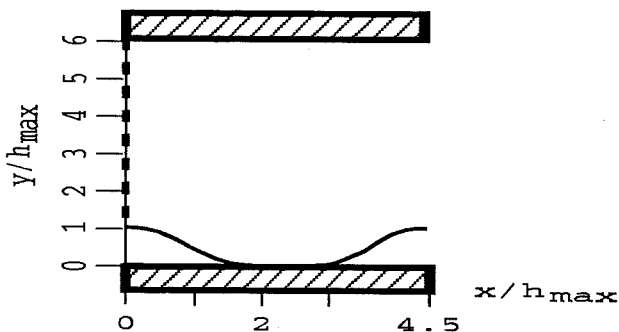


- Experiments \square
- CompDyna hKE RNG+wf $---$
- UPorto hKE LeRo+wf $---$
- EDFLNHLa lKE LaSh $---$
- IOlomouc hKE std+Gol $---$
- UKarlsru hKE std+NoRe $---$
- DLRGoett kOm Wil $---$
- IOlomouc nKE Spez+wf $---$

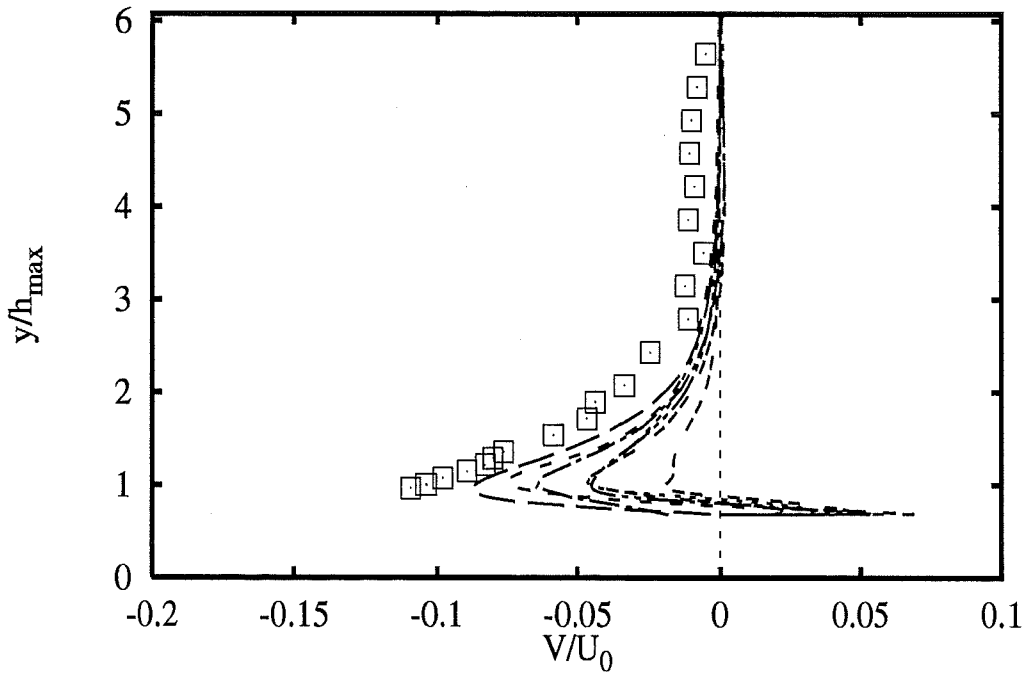
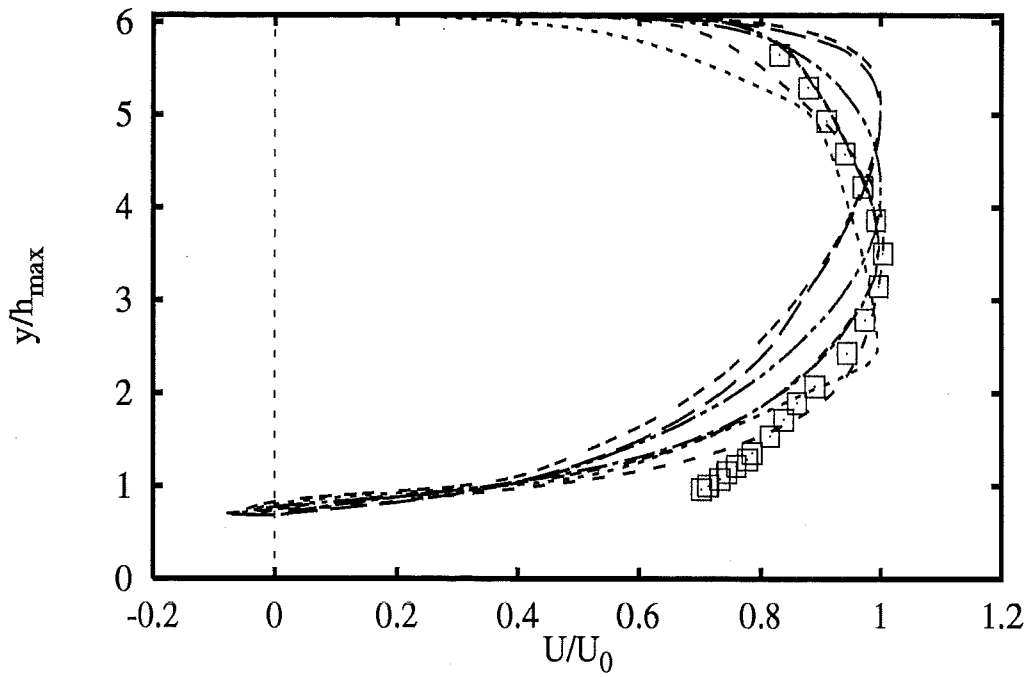
2B - 17



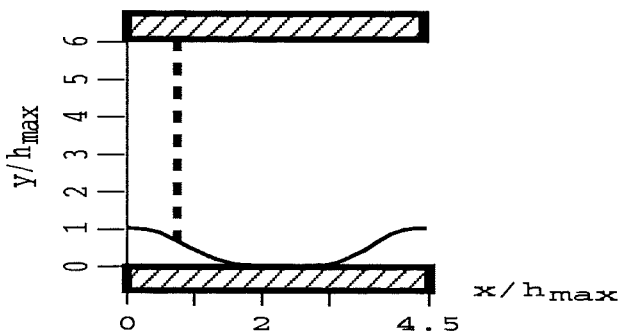
Profiles at $x/h_{max} = 0$



- Experiments \square
- CompDyna hKE RNG+wf ---
- UPorto hKE LeRo+wf - - -
- EDFLNHLA lKE LaSh (dotted)
- IOlomouc hKE std+Gol - · - · -
- UKarlsru hKE std+NoRe - · - · -
- DLRGoett kOm Wil - · - · -
- IOlomouc nKE Spez+wf - · - · -

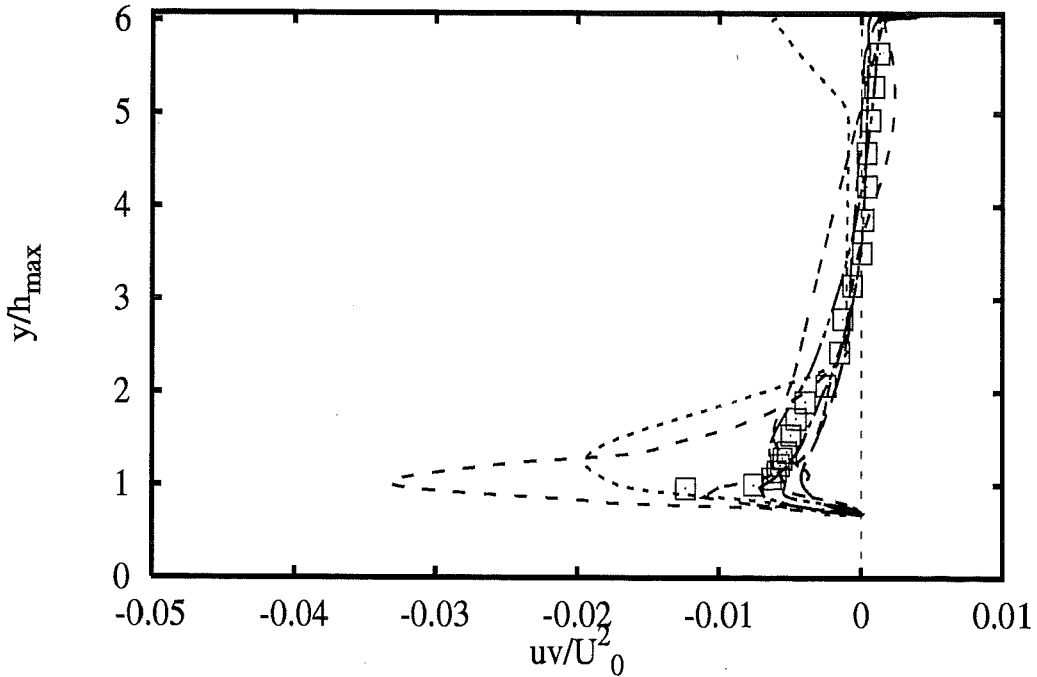
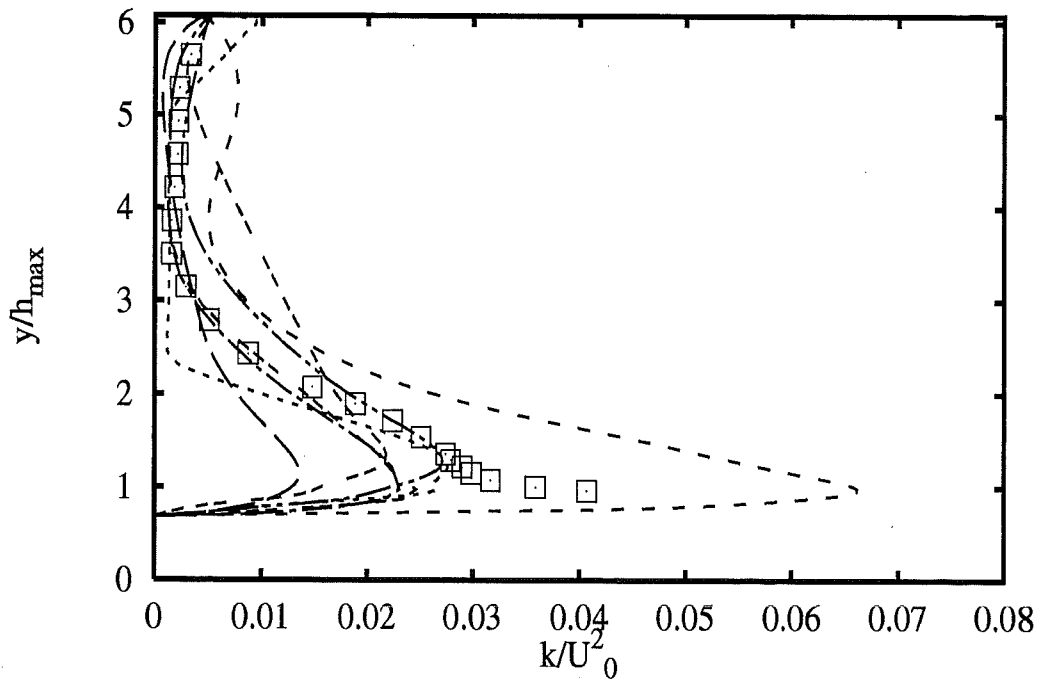


Profiles at $x/h_{max} = 0.71$

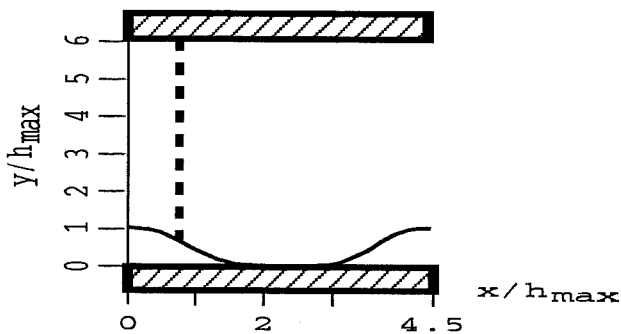


- Experiments □
- CompDyna hKE RNG+wf ---
- UPorto hKE LeRo+wf ---
- EDFLNHLA lKE LaSh ---
- IOlomouc hKE std+Gol ---
- UKarlsru hKE std+NoRe ---
- DLRGoett kOm Wil ---
- IOlomouc nKE Spez+wf ---

2B - 19

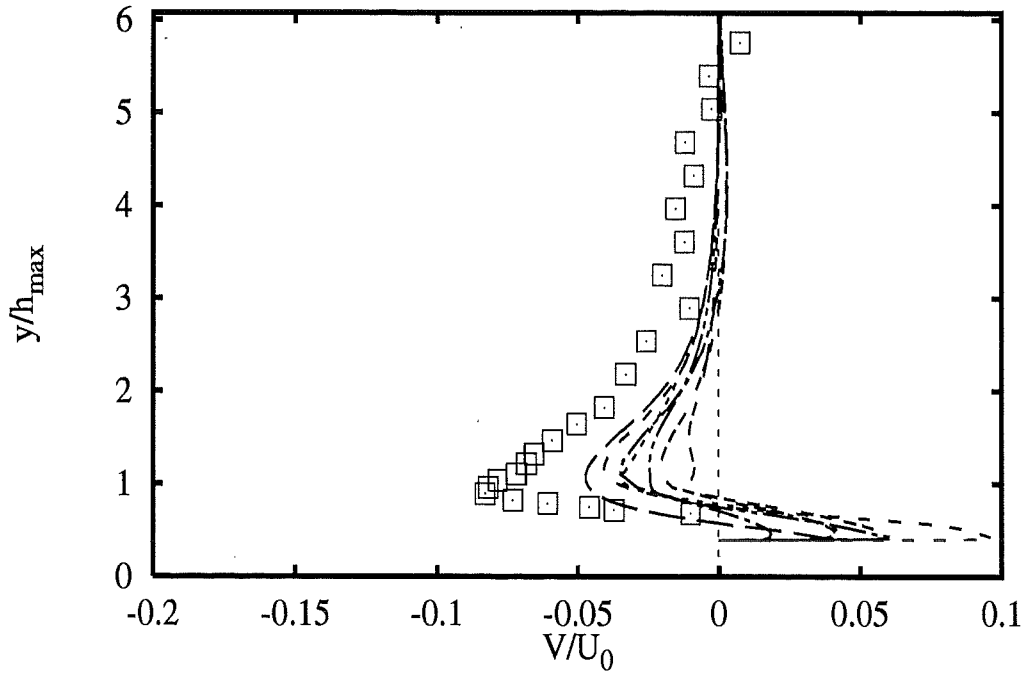
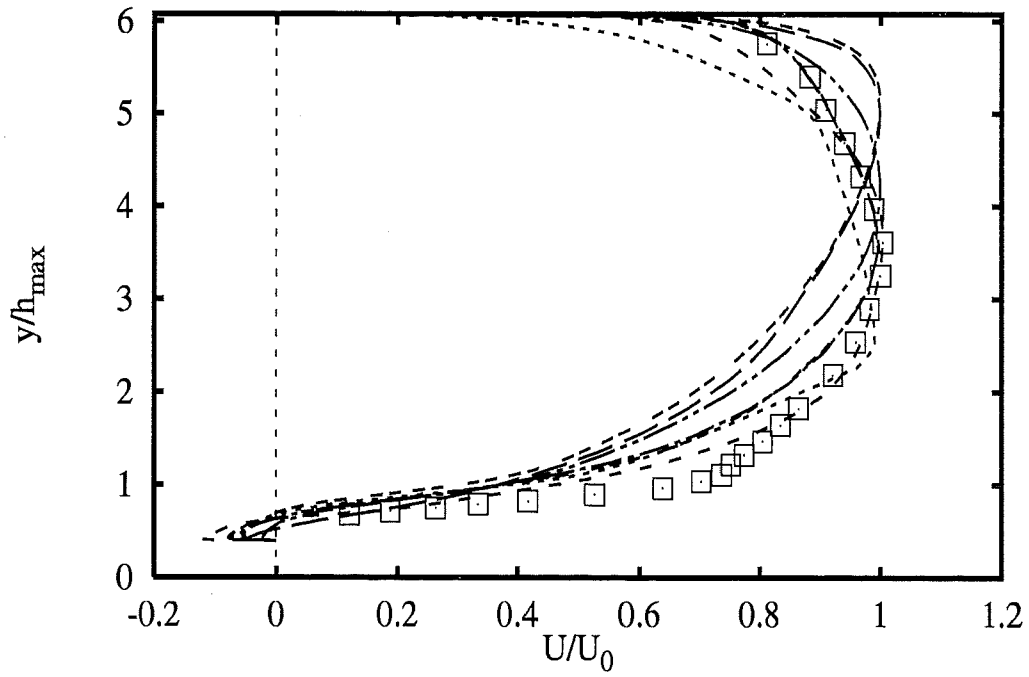


Profiles at $x/h_{max} = 0.71$

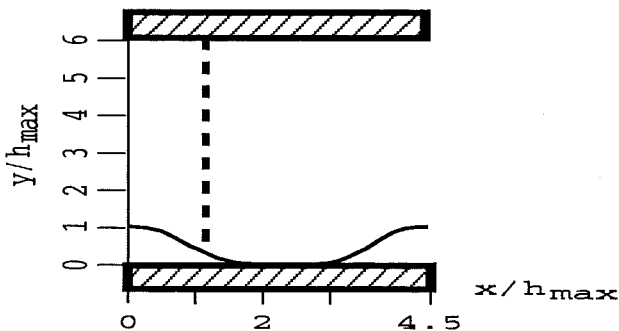


- | | |
|-----------------------|-------|
| Experiments | □ |
| CompDyna hKE RNG+wf | --- |
| UPorto hKE LeRo+wf | ---- |
| EDFLNHLA lKE LaSh | |
| IOlomouc hKE std+Gol | ---- |
| UKarlsru hKE std+NoRe | ---- |
| DLRGoett kOm Wil | ---- |
| IOlomouc nKE Spez+wf | ---- |

2B - 20

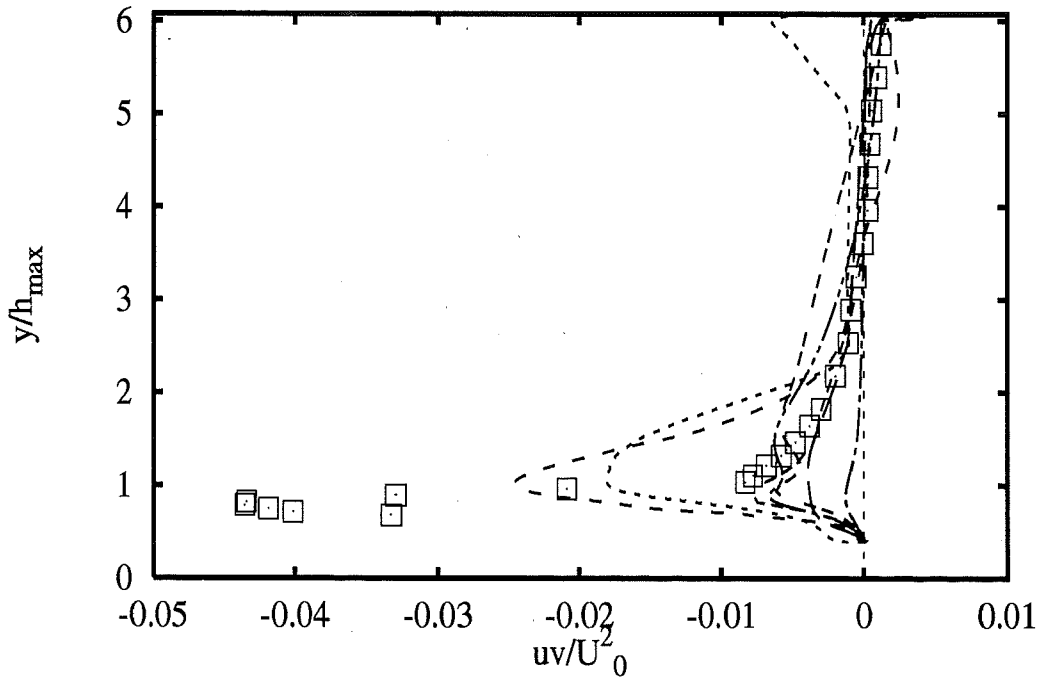
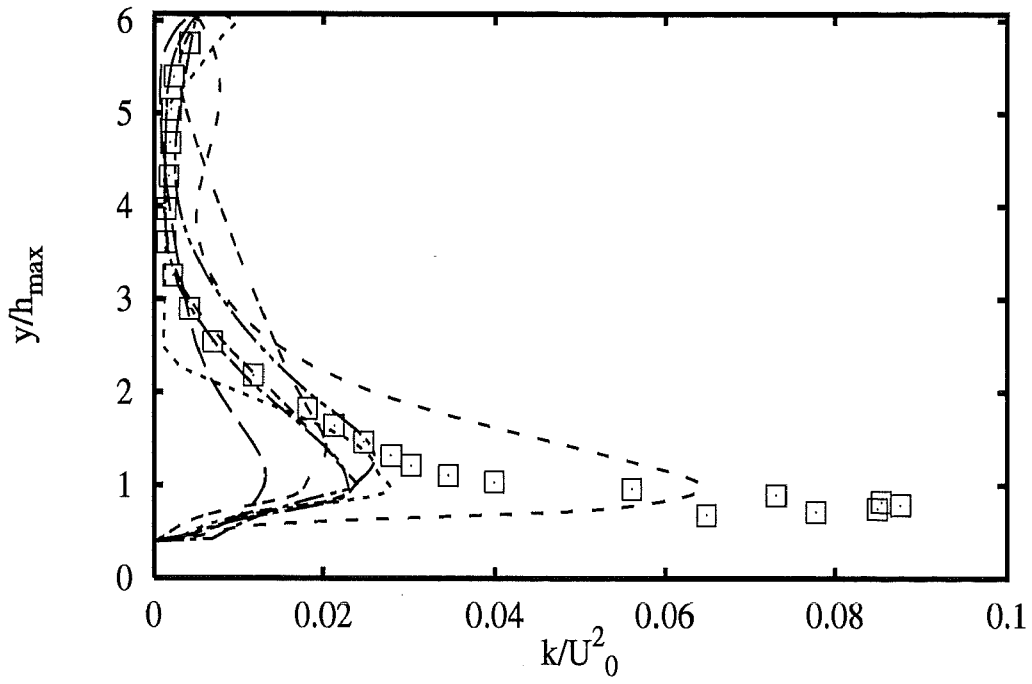


Profiles at $x/h_{max} = 1.07$

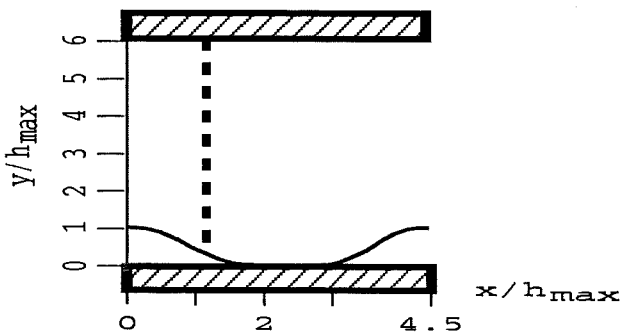


- Experiments \square
- CompDyna hKE RNG+wf $---$
- UPorto hKE LeRo+wf $---$
- EDFLNHLA lKE LaSh $---$
- IOlomouc hKE std+Gol $---$
- UKarlsru hKE std+NoRe $---$
- DLRGoett kOm Wil $---$
- IOlomouc nKE Spez+wf $---$

2B - 21

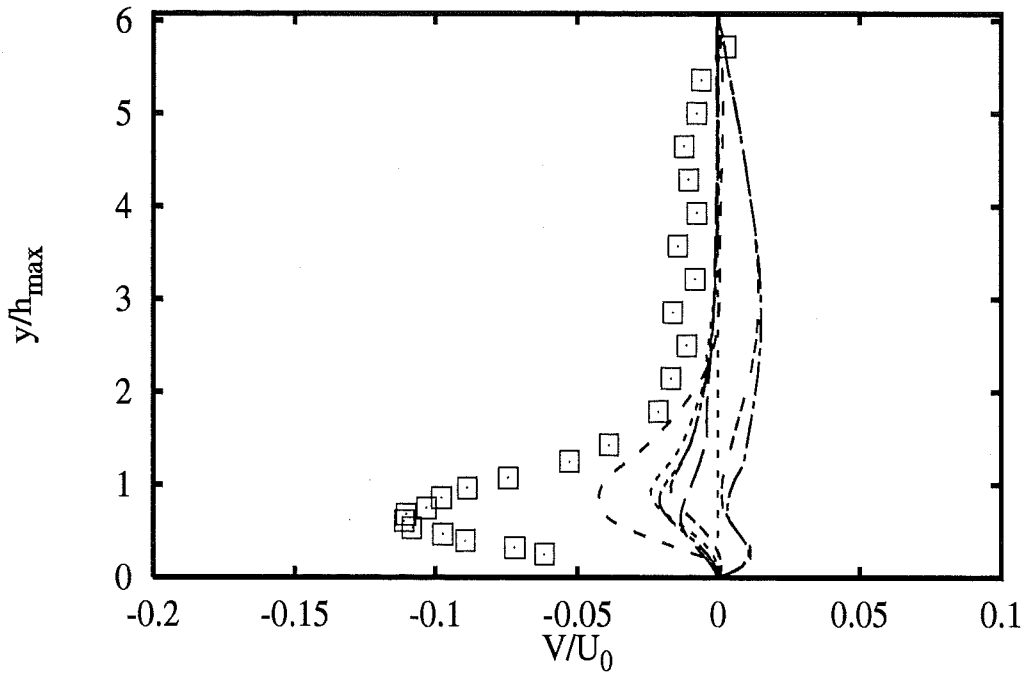
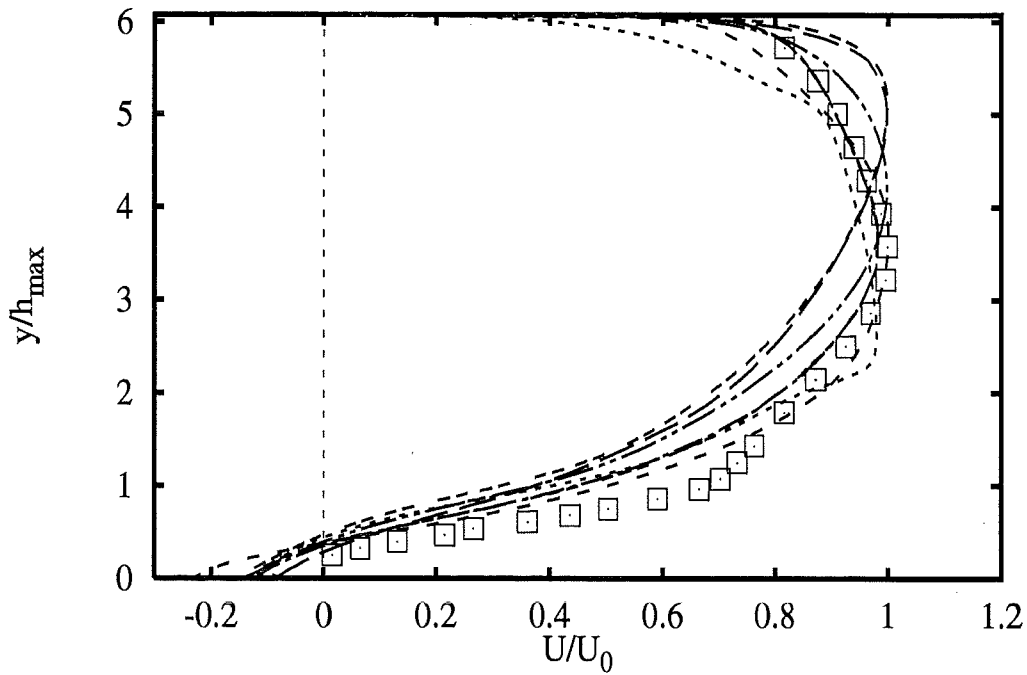


Profiles at $x/h_{max} = 1.07$

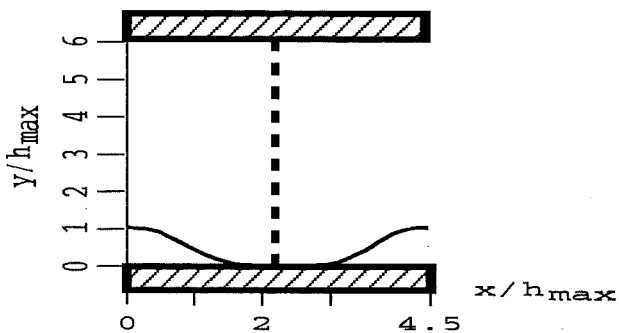


- | | |
|-----------------------|-------|
| Experiments | □ |
| CompDyna hKE RNG+wf | --- |
| UPorto hKE LeRo+wf | ---- |
| EDFLNHLA lKE LaSh | |
| IOlomouc hKE std+Gol | -.-.- |
| UKarlsru hKE std+NoRe | ---- |
| DLRGoett kOm Wil | ---- |
| IOlomouc nKE Spez+wf | ---- |

2B - 22

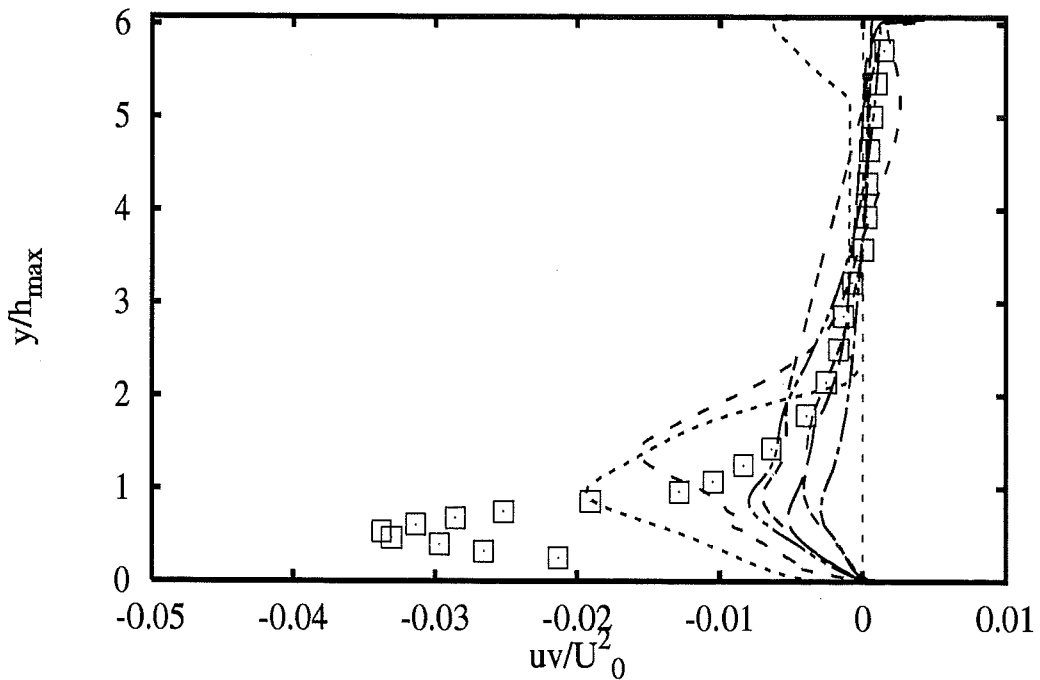
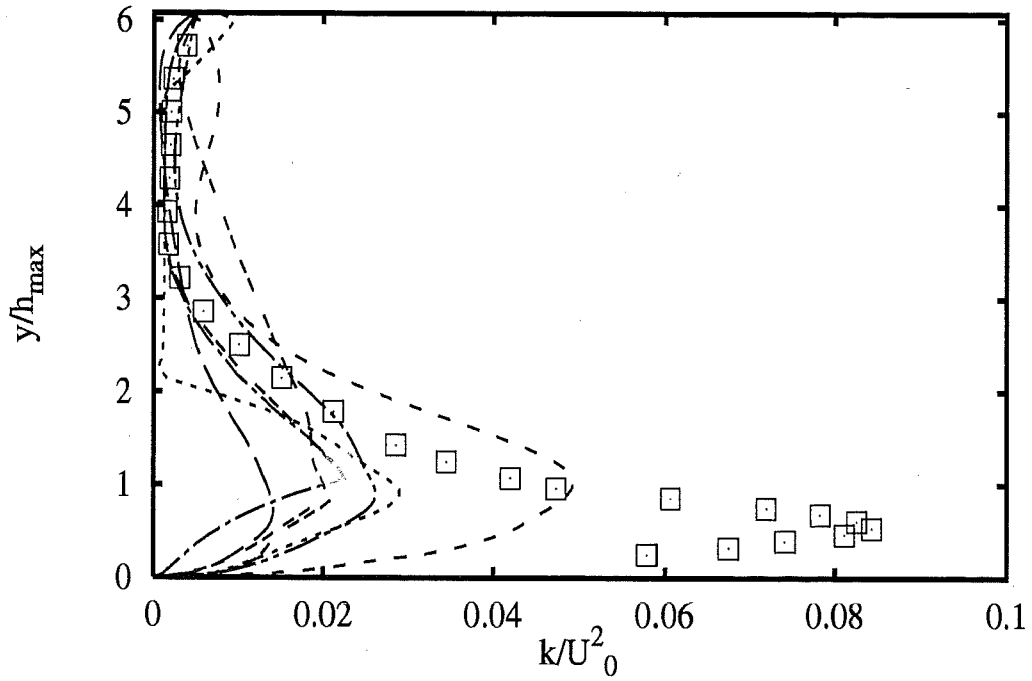


Profiles at $x/h_{max} = 2.25$

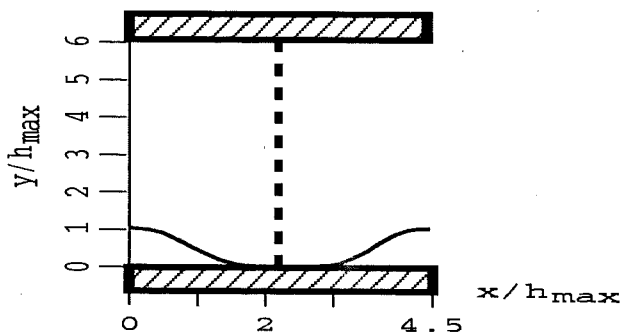


- Experiments \square
- CompDyna hKE RNG+wf $---$
- UPorto hKE LeRo+wf $---$
- EDFLNHLA lKE LaSh $---$
- IOlomouc hKE std+Gol $---$
- UKarlsru hKE std+NoRe $---$
- DLRGoett kOm Wil $---$
- IOlomouc nKE Spez+wf $---$

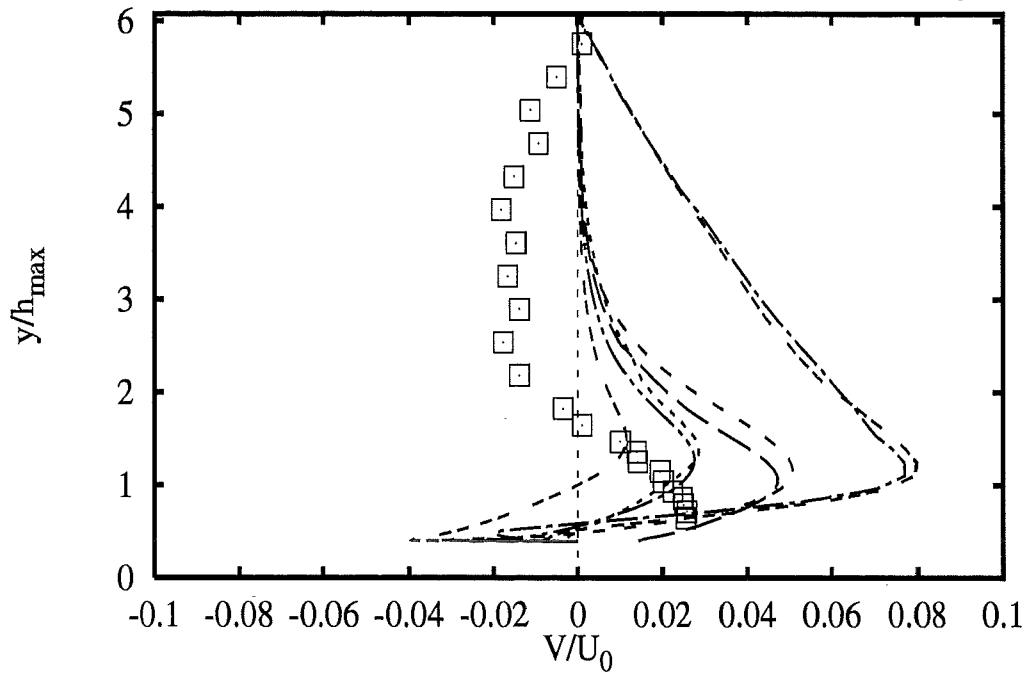
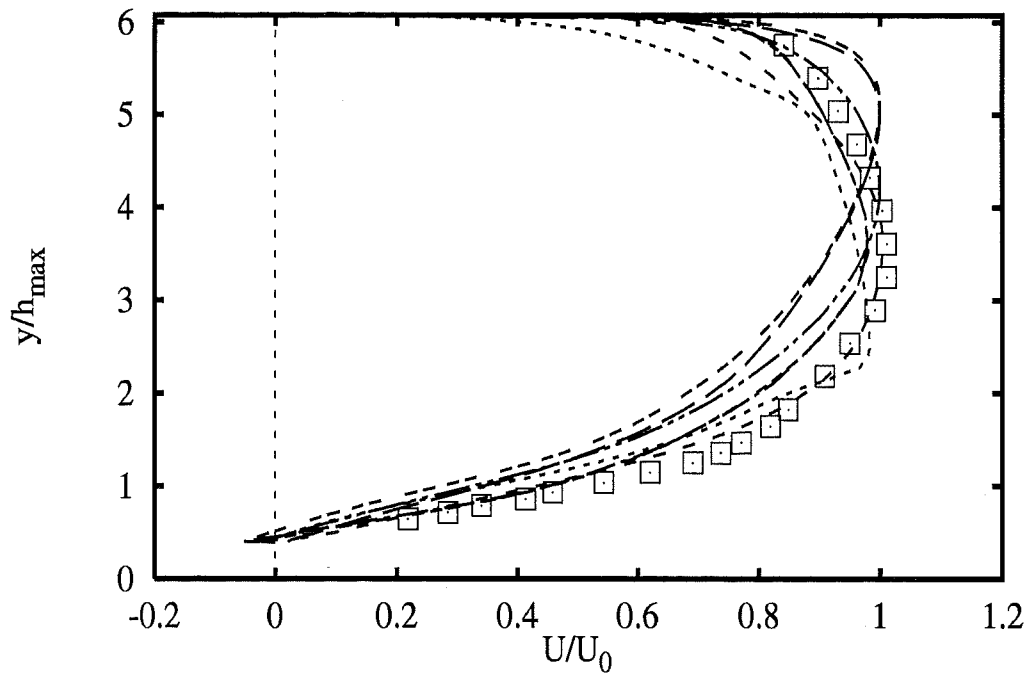
2B - 23



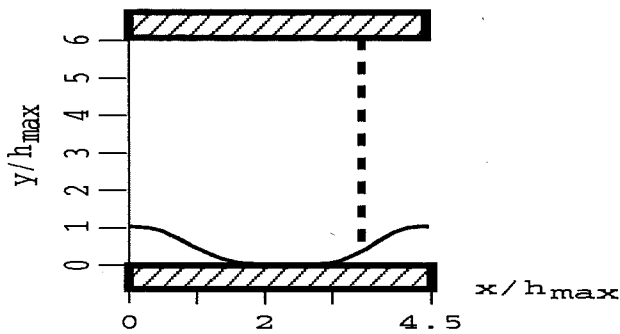
Profiles at $x/h_{max} = 2.25$



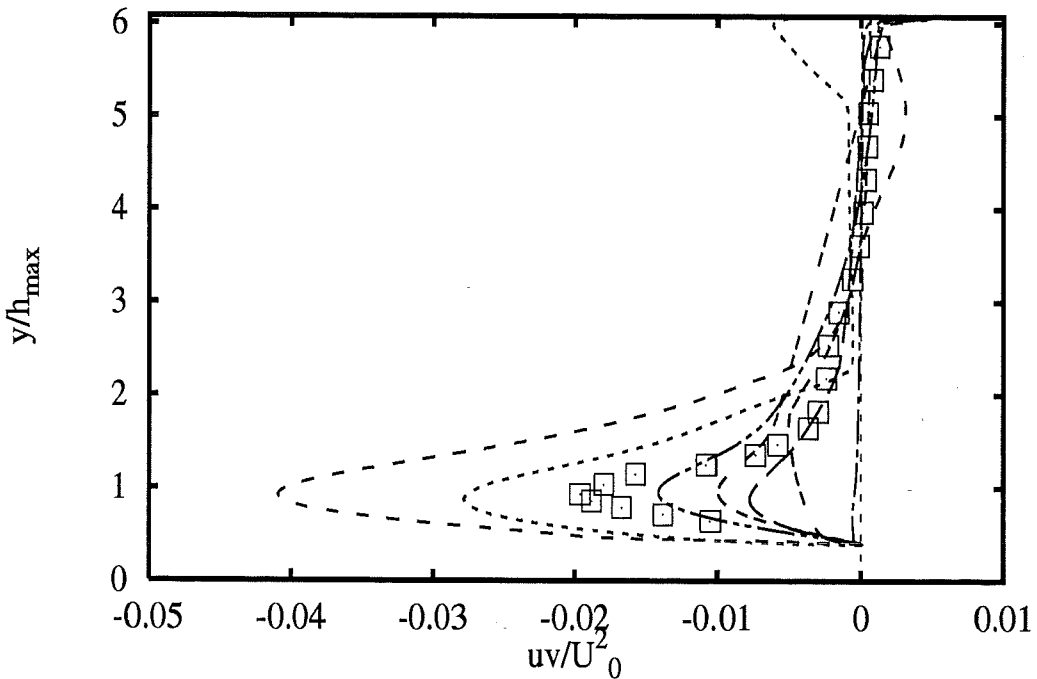
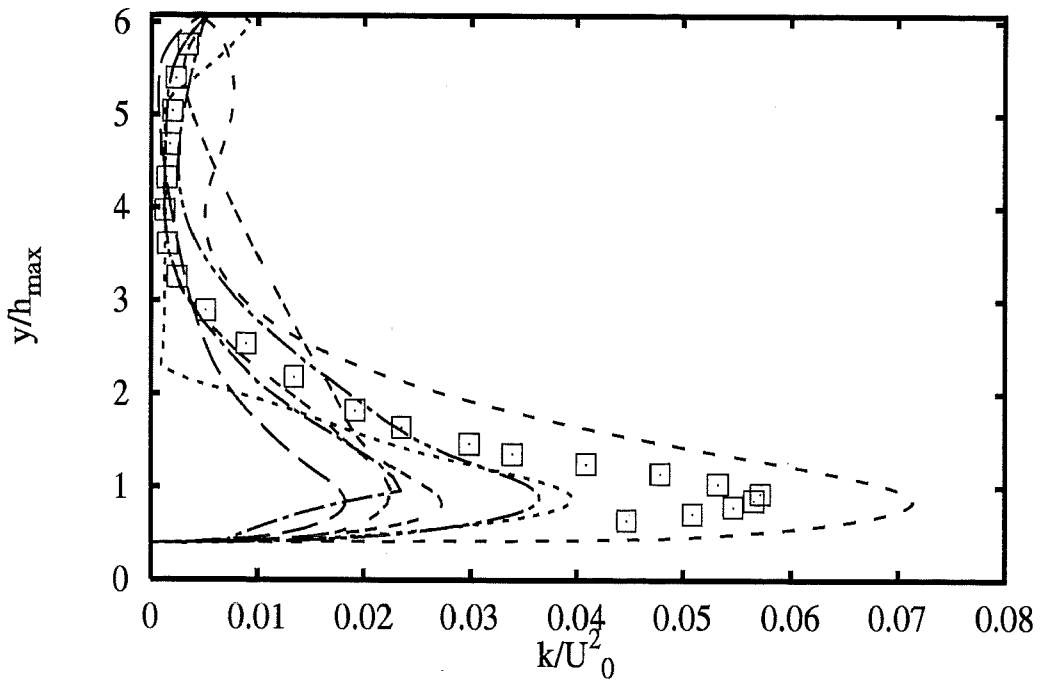
- | | |
|-----------------------|-------|
| Experiments | □ |
| CompDyna hKE RNG+wf | --- |
| UPorto hKE LeRo+wf | --- |
| EDFLNHLA lKE LaSh | |
| IOlomouc hKE std+Gol | --- |
| UKarlsru hKE std+NoRe | --- |
| DLRGoett kOm Wil | --- |
| IOlomouc nKE Spez+wf | --- |



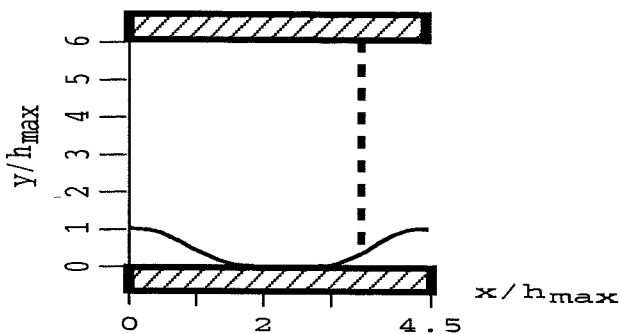
Profiles at $x/h_{max} = 3.43$



- Experiments \square
- CompDyna hKE RNG+wf $---$
- UPorto hKE LeRo+wf $---$
- EDFLNHLA lKE LaSh $---$
- IOlomouc hKE std+Gol $---$
- UKarlsru hKE std+NoRe $---$
- DLRGoett kOm Wil $---$
- IOlomouc nKE Spez+wf $---$

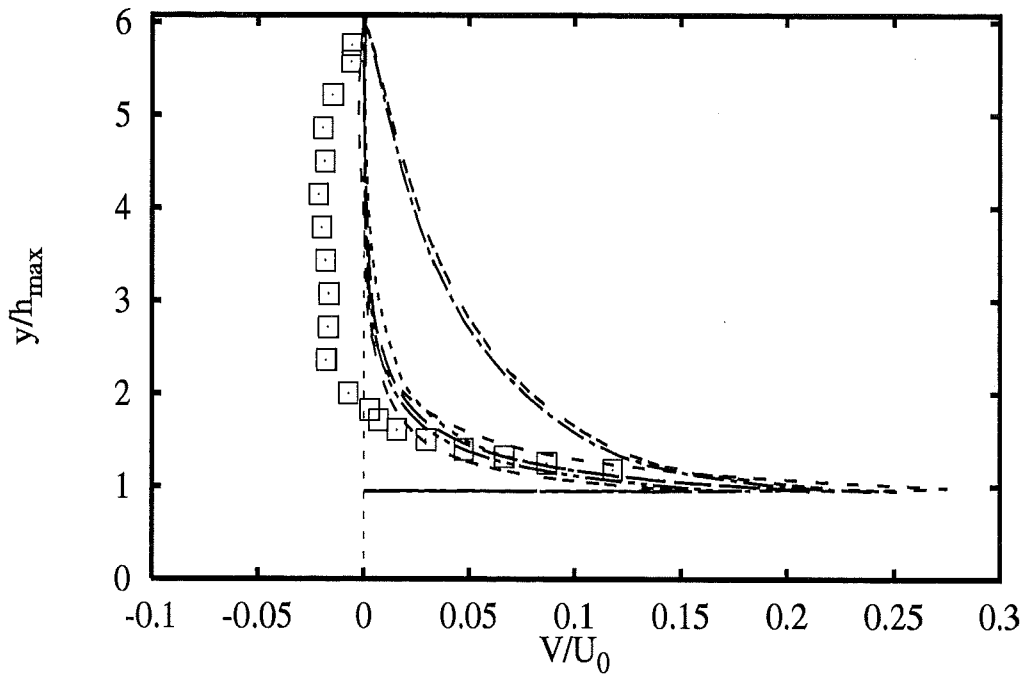
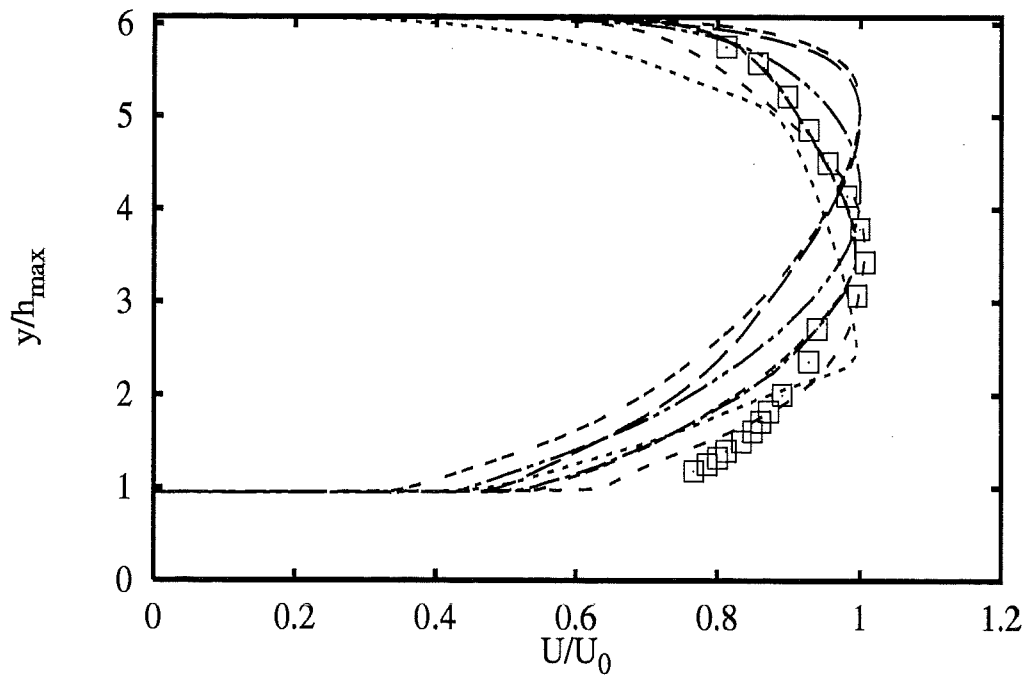


Profiles at $x/h_{max} = 3.43$

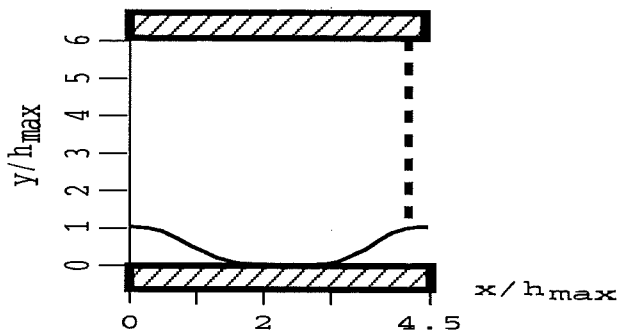


- Experiments** □
- CompDyna** *hKE* RNG+wf ---
- UPorto** *hKE* LeRo+wf - - -
- EDFLNHLA** *lKE* LaSh ·····
- IOlomouc** *hKE* std+Gol - · - · -
- UKarlsru** *hKE* std+NoRe - · - · -
- DLRGoett** *kOm* Wil - - -
- IOlomouc** *nKE* Spez+wf - - -

2B - 26

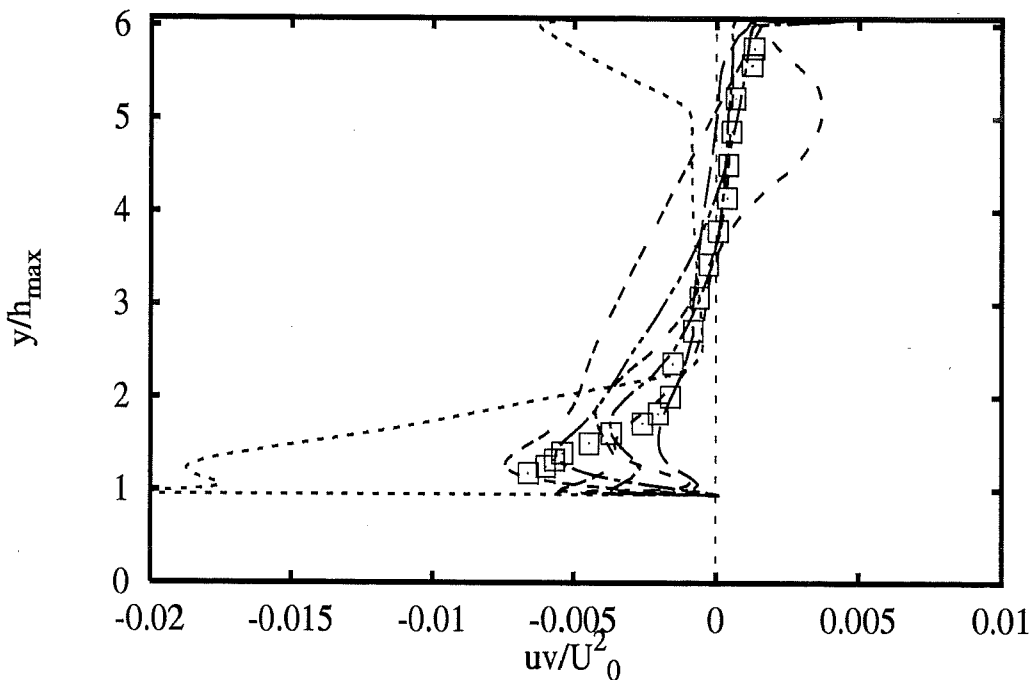
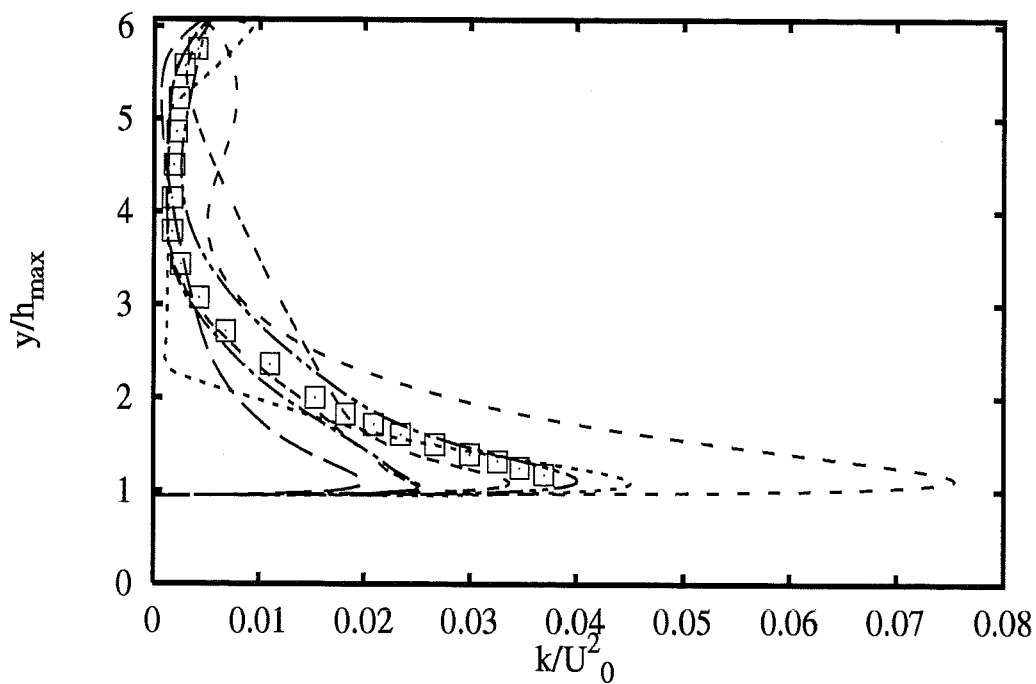


Profiles at $x/h_{max} = 4.14$

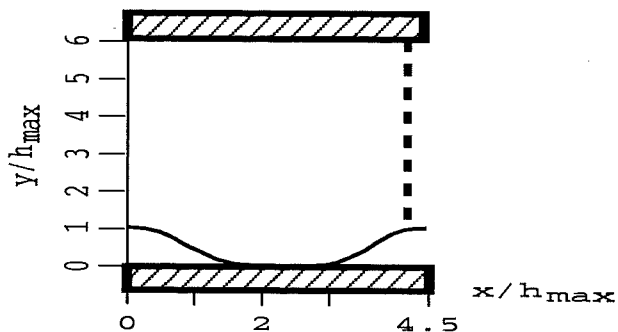


- Experiments \square
- CompDyna hKE RNG+wf ---
- UPorto hKE LeRo+wf - - -
- EDFLNHLa lKE LaSh (dotted)
- IOlomouc hKE std+Gol - - - -
- UKarlsru hKE std+NoRe - - - -
- DLRGoett kOm Wil - - - -
- IOlomouc nKE Spez+wf - - - -

2B - 27



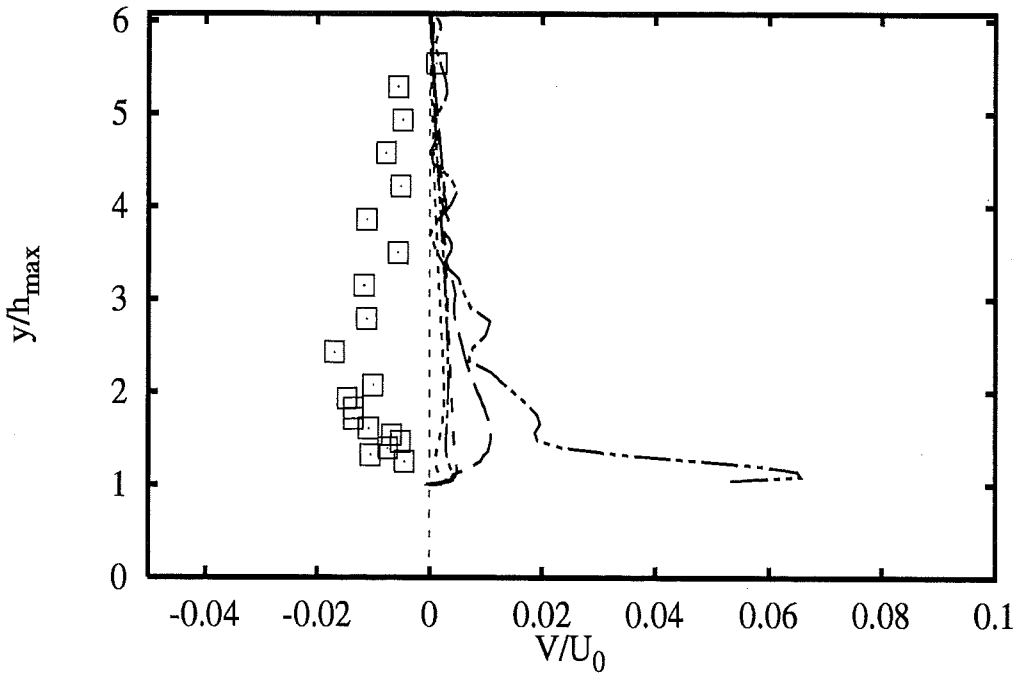
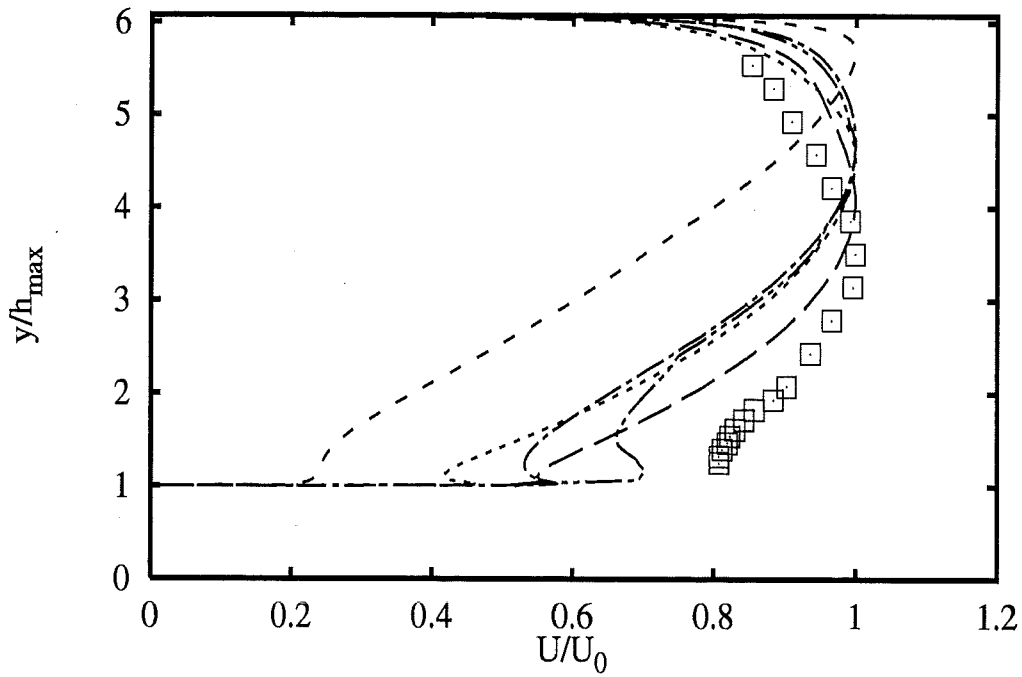
Profiles at $x/h_{max} = 4.14$



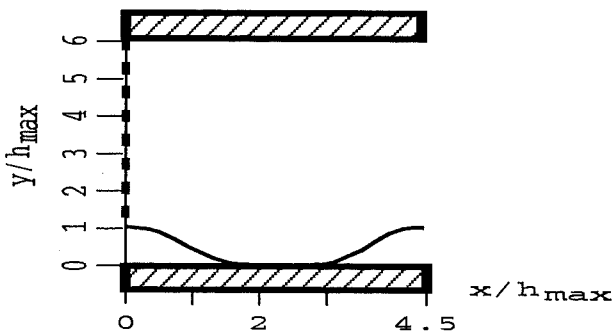
- Experiments \square
- CompDyna hKE RNG+wf ---
- UPorto hKE LeRo+wf - - -
- EDFLNHLA lKE LaSh (dotted)
- IOlomouc hKE std+Gol --- (dash-dot)
- UKarlsru hKE std+NoRe - - - (long-dash)
- DLRGoett kOm Wil - - - (short-dash)
- IOlomouc nKE Spez+wf - - - (dash-dot-dot)



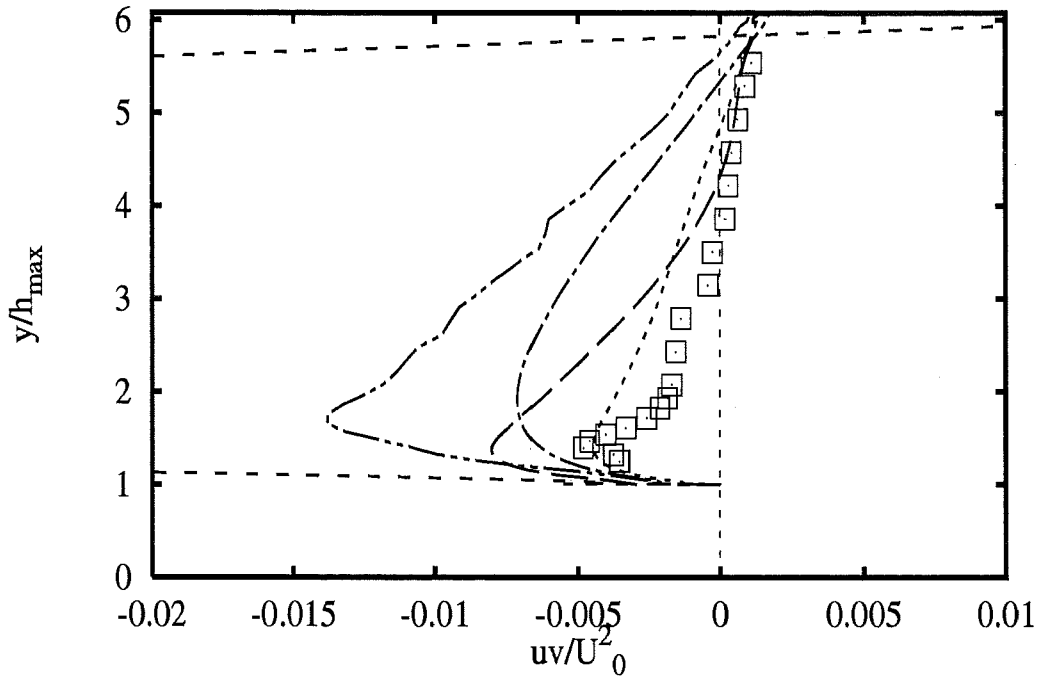
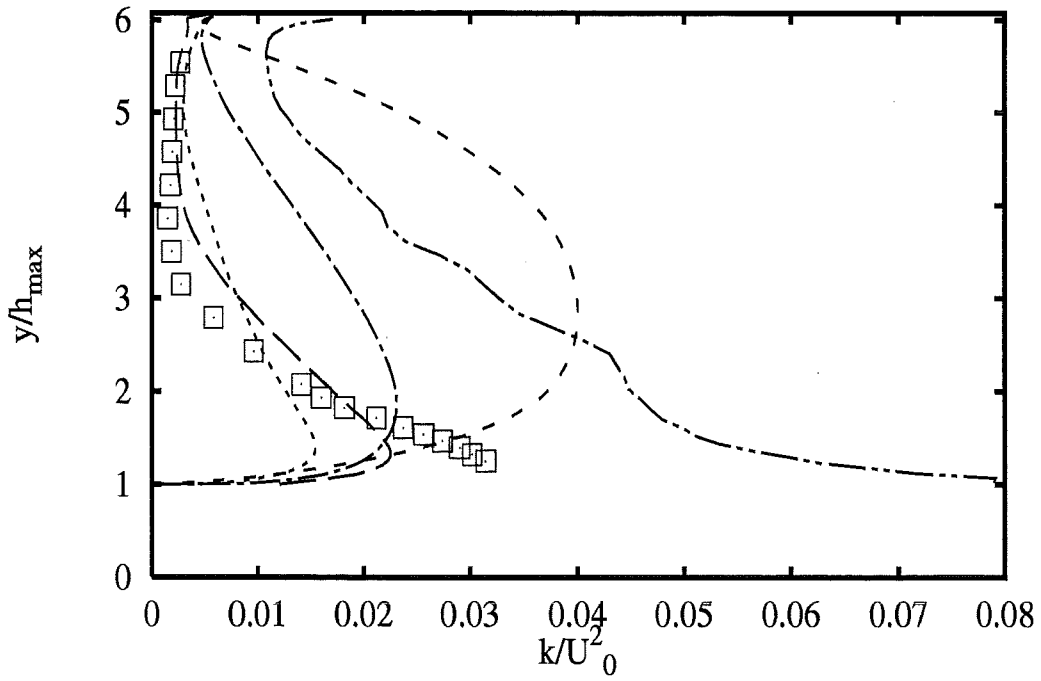




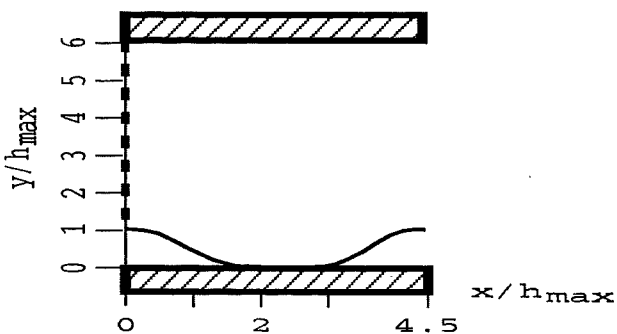
Profiles at $x/h_{max} = 0$



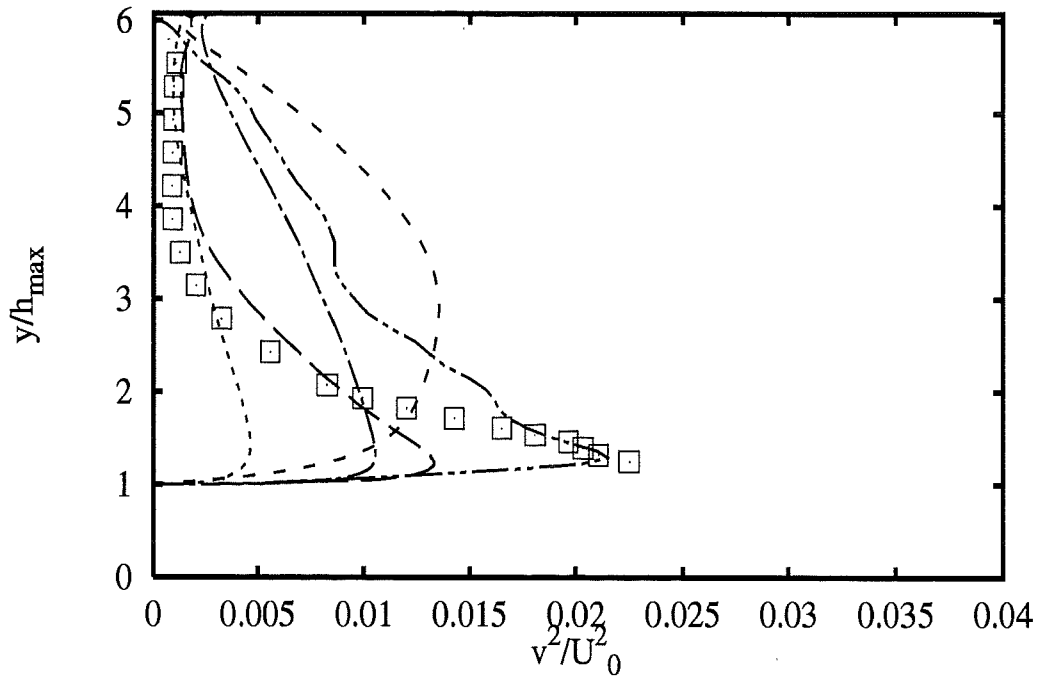
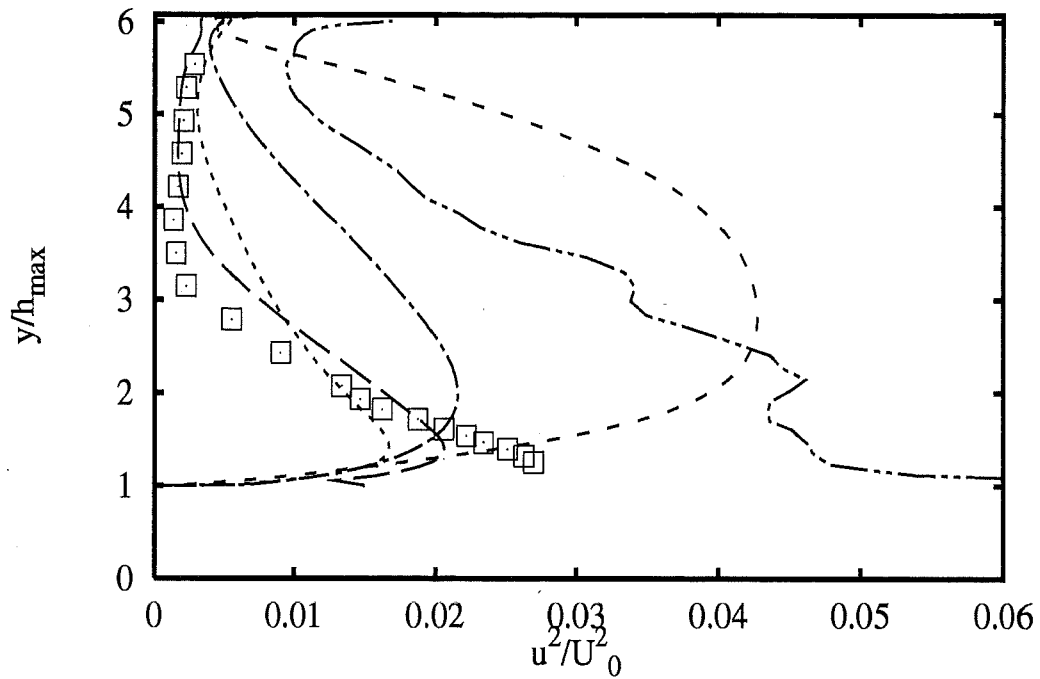
- Experiments \square
- EDFLNHLa RSM LRR+wf $---$
- UdelftHa RSM LRR+wf $----$
- UMISTCra RSM CrLa+2eq $\cdots\cdots$
- UMISTCra RSM Cub+2eq $- \cdot - \cdot -$
- DLROberp LES $-\cdot-\cdot-$



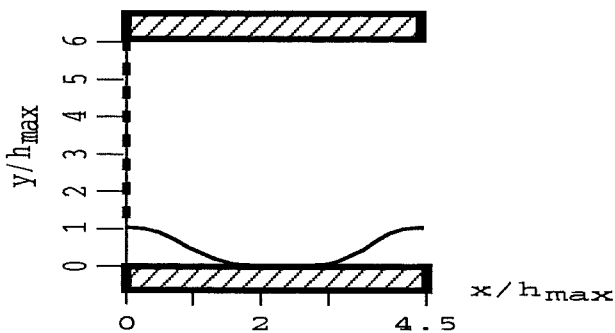
Profiles at $x/h_{max} = 0$



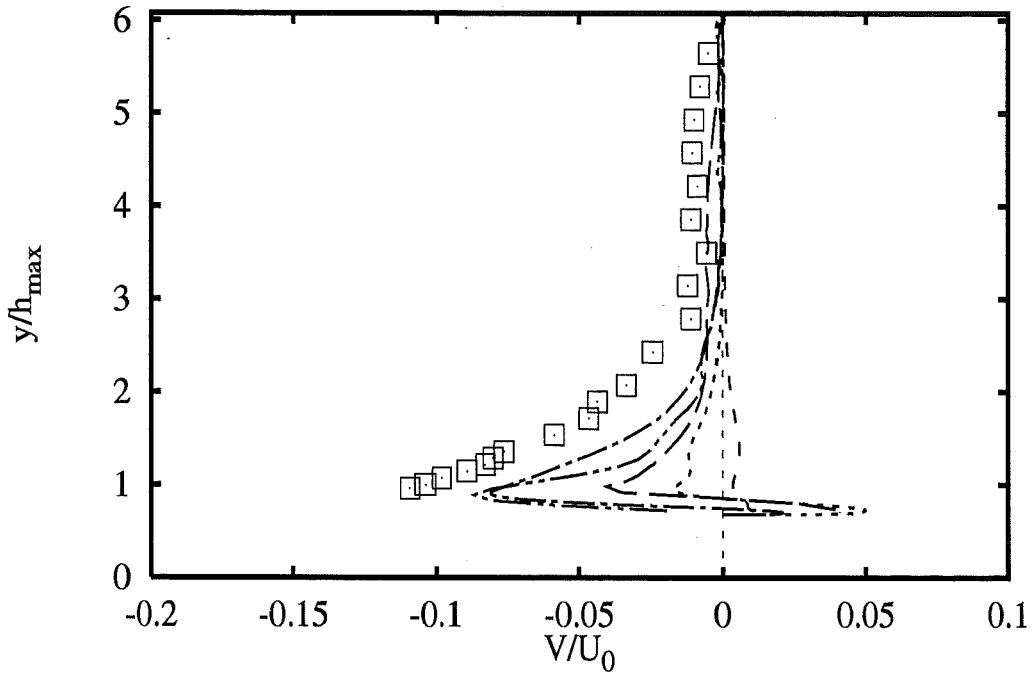
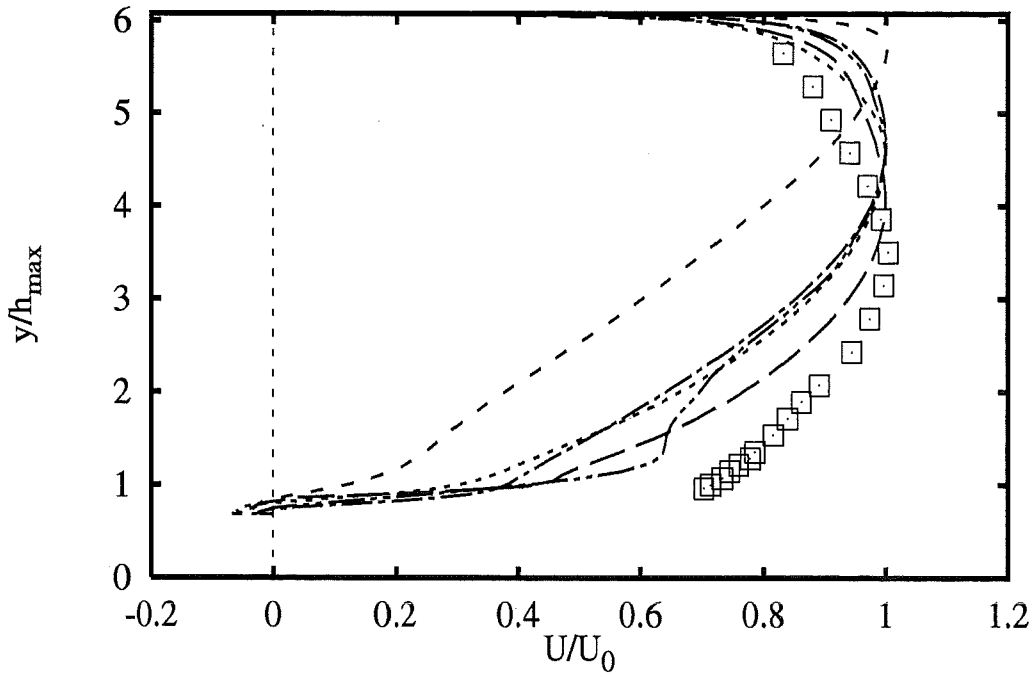
- | | |
|--------------------|-----------------------------|
| Experiments | \square |
| EDFLNHLa | RSM LRR+wf --- |
| UdelftHa | RSM LRR+wf - - - |
| UMISTCra | RSM CrLa+2eq (dotted) |
| UMISTCra | RSM Cub+2eq - · - · - |
| DLROberp | LES - · - · - |



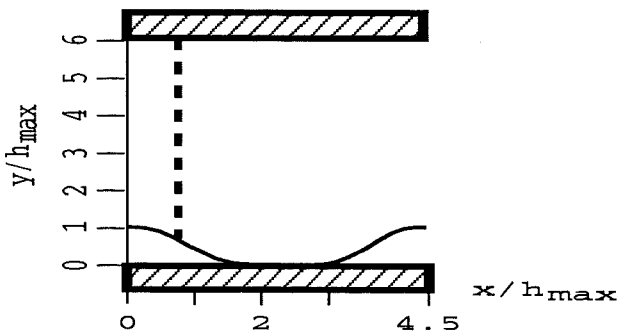
Profiles at $x/h_{max} = 0$



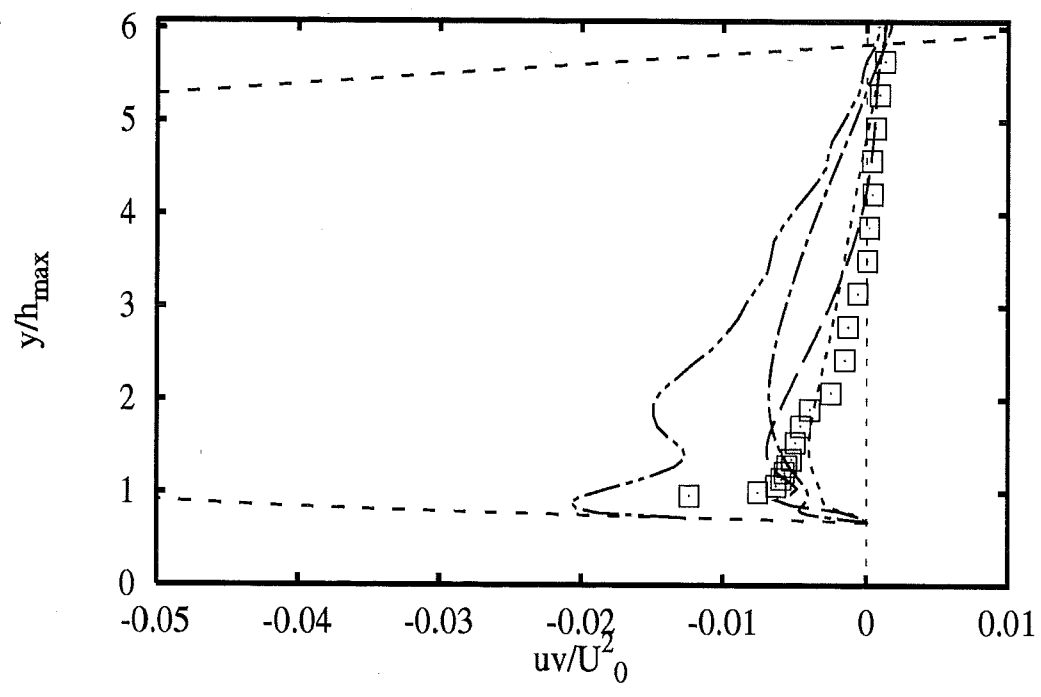
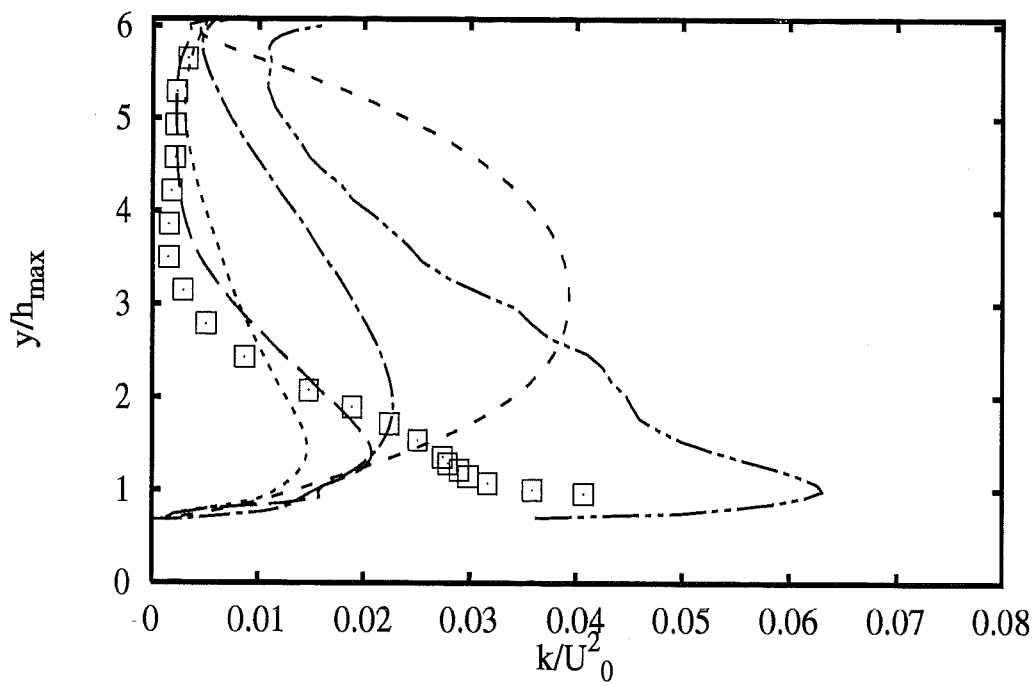
- | | |
|------------------------------|-----------|
| Experiments | □ |
| EDFLNHLa RSM LRR+wf | — — — |
| UdelftHa RSM LRR+wf | - - - - - |
| UMISTCra RSM CrLa+2eq | · · · · · |
| UMISTCra RSM Cub+2eq | — · — · — |
| DLROberp LES | — · — · — |



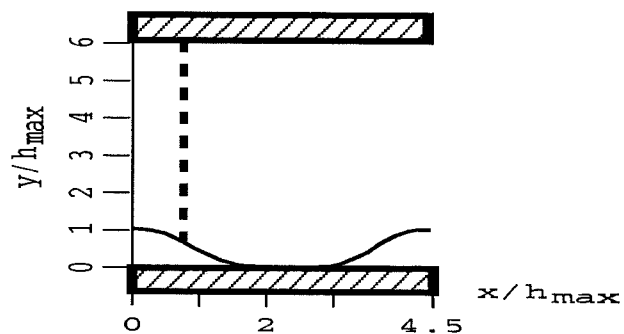
Profiles at $x/h_{max} = 0.71$



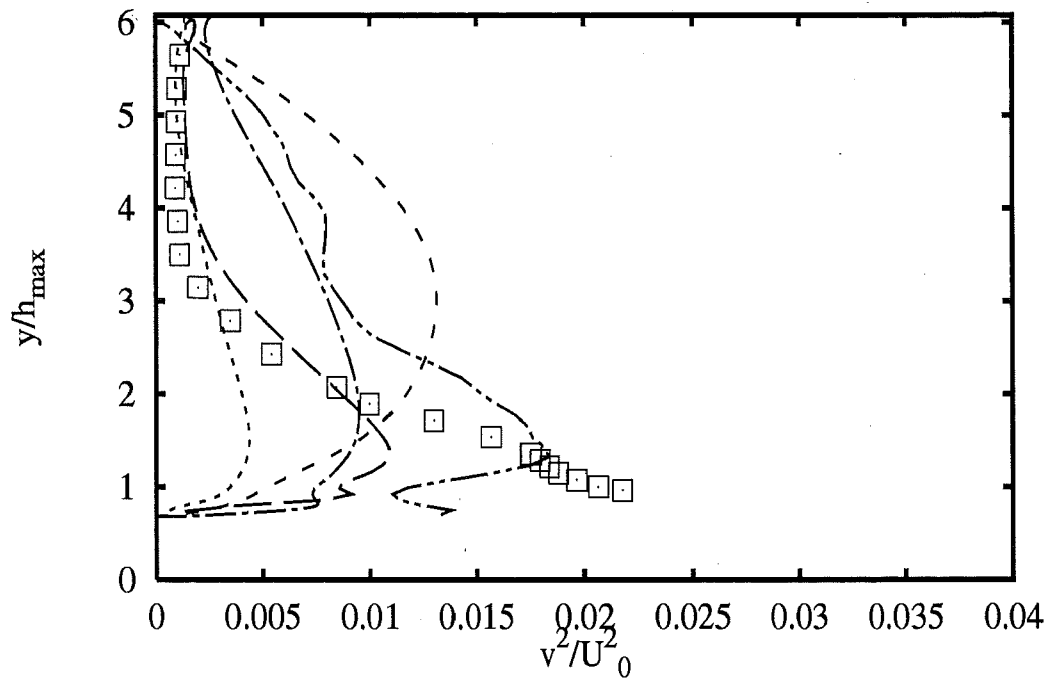
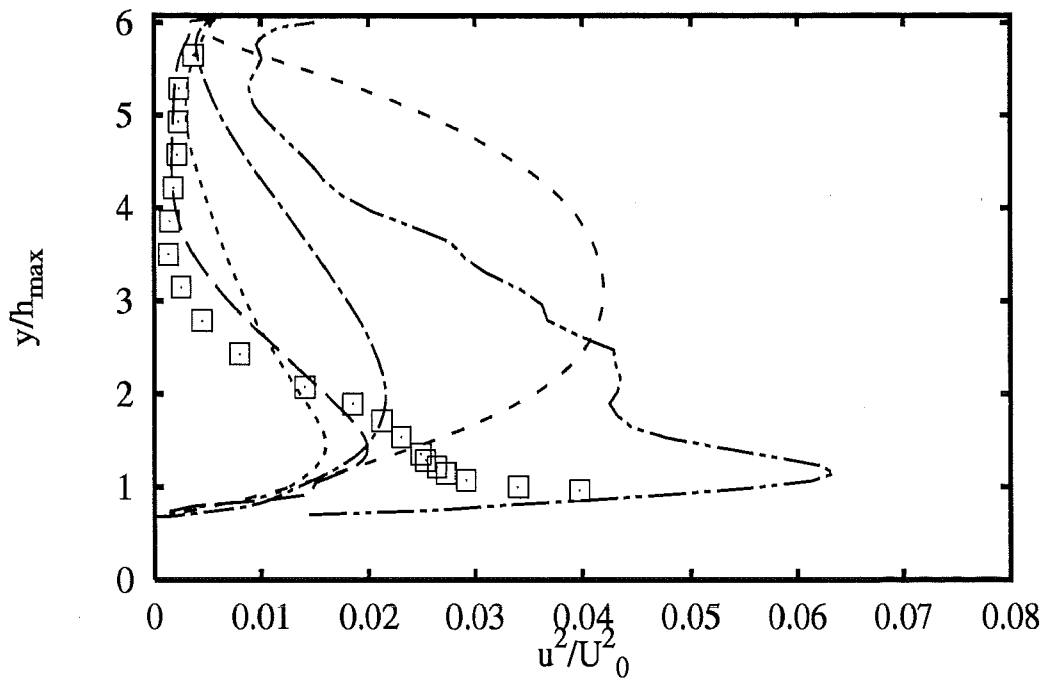
- Experiments \square
- EDFLNHLa RSM LRR+wf $---$
- UdelftHa RSM LRR+wf $----$
- UMISTCra RSM CrLa+2eq $\cdots\cdots$
- UMISTCra RSM Cub+2eq $-.-.-$
- DLROberp LES $-\cdot-\cdot-$



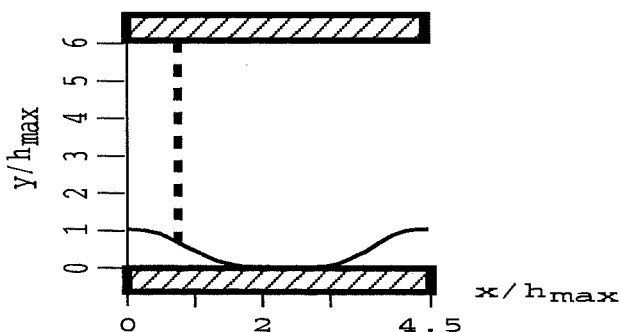
Profiles at $x/h_{max} = 0.71$



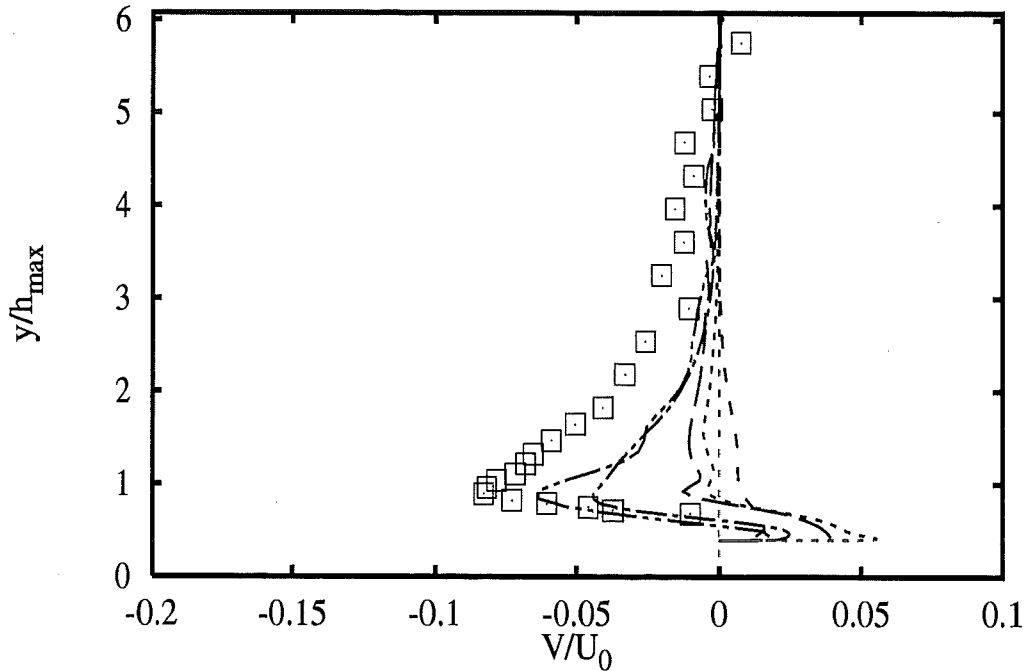
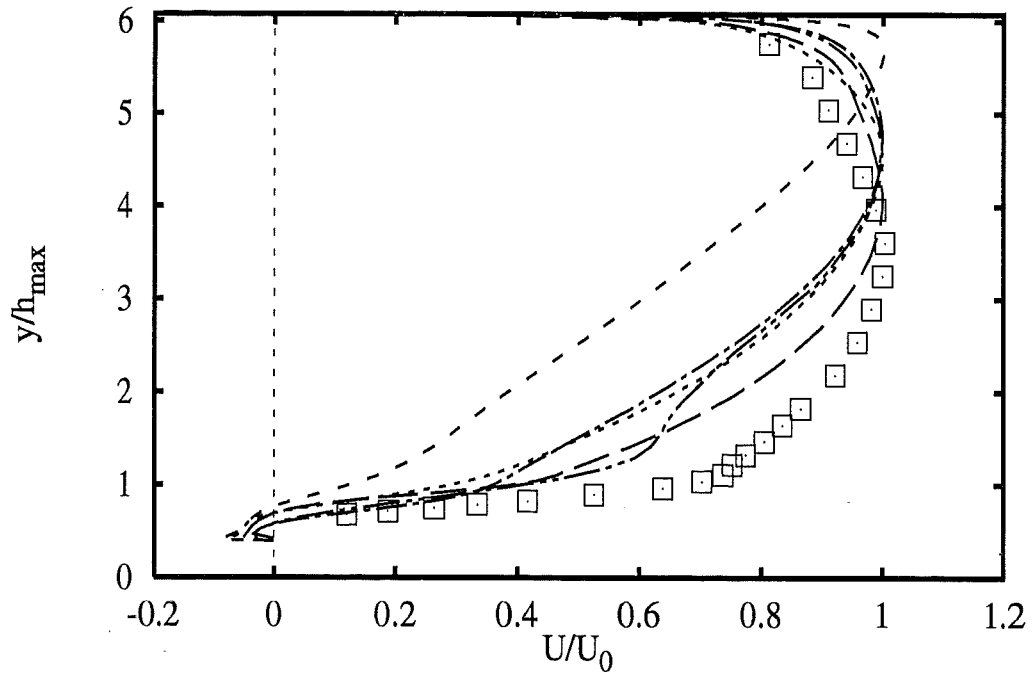
- Experiments \square
- EDFLNHLa RSM LRR+wf $---$
- UdelftHa RSM LRR+wf $----$
- UMISTCra RSM CrLa+2eq $\cdots\cdots$
- UMISTCra RSM Cub+2eq $-\cdot-\cdot-$
- DLROberp LES $-\cdot-\cdot-$



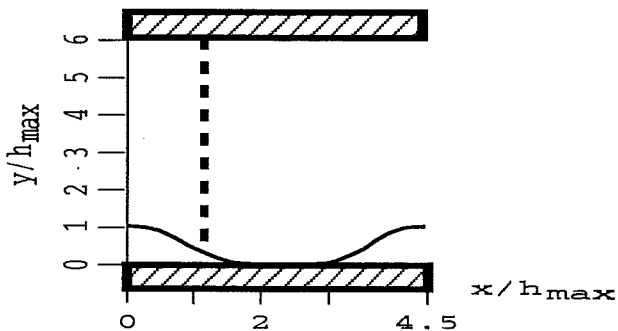
Profiles at $x/h_{max} = 0.71$



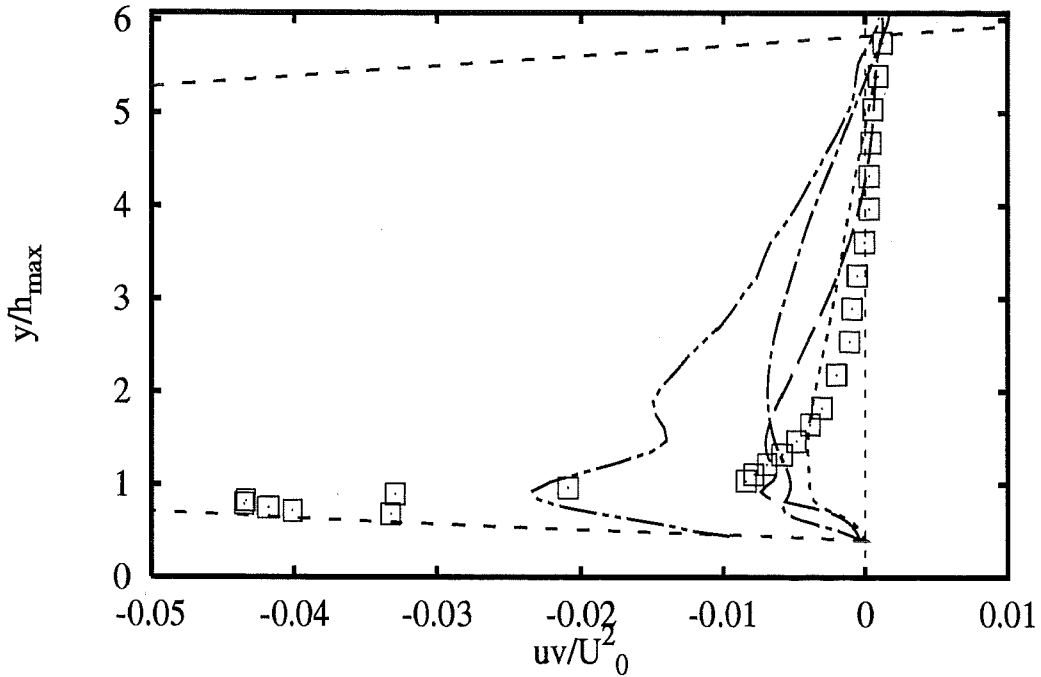
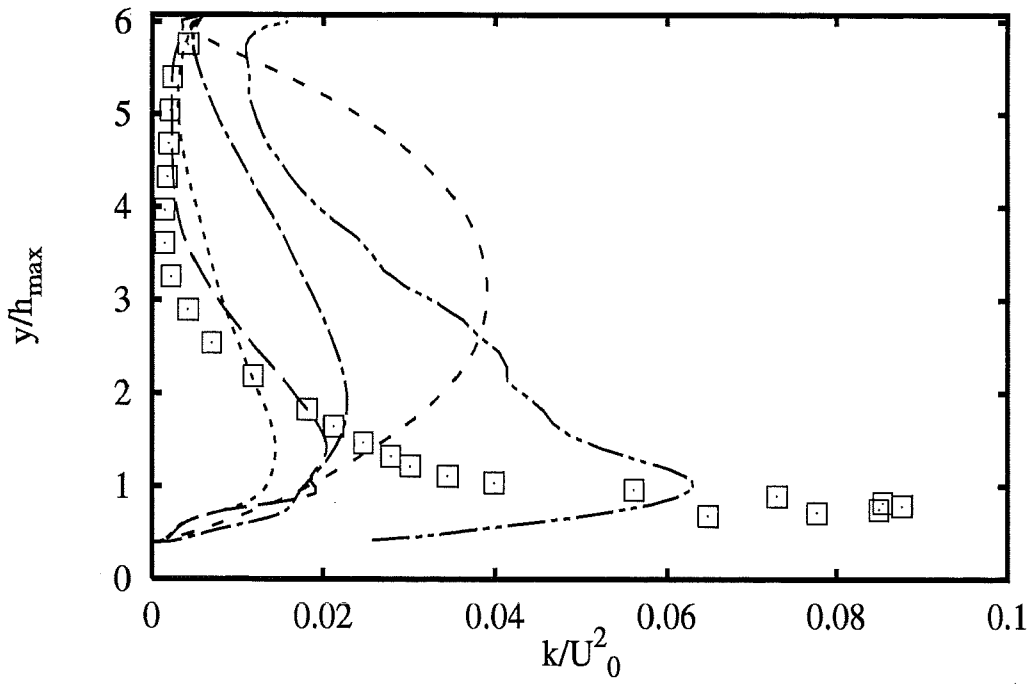
- Experiments \square
- EDFLNHLa RSM LRR+wf $---$
- UDelftHa RSM LRR+wf $---$
- UMISTCra RSM CrLa+2eq $\cdots\cdots\cdots$
- UMISTCra RSM Cub+2eq $---$
- DLRoberp LES $---$



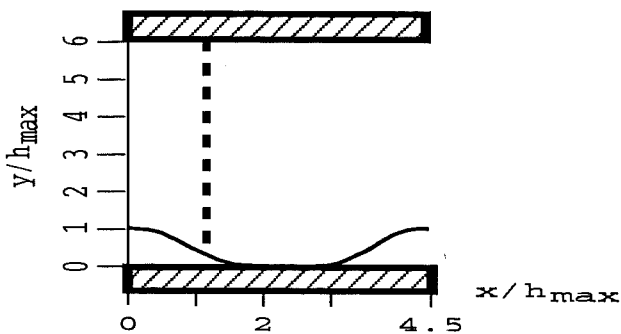
Profiles at $x/h_{max} = 1.07$



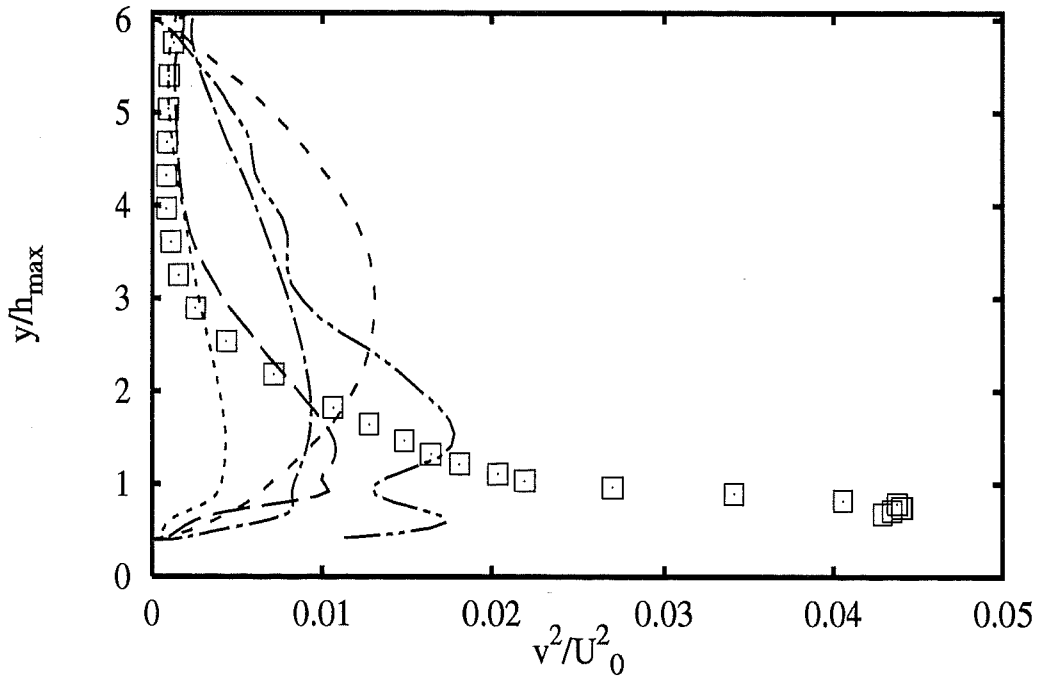
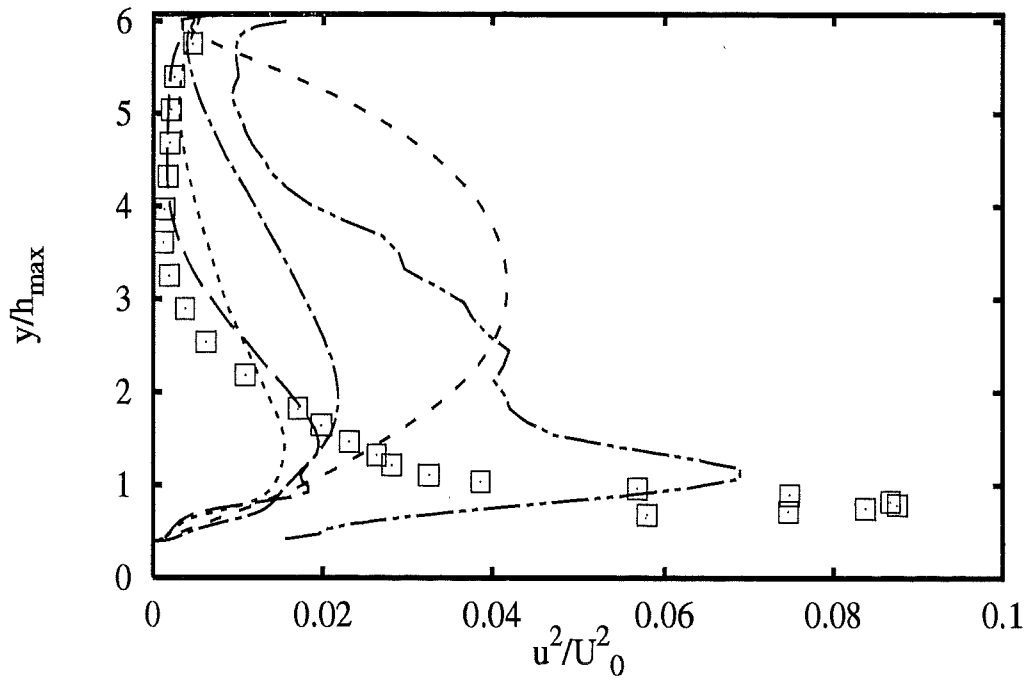
- Experiments \square
- EDFLNHLa RSM LRR+wf ---
- UDeftHa RSM LRR+wf - - -
- UMISTCra RSM CrLa+2eq
- UMISTCra RSM Cub+2eq ---
- DLROberp LES - . - .



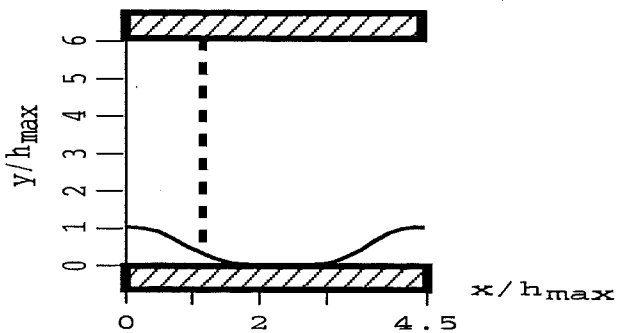
Profiles at $x/h_{max} = 1.07$



- | | |
|--------------------|-----------------------------|
| Experiments | \square |
| EDFLNHLa | RSM LRR+wf --- |
| UdelftHa | RSM LRR+wf - - - |
| UMISTCra | RSM CrLa+2eq (dotted) |
| UMISTCra | RSM Cub+2eq - · - · - |
| DLROberp | LES - · - · - |

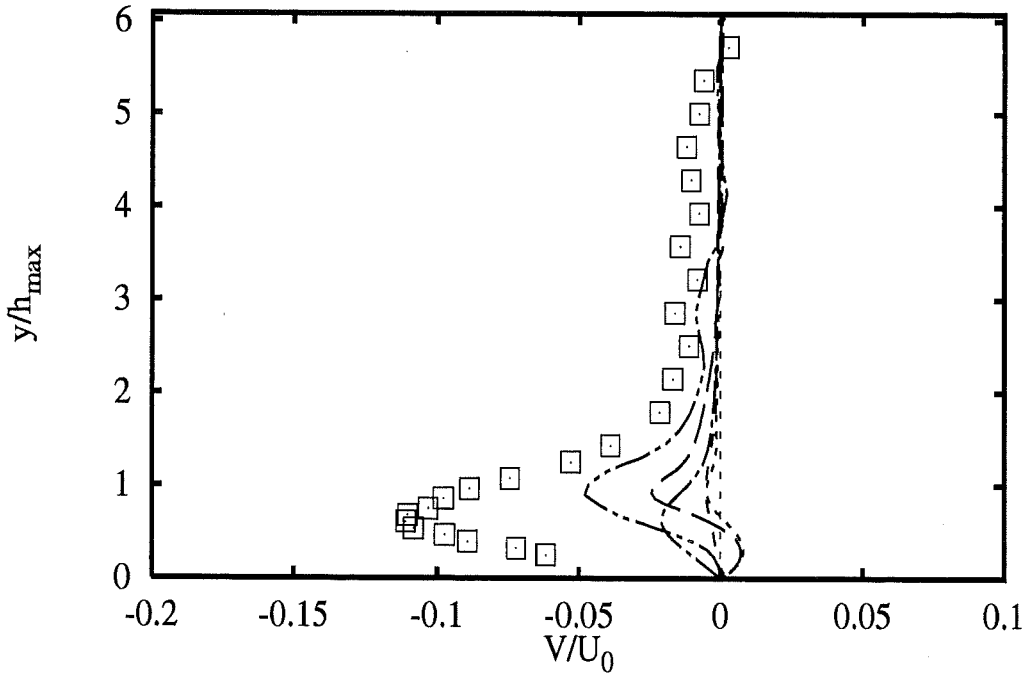
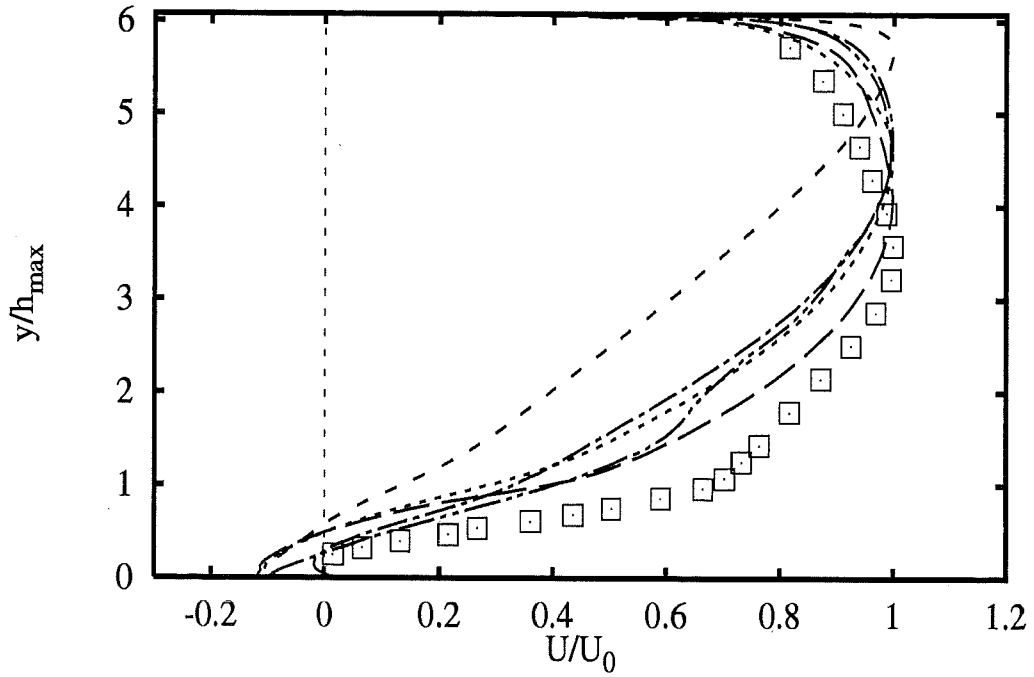


Profiles at $x/h_{max} = 1.07$

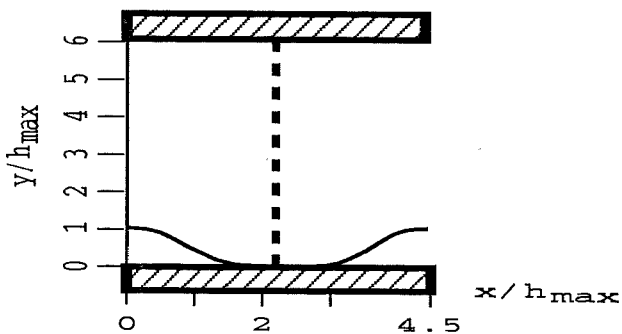


- Experiments \square
- EDFLNHLA RSM LRR+wf $---$
- UDeftHa RSM LRR+wf $---$
- UMISTCra RSM CrLa+2eq $\cdots\cdots\cdots$
- UMISTCra RSM Cub+2eq $---$
- DLROberp LES $---$

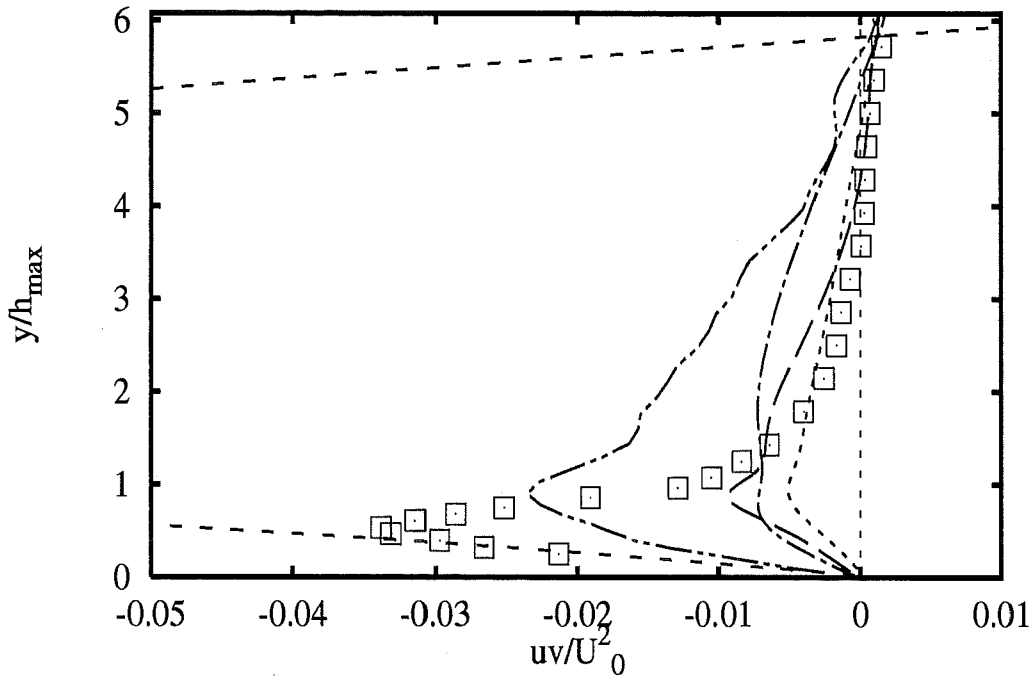
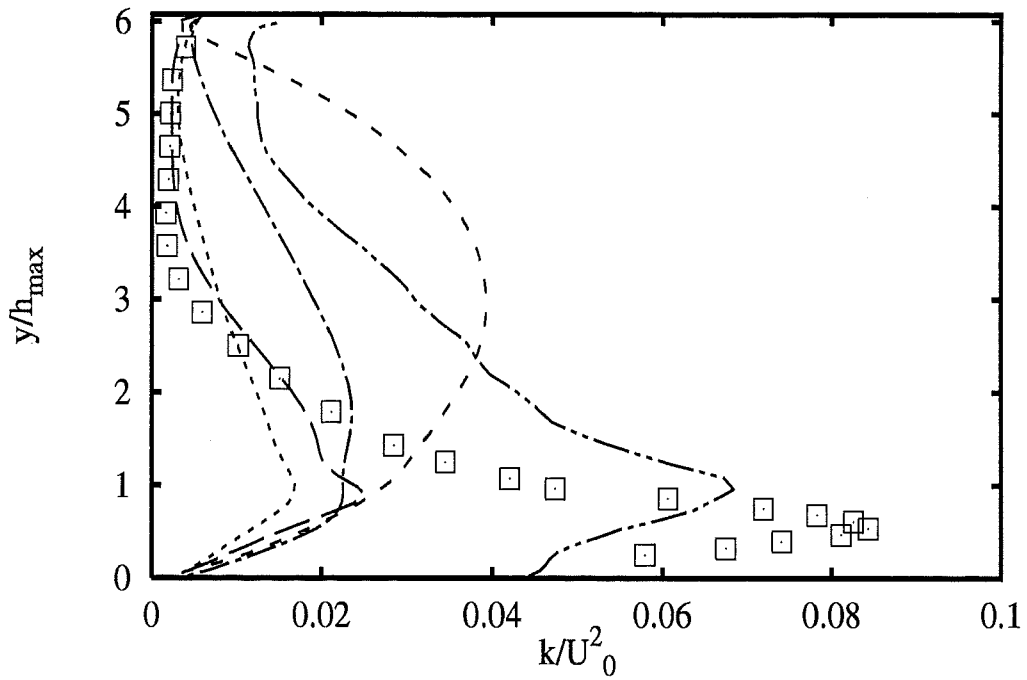
2B - 37



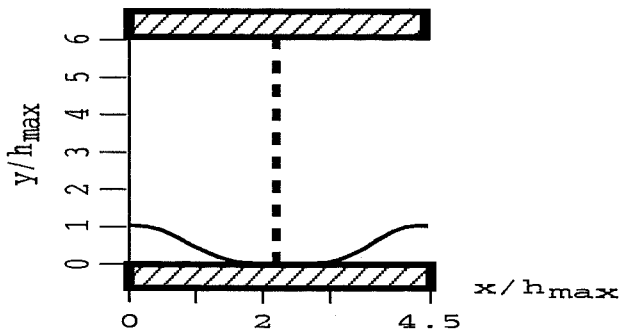
Profiles at $x/h_{max} = 2.25$



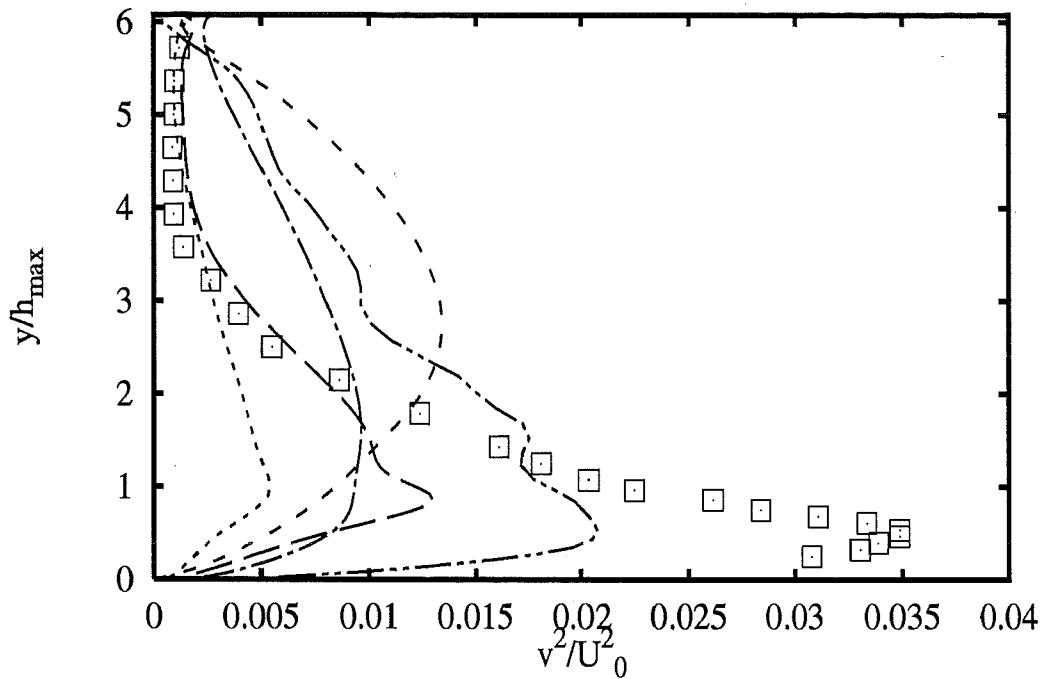
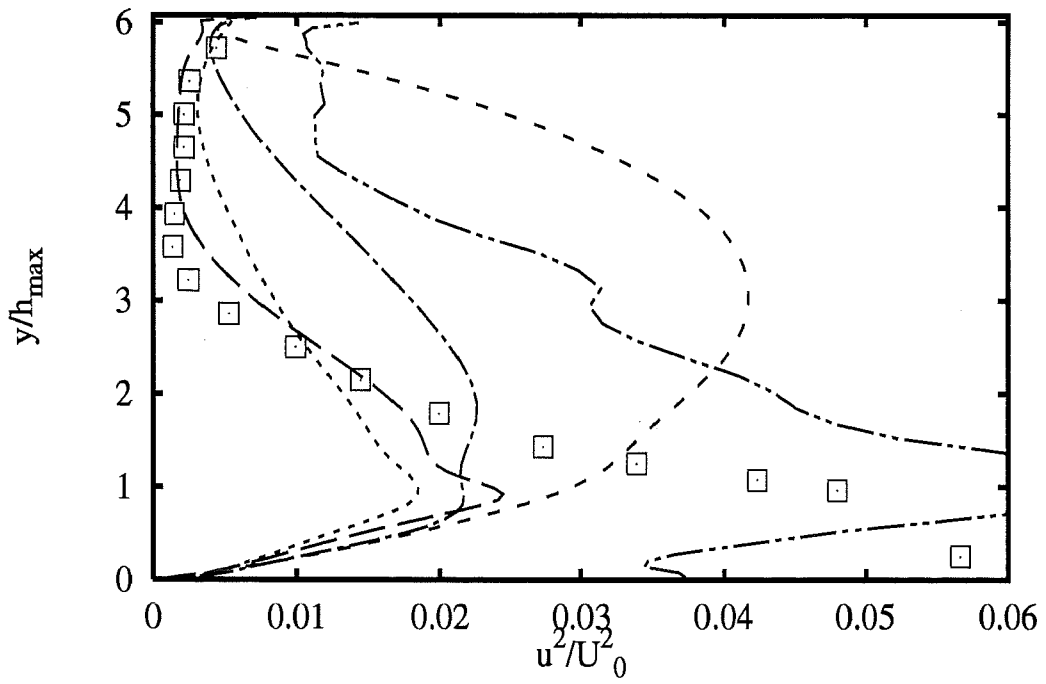
- Experiments \square
- EDFLNHLa RSM LRR+wf ---
- UDeIfthHa RSM LRR+wf - - -
- UMISTCra RSM CrLa+2eq (dotted)
- UMISTCra RSM Cub+2eq - · - · -
- DLROberp LES - · - · -



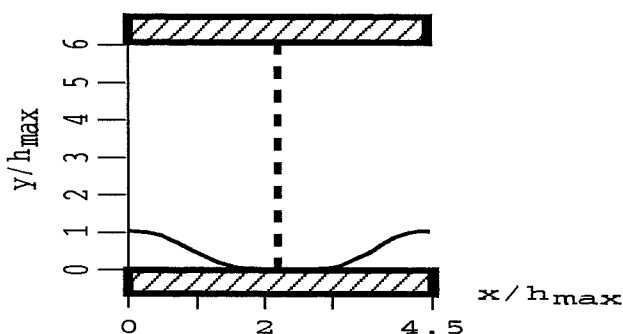
Profiles at $x/h_{max} = 2.25$



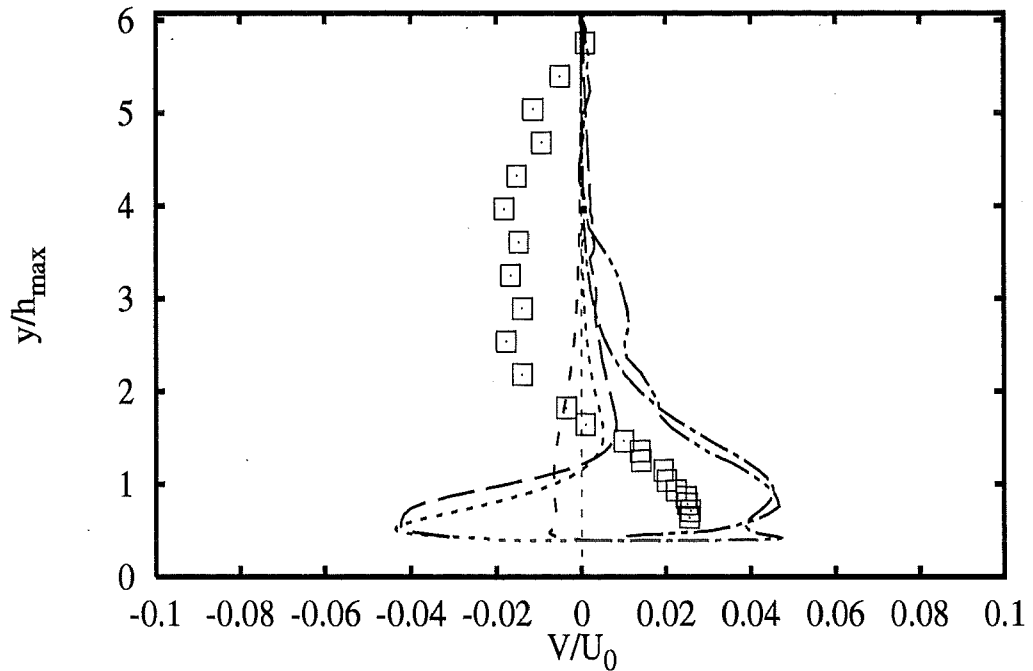
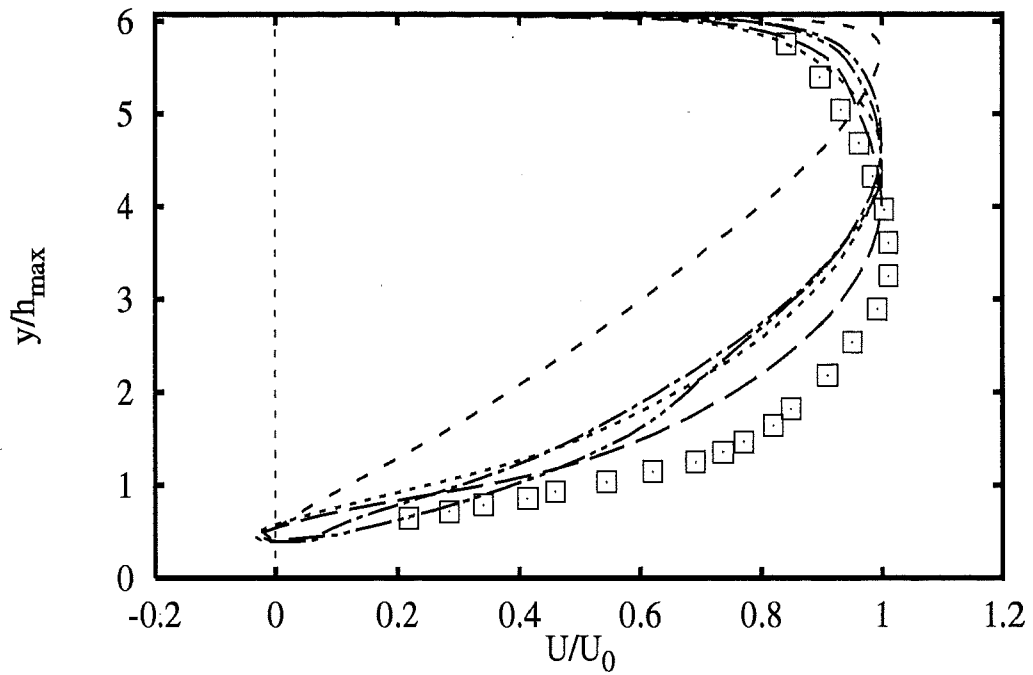
- Experiments \square
- EDFLNHLa RSM LRR+wf $---$
- UdelftHa RSM LRR+wf $----$
- UMISTCra RSM CrLa+2eq $\cdots\cdots$
- UMISTCra RSM Cub+2eq $----$
- DLROberp LES $----$



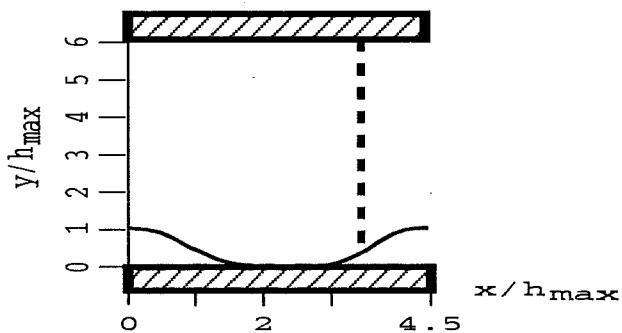
Profiles at $x/h_{max} = 2.25$



- | | |
|------------------------------|-----------|
| Experiments | \square |
| EDFLNHLa RSM LRR+wf | --- |
| UdelftHa RSM LRR+wf | --- |
| UMISTCra RSM CrLa+2eq | |
| UMISTCra RSM Cub+2eq | --- |
| DLROberp LES | --- |

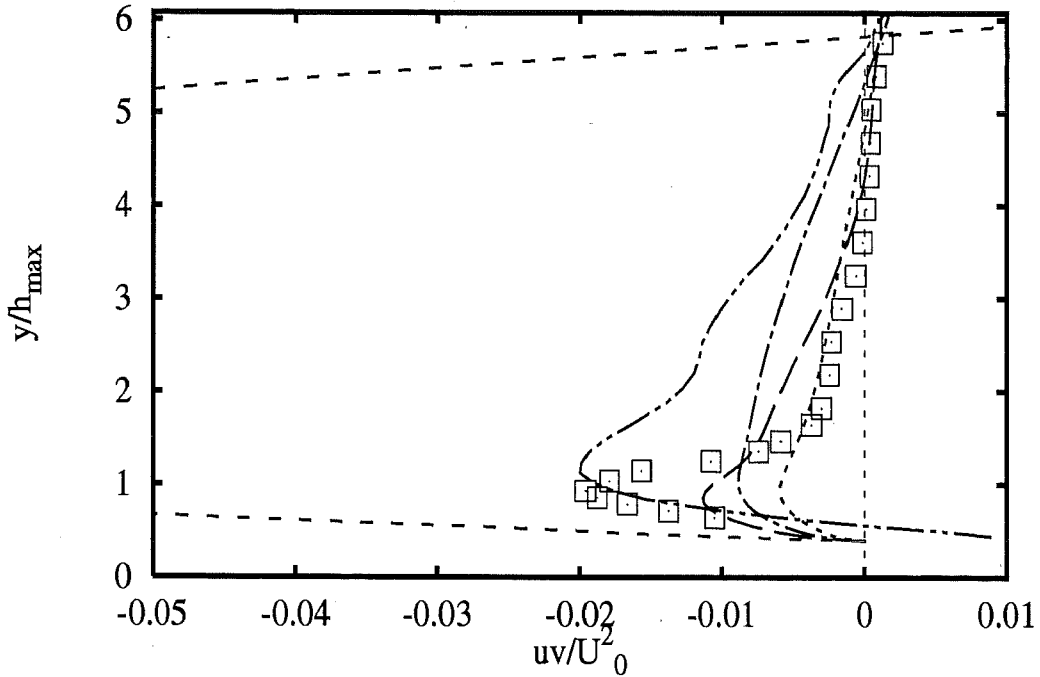
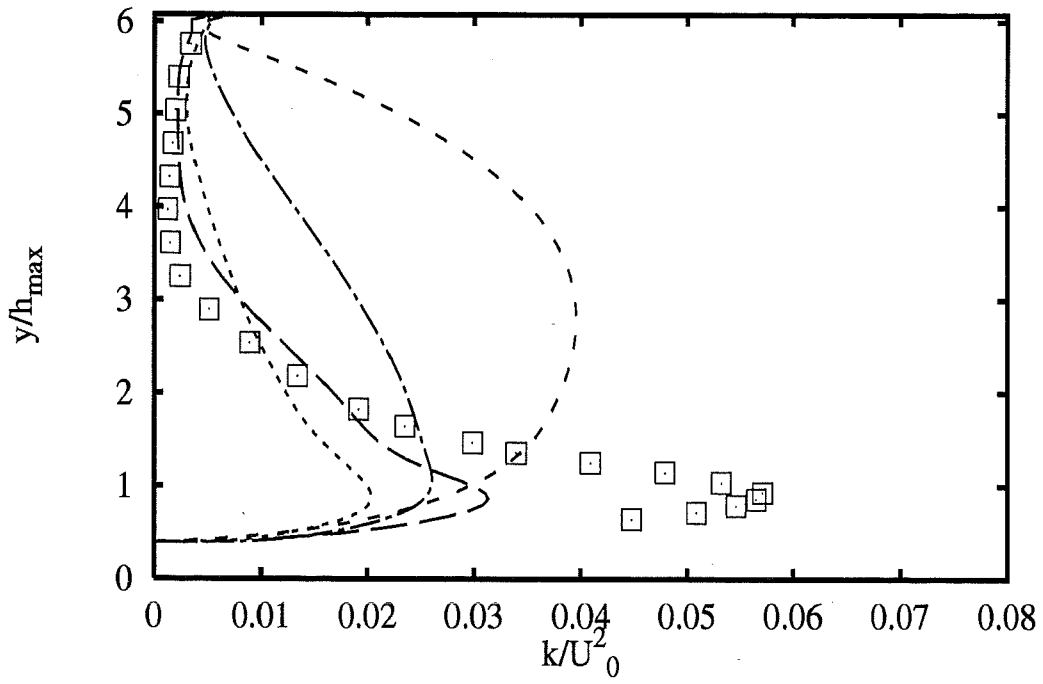


Profiles at $x/h_{max} = 3.43$

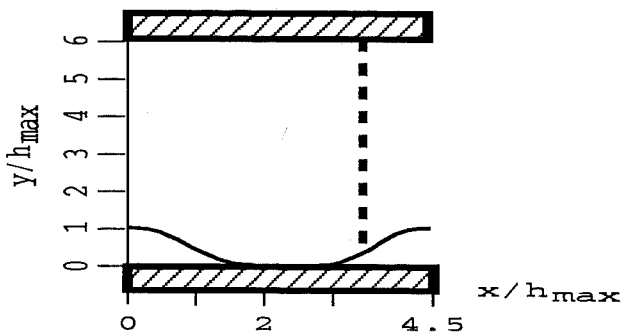


- Experiments \square
- EDFLNHLa RSM LRR+wf $---$
- UDeftHa RSM LRR+wf $---$
- UMISTCra RSM CrLa+2eq $\cdots\cdots\cdots$
- UMISTCra RSM Cub+2eq $-\cdot-\cdot-\cdot-$
- DLROberp LES $-\cdot-\cdot-\cdot-$

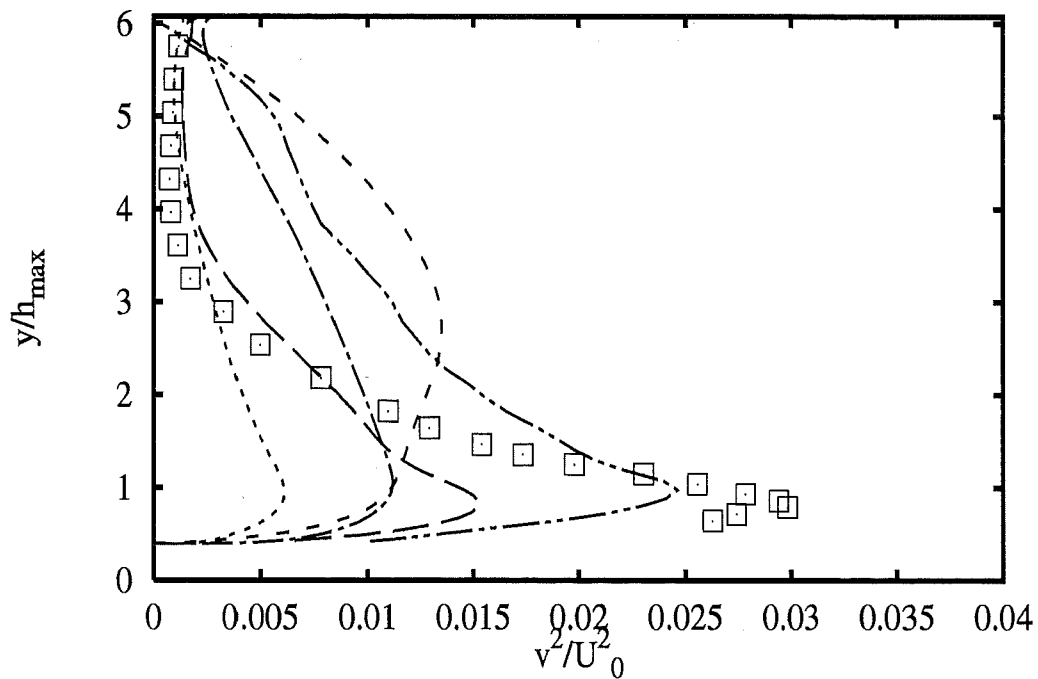
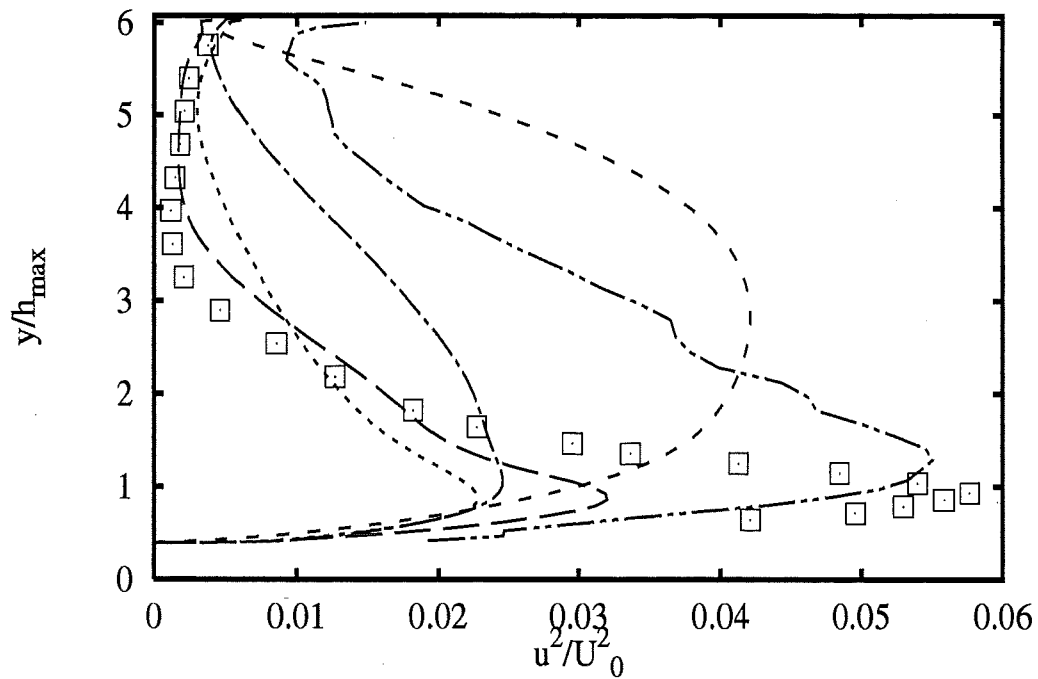
2B - 41



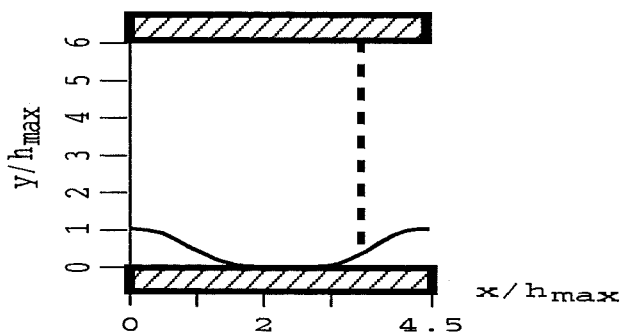
Profiles at $x/h_{max} = 3.43$



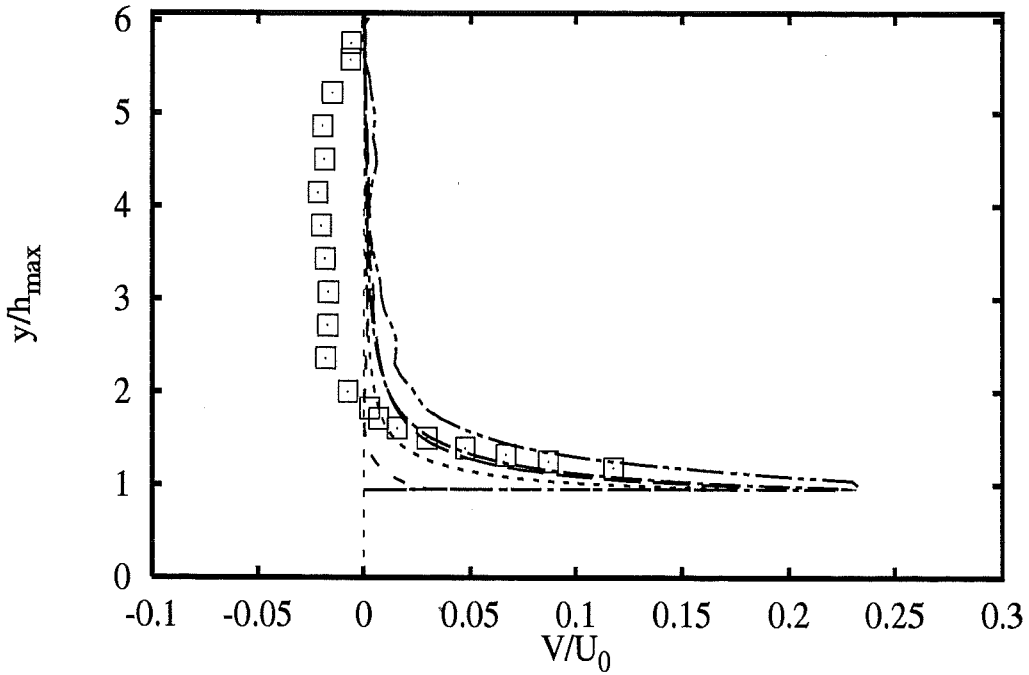
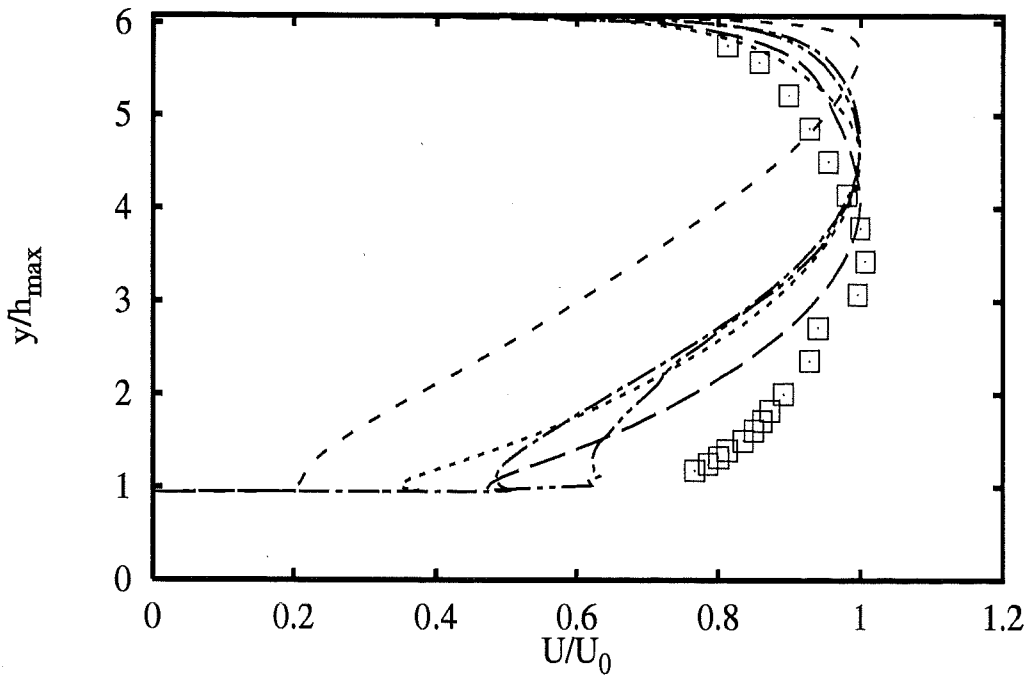
- Experiments \square
- EDFLNHLa RSM LRR+wf ---
- UdelftHa RSM LRR+wf - - -
- UMISTCra RSM CrLa+2eq (dotted)
- UMISTCra RSM Cub+2eq - · - · -
- DLROberp LES - · - · -



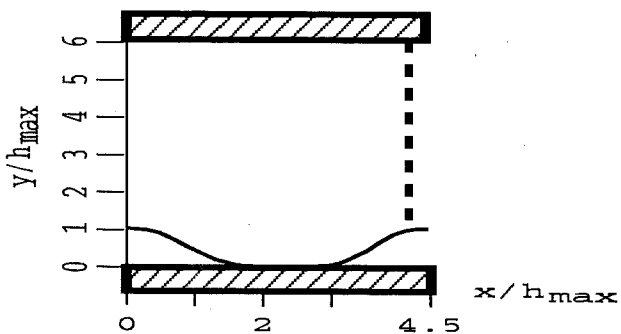
Profiles at $x/h_{max} = 3.43$



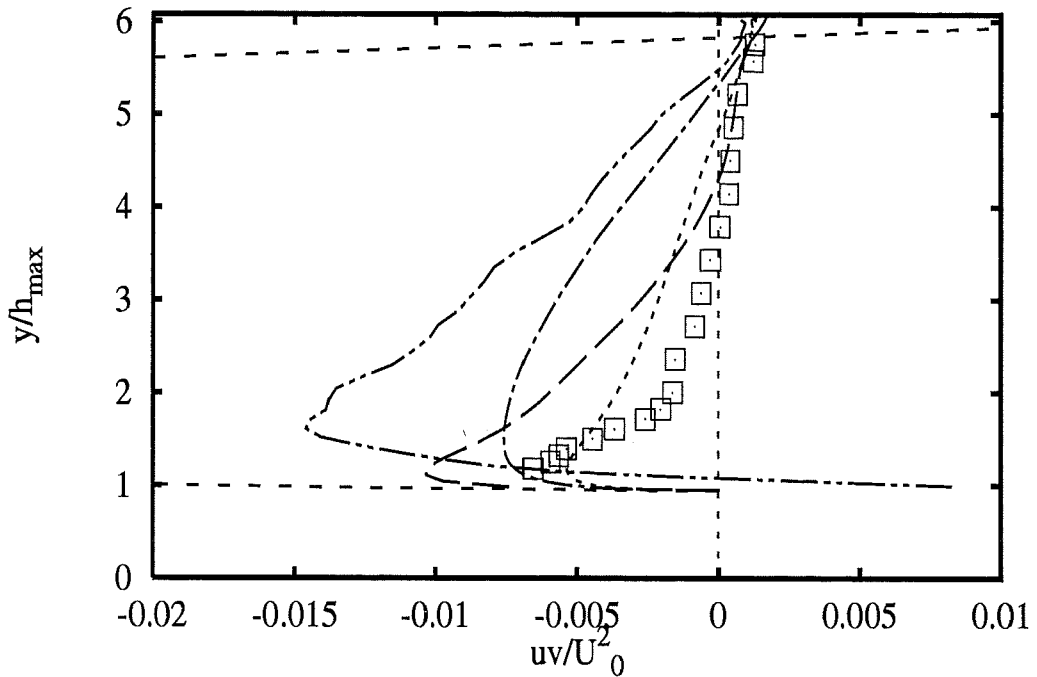
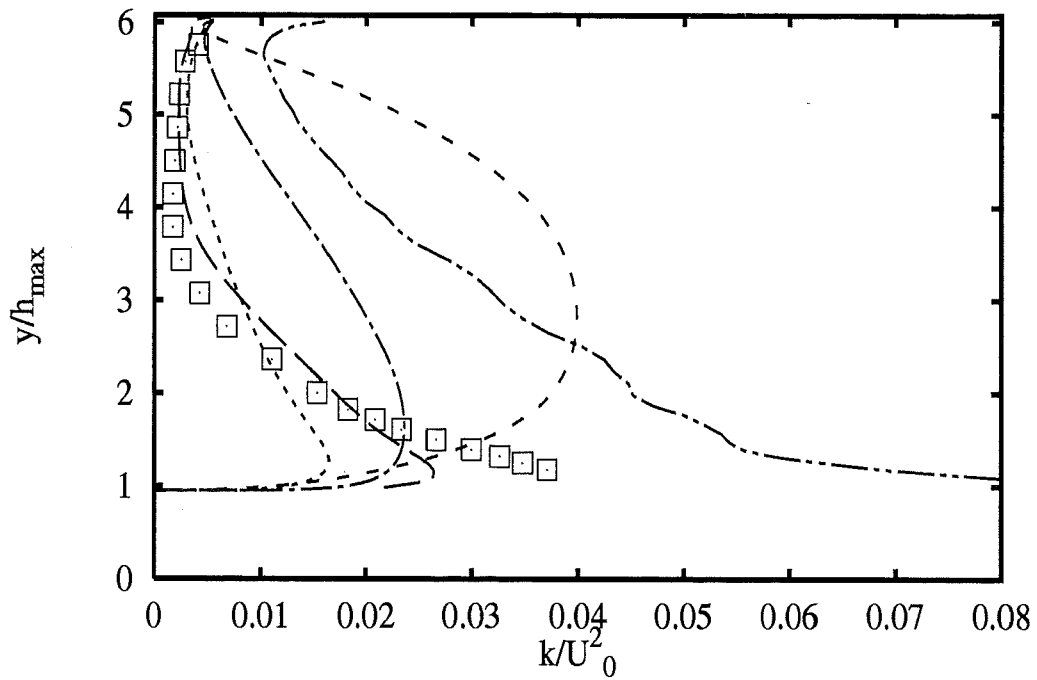
- | | |
|------------------------------|---------|
| Experiments | □ |
| <i>EDFLNHLa</i> RSM LRR+wf | — — |
| <i>UdelftHa</i> RSM LRR+wf | - - - |
| <i>UMISTCra</i> RSM CrLa+2eq | · · · · |
| <i>UMISTCra</i> RSM Cub+2eq | - · - · |
| <i>DLROberp</i> LES | · · · · |



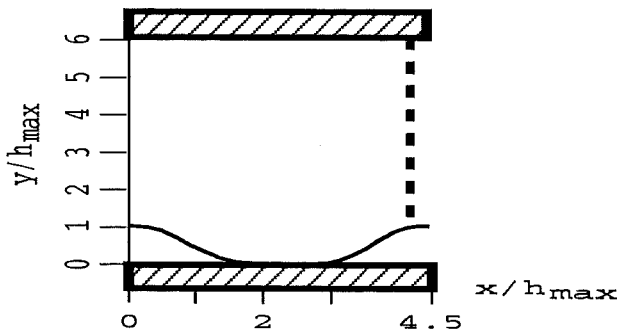
Profiles at $x/h_{max} = 4.14$



- Experiments \square
- EDFLNHLa RSM LRR+wf ---
- UDeftHa RSM LRR+wf - - -
- UMISTCra RSM CrLa+2eq (dotted)
- UMISTCra RSM Cub+2eq - · - · -
- DLROberp LES - - - -

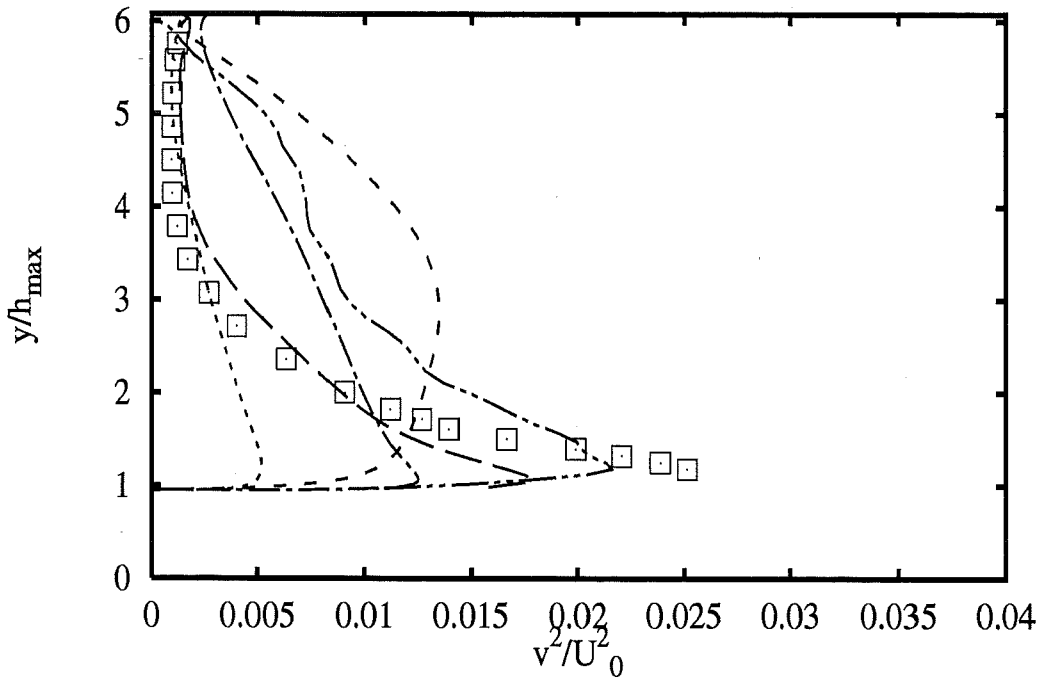
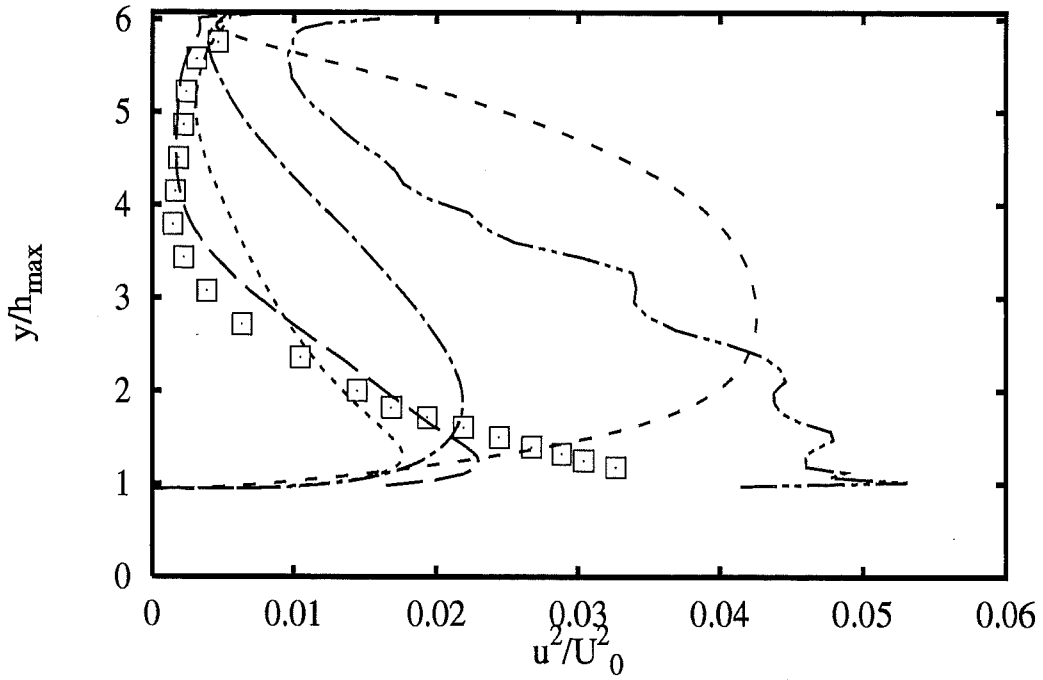


Profiles at $x/h_{max} = 4.14$

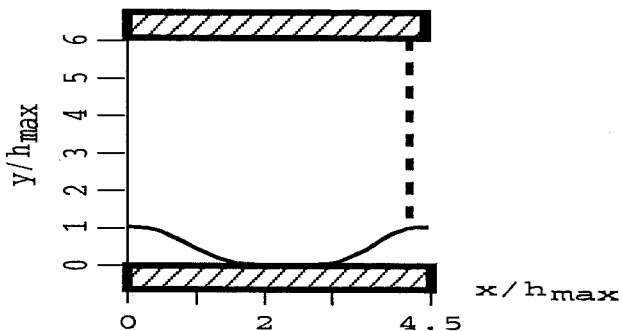


- Experiments \square
- EDFLNHLa RSM LRR+wf —
- UDeftHa RSM LRR+wf - - -
- UMISTCra RSM CrLa+2eq ·····
- UMISTCra RSM Cub+2eq - · - · -
- DLROberp LES - - - -

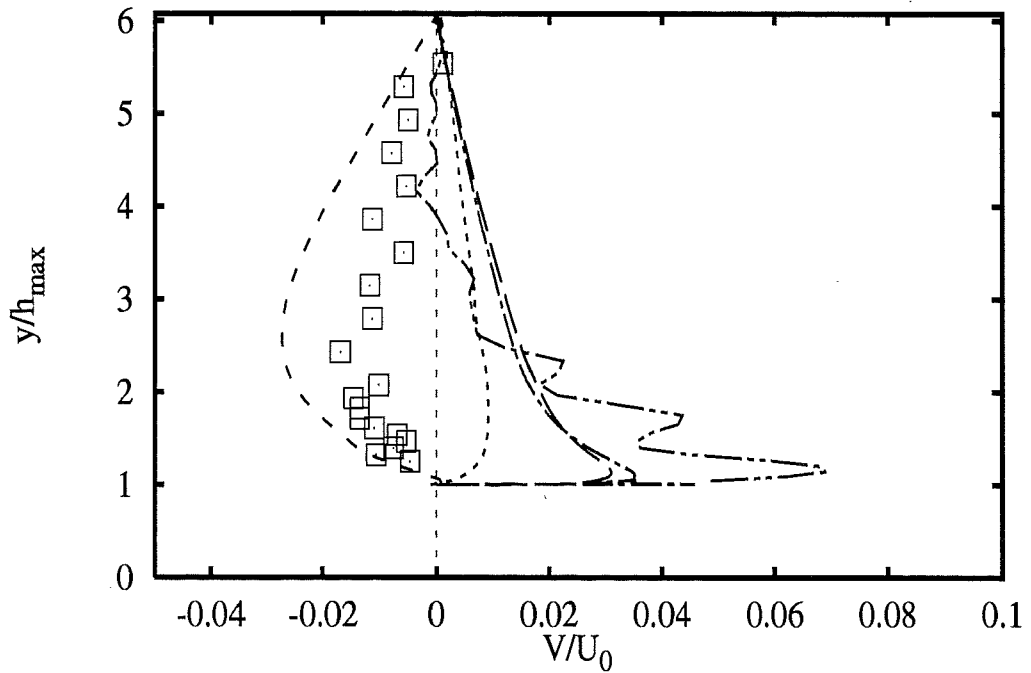
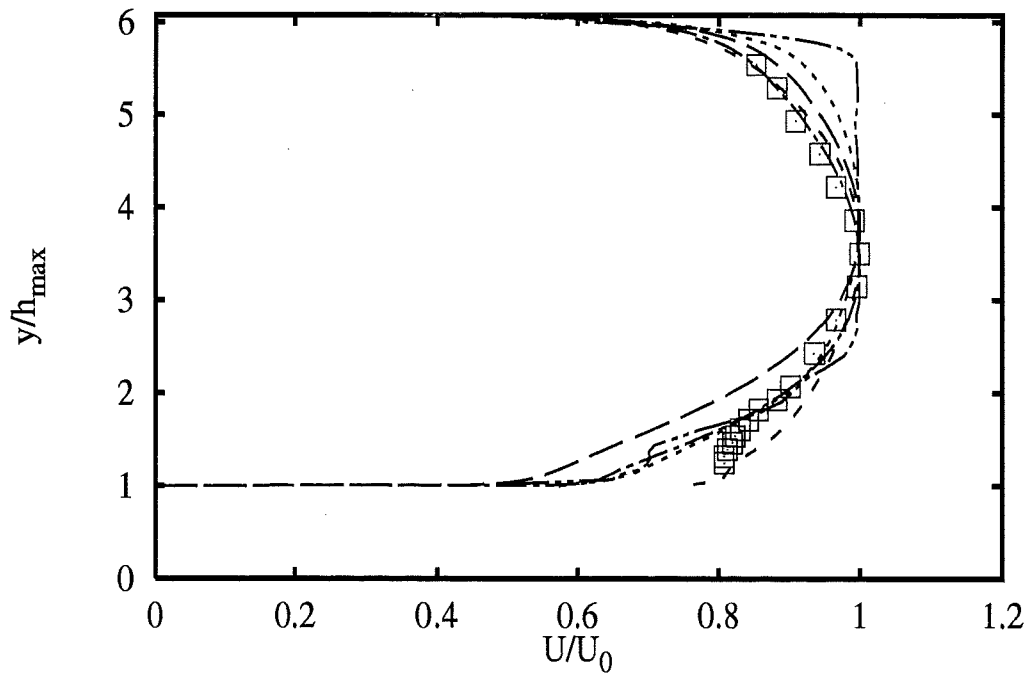
2B - 45



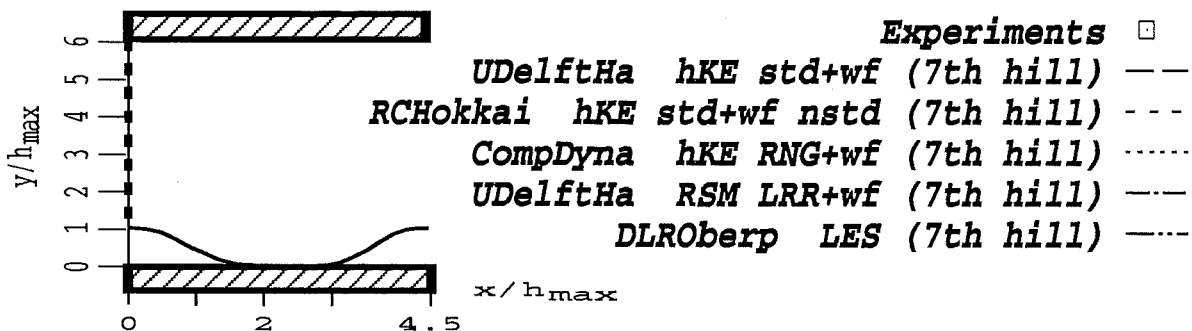
Profiles at $x/h_{max} = 4.14$

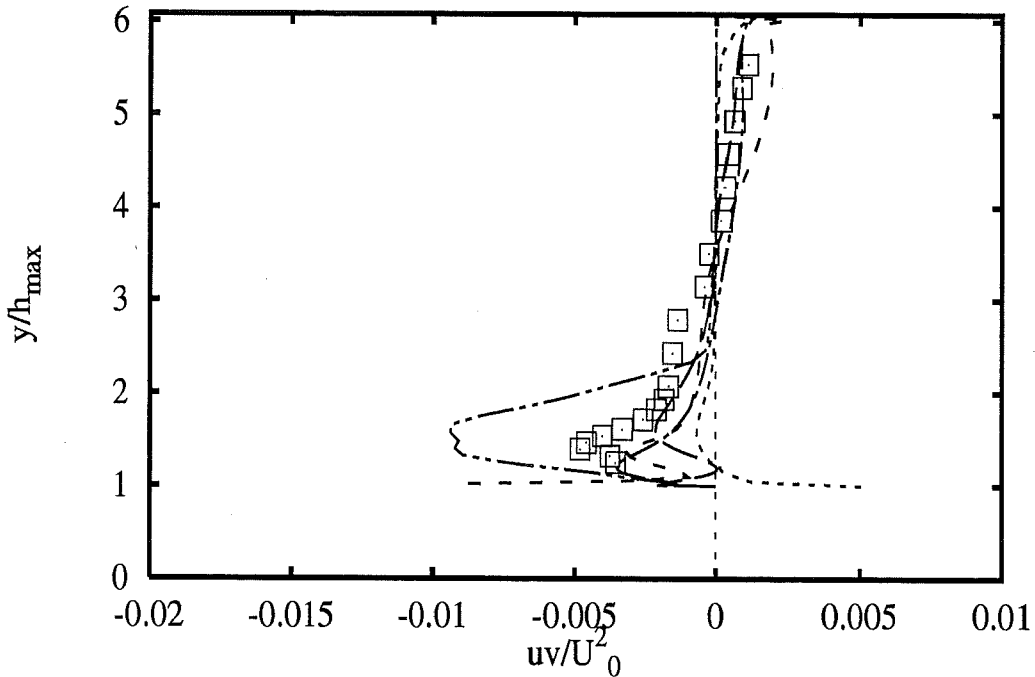
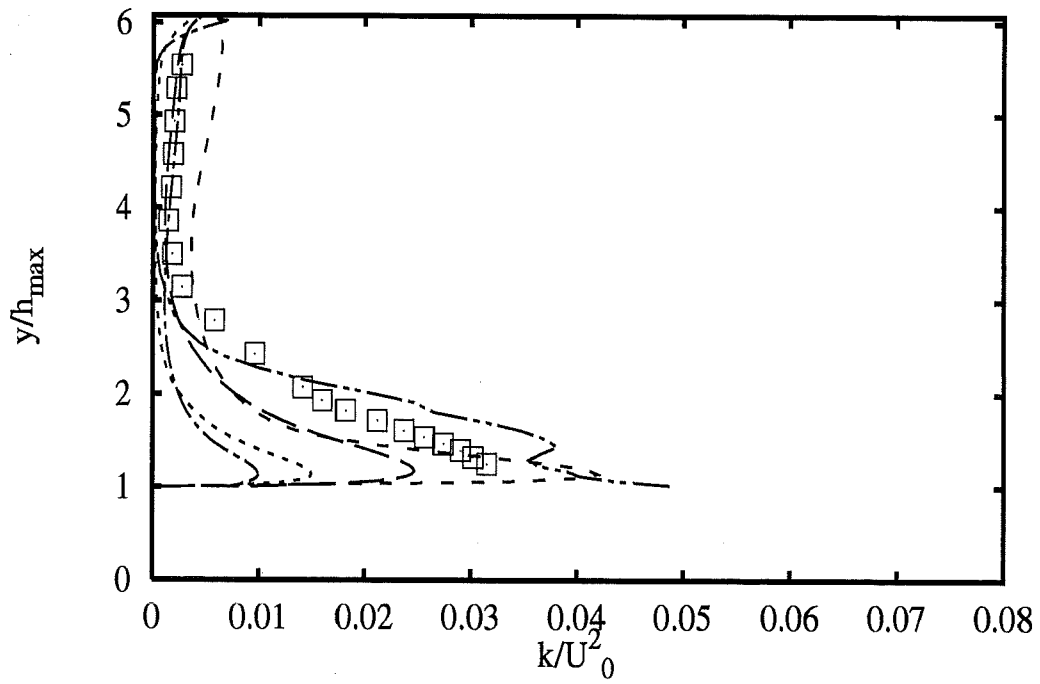


- Experiments** \square
- EDFLNHLa RSM LRR+wf** ---
- UDeftHa RSM LRR+wf** - - -
- UMISTCra RSM CrLa+2eq** ·····
- UMISTCra RSM Cub+2eq** - · - · -
- DLROberp LES** - - - -

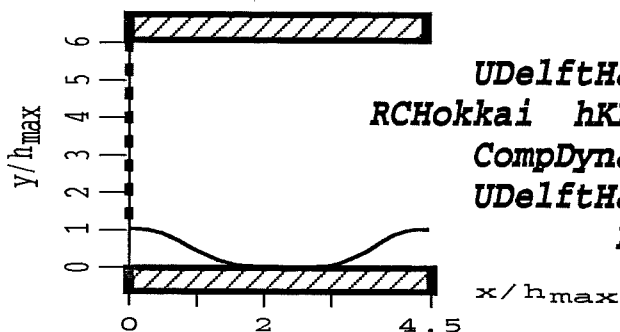


Profiles at $x/h_{max} = 0$

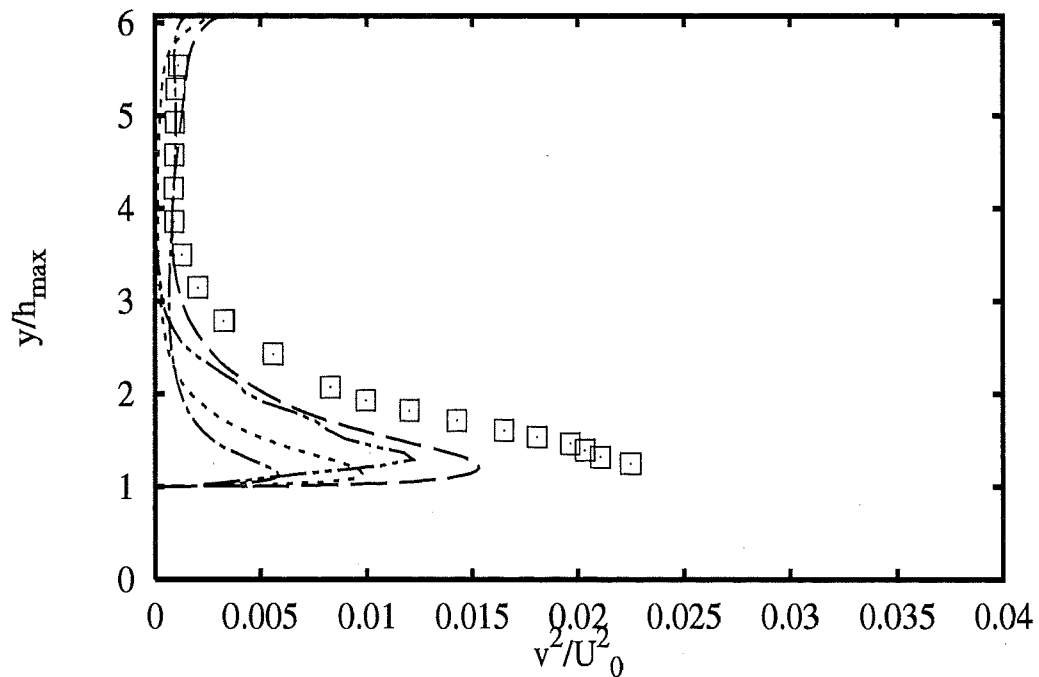
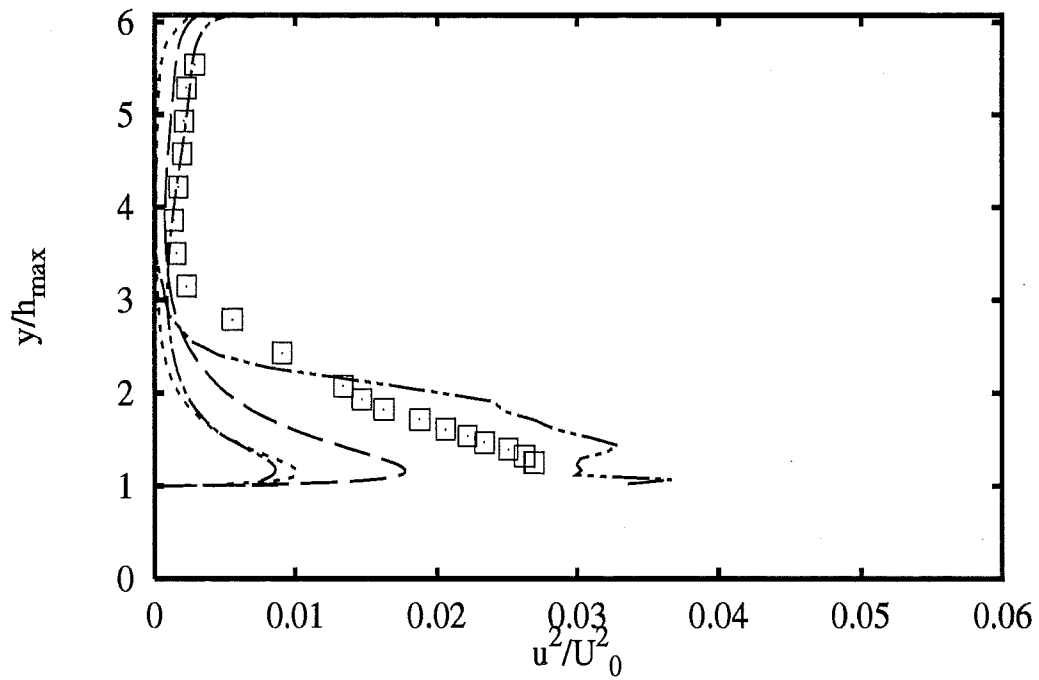




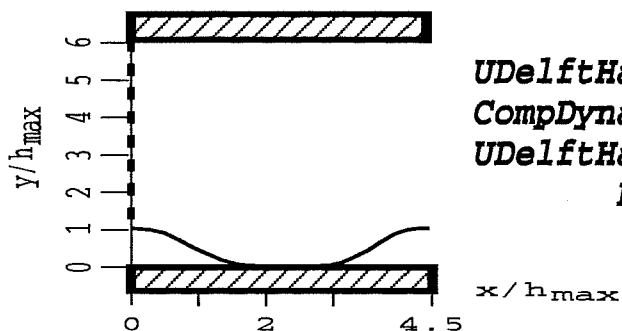
Profiles at $x/h_{max} = 0$



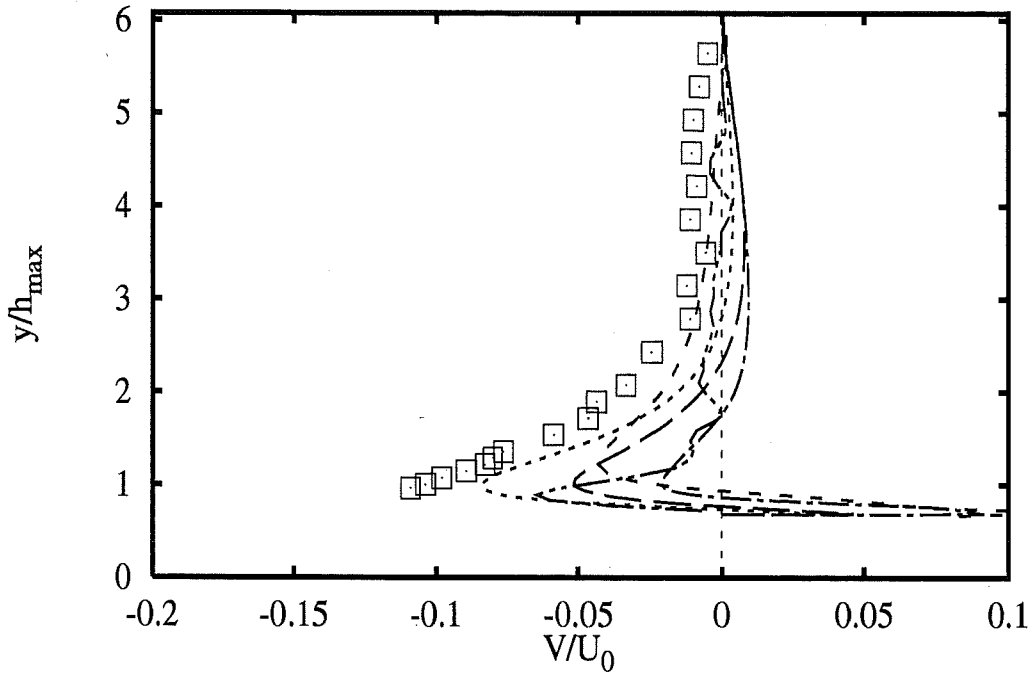
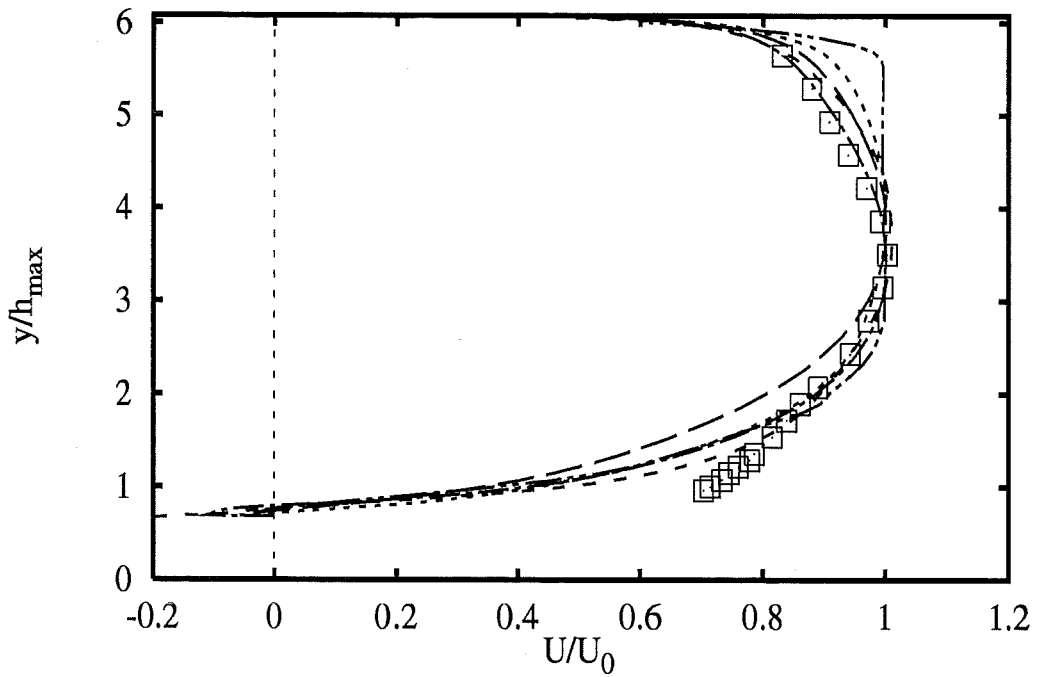
- Experiments** □
- UDelftHa hKE std+wf (7th hill) ---
 - RCHokkai hKE std+wf nstd (7th hill) - - -
 - CompDyna hKE RNG+wf (7th hill) ·····
 - UDelftHa RSM LRR+wf (7th hill) - · - · -
 - DLROberp LES (7th hill) — · — · —



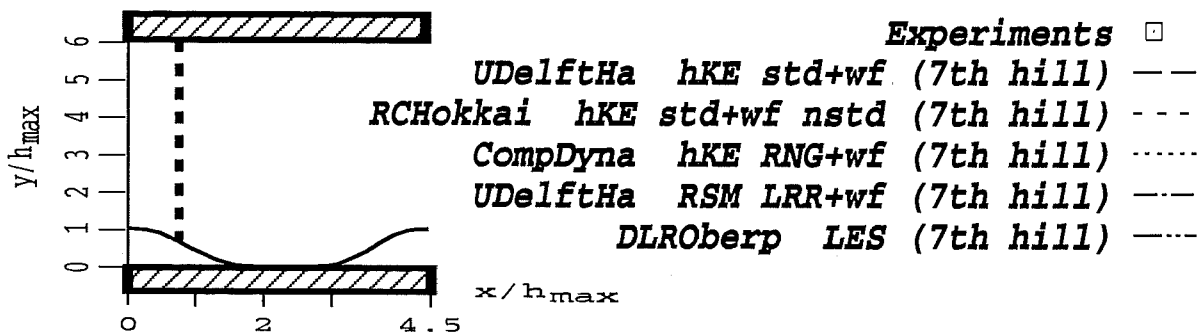
Profiles at $x/h_{max} = 0$

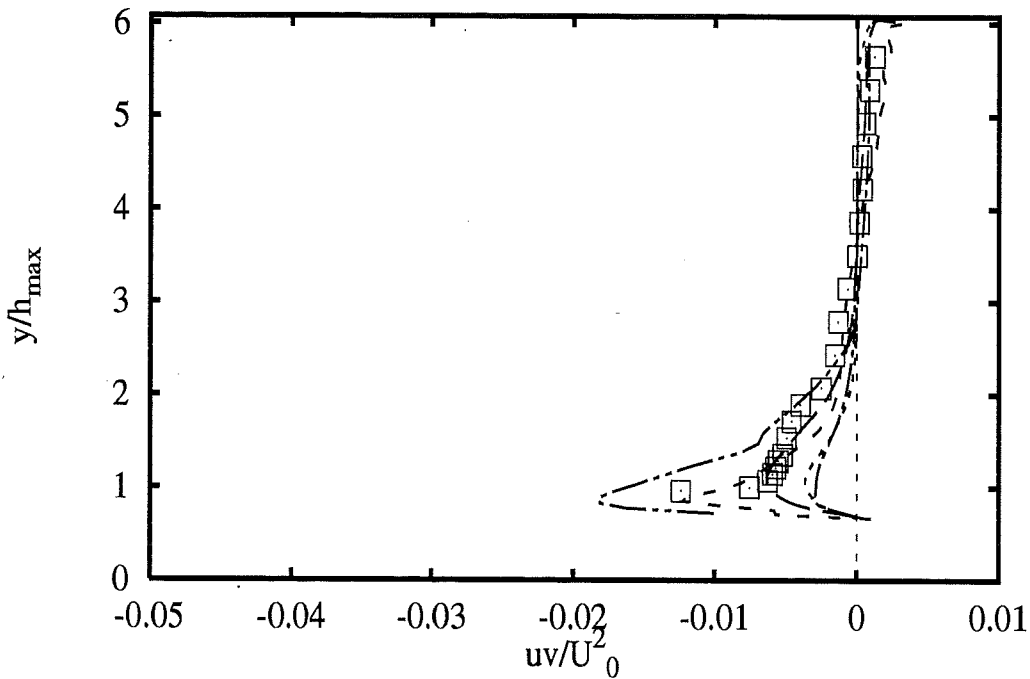
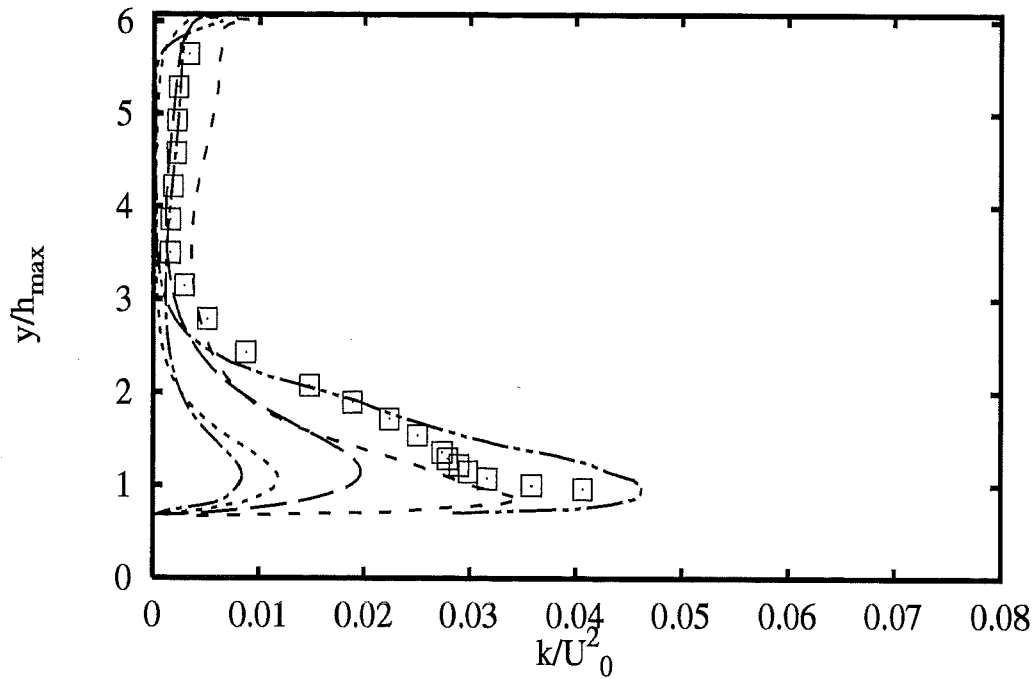


- | | | |
|------------------|------------------------------|-------|
| | Experiments | □ |
| <i>U</i> DelftHa | <i>hKE std+wf</i> (7th hill) | --- |
| <i>Comp</i> Dyna | <i>hKE RNG+wf</i> (7th hill) | |
| <i>U</i> DelftHa | <i>RSM LRR+wf</i> (7th hill) | -.-.- |
| <i>DLR</i> Oberp | <i>LES</i> (7th hill) | ---- |

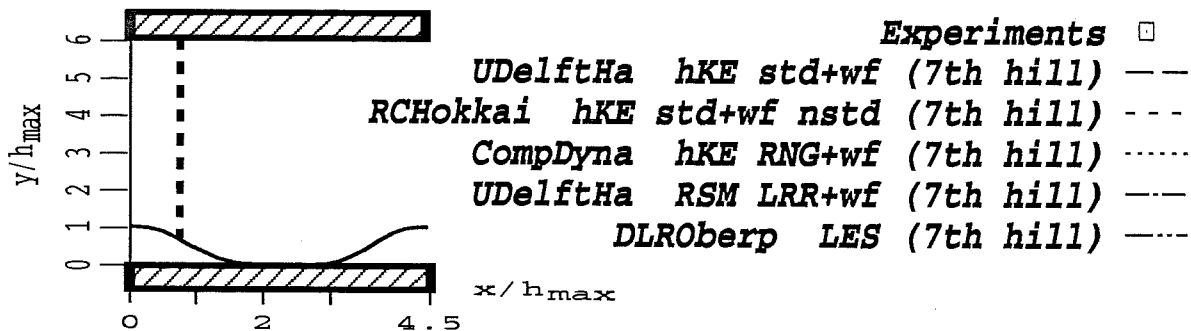


Profiles at $x/h_{max} = 0.71$

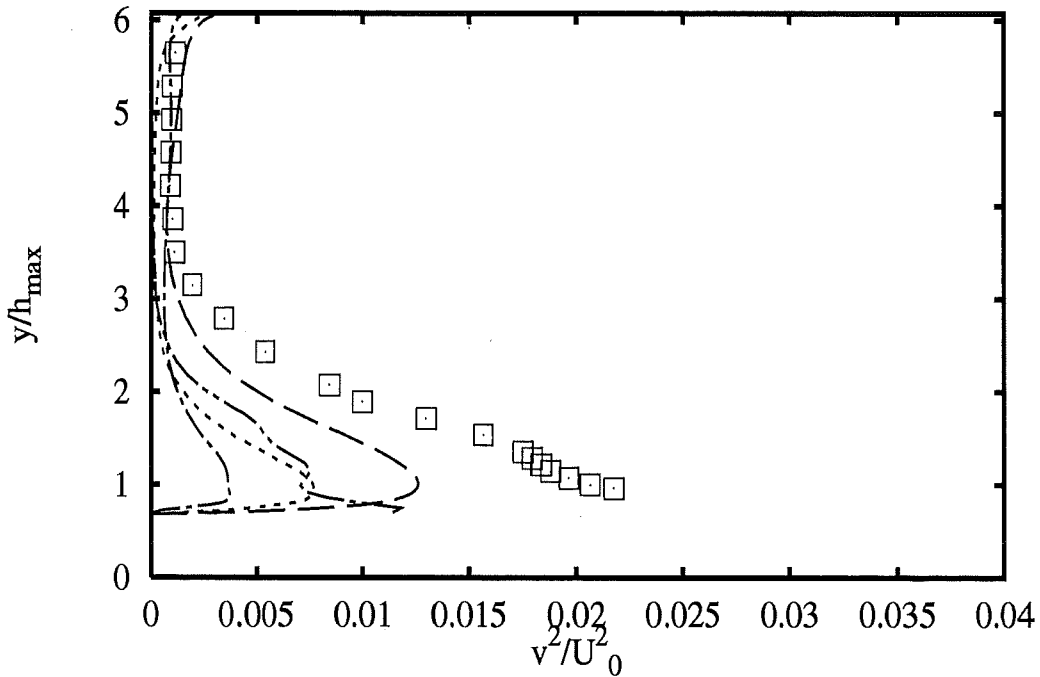
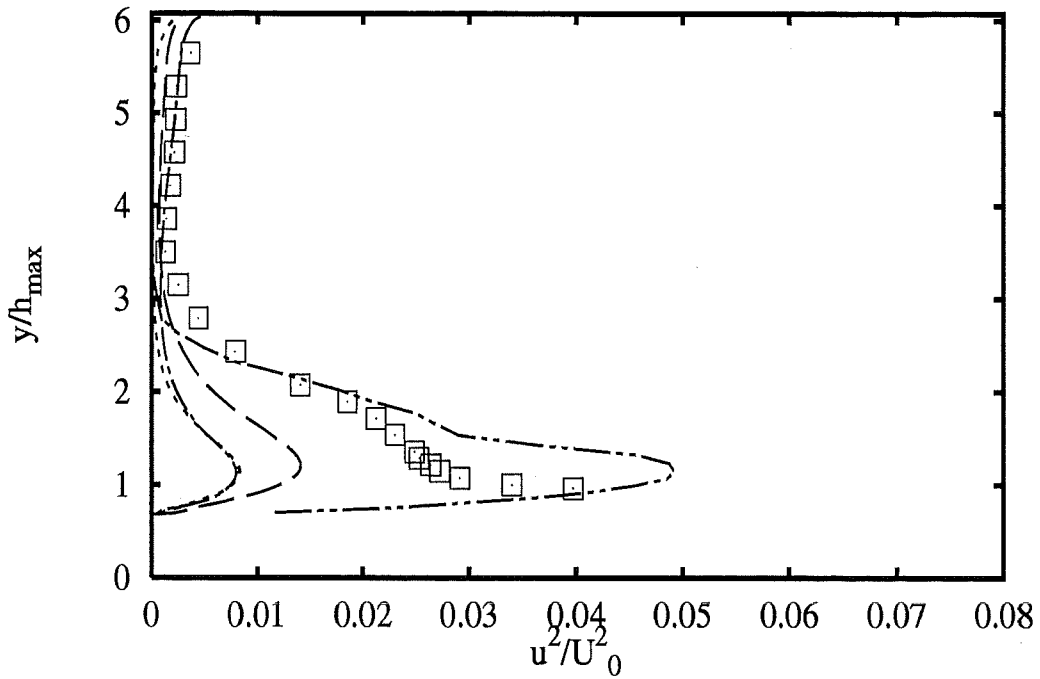




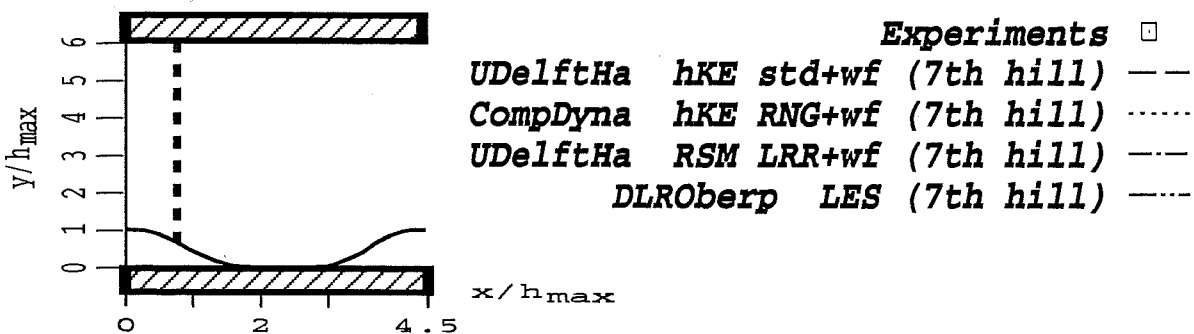
Profiles at $x/h_{max} = 0.71$

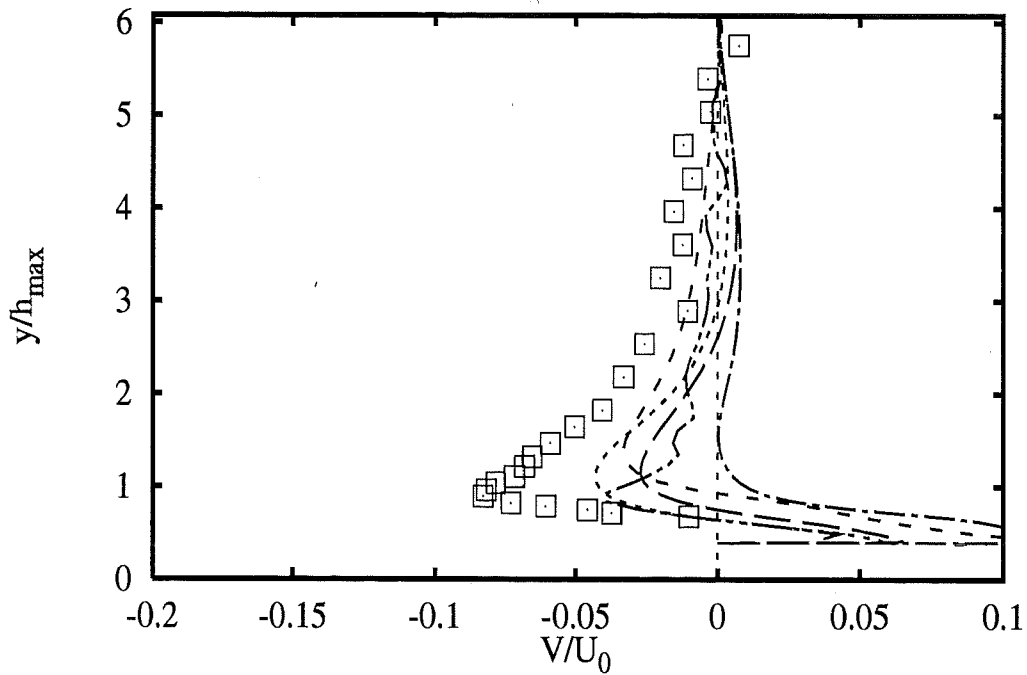
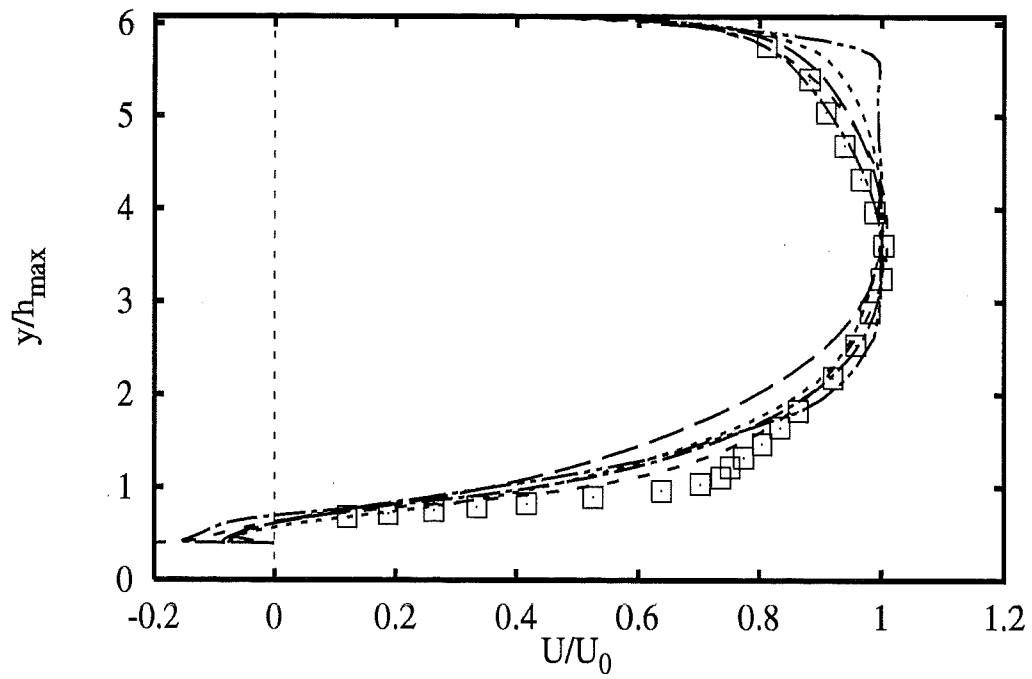


2B - 51

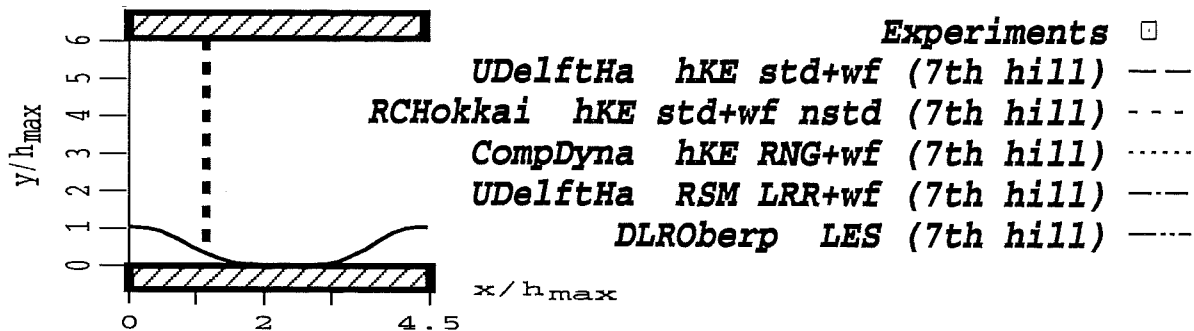


Profiles at $x/h_{max} = 0.71$

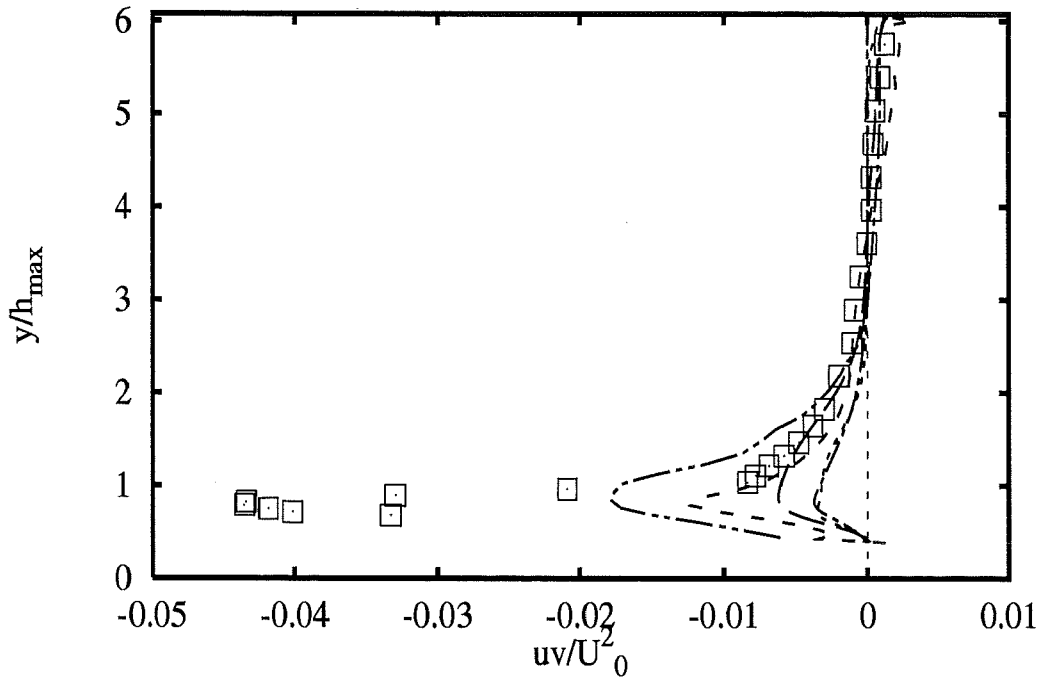
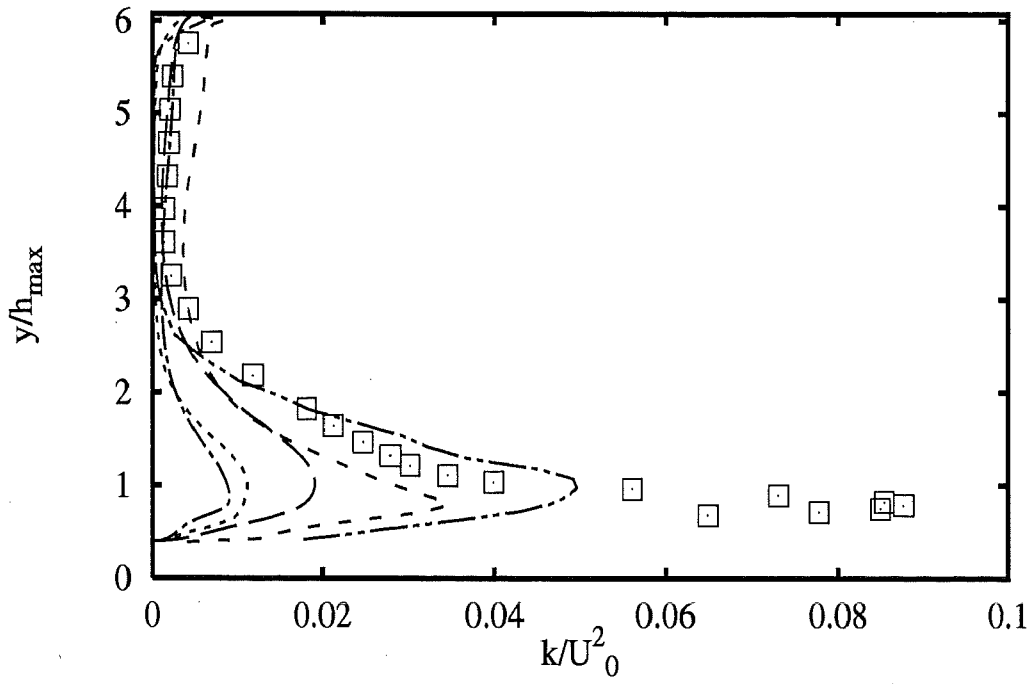




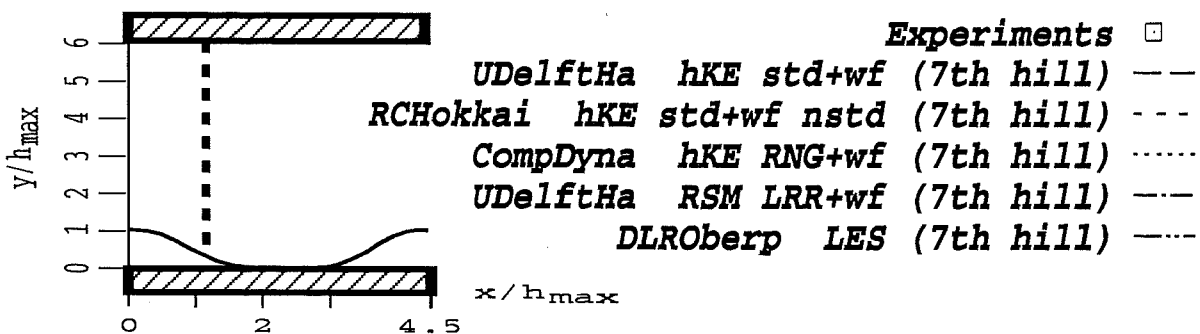
Profiles at $x/h_{max} = 1.07$

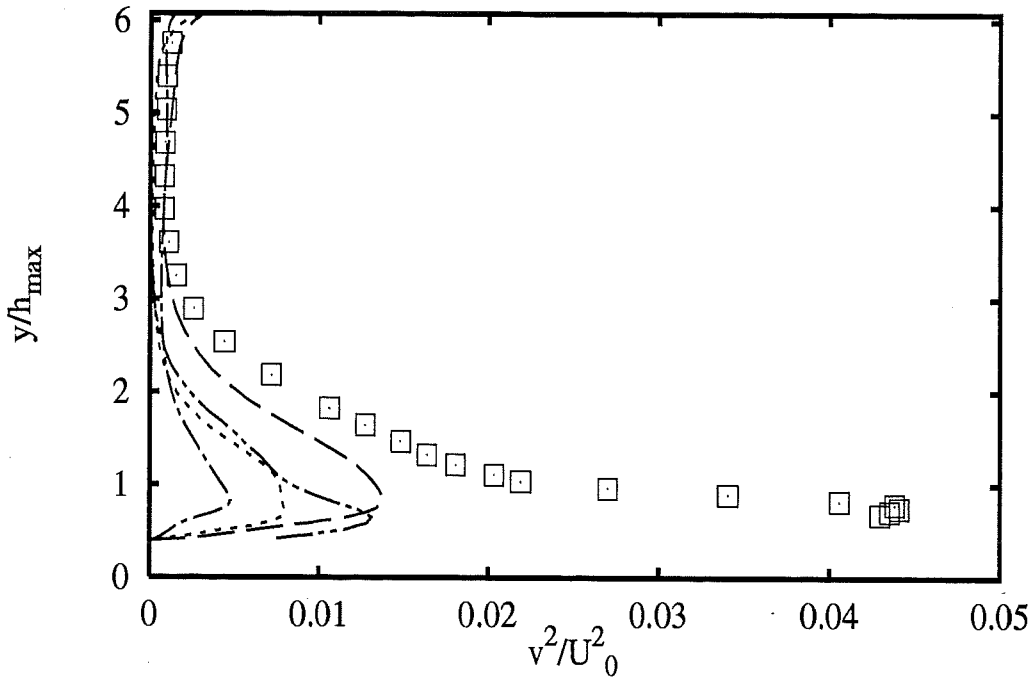
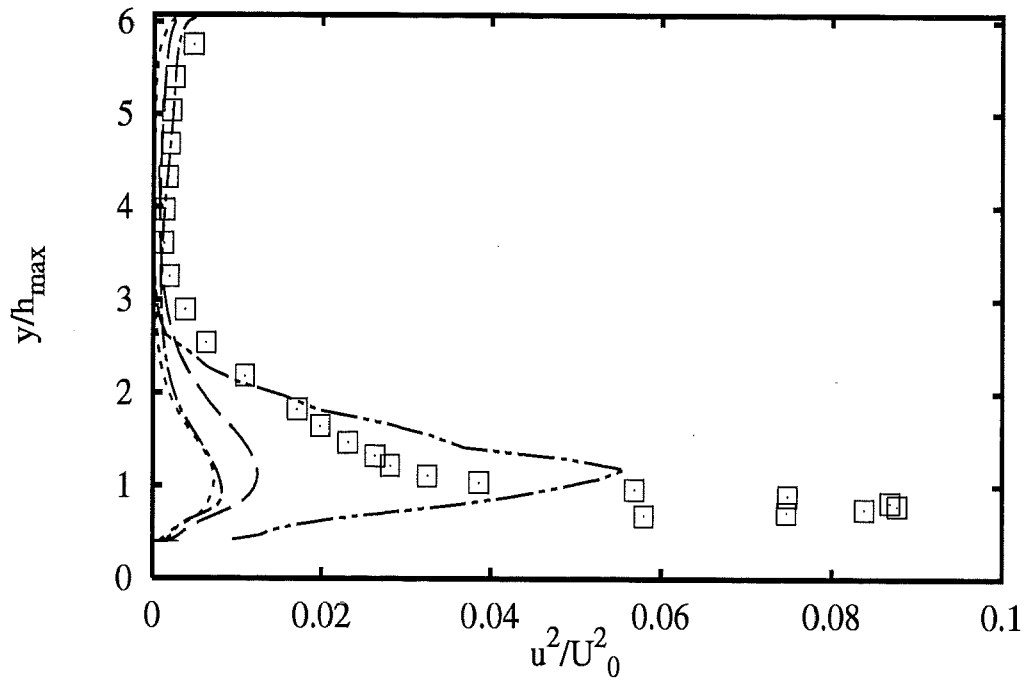


2B - 53

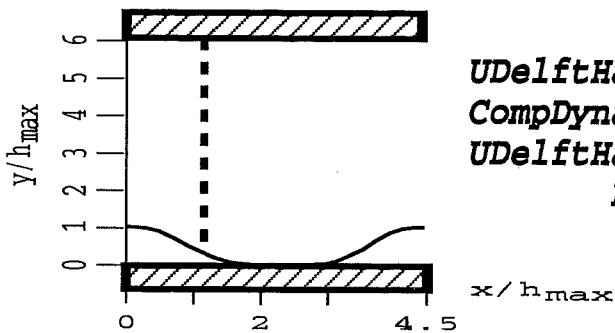


Profiles at $x/h_{max} = 1.07$

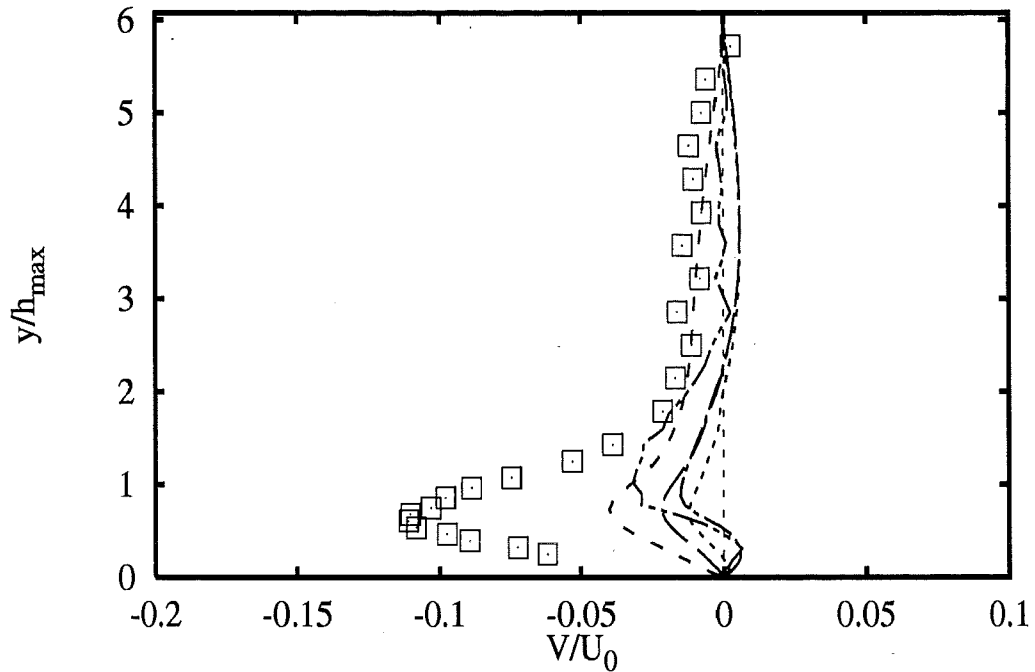
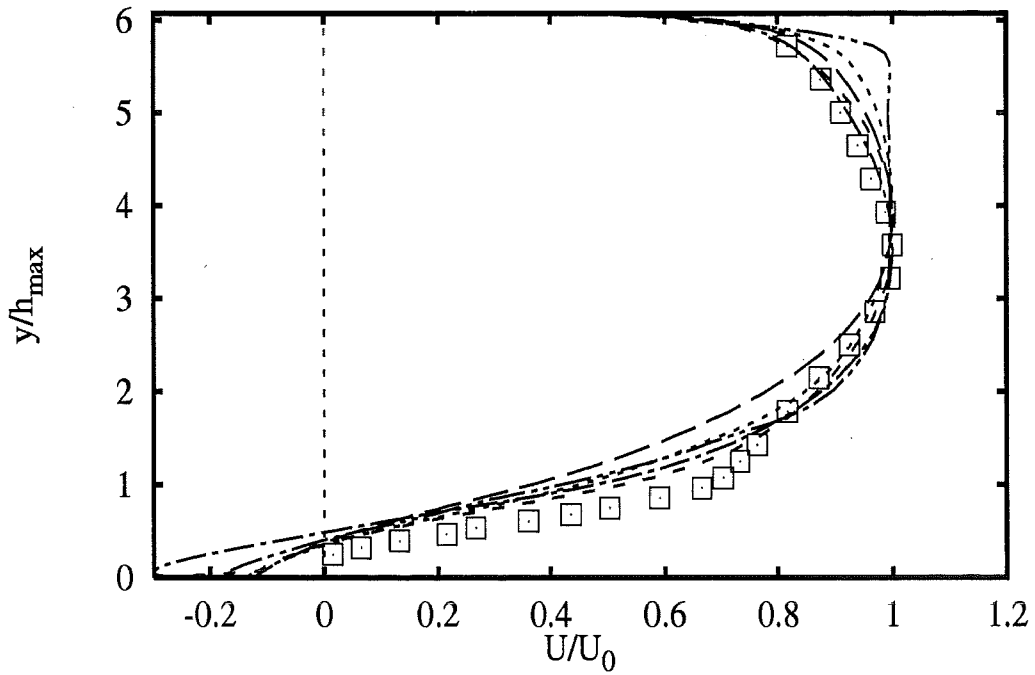




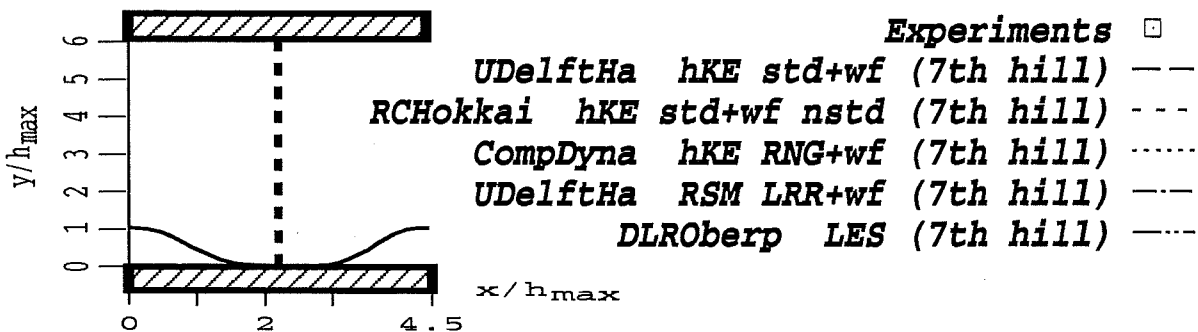
Profiles at $x/h_{max} = 1.07$

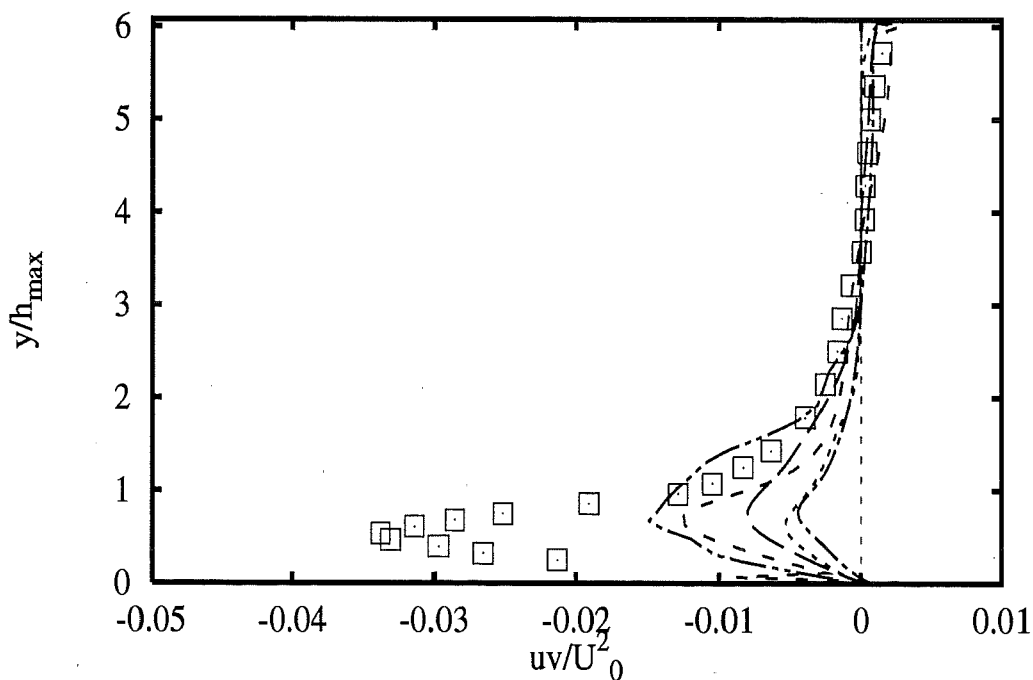
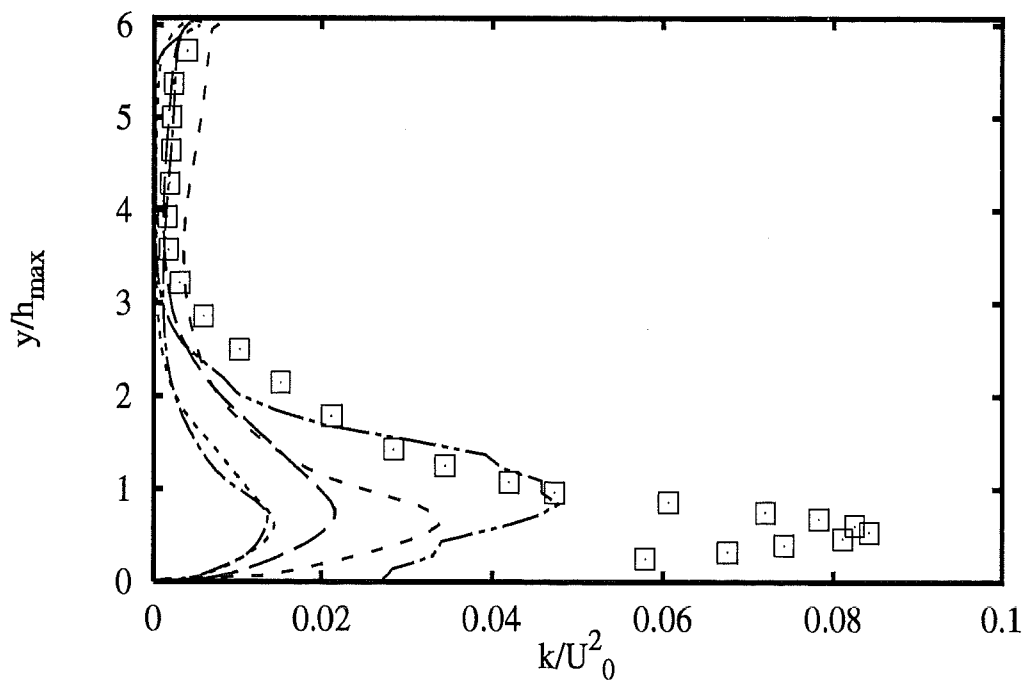


- Experiments** □
- UDelftHa hKE std+wf (7th hill) — —
 - CompDyna hKE RNG+wf (7th hill) ·····
 - UDelftHa RSM LRR+wf (7th hill) - - -
 - DLROberp LES (7th hill) - · - ·

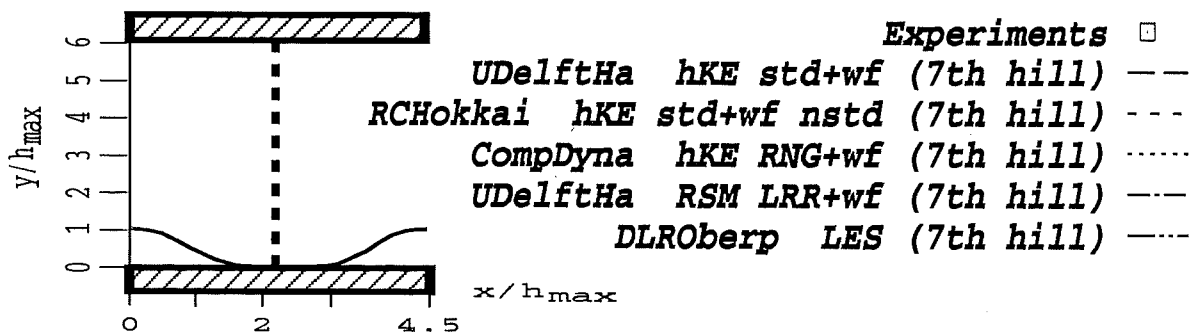


Profiles at $x/h_{max} = 2.25$

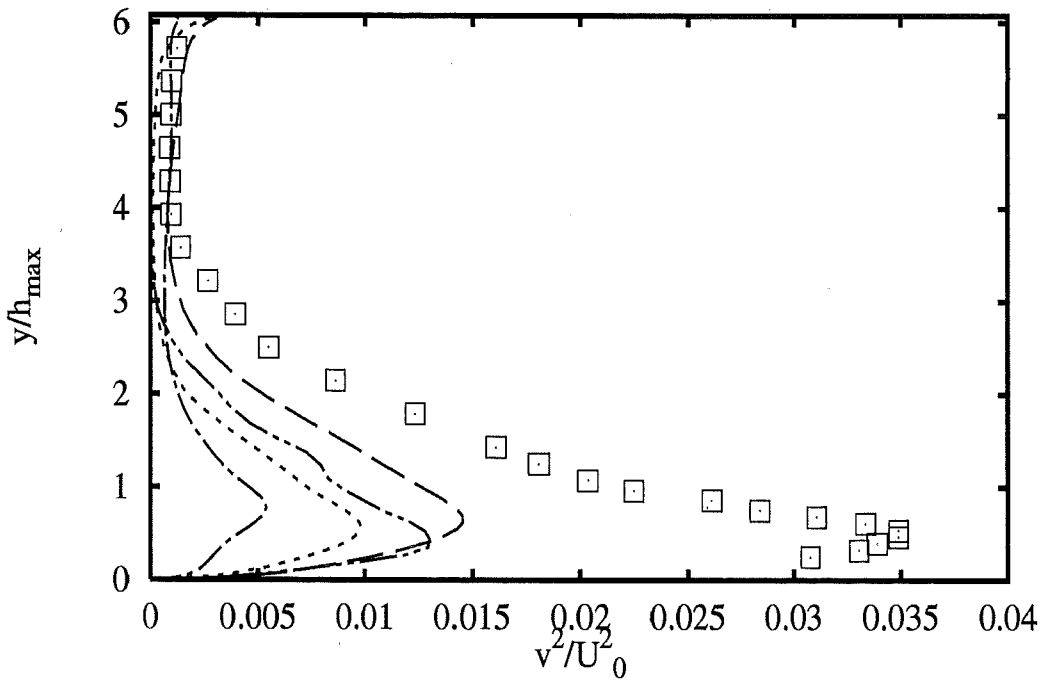
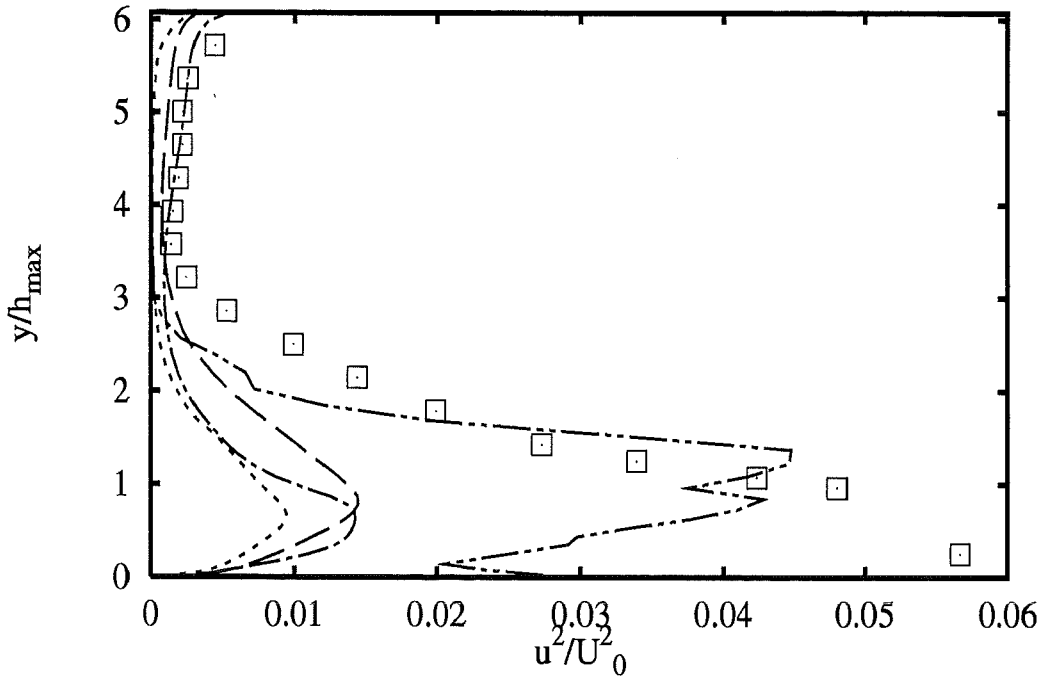




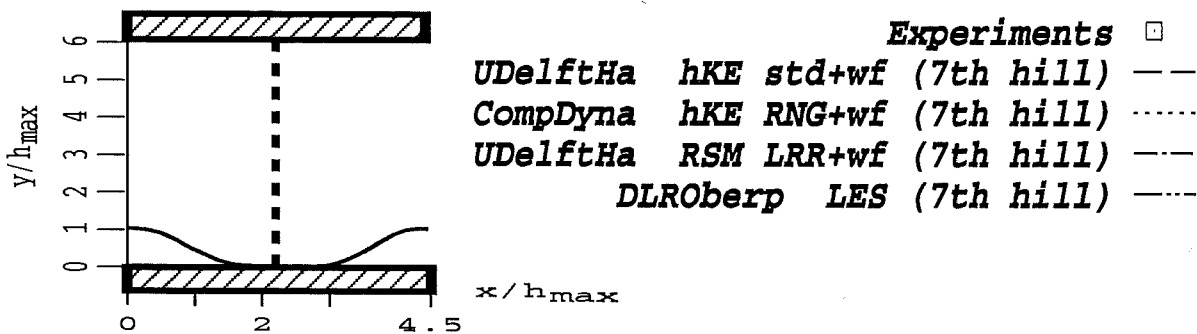
Profiles at $x/h_{max} = 2.25$



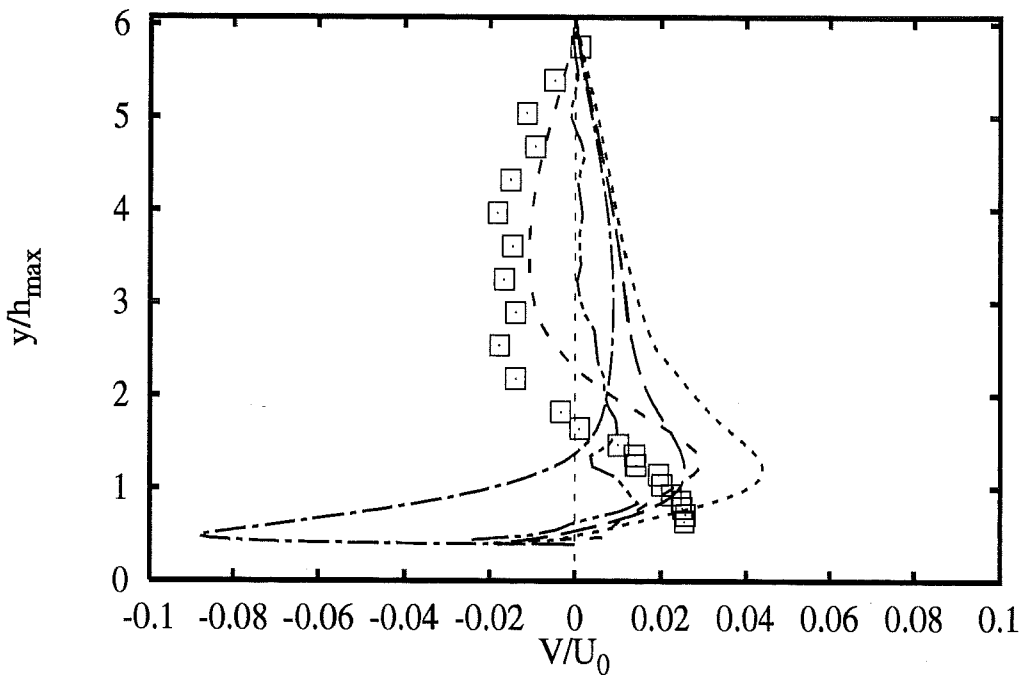
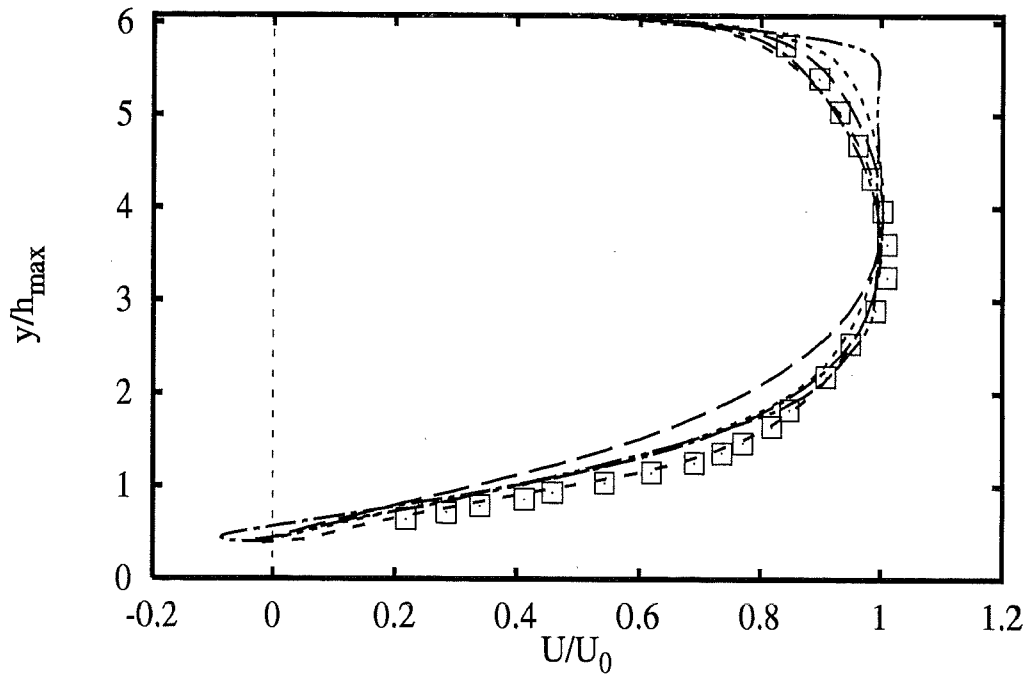
2B - 57



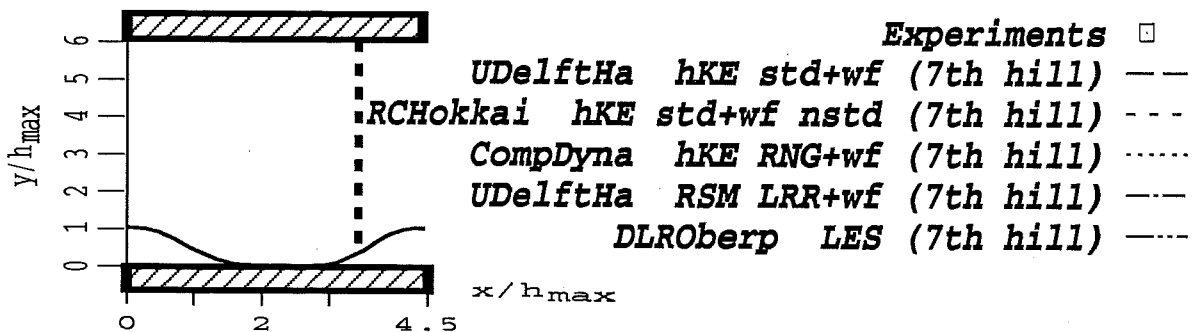
Profiles at $x/h_{max} = 2.25$

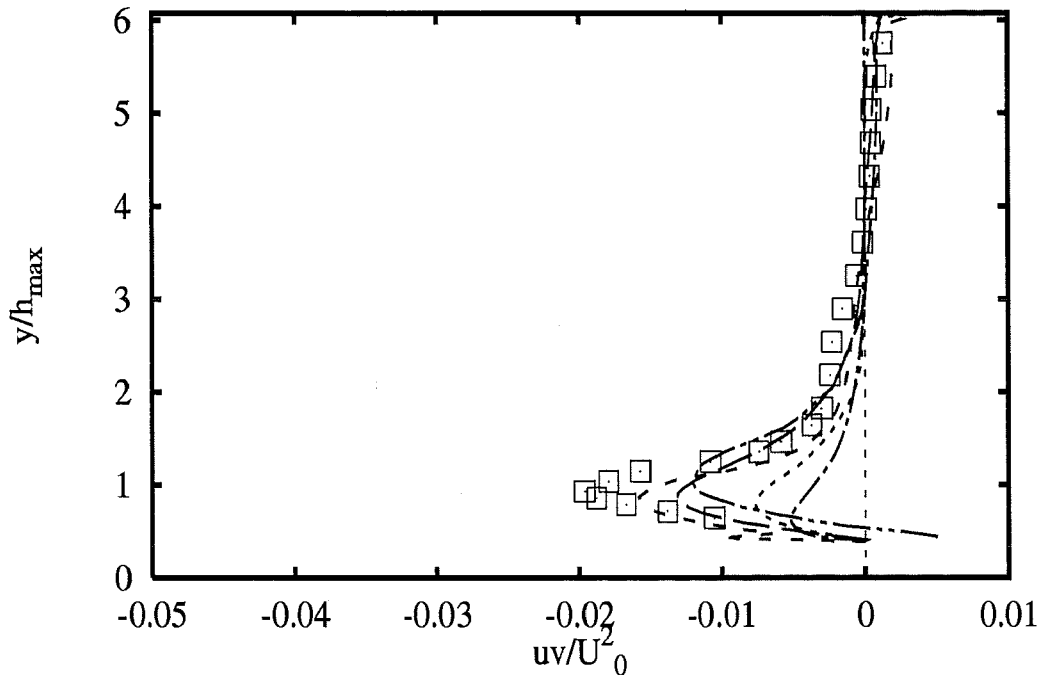
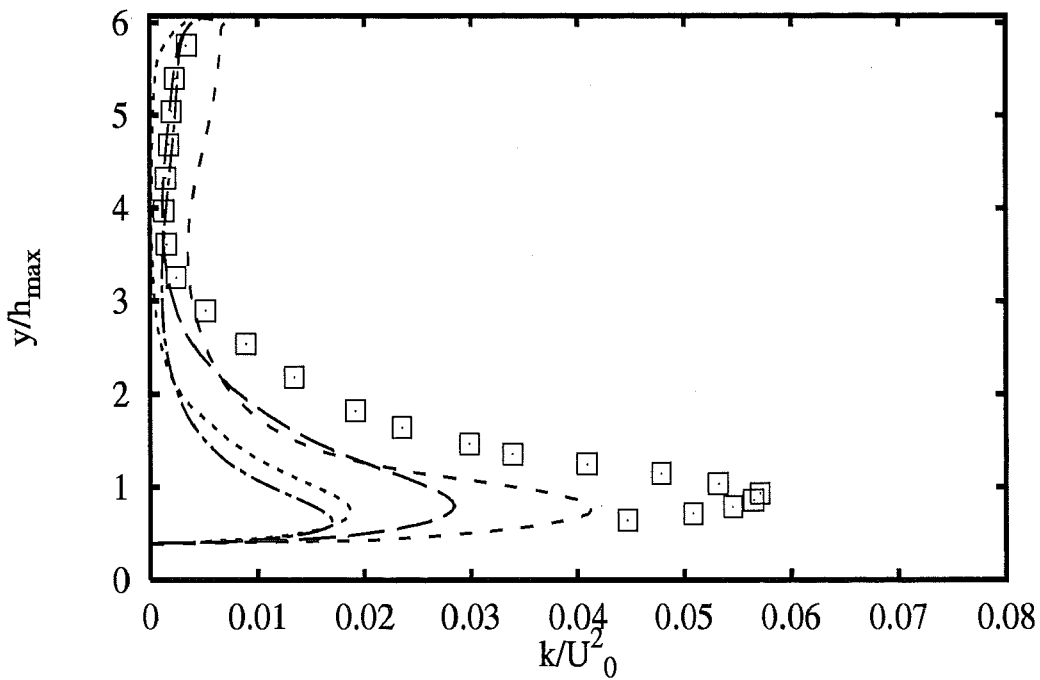


2B - 58

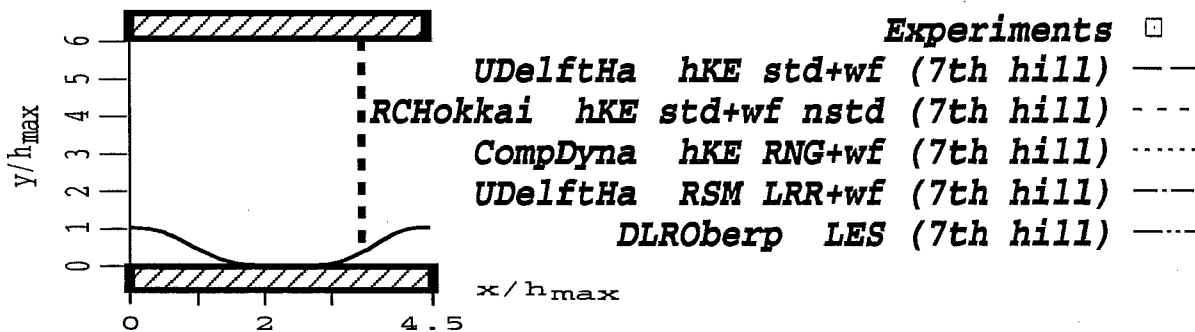


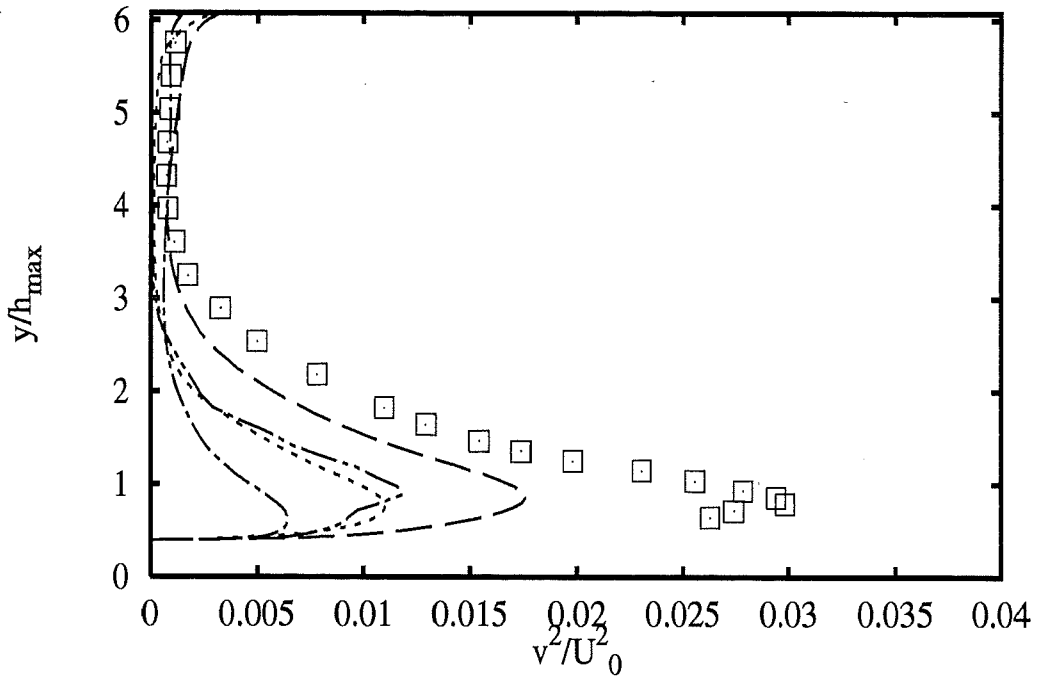
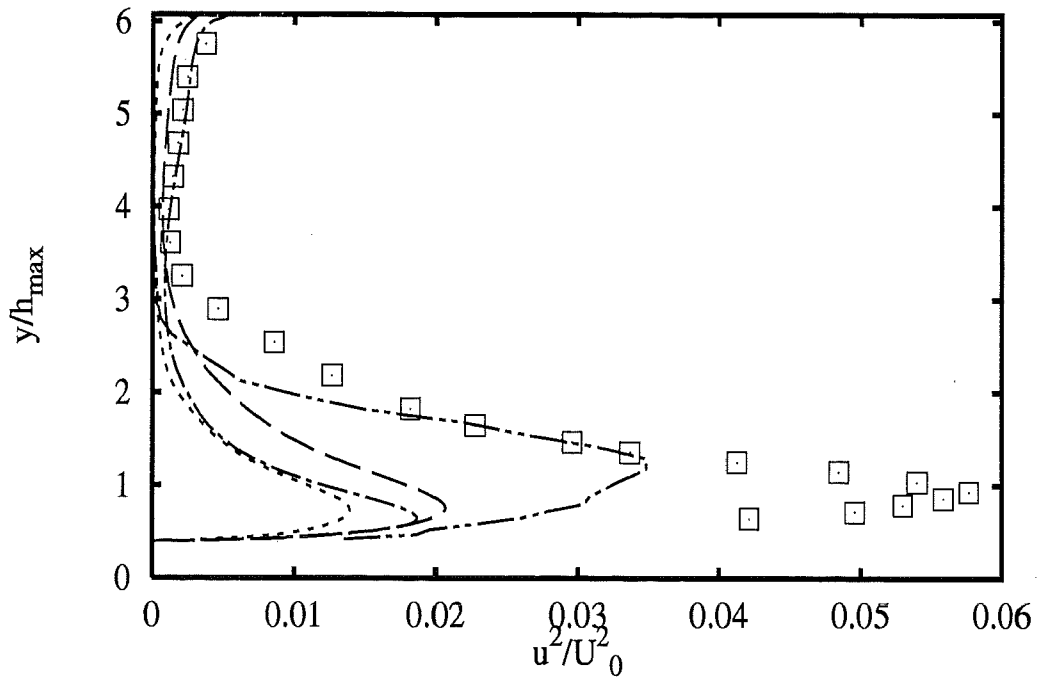
Profiles at $x/h_{max} = 3.43$



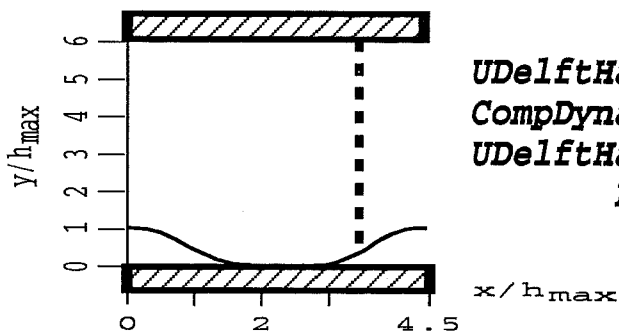


Profiles at $x/h_{max} = 3.43$



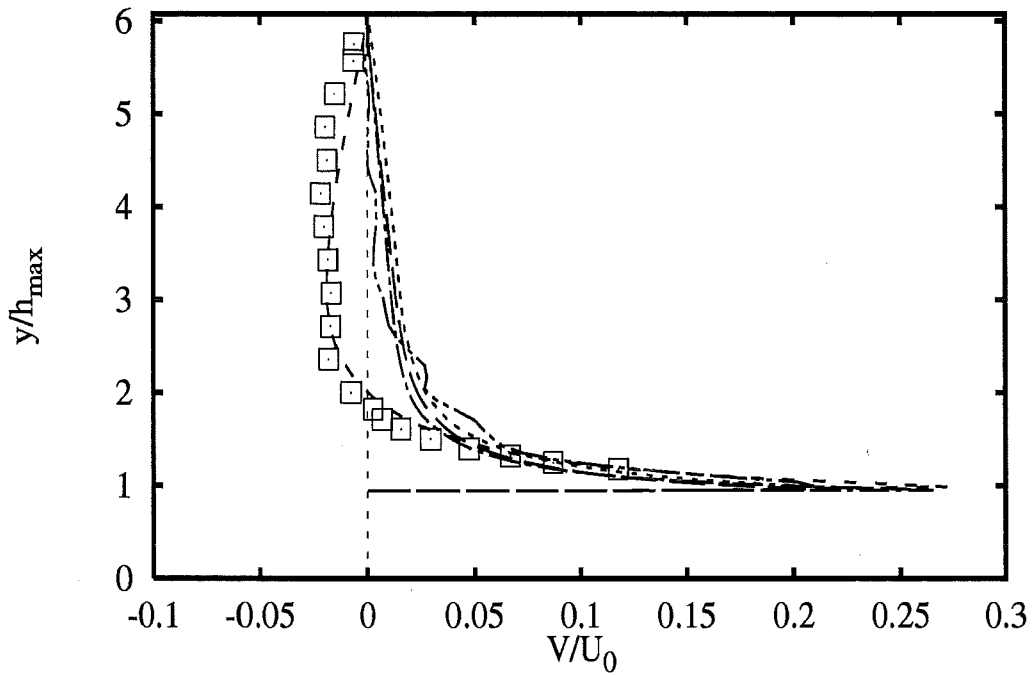
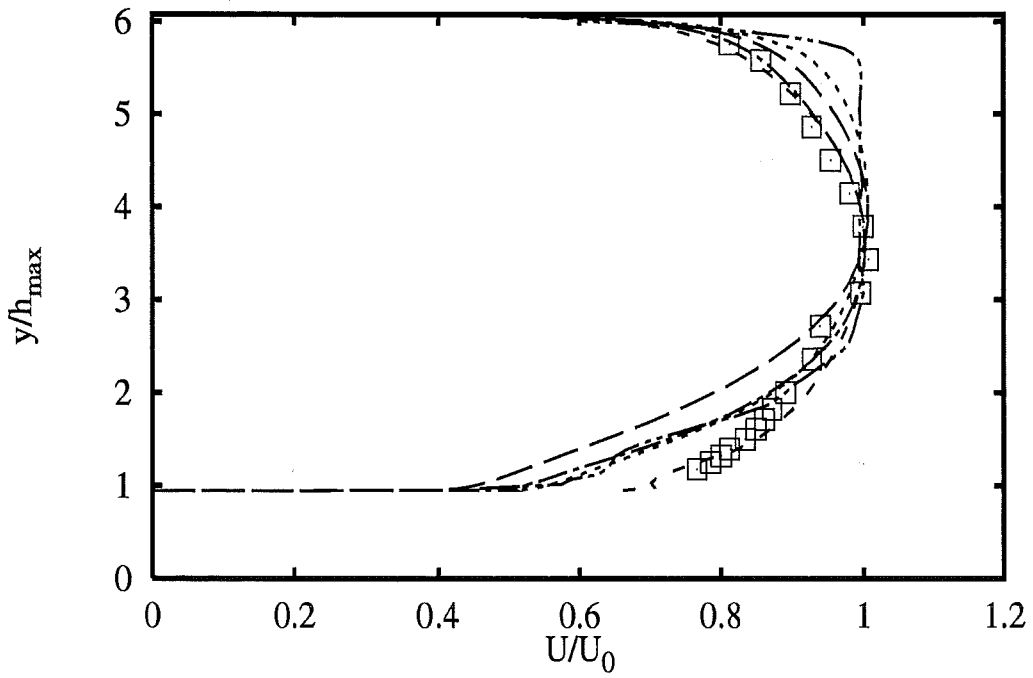


Profiles at $x/h_{max} = 3.43$

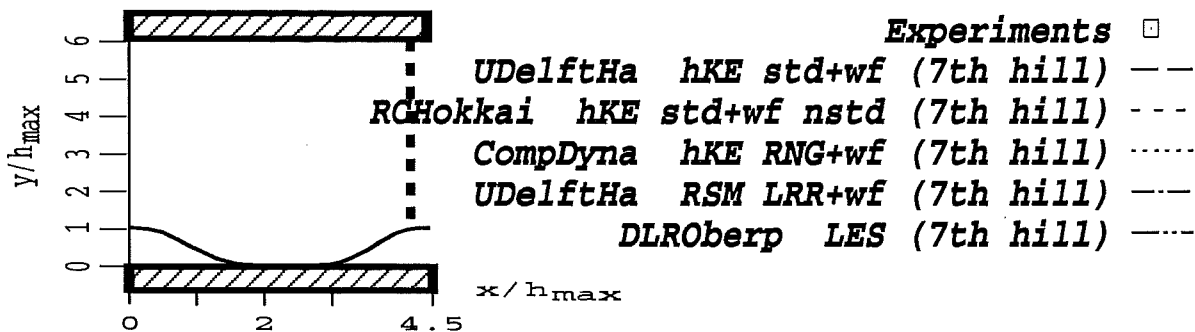


- | | | |
|----------|-----------------------|---------|
| | Experiments | □ |
| UDelftHa | hKE std+wf (7th hill) | — — |
| CompDyna | hKE RNG+wf (7th hill) | · · · · |
| UDelftHa | RSM LRR+wf (7th hill) | - - - - |
| DLROberp | LES (7th hill) | — · — · |

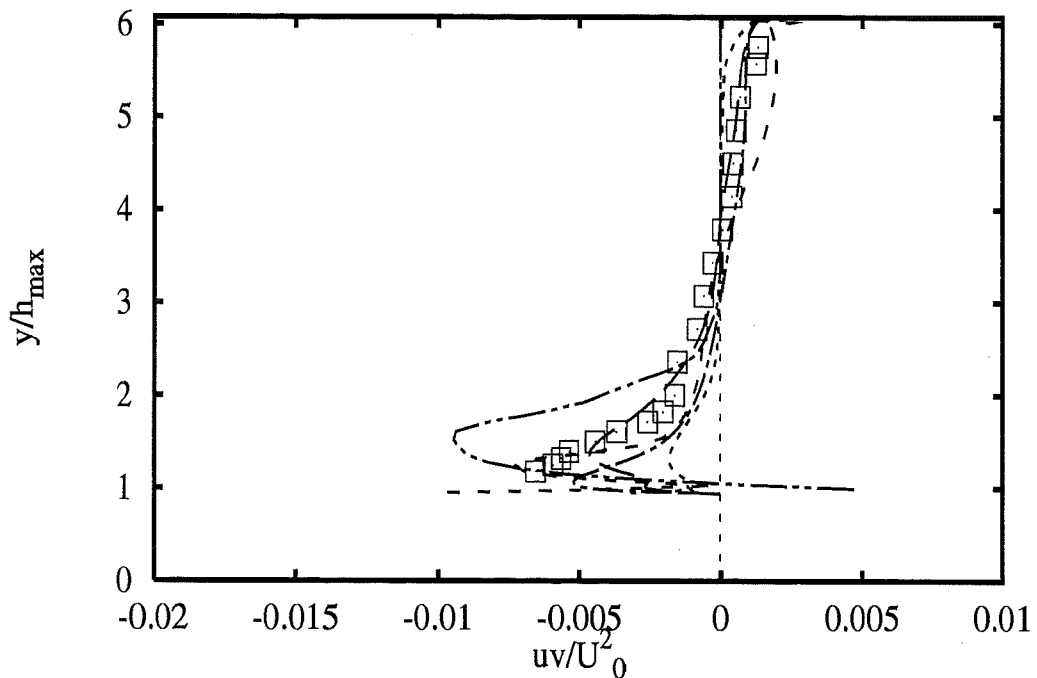
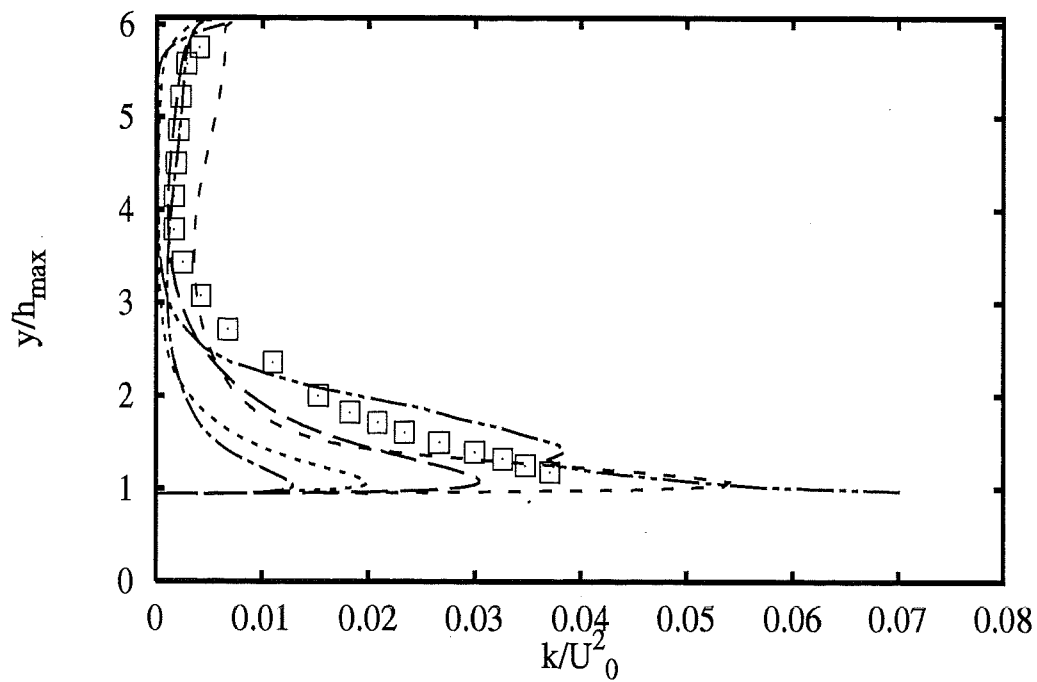
2B - 61



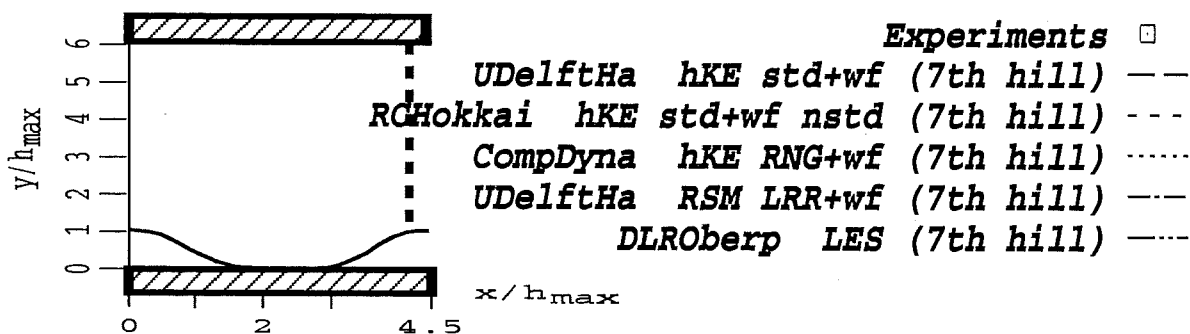
Profiles at $x/h_{max} = 4.14$



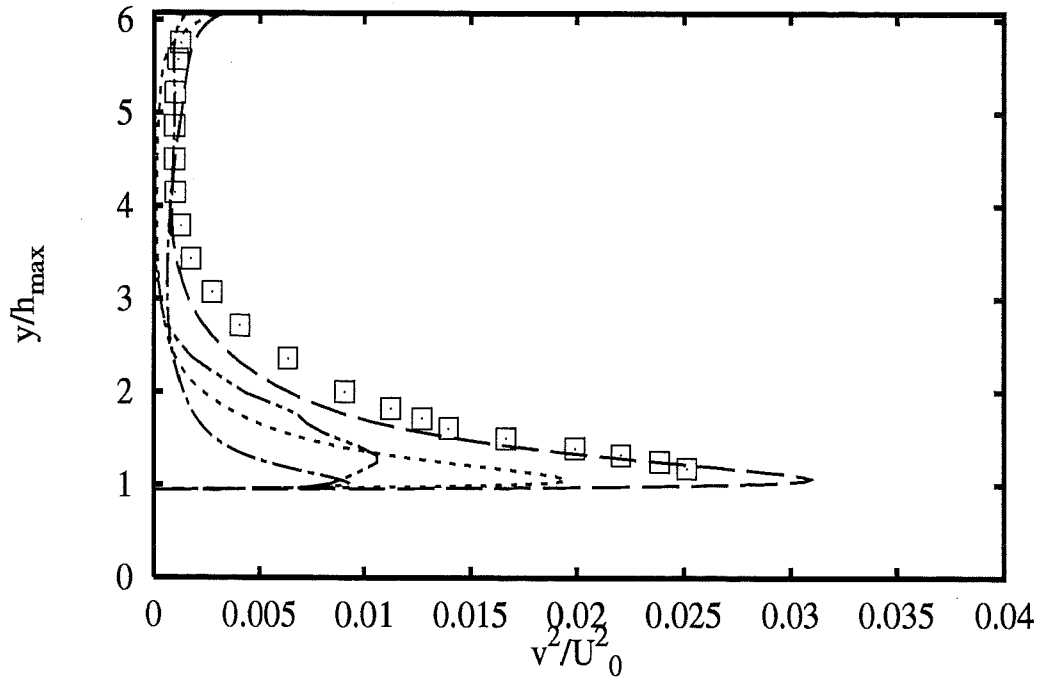
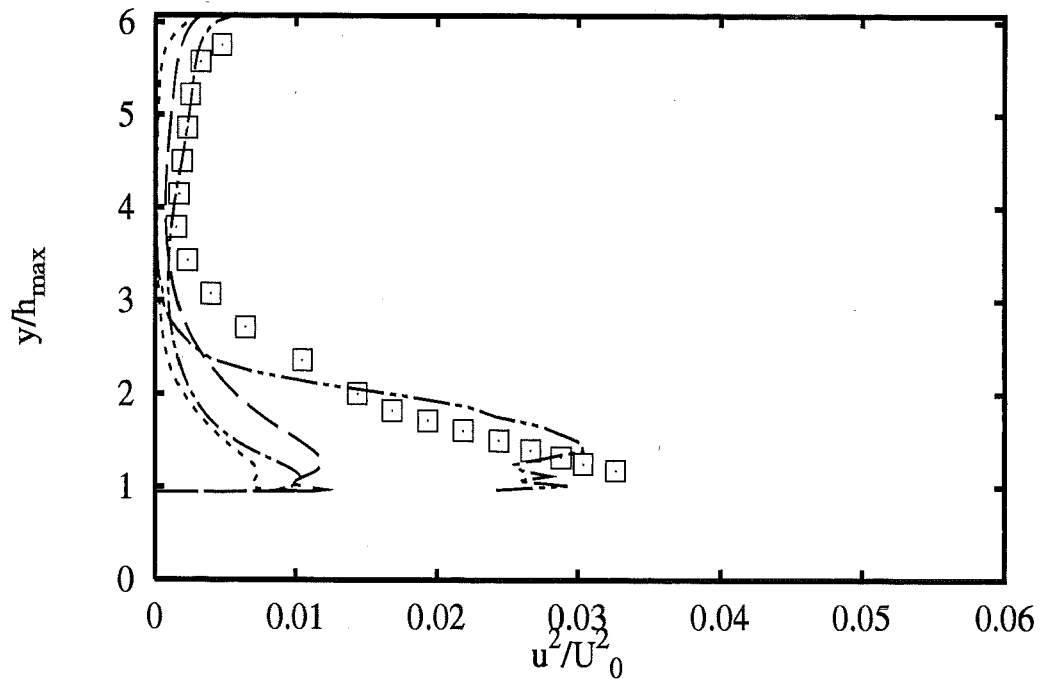
2B - 62



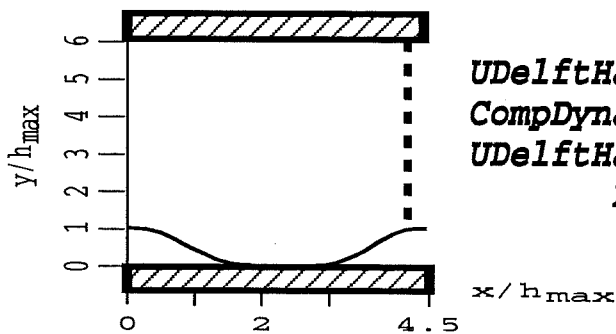
Profiles at $x/h_{max} = 4.14$



2B - 63



Profiles at $x/h_{max} = 4.14$



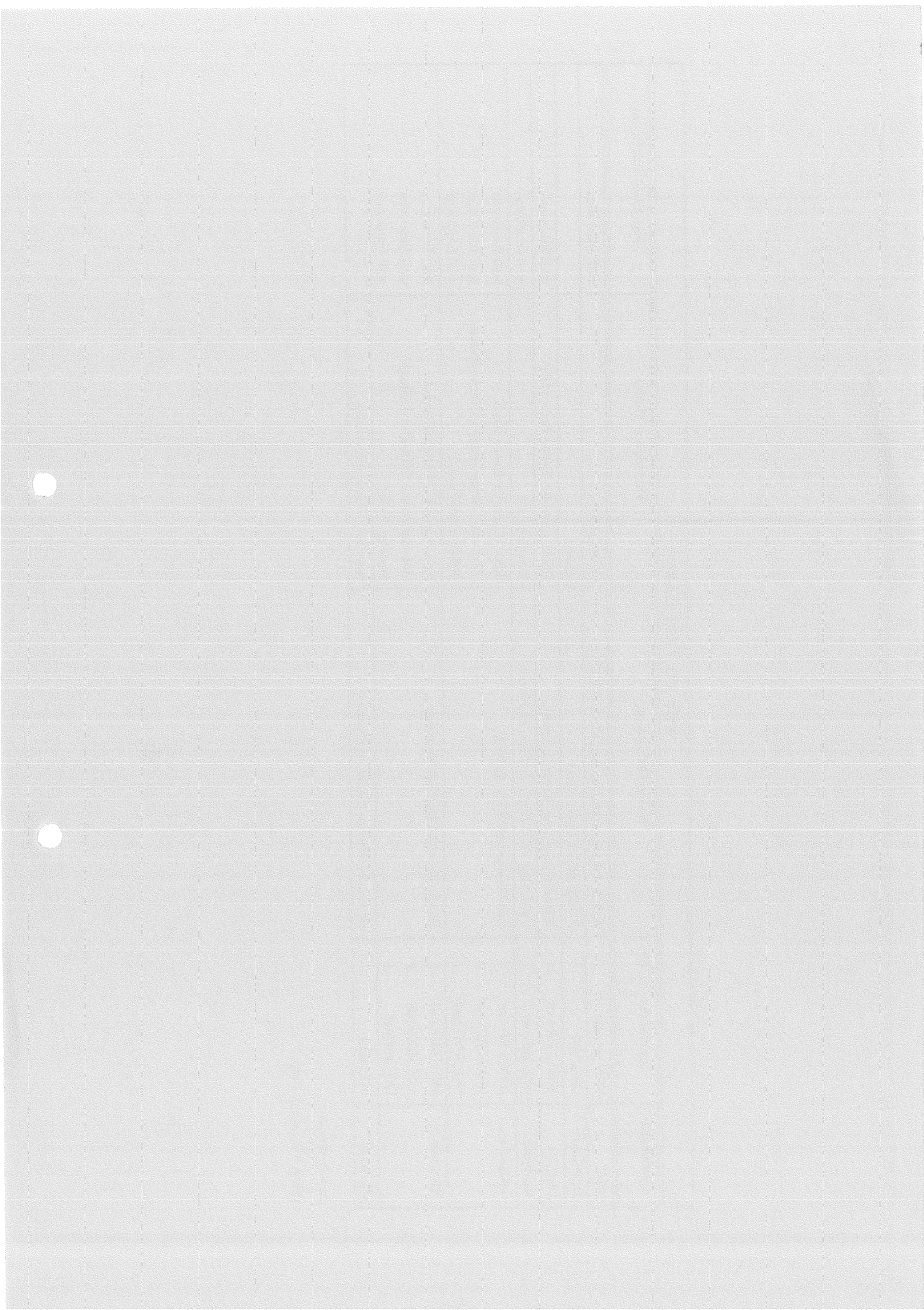
- Experiments** □
- UDelftHa hKE std+wf (7th hill) — —
 - CompDyna hKE RNG+wf (7th hill) ·····
 - UDelftHa RSM LRR+wf (7th hill) - - -
 - DLROberp LES (7th hill) - - -

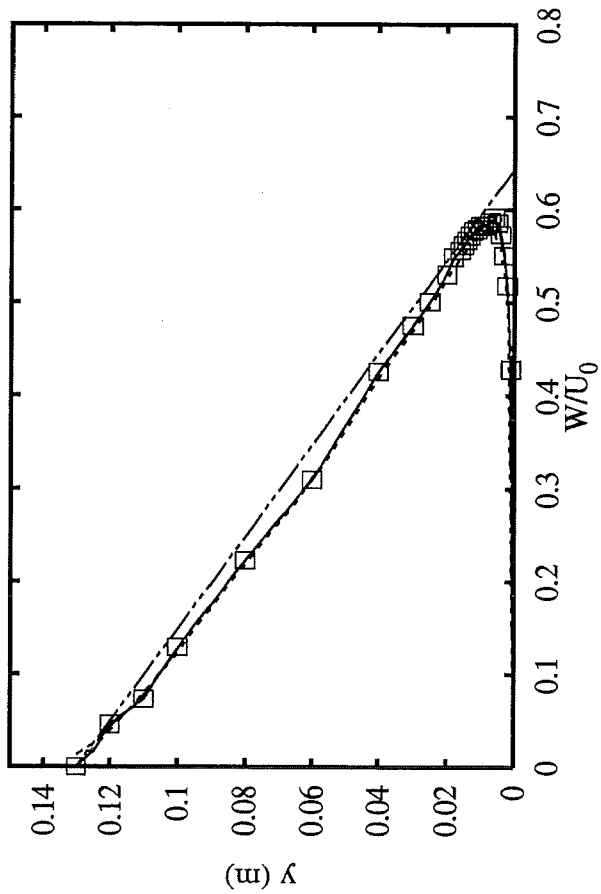
KEY TO TEST CASE 3

| Contributor | Key-Name | Gr. | Name (Affiliation) | Turbulence Model | Near-Wall Treatment |
|-------------|-------------|-----|---|--|---------------------|
| ASC | hKE_std+wf | 1 | Sick & Scheuerer (Sulzer Innotec & ASC) | standard k- ϵ | wall functions |
| DLRGoett | kOm_Wil | 1 | Kessler (DLR Goettingen) | k- ω | — |
| ECLyon | RSM_LRR+wf | 2 | Brison et al. (Ecole Centrale Lyon) | RSM Launder-Reece-Rodi (IP) | wall functions |
| GEHydro | hKE_std+wf | 1 | Vu & Shyy (GE Hydro & Univ. of Florida) | standard k- ϵ | wall functions |
| THAachen | RSM_LRR+wf | 2 | Gier/Krueger (RWTH Aachen) | RSM Launder-Reece-Rodi | wall functions |
| | ASM_CiWi+wf | 2 | | Algebraic-Stress Model Clarke-Wilkes | wall functions |
| | hKE_RNG+wf | 1 | | RNG-modified k- ϵ | wall functions |
| Ubrussel | nKE_HiKh+wf | 2 | Hirsch/Khodak (Univ. of Brussels) | non-linear k- ϵ Hirsch-Khodak | wall functions |
| | nKE_HiKh+wf | 2 | | non-linear k- ϵ Shih-Zhu-Lumley | wall functions |
| | hKE_std+wf | 1 | | standard k- ϵ | wall functions |
| UFlorenc | IKE_JoLa | 1 | Michelassi/Mugnai (Univ. of Florence) | low-Re k- ϵ Jones-Launder | — |

In key-names:

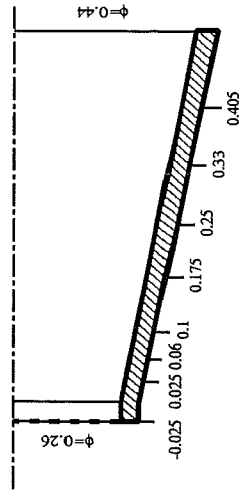
(3D): 3D calculations



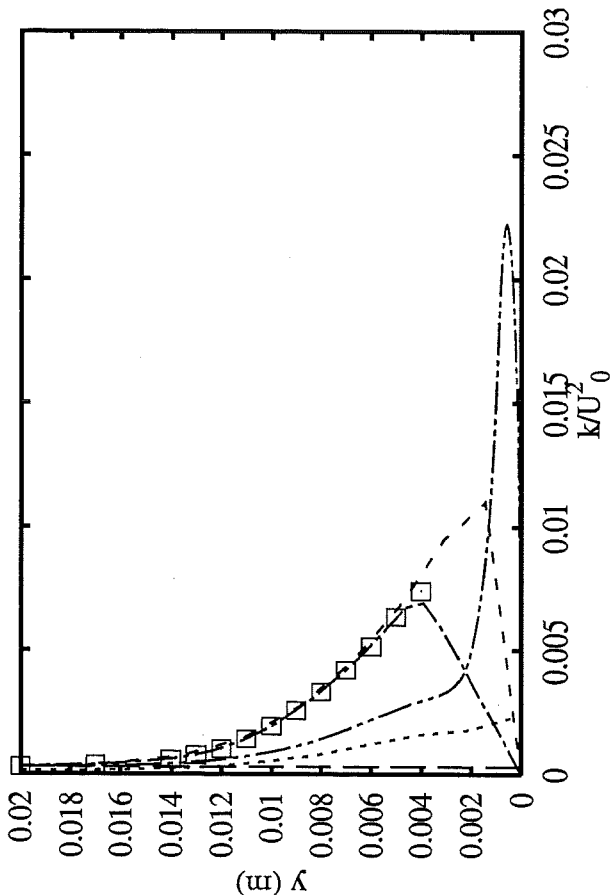
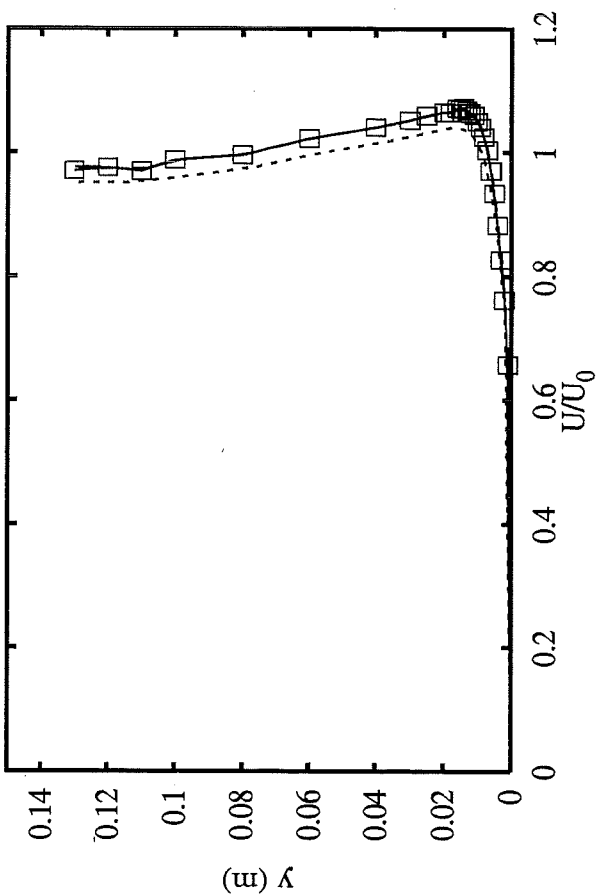


Profiles at $x = -0.025 \text{ m}$

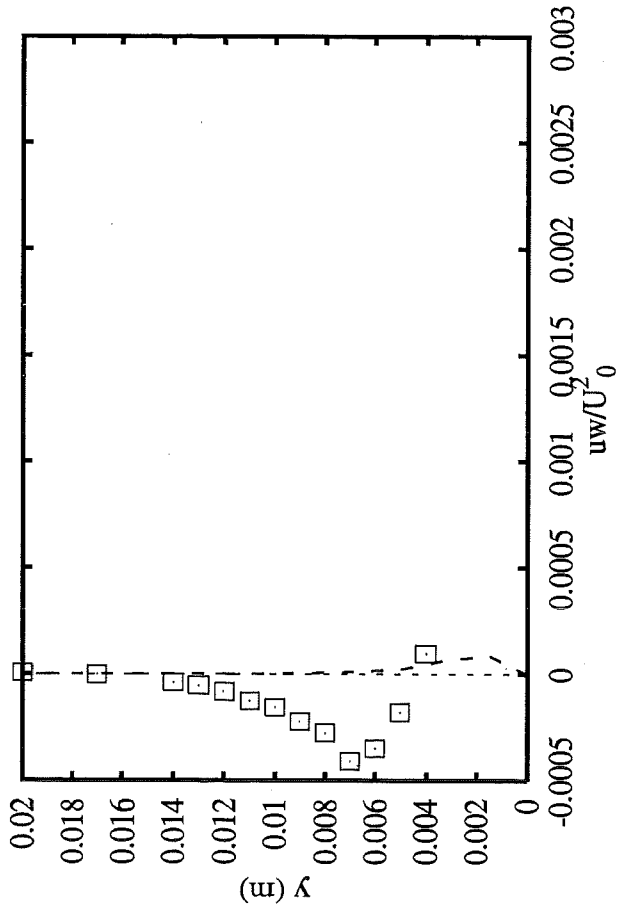
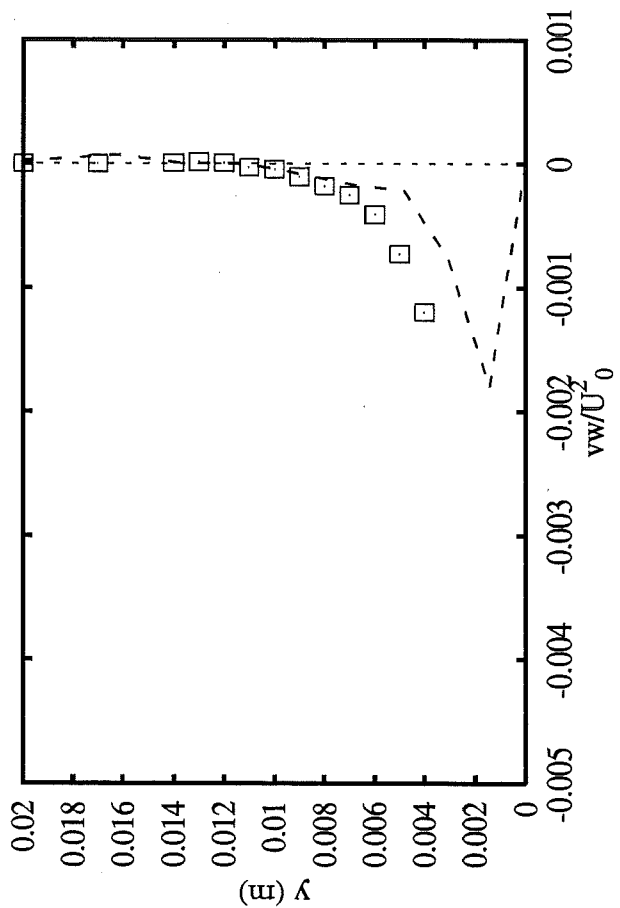
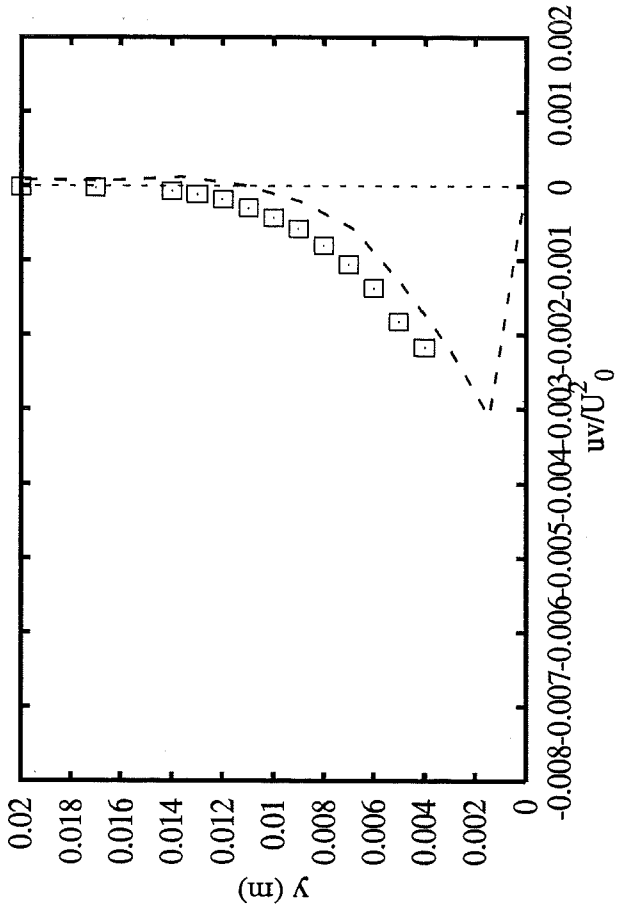
- Experiments \square
- ASC hKE std+wf ---
- UBrussel hKE std+wf - - -
- GEHydro hKE std+wf (3D) ·····
- THAachen hKE RNG+wf - · - ·
- UFlorenc IKE JoLa - - -



Swirling boundary layer in conical diffuser
Group 1: k-epsilon and k-omega models

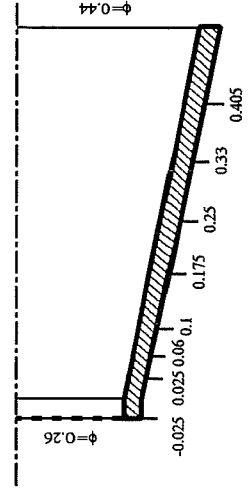


4th ERCOFTAC/IAHR Workshop on Refined Flow Modelling
April 3-7, 1995, University of Karlsruhe, Germany

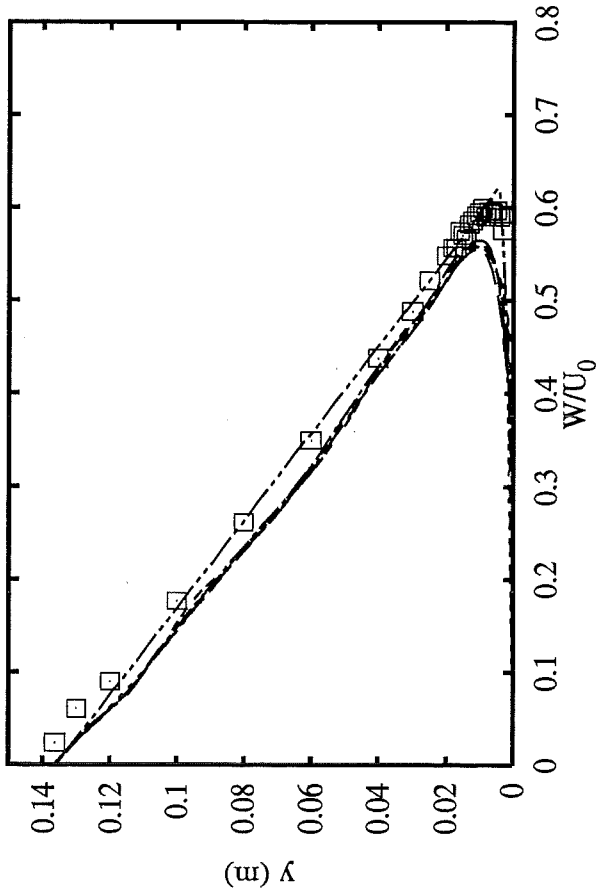


Profiles at $x=-0.025$ m

Experiments \square
UBrunsel hKE std+wf ---

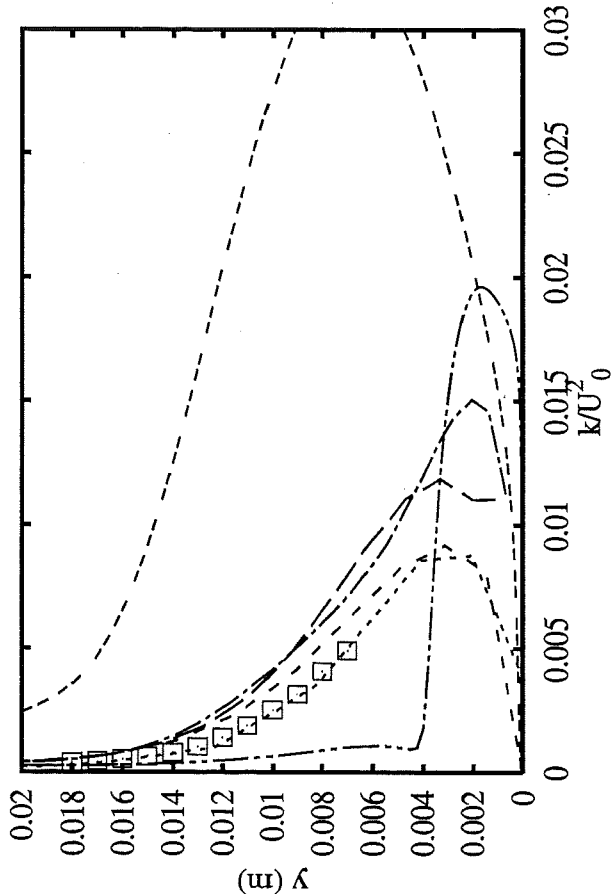
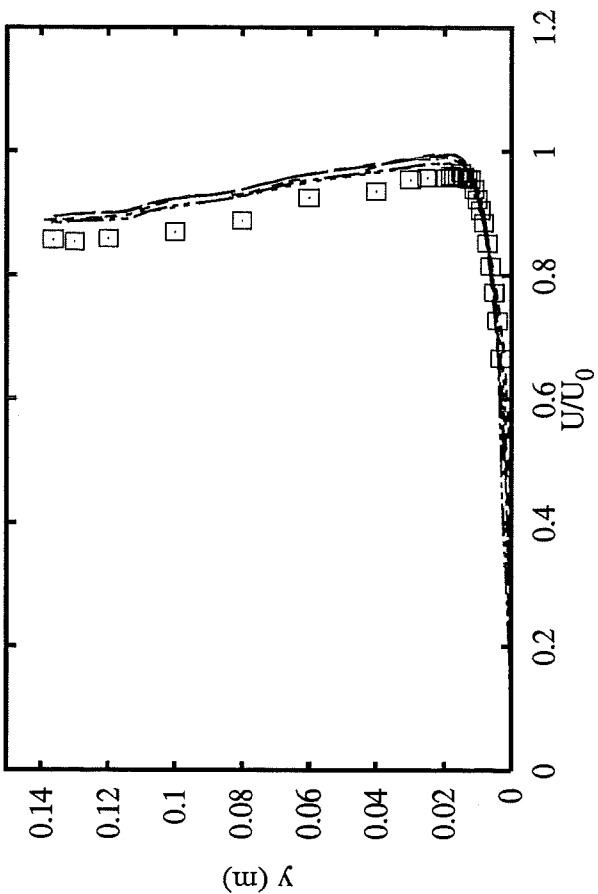
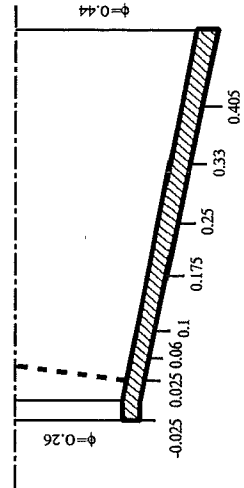


Swirling boundary layer in conical diffuser
Group 1: k-epsilon and k-omega models



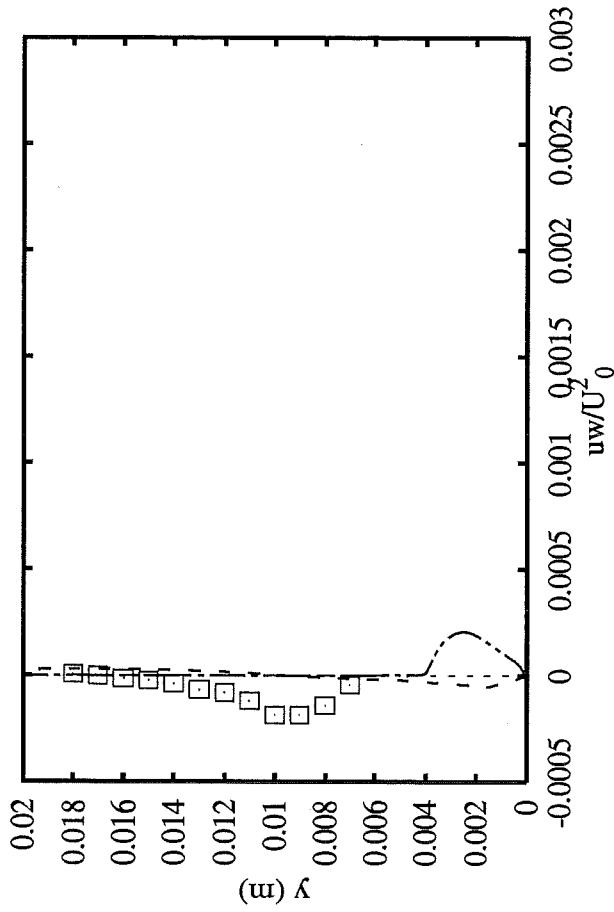
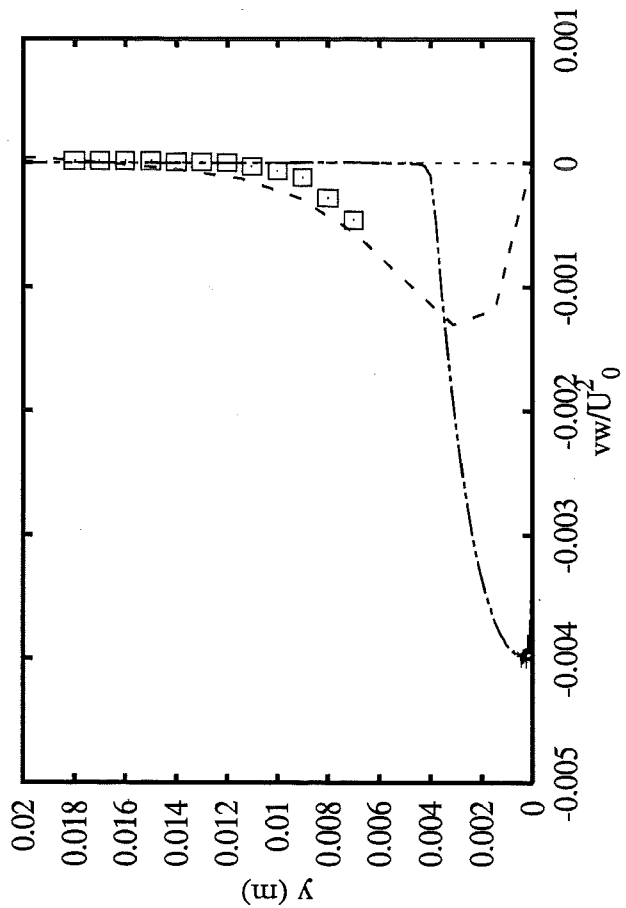
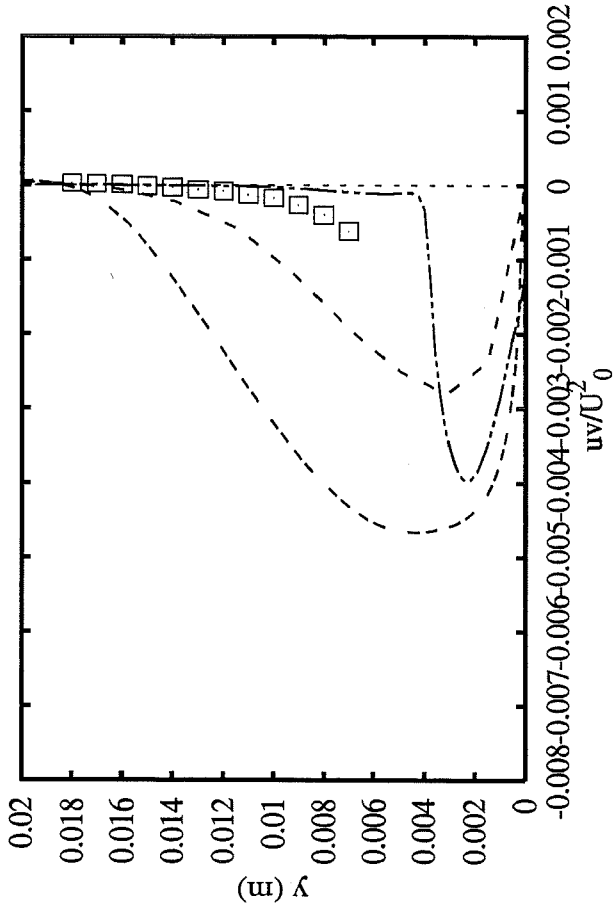
Profiles at $x=0.025$ m

- Experiments \square
- ASC hKE std+wf $---$
- UBrusse1 hKE std+wf $----$
- GEHydro hKE std+wf (3D) $-----$
- THAachen hKE RNG+wf $-----$
- UFlorenc IKE JOLA $-----$
- DLRGoett kOm Wil $-----$



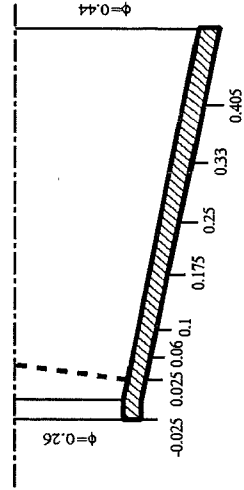
Swirling boundary layer in conical diffuser
Group 1: k-epsilon and k-omega models

4th ERCOFTAC/IAHR Workshop on Refined Flow Modelling
April 3-7, 1995, University of Karlsruhe, Germany



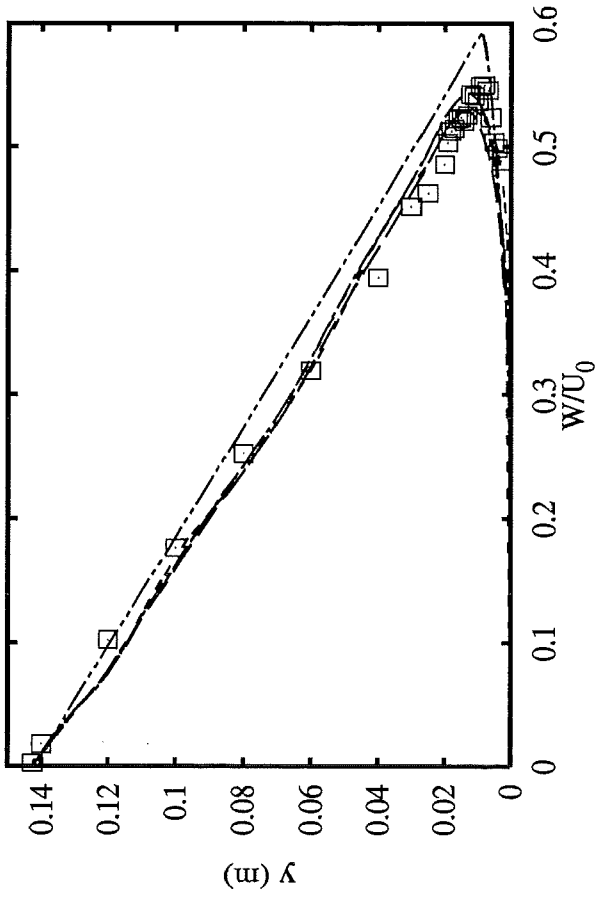
Profiles at $x=0.025$ m

- Experiments \square
- UBrusse1 hKE std+wf ---
- UFlorenc IKE JoLa - - -
- DLRGoett kOm Wil - - -



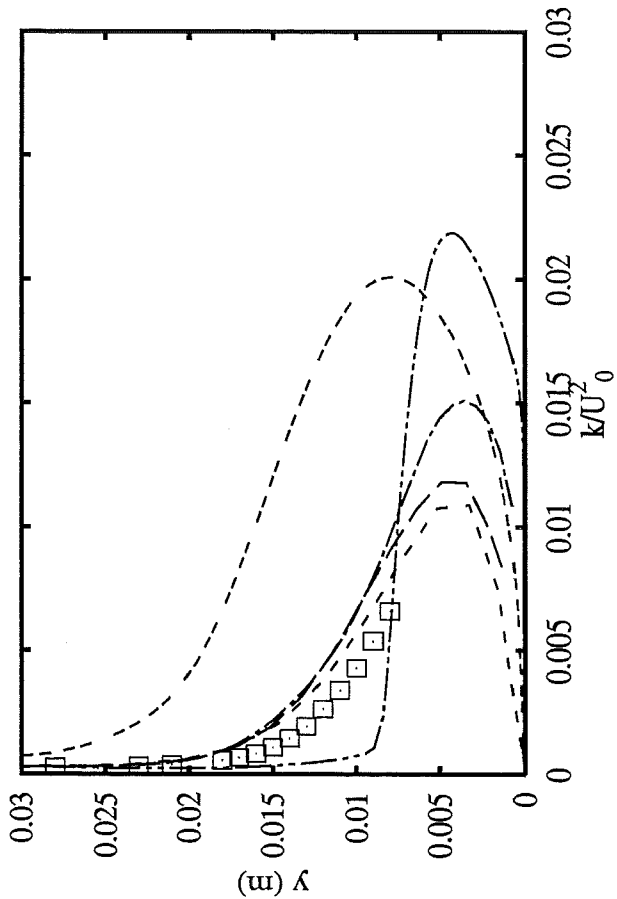
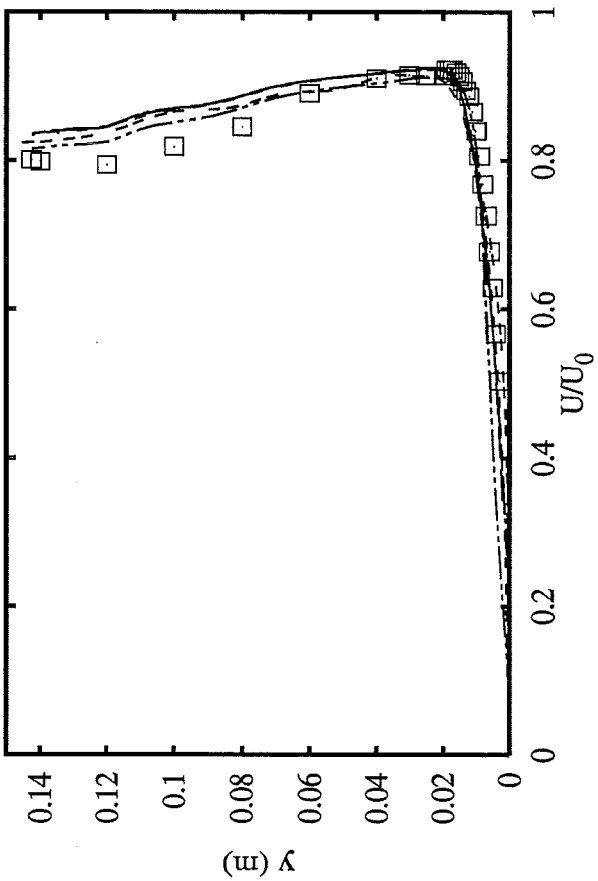
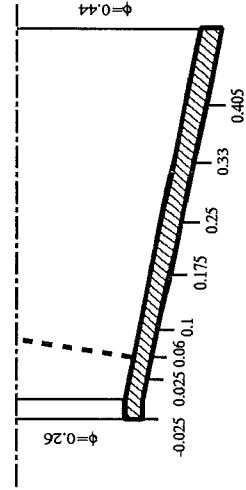
4th ERCOFTAC/IAHR Workshop on Refined Flow Modelling
 April 3-7, 1995, University of Karlsruhe, Germany

Swirling boundary layer in conical diffuser
 Group 1: k-epsilon and k-omega models



Profiles at $x=0.060$ m

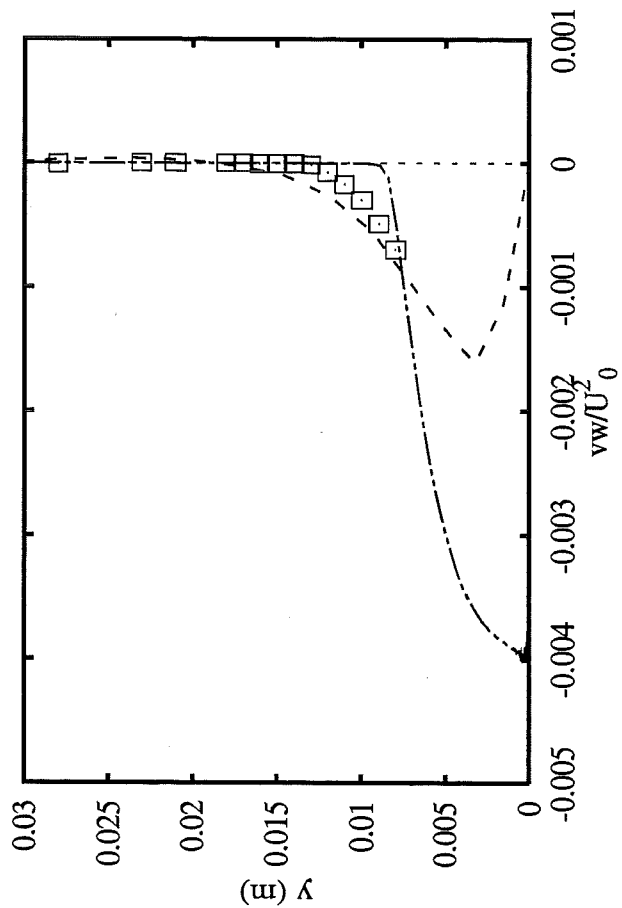
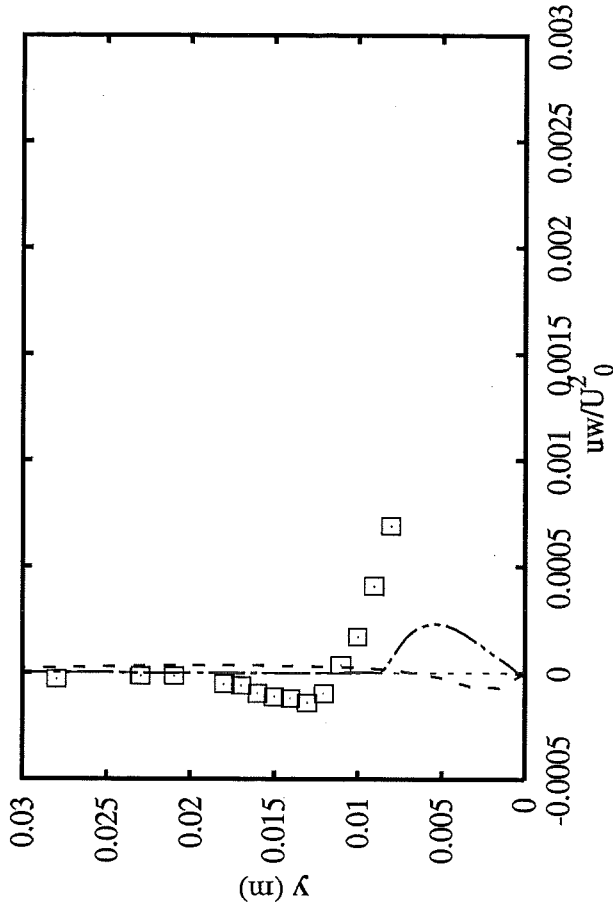
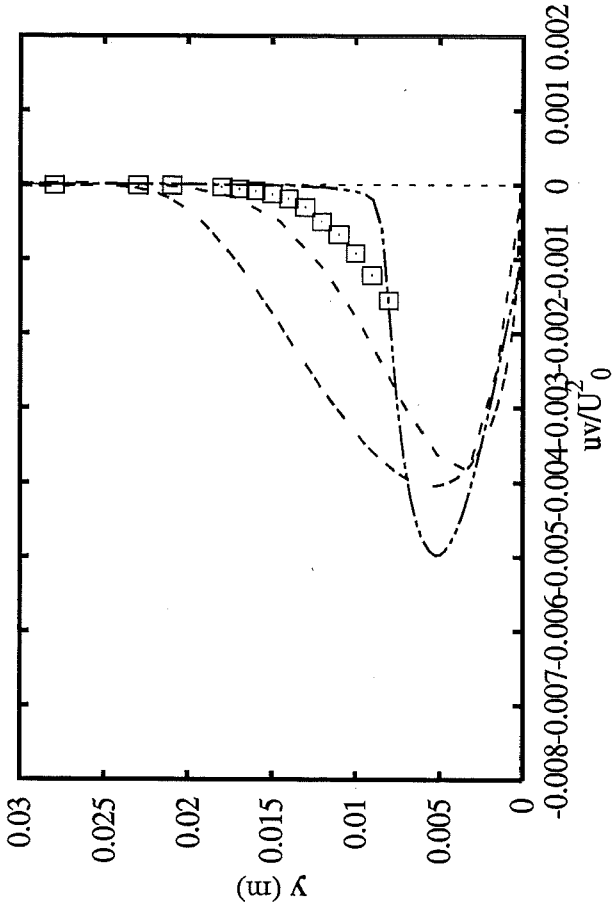
- Experiments \square
- ASC hKE std+wf ---
- UBrussel hKE std+wf - - -
- THAachen hKE RNG+wf - - -
- UFlorenc IKE JOLA - - -
- DLRGoett kOm Wil - - -



Swirling boundary layer in conical diffuser
Group 1: k-epsilon and k-omega models

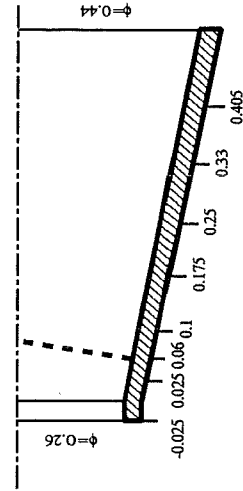
3 - 5

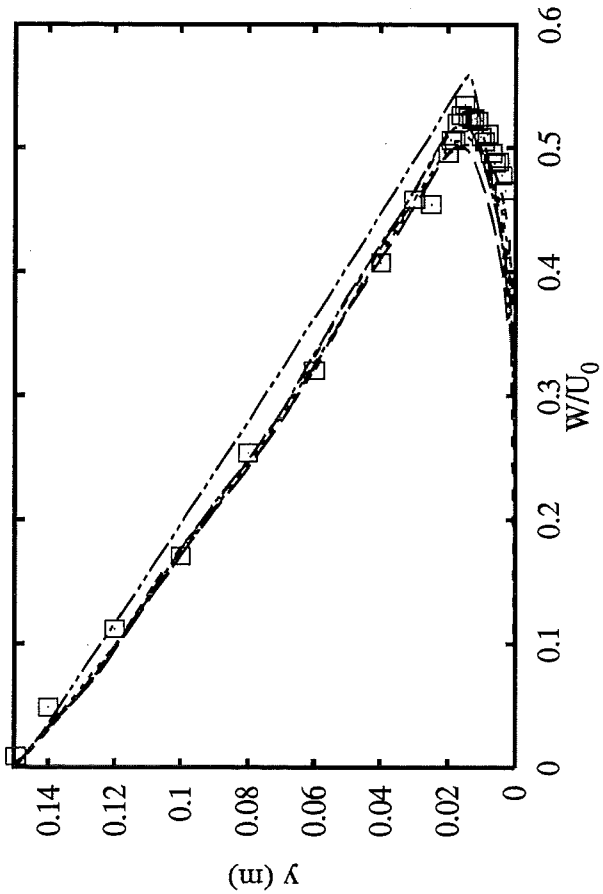
4th ERCOFTAC/IAHR Workshop on Refined Flow Modelling
April 3-7, 1995, University of Karlsruhe, Germany



Profiles at $x=0.060$ m

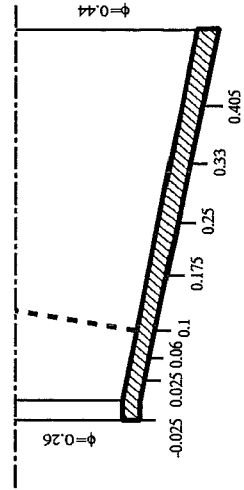
- Experiments \square
- UBrussel hKE std+wf - - -
- UFlorenc IKE JoLa - - -
- DLRGoett kOm Wil - - -



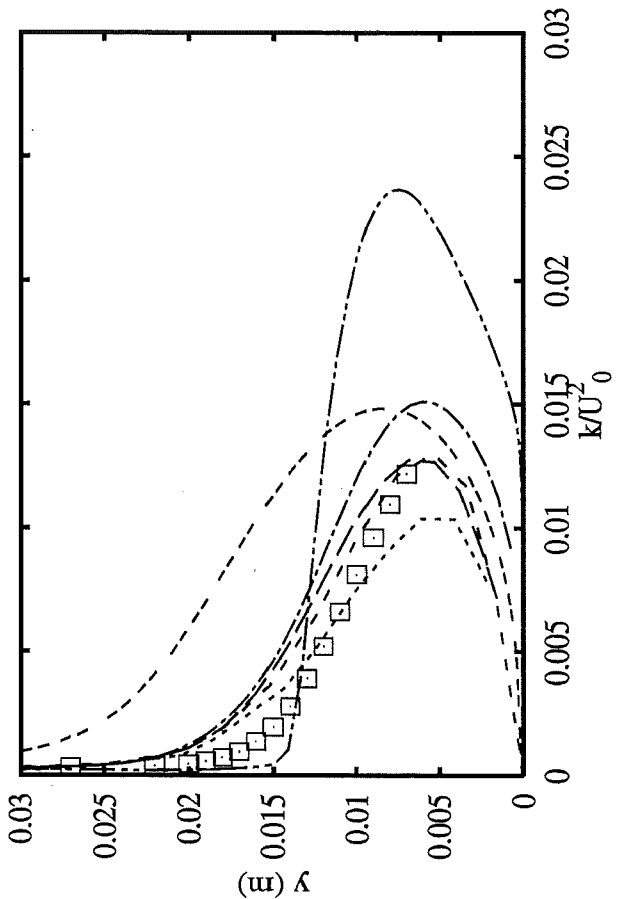
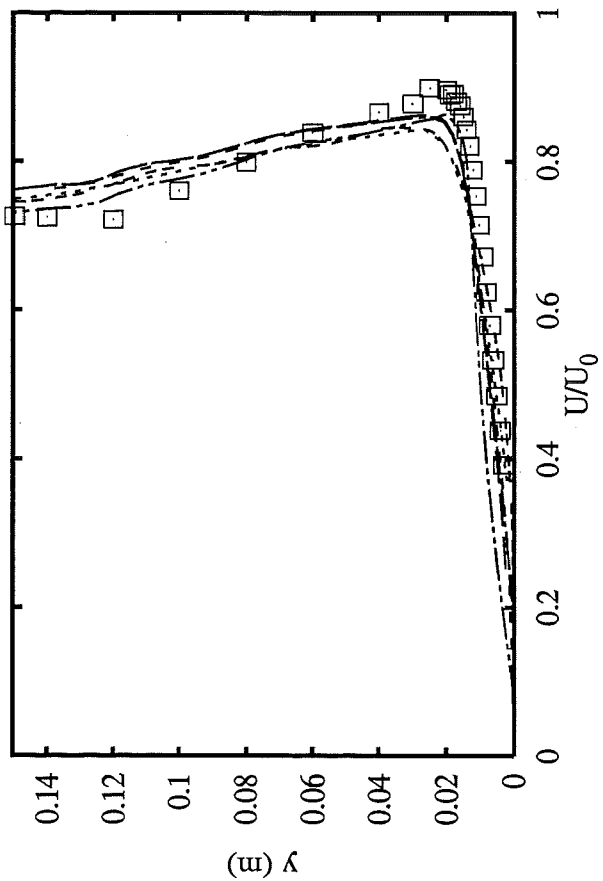


Profiles at $x=0.100$ m

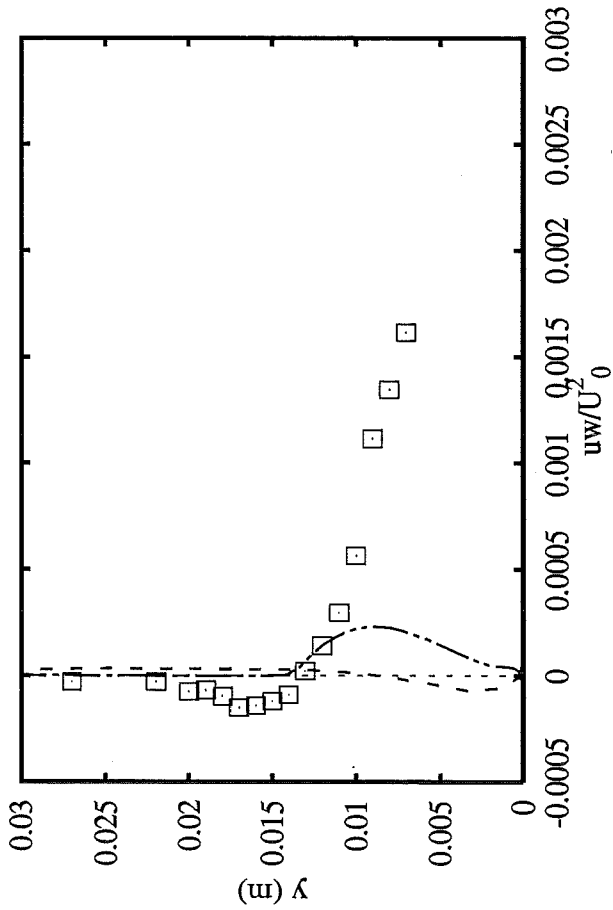
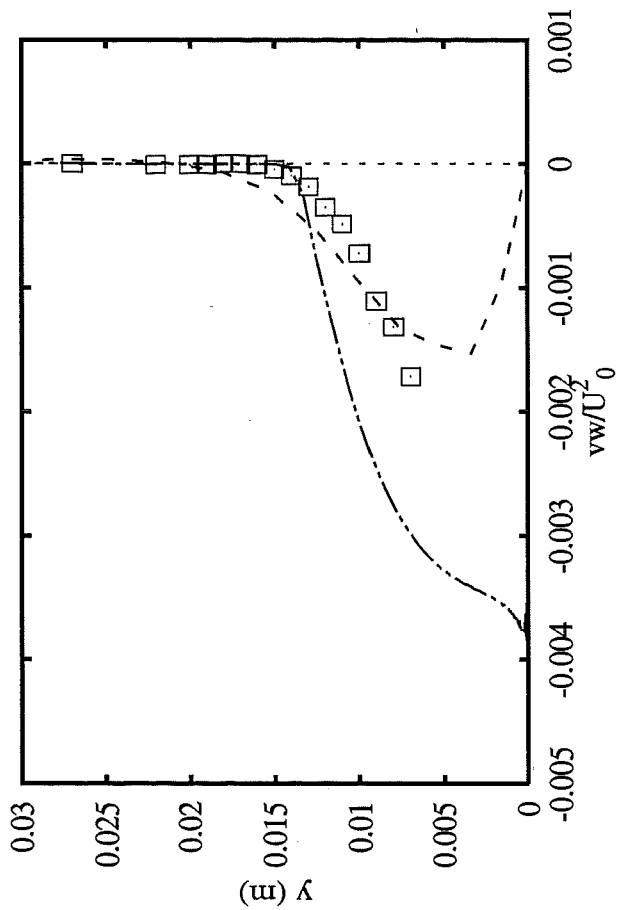
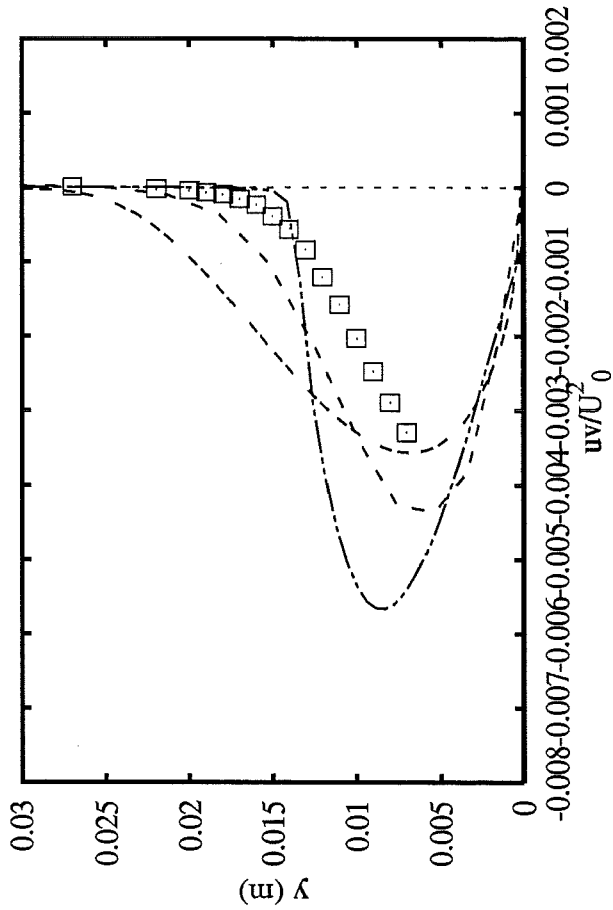
- Experiments \square
- ASC hKE std+wf
- UBrussel hKE std+wf
- GEHydro hKE std+wf (3D)
- THAachen hKE RNG+wf
- UFlorenc IKE JOLA
- DLRGoett kOm Wil



Swirling boundary layer in conical diffuser
Group 1: k-epsilon and k-omega models

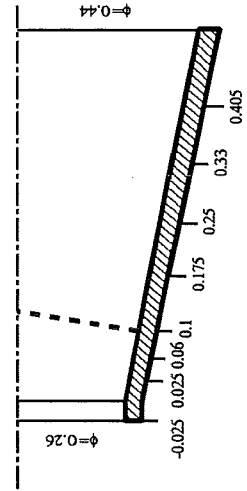


4th ERCOFTAC/IAHR Workshop on Refined Flow Modelling
April 3-7, 1995, University of Karlsruhe, Germany



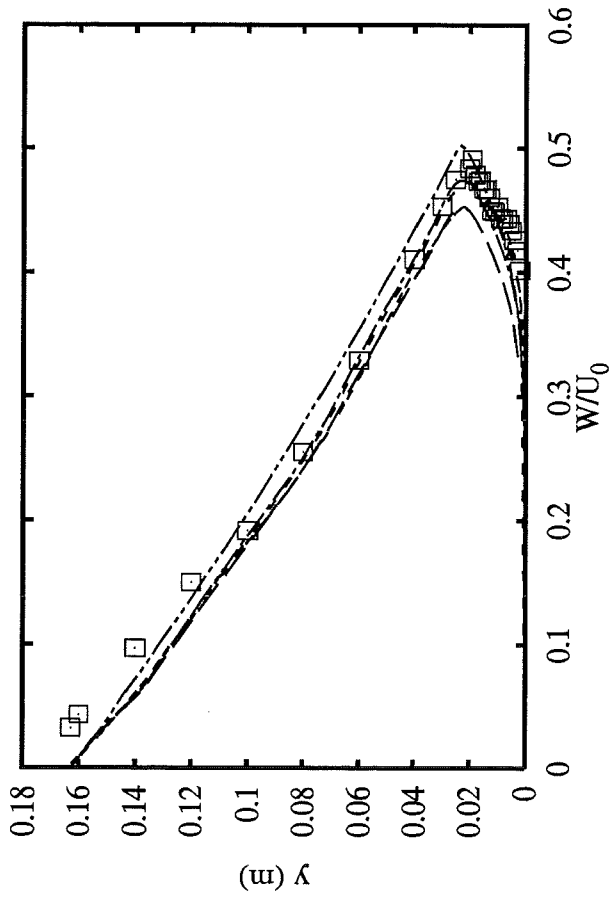
Profiles at $x=0.100$ m

- Experiments \square
- UBrusse1 hKE std+wf - - -
- UFlorence IKE JoLa - - -
- DLRGoett kOm Wil - - -



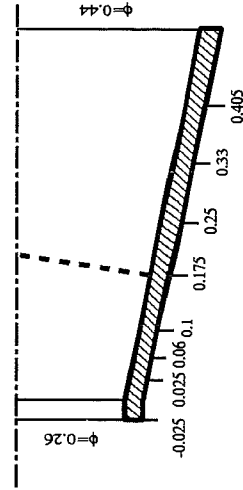
4th ERCOFTAC/IAHR Workshop on Refined Flow Modelling
 April 3-7, 1995, University of Karlsruhe, Germany

Swirling boundary layer in conical diffuser
 Group 1: k-epsilon and k-omega models

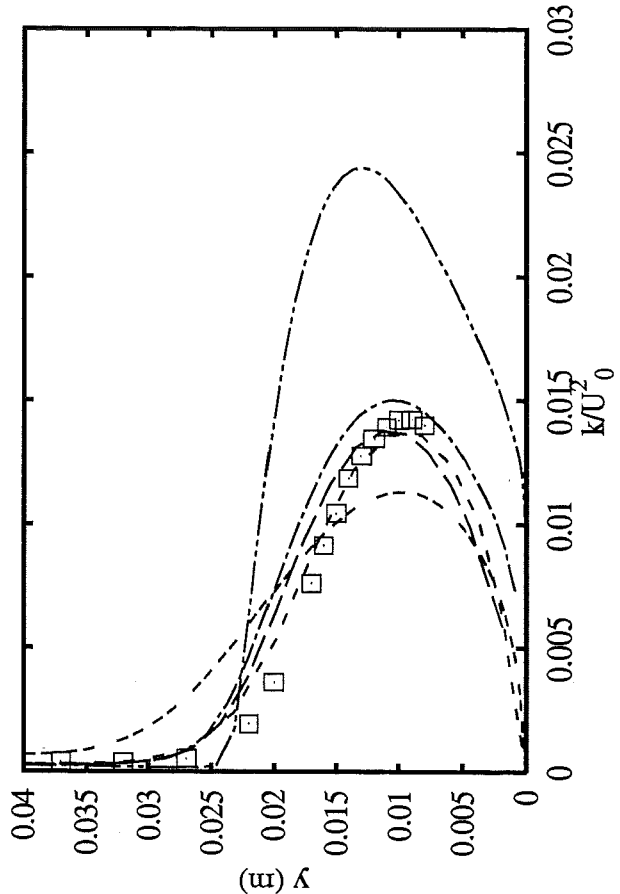
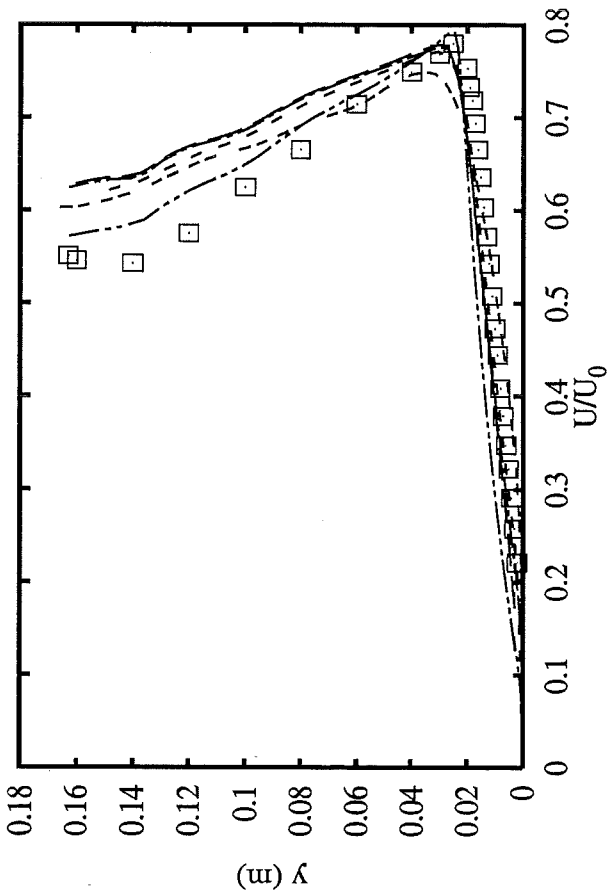


Profiles at $x=0.175$ m

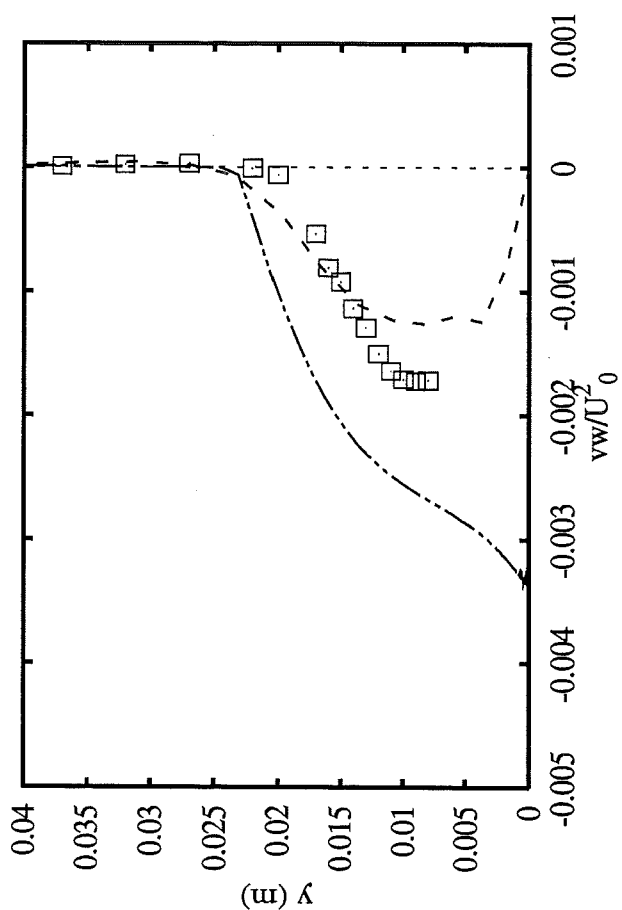
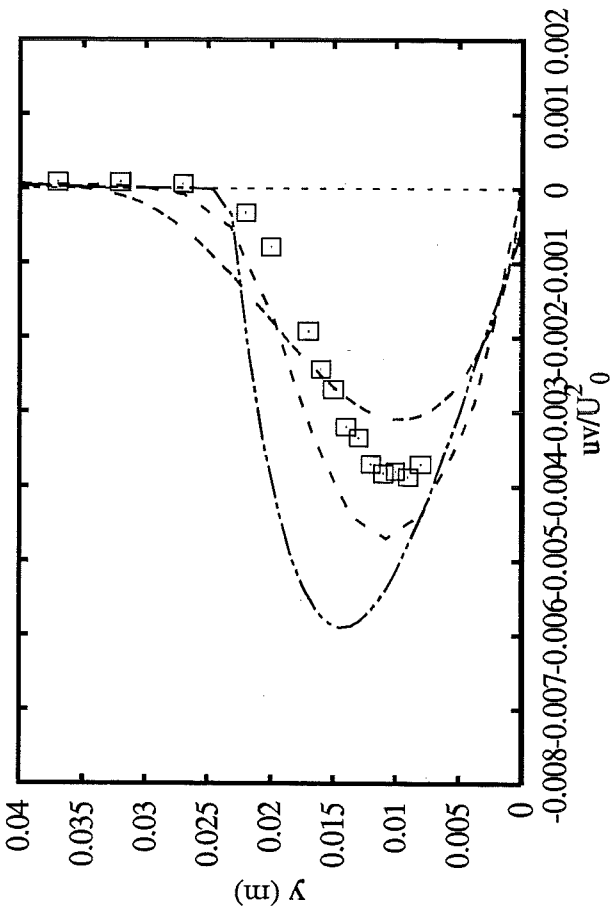
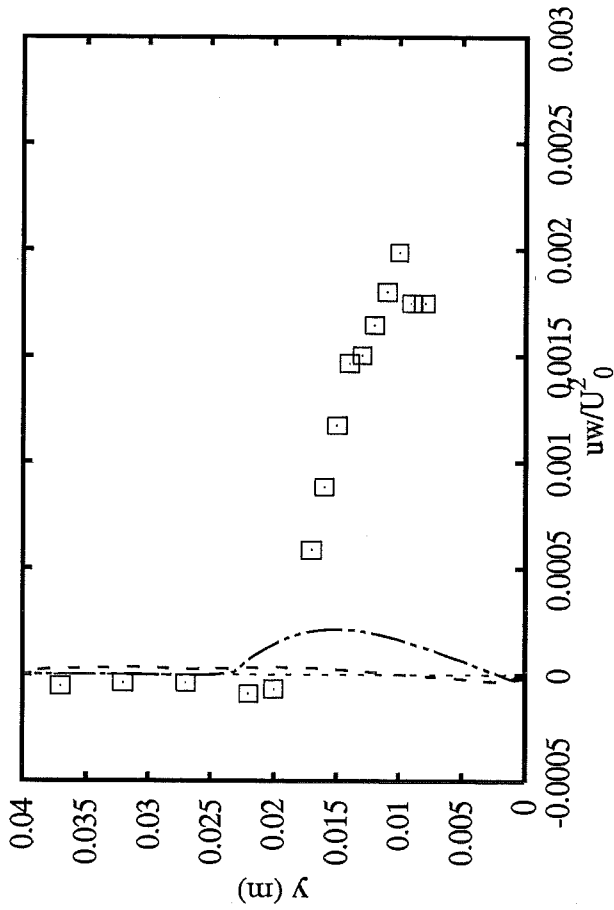
- Experiments \square
- ASC hKE std+wf ---
- UBrusse1 hKE std+wf -.-
- THAachen hKE RNG+wf ...
- UFlorenc IKE JOLA -.-.-
- DLRGoett kOm Wil -.-.-



Swirling boundary layer in conical diffuser
Group 1: k-epsilon and k-omega models

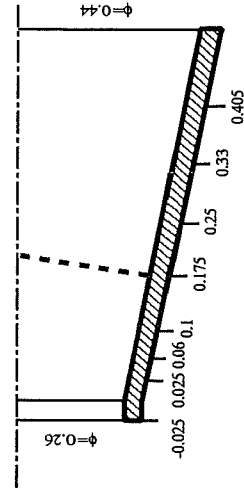


4th ERCOFTAC/IAHR Workshop on Refined Flow Modelling
April 3-7, 1995, University of Karlsruhe, Germany

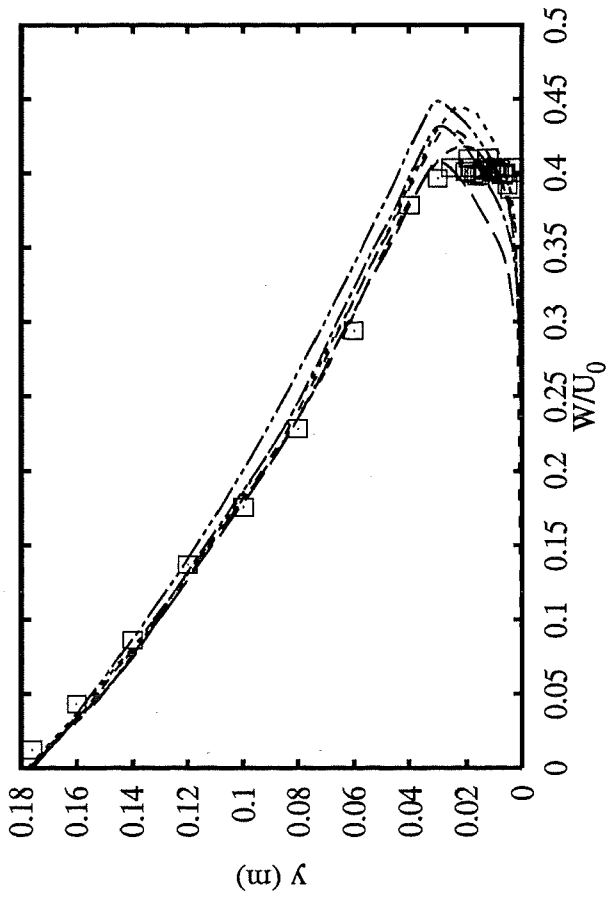


Profiles at x=0.175 m

- Experiments \square
- UBrusse1 hKE std+wf - - -
- UFlorenc IKE JOLA - - -
- DLRGoett kOm Wil - - -

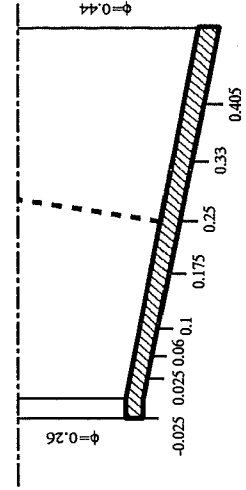


Swirling boundary layer in conical diffuser
Group 1: k-epsilon and k-omega models



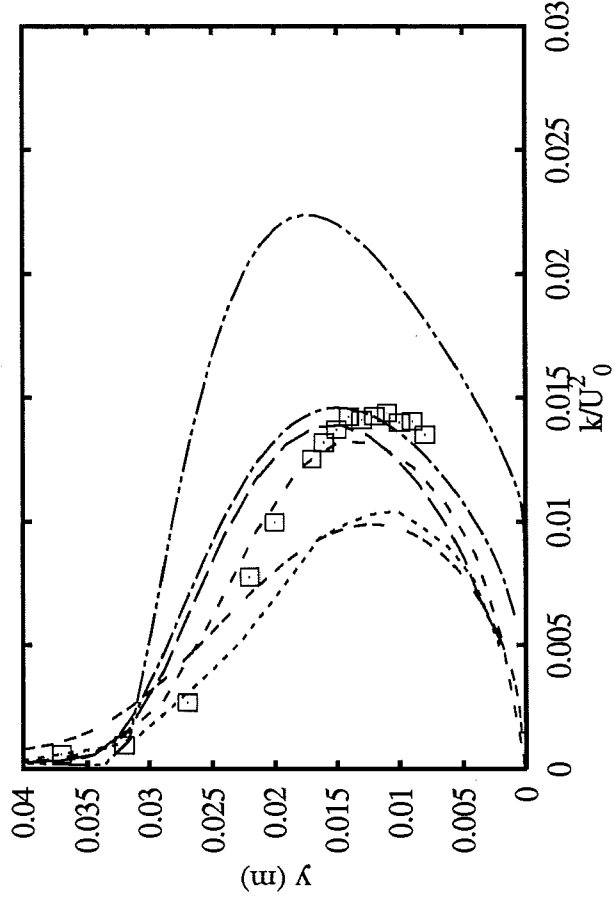
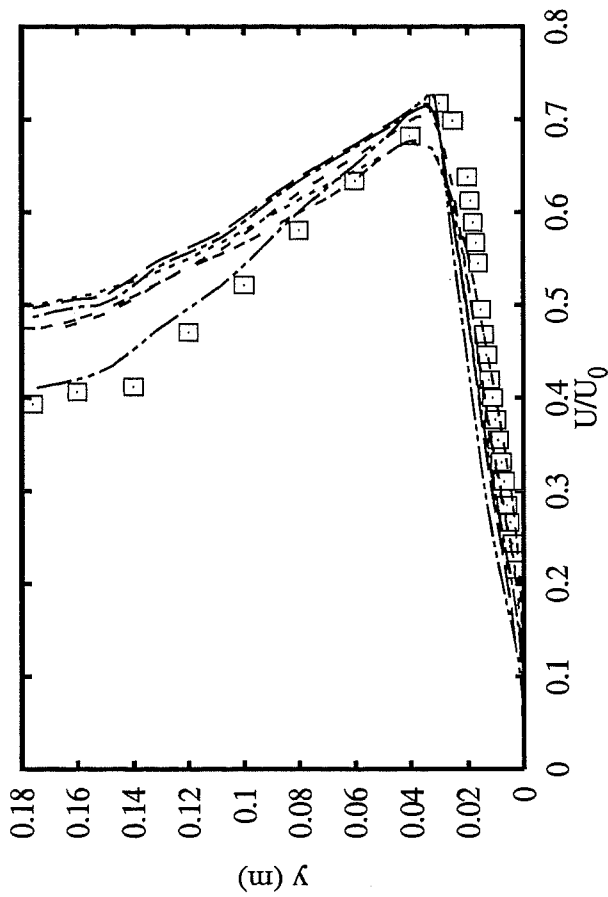
Profiles at $x=0.250$ m

- Experiments \square
- ASC hKE std+wf $---$
- UBrussel hKE std+wf $---$
- GEHydro hKE std+wf (3D) $---$
- THAachen hKE RNG+wf $---$
- UFlorenc IKE JoLa $---$
- DLRGoett kOm Wil $---$

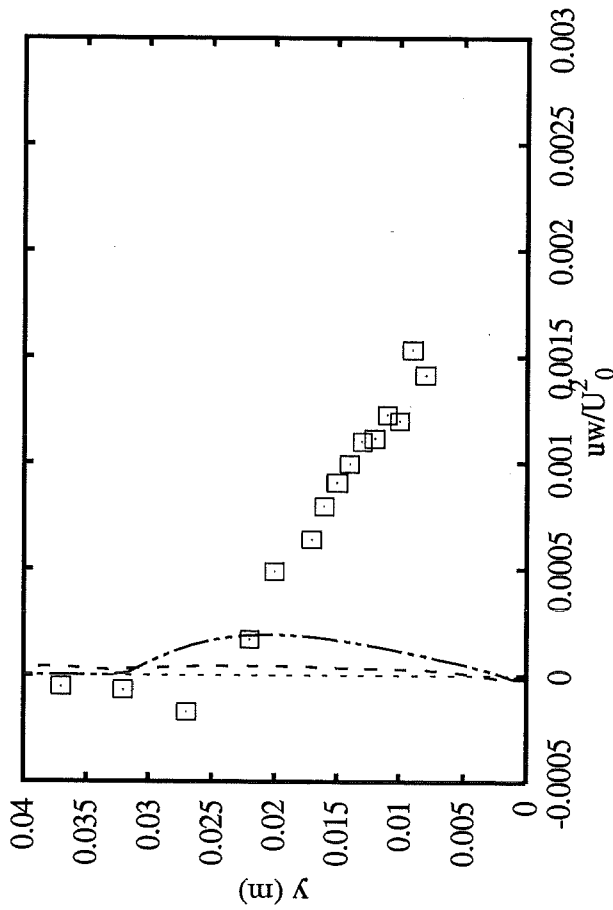
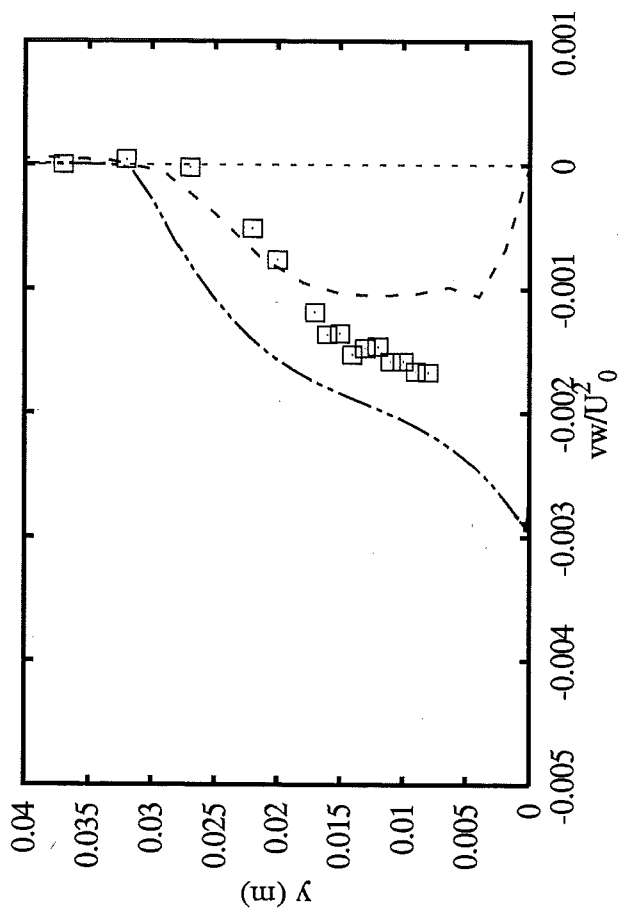
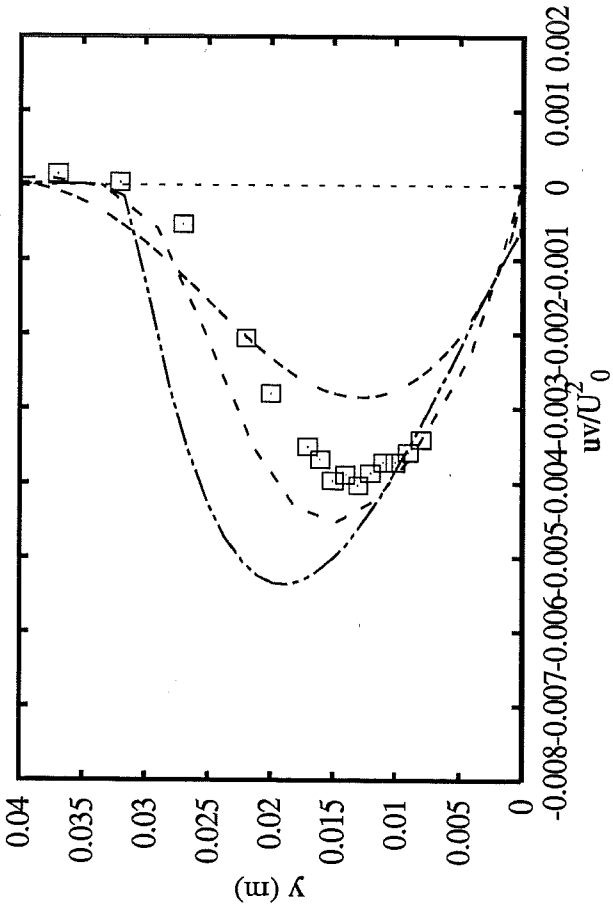


Swirling boundary layer in conical diffuser
Group 1: k-epsilon and k-omega models

3 - 11

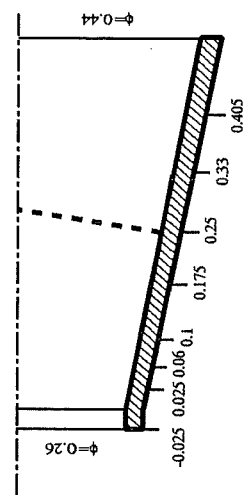


4th ERCOFTAC/IAHR Workshop on Refined Flow Modelling
April 3-7, 1995, University of Karlsruhe, Germany



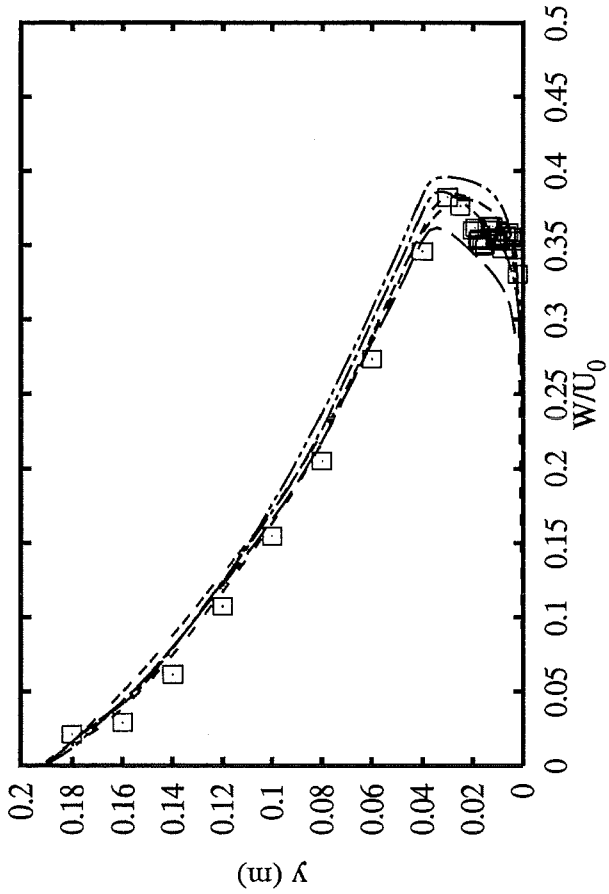
Profiles at $x=0.250$ m

- Experiments \square
- UBrussel hKE std+wf - - -
- UFlorenc IKE Jola - - -
- DLRGoett kOm Wil - - -



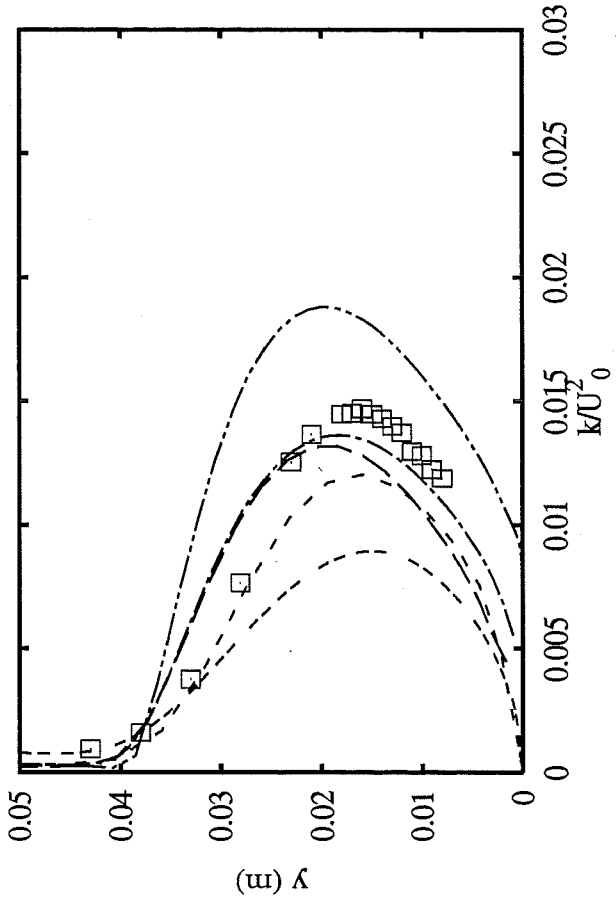
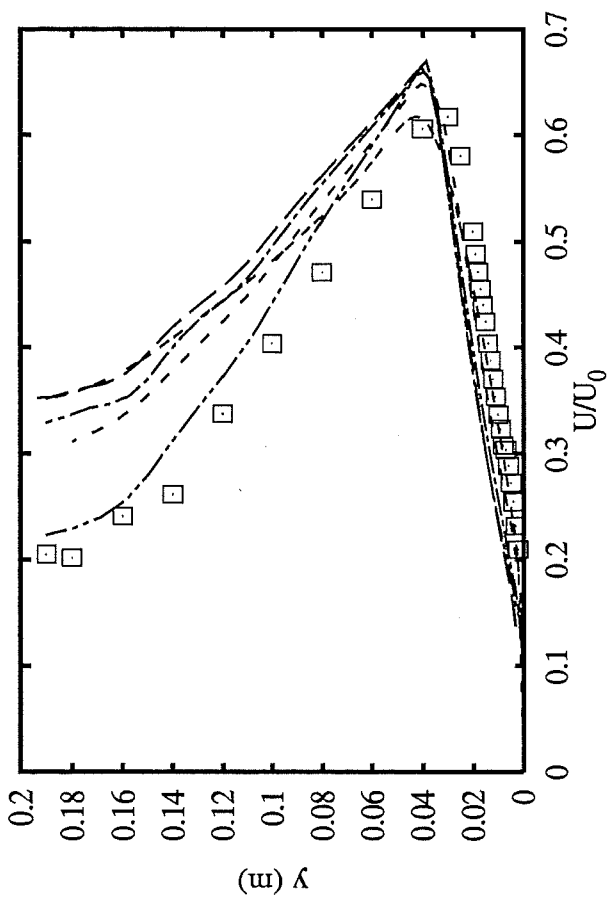
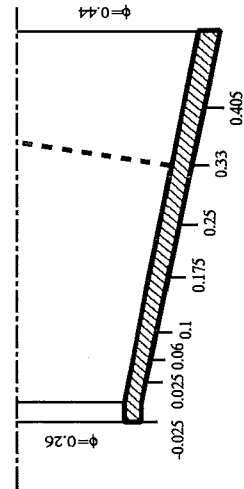
Swirling boundary layer in conical diffuser
Group 1: k-epsilon and k-omega models

4th ERCOFTAC/IAHR Workshop on Refined Flow Modelling
April 3-7, 1995, University of Karlsruhe, Germany

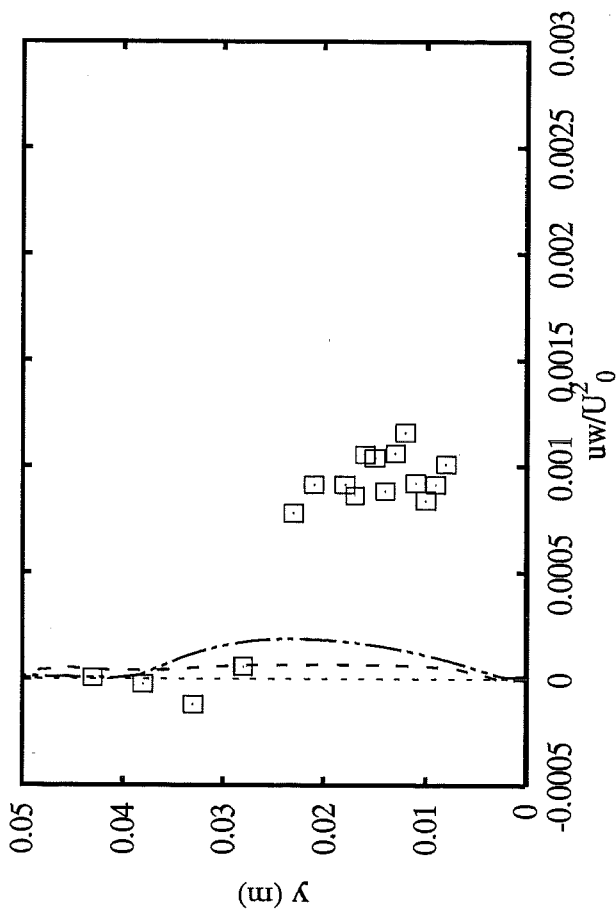
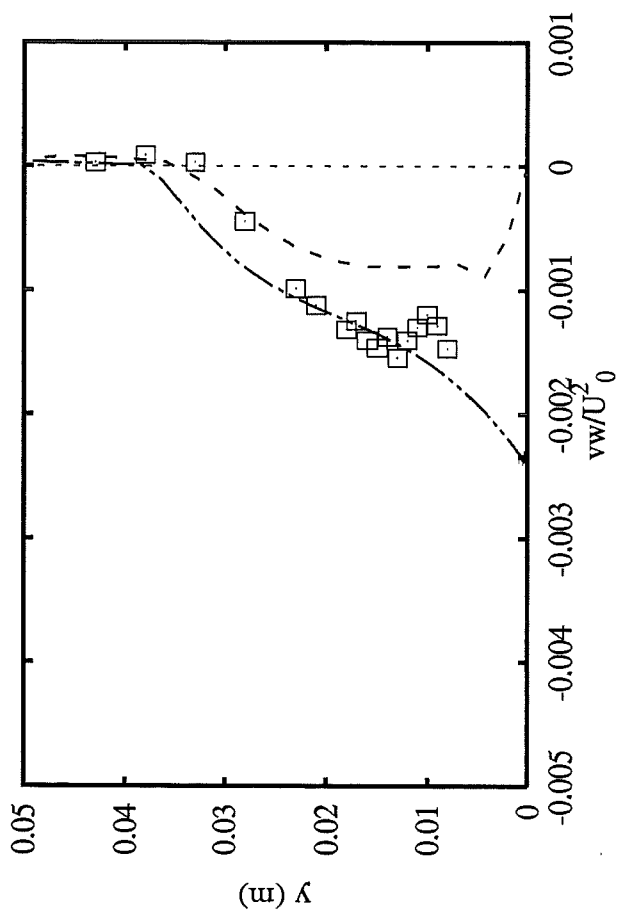
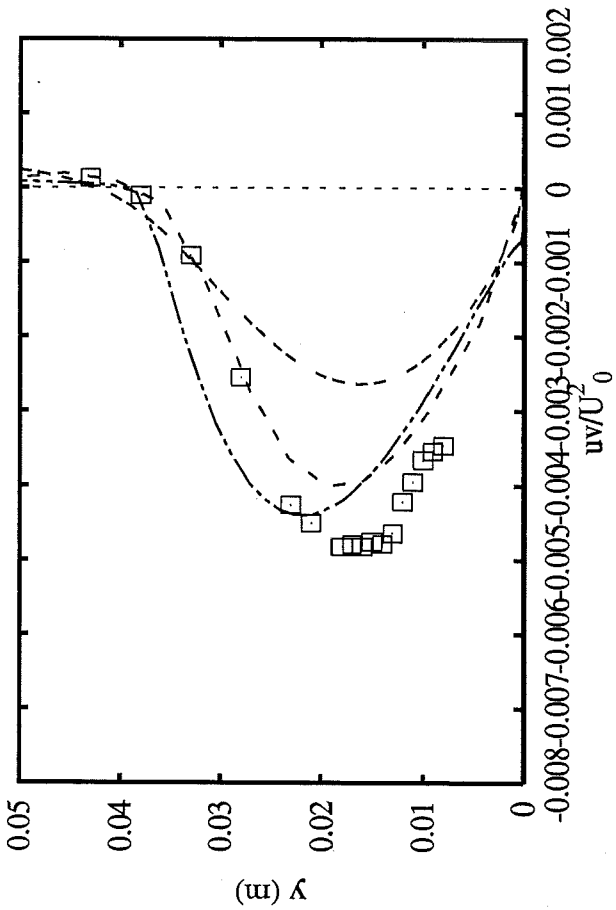


Profiles at $x=0.330$ m

- Experiments \square
- ASC hKE std+wf $---$
- Ubrussel hKE std+wf $---$
- THAachen hKE RNG+wf $---$
- UFlorenc IKE JOLA $---$
- DLRGoett kOm Wil $---$

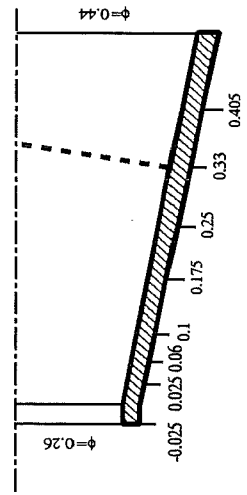


Swirling boundary layer in conical diffuser
Group 1: k-epsilon and k-omega models

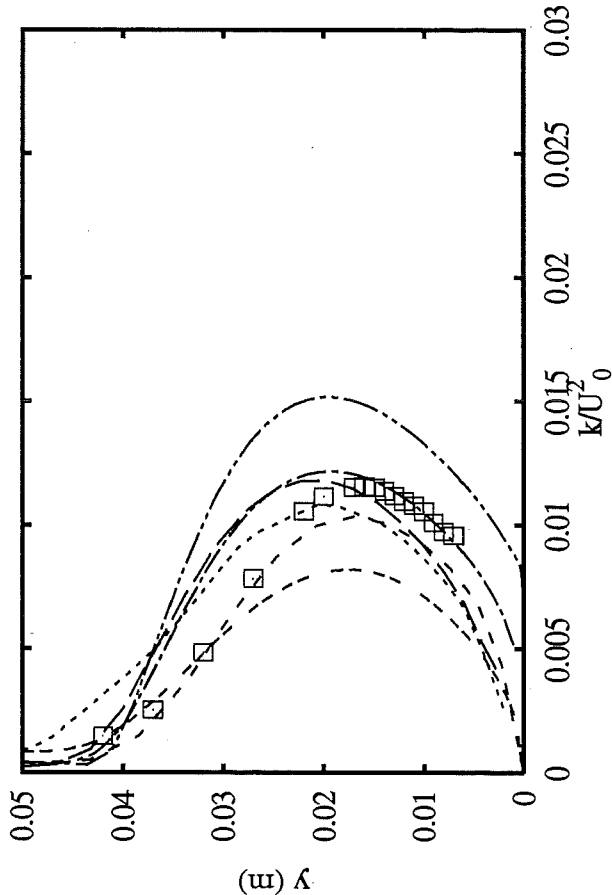
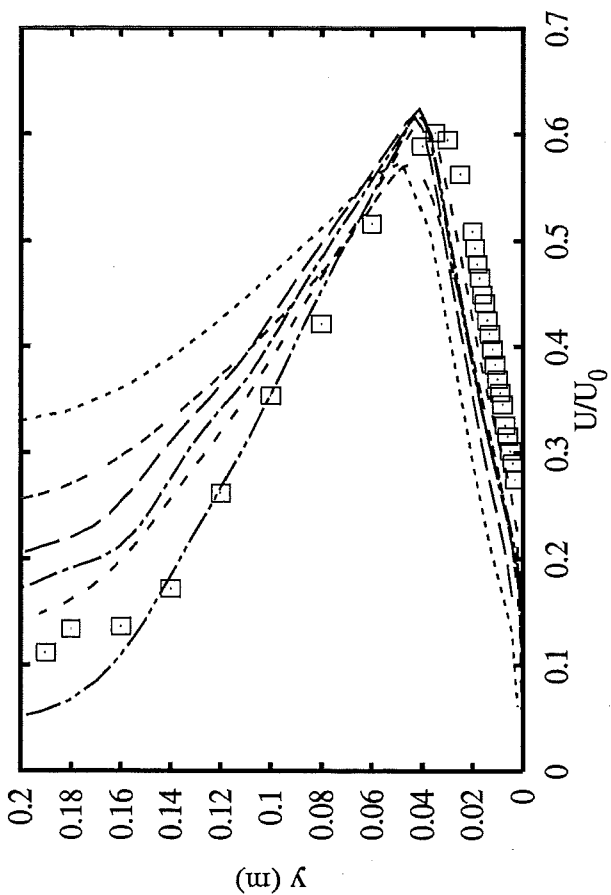
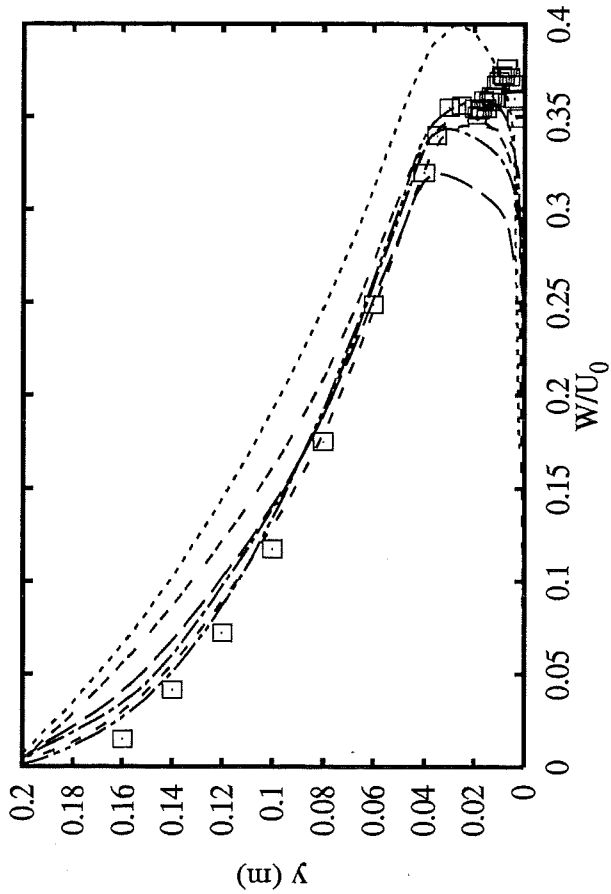


Profiles at $x=0.330$ m

- Experiments \square
- UBrussel hKE std+wf - - -
- UFlorenc IKE Jola - - -
- DLRGoett kOm Wil - - -

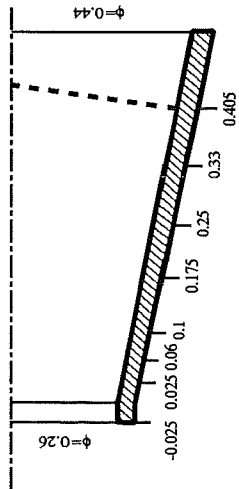


Swirling boundary layer in conical diffuser
Group 1: k-epsilon and k-omega models



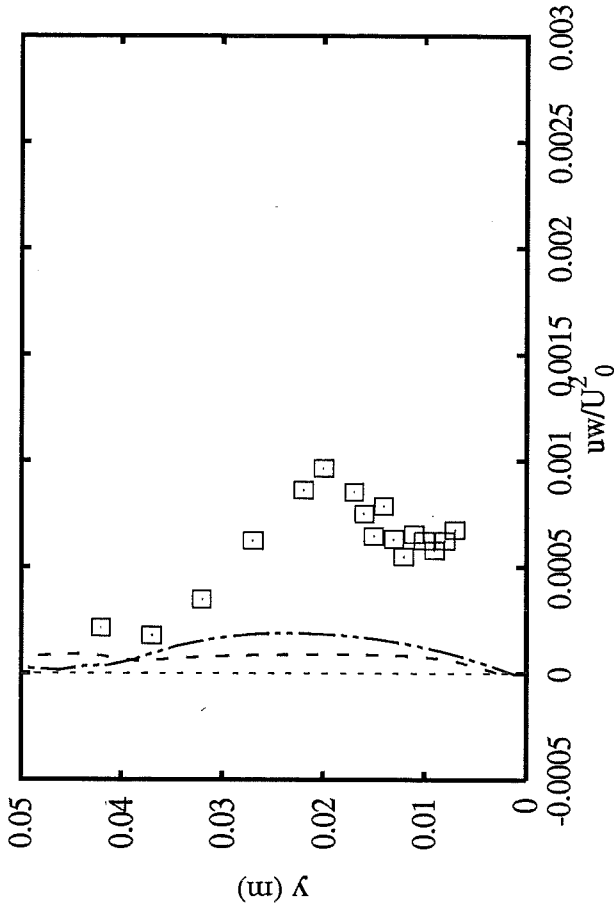
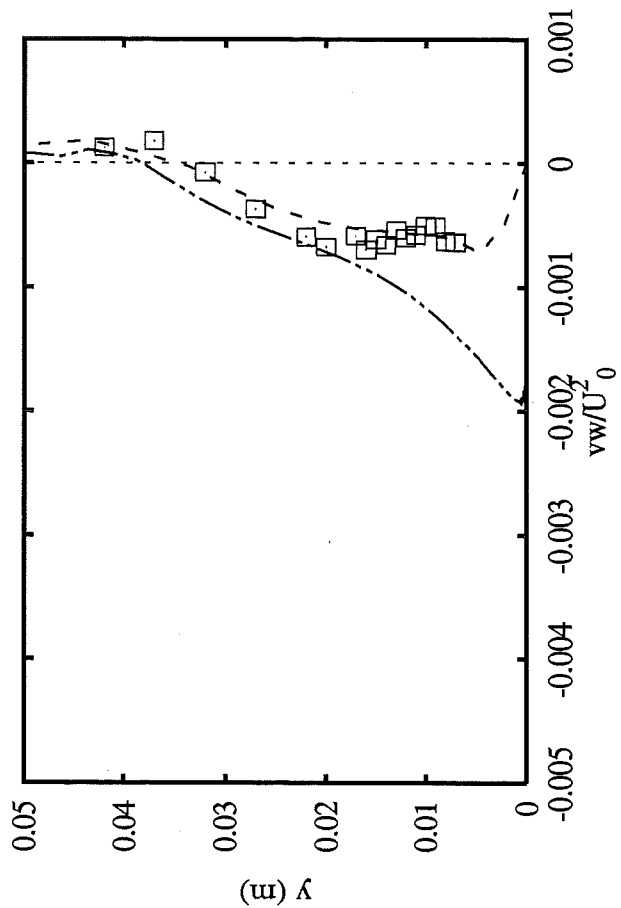
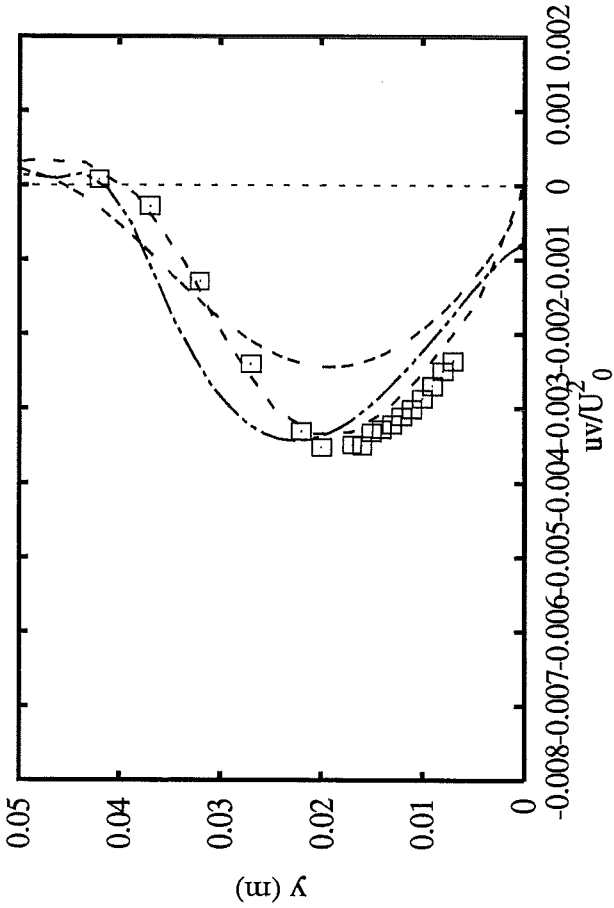
Profiles at $x=0.405$ m

- Experiments \square
- ASC hKE std+wf $---$
- UBrussel hKE std+wf $---$
- GEHydro hKE std+wf (3D) $---$
- THAachen hKE RNG+wf $---$
- UFlorenc IKE JoLa $---$
- DLRGoett kOm Wil $---$



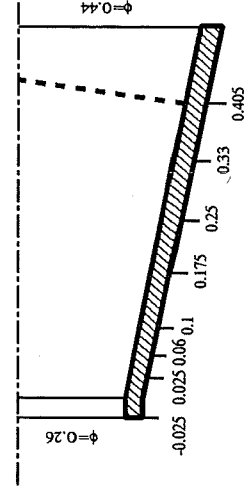
Swirling boundary layer in conical diffuser
Group 1: k-epsilon and k-omega models

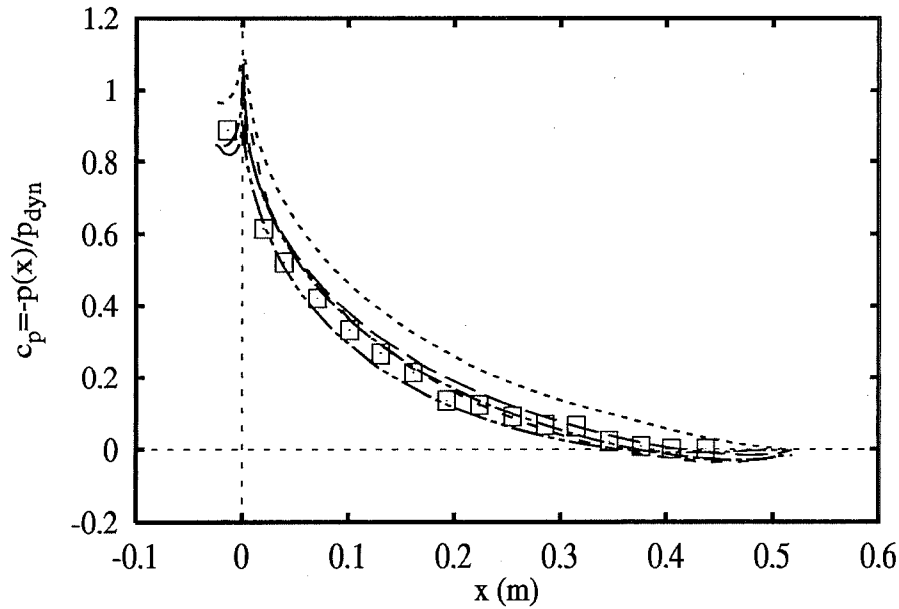
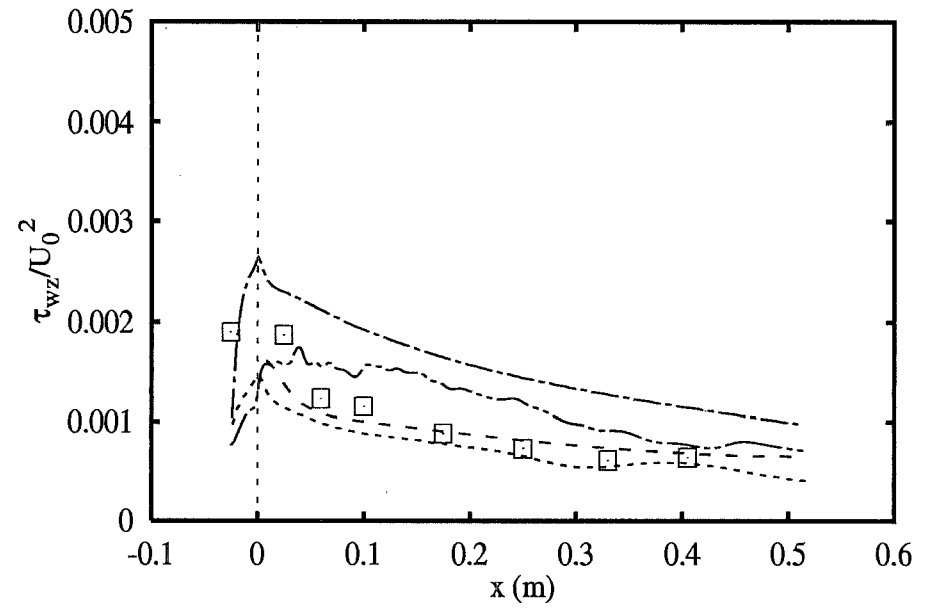
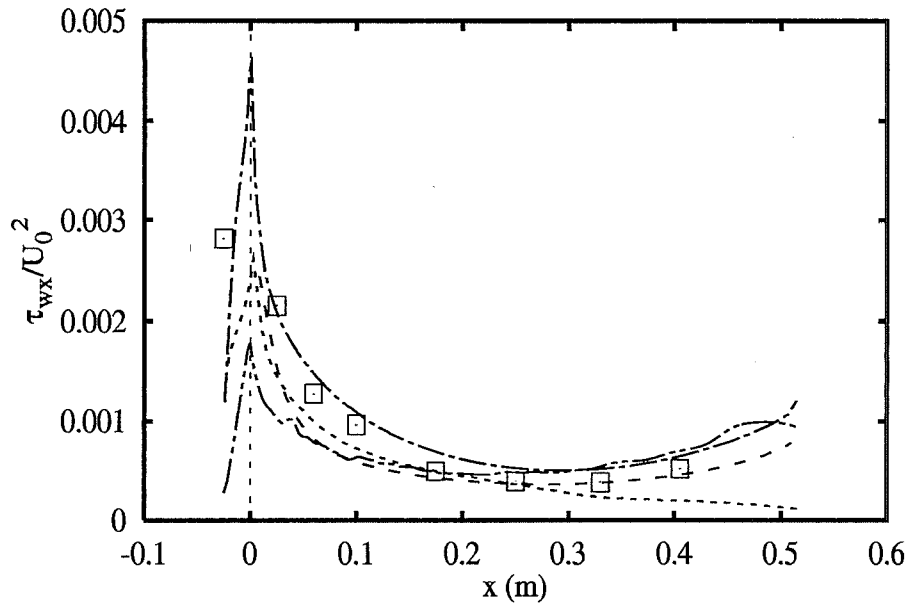
4th ERCOFTAC/IAHR Workshop on Refined Flow Modelling
April 3-7, 1995, University of Karlsruhe, Germany



Profiles at $x=0.405$ m

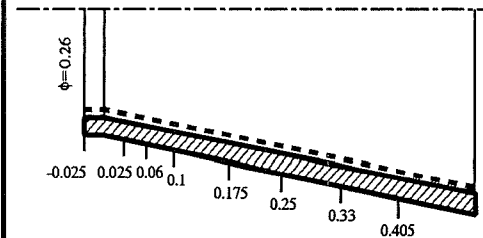
- Experiments \square
- UBrussel hKE std+wf - - -
- UFlorenc lKE JoLa - · - · -
- DLRGoett kOm Wil - - -

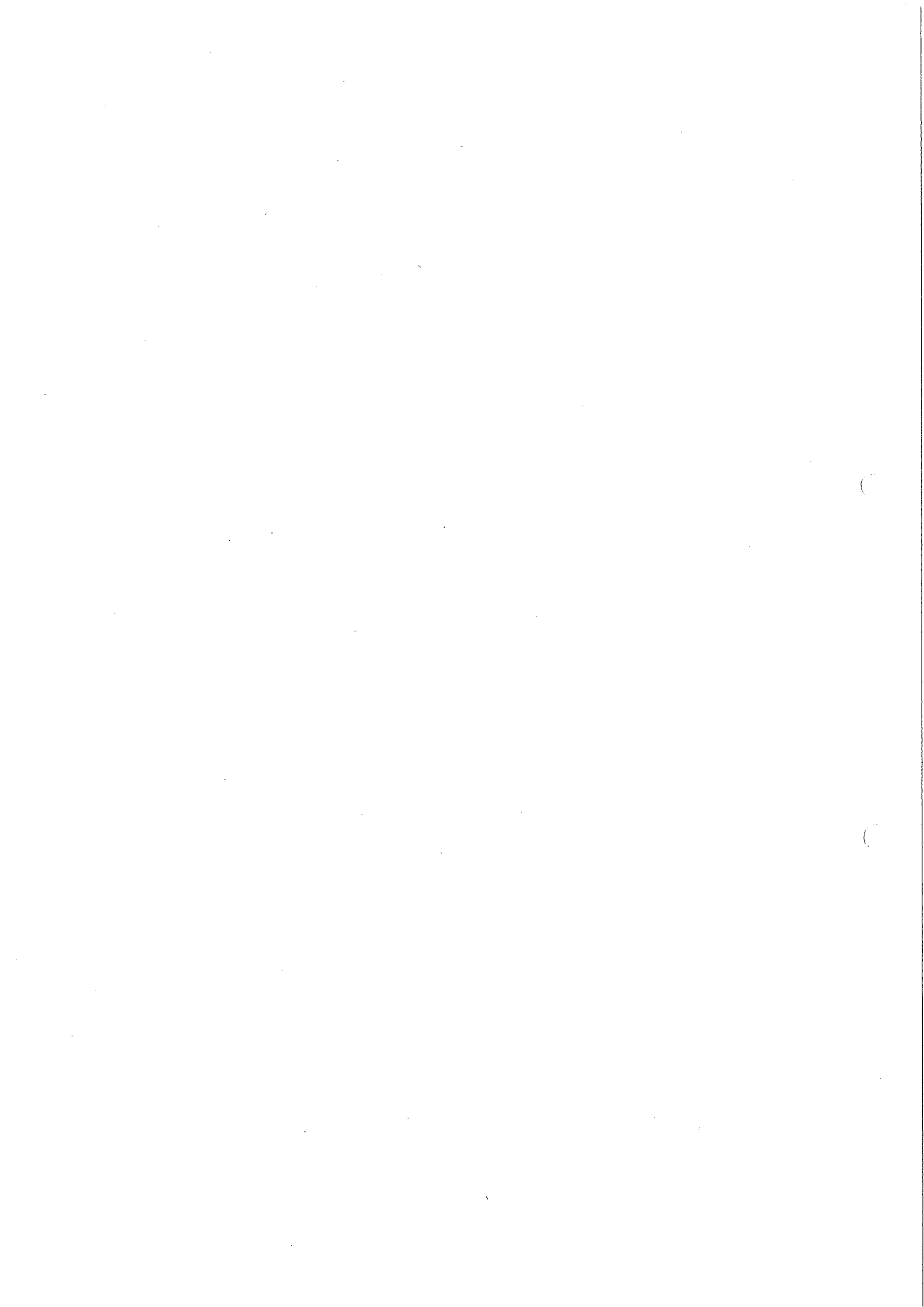


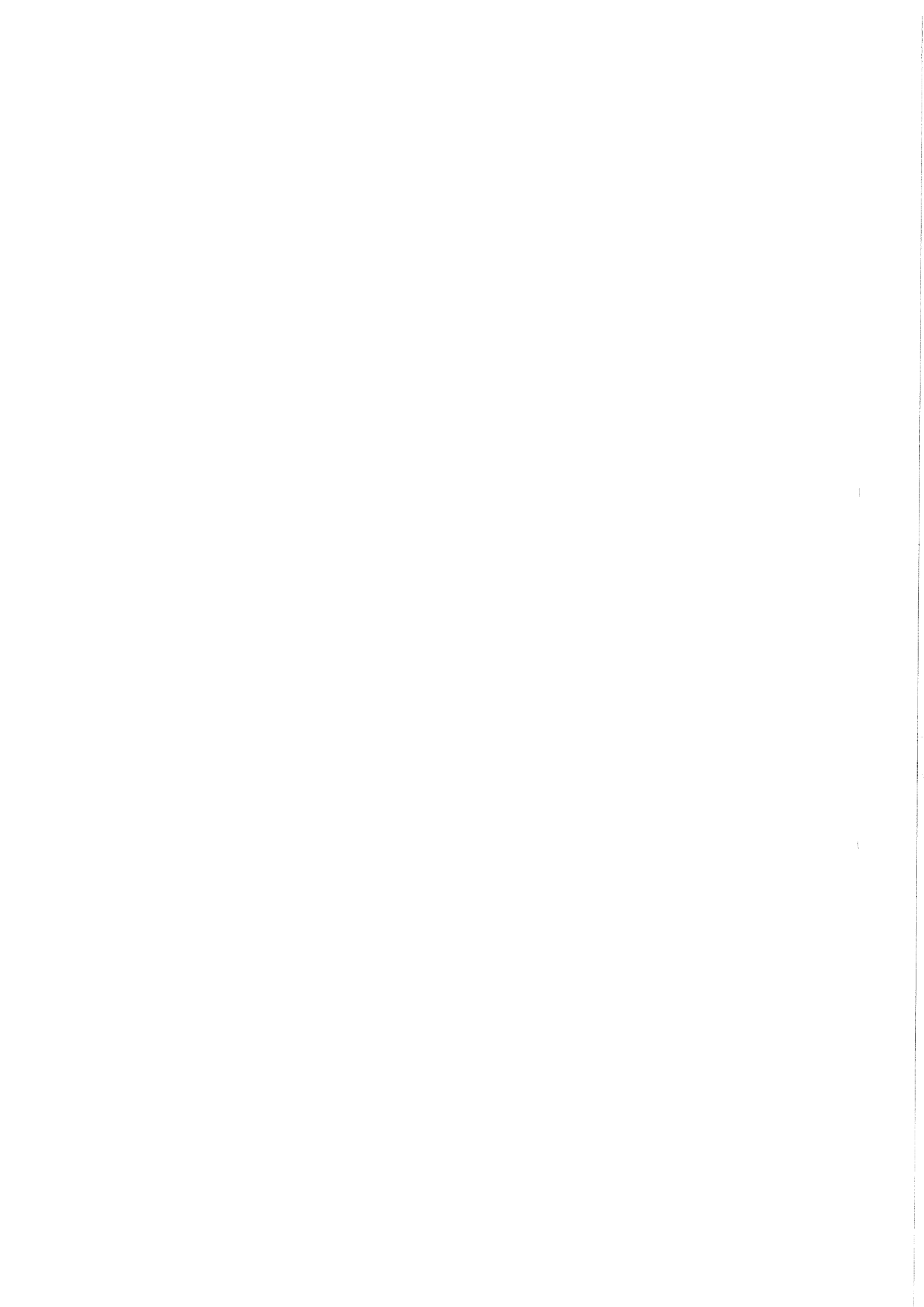


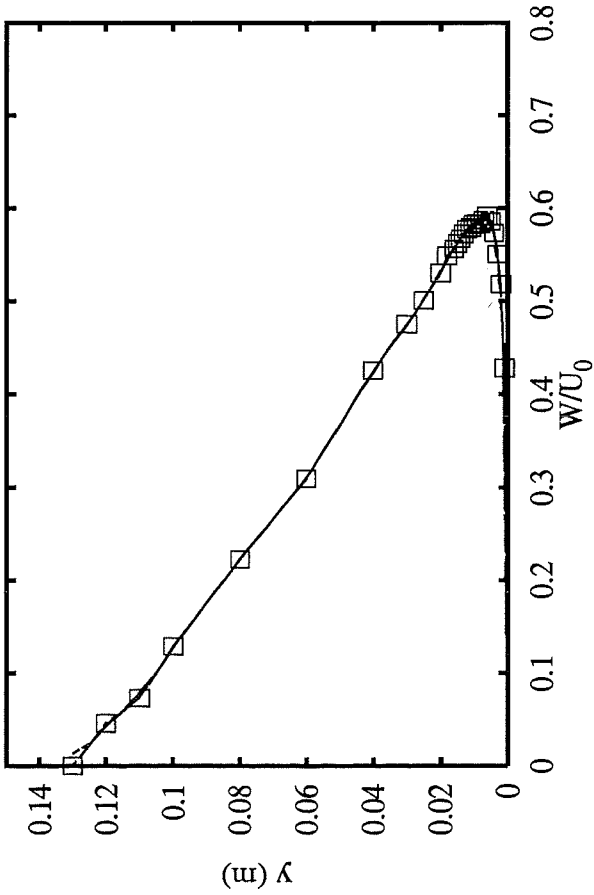
Distributions along wall

- Experiments** □
- ASC hKE std+wf** —
- UBrussel hKE std+wf** - - -
- GEHydro hKE std+wf (3D)** · · · · ·
- THAachen hKE RNG+wf** - · - · -
- UFlorenc lKE JoLa** - - - - -



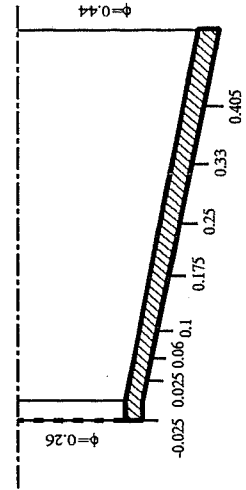




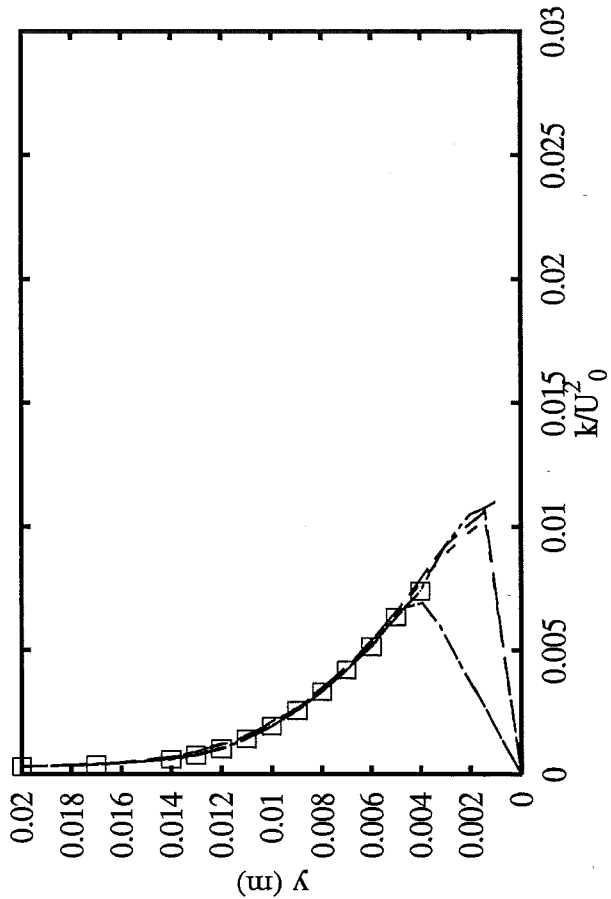
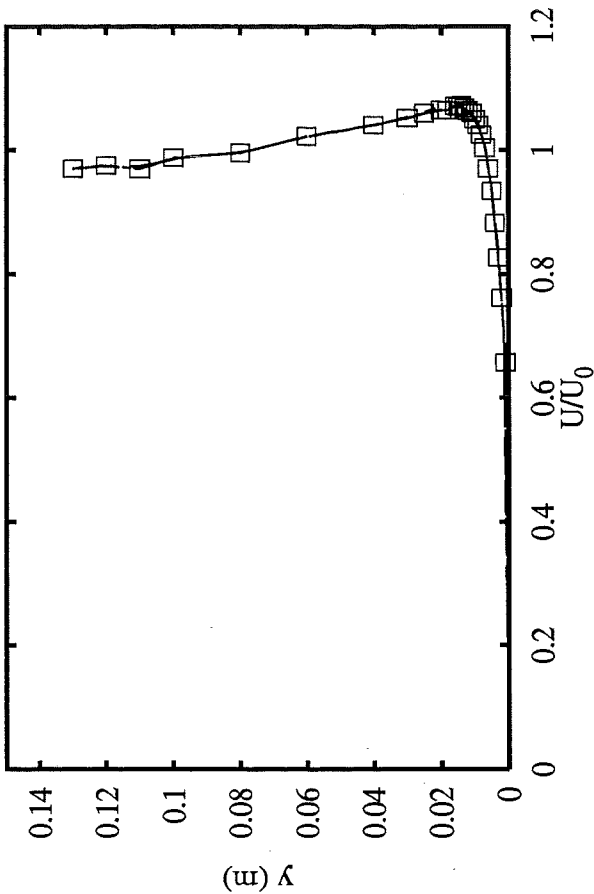


Profiles at $x = -0.025$ m

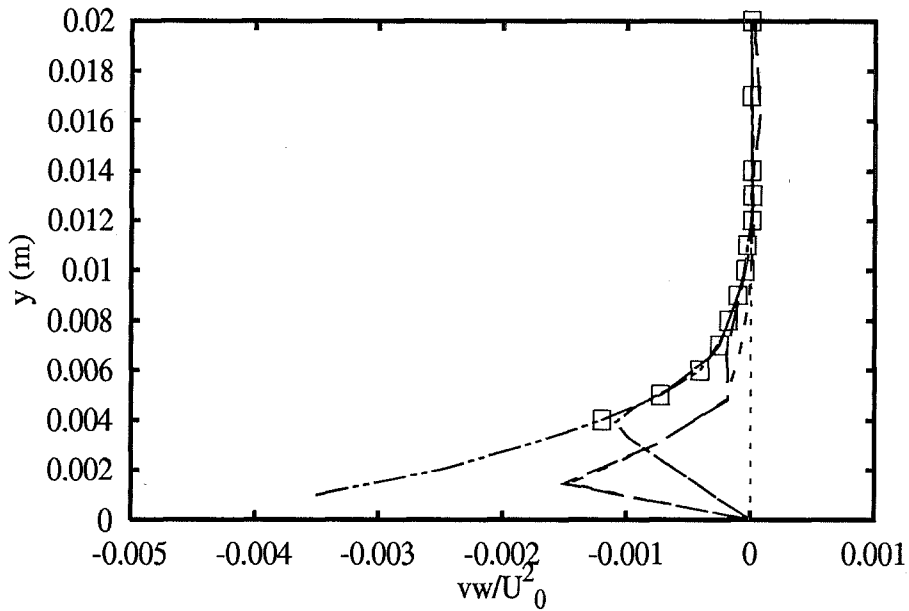
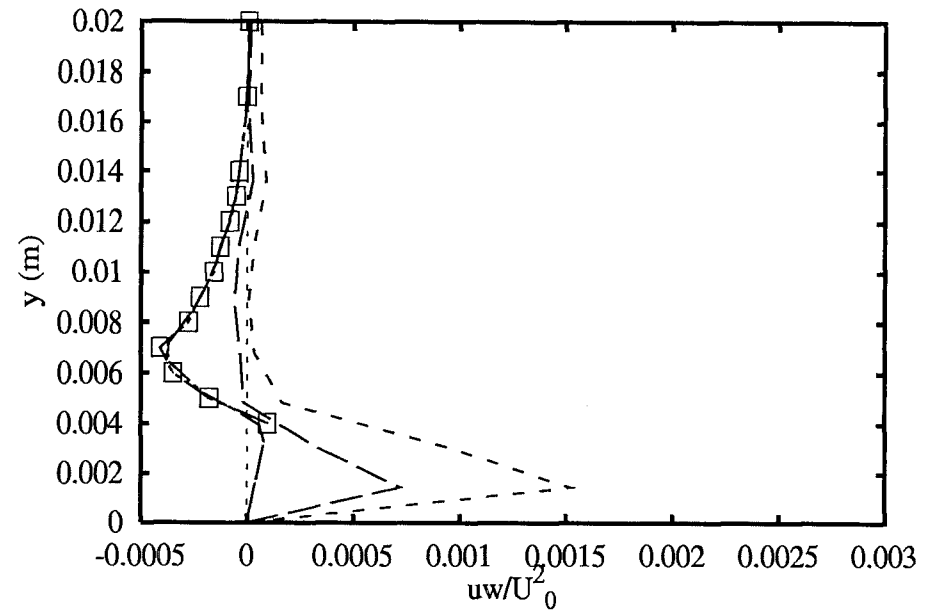
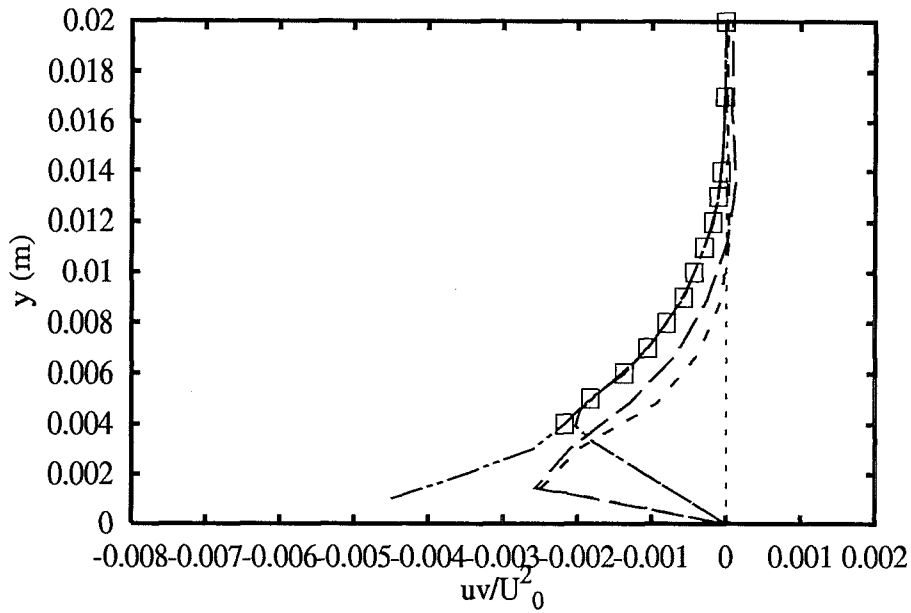
- Experiments \square
- UBrusse1 nKE SZL+wf
- UBrusse1 nKE HiKh+wf
- THAachen ASM ClWi+wf
- THAachen RSM LRR+wf
- ECLyon RSM LRR+wf



Swirling boundary layer in conical diffuser
Group 2: other models

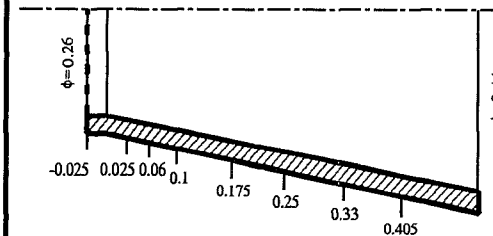


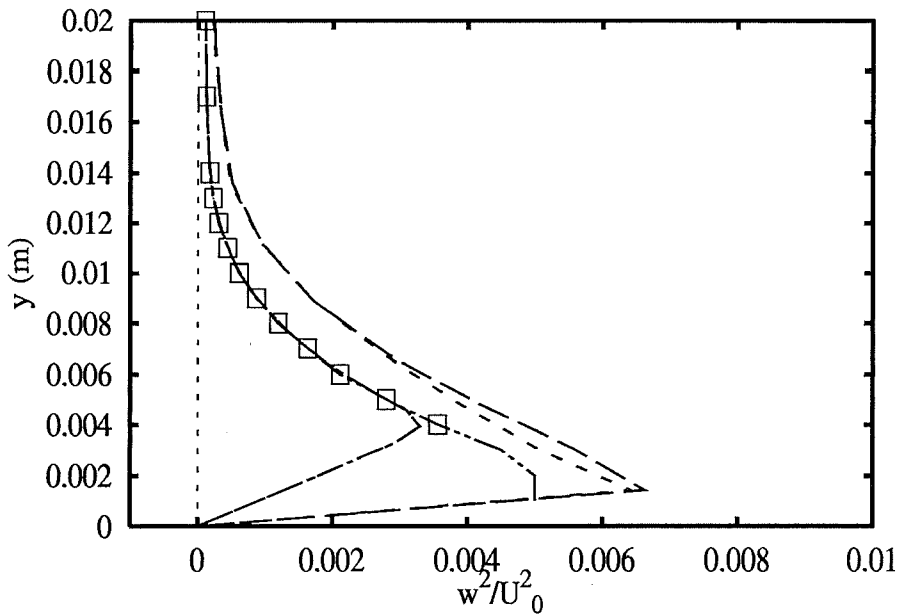
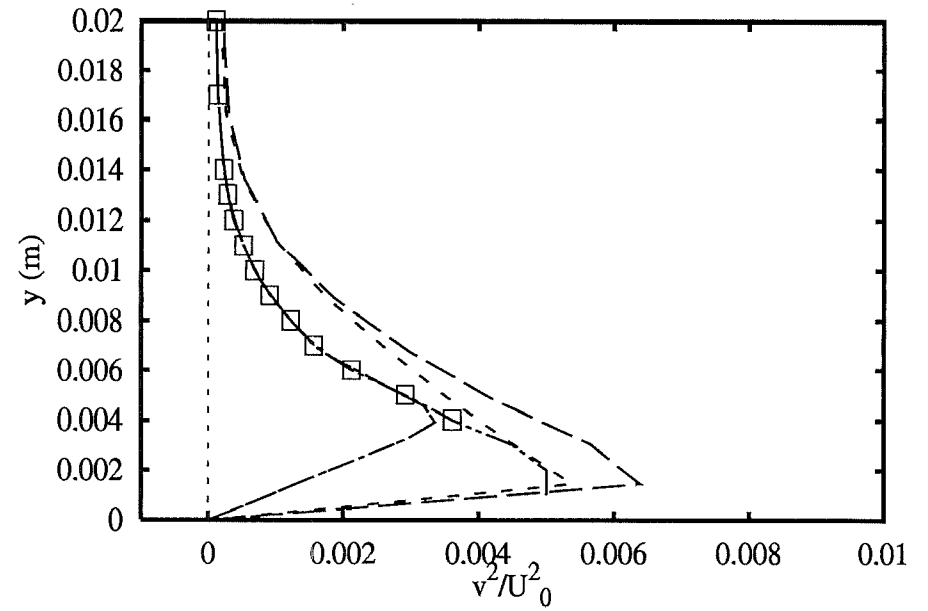
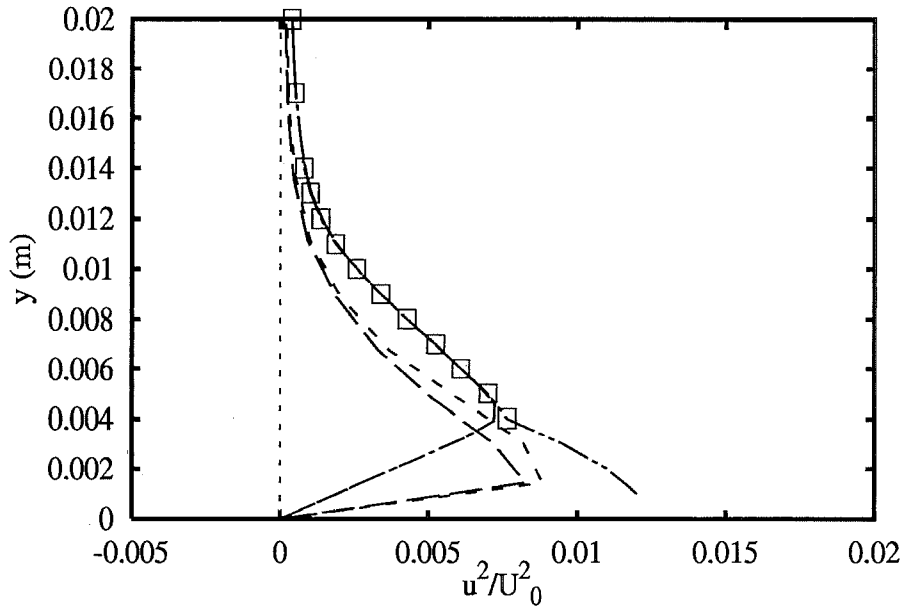
4th ERCOFTAC/IAHR Workshop on Refined Flow Modelling
April 3-7, 1995, University of Karlsruhe, Germany



Profiles at $x = -0.025$ m

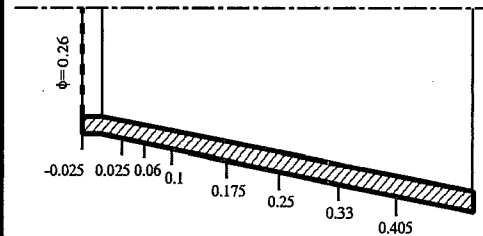
- | | | |
|----------|----------------------------|-------|
| | Experiments | □ |
| U | Brussel nKE SZL+wf | — — |
| U | Brussel nKE HiKh+wf | - - - |
| T | Aachen ASM ClWi+wf | · · · |
| T | Aachen RSM LRR+wf | - · - |
| E | CLyon RSM LRR+wf | - · - |

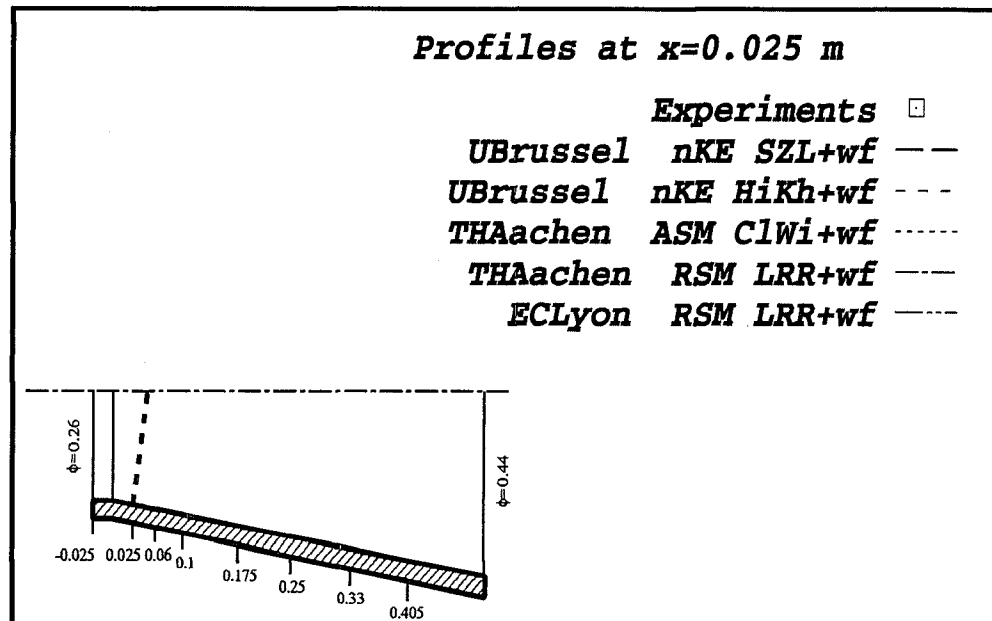
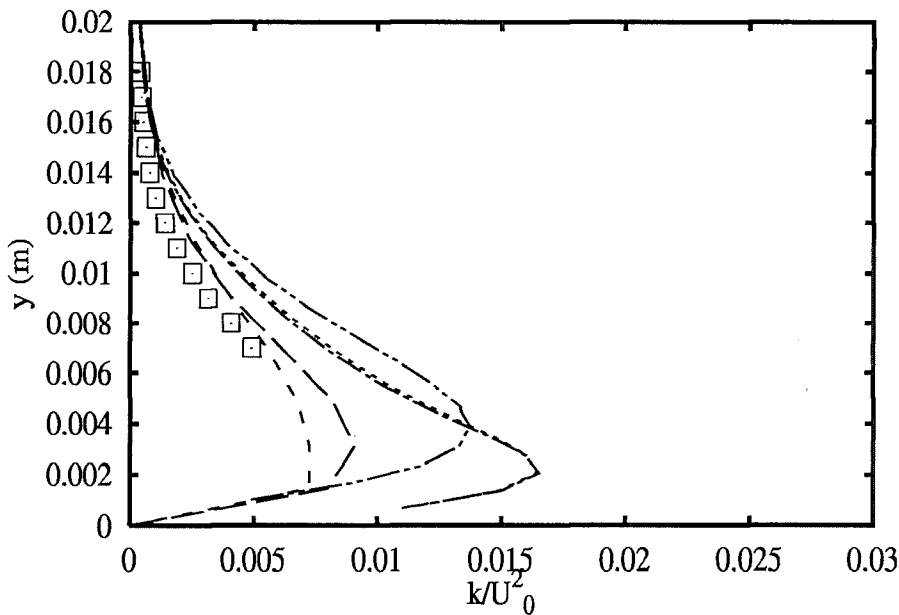
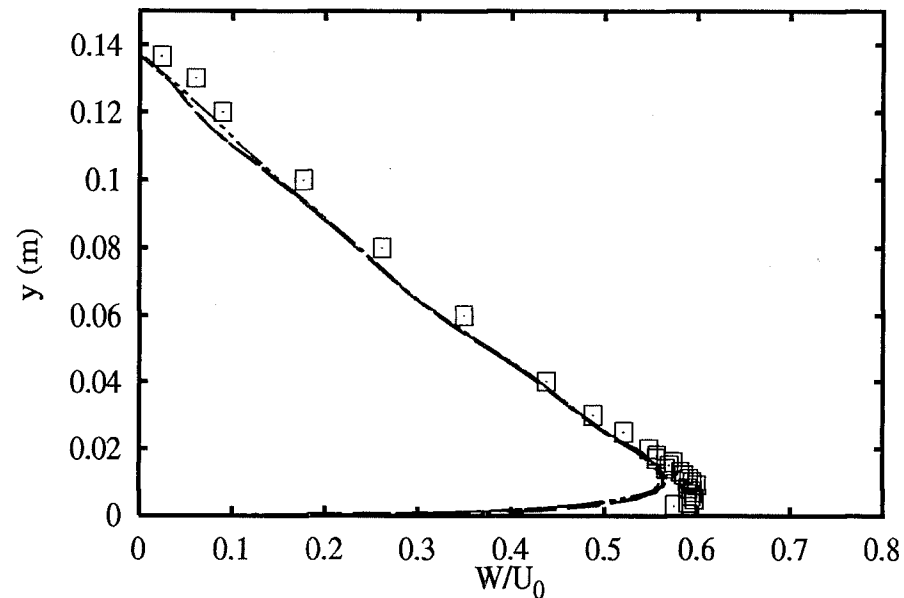
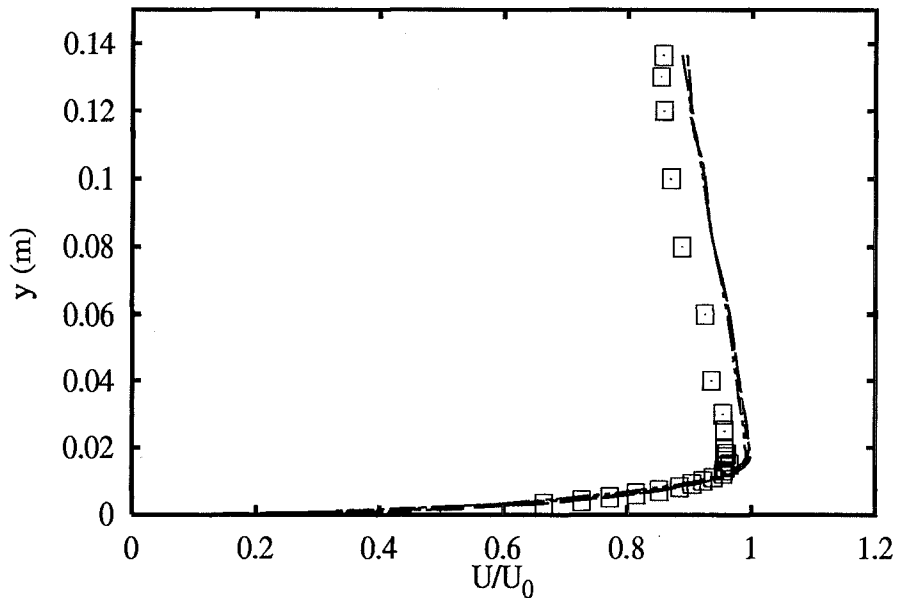


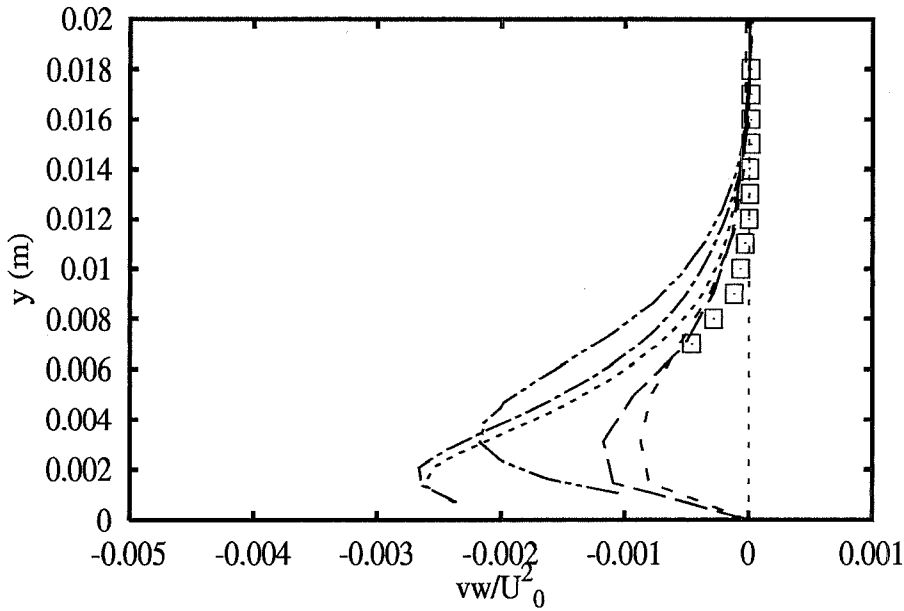
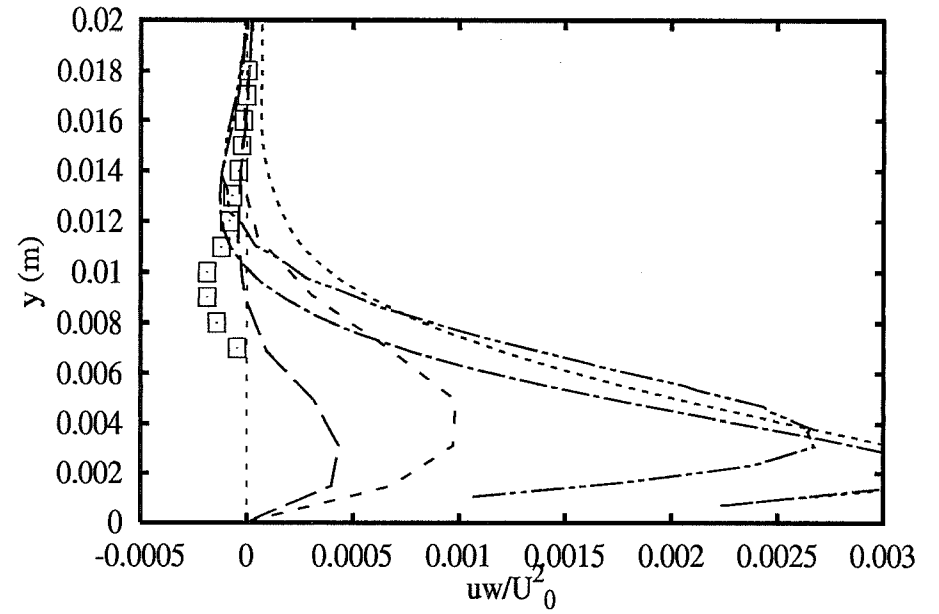
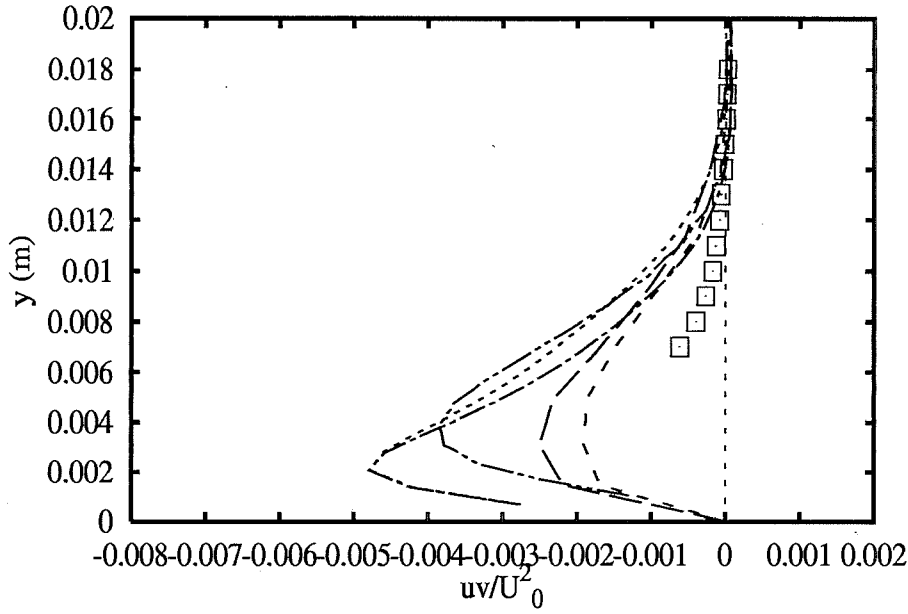


Profiles at $x = -0.025$ m

- | | | |
|----------|----------------------------|-----------|
| | Experiments | □ |
| U | Brussel nKE SZL+wf | — |
| U | Brussel nKE HiKh+wf | - - - |
| T | Aachen ASM ClWi+wf | · · · · · |
| T | Aachen RSM LRR+wf | - · - · - |
| E | CLyon RSM LRR+wf | — · — · — |

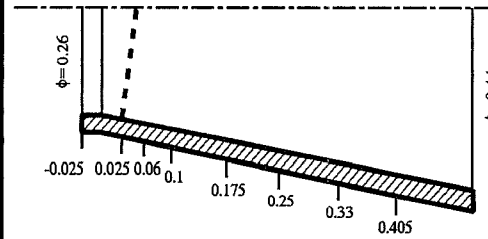


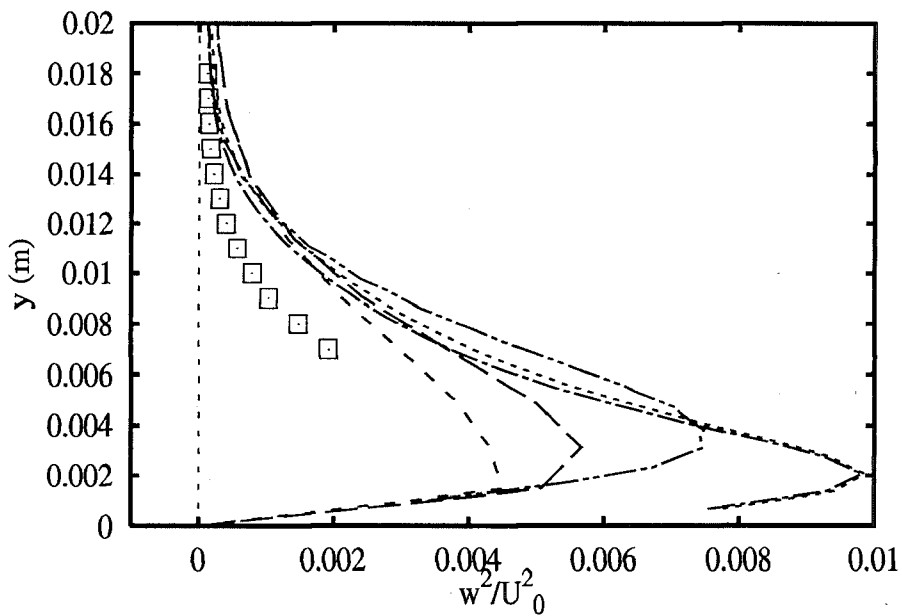
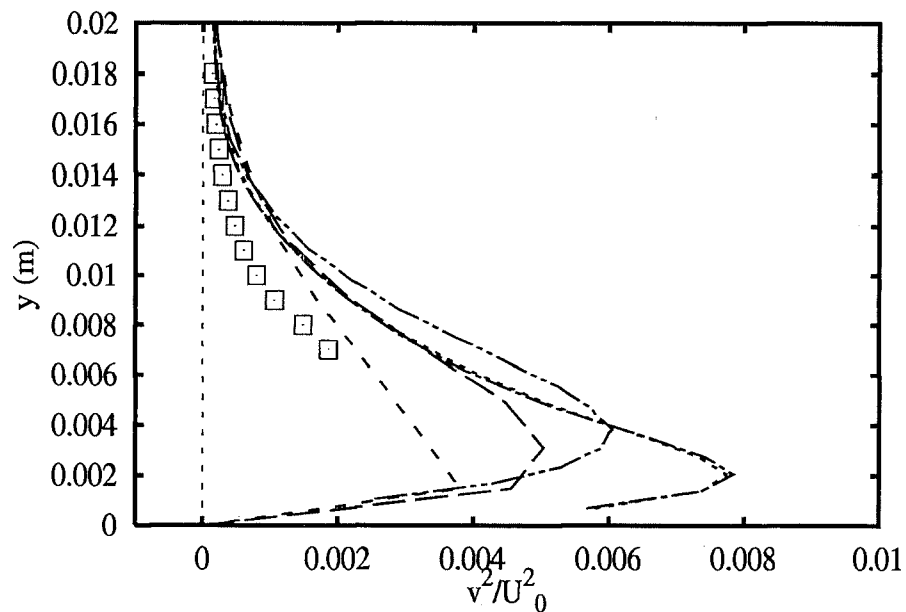
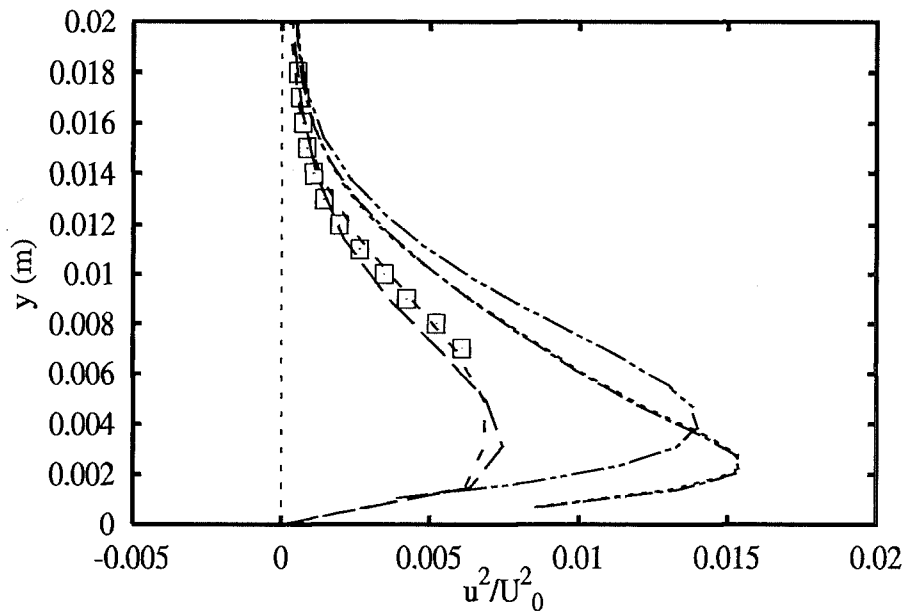




Profiles at $x=0.025$ m

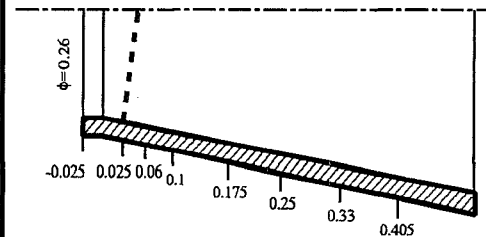
- Experiments** □
- Ubrussel nKE SZL+wf** —
- Ubrussel nKE HiKh+wf** - - -
- THAachen ASM ClWi+wf** - · - · -
- THAachen RSM LRR+wf** - - -
- ECLyon RSM LRR+wf** - · - · -

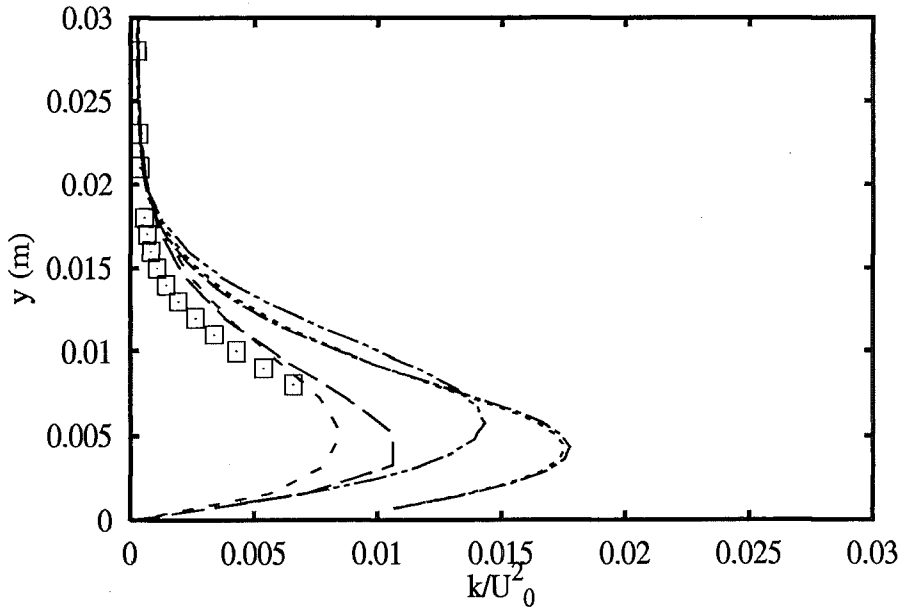
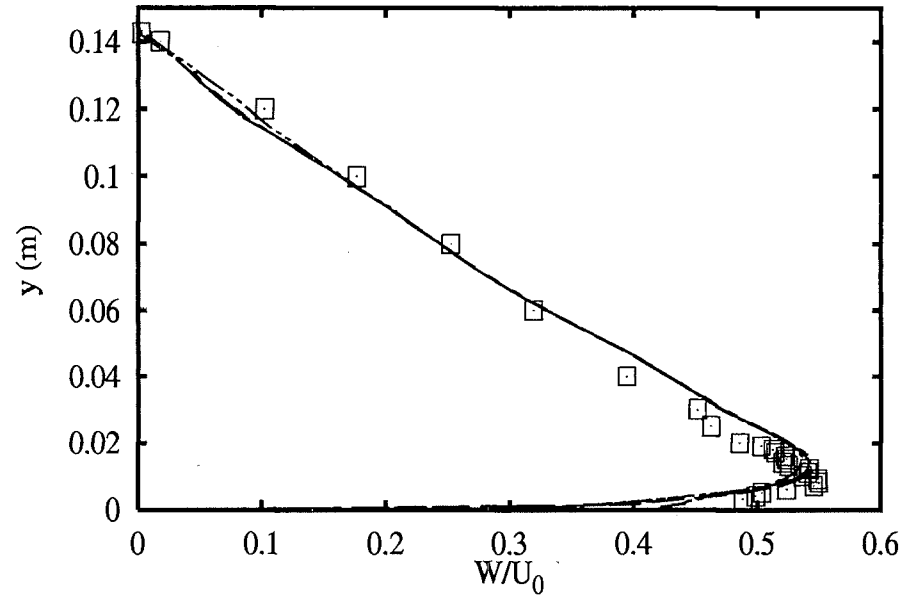
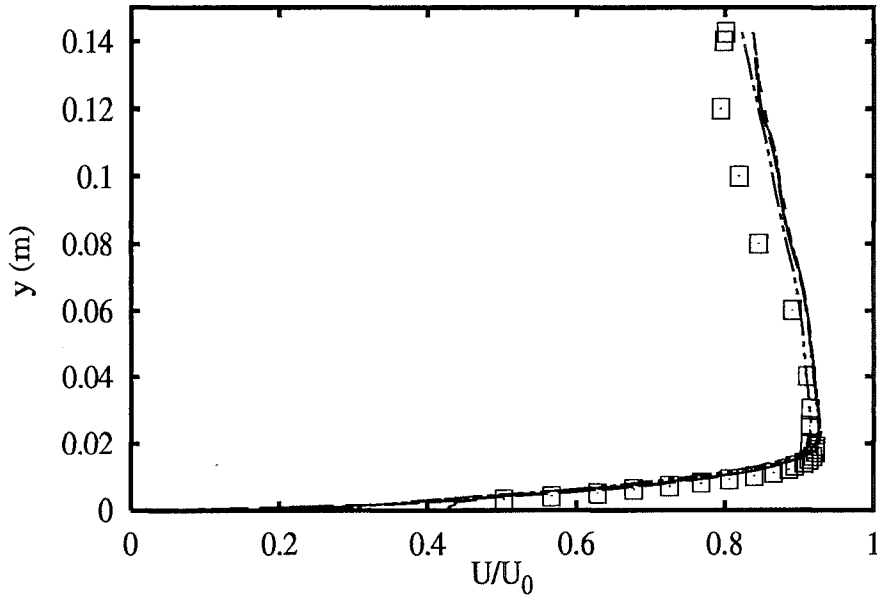




Profiles at $x=0.025$ m

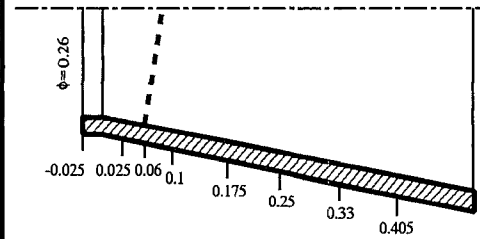
- | | |
|-----------------------------|-----------|
| Experiments | □ |
| UBrussel nKE SZL+wf | — |
| UBrussel nKE HiKh+wf | - - - |
| THAachen ASM ClWi+wf | · · · · · |
| THAachen RSM LRR+wf | - · - · - |
| ECLyon RSM LRR+wf | - · - · - |

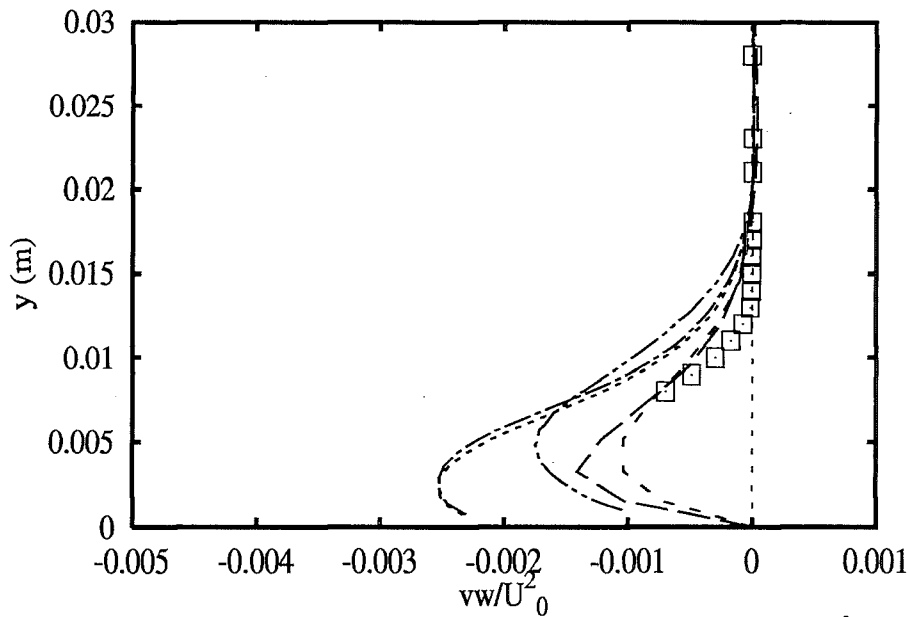
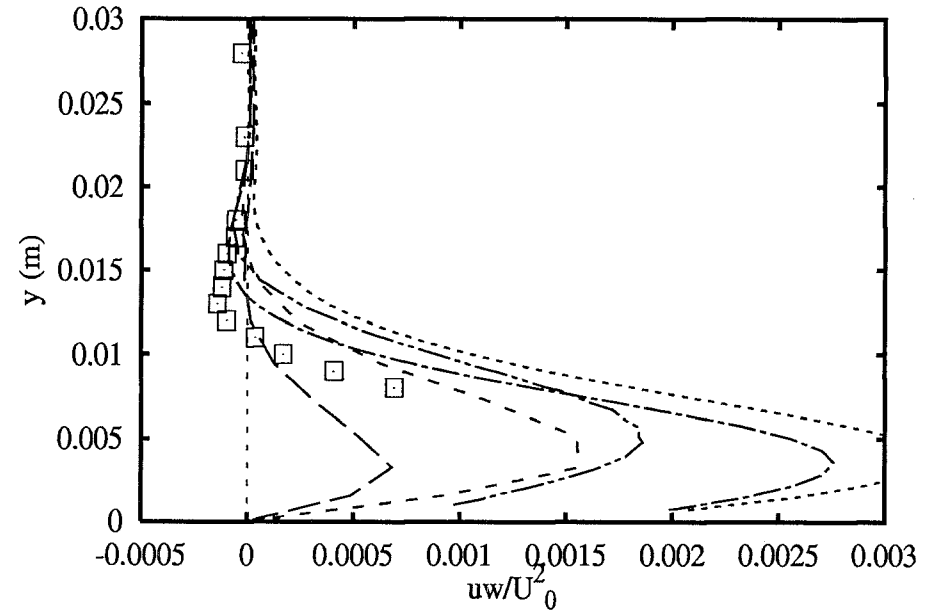
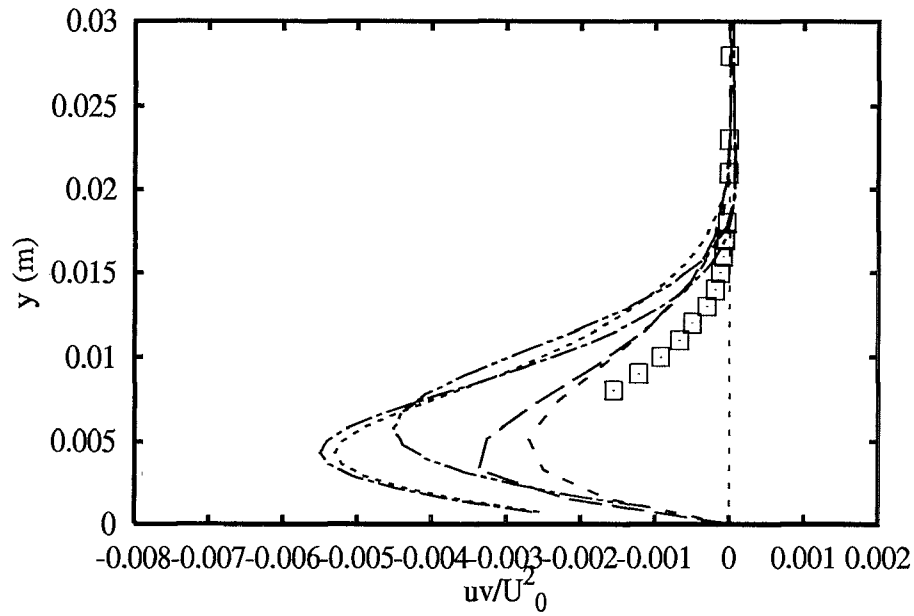




Profiles at $x=0.060$ m

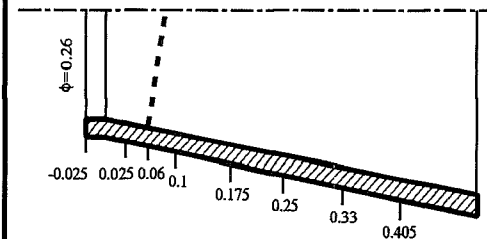
- Experiments \square
- Ubrussel nKE SZL+wf $---$
- Ubrussel nKE HiKh+wf $----$
- THAachen ASM ClWi+wf $.....$
- THAachen RSM LRR+wf $----$
- ECLyon RSM LRR+wf $----$

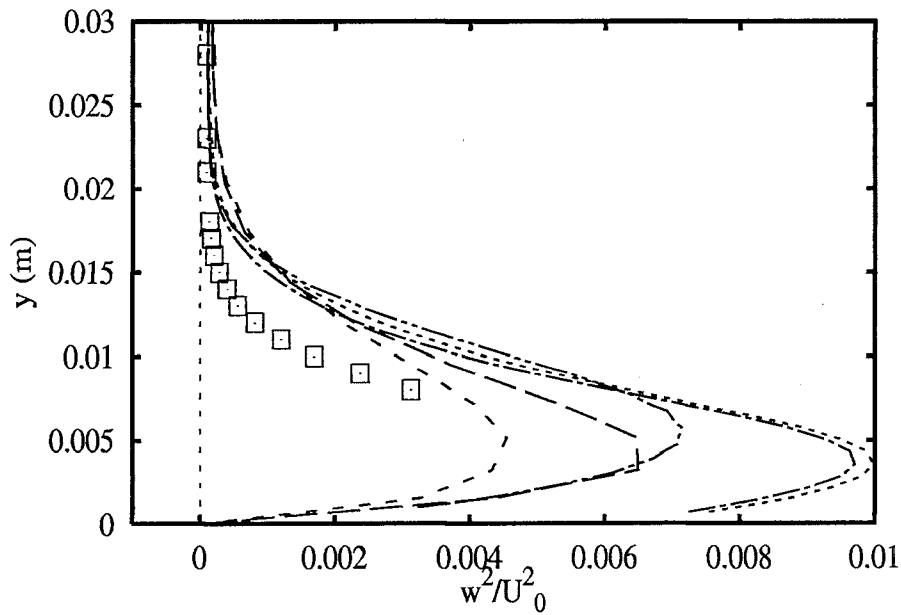
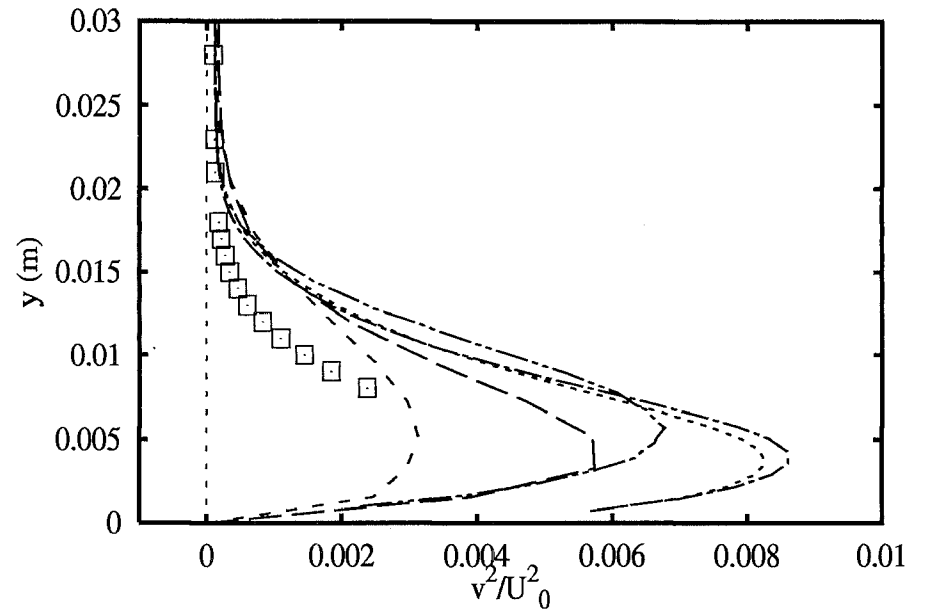
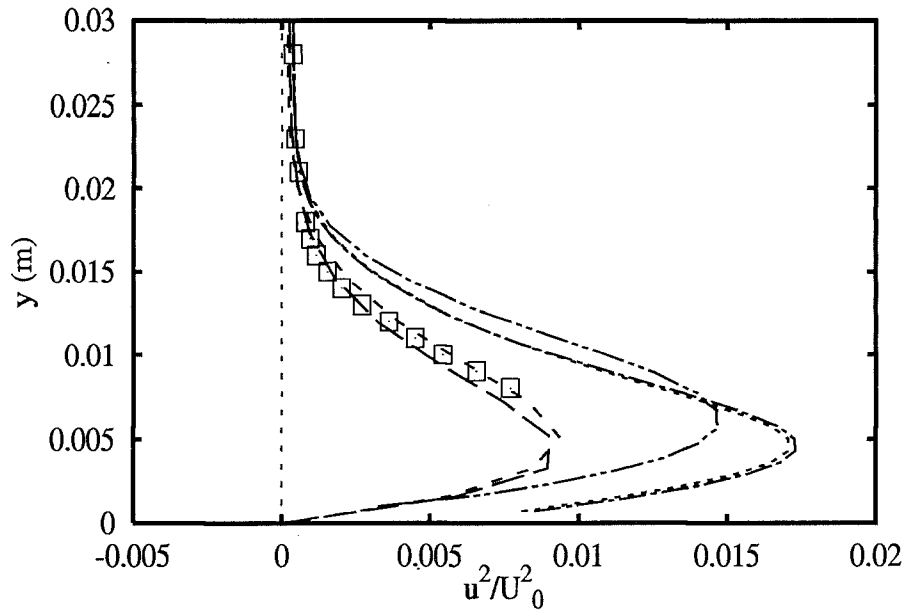




Profiles at $x=0.060$ m

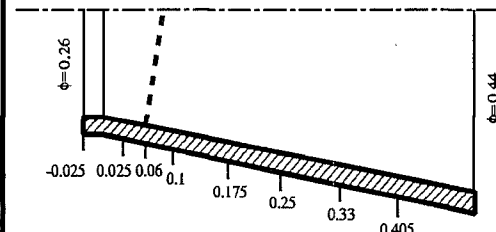
- | | | |
|-----------------|----------------------------|-----------|
| | Experiments | □ |
| U | Brussel nKE SZL+wf | — |
| U | Brussel nKE HiKh+wf | - - - |
| THAachen | ASM ClWi+wf | · · · · · |
| THAachen | RSM LRR+wf | - - - |
| ECLyon | RSM LRR+wf | - - - |

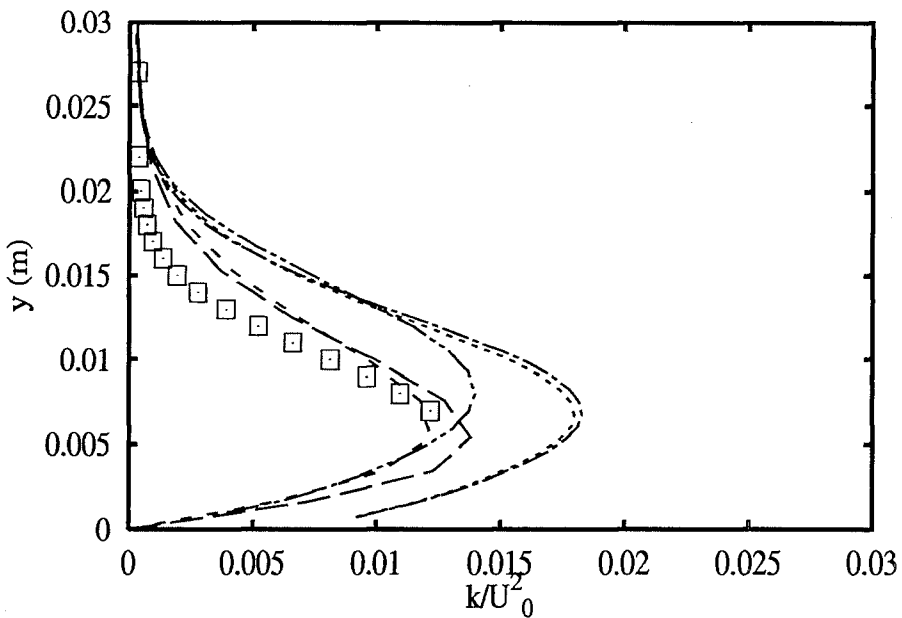
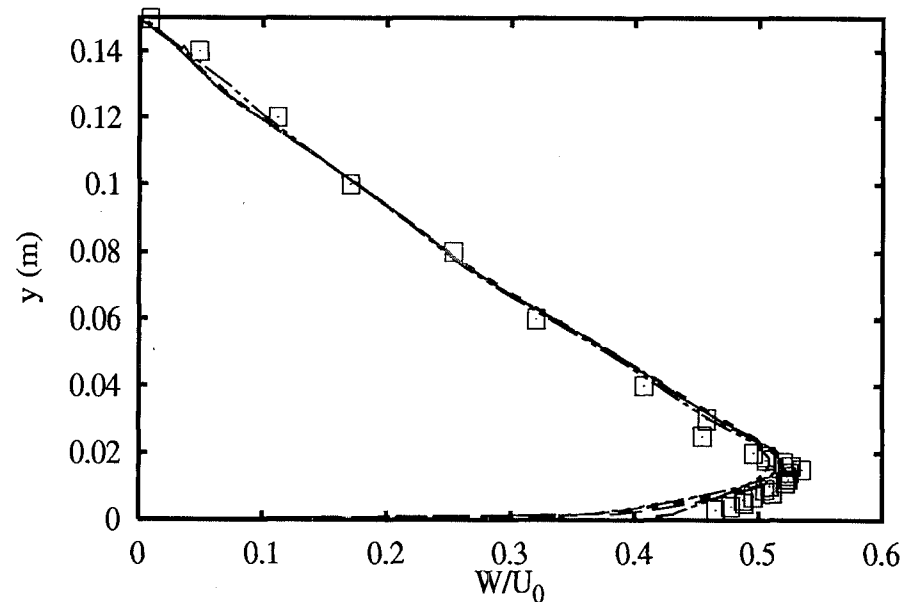
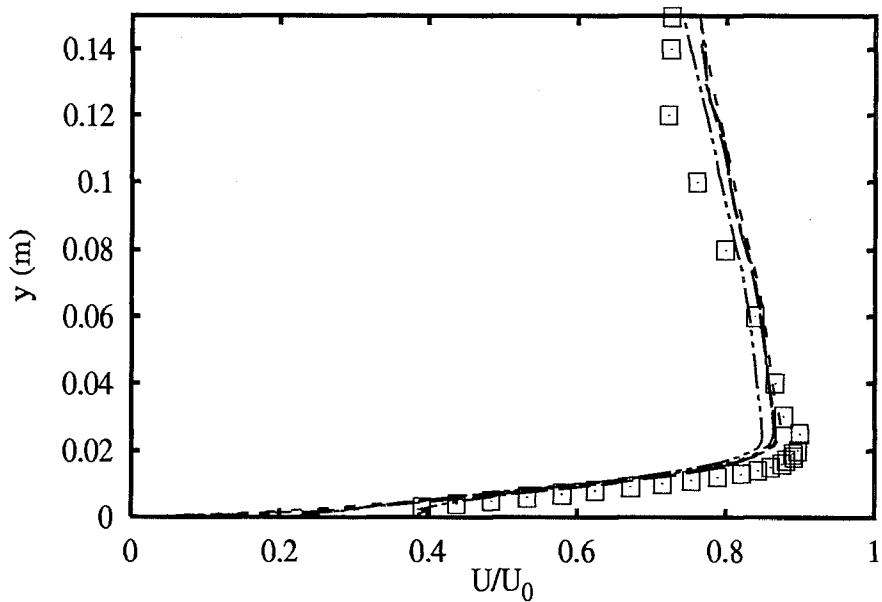




Profiles at $x=0.060$ m

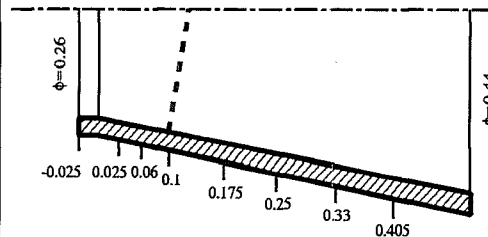
- | | |
|--|-----------|
| Experiments | □ |
| U Brussel nKE SZL+wf | — — — |
| U Brussel nKE HiKh+wf | - - - - - |
| THA achen ASM ClWi+wf | · · · · · |
| THA achen RSM LRR+wf | - · - · - |
| ECL yon RSM LRR+wf | · · · · · |

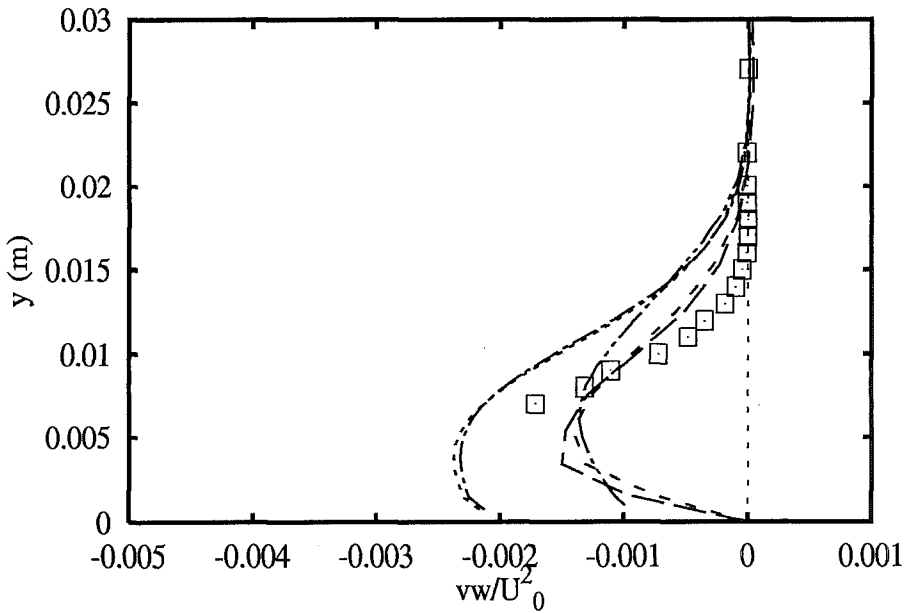
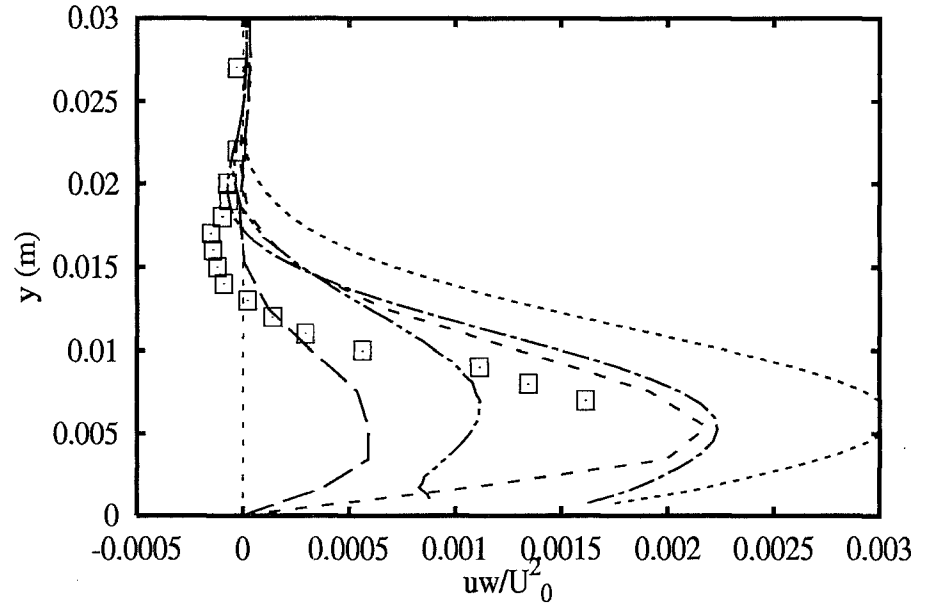
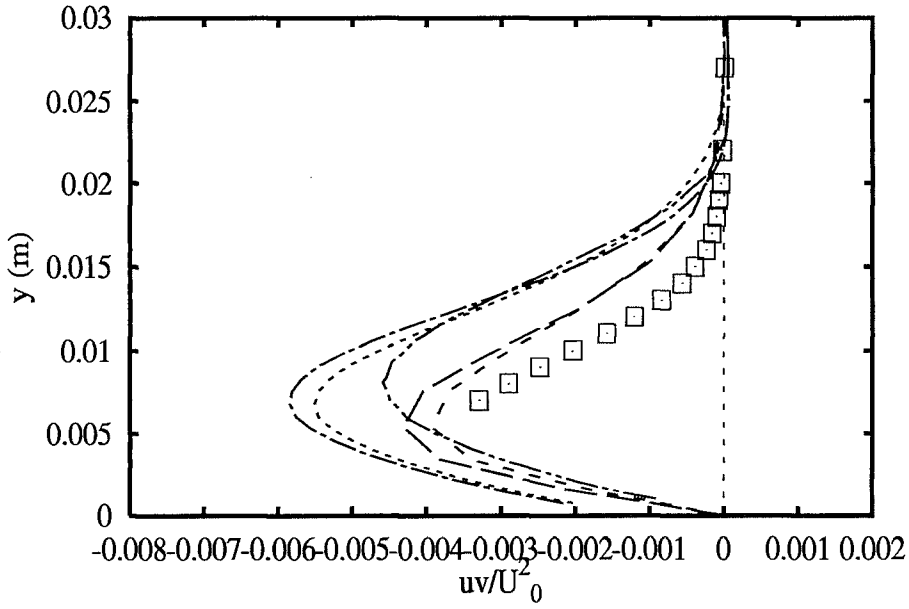




Profiles at $x=0.100$ m

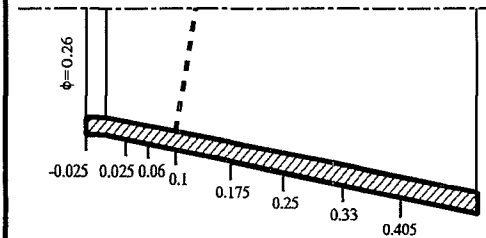
- | | | |
|-----------------|--------------------|---------|
| | Experiments | □ |
| UBrussel | nKE SZL+wf | — — |
| UBrussel | nKE HiKh+wf | - - - |
| THAachen | ASM ClWi+wf | · · · · |
| THAachen | RSM LRR+wf | - · - · |
| ECLyon | RSM LRR+wf | - · - · |

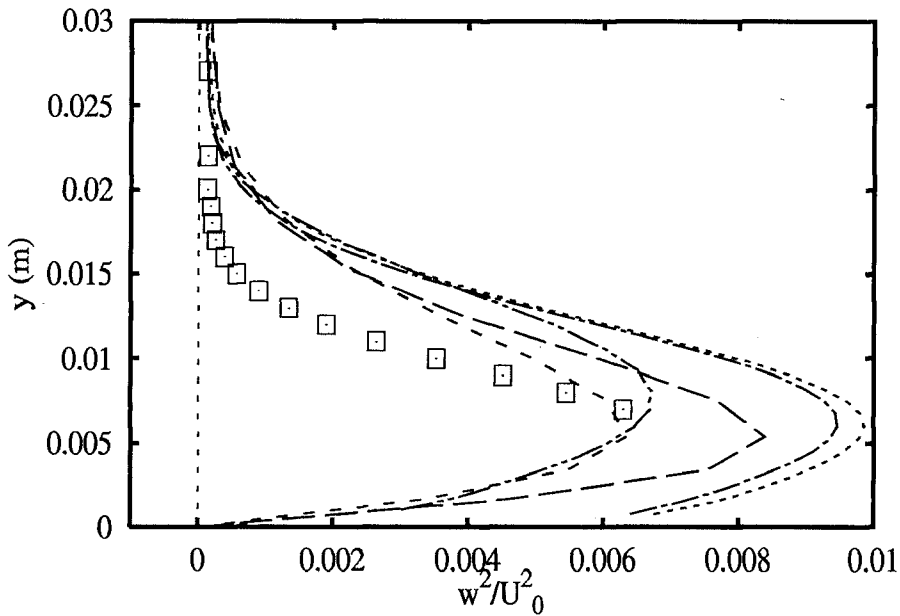
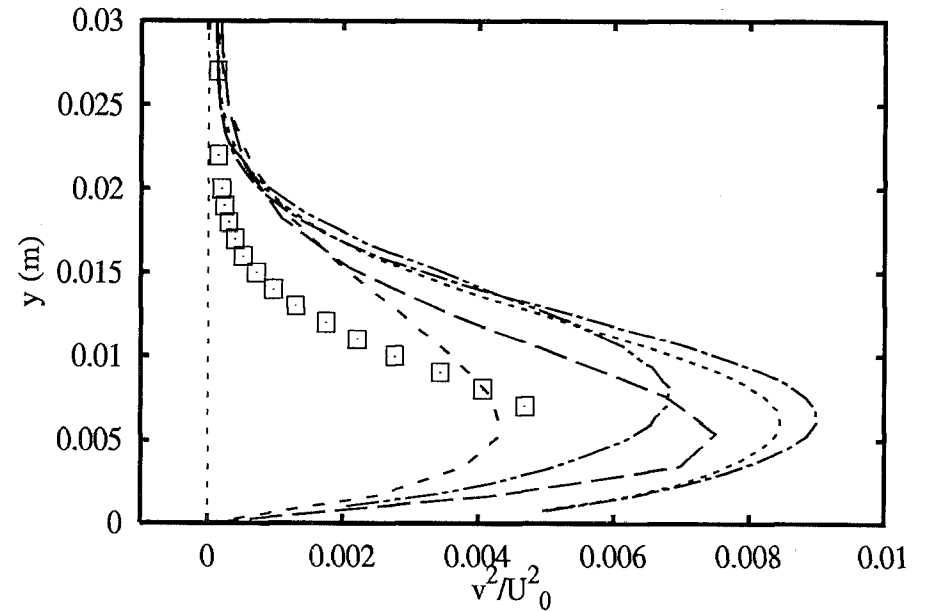
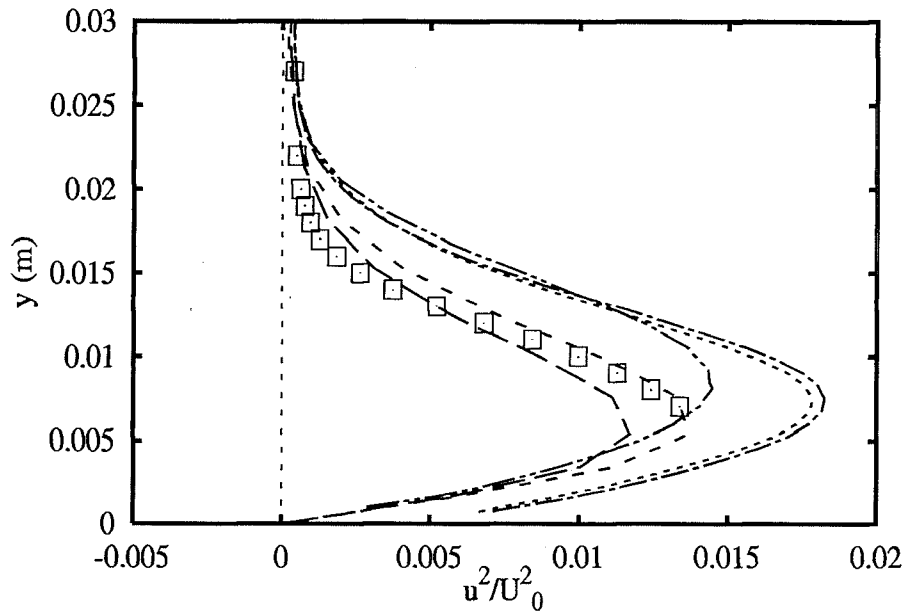




Profiles at $x=0.100$ m

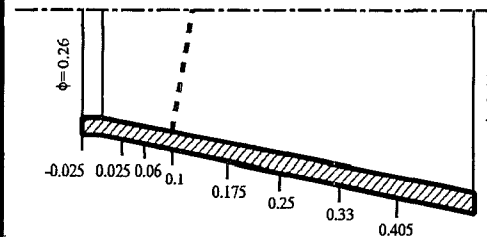
- | | | |
|------------|----------------------------|-----------|
| | Experiments | □ |
| U | Brussel nKE SZL+wf | --- |
| U | Brussel nKE HiKh+wf | - - - |
| THA | achen ASM ClWi+wf | · · · · · |
| THA | achen RSM LRR+wf | - · - · - |
| ECL | yon RSM LRR+wf | - · - · - |

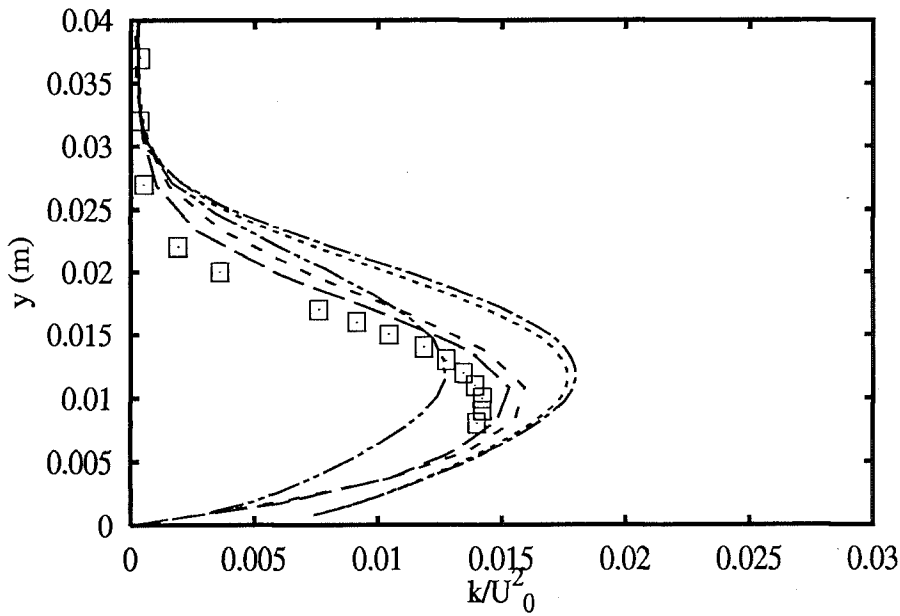
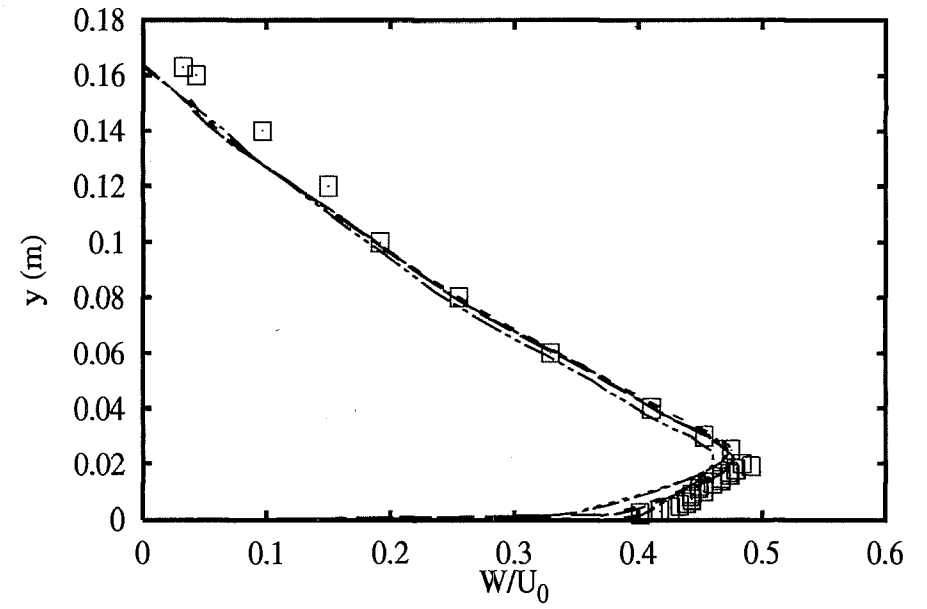
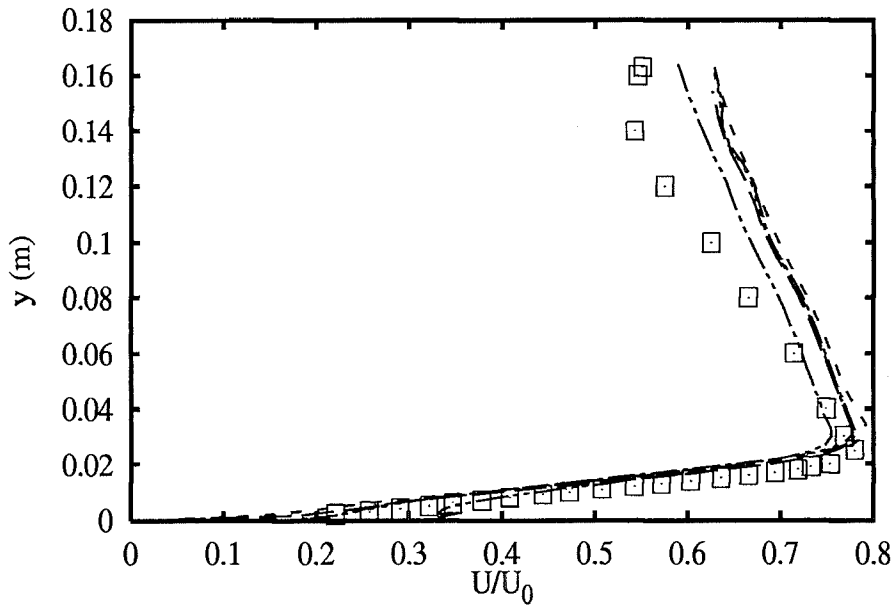




Profiles at x=0.100 m

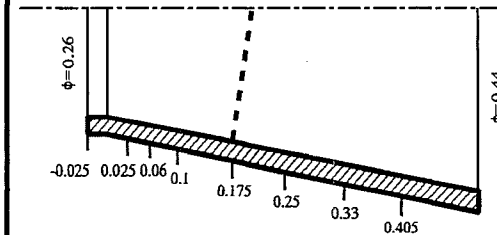
- | | |
|-----------------------------|-----------|
| Experiments | □ |
| Ubrussel nKE SZL+wf | — |
| Ubrussel nKE HiKh+wf | - - - |
| THAachen ASM ClWi+wf | · · · · · |
| THAachen RSM LRR+wf | - · - · - |
| ECLyon RSM LRR+wf | - · - · - |

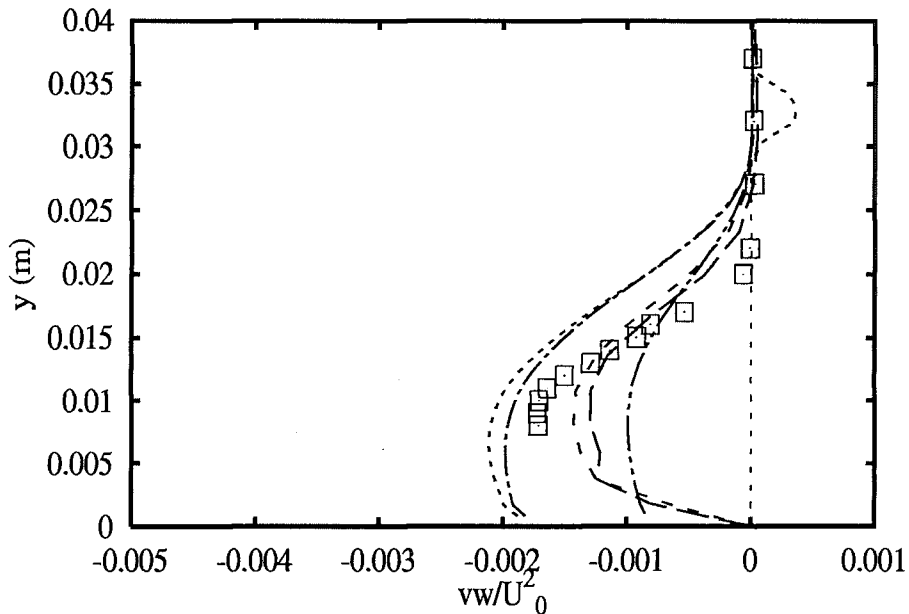
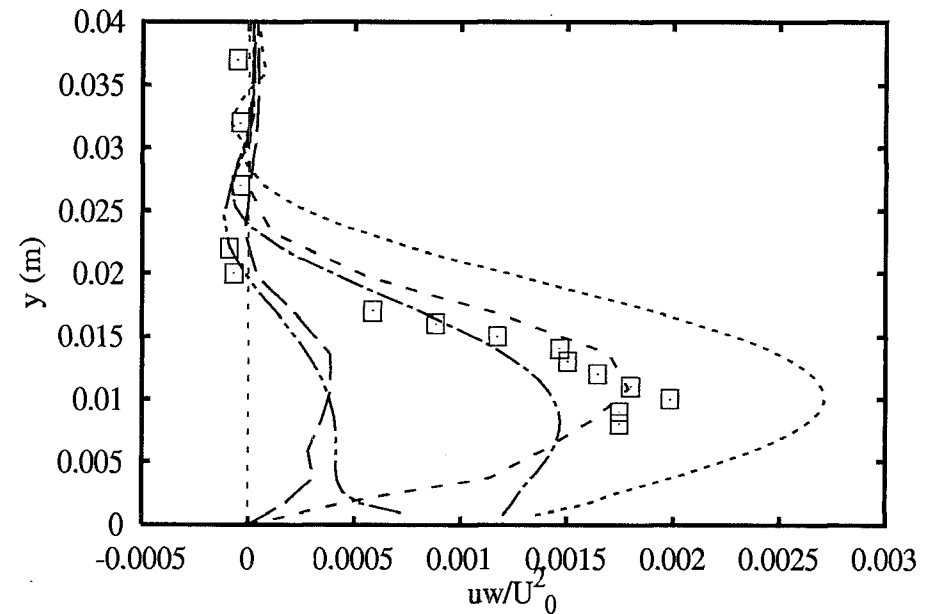
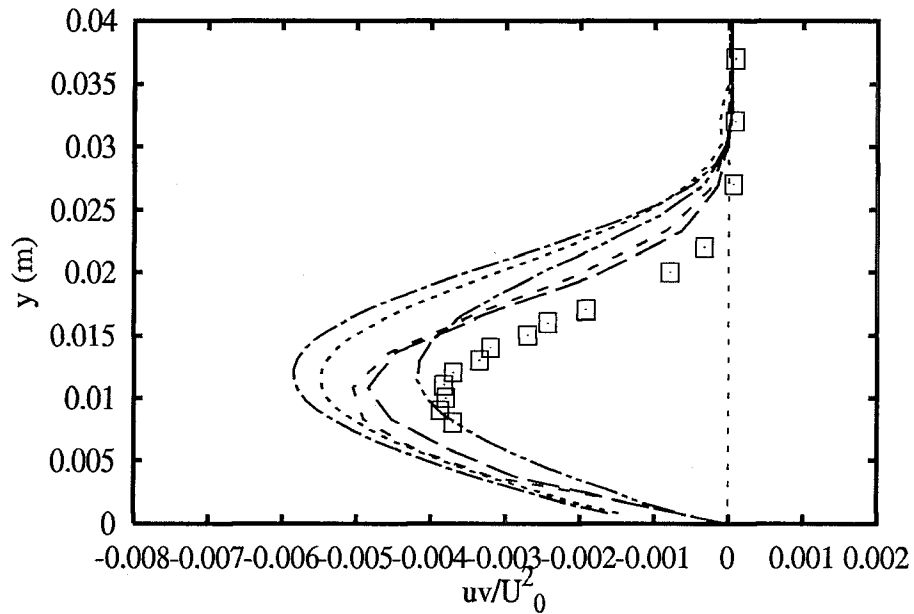




Profiles at $x=0.175$ m

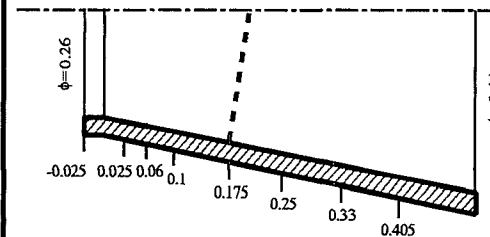
- | | | |
|------------|----------------------------|-----------|
| | Experiments | □ |
| U | Brussel nKE SZL+wf | — |
| U | Brussel nKE HiKh+wf | - - - |
| THA | achen ASM ClWi+wf | · · · · · |
| THA | achen RSM LRR+wf | - · - · - |
| ECL | yon RSM LRR+wf | · · · · · |

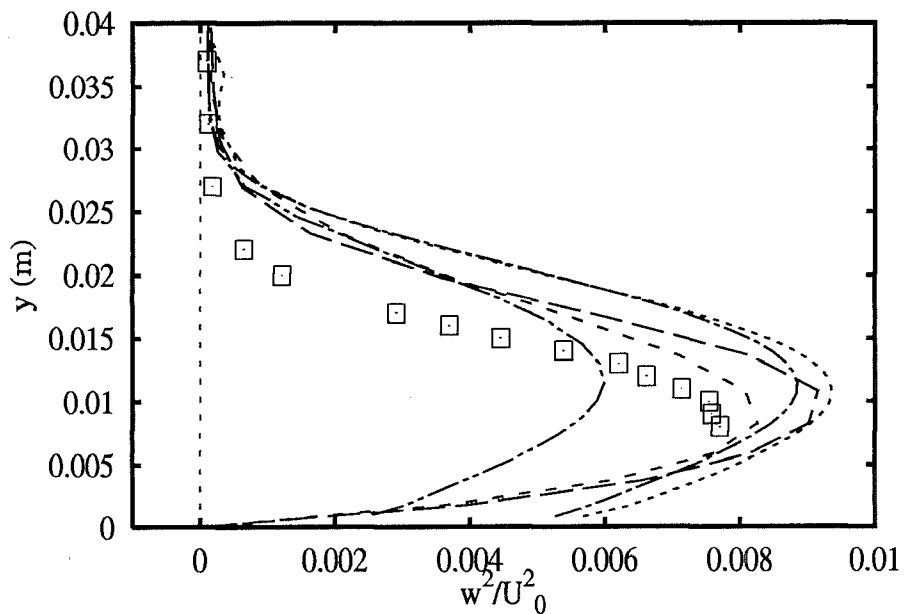
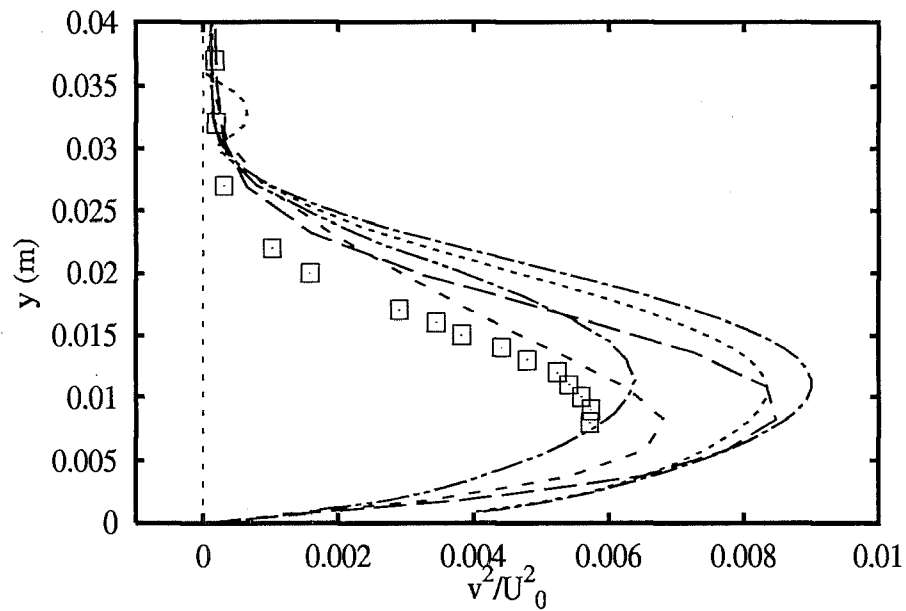
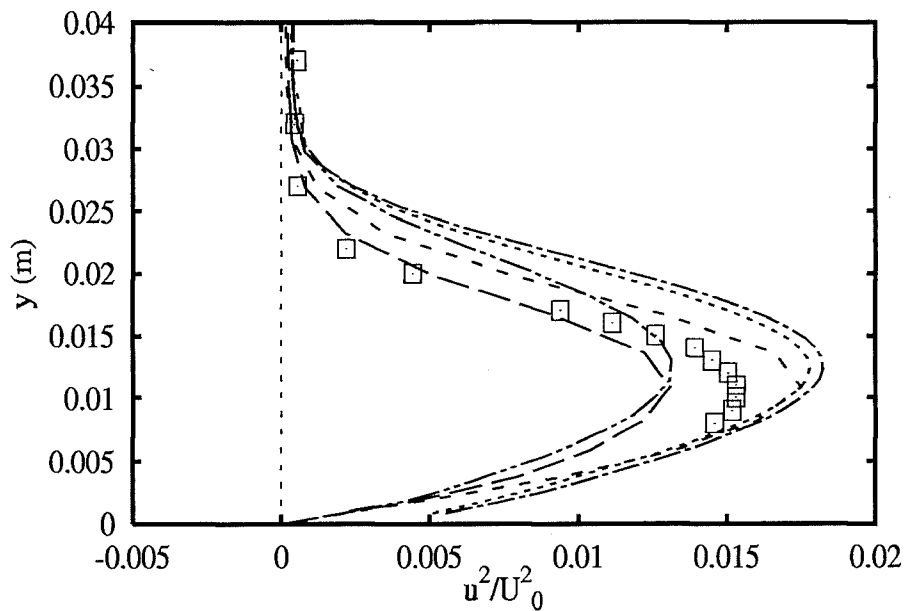




Profiles at $x=0.175$ m

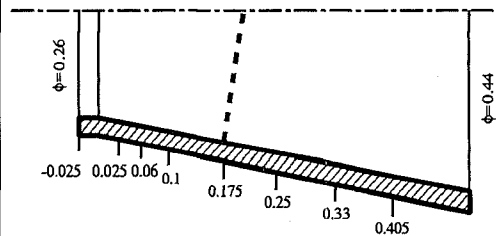
- Experiments \square
- Ubrussel nKE SZL+wf $---$
- Ubrussel nKE HiKh+wf $----$
- THAachen ASM ClWi+wf $.....$
- THAachen RSM LRR+wf $-----$
- ECLyon RSM LRR+wf $-----$

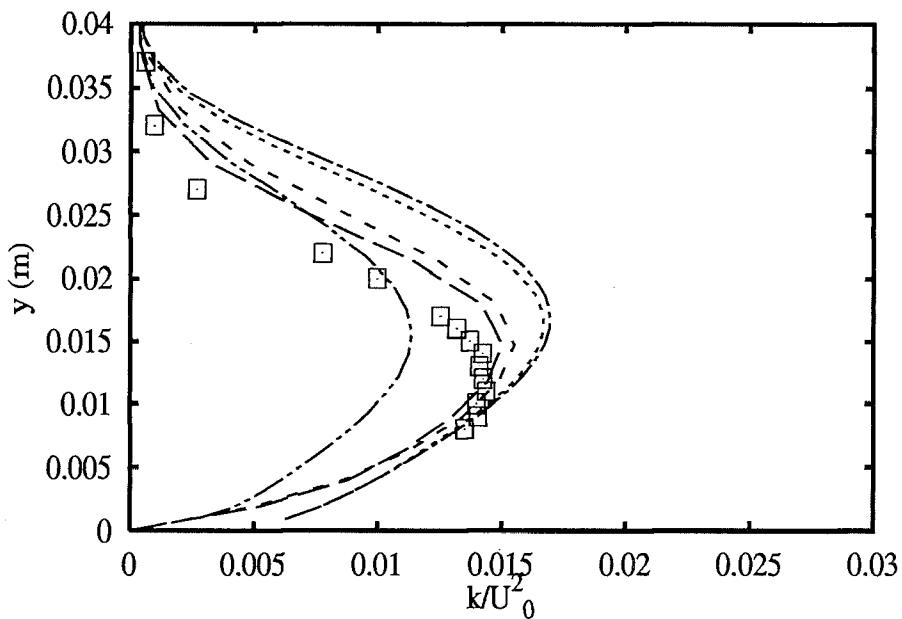
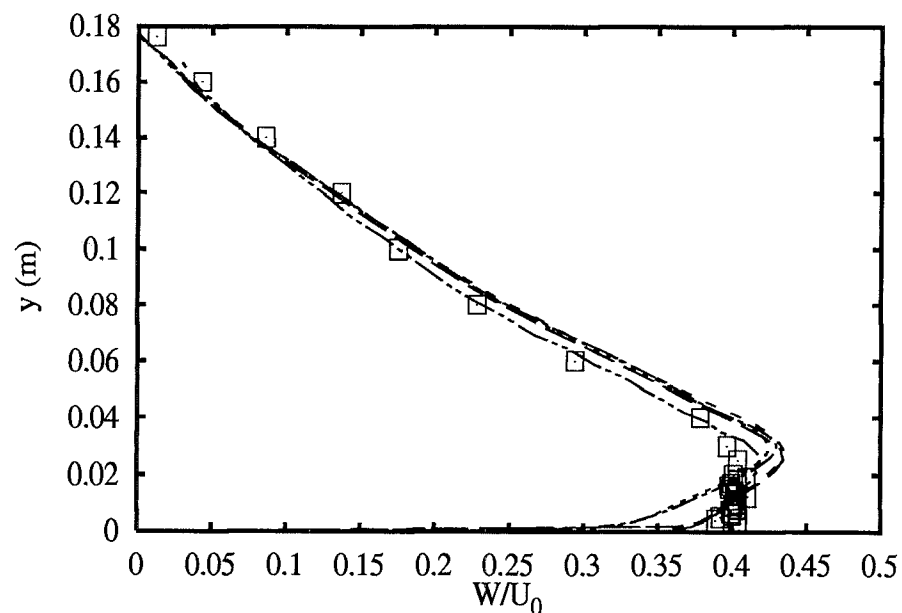
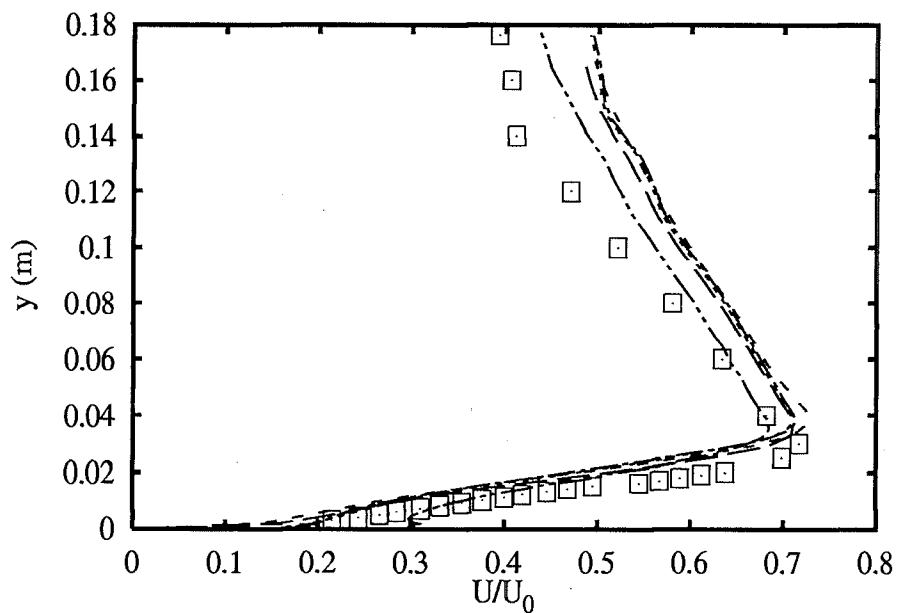




Profiles at $x=0.175$ m

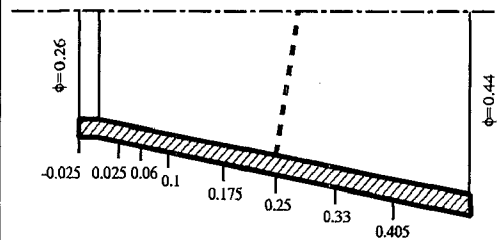
- | | | |
|-----------------|----------------------------|-----------|
| | Experiments | □ |
| U | Brussel nKE SZL+wf | --- |
| U | Brussel nKE HiKh+wf | - - - |
| THAachen | ASM ClWi+wf | · · · · · |
| THAachen | RSM LRR+wf | - · - · - |
| ECLyon | RSM LRR+wf | - · - · - |

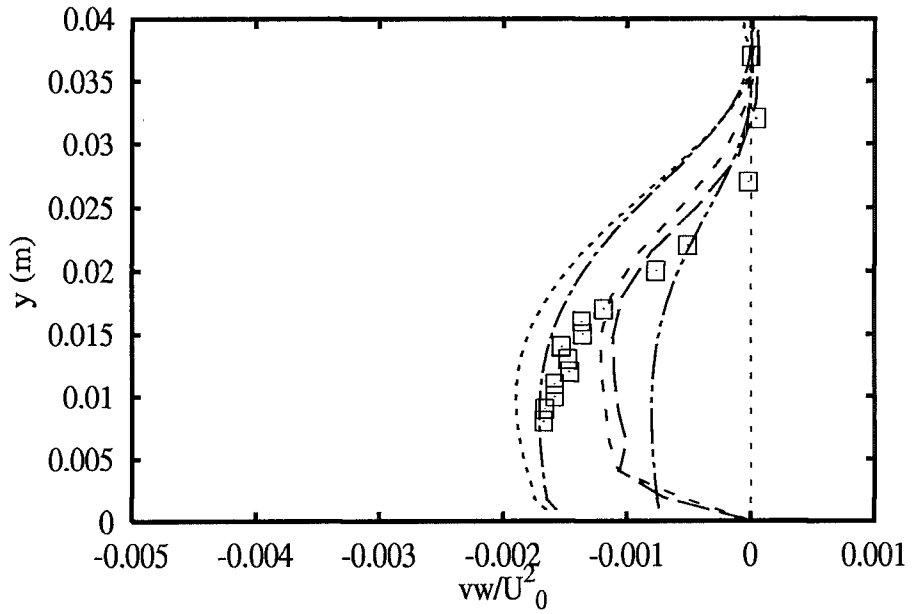
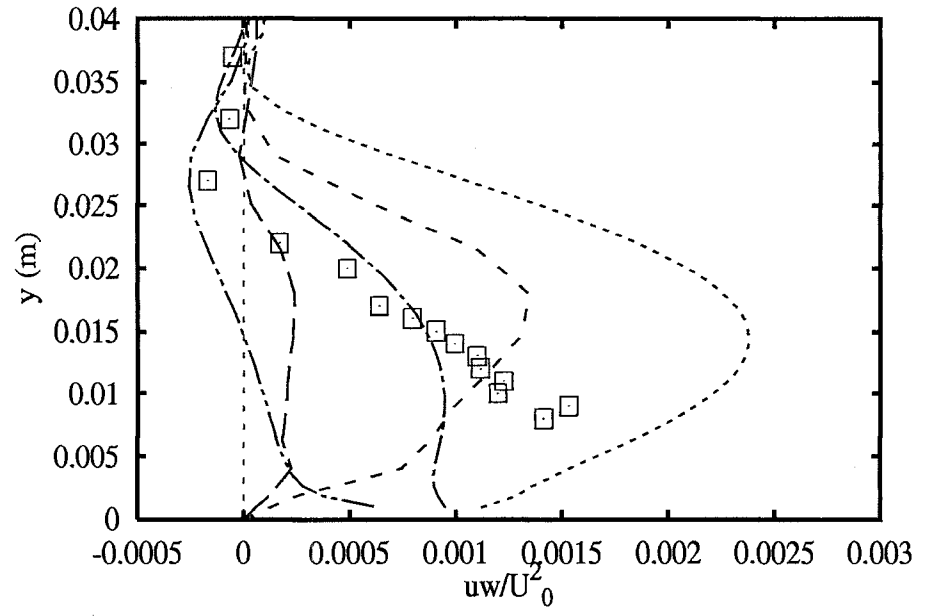
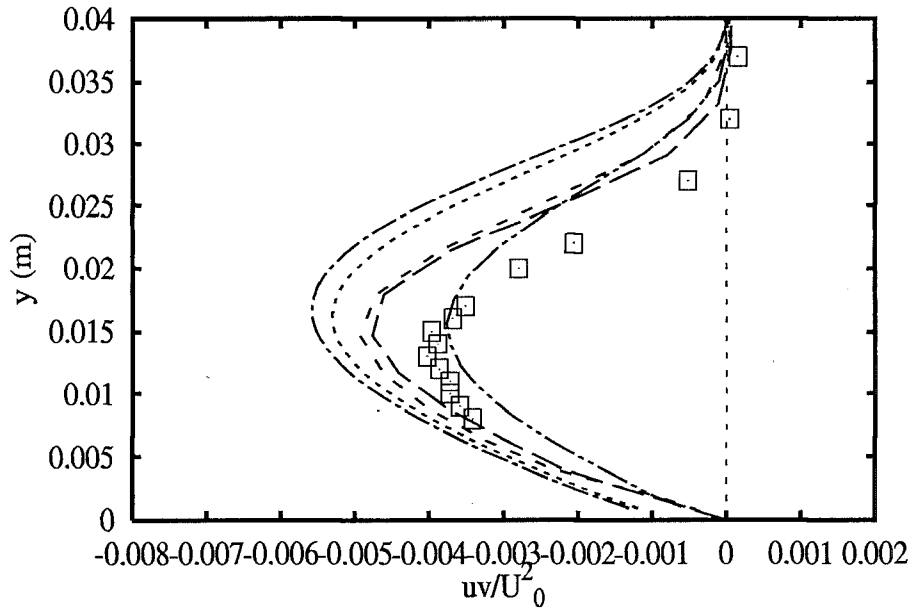




Profiles at $x=0.250$ m

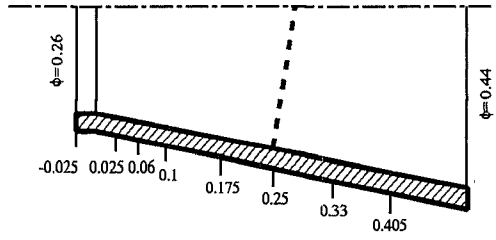
- Experiments \square
- Ubrussel nKE SZL+wf $---$
- Ubrussel nKE HiKh+wf $----$
- THAachen ASM ClWi+wf $.....$
- THAachen RSM LRR+wf $----$
- ECLyon RSM LRR+wf $----$

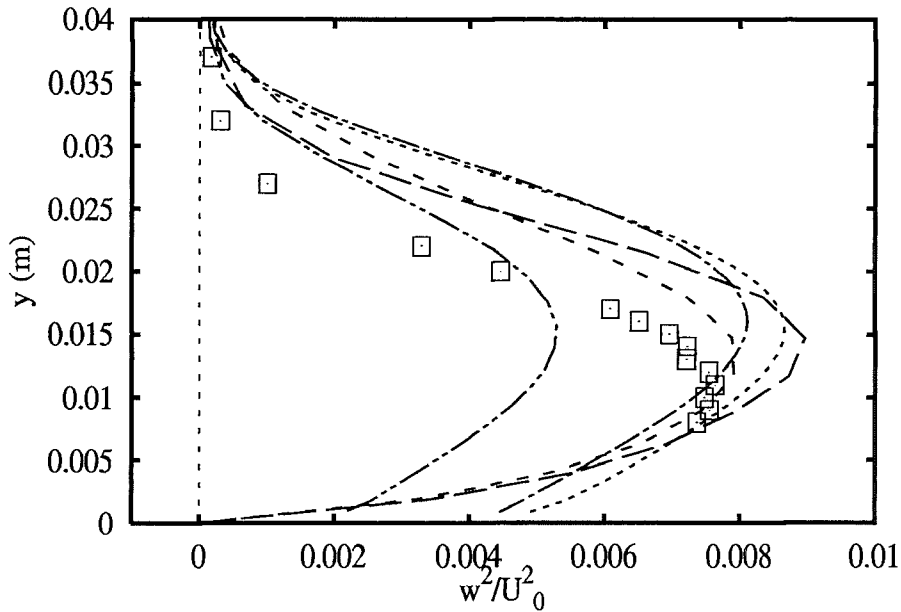
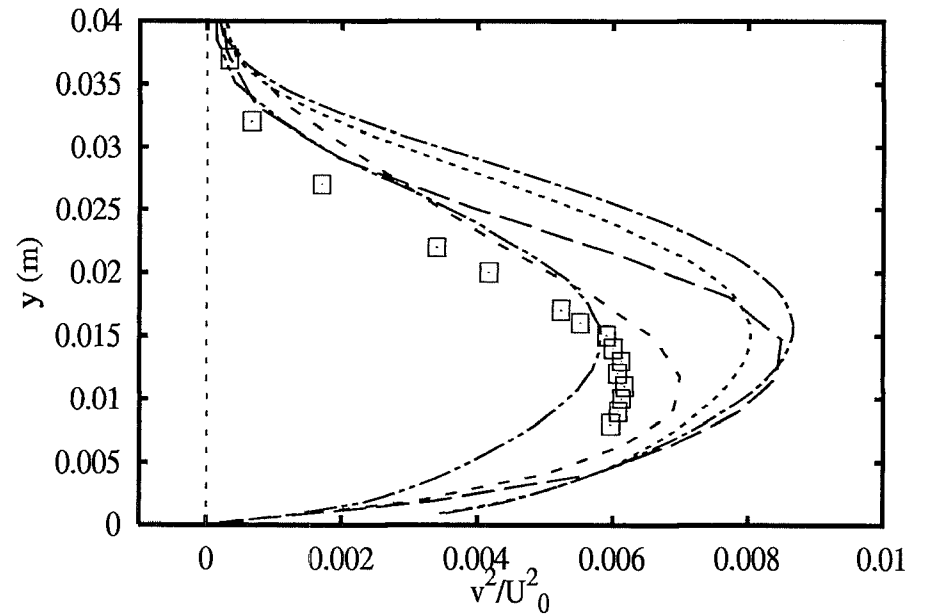
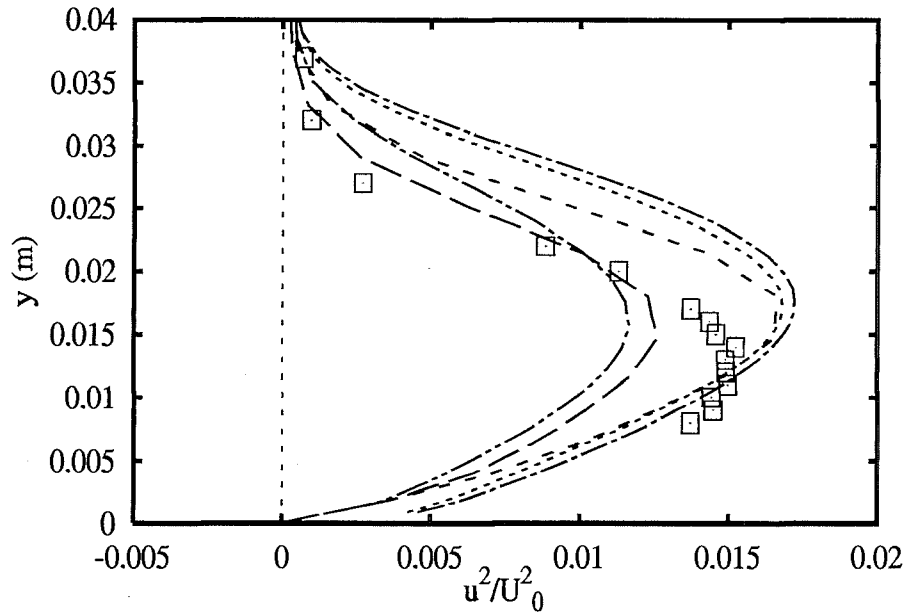




Profiles at $x=0.250$ m

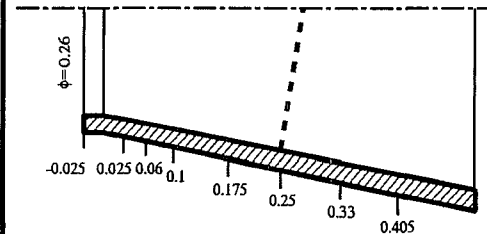
- Experiments \square
- Ubrussel nKE SZL+wf ---
- Ubrussel nKE HiKh+wf - - -
- THAachen ASM ClWi+wf ·····
- THAachen RSM LRR+wf - · - · -
- ECLyon RSM LRR+wf - · - · -

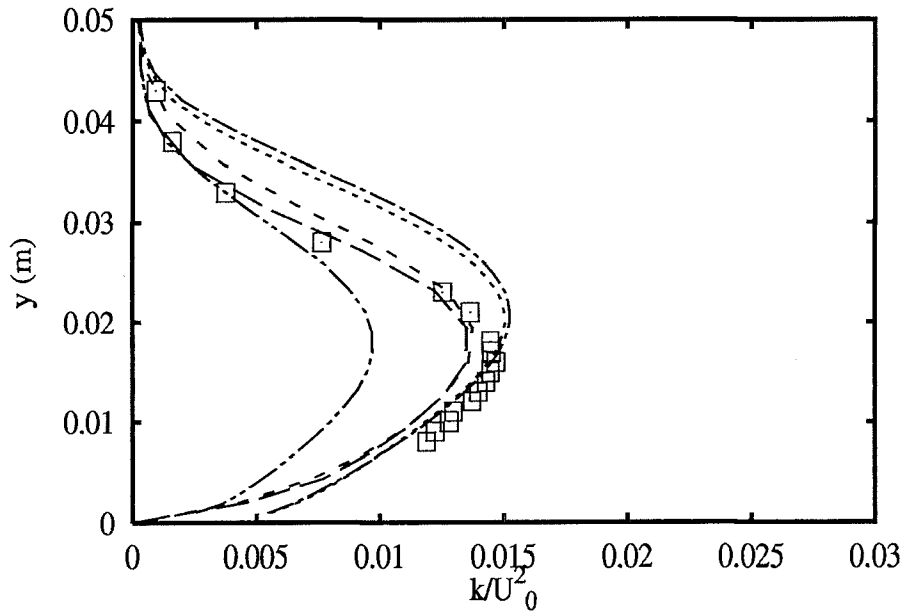
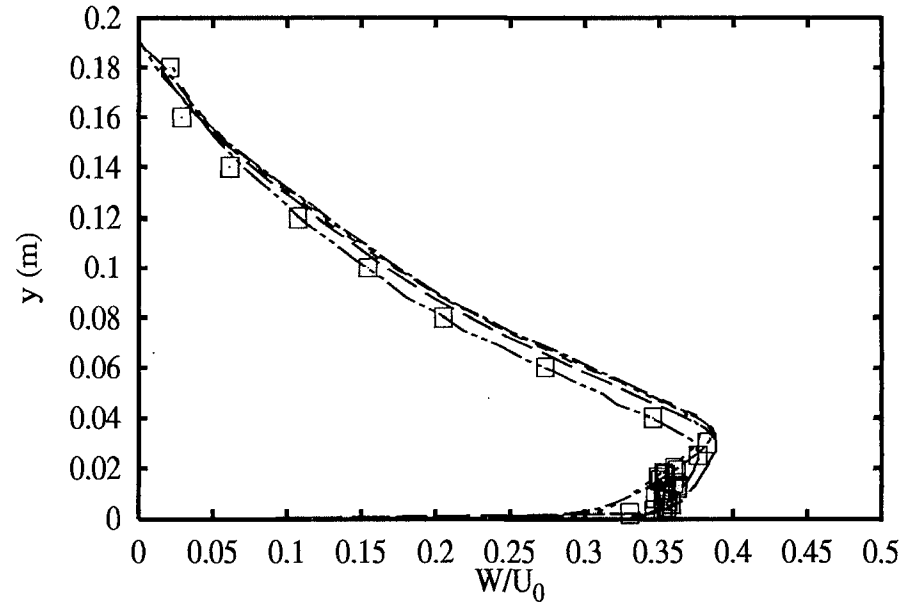
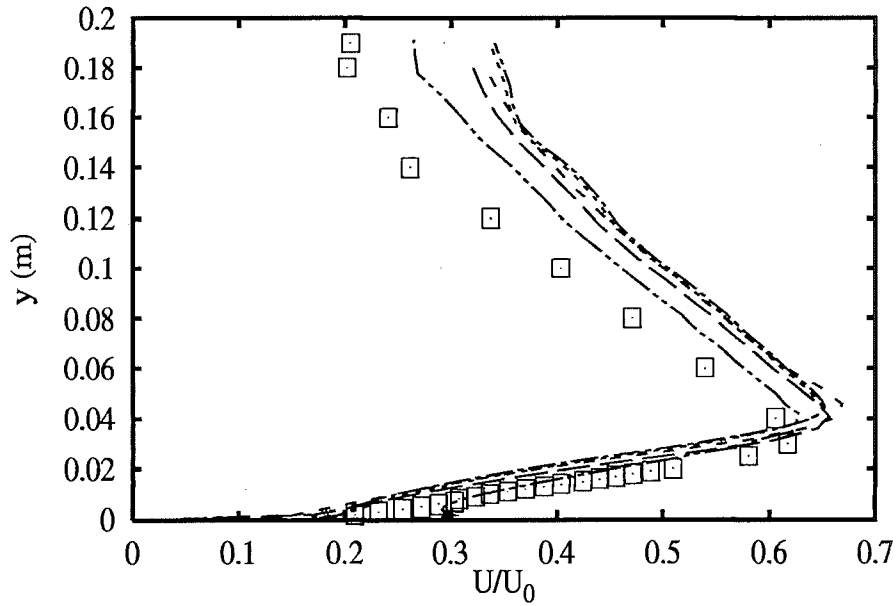




Profiles at $x=0.250$ m

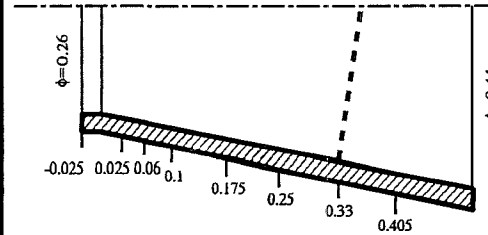
- | | | |
|----------|----------------------------|-----------|
| | Experiments | □ |
| U | Brussel nKE SZL+wf | — |
| U | Brussel nKE HiKh+wf | - - - |
| T | Aachen ASM ClWi+wf | - · - · - |
| T | Aachen RSM LRR+wf | - - - |
| E | CLyon RSM LRR+wf | - · - · - |

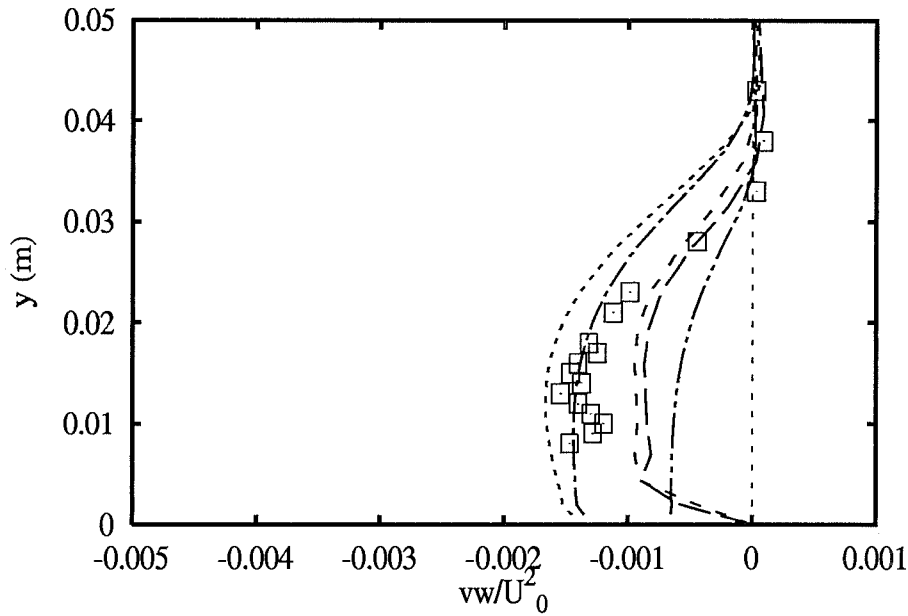
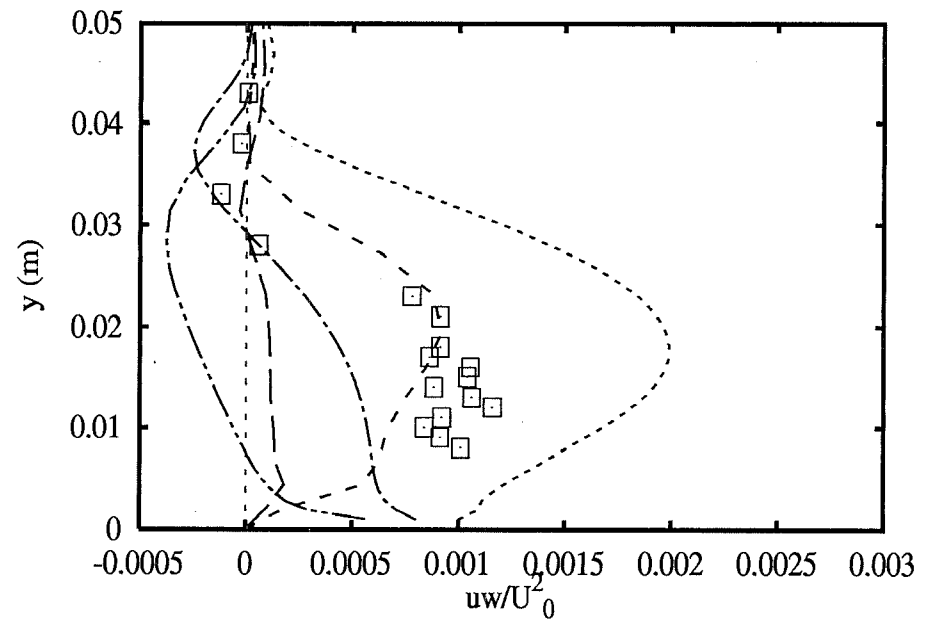
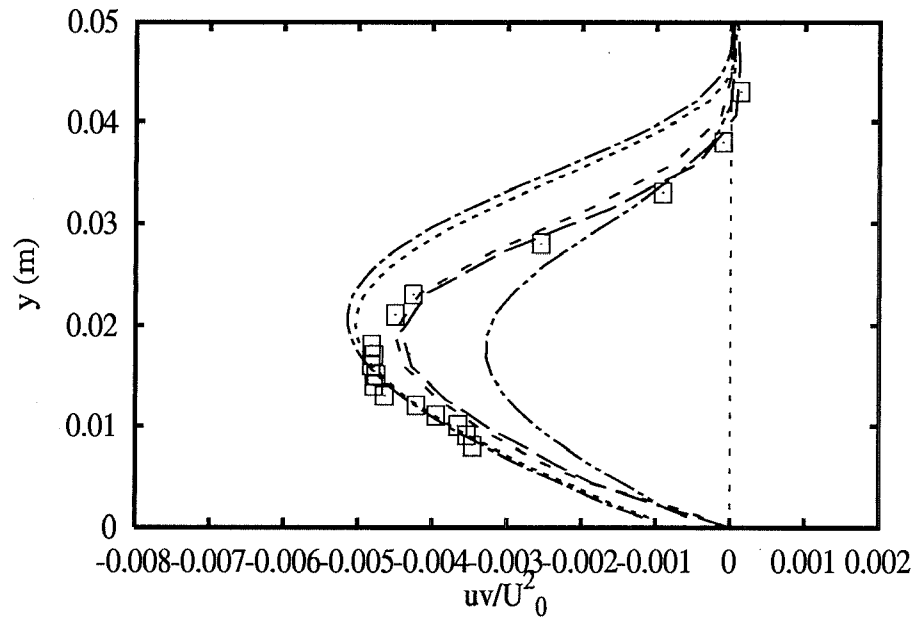




Profiles at $x=0.330$ m

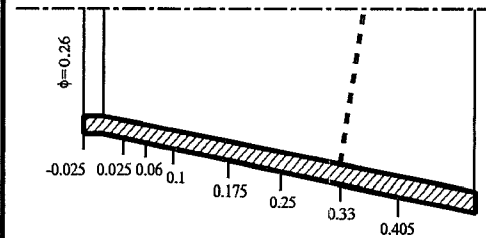
- | | | |
|----------|----------------------------|-----------|
| | Experiments | □ |
| U | Brussel nKE SZL+wf | — |
| U | Brussel nKE HiKh+wf | - - - |
| T | Aachen ASM ClWi+wf | · · · · · |
| T | Aachen RSM LRR+wf | - · - · - |
| E | CLyon RSM LRR+wf | - · - · - |

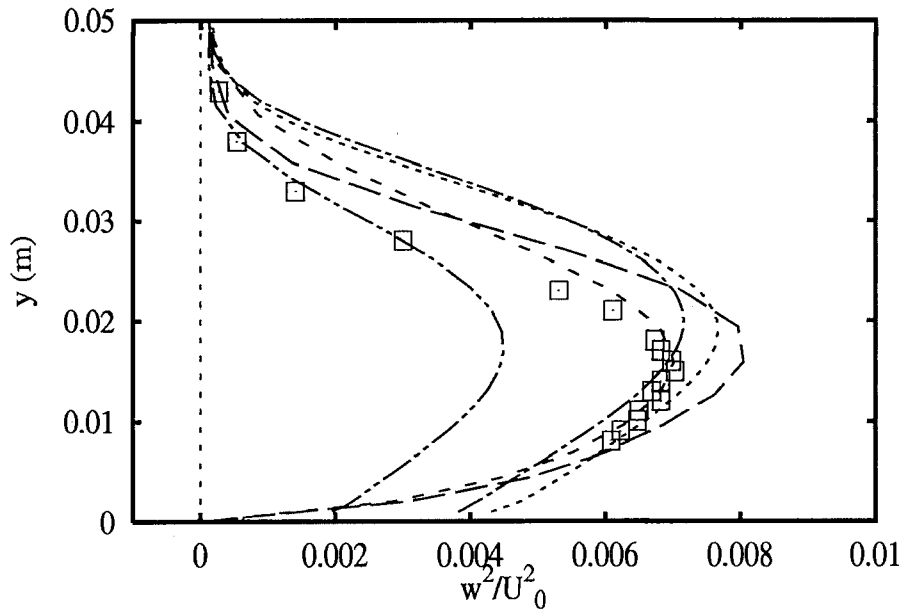
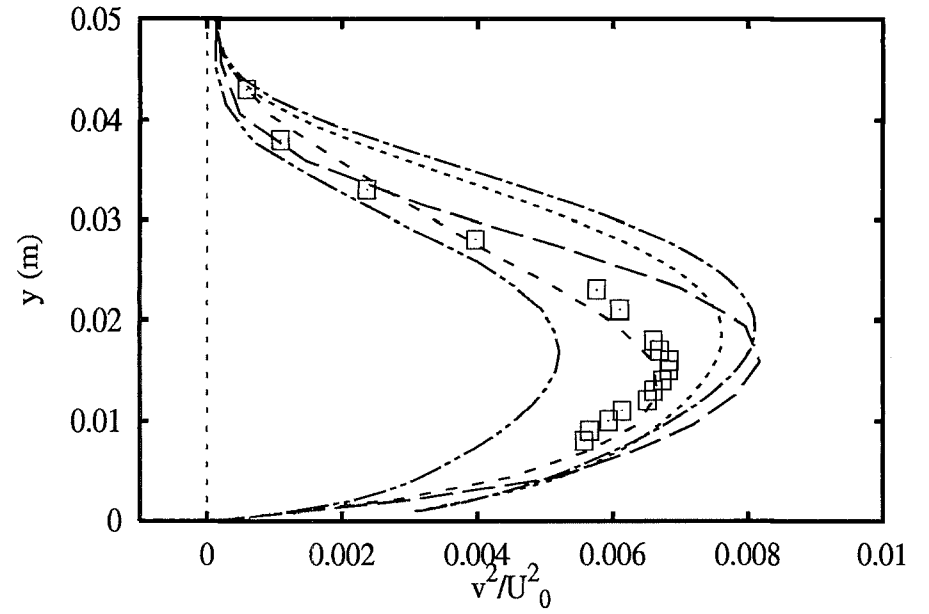
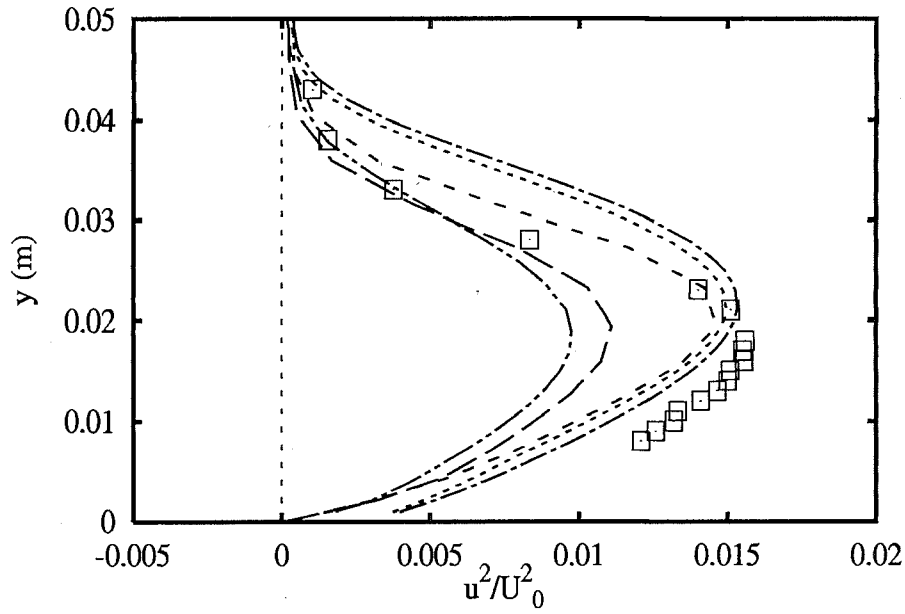




Profiles at x=0.330 m

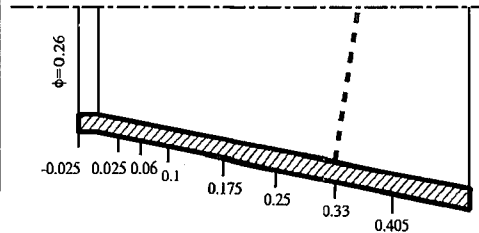
- Experiments** □
- Ubrussel nKE SZL+wf** ---
- Ubrussel nKE HiKh+wf** - - -
- THAachen ASM ClWi+wf** - · - · -
- THAachen RSM LRR+wf** - · - -
- ECLyon RSM LRR+wf** - · - · -

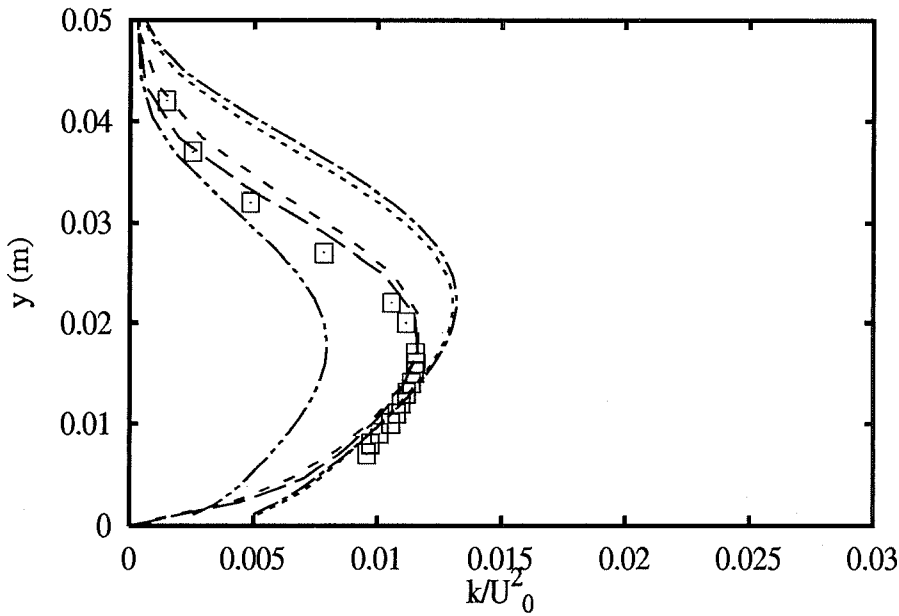
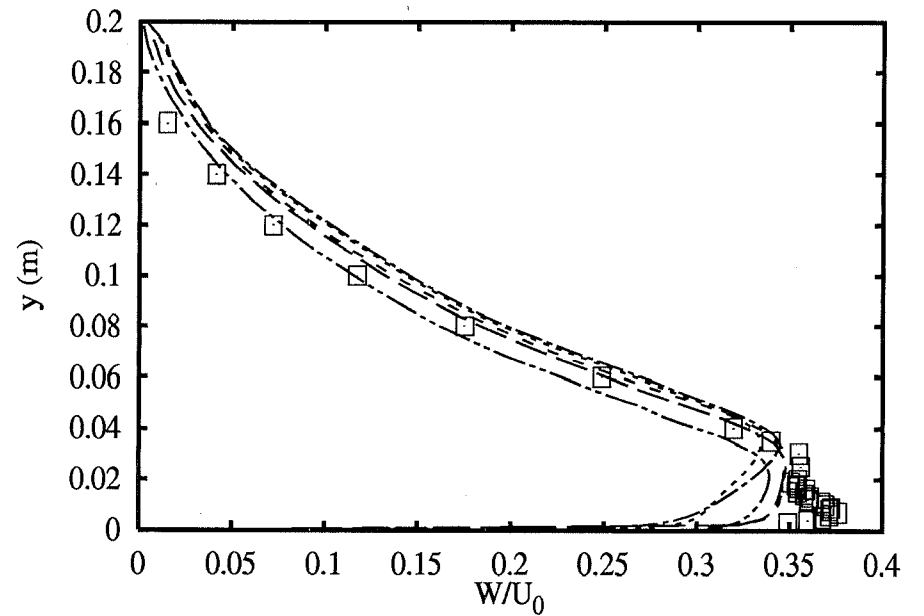
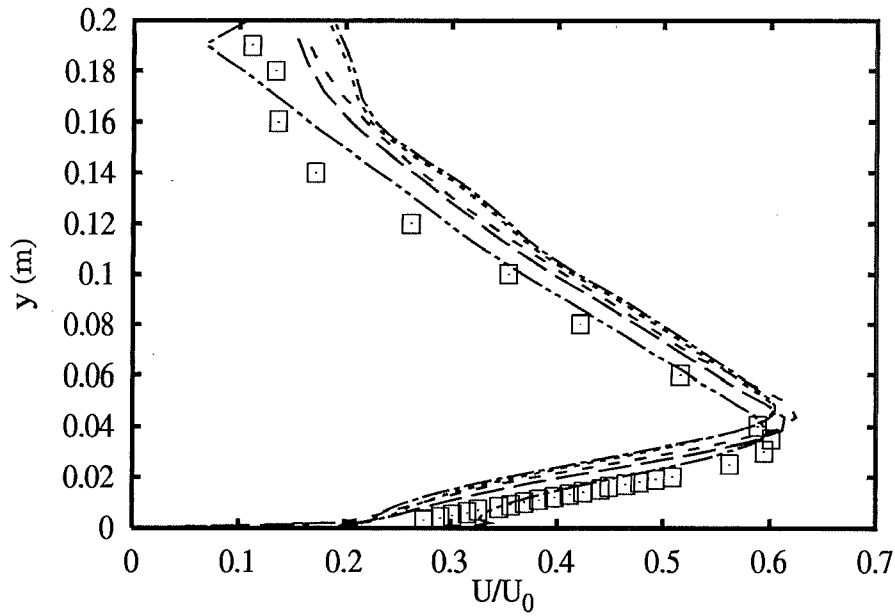




Profiles at $x=0.330$ m

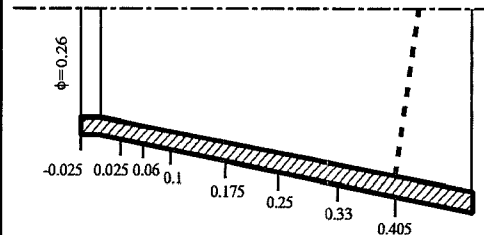
- | | |
|-----------------------------|-----------|
| Experiments | □ |
| Ubrussel nKE SZL+wf | — |
| Ubrussel nKE HiKh+wf | - - - |
| THAachen ASM ClWi+wf | · · · · · |
| THAachen RSM LRR+wf | - · - · - |
| ECLyon RSM LRR+wf | - · - · - |

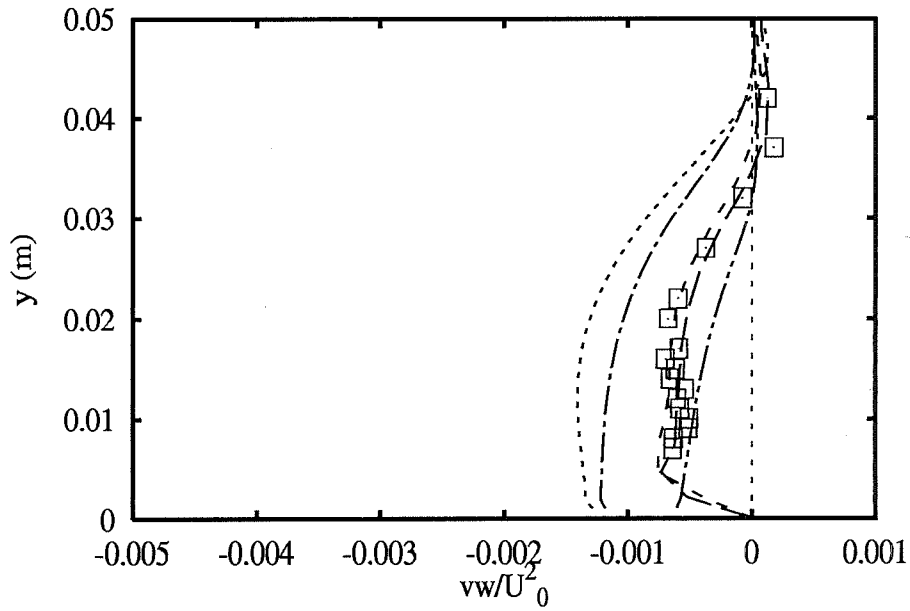
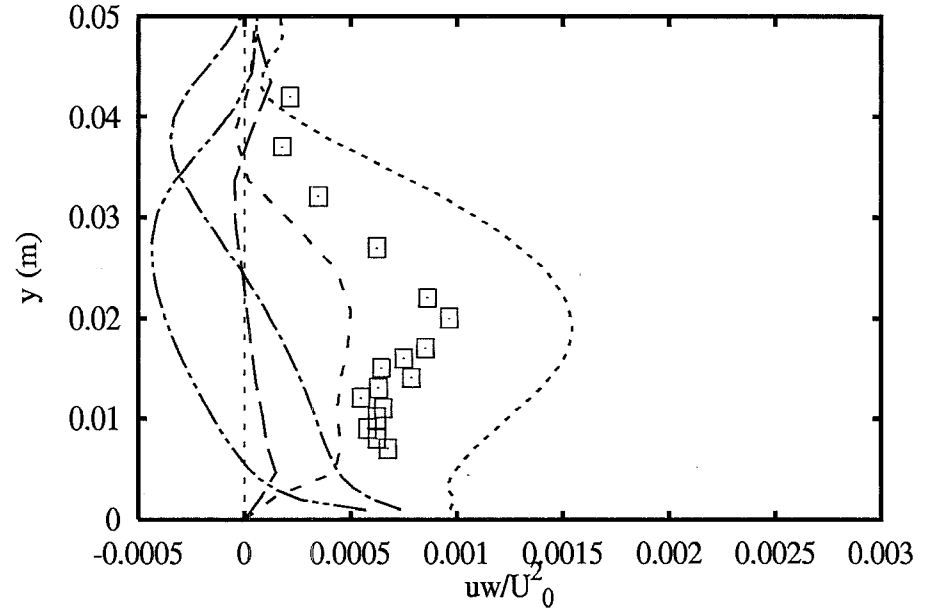
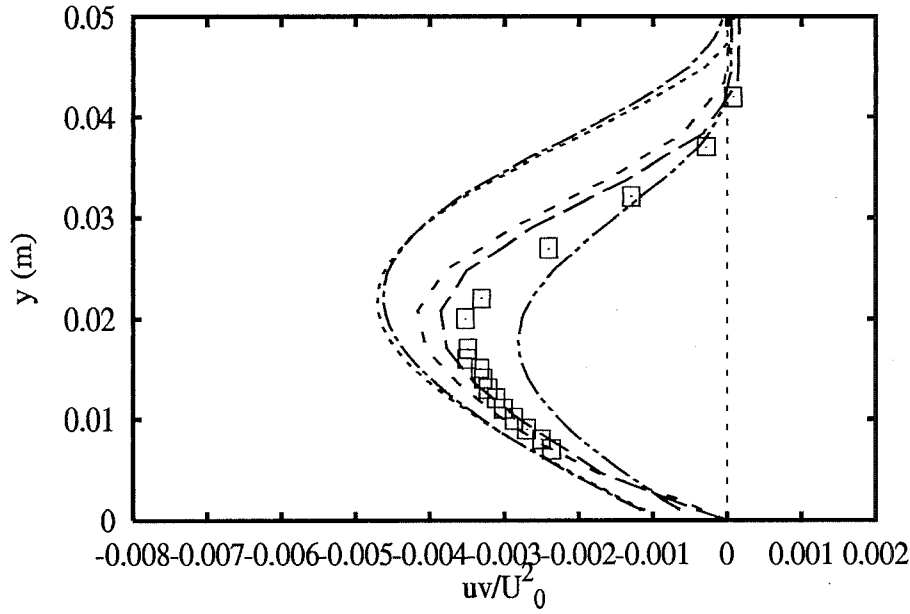




Profiles at $x=0.405$ m

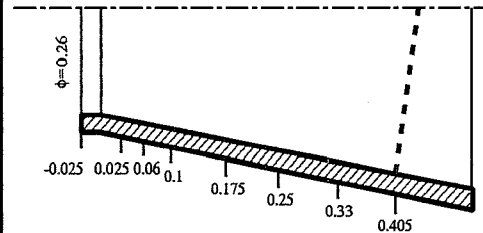
- | | | |
|-----------------|----------------------------|---------|
| | Experiments | □ |
| U | Brussel nKE SZL+wf | — — |
| U | Brussel nKE HiKh+wf | - - - |
| THAachen | ASM ClWi+wf | · · · · |
| THAachen | RSM LRR+wf | - · - · |
| ECLyon | RSM LRR+wf | · · · · |

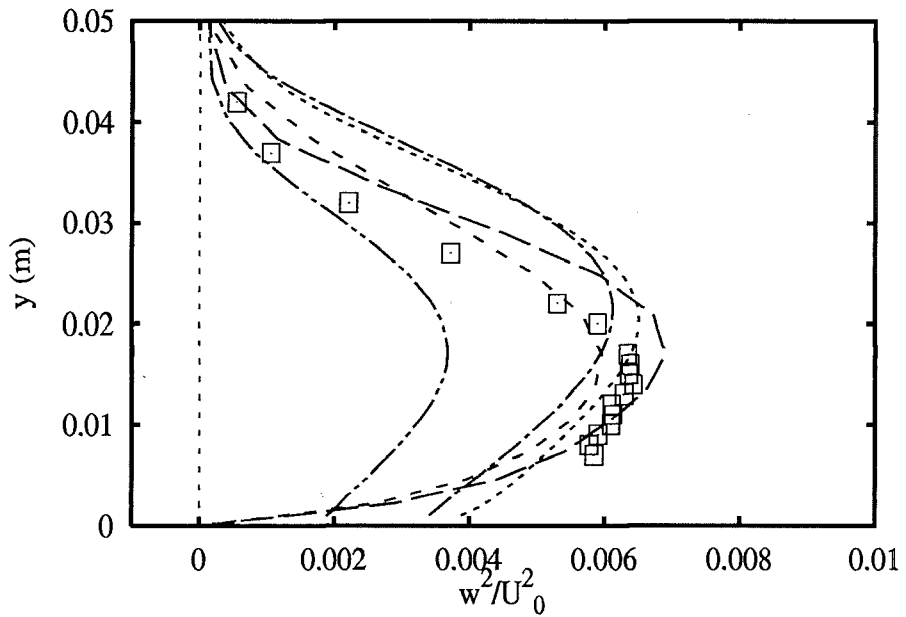
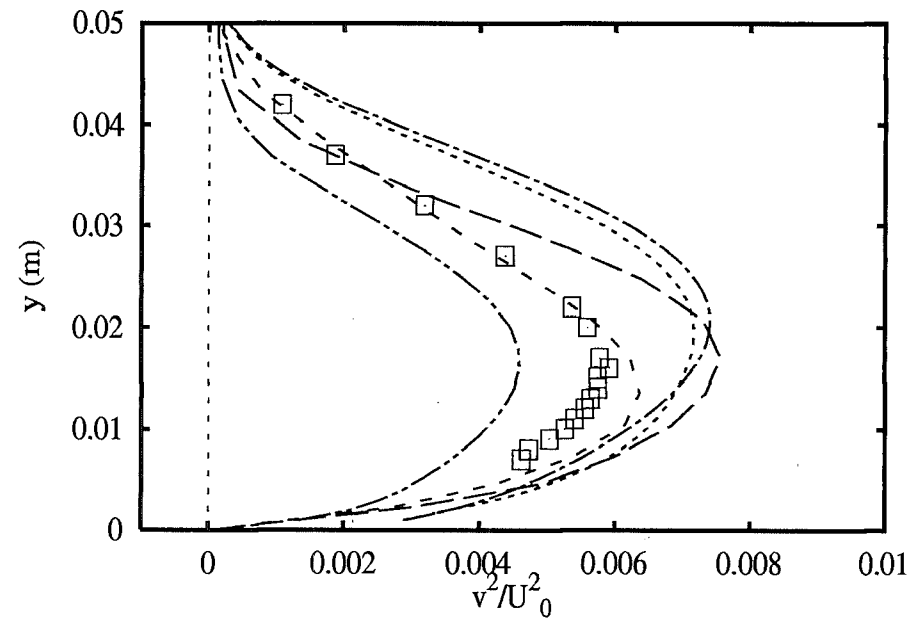
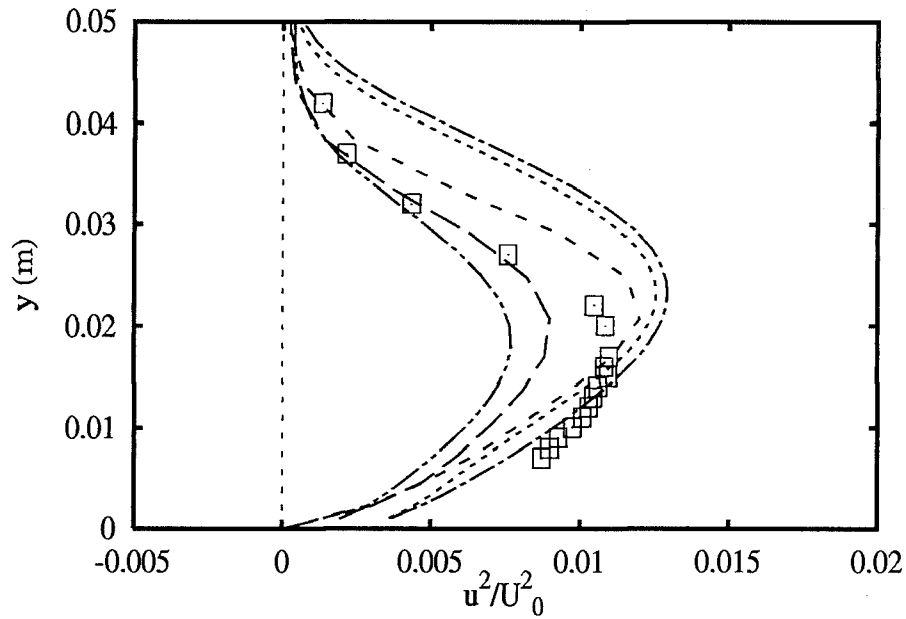




Profiles at $x=0.405$ m

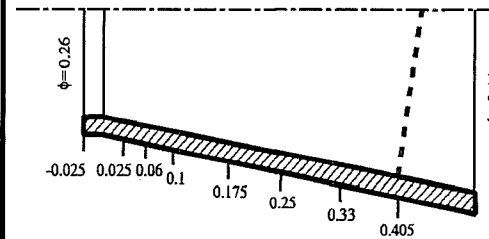
- | | | |
|----------|----------------------------|-----------|
| | Experiments | □ |
| U | Brussel nKE SZL+wf | — |
| U | Brussel nKE HiKh+wf | - - - |
| T | Aachen ASM ClWi+wf | · · · · · |
| T | Aachen RSM LRR+wf | - · - · - |
| E | CLyon RSM LRR+wf | · · · · · |

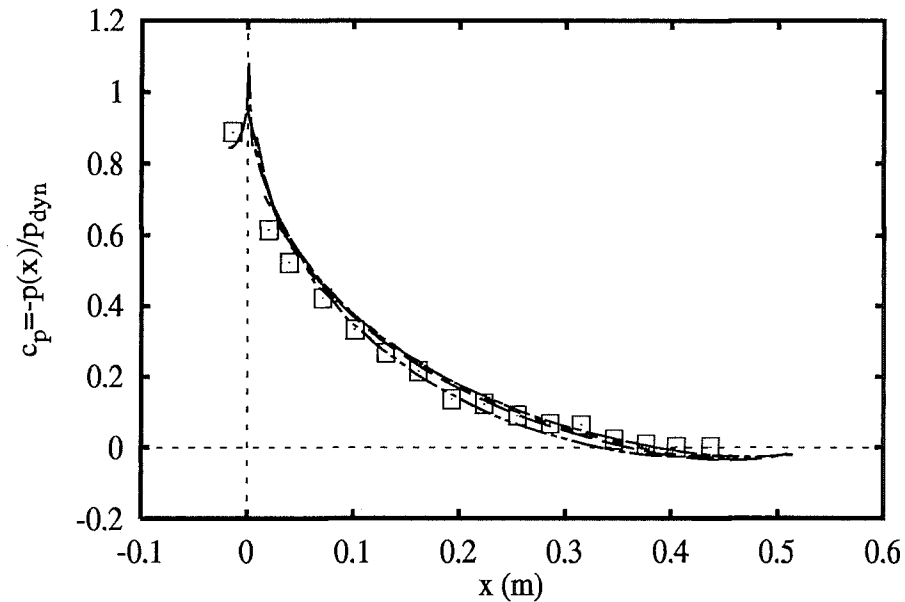
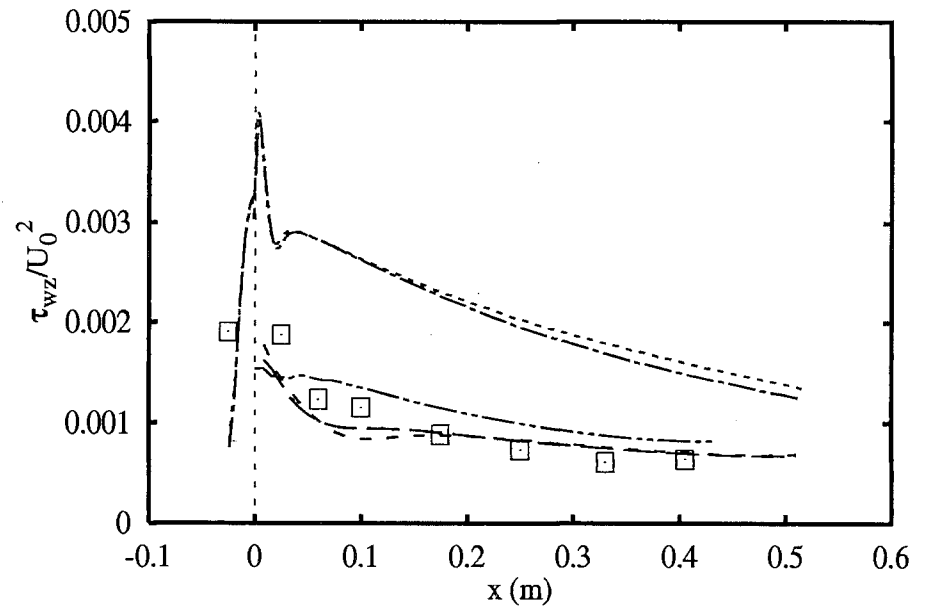
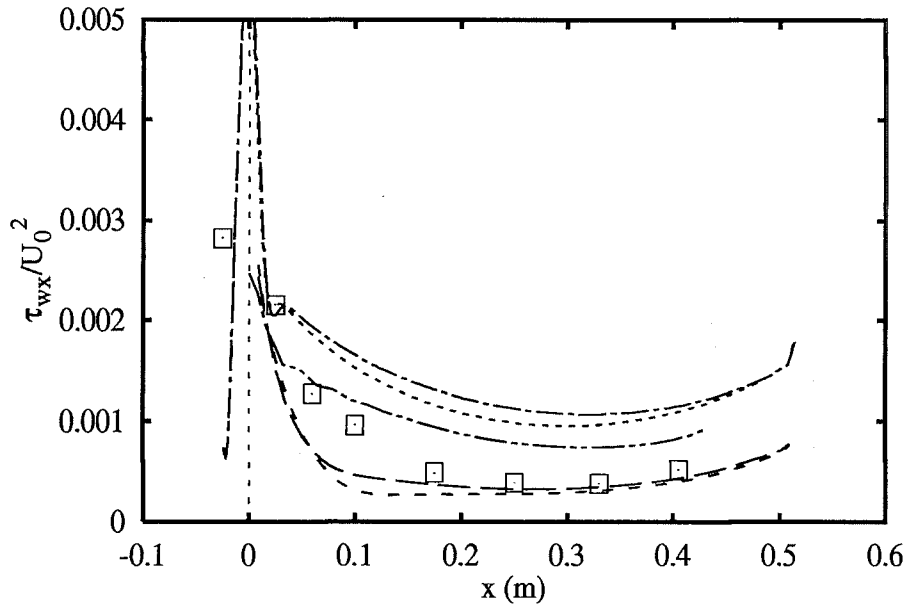




Profiles at $x=0.405$ m

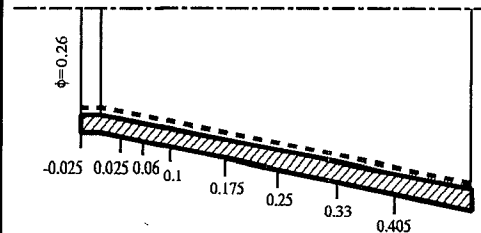
- | | |
|-----------------------------|-----------|
| Experiments | □ |
| Ubrussel nKE SZL+wf | — |
| Ubrussel nKE HiKh+wf | - - - |
| THAachen ASM ClWi+wf | · · · · · |
| THAachen RSM LRR+wf | - · - · - |
| ECLyon RSM LRR+wf | - · - · - |

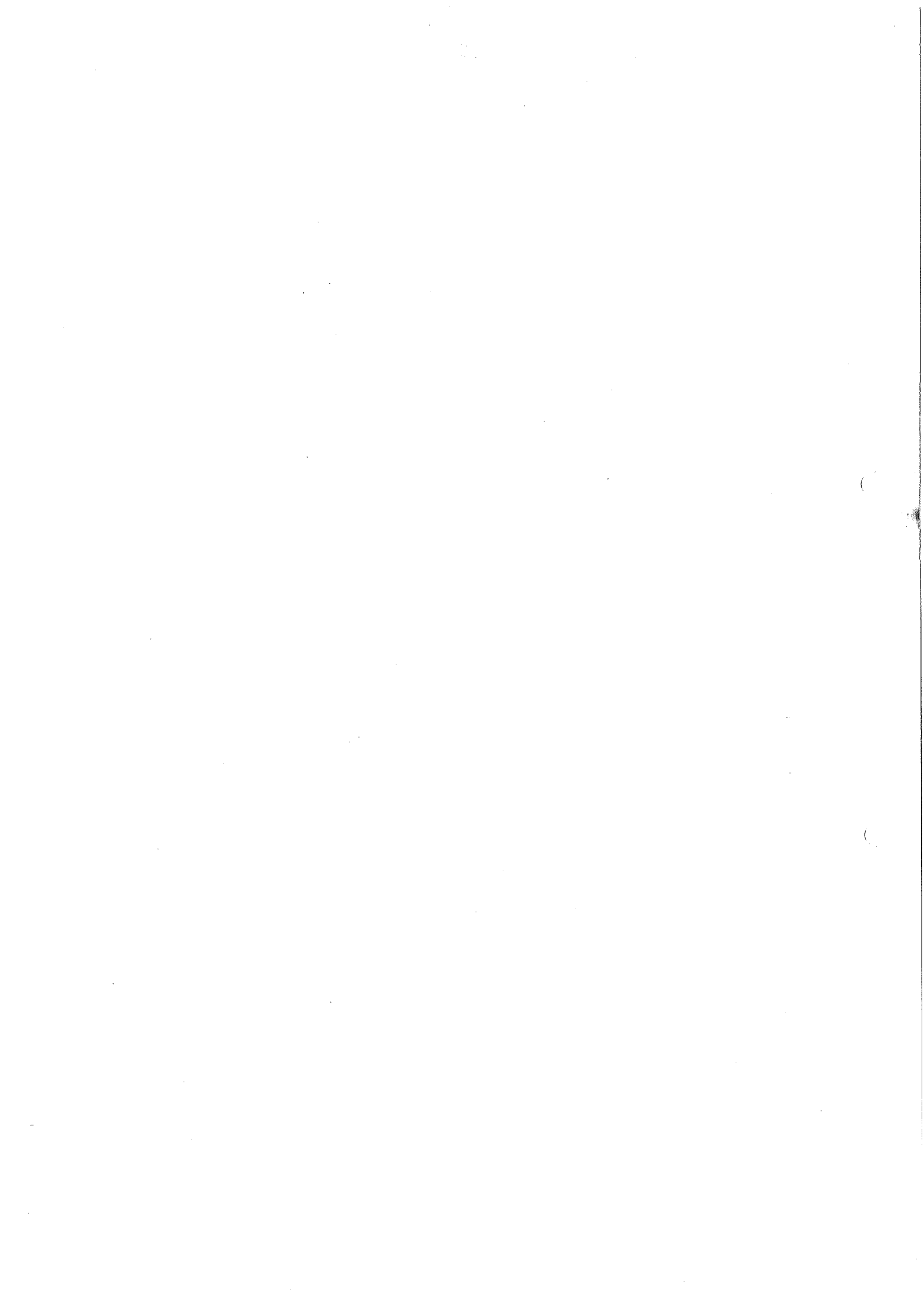




Distributions along wall

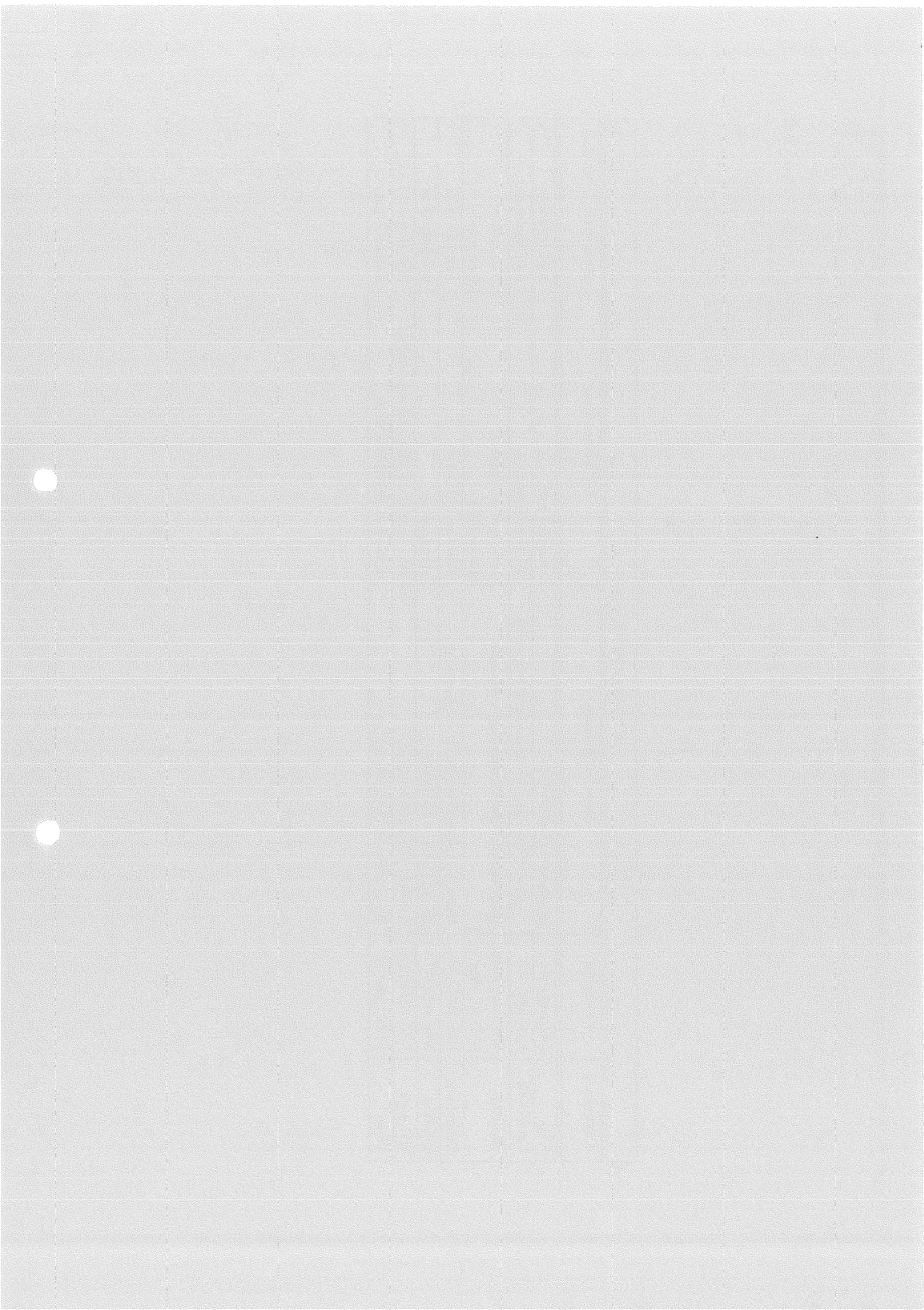
- Experiments** \square
- UBrussel nKE SZL+wf** —
- UBrussel nKE HiKh+wf** - - -
- THAachen ASM Clwi+wf** ·····
- THAachen RSM LRR+wf** - · - ·
- ECLyon RSM LRR+wf** - · - ·





KEY TO TEST CASE 4

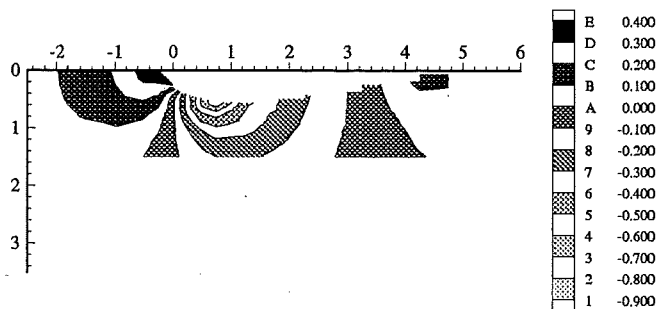
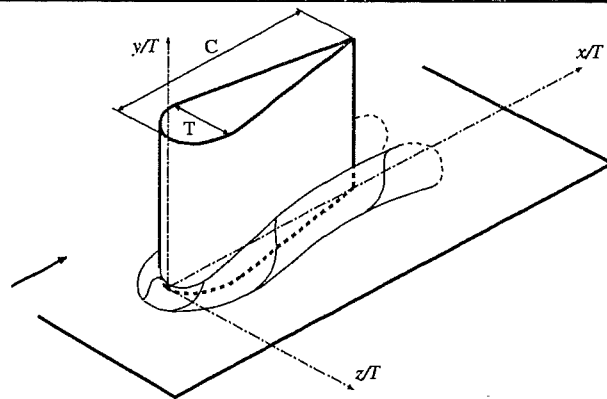
| Contributor | Key-Name | Name (Affiliation) | Turbulence Model | Near-Wall Treatment |
|-------------|--------------|--|---|---------------------|
| ASC | hKE_std+wf | Scheuerer/Holzwarth (ASC) | standard $k-\varepsilon$ | wall functions |
| CompDyna | hKE_RNG+wf | Issa/Leong/Sanatian (Computational Dynamics) | RNG-modified $k-\varepsilon$ | wall functions |
| FluiDyna | hKE_mod+0eq | Haroutunian (Fluid Dynamics International) | two-layer modified $k-\varepsilon$ | 0 eq.-model |
| | hKE_std+0eq | | two-layer $k-\varepsilon$ | 0 eq.-model |
| UHamburg | hKE_RNG+wf | Mains/Muzaferija/Peric (Univ. of Hamburg) | RNG-modified $k-\varepsilon$ | wall functions |
| UKarlsru | hKE_std+wf | Buchal (Univ. of Karlsruhe) | standard $k-\varepsilon$ | wall functions |
| UStuttg2 | hKE_KaLa+1eq | Ruprecht (Univ. of Stuttgart) | two-layer $k-\varepsilon$ + Kato-Launder modif. | Mohammadi 1 eq. |
| Volvo | RSM_LRR+wf | Daunius (Volvo Data AB) | RSM Launder-Reece-Rodi | wall functions |



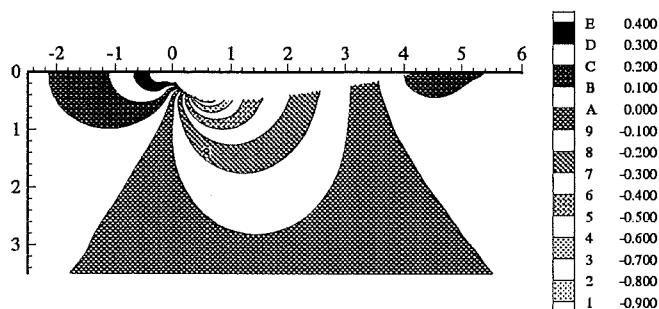
Wing/Body Junction with Separation

Mean pressure coefficient

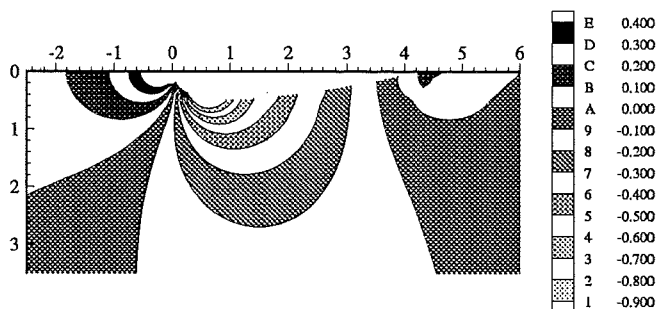
On ground plate



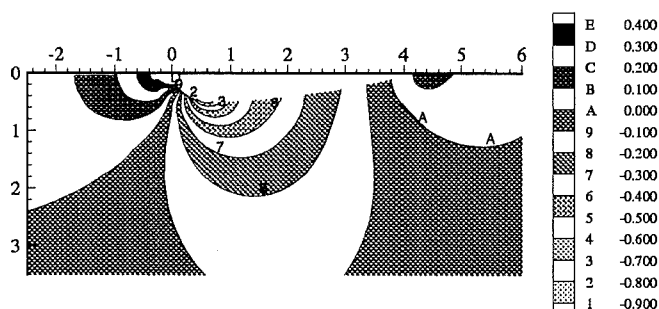
Exp



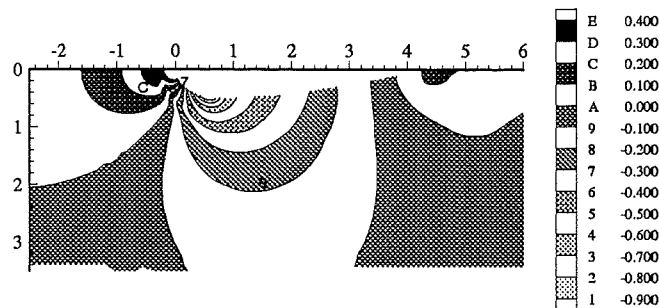
ASC:hKE_std+wf



UKarlsru:hKE_std+wf



CompDyna:hKE_RNG+wf

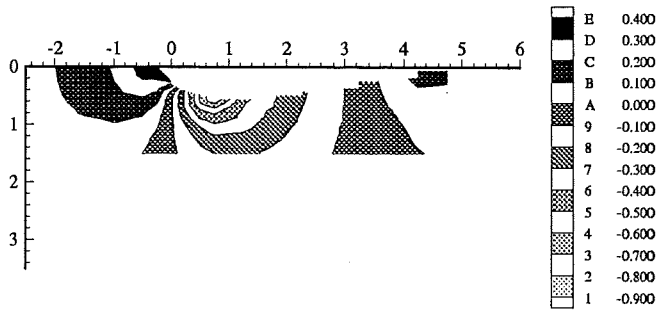
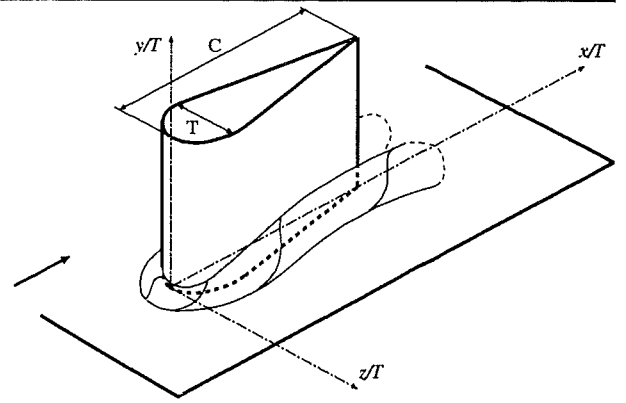


UHamburg:hKE_RNG+wf

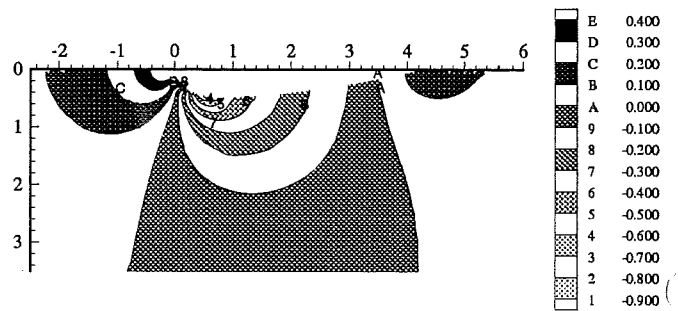
Wing/Body Junction with Separation

Mean pressure coefficient

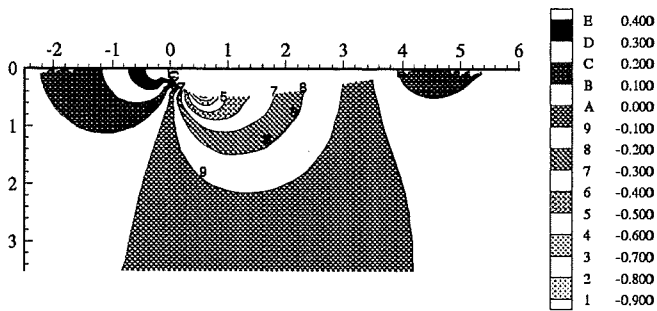
On ground plate



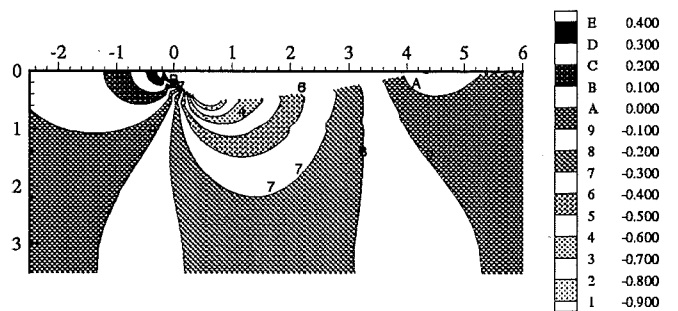
Exp



FluiDyna:hKE_std+0eq



FluiDyna:hKE_mod+0eq

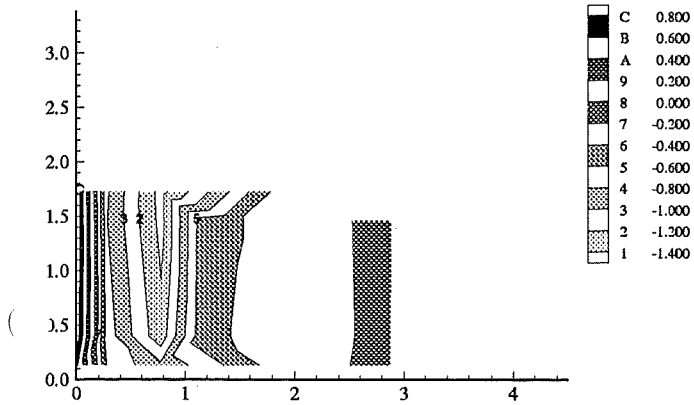
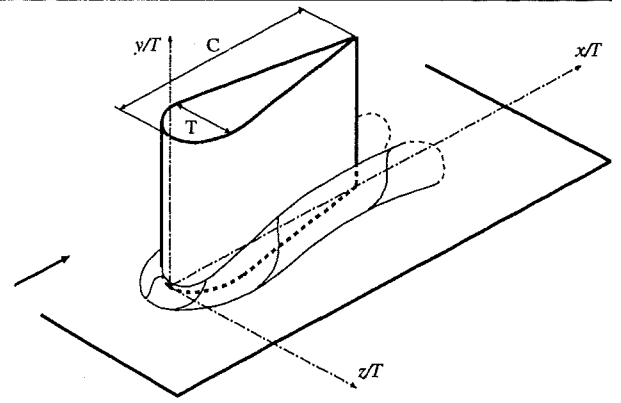


Volvo:RSM_LRR+wf

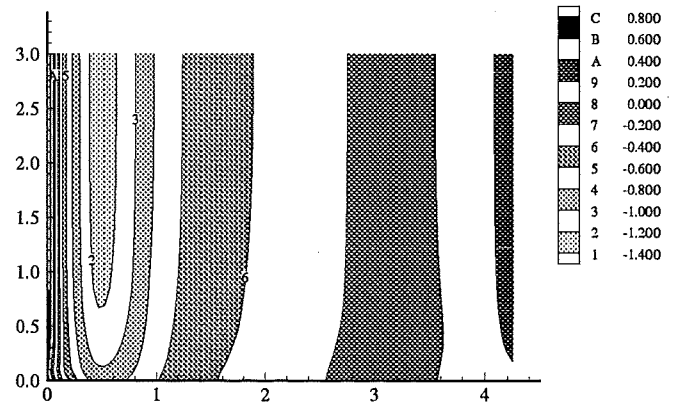
Wing/Body Junction with Separation

Mean pressure coefficient

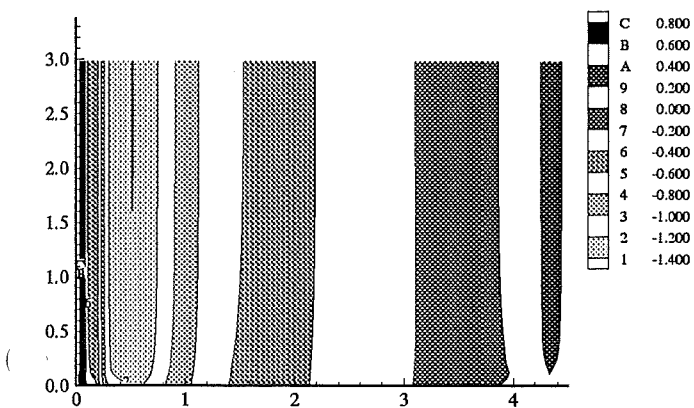
Around wing (projection)



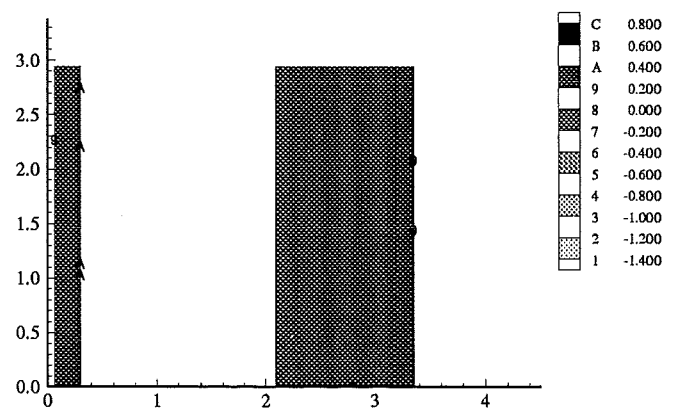
Exp



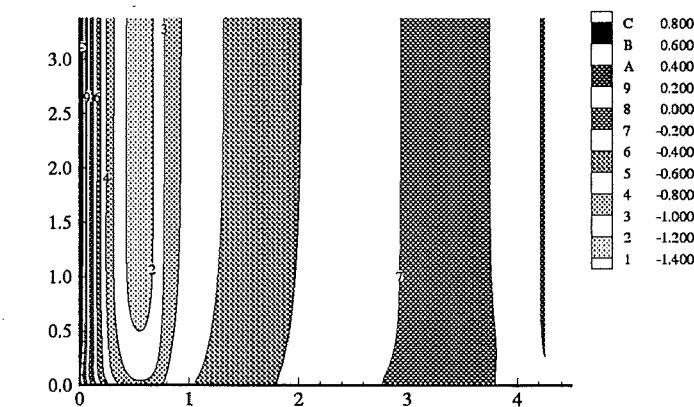
ASC:hKE_std+wf



UKarlsru:hKE_std+wf



CompDyna:hKE_RNG+wf

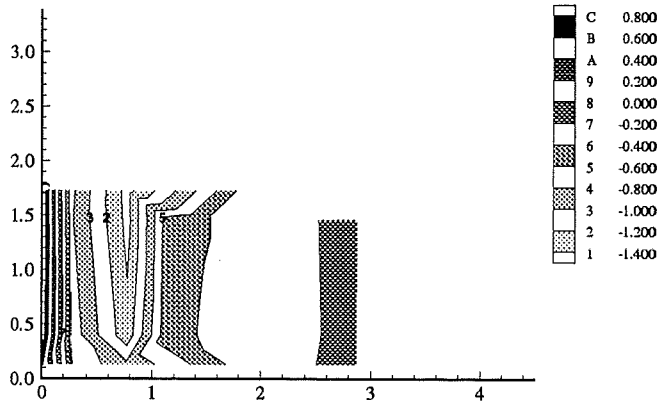
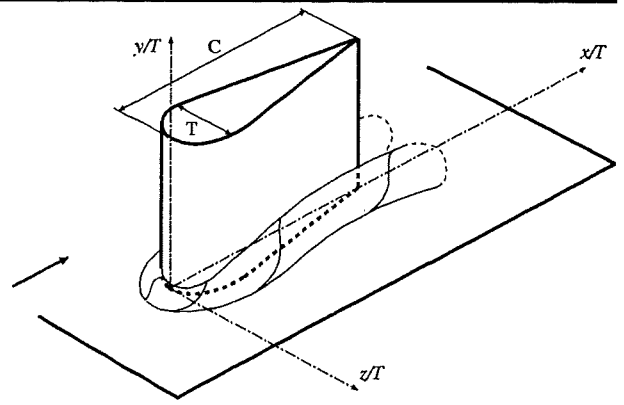


UHamburg:hKE_RNG+wf

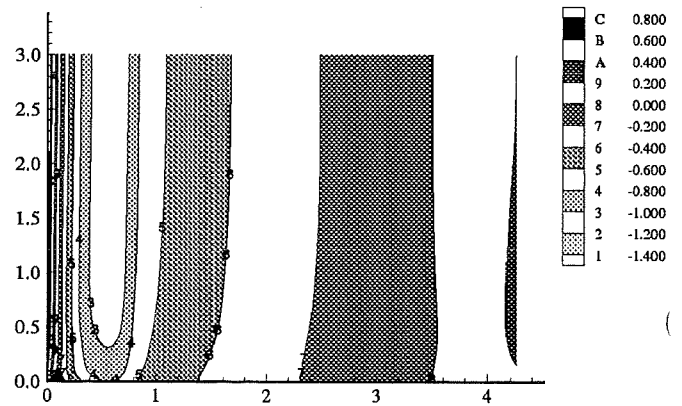
Wing/Body Junction with Separation

Mean pressure coefficient

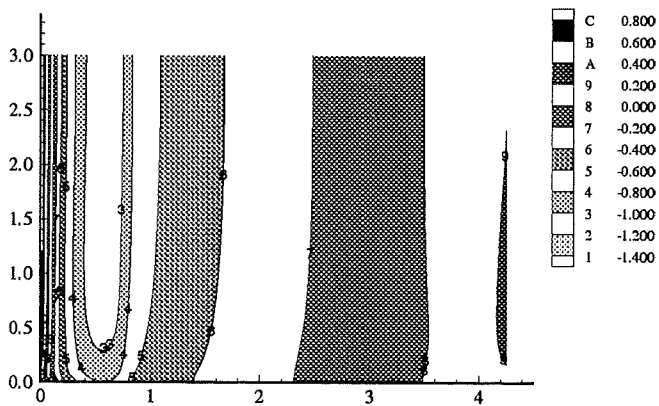
Around wing (projection)



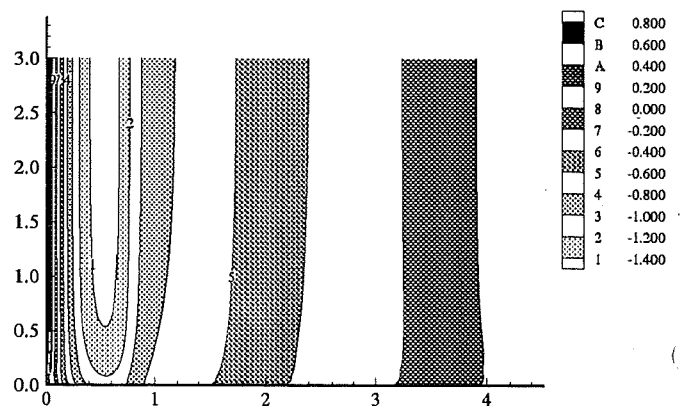
Exp



FluiDyna:hKE_std+0eq



FluiDyna:hKE_mod+0eq

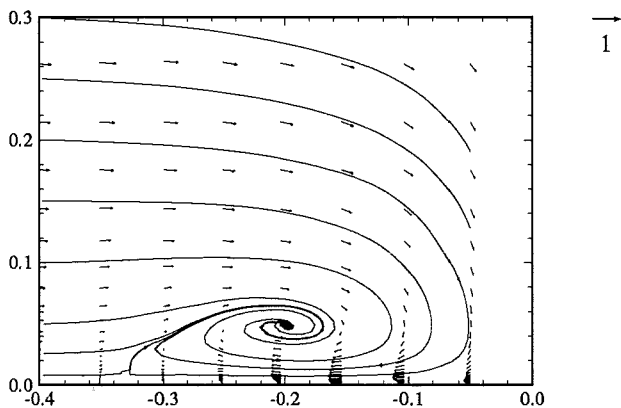
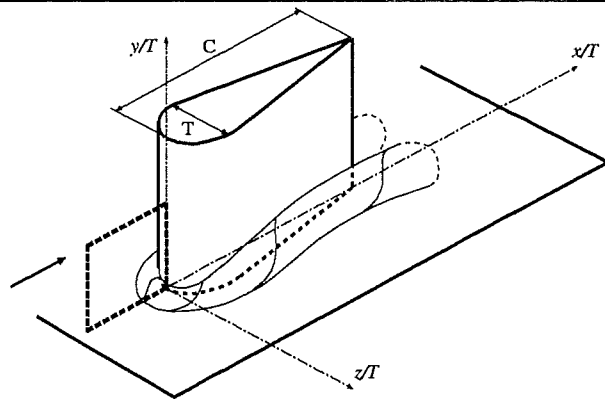


Volvo:RSM_LRR+wf

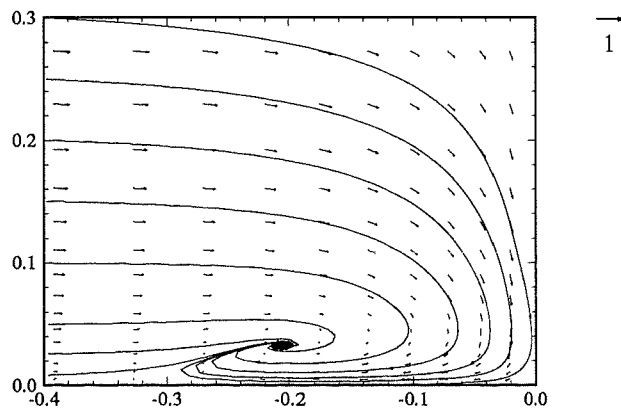
Wing/Body Junction with Separation

Streamwise velocity vectors

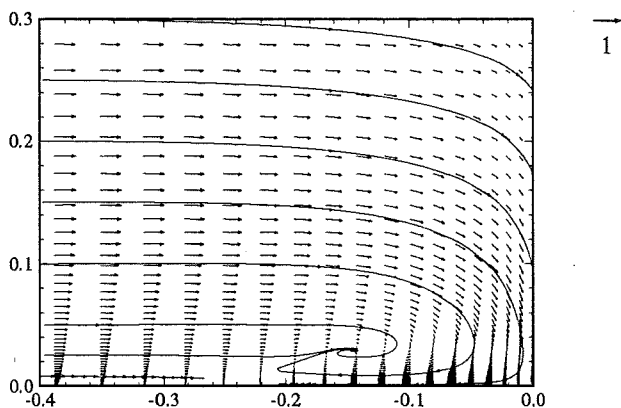
Symmetry plane in front of the wing



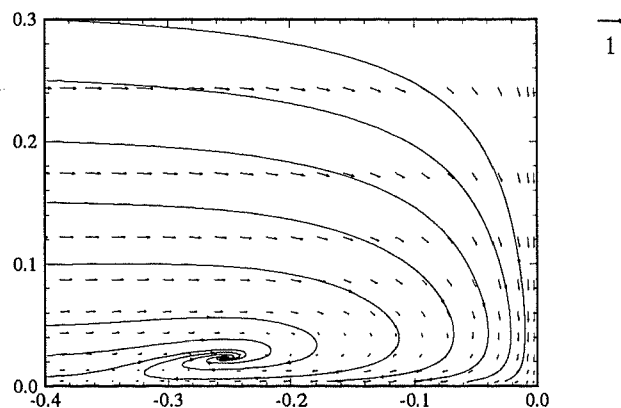
Exp



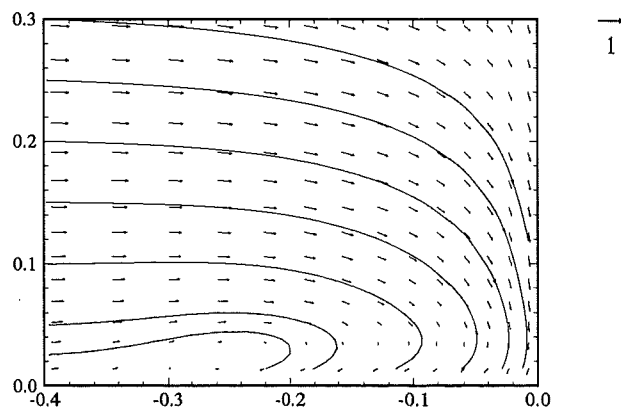
ASC:hKE_std+wf



UKarlsruhe:hKE_std+wf



CompDyna:hKE_RNG+wf

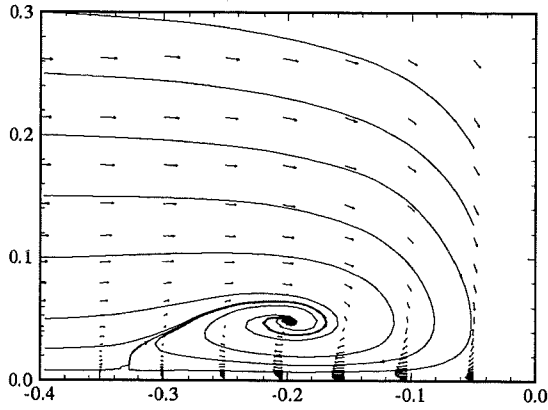
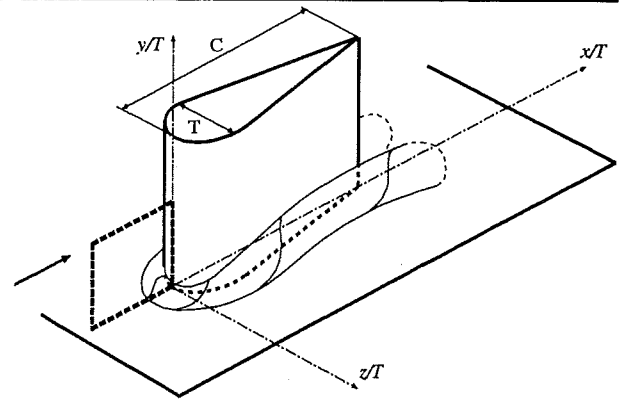


UHamburg:hKE_RNG+wf

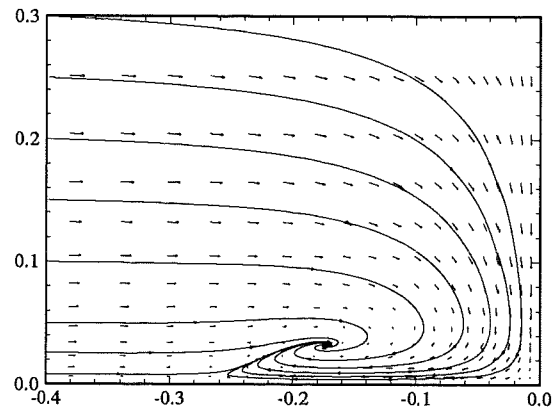
Wing/Body Junction with Separation

Streamwise velocity vectors

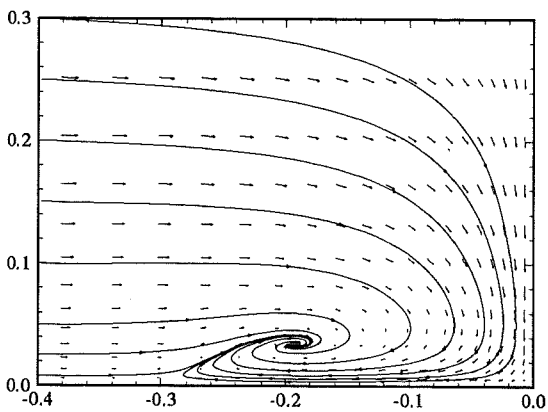
Symmetry plane in front of the wing



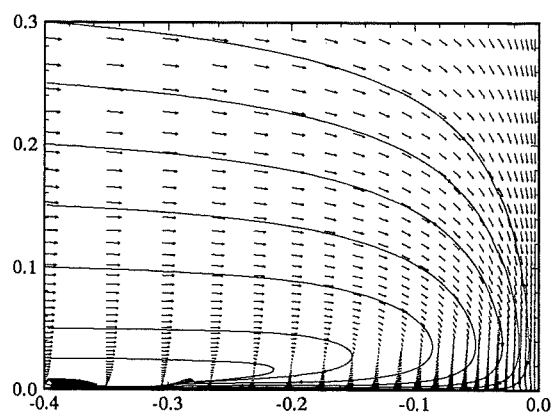
Exp



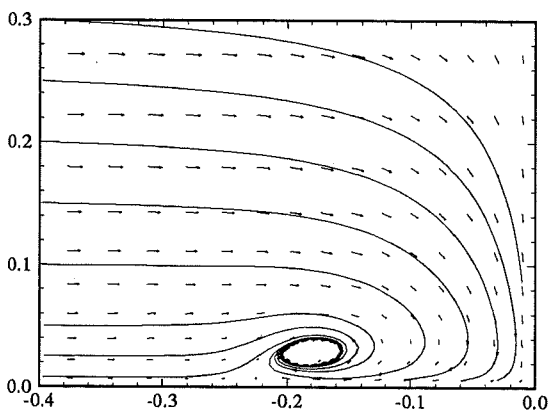
Fluidyna:hKE_std+0eq



Fluidyna:hKE_mod+0eq



UStuttg2:hKE_KaLa+1eq

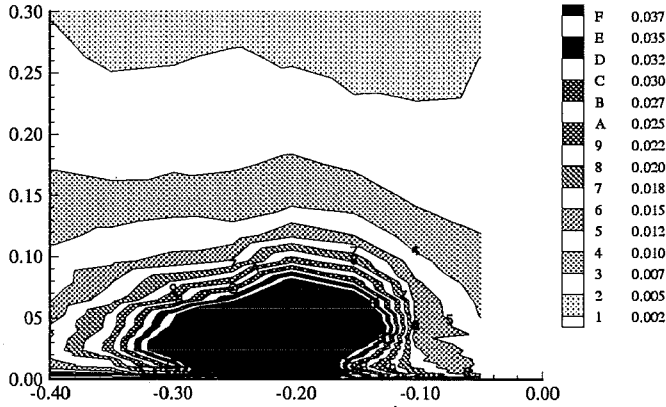
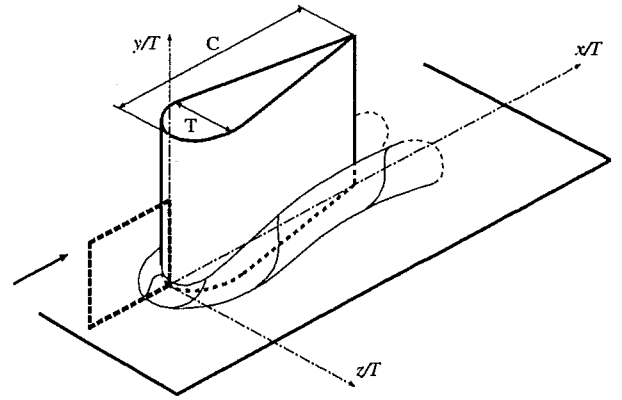


Volvo:RSM_LRR+wf

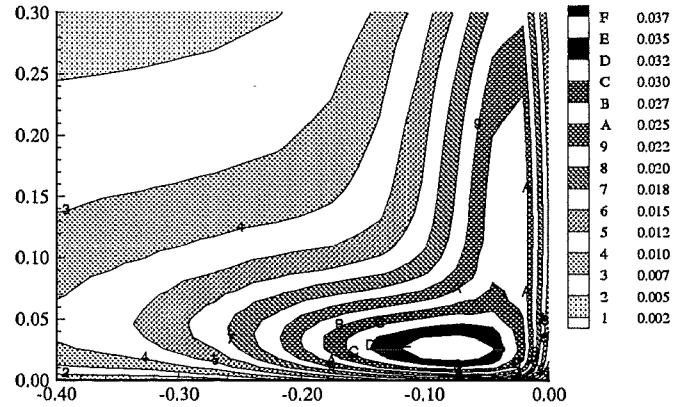
Wing/Body Junction with Separation

Turbulent kinetic energy k

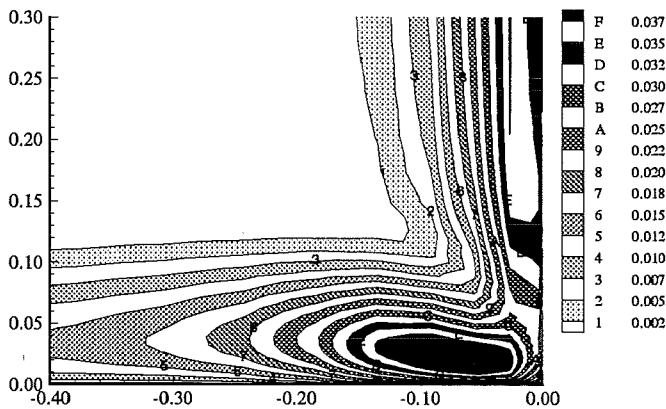
Symmetry plane in front of the wing



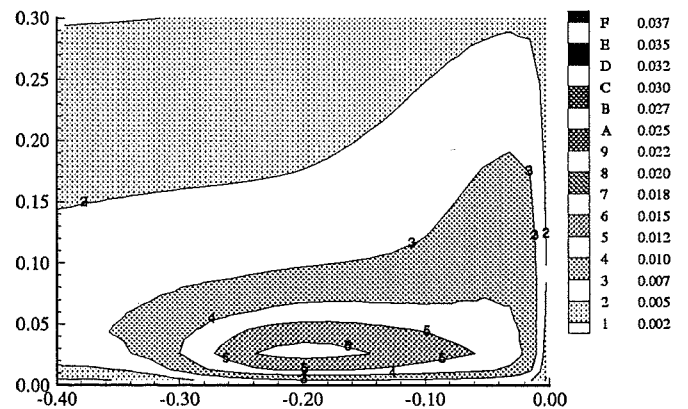
Exp



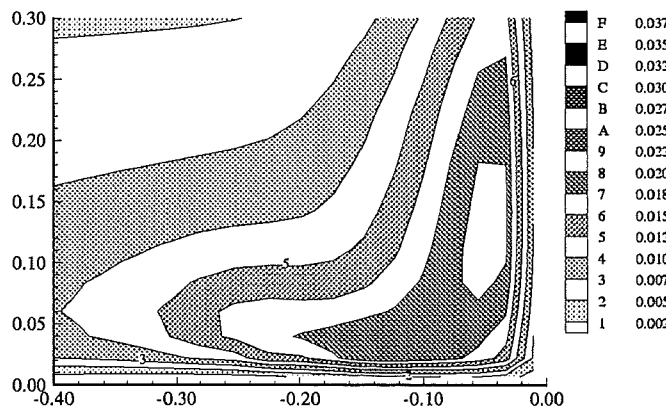
ASC:hKE_std+wf



UKarlsru:hKE_std+wf



CompDyna:hKE_RNG+wf

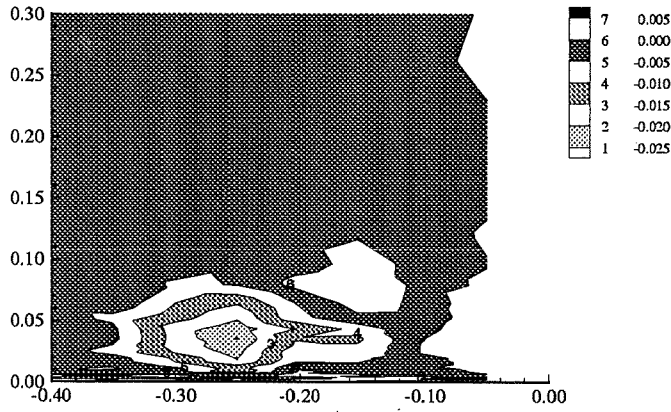
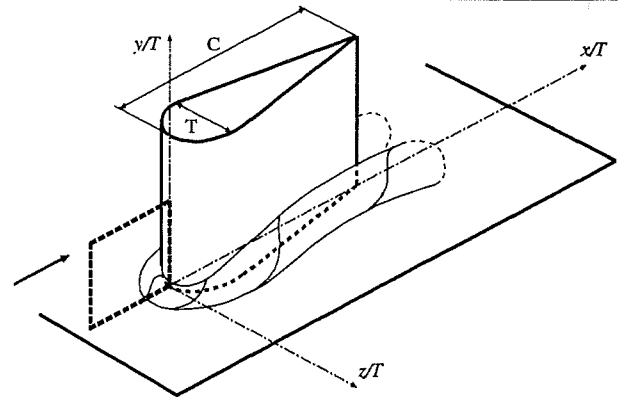


Volvo:RSM_LRR+wf

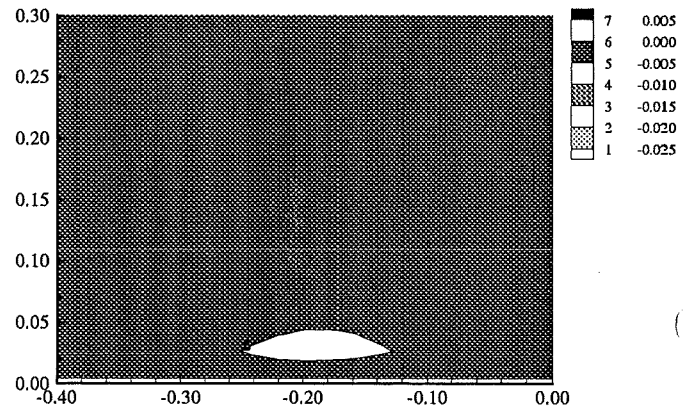
Wing/Body Junction with Separation

Reynolds shear stress uv

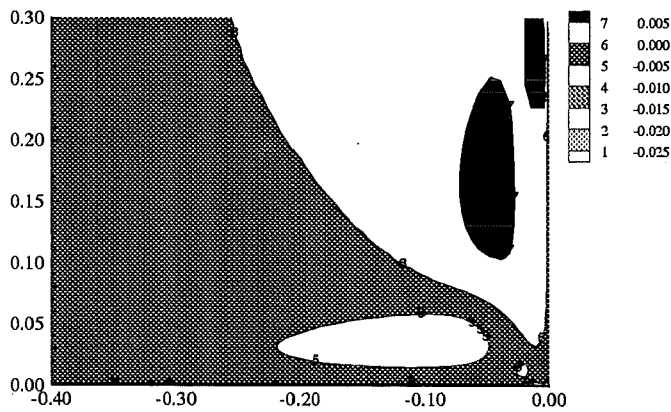
Symmetry plane in front of the wing



Exp



CompDyna:hKE_RNG+wf

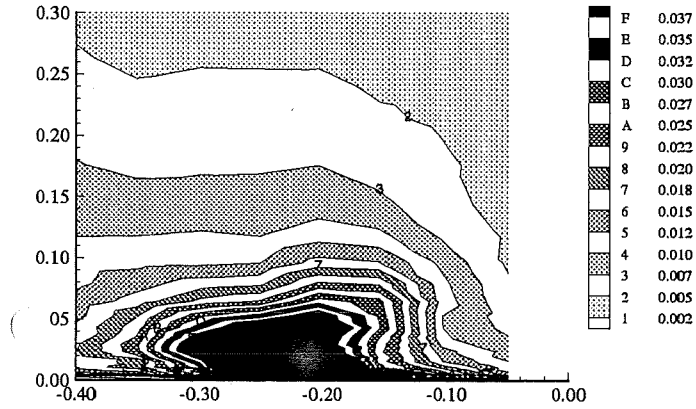
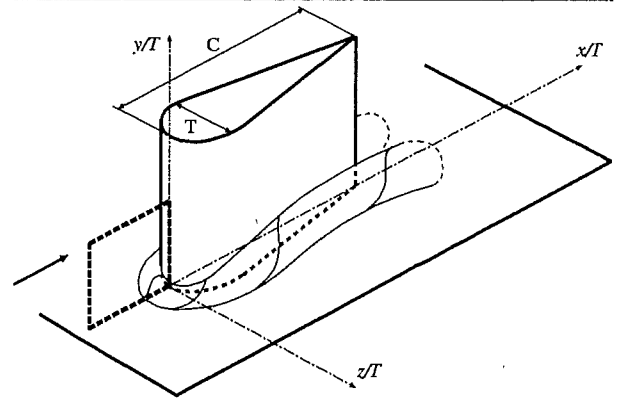


UStuttg2:hKE_KaLa+1eq

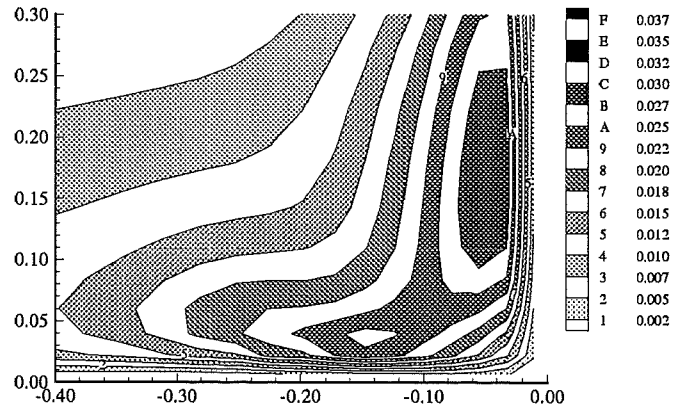
Wing/Body Junction with Separation

Reynolds normal stress uu

Symmetry plane in front of the wing



Exp

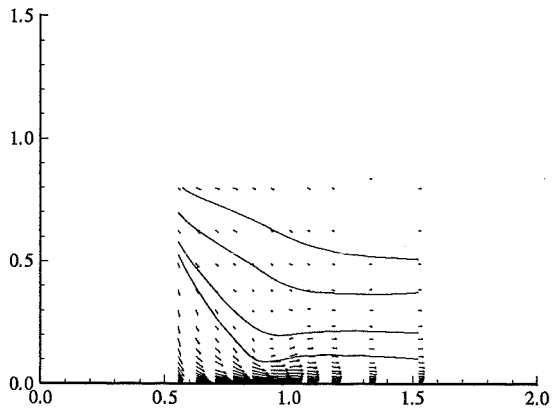
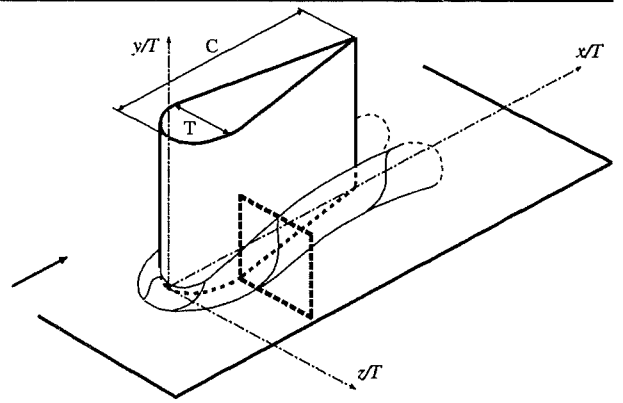


Volvo:RSM_LRR+wf

Wing/Body Junction with Separation

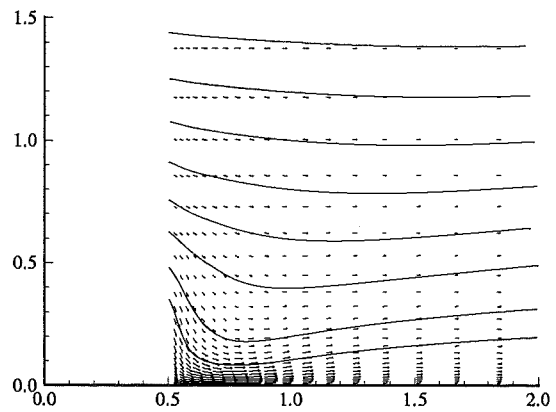
Secondary velocity vectors

Plane $x/C = 0.18$



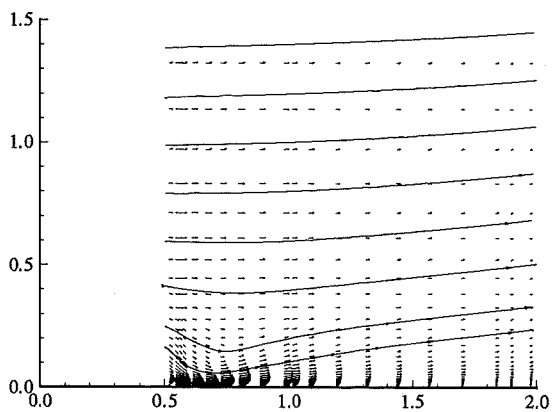
Exp

→
0.5



ASC:hKE_std+wf

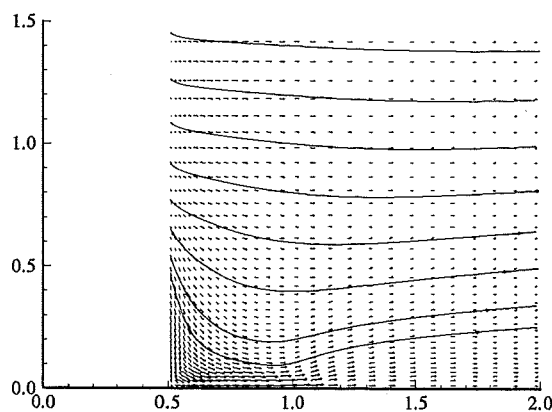
→
0.5



UKarlsru:hKE_std+wf

→
0.5

CompDyna:hKE_RNG+wf



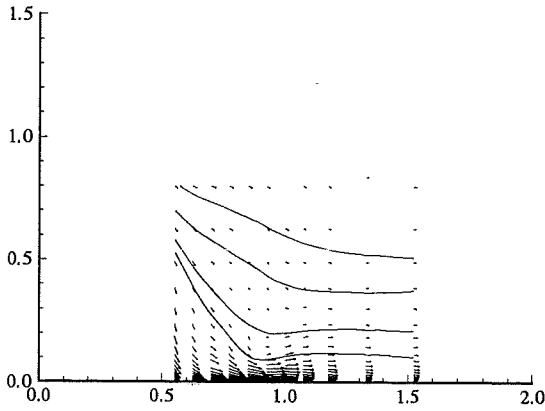
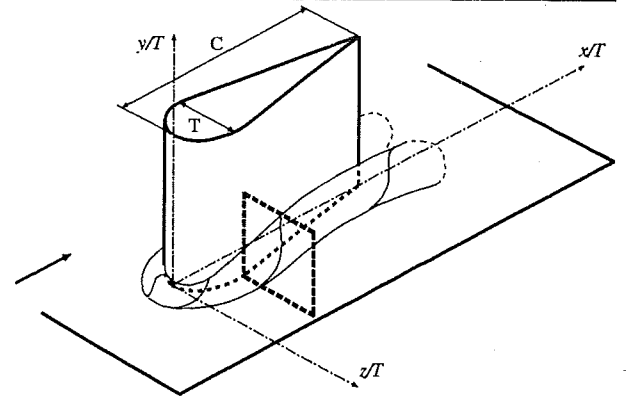
UHamburg:hKE_RNG+wf

→
0.5

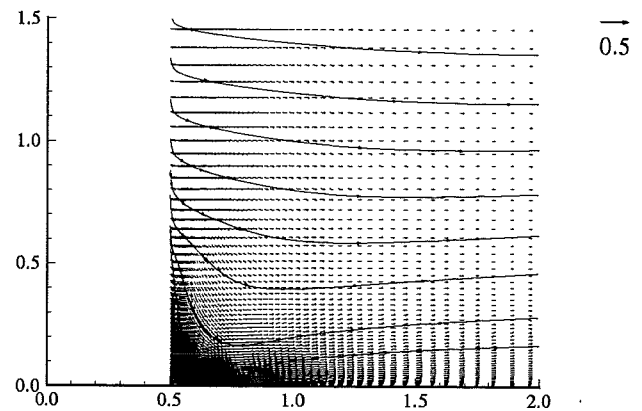
Wing/Body Junction with Separation

Secondary velocity vectors

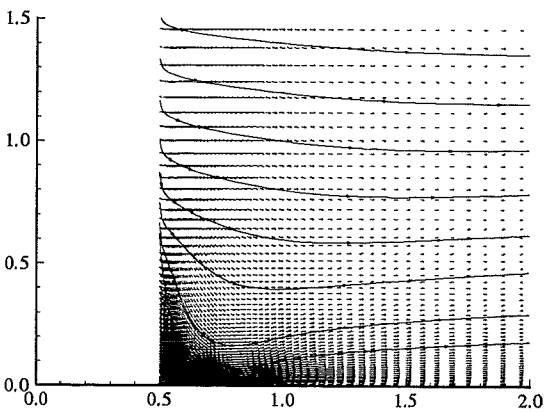
Plane $x/C = 0.18$



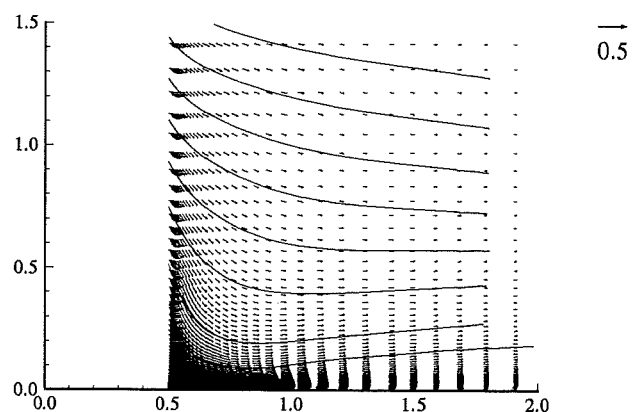
Exp



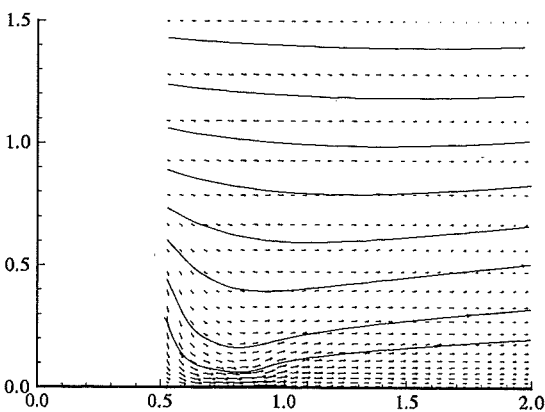
FluiDyna:hKE_std+0eq



FluiDyna:hKE_mod+0eq



UStuttg2:hKE_KaLa+1eq

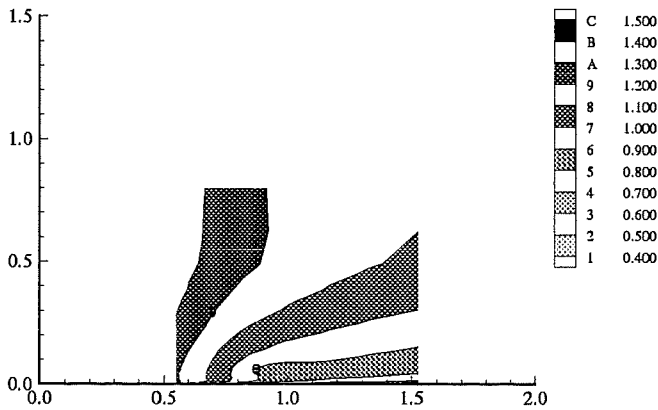
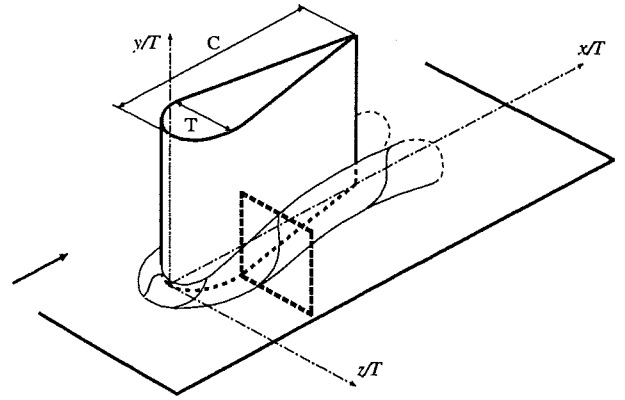


Volvo:RSM_LRR+wf

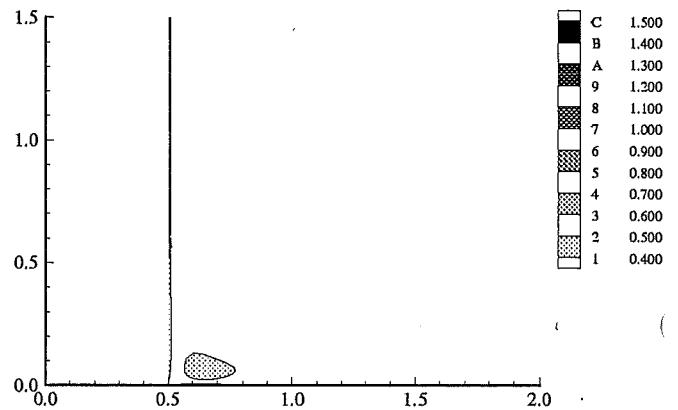
Wing/Body Junction with Separation

Streamwise mean velocity

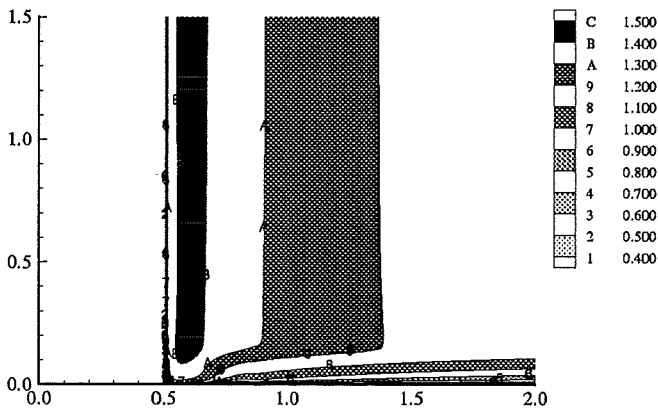
Plane $x/C = 0.18$



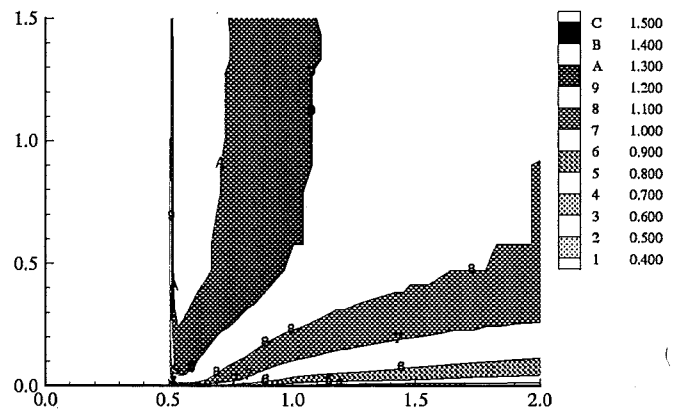
Exp



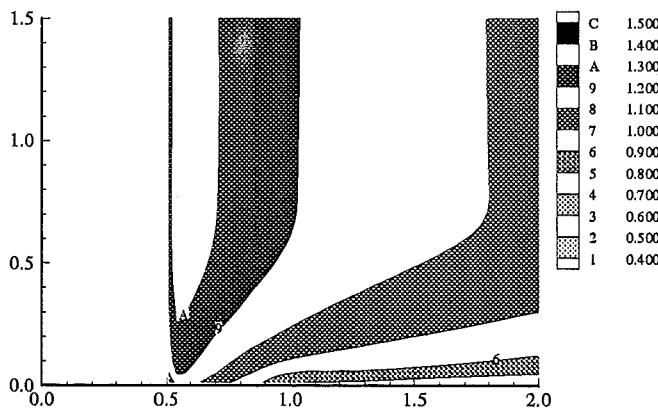
ASC:hKE_std+wf



UKarlsruhe:hKE_std+wf



CompDyna:hKE_RNG+wf

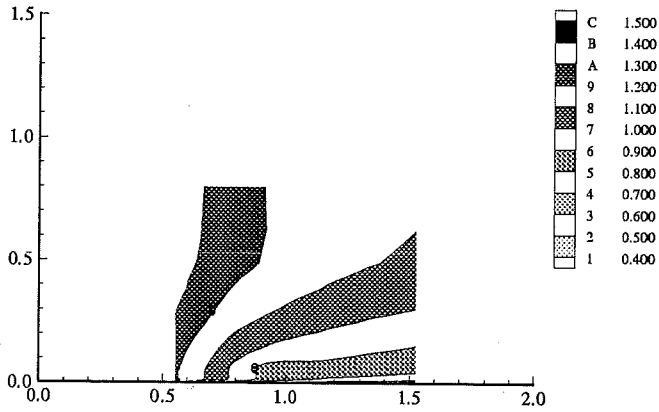
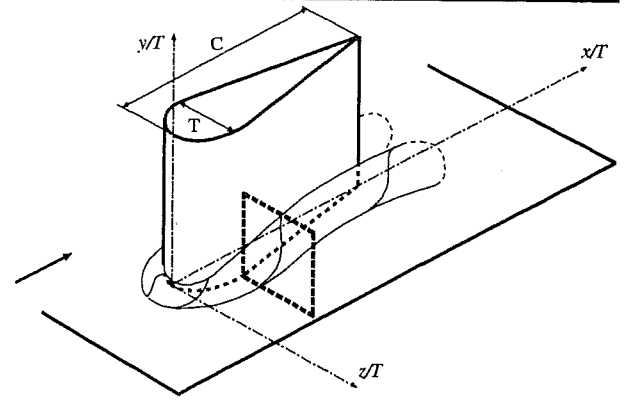


UHamburg:hKE_RNG+wf

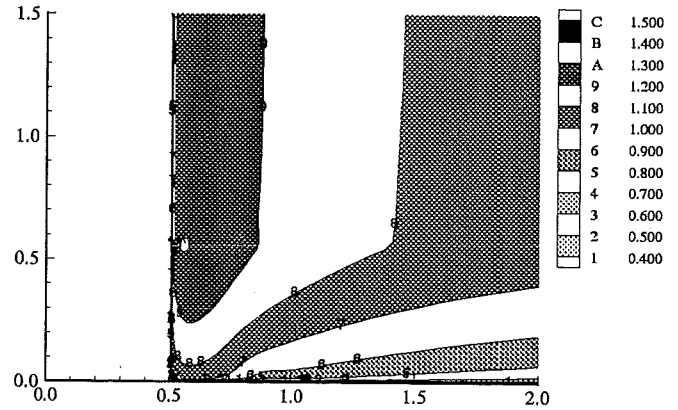
Wing/Body Junction with Separation

Streamwise mean velocity

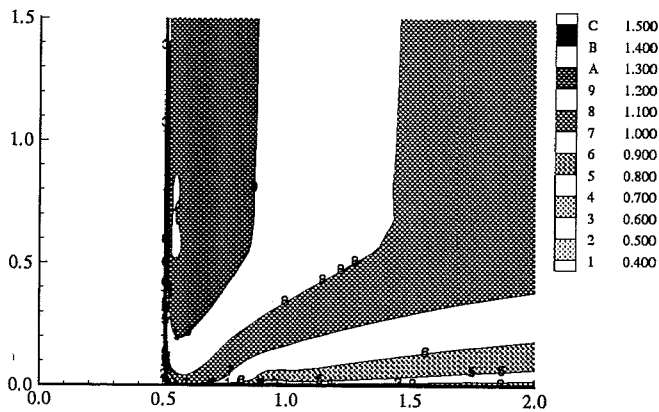
Plane $x/C = 0.18$



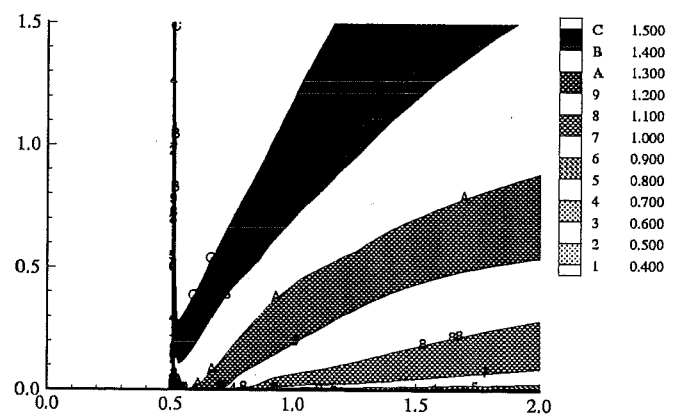
Exp



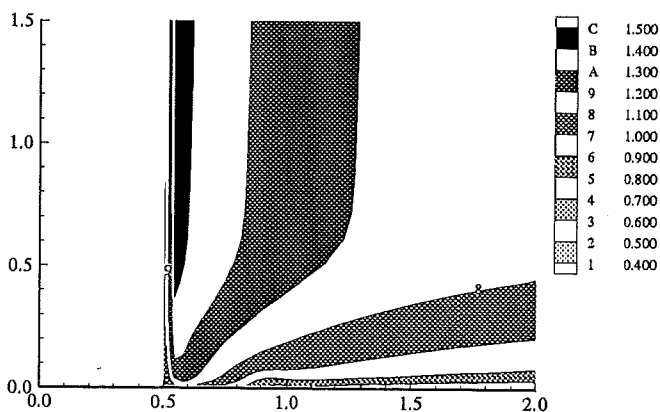
FluiDyna:hKE_std+0eq



FluiDyna:hKE_mod+0eq



UStuttg2:hKE_KaLa+1eq

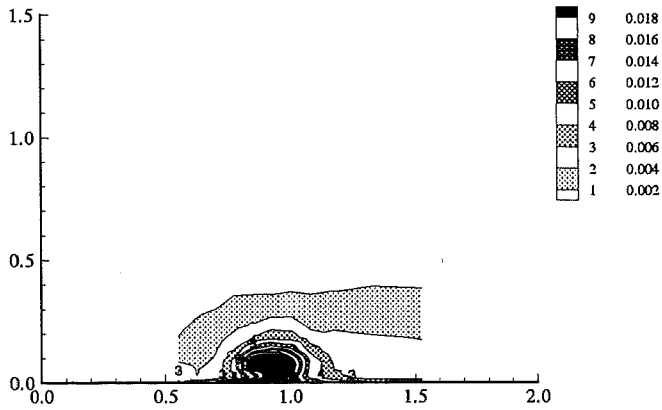
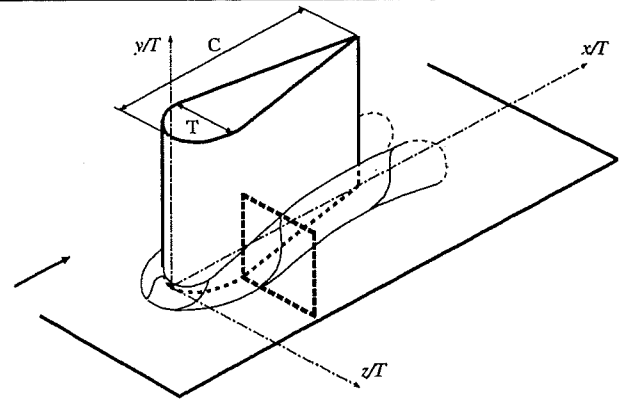


Volvo:RSM_LRR+wf

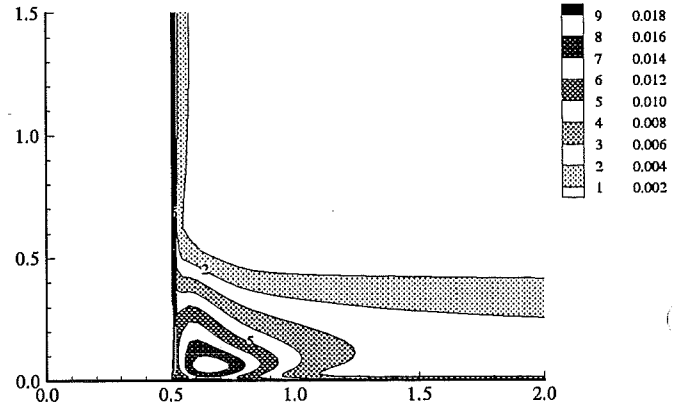
Wing/Body Junction with Separation

Turbulent kinetic energy k

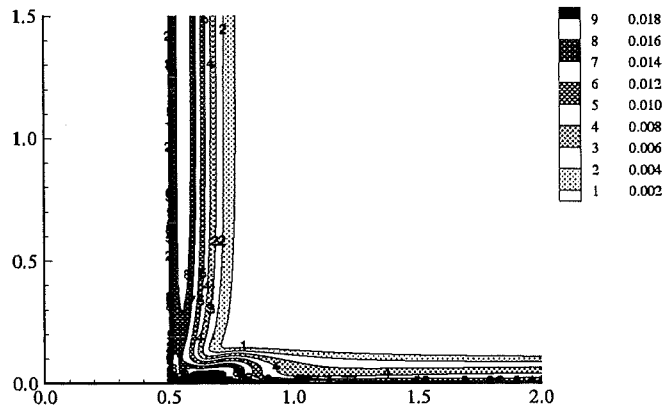
Plane $x/C = 0.18$



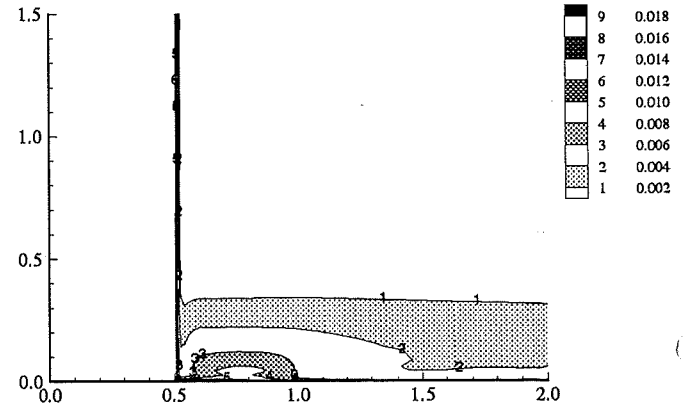
Exp



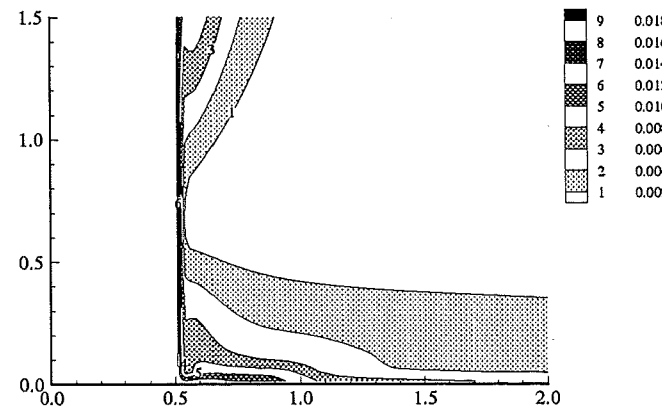
ASC:hKE_std+wf



UKarlsruhe:hKE_std+wf



CompDyna:hKE_RNG+wf

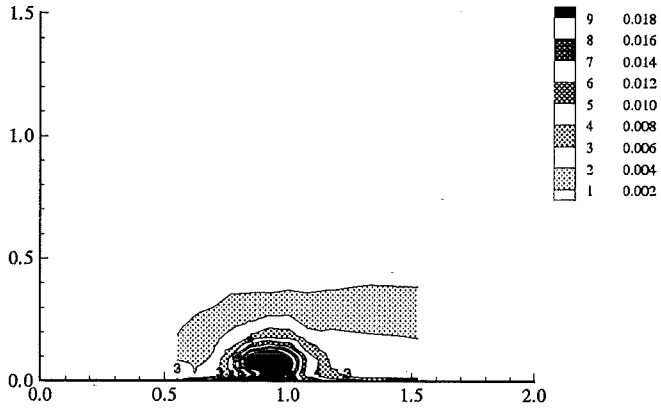
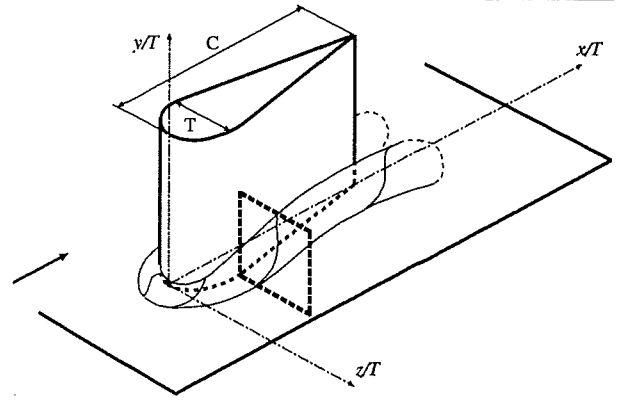


UHamburg:hKE_RNG+wf

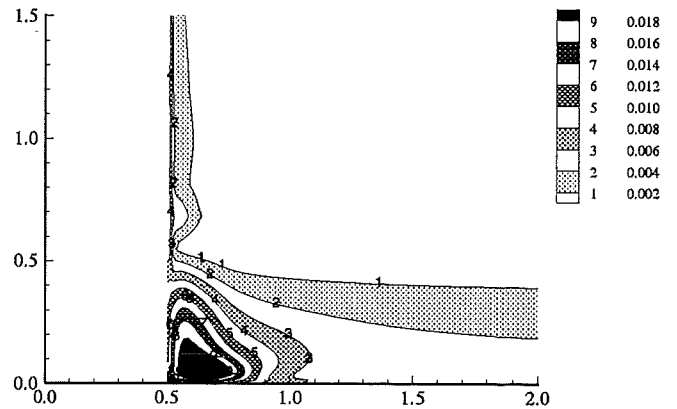
Wing/Body Junction with Separation

Turbulent kinetic energy k

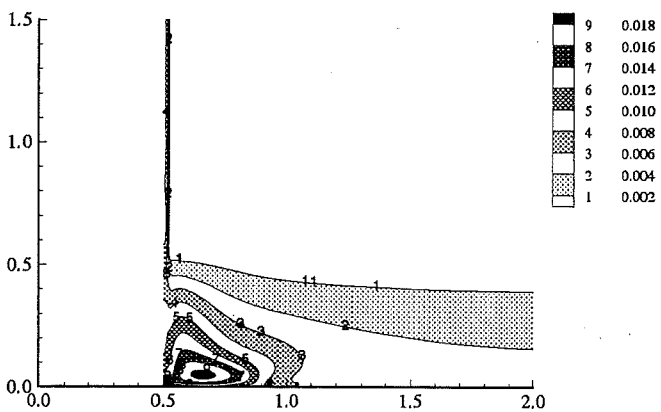
Plane $x/C = 0.18$



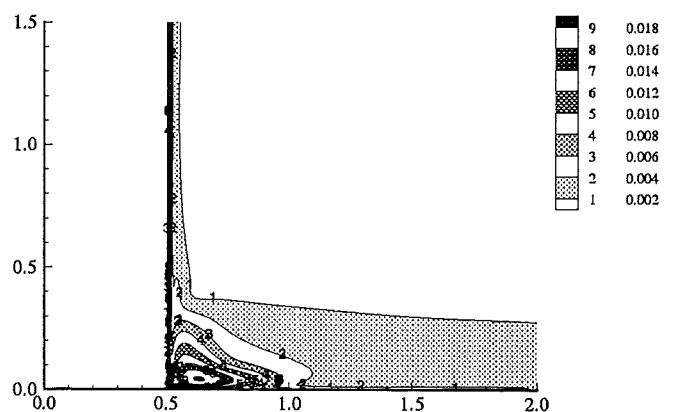
Exp



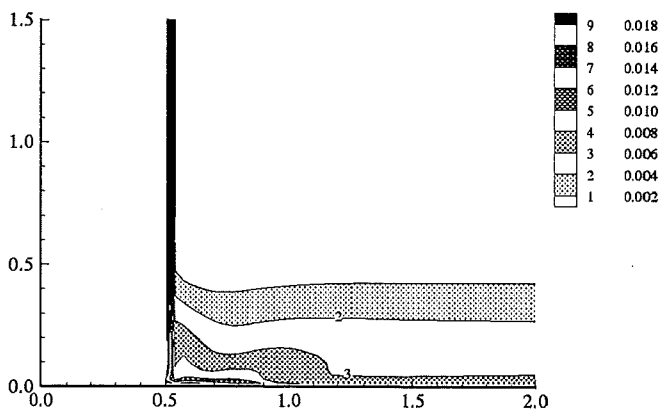
FluiDyna:hKE_std+0eq



FluiDyna:hKE_mod+0eq



UStuttg2:hKE_KaLa+1eq

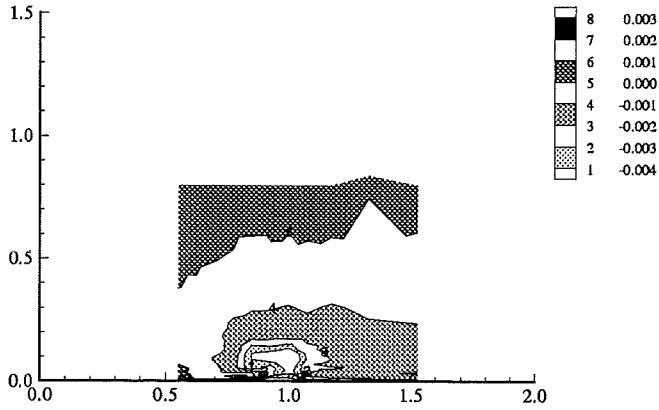
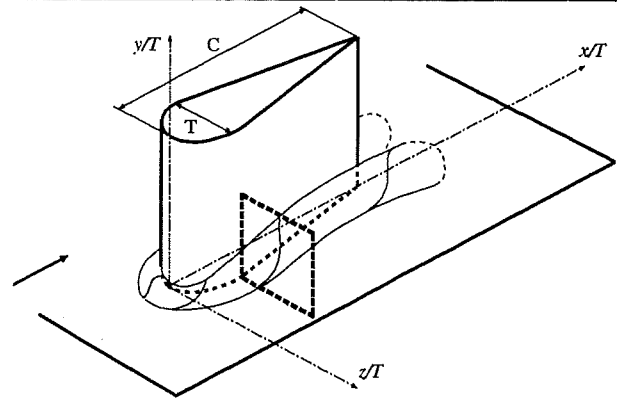


Volvo:RSM_LRR+wf

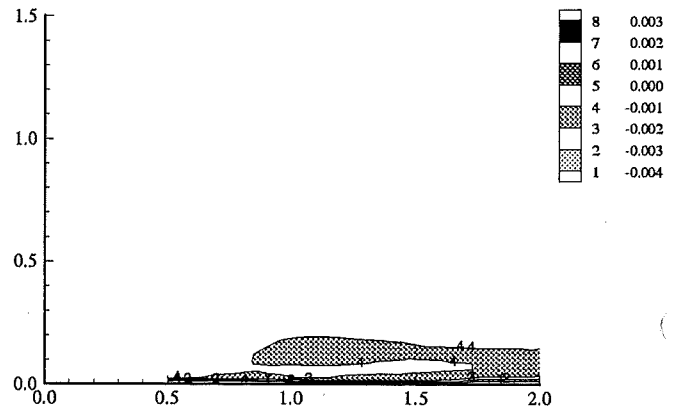
Wing/Body Junction with Separation

Reynolds shear stress uv

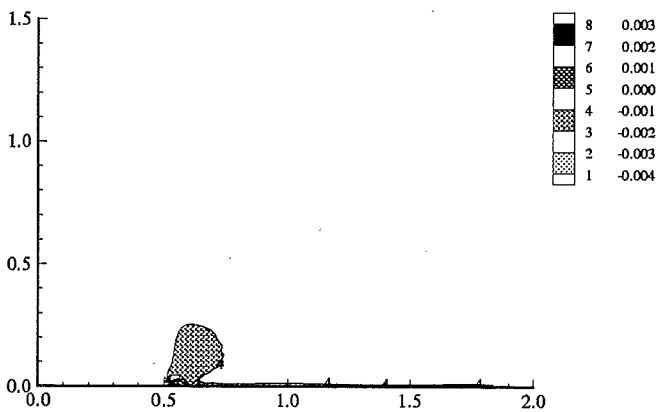
Plane $x/C = 0.18$



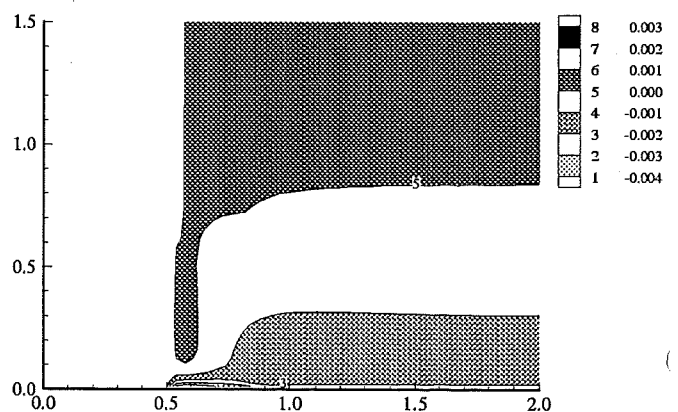
Exp



CompDyna:hKE_RNG+wf



UStuttg2:hKE_KaLa+1eq

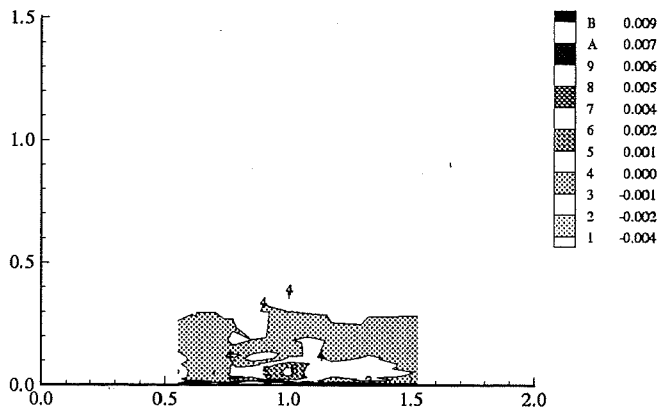
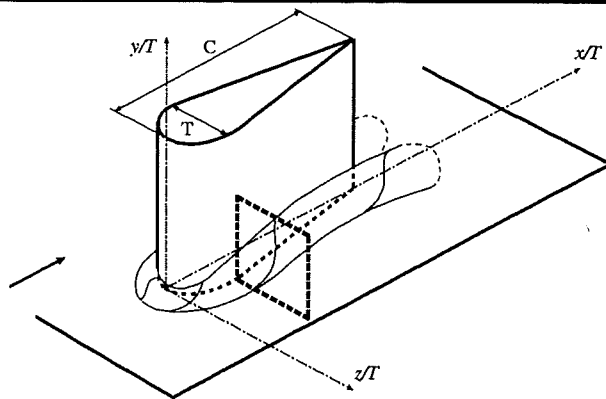


Volvo:RSM_LRR+wf

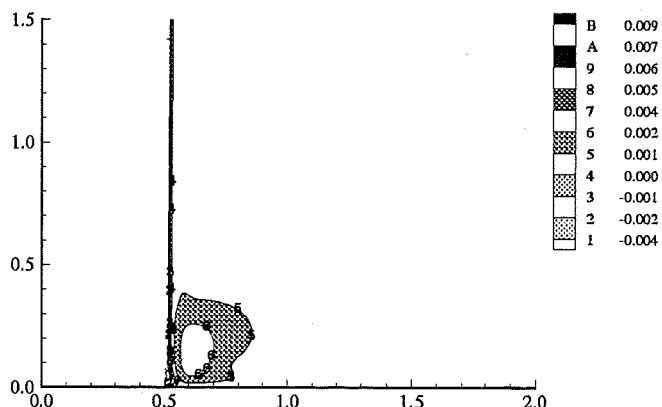
Wing/Body Junction with Separation

Reynolds shear stress uw

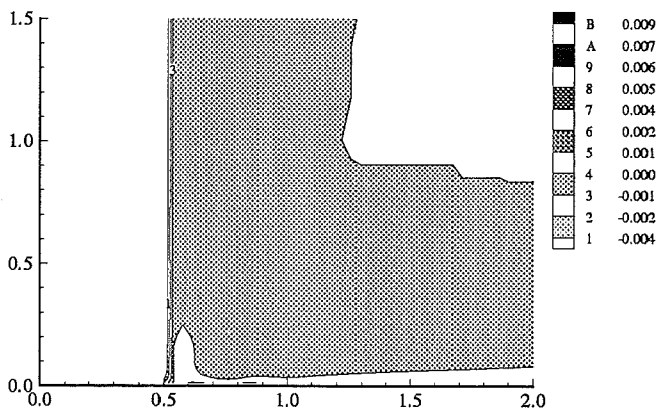
Plane $x/C = 0.18$



Exp



UStuttgart2:hKE_KaLa+1eq

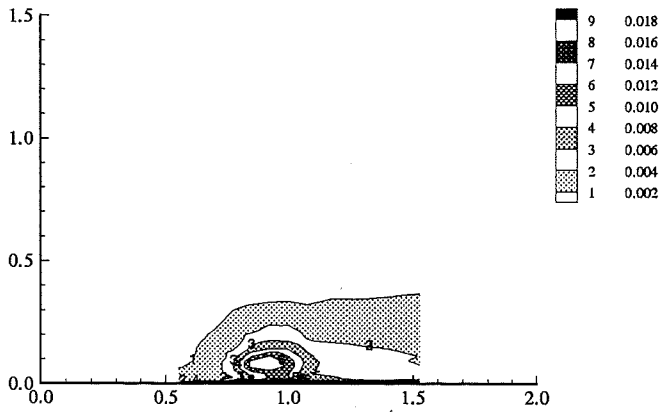
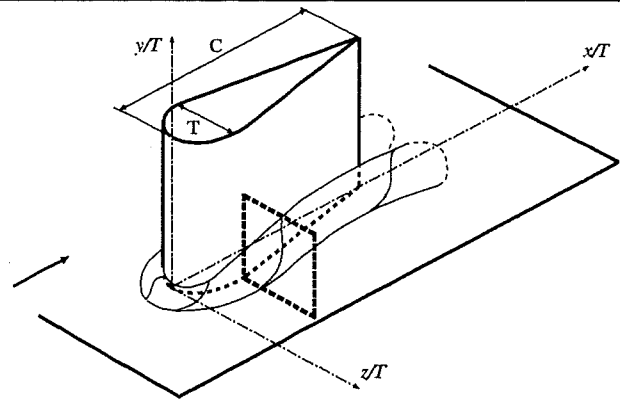


Volvo:RSM_LRR+wf

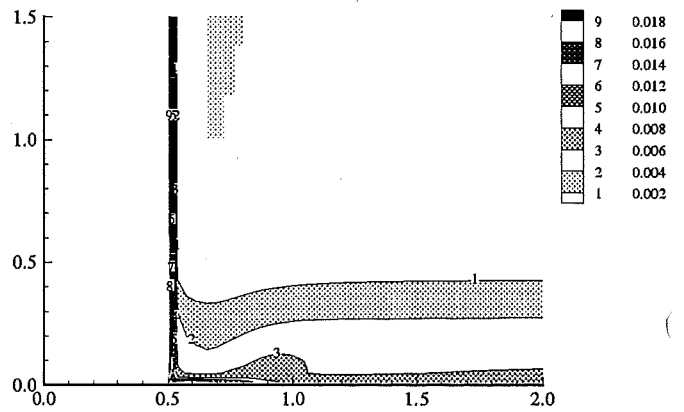
Wing/Body Junction with Separation

Reynolds normal stress uu

Plane $x/C = 0.18$



Exp

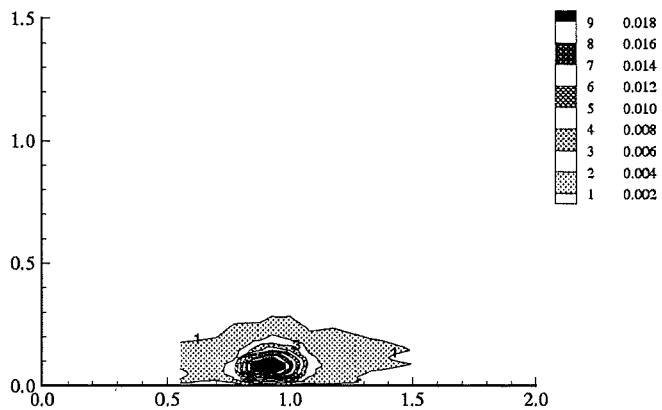
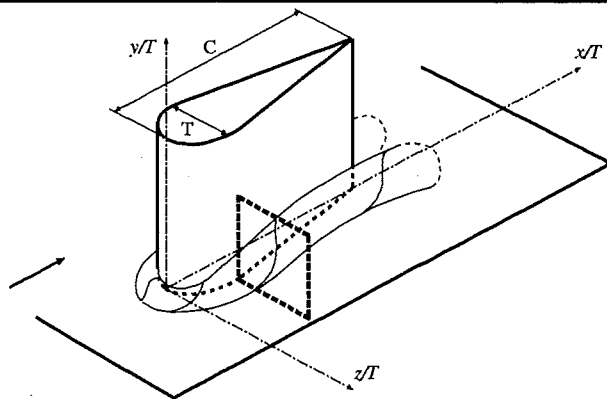


Volvo:RSM_LRR+wf

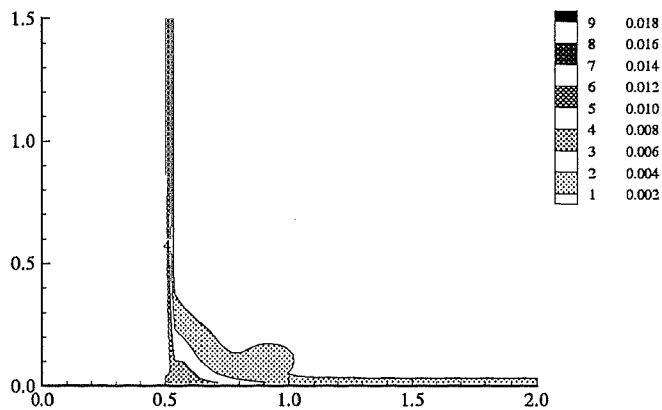
Wing/Body Junction with Separation

Reynolds normal stress $v'v'$

Plane $x/C = 0.18$



Exp

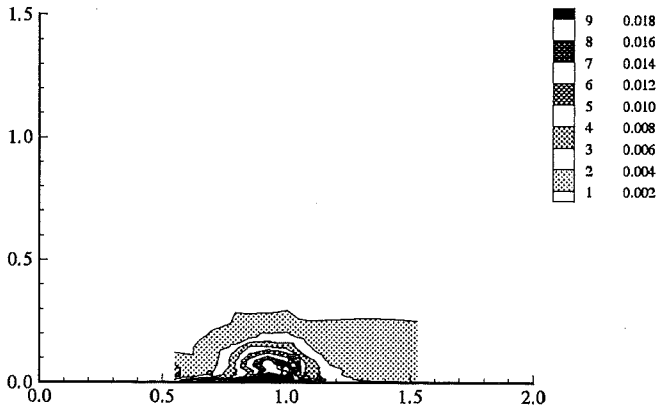
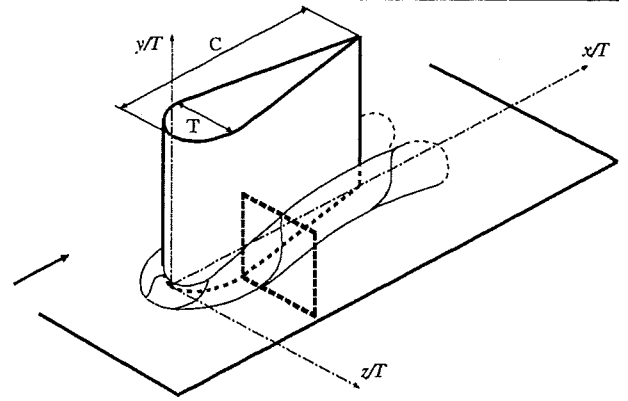


Volvo:RSM_LRR+wf

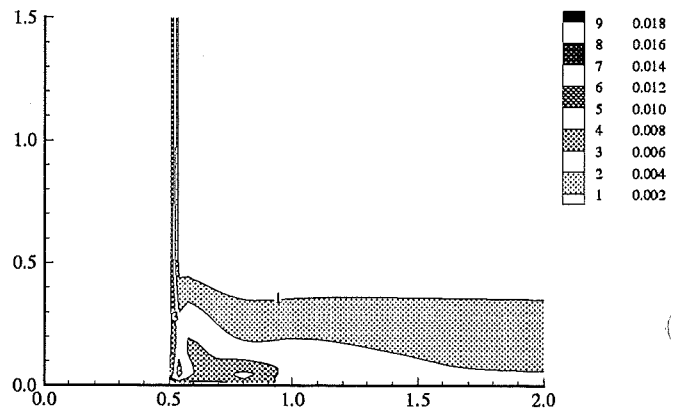
Wing/Body Junction with Separation

Reynolds normal stress $w w$

Plane $x/C = 0.18$



Exp

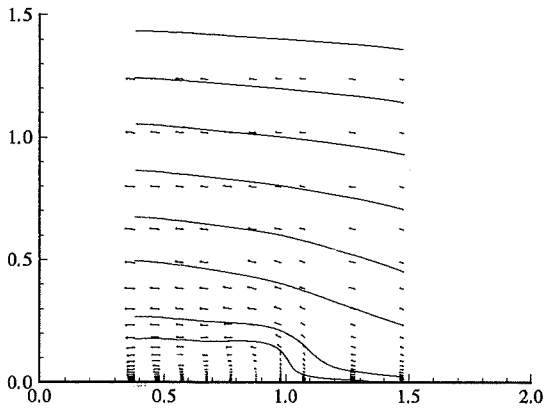
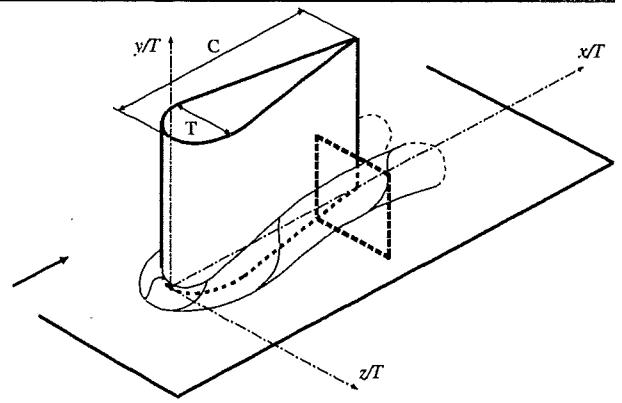


Volvo:RSM_LRR+wf

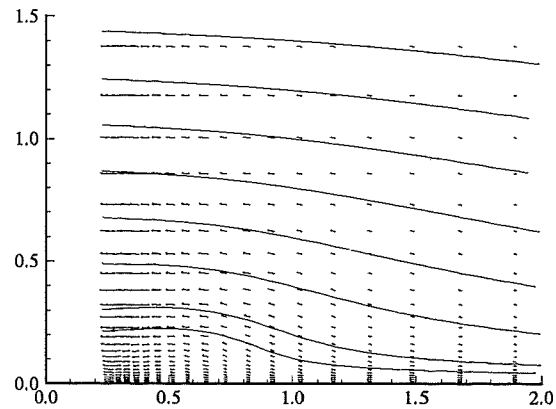
Wing/Body Junction with Separation

Secondary velocity vectors

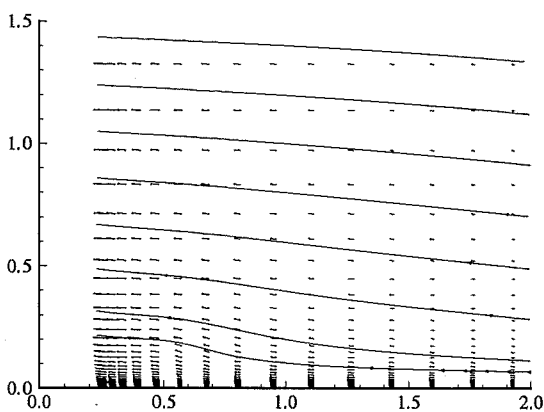
Plane $x/C = 0.75$



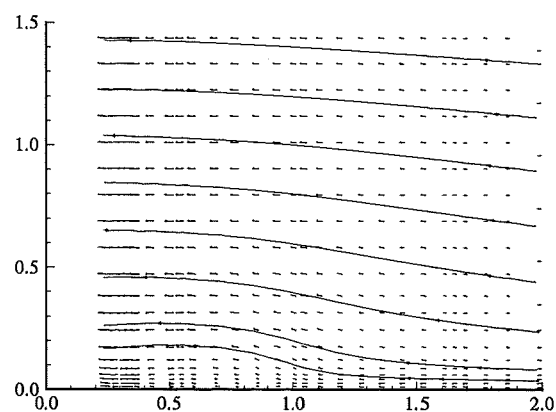
Exp



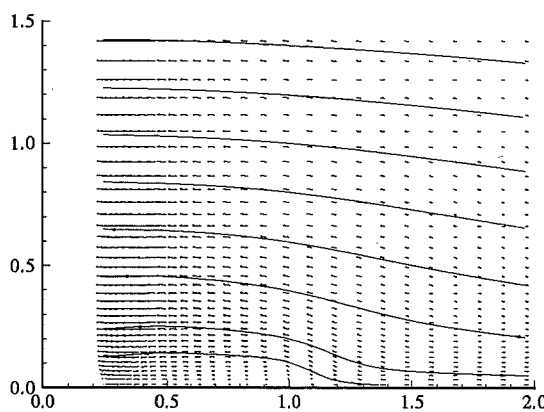
ASC:hKE_std+wf



UKarlsruhe:hKE_std+wf



CompDyna:hKE_RNG+wf

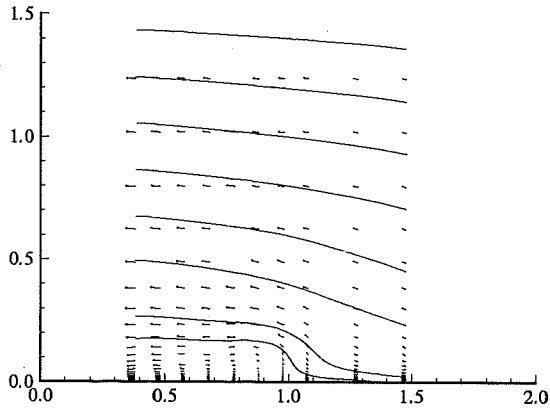
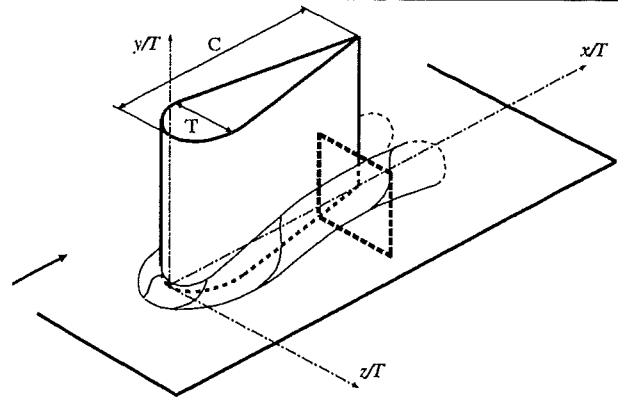


UHamburg:hKE_RNG+wf

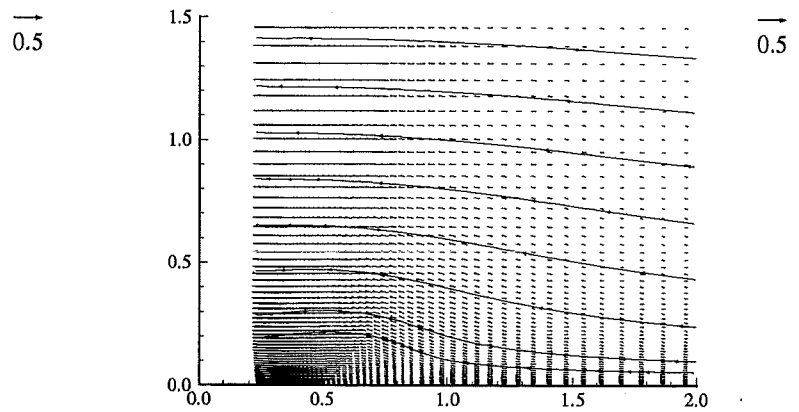
Wing/Body Junction with Separation

Secondary velocity vectors

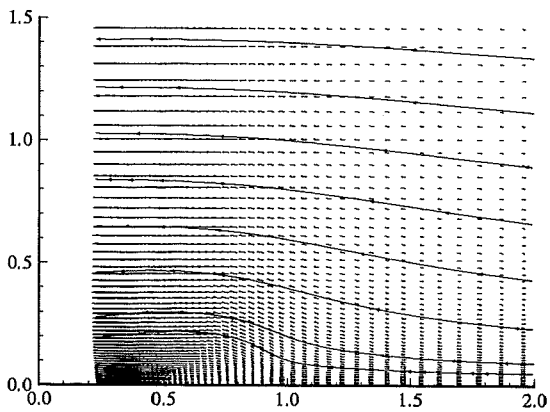
Plane $x/C = 0.75$



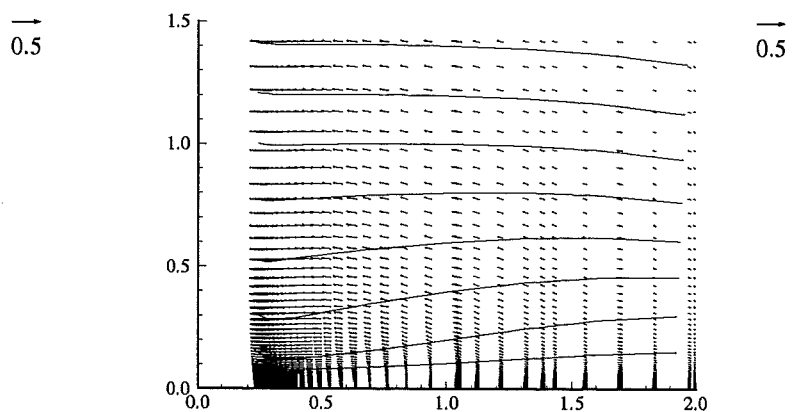
Exp



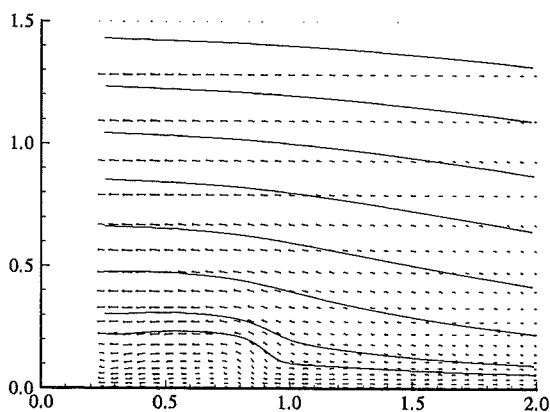
Fluidyna:hKE_std+0eq



Fluidyna:hKE_mod+0eq



UStuttgart2:hKE_KaLa+1eq

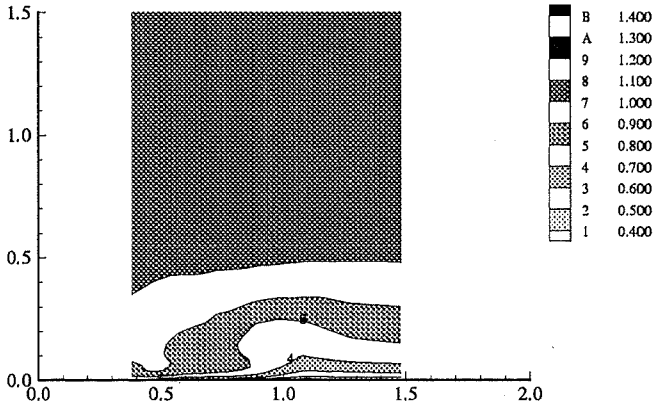
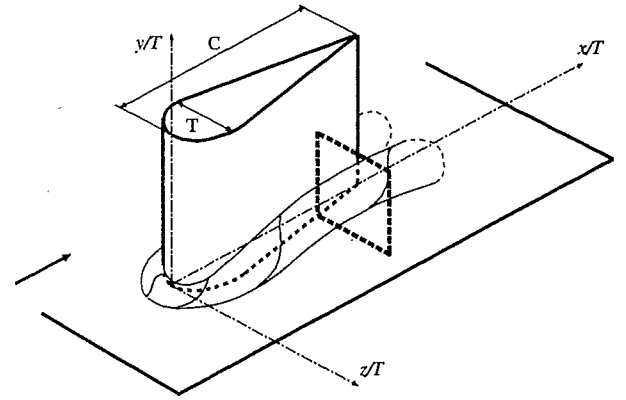


Volvo:RSM_LRR+wf

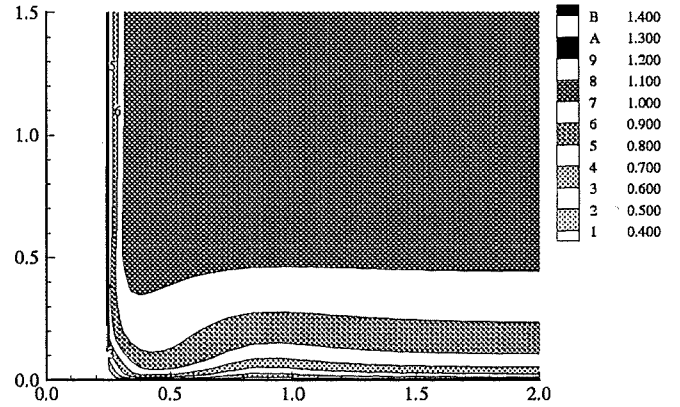
Wing/Body Junction with Separation

Streamwise mean velocity

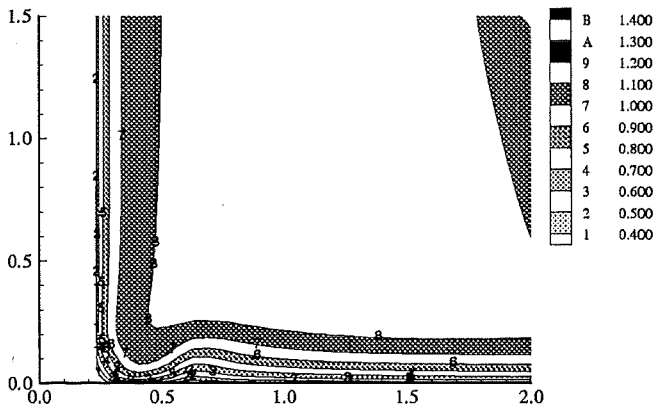
Plane $x/C = 0.75$



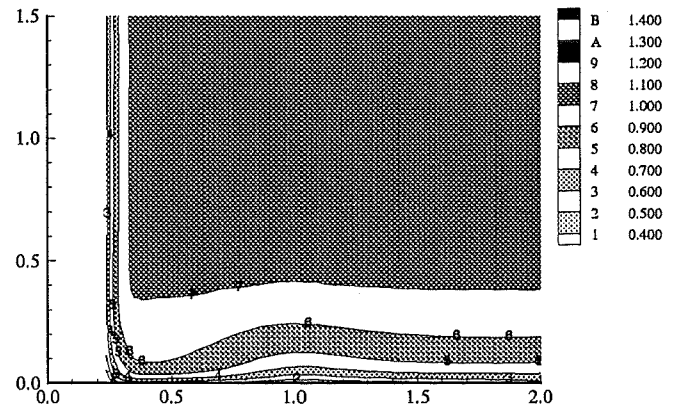
Exp



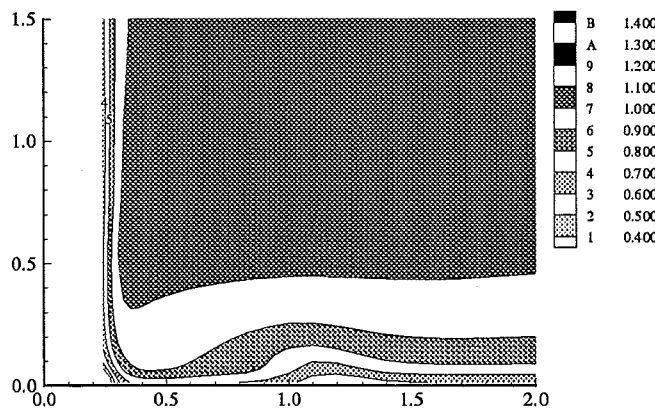
ASC:hKE_std+wf



UKarlsru:hKE_std+wf



CompDyna:hKE_RNG+wf

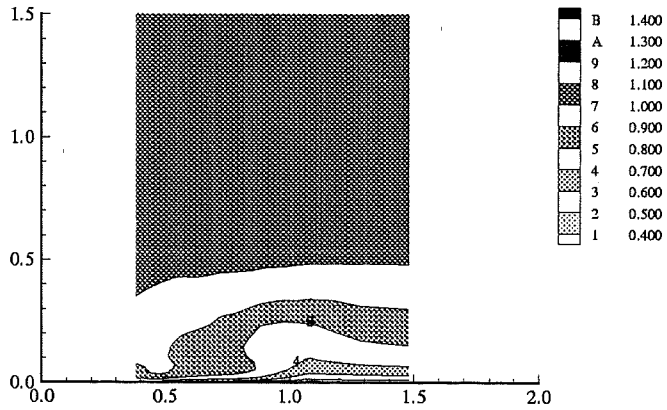
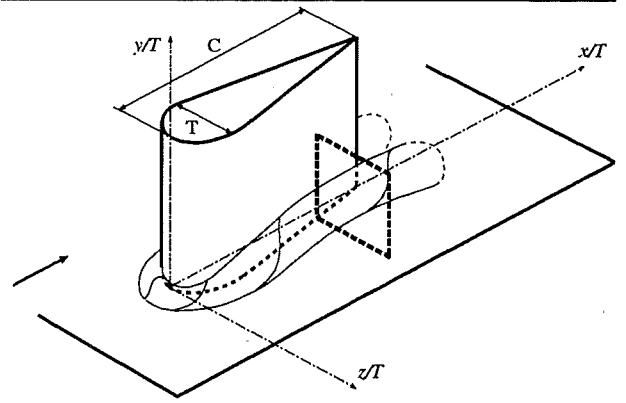


UHamburg:hKE_RNG+wf

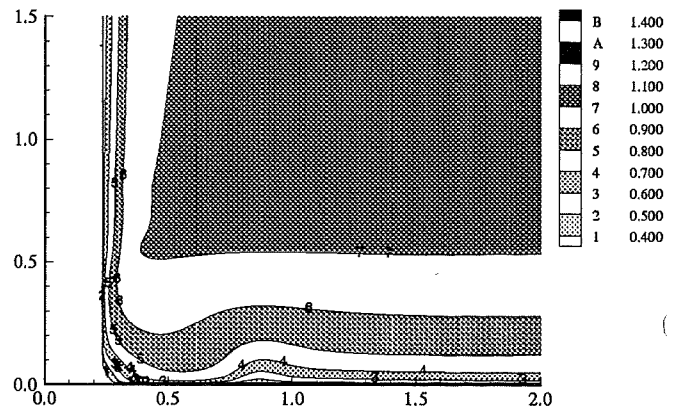
Wing/Body Junction with Separation

Streamwise mean velocity

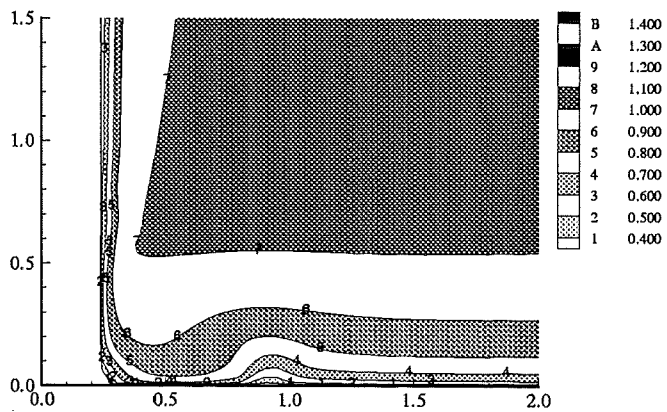
Plane $x/C = 0.75$



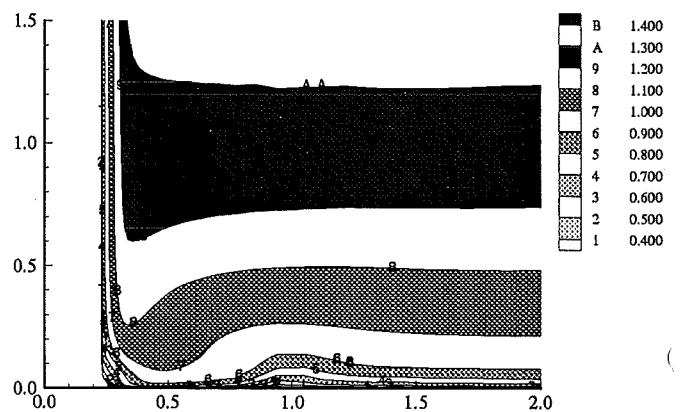
Exp



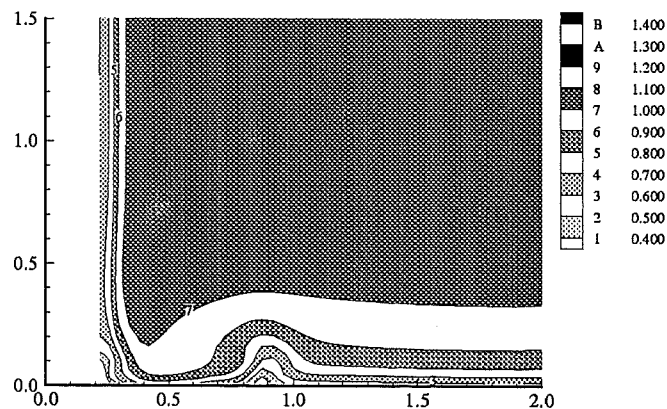
FluiDyna:hKE_std+0eq



FluiDyna:hKE_mod+0eq



UStuttg2:hKE_KaLa+1eq

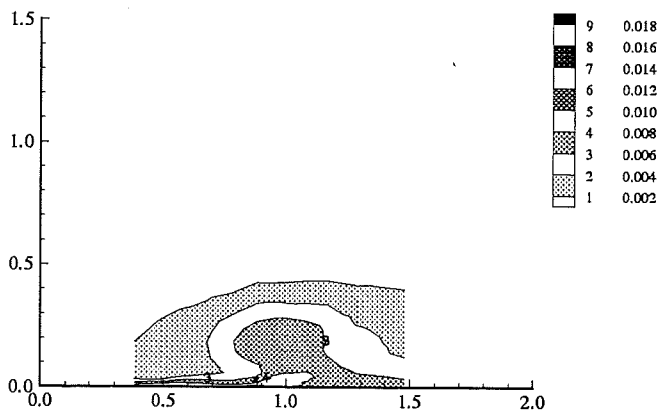
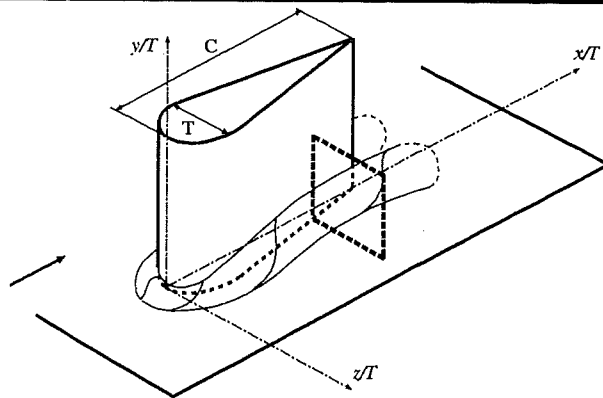


Volvo:RSM_LRR+wf

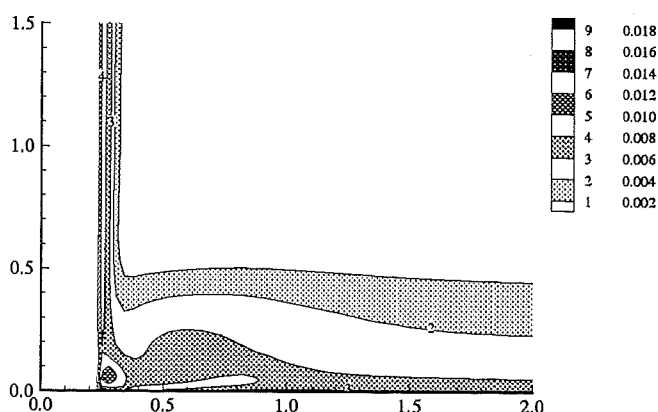
Wing/Body Junction with Separation

Turbulent kinetic energy k

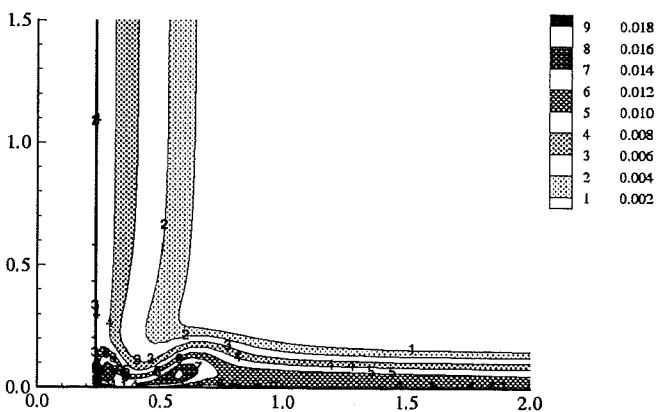
Plane $x/C = 0.75$



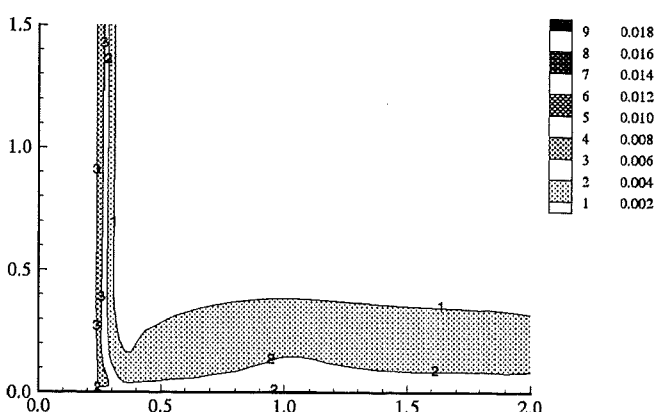
Exp



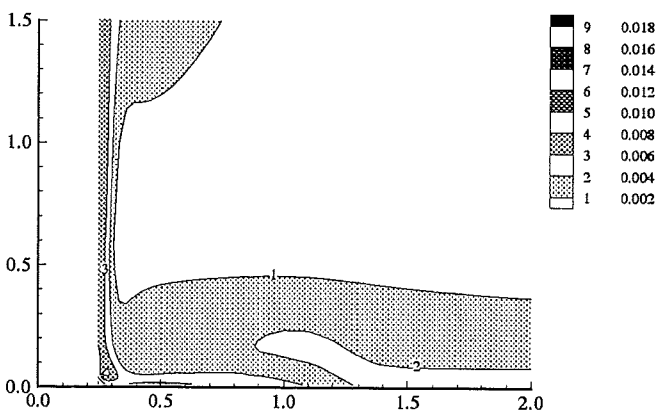
ASC:hKE_std+wf



UKarlsru:hKE_std+wf



CompDyna:hKE_RNG+wf

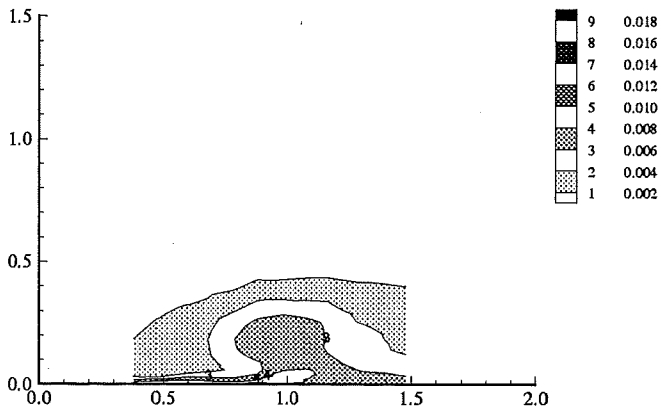
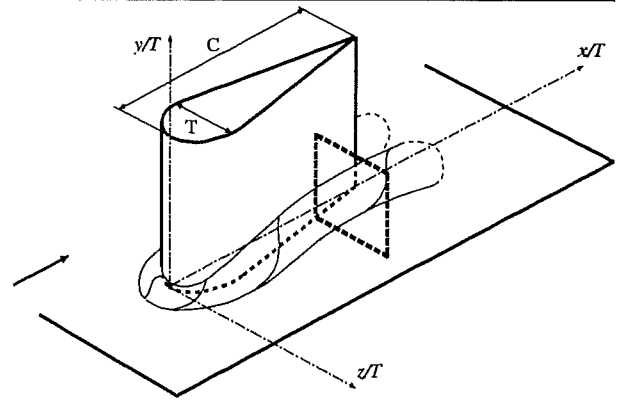


UHamburg:hKE_RNG+wf

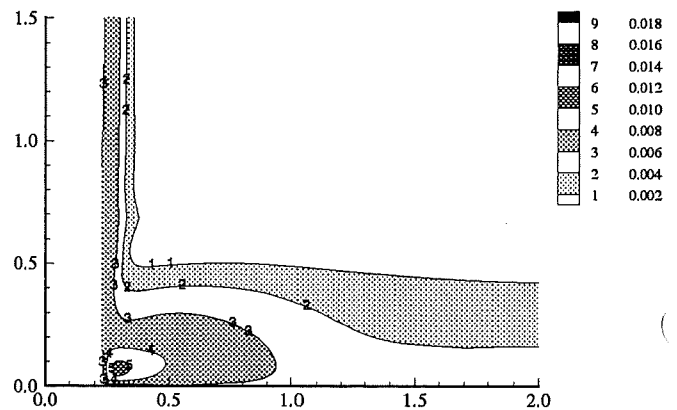
Wing/Body Junction with Separation

Turbulent kinetic energy k

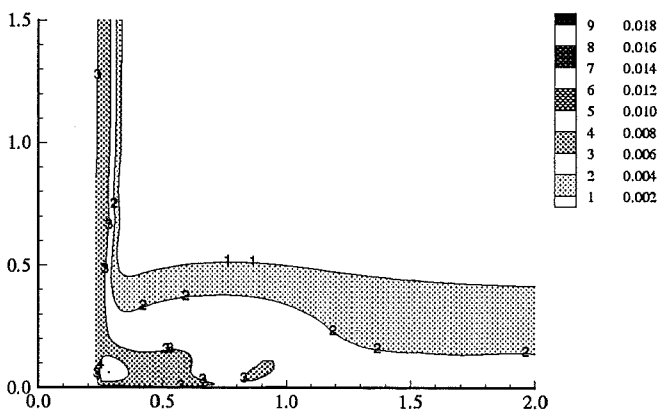
Plane $x/C = 0.75$



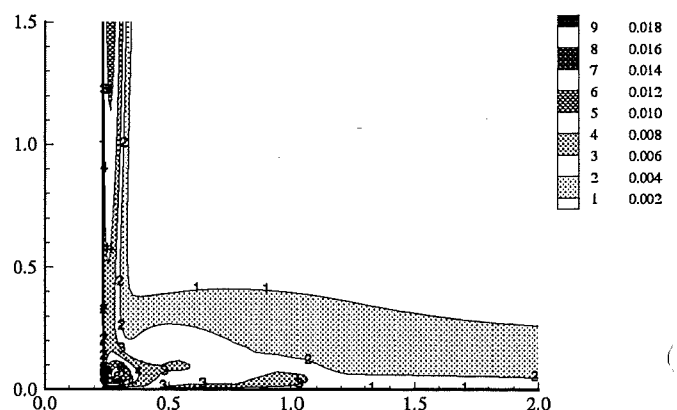
Exp



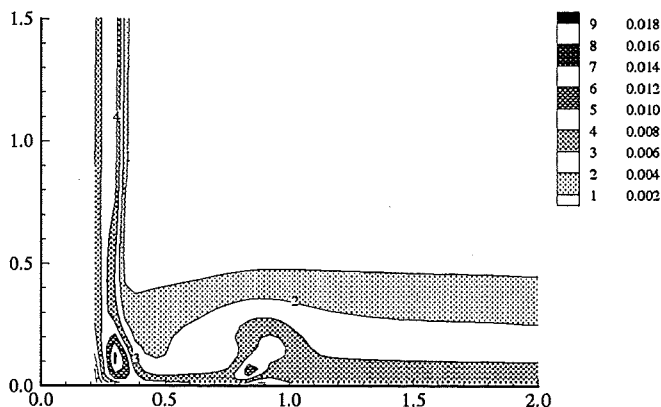
FluiDyna:hKE_std+0eq



FluiDyna:hKE_mod+0eq



UStuttg2:hKE_KaLa+1eq

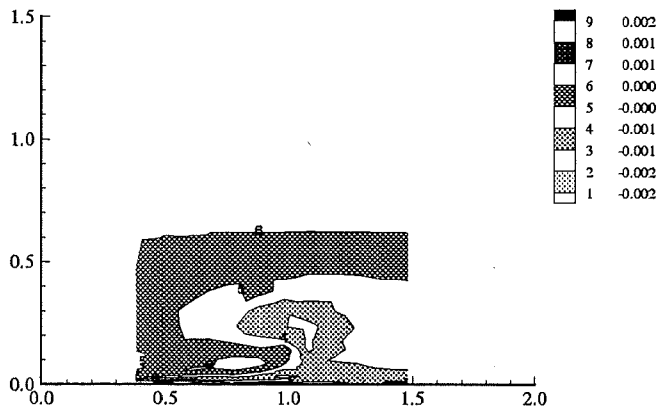
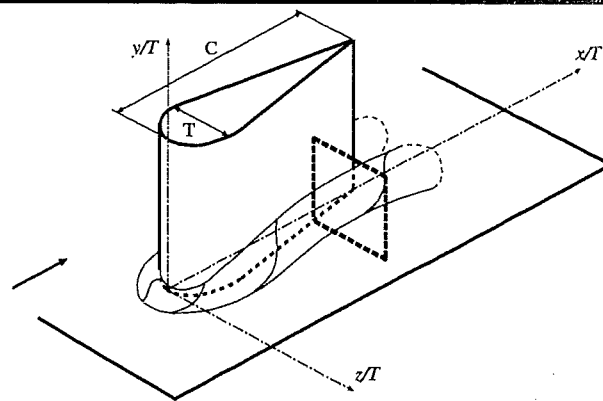


Volvo:RSM_LRR+wf

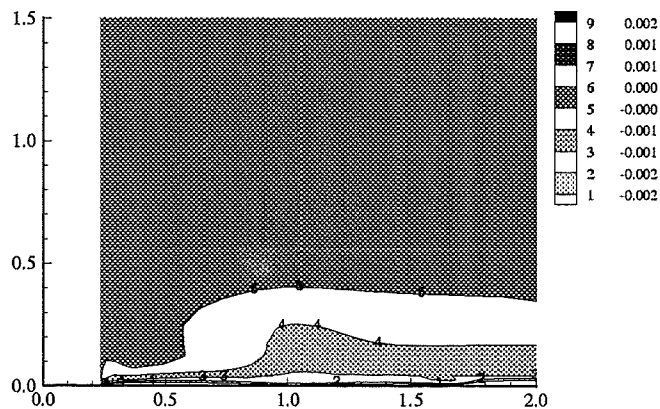
Wing/Body Junction with Separation

Reynolds shear stress uv

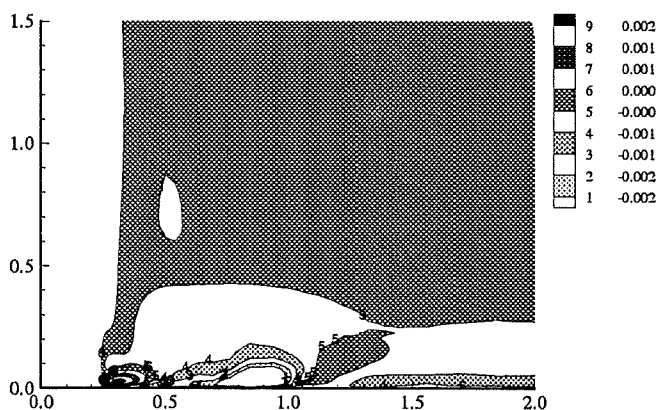
Plane $x/C = 0.75$



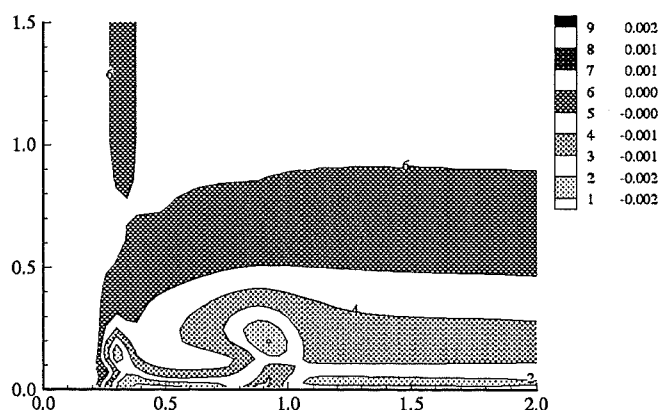
Exp



CompDyna:hKE_RNG+wf



UStuttg2:hKE_KaLa+1eq

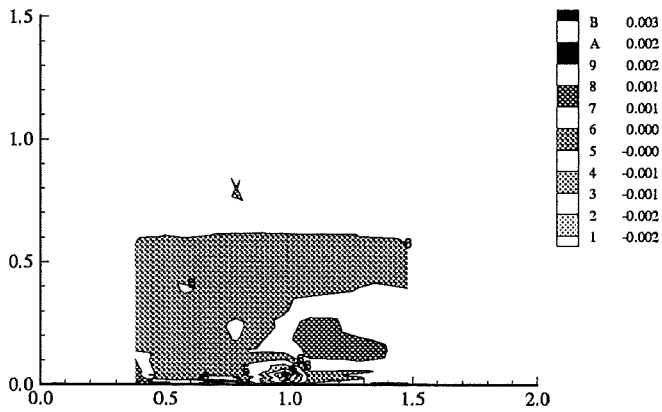
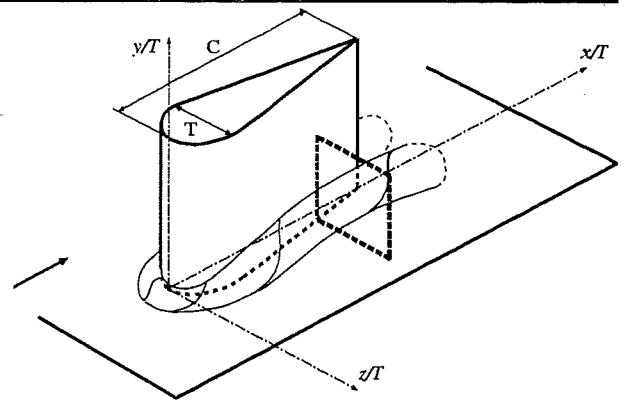


Volvo:RSM_LRR+wf

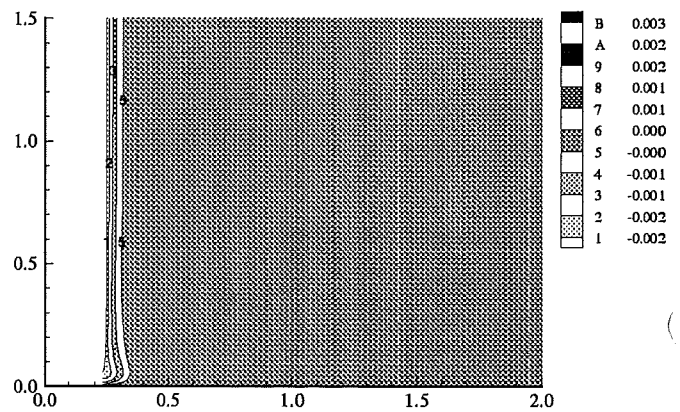
Wing/Body Junction with Separation

Reynolds shear stress $u'w'$

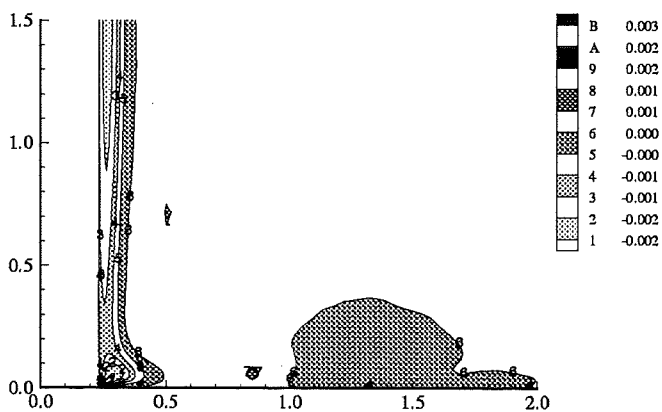
Plane $x/C = 0.75$



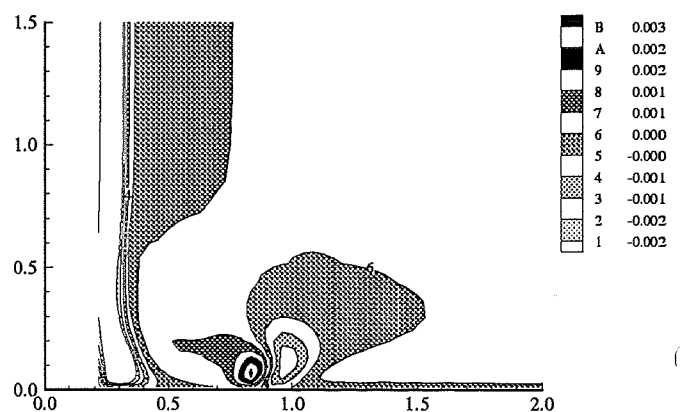
Exp



CompDyna:hKE_RNG+wf



UStuttg2:hKE_KaLa+1eq

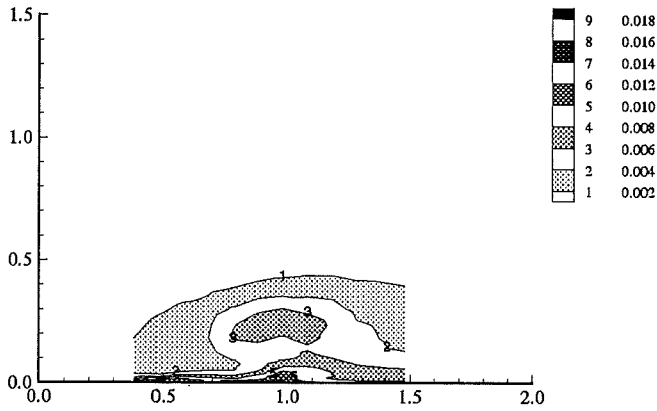
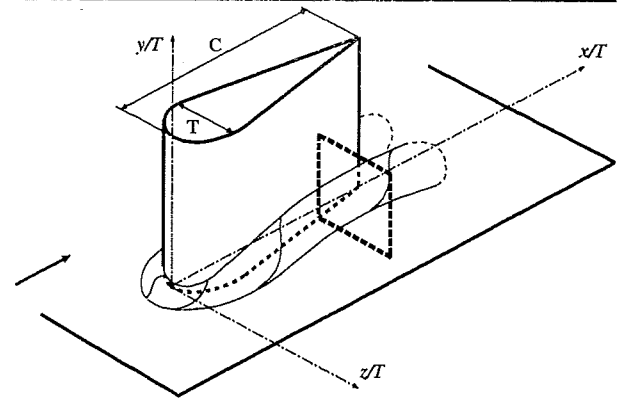


Volvo:RSM_LRR+wf

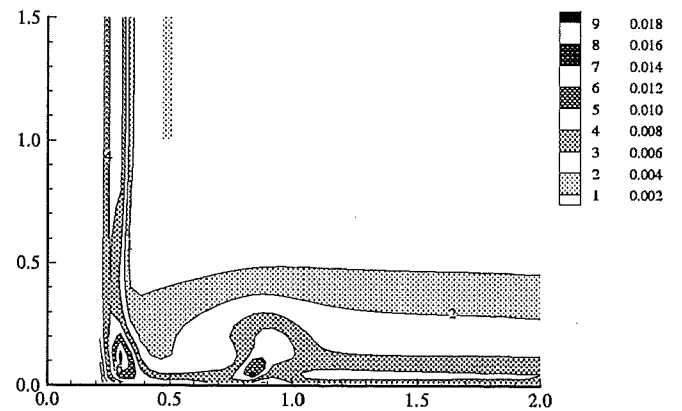
Wing/Body Junction with Separation

Reynolds normal stress uu

Plane $x/C = 0.75$



Exp

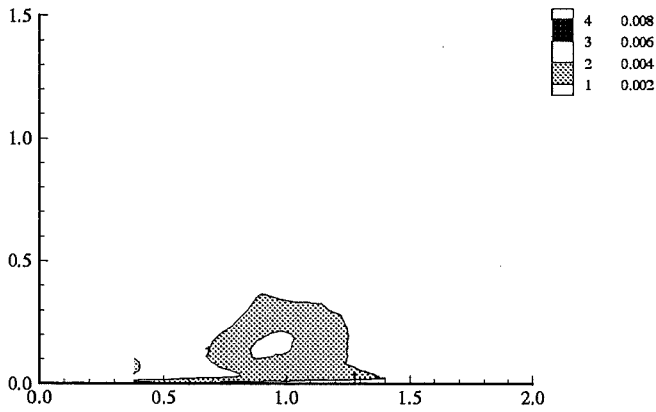
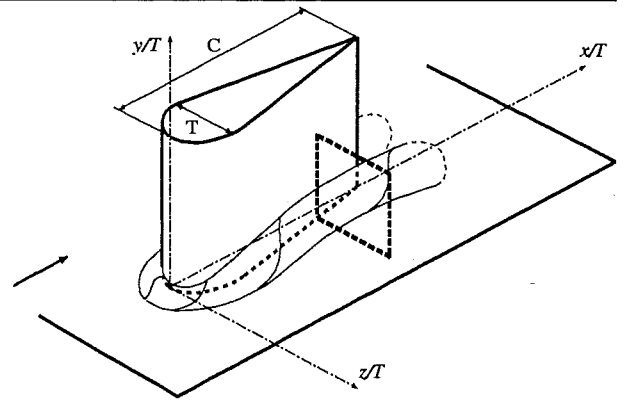


Volvo:RSM_LRR+wf

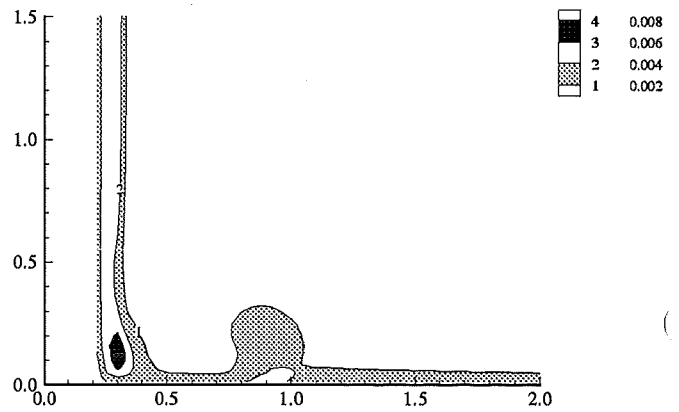
Wing/Body Junction with Separation

Reynolds normal stress $\overline{v'v'}$

Plane $x/C = 0.75$



Exp

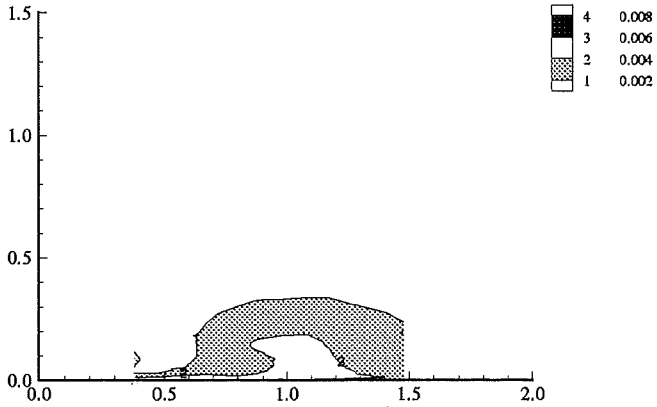
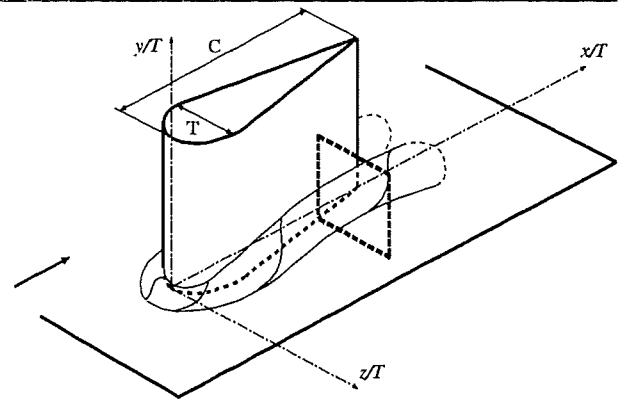


Volvo:RSM_LRR+wf

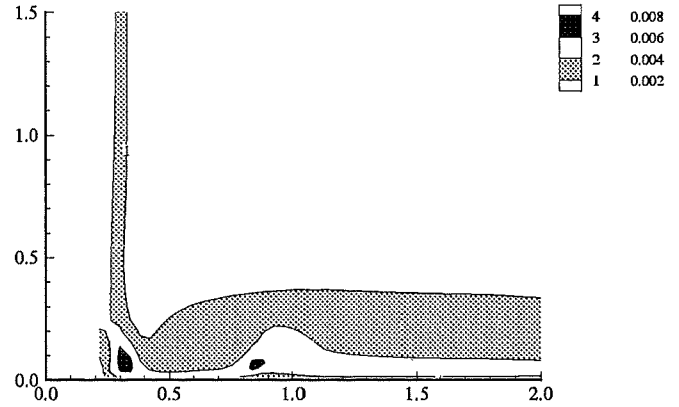
Wing/Body Junction with Separation

Reynolds normal stress $w w$

Plane $x/C = 0.75$



Exp

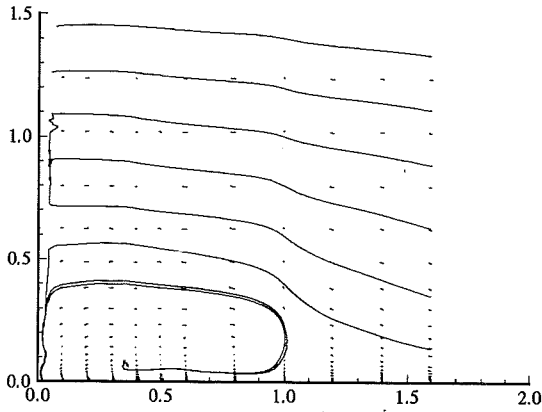
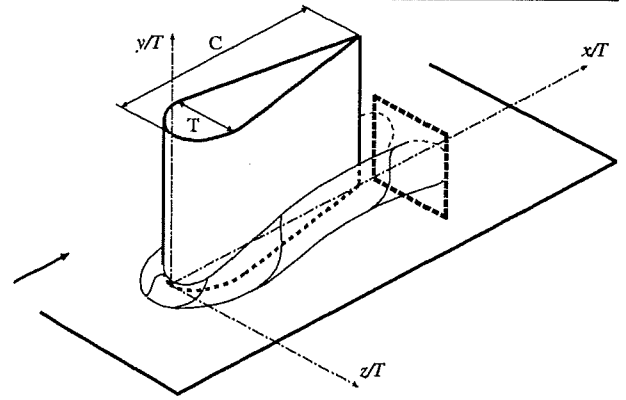


Volvo:RSM_LRR+wf

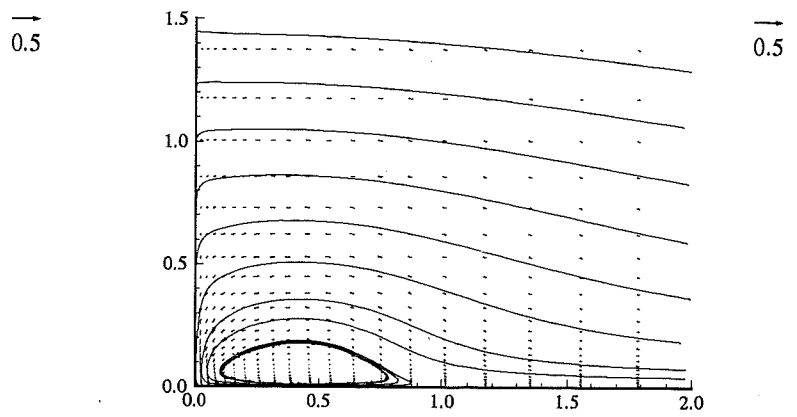
Wing/Body Junction with Separation

Secondary velocity vectors

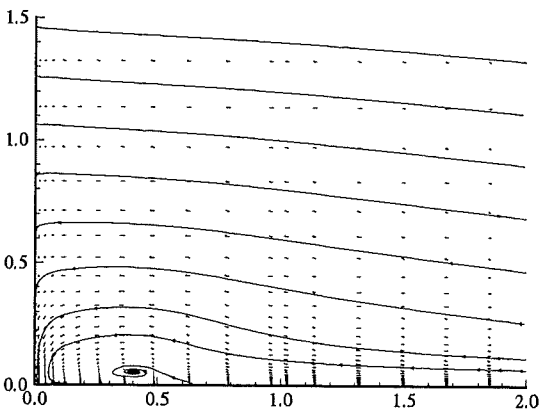
Plane $x/C = 1.05$



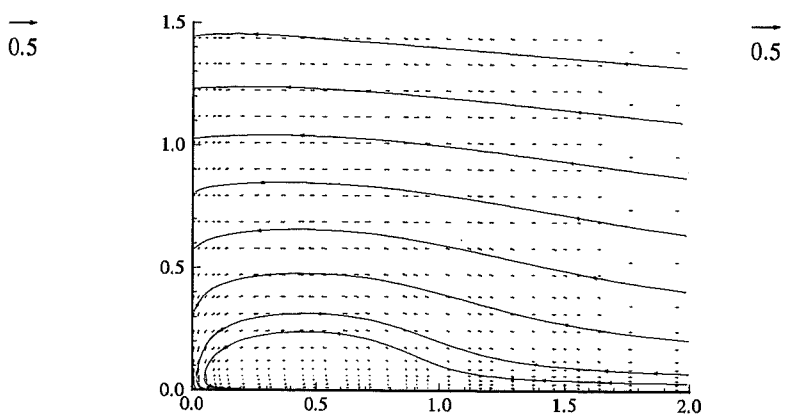
Exp



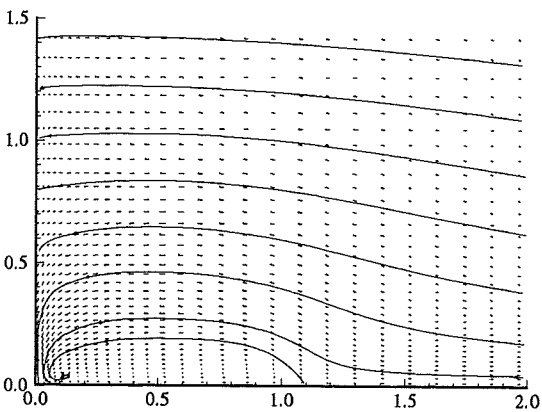
ASC:hKE_std+wf



UKarlsruhe:hKE_std+wf



CompDyna:hKE_RNG+wf

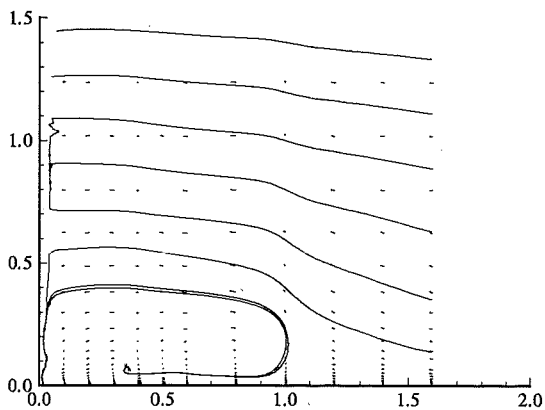
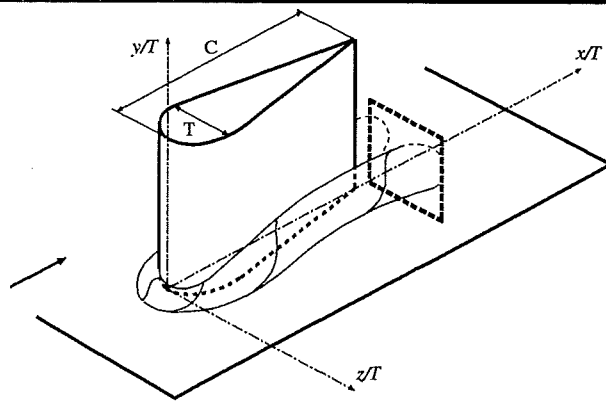


UHamburg:hKE_RNG+wf

Wing/Body Junction with Separation

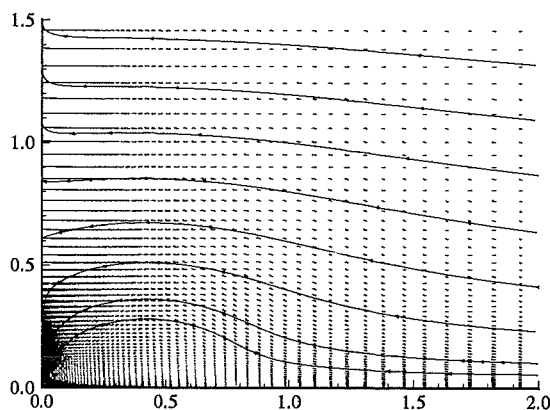
Secondary velocity vectors

Plane $x/C = 1.05$



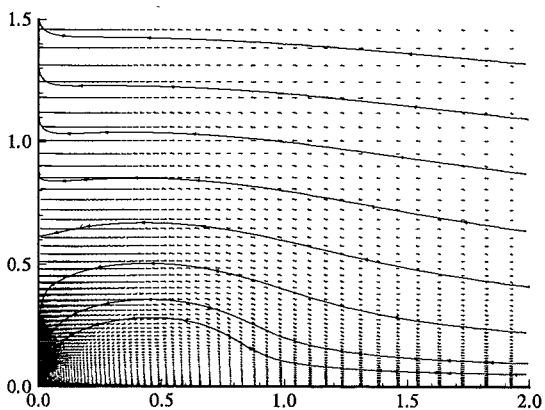
Exp

→
0.5



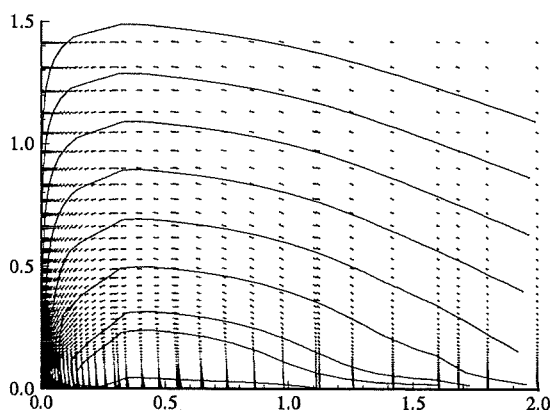
FluiDyna:hKE_std+0eq

→
0.5



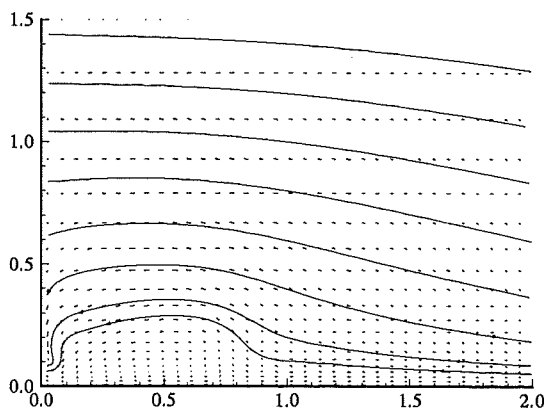
FluiDyna:hKE_mod+0eq

→
0.5



UStuttg2:hKE_KaLa+1eq

→
0.5



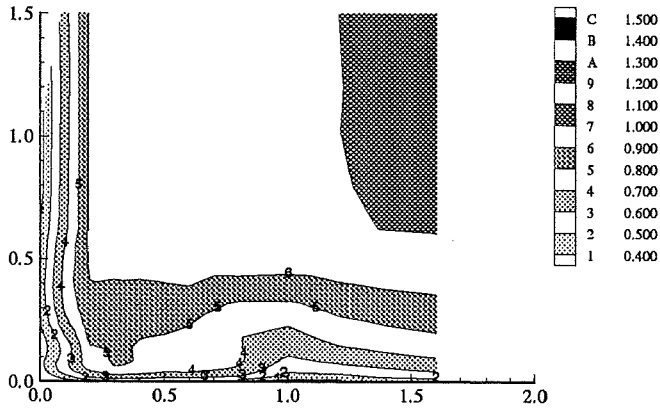
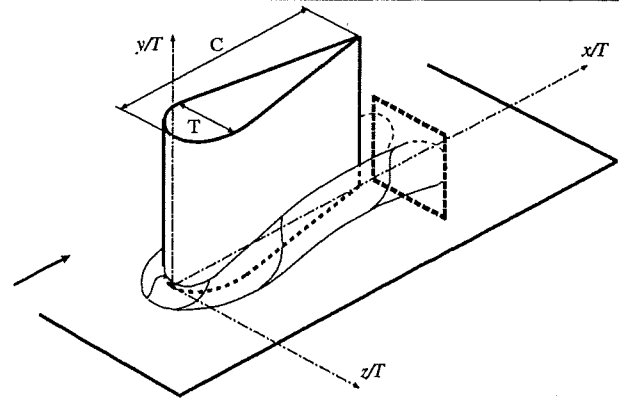
Volvo:RSM_LRR+wf

→
0.5

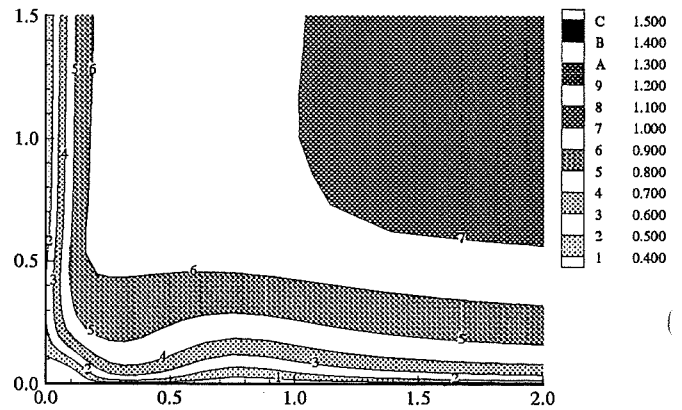
Wing/Body Junction with Separation

Streamwise mean velocity

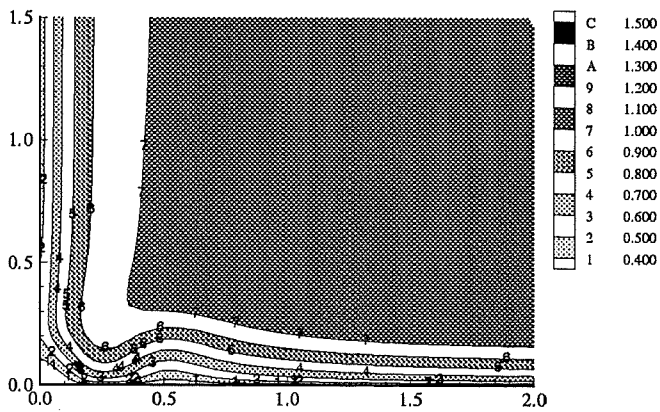
Plane $x/C = 1.05$



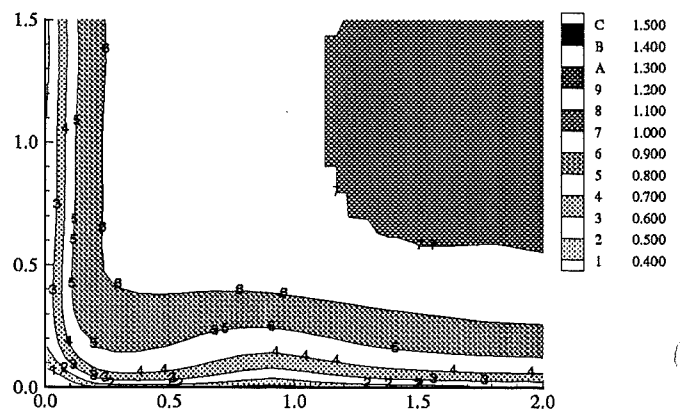
Exp



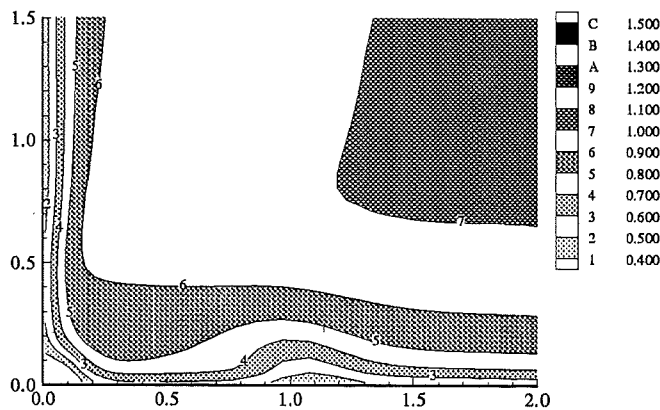
ASC:hKE_std+wf



UKarlsruhe:hKE_std+wf



CompDyna:hKE_RNG+wf

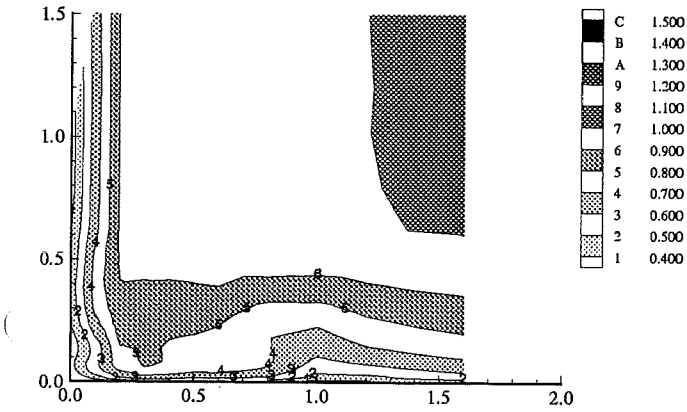
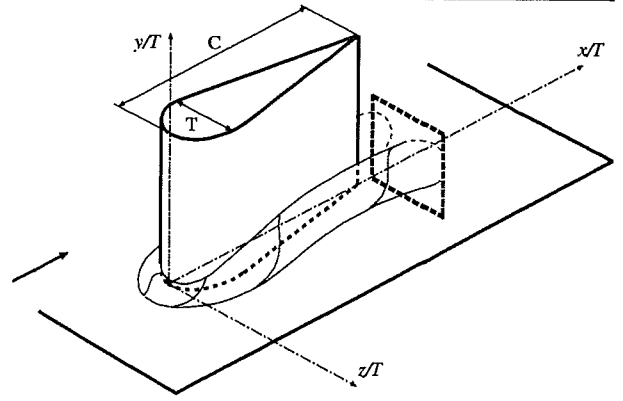


UHamburg:hKE_RNG+wf

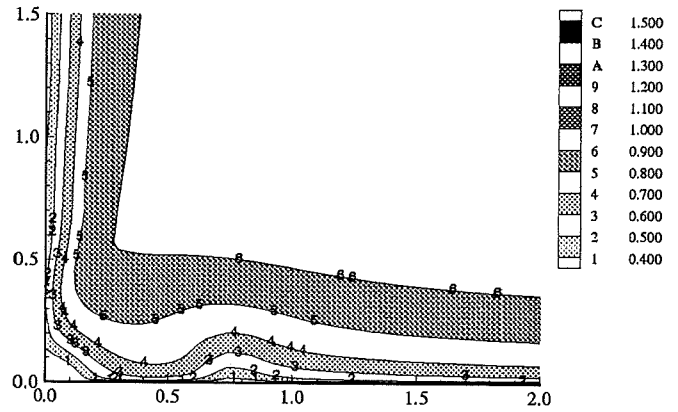
Wing/Body Junction with Separation

Streamwise mean velocity

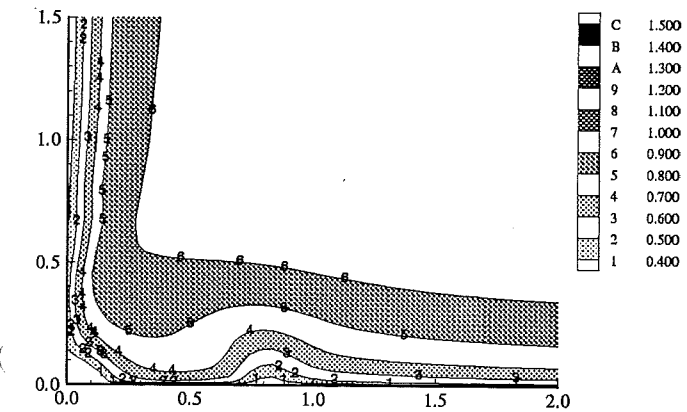
Plane $x/C = 1.05$



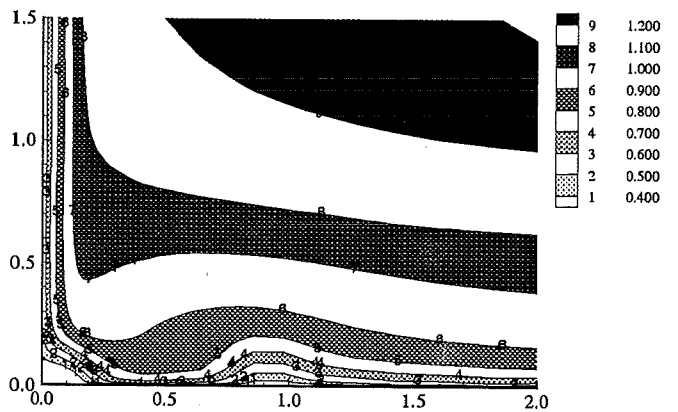
Exp



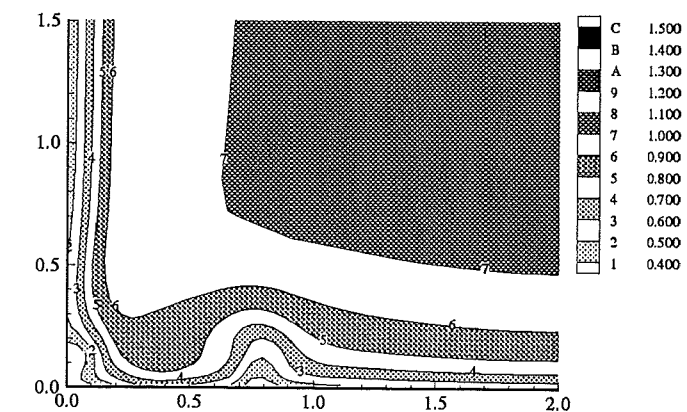
FluiDyna:hKE_std+0eq



FluiDyna:hKE_mod+0eq



UStuttg2:hKE_KaLa+1eq

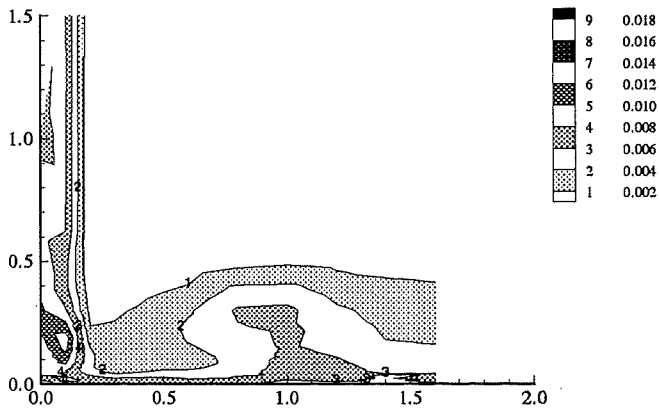
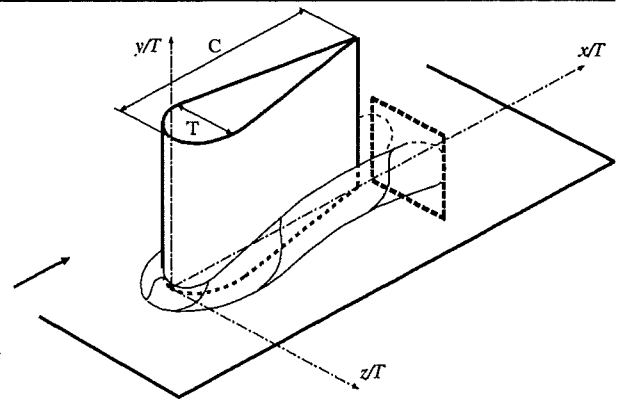


Volvo:RSM_LRR+wf

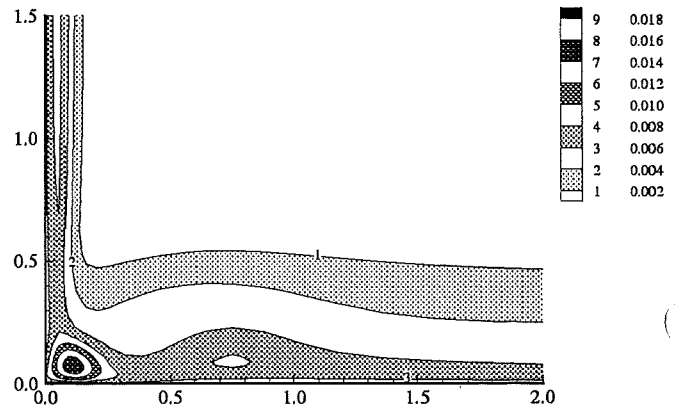
Wing/Body Junction with Separation

Turbulent kinetic energy k

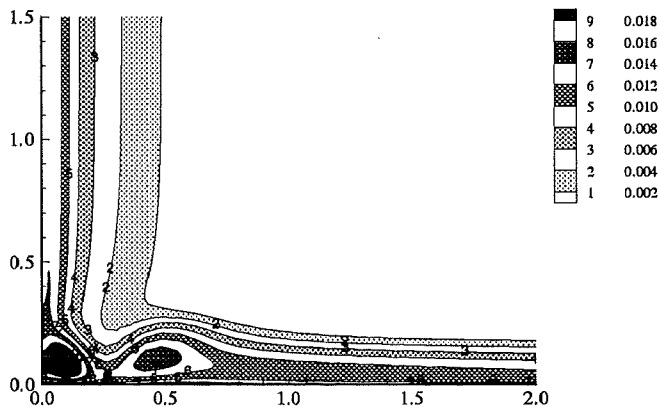
Plane $x/C = 1.05$



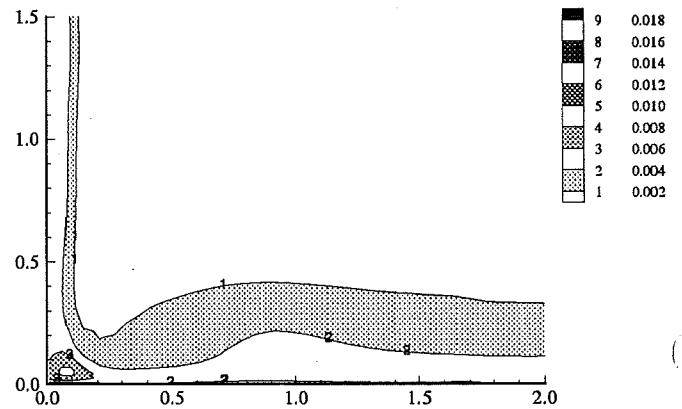
Exp



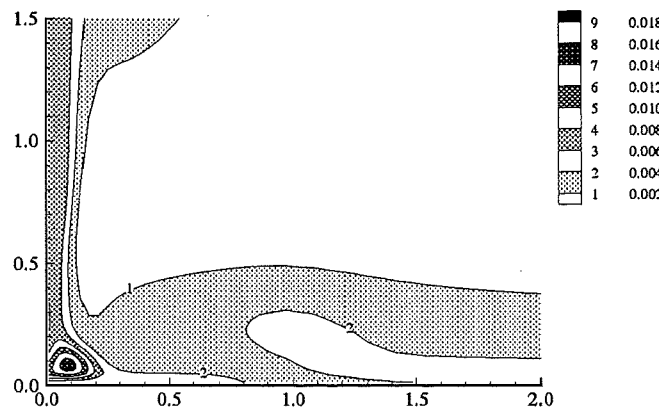
ASC:hKE_std+wf



UKarlsruhe:hKE_std+wf



CompDyna:hKE_RNG+wf

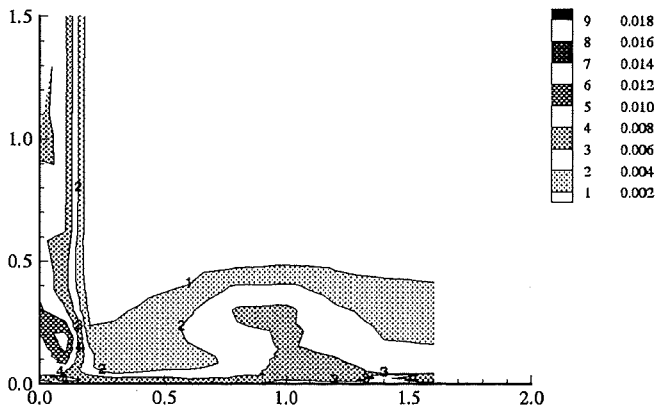
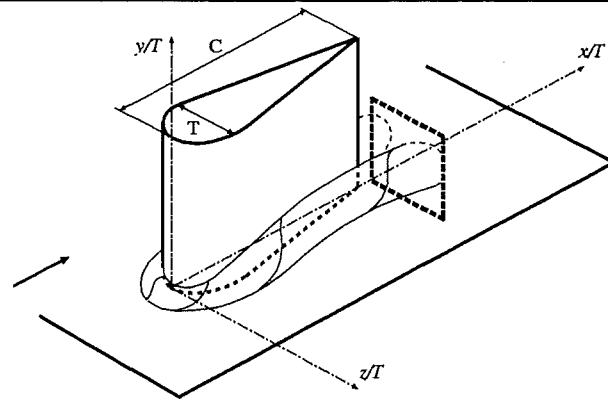


UHamburg:hKE_RNG+wf

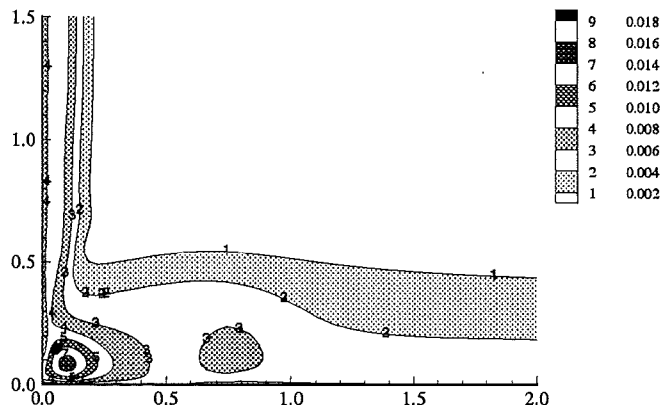
Wing/Body Junction with Separation

Turbulent kinetic energy k

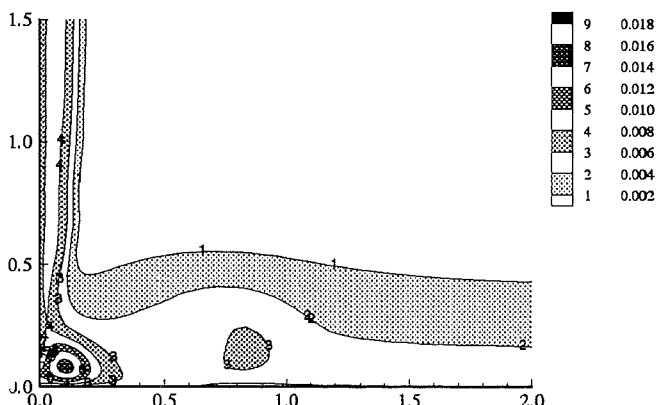
Plane $x/C = 1.05$



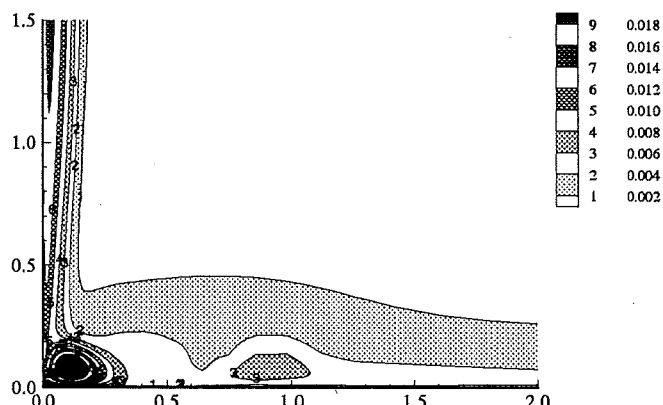
Exp



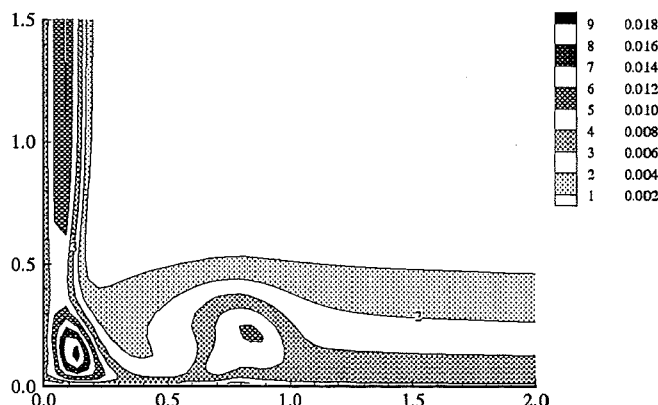
Fluidyna:hKE_std+0eq



Fluidyna:hKE_mod+0eq



UStuttg2:hKE_KaLa+1eq

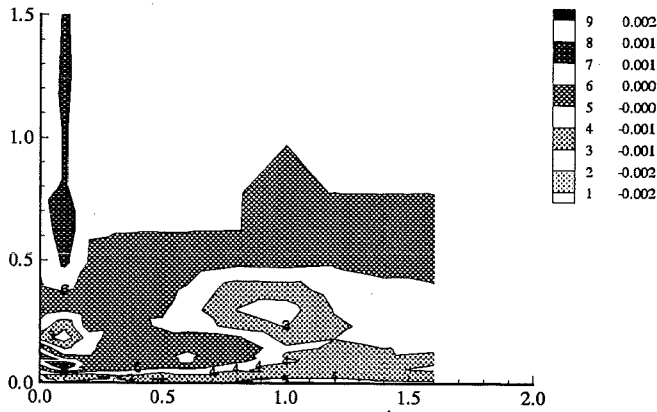
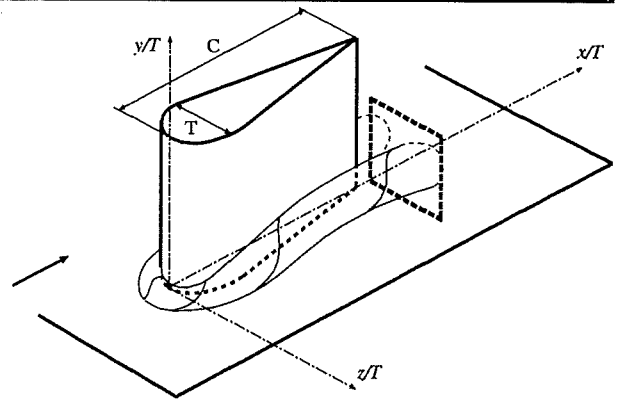


Volvo:RSM_LRR+wf

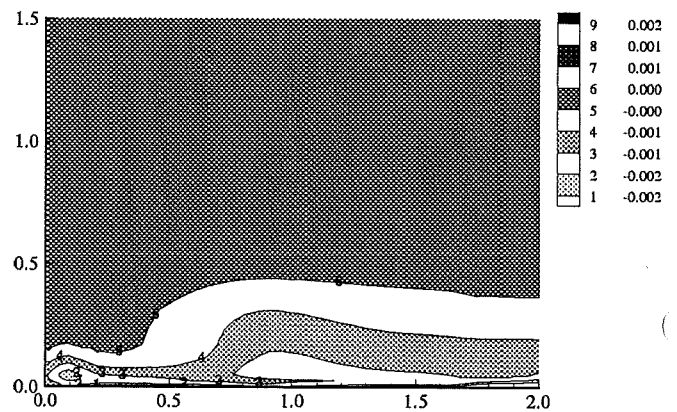
Wing/Body Junction with Separation

Reynolds shear stress uv

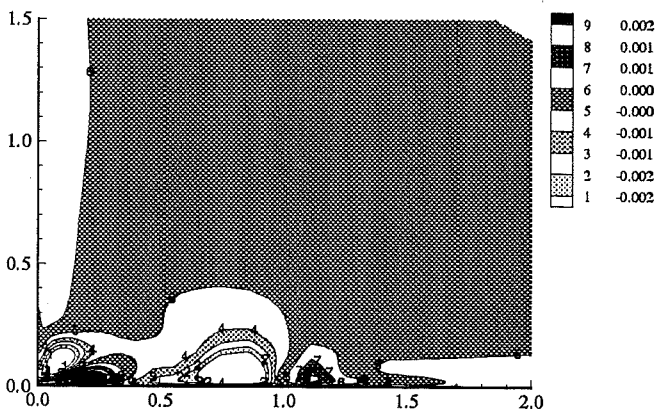
Plane $x/C = 1.05$



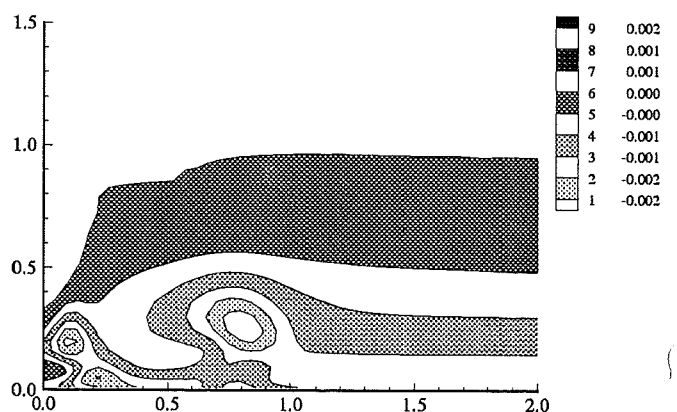
Exp



CompDyna:hKE_RNG+wf



UStuttg2:hKE_KaLa+1eq

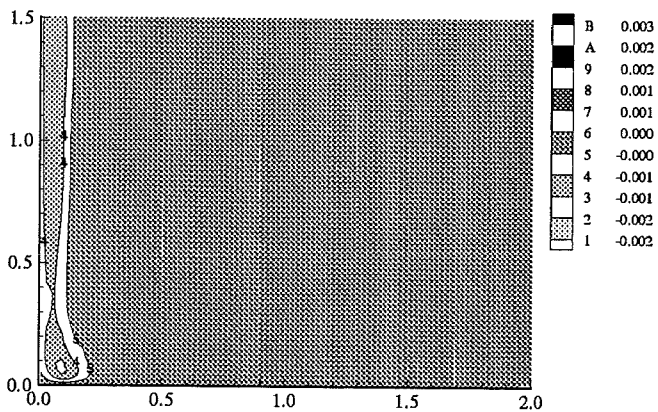
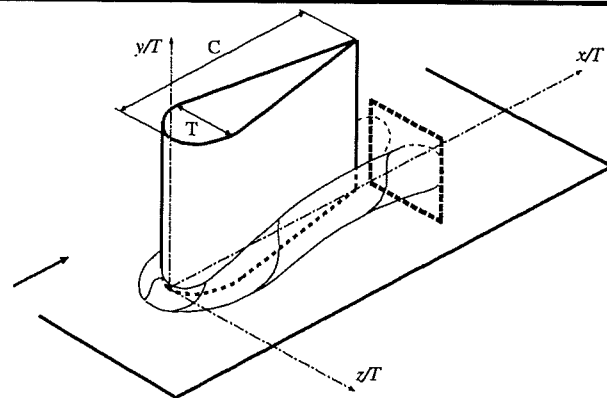


Volvo:RSM_LRR+wf

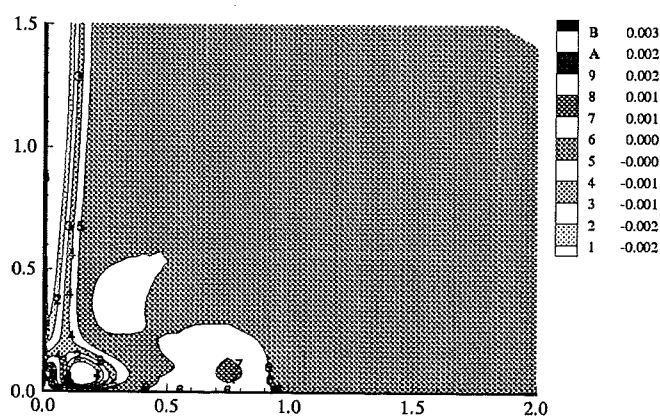
Wing/Body Junction with Separation

Reynolds shear stress uw

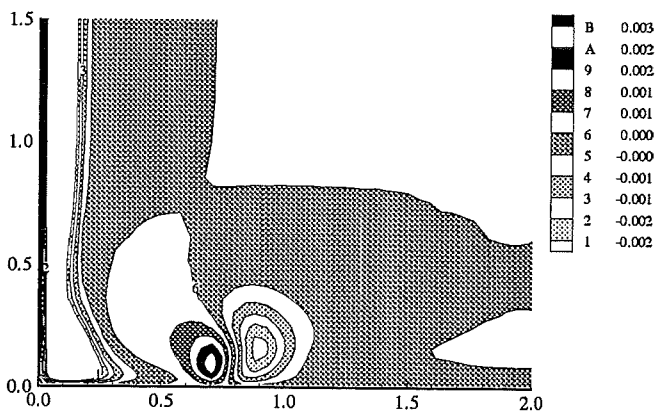
Plane $x/C = 1.05$



CompDyna:hKE_RNG+wf



UStuttg2:hKE_KaLa+1eq

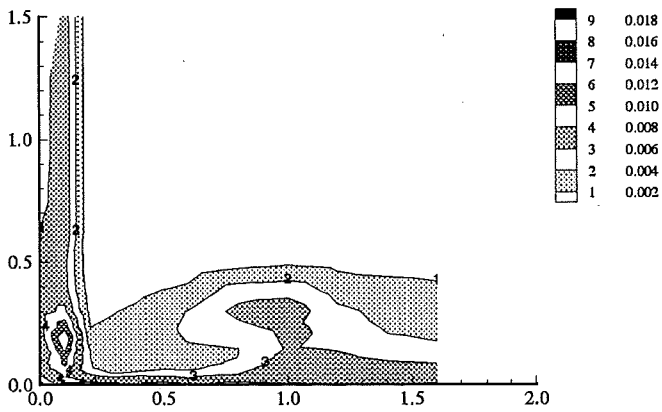
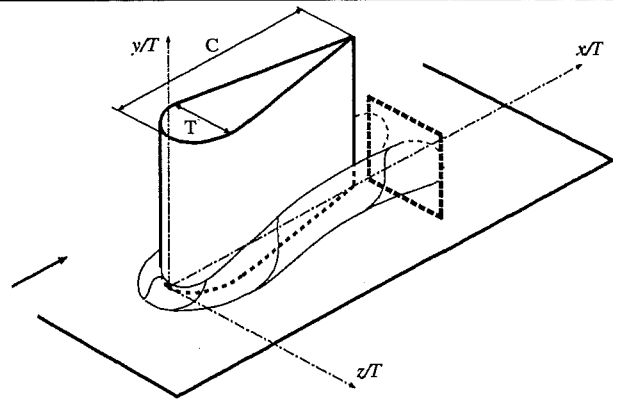


Volvo:RSM_LRR+wf

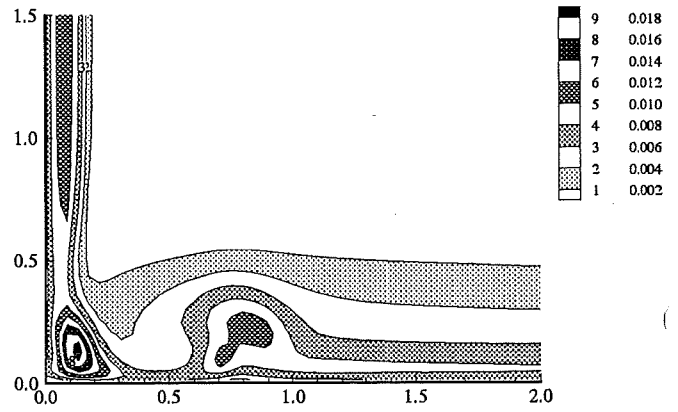
Wing/Body Junction with Separation

Reynolds normal stress uu

Plane $x/C = 1.05$



Exp

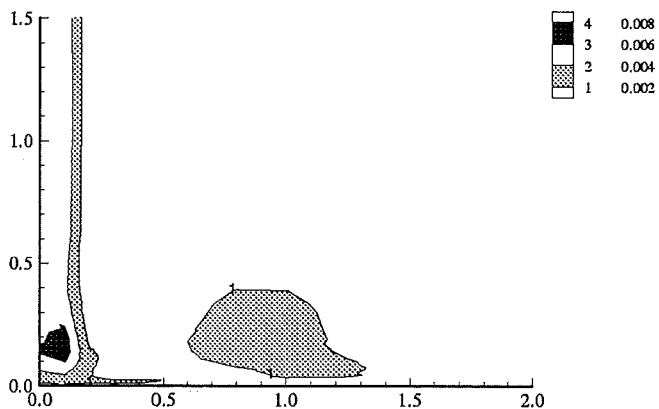
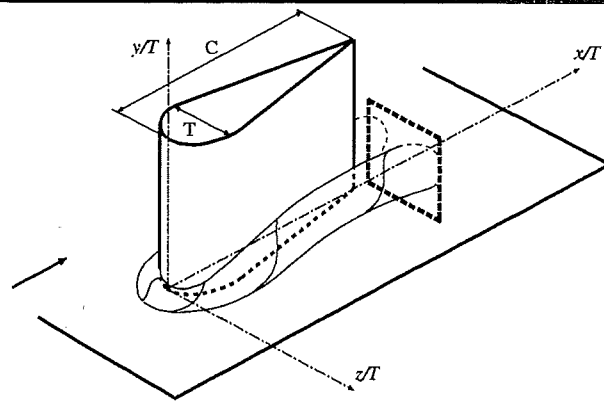


Volvo:RSM_LRR+wf

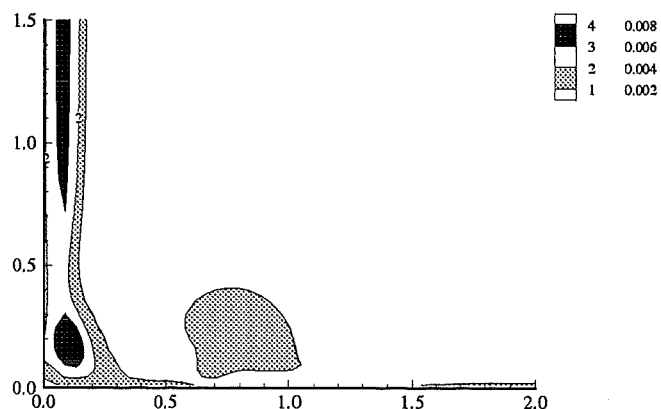
Wing/Body Junction with Separation

Reynolds normal stress $\overline{v'v'}$

Plane $x/C = 1.05$



Exp

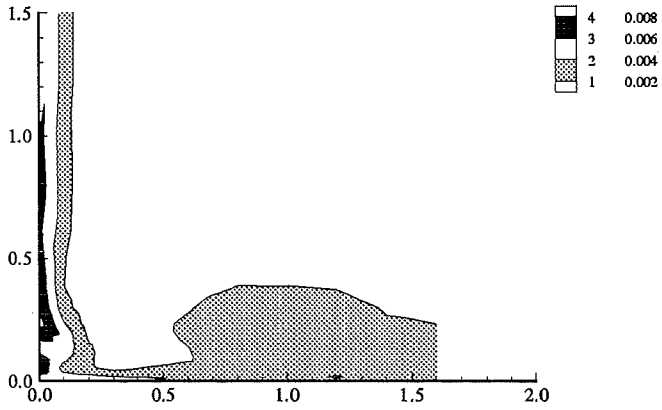
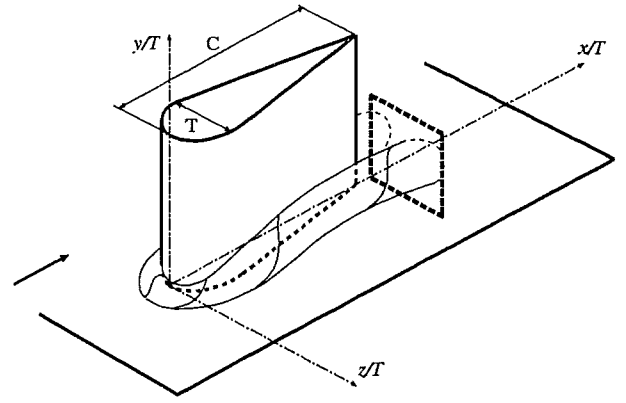


Volvo:RSM_LRR+wf

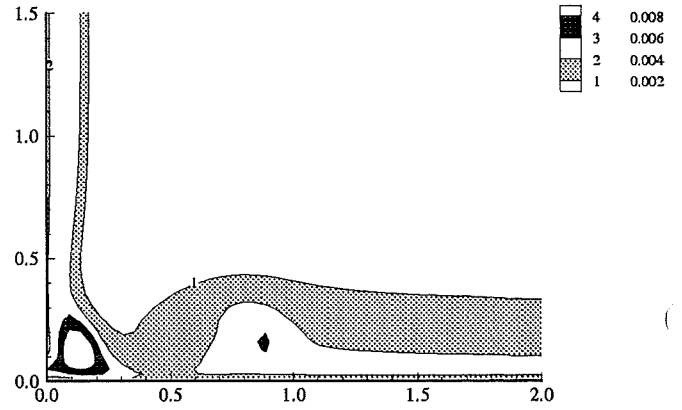
Wing/Body Junction with Separation

Reynolds normal stress $w'w'$

Plane $x/C = 1.05$



Exp

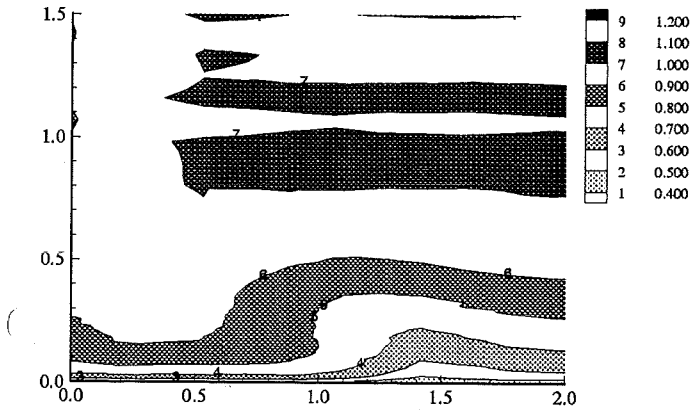
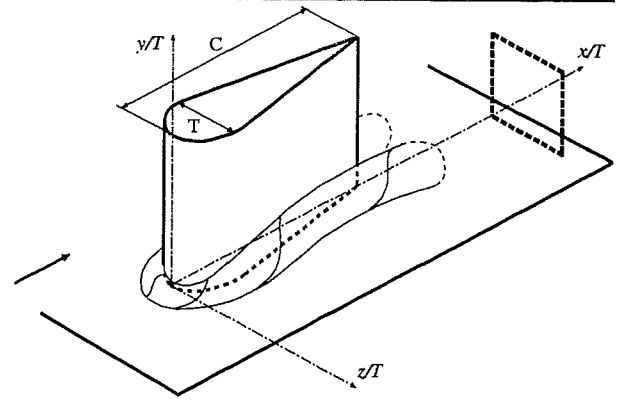


Volvo:RSM_LRR+wf

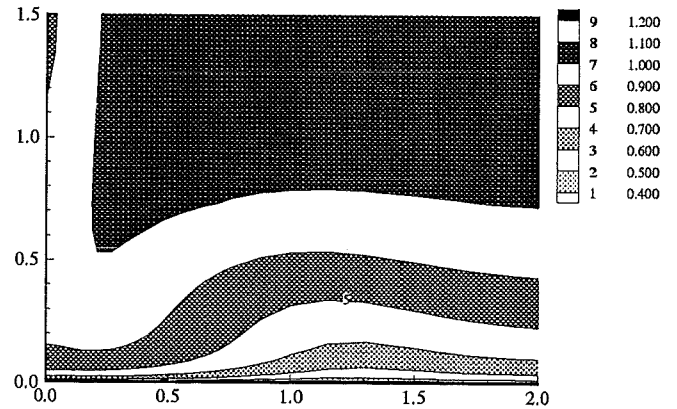
Wing/Body Junction with Separation

Streamwise mean velocity

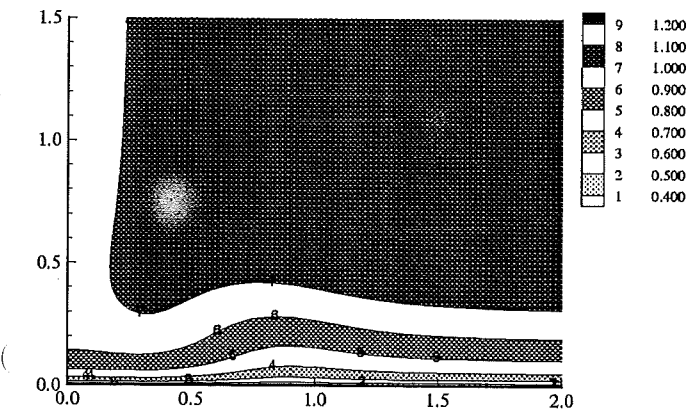
Plane $x/C = 3.00$



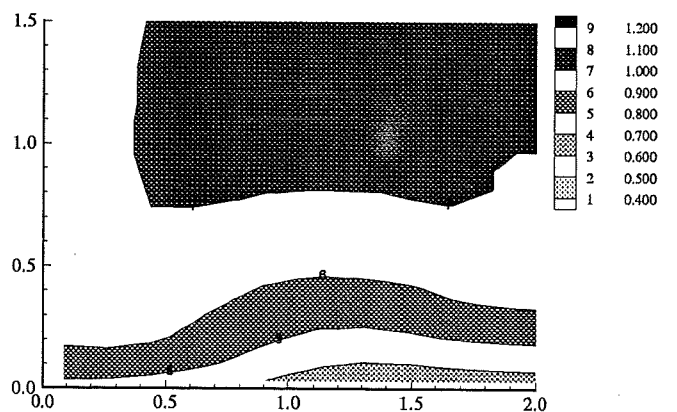
Exp



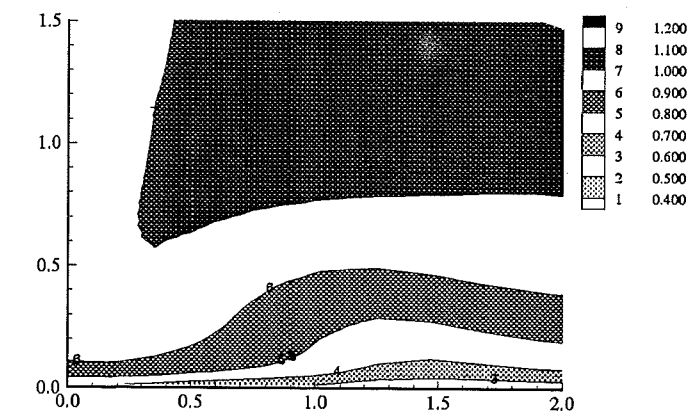
ASC:hKE_std+wf



UKarlsruhe:hKE_std+wf



CompDyna:hKE_RNG+wf

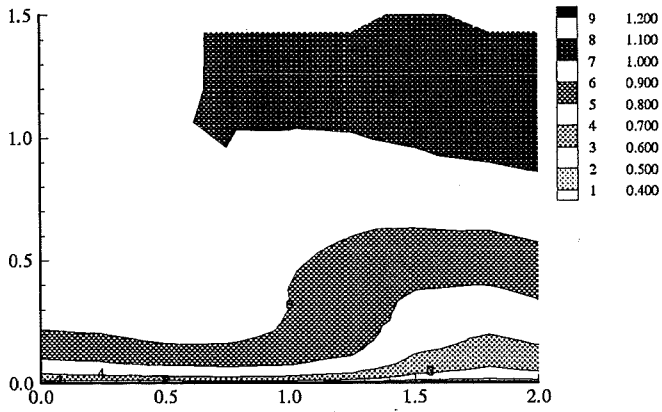
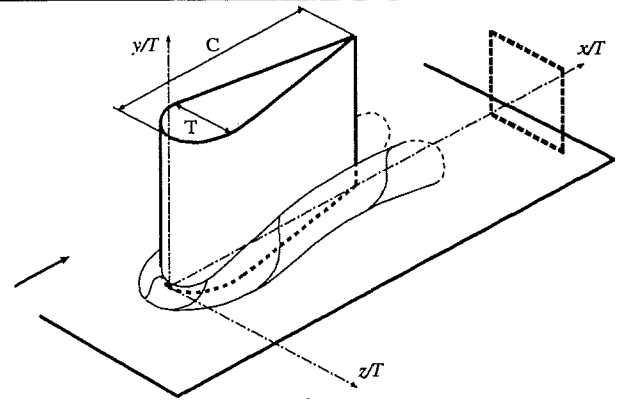


UHamburg:hKE_RNG+wf

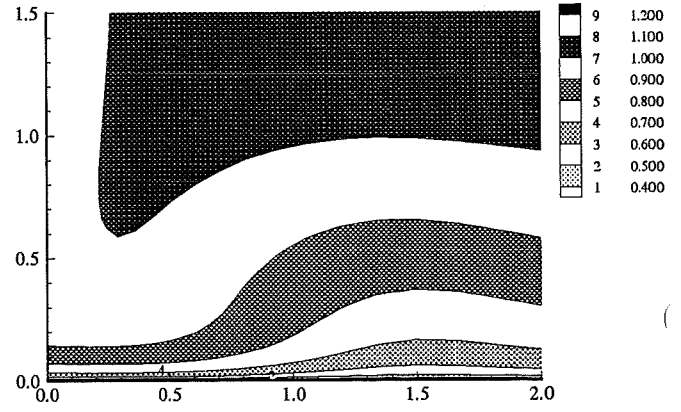
Wing/Body Junction with Separation

Streamwise mean velocity

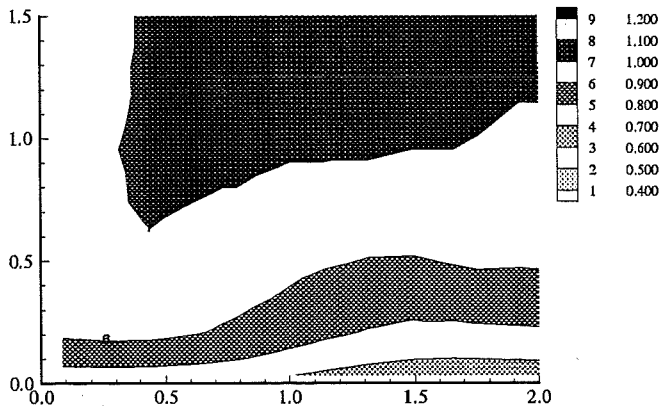
Plane $x/C = 5.89$



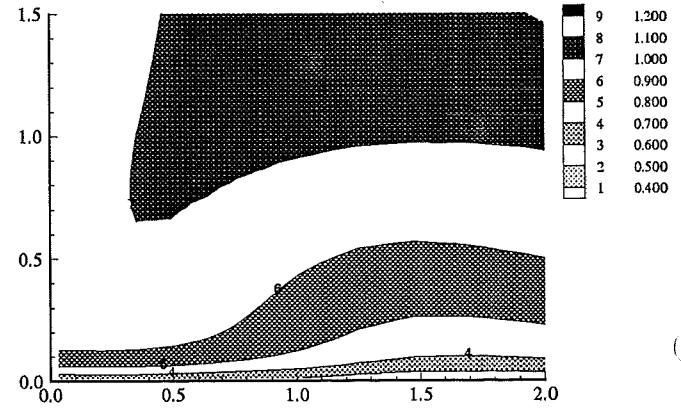
Exp



ASC:hKE_std+wf



CompDyna:hKE_RNG+wf

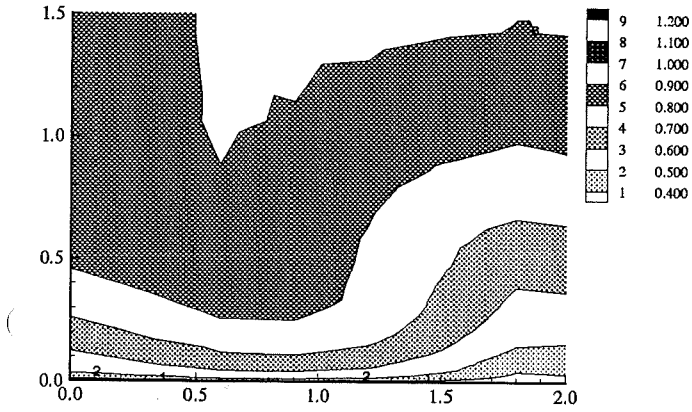
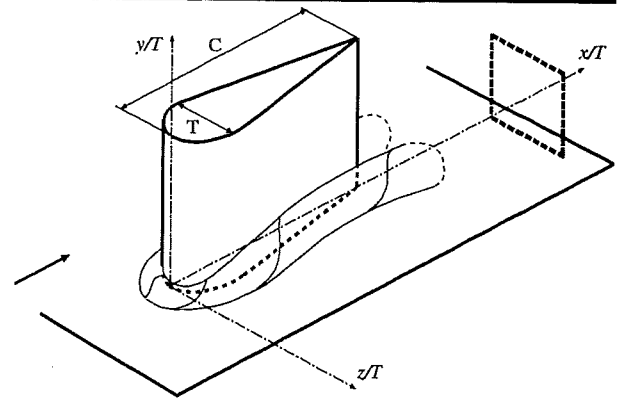


UHamburg:hKE_RNG+wf

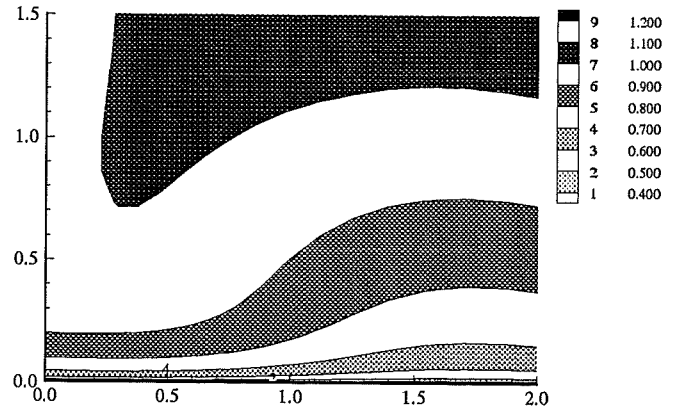
Wing/Body Junction with Separation

Streamwise mean velocity

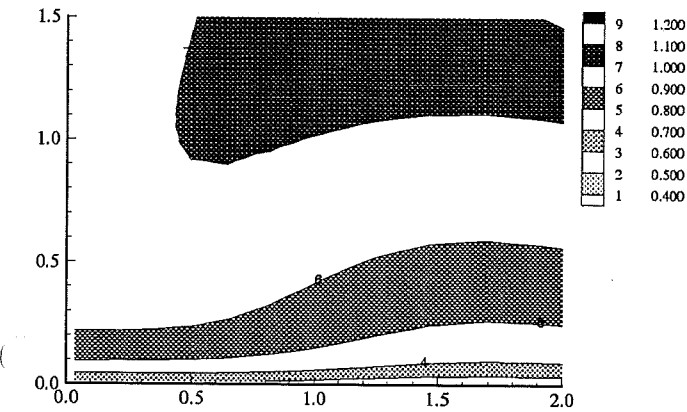
Plane $x/C = 9.14$



Exp



ASC:hKE_std+wf

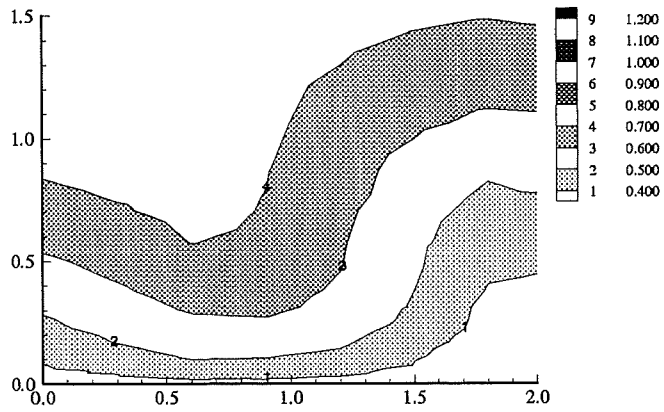
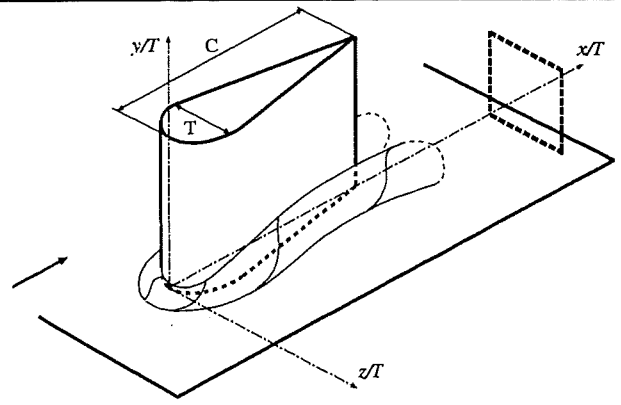


UHamburg:hKE_RNG+wf

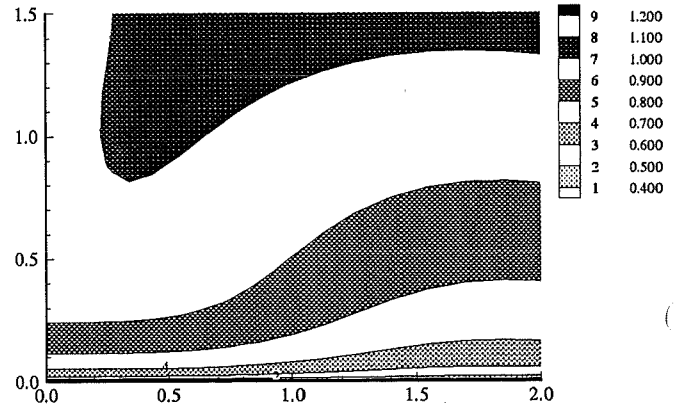
Wing/Body Junction with Separation

Streamwise mean velocity

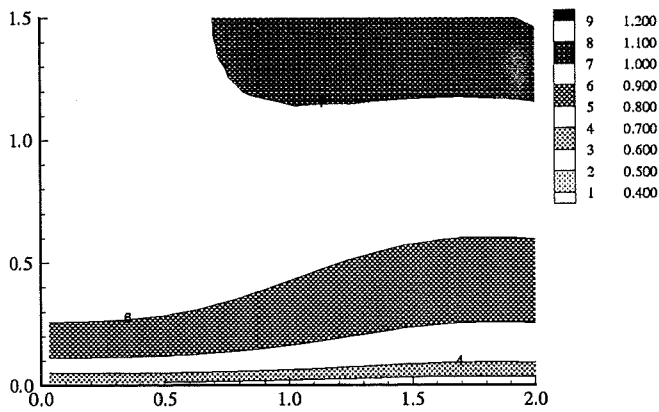
Plane $x/C = 11.6$



Exp



ASC:hKE_std+wf



UHamburg:hKE_RNG+wf

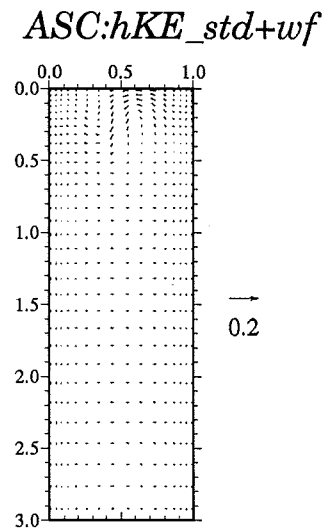
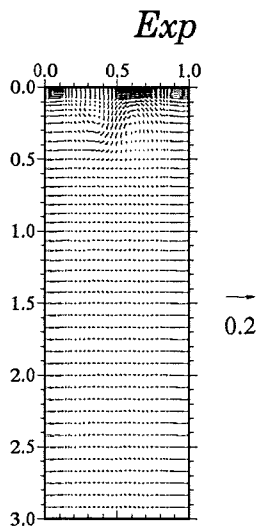
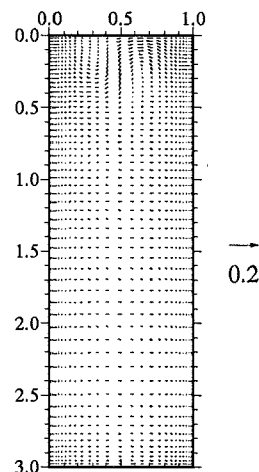
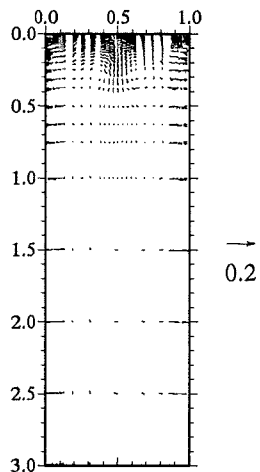
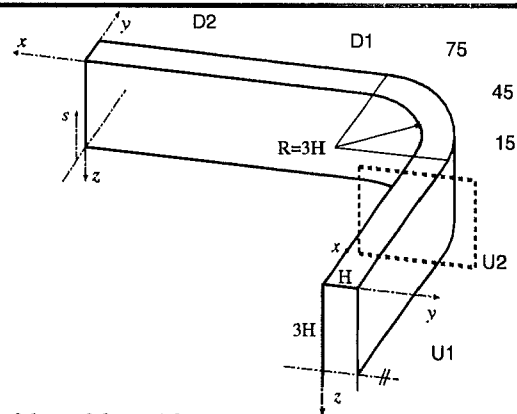
KEY TO TEST CASE 5

| Contributor | Key-Name | Name (Affiliation) | Turbulence Model | Near-Wall Treatment |
|-------------|-------------|---|--|---------------------|
| ASC | hKE_std+wf | Sick & Scheuerer (Sulzer Innotec & ASC) | standard k- ϵ | wall functions |
| EDFLNHMi | hKE_std+wf | Mattei/Minier (EDP-DER-LNH) | standard k- ϵ | wall functions |
| UBrussel | nKE_HiKh+wf | Hirsch/Khodak (Univ. of Brussels) | non-linear k- ϵ Hirsch-Khodak | wall functions |
| | nKE_SZL+wf | | non-linear k- ϵ Shih-Zhu-Lumley | wall functions |
| | hKE_std+wf | | standard k- ϵ | wall functions |
| UMcGill | RSM_GiLa+wf | Hedbergh/Chung (CERCA, McGill, Univ) | Reynolds-Stress Model Gibson-Launder | wall functions |
| USoutham | ASM_CiWi+wf | Zhang/Zhang (Univ. of Southampton) | Algebraic-Stress Model Clarke-Wilkes | wall functions |
| | | | | |

Developing Flow in a Curved Rectangular Duct

Secondary velocity vectors

Plane $x/H = -0.5$



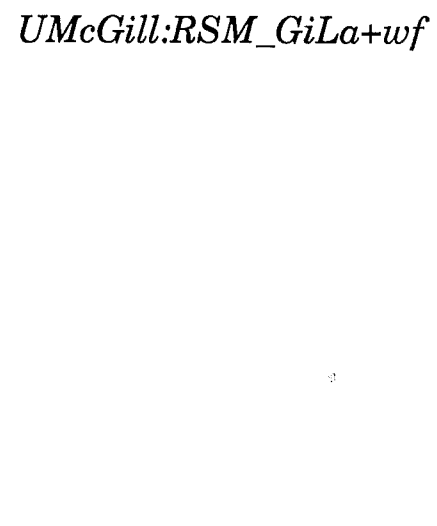
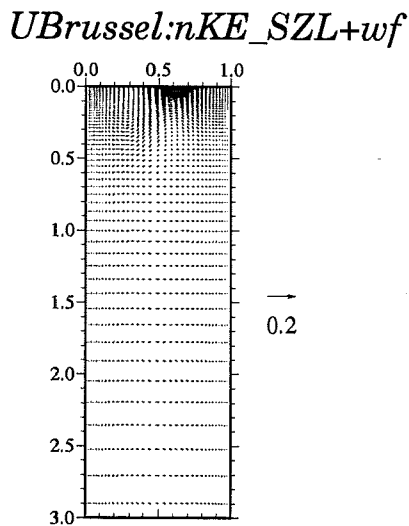
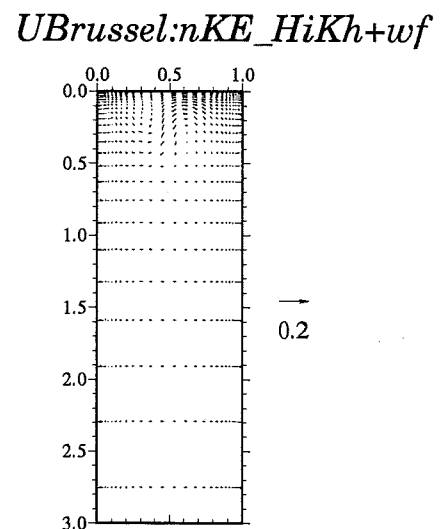
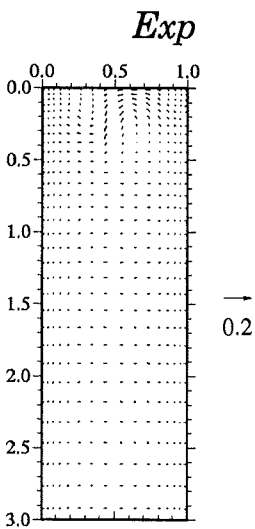
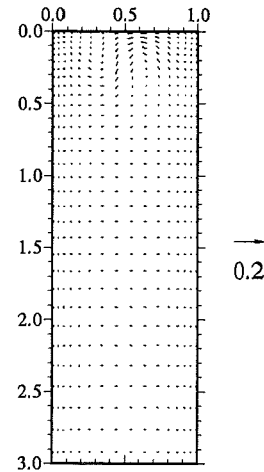
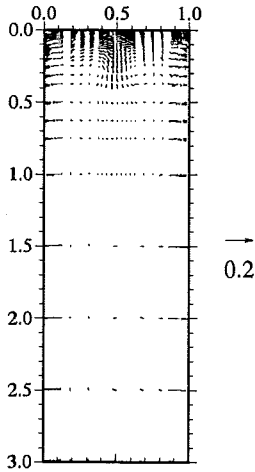
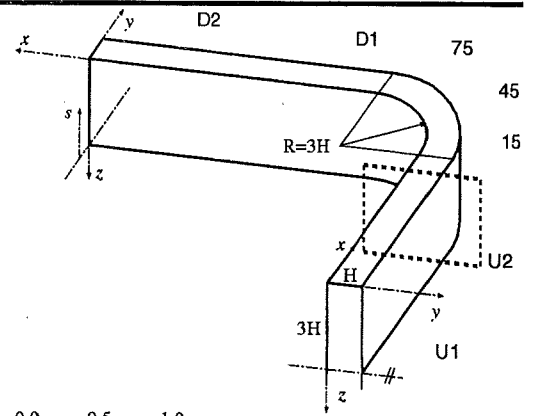
EDFLNHMi:hKE_std+wf

UBrussel:hKE_std+wf

Developing Flow in a Curved Rectangular Duct

Secondary velocity vectors

Plane $x/H = -0.5$

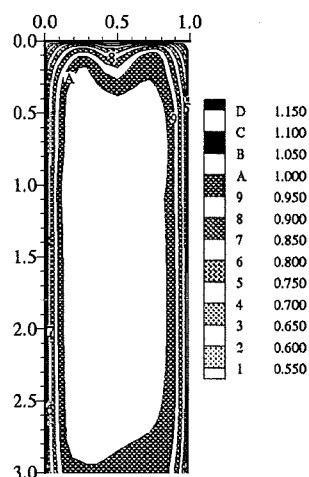
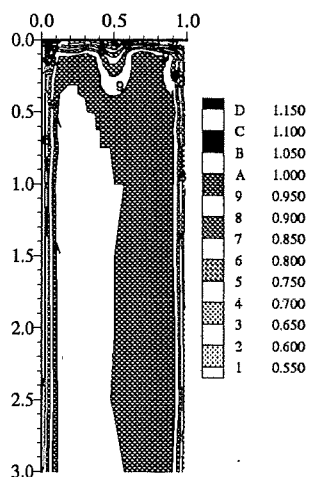
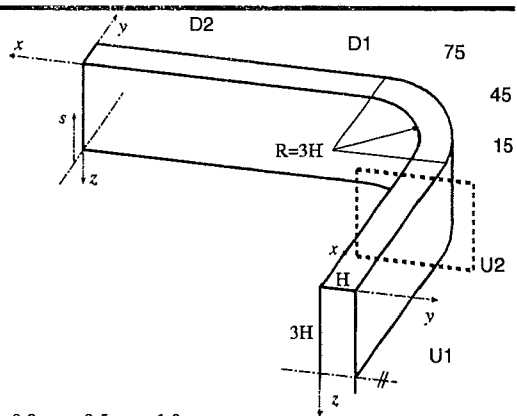


USoutham:ASM_ClWi

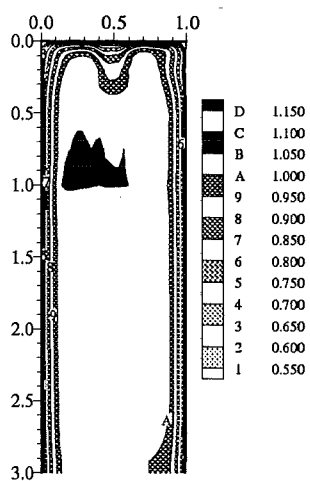
Developing Flow in a Curved Rectangular Duct

Streamwise mean velocity

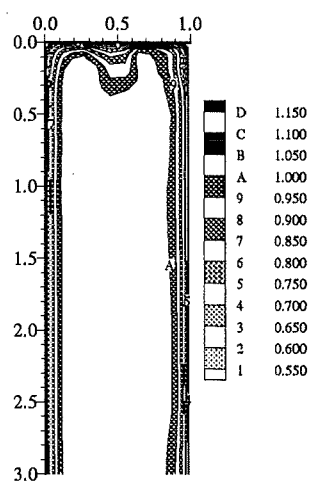
Plane $x/H = -0.5$



Exp



ASC:hKE_std+wf



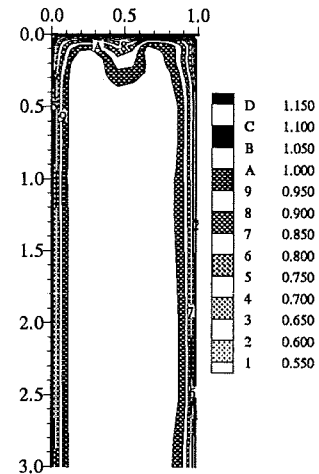
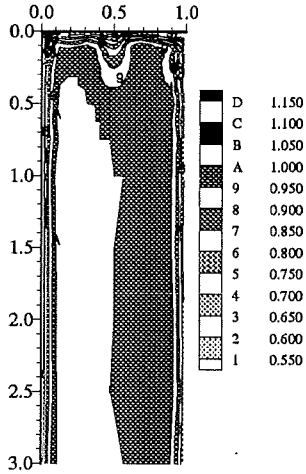
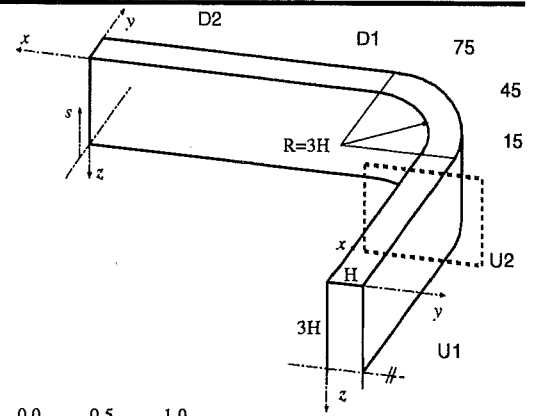
EDFLNHMi:hKE_std+wf

UBrussel:hKE_std+wf

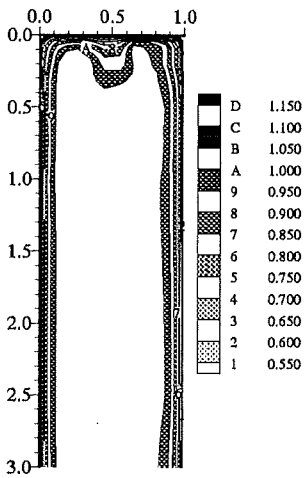
Developing Flow in a Curved Rectangular Duct

Streamwise mean velocity

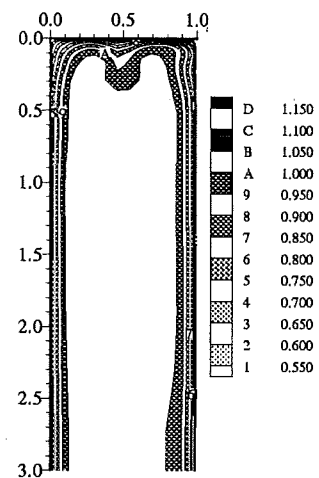
Plane $x/H = -0.5$



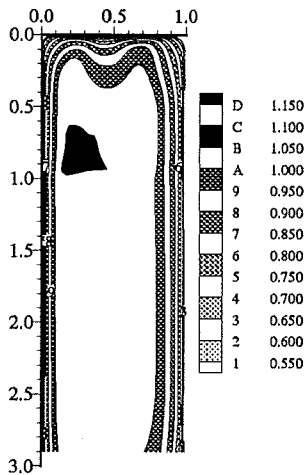
Exp



UBrussel:nKE_HiKh+wf



UBrussel:nKE_SZL+wf



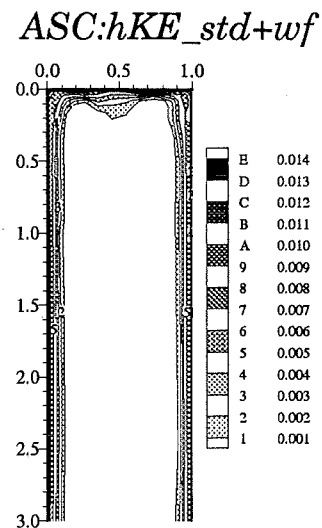
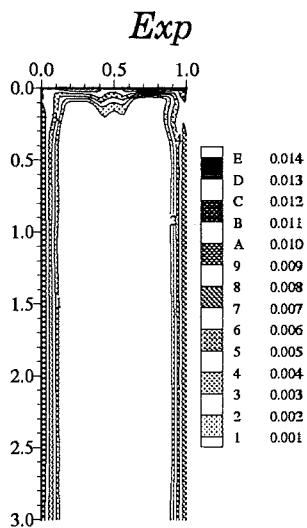
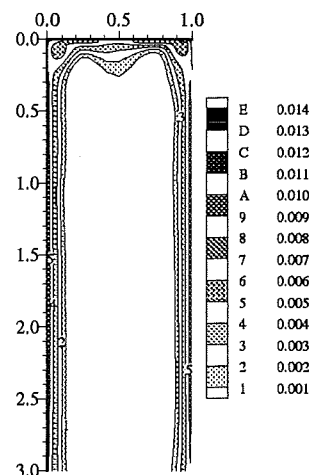
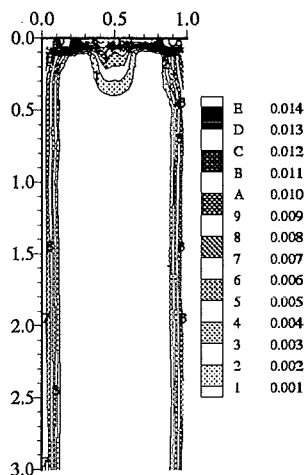
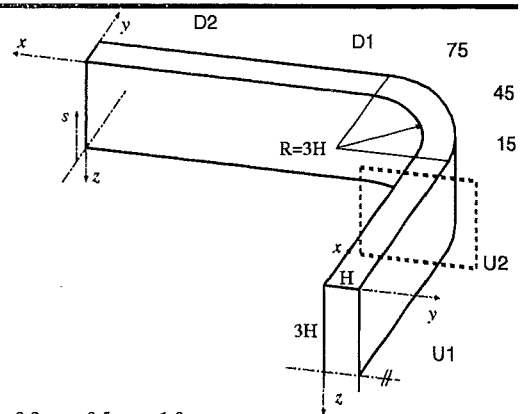
UMcGill:RSM_GiLa+wf

USoutham:ASM_CiWi

Developing Flow in a Curved Rectangular Duct

Turbulent kinetic energy k

Plane $x/H = -0.5$



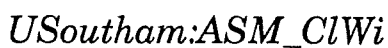
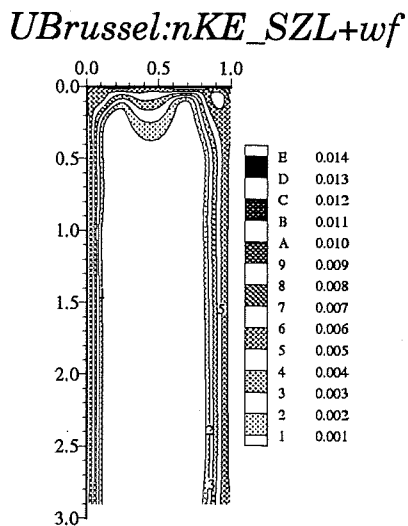
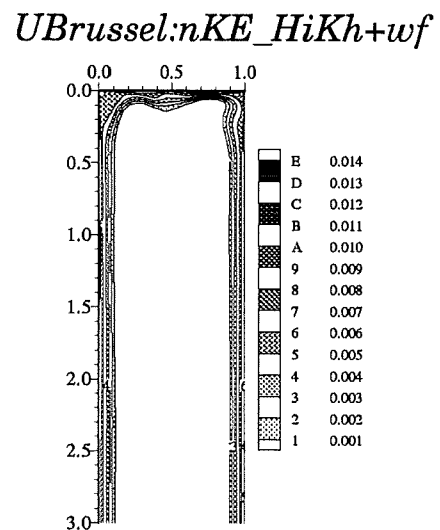
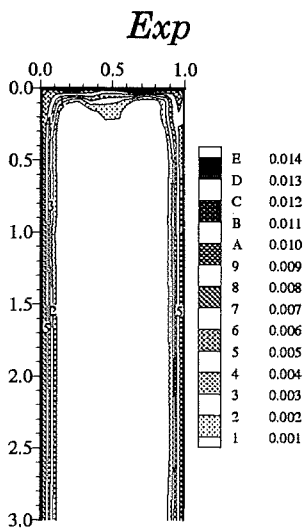
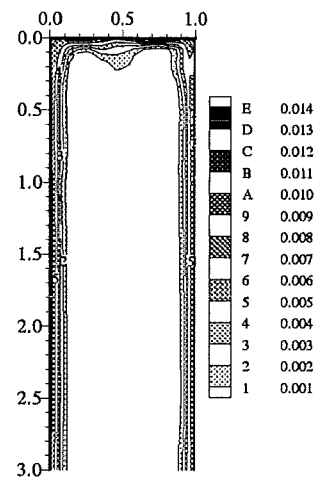
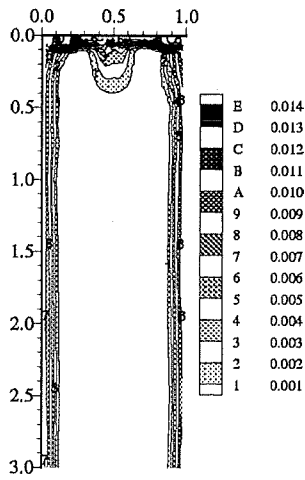
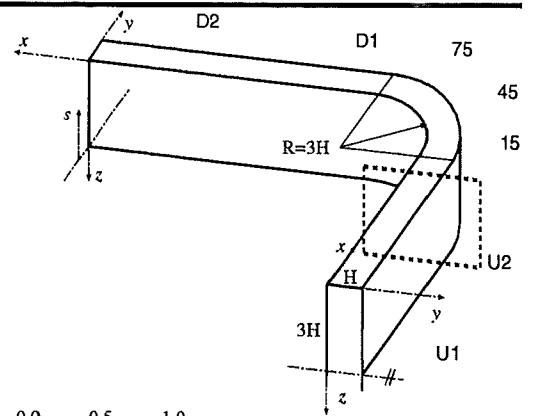
EDFLNMI:hKE_std+wf

UBrussel:hKE_std+wf

Developing Flow in a Curved Rectangular Duct

Turbulent kinetic energy k

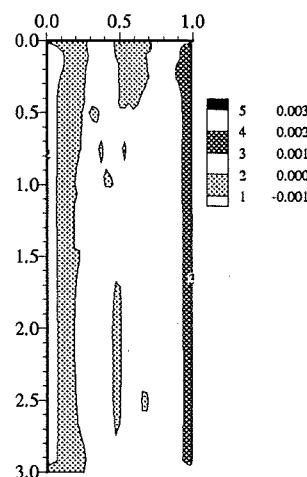
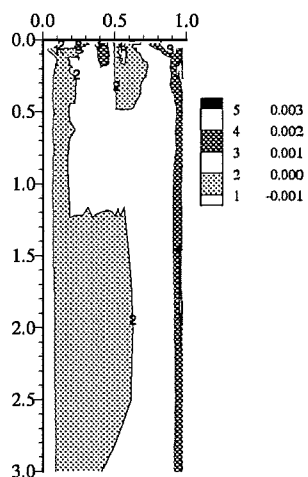
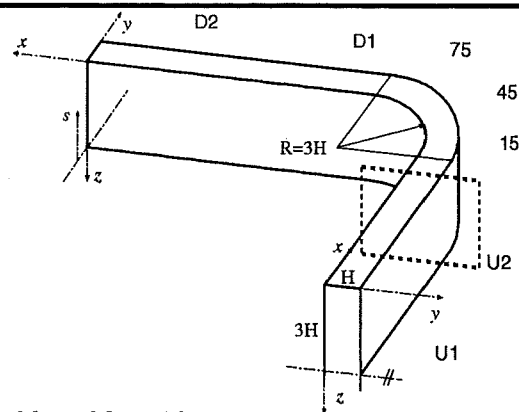
Plane $x/H = -0.5$



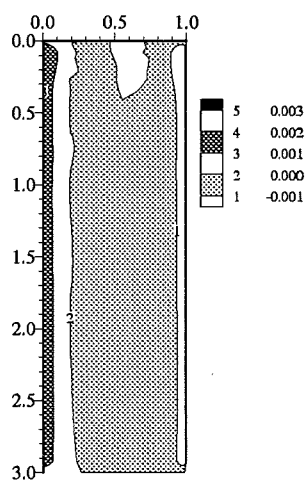
Developing Flow in a Curved Rectangular Duct

Reynolds shear stress uv

Plane $x/H = -0.5$



Exp



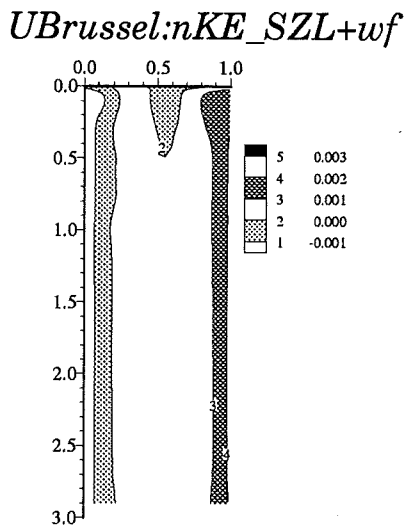
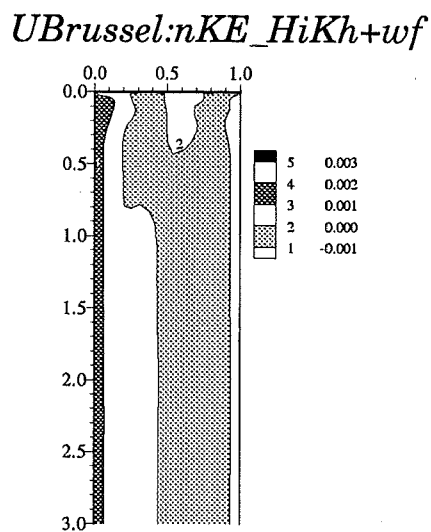
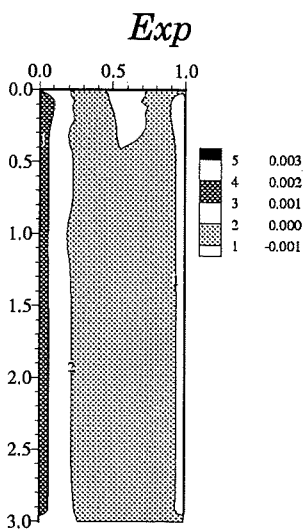
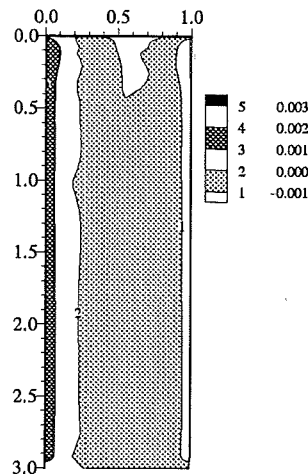
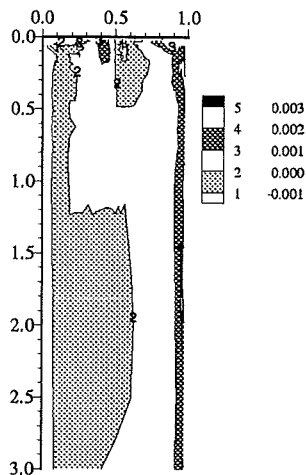
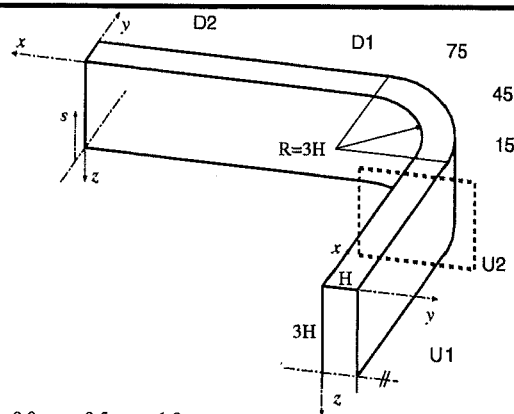
EDFLNHi:hKE_std+wf

UBrussel:hKE_std+wf

Developing Flow in a Curved Rectangular Duct

Reynolds shear stress uv

Plane $x/H = -0.5$

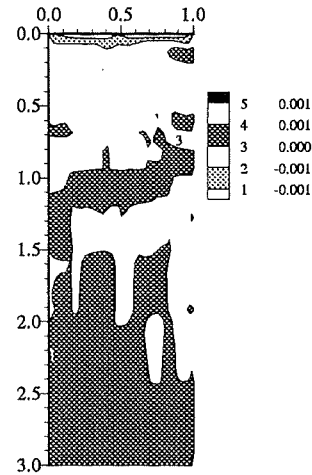
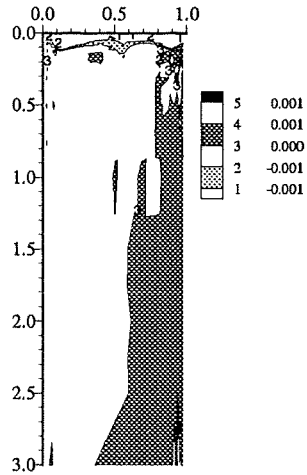
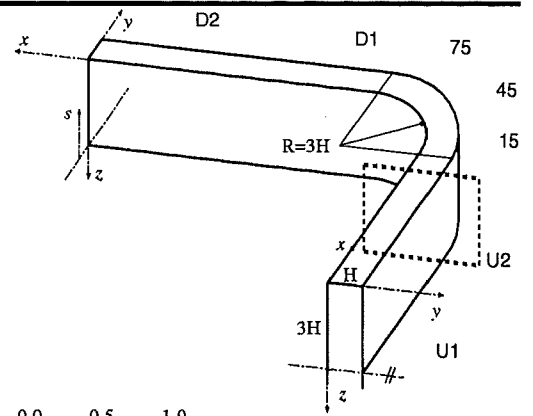


USoutham:ASM_CiWi

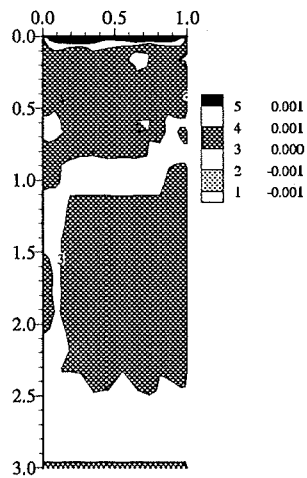
Developing Flow in a Curved Rectangular Duct

Reynolds shear stress uw

Plane $x/H = -0.5$



Exp



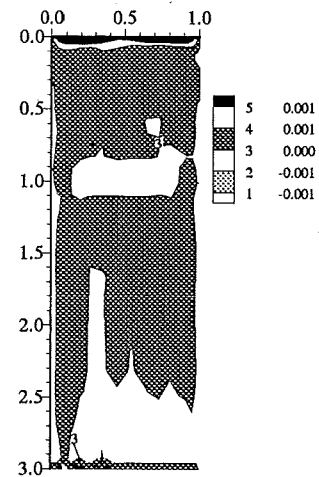
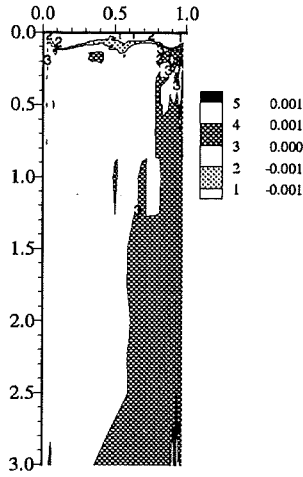
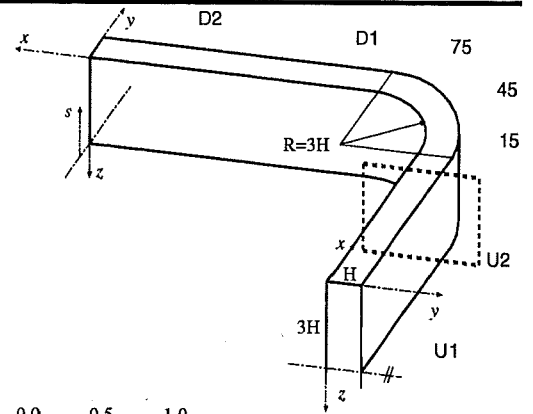
EDFLNHMi:hKE_std+wf

UBrussel:hKE_std+wf

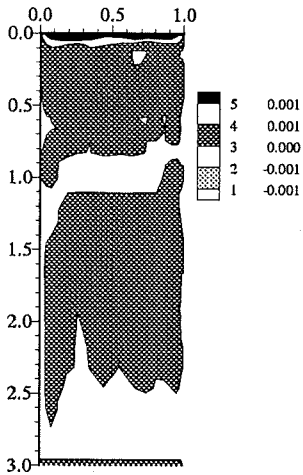
Developing Flow in a Curved Rectangular Duct

Reynolds shear stress uw

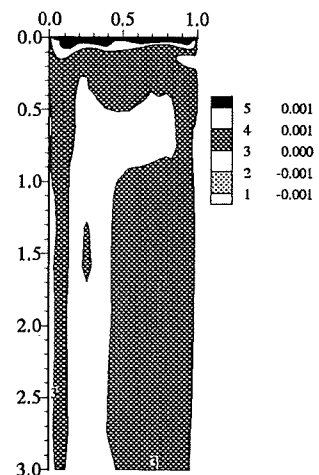
Plane $x/H=-0.5$



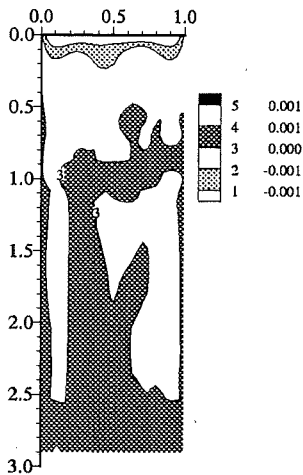
Exp



UBrussel:nKE_HiKh+wf



UBrussel:nKE_SZL+wf



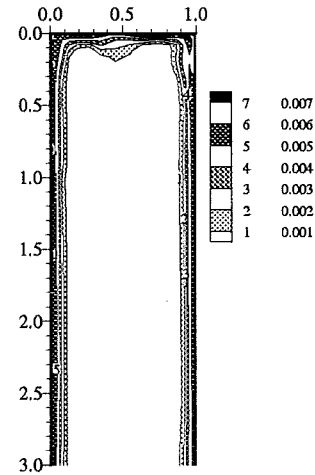
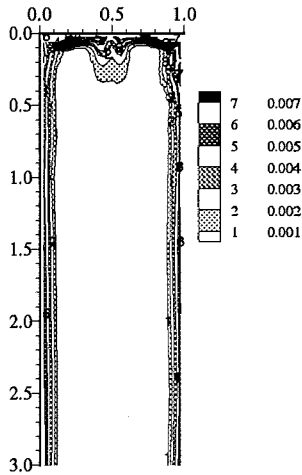
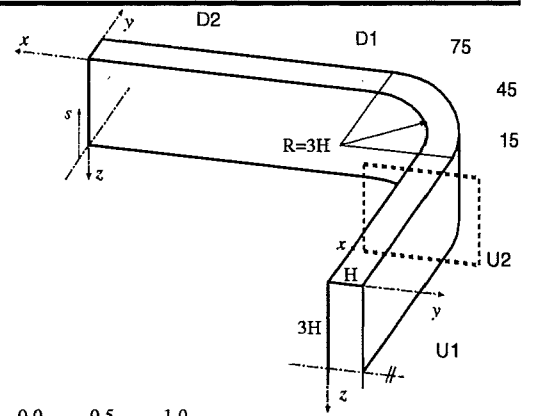
UMcGill:RSM_GiLa+wf

USoutham:ASM_CiWi

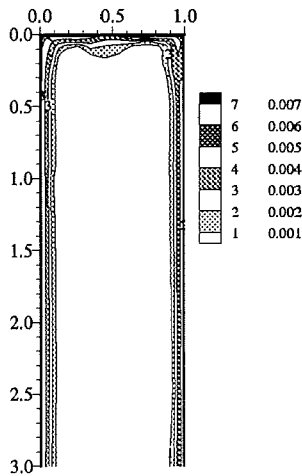
Developing Flow in a Curved Rectangular Duct

Reynolds normal stress uu

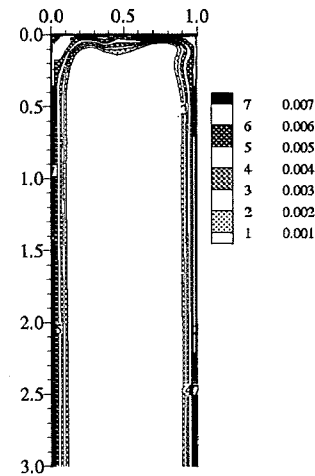
Plane $x/H = -0.5$



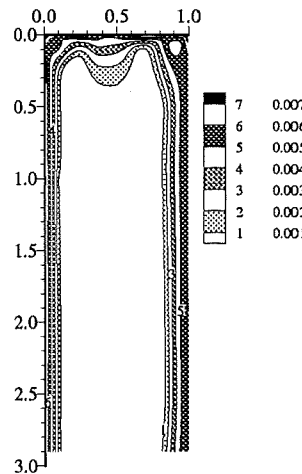
Exp



UBrussel:nKE_HiKh+wf



UBrussel:nKE_SZL+wf



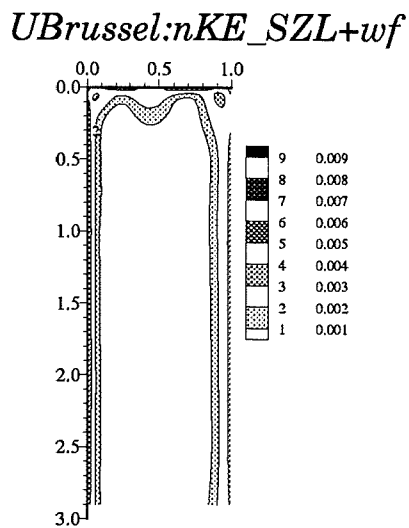
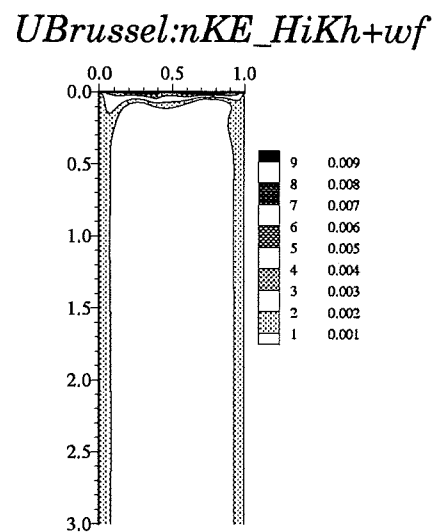
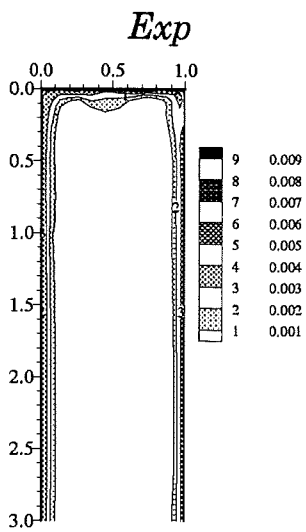
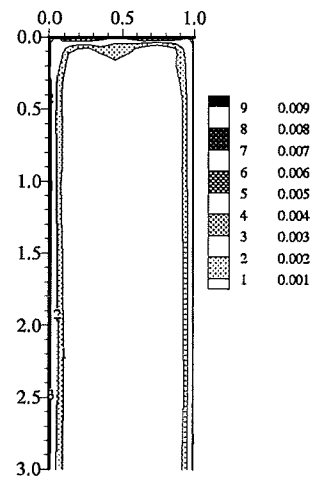
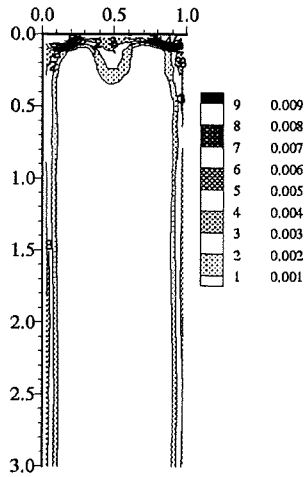
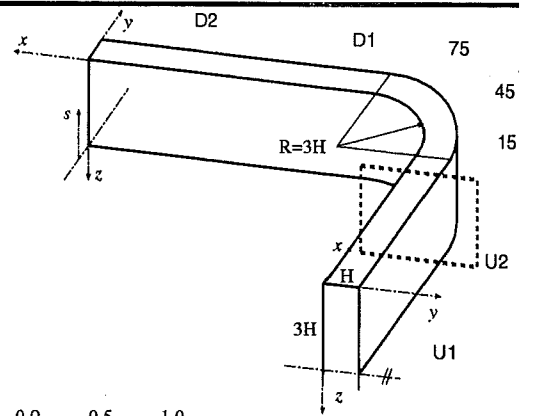
UMcGill:RSM_GiLa+wf

USoutham:ASM_ClWi

Developing Flow in a Curved Rectangular Duct

Reynolds normal stress $\overline{v'v'}$

Plane $x/H = -0.5$

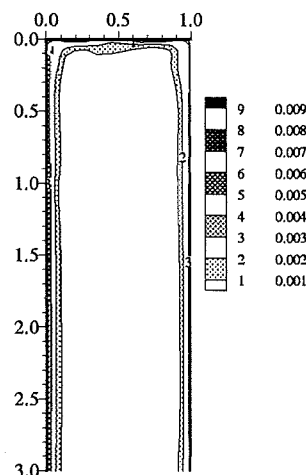
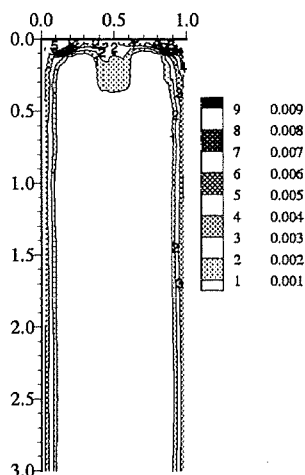
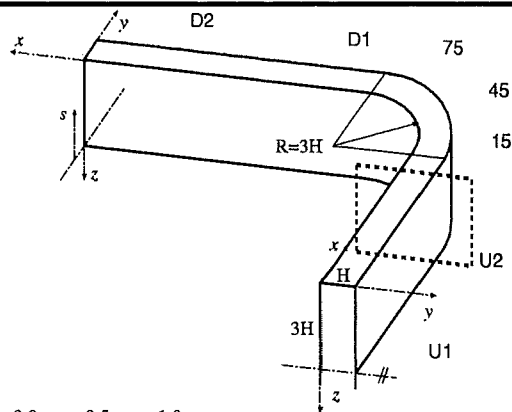


USoutham:ASM_ClWi

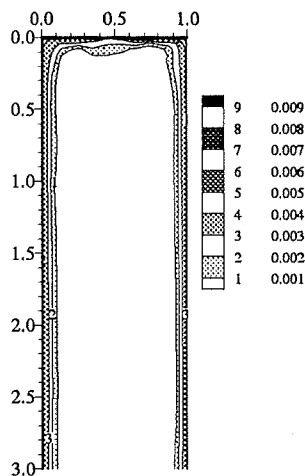
Developing Flow in a Curved Rectangular Duct

Reynolds normal stress $w w$

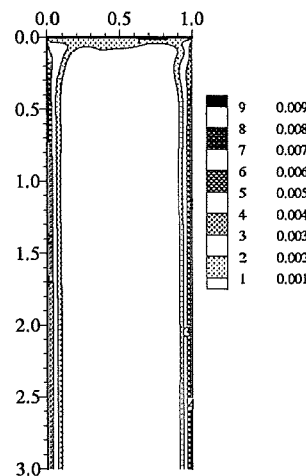
Plane $x/H = -0.5$



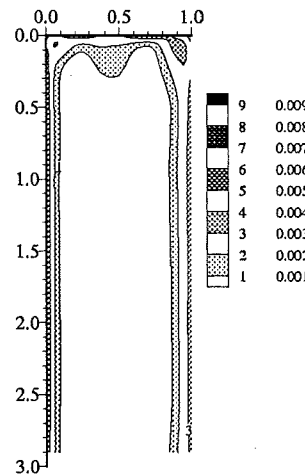
Exp



UBrussel:nKE_HiKh+wf



UBrussel:nKE_SZL+wf



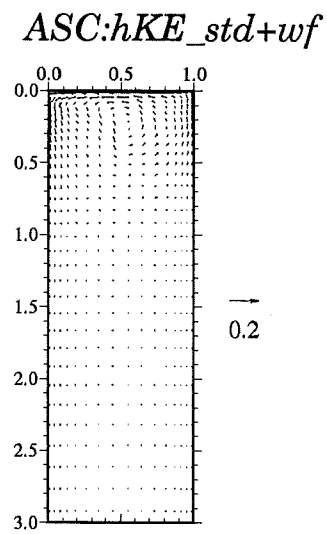
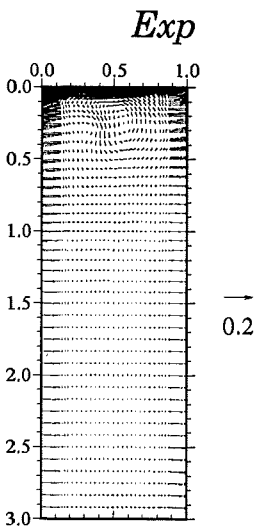
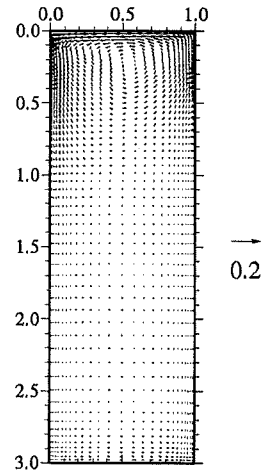
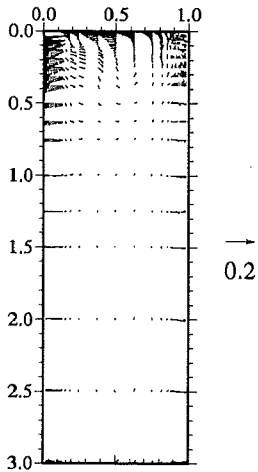
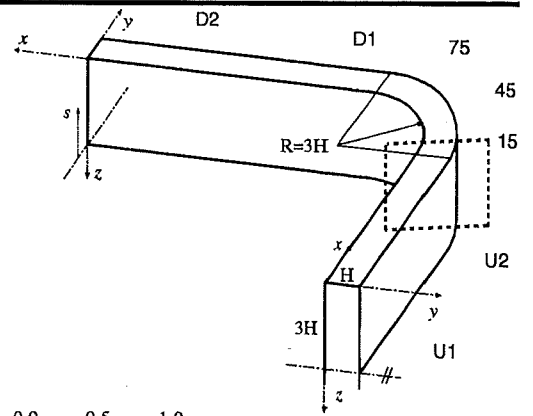
UMcGill:RSM_GiLa+wf

USoutham:ASM_ClWi

Developing Flow in a Curved Rectangular Duct

Secondary velocity vectors

Plane alpha=15 deg.



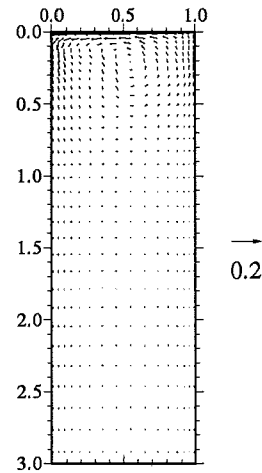
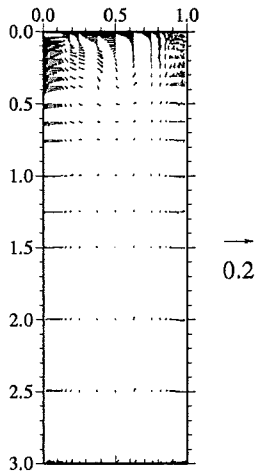
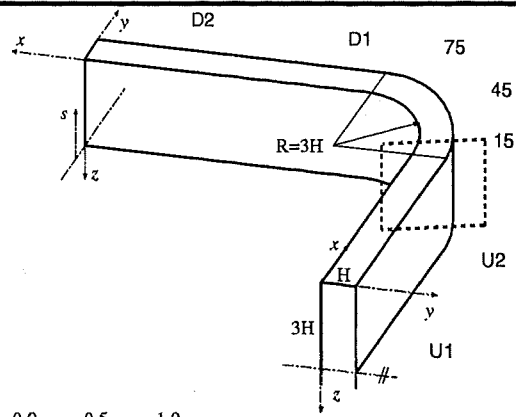
EDFLNHMi:hKE_std+wf

UBrussel:hKE_std+wf

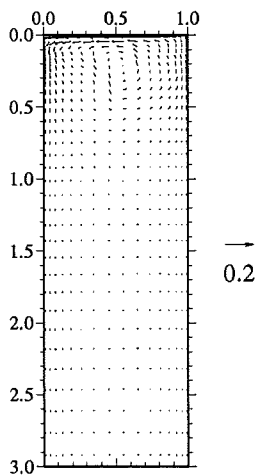
Developing Flow in a Curved Rectangular Duct

Secondary velocity vectors

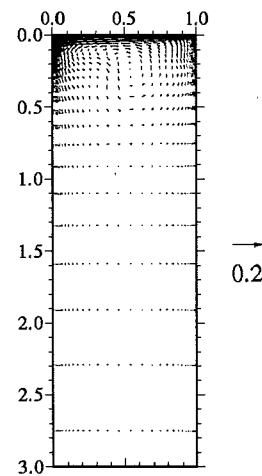
Plane alpha=15 deg.



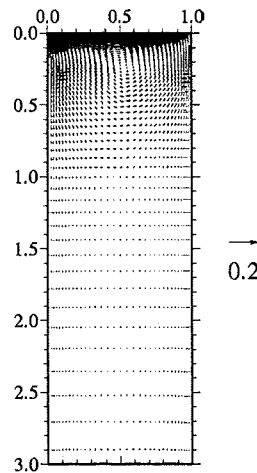
Exp



UBrussel:nKE_HiKh+wf



UBrussel:nKE_SZL+wf



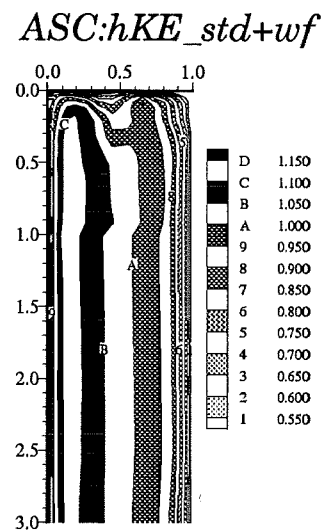
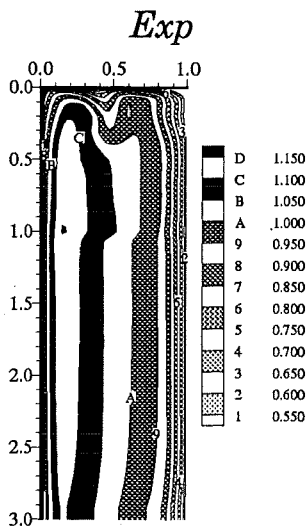
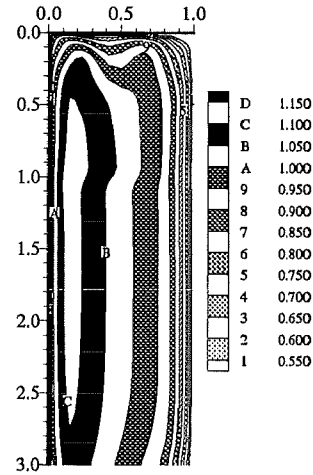
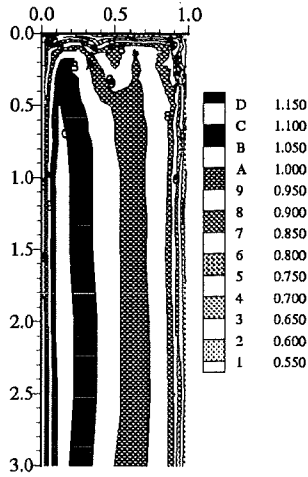
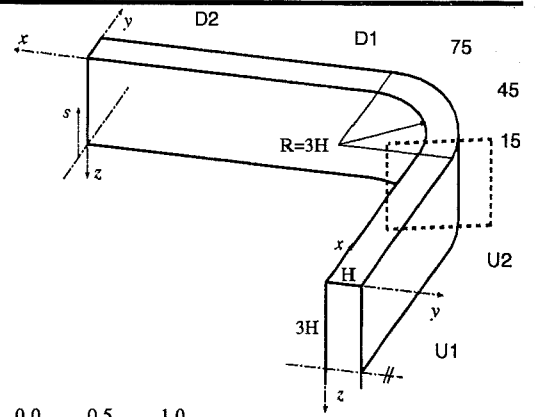
UMcGill:RSM_GiLa+wf

USoutham:ASM_ClWi

Developing Flow in a Curved Rectangular Duct

Streamwise mean velocity

Plane $\alpha=15$ deg.



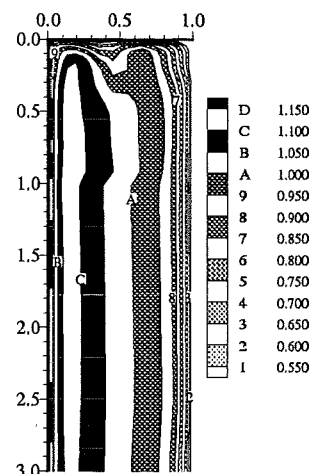
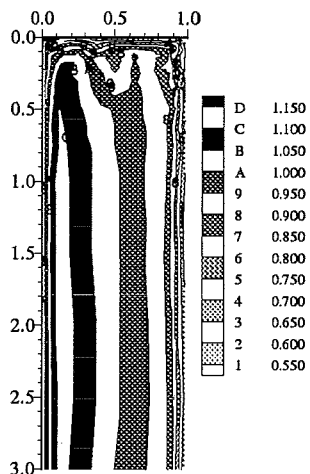
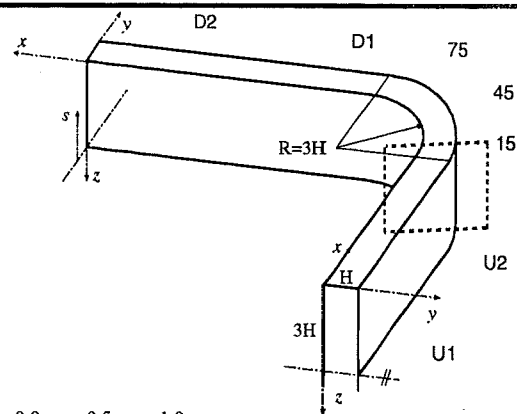
EDFLNHMi:hKE_std+wf

UBrussel:hKE_std+wf

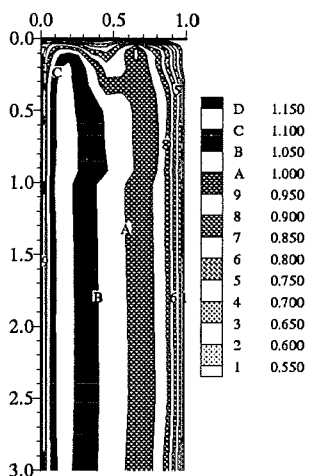
Developing Flow in a Curved Rectangular Duct

Streamwise mean velocity

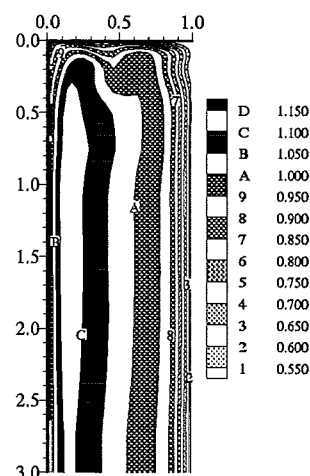
Plane alpha=15 deg.



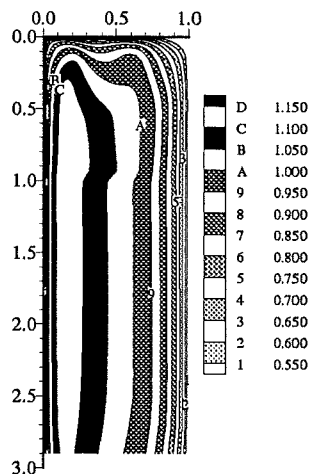
Exp



UBrussel:nKE_HiKh+wf



UBrussel:nKE_SZL+wf



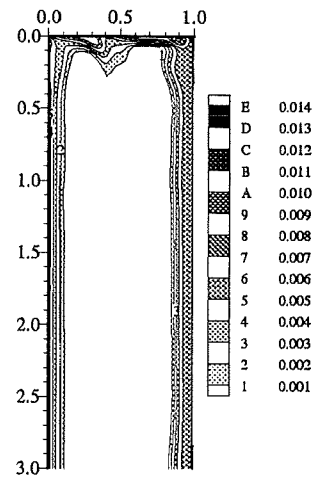
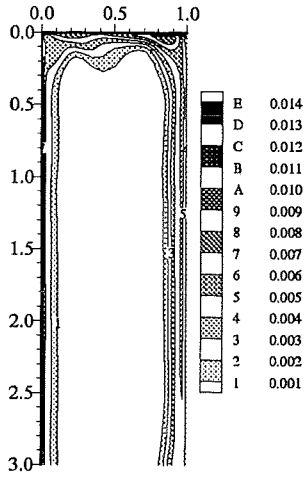
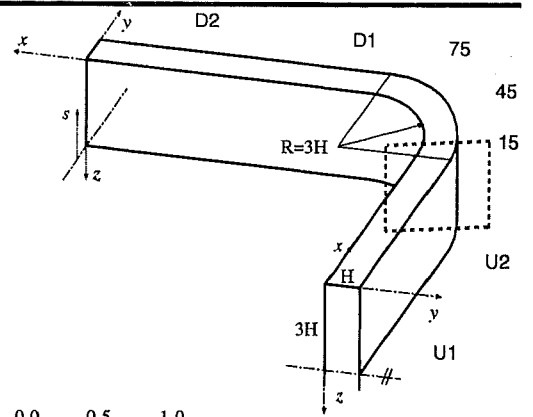
UMcGill:RSM_GiLa+wf

USoutham:ASM_ClWi

Developing Flow in a Curved Rectangular Duct

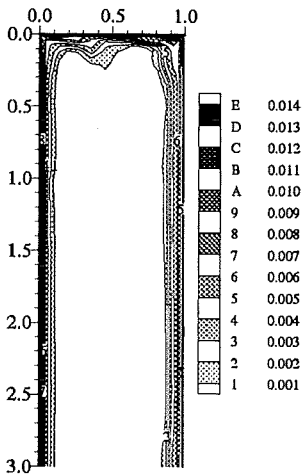
Turbulent kinetic energy k

Plane $\alpha=15$ deg.



ASC:hKE_std+wf

EDFLNHMi:hKE_std+wf

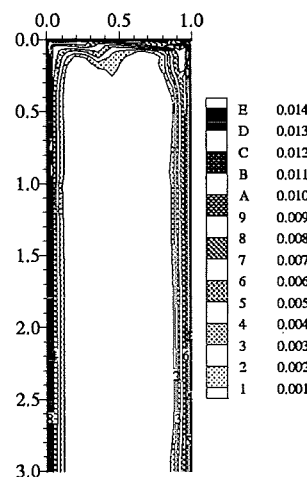
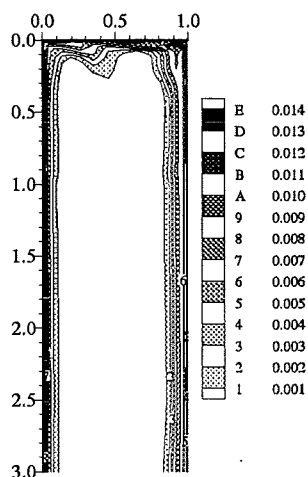
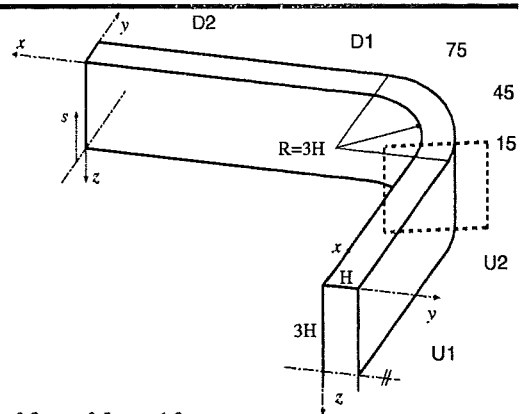


UBrussel:hKE_std+wf

Developing Flow in a Curved Rectangular Duct

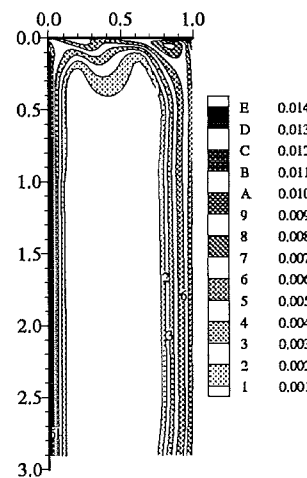
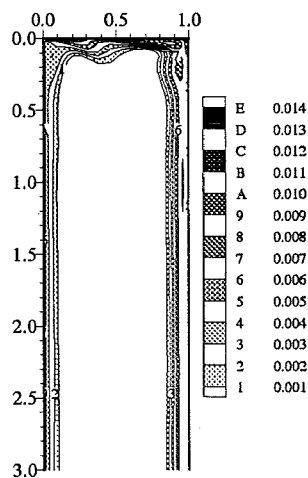
Turbulent kinetic energy k

Plane $\alpha=15$ deg.



UBussel:nKE_HiKh+wf

UBussel:nKE_SZL+wf



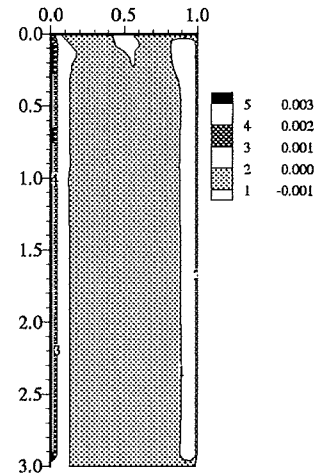
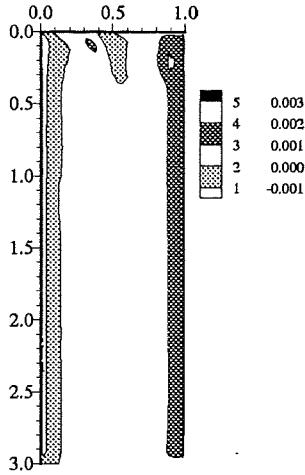
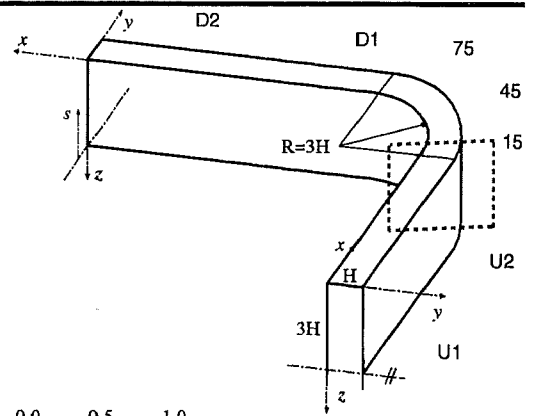
UMcGill:RSM_GiLa+wf

USoutham:ASM_ClWi

Developing Flow in a Curved Rectangular Duct

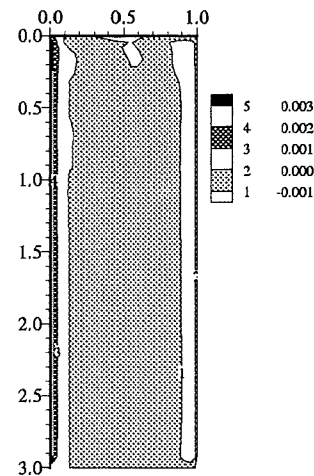
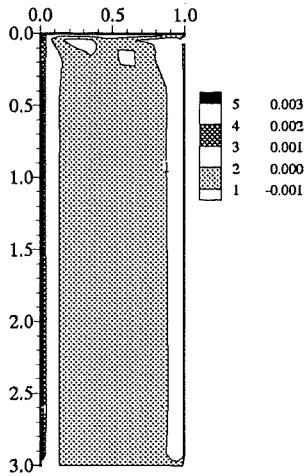
Reynolds shear stress uv

Plane $\alpha=15$ deg.



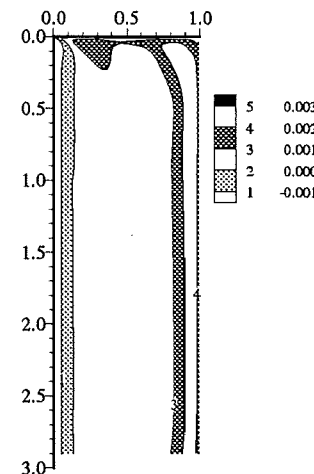
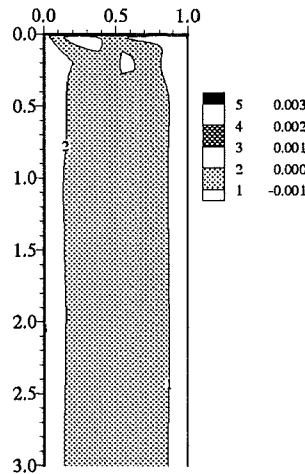
EDNLNHi:hKE_std+wf

UBrussel:hKE_std+wf



UBrussel:nKE_HiKh+wf

UBrussel:nKE_SZL+wf



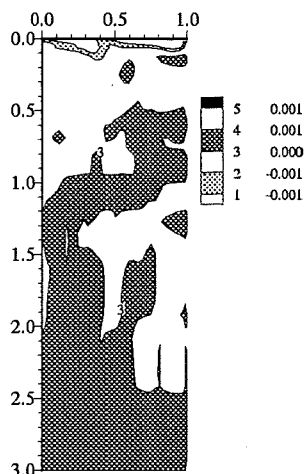
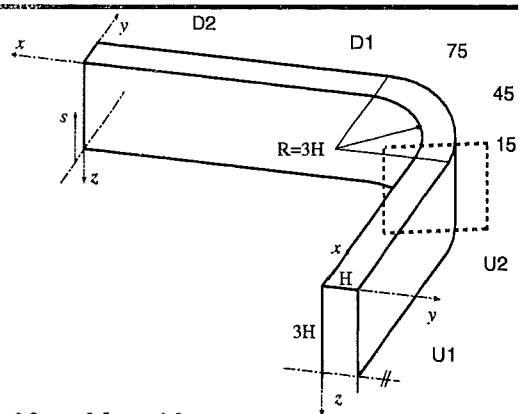
UMcGill:RSM_GiLa+wf

USoutham:ASM_CiWi

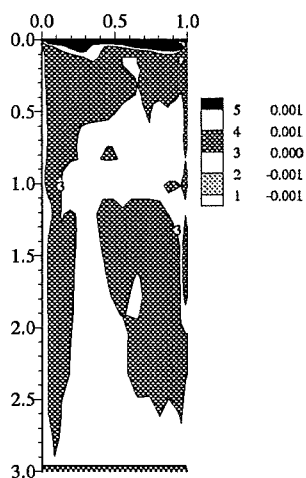
Developing Flow in a Curved Rectangular Duct

Reynolds shear stress uw

Plane $\alpha=15$ deg.



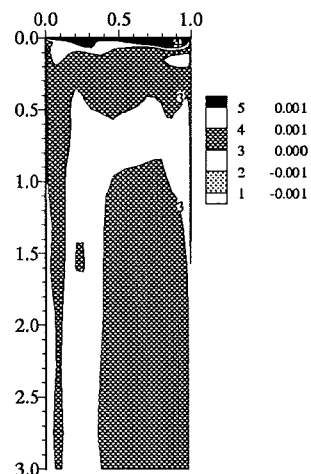
EDFLNMi:hKE_std+wf



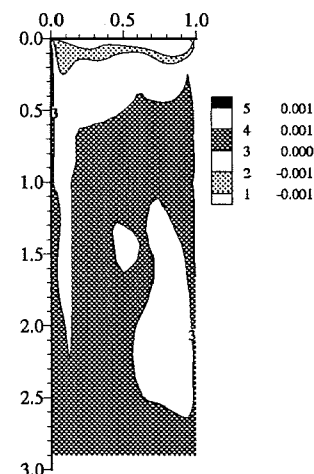
UBrussel:hKE_std+wf



UBrussel:nKE_HiKh+wf



UBrussel:nKE_SZL+wf



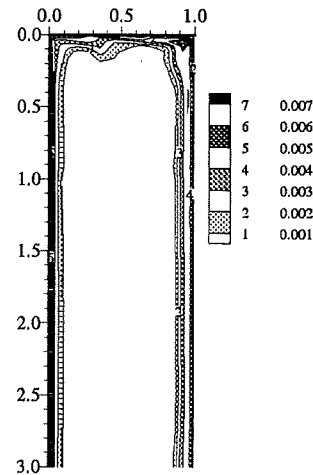
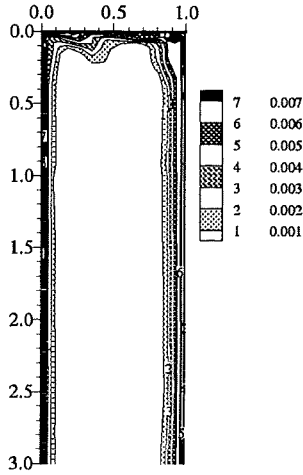
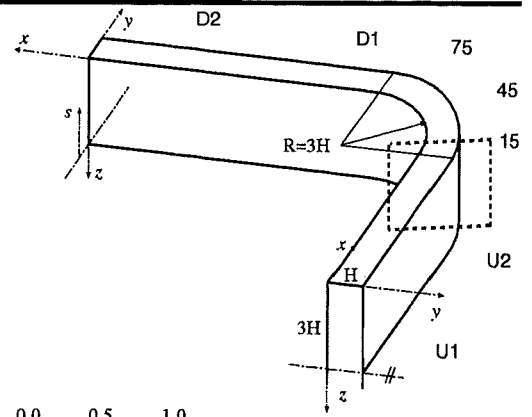
UMcGill:RSM_GiLa+wf

USoutham:ASM_ClWi

Developing Flow in a Curved Rectangular Duct

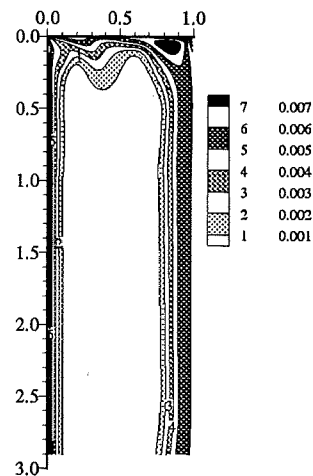
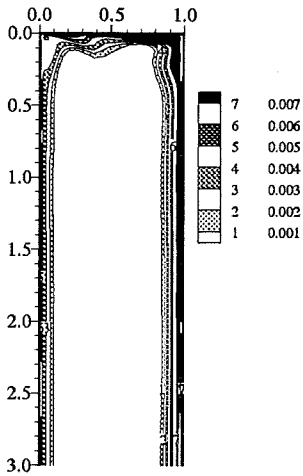
Reynolds normal stress uu

Plane $\alpha=15$ deg.



UBrunsel:nKE_HiKh+wf

UBrunsel:nKE_SZL+wf



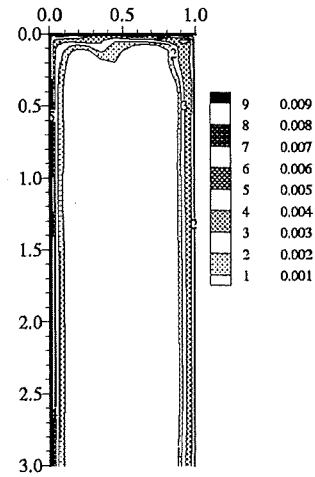
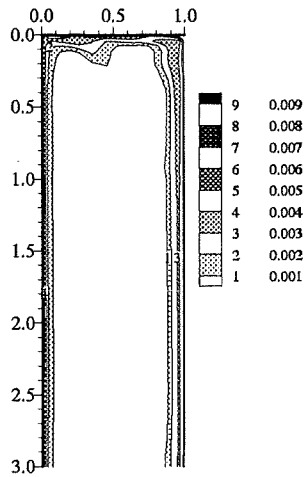
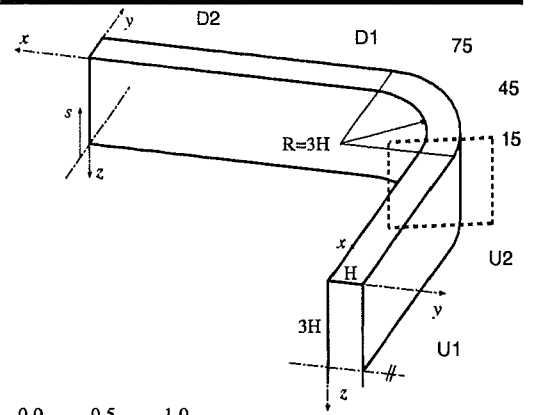
UMcGill:RSM_GiLa+wf

USoutham:ASM_ClWi

Developing Flow in a Curved Rectangular Duct

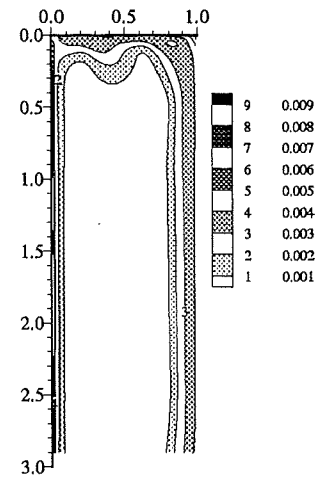
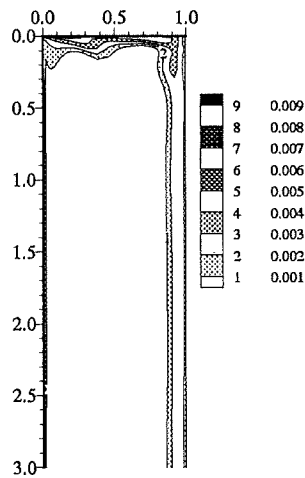
Reynolds normal stress $\overline{v'v'}$

Plane $\alpha=15$ deg.



UBussel:nKE_HiKh+wf

UBussel:nKE_SZL+wf



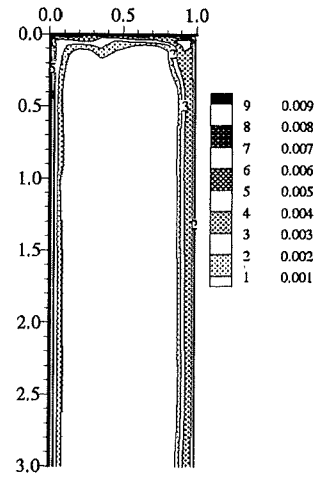
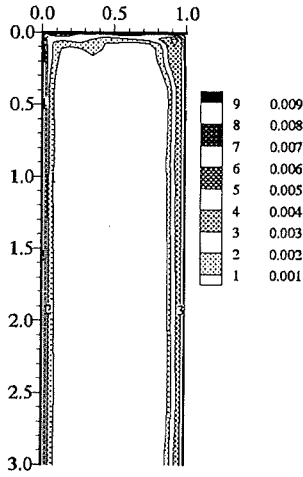
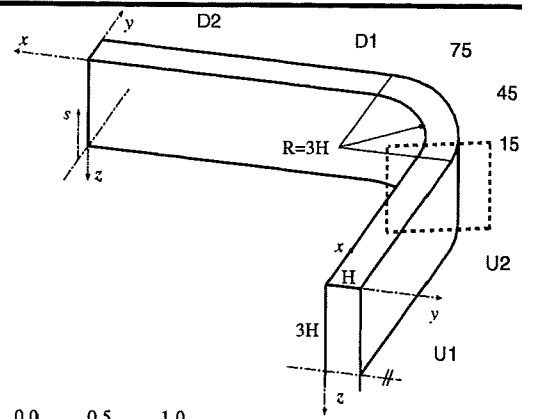
UMcGill:RSM_GiLa+wf

USoutham:ASM_ClWi

Developing Flow in a Curved Rectangular Duct

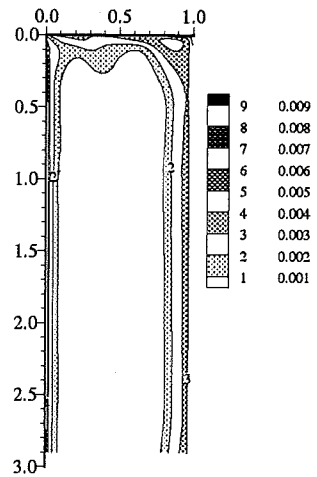
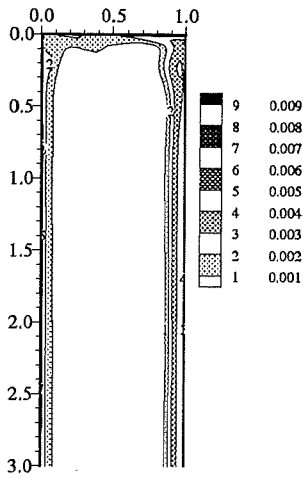
Reynolds normal stress $\overline{w'w'}$

Plane $\alpha=15$ deg.



UBussel:nKE_HiKh+wf

UBussel:nKE_SZL+wf



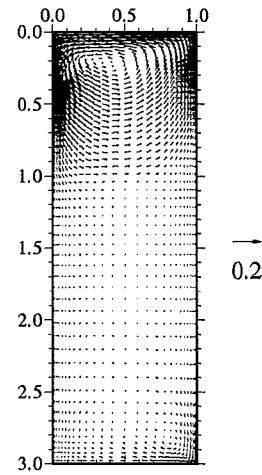
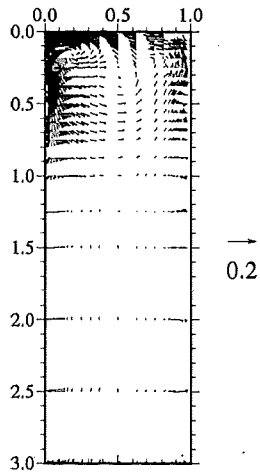
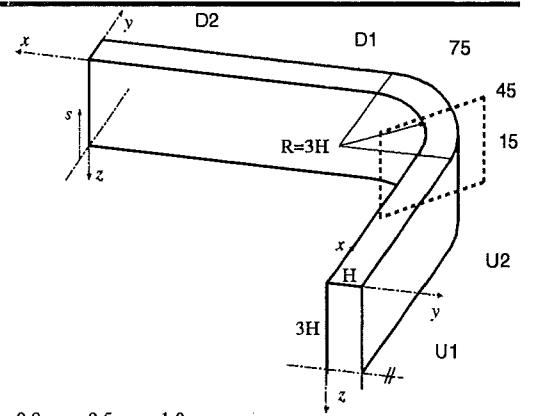
UMcGill:RSM_GiLa+wf

USoutham:ASM_ClWi

Developing Flow in a Curved Rectangular Duct

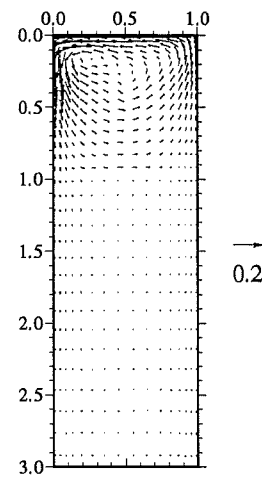
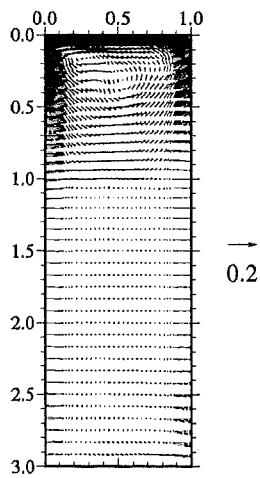
Secondary velocity vectors

Plane $\alpha=45$ deg.



Exp

ASC:hKE_std+wf



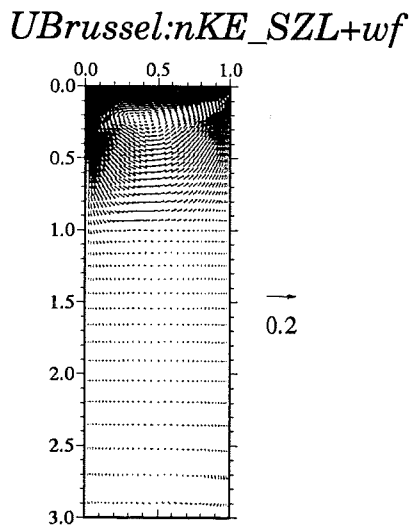
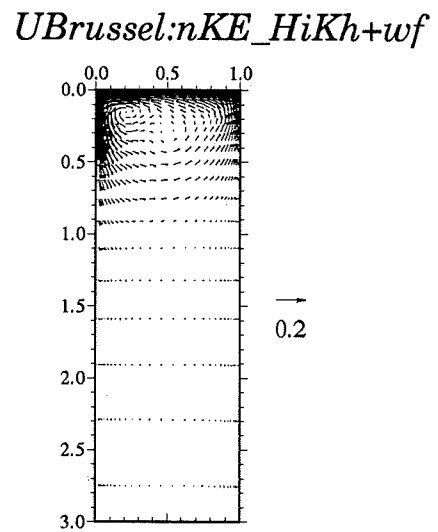
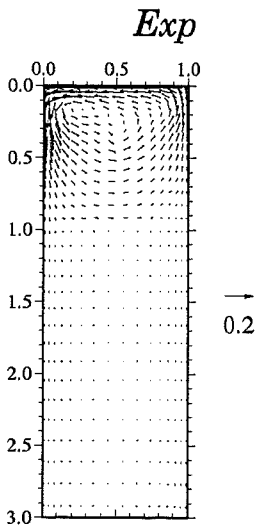
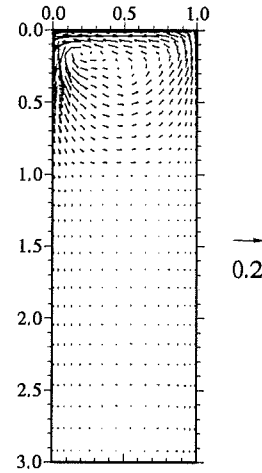
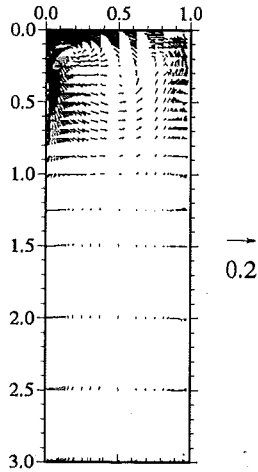
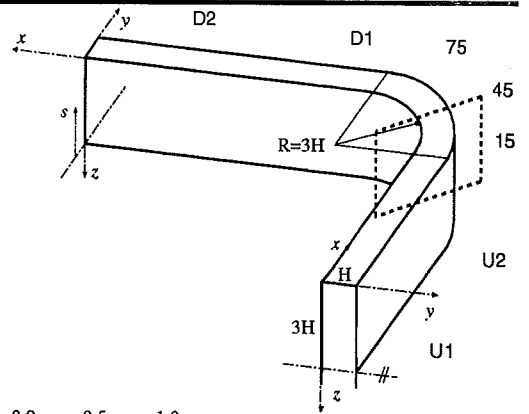
EDFLNHMi:hKE_std+wf

UBrussel:hKE_std+wf

Developing Flow in a Curved Rectangular Duct

Secondary velocity vectors

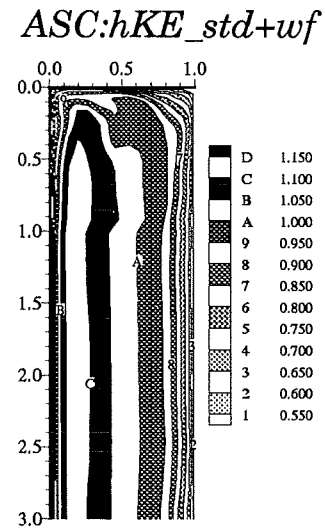
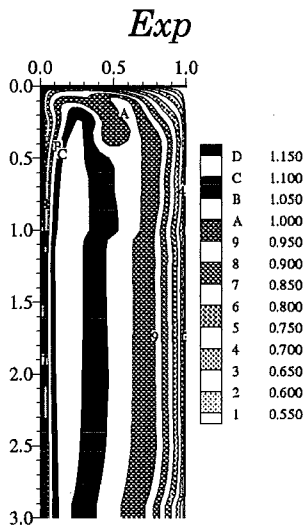
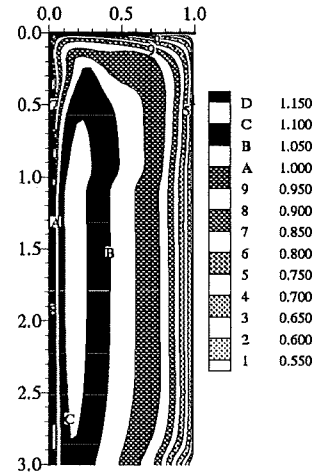
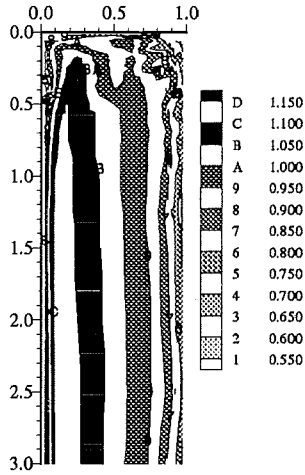
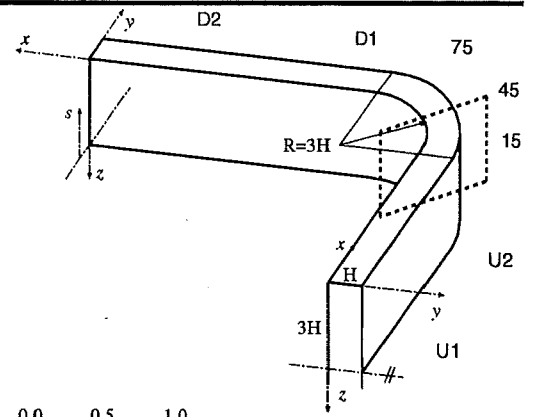
Plane alpha=45 deg.



Developing Flow in a Curved Rectangular Duct

Streamwise mean velocity

Plane alpha=45 deg.



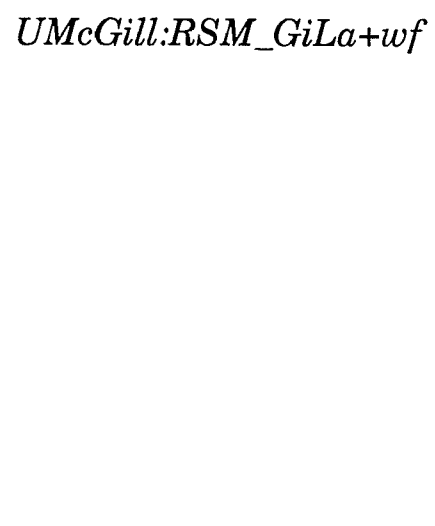
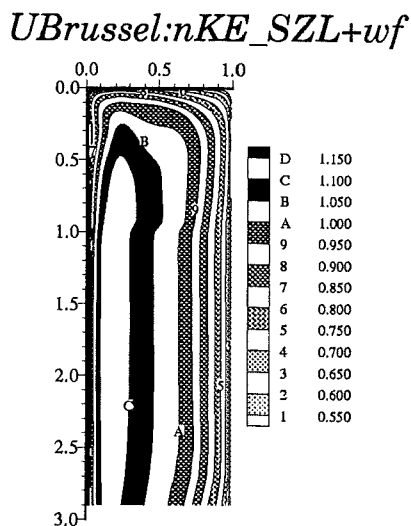
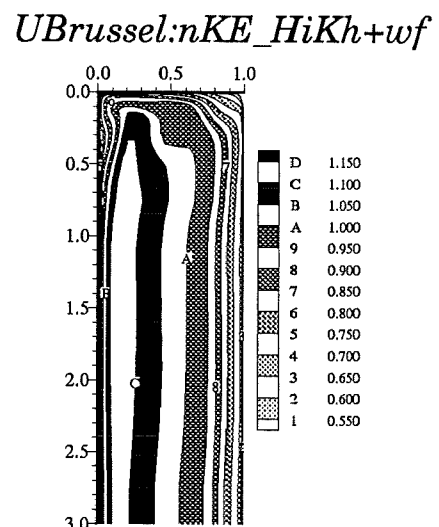
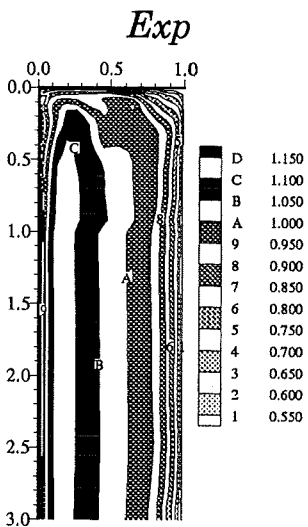
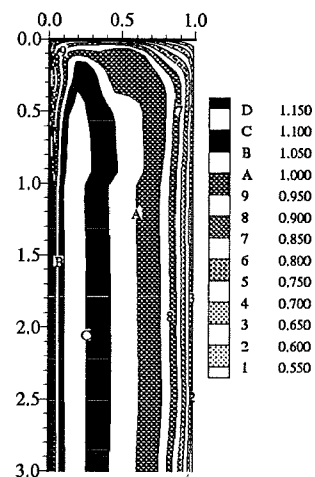
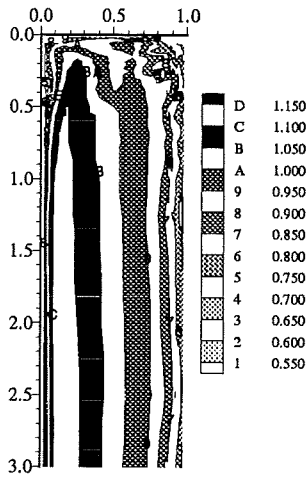
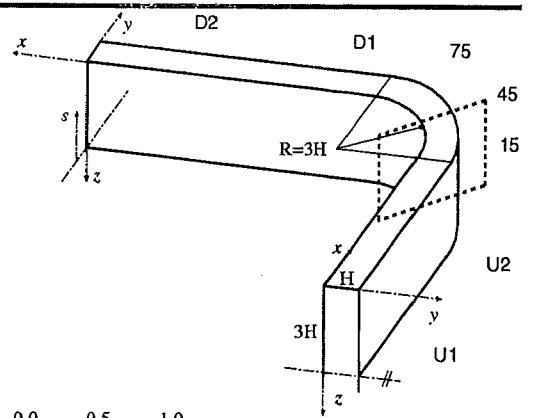
EDFLNHMi:hKE_std+wf

UBrussel:hKE_std+wf

Developing Flow in a Curved Rectangular Duct

Streamwise mean velocity

Plane alpha=45 deg.

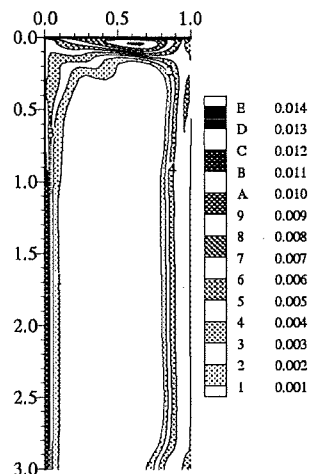
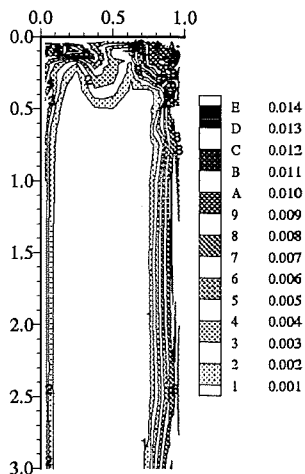
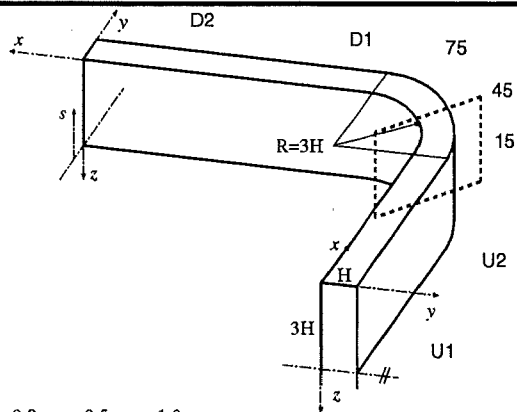


USoutham:ASM_ClWi

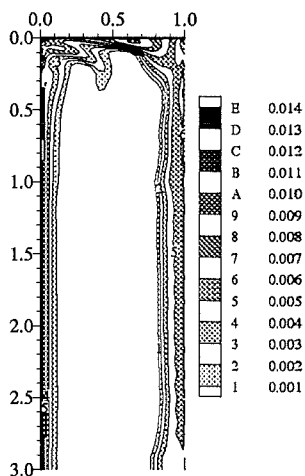
Developing Flow in a Curved Rectangular Duct

Turbulent kinetic energy k

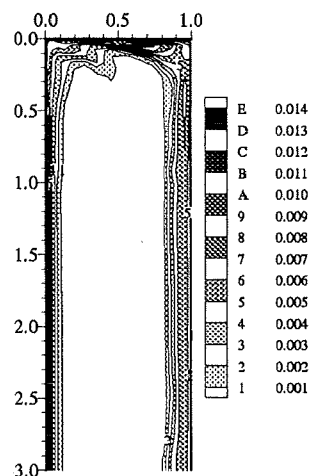
Plane $\alpha=45$ deg.



Exp



ASC:hKE_std+wf



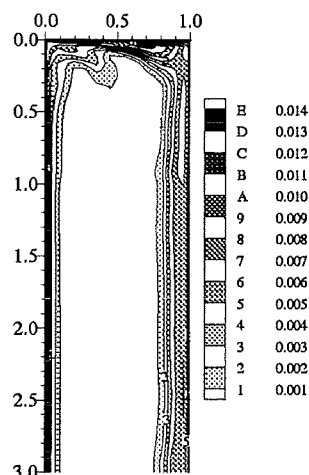
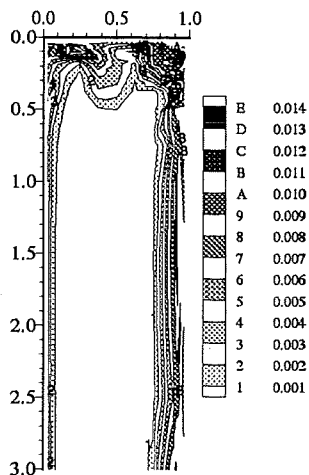
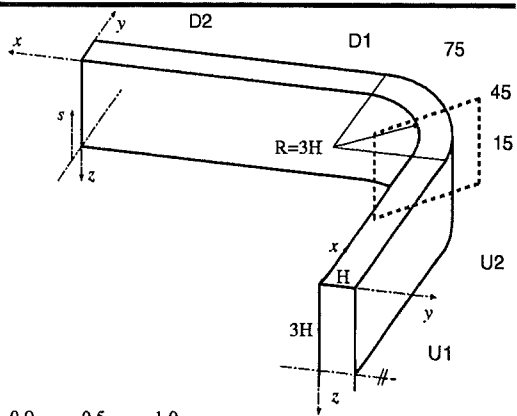
EDFLNHMi:hKE_std+wf

UBrussel:hKE_std+wf

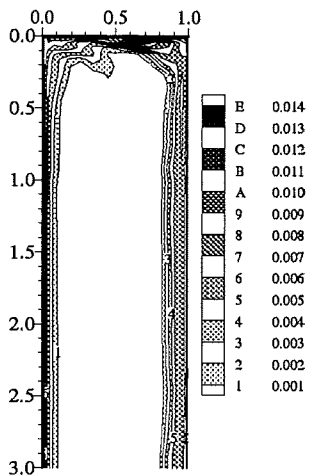
Developing Flow in a Curved Rectangular Duct

Turbulent kinetic energy k

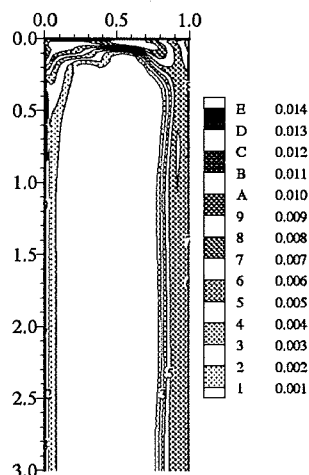
Plane $\alpha=45$ deg.



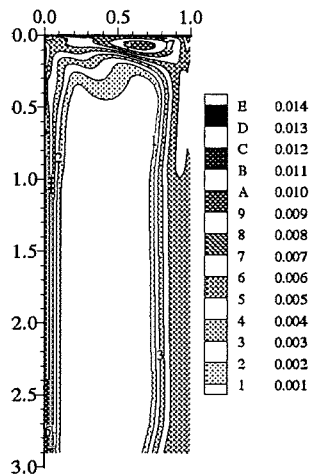
Exp



UBrussel:nKE_HiKh+wf



UBrussel:nKE_SZL+wf



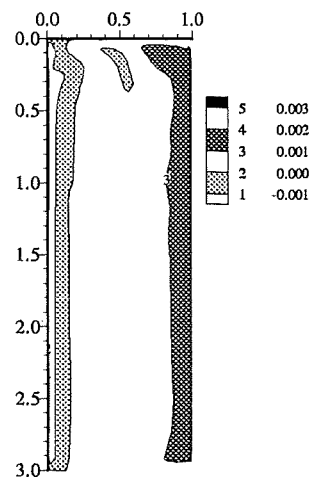
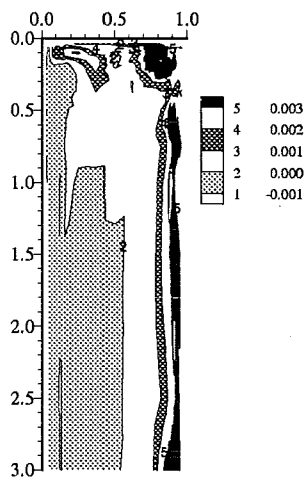
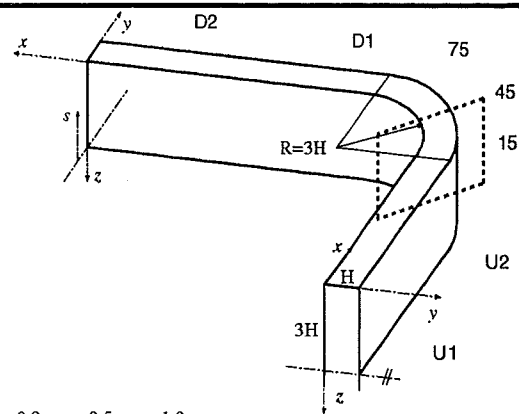
UMcGill:RSM_GiLa+wf

USoutham:ASM_ClWi

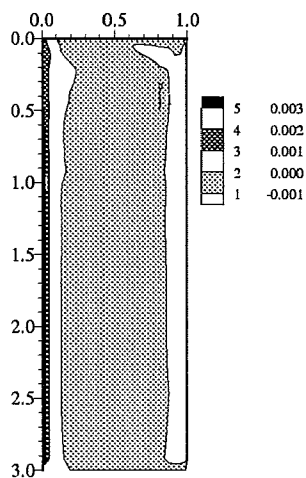
Developing Flow in a Curved Rectangular Duct

Reynolds shear stress uv

Plane $\alpha=45$ deg.



Exp



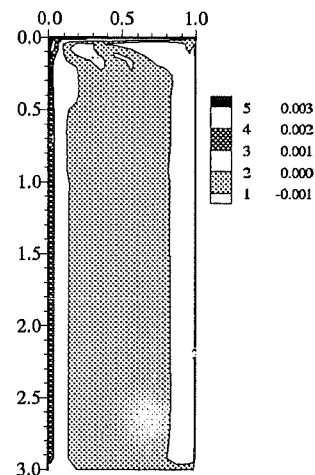
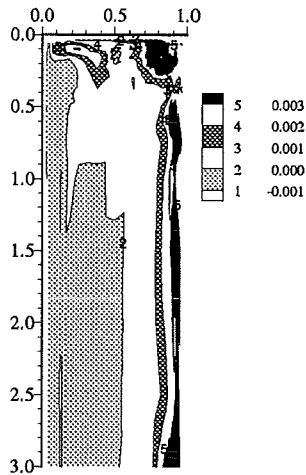
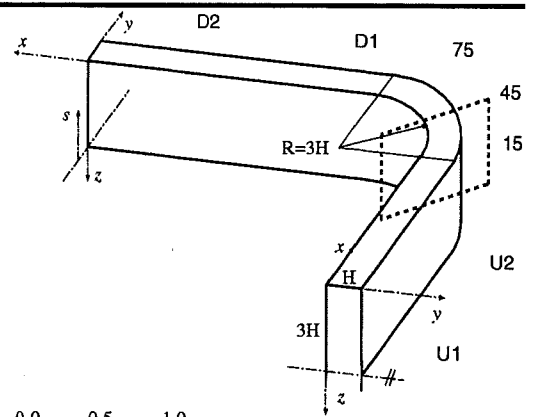
EDfLNHMi:hKE_std+wf

UBrussel:hKE_std+wf

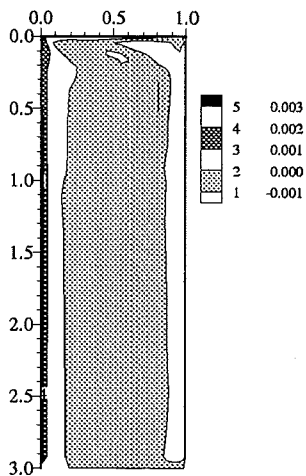
Developing Flow in a Curved Rectangular Duct

Reynolds shear stress uv

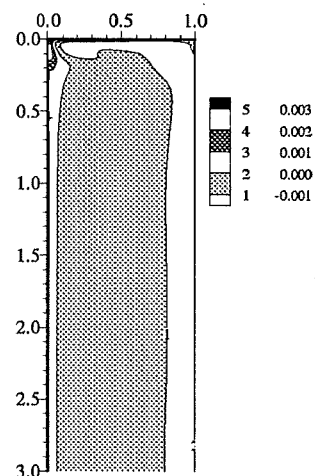
Plane $\alpha=45$ deg.



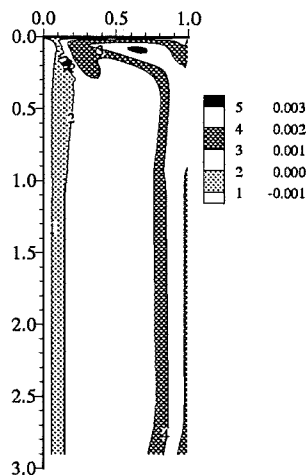
Exp



UBrusseL:nKE_HiKh+wf



UBrusseL:nKE_SZL+wf



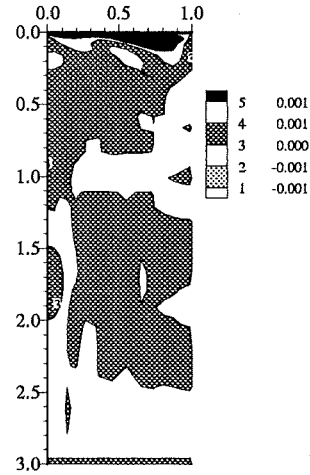
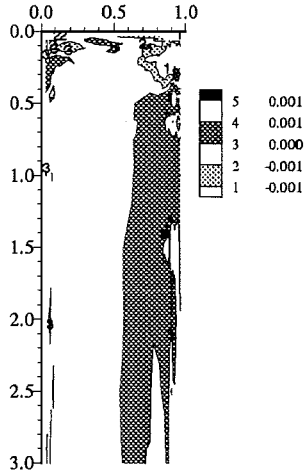
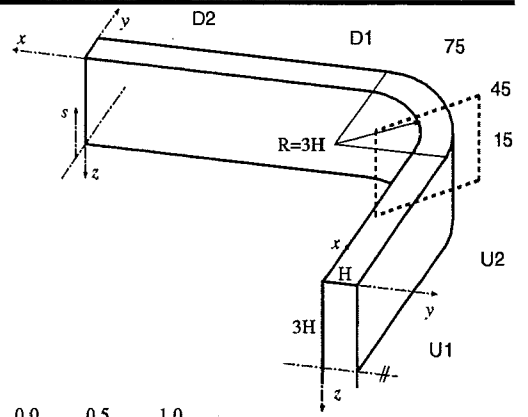
UMcGill:RSM_GiLa+wf

USoutham:ASM_ClWi

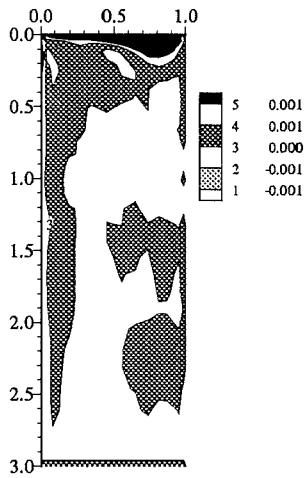
Developing Flow in a Curved Rectangular Duct

Reynolds shear stress uw

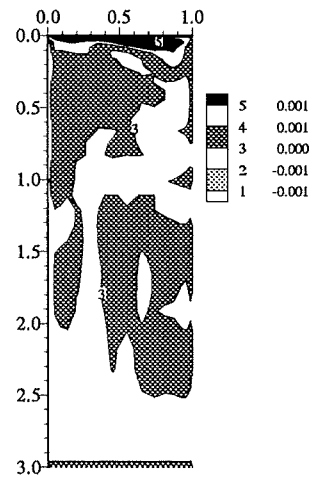
Plane $\alpha=45$ deg.



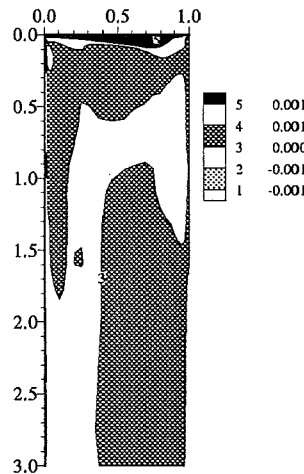
Exp



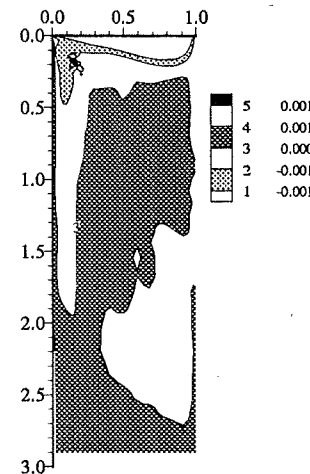
UBussel:hKE_std+wf



UBussel:nKE_HiKh+wf



UBussel:nKE_SZL+wf



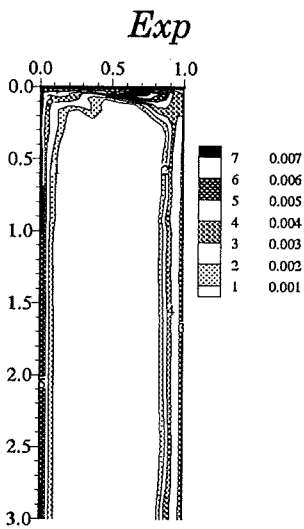
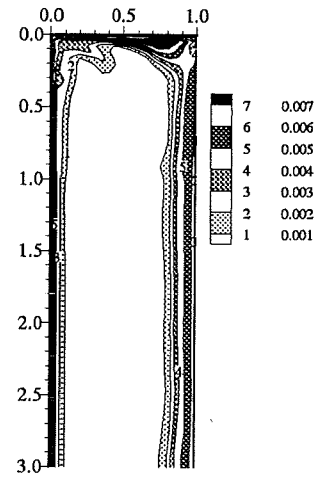
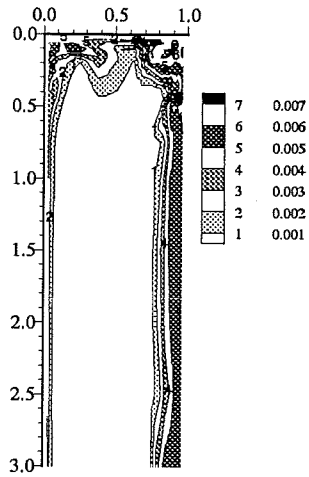
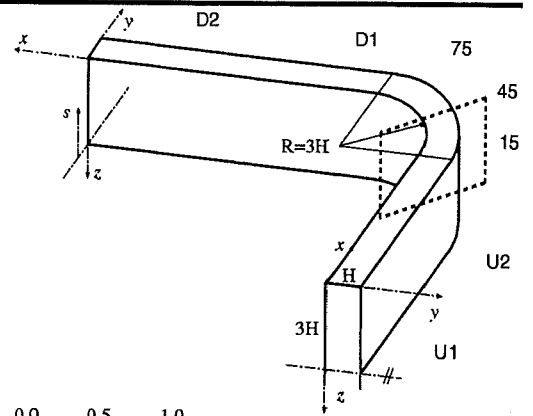
UMcGill:RSM_GiLa+wf

USoutham:ASM_ClWi

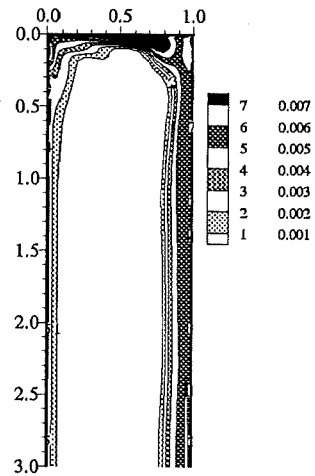
Developing Flow in a Curved Rectangular Duct

Reynolds normal stress uu

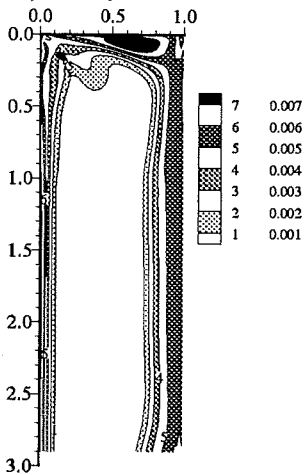
Plane $\alpha=45$ deg.



UBrussel:nKE_HiKh+wf



UBrussel:nKE_SZL+wf



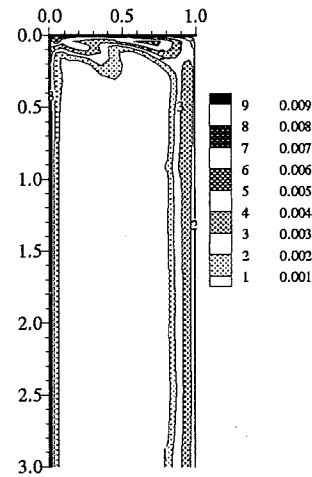
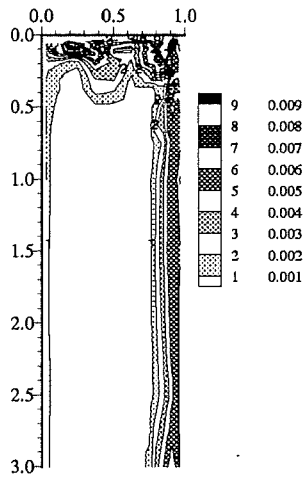
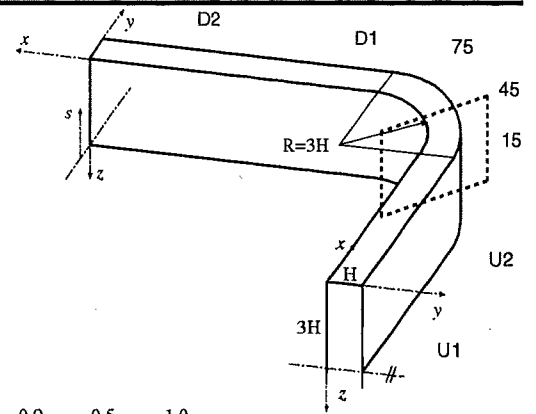
UMcGill:RSM_GiLa+wf

USoutham:ASM_ClWi

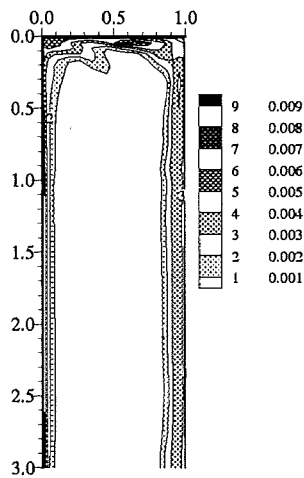
Developing Flow in a Curved Rectangular Duct

Reynolds normal stress $\overline{v'v'}$

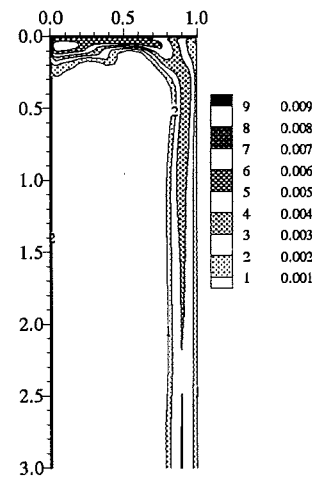
Plane $\alpha=45$ deg.



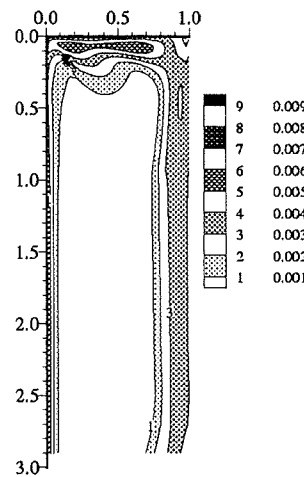
Exp



UBrussel:nKE_HiKh+wf



UBrussel:nKE_SZL+wf



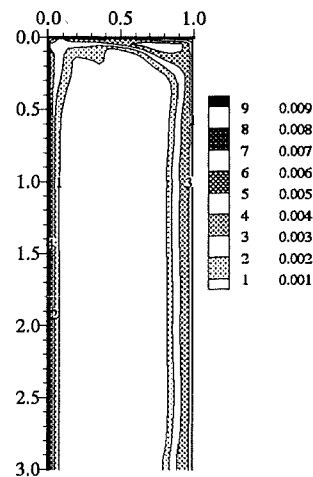
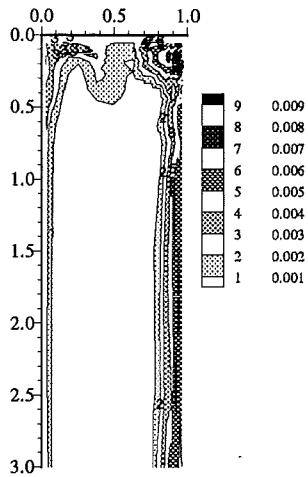
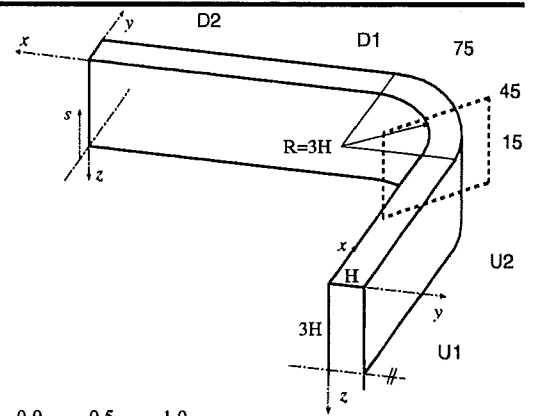
UMcGill:RSM_GiLa+wf

USoutham:ASM_CiWi

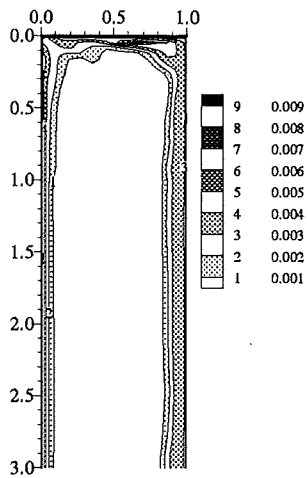
Developing Flow in a Curved Rectangular Duct

Reynolds normal stress $\overline{w'w'}$

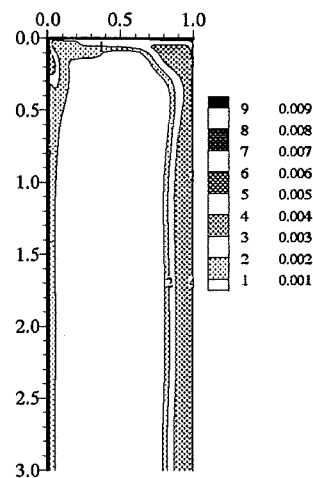
Plane $\alpha=45$ deg.



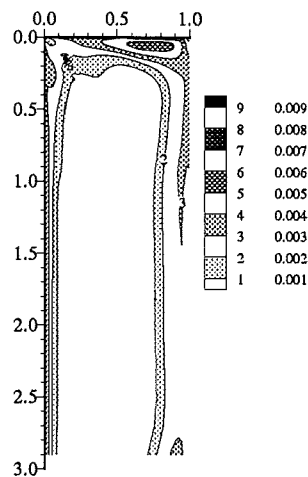
Exp



UBrussel:nKE_HiKh+wf



UBrussel:nKE_SZL+wf



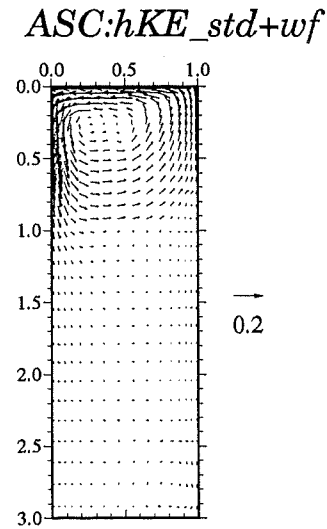
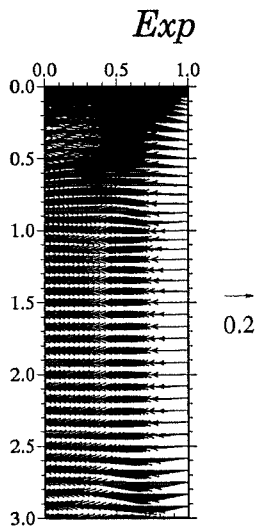
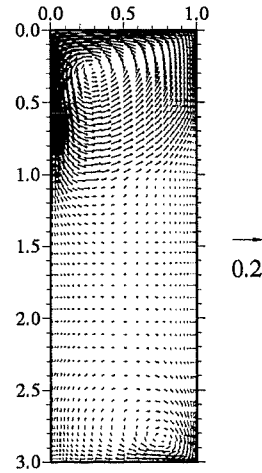
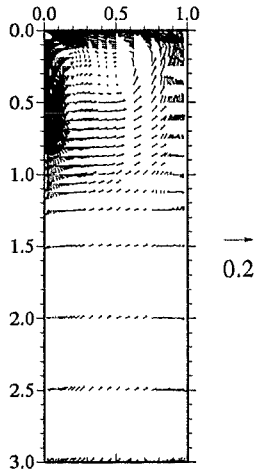
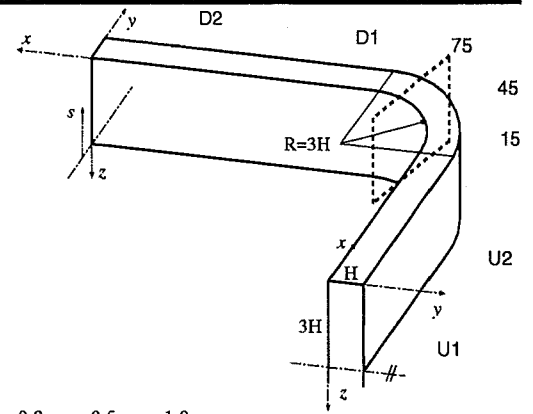
UMcGill:RSM_GiLa+wf

USoutham:ASM_ClWi

Developing Flow in a Curved Rectangular Duct

Secondary velocity vectors

Plane $\alpha=75$ deg.



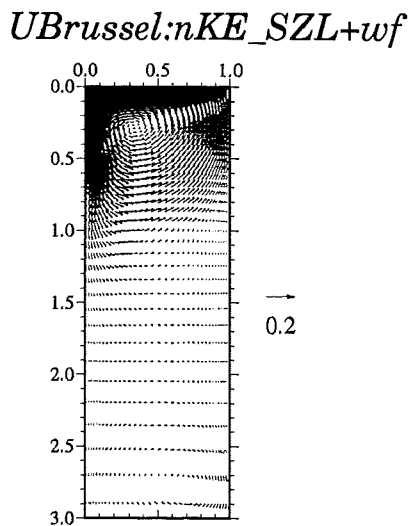
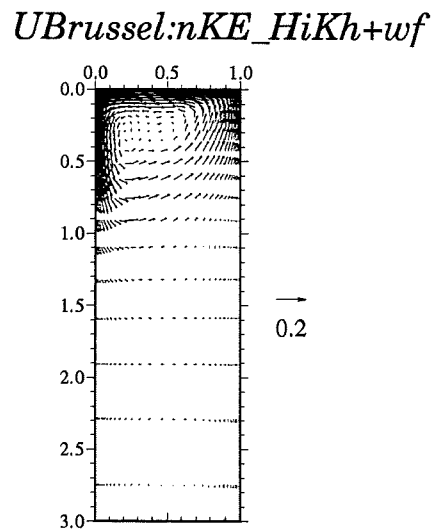
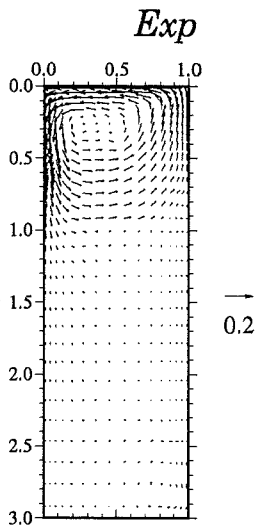
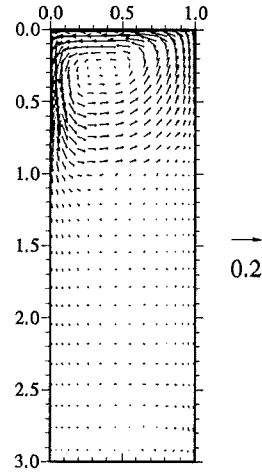
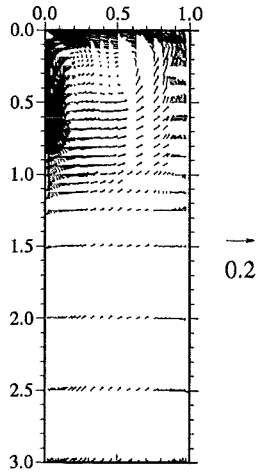
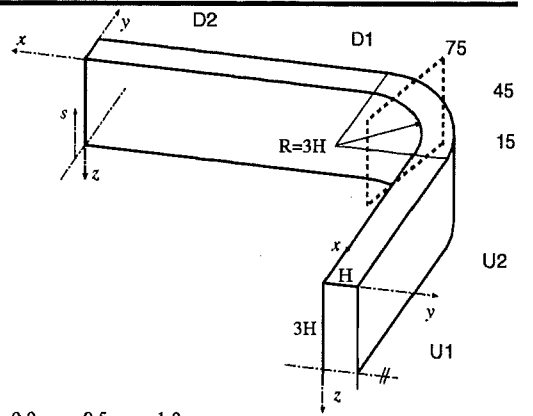
EDFLNHMi:hKE_std+wf

UBrussel:hKE_std+wf

Developing Flow in a Curved Rectangular Duct

Secondary velocity vectors

Plane $\alpha=75$ deg.

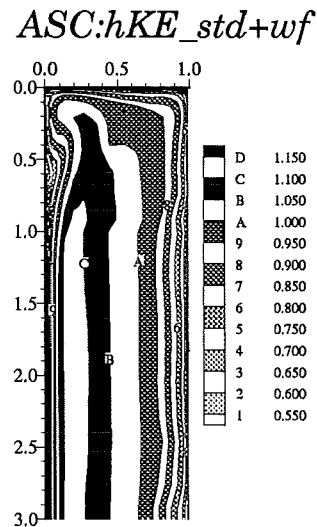
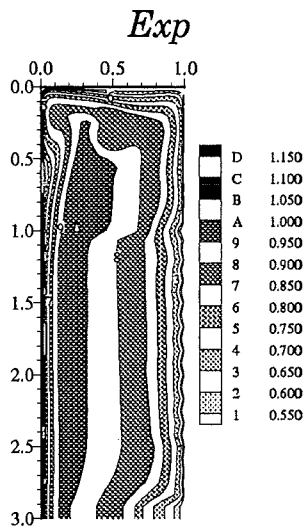
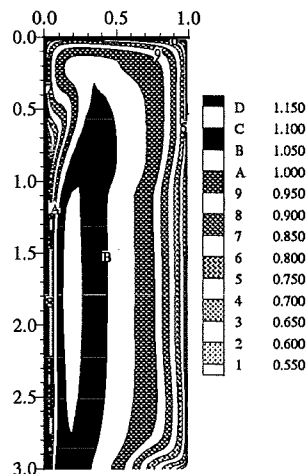
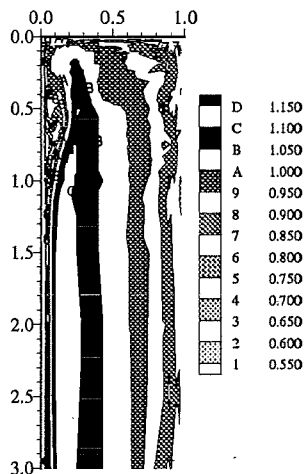
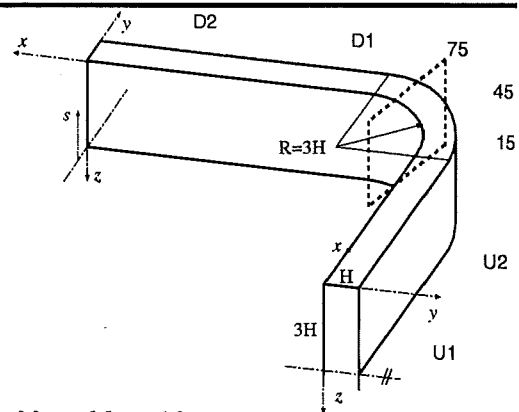


USoutham:ASM_ClWi

Developing Flow in a Curved Rectangular Duct

Streamwise mean velocity

Plane $\alpha=75$ deg.



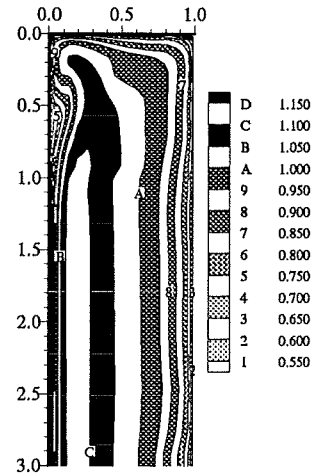
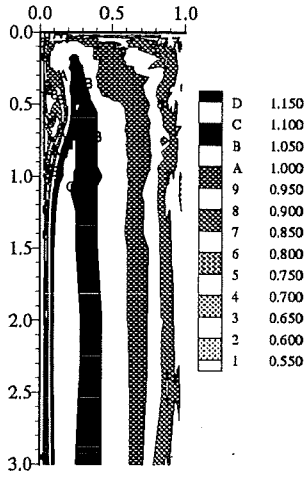
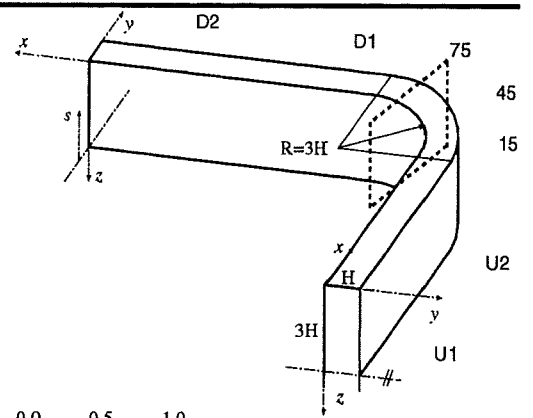
EDFLNMI:hKE_std+wf

UBrussel:hKE_std+wf

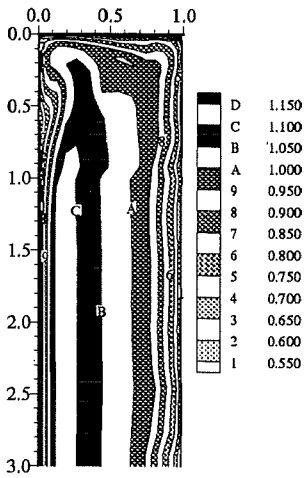
Developing Flow in a Curved Rectangular Duct

Streamwise mean velocity

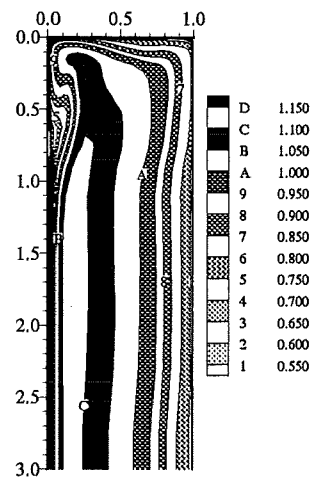
Plane alpha=75 deg.



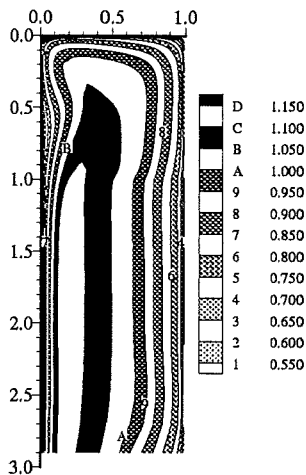
Exp



UBrussel:nKE_HiKh+wf



UBrussel:nKE_SZL+wf



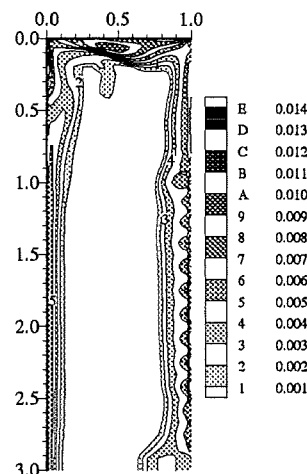
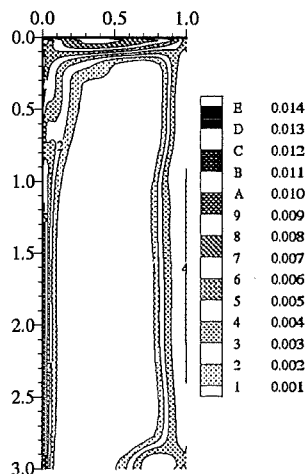
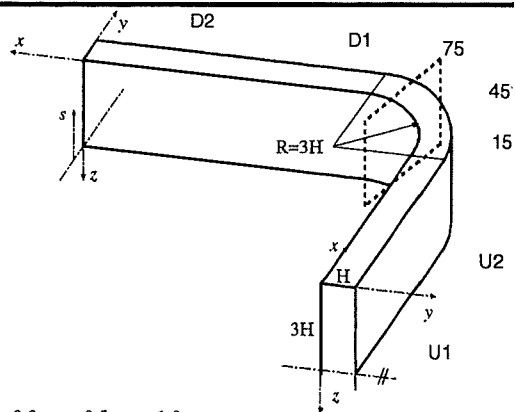
UMcGill:RSM_GiLa+wf

USoutham:ASM_ClWi

Developing Flow in a Curved Rectangular Duct

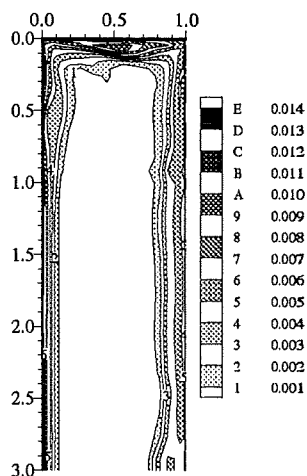
Turbulent kinetic energy k

Plane $\alpha=75$ deg.



ASC:hKE_std+wf

EDFLNHM:i:hKE_std+wf

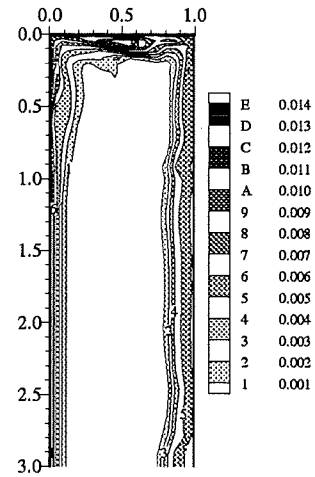
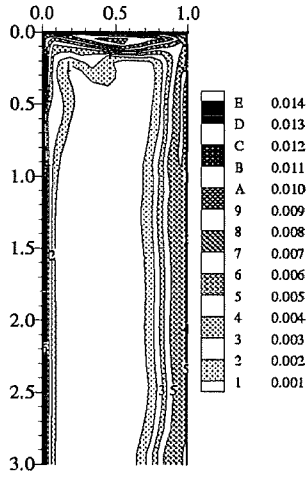
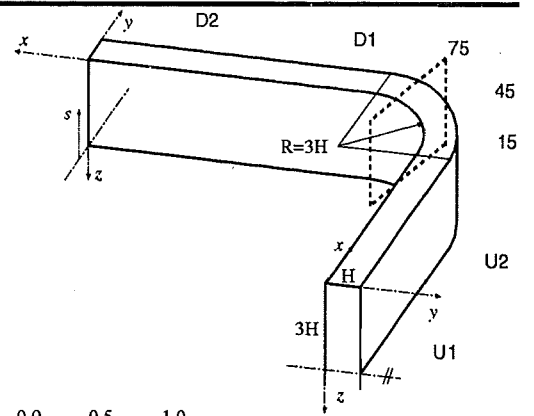


UBrussel:hKE_std+wf

Developing Flow in a Curved Rectangular Duct

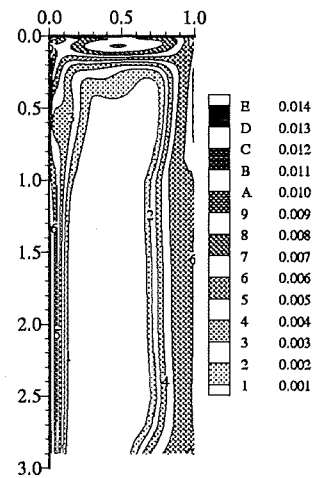
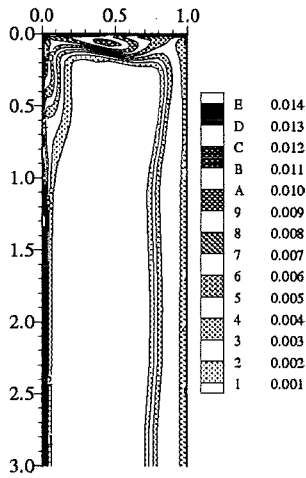
Turbulent kinetic energy k

Plane $\alpha=75$ deg.



UBussel:nKE_HiKh+wf

UBussel:nKE_SZL+wf



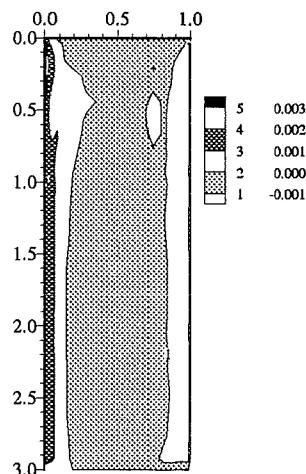
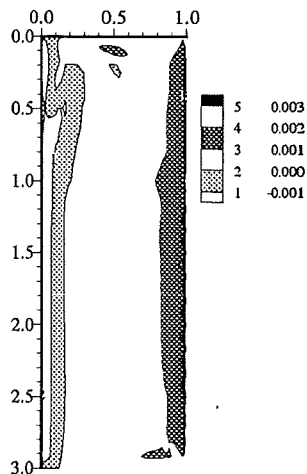
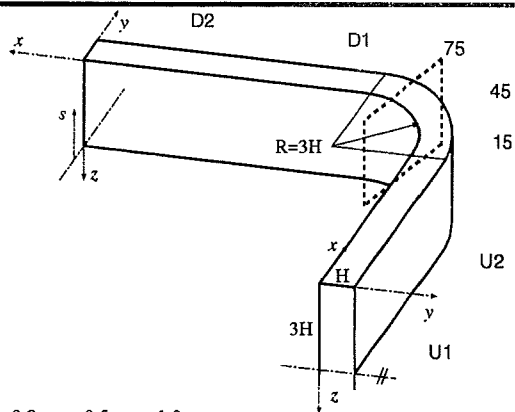
UMcGill:RSM_GiLa+wf

USoutham:ASM_CiWi

Developing Flow in a Curved Rectangular Duct

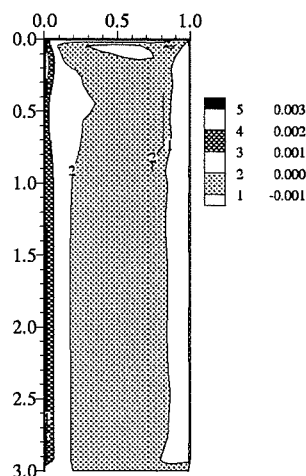
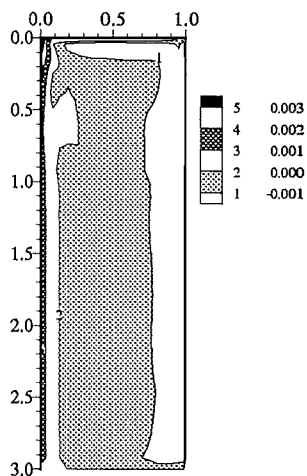
Reynolds shear stress uv

Plane $\alpha=75$ deg.



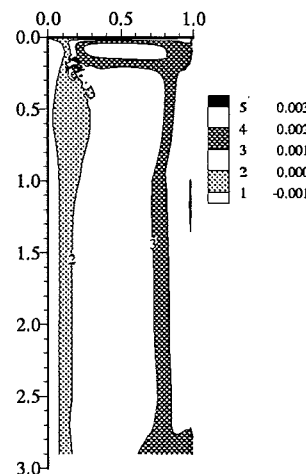
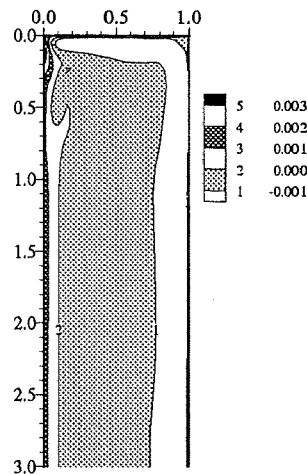
EDNLNHi:hKE_std+wf

UBrussel:hKE_std+wf



UBrussel:nKE_HiKh+wf

UBrussel:nKE_SZL+wf



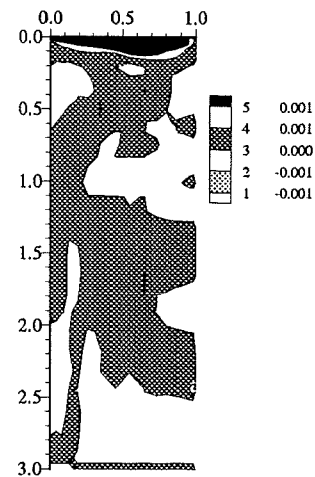
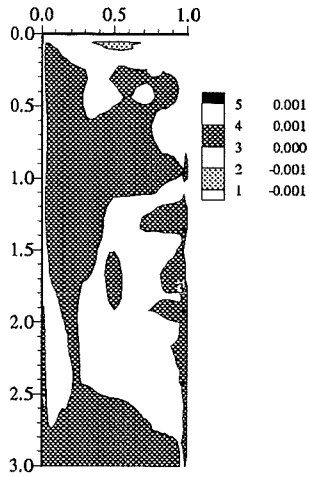
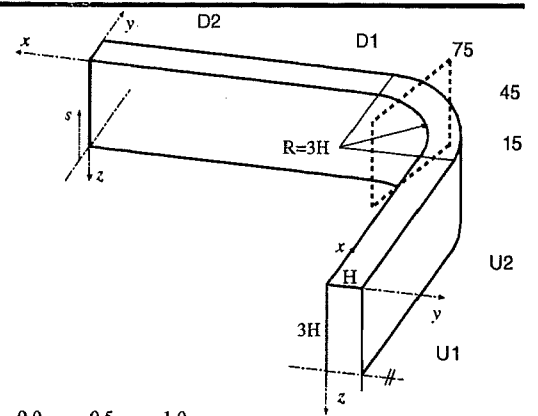
UMcGill:RSM_GiLa+wf

USoutham:ASM_ClWi

Developing Flow in a Curved Rectangular Duct

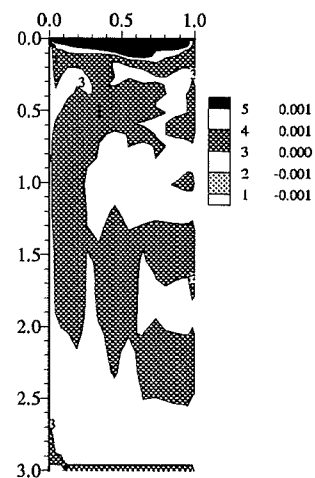
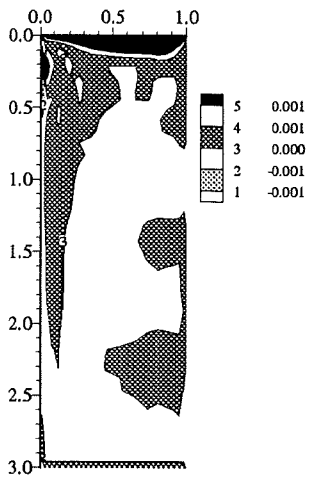
Reynolds shear stress uw

Plane $\alpha=75$ deg.



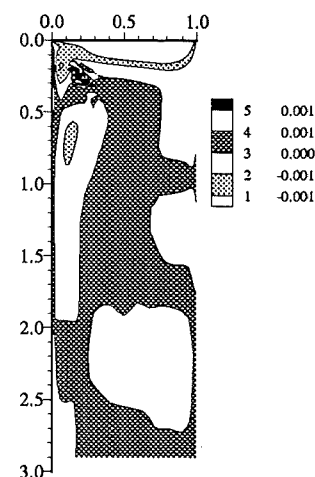
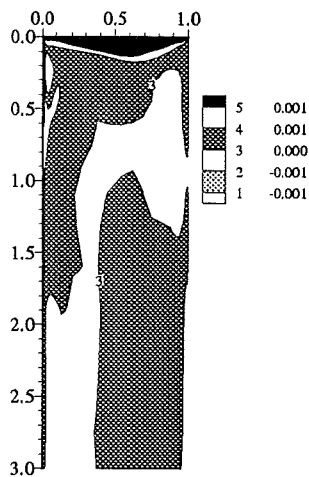
EDFLNHi:hKE_std+wf

UBrussel:hKE_std+wf



UBrussel:nKE_HiKh+wf

UBrussel:nKE_SZL+wf



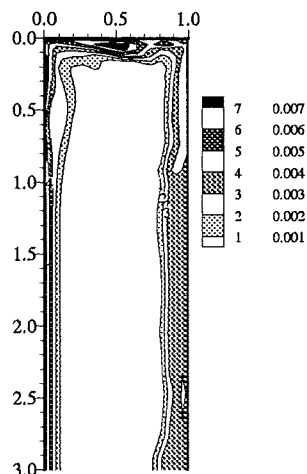
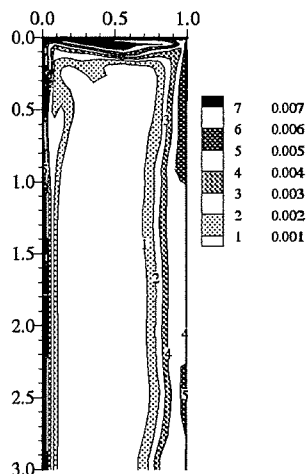
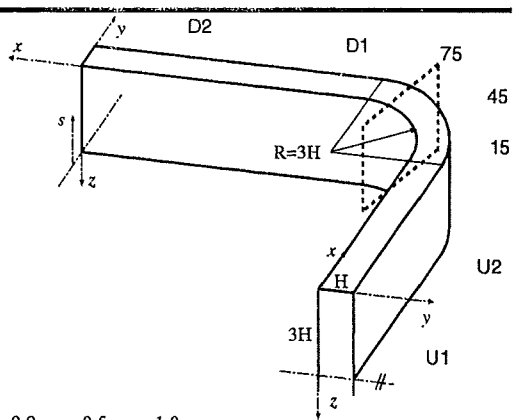
UMcGill:RSM_GiLa+wf

USoutham:ASM_ClWi

Developing Flow in a Curved Rectangular Duct

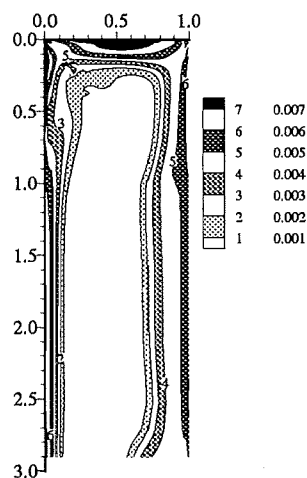
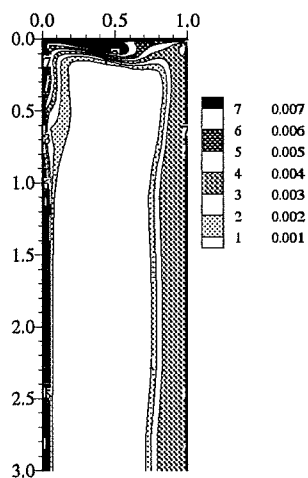
Reynolds normal stress uu

Plane $\alpha=75$ deg.



UBussel:nKE_HiKh+wf

UBussel:nKE_SZL+wf



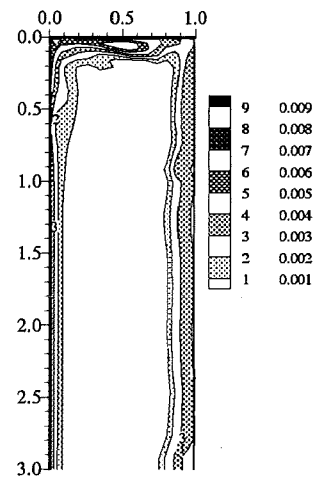
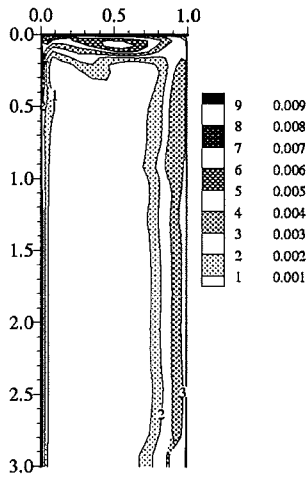
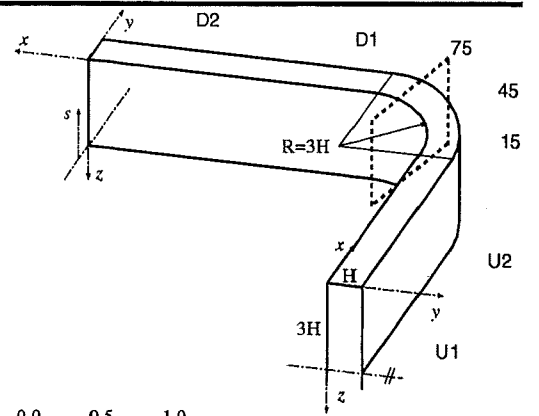
UMcGill:RSM_GiLa+wf

USoutham:ASM_ClWi

Developing Flow in a Curved Rectangular Duct

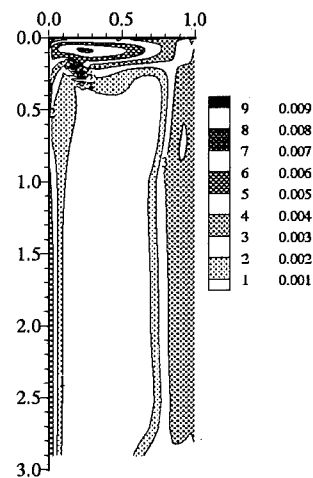
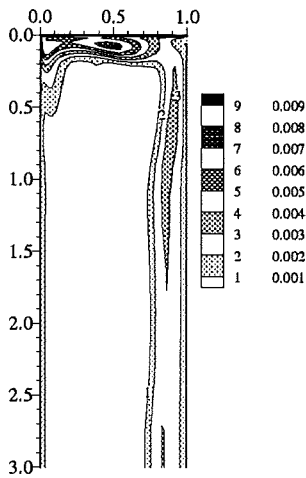
Reynolds normal stress $\overline{v'v'}$

Plane $\alpha=75$ deg.



UBrussel:nKE_HiKh+wf

UBrussel:nKE_SZL+wf



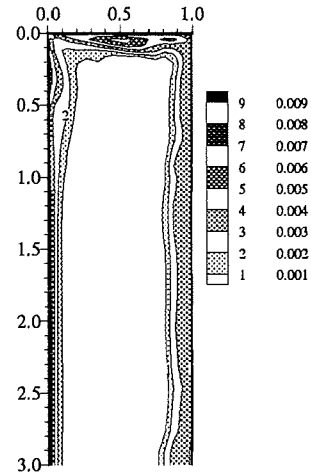
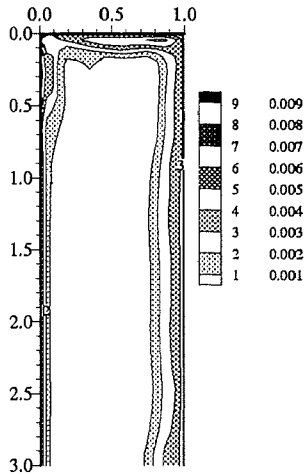
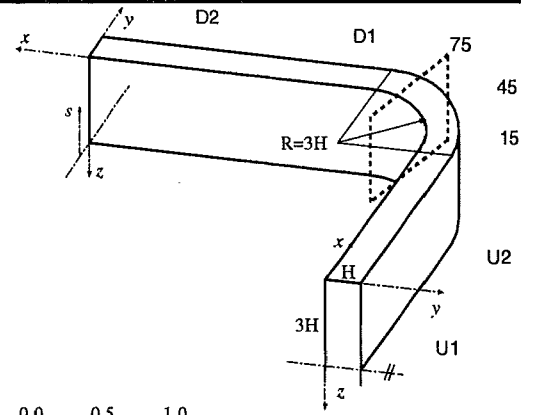
UMcGill:RSM_GiLa+wf

USoutham:ASM_CiWi

Developing Flow in a Curved Rectangular Duct

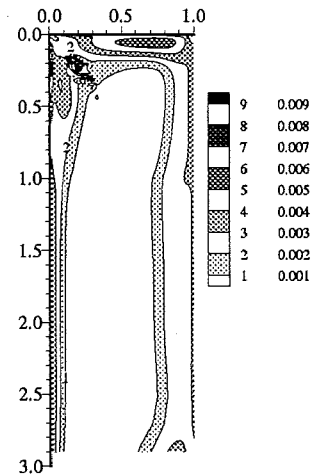
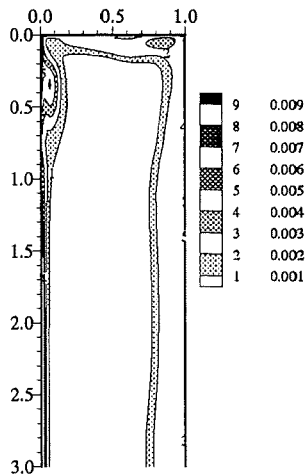
Reynolds normal stress w_w

Plane $\alpha=75$ deg.



UBussel:nKE_HiKh+wf

UBussel:nKE_SZL+wf



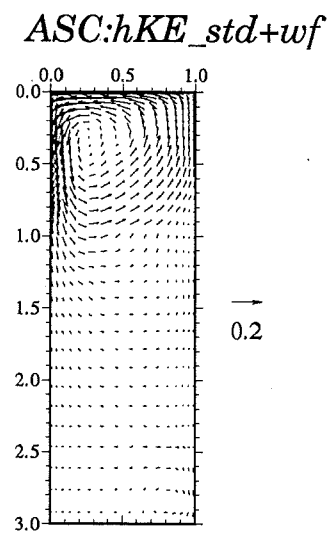
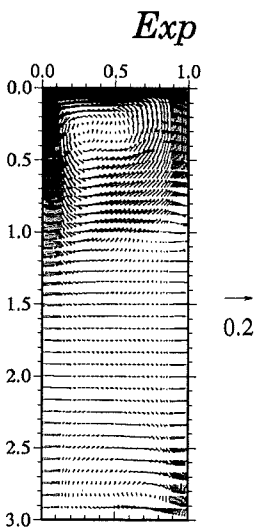
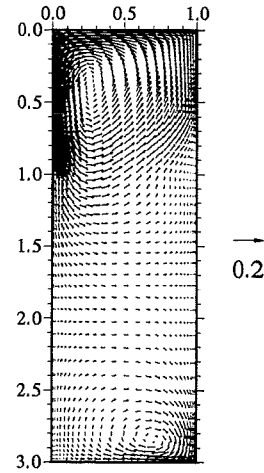
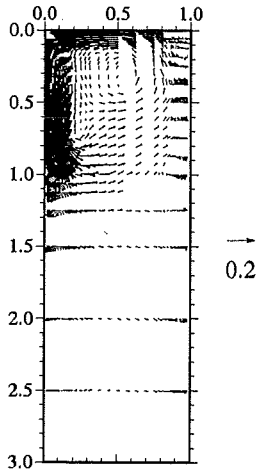
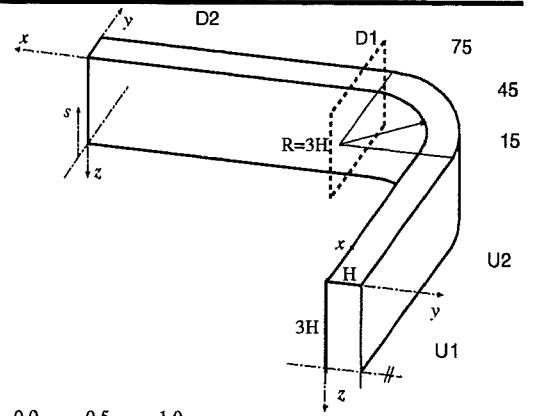
UMcGill:RSM_GiLa+wf

USoutham:ASM_ClWi

Developing Flow in a Curved Rectangular Duct

Secondary velocity vectors

Plane $x/H=0.5$



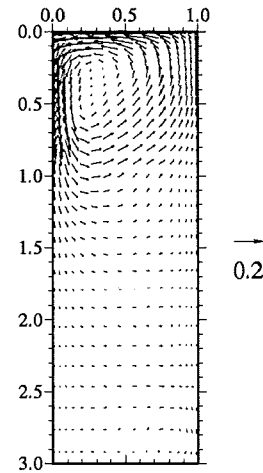
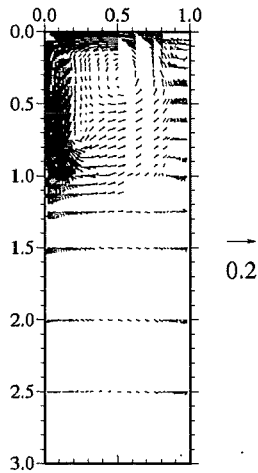
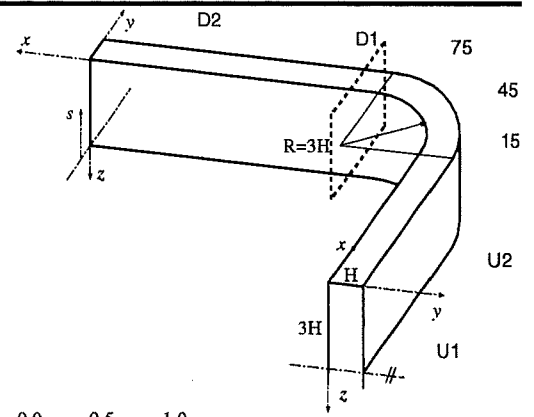
EDFLNHMi:hKE_std+wf

UBrussel:hKE_std+wf

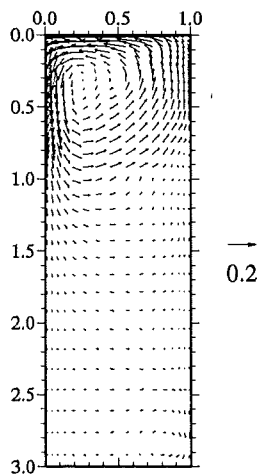
Developing Flow in a Curved Rectangular Duct

Secondary velocity vectors

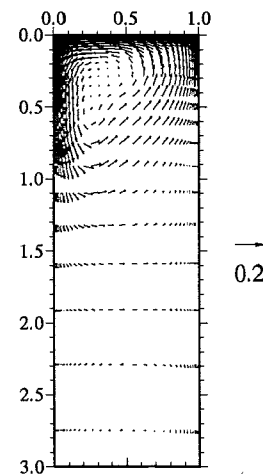
Plane $x/H=0.5$



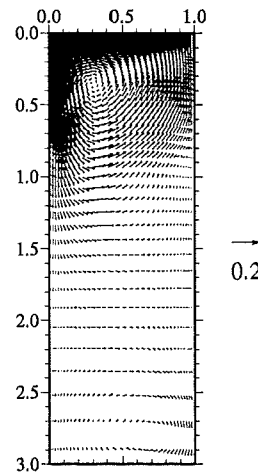
Exp



UBussel:nKE_HiKh+wf



UBussel:nKE_SZL+wf



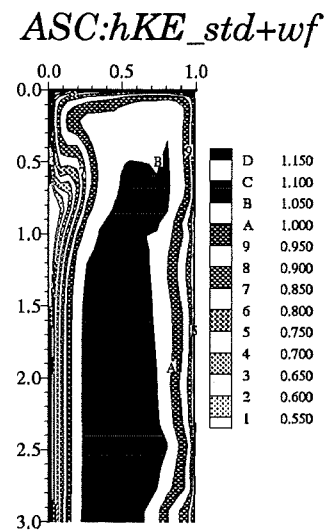
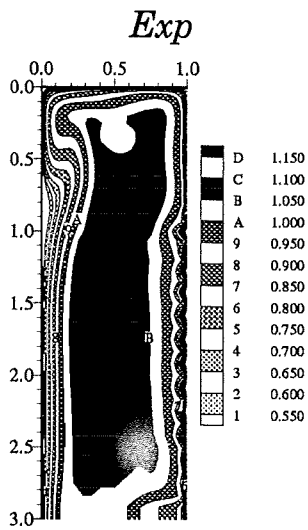
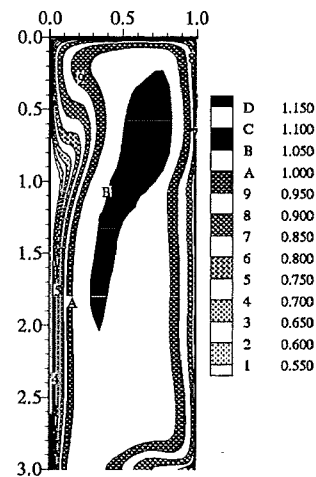
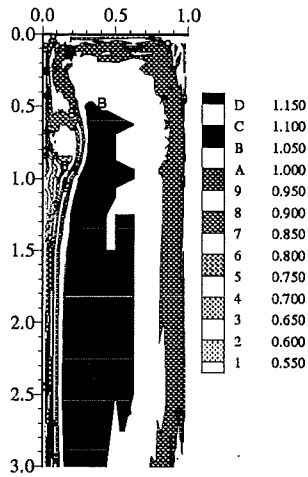
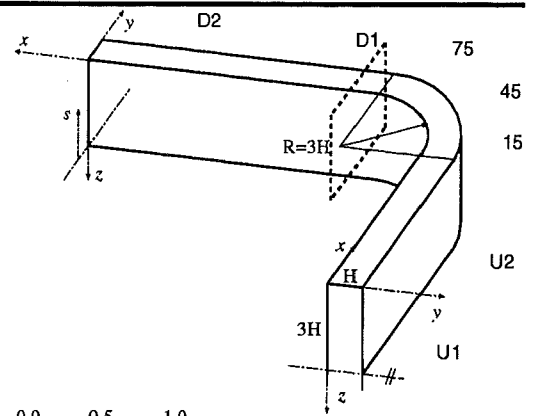
UMcGill:RSM_GiLa+wf

USoutham:ASM_CiWi

Developing Flow in a Curved Rectangular Duct

Streamwise mean velocity

Plane $x/H=0.5$



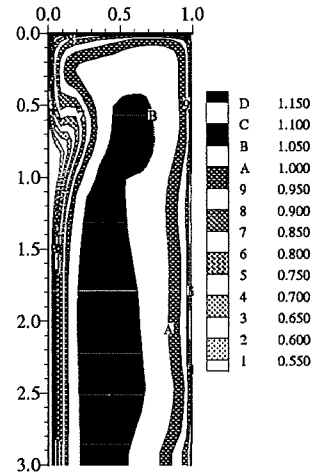
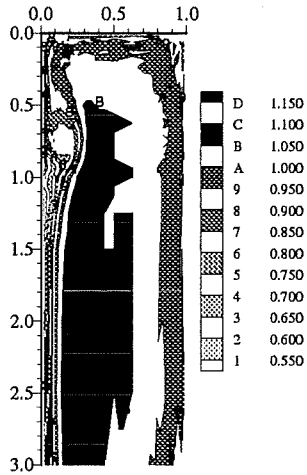
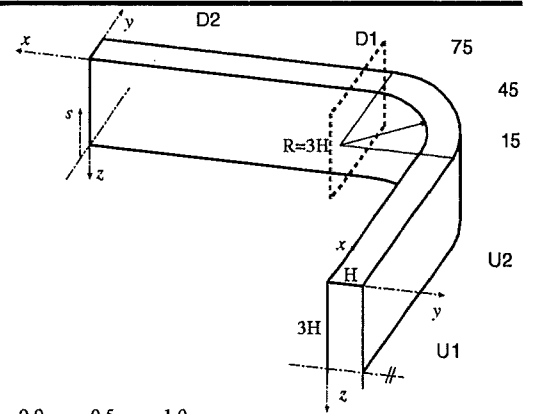
EDFLNHMi:hKE_std+wf

UBrussel:hKE_std+wf

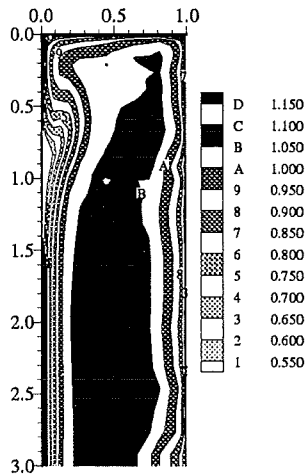
Developing Flow in a Curved Rectangular Duct

Streamwise mean velocity

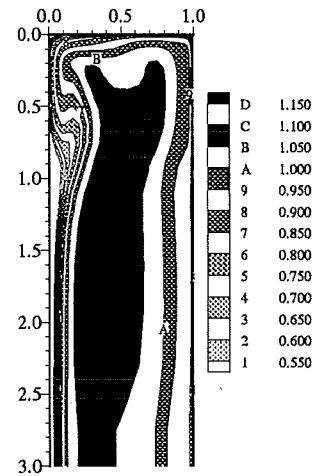
Plane $x/H=0.5$



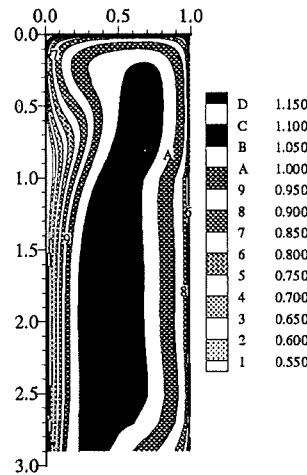
Exp



UBrussel:nKE_HiKh+wf



UBrussel:nKE_SZL+wf



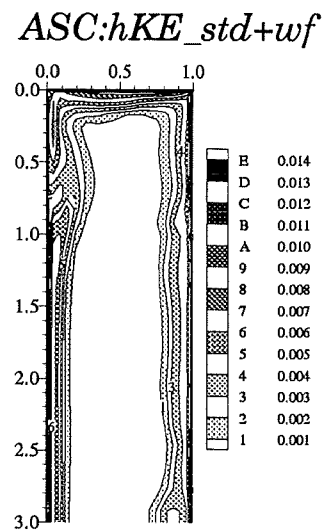
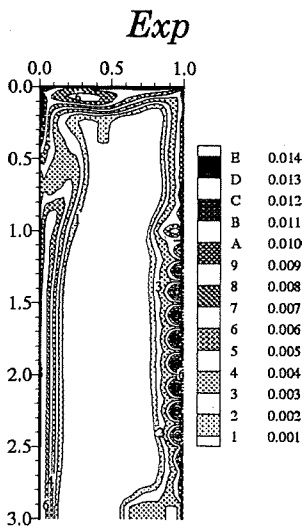
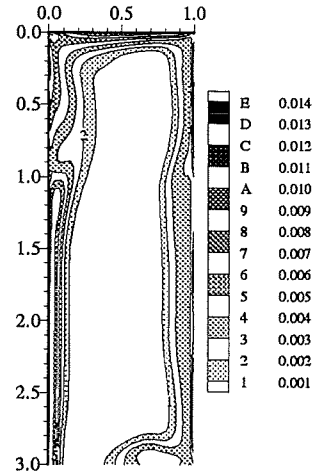
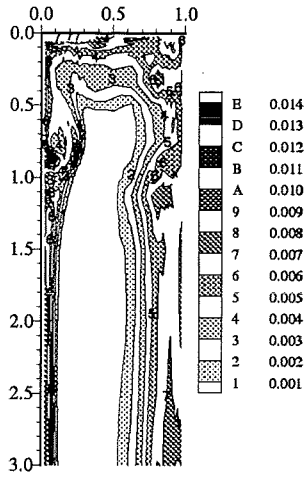
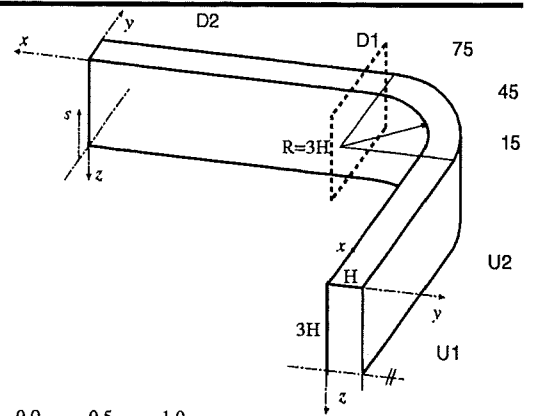
UMcGill:RSM_GiLa+wf

USoutham:ASM_CiWi

Developing Flow in a Curved Rectangular Duct

Turbulent kinetic energy k

Plane $x/H=0.5$



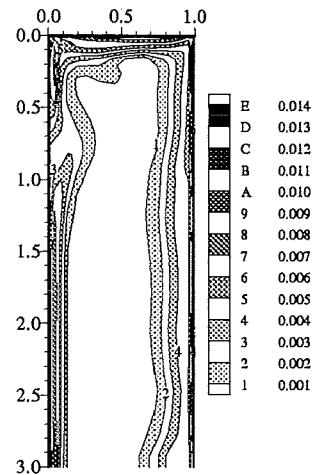
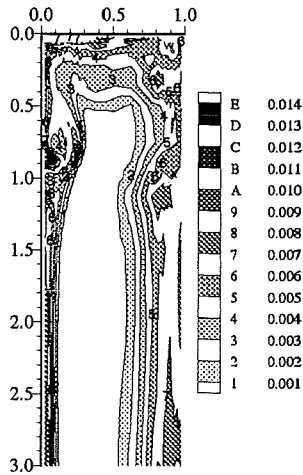
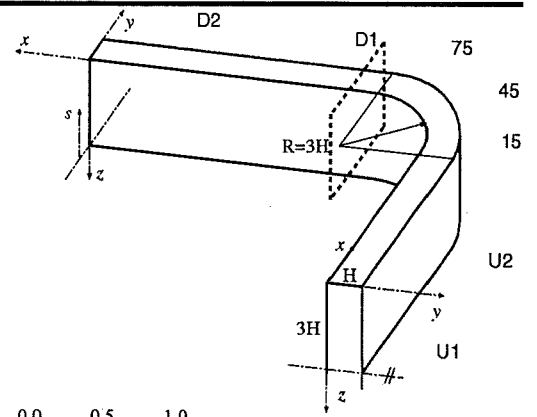
EDFLNHMi:hKE_std+wf

UBrussel:hKE_std+wf

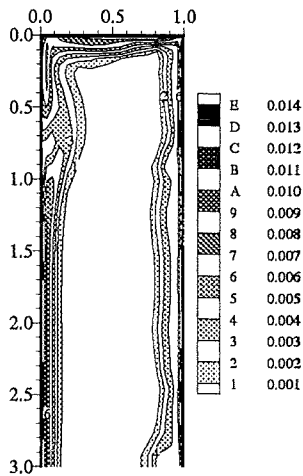
Developing Flow in a Curved Rectangular Duct

Turbulent kinetic energy k

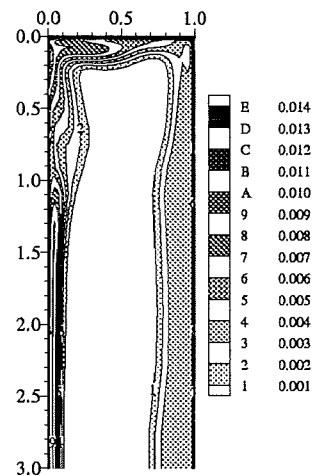
Plane $x/H=0.5$



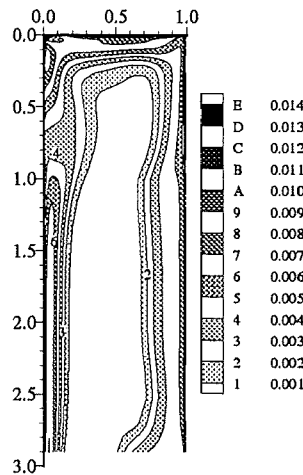
Exp



UBrussel:nKE_HiKh+wf



UBrussel:nKE_SZL+wf



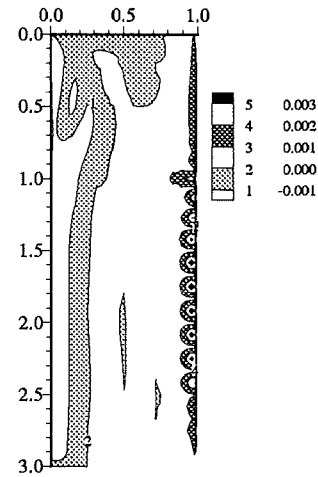
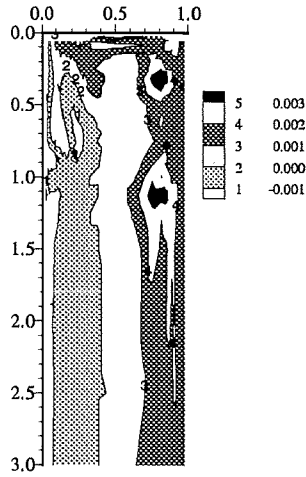
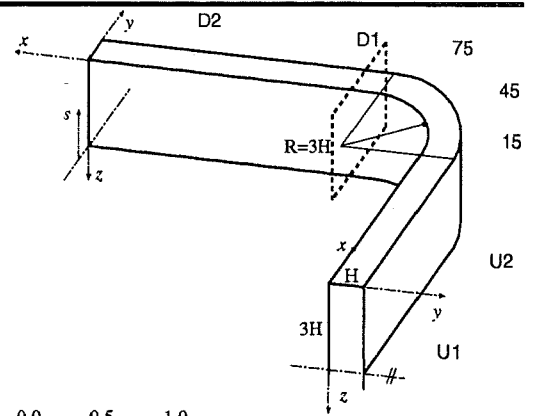
UMcGill:RSM_GiLa+wf

USoutham:ASM_CiWi

Developing Flow in a Curved Rectangular Duct

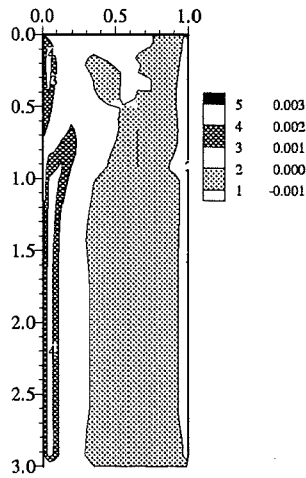
Reynolds shear stress uv

Plane $x/H=0.5$



EDFLNMI:hKE_std+wf

Exp

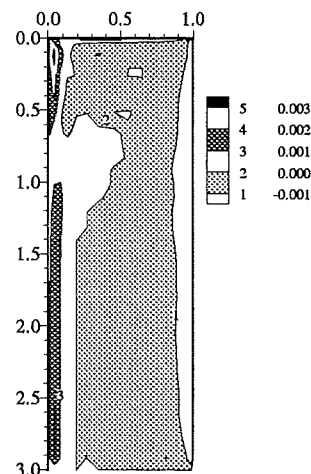
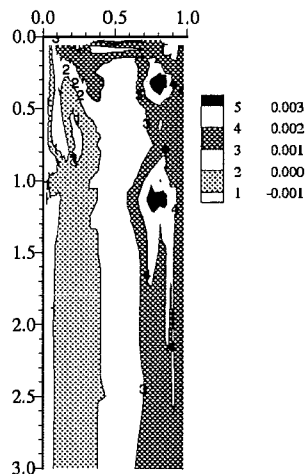
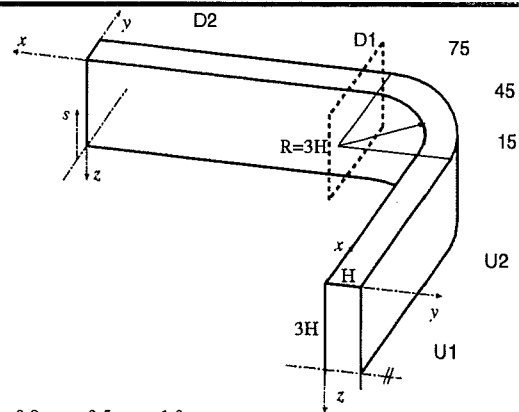


UBrussel:hKE_std+wf

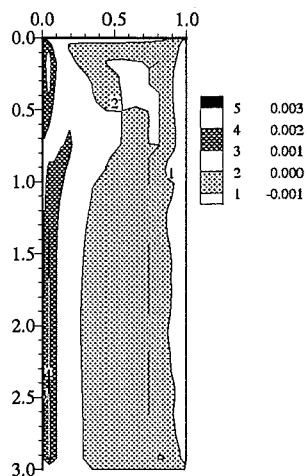
Developing Flow in a Curved Rectangular Duct

Reynolds shear stress uv

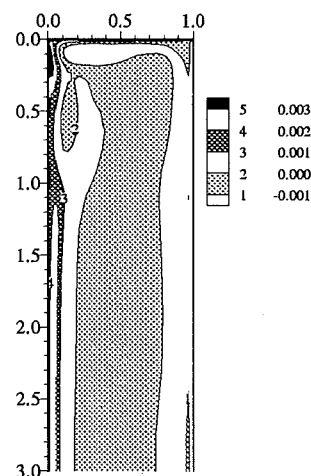
Plane $x/H=0.5$



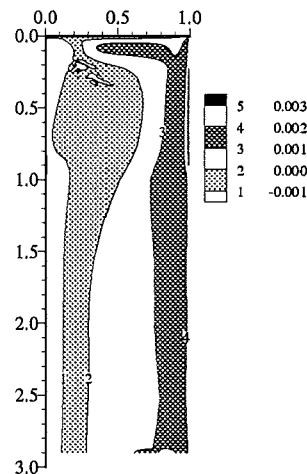
Exp



UBrusseL:nKE_HiKh+wf



UBrusseL:nKE_SZL+wf



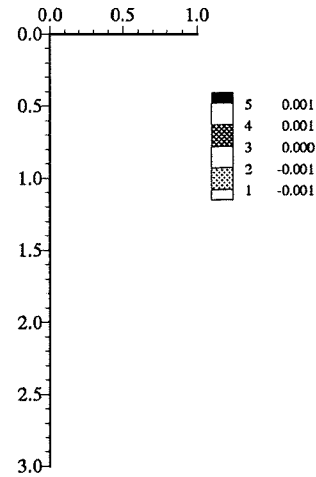
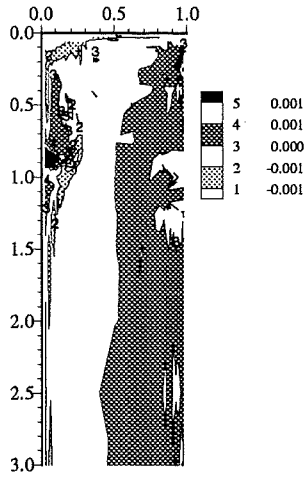
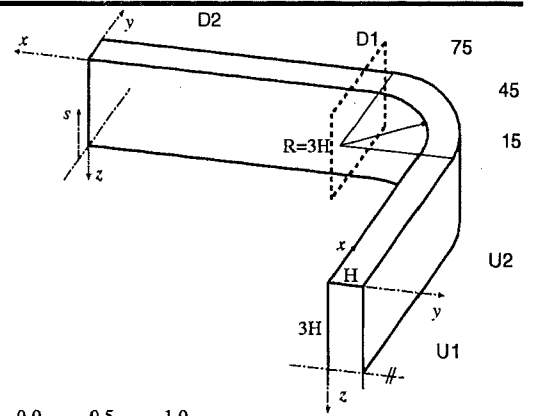
UMcGill:RSM_GiLa+wf

USoutham:ASM_ClWi

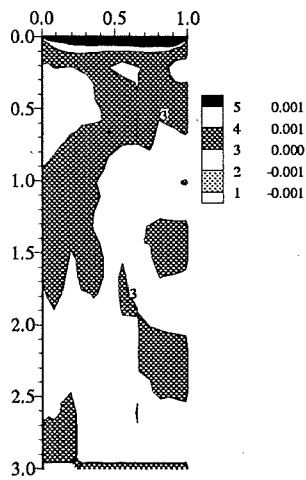
Developing Flow in a Curved Rectangular Duct

Reynolds shear stress uw

Plane $x/H=0.5$



Exp



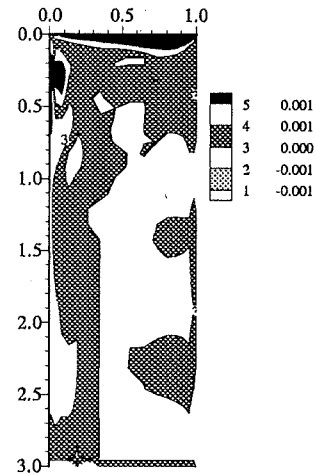
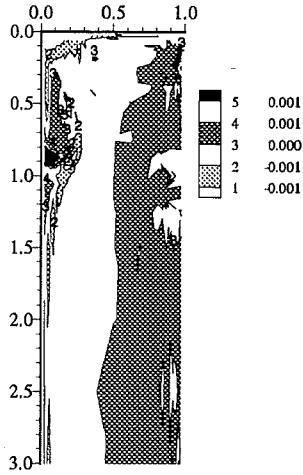
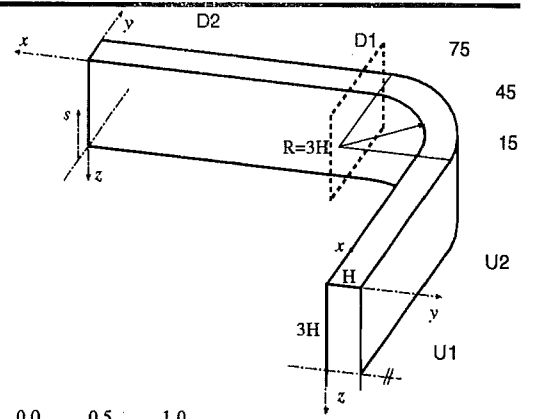
EDFLNMI:hKE_std+wf

UBrussel:hKE_std+wf

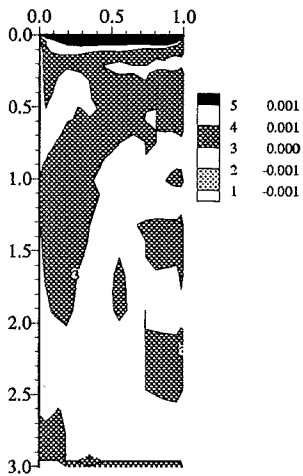
Developing Flow in a Curved Rectangular Duct

Reynolds shear stress uw

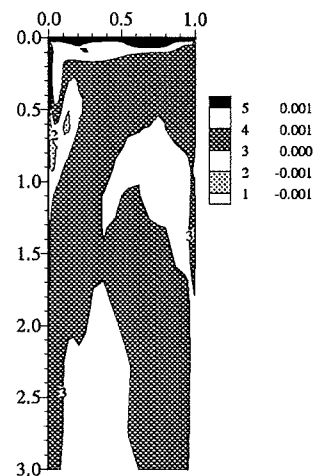
Plane $x/H=0.5$



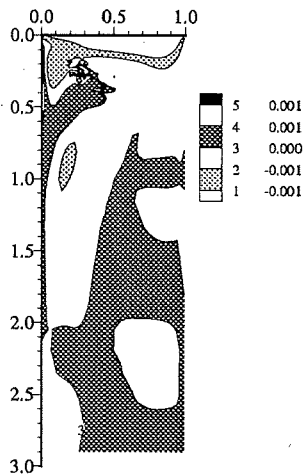
Exp



UBrusseL:nKE_HiKh+wf



UBrusseL:nKE_SZL+wf



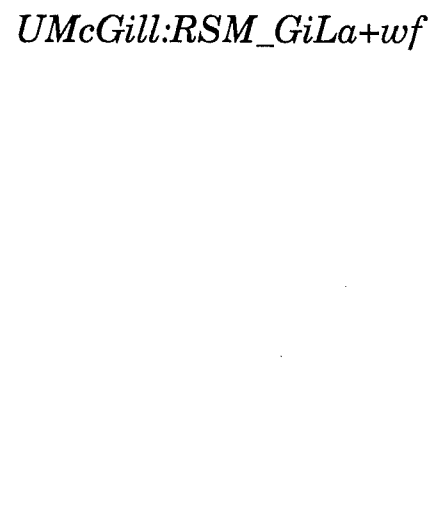
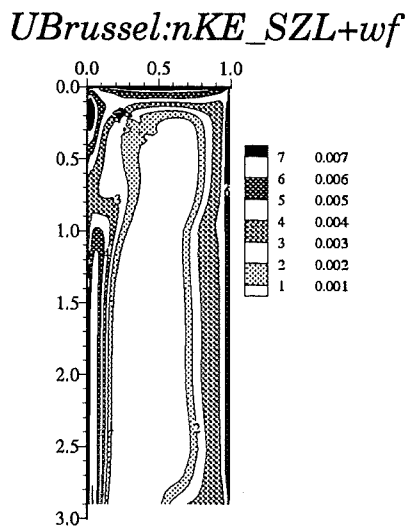
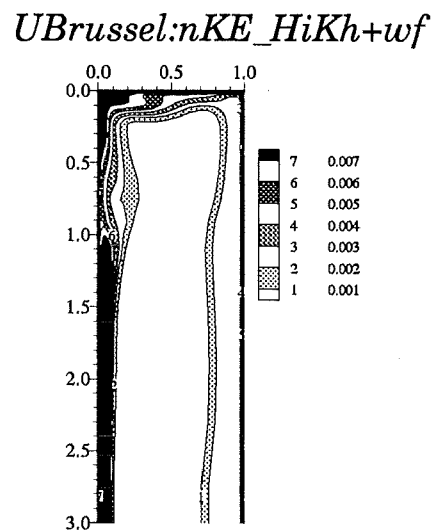
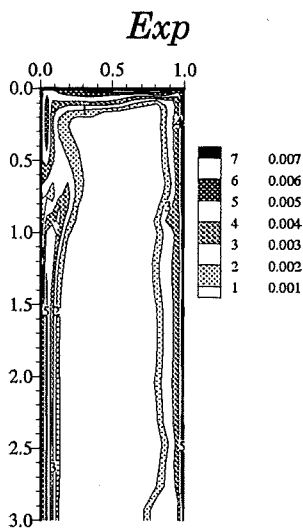
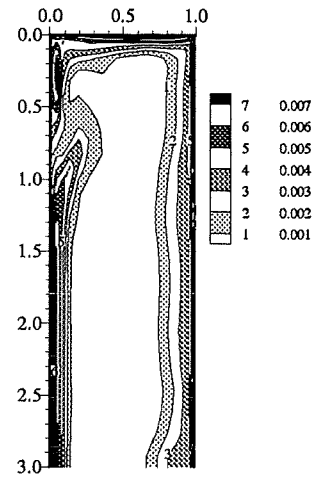
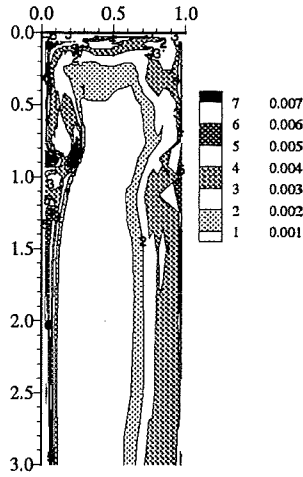
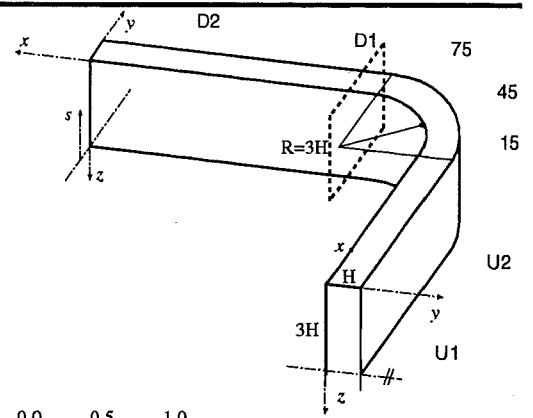
UMcGill:RSM_GiLa+wf

USoutham:ASM_CiWi

Developing Flow in a Curved Rectangular Duct

Reynolds normal stress uu

Plane $x/H=0.5$

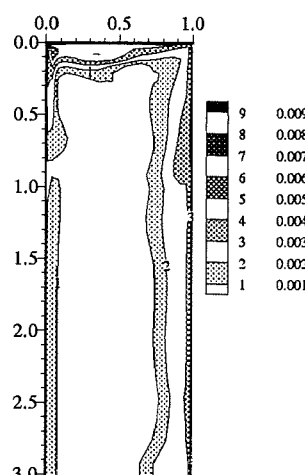
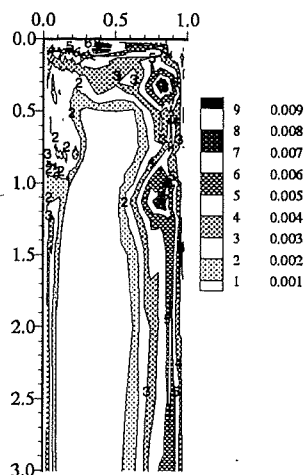
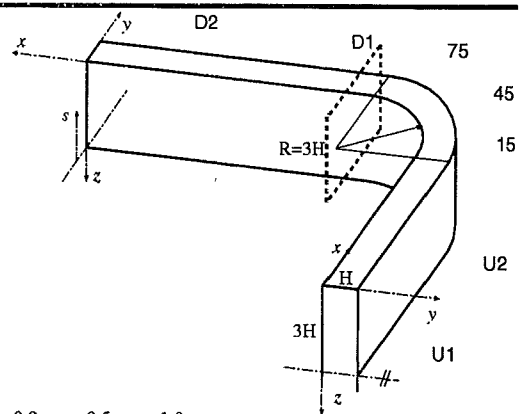


USoutham:ASM_ClWi

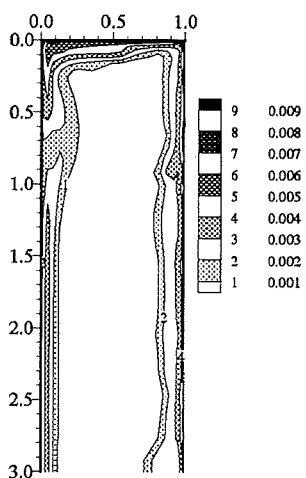
Developing Flow in a Curved Rectangular Duct

Reynolds normal stress $\overline{v'v'}$

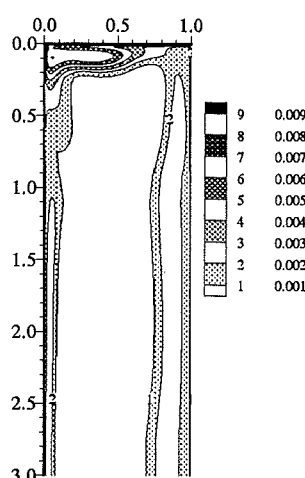
Plane $x/H=0.5$



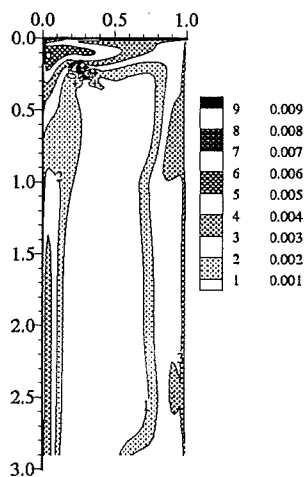
Exp



UBrussel:nKE_HiKh+wf



UBrussel:nKE_SZL+wf



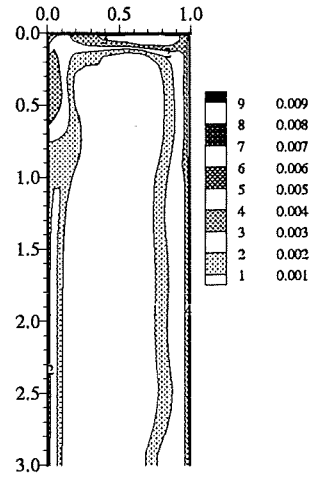
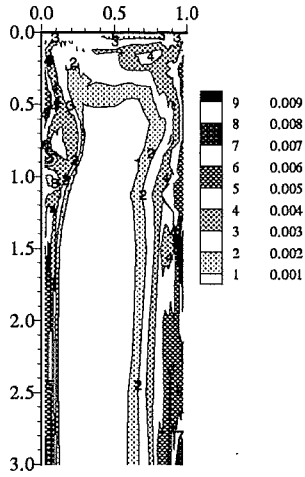
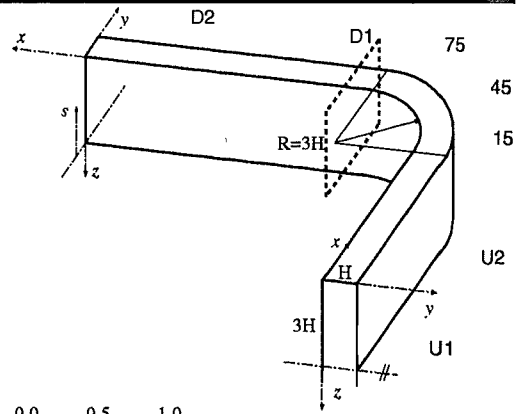
UMcGill:RSM_GiLa+wf

USoutham:ASM_ClWi

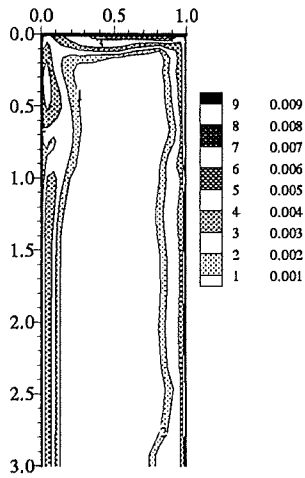
Developing Flow in a Curved Rectangular Duct

Reynolds normal stress $w w$

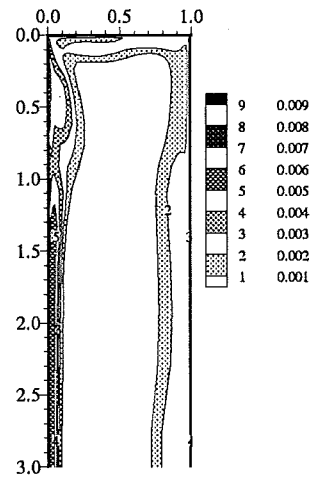
Plane $x/H=0.5$



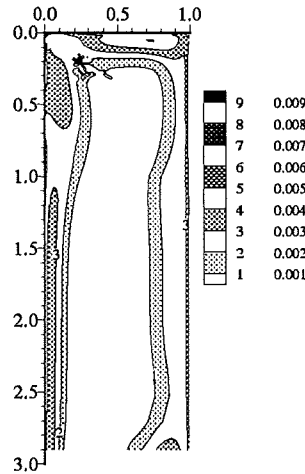
Exp



UBussel:nKE_HiKh+wf



UBussel:nKE_SZL+wf



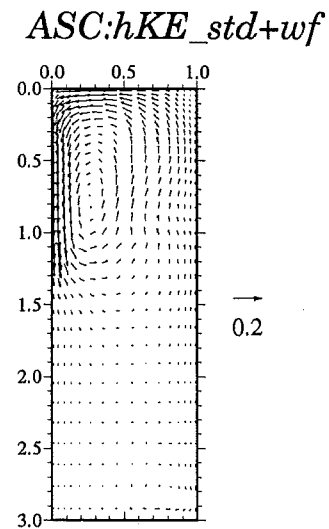
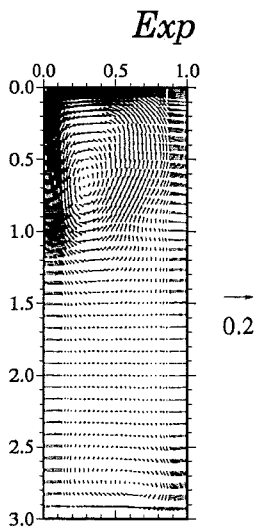
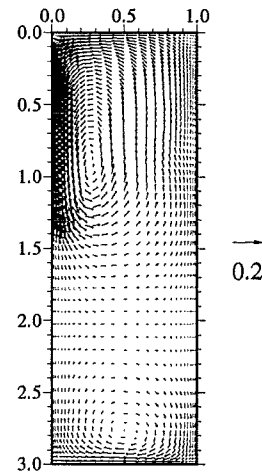
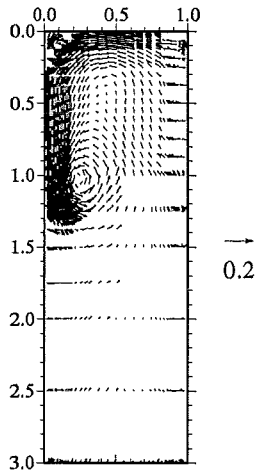
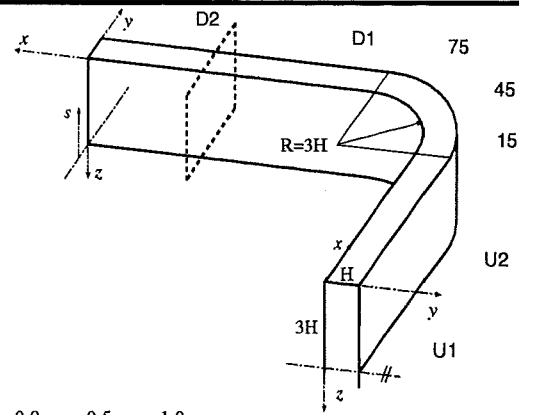
UMcGill:RSM_GiLa+wf

USoutham:ASM_ClWi

Developing Flow in a Curved Rectangular Duct

Secondary velocity vectors

Plane $x/H=4.5$



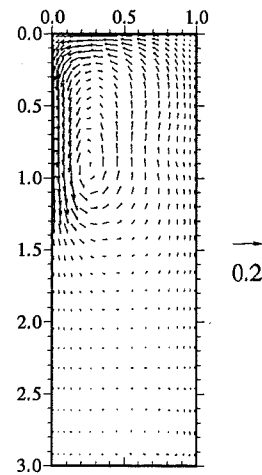
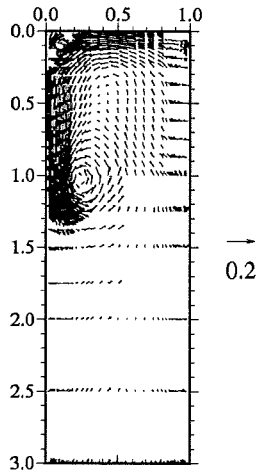
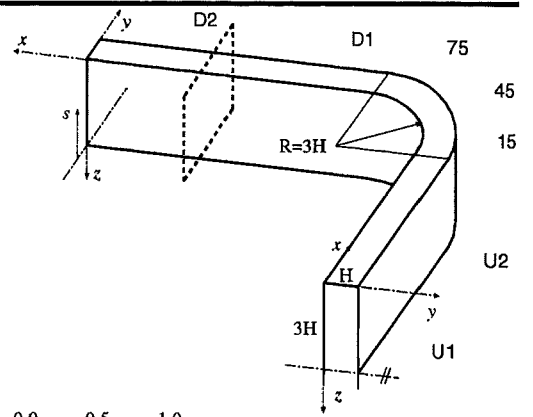
EDFLNHMi:hKE_std+wf

UBrussel:hKE_std+wf

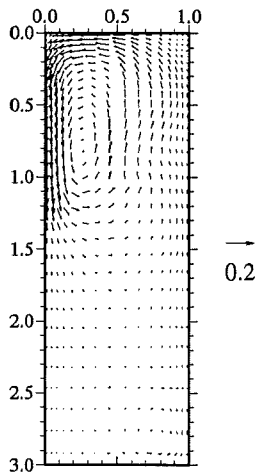
Developing Flow in a Curved Rectangular Duct

Secondary velocity vectors

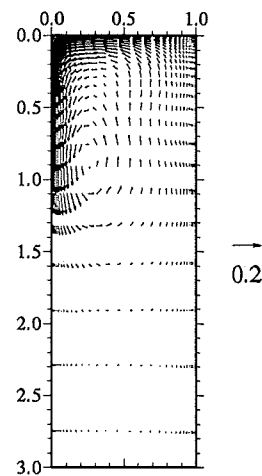
Plane $x/H=4.5$



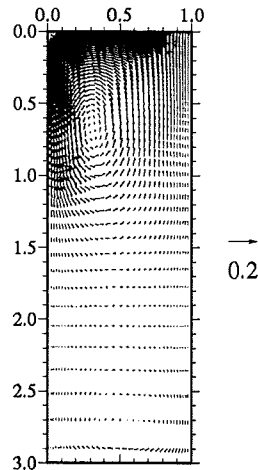
Exp



UBrusseL:nKE_HiKh+wf



UBrusseL:nKE_SZL+wf



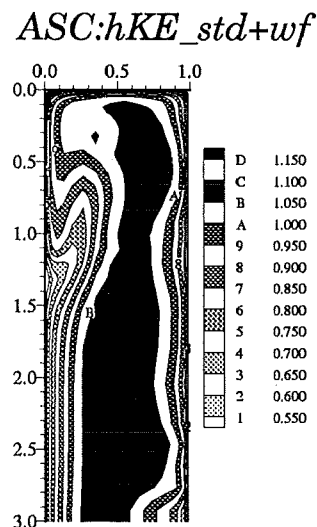
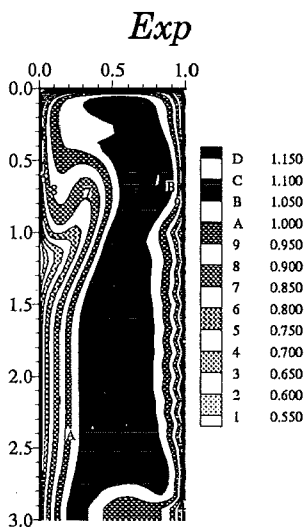
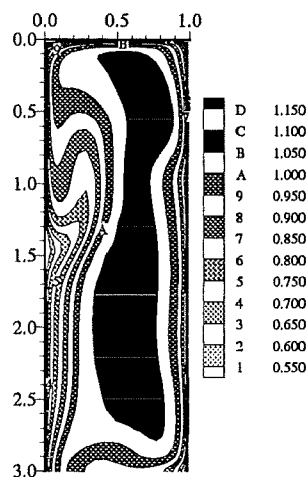
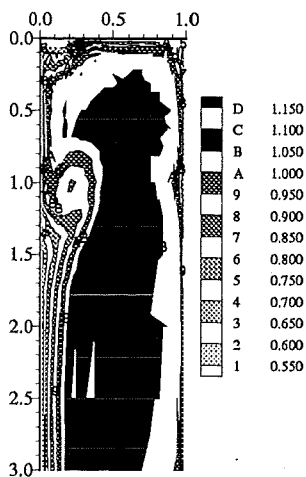
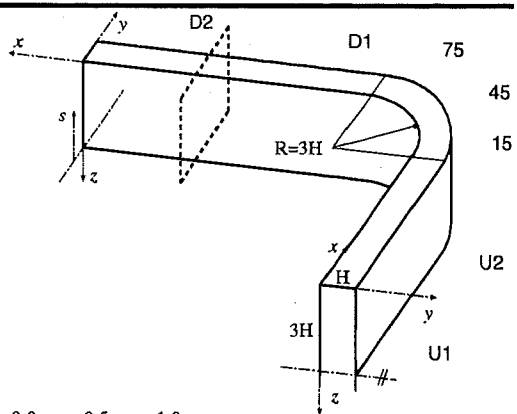
UMcGill:RSM_GiLa+wf

USoutham:ASM_ClWi

Developing Flow in a Curved Rectangular Duct

Streamwise mean velocity

Plane $x/H=4.5$



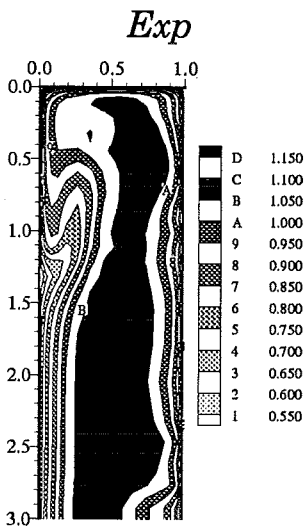
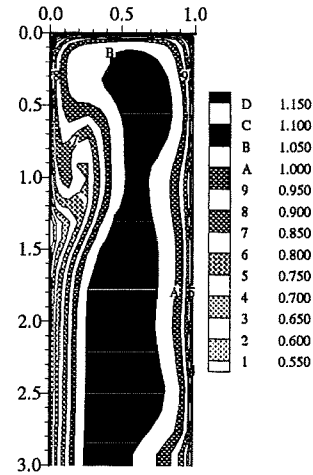
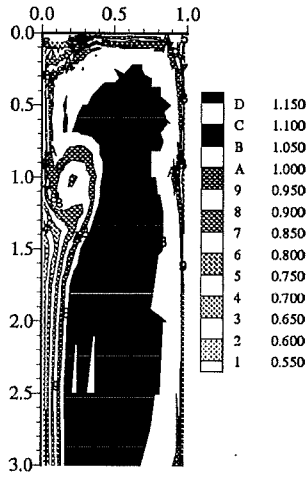
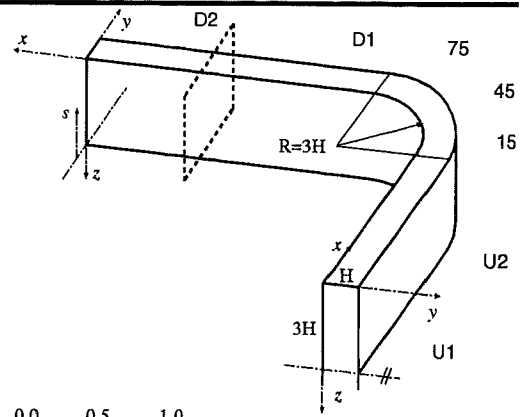
EDFLNHMi:hKE_std+wf

UBrussel:hKE_std+wf

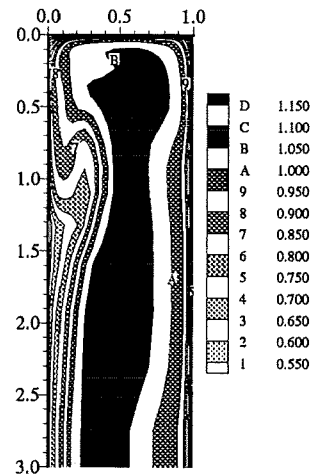
Developing Flow in a Curved Rectangular Duct

Streamwise mean velocity

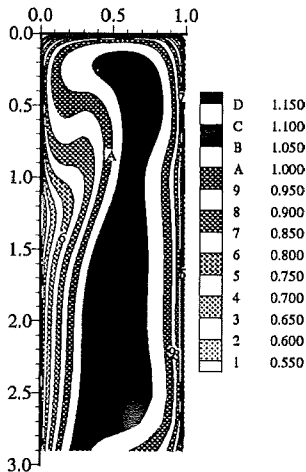
Plane $x/H=4.5$



UBrussel:nKE_HiKh+wf



UBrussel:nKE_SZL+wf



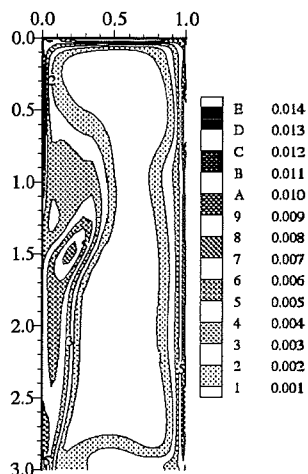
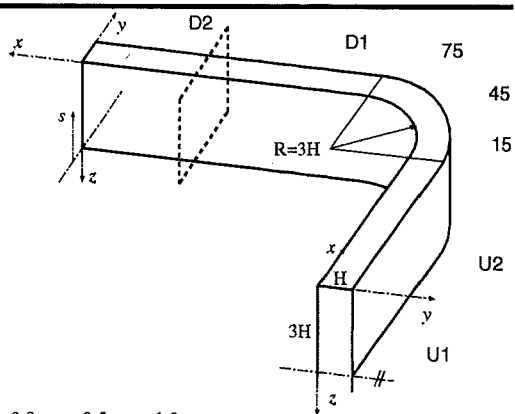
UMcGill:RSM_GiLa+wf

USoutham:ASM_CiWi

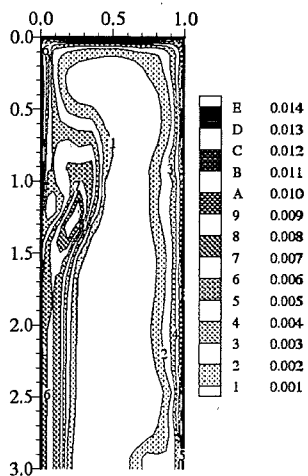
Developing Flow in a Curved Rectangular Duct

Turbulent kinetic energy k

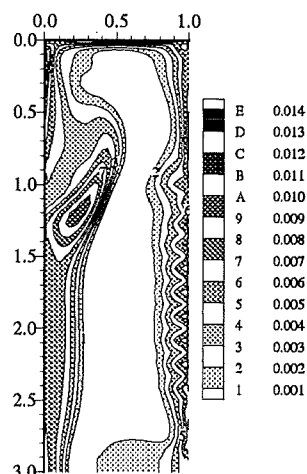
Plane $x/H=4.5$



ASC:hKE_std+wf



UBrussel:hKE_std+wf

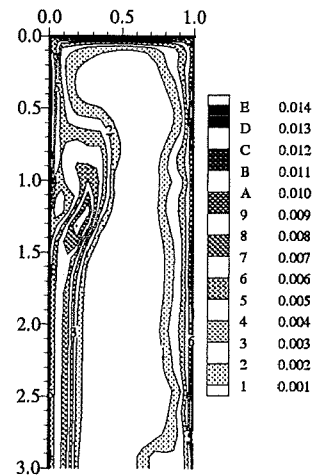
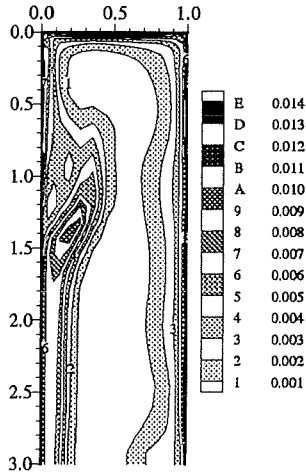
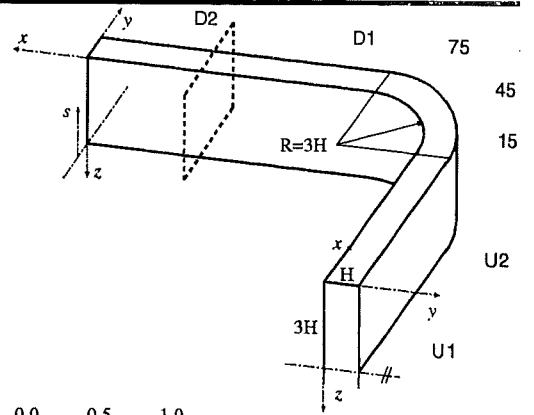


EDFLNHi:hKE_std+wf

Developing Flow in a Curved Rectangular Duct

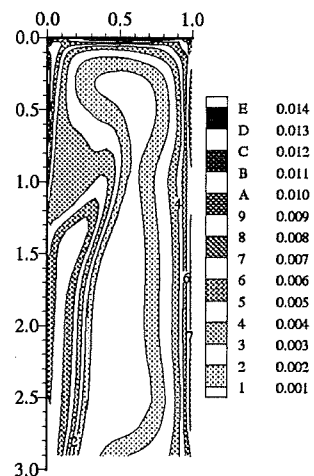
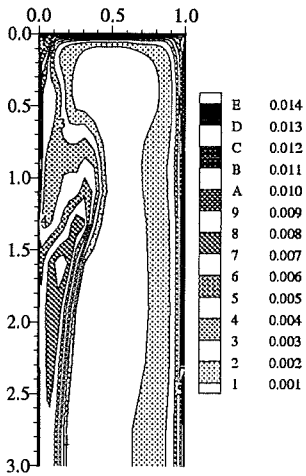
Turbulent kinetic energy k

Plane $x/H=4.5$



UBrussel:nKE_HiKh+wf

UBrussel:nKE_SZL+wf



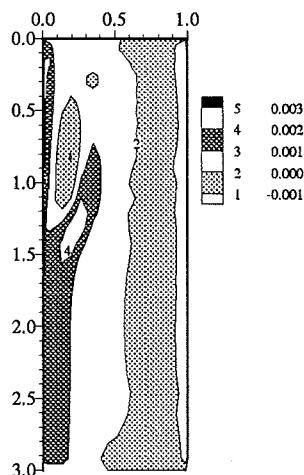
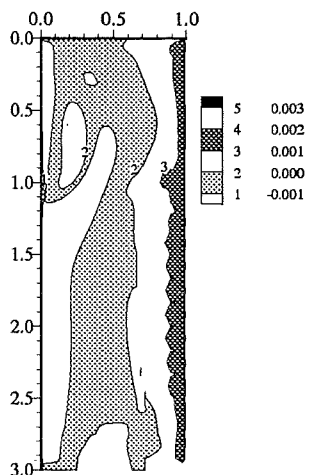
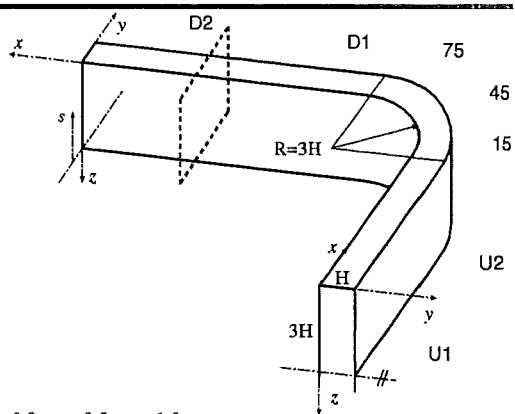
UMcGill:RSM_GiLa+wf

USoutham:ASM_CiWi

Developing Flow in a Curved Rectangular Duct

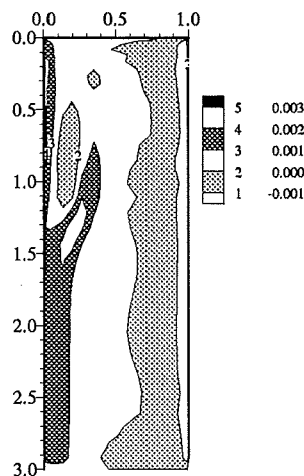
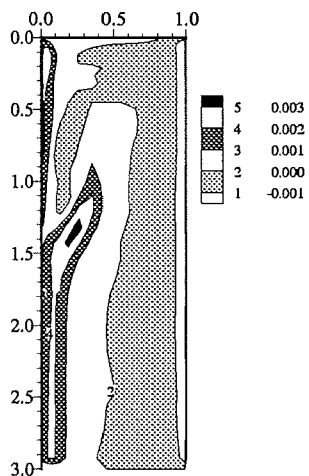
Reynolds shear stress uv

Plane $x/H=4.5$



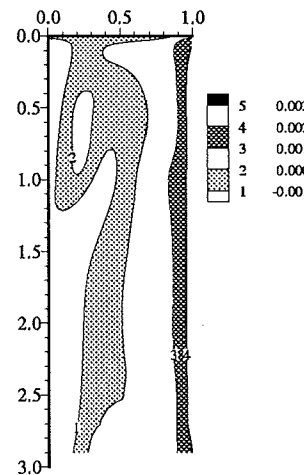
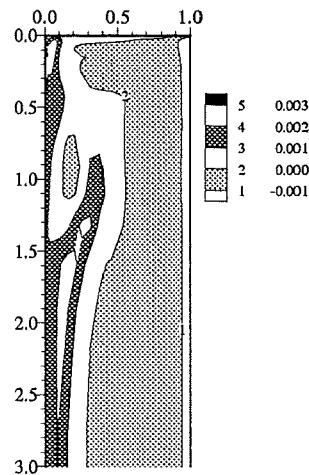
EDNLNHi:hKE_std+wf

UBrussel:hKE_std+wf



UBrussel:nKE_HiKh+wf

UBrussel:nKE_SZL+wf



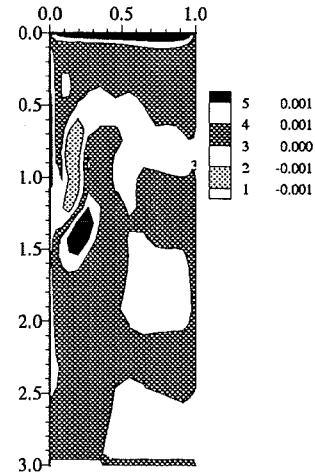
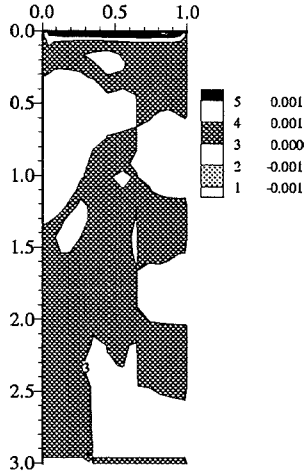
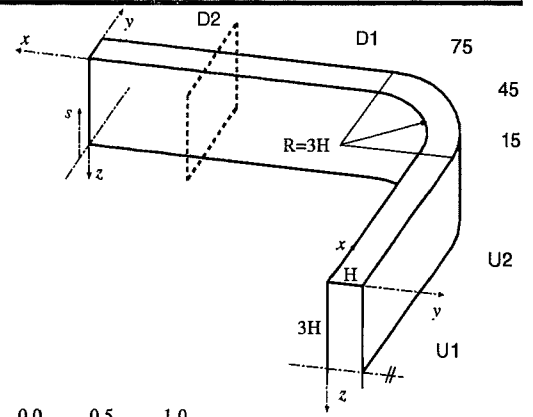
UMcGill:RSM_GiLa+wf

USoutham:ASM_ClWi

Developing Flow in a Curved Rectangular Duct

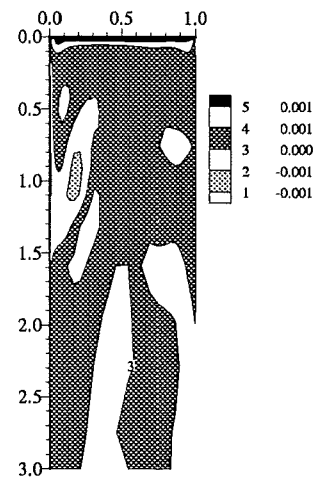
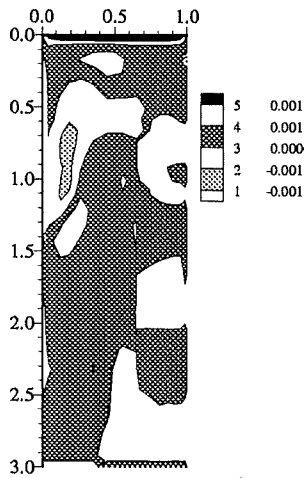
Reynolds shear stress uw

Plane $x/H=4.5$



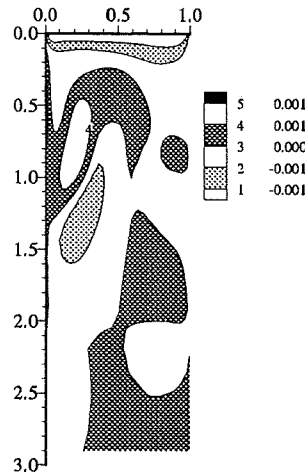
UBussel:hKE_std+wf

UBussel:nKE_HiKh+wf



UBussel:nKE_SZL+wf

UMcGill:RSM_GiLa+wf

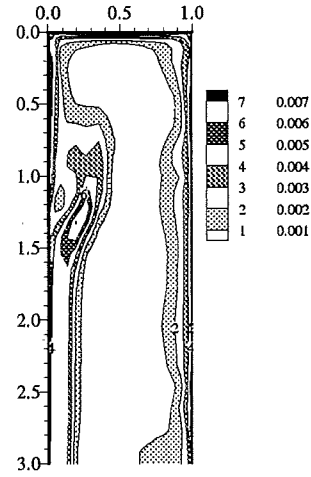
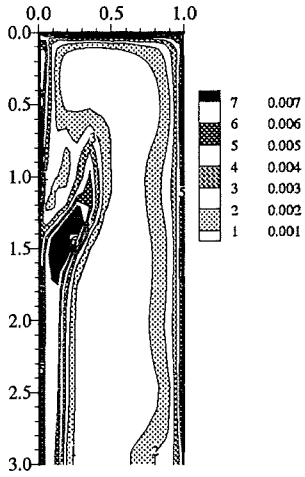
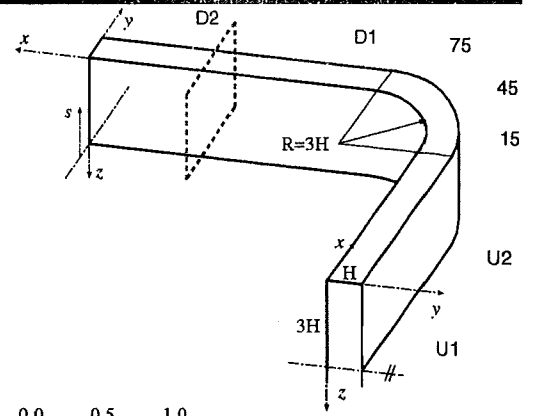


USoutham:ASM_CiWi

Developing Flow in a Curved Rectangular Duct

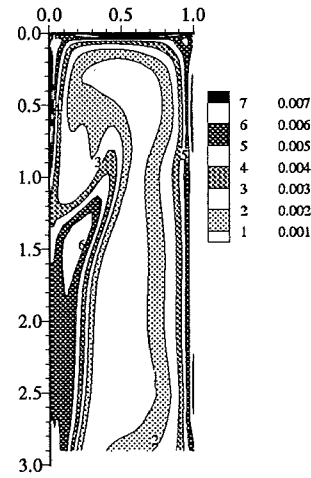
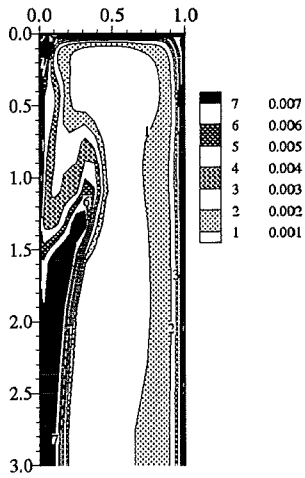
Reynolds normal stress uu

Plane $x/H=4.5$



UBrussel:nKE_HiKh+wf

UBrussel:nKE_SZL+wf



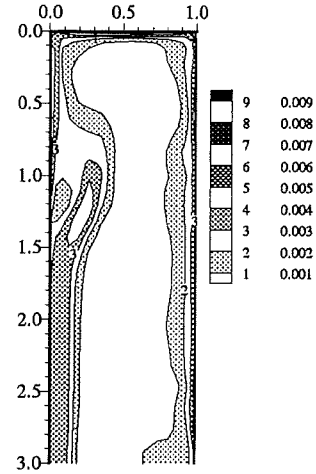
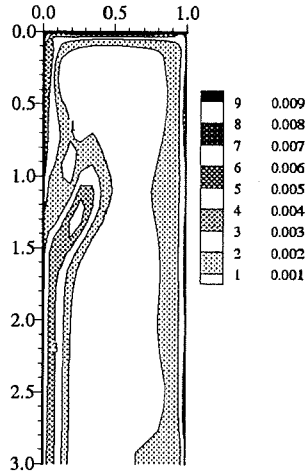
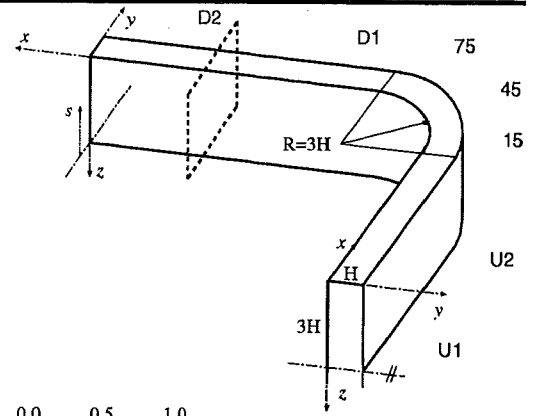
UMcGill:RSM_GiLa+wf

USoutham:ASM_ClWi

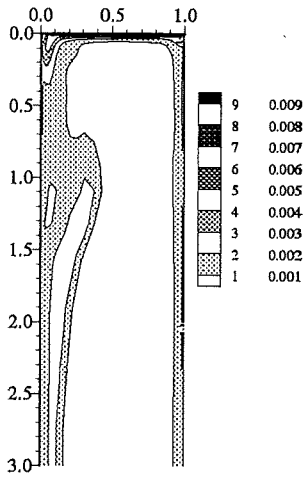
Developing Flow in a Curved Rectangular Duct

Reynolds normal stress v_v

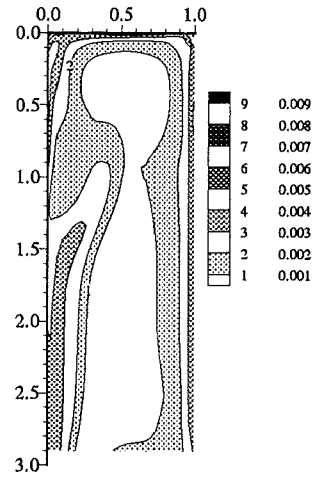
Plane $x/H=4.5$



UBrussel:nKE_HiKh+wf



UBrussel:nKE_SZL+wf



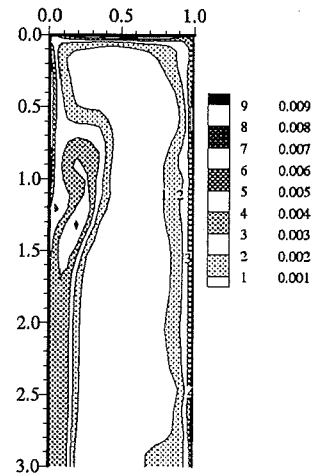
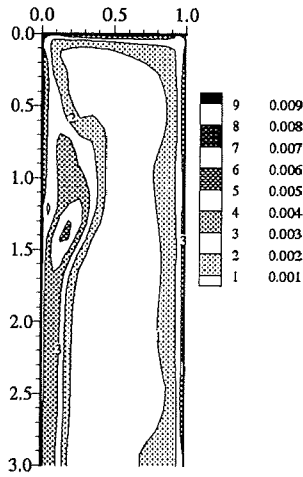
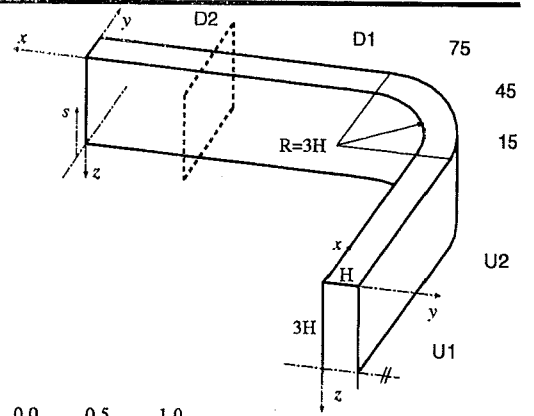
UMcGill:RSM_GiLa+wf

USoutham:ASM_CiWi

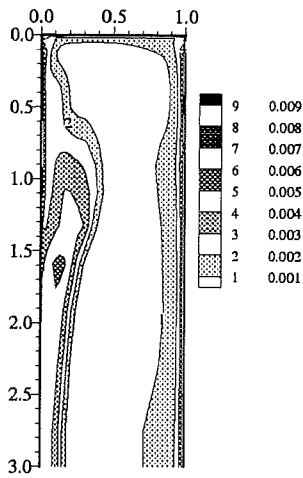
Developing Flow in a Curved Rectangular Duct

Reynolds normal stress $w w$

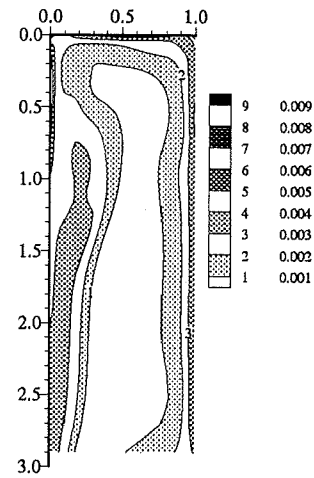
Plane $x/H=4.5$



UBrunsel:nKE_HiKh+wf



UBrunsel:nKE_SZL+wf

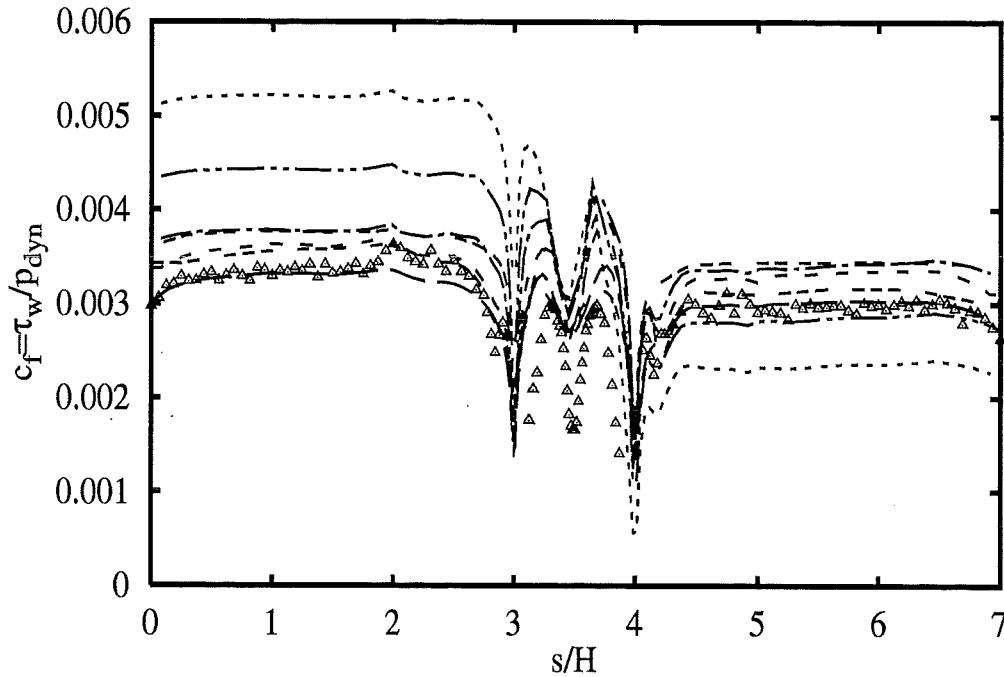


UMcGill:RSM_GiLa+wf

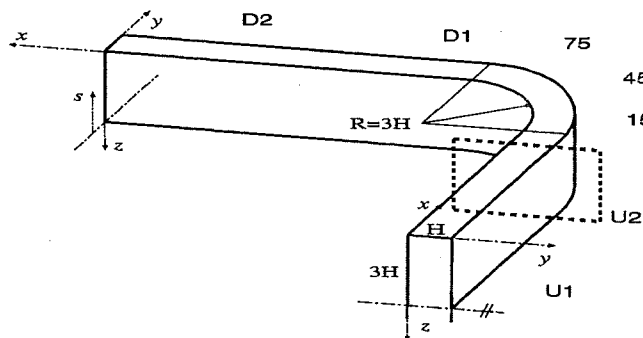
USoutham:ASM_ClWi





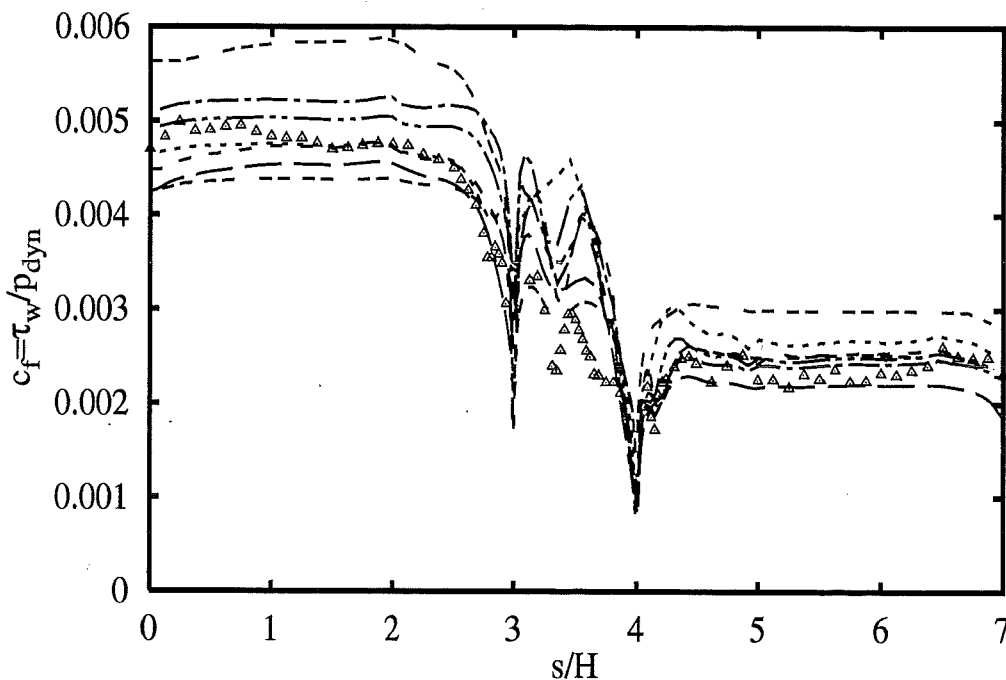


Distribution at $x/H = -0.5$

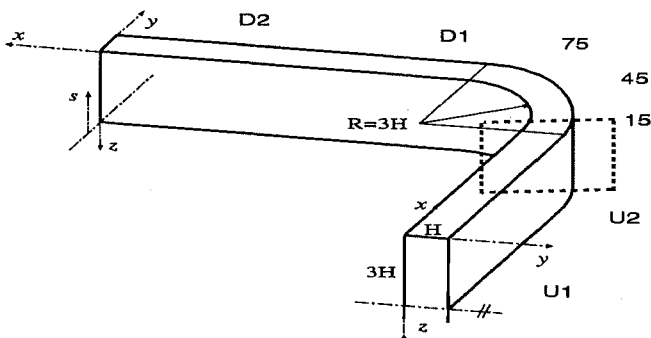


| Experiments | | | △ |
|-------------|-----|---------|-----|
| ASC | hKE | std+wf | --- |
| EDFLNHi | hKE | std+wf | --- |
| UBrussel | hKE | std+wf | --- |
| UBrussel | nKE | HiKh+wf | --- |
| UBrussel | nKE | SZL+wf | --- |
| USoutham | ASM | Clwi | --- |
| UMcGill | RSM | GiLa+wf | --- |

5 - 73

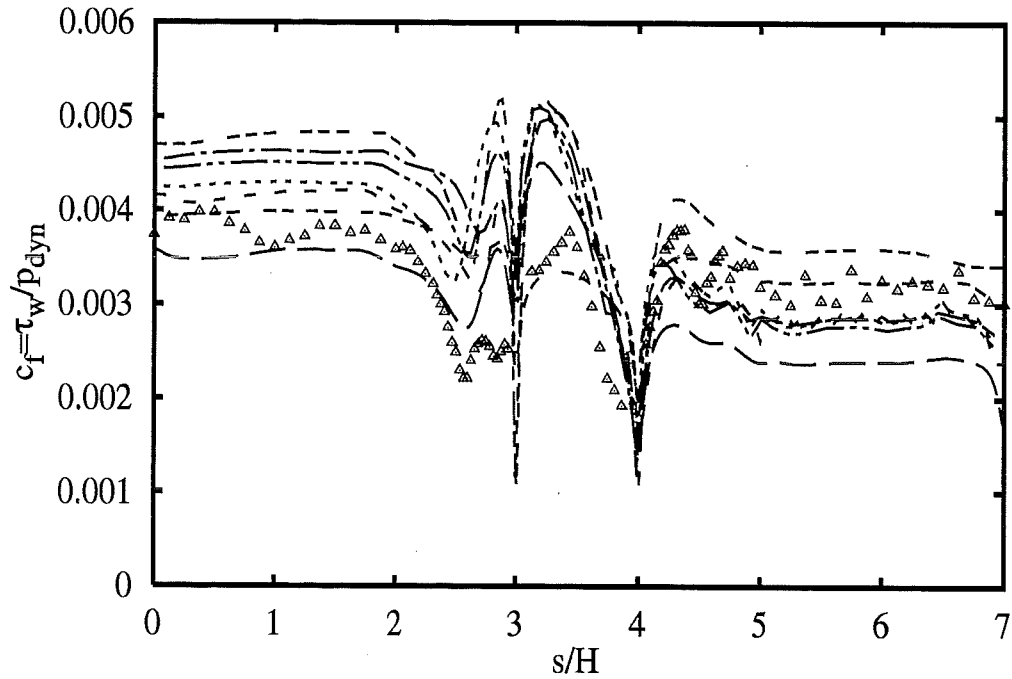


Distribution at $\alpha=15^{\circ}$

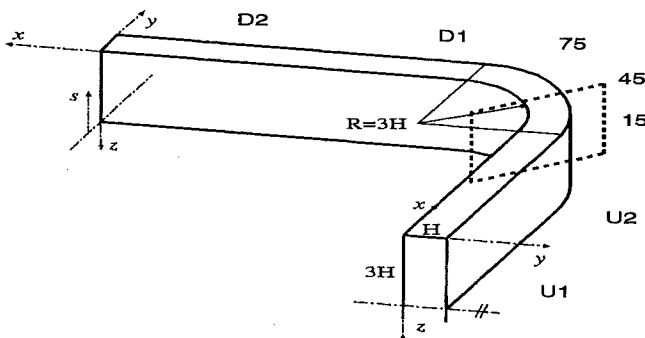


| Experiments | | |
|-------------|-------------|-----|
| ASC | hKE std+wf | --- |
| EDFLNHi | hKE std+wf | --- |
| UBrussel | hKE std+wf | --- |
| UBrussel | nKE HiKh+wf | --- |
| UBrussel | nKE SZL+wf | --- |
| USoutham | ASM ClWi | --- |
| UMcGill | RSM GiLa+wf | --- |

5 - 74

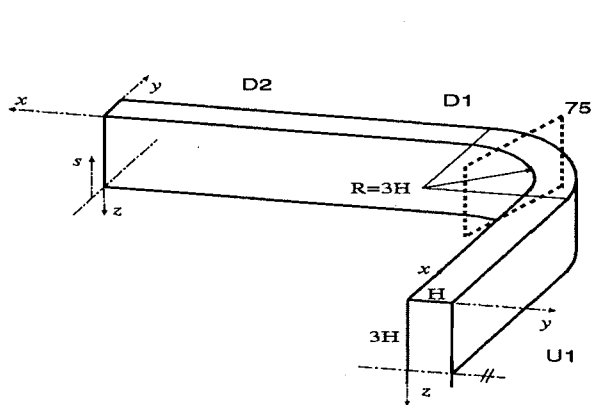
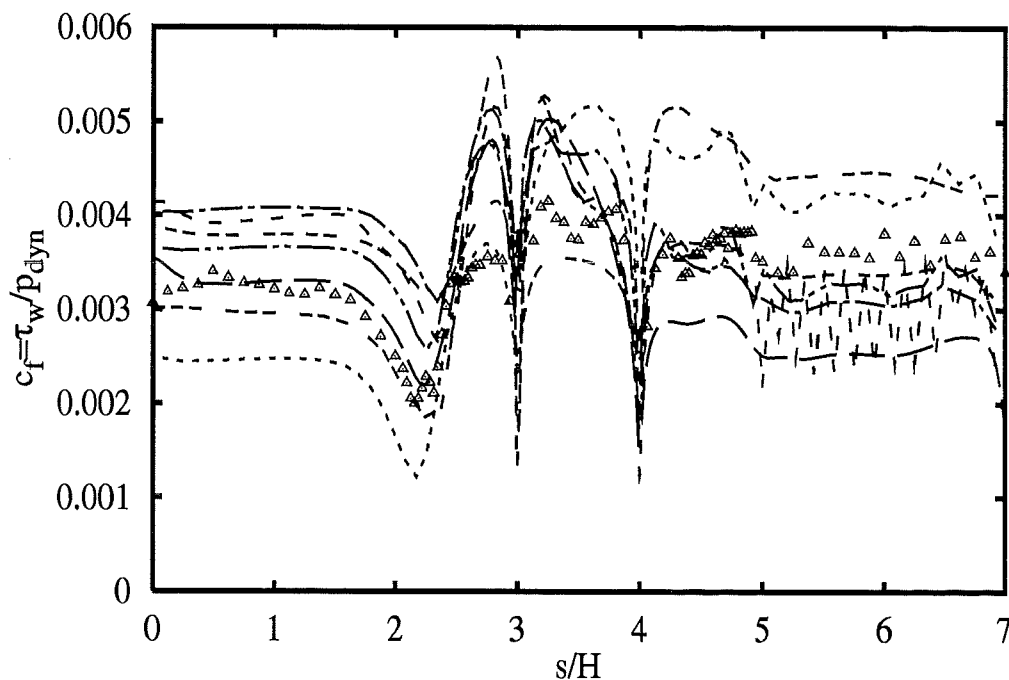


Distribution at $\alpha=45^\circ$



| Experiments | | | △ |
|-------------|-----|---------|-----|
| ASC | hKE | std+wf | --- |
| EDFLNHi | hKE | std+wf | --- |
| UBrussel | hKE | std+wf | --- |
| UBrussel | nKE | HiKh+wf | --- |
| UBrussel | nKE | SZL+wf | --- |
| USoutham | ASM | Clwi | --- |
| UMcGill | RSM | GiLa+wf | --- |

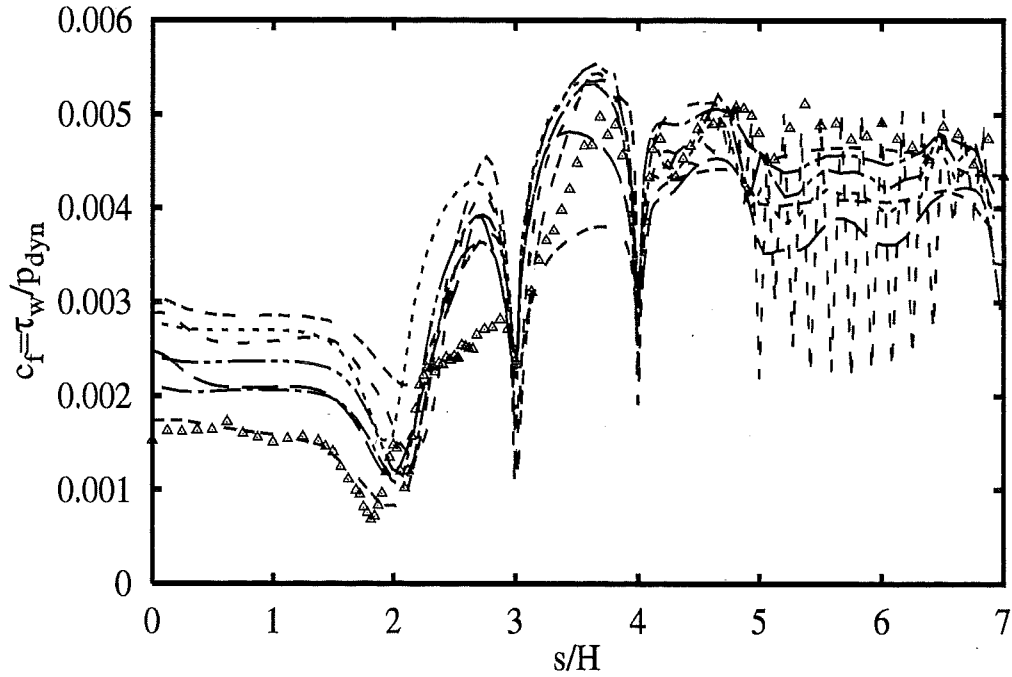
5 - 75



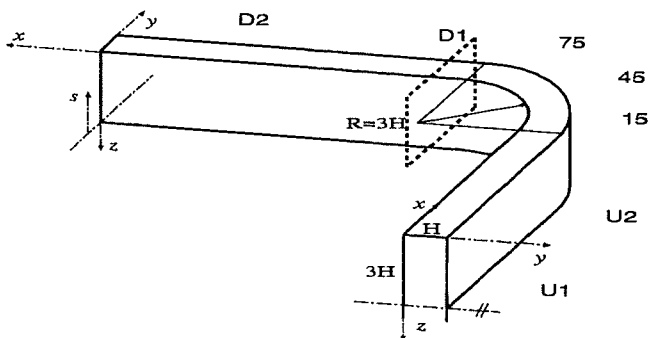
Distribution at $\alpha=75^0$

| Experiments | | |
|-------------|-------------|-----|
| ASC | hKE std+wf | --- |
| EDFLNHi | hKE std+wf | --- |
| Ubrussel | hKE std+wf | --- |
| Ubrussel | nKE HiKh+wf | --- |
| Ubrussel | nKE SZL+wf | --- |
| USoutham | ASM ClWi | --- |
| UMcGill | RSM GiLa+wf | --- |

5 - 76

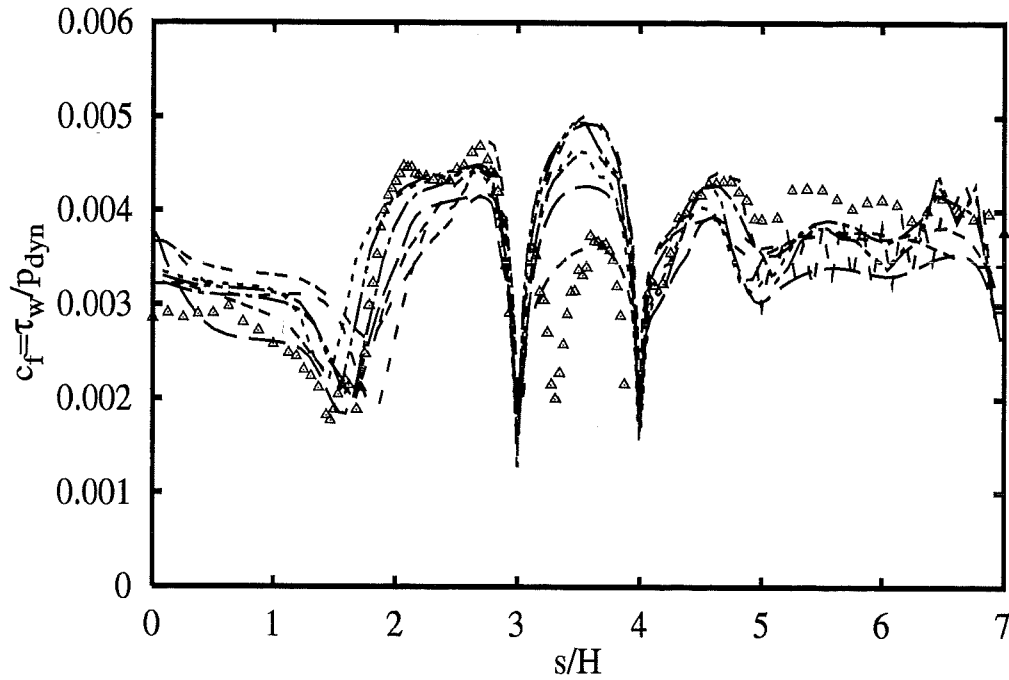


Distribution at $x/H=0.5$

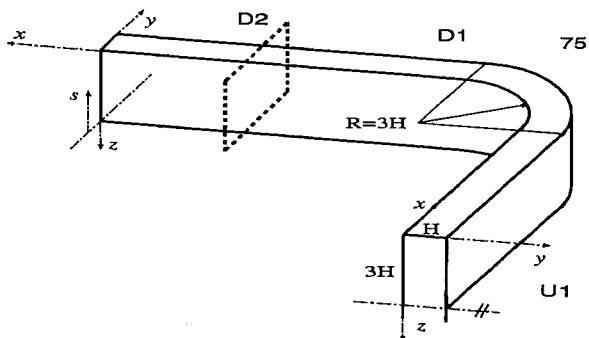


| | | Experiments Δ |
|----------|--------------------|----------------------|
| ASC | <i>hKE std+wf</i> | --- |
| EDFLNHi | <i>hKE std+wf</i> | --- |
| UBrussel | <i>hKE std+wf</i> | --- |
| UBrussel | <i>nKE HiKh+wf</i> | --- |
| UBrussel | <i>nKE SZL+wf</i> | --- |
| USoutham | <i>ASM ClWi</i> | --- |
| UMcGill | <i>RSM GiLa+wf</i> | --- |

5 - 77

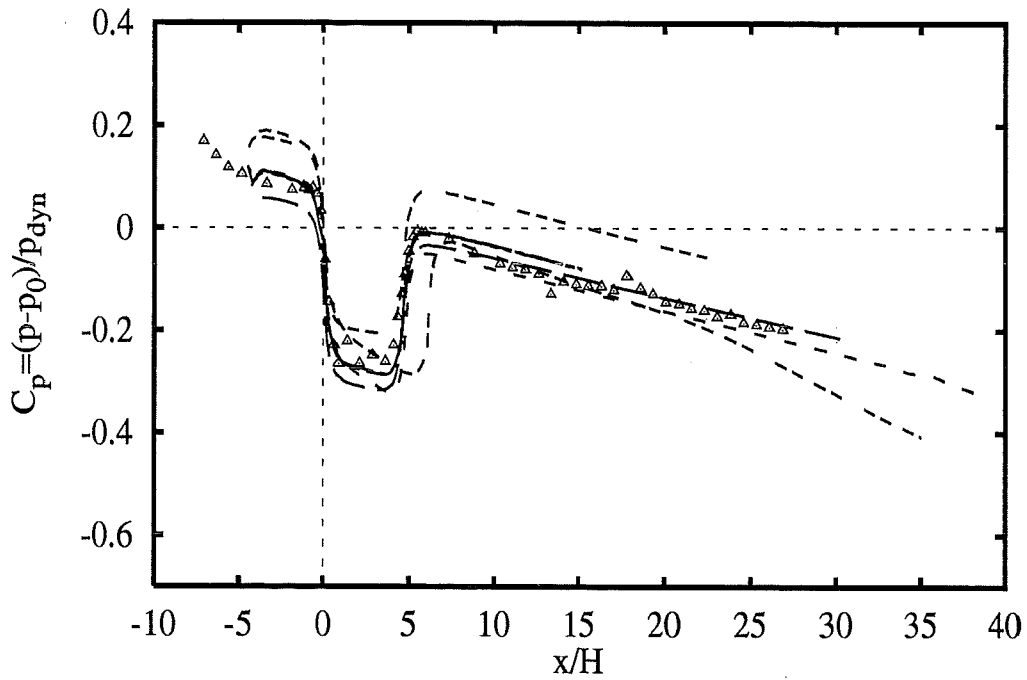


Distribution at $x/H=4.5$

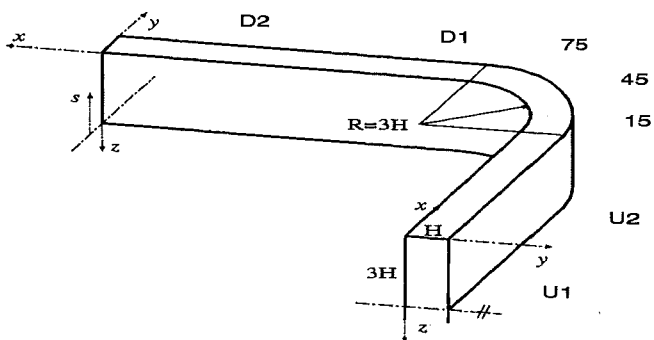


| | | Experiments | Δ |
|----------|-------------|-------------|----------|
| ASC | hKE std+wf | --- | |
| EDFLNHi | hKE std+wf | --- | |
| UBrussel | hKE std+wf | --- | |
| UBrussel | nKE HiKh+wf | --- | |
| UBrussel | nKE SZL+wf | --- | |
| USoutham | ASM ClWi | --- | |
| UMcGill | RSM GiLa+wf | --- | |

5 - 78

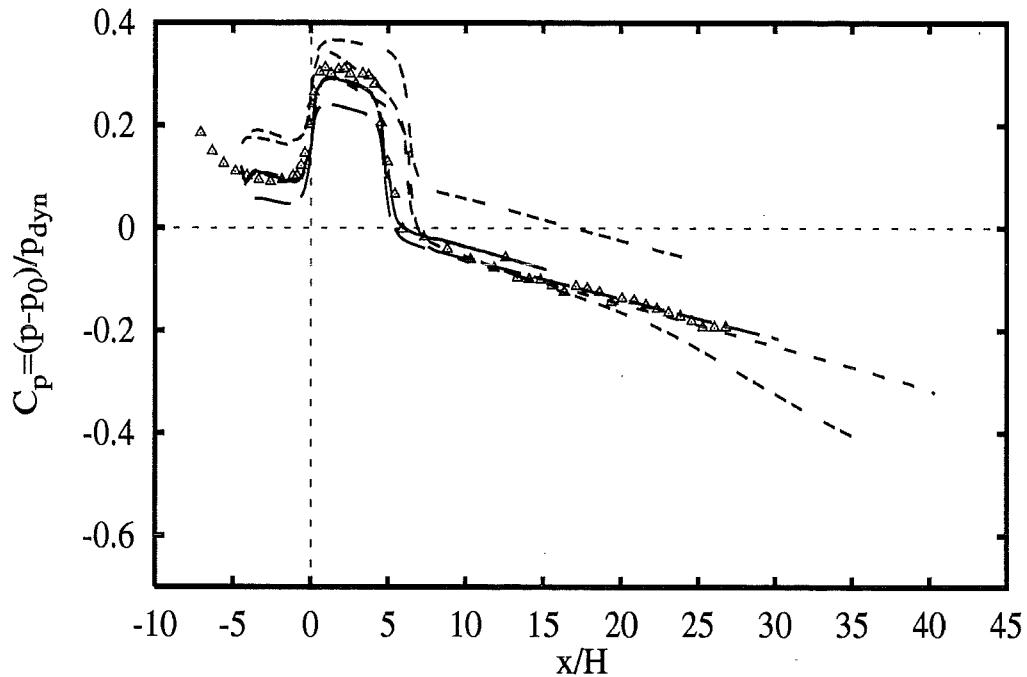


Distribution along inner wall

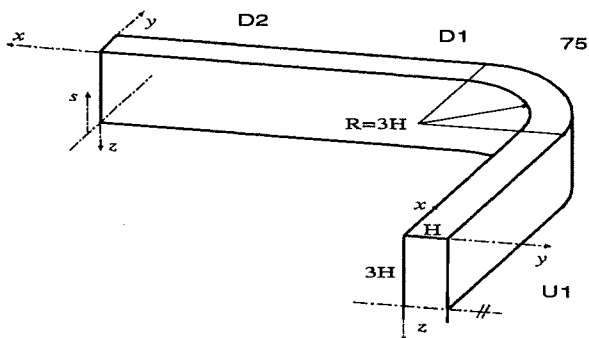


| Experiments | | △ |
|-------------|-------------|-------|
| ASC | hKE std+wf | --- |
| EDFLNHMi | hKE std+wf | --- |
| UBrussel | hKE std+wf | |
| UBrussel | nKE HiKh+wf | --- |
| UBrussel | nKE SZL+wf | |
| USoutham | ASM ClWi | --- |
| UMcGill | RSM GiLa+wf | --- |

5 - 79



Distribution along outer wall



| | | | △ |
|----------|-----|---------|-----|
| ASC | hKE | std+wf | --- |
| EDFLNHi | hKE | std+wf | --- |
| UBrussel | hKE | std+wf | --- |
| UBrussel | nKE | HiKh+wf | --- |
| UBrussel | nKE | SZL+wf | --- |
| USoutham | ASM | ClWi | --- |
| UMcGill | RSM | GiLa+wf | --- |

5 - 80